Probing the Mode of Action of eW5 - A Small Molecule Plant Growth Promoter

JONATHAN AVRAHAM REUVEN

Probing the Mode of Action of eW5 - A Small Molecule Plant Growth Promoter

Reuven Jonathan Avraham

PhD Thesis

Supervisor: Professor Patrick G. Steel

Durham University

Department of Chemistry

2021

“Managing expectations” Durham University 2020-

Thesis Abstract:

The work described in this thesis cover two distinct areas of chemistry. The primary body of this thesis looks at a small molecule *N-(2-aminoethyl)naphthalene-1-sulfonamide* (named eW5, **1**) which has been shown to promote various aspects of plant growth (Volume I, Chapters 1-4). Plant hormonal pathways control almost every aspect of plant development and growth. Small molecules can selectively perturb these highly complex and interconnected pathways and have thus demonstrated to be effective tools for the study of plant hormonal signalling. In order to determine the mode of action of eW5, two lines of research were undertaken and are described in the thesis. In the first approach, target identification of **1** was initiated by SAR studies that showed that C–4 substituents were viable, indicating viable incorporation of a photoaffinity tag. Three synthetic approaches towards a chemical probe were explained–ultimately affording *N-{2-[2-({4-[(2-aminoethyl)sulfamoyl] naphthalen-1-yl}oxy)ethoxy]ethyl}-3-tert-butyl-N-(pent-4-yn-1-yl) benzamide hydrochloride* (**145**) which was shown to retain the growth promoting abilities of **1**. A complementary approach using a genetic screen of EMS mutants was also employed to identify the causative gene mutation for eW5-resistance.

In the second aspect of the thesis (Volume II), two separate studies on Ir catalysed aromatic C–H activation are described. The development of the transformation of C–H bonds to form organoboron compounds has allowed for the formation of highly functionalised aromatics and late-stage functionalisation of compounds, making it of significance to the fields of natural product synthesis and medicinal chemistry. In the first of these studies, tandem Ir catalysed borylation – Suzuki-Miyaura cross coupling to 2-halo nicotinates was developed to afford trifunctional pyridines. Fluoro-aromatics represent another interesting class of substrates and as such, the second report describes a systematic study on the regioselectivity of Ir catalysed borylation. It was shown that the fluorine substitution pattern and the boron source were able to alter the standard steric controlled regioselectivity subtly yet distinctly in various substrates.

Table of Contents

Abbreviations

ABA	Abscisic acid
ABF	ABA-responsive element binding factors
Alloc	Allyloxycarbonyl
ASAP	Atmospheric solids analysis probe
B_2Pin_2	Bis(pinacolato)diboron
bHLH	Basic helix-loop-helix
bpy	2,2'-Bipyridine
CaM	Calmodulin
cod	1,5-Cyclooctadiene
coe	Cyclooctene
COSY	Correlation spectroscopy
CRISPR	Clustered regularly interspaced short palindromic repeats
DABCO	1,4-diazabicyclo[2.2.2]octane
DCC	N,N'-Dicyclohexylcarbodiimide
DCM	Dichloromethane
DIPEA	N,N-Diisopropylethylamine
DMAc	Dimethylacetamide
DMAP	4-Dimethylaminopyridine
DMF	Dimethylformamide
DMPE	1,2-Bis(dimethylphosphino)ethane
DMS	Dimethyl sulfate
DMSO	Dimethyl sulfoxide
dppf	1,1'- Bis(diphenylphosphanyl)ferrocene
dtbpy	4,4'-Di-tert-butyl-2,2'dipyridyl
eg	Ethylene glycol
EI	Electron ionisation
EMS	Ethyl methanesulfonate
eq	Equivalents
ES	Electropray
GA	Gibberellic acid

GAI	Gibberellic-Acid Insensitive
GCMS	Gas chromatography–mass spectrometry
GFP	Green fluorescent protein
HAB	Homology to ABA1
HBpin	Pinacolborane
HBTU	Hexafluorophosphate benzotriazole tetramethyl uronium
HMBC	Heteronuclear multiple-bond correlation spectroscopy
HOBt	Hydroxybenzotriazole
HPLC	High-performance liquid chromatography
HRMS	High-resolution mass spectrometry
HSL	Hormone-sensitive lipase
HSQC	Heteronuclear single quantum coherence spectroscopy
ITC	Isothermal titration calorimetry
JA	Jasmonic Acid
LC-MS	Liquid chromatography–mass spectrometry
LED	Light emitting diode
MMS	Methyl methanesulfonate
MOM	Methoxymethyl
mtbe	Methyl tert-butyl ether
NBD	Nitrobenzoxadiazole
NMR	Nuclear magnetic resonance
NOESY	Nuclear Overhauser effect spectroscopy
PAC	Paclobutrazol
PCR	Polymerase chain reaction
PEG	Poly-ethylene glycol
PG	Protecting group
PIF	Phytochrome Interacting Factor
PP2Cs	Protein phosphatase type C
Pybop	Benzotriazol-1-yloxytripyrrolidinophosphonium hexafluorophosphate
PYR	Pyrabactin Resistance
RCAR	Regulatory component of ABA receptor
RGA	Repressor of Gibberellic Acid

rt	Room temperature
SA	Salicylic acid
SAR	Structural Activity Relationship
SCR	Scarecrow
SEM	2-(Trimethylsilyl)ethoxy]methyl
SLY	Sleepy
SnAr	Nucleophilic aromatic substitution
SnRK	SNF1-related protein kinase
START	Steroidogenic acute regulatory related lipid transfer
TBAF	Tetra-n-butylammonium fluoride
TBAI	Tetra-n-butylammonium iodide
tBu	*tert*-Butyl
TFA	Trifluoroacetic acid
THF	Tetrahydrofuran
TIPS	Triisopropylsilyl
TLC	Thin layer chromatography
TMS	Trimethylsilane
TSA	Thermal shift assay
UV	Ultraviolet
WT	Wildtype
Y2H	Yeast two hybrid
YAC	Yeast artificial chromosomes

Declaration and Statement of Copyright

The work described in this thesis was carried out in the Department of Chemistry, Durham University between October 2018 and October 2021. All work is the author's own, unless otherwise stated. This work has not been previously submitted for a degree at this or any other institution.

Acknowledgements

First and foremost, I would like to thank my primary supervisor, Professor Patrick Steel. Your tireless dedication to research was a feat to watch and it motivated me to be the best chemist I could be. No matter how challenging things became, I always looked forward to coming in everyday as I knew you enjoyed solving any problem that might have arisen. I will always be grateful for the having worked with you.

To my second supervisor, Professor Marc Knight, thank you for all you have done to aid me in this process. During induction on my first day, I was told a second supervisor was usually nothing more than a formality, but you have been integral to my PhD journey. Your endless optimism was much needed especially in these challenging times, and I will always appreciate the time you gave to guide me in biology and to just have a friendly chat.

I would also like to extend my thanks to everyone who has worked in CG001, past and present. There are far too many of you to mention by name but whether as a Post Doc., PhD student, final year undergraduate or a placement student, this thesis would not have been possible without your collaboration and support. Courtney, you always managed to find the balance between keeping the atmosphere loose and tough love and I will always appreciate how you took your time to show me the ropes when I first joined, despite how stubborn I was. Thank you, Jaime, for always keeping things in perspective, your life lessons will follow me wherever I go. Exe, I cannot thank you enough for your endless support over the past three years. No matter how much you had on your plate, you were always happy to help, and I hope that some of that enthusiasm for chemistry has rubbed off on me. Thank you, Vanessa, and Michaela, for always keeping me grounded and reminding me that there was always time for a laugh no matter how dire the situation was. Dan, I couldn't have asked for a better person to have spent doing "a bit of grunt work" with, thank you for keeping me sane during our countless hours in biology. And last but certainly not least, thank you, Victor, for not only tolerating me in the lab, but out of it as well. You were always there whenever I needed a good rant, and your sense of joy was always infectious.

To everyone in Biosciences, especially Lab 19 who went out of their way to accommodate me, I cannot thank you enough. No matter how busy everyone was, they were always willing to coordinate and, in some instances, take on a proactive role in my experiments. The last 18 months were very challenging and without the help of Bryony, Nathan, Roland and Dr. Heather Knight, the biological assays you see in this thesis would not have been possible.

Thank you to Durham's analytical staff in both the Department of Chemistry and the Department of Biosciences who's committed hard work was also essential to the completion of this project. To Juan Aguilar, Catherine Heffernan and Eric Hughes, thank you for keeping the NMR services running smoothly despite all of the challenges. Thank you to Pete Stokes and Dave Parker for all your work in maintaining a running mass-spectrometry service during these challenging times. And finally, thank you to Joanne Robson in Biosciences who very patiently guided me through the process of imaging root tips.

Finally, I would like to thank my partner Victoria and my family back in Hong Kong for their unconditional love and support over the past three years. Thank you for continuing to push me no matter how difficult the circumstances were, I owe all my successes to you all.

Volume I: Probing the Mode of Action of eW5 - A Small Molecule Plant Growth Promoter

Chapter 1: Introduction

1.1: Thesis Introduction

This primary aim of this thesis is to discuss the two approaches undertaken in the identification of the target of plant growth promoter eW5 (**1**). The first was a forwards chemical genetics approach which involved the exploration of the SAR of the compound and subsequent development into a chemical probe, the second being a forwards genetics approach through an EMS mutant screen.

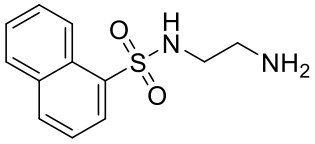

1

Figure 1: Structure of eW5.

This thesis comprises of two distinct volumes. Volume I contains four chapters focussing on target identification of eW5 (**1**). Chapter 1 introduces the use of chemical probes in a plant biology context, the relevant plant hormonal pathways, previous work conducted in the group and the aims of this research. Chapter 2 presents the initial synthesis of analogues and SAR studies. Chapter 3 describes the methods employed in the development of the chemical probes targeted. Chapter 4 discusses a complementary genetic approach in the identification of the target of eW5. Chapter 5 provides the data supporting compound characterisation and experimental methodology. Volume II discusses a separate line of research in the investigation of aromatic Ir catalysed C–H activation. This volume will outline the rationale and results behind two studies and present the respective manuscripts.

1.2: Use of Small Molecules as Chemical Probes within Plant Systems

1.2.1: Introduction to Chemical Genetics

Due to the advancements of genetic approaches, the last 20 years has seen significant progress in the study and elucidation of hormonal pathway mechanisms within plants.[1] These classical methodologies can be divided into two major groups: forward and reverse genetics. Forward genetic approaches aim to identify novel proteins by studying phenotypic responses on randomly mutagenized populations whilst reverse genetic approaches aim to identify a phenotype through targeted mutation of a specific gene.[2] In plants, genetic studies over the past decade have mainly been applied on the model organism *Arabidopsis thaliana* and elucidated the highly complex and interwoven hormonal pathways which modulate growth at various stages of the plant lifecycle.

Despite the vast inroads made through genetic studies, the issue of genetic redundancy is a recurring limitation of these approaches. This issue arises from the highly similar function of several genes responsible for a specific phenotype.[3] To compound this, the highly interdependent relationship of genes not only increases the difficulty of identifying protein function, but also introduces the issue of lethality and pleiotropic effects which are commonly observed in genetic mutants.[4]

Small bioactive molecules are able to address these issues by acting as a general antagonist that inhibits multiple components within a network or by acting as a specific agonist which triggers a specific component within a network. This principle does not work in reverse as specific antagonists would not affect similar responses from a redundant system and a general agonist would activate too many components to be identified accurately through genetics.[5] Introducing small molecules in plant systems allows for instantaneous and reversible phenotypic response thereby making them good tools to study the often complex, and highly dynamic pathways without the issues of lethality and gene redundancy. This approach is like genetic mutant analysis as inhibition of protein function can be understood to be the same as loss-of-function alleles whereas compounds acting as agonists are equivalent to gain-of-function phenotype.[6] Investigation of plant hormonal responses with these small molecules lead to a wide array of possibilities, from the rational development of related bioactive analogues and probes which will further our understanding of the modes of action of plant hormones to the identification of novel molecules with agricultural applications.

The field of chemical genetics combines classical genetic approaches with the use of small bioactive molecules.[7,8,9] As with classical genetics, these studies can be conducted in a forwards and reverse manner. In forward chemical genetics, randomly mutagenized populations are replaced with screening against a compound library (chemical toolbox).[1] As with forward genetics, a phenotypic response is

measured and the compound(s) that induce this are selected and used to identify the target protein. In chemical genetics an additional step of target enrichment, prior to identification is needed, often requiring the development of a method of binding the small molecule with its biological target.[10,11] Compound libraries are also used in reverse chemical genetics but on a known protein target to identify bioactive ligands that have agonistic or antagonistic properties. Viable ligands are then introduced back into an *in vivo* system to identify the phenotypic change.[12,13] As the use of chemical probes to identify protein targets fall within forward chemical genetics, this review will focus on this approach.

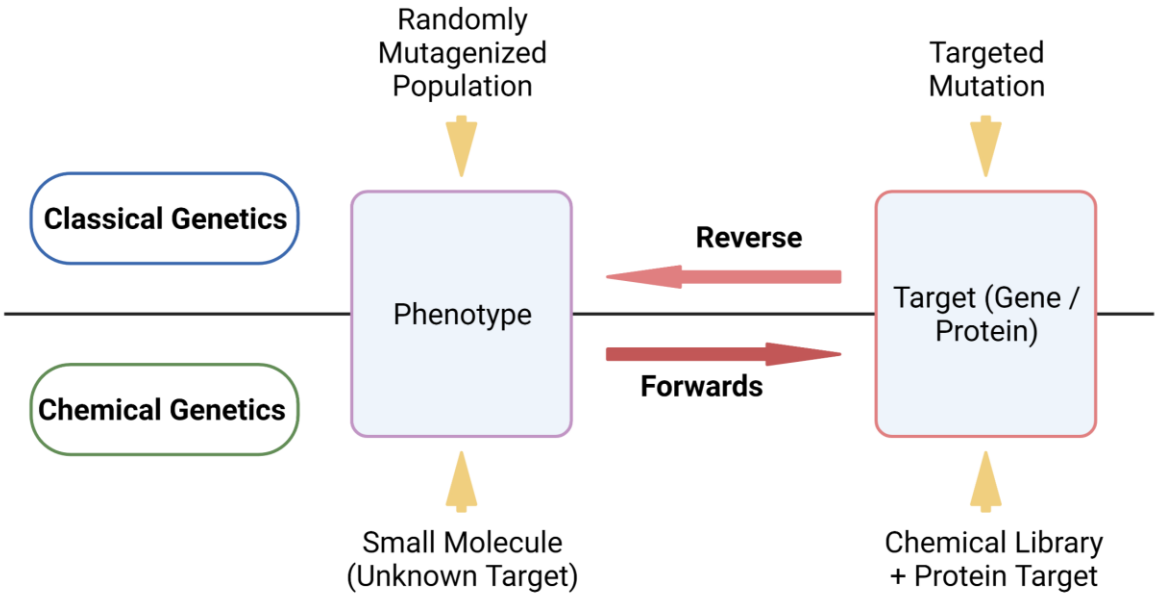

Figure 2: Forward and reverse classical and chemical genetic approaches.

1.2.2: Introduction to Chemical Probes

The determination of targets of small molecules is vital in understanding the mode of action of the molecule. This not only aids research in the particular pathway but can ultimately lead to enhanced phenotypic responses through rational (re)design of the molecule. Although important, identification of a target poses the greatest difficulty in forward chemical genetics. This involves a strategy to develop the small molecule of interest into a chemical probe. In recent times, there has been extensive use of chemical probes in the interface of biology and chemistry and thus the term has garnered a large range of definitions, covering all molecules that can be used as chemical tools.[14] The definition given by Arrowsmith *et al*. describing a chemical probe as a "a selective small-molecule modulator of a protein's function that allows the user to ask mechanistic and phenotypic questions about its molecular target" is best suited for this discussion.[15]

A chemical probe usually has to achieve two main functions; to bind to its target and to provide a method of extracting the probe-target complex. This review will focus on the latter – methods of attachment within a plant context. Due to the structural and biological diversity of small molecules and their respective targets, numerous methods have been developed to bind the two. In this overview, these probes have been divided into three general categories: affinity-based probes which exploit the small molecule's interaction with its target, reactivity-based probes which utilise an additional reactive module and photoaffinity-based probes which require the use of a photo-reactive tag.

It is worth noting that another common strategy for target identification is through the use of imaging. This usually involves the attachment of fluorophores or the alteration of the lead molecule in such a way that it itself is fluorescent, allowing for localisation of the compound to be observed within a biological system.[16] Although these methods may provide better initial approach for target identification by allowing for the visualisation of small molecule localisation, they do not necessarily lead to the identification of biomolecular targets and thus will not be covered in this review.

1.2.3: Affinity Based-Probes

The simplest approach in target identification is by utilizing the inherent binding affinity between the small molecule and its target.[17] Often non-covalent in nature, these transient interactions can be exploited as competition experiments with known inhibitors to allow for validation of an on-target effect. There have been several reported cases where the small molecule in question forms a strong enough reversible interaction that it allows for target enrichment and identification as described below.

1.2.3.1: Affinity Probes in Plants

Although there are numerous reports of this methodology being used to elucidate mammalian cell mechanisms, only a few successful examples of affinity-based probes used within a plant context exist.[17] One notable report of this approach being used in plants was described by Uehara *et al*. in the study of the casein kinase 1 like (CKL) family in *Arabidopsis*.[18] Previous studies have shown that CKL kinases regulate stomatal aperture, blue light signalling and ethylene production. They have also been heavily implicated in the control of the circadian clock which allows for adaptation to daily and seasonal cycles.[19] Although several lines of protein sub-families have been identified, the issue of genetic redundancy has been an issue, resulting in the need for small molecule modulators.

Preliminary affinity-proteomics data had suggested that PHA767491 (**2**) interacts with 13 members of the CKL family in *Arabidopsis*. SAR studies found that N-alkylation of the pyrrole retained the ability

to lengthen the circadian period, leading to the development of probe **5** which was then linked to agarose beads. Proteins that bound to the affinity resin were analysed through LC-MS and to confirm on target binding, **2** was used in competition assays. Proteins identified included members of the CKL family, shaggy-related protein kinases (GSK3) family and 5-METHYLTHIORIBOSE KINASE1 (MTK1), confirming initial proteomic data.

In further studies described by Saito *et al*., SAR studies of **2** led to the synthesis of pyrrole based **4** which was found to be 100-fold more inhibitory towards kinase activity.[20] From this lead molecule, probe **6** was developed with a primary amine allowing for the covalent linkage onto agarose beads (Figure 3).

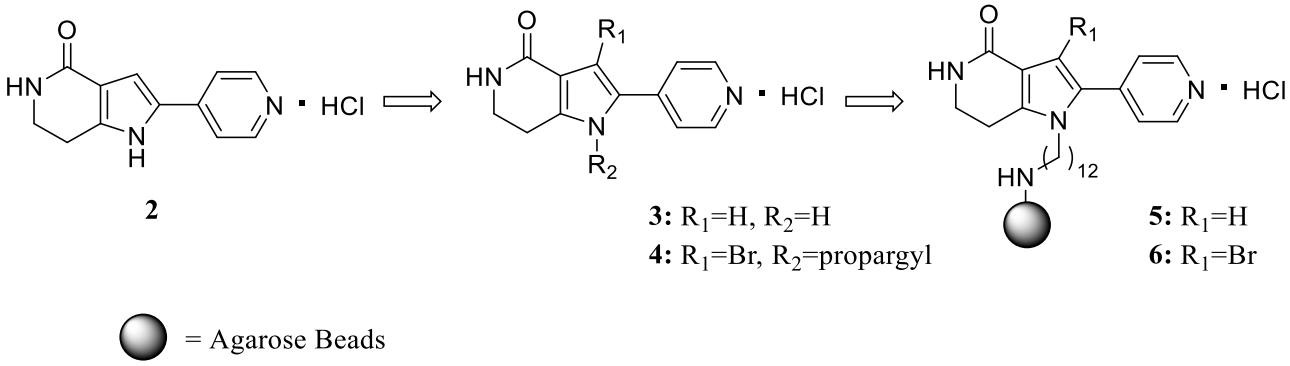

Figure 3: Development of PHA767491 (**2**) into an affinity-based probe.

Despite the molecule not containing any obvious reactive component capable of forming covalent interactions with a protein, target enrichment and identification was still possible. Using similar methodology as described above, mass spectrum analysis was able to identify a set of 23 proteins in the CK1 family as well as 10 additional non-CK1 proteins, demonstrating that the new analogue was highly selective for the CK1 family. This ultimately opens possibilities of these pyrrole-based compounds functioning as agricultural agents in the control of stress responses, flowering and circadian clock modulators.

Although this approach was advantageous in its simplicity, it cannot be applied to all cases. The lead molecule was previously known as an inhibitor of the mammalian cell division cycle (CDC) 7 kinase and as such, a robust biological assay was able to be developed for compound evaluation. In studies where the target(s) of the small molecule involved have not been narrowed down to a particular protein family, an observed increase in *in vivo* activity cannot be directly correlated to enhanced binding efficiency. This ultimately prevents protein enrichment and identification as the interaction between the small molecule and its target may remain transient in nature.

1.2.4: Activity Based Probes

Activity based probes take advantage of reactive residues within the binding site of the small molecule to form an interaction. Unlike affinity-based probes, this approach makes use of an additional reactive component that is able to form an irreversible covalent bond with the target.[21] Once a covalent linkage has been established, target enrichment can be carried out via the reporting unit facilitating target identification which can be carried out in a similar manner as discussed above. Reactive groups on their own label the most reactive residues without selectivity.[22] Selectivity can be introduced by combining these groups with a ligand that acts as a directing group to the target, these probes are known as mechanism-based probes.

Mechanism-based probes take advantage of the fact that during the catalysis of reactions, most enzymes form a covalent complex with its respective substrate.[23] Probes that fall into this category usually mimic these substrates but prevent the catalytic cycle from progressing past the covalent complex intermediate. There are a wide range of reactive groups, all specifically targeting active nucleophilic residues that have been used in the development of plant probes. These groups include but are not exclusive to epoxides (**7**), fluorophosphonates (**8**) which target serine residues, iodoacetamides (**9**) and β-lactones (**10**) which target cysteine residues, and aryl fluorosulfonates (**11**) which target active lysine residues.[22]

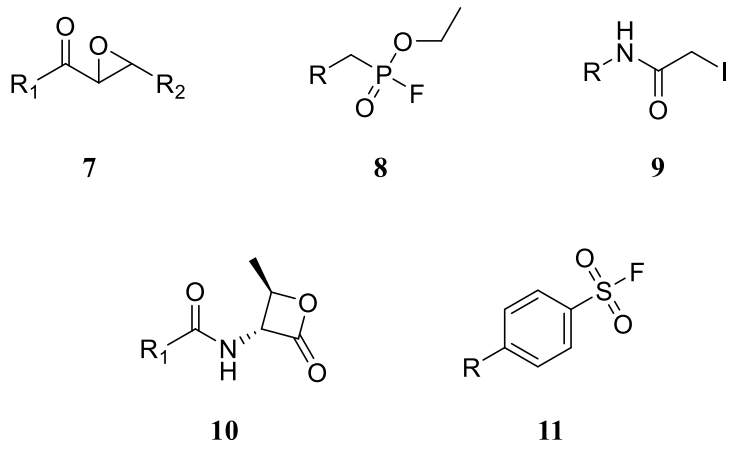

Figure 4: Selected reactive groups used within activity based probes.[22]

1.2.4.1: Activity Based Probes in Plants

One notable example of activity base probes being employed to identify plant protein targets was reported by Morimoto *et al*, in the study of 1,3,5-triazines.[24] Although these structures are not commonly found in nature, they have been used extensively in herbicides. Some plants have been shown

to be able to degrade these scaffolds into intermediates that accumulate, posing a threat to nearby algae and plants. It was thus of interest to identify the protein targets of these compounds to better understand the mode of action of triazine-containing agrochemicals as well as allow for the rational design of compounds containing less persistent scaffolds. Two approaches using reactive groups were undertaken in parallel. The first approach connected a chloroacetamide as the reactive group via an ethylenediamine linker to the triazine core affording probe **13**. The second approach attached a chlorine directly onto the triazine scaffold, forming a chloro-triazine reactive group forming probe **14** which would be able to form a covalent linkage via SnAr substitution by a nucleophilic residue. It was shown that chloro-triazine **14** gave the strongest signal when tested on Arabidopsis extracts and also gave specific binding even at higher concentrations. Following coupling of the probe to biotin azide via copper(I)-catalysed alkyne-azide cycloaddition (CuAAC), and enrichment on protein gels, LCMS analysis was able to identify ascorbate peroxidase 1 (APX1) as the main target of the probe, furthering the understanding of the mode of action of 1,3,5-triazine-containing herbicides.

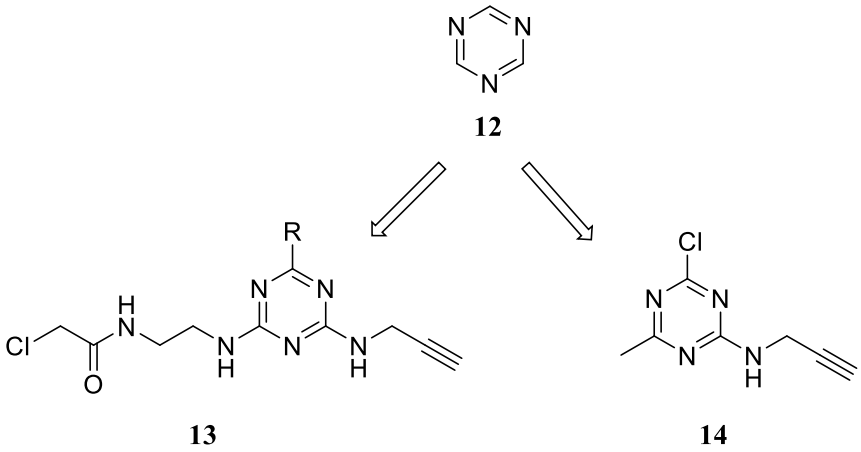

Figure 5: Development of activity-based probes **13** & **14**.

In addition to an increased probability in target identification, one of the primary advantages of this approach is that the range of available reactive groups allows for the targeting of specific protein families due to the conservation of catalytic residues.[25] Despite this advantage, this approach can be limited in the identification of unknown targets as it assumes reactive residues are present in the binding site. The propensity to bind to certain residues over others also can limit this approach, especially if the small molecule in question has multiple targets.

1.2.5: Photoaffinity Based Probes

Photo-affinity probes belong in a subset of the activity-based probes, where the reactive group is formed *in situ* under a specific wavelength of light. This is a commonly used when either the affinity of the molecule in question is too transient to allow for target isolation and identification, or if very little is understood about the interaction between it and the target.[26] In principle, the photoactive component is stable in the absence of UV light, allowing the probe to form a covalent interaction with the target. Irradiation at a specific wavelength activates the reactive component forming a highly reactive intermediate. This gives rise to the most significant advantage of these probes which is their ability to bind to targets even if the interaction is transient.[27–29] The reactive intermediate generated (carbenes, nitrenes and excited ketyl diradicals) are able to bind indiscriminately, even inserting into C–H bonds, making them ideal for forming an irreversible covalent interaction. Importantly, the wavelength required to generate these reactive intermediates are usually > 330 nm, ensuring that protein integrity is not compromised.[30] The inert nature of these compounds in the absence of UV light also allows for equilibrium to be established prior to target-crosslinking, increasing on target binding as well as binding efficiency.[31]

The approach shares the same drawback that arise from activity based-probes wherein the modified molecule needs to retain the same binding behaviour with its respective target prior to photo-crosslinking to ensure on-target binding.[32] Photoaffinity based probes are widely used in plant chemical genetic approaches and exclusively make use of three photoreactive groups; benzophenones, diazarines and aryl azides.

1.2.5.1: Benzophenones

Benzophenones are commercially available, easily incorporated into synthetic routes, activated at 365 nm and chemically stable in the absence of UV light.[33] These properties make it a popular photo-reactive tag despite the steric bulk it introduces into a probe. During activation by UV light, a non-binding oxygen electron is promoted into the carbonyl π^* orbital generating two possible triplet excited states and two singlet excited states.[34] The excited biradical (**16**) is able to undergo various chemical reactions namely H–atom abstraction and insertion into C–C bonds. This reactive biradical gives rise to one of benzophenone's advantages as a photo-crosslinking tag as it is able to react reversibly with water.[32] The formed hydrate (**18**) eliminates rapidly to reform original benzophenone **15** which can be excited again. Benzophenones are also significantly more stable than diazarines and aryl azides in ambient light, allowing for easier manipulation.[34]

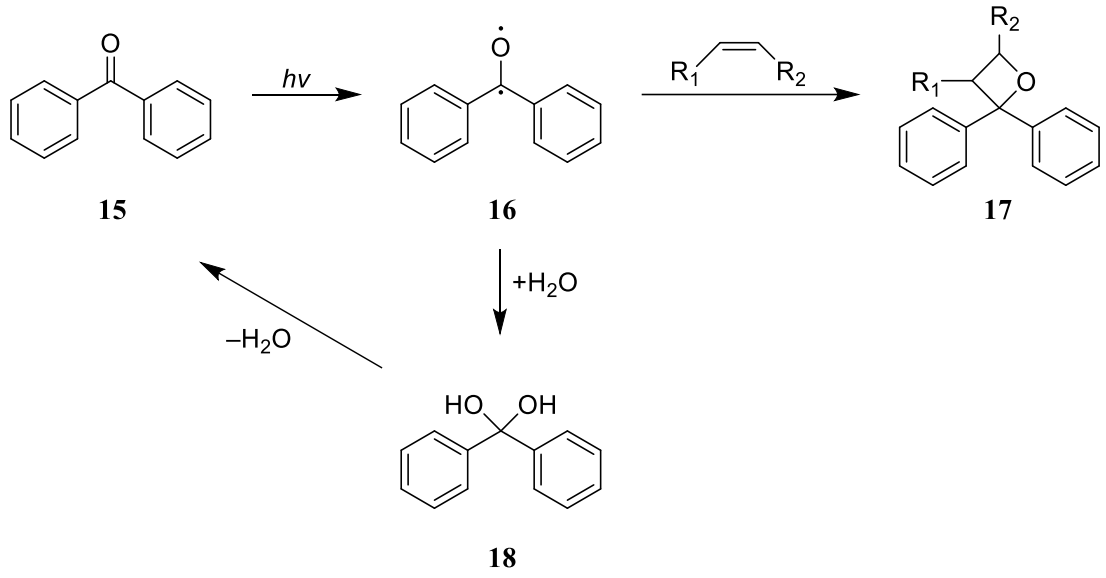

Scheme 1: Mechanism of insertion of benzophenones and reversible reaction with water.

Despite the advantages of the benzophenone moiety, there are several factors that limit utility in photoaffinity probes. A study conducted by Weber *et al*. found that C–H insertions by a benzophenone containing peptide were much higher yielding in the presence of water than in isopropanol, indicating the efficiency of photo-crosslinking is highly dependent on the hydrophilicity of the binding site.[35] As photo-affinity probes are primarily used for the purpose of target identification, this limitation poses an issue as the nature of the binding site is almost always unknown. Additional limitations are with respect to the orthogonality of benzophenones to amines. Although benzophenones are generally stable in the absence of UV light, the carbonyl group is able to form imines with biologically active amines. In a report by Shultz *et al*, it observed that a benzophenone containing peptide was able to covalently bind with a lysine residue of HIV protease.[36] Although this interaction was reversible, it demonstrated the possibility of increased non-specific interactions with increasing concentration of the photoaffinity probe. Another limitation of this group is the steric size it introduces to the small molecule, possibly altering the mode of binding. As mentioned above, photoaffinity probes often need to retain biological activity to validate on-target photo-capture and the introduction of a large group could result in off-target labelling.

The most significant limitation of benzophenones is the low reactivity of the excited biradical which often requires a long irradiation time to achieve binding.[34] This low rate of activation thus becomes comparable with the rate of ligand-binding site dissociation increasing the possibility of non-specific binding, especially if the interaction is inherently weak. This combined with its steric size limits its use

as alteration of the molecule can lead to reduced target interactions again resulting in increased non-specific binding.[37]

1.2.5.2: Diazarines

Diazarines are widely used as photo-crosslinking tags in photoaffinity probes. Liberating nitrogen in the presence of UV light (335 nm), ultrasonication or heat generates a reactive carbene.[38] There are two possible mechanistic routes to which this occurs; directly or through photoisomerization to the non-cyclic diazo species (Scheme 2). Both singlet and triplet forms of the carbene can be formed, with the singlet being the one of major interest due to its ability to undergo C–H bond insertion.[39]

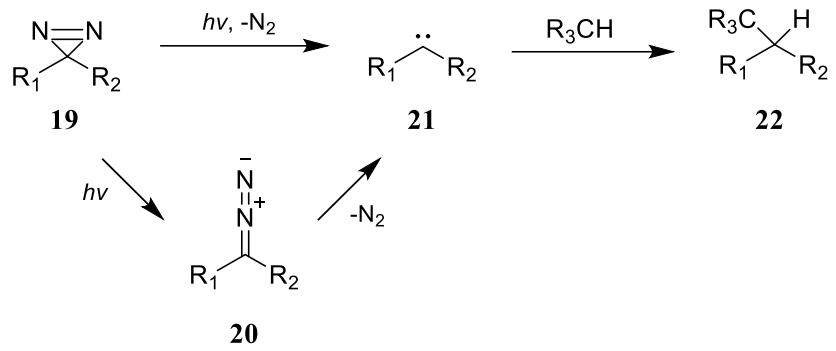

Scheme 2: Mechanism of diazarine carbene formation and C–H bond insertion.[40]

Early diazarines were aliphatic which gave rise to issues when being used in photoaffinity probes due to their propensity to undergo 1,2-hydrogen rearrangements (Scheme 3, **A**).[41] Despite this limitation, this group has been developed into several fundamental building blocks in the development of photoaffinity probes namely, the minimalist linker and photo-amino acids. Minimalist linker **26** was first reported by Li *et al*, combining the aliphatic diazarine, an alkyne reporting unit and a primary alcohol for attachment in a small module.[42] Several amino acids incorporating aliphatic diazarines into their respective side chains have been reported, such as photo-leucine (**27**) and photo-lysine (**28**).[43] In addition to synthetic approaches to access these photoactive amino acids, they have also been introduced via genetic code expansion.[44] Reports published by Shultz *et al*. outline the ability to specifically incorporate these functionalized amino acids into specific sites within native environments which allow for the study of transient protein-protein interactions.[45][46] Both these examples of aliphatic diazarine functionalization aim to address the issue of large appendage groups negatively affecting biological activity of the small molecule and have been extensively used in the development of chemical probes.

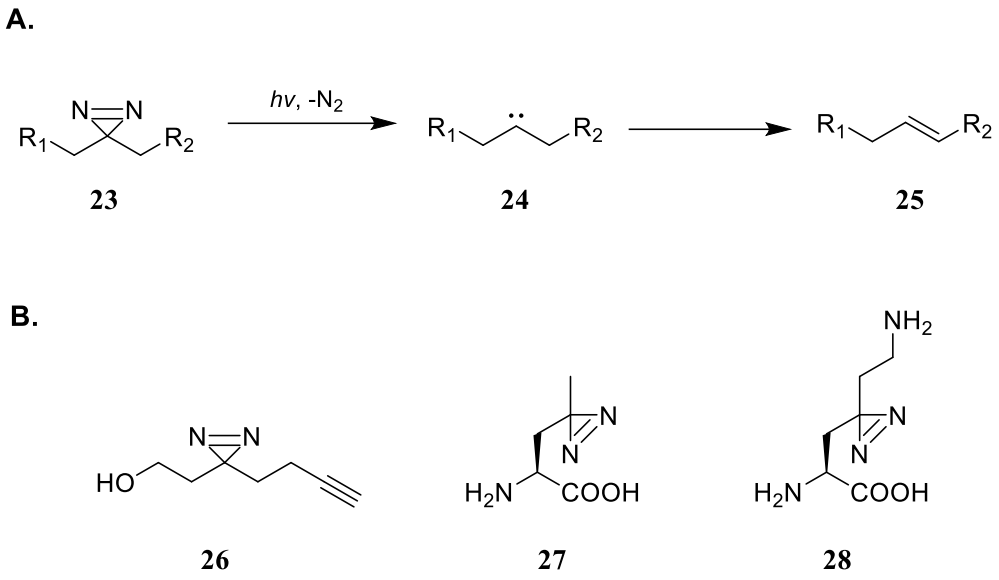

Scheme 3: **A**. 1,2-hydrogen rearrangement of aliphatic dizaraines. **B**. Photo-reactive modules containing aliphatic diazarines.

Phenyl diazarines were first identified as more efficient photolabeling groups by Knowles *et al*. due to the reduced tendency to undergo 1,2-hydrogen rearrangements.[47] Upon further studies phenyl diazarines were shown to form the carbene via linear diazo species **20**.[48] This ultimately resulted in non-specific binding as the slow photoisomerization process allowed for dispersion of the probe from the binding site before insertion could take place.[49] A proposed solution was reported by Brunner *et al* using a trifluoromethyl group flanking the phenyl diazarine. Although still not fully understood, the electron withdrawing nature of the trifluoromethyl group reduces the reactivity and abundance of the diazo intermediate, resulting in increased binding to the active site of interest.[50]

1.2.5.3: Aryl Azides

Although not as prevalent as benzophenones and diazarines, aryl azides still make up a significant proportion of photoactive labels within plant chemical probes. When irradiated with UV light (330 – 370 nm), aryl azides readily convert to nitrenes via the loss of N_2.[30] As with carbenes, this highly reactive intermediate (**30**) can readily insert into C–H or hetero–H bonds to form the secondary amine adduct (**31**). The main advantage of this approach is that the aryl azide can be directly linked onto an existing aromatic core of the small molecule, minimizing the disruption to binding and biological activity. [51] Despite the small steric bulk introduced by this photo affinity group, its lower reactivity to C–H bonds compared to benzophenones and diazarines limit its use in photoaffinity probes.[52]

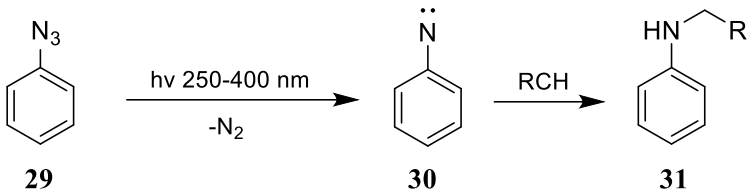

Scheme 4: Mechanism of aryl azide photo-crosslinking reaction.[30]

1.2.5.4: Photoaffinity Based Probes in Plants

There have been extensive reports on the use of photoaffinity based probes in the study of plant targets and pathways. One such example is a report by Li *et al*. which demonstrated the effectiveness of this approach in the elucidation of plant biosynthetic pathways.[53] Unlike prokaryotes, eukaryotes do not contain gene clusters of biosynthetic genes, making it challenging to identify the biosynthetic pathway of novel natural products. This study aimed to circumvent this issue by coupling minimalist probe **26** attached via an ester linkage to steviol (**32**), a natural sweetener isolated from the leaves of *Stevia rebaudiana*.

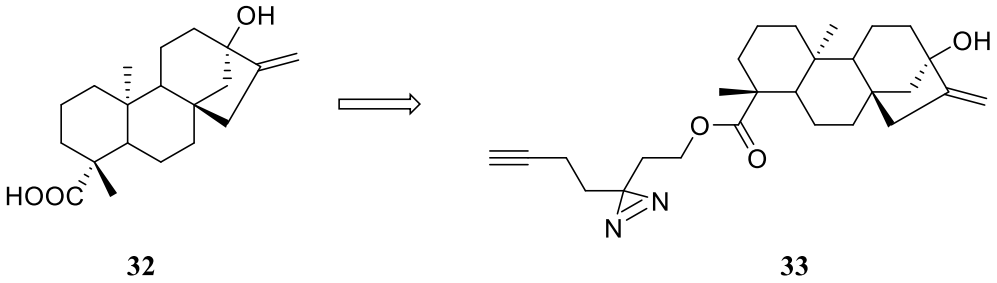

Figure 6: Development of steviol into a photoaffinity probe.

Probe **33** was incubated with plant lysate and following a large-scale pull-down experiment, biotin enrichment and mass spec analysis, UPD-glycosytransferase UGT73E1 was identified as being involved in steviol glycoside biosynthesis. Interestingly, an affinity-based approach was initially attempted through the use of a biotinylated steviol probe, but binding affinity was shown not to be sufficient for this. This demonstrates the benefits in covalently capturing the target via photo-crosslinking, overcoming the issues posed by reversible interactions.

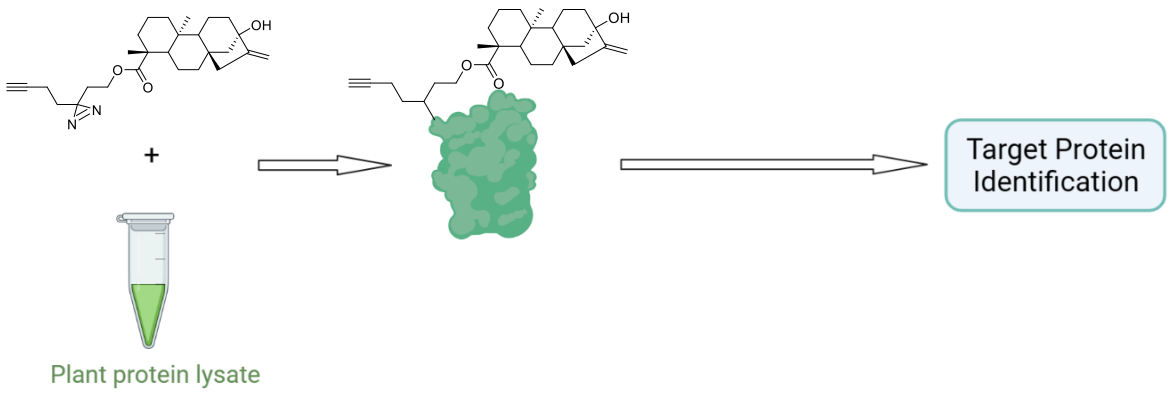

Figure 7: Workflow for target protein identification of steviol.[53]

Another example of photoaffinity probes being used in the study of small molecule targets in plants was reported by Fujii *et al*, investigating circadian rhythm-controlled leaf movement.[54] This was achieved through the development of potassium isolespedezate (**34**), a known promotor of leaf-opening in *Cassia minosoides* L., into a chemical probe. Modifications of the glycon moiety in initial SAR studies found comparable activities to **34**, resulting in the assumption that the phenol component of the molecule was in closer proximity to the binding site.[55] The addition of the aromatic trifluoromethyl diazarine group to either the 2' or 6' positions resulted in probes **35** and **36**, and subsequent photo-labelling experiments were able to identify unknown binding proteins of mass 210 and 180 kDa.[56]

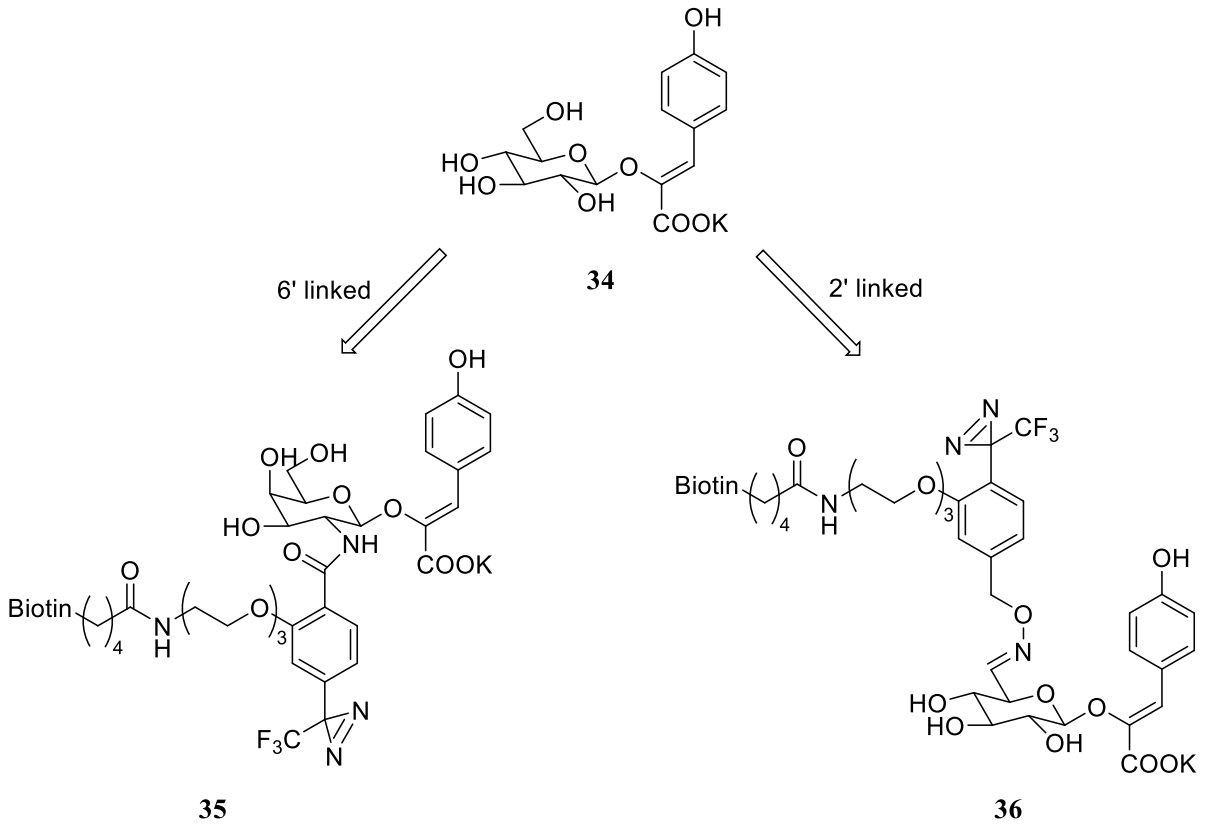

Figure 8: Development of trifluoromethyl diazarine probes from potassium isolespedezate (**34**).

One observation made in this report was that the addition of the large photoaffinity group meant that both high labelling yield and biological activity was not achievable. Previous SAR studies supported the proposal that the 2' position was closer to the binding site, and it was expected that the attachment of a sterically demanding photoaffinity tag in this position would result in decreased biological activity. This hypothesis was confirmed via leaf opening assays as 6' modified probe **35** retained greater biological activity, but no specific band was identified following pull-down experiments suggesting inefficient photo-crosslinking. Conversely, although 2' modified probe **36** showed reduced biological activity, it gave greater labelling yields in photoaffinity labelling experiments identifying 2 specific bands. On target binding was confirmed through competition assays using leaf opening factor **34**. These results indicate that although a balance is needed to be achieved between biological activity and labelling efficiency, the vicinity of the photolabeling group to the binding site should take primary consideration in the development of a chemical probe.

Similar issues were of concern in the investigation into a similar leaf opening factor LOF (**37**) reported by Okada *et al*.[57] Given the high degree of non-specific binding that can arises from endogenous biotinylated proteins, the purification method chosen was through the use of the FLAG peptide and the anti-flag monoclonal antibody. Given the large size of the peptide, a small photoactive group was

needed as to not further disrupt binding. Consequently, probe **38** was synthesised, incorporating the aryl azide photoaffinity label into the aromatic core of the molecule. Despite the large size of the peptide, the compact photo-active portion allowed the molecule to retain biological activity albeit at about half the effect of the lead. Using lead molecule **37** as a competitive ligand, photoaffinity experiments using probe **38** ultimately identified an unknown membrane-bound receptor protein located specifically in the motor cells of leaf and stem joints.

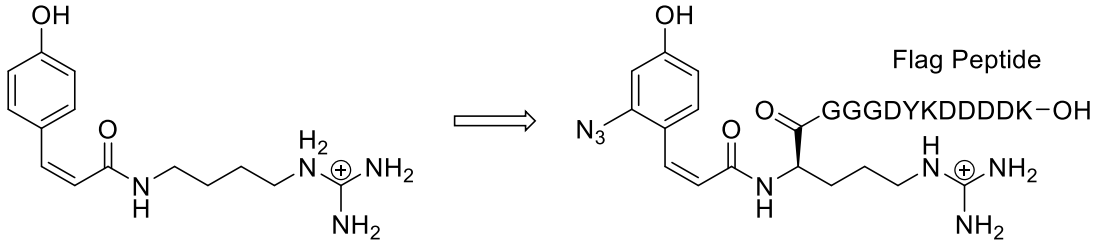

LOF **37** **38**

Figure 9: Development of LOF (**37**) into an aryl azide containing photoactive probe.

1.2.6: Conclusion

Target identification of small molecules remains the most challenging aspect of forwards chemical genetics and although a vast array of strategies has been developed for capture of these targets. The discussion above outlined the three primary methods of doing this: using the small molecule's inherent affinity to its target, using electrophilic reactive groups, and using photo-crosslinking groups. Due to the diversity of small molecules used within plant chemical biology, the approach adopted is dependent on the structure of the small molecule and what is already known about its target(s). Affinity based probes provide the simplest approach but are dependent on a strong interaction between the small molecule and its target. Probes containing a reactive group or photoaffinity tag can overcome this limitation through the formation of irreversible covalent linkages with the target. Despite this, these approaches are also constrained with electrophilic reactive groups requiring the presence of active residues and photoaffinity probes needing to retain binding in the presence of the large photoaffinity group to ensure on-target cross-linking. The examples highlighted above show the diverse approaches in which chemical probes can identify small molecular targets. This ultimately allows for the limitations of traditional genetic approaches to be circumvented, leading to advancements in our understanding of complex pathways in plants.

1.3: Plant Hormones

1.3.1: Introduction to Plant Hormones

Plants have developed the ability to continuously adjust in response to external factors. These processes are regulated by the integration of environmental, genetic, and chemical signals that together dictate plant growth and development. A fundamental component of this process are molecules collectively known as hormones. These small molecules regulate almost every aspect of plant development with one hormone having the ability to perturb a vast range of cellular processes whilst simultaneously multiple hormones being needed to affect one aspect of growth.[58] The perception of these small molecules is fast and sensitive at low concentrations further contributing to their fundamental role in the regulation of developmental processes.

Although each plant hormone is responsible for a range of responses, they can be loosely classified into two groups; those which regulate growth and developmental processes, and those which regulate stress responses. Hormones such as cytokinin, ethylene, gibberellic acid (GA) and brassinosteroids are involved in multiple aspects of plant growth whilst stress hormones include those such as abscisic acid (ABA), salicylic acid (SA) and jasmonic acid (JA).[59,60] These groups of hormones combine to form a complex, interconnected signalling network allowing for the regulation of multiple metabolic processes and plant development pathways. As noted above, a single hormone can be responsible for several aspects of plant responses. For example, GA is implicated in the regulation of cell elongation, cell division, floral development and seed germination. Their roles are not mutually exclusive as both auxin and cytokinin are also involved in the establishment of meristems.[58,61] These relationships can be antagonistic as is the case with the interrelation of GA and ABA in seed dormancy and germination or they can be synergistic as observed with auxin and brassinosteroids in the processes of cell elongation and division. With structural and biological data suggesting the perturbation of the ABA and GA pathways by novel compound eW5, this overview will focus on these two hormones.

1.3.2: Abscisic Acid

Best known as a plant's "stress hormone", ABA is central to a plant's ability to respond to environmental pressures through the regulation of a wide range of processes including dormancy, germination, stomatal opening, and root growth. For example, under stress conditions of drought or high salinity, ABA promotes stomatal closure, reducing water loss via transpiration. In addition to the regulation of stress processes, ABA also acts as a suppressor of seed germination, delaying the process until seeds have fully developed and conditions are favourable. The transition between dormancy and

germination is controlled by the antagonistic hormone pair of ABA and GA where a higher ratio of GA promotes germination and reduces the duration of dormancy.[62]

ABA is an isoprenoid molecule synthesized from zeaxanthin; one of the most common naturally occurring carotenoid alcohols. The relationship between the stereocenter of ABA and its biological activity has been extensively documented with the (R)-cis enantiomer displaying weak activity compared to the naturally occurring (S)-cis isomer (**39**). Although readily isomerized on exposure to UV light, geometric isomerism has also been explored within the molecule with assays conducted under low light conditions have shown that the (S) 2-*trans* form is inactive.[63]

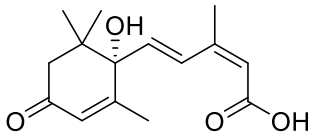

39

Figure 10: Structure of (S)-cis-ABA.

1.3.2.1: Abscisic Acid Hormonal Pathway

The core model of ABA function can be separated into four distinct portions; the pyrabactin resistance 1 (PYR1) and PYR1-like (PYL) proteins, type 2C protein phosphatases (PP2Cs), Snf1-related protein kinases 2 (SnRK2s) and ABA-responsive element binding factors (ABFs). SnRK2s are positive regulators of the ABA pathway, phosphorylating downstream effectors including ABFs, leading to the activation of ABA responses. High ABA concentrations induce binding between the PYR/PYL proteins and PP2Cs, inhibiting its action, resulting in the accumulation of phosphorylated SnRK2s which can then phosphorylate ABFs. Conversely, in the absence of ABA, the PYR/PYL proteins are not bound to the PP2Cs, increasing the activity of the phosphatase, inhibiting SnRK2 function (Figure 11).

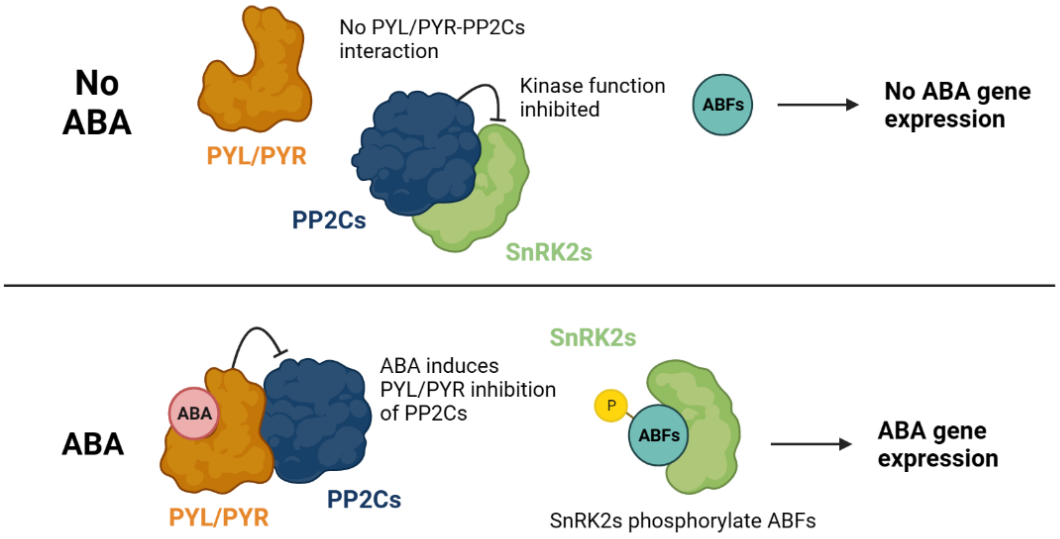

Figure 11: Schematic diagram of ABA signalling pathway in absence and in presence of ABA.[64]

1.3.2.2: PYR/PYL Proteins

It was only in 2014 that two independent reports described the identification of ABA receptor proteins. These involved a forward chemical genetic approach (outlined in section 1.2.1) and a Yeast-2-hybrid (Y2H) screen which observed two PP2Cs (ABA INSENSITIVE 1/2 (ABI1/2)). This identified members of the steroidogenic acute regulatory related lipid transfer (START) superfamily as ABA receptors and ultimately led to the discovery of the ABA receptor proteins Pyrabactin Resistance 1 (PYR1) and PYR1-like 1-13 (PYL1-13) which have been subsequently named as regulatory components of ABA receptor (RCARs) but for simplicity will be referred to as PYRs and PYLs in this thesis.

There is a high degree of similarity between the primary structures of the 14 members of the PYR/PYL gene family. Initial structural studies were conducted on PYR1, PYL1 and PYL 2 and since then the structures of PYL3, PYL5, PYL9, PYL10 and PYL13 have also been reported. They are characteristically small proteins, between 159 and 211 amino acids in length and all contain a seven-stranded beta-sheet along with a C-terminus alpha helix enfolded by two additional alpha helices.[65,66] These distinctive motifs combine to form a “helix-grip” fold structure, a common feature of START domain proteins and results in a hydrophobic ligand-binding pocket (Figure 12).

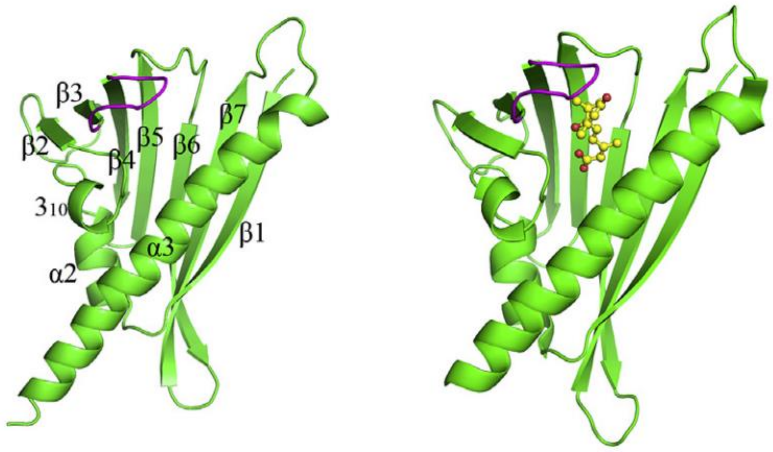

Figure 12: X-ray crystal structures of **A**. apo-PYL10 and **B**. ABA-PYL10 interaction via hydrogen bonding. Ball and stick model represents (S)-cis-ABA. Common features shared by members of this gene family include the C-terminus alpha helix surrounded by 2 additional alpha helices. Image replicated from Sun *et al.* [67]

The structure of the receptors plays an important role in the protein's ability to perceive ABA. Structural data has shown the PYL proteins contain 2 highly conserved loops which have been dubbed as the "gate and latch" allowing the protein to adopt an open and closed confirmation.[68] These two loops rearrange upon binding with ABA which induces the closed conformation, blocking the entry. This forms the surface that allows the receptor to interact with PP2Cs, inhibiting phosphatase activity (Figure 12, A). The phosphatase contains a conserved tryptophan residue which can then slide between the two loops, locking the receptor-PP2Cs complex in the closed conformation.[69] Receptor recognition of ABA is possible through a mixture of hydrogen bond networks and hydrophobic contacts (Figure 12, B/C). Structural studies with PYL1 have shown binding to occur between a Lys residue and the carboxyl group of ABA through the formation of an ion pair and hydrogen bonds mediated with three water molecules. Hydrophobic interactions are observed between the pentadienoic acid group of ABA and residues Phe 135, Leu 144 and Val 193.[70–72] These interactions are predicted to be conserved between other homologous ABA-specific receptor proteins.

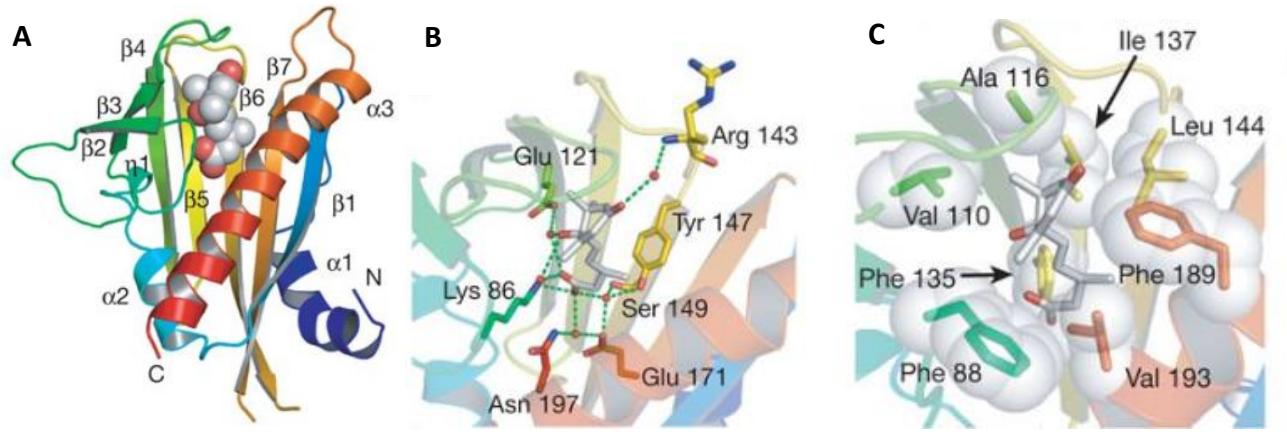

Figure 13: **A**. Ribbon diagram and annotations of secondary structures. Blue indicates N-terminus and red indicates the C-terminus. **B**. Hydrogen bond networks between ABA and residues of PYL1. Water molecules are illustrated by red spheres and hydrogen bonds are drawn as green dotted lines. **C**. Hydrophobic interactions between ABA and PYL1. Images from Miyazono *et al.*[70]

Further structural studies have shown that the ABA receptors can be grouped based on their oligomeric configuration. With the exception of PYL7, PYL4-12 are monomeric whilst PYR1 and PYL1-3 are homodimers but will dissociate in the presence of ABA. The conformation of the receptors has an effect on their respective binding affinities to ABA as structural analysis of the dimeric proteins has shown a cis-homodimer arrangement, blocking access to the ligand binding pockets. As a result, dimeric receptors display a significantly lower binding affinity with ABA with Kd values ≥50 μM whilst the monomeric receptors display much greater binding affinities with binding constants of ~1 μM as determined through ITC.[62]

The PYL-ABA affinity is reflected in the PYL-PP2Cs affinity with dimeric receptors displaying an intrinsic ability to inhibit PP2Cs whilst this interaction is undetectable with the monomeric ABA receptors in the absence of ABA. Although the dimeric receptors are able to independently inhibit PP2Cs, ABA significantly enhances this interaction, as was observed for PYL10-PP2C in which affinity was increased to from 1.2 μM to 18 nM in the presence of ABA.[70] This observation has led to the hypothesis of the monomeric PYLs functioning as ABA sensitive receptors whereas dimeric PYL's inhibitory activity on PP2Cs activity is ABA dependent.

1.3.2.3: PP2Cs & SnRKs

As mentioned previously (Section 1.3.2.1), protein phosphatase type C (PP2Cs) makes up a component of the negative regulation of the ABA pathway. The genes that encode for PP2Cs are arranged into 10 groups (A-J), where members belonging to Group A have a function within the ABA pathway. The

most extensively studied elements within this group include ABA insensitive 1 and 2 (ABA1/2) which code for homologous PP2Cs and hypersensitive to ABA 1 (HAB1) which was identified from its sequence homology to ABA1/2.[73,74] In both germination and root growth studies, *abi1-1* and *abi2-1* mutants are ABA insensitive, whilst *hab1-1* mutants display increased ABA-mediated stomatal closure and the inhibition of growth and germination, supporting the notion that PP2Cs are negative regulators of the ABA pathway.[75]

Another major regulator of the ABA hormonal pathway are the serine/threonine protein kinases (SnRKs) which are negatively regulated by PP2Cs. In the absence of ABA, the activity of SnRKs are inhibited, preventing the binding and phosphorylation of ABFs (Figure 11). Of the three classes of kinases (SnRK1, SnRK2, SnRK3), SnRK2 and SnRK3 play a role in stress responses and plant growth. Members of the SnRK2 have shown to be the main positive regulators of the ABA pathway with specifically SnRK2.6 being expressed within guard cells. This results in the closure of the stomata as a response to the presence of ABA, an observation supported by the inability of *snrk2.6* mutants to retain water due to the inability to regulate the closure of the stomata.[69,76]

Members of the SnRK2 subclass share a highly conserved catalytic domain and it has been widely reported that the phosphorylation of SnRK2s are important for its activation. Several phosphorylation sites have been identified using SnRK2.6 recombinants, most notably Ser 175 which has been determined to be critical in the activity of the kinase. When active, SnRK2s phosphorylate downstream effectors such as ion channels and transcription factors resulting in the ABA mediated response.

1.3.2.4: Known ABA Agonists/Antagonists

The problem of genetic redundancy has been the main issue with using classical forwards genetic in the identification of ABA signalling components. As discussed in section 1.2.1, with the use of a specific agonist that selectively activates part of the ABA pathway, classical forwards genetics can now be used in tandem to identify specific signalling components. This has resulted in a range of small ABA related compounds which had been screened for, or rationally designed with the aim of studying the mode of action of ABA (Figure 14).

The most notable example of this was the use of a synthetic seed germination inhibitor named pyrabactin (**41**). The compound was first identified by Cutler *et al.* as a synthetic seed germination inhibitor and was subsequently used in a mutant screen which isolated and sequenced pyrabactin insensitive individual plants, leading to the identification of the PYR1 gene.[62] Through additional sequence analysis, the 13 additional PYL genes were identified. Detection of binding between ABA

and PYR1 was supported by ^{1}H-NMR spectral HSQC data and this coupled with results from a Y2H screen suggested PYR1 is an ABA receptor that interacts with PP2Cs upon ABA binding. Although there is no obvious structural resemblance between pyrabactin and ABA, it has been shown to be a selective agonist of PYR-1 and PYL-1 and an antagonist of PYL2. The discovery of pyrabactin as a specific agonist has led to the identification of four additional novel pyrabactin-like agonists **43**-**46** through rational design and docking analysis followed by in vitro confirmation Melcher *et al.*[77]

One limitation of pyrabactin (**41**) is its relatively low bioactivity and narrow receptor activation. Derived from a screen aimed to address these limits, quinabactin (**42**) was identified as possessing similar agonistic properties on a wider range of the PYL/PYR family.[78] Whilst pyrabactin (**41**) selectively alters the seed germination phenotype, application of quinabactin (**42**) results in broad spectrum ABA effects such as drought tolerance in adult plants.[63] The two compounds are sulfonamides but do have significant differences in their chemical structures. This is most notable to the groups attached to each end of the sulphonamide; pyrabactin has naphthalene and pyridine bonded to the sulfonamide moiety whilst quinabactin contains a benzyl group and a dihydroquinolinone ring. Quinabactin was found to display similar biological effects including survival of *Arabidopsis* following extended water deficiency and the inhibition of seed germination. More specifically, quinabactin's ABA mimicking effects were found to be mediated by the dimeric ABA receptors; PYR1, PYL1, PYL2, PYL3, allowing for further studies in to the role of the homodimer receptors in ABA responses.[79]

ABA Agonists

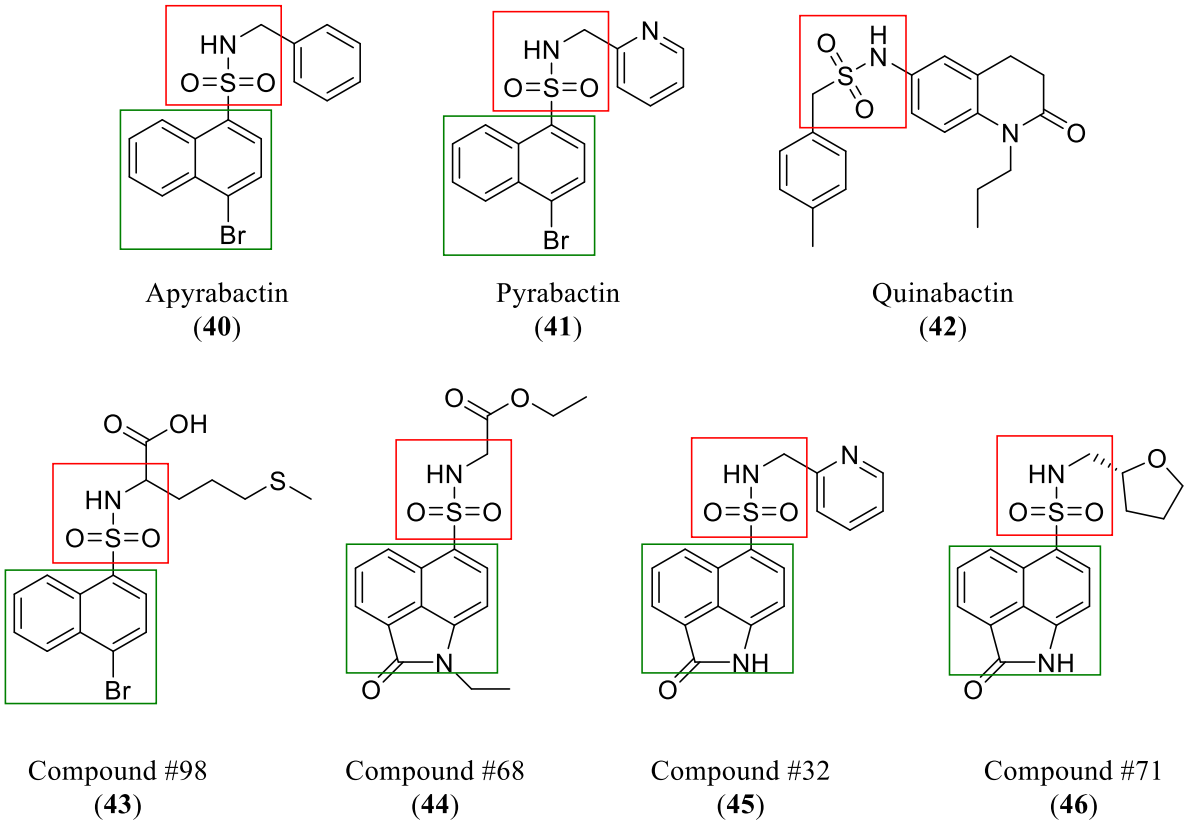

Figure 14: Known agonists of ABA. (Red) The sulphonamide moieties shared between the compounds. (Green) The 4-substituted naphthalene moieties shared by the compounds.

Interestingly, although the known ABA agonists share similar structural properties including an aromatic sulphonamide, none share any obvious structural resemblance to ABA (**39**). This is contrary to known ABA antagonists as AS6 (**49**) was identified through rational design as a potent ABA antagonist by Takeuchi.[80] With the exception of the hexane chain linked to the thioester, the compound is almost identical to ABA, allowing it to bind to PYL with a similar affinity and binding mode as ABA. The long alkyl chain gives the molecule its antagonistic properties as it protrudes out onto the PP2C interaction surface of the PYL receptors, blocking further ABA responses.

ABA antagonists have also shown to be useful tools in the study of hormone crosstalk responses. Despite the significant structural overlap between DFPM (**48**) and ABA (**39**), the discovery of **48** as a selective antagonist by Kim *et al*., (2011) could indicate that a direct structural relationship is not entirely necessary. PBI-51 (**47**) was identified by Wilen (2009) as an antagonist inhibiting ABA-regulated gene expression in seed germination, allowing for the study of the relationship between osmotic stress and ABA regulated seed development.[81] This example of crosstalk elucidation through

ABA antagonists was also seen in the development of DFPM. **48** was initially characterized as a selective ABA antagonist for a small set of ABA responses such as the regulation of stomatal aperture.

ABA Antagonists

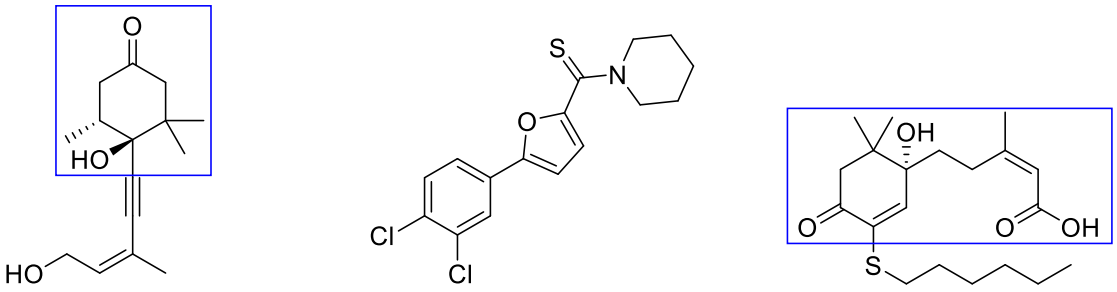

PBI-51 (**47**) DFPM (**48**) AS6 (**49**)

Figure 15: Known antagonists of ABA. Blue boxes highlight portions of the compounds which structurally overlap with ABA.

1.3.3: Gibberellic Acid (GA)

Gibberellic acid (GA) is involved in the regulation of diverse aspects of plant growth and development at various stages throughout the plant life cycle. Although primarily involved in the promotion of organ growth through the stimulation of cell division and elongation, it has also been implicated in other transitional processes such as seed germination, shoot growth, sex determination and flowering.[82,83] The class of Gibberellins contain over a hundred identified GAs, with only a small subset being bioactive within plants, namely GA1, GA3, GA4 and GA7 (**50**-**53**, Figure 16). These bioactive molecules are pentacyclic diterpene isoprenoid phytohormones and share several common structural moieties including a lactone bridging C-4 and C-10, a C-6 carboxylic acid and a hydroxyl group at C-3.

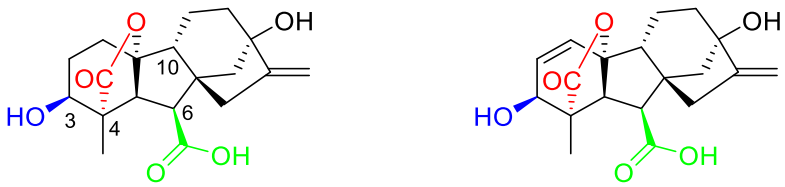

GA1
50

GA3
51

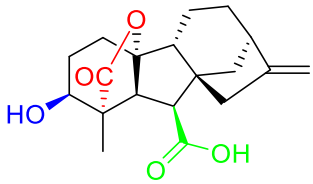

GA4
52

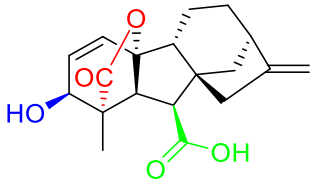

GA7
53

Figure 16: Structures of bioactive GAs; GA1, GA3, GA4 and GA7 (**50**-**53**) displaying common functional groups. **A.** (Red) Gamma-lactones between C-4 and C-10. **B.** (Blue) Hydroxy group on C-3. **C.** (Green) Carboxylic acid on C-6

1.3.3.1: GA Hormonal Pathway

The GA signalling pathway is comprised of four major components; GA itself, the associated receptors (namely GIBBERELLIN INSENSITIVE 1, GID1), DELLA proteins and the F box protein SLEEPY1 (SLY1). The most important mechanism associated with the GA hormonal pathway is the repression of DELLA protein function. DELLA proteins are part of the GRAS superfamily of proteins and act as negative regulators of growth through the interaction with transcription factors such as PHYTOCHROME INTERACTING FACTOR 3 (PIF3), PIF4 and SCARECROW-LIKE 3 (SCL3), inhibiting their function. In the presence of GA, DELLAs undergo rapid degradation via the ubiquitin-proteasome pathway. GA binding to GID1 promotes conformational changes within the receptor, forming the GA-GID1-DELLA complex. The formation of this complex promotes binding of SLY1 (as part of the SCF^{SLY1} complex) to the GRAS domain of the DELLA proteins, triggering polyubiquitination and subsequent degradation of the DELLAs by the 26S proteasome. With DELLAs acting as negative regulators of growth, degradation leads to the activation of downstream transcription factors, resulting in growth.

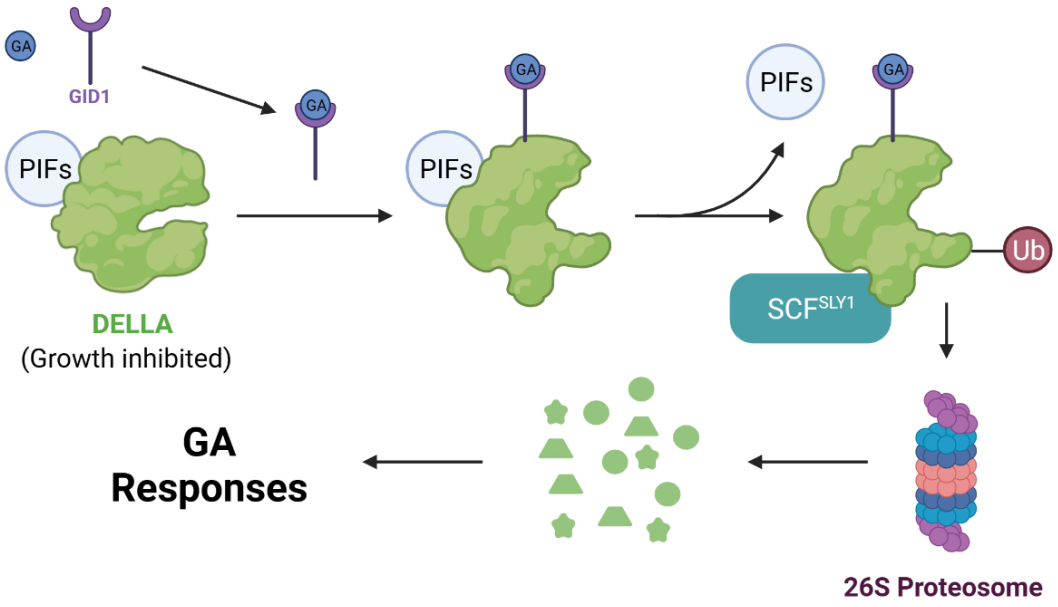

Figure 17: Model of GA hormonal pathway in plants.[84]

1.3.3.2: GA Receptors

First identified in *Oryza sativa*, the *OsGID1* gene encodes for the GID1 protein that forms a specific interaction with GA. The GA receptors in *Arabidopsis* were identified though map based cloning where it was shown that three homologues existed that were similar to *OsGID1*; *AtGID1a*, *AtGID1b* and *AtGID1c*.[85] The interaction between the GID1 receptors and GA leads to the degradation of the DELLA protein SLENDER RICE1 (SLR1) involving the F-box protein GID2.[84]

Results of single mutant studies of homologues GID1a, GID1b and GID1c have indicated redundancies between the receptors as they do not result in differed phenotypes when compared with wild-type individuals. In contrast, studies of double mutants enable the specificity of the receptors to be differentiated. Although the *gid1a-1*, *gid1b-1* and *gid1b-1*, *gid1c-1* double mutants show no change in phenotype, the *gid1a-1 gid1c-1* double mutation results in the observation of a dwarfed phenotype, indicating that the GID1b receptor plays a lesser role in stem elongation.[86,87] The triple mutant results in significant GA-insensitivity leading to severe dwarfism and infertility which cannot be recovered through treatment with GA, indicating that the perception of GA by the GID receptors is an important step in the GA hormonal pathway.

Ultimately, this hormonal pathway is activated through the interaction between GA and GID1 which results in the conformational change of the receptor. The primary sequence of GID1 shows similarity to hormone sensitive lipases (HSL), sharing two conserved motifs. Despite the current lack of

confirmation from x-ray crystal structures, current models suggest that the GA binding to GID1 is aided with a lid which traps the substrate in the binding pocket.[88] This conformational change then allows for binding to DELLA proteins via the N-terminal motifs, stabilizing the GA-GID1-DELLA complex. Despite the similarities in sequence and structure, HSL-enzymatic activity is not observed with GID1, primarily due to the substitution of a His residue for Val or Ile in the C-terminus region that is essential for HSL function.

1.3.3.3: DELLA Proteins

There are five DELLA repressor genes that have been identified in *Arabidopsis*; REPRESSOR OF GIBBERELLIC ACID (RGA), GA-INSENSITIVE (GAI), and the RGA-Like Proteins (RGL1), RGL2, RGL3. RGA and GAI transcripts are present in all tissues and RGL1-3 are expressed only in germinating seeds and flowers, showing the distinct functions between the DELLA genes despite the redundant nature of these genes as suppressors of the GA responses. Additional genetic studies have shown some of the genes are responsible for varying functions in relation to plant growth. These studies were conducted on the GA biosynthesis mutant *ga1-3* and the proteins were observed for their ability to rescue the phenotypes.[84] This loss-of-allele study showed that mutations to RGA, RGA1 and GAI were able to rescue height of the plant, mutations to RGL, RGL1 and RGL2 were able to rescue flowering and mutations to RGL2, RGA, GAI and RGL3 were able to rescue seed germination[89].

As members of the GRAS super family, the DELLAs have a conserved C-terminal GRAS domain. However, the N-terminal regional domain is more significant to the function of the DELLAs. These areas are Ser and Thr rich acting as the regulatory domain of the protein and contains two highly conserved motifs (DELLA and VHYNP). The importance of these DELLA motifs to the protein's interaction with the GID1 receptor has been shown through genetic studies conducted by Sun *et al.*[90] It was shown that mutation in this motif through the deletion of Ser/Thr and VHYNP residues inhibits the phosphorylation of DELLA proteins. The phosphorylation of DELLA ortholog found in rice (SLR1) is a crucial process as GID2 (an F-box subunit) forms a specific interaction with the phosphorylated protein, thereby regulating the gibberellin-dependent degradation of DELLAs.[91] The result of this mutant is a semi-dwarfed phenotype which cannot be reversed with the treatment of GA as the mutation interferes with DELLA-GID1 interaction, leading to the inability to regulate the DELLA repressor. In addition to the necessity of the conserved N-terminus motifs, the GRAS domain also plays a vital role in DELLA function as it is required for SLY1 binding. Although yet to be confirmed by crystal structures, current hypotheses suggest that a conformational change of the DELLAs occur upon GA-GID1 binding thereby allowing SLY1 interaction and subsequent polyubiquitination.[92]

1.3.3.4: F-Box Proteins

The protein named SLEEPY1 (SLY1) acts as a positive regulator of GA signalling, catalysing the polyubiquitylation of and ultimately the degradation of DELLA proteins.[93] SLY1 encodes for a protein highly homologous to F-box proteins, both functioning as components of a ubiquitin ligase complex, recruiting specific proteins for polyubiquitination. As reported by Steber, the unfunctional *sly-1-10* mutant accumulates high concentrations of RGA and GAI proteins resulting in a dwarfed phenotype which is unable to be rescued through treatment with GA, indicating the vital role F-box proteins play in GA signalling.[94]

Through Y2H assays, it was observed that SLY1 in the absence of GA interacts weakly with all *Arabidopsis* DELLA proteins indicating the function of GA is that of an enhancer, strengthening the SLY1-DELLA interaction. SLY1 binds to the GRAS domain of the DELLA proteins as part of SCF^{SLY1} E3 ligase, promoting polyubiquitination and degradation by the 26s proteasome. As DELLAs inhibit growth through the inhibition of PHYTOCHROME INHIBITING FACTOR 3 and 4 (PIF3-4), the degradation of these negative regulators ultimately results in GA responses.

1.3.3.5: Light Regulation of the GA Pathway

Under light conditions, seedlings undergo photomorphogenesis, resulting in expanded cotyledons and short hypocotyls. This is due to the increased activity of phytochrome in light conditions, inhibiting the accumulation of GA. The converse result is observed for seedlings grown in dark conditions as they undergo skotomorphogensis, resulting in closed cotyledons and longer hypocotyls. Phytochrome interacting factors (PIFs) mediate cell elongation and are part of the basic helix-loop-helix (bHLH) subset of transcription factors, regulating seedlings when they are etiolated. Under dark conditions, the red light photoreceptor phyB and DELLA proteins both negatively regulate PIFs which acts as a suppressor of the overall GA hormonal pathway.[95] Activation of phyB under light conditions result in the destabilization of PIFs whilst the increase in DELLA protein levels lead to the inhibition of the DNA-recognition domain of the PIFs, thereby blocking its binding.

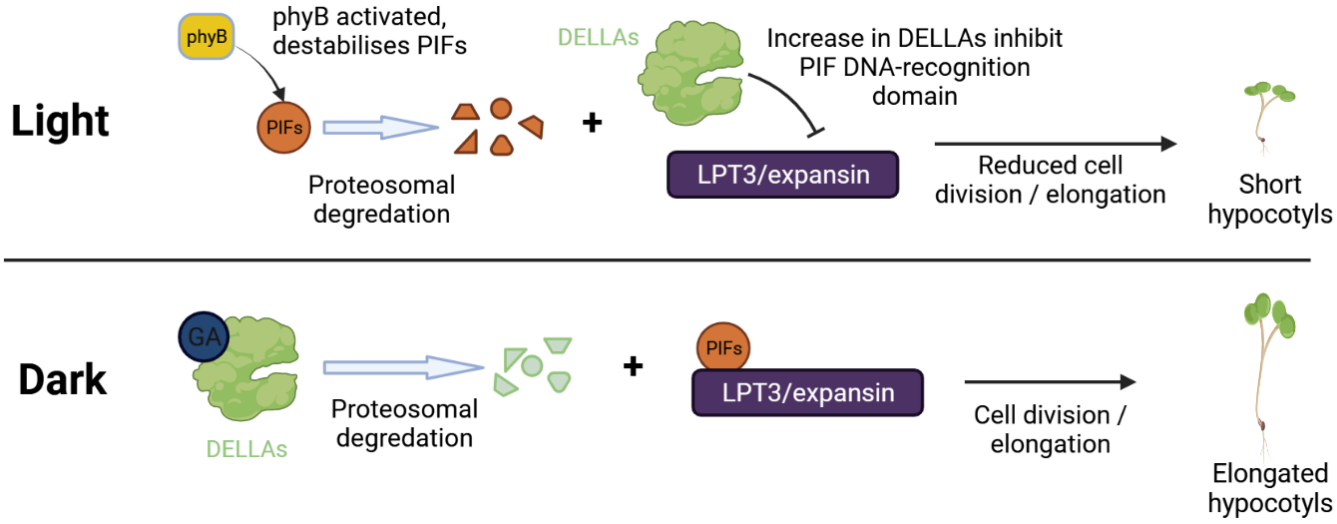

Figure 18: Illustration of cell elongation mechanism in light and dark conditions. In dark conditions, PIF4 mediates cell elongation. Degradation of PIF4 in light by phyB inhibits cell elongation.[96]

When grown in dark conditions, the transcription levels of GA biosynthetic enzymes (*GA3ox1* and *GA20ox1*) are high whilst the transcription of GA catabolic enzymes (*GA2ox1*) are low. The reverse is true for hypocotyls grown in light conditions. The low levels of GA catabolic enzymes when plants are grown in the dark result in a higher concentration of GA.[97] This increases DELLA degradation, leading to the promotion of increased hypocotyl growth, illustrating the agonistic relationship between light and GA.

1.3.3.6: Small Molecule GA Antagonists

Unlike with the ABA pathway, chemical genetics have not been used to the same extent in the perturbation of the GA pathway. Nevertheless, there are still salient examples of small molecules being used in the study of GA crosstalk with other plant hormones and in agriculturally significant applications.

One reported antagonist was by Phinney *et al*. where it was shown that tannins were able to inhibit gibberellin-induced growth in pea and cucumber seedlings. Tannins make up a diverse group of chemicals but can be loosely defined as phenylpropanoid compounds and their respective condensed polymers.[98] This study was able to show that chemically defined tannins (Examples **54**-**56**, Figure 19) were able to inhibit growth that was caused with the addition of GA_3.[99] By increasing the concentration of GA_3 the inhibitory effect of the tannins was reversed, indicating that the two were involved in the

same pathway. Although some of the tannins push the boundaries on the classification of "small molecules", the antagonistic role they play lead to the proposal that they act as growth-regulators acting along the GA pathway.

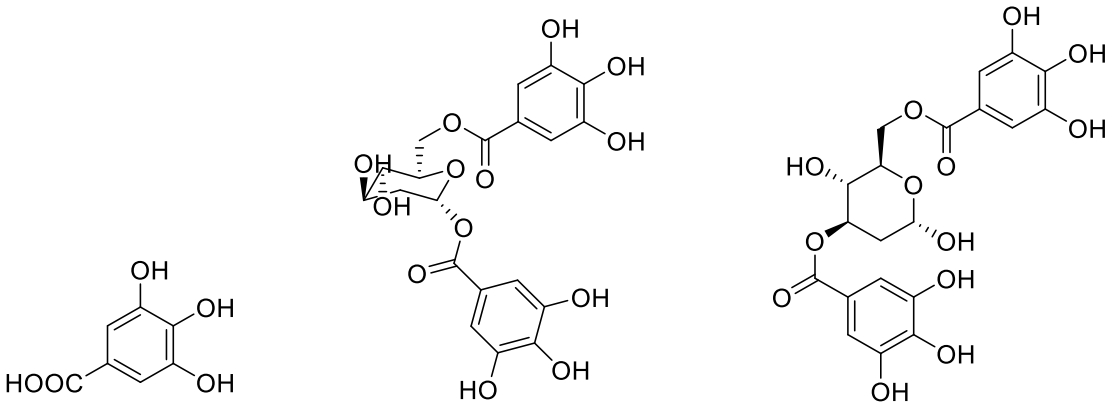

Gallic Acid **54** | beta-D-1,6-di-O-Galloyl Glucose **55** | 3,6-Digalloyl Glucose **56**

Figure 19: Examples of inhibitory tannins reported by Phinney *et al.*[99]

Another reported example of a small molecule GA antagonist is the synthetic cytokinin 6-benzyladenine (**57**). In a report by Li *et al*. which looked to elucidate the mechanism by which cytokinins promote flower bud formation in apple trees, the transcriptomic response to treatment with **57** was conducted. The results identified 84 genes that were highly correlated with genes relating to flowering time and it was found that there was a significant upregulation of a GA signal repressor.[100] This study not only identified **57** as an antagonist of GA by downregulating GA signalling pathway related genes, but also elucidated part of the crosstalk mechanism between the two hormones, again illustrating the effectiveness of small molecules as tools.

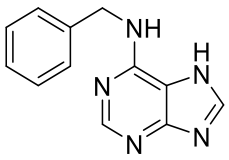

6-benzyladenine **57**

Figure 20: Structure of 6-benzyladenine (**57**).

Section 1.4: Previous work

1.4.1: Introduction to eW5

In an early report, Kaplan *et al*. had described a study exploring the effect of two known calmodulin inhibitors N-(6-Aminohexyl)-1-naphthalenesulfonamide (W5) and N-(6-Aminohexyl)-5-chloro1-naphthalenesulfonamide (W7) on the secondary calcium signalling pathway in plants. Calmodulin is a positive regulator of calcium pumps which pump Ca^{2+} against a strong calcium gradient in the main body of the cell. Inhibition of calmodulin results in inhibition of the pumps, resulting in the diffusion of the ions back along against the concentration gradient, increasing cytosolic [Ca^{2+}]. The introduction of these two compounds into seedlings ledd to the identification of touch-responsive genes (*TOUCH3*) and dehydration responsive genes (*ERD15*) regulated by Ca^{2+}.[101]

As mentioned in Section 1.2.1, chemical genetics can be a powerful tool in the study of hormonal pathways when classical genetic approaches are limited. Unfortunately, **58** and **59** were found to be broad spectrum inhibitors targeting all 7 plant calmodulins, the almost 100 calmodulin-like proteins and other protein kinases. It was proposed that a small library of analogues (Figure 32) could be synthesized for the purpose of identifying compounds that specifically targeted a subset of these proteins. This approach would allow for more precise detection of such calcium binding proteins involved in the specific pathways. All analogues tested led to an increase in cellular calcium concentrations, supporting the hypothesis that they could potentially be CaM antagonists.

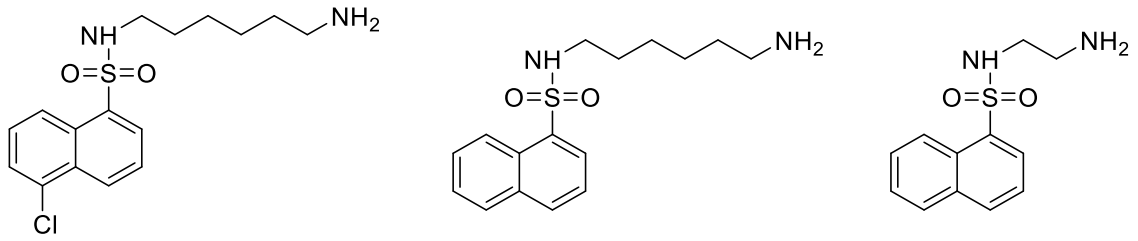

W7 (**58**) W5 (**59**) eW5 (**1**)

Figure 21: Structures of known calmodulin inhibitors **58** & **59** and novel compound eW5 (**1**). All contain a naphthyl sulfonamide core along with a hydrocarbon tail with a primary amine.

In contrast to the rest of the series which resulted in root growth inhibition, eW5 (**1**) displayed the opposite effect, leading to root growth promotion (Figure 22). The apparent growth promoting effect was of interest and a series of genetic and growth assays were undertaken to identify the compound's binding interactions and the mode of action underlying the growth promoting effects of eW5.

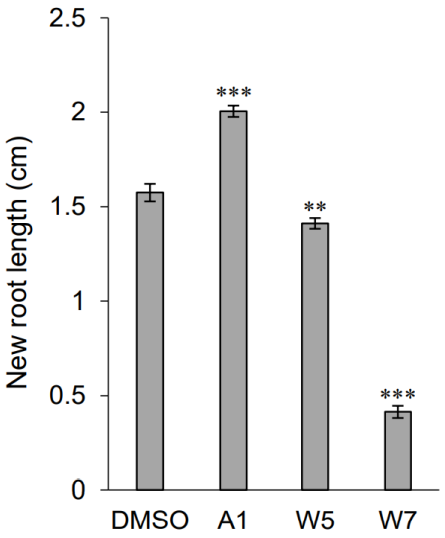

Figure 22: Root growth analysis of 7-day old seedlings after 5 days of chemical treatment with known calmodulin inhibitors W5 (**59**), W7 (**58**) and A1/eW5 (**1**) at 100 µM. Error bars represent standard error of 18 seedlings. Asterisks indicate statistically significant differences to DMSO (independent t-test, ** P<0.005, *** P<0.001) between DMSO and chemical treatment. Replicated from Sukiran.[102]

1.4.2: eW5 Effect on ABA Pathway

Despite eW5 (**1**) apparently operating in an inverse fashion to ABA, which inhibits root growth via the promotion of ethylene biosynthesis,[69] it shares significant structural similarities with the ABA agonist pyrabactin. As introduced in Section 1.3.2.4, pyrabactin (**41**) was essential in the identification of the 13 PYL receptors and the gate-latch-lock mechanism involved in ABA recognition. Despite pyrabactin having yet to display ABA like effects past seed germination, it was hypothesized that its interaction with several members of the PYR and PYL family could be mimicked by eW5 (**1**). Consequently, initial studies explored the PYR and PYL family as potential targets of eW5.

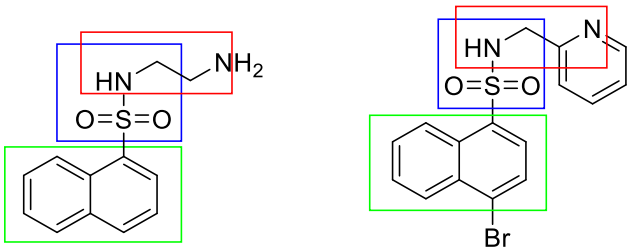

eW5 (**1**) pyrabactin (**41**)

Figure 23: Structural relationships between pyrabactin (**41**) and eW5 (**1**). (Blue) The Sulfonamide shared between eW5, pyrabactin and quinabactin. (Green) The naphthyl-sulfonamide moiety shared by pyrabactin and quinabactin. (Red) The two carbon atoms between nitrogen atoms.

One noticeable structural difference between eW5 (**1**) and pyrabactin (**41**) is the presence of the bromine substituent in the 4-position. The presence of the bromine is important for the Van Der Waals interactions with Leu-Pro-Ala residues at the ligand entry gate.[68] With the lack of substituent para to the sulfonamide moiety and the ability to display root growth promotion, it was hypothesized that the compound had a different interaction with PYL receptors, resulting in a reversal in the expected root growth inhibition that arise from ABA responses.

This theory was initially supported through preliminary thermal shift assays and MicroScale Themophoresis studies which suggested that eW5 (**1**) had an ability to interact with PYL1, PYL2, PYL5 and PYL8. As outlined in section 1.3.2, at low ABA concentrations, the ABA signalling pathway is negatively regulated through the inhibition of the SnRK2 kinase protein by PP2Cs. The level of phosphatase activity of the PP2C HAB1 was used to explore the possible antagonistic effect of eW5 (**1**) through co-application with ABA (**39**).

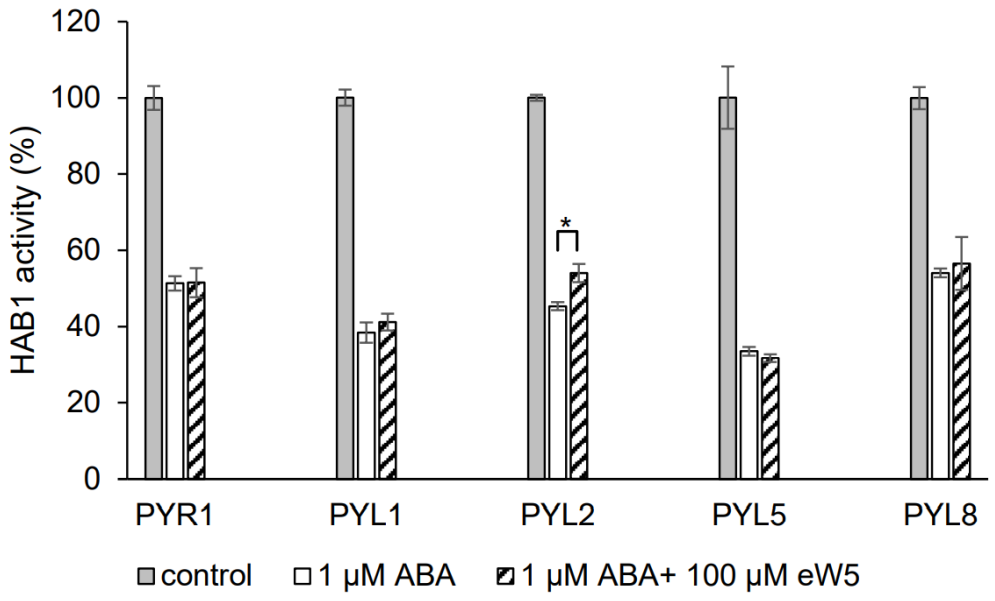

Figure 24: Measurement of the activity of HAB1 on various PYL receptors. Error bars represent standard error and asterisks show significant differences (independent t-test, * P<0.05) between treatment with ABA and eW5. Replicated from Sukiran.[102]

However, in contrast to the initial TSA data, co-application of eW5 was unable to restore the activity of PP2Cs for any of these receptors contradicting previous data suggesting its role as an antagonist of PYR/PYLs. This led to the hypothesis that eW5 was playing an agonistic role. Unfortunately, further studies on HAB1 showed no observable difference in phosphatase activity between the control and treatment with the compound, suggesting the relationship was not agonistic either (Figure 25). Although

there was preliminary data suggesting eW5 interacted with the PYL proteins, subsequent studies conducted by Sukiran and additional thermodynamic experiments were unable to support this and further investigation into this was not taken further.

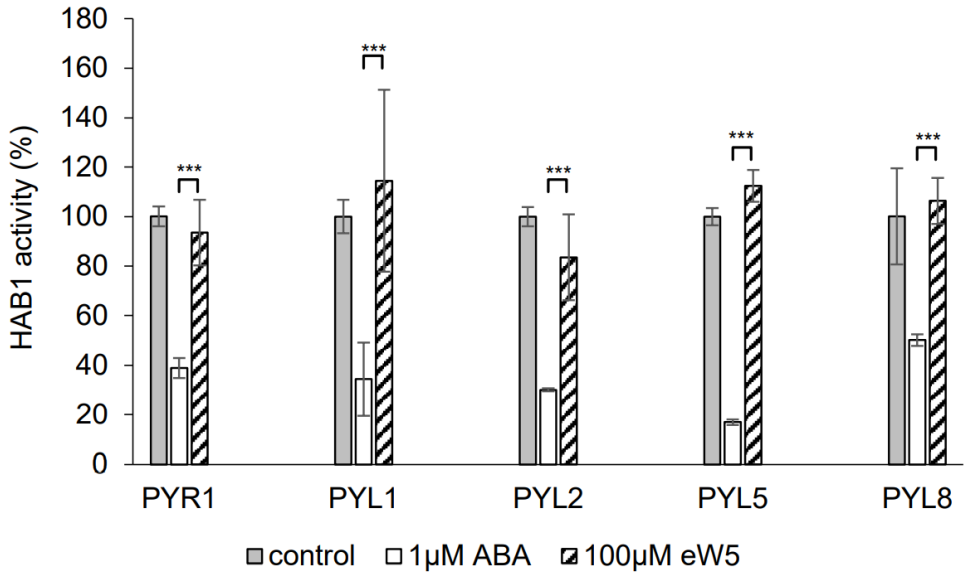

Figure 25: HAB1 activity on various PYL receptors following treatment with eW5. Asterisks show significant differences (independent t-test, * P<0.05) between treatment with ABA and eW5. Replicated from Sukiran.[102]

1.4.3 eW5 on GA Pathway

With the failure to identify a link between the ABA signalling pathway and eW5, an alternative possibility was considered; that eW5 (**1**) could be targeting components of GA signalling and recognition. The GA pathway is the most implicated pathway in plant growth and as outlined in section 1.3.3, the fundamental process involved is the proteasomal degradation of the growth repressor DELLA proteins which results in various growth processes such as leaf expansion and stem elongation.

To observe the effect of eW5 on DELLA protein stability, an assay developed by Silverstone *et al*. (2001) was employed. In this assay, the degradation of the DELLA protein RGA was observed through the loss of fluorescence of an RGA-GFP fusion protein. With GA as a positive control and paclobutrazol; a well-documented inhibitor of GA biosynthesis as a negative control, transgenic *Arabidopsis thaliana* seedlings expressing the fusion protein RGA-GFP were treated with eW5 and imaged after 2- and 24-hours. The results showed a loss in fluorescence in response to chemical treatment with both GA and eW5 (**1**) indicating the degradation of DELLA proteins whilst application

of PAC resulted in increased fluorescence, indicating the stabilisation of DELLA proteins (Figure 26). This provided strong evidence supporting the hypothesis that a possible mode of action for eW5 was through DELLA mediated activation of the GA signalling pathway.

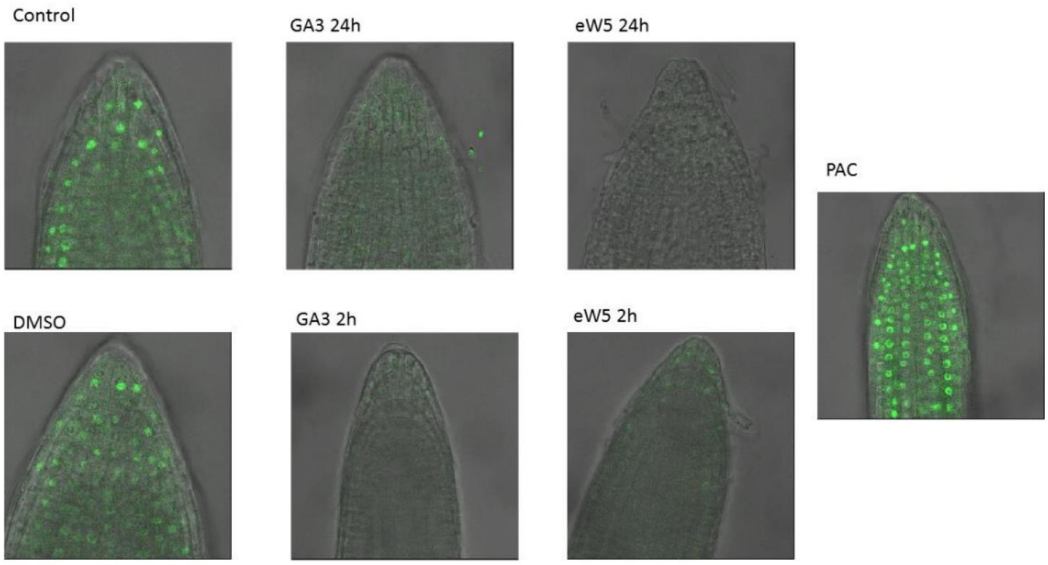

Figure 26: Transgenic Arabidopsis expressing RGA-GFP imaged 2- and 24-hours following treatment with eW5 and GA (both at 100µM). Seedlings imaged for the negative control were treated with Paclobutrazol (PAC) at 100µM for 48-hours. Image replicated from Sukiran.[102]

Additional studies on the effect of eW5 on DELLA degradation were conducted through hypocotyl growth assays. The interplay between GA and DELLA proteins have been well established and using GA as a positive control and PAC as a negative control, eW5 was tested for its effect on hypocotyl growth. It was observed that treatment with eW5 and GA lead to significantly greater hypocotyl lengths whilst treatment of PAC results in significantly dwarfed hypocotyls (Figure 27), supporting the hypothesis that the compound promoted growth through the degradation of DELLA proteins.

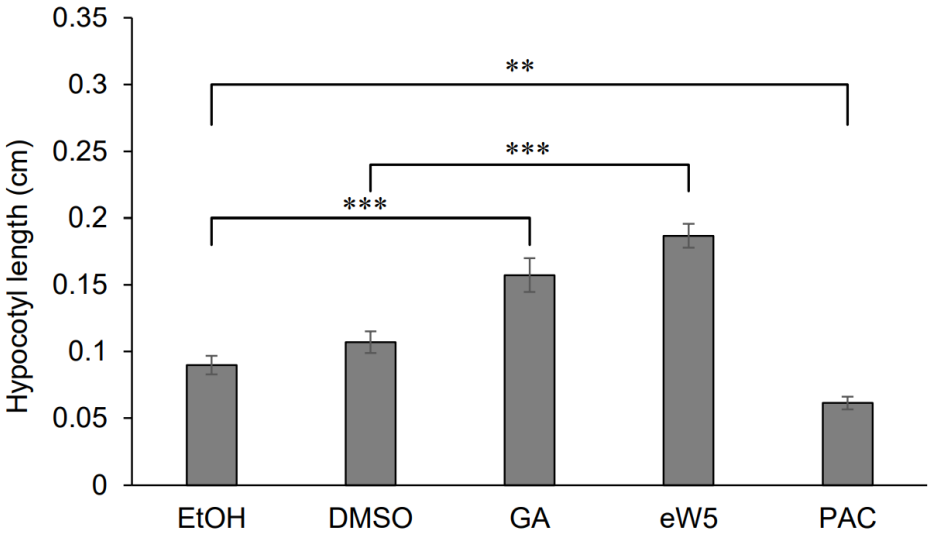

Figure 27: Hypocotyl length of Arabidopsis following treatment with eW5. Error bars represent the standard error from 30 individuals and asterisks show significant differences (independent t-test, ** P<0.005, *** P<0.001) between different treatments. Replicated from Sukiran.[102]

With results indicating the DELLA dependency of eW5's ability to promote growth, the compound was then tested against a mutant line that was deficient in all DELLA (GAI, RGA, RGL1, RGL2 & RGL3) function. Treatment of the mutants with eW5 resulted in no significant difference in root or hypocotyl growth when compared with the control, further supporting the hypothesis that eW5 requires the presence of DELLA proteins for its mode of action (Figure 28).

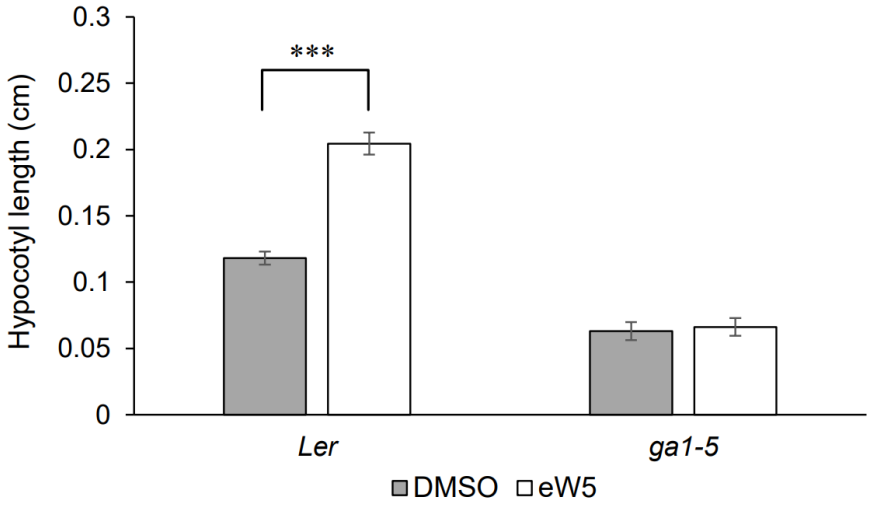

Figure 28: Hypocotyl growth assay for DELLA quintuple mutant. Error bars represent standard error, based on three biological replicates. Asterisks indicate statistically significant differences (independent t-test, *** P<0.001) between chemical treatment. Figure replicated from Sukiran.[102]

The significant overlap between the observed effects of eW5 and GA lead to assumption that eW5 was operating through the GA hormonal pathway. To test this proposal, an experiment was conducted on mutants lacking one or more of the three *Arabidopsis* GA receptors; GID1a, GID1b and GID1c. The double mutant *gid1a1c* and triple mutant *gid1a1b1c* both display the phenotype of significantly dwarfed stems which cannot be reversed with treatment of GA and were not used in this study. eW5 was unable to display its growth promotion effects in *gid1a1c*, *gid1a1b* and *gid1b1c* double mutants, indicating that the presence of the GA receptors was required for the growth promoting effects of eW5 to be observed.

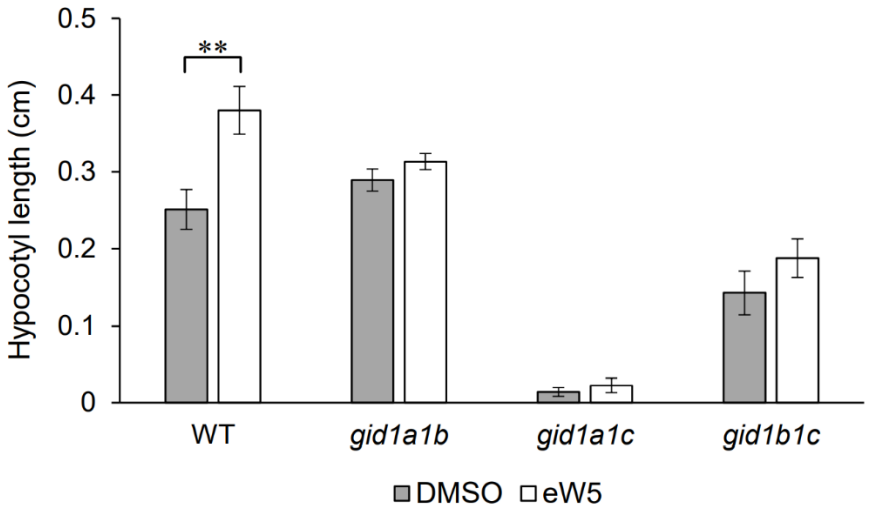

Figure 29: Hypocotyl length of GA double mutants Error bars represent the standard error from 30 individuals and asterisks show significant differences (independent t-test, ** P<0.005) between different treatments. Figure replicated from Sukiran.[102]

With evidence suggesting the GA receptors were required for the mode of action of eW5, it was then hypothesized that the compound might be mimicking GA. This was studied further using *ga1-5* mutants, which display the dwarfed phenotype due to low GA levels. Treatment with eW5 failed to restore the hypocotyl elongation effects seen with GA, indicating that the compound's mode of action was not identical to that of GA and further suggested that endogenous GA was required for its growth promotion effects.

With GA being required for the growth promoting effects of eW5 to be observed, it was then proposed that the compound was affecting GA sensitivity or upregulating biosynthesis of the hormone. To study the possibility of eW5 enhancing GA sensitivity, an additional hypocotyl assay was conducted where eW5 was co-applied with varying low concentrations of GA (Figure 30). It was observed that treatment of eW5 alongside GA resulted in increased hypocotyl growth for all concentrations tested (1-10 μM),

supporting the hypothesis that eW5's growth promoting effect was additive to the GA hormonal pathway.

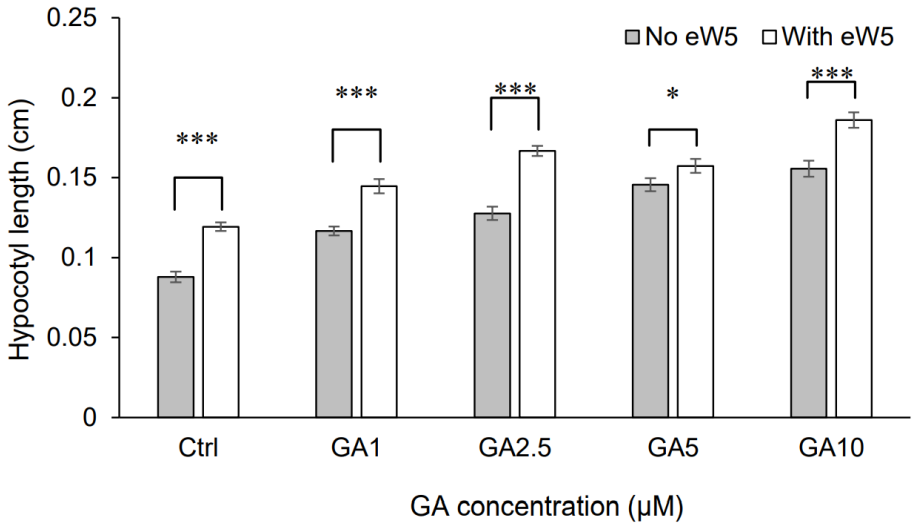

Figure 30: Hypocotyl growth at varying GA concentrations with and without additional eW5 treatment. Error bars represent the standard error of at least 30 individuals and asterisks show significant differences (independent t-test, * P<0.05, *** P<0.001) between treatment with ABA and eW5. Replicated from Sukiran.[102]

Investigation on the effect of eW5 on the biosynthesis of GA was carried out through the real-time quantitative PCR (qPCR) monitoring of the expression of the *AtGA20ox1-AtGA20ox5* gene family which encode for the GA biosynthetic enzymes. When observed at 1-, 3- and 6- hours after treatment of eW5, there was no significant difference in the expression levels of the three GA metabolic enzymes *GA20ox1*, *GA20ox2* and *GA20ox3*. Despite qPCR indicating eW5 had no effect on GA biosynthesis through the up- or downregulation of gene expression, the effect of the compound on this pathway cannot be entirely ruled out as there remains a possibility that regulation could be occurring at a different level, such as on enzyme activity itself.

A phenotypic analysis of the dwarfed *GA20ox1*, *GGA20ox2* and *GA20ox1*/2 mutants was then carried out as a confirmation on whether eW5 can act as a substitute in the absence of biosynthetic GA. Application of GA is known to recover the phenotype but application with eW5 failed to result in the same effect, supporting initial observations that the compound did not increase expression of GA biosynthetic related genes. This was supported by additional real time qualitative PCR measurements of the *GA20ox3* gene in GA deficient mutants. Unlike GA which unexpectedly showed a low level of *GA20ox3* expression at 30- and 60-minutes following treatment, eW5 showed greater expression of the

gene when compared with the DMSO control, further supporting that eW5 had no effect on GA concentration.

1.4.4: Epigenetic Effect of eW5

In addition to the studies on plants treated with eW5, it was also noted that in seeds treated with the compound but grown in control conditions in the absence of eW5, the growth promoting effects were retained. This led to the hypothesis that eW5 could have an additional epigenetic effect on the plant's growth mechanism. The perception of environmental signals can involve changes in gene expression and results in a variation of phenotype without modification to the DNA sequence.[103] The most widely studied epigenetic mechanism is through DNA methylation and histone modification which can either suppress or enhance gene expression either through the blocking of transcription factors or through the attraction of methylcytosine-binding proteins which ultimately results in the compaction of the chromatin.

To observe the epigenetic effect of eW5, Methylation Sensitive-Random Amplified Polymorphic Chain Reaction (MS-RAPD-PCR) was carried out on the genome of Arabidopsis treated with the compound. With DMSO as a control, the methylation-sensitive restriction enzymes Hpall and Mspl were used to cleave the specific sequence 5'-CCGG-3' followed by sample amplification through PCR. Following separation on an agarose gel, a differentiation between band profiles between DMSO and eW5 was observed, indicating that eW5 could potentially have a regulatory effect on the epigenetic mechanism.

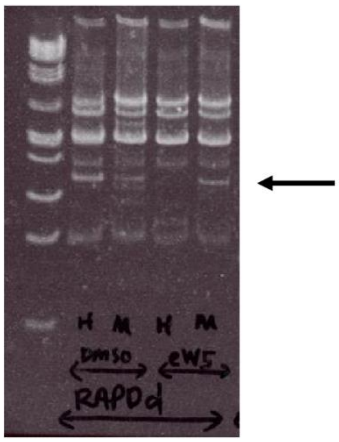

Figure 31: Agarose gel of PCR products following Random Amplified Polymorphic DNA primer amplification. H and M represent Hpall and Mspl respectively, the comparison between the methylated or unmethylated site are seen from the bands of the HpaII and MspI products. Figure replicated from Sukiran.[102]

Though the methylation study did indicate the possibility of eW5 having an effect through epigenetics, further RNA-seq analysis did not give as definitive conclusions on the potential regulatory pathway of the compound. Correlation graphs were constructed to observe any effect of eW5 on the expression of genes involved in plant growth and development and when compared with W5, eW5 only showed an effect in ethylene production. Attempts to measure the transcript level of individual genes that displayed the difference between the two compounds showed no significant deviation in expression, suggesting the growth promoting effect could be via protein activity as opposed to gene expression. Additional epigenetic studies such as bisulfate profiling which looks at conversion of unmethylated cytosine to uracil to probe further into the mode of action of eW5's growth promoting effects was not undertaken.

1.4.5: Current Structural Activity Relationship

With very little known about binding mode and target of eW5, and with the compound being very structurally similar to its parent molecules W5 and W7, a series of simple analogues were synthesized with the aim of developing a structural activity relationship (SAR). The initial set of analogues from which eW5 was derived can be classed into two distinct series; the A-series which has an identical aromatic core to W5, and the AC-series which has a 5-chloro substituent on its naphthalene core like W7.

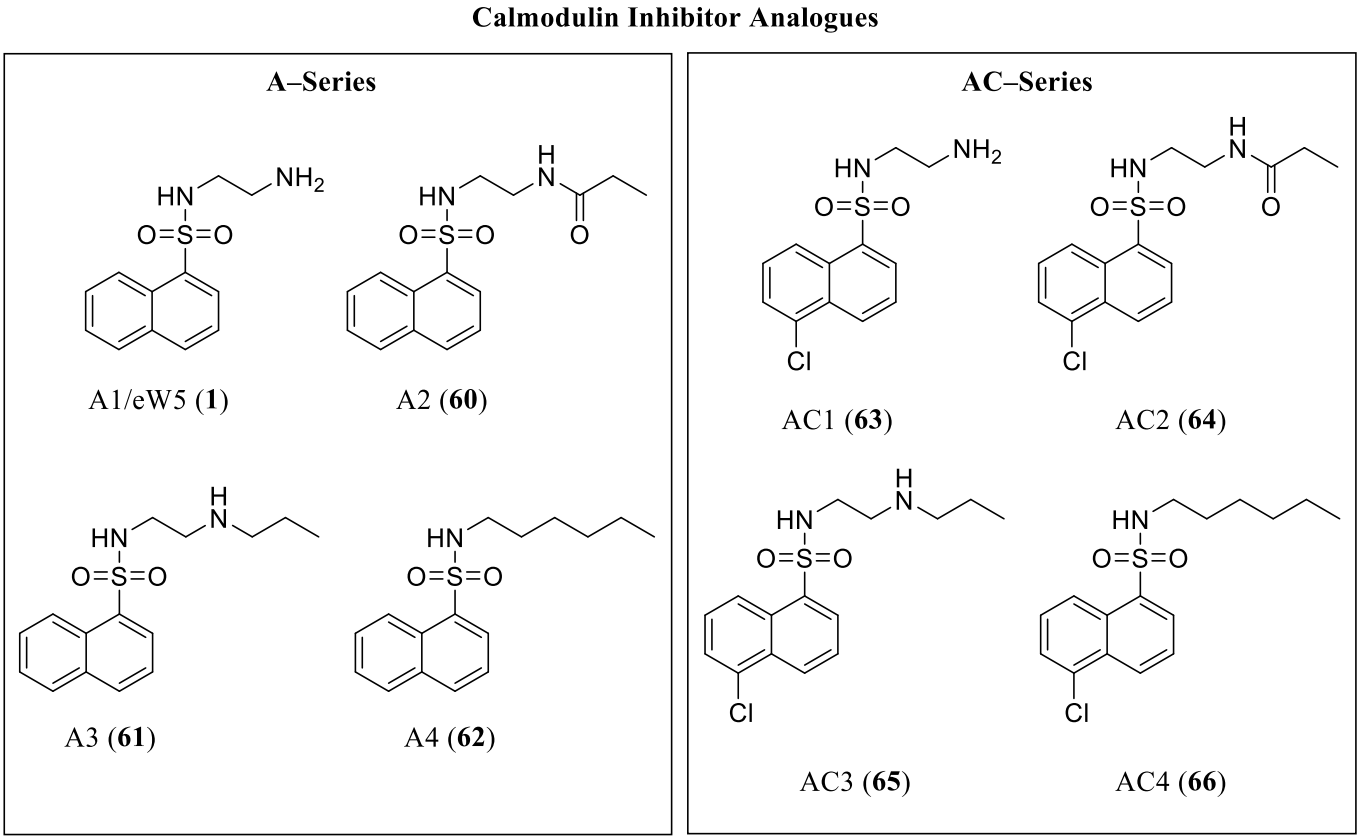

Figure 32: Structures of previously synthesized calmodulin inhibitor analogues **60**-**66**.

In addition to the original series of calmodulin inhibitor analogues a second series of molecules based on the structure of eW5 were synthesized (e-series) by using sulfonyl chloride substituted aromatic compounds were as starting materials and a range of primary amines. **67** was synthesized with the aim of investigating the functionality of the naphthalene core, **69** was aimed at looking the moving the sulphonamide moiety to a benzylic position, **68** & **70** were to investigate the effect of a para-substituent in the aromatic core and **71-72** were synthesized to probe the function of the primary amine and sulphonamide moieties respectively. These newly synthesized compounds along with the initial set of analogues of calmodulin inhibitors help create a preliminary SAR allowing for connections to be made between the structure of eW5 and its biological function.

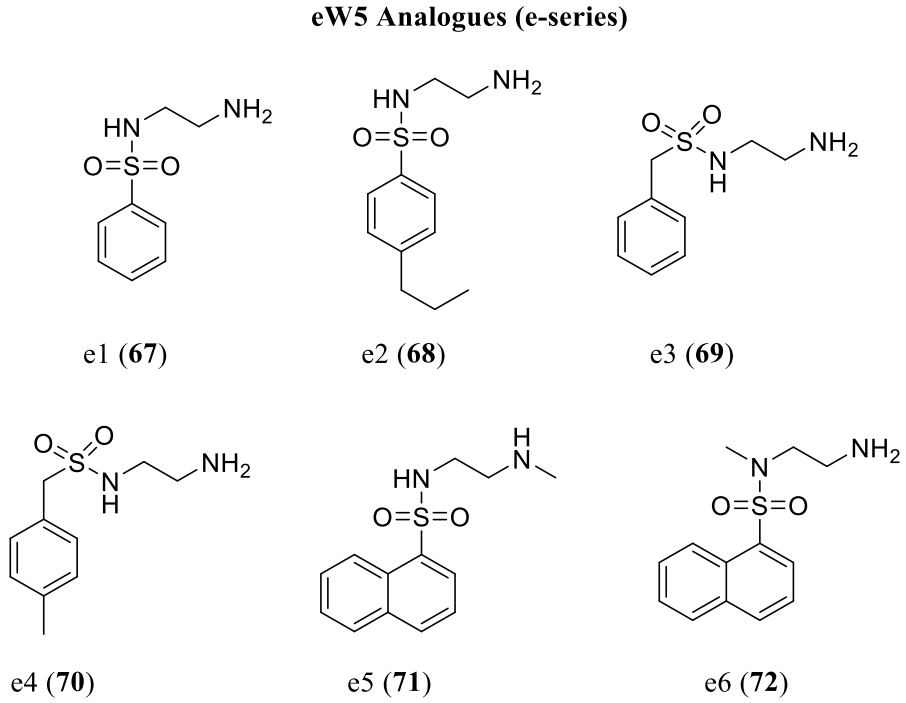

Figure 33: Structures of previously synthesized eW5 based analogues **67-72**.

The analogues were tested for their effect on new root growth on 7-day old seedlings and measured following an additional 5 days of growth.

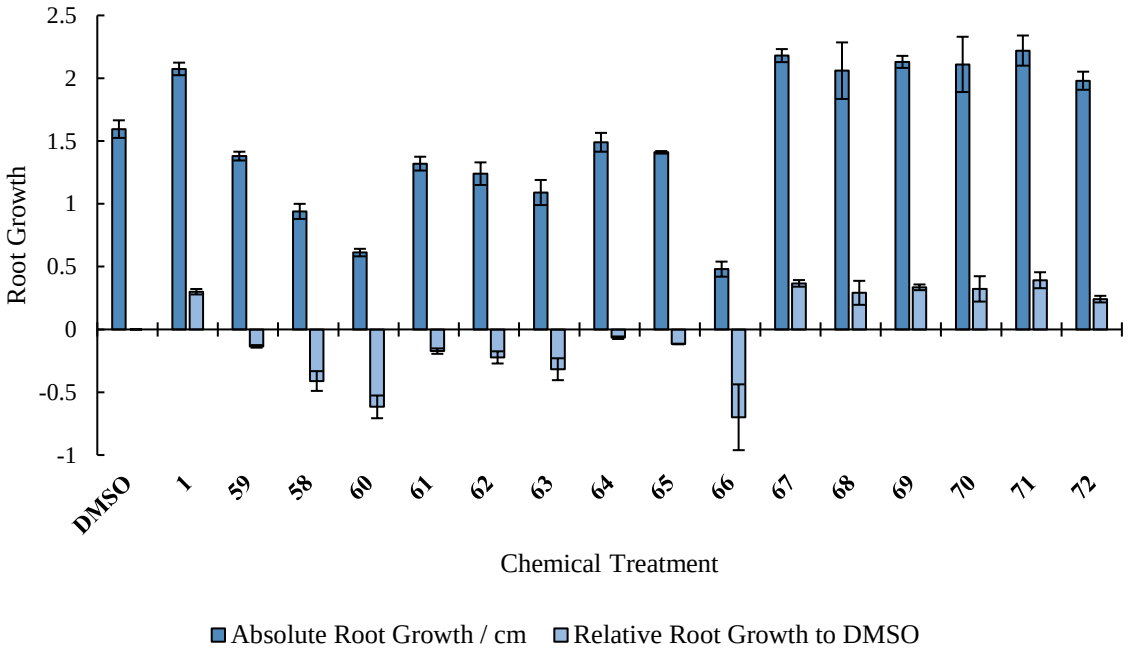

Figure 34: New root growth following treatment with respective compounds W5 (**59**), W7 (**58**), eW5 (**1**) and analogues **60**-**72** with DMSO set as the negative control; Error bars represent the standard error of at least 30 individuals. Graph showing relative new root growth of seedlings treated with compound against the negative control of DMSO.[102]

When combining the data for new root growth of all the synthesized analogues, some general observations about the SAR of eW5 could be made namely in simplifying the naphthalene core to a benzyl ring, moving the sulphonamide moiety to the benzylic position and alkyl substituents in the 4-position all had no significant difference to the growth promoting effect of these compounds.

Ultimately the major structural difference that could be observed between the original set of growth inhibiting calmodulin antagonists and growth promoting e-series analogues was the presence of the primary amine, indicating the importance of this motif in the function of eW5 (**1**). The only exception to this was secondary amine **71**, which retained the original effects of **1** in both the hypocotyl and root growth assays. **71** & **61** only differ by the secondary amide alkyl chain yet display vastly different growth promoting effects. **71** showed the greatest root promoting effect out of the e-series of analogues and contains a methyl group attached to the diamine moiety whereas **61** has a propyl group. The opposite effects of these compounds on root growth could indicate that a longer alkyl chain would be inhibitory as **61** acts as an antagonist for root growth. It may be hypothesized that this is similar to the effect reported by Hayashi *et al*. (2008) where it was shown that compounds containing longer alkyl chains block the access of Aux/IAA to TRANSPORT INHIBITOR RESPONSE 1 (TIR).[104]

Further investigations of the analogues were conducted through hypocotyl growth assays (Figure 35). Although each e-series analogue was able to promote growth in the root growth assays, this did not directly correlate with the analogue's ability to increase hypocotyl growth. An example of this was with analogues **69** & **70** as these two compounds displayed new root growth to eW5 (**1**) but were unable to yield the same growth promoting effects in relation to hypocotyl growth. The varying effects that result from moving the sulphonamide position to the benzylic position could indicate the possibility of polypharmacology.

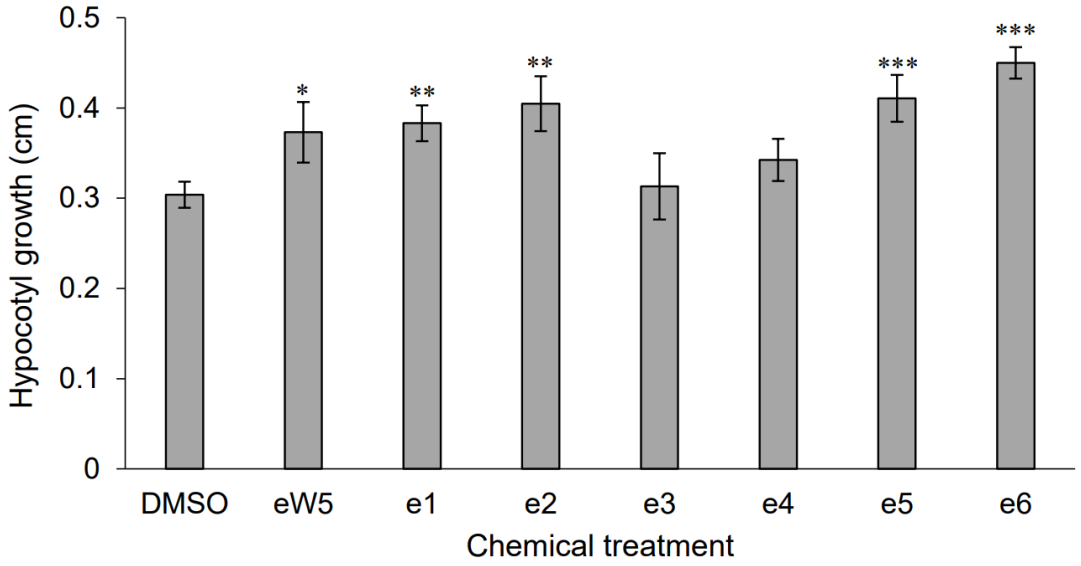

Figure 35: Hypocotyl growth assay for e-series of analogues **67-72** with eW5 (**1**) as a positive control at 100µM concentration. Asterisks indicate statistically significant differences (independent t-test, P<0.05, ** P<0.005, *** P<0.001) between DMSO and chemical treatment. The error bars represent standard error based on three biological replicates. Replicated from Sukiran.[102]

Although this initial library of analogues gave some initial indications of SAR, additional questions need to be asked about the functional groups of eW5 (**1**) and their relation to its biological activity. In particular, further analogues can be synthesized to probe the function of the aromatic core, the length of the alkyl chain between the diamine and possibility of substituents on other positions around the naphthalene core.

1.5: Aims of the Project

As discussed in Section 1.4, although studies along ABA and GA pathway elucidated some aspects of the mode of action of eW5, they ultimately failed to definitively identify the target. Thus, the principal aim of this project was to elucidate the target(s) of the compound.

Two independent strategies were envisioned. The first approach was to develop the eW5 scaffold into a chemical probe. In reviewing the strategies for chemical probes and target identification, it was proposed that a photoaffinity probe would be the best approach in situations where binding affinity is low or when little is understood of the target of the small molecule. It was also worth taking into consideration the possibility that eW5 is targeting a non-proteinaceous entity. These two factors mean that the reactive species formed from photo-crosslinking tags would have an advantage over reactive electrophilic groups as active nucleophilic residues would be required for covalent capture.

The initial area of interest was to explore structural variation in various parts of the molecule to further develop the current SAR. Through the synthesis and biological testing of analogues our aim was to better understand the role of the various components of the molecule in relation to its biological effect and to identify "hot-spots" on the molecule which could be targeted for photo affinity conjugation without being detrimental to the biological activity of eW5. Building on the SAR data developed by Sukiran which indicated tolerances for structural variation in the aromatic core, it was decided that the naphthalene ring would be examined as an initial site of attachment for a photoaffinity moiety.[102]

It was proposed to develop a modular approach to our photoprobe design where we aimed to attach various photoaffinity components to a core molecule without significant variation in synthetic strategies. As previously discussed in section 1.2.5.4 this strategy is similar to photoprobe designs employed by Fujii *et al*.

Although synthetically attractive, this method faces similar issues as encountered by Fujii where the steric bulk introduced by the photoaffinity and reporting module could affect the small molecule's interaction with its target, resulting in reduced biological activity and non-specific covalent linkages. To address this concern a more hybrid design was envisaged where the size of the probe would be reduced by incorporating the photo-active and reporting group into the molecule without the use of a linker. This approach has the additional benefit of having the photoaffinity tag closer to the core of the molecule, increasing binding efficiency to the target. Again, SAR studies would initially be required to inform the designs of this alternate approach in the development of a chemical probe.

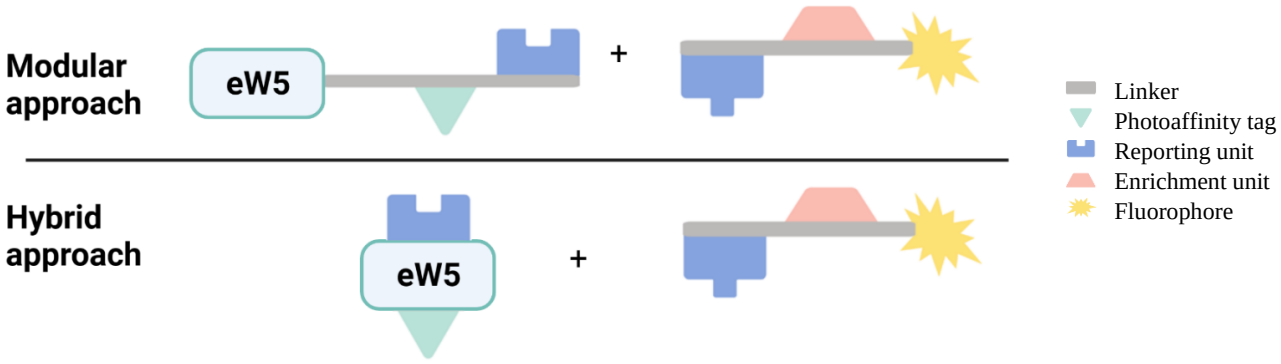

Figure 36: Proposed eW5-based photo affinity probe

In a complementary approach, a forwards genetics approach was also proposed as a viable method for target identification of eW5. This would be similar to the approach used with the ABA agonist pyrabactin which selected for mutants which were able to germinate in the presence of the compound and led to the identification of the PYR1 gene (Section 1.3.2). Using an EMS mutated A*arabidopsis thaliana* population, the screen would select for individuals which fail to display enhanced growth in the presence of eW5. These could then be sequenced to identify the mutation(s) involved in eW5 insensitivity. Although this approach may not definitively yield the protein target of eW5, it could elucidate the mechanism of action of the molecule as mutants of downstream factors could be identified, allowing for additional insight into the affected pathway.

Chapter 2: Developing the SAR of eW5

2.1: Chapter Introduction

This chapter describes the development of the SAR of eW5 for the purpose of probe development. As discussed in section 1.2.5, probes containing a photo-affinity unit need to retain biological activity to ensure on-target crosslinking. The relatively small size of eW5 provides no natural locations to which a photo-crosslinking group and reporting unit could be covalently attached. With the aim being the development of a chemical probe, the SAR of eW5 would need to be developed to enable the identification of sites of derivatisation and inform the design and location of the photo-crosslinking group and the reporting unit.

The initial approach involved synthesis from commercially available sulfuryl chlorides but was limited in terms of further derivatisation. A new strategy to synthesise sulfonamides via the lithiation of respective aryl bromides was then established, affording numerous alkoxy-substituted analogues. Evaluation of the compounds through a hypocotyl growth assay demonstrated the feasibility of monocyclic aromatic cores, various electron withdrawing substituents and simple N- substituents. Towards the goal of probe development, the assay also demonstrated the tolerance of alkoxy chains in the 2- and 4-position supporting the proposition that linkers could be attached to the aromatic core.

2.2: Synthesis of eW5 Analogues

As outlined in section 1.4.5, understanding of the SAR of eW5 to this point was relatively limited. Analogues that were synthesised (**67**-**72**) questioned only fundamental aspects of the compound's structure in relation to its growth promoting effects, namely the effect of monocyclic aromatic cores, benzylic sulfonamides, N–H methylation and simple substituents in the 4-position. Despite the small number of analogues, one common thread that was identified was the N–aminoethyl sulphonamide moiety being present amongst all compounds displaying eW5-like growth promoting properties, leaving possible linker attachment sites limited to the sulphonamide N–R and naphthalene core.

Previously synthesized sulfonamide analogues had been generated via the coupling of a commercially available sulfonyl chloride with a primary amine and was the approach taken in the synthesis of the initial set of eW5 analogues. Although this strategy is well established in the synthesis of sulfonamides, purification consistently proved challenging due to the presence of a free amine. This problem was bypassed by Boc-protection of the amine, forming carbamate **74** which could then be purified through

flash column chromatography. Subsequent Boc-deprotection using 4M HCl in dioxane quantitatively yielded desired amine **1** which could then be used without further purification (Scheme 1).

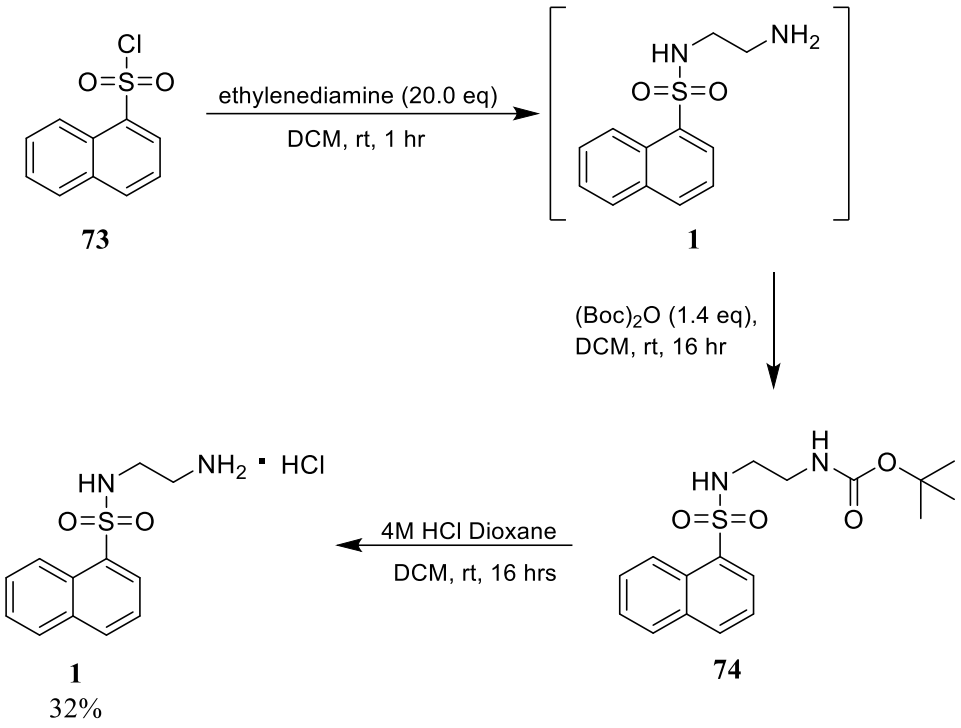

Scheme 1: Previous preparation of eW5.

With a wide range of commercially available aromatic-sulfonyl chlorides, this synthetic route was initially chosen as a method of generating eW5 analogues. The successful synthesis of eW5 (**1**) described above suggested that the direct use of Boc-protected amines would allow easier purification and increased yields due to the reduced number of synthetic steps. As an initial proof of concept, eW5 was synthesized from 1-napthalene sulfonyl chloride and N-Boc ethylene diamine to give carbamate **74** characterised by a characteristic sharp singlet in the ^{1}H–NMR at δ 1.35 (9H). This was then treated with 4M HCl in dioxane, giving eW5 (**1**) in 81% yield over the 2 steps (Scheme 2).

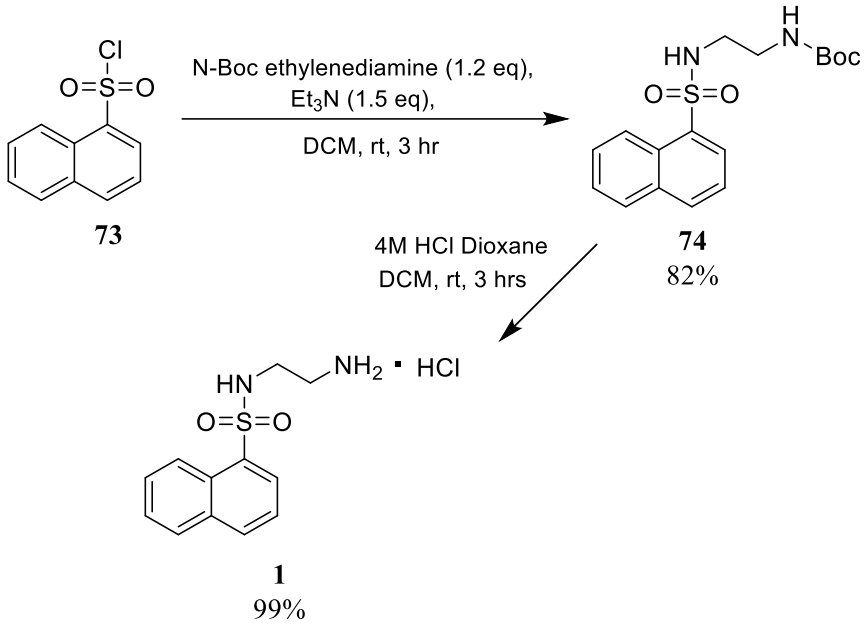

Scheme 2: Synthesis of eW5 via Boc-carbamate **74**.

Having established an effective synthetic method for the synthesis of eW5, focus then shifted to exploring the SAR of the sulfonamide. In the original set of analogues prepared by Sukiran *et al*, it was identified that mono cyclic cores and alkyl substituents in the 4-position did not adversely affect the growth promoting properties of the compounds, with analogues **68** and **70** being comparable to eW5.[102] Although these compounds did indicate that modification of these sites would be feasible, alkyl substitutions were synthetically challenging as it provides no direct method of attachment of a photo-affinity module.

The initial set of analogues that were synthesized looked to expand on these findings by exploring the effect of various substituents and substitution patterns on monocyclic cores as well as varying alkyl substituents in the 4-position. The first area of study was the position of the sulfonamide on the naphthalene ring and whether it needed to be in the 1-position. This led to the synthesis of **75** from 2-naphthalene sulfonyl chloride which was obtained in 64% yield over the two steps.

Simple analogues containing electron-withdrawing substituents were then synthesized with **76**, **77**, containing 2- and 3- fluoro- substituents and a 4-nitro analogue **78** being synthesized in appreciable yields. To further investigate the tolerance of substituents in the 4-position, large bulky groups were chosen. This would not only give a better understanding of the binding pocket of eW5 but also give a good indication on whether or not this space was available for the addition of a photo-crosslinker. As a result, tert-butyl analogue **79** and biphenyl analogue **80** were synthesized. Another question regarding the naphthalene core was whether it needed to be directly attached to the sulfonamide. Of the e-series

analogues (**67-72**, Figure 33), none of the benzylic sulfonamides were able to promote hypocotyl growth. As this was only tested on monocyclic compounds a naphthalene analogue was synthesised with an ethyl chain between the aromatic core and the sulfonamide giving analogue **81**.

In addition to the study of the aromatic core and its substituents, it was of interest to whether two carbons were the optimal length for the diamine tail. From the original series, it was shown that six carbons led to root growth inhibition (W5, **59**), but other lengths had not been explored. To address this, compound **82** was synthesised using N-Boc propyl-1,3-diamine.

Additionally, substitution of the primary amine remained an open question. At this point, only mono methylation of the primary amine tail had been studied and this showed comparable growth promoting effects to eW5. This naturally pointed to the question of a tertiary amine and if a similar effect would be observed. To answer this, compound **83** was synthesized directly through the reaction of 1-naphthalene sulfonyl chloride and N,N dimethyl ethylene diamine.

Finally, remaining on the diamine tail, the role of the amine itself was questioned. It was proposed that substitution of the nitrogen to an oxygen atom would be a good initial modification to determine the importance of the primary amine. Thus, primary alcohol **84** and ether **85** were synthesised directly through the same method as outlined above using ethanolamine and 2-methoxyethan-1-amine.

Other analogues synthesized from this strategy aimed to investigate the role of the aromatic core itself. With the ethylene diamine tail seemingly the common feature of all growth promoting analogues, it then became of interest to confirm the essentiality of the aromatic ring. This was elucidated through equivalent conditions using various alkyl sulfonyl chlorides to afford **86** and **87**.

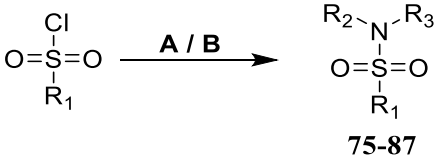

75-87

Condition **A**: i. NHR_2R_3 (1.2 eq), NEt_3 (1.5 eq) DCM, rt, 3 hrs
ii. 4M HCl, dioxane, rt, 3 hrs

Condition **B**: NHR_2R_3 (1.2 eq), NEt_3 (1.5 eq) DCM, rt, 3 hrs

Entry	R_1	NHR_2R_3	Condition	Compound
1	2-naphthalene	N-Boc ethylenediamine	**A**	**75** 64% 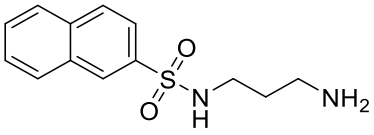

2	2-fluorobenzene	N-Boc ethylenediamine	**A**	**76** 82% 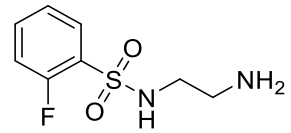
3	3-fluorobenzene	N-Boc ethylenediamine	**A**	**77** 54% 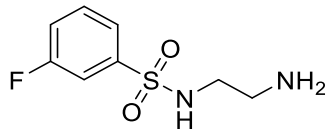
4	4-nitrobenzene	N-Boc ethylenediamine	**A**	**78** 54% 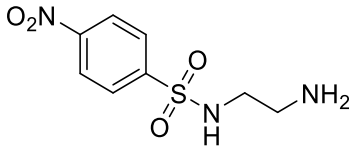
5	4-*tBu* benzene	N-Boc ethylenediamine	**A**	**79** 45% 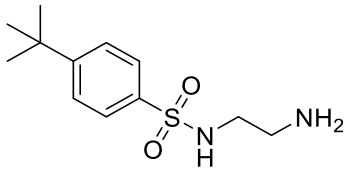
6	1-1'diphenyl	N-Boc ethylenediamine	**A**	**80** 73% 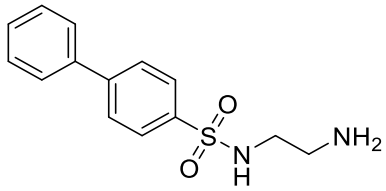
7	2-(naphthanlene-1-yl) ethanesulfonyl chloride	N-Boc ethylenediamine	**A**	**81** 60% 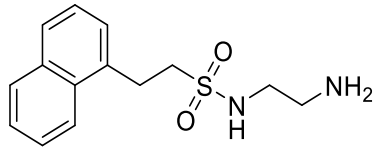
8	1-naphthalene	N-Boc propyldiamine	**A**	**82** 83% 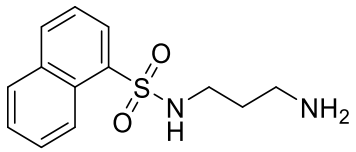
9	1-naphthalene	N,N-dimethyl ethylenediamine	**B**	**83** 85% 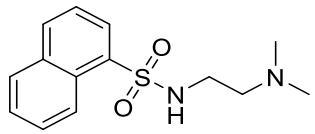
10	1-naphthalene	ethanolamine	**B**	**84** 82% 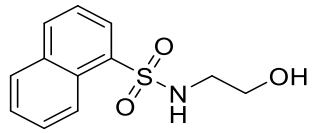
11	1-naphthalene	2-methoxyethlamine	**B**	**85** 87% 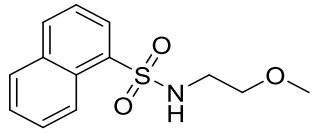
12*	Mesyl chloride	N-Boc ethylenediamine	**A**	**86** 81% 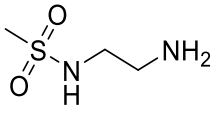

13	Cyclohexyl sulfonyl chloride	N-Boc ethylenediamine	**A**	**87** 80% 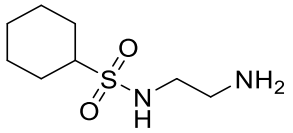
14	1-naphthalene	N-(2-Aminoethyl)-N,N-Boc methyl	**A**	**71** **67%** 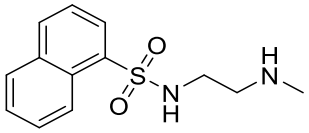
15	1-naphthalene	N-Boc-2-methylamino-ethylamine	**A**	**72** 89% 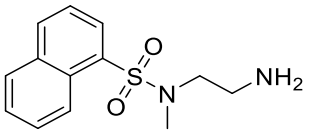
16	4-*n*-propylbenzene	N-Boc ethylenediamine	**A**	**68** 61% 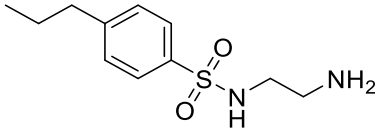
17	5-chloro, 1-naphthalene	N-Boc ethylenediamine	**A**	**63** 70% 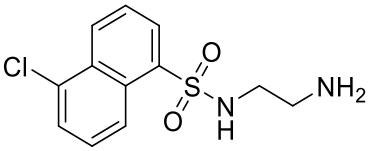

Table 1: Generic synthesis of eW5-analogues **63**, **68**, **71**-**72**, **75**-**87** from commercial sulfonyl chlorides. Values reported represent overall yields. *Compound prepared by Harry Peachment.

Alongside these novel analogues, **63**, **68**, **71** & **72** were resynthesized using this synthetic strategy.

Although this strategy was able to generate a diverse range of analogues efficiently, it was limiting in terms of the structural diversity of commercially available sulfonyl chlorides. Furthermore, additional functionalization of such electron deficient arenes is challenging as it prevents the use of standard Friedel Crafts conditions and C–H activation strategies could possibly encounter selectivity issues. Consequently, strategies to address these issues were sought and discussed in the next section.

2.3: Synthesis of Sulfonamides from Aryl-Bromides

As discussed above, a strategy to introduce greater diversity of substituents into an aryl sulfonamide was required. It was initially proposed that the sulfonyl chloride could be installed via an aryl halide. This would allow for a wider range of simple di-substituted aromatic cores to be used as functionalized starting material.

A review of the literature revealed a method described by Willis *et al*. using DABCO-bis(sulfur dioxide) (DABSO, **89**) (Scheme 3).[105] This one pot reaction to synthesize a sulphonamide begins with the

combination of DABSO (**89**) and a Grignard reagent to form a sulfonate intermediate which is transformed into the sulfonyl chloride with the addition of sulfuryl chloride. The coupling of the amine to this intermediate completes the synthesis.

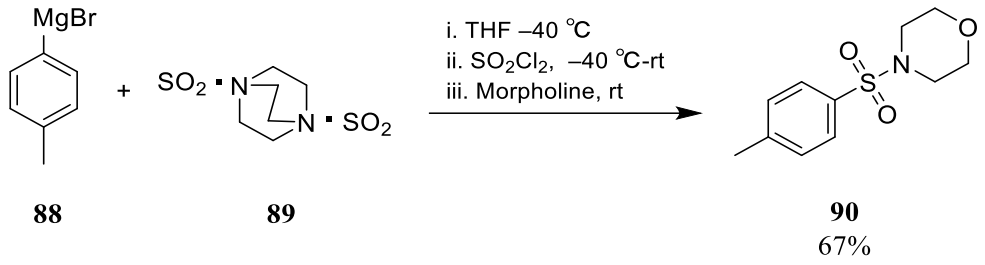

88 **89** **90**
67%

Scheme 3: Synthesis of sulfonamide **90** using DABSO (**89**) as described by Willis *et al*.

To verify the methodology, a model reaction using phenyl magnesium bromide (**91**) and diethylamine was undertaken to give sulfonamide **92**.

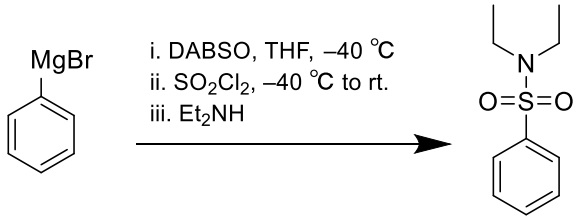

91 **92**
77%

Scheme 4: Synthesis of sulfonamide **92** following method described by Willis.

This reaction gave the desired product in an equivalent yield to that reported by Willis as confirmed by peaks in the ^{1}HNMR spectrum at δ 7.84, 7.57 and 7.53 integrating to 2, 1 and 2 protons corresponding with aromatic protons whilst peaks at δ 3.27 and 1.14 integrate to 4 and 6 hydrogens, corresponding with the aliphatic protons. Subsequently this procedure was attempted with the Grignard reagent prepared in situ from magnesium and 1-bromonaphthalene. Disappointingly, despite multiple attempts, this failed to give the desired product in significant yields or purity. Given the previous success of the Willis reaction, the reasons for this were not obvious but were attributed to the quality of the in situ generated Grignard. To circumvent this difficulty, efforts then turned to explore alternative organometallic reagents.

Towards this goal, an alternative two step synthesis was adopted based on the reported reaction of an aryl-lithium with sulfuryl chloride by Ishihara *et al*.[106] This was initially tested on the synthesis of model compound **94** by adding n-BuLi to 1-bromonaphthalene (**93**) and trapping the subsequent aryl-lithium

intermediate with sulfuryl chloride. This yielded the sulfuryl chloride intermediate **73** which without further purification was coupled with diethylamine forming the aryl sulfonamide **94** in 23% yield, characterized by an LC-MS peak at 2.54 mins corresponding to ES^+ *m/z* 352.04 $[M+H]^+$. Despite the low yield, the desired product was isolated. Given the ease of synthesis, it was believed that adopting this method would allow for the rapid assembly of SAR data from readily available aryl halides.

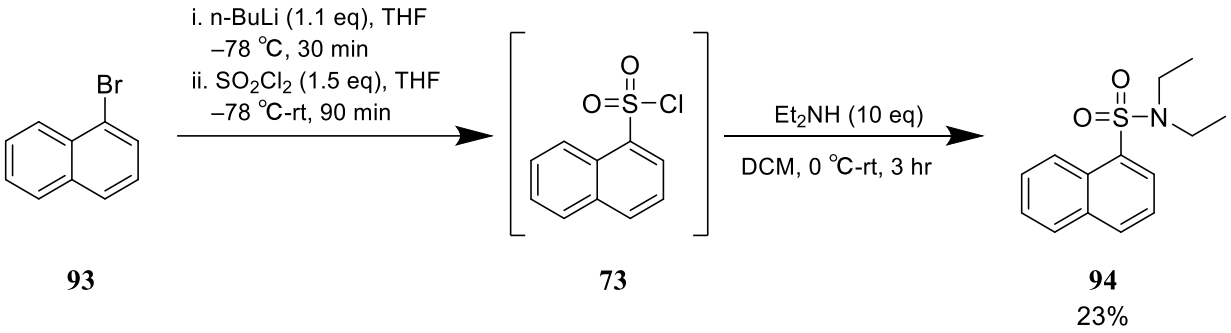

Scheme 5: Synthetic route for model sulfonamide **94** from aryl bromide.

Having established a general procedure for the formation of sulfonamides through the lithiation of aryl-bromides, the synthesis of eW5 was attempted to validate the entire synthetic route. eW5 (**1**) was prepared using N-Boc ethylene diamine as a coupling partner for the sulfonyl chloride intermediate. This afforded the Boc-protected species **74** and treatment of the carbamate with 4M HCl in dioxane afforded **1** as an HCl salt in 36% yield over the 3 steps.

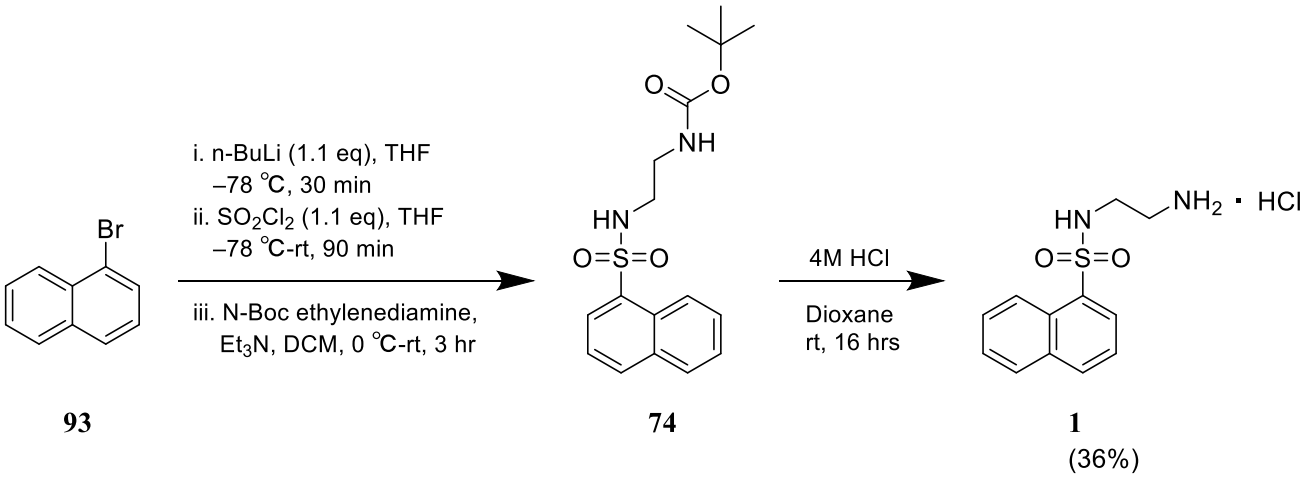

Scheme 6: Synthetic route for lead compound eW5 (**1**)

2.4: Heterocyclic Analogues

To this point, there were no heterocyclic analogues of eW5 and the effects of electronics of the aromatic core were unknown. It was proposed a simple study of "walking" a nitrogen around the naphthalene core would address this question. Using the same method as described above enabled the synthesis of quinoline and isoquinoline analogues of eW5.

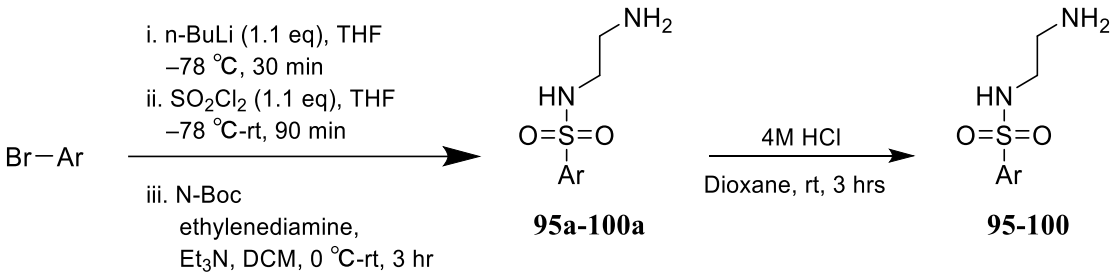

Entry	Compound	Ar	Yield* (%)
1	**95**	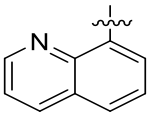	13
2	**96**	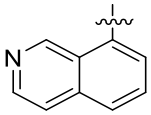	37
3	**97**	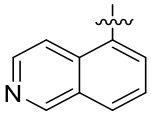	28
4	**98**	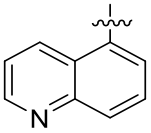	40
5	**99**	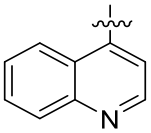	0
6	**100**	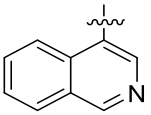	60

Table 2: Synthesis of (Iso)quinoline analogues **95-100**. *Values represent overall yields.

Although this pathway allowed for the access of (iso)quinoline analogues **95-98** and **100** in good yields, attempts to prepare 4-quinoline analogue **99** was not successful and no attempt was made to develop alternative routes to this compound.

In addition to the (iso)quinoline series of analogues, fluorescent heterocycles were also briefly explored. NBD sulfonamides have shown to be fluorescent and given the structural similarities between it and eW5 (**1**), synthesis of an NBD-eW5 hybrid analogue was attempted. This analogue had the additional benefit of allowing for localization experiments to be conducted, giving a better understanding of eW5's mode of action.

The synthesis of fluorescent analogue **104** began by treating 4-chloro-7-chlorosulfonyl-2,1,3-benzoxadiazole (**101**) with N-Boc ethylenediamine using the conditions described in Scheme 2. to afford compound **102** in 69% yield. The NBD core required a lone pair of electrons feeding into the system for it to be fluorescent. As a result, **102** underwent SnAr with methylamine to afford the boc-protected analogue **103** giving the characteristic singlet at δ 4.15 integrating to 3 protons, corresponding to the methylated amine. This was followed by Boc-deprotection using 4M HCl in dioxane to give fluorescent analogue **104**.

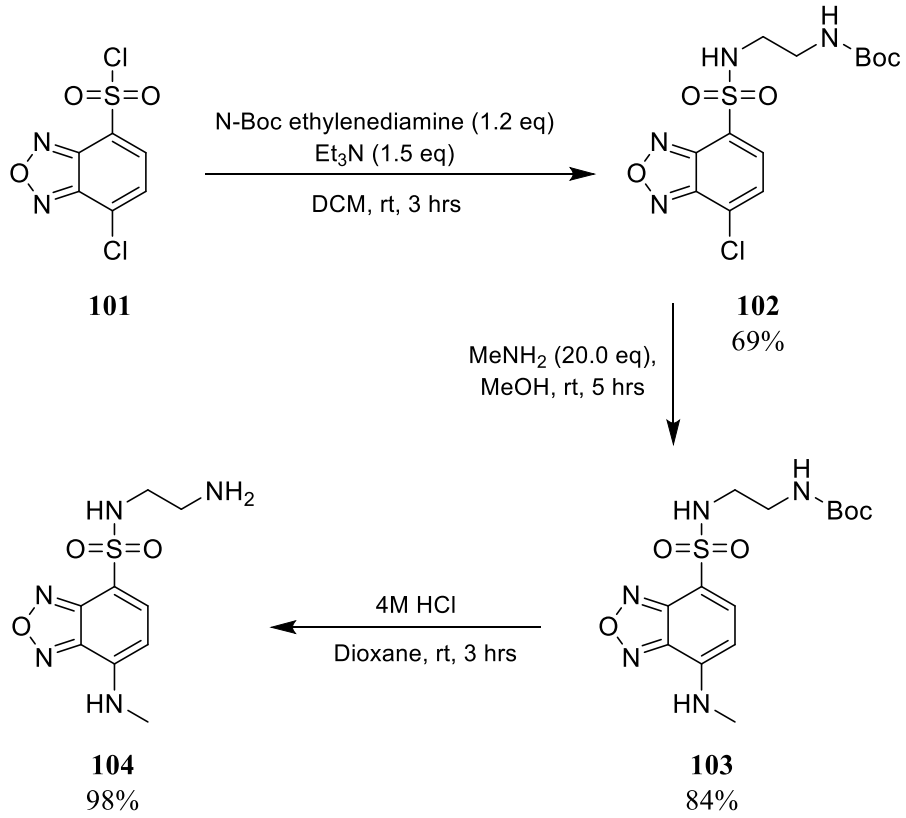

Scheme 7: Synthesis of NBD analogue **104**.

2.5: Alkoxy-Substituted Analogues

As mentioned previously, although 4-alkyl substituents were shown to be feasible, the scope for further variation was synthetically limited. Consequently, it was proposed that an alkoxy substituent would

provide greater synthetic scope for the attachment of a diverse linker groups. Commercial availability limited alkoxy substitutions on the primary ring but nevertheless this approach was initially undertaken due to the trivial nature of phenol alkylation.

Following methylation of the naphthol as the methyl ether, lithiation and reaction with sulfuryl chloride and N-Boc ethylenediamine, as before, afforded derived eW5 analogue **110** in 35% yield over 4 steps. With an established protocol, it was of further interest to explore the corresponding 2- and 3- substituted regioisomers. However, whilst 1-bromonapth-2-ol was also commercially available, the corresponding naphth-3-ol was not and required synthesis.

On the basis that more electron deficient aryls are borylated faster, it was suggested that the naphthol could be synthesized via sequential Ir catalysed C-H borylation-oxidation of 1-bromonaphthalene. Unfortunately, GCMS analysis of the crude mixture following oxidation showed a mixture of 3 naphthols which were suggested to be the 3-, 6- and 7- substituted (**105**-**107**). Although it was suspected that the 1,3- substituted naphthol was the major product, attempts to separate the isomers were unsuccessful. As a result, synthesis of 3-alkoxy substituted naphthalene sulfonamides was not taken further at this stage.

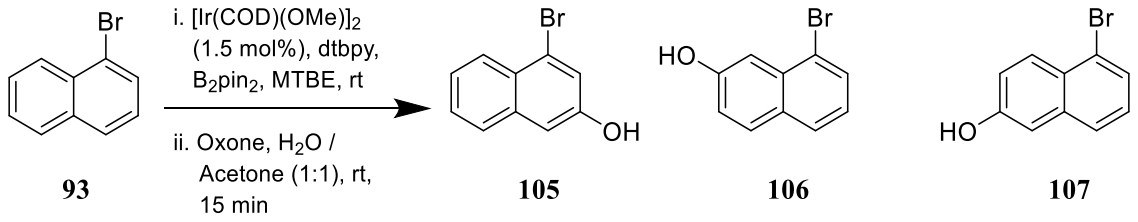

Scheme 8: Borylation then oxidation of 1-bromonaphthalene (**93**).

Following protection of 1-bromonaphth-2-ol and 1-bromonaphth-4-ol as the respective methyl esters, sulfonamide generation as before gave N-Boc protected methoxy substituted naphthalene sulfonamides **108** and **110**. Having successfully shown methoxy substituted naphthalene sulfonamides could be accessed via this synthetic route, attention turned to monocyclic aromatic cores as earlier eW5 analogues showed the ability of phenyl-based compounds to retain growth promoting properties. Consequently 1,2-, 1,3- and 1,4- bromo anisoles were treated in an identical fashion to afford sulfonamides **112**, **114** and **116** in acceptable yields of 40-52%.

Longer chain alkoxy substituted naphthalene and phenyl analogues were accessed in a similar manner. Whilst the coupling of naphthols with iodoalkanes proceeded uneventfully, the use of bromoalkanes

required the presence of catalytic TBAI. Each bromoaryl-alkyl ether was then converted to Boc-protected sulfonamides **109**, **111**, **113**, and **115** following the procedure described in Scheme 5.

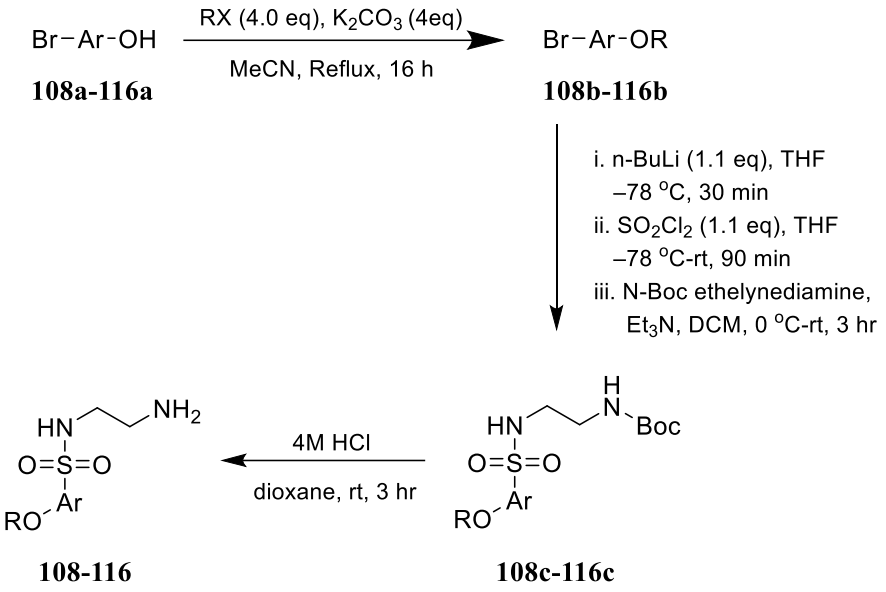

Entry	a	RX	b	Analogue*
1	1-bromonaphth-2-ol	MeI	**108b.** *1-bromo, 2 methoxy naphthalene* 93%	**108** 34% 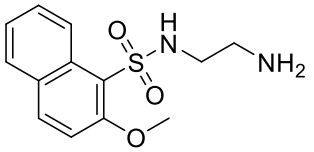
2	1-bromonaphth-2-ol	1-iodopentane	**109b.** *1-bromo, 2-pentoxy naphthalene* 91%	**109** 24% 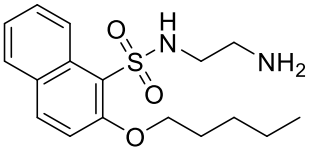
3	1-bromonaphth-4-ol	MeI	**110b.** *1-bromo, 2-methoxy naphthalene* 96%	**110** 36% 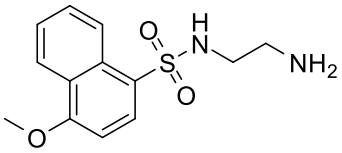
4	1-bromonaphth-4-ol	1-iodopentane	**111b.** *1-bromo, 2 pentoxy naphthalene* 93%	**111** 38% 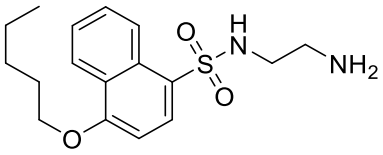
5	2-bromophenol	MeI	**112b.** 2-bromo anisole 95%	**112** 52% 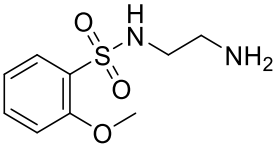
6	2-bromophenol	1-bromohexane	**113b.** *1-bromo, 2-hexoxy benzene* 93%	**113** 37% 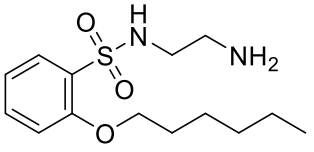

7	4-bromophenol	MeI	**114b.** 4-bromo anisole 96%	**114** 40% 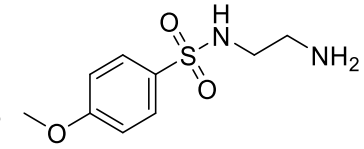
8	4-bromophenol	1-bromohexane	**115b.** 1-bromo, 4-hexoxy benzene (95)[i]	**115** 46% 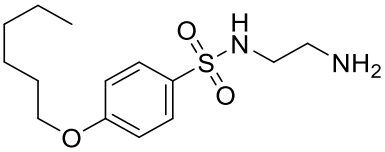
9	/	/	**116b.** 3-bromo anisole	**116** 48% 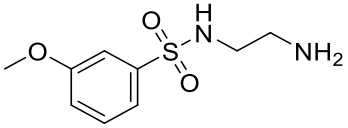

Table 3: General Procedure for synthesis of alkoxy analogues 108-116. [i]0.1 mol% TBAI was added in addition to standard procedure. *Values reported represent yields over 2 steps.

In a similar fashion, 2-ethoxyethoxy-analogues were prepared using 2-ethoxyethyl methanesulfonate (**117**) as the electrophile. Interestingly, initial attempts to prepare the 4-substituted 2-ethoxyethyl compound **122**, unexpectedly produced trisubstituted compound **121**. This was characterized by an observable chlorine isotopic pattern in LC-MS and a singlet at δ 8.22 in HNMR corresponding to 2–H.

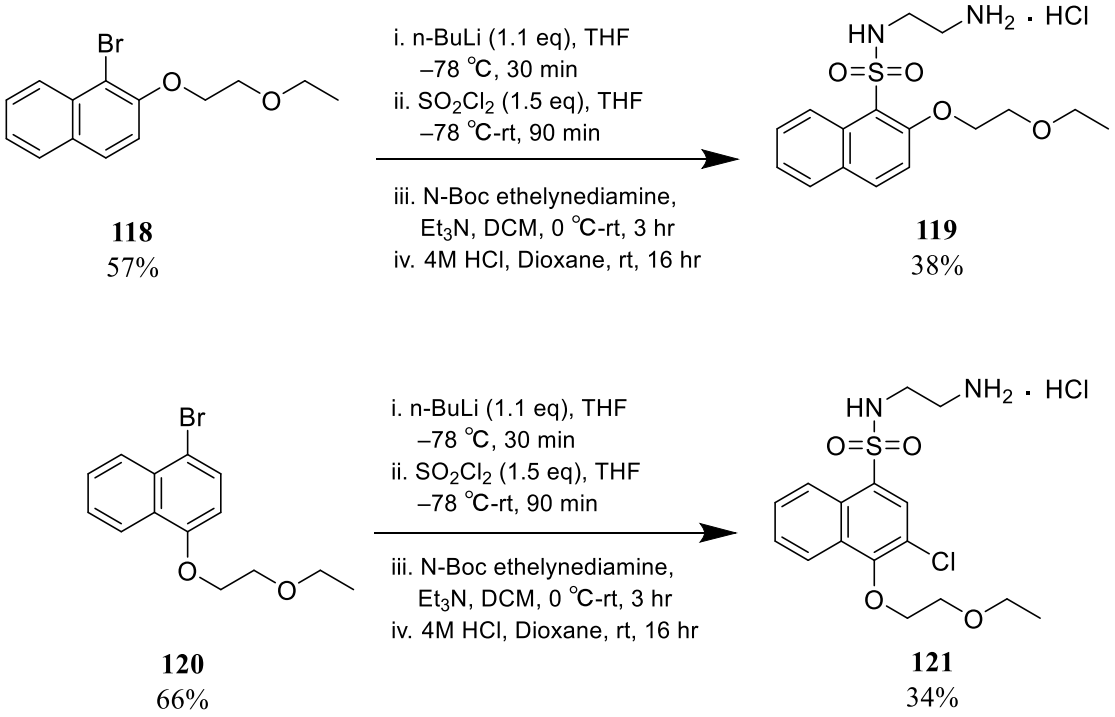

118 57%

119 38%

120 66%

121 34%

Scheme 9: Synthetic route for compounds **119** and **121** from respective 2-ethoxyethoxy, bromonaphthalenes **118** and **120**.

It was suspected that the 2-ethoxyethoxy- substituent in **120** was acting as direct metalating group, resulting in ortho lithiation of the 3-position. Sulfuryl chloride has been shown to be an electrophilic source of chlorine and addition of this to the organolithium intermediate resulted in a chlorine substitution ortho to the 2-ethoxyethoxy group. To overcome this issue, the reaction was repeated with 0.95 eq of both n-Buli and sulfuryl chloride which resulted in desired sulfonamide **120**, albeit with a significantly reduced yield.

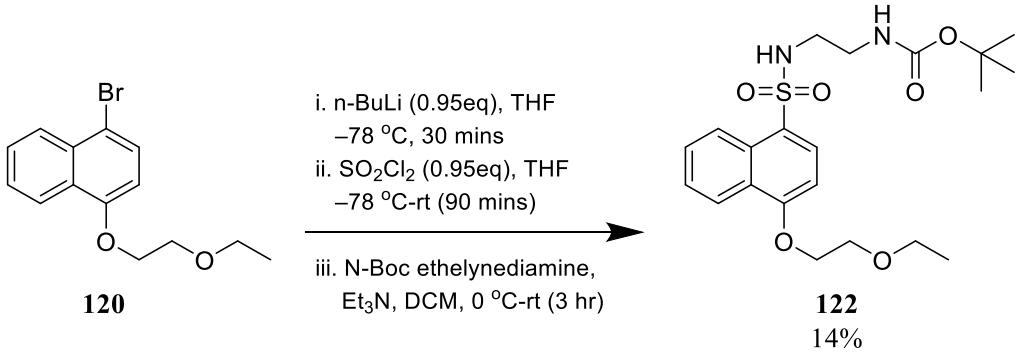

Scheme 10: Revised conditions for synthesis of 4-(2'-ethoxyethoxy) sulfonamide **122**.

2.6: Hypocotyl Assay of Analogues

Having synthesized a diverse range of analogues, focus shifted to biological evaluation of these compounds. As previously discussed in Section 1.4, eW5 results in multiple observable phenotypes, including increased root growth, hypocotyl growth, stomatal aperture, and fresh and dry weight. As the simplest and most reproducible of these assays in assessing eW5-like properties, hypocotyl growth was chosen as the primary metric in the assessment of the biological activity of the analogues. With the current hypothesis of the mode of action of eW5 being that it is linked with the GA hormonal pathway, the hypocotyl assay had an additional benefit in that it was the most diagnostic for gibberellins. In brief, using DMSO as the negative control and eW5 as the positive control, seeds were placed on agar plates which had been treated with the respective analogue and allowed to grow for 5 days in reduced light conditions. Following this, the plates were imaged, and plant hypocotyl lengths were recorded using ImageJ software (for complete table of results, see Appendix B).

2.6.1: General SAR

Analogues with alterations on the diamine tail were first tested. In order to account for the natural variation in absolute hypocotyl lengths between trials, the ratio of the growth relative to the controls

was used to compare analogues. As a result, the analogues' growth promoting effect will be discussed in terms of their relative growth compared to DMSO and eW5.

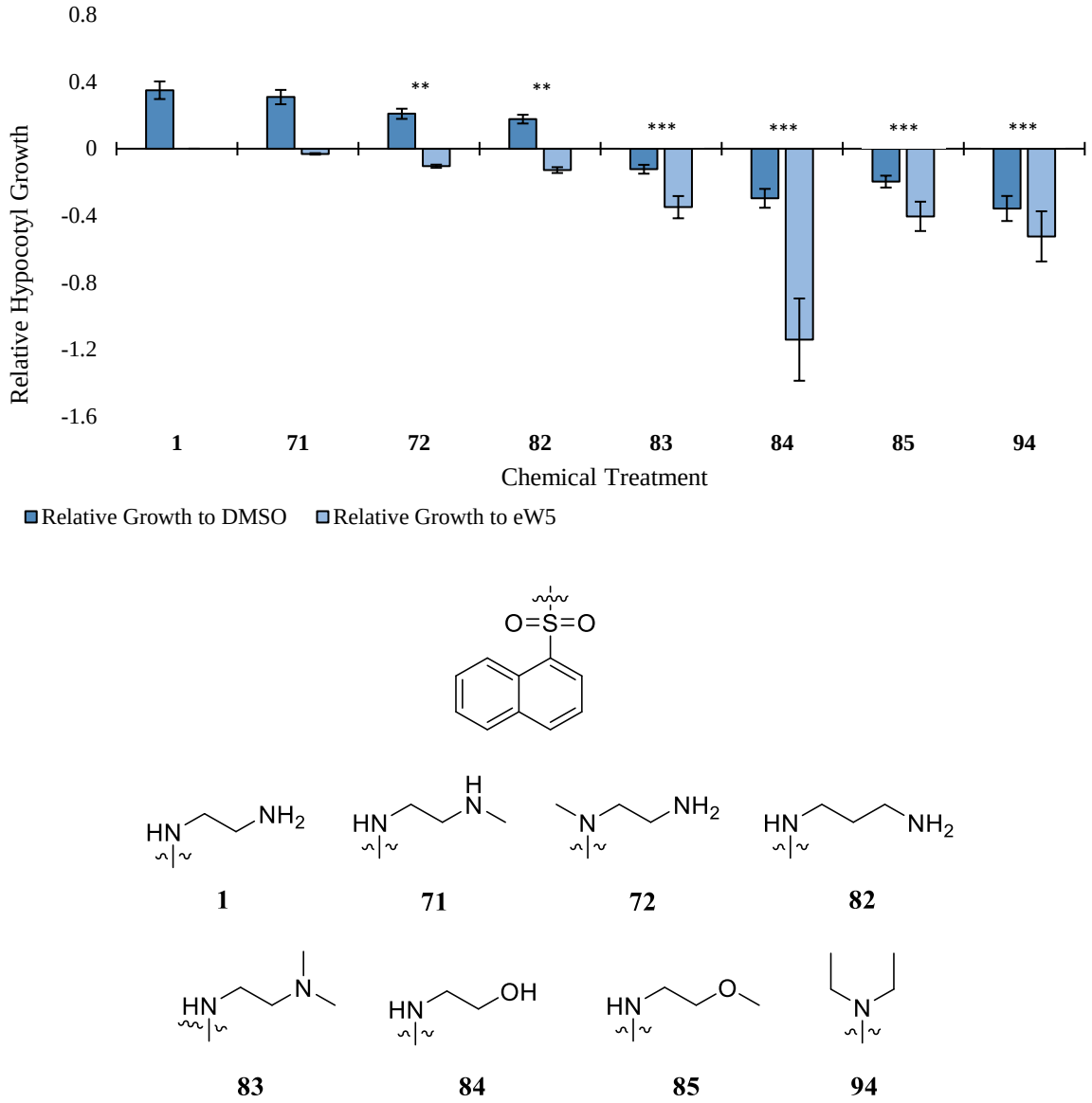

Figure 37: Relative hypocotyl growth of Aribidopsis seedlings treated with **71**, **72**, **82**-**85** and **94** to eW5 (**1**) and DMSO. Values were calculated from three biological replicates. Error bars represent standard error from a population of at least 40 seedlings. Asterisks indicate statistically significant differences (independent t-test, ** P<0.05, ***P<0.005) between chemical treatment and eW5.

One of the most notable aspects of these diamine modified analogues was that the majority inhibited growth compared to the DMSO control. The only positive growth promoters were **82**, **71** and **72**. Propyldiamine analogue **82** was less effective than eW5, indicating that the ethylene diamine motif is the best for growth promotion. This supports the observations made in the synthesis of the original calmodulin inhibitors where hexyldiamine (W5, **59**) was found to inhibit root growth. N-methyl

substituted analogues **71** and **72** showed similar growth promoting effects to eW5, agreeing with previously acquired data (Section 1.4.5, Figure 35), indicating that simple N-substitutions are tolerated. One common feature shared between inhibiting analogues **83**-**85**, and **94** was that they did not possess a nucleophilic amine at the end of the tail, indicating that this feature might be vital for growth enhancement. After identifying tolerable modifications on the diamine tail, focus shifted to looking at analogues with modified aromatic cores.

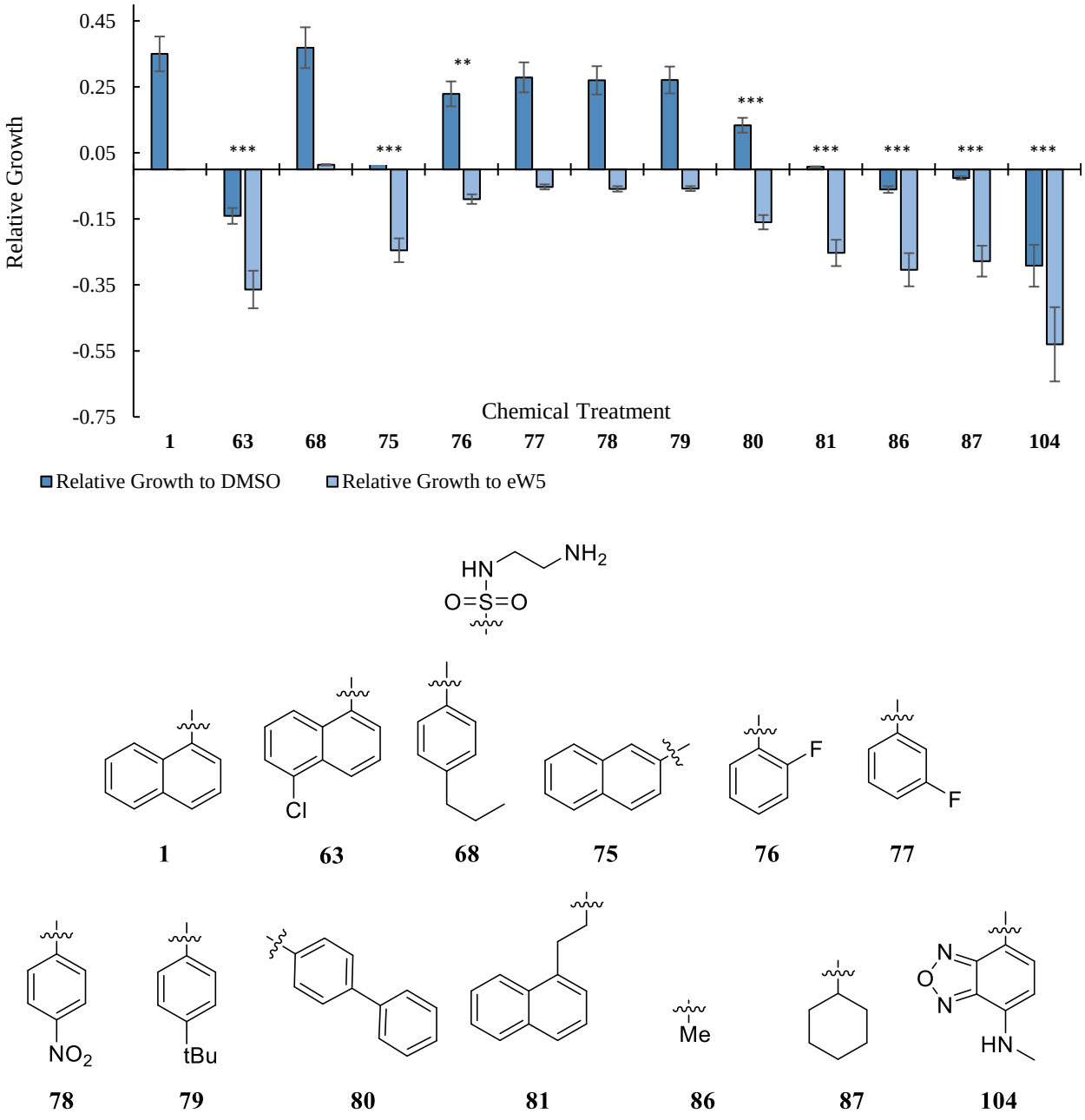

Figure 38: Relative hypocotyl growth of Aribidopsis seedlings treated with analogues varying the naphthalene core. Values were calculated from three biological replicates. Error bars represent standard error from a population of at least 40 seedlings. Asterisks indicate statistically significant differences (independent t-test, ** P<0.05, ***P<0.005) between chemical treatment and eW5.

Compounds **76-80** displayed significant hypocotyl growth promoting activity albeit in lower efficacy compared to eW5. More noticeably, bulky substituent analogue **79** retained eW5-like effects, supporting the proposal of using the 4-position as a site of attachment in the development of a probe. Further conclusions that were drawn from these analogues include the importance of the 1-substituted aryl sulfonamide motif with **75** and **81** showing negligible growth promoting capabilities when compared to DMSO.

Addressing the function of the aromatic ring itself, aliphatic analogues **86** and **87** showed slight growth inhibiting effects compared to DMSO, suggesting that an aromatic core is essential to the function of eW5. This was further supported by the results observed in NBD-hybrid analogue **104** where a significant inhibitory effect was observed, again highlighting the importance of an aromatic core to retain growth promoting properties. As with the earlier series, there was little evidence to enhanced growth promotion. The most active analogues contained substituents in the 2- and 4-positions, supporting proposals for the development of probes through derivatization at these sites.

2.6.2: (Iso)quinoline Series

Once the structural modifications were evaluated, attention turned to looking at the heteroaromatic series to assess if the electronics of the aromatic ring played a role in the compound's activity.

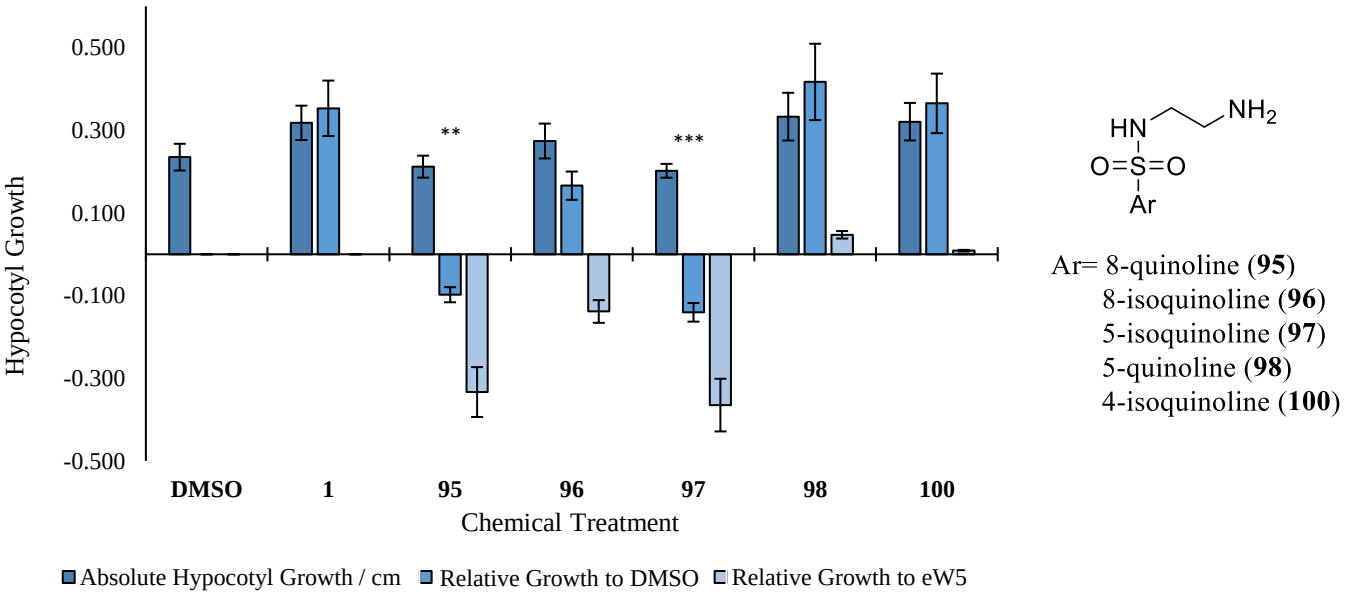

Figure 39: Hypocotyl growth of Aribidopsis seedlings treated with (iso)quinoline analogues **95-98** and **100**. Values were calculated from three biological replicates. Error bars represent standard error from a population of at least 40 seedlings. Asterisks indicate statistically significant differences (independent t-test, ** P<0.05, ***P<0.005) between chemical treatment and eW5.

With the quinoline/isoquinoline series of analogues, there is no defined pattern to explain the observed results. **96**, **98**, and **100** showed increased growth from the control, with **100** showing the most similar effects to eW5 (**1**) and **98** showing slightly greater effects. Although **96** was growth promoting, its effects were not as great as eW5 and led to a reduction in growth promotion. **95** and **97**, showed reduced growth effects when compared with the DMSO control. The effects displayed by **98** were especially surprising as the original 5-chlorine substituted series of analogues proved to be inhibitors of growth. The growth promotion observed with the substitution of nitrogen for the 5-carbon suggests that the effect of the chlorine in the initial series of analogues could be a steric one or that the nitrogen in the quinoline core could be acting as a hydrogen bond acceptor. Ultimately, the retention of eW5-like properties by several analogues in this series indicates a tolerance for varying aromatic systems. However, the varying effects shown by moving the nitrogen around the ring also indicate that the core may be involved in a specific binding interaction.

An additional effect of the substitution of the naphthalene to the quinoline/isoquinoline cores was the significantly improved aqueous solubility. With a drop in theoretical logP values from 0.97 in lead compound eW5 to 0.07 to -0.12 in compounds **95-98**, the change in biological activity could also be due to the change in solubility.[1] In addition to this, it was predicted that the nitrogen in the aromatic system would be protonated in vivo which could affect the absorption of the compound into the cell. Ultimately, with the isoquinoline and quinoline series, even though individual analogues yielded interesting results, the subtle change to the electronics of the aromatic core was not enough to give substantial information regarding the SAR of the lead molecule.

2.6.3: Alkoxy Substituted Analogues

Having shown that a wide range of structural variation was tolerated, focus shifted to looking at alkoxy-substituted analogues. These compounds were of particular interest as they explored the feasibility of an ether group as strategy for attaching a linker. Simple methoxy substituted analogues **108** and **110** were assessed first.

[1] logP values calculated using www.swissadme.ch

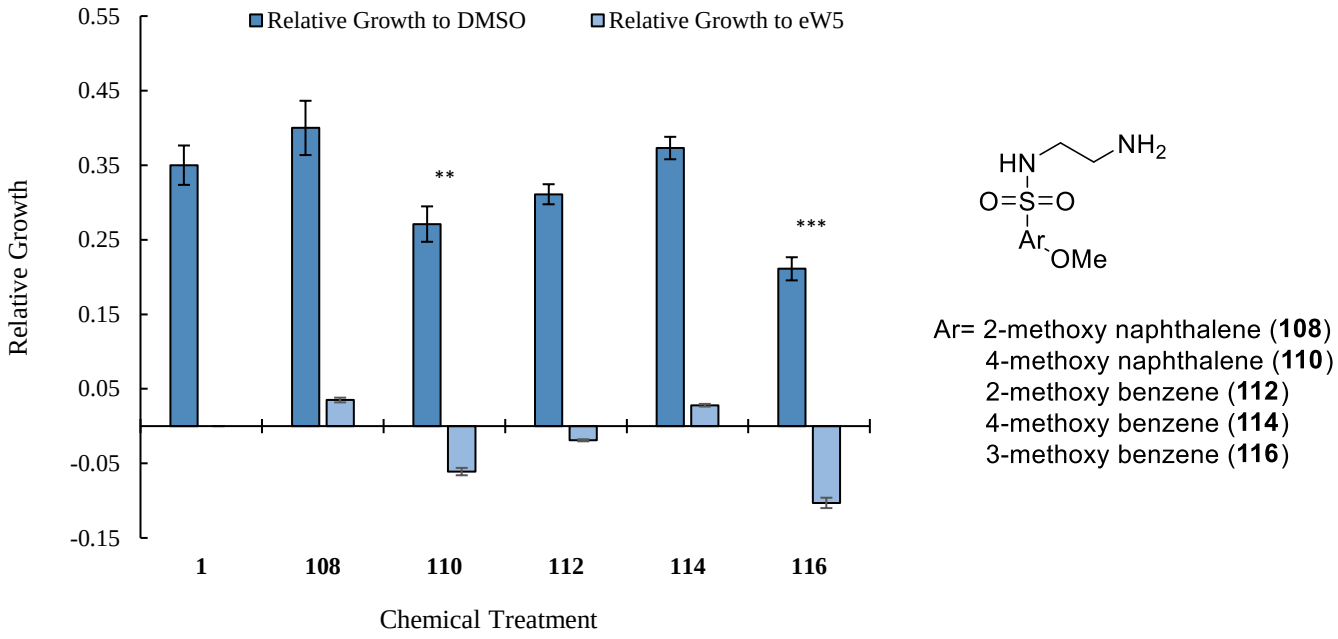

Figure 40: Relative hypocotyl growth of Aribidopsis seedlings treated with **108**, **110**, **112**, **114** and **116**. Values were calculated from three biological replicates. Error bars represent standard error from a population of at least 40 seedlings. Asterisks indicate statistically significant differences (independent t-test, ** P<0.05, ***P<0.005) between chemical treatment and eW5.

Initial results from the hypocotyl assay were encouraging as previous results obtained by Sukiran were replicated and eW5 displayed significant growth promoting effects when compared with the control.[102] 1,4-substituted monocycle **114** showed comparable growth promoting properties to propyl-substituted benzene analogue **68** indicating the change in electronics caused by the substituents was not an area of concern as initially thought. Ultimately all four methoxy-substituted analogues retained eW5-like effects, indicating that both 1,2- and 1,4- substitution patterns could be further studied as sites of linker attachment. It is also worth noting that all five compounds not only retained growth promoting activity but this activity was comparable, corroborating previous SAR data that monocyclic derivatives resulted in similar hypocotyl growth promotion. Interestingly, the compound which showed the least growth promoting effect was 1,3-substituted **116**, and as a result, further study into this substitution pattern was not undertaken.

Once the feasibility of inserting small substituents in the 2- and 4-position of the aromatic core was established, subsequent experiments were conducted with long chain alkoxy analogues **109**, **111**, **113** and **115** to further explore these two positions as sites for linker attachment.

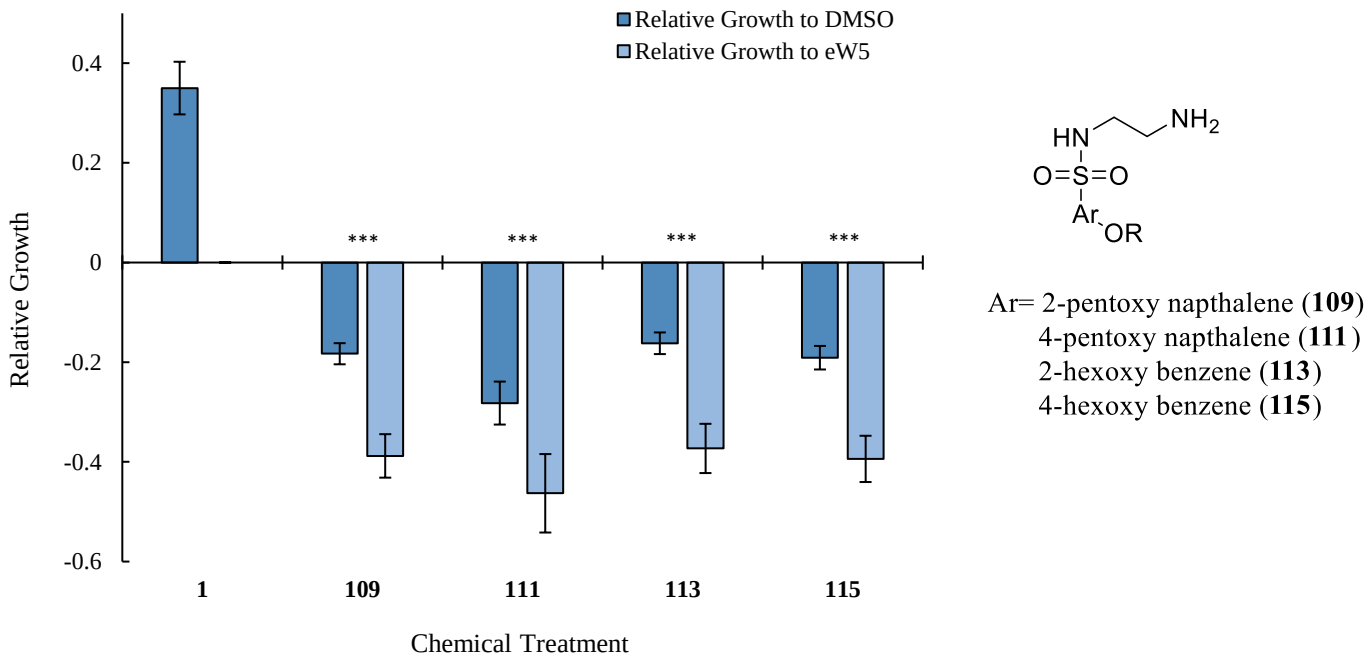

Figure 41: Hypocotyl growth of Aribidopsis seedlings treated with long chain alkoxy-substituted analogues **109**, **111**, **113** and **115**. Values were calculated from three biological replicates. Error bars represent standard error from a population of at least 40 seedlings. Asterisks indicate statistically significant differences (independent t-test, ***P<0.005) between chemical treatment and eW5.

Not only were the long chain variants not able to retain the activity of eW5, the compounds were inhibitory to hypocotyl growth when compared with the control. Interestingly, there was no significant difference observed in the effect on hypocotyl growth between the benzene and naphthalene core, supporting the initial observation made with the methoxy-substituents.

As there had been precedent for 2- and 4- naphthyl-substituents to be tolerated, the lack of effect of the long chain alkyl substituents was unexpected. Two competing hypotheses were developed to explain the inability of the long chain alkyl- substituted analogues **109, 111, 113** and **115** to display eW5-like effects. The initial hypothesis was that the binding pocket of eW5 simply did not tolerate a long alkyl chain, but this seemed unlikely as previous analogue **68** containing a propyl substituent para to the sulfonamide was able to display eW5 like effects.

The alternative proposal was that this set of analogues were present in higher concentrations within the cytoplasm, enhancing the observed inhibition over the expected growth promotion. The theoretical logP of long chain alkoxy analogues **109, 111, 113** and **115** range from 2.56 to 2.80, significantly greater than 0.97 of eW5 (**1**), allowing for greater membrane permeability. To test if lipophilicity was a factor

in the inhibitory effects of the long chain alkoxy substituted analogues, an ethyl ethoxy substituent was investigated with the aim of increasing the overall polarity of the compound.

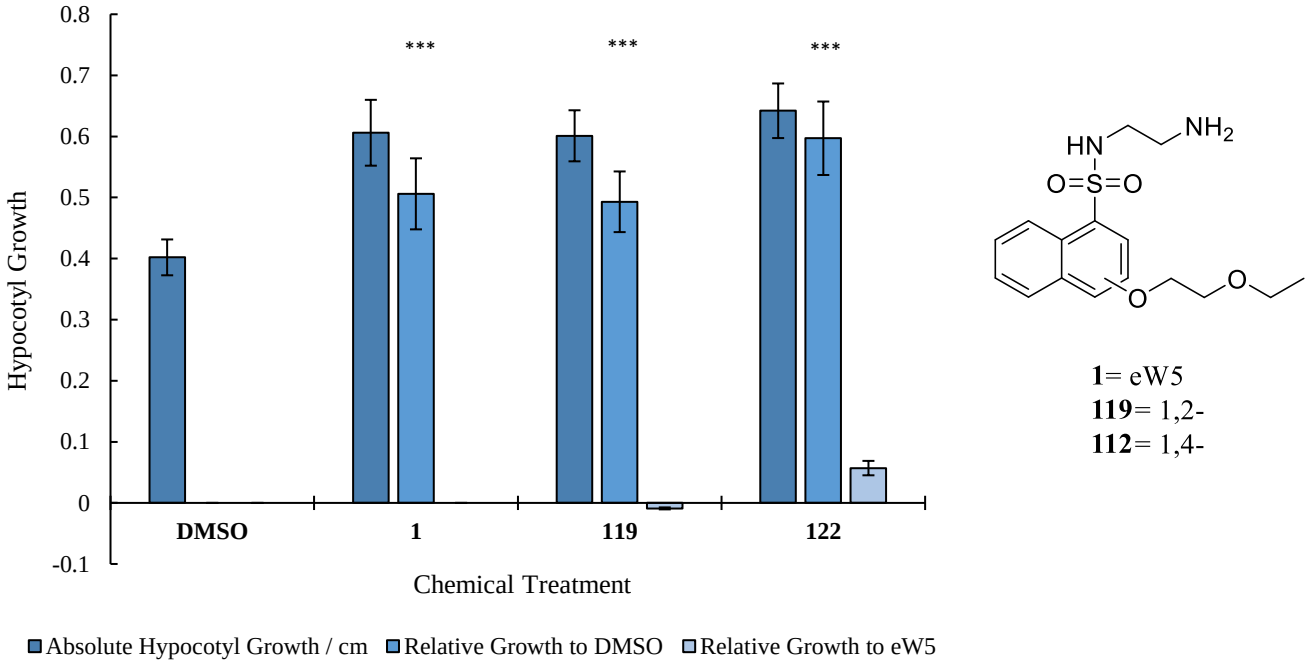

Figure 42: Hypocotyl growth of Aribidopsis seedlings treated with ethyl-ethoxy substituted **119** and **122**. Values were calculated from three biological replicates. Error bars represent standard error from a population of at least 40 seedlings. Asterisks indicate statistically significant differences (independent t-test, ***P<0.005) between chemical treatment and DMSO.

Both compounds **119** and **122** showed comparable hypocotyl growth promoting abilities to eW5 (**1**). 2- and 4- ethyl ethoxy substituents **119** and **122** had theoretical logP values of 1.75 and 1.84 respectively, falling between **1** and the long chain alkoxy analogues **109, 111, 113** and **115**. The ability of this substituent to retain growth promoting properties ultimately supported the hypothesis that the increased hydrophobicity of the pentoxy- substituted analogues were a contributing factor to their inhibitory effect.

Hypocotyl growth is a combination of multiple signals and with the mechanism of eW5 unknown, the possibility of multiple proteins being targeted must be considered. As outlined in Section 1.3.1, plant hormones often play more than one role in physiological processes, and it has been well established that responses are dictated by both their location and concentration. As a result, to further test the hypothesis that the increased membrane permeability and the resulting high cytoplasmic concentration of the long hydrocarbon alkoxy-substituents was enhancing one effect over another, the hypocotyl assay was conducted again using long chain naphthalene analogues **109** and **111** at varying concentrations.

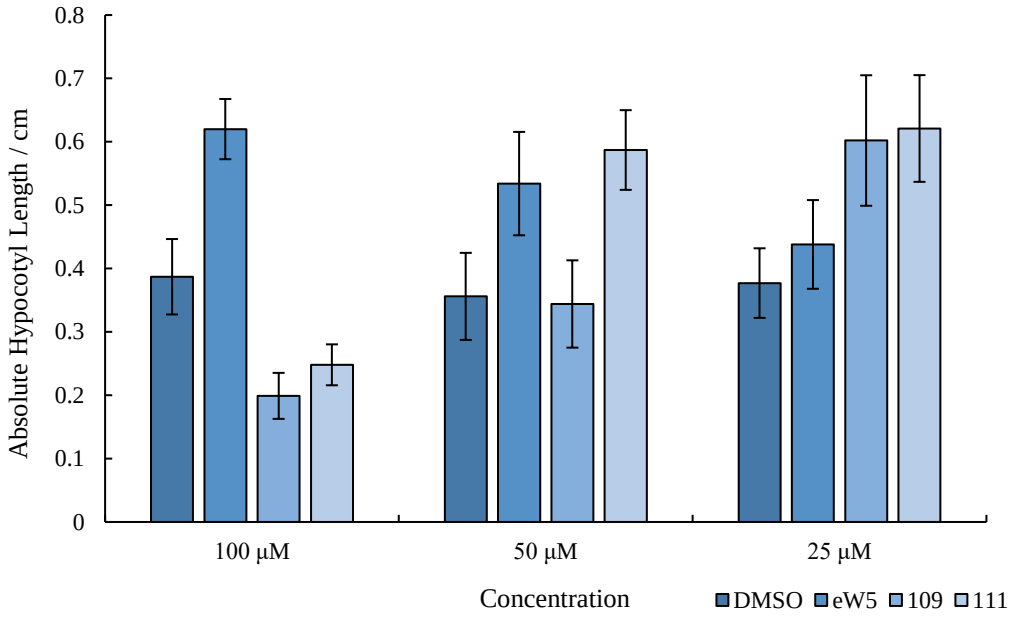

Figure 43: Hypocotyl growth of Arabidopsis treated with 109 and 111 at varying concentrations. Values were calculated from three biological replicates. Error bars represent standard error from a population of at least 40 seedlings.

At reduced concentrations, growth promoting effects were restored to the point where it became comparable to eW5 at 100 µM. This supports the hypothesis that the observed effect of **109** and **111** at 100 µM was due to increased cytosolic concentrations leading to reversed effects. This ultimately supports additional data gathered in this section supporting the tolerance of linker-like substituents in the 2- and 4-position of the aromatic core. Given **122** showed the greatest growth promoting effects, leading to more hypocotyl growth over eW5, the 4-position on the naphthalene ring would seem to be the most suitable for this function.

2.7: RGA-GFP Assay

As discussed in Section 1.3, DELLA proteins are negative regulators of PIFs, preventing their binding to target promoters and inhibiting hypocotyl growth. Thus, the hypocotyl growth assay conducted in reduced light is primarily diagnostic for the GA pathway. Although the results discussed above indicate that the growth promoting analogues tested operate along the GA pathway, no conclusions can be made on the specific mechanism, namely on whether these compounds result in DELLA degradation specifically. As such, the fluorescent assay outlined in Section 1.4 using an RGA-GFP transgenic line was conducted on representative analogues. Compound **98** was chosen to represent heterocyclic analogues, and **114** was chosen as a substituted monocyclic representative.

7-day old *Arabidopsis thaliana* seedlings expressing RGA-GFP were treated with the respective compounds for 2-hours and root tips were imaged through confocal microscopy. eW5 (**1**) and GA 4+7 (**52**+**53**) were used as positive controls and DMSO and paclobutrazol (PAC), a known inhibitor of GA synthesis, were used as negative controls.

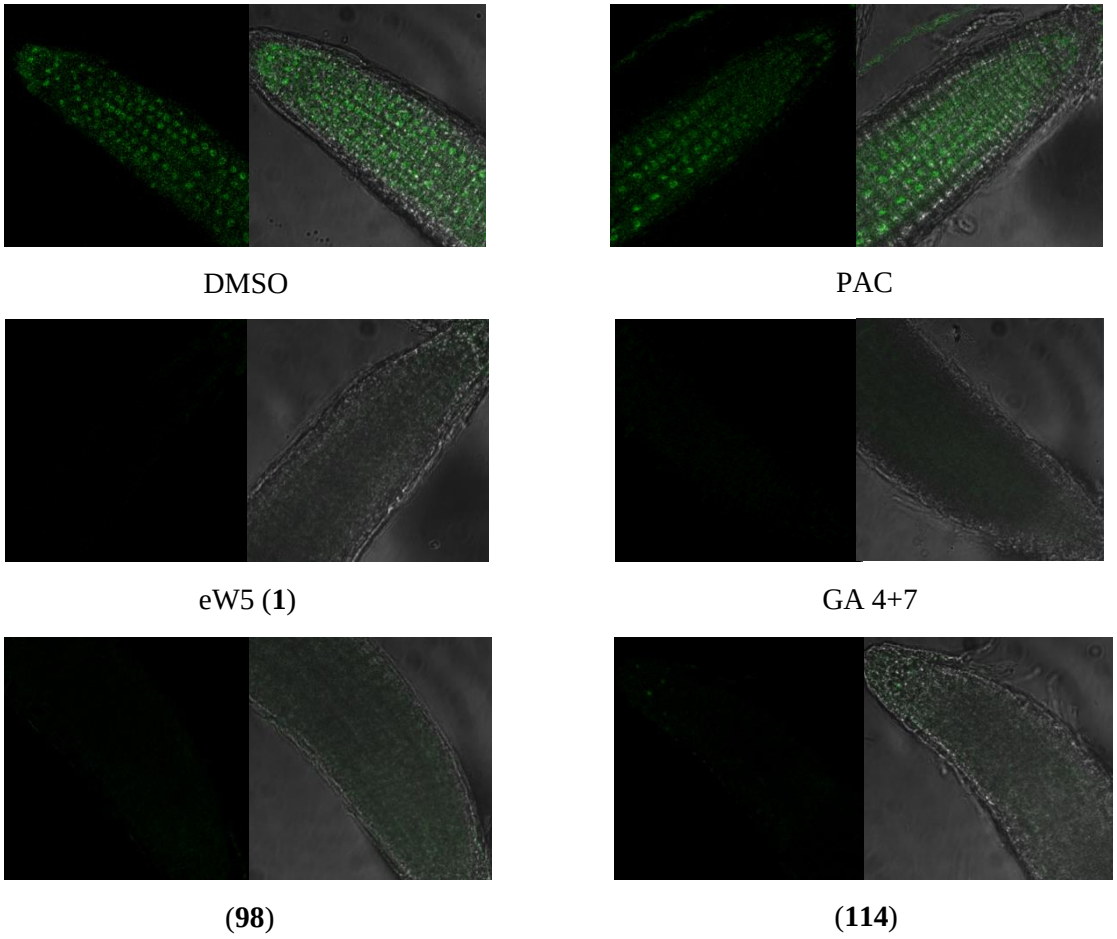

Figure 44: Fluorescence in root tips of 7-day old transgenic Arabidopsis seedlings expressing RGA-GFP with (right) and without (left) backlight. Seedlings were treated at 100 μM concentration for 2-hours. At least 3 root tips were imaged per chemical treatment, images shown above are representative of sample.

When compared to the negative controls which show concentrated pockets of fluorescencefrom the presence of DELLAs within the nucleus, images of the analogues show a much more diffused GFP-"haze" indicating a degree of DELLA degradation had taken place. The images clearly show the analogues result in a decrease in fluorescence, but not to the extent seen with eW5 (**1**). This suggests that although the analogues are also promoting growth via DELLA degradation, there may be a difference in the timescale that the compounds are operating on or that their specific mode of action differs slightly.

2.8: SAR Conclusions and Future Work

Ultimately, study of the SAR of eW5 was able to identify six analogues that were able to display slightly increased hypocotyl growth promoting abilities. This included methoxy analogues **108** and **110** and ethyl ethoxy substituted analogue **122**, indicating the feasibility of attaching a photoaffinity tag on the aromatic core via an ether linkage.

Additional analogues that investigated other aspects of the molecule were able to demonstrate the tolerance for simple substitutions on the sulfonamide and primary amine, various electron-withdrawing groups on the aromatic core and even some heterocycles. Substitution of the amine to a primary alcohol and the aromatic core for non-aromatic substitutes resulted in inhibitory effects, indicating that both these moieties were vital to growth promoting function.

With the assay judging the compounds purely based on the phenotypic response, conclusions on the role that the modifications (such as an aromatic nitrogen plays) are limited. Current explanations for the growth promoting ability of the compounds in relation to the structure are restricted to solubility and loose hypotheses on the binding mode of eW5. It should be noted that the mode of action of these compounds may differ from eW5 due to the possibility of multiple targets as certain interactions could be enhanced or hindered yet result in the summative effect of growth promotion. To address this, additional biological assays were conducted on heterocyclic analogue **98** and substituted monocyclic analogue **114** using a transgenic RGA-GFP line. Following 2-hours of chemical treatment, confocal microscopy was able to show a decrease in fluorescence, indicating that these analogues were operating along the same pathway as eW5, resulting in the degradation of DELLA proteins.

Having synthesized a library of analogues, future work should focus on biological evaluation of these analogues to assess if they promote growth along the same pathway as eW5. The GFP assay should be repeated using different time-points to assess if the analogues are able to induce complete DELLA degradation as observed with eW5. In addition to this, a more qualitative assay can also be conducted through rt-PCR. Transcriptomic analysis conducted by Nur Afikah Sukiran has identified 5 candidate genes most upregulated in response to eW5. Conducting qPCR on RNA extracted from seedlings treated with eW5 at various time points would allow for the experimental confirmation of the upregulation of these marker genes. This could be repeated using the analogues, allowing for a quantitative comparison against eW5 assessing whether these compounds are acting along the same pathway and to what extent they regulate the same genes.

Chapter 3: Synthesis of Photoaffinity Probes

3.1: Chapter Introduction

This chapter outlines the synthetic routes attempted in the synthesis of eW5-based photoaffinity probes. Having identified the 4-position as a site for the derivatisation in the previous chapter, efforts were focused on the attachment of a photoaffinity and reporting units. Initial attempts employed a highly convergent approach where the probe components were synthesised as individual modules and joined to the eW5 core via an appendage linker. A parallel approach was also explored where the photoaffinity tag was directly conjoined to the naphthalene core, reducing the physical distance between the two.

As a proof of concept for the first approach and to facilitate biological evaluation, model probes were first synthesised substituting a *tert*-butyl group for the diazarine moiety. Hypocotyl growth assays demonstrated eW5-based probes with an appendage linker were able to retain significant growth promoting effects. Although the respective photoactive probes were not successfully synthesised, this chapter discusses the efforts undertaken towards this goal and towards the second approach of attaching the photoaffinity tag directly onto the core of eW5.

3.2: Design and of Photoaffinity Probes

Having developed an understanding of the SAR for eW5 as described in the previous chapter, focus shifted to the design and synthesis of chemical probes to identify the target of the molecule. The structure of eW5 has no obvious reactive moiety and therefore it was proposed that the development of a photoaffinity-based probe would be most suitable. With little known about the target protein profile and thus the mode of binding of eW5, a range of structurally diverse probes were designed. It was advantageous to design a set of probes with photoactive groups at different positions as the structural variation could lead to differences in target affinity.

It was shown that analogues **68**, **110**, **111**, **114**, **115** and **122** (Figure 45) retained eW5-like properties and as a result it was proposed that the 4-position would be most suitable to introduce substituents. It is worth noting that although long chain alkoxy analogue **111** initially showed growth inhibiting effects at 100 μM, lowering the concentration of the chemical treatment reversed this effect, showing that flexible hydrophobic groups were also tolerated at certain concentrations (Section 2.6, Figure 41).

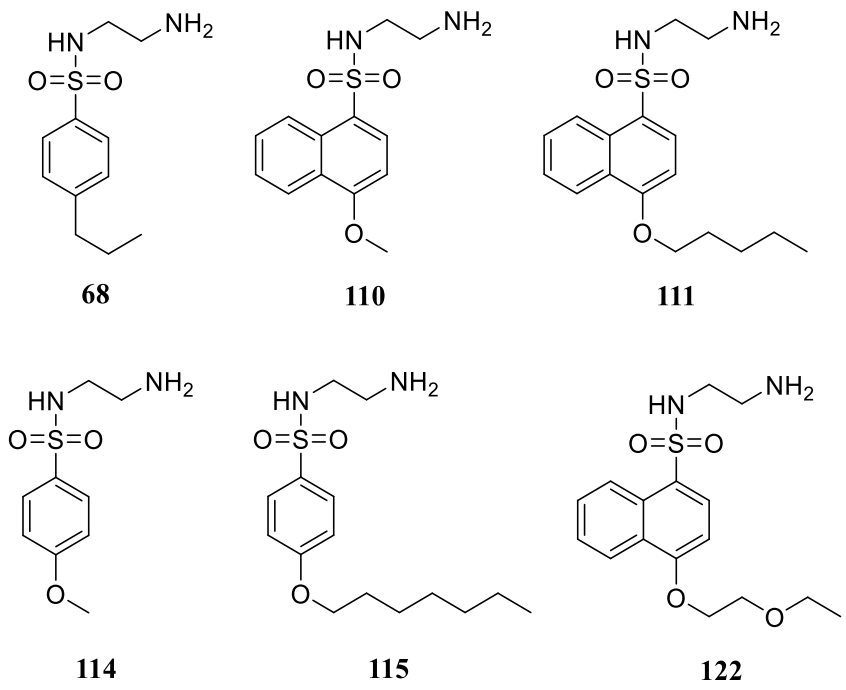

Figure 45: Structures of 4-substituted eW5 analogues.

Ethoxy-ethoxy-substituted naphthol **122** showed the greatest growth promoting effects and was selected as the lead compound to develop into a probe. There were two initial strategies for the attachment of a photoaffinity tag; on a pendant arm (Probe **I**) or directly attached to the naphthalene core (Probe **II**). These approaches were explored in parallel.

3.3: Probe Design I

With the ethoxy-ethoxy chain effectively acting as a linker, the simplest approach was to attach the photoaffinity moiety directly onto the chain. It was proposed that an amide linkage would be the most synthetically feasible method of conjoining the two sections. Focus then turned to the attachment of a terminal alkyne to facilitate enrichment via click-reaction with a complementary azide. Two sites of attachment were envisaged for the design of Probe **I**. They were either on the amide nitrogen (Probe **Ia**) or *meta*- to the trifluoromethyl diazirine (Probe **Ib**).

As outlined in section 1.2.5.4, a report by Fujii *et al*. was able to demonstrate that extensive modifications to the structure of the lead compound including the addition of an appendage linker and photoaffinity module significantly affected the on-target binding ability of the probe (Figure 8). To pre-empt this issue, it was it was hypothesized that a secondary amide would be more favourable than a

primary amide as not to introduce a hydrogen bond doner through this linkage connection, reducing interactions with non-target proteins.

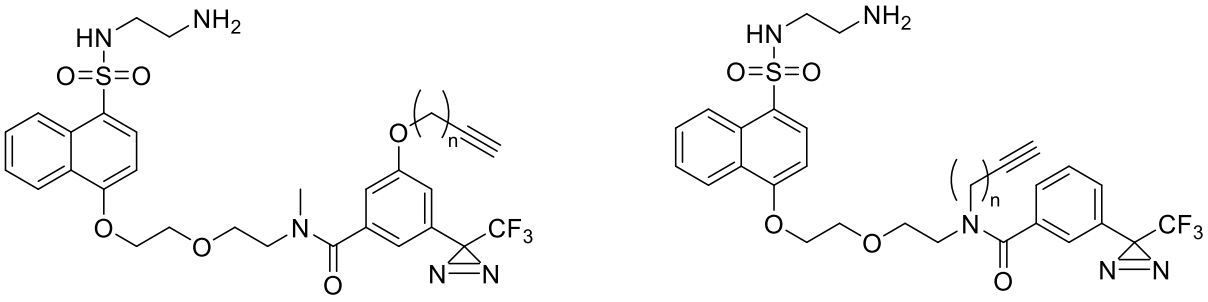

Figure 46: Probe designs **Ia** and **Ib**.

3.3.1: Retrosynthesis of Probe Designs Ia and Ib

An advantage of Probe design **I** was the natural divide into three components: the core of eW5, the linker, and the photoaffinity group. Retrosynthetic analysis showed the most natural disconnection of the probe design was the amide bond connecting the linker to the photoaffinity module, giving secondary amine **123** and acid **124** which could be coupled using standard conditions. This disconnection also had the extra advantage of installing the photoaffinity module last, minimizing the number of synthetic steps where the diazirine would need to be handled, thus reducing the possibility of degradation from sources of UV light. With conditions for the nucleophilic substitution using naphthols already established (Section 2.4, Table 3), it was proposed that the linkage between linker **126** and eW5 portion **125** could be achieved in a similar manner.

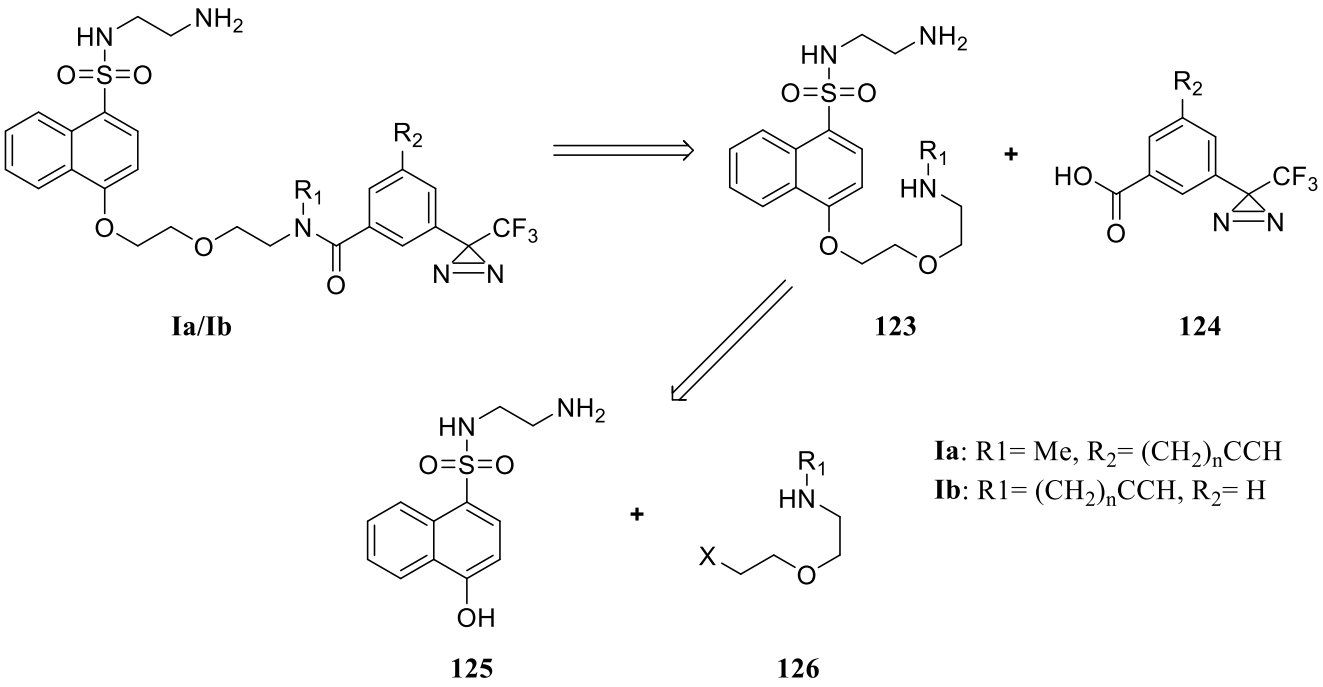

Scheme 11: Retrosynthetic analysis of Probe design **I**.

3.3.2: Synthesis of Probe Design I

One possible issue with the addition of the photoaffinity labelling group was the steric size introduced to the molecule. To confirm that the probes would still bind to the same proteins as eW5, biological validation was required. This itself presented its own challenges as the biological conditions employed posed a risk to the stability of the diazirine labelling group. To address this issue, a simple and more stable model system was proposed using a *tert*-butyl group as an isostere for the trifluoromethyl diazarine.

3.3.2.1: Synthesis of eW5-naphthol

It was proposed that the synthesis of the eW5 portion of the molecule (**125**) could be achieved simply through the installation of the N-Boc ethylenediamine sulphonamide moiety via lithium-halogen exchange, on a protected derivative of 4-bromonaphth-1-ol (**108a**), a process described in Section 2.4 (Table 3). Subsequent deprotection to give the naphthol-sulfonamide would then yield the nucleophile required to facilitate substitution. Given the previous success in using Boc protected ethylenediamine, the initial focus was to determine the corresponding phenol protecting group. Consequently, an initial screen of orthogonal protecting groups for their stability under the lithiation conditions was undertaken (Table 4).

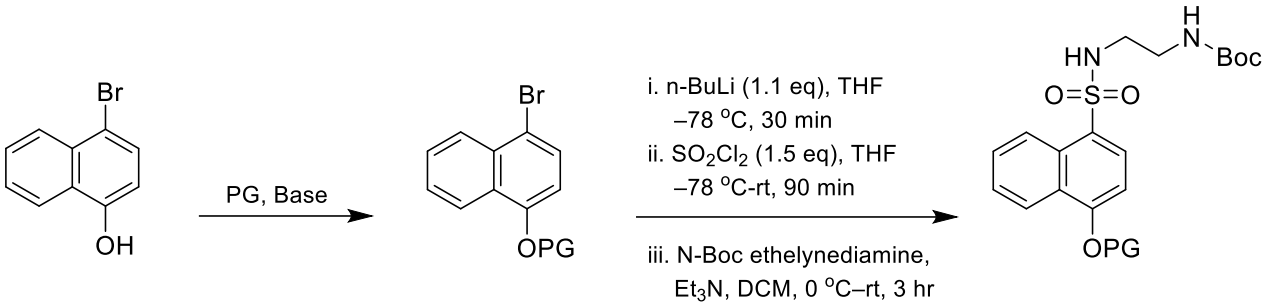

108a **127a-130a** **127-130**

Entry	PG	Protection Conditions	Protected Naphthol	Sulfonamide
1	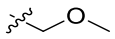	MOM-Cl (1.1 eq), NaH (1.1 eq), THF, 0 °C-rt, 90 min	**127a** (80)	**127** (44)
2	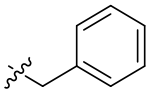	Bn-Br (1 eq), K_2CO_3 (4eq), TBAI (0.1 eq), THF, rt, 16 h	**128a** (89)	**128** (0)
3	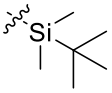	TBDMS-Cl (1.1 eq), imidazole (2 eq), DMF, rt, 16 h	**129a** (93)	**129** (0)
4	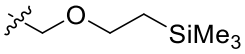	SEM-Cl (1.1 eq), NaH, (1.1 eq), THF, 0 °C-rt, 90 min	**130a** (83)	**130** (38)

Table 4: Screen of naphthol protecting groups for their stability under lithiation conditions.

Of the 4 groups tested, MOM and SEM proved to be stable under lithiation conditions and were further investigated for their orthogonality to Boc. Although no standard conditions were found for the cleavage of MOM in the presence of Boc, it was proposed that a global deprotection followed by a selective reprotection of the primary amine could afford the desired product. Treatment of **127** with TFA followed by the addition of Boc_2O unfortunately gave a mixture of mono and di-protected compounds (**131** and **132**) as shown by the formation of two major products in LCMS 367.205 $[M(\mathbf{131})+H]^+$, 467.253 $[M(\mathbf{132})+H]^+$. Although carbonate **132** was selectively hydrolysed during workup with 1M $NaHCO_3$, subsequent isolation of **131** was not possible.

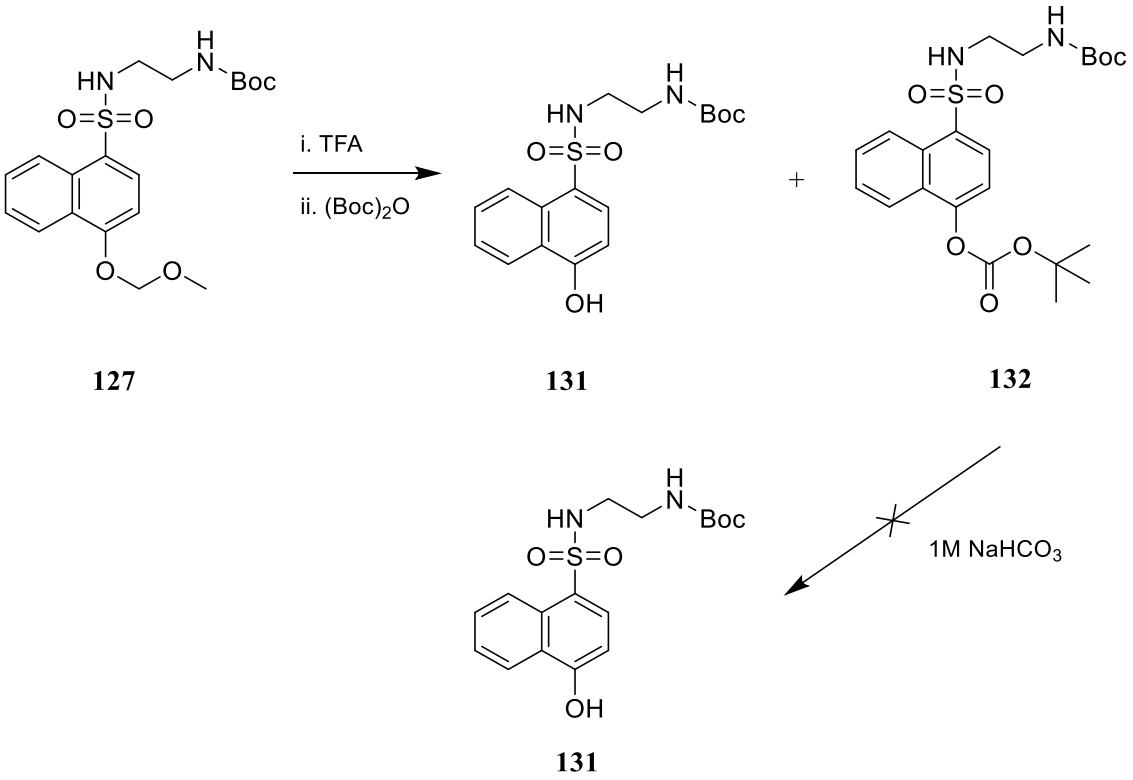

127 **131** **132**

131

Scheme 12: Attempted selective MOM deprotection of deprotected compound **127**.

The SEM protecting group proved to be more viable as standard TBAF deprotection conditions afforded desired naphthol **131** from **130** in 78% yield as characterized by LCMS where the distinctive $[M–H]^-$ ion 365.348 *m/z* was observed.

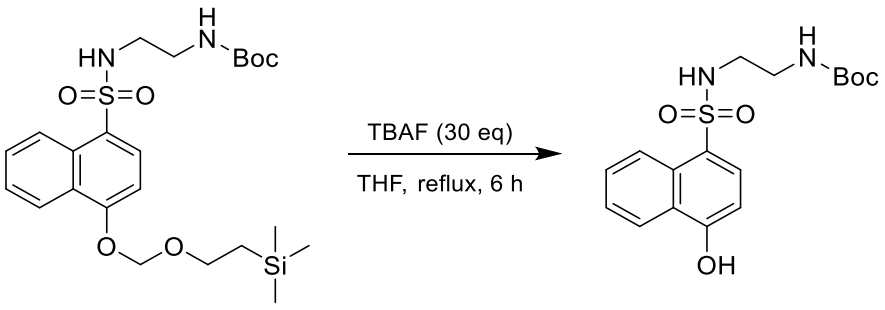

130 **131** (78)

Scheme 13: SEM deprotection of **130** to form naphthol **131**.

3.3.2.2: Linker Synthesis

The linkers of model Probe designs **Ia** and **Ib** both share an ethoxy-ethoxyamine chain, which prompted a search for viable PEG-like chains that were capped with a primary amine and electrophilic group

respectively to facilitate nucleophilic substitution with naphthol **131**. 2-(2-Aminoethoxy)ethanol (**132**) proved to be a good candidate for the synthesis of both linkers.

As proposed above, it was hypothesised that the most optimal strategy to combine the 3 module components of the two variants of Probe design **I** was to first form the eW5-linker intermediate (**133**). To allow for subsequent amide bond formation between **133** and the respective photoaffinity modules, an amine protecting group orthogonal to Boc would have to be used. It was proposed that following the formation of the respective secondary amine, Alloc protection would allow for further functionalization of the alcohol whilst providing an orthogonal group to Boc.

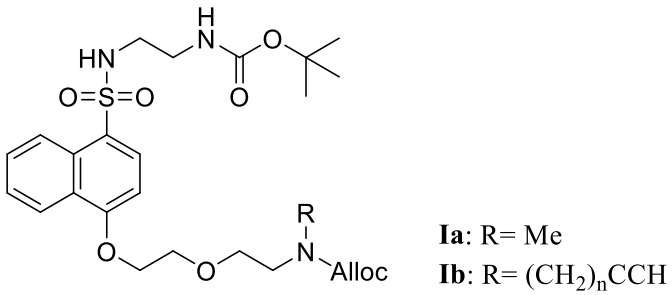

133

Figure 47: Proposed structure of eW5-linker intermediate with orthogonal amine protecting groups.

3.3.2.2.1: Probe Ia Linker Synthesis

For the linker of Probe design **Ia**, it was proposed that mono-methylation of the primary amine could be achieved by reaction with methyl chloroformate followed by reduction of the carbamate. Treatment of the resulting secondary amine **135** with Alloc-Cl gave protected linker **136** in 69% overall yield, as characterized by a distinctive multiplet at δ 5.93 integrating to 1 proton, corresponding to the non-geminal vinylic hydrogen.

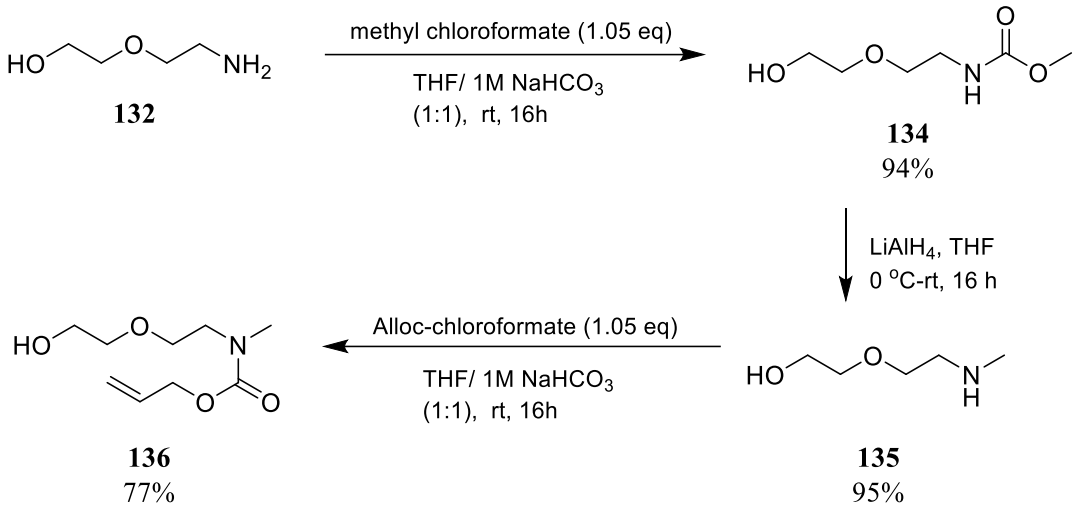

Scheme 14: Synthesis of Alloc-protected linker **136**.

3.3.2.2.2: Linker synthesis of Probe Design Ib

It was hypothesized that the Alloc-protected linker for model Probe design **Ib** could be synthesized in a similar fashion via protection of the secondary amine. To form the desired secondary amine intermediate, initial experiments explored reductive amination.

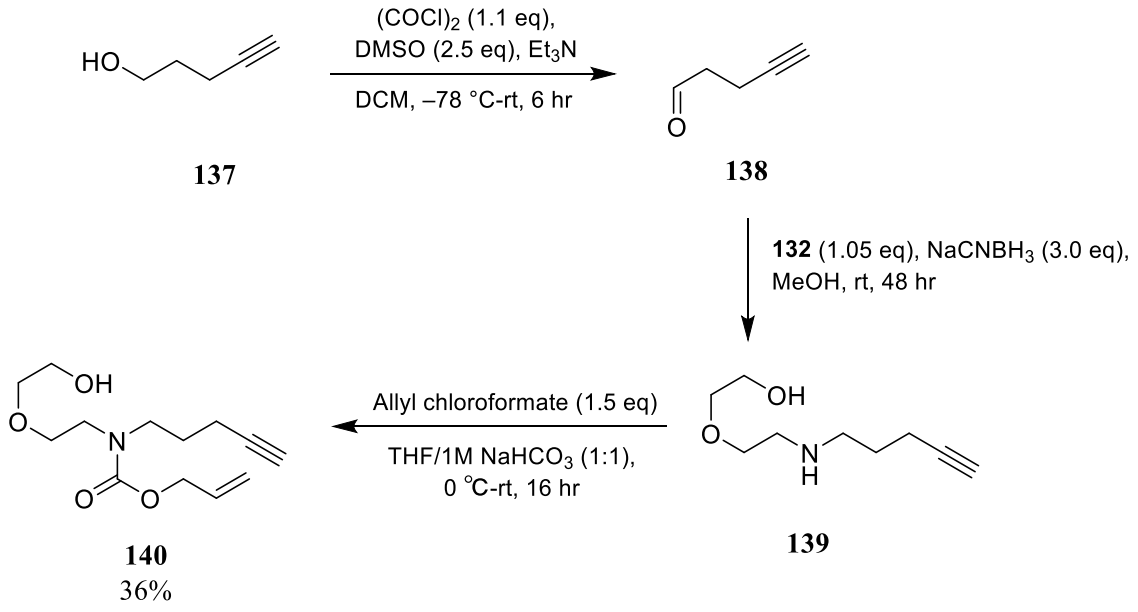

Scheme 15: Synthetic route to form Probe **Ib** linker **140**.

However, purification of the secondary amine proved not to be possible and as result, the crude mixture was reacted immediately with Alloc-Cl. This allowed for the isolation of Alloc carbamate **140** in 36% yield over the 3 steps.

3.3.2.3: Model Photoaffinity Module Synthesis

As no 1,3,5-substituted benzenes containing *tert*-butyl and acid substituents were commercially available, it was proposed that the basic scaffold of the model photoaffinity module of Probe **Ia** could be obtained through selective C-H activation of meta-substituted methyl benzoate.

To facilitate C-H activation, acid **141** was protected using MeI to give the desired methyl benzoate **142**. Ir catalysed borylation followed by oxidation of the boronate ester gave phenol **143** in 62% yield as characterized by a broad singlet at δ 6.54 corresponding to the phenolic proton. With concerns that alkylation of a 4-carbon alkyne would favour elimination to form the conjugated ene-yne, it was hypothesized that 1-chloropent-4yne would be a more suitable electrophile. To add the linker to the model, phenol **143** was then alkylated using 1-chloro-pent-4-yne following the conditions described in Section 2.4 (Table 3). Finally, the resulting ester was hydrolysed to form the deprotected acid **145**.

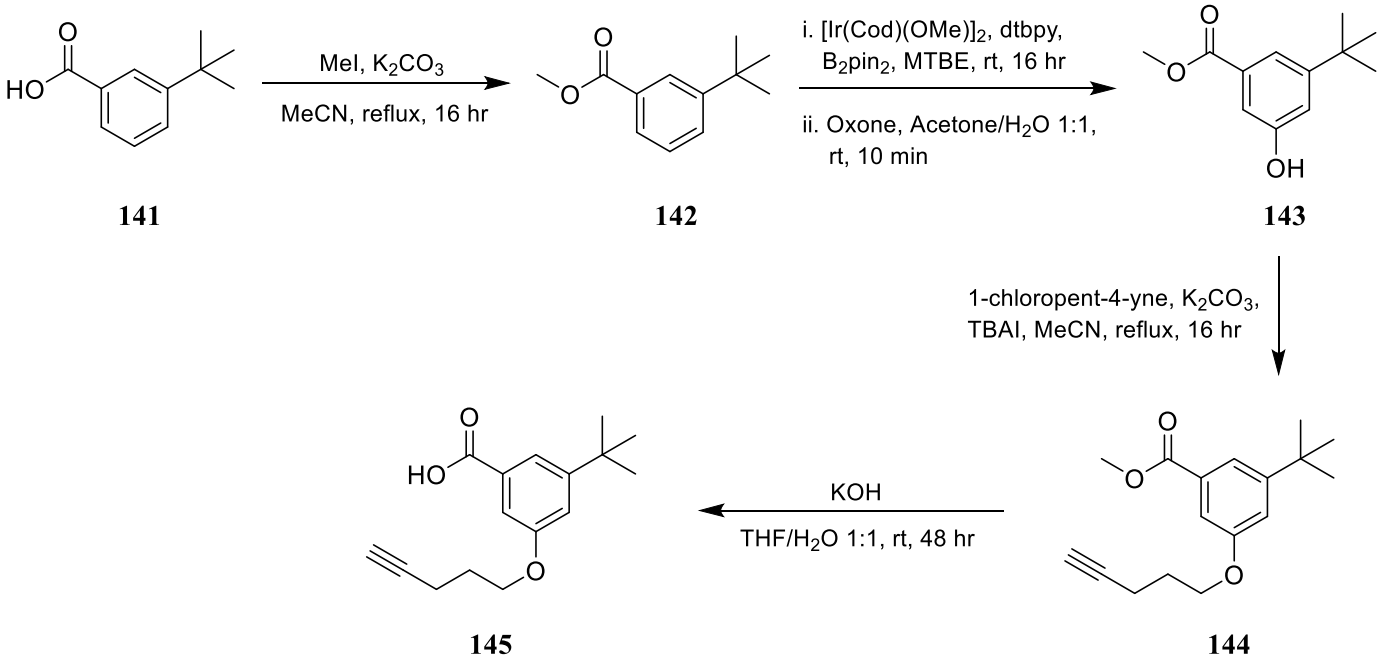

Scheme 16: Synthetic route for model photoaffinity module of Probe **Ib**.

With acids **141** and **145** available, attention was turned toward amide bond formation with the N-terminus of the respective linkers.

3.3.2.4: Synthesis of Model Probes Ia and Ib

It was hypothesized that coupling of naphthol **131** to a linker could be achieved through the activation of the primary alcohol to a leaving group. Linker **140** was treated with mesylate chloride to afford intermediary mesylate (**146**) as characterized by a distinctive singlet at 3.05 ppm integrating to 3 protons. This was then coupled to **131** using the naphthol substitution conditions described in Section 2.4. Disappointingly, stirring under reflux for 16 hours failed to afford the desired substitution product and instead resulted in the elimination product **147** as observed by GCMS (237.31, $[M+H]^+$).

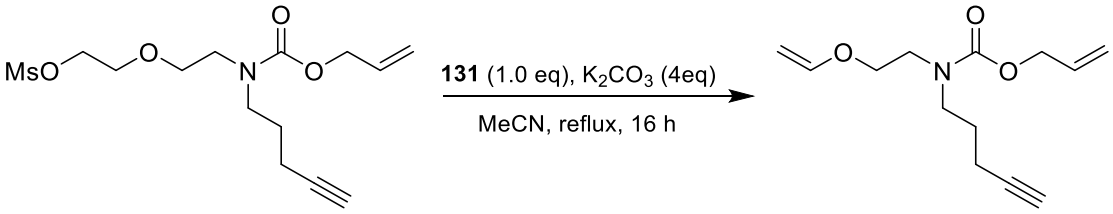

146 **147**

Scheme 17: Attempted alkylation of naphthol **131** with mesylate

To overcome this issue, it was thought that alteration of the electrophile to a halide would better favour formation of the substitution product. To test this, a model experiment was set up using naphthol **131** and MeI to form **148** (Scheme 18). Surprisingly, not only was substitution observed on the naphthol, but also on the sulfonamide, as observed through a single major product on LCMS (395.341, $[M+H]^+$), indicating the feasibility of this S_N2 when using a halide as the leaving group.

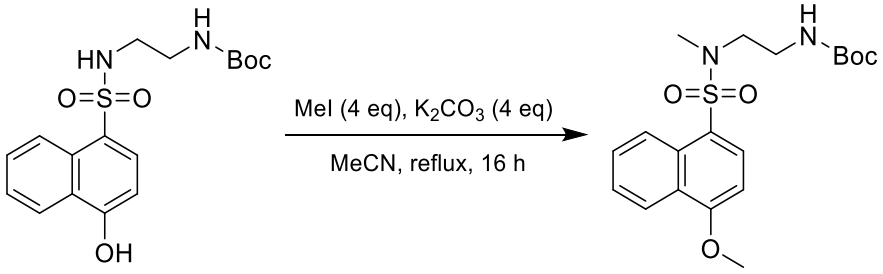

131 **148**

Scheme 18: Model alkylation of naphthol **131** with methyl iodide.

The original procedure was modified so that previously obtained mesylate **146** was pre-stirred with a stochiometric amount of TBAI followed by the addition of naphthol **131**. This afforded the desired substitution product **149** in 58% yield following column chromatography.

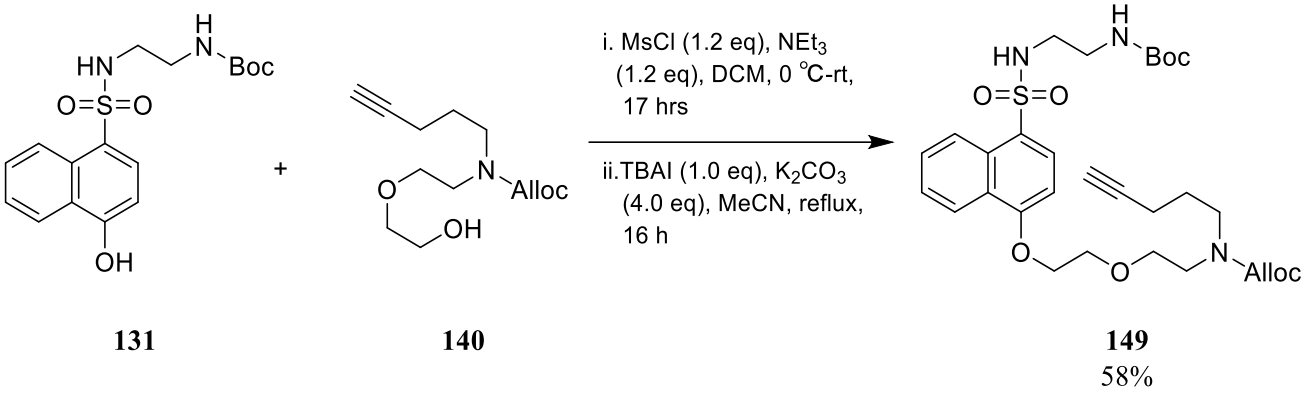

131 **140** **149**
58%

Scheme 19: Nucleophilic substitution of mesylate linker **140** to naphthol **131**

The final step in the synthesis of model Probe **Ia** was the cleavage of the Alloc carbamate and coupling the resulting secondary amine with 3-*tert*-butyl benzoic acid (**141**). Deprotection to form the secondary amine was carried out using standard Alloc deprotection conditions and was monitored using TLC. As the final photoactive probe was going to be synthesized via the same route, it was of interest to find an amide coupling reaction that could be carried out in the presence of a diazirine. It was initially proposed that HOBt would be a suitable coupling reagent to form the final Boc-protected compound due to the mild conditions employed in the reaction. Unfortunately, no product was observed by LCMS following 16-hours of stirring. It was hypothesized that this was possibly a result of the steric constraints of coupling a secondary amine to a benzoic acid.

A search through the literature found precedent for the formation of an intermediary acid chloride in the presence of diazirines using oxalyl chloride which could then be coupled to a secondary amine.[40] This route was employed using **141** and **149** but no formation of desired amide **150** was observed.

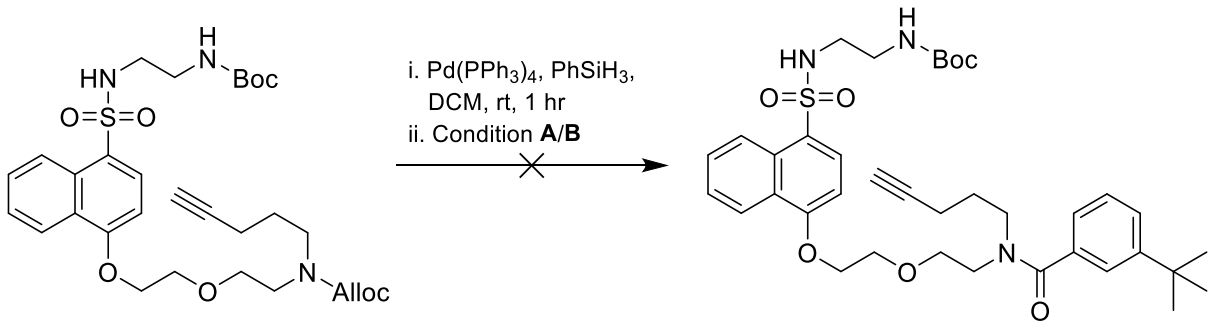

149 **150**

Condition **A**: HOBt, DMAP, Et_3N, DCM, rt, 16 hr
Condition **B**: i. **141** $(COCl)_2$, DMF, DCM, rt, 2 hr.
ii. Et_3N, DCM, rt, 16 hr

Scheme 20: Attempted Alloc deprotection and amide coupling of **149** to **141**.

As synthesis of linkers **136** and **140** have demonstrated that secondary amines readily react with chloroformates to give carbamates, it was proposed that the problematic step involved the deprotection of the Alloc carbamate of **149**. Despite the observation of complete conversion using TLC, the inability to observe even trace amounts of the desired amide suggested issues in forming the secondary amine intermediate. Having attempted several methods of coupling with no success, an alternative route to the formation of model probe **150** were then considered. No further work was conducted to resolve issues in this step and synthesis of Probe **Ia** via this route was also abandoned.

To overcome the issues arising from the final coupling, a different synthetic route was proposed where the amide linkage between the linker and the model photoaffinity module would be formed first. Although this route would increase the number of steps involving the diazirine moiety if used in the formation of the photoactive probe, it was nevertheless undertaken. It was proposed that following the formation of the amide bond between the model photoaffinity modules and the respective linkers, the resultant primary alcohol could then be converted into an electrophile and connected to naphthol **131** through nucleophilic substitution using the same procedure as described above (Scheme 19).

Again, due to the commercial availability of the model photoaffinity module **141**, synthesis of Probe **Ib** was attempted first. As outlined above in Section 3.3.2.2.2, the initial strategy to form the secondary amine intermediate of the linker through reductive amination failed yielded a complex mixture. As the secondary amine in the new synthetic route is no longer an intermediate and would be used in an amide coupling, a new strategy was needed for the synthesis of the linker. It was hypothesized that this could be achieved by first forming an amide between 2-(2-Aminoethoxy)ethanol (**132**) and 4-pentynoic acid (**151**) followed by a reduction to form the secondary amine (Scheme 21).

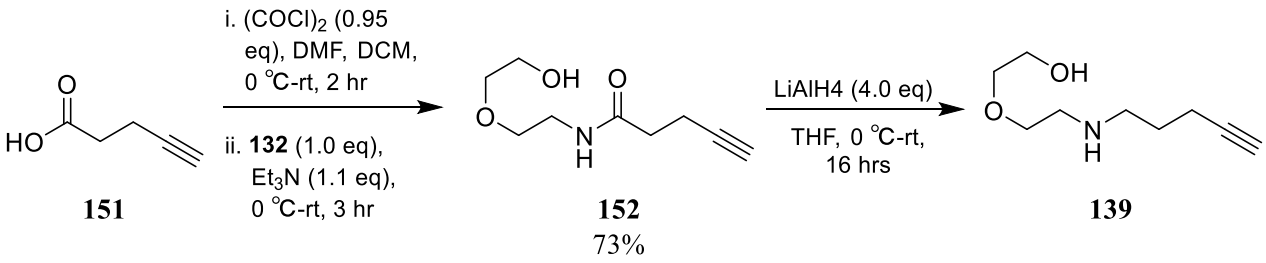

Scheme 21: Alternative synthesis of secondary amide **139**.

4-pentynoic acid (**151**) was first pre-treated with oxalyl chloride and DMF to give the intermediary acid chloride which was reacted immediately with **132** to form amide **152** in 73% yield as characterized by a triplet at δ 1.98 integrating to 1 proton corresponding to the alkyne proton. **152** was then reduced using $LiAlH_4$ to secondary amide **139** as characterized by LCMS (172.424, $[M+H]^+$). **139** was used without

further purification in the formation of the amide bond between the linker and model photoaffinity module **141**.

A modification on the method described by Lehman *et al*. used in the formation of amide bonds in the presence of diazirines was employed in the formation of an amide bond.[107] Using DMF as a catalyst, benzoic acid **141** was treated with oxalyl chloride to form the acid chloride intermediate which was immediately coupled with amine **139** to form amide **153** in appreciable yields.

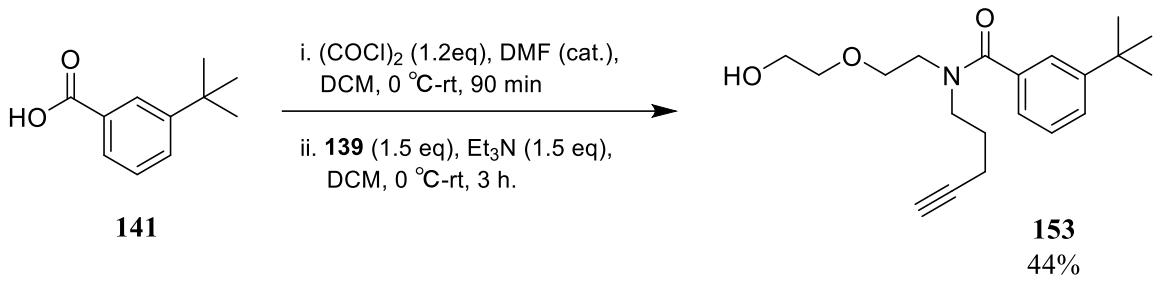

Scheme 22: Amide coupling conditions to form photoaffinity-linker module **153**.

Once the linker-photoaffinity bond was formed, focus shifted to connecting naphthol **131**. Having already established a protocol for the nucleophilic substitution of mesylates using TBAI in Scheme 19, the same conditions were employed (Scheme 23). Boc deprotection using 4M HCl in dioxane gave the final model probe **154**, characterized by LCMS where 580.285 *m/z* was observed, corresponding to $[M+H]^+$.

Scheme 23: Synthesis of final model Probe **Ib** (**154**).

Similar conditions were employed in the synthesis of the model of Probe **Ia**. Linker **135** (formed from reduction of carbamate as outlined in Scheme 14) was coupled to model affinity module **145** by first preforming the intermediary acid chloride forming primary alcohol **155**. Alkylation was carried out

using the same conditions as described above in the synthesis of model Probe **Ib,** yielding Boc protected compound **156a** following purification by HPLC. Subsequent treatment with HCl gave final probe model **156**, again characterized by LCMS where 580.285 *m/z* was observed, corresponding to $[M+H]^+$.

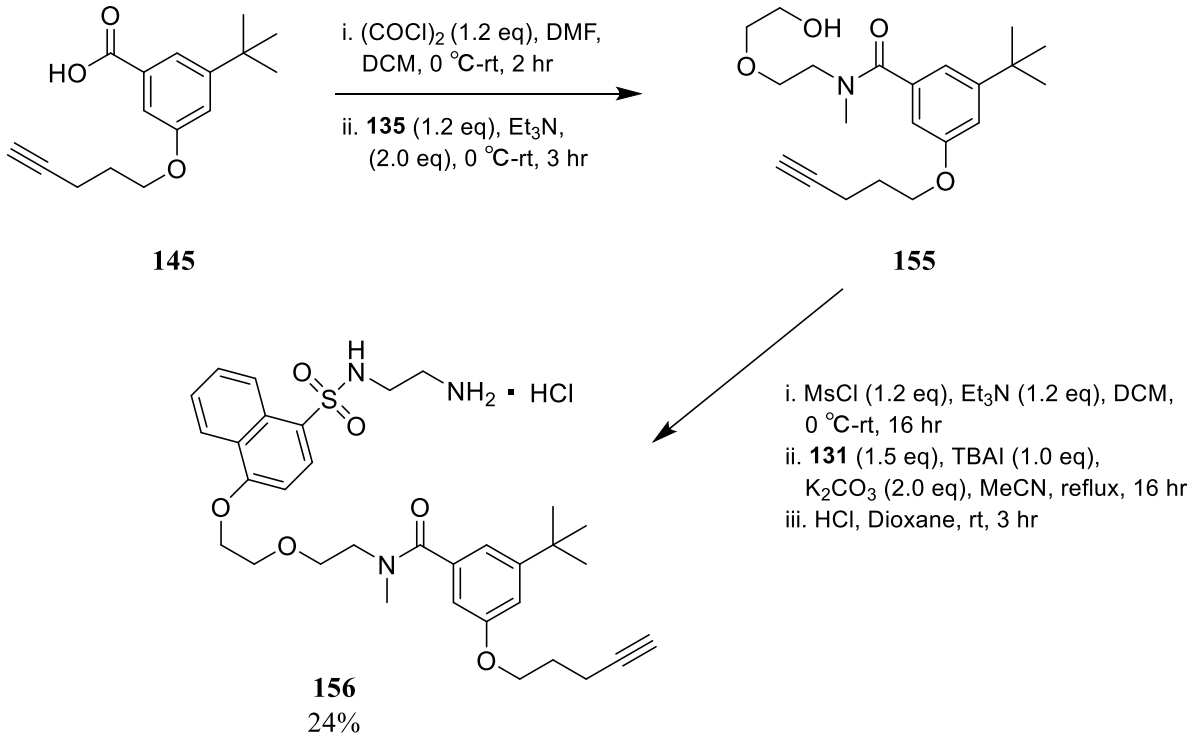

Scheme 24: Synthetic route for model Probe **Ia** (**156**).

3.3.2.5: Biological Evaluation of Model Probes

With model probes in hand, it was necessary to verify that they retained the growth promoting behaviour of eW5. To achieve this, biological evaluation of model Probes **154** and **156** were conducted in an identical manner as described in Section 2.6 and hypocotyls of *Arabidopsis* seedlings were imaged after 5 days of growth in reduced light conditions.

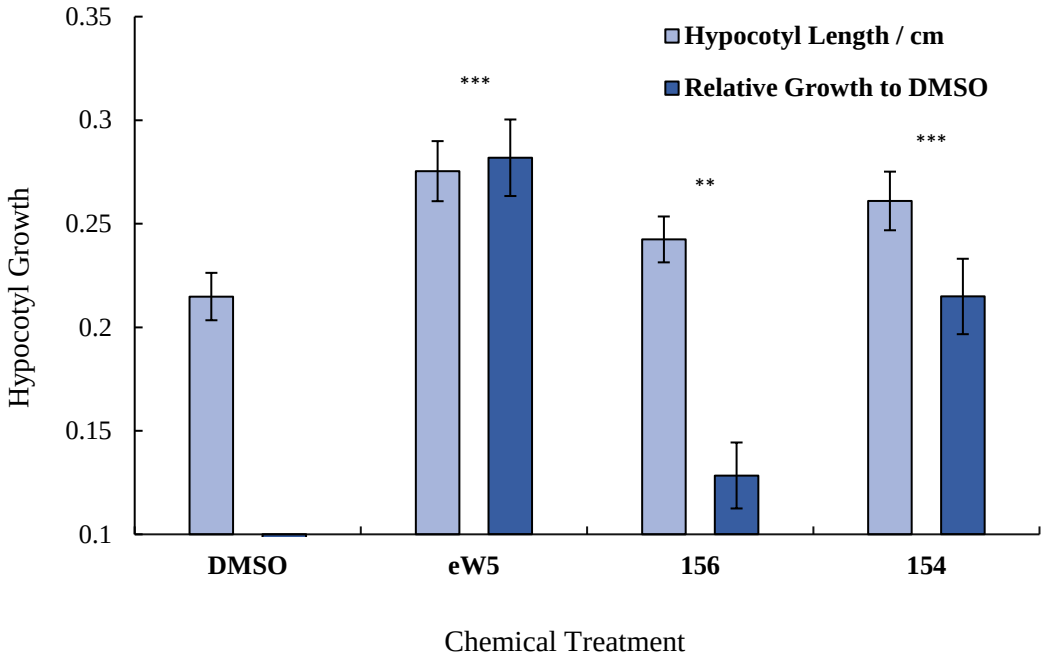

Figure 48: Hypocotyl growth of Arabidopsis treated with model Probes **156** and **154**. Values were calculated from three biological replicates. Error bars represent standard error from a population of at least 40 seedlings. Asterisks indicate statistically significant differences (independent t-test, **P<0.05, ***P<0.005) between chemical treatment and DMSO.

Pleasingly, both models showed significant growth promoting effects over the control, supporting the hypothesis that the probes would share the same targets as eW5 despite the addition of the model photo-crosslinking group and the linker. An additional concern with the addition of steric size was the issue of membrane permeability. This study also confirmed that these relatively large molecules retain cell permeability.

Although both models were found to be growth promoting, neither **154** nor **156** were found to be as effective growth promoters as eW5, suggesting the addition of the model components were hindering target affinity in some way. N-linked alkyne model Probe **Ib (154)** displayed significantly greater growth promoting effects over model Probe **Ia (156)**. A possible rationalisation for this observation was that the di-substituted benzene introduced less bulk concentrated in a single area, leading to more efficient binding with its target. Having demonstrated that the model probes show eW5-like effects in *Arabidopsis* seedlings, efforts shifted to the synthesis of the photoactive versions of Probes **Ia** and **Ib**.

3.3.2.6: Synthesis of Photo Active Probes Ia and Ib

With the other two components of the molecule; the linker and ew5 core remaining identical, the only additional synthesis required was in the formation of photoaffinity modules **157** and **158** for Probe

designs **Ia** and **Ib** respectively. With the model for Probe design **Ib** showing greater growth promoting effects, the initial focus was placed on the synthesis of disubstituted module **158**.

157 **158**

Figure 49: Active photoaffinity modules of Probe **Ia** and **Ib**.

3.3.2.6.1: Synthesis of Disubstituted Photoaffinity Module 158

As discussed above, there are many reports describing the transformation of an aromatic trifluoromethyl ketone to an aromatic trifluoromethyl diazarine. A method reported by Rennhack et al.[108] describing the synthesis of the 1,4-substituted isomer of module **158** was chosen as the reference for the route outlined below (Scheme 25). The route started with a standard esterification of 3 formyl benzoic acid (**159**) using DCC, DMAP and methanol to yield ester **160** in 89% yield as characterized by ^{1}H NMR where the appearance of a singlet at δ 3.97 (3H, s, –OC*H*$_3$) was observed. Ruppert's reagent was then used to form an intermediary trifluoromethyl alcohol which was oxidized to afford trifluoromethyl ketone **161** in 62% yield as characterized by the appearance of a ^{19}FNMR peak at δ –71.58.

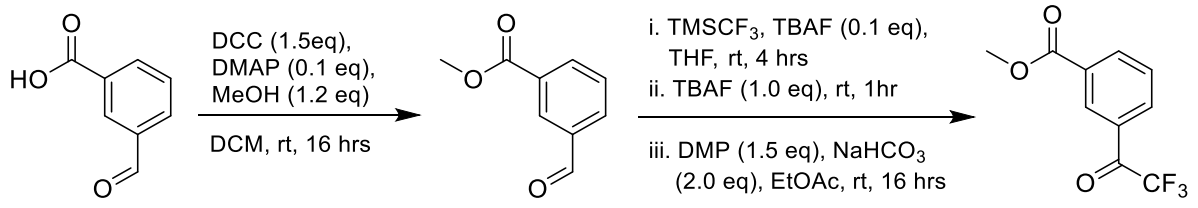

159 **160** 89% **161** 63%

Scheme 25: Synthesis of trifluoromethyl ketone **161**.

Having formed the trifluoromethyl ketone, subsequent synthetic steps were focused on conversion of an aromatic trifluoromethyl ketone into an aromatic trifluoromethyl diazarine, a transformation which has been outlined in numerous literature reports. The majority describe the same synthetic strategy which comprises of four distinct steps: the formation of the oxime (**163**), tosylation of the oxime (**164**),

formation of the diaziridine (**165**) using condensed ammonia, and oxidation of the diaziridine to form the diazarine (**166**).

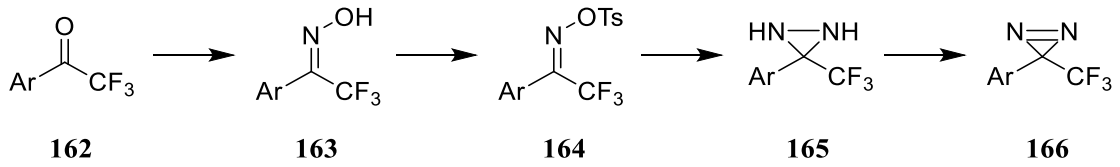

162 **163** **164** **165** **166**

Scheme 26: General synthetic route for synthesis of aromatic trifluoromethyl diazarines

Ketone **161** was stirred with hydroxylamine hydrochloride in pyridine at 70 °C to afford oxime **167** in 96% yield as characterised by two peaks in ^{19}FNMR δ –63.89, –67.64 corresponding to the two oxime isomers. **167** was then tosylated and mixed with condensed ammonia for 6-hours to give diaziridine **169**. **169** was isolated in 32% yield as characterised by ^{1}H-NMR where two peaks observed at δ 2.85 and 2.27 corresponded with the two diaziridine protons.

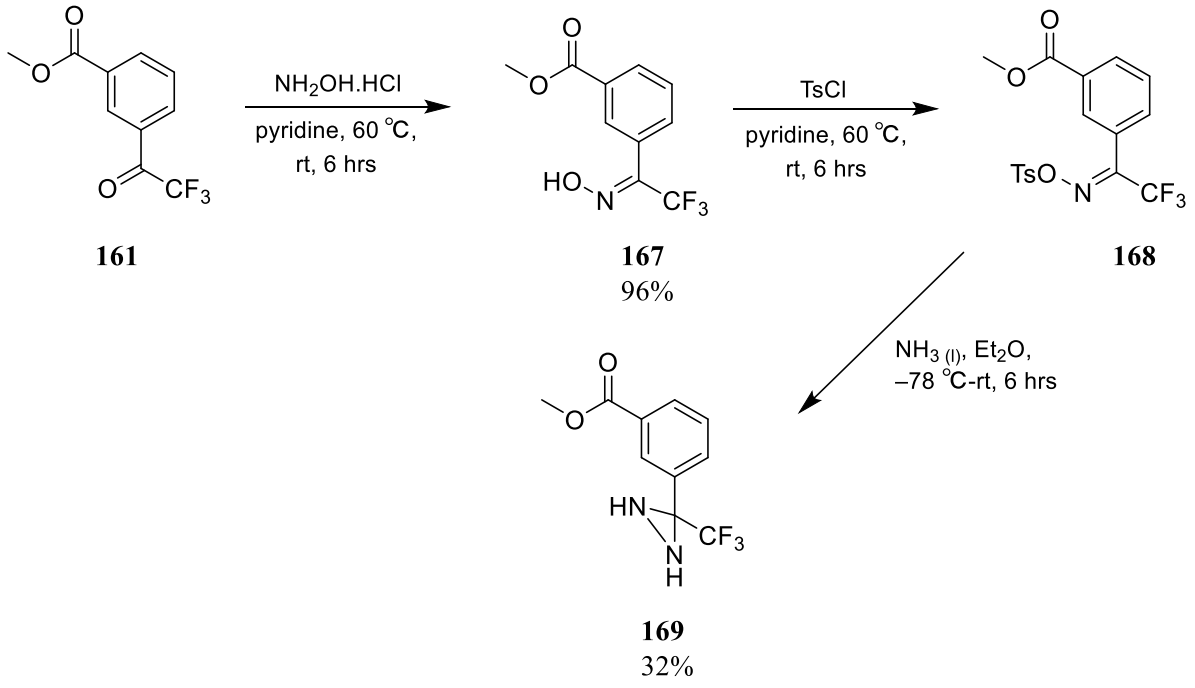

161 **167** 96% **168**

169 32%

Scheme 27: Formation of diazridine **169** from trifluoromethyl ketone **161**

Oxidation of **169** to the desired diazarine was conducted using I_2 at room temperature for 4-hours. This afforded **170** as characterised by ^{1}HNMR where loss of the two diaziridine proton peaks at δ 2.85 and 2.27 were observed. **170** was then treated with LiOH, giving the hydrolysis product **158** in 95% yield ready for coupling to the linker.

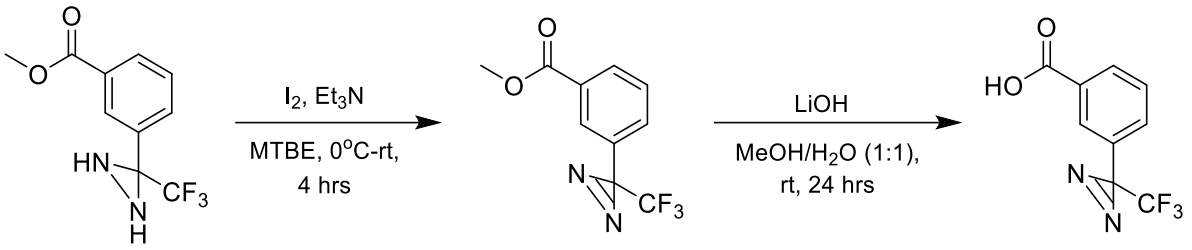

169 **170** 76% **158** 95%

Scheme 28: Synthesis of disubstituted photoaffinity module **158**.

3.3.2.6.2: Model Photo-Insertion Reaction

Once photoaffinity module **158** was synthesised, a simple model photo-labelling experiment was carried out to confirm the generated carbene would be able to perform an insertion. A search through the literature found that activation of an aromatic trifluoromethyl diazarine is typically conducted by exposing the compound to a UV source (365-315 nm) for 5-10 minutes. It was predicted that a simple sp^2-containing molecule would best facilitate insertion. Ester **170** was chosen as the model diazarine and dissolved in cyclohexene. The solution was exposed to a 365 nm LED lamp for 5 minutes after which volatiles were removed and the resulting residue was analysed by ^{19}F NMR.

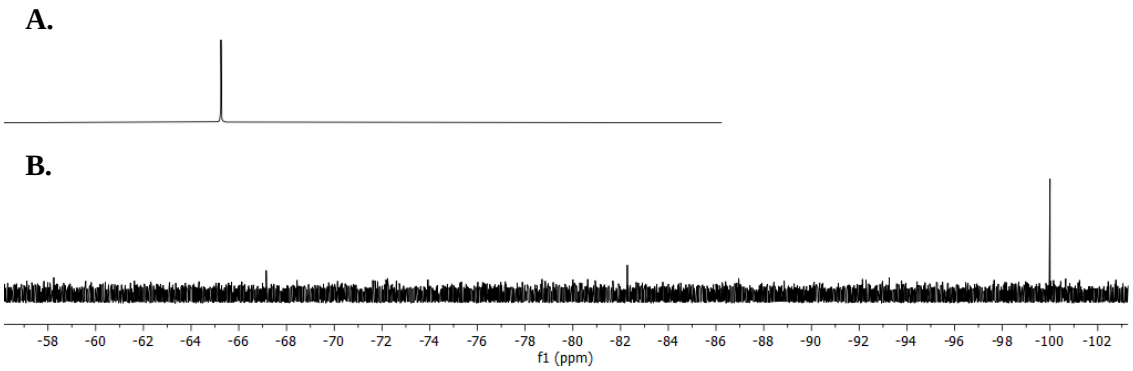

Figure 49: **A**. ^{19}F-NMR of diazarine **170**. **B**. ^{19}F-NMR of crude reaction mixture of **170** and cyclohexene in the presence of UV light.

Following exposure to a UV light for 5 minutes, ^{19}F–NMR analysis showed the consumption of the starting material and the formation of three major products. Having confirmed the formation of the carbene through ^{19}F-NMR, LCMS analysis was conducted to confirm whether insertion had occurred. Although LCMS showed the model reaction had formed a complex mixture, the insertion product was observed (*m/z* 299.371 $[M+H]^+$), supporting the hypothesis that diazarine **158** was a viable photoaffinity tag.

3.3.2.6.3: Synthesis of Photoactive Probe Design Ib

Having synthesised photoactive probe module **158**, work began on synthesising photoaffinity Probe **Ib**. As a route had been established in the synthesis of the models (Section 3.3.2.4), it was proposed that similar methodologies could be employed to synthesise the photoactive version. The initial step was the formation of the amide bond, connecting module **158** with linker **139**. The synthesis was carried out using the same conditions described in Scheme 24 where **158** was treated with oxalyl chloride to form the intermediary acid chloride which was then added to a solution containing secondary amine **139** and triethylamine.

Scheme 29: Initial attempts at synthesis of amide **171**.

Unfortunately, despite numerous reports of diazarines being stable in acid chloride formation and subsequent amide coupling conditions, no evidence of the desired compound was observed in LCMS or NMR. It was then proposed that direct coupling of amine **139** and acid **158** would be more viable. Pybop was selected as a coupling reagent and used to pre-treat acid **158** to which amine **139** and DIPEA were added to form amide **171** in 57% yield as characterized by LCMS where *m/z* 384.565 $[M+H]^+$ was observed.

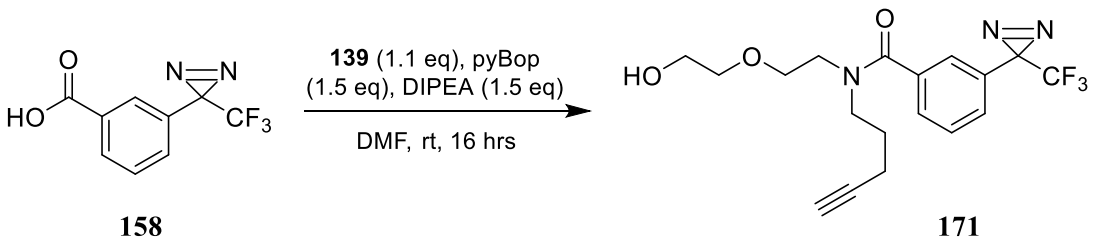

Scheme 30: Revised synthetic method for synthesis of amide **171**

Despite evidence for the formation of the compound, **171** was obtained as a mixture with a by-product of the pybop coupling. Given the high polarity of the compound due to the primary alcohol, it was proposed that the mixture could be telescoped through subsequent steps. As a result, alcohol **171** was

mesylated to form the intermediary mesylate and then underwent nucleophilic substitution with naphthol **131** to form the Boc-protected photoactive probe **172**.

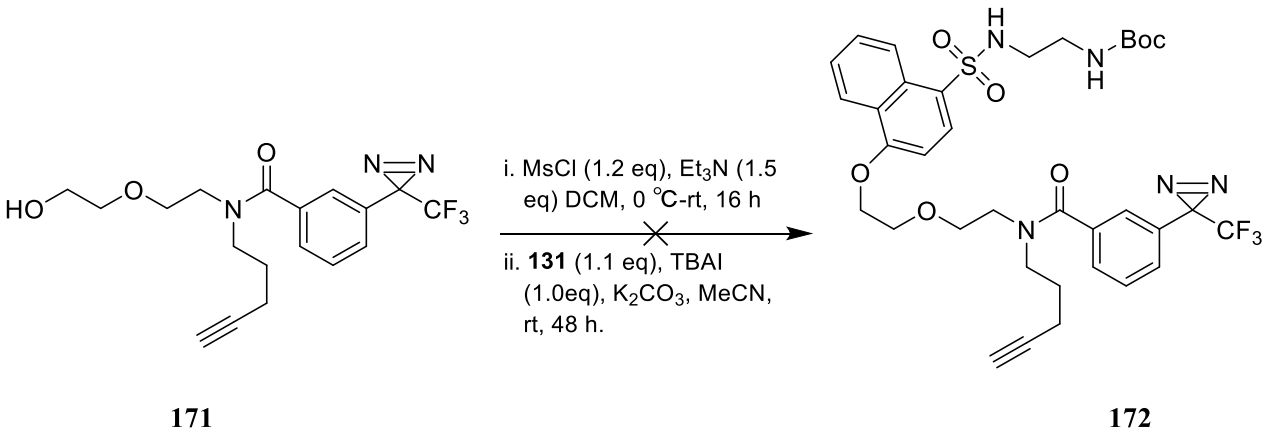

Scheme 31: Attempted synthesis of Boc-protected photoactive probe **172**

LCMS of the crude reaction gave evidence for formation of the desired diazarine (693.442 $[M–N_2+H]^+$, 732.390 $[M–N_2+MeCN+H]^+$. Despite LCMS showing evidence for the formation of the final probe as the major product of the nucleophilic substitution, the compound was not able to be isolated through normal phase flash chromatography. Time limited further work on this line of synthesis and future work should explore HPLC as a viable method of separation following the reaction.

3.3.2.6.1: Synthesis of Trisubstituted Photoaffinity Module 157

With efforts to isolate Probe **Ib** unsuccessful, focus shifted to the synthesis of Probe **Ia**. Again, as the rest of the molecule is identical with the model probe, only the synthesis of the photo-active module was needed to be developed. Retrosynthetic analysis of highly functionalized photoactive module **157** identified several key areas of concern, namely the order of addition of the various substituents as well as the use of orthogonal protecting groups at multiple stages throughout the synthesis.

Working backwards from **157**, the aromatic trifluoromethyl diazirine moiety could be accessed via 4 steps from the respective aromatic trifluoromethyl ketone compound **173** using the steps outlined in Scheme 26. This in turn could be installed via lithiation of aromatic halide **174** followed by treatment with ethyl trifluoroacetate. Accessing 1,3,5 substituted benzene **174** proved to be a challenge as no suitable commercially available compounds were found. It was therefore proposed that this scaffold could be achieved through Ir-catalysed C-H activation; the same strategy employed in the formation of model photoaffinity module **146** (Scheme 16). As previous work conducted in the group had shown

that Ir-catalysed C-H activation in the presence of an aromatic trifluoromethyl ketone leads to the reduction of the ketone to the alcohol, it was decided that the substitution pattern had to be set prior to installation of the trifluoromethyl ketone. Once the order of addition for the substituents was finalized, it was shown that tri substituted phenol **175** could be accessed from commercially available 3-halo benzoic acid **176** and its derivatives.

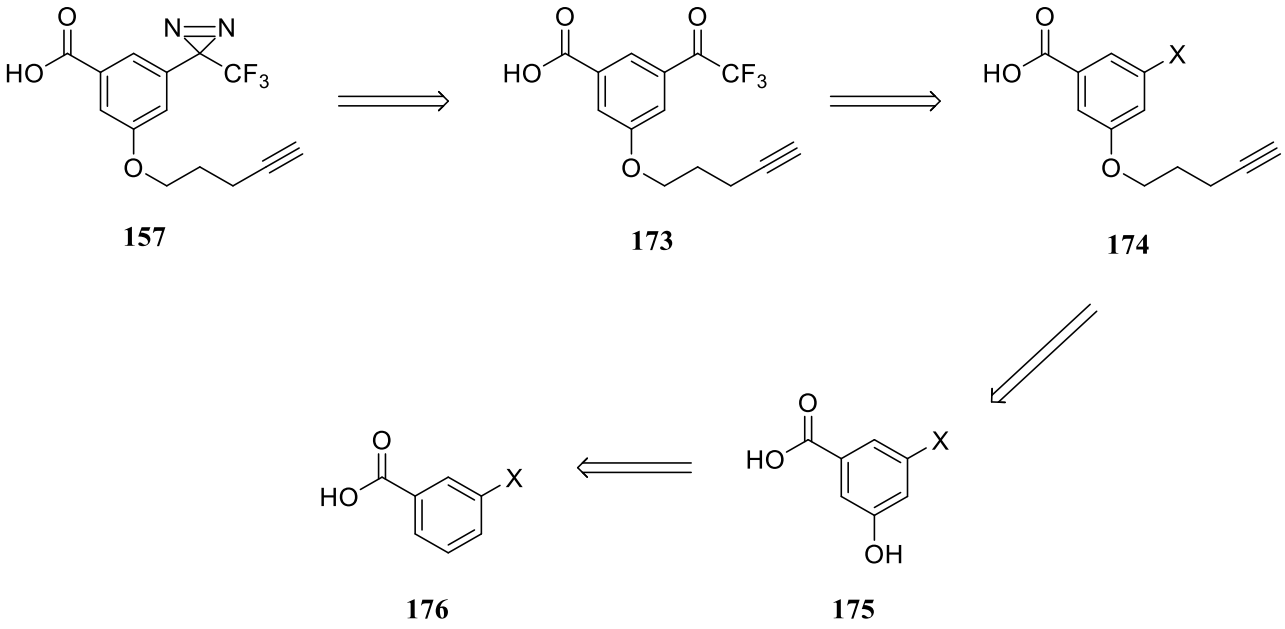

Figure 49: Retrosynthetic analysis of photoactive module **157**.

The initial focus was in finding a suitable acid protecting group that would be stable in the presence of nBuLi which was required in the installation of the trifluoromethyl ketone group. It was hypothesized that a tert-butyl ester would provide the sufficient bulk required to protect against nucleophilic attack. To generate this group, commercially available methyl-3 bromo benzoic acid was first hydrolysed to give the free acid and treated with $(Boc)_2O$ to give *tert*-butyl benzoate **178** characterized by a singlet at δ 1.59 integrating to 9 protons corresponding to the *tert*-butyl hydrogens.

Using conditions described in Scheme 16, Ir Catalysed C-H activation of **178** followed by oxidation of the boronate ester yielded 1,3,5 substituted phenol **179** in 88% yield, observed by a characteristic singlet at δ 6.76 corresponding to the phenolic proton. Following the formation of phenol **179**, focus then shifted onto the attachment of the reporting alkyne. As subsequent steps involved the use of nBuLi, it was proposed that the use of a TMS group would prevent deprotonation of the alkynal proton. Nucleophilic substitution with (5-chloropent-1-yn-1-yl)trimethylsilane using TBAI as a nucleophilic catalyst gave **180** in 61% yield (Scheme 32).

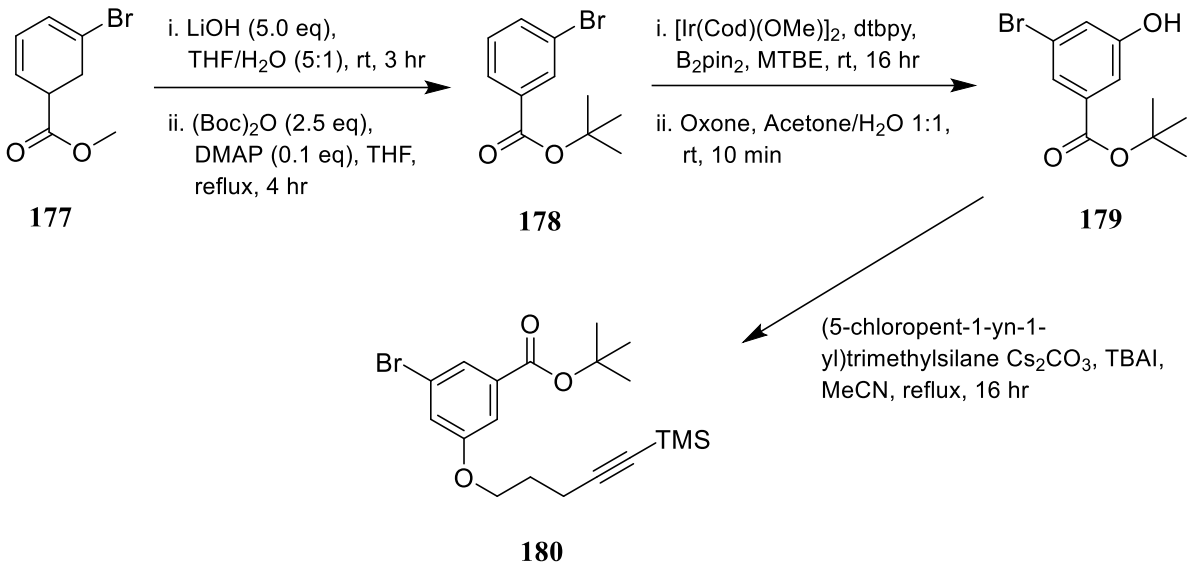

Scheme 32: Synthesis of 1,3,5-trisubstituted benzene 180

Having synthesized trisubstituted benzene **180**, the next step was to install the trifluoromethyl ketone moiety. A modified procedure described by Dolman *et al*. was used in which aryl bromide **180** was treated with n-BuLi for 30-minutes at –78 °C.[109] The aryl lithium intermediate was then quenched with ethyl trifluoroacetate and the mixture was allowed to reach ambient temperature and stirred for a further 2 hours (Scheme 33). Although it was thought that the *tert*-butyl ester would be sufficient in protecting against nucleophilic attack, LCMS of the crude reaction failed to show any evidence for the formation of aromatic trifluoromethyl ketone **181**. The reaction had instead yielded a highly complex mixture.

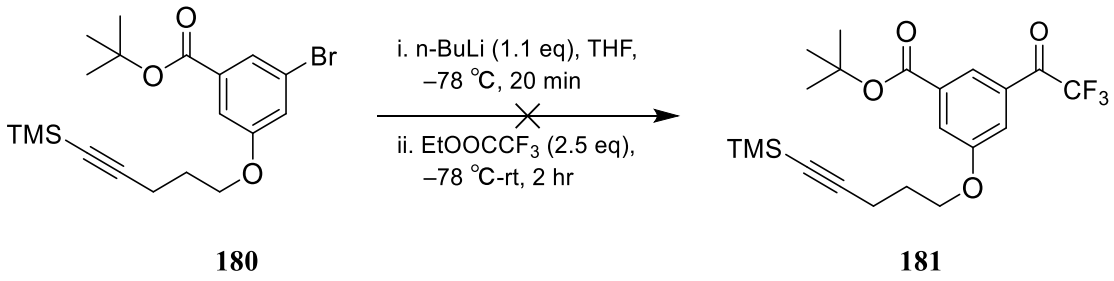

Scheme 33: Initial attempt at installing trifluoromethyl ketone group on tert-butyl ester **180**.

With the *tert*-butyl ester being unstable in lithiation conditions, it was hypothesized that using the carboxylic salt as a temporary protecting group might provide a solution. This required access to the respective acid. Unfortunately, treatment of **180** with 1M HCl in a 1:1 mixture of THF and H_2O to hydrolyse the *tert*-butyl ester yielded a mixture of two major products as observed by LCMS, (*m/z*

281.348 [**180** (^{79}Br)–*tBu*–TMS]$^-$, 353.281 [**180** (^{79}Br)–*tBu*]$^-$). As **180** failed to hydrolyse into a single benzoic acid, no further work was conducted on this synthetic route.

With the feature to generate the desired acid, it was conjectured that the starting methyl ester **177** could be used directly without any manipulation of protecting groups. Similar conditions as described in Scheme 32 were employed to form 1,3,5 substituted methyl-benzoate **185** (Scheme 34, **B**). However, as the TMS group was shown to be unstable in acidic conditions, a more robust silyl-group was chosen. Lithiating 1-chloropent-4-yne (**182**) with n-BuLi and treating with TIPS-Cl gave the corresponding protected alkyne **183** in 82% yield as characterized by a multiplet integrating to 21 protons between δ 1.16 – 0.92, corresponding to the isopropyl groups (Scheme 34, **A**).

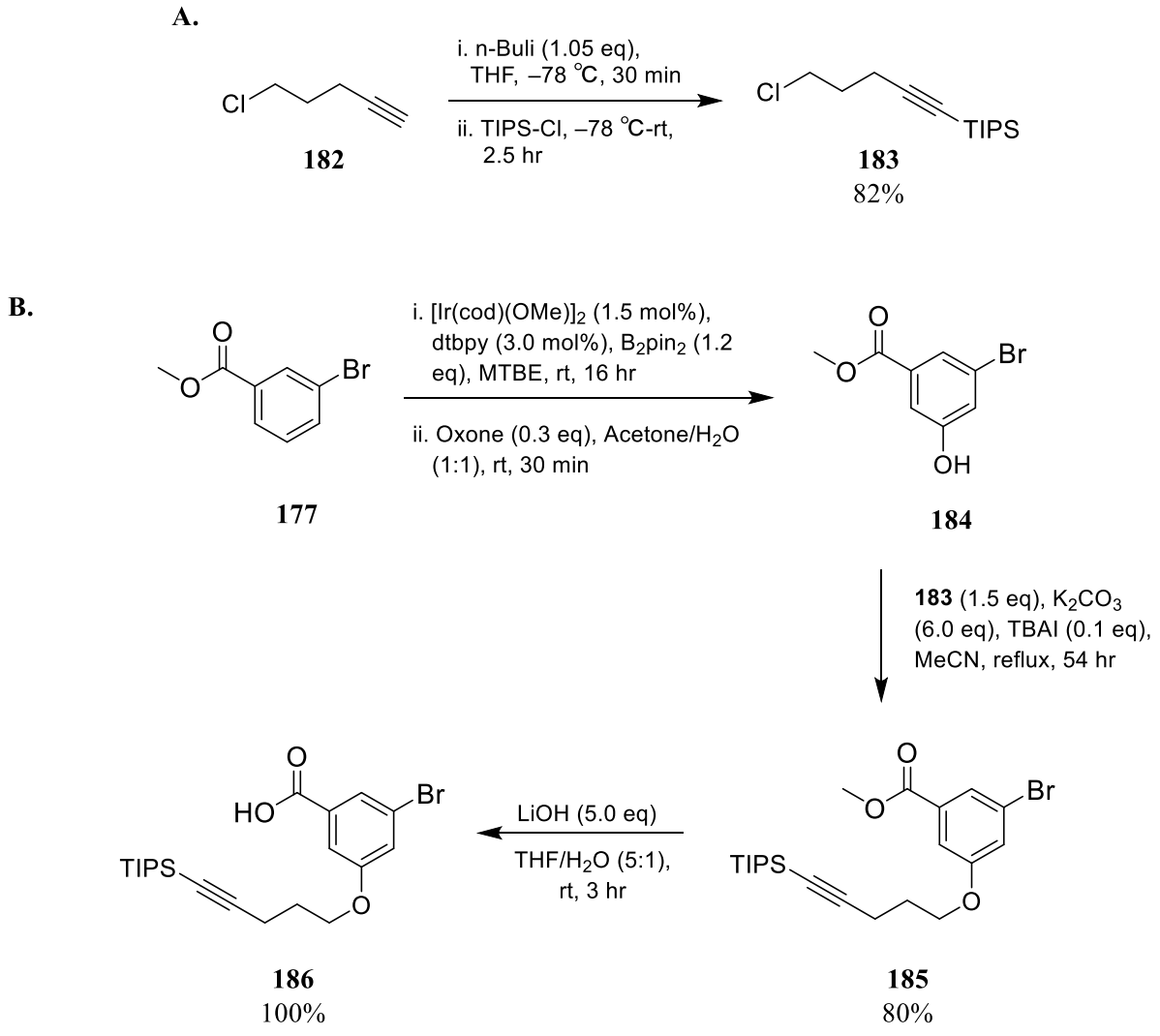

Scheme 34: **A.** Synthesis of TIPS-protected 1-chloro, pent-4-yne **183**. **B.** Synthesis of 1,3,5-trifunctional benzoic acid **186**.

Treatment of methyl-benzoate **185** with LiOH yielded the desired free acid characterized by the loss of the methoxy singlet at δ 3.91 from the starting ester. Lithiation of **185** using one extra equivalent of nBuLi enabled deprotonation of the benzoic acid whilst simultaneously facilitating the lithium-halogen exchange. Despite LCMS giving evidence for formation of **186** as the major product (*m/z* 455.293 $[M–H]^-$), the poor yield meant that it was not possible to isolate the compound following workup.

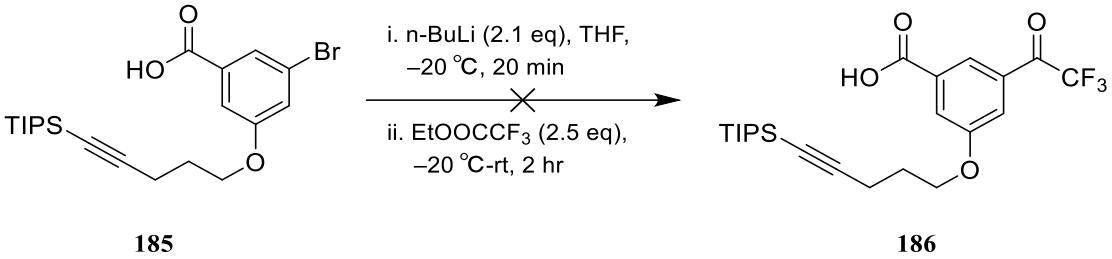

185 **186**

Scheme 35: Initial lithiation attempt on benzoic acid **185**

Despite the low yields, the hypothesis that the lithiation would yield the desired trifluoromethyl ketone was supported. A search through the literature was conducted to identify methods in which yields of lithiation reactions in the presence of benzoic acids could be improved. One possible method was described by Kato *et al*. where they reported the use of dibutylmagnesium as an additive in the metalation of aryl bromides containing proton donating groups.[110] They proposed initially quenching a carboxylic acid using a dialkylmetal to form a metal dibenzoate, allowing for direct lithium halogen exchange of the aryl bromide.

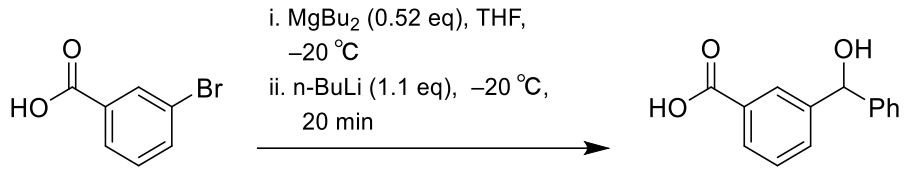

187 **188**
68%

Scheme 36: Example of lithiation of benzoic acid from Kato *et al*.

Using the procedure established by Kato, aryl bromide **185** was first treated with 0.5 equivalence of dibutylmagnesium until the formation of a precipitate. n-BuLi was then added and the resulting aryl lithium was quenched with $EtOOCCF_3$. LCMS analysis of the crude mixture revealed that the major product formed was trifluoromethyl ketone **186**. Attempts at isolation of this compound proved not to be possible.

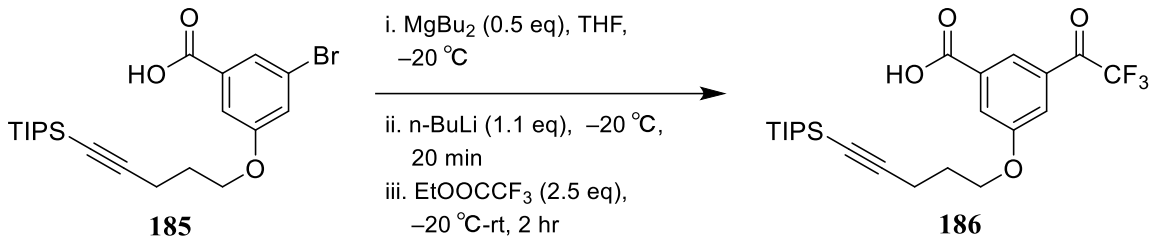

Scheme 37: Synthesis of trifluoromethylketone **186** using modified method from Kato *et al*.

As purification of **186** from the reaction mixture did not prove to be viable, consequently, the subsequent steps were telescoped through the following protection and deprotection steps. The mixture was first esterified using K_2CO_3 and MeI and following workup, TBAF was added to remove the silyl protecting group to give **187**. Despite the significant changes in polarity to the compound, purification still proved difficult due to the highly hydrophobic nature of the molecule and a spectroscopically pure sample was not obtained.

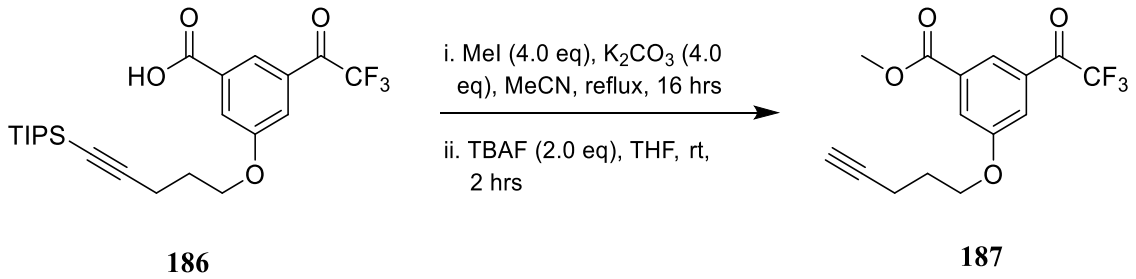

Scheme 38: Ester protection and alkyne deprotection of **186**.

Finally, treatment of this last mixture with hydroxylamine hydrochloride in pyridine afforded oxime **188**. Flash chromatography enabled the isolation of **188** as a mixture of isomers, characterized by ^{19}F NMR where two peaks at -63.82 and -67.65 ppm, in 21% yield over the previous four steps.

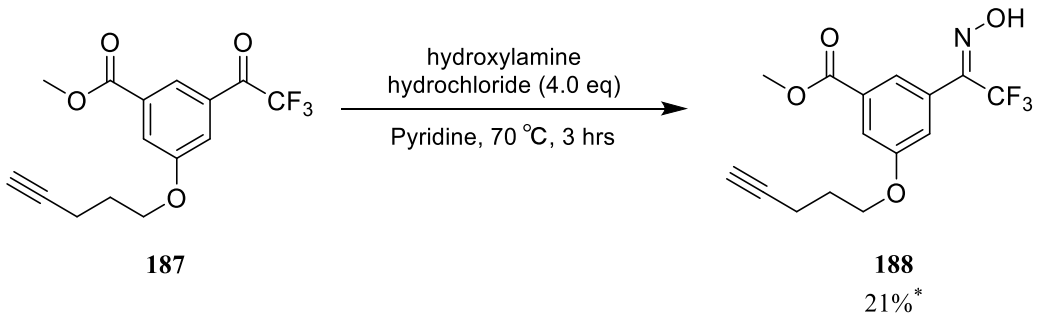

Scheme 39: Synthesis of oxime **188**. *Value represents yield over previous 4 steps.

Oxime **188** was then tosylated and without further purification was treated with condensed ammonia for 5-hours. This yielded **190** in 69% yield as characterized by ^{1}HNMR where the two diaziridine protons were observed at δ 2.81 (1H, d, *J* = 8.8 Hz), 2.24 (d, *J* = 8.8, Hz). Oxidation of **190** was conducted using I_2 at room temperature for 4-hours and chromatography gave the desired diazarine **191** in 81% yield as a colourless oil.

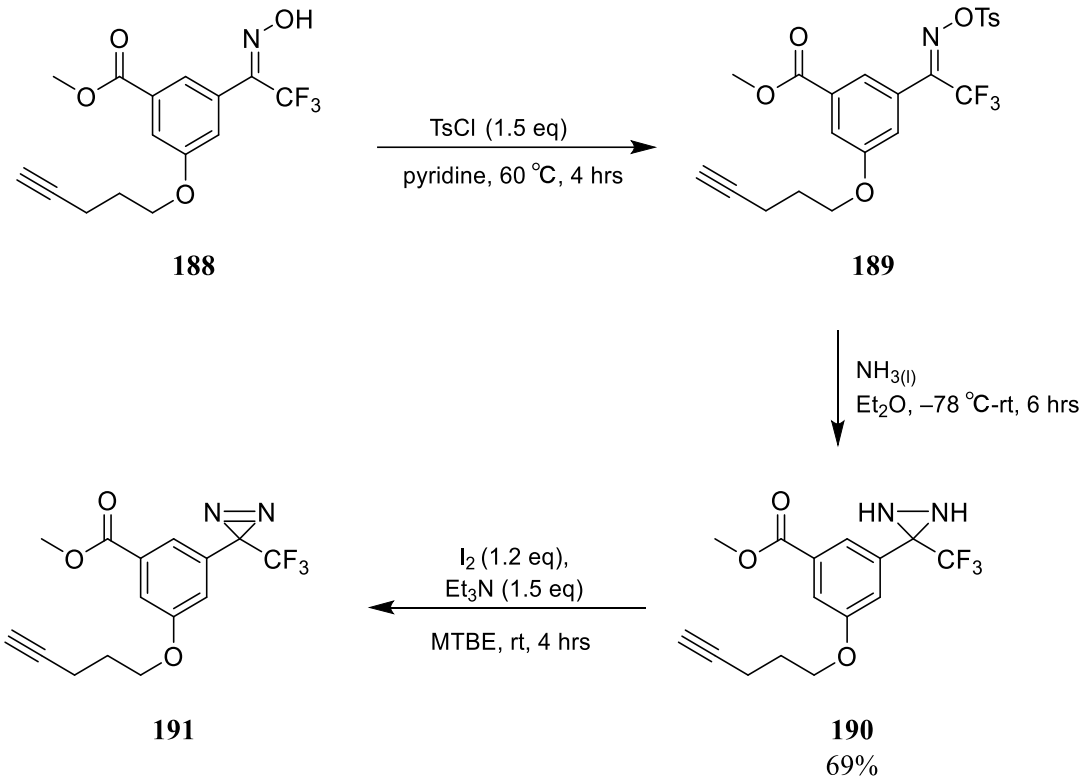

188 **189** **190** 69% **191**

Scheme 40: Synthesis of diazarine **191**.

Despite preliminary NMR data showing the loss of the diaziridine protons, supporting the formation of the diazarine, the isolated compound was found to be unstable under high vacuum. Proton NMR after being under high vacuum for 3-hours showed the appearance of additional peaks as well as the disappearance of the distinct aromatic peaks observed earlier showing a 1,3,5 substituted system. As a result of compound degradation and the limited time available no additional work has yet been conducted on the synthesis of photoactive Probe **Ia**.

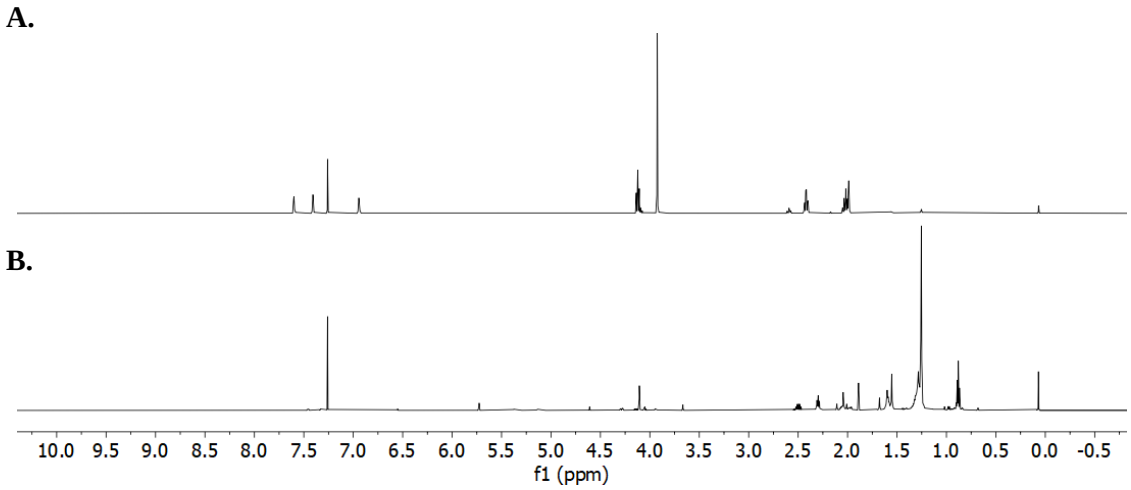

Figure 50: **A**. ^{1}H-NMR spectra of **191** post-column chromatography. **B**. ^{1}H-NMR spectra of 191 after high-vacuum for 3-hours.

3.4: Probe Design II

One potential issue with Probe design **I** was with regards to target binding as there was a significant distance between the trifluoromethyldiazarine group and the core of the molecule. Currently there is no model for the binding conformation of eW5 to its target and as such, it is possible that the tolerance for 4-substituted long chains is due to this group being orientated in solvent exposed space. Consequently, to address this concern, in a concurrent approach, another probe design attaching a photo-crosslinking group directly onto the naphthalene core was explored.

The SAR developed in Section 2.2 had revealed that analogues **79** and **80** containing bulky groups in the 4-position (*tBu*, Ph) retained eW5-like growth promoting effects. It was therefore proposed that a diazirine moiety directly attached to the naphthalene core would also be tolerated, resulting in Probe design **II.** As long alkane substituted analogues **109** and **111** posed issues at the standard concentration of 100 μM, it was proposed that an ether linkage between the diazarine and reporting unit would provide greater solubility as well as increase the synthetic scope.

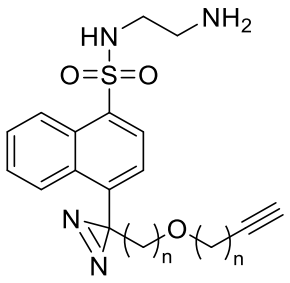

Probe II

Figure 51: Structure of Probe design **II**

3.4.1: Retrosynthesis of Probe Design II

Retrosynthetic analysis of **Probe II** showed that the aromatic diazarine can be obtained through the corresponding aromatic carbonyl compound **191** via the steps outlined in previous probe designs (Scheme 26). Having established a procedure for the installation of aryl sulfonamides from the respective aryl bromide in Section 2.3, it was hypothesized that **191** could be obtained from **192**, which in turn could be obtained from a nucleophilic substitution of halo-carbonyl **193**. The limited availability of 1-4 substituted naphthalenes meant that a strategy for the selective substitution in the 4-position would need to be developed. Fortunately, a search through the literature found precedent for Friedel-Crafts acylations of simple acyl chlorides on 1-bromonaphthalene (**93**) to be selective for the 4-position and it was hypothesized that this would allow for the formation of intermediate **193**.

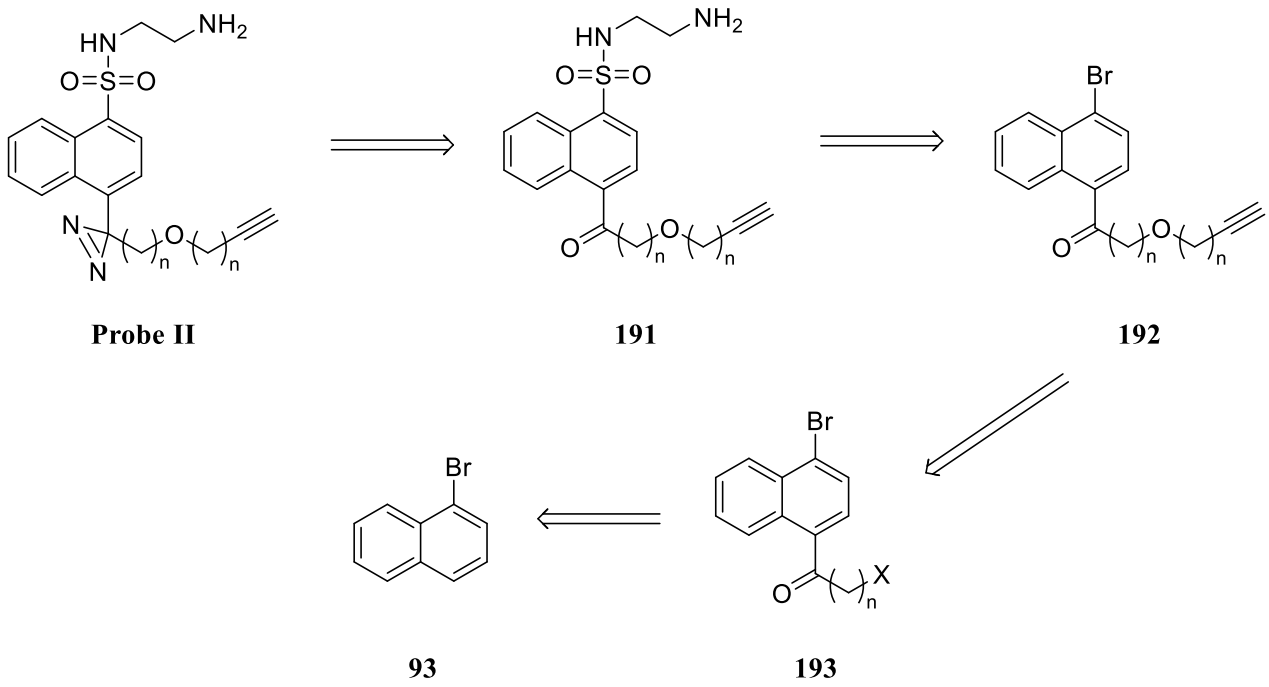

Figure 52: Retrosynthetic analysis for Probe **II**.

3.4.2: Friedel Crafts Strategies.

Although it was initially hypothesized that Friedel-Crafts conditions would result in a 4-acylated product, the presence of the second aromatic ring meant that it was also possible to obtain a 5-subsituted naphthalene. To test the specificity of acylation, a model literature procedure described by Dixon et al. using a simple acid chloride was attempted.[111] 1-bromonaphthalene **93** was treated with acetyl chloride and $AlCl_3$ for 3 hours at room temperature yielding 4-substituted naphthalene **194** as the major product

as determined by ^{1}H-NMR where a characteristic singlet at δ 2.74 integrating to 3 protons was observed and a single peak in LCMS [M(^{79}Br)+H]$^{+}$ 249.166, [M(^{81})Br)+H]$^{+}$ 251.143.

93 **194** 95%

Scheme 41: Model Friedel-Crafts reaction to form 4-substitued naphthalene **194**.

Having demonstrated that Friedel-Crafts acylation of 1-bromonaphthalene using acetyl chloride favours the 4-substituted product, it was then hypothesised that acylation using chloro-acetyl chloride would form a potent electrophile, allowing for the simple formation of the ether linkage to the reporter unit. α-chloro ketone **195** was prepared using the same conditions as described in Scheme 41, but despite evidence for the formation of the compound from LCMS, purification by column chromatography failed to isolate the product.

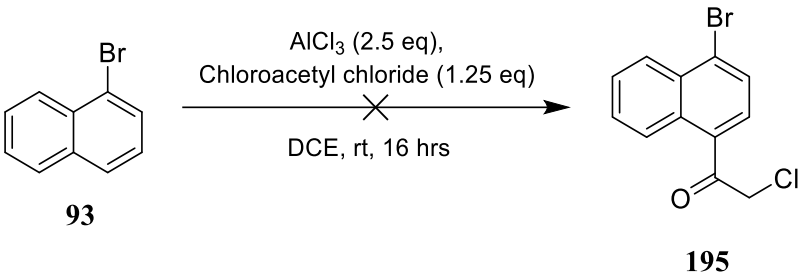

93 **195**

Scheme 42: Attempted synthesis of α-chloro ketone **95**.

It was hypothesized that α-chloro ketone **195** was unstable and that reacting the compound on crude to form the α-alkoxy ketone would then allow for isolation of the compound. As subsequent reactions involved the use of n-BuLi, a protected alkyne-ol would be needed to prevent abstraction of the alkyne proton. TIPS-protected alkyne **197** was made by treating butyne-ol (**196**) with two equivalents of nBuLi to first form the dianion to which equivalents of TIPS-Cl were subsequently added. Treating the intermediate with 1M HCl for 2-hours selectively deprotected the silyl ester to give **197** in 69% yield as characterized by ^{1}H-NMR where a peak at δ 1.21 – 0.98 integrating to 21 protons was observed.

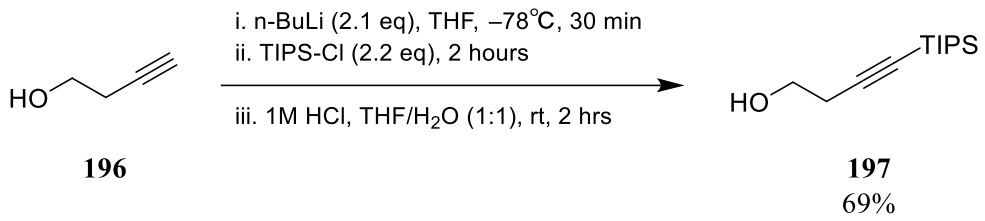

Scheme 43: Synthesis of TIPS-protected alkyne-ol **197**.

Initial attempts to alkylate **195** with **197** used NaH to pre-form the alkoxide but unfortunately no desired compound was obtained as determined by LCMS. TLC analysis following stirring for 16-hours at room temperature showed presence of the starting alcohol **197** but naphthalene **195** was consumed, leading to the belief that it had decomposed. Milder conditions using NaOH were subsequently employed but also failed to yield α-alkoxy ketone **198**, again with TLC and LCMS indicating starting α-chloro ketone **195** had decomposed.

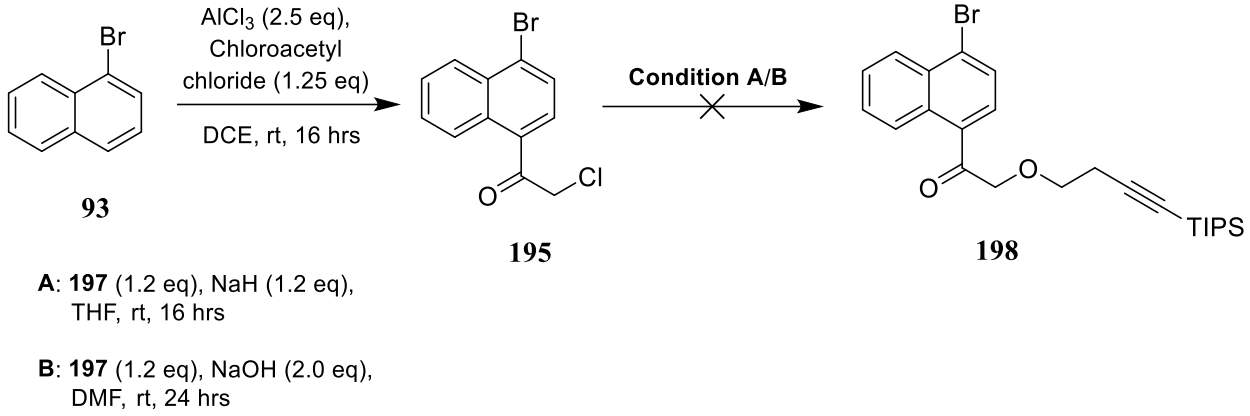

Scheme 44: Attempted alkylation of α-chloro ketone **195**.

An extensive search through the literature failed to yield any examples of nucleophilic substitutions from aliphatic alcohols to form an α-alkoxy aromatic ketone. One of the common methods to form α-alkoxy ketones is via the O–H insertion of α-diazoketones which can be catalysed by rhodium or copper complexes and dilute acids. Unfortunately, this strategy poses its own issues as esters can be formed as a by-product from the competing Wolff rearrangement and as a result, work along this synthetic route was halted.[112]

It was then proposed that a Friedel-Crafts acylation could be performed using an acid chloride with a preformed α-alkoxy bond. To form the desired acid chloride, ethyl bromoacetate was alkylated using TIPS-protected alcohol **197** giving ester **199**. The ester was then hydrolysed and resulting acid **200** was

treated with oxalyl chloride to give the desired acid chloride **201**. Unfortunately, reaction of **201** with 1-bromonaphthalene (**93**) turned black instantaneously upon addition of $AlCl_3$. Despite TLC analysis of the mixture after 5-minutes showing complete consumption of the starting acid chloride, LCMS revealed a complex mixture where no evidence of the desired compound was detected. This was further confirmed by NMR of the crude mixture which showed a highly complicated mixture of peaks in the aromatic region.

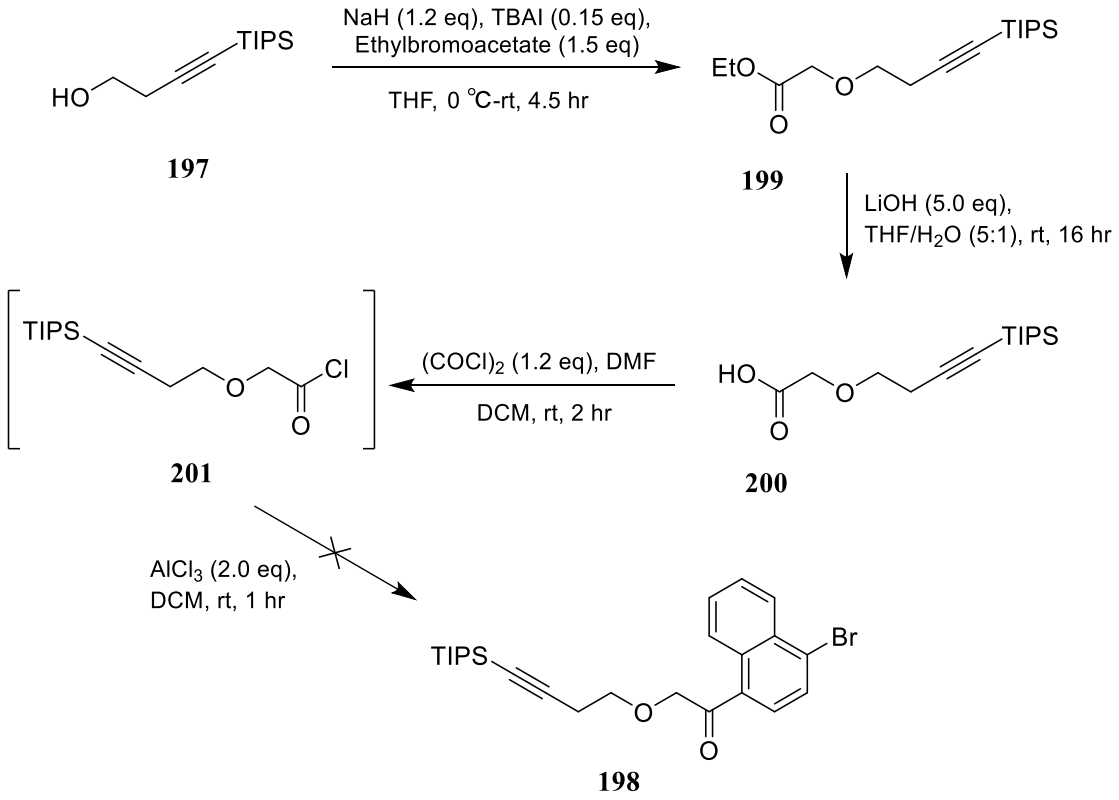

Scheme 45: Attempted Friedel-Crafts reaction with preformed α-alkoxy bond.

To overcome the issue of a complex mixture being formed from Friedel Crafts conditions, it was hypothesized that a trimethylsilyl-substituted naphthalene would give greater selectivity to acylation. A modification of the scheme outlined by Offner *et al*. was employed and 1-4 dibromonaphthalene **202** was monolithiated and treated with TMS–Cl to give aromatic trimethyl silyl compound **203** in 90% yield characterised by a characteristic singlet in the ^{1}H-NMR spectra at δ 0.46 integrating to nine protons.[113] Unfortunately, TLC analysis of the subsequent reaction with $AlCl_3$ and acid chloride **201** also showed the formation of a highly complex mixture and again, no desired compound was detected by LCMS.

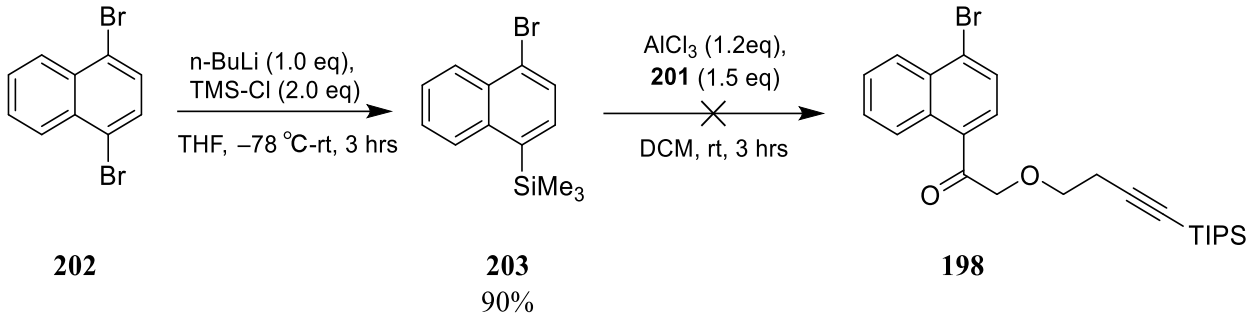

202 **203** 90% **198**

Scheme 46: Attempted synthesis of α-alkoxy-ketone **198** from aromatic trimethylsilyl **203**.

It was hypothesized that the combination of the α-oxygen and the alkyne group were interfering with the Friedel Crafts reaction, explaining why the complex acid chlorides failed to yield the desired 4-subtituted naphthalenes despite test reactions with simple reagents showing promise. With multiple strategies involving Fridel Crafts acylating conditions all failing to give the desired 4-substituted naphthalene, this approach was abandoned.

3.4.3: Mono-Lithiation Strategies

With Friedel-Crafts acylations of more complex acid chlorides yielding complex mixtures, alternative strategies which gave greater regioselective control were considered. It was proposed that mono-lithiation of 1-4-dibromonaphthalene (**202**) would generate a suitable nucleophile for the formation of the aromatic acyl bond. As the creation of an aromatic ketone would yield a product more reactive than the respective starting electrophile, it was proposed that the use of a Weinreb amide would prevent nucleophilic substitution into the ketone and the formation of tertiary alcohol by-products.

Acid **200** formed in Scheme 45 was treated with N-O-dimethylamine and DCC as a coupling reagent to form Weinreb amide **204**. **204** was obtained as a colourless oil in 72% yield characterized by ^{1}H-NMR where two singlets each integrating to 3 protons 3.23 and 3.72 ppm were observed.

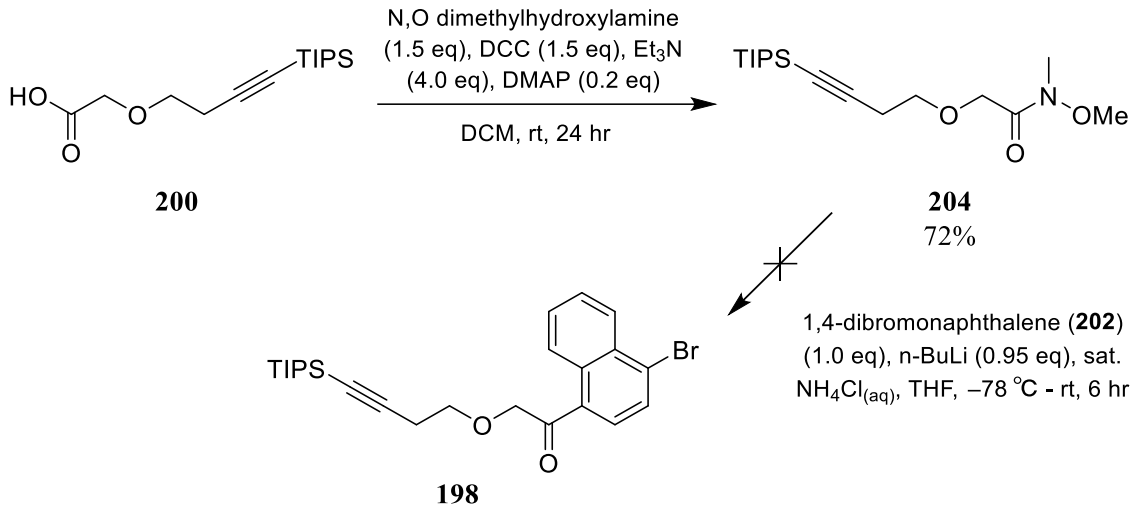

Scheme 47: Attempted synthesis of **198** via Weinreb amide **204**.

Unfortunately, treatment of the mono-lithiated naphthalene with Weinreb amide **204** at 0°C failed to yield the desired compound. Analysis of the crude proton NMR spectrum showed that the major product formed was 1-bromonaphthalene (**93**), suggesting that although lithiation was possible, the acylation step was not efficient.

Having established a protocol for monolithiation of dibromonaphthalene **202**, further exploration into whether this step was a viable method of accessing the 1-bromo, 4-oxo scaffold required for Probe design **II** was needed. A literature search identified a report by List et al. where such a structure was formed via monolithiation of a dibromo aromatic compound. γ-butrylactone **206** was added to monolithiate 1,4-dibromobenze **205** to form 4-(4'-Bromophenyl)-4-oxobutanal **207** in 26% yield.[114]

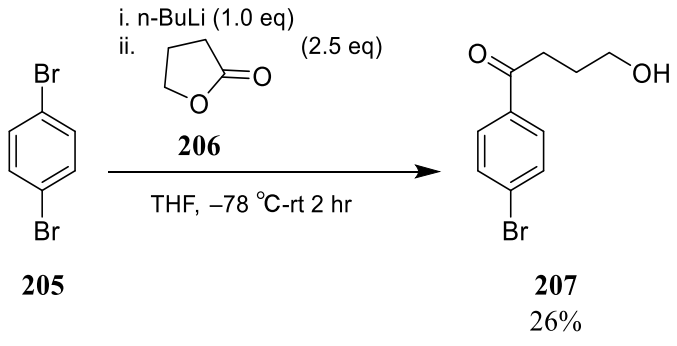

Scheme 48: Example of monolithiation to form aryl-oxo compound **207** as described by List *et al.*

This approach was attractive not only because it controlled the regioselectivity of then substituents, but also the primary alcohol generated made for a natural attachment site for an alkyne reporting unit. To

form 1-bromo, 4-oxo-naphthalene **208**, monolithiation of dibromonaphthalene **202** was performed using 0.95 equivalence of n-BuLi. To this mixture, lactone **206** was added which afforded desired compound **208** as characterized by LCMS where *m/z* peaks of 293.329 ([M+H (^{79}Br)]$^+$, 27) and 295.267 ([M+H (^{81}Br)]$^+$, 43) were observed. Unfortunately, this compound was not separable from excess lactone **206** and attempts to remove it under high vacuum resulted in polymerization of the primary alcohol, seen through the appearance of additional aromatic peaks in ^{1}HNMR. As a result, **208** was moved on to the next step without further purification.

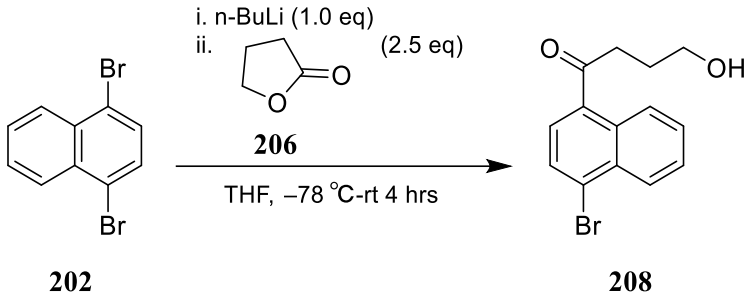

202 **208**

Scheme 49: Monolithiation to form naphthyl-oxo compound **208**.

Although the primary alcohol allowed for immediate alkylation to a reporting unit, it was believed the aromatic ketone could have interfered with this step. To overcome this potential issue, a series of protection and deprotection steps were conducted prior to alkylation of the alcohol. Alcohol **208** was first acyl-protected by treating the naphthalene with AcCl to form ester **209** as characterised by a singlet in ^{1}H-NMR at δ 2.04 integrating to 3 protons, corresponding to the acyl group. This transformation had the additional benefit of allowing for the purification of the desired compound from the telescoped mixture of **208**, giving the protected alcohol in 33% yield over the two steps. Following the alcohol protection, **209** was stirred under reflux with ethylene glycol to protect the ketone as an acetyl. Mixing the resulting crude mixture of this reaction with NaOH yielded acetyl **210** as characterised by ^{1}H-NMR where a multiplet at δ 4.21 – 3.78 integrating to 4 protons corresponding to the acetyl protons was observed.

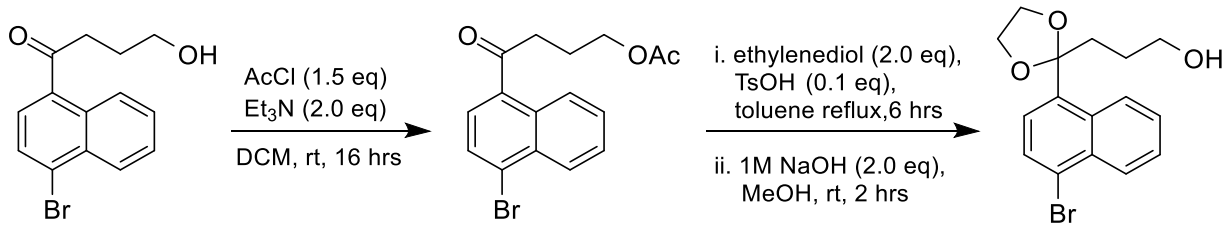

208 **209** 33% **210** 54%

Scheme 50: Synthesis of acetyl **210**.

It was then proposed that TIPS-protected alkyne **197** could be used directly to attach the reporting unit onto **210**. There was concern that nucleophilic substitution using **197** as the electrophile would result in the conjugated ene-yne and thus it was proposed that TIPS-protected alcohol **197** would be better suited as a nucleophile. Alcohol **210** was first treated with TsCl to give the intermediary tosylate which was then alkylated with **197** using similar conditions as described in Scheme 44, Condition **A**.

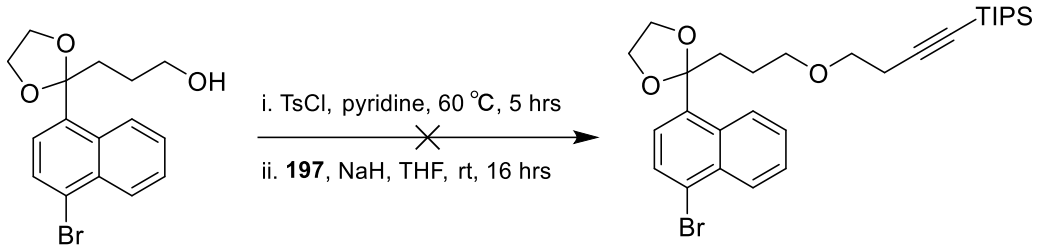

210 **211**

Scheme 51: Attempted alkylation of **210** with alkyne **197**.

Unfortunately, despite ASAP data supporting the formation of the tosylate, no evidence for the alkylated product was observed after stirring overnight. Time has prevented further investigation to date but future reactions along this route should ensure optimisation of these alkylating conditions and the exploration of diazarine formation.

3.5: Conclusions and Future Work

This chapter has described routes to synthesise model probes **154** and **156** in a highly convergent manner, with the eW5-core, linker and photoaffinity model modules being synthesised separately. Although there were concerns that the large size of these models would affect cell permeability and thus growth promoting activity, this proved not to be the case and biological validation via the hypocotyl assay was able to show that both model probes **154** and **156** were significant growth promoters, with seedlings treated with **154** showing comparable absolute hypocotyl length values to those treated with eW5.

Despite being able to synthesise the various modules of the photoactive probes, synthesis of the entire molecule was unsuccessful with the coupling of aryl trifluoromethyl diazarine-linker unit **158** to eW5-naphthol **131** failing to afford any isolatable probe. With time limiting further progress along this route, future work along the synthesis of photo active Probes **Ia** and **Ib** should be focused on optimising conditions for the alkylation of the naphthol. With **Probe II**, it was demonstrated that monolithiation

of 1,4-dibromonaphthalene (**202**) proved to be a much more viable strategy of obtaining the desired, 1-bromo 4-keto scaffold over standard Friedel-Crafts acylations. Again, with time limiting further progress along this route, additional work along this synthetic route should be focused on the alkylation of primary alcohol **210** with protected alkyne **197**. Once afforded, the sulfonamide moiety can be installed via lithiation as developed in Section 2.3 and subsequent acetyl deprotection would yield the desired aryl ketone scaffold, allowing for transformation into a diazarine (Scheme 52).

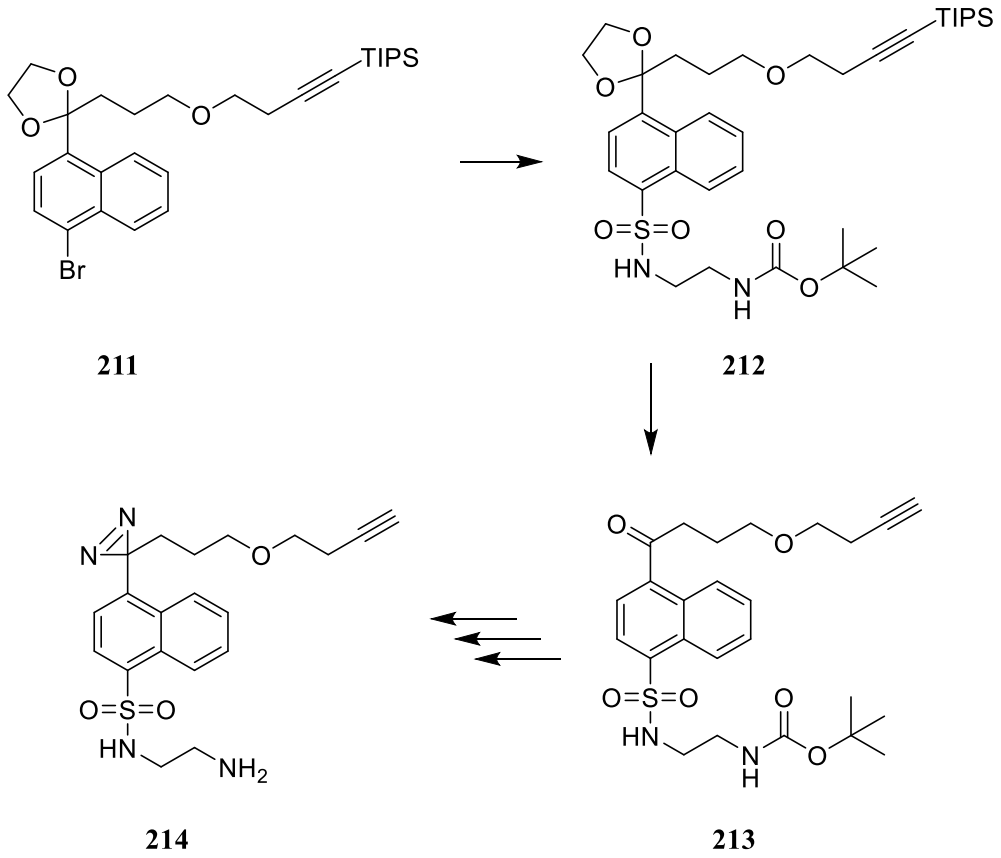

Scheme 52: Proposed future work for synthesis of **Probe II**.

Following the synthesis of the photoactive probes, biological evaluation can be conducted via the hypocotyl assay to assess if the probes retain eW5-like growth promoting abilities. Given the instability of diazarines to UV light, optimisation of growth conditions would be first required; namely growth under red light conditions to minimise the possibility of the reactive carbene species being formed. Once biological activity has been validated, the probes can then be used for target identification. This process would require incubation of the probes with *Arabidopsis* protein lysate followed by exposure to UV light to facilitate target protein capture. Following biorthogonal reaction with a biotin reporting unit, a protein gel can then be run to identify if a distinctive protein band can be observed. As an additional validation of on-target binding, eW5 (**1**) can be used as a competitive inhibitor as reduction

in the fluorescent intensity of a certain band with increasing eW5 concentrations would indicate that the probe is being out-competed. Once a distinct band has been identified, identification of the target protein can be conducted via mass-spec analysis.

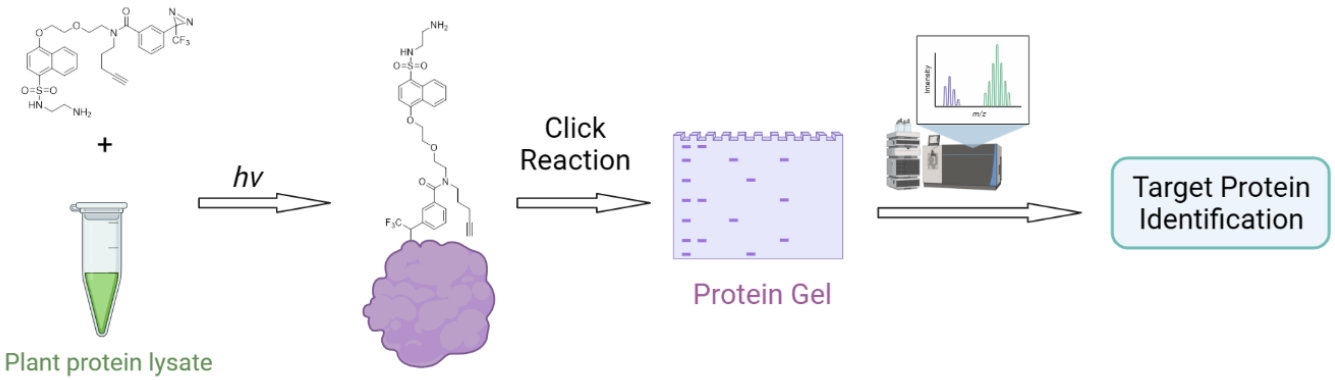

Figure 53: Workflow for target identification of eW5 following synthesis of photoactive probes

Chapter 4: Genetic Mutant Screen

4.1: Chapter Introduction

In a complementary approach to identify the target of eW5, a genetic screen was employed. As it had been well established treatment with eW5 results in elongated hypocotyls in *Arabidopsis*, the aim of this screen was to select mutants with displaying the dwarfed hypocotyl phenotype from an EMS-mutagenized population. Subsequent genome sequencing and mapping of the selected mutants would find the mutation responsible for the phenotype of eW5-insensitivity. This chapter briefly reviews the literature of forward genetic approaches for gene/protein target identification, outlines the workflow employed to identify mutants that displayed the desired phenotypic response and future work that can be employed following genome sequencing. This work was conducted alongside Dan Bruce (University of Durham, Department of Biosciences) and full data can be found in Appendix C.

4.2: Introduction to Genetic Screening

4.2.1: Chemical Mutagens

As outlined in section 1.2, forward genetics is a widely used approach for the identification of target genes or proteins. This method requires the screening of mutagenized populations for individuals displaying a desired phenotype. A wide range of mutagens have been used to generate mutant libraries including but not limited to x-rays, N-ethyl-N-nitrosourea (**215**), trimethylpsoralen (**216**) and UV light.[115] The most commonly used mutagen in the formation of mutagenized screening populations is ethyl methane sulfonate (EMS (**214**)) due to its ability to promote single-base mutations over insertions/deletions, whilst limiting lethality and sterility.[116] First reported in 1961 by Brookes *et al*., the alkylating agent has been shown to primarily react with guanine nucleotides, leading to mispairings with thymine in DNA replication.[117] EMS is able to alkylate two positions on guanine nucleotides; N-7 and O-6. Although it was initially believed that the N-7 alkylation was responsible for DNA mispairing, the ability for weaker chemical mutagens such as dimethyl sulfate (DMS) and methyl methane sulfonate (MMS) to also alkylate the N-7 position effectively has led to the current hypothesis that mutagenesis correlates with O-6 alkylation.[118,119] As EMS is able to react non-selectively, the entire genome can be mutagenized resulting in a wide range of mutants including loss- or gain-of function mutants.[120]

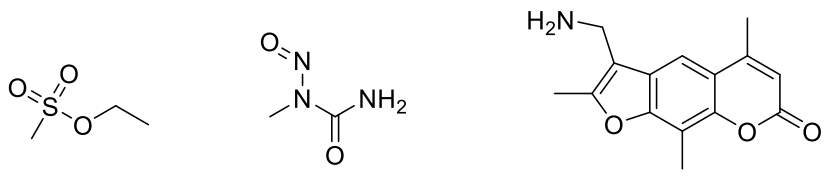

EMS **214** | N-Methyl-N-nitroso Urea **215** | Trimethylpsoralen **216**

Figure 54: Structures of selected chemical mutagens.

Prior to the introduction of genome sequence-based methods, the primary technique used for the identification of the mutated gene of interest in a mutagenized individual involved the process of "chromosome walking". Using yeast artificial chromosomes (YACs), a physical map had to be built with markers being identified individually to link the mutation to a specific location. This is a highly labour-intensive process, limiting applications of the methodology.[116] Traditionally, identification of causal mutations was carried out via recombinant genotyping followed by candidate gene sequencing. Nowadays with genome sequencing being relatively routine, causative gene mutations can be easily identified. One way in which this can be achieved is through simultaneous mapping and mutation identification by deep sequencing (SHOREmap). Through whole-genome resequencing of recombinant mutant genomes, the mutation is mapped through identification of the highest frequency mutation, allowing for a direct link between a phenotype of interest and the causal mutation to be made.[121,122] This combined with the introduction of next-generation genome sequencing, a highly parallel approach that allows for quick and high-throughput sequencing has made forwards genetics a powerful tool in the identification for causative mutations.

4.2.2 General Procedure to Identify Causative Mutation.

Most genetic screens involving EMS mutants follow the same general protocol. An EMS mutant library can be prepared easily by treating WT seeds in EMS solution for 3-12 hours giving the first generation of mutants labelled M_1. The chemically treated seeds are then self-crossed and the M_2 progeny collected. This serves 3 major functions; to bulk up the sample, to eliminate lethal mutations or mutations resulting in sterility and to create homozygous recessive mutants. The final reason is significant as the random mutations will one occur on one allele. With most mutations being recessive and requiring to be homozygous to show the phenotype, a self-cross is required to generate mutants which are suitable for a phenotypic screen.[116,123]

Once mutant individuals with the desired phenotype are identified, they are crossed with WT *Arabidopsis*. The progeny of this cross generates F_1, and this is the generation that will be used for identification of the causative mutation. In standard mapping procedures which rely on genetic markers, the crosses would involve different ecotypes to ensure a high density of these molecular markers, giving better resolution when mapping. The cross between WT ecotypes Col-0 and *Ler* are the most commonly used in genetic mapping due to the presence of divergent sequences in both, naturally resulting denser molecular markers in F_1 and increased mapping resolution.[116,124,125] With SHOREmapping, the causative mutation is identified through its frequency rather than through molecular markers and as such, the crosses are conducted with the same ecotype.

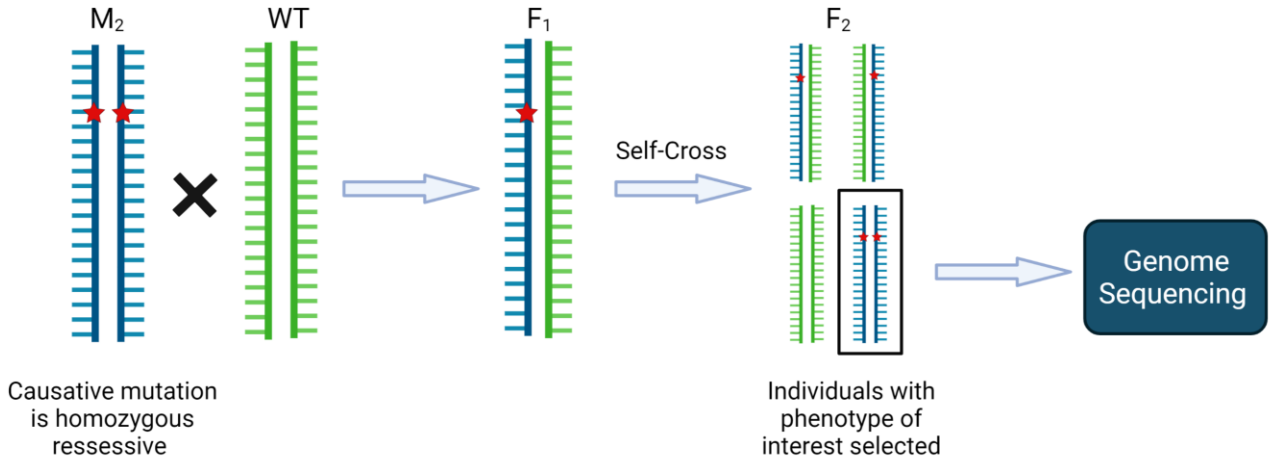

Figure 55: General procedure for identification of causative mutations using EMS libraries. Image adopted from Zhang *et al.*[124]

There are two fundamental stages in this forward genetics method that are critical to successfully identify the target gene; selection of mutants with the desired phenotype and the cross of these mutants with a WT Arabidopsis to generate F_1. Although multiple target genes are commonly identified, a report by Cuperus *et al*. demonstrate that with a robust phenotypic screen, the mutation can be linked to a single gene.[126] The introduction of false positives into the F_1 population creates noise and can result in non-relevant genes being identified as possible candidates.

Assuming the mutated gene of interest is homozygous in individuals displaying the desired phenotype, the progeny of WT and M_2 will display both the homozygous and heterozygous phenotype.[127] F_2 plants displaying the desired phenotype are selected and then sequenced. In brief, via next-generation sequencing, the sequence reads are filtered and computationally processed. Traditional mapping methods to identify were advantageous in that they were able to causative identify mutations of all forms including insertions and deletions of large DNA fragments but as mentioned above, were limiting in the

time took to carry out. SHOREmapping is a whole genome mapping method that significantly by simultaneously defining the mapping regions and identifying the genetic variants to identify mutations that occur with the greatest frequency.[128] As the screening process enriches the causative mutation, the mutation that occurs with the greatest frequency can be identified as the mutation of interest.

4.3 Workflow in Identification of eW5-insentitive Mutants

As the phenotype observed with eW5 treatment is growth promotion, mutant screening would select for individuals which do not display increased growth. It was proposed that sequencing of eW5-insensitive mutants would then allow for identification of the mutated gene of interest and ultimately the protein target(s) of eW5. Hypocotyl growth was chosen as the assay for this study due to its combination of replicability and ease of scale up, allowing for the high throughput screening of the mutants. Starting with EMS mutants obtained from the Farmer group at the Université de Lausanne, this mutant screen consisted of 4 generations: M_2, M_3, F_1, and F_2. M_2 and M_3 served as the screen to identify mutants displaying the phenotype of interest. M_2 serves as the initial screen where mutants displaying the dwarfed hypocotyl phenotype are selected and M3 serves as the control where the mutants are grown in eW5 and DMSO to confirm if the observed phenotype is a response to eW5 or other to other random mutations.

M_3 was then crossed with WT (*Col0*) *Arabidopsis* to give F_1 and to bulk up the product of this backcross, F_2 was grown to seed, affording F_3. A small proportion of each population underwent hygromycin selection. This was done to confirm if the crosses between M_3 and WT F_1 had taken. Hygromycin B is an aminoglycosidic antibiotic with broad spectrum activity against both procaryotic and eucaryotic cells. Its mode of action is through the inhibition of protein synthesis through the promotion of mistranslation and disrupting translocation in the 80S ribosome.[129] When grown in plates dosed with hygromycin, WT *Arabidopsis* seedlings will display short hypocotyls and are easily distinguished from hygromycin B-resistant seedlings which display long hypocotyls (0.2-0.4 cm against 0.8-1.0 cm depending on conditions).[130] With the original M_1 line of mutants containing a transgene for hygromycin B-resistance, F_1 populations which are the result of successful crosses should also contain this gene, providing a simple method to identify if the crosses had taken. Having confirmed the success of the crosses, F_2 plants displaying the desired phenotype were then selected and sequenced via next-generation sequencing.

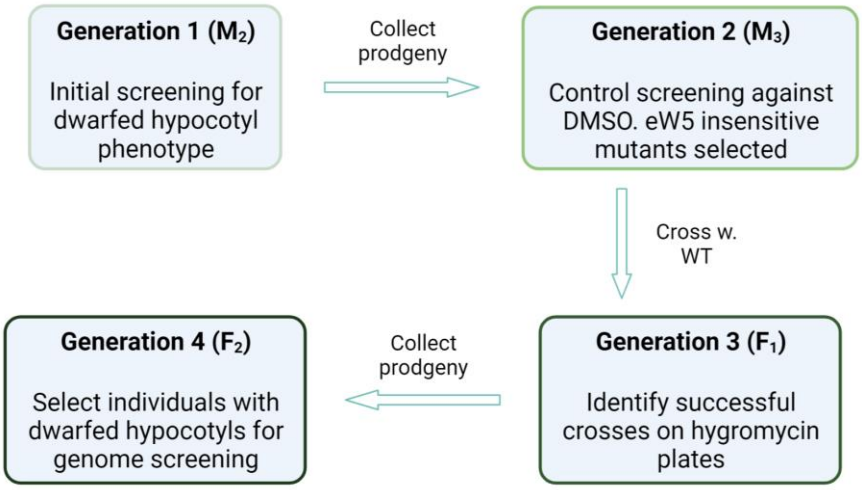

Figure 56: Workflow adopted for the identification of eW5 insensitive mutants and enrichment of causative mutation.

4.3.1. Generation 1 (M_2)

Prior to the initial screening for eW5-insensitive individuals in the M_2 population, the hypocotyl assay was first run on WT Arabidopsis at varying concentrations of eW5. This was to optimise the conditions for the initial screening for the desired phenotype ensuring that difference in hypocotyl length observed between eW5-insensitive mutants and the expected response was as large as possible.

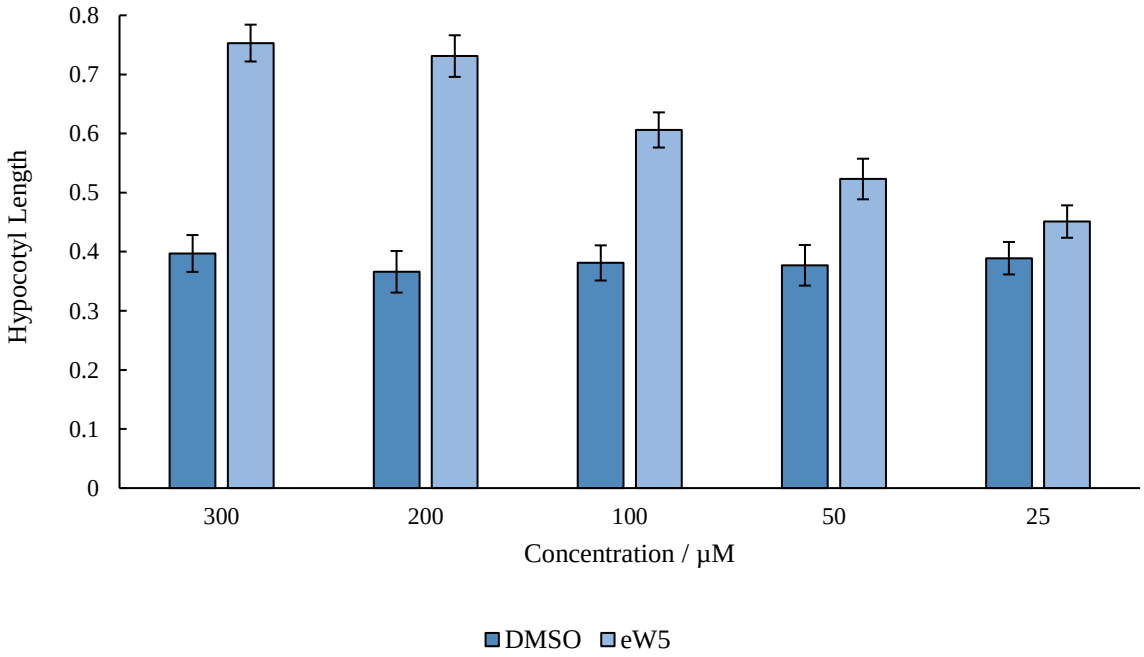

Figure 57: Hypocotyl growth of Arabidopsis treated with eW5 at varying concentrations. Values were calculated from three biological replicates. Error bars represent standard error from a population of at least 40 seedlings

Although dosing the agar plates at 300 µM eW5 gave the greatest absolute hypocotyl length values, hypocotyl growth promotion at this concentration was not significantly different to that observed at 200 µM. To better facilitate the high-throughput screen, 200 µM was chosen as the concentration of chemical treatment for the initial screening of mutants displaying the desired phenotype.

As reported in Lukowitz *et al*, when identifying a mutation through mapping, as few as 1000 individual mutants are required to identify a mutated gene of interest if there is a high density of molecular markers.[131] As SHOREmapping would be used as the method for the identification of a causative mutation, significantly more mutants were required to increase the frequency of the mutation within the population. In a study by Mercier et al, it reported that genome sequencing of 897 mutant lines showed an average of 696 homozygous mutations per line, of which 195 modified a protein sequence, resulting in over 170000 mutations.[132] Assuming the genome for Arabidopsis contains 25000 encoding genes, this ensures that each gene is being mutated roughly 6-7 times within the population.

Assuming a similar mutation rate, 114 pooled mutant lines (consisting of between 10-15 separate mutant lines each), roughly equates to each gene within the population being mutated 10 times. To account for the possibility of a lower absolute mutation rate, false-positives and negatives, loss of plant material and random variation, it was proposed that roughly 10 individual mutants per line would strike the balance between ensuring that the same gene is mutated several times throughout the population and the management of time and material resources. A total of 23684 individual seeds were tested. M_2 seeds were screened via the hypocotyl assay described in Section 2.6 at 200 µM of eW5. Individuals displaying the dwarfed hypocotyl phenotype were selected with the aim of not only selecting for the mutation responsible for eW5-resistance, but also for mutations that result in an inhibitory effect being observed.

Given vast amount of plant material, this screening of M_2 seeds was conducted over multiple trials. As with the hypocotyl assays in the investigation of the SAR of eW5, variation between the batches of M_2 mutants was observed. To account for this significant difference in the mean absolute hypocotyl lengths between various trials, a percentage, rather than an absolute value was chosen as the cut-off point for selection. Following imaging and measurement of the hypocotyls, the bottom 1.5% of mutants in each trial were selected. This extreme percentage was chosen to ensure that enough mutants were represented in the secondary screening for the desired phenotype, whilst again, managing the impact on time and human resources.

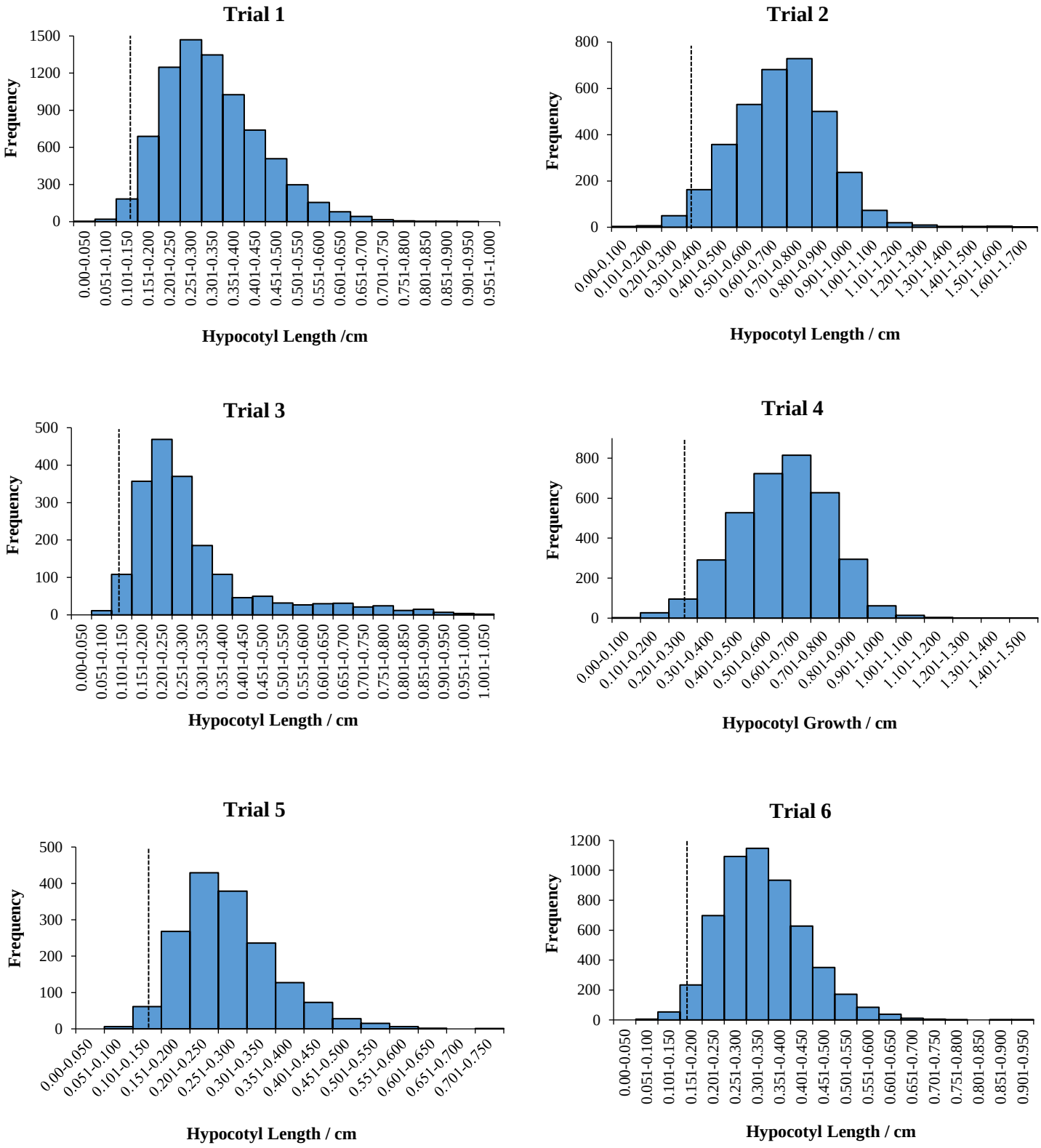

Figure 58: Hypocotyl lengths of 5-day old EMS mutant seedlings grown on agar plates treated with 200 µM eW5. Dashed lines represent 1.5th percentile.

A total of 317 individual mutants were selected and planted into peat plugs, grown to seed and the progeny (M_3) harvested. The progeny of 34 individual mutants were not collected due to primarily due to sterility issues that most likely arose from other induced mutations.

4.3.2 Generation 2 (M_3)

As hypocotyl growth is an amalgamation of various biological processes, a control would be required to determine if the dwarfed hypocotyl phenotype was a result of eW5-insensitivity. Given the population consisted of mutants, it was very likely that there would have been a greater portion of individuals displaying the dwarfed hypocotyl phenotype due to unrelated mutations, increasing the need for a separate screen to eliminate false positives. M_3 seeds were grown on two separate agar plates, one dosed with 200 µM eW5, and one DMSO control. Again, following the hypocotyl assay, the plates were imaged, and the hypocotyls measured. Individual mutants that yielded less than 30 seeds were discarded as the low population size complicated the statistical analysis and it was probable that a mutation related to fertility was involved.

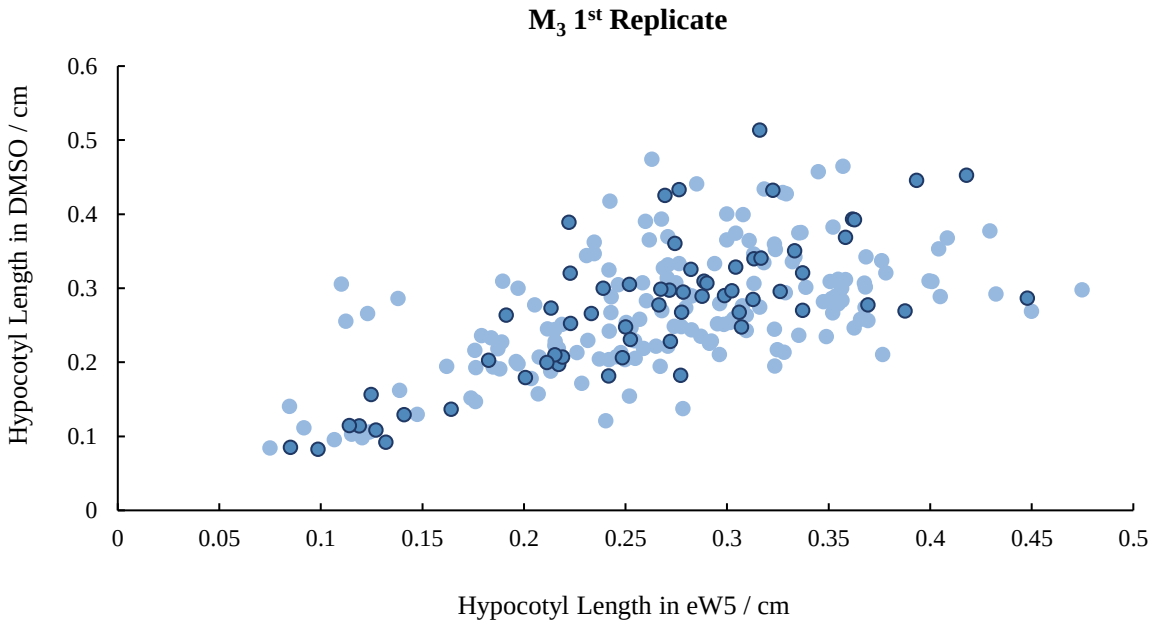

Figure 59: 1st replicate of M3 seed screening. Average hypocotyl lengths of individual mutant populations in eW5 (200 µM) and DMSO. Mean was determined by measurement of at least 15 seedlings. Dark blue points represent mutant populations selected as determined by statistical T-test; $p < 0.005$.

For individual mutants with mutations leading to eW5 insensitivity, it should be expected that there is no significant difference in hypocotyl length between chemical treatment with eW5 and the DMSO control. The statistical test chosen was the student T-test and the critical value chosen was 0.95, i.e., populations with values under this showed no significant difference in hypocotyl growth when treated with eW5 and DMSO and were thus selected. To further eliminate false positives from the mutant pool, the assay was repeated two more times. Individual mutants that yielded a T-value of under 0.95 over the 3 replicates were then selected and transferred to peat plugs. As 5 mutant populations would be taken forward for genome sequencing, it was proposed that ~2X this amount should be taken forward to account for unsuccessful crosses and loss of plant material. Thus, a total of 12 mutants were selected for the next stage of the screen.

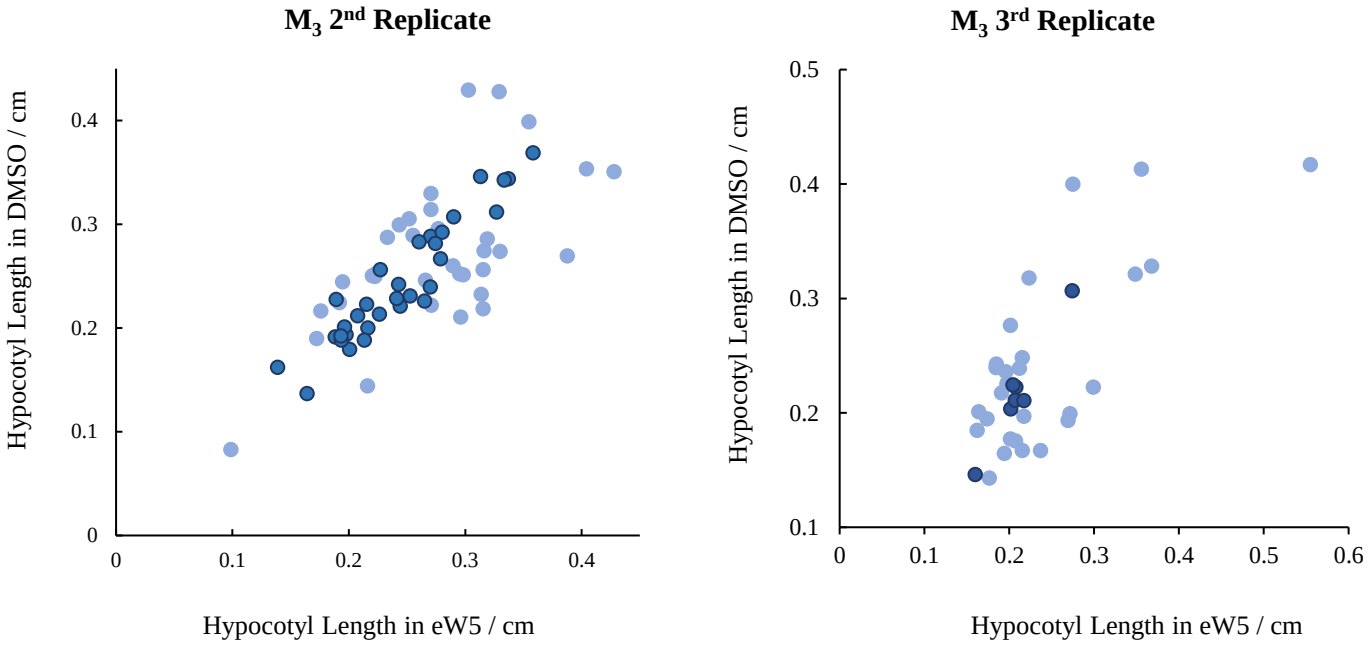

Figure 60: 2nd and 3rd replicates of M3 seed screening. Average hypocotyl lengths of individual mutant populations in eW5 (200 µM) and DMSO. Mean was determined by measurement of at least 15 seedlings. Dark blue points represent mutant populations selected as determined by statistical T-test; $p < 0.005$.

4.3.3: Generation 3 (F_1)

Having selected eW5-insensitive mutants, the next step of the screen was to backcross the mutants with WT *Arabidopsis*. Budding flowers of WT *Arabidopsis* were emasculated and pollinated by the respective mutants. Successful crosses generated a seed pod which was then harvested to afford F_1 seeds. F_2 seeds were then planted directly into peat plugs and allowed to self-pollinate to generate F_2 seeds.

4.3.4 Generation 4 (F_2)

Following the harvesting of F_2 seeds, the final stage of the screen was to identify mutants for genome sequencing. The first step was to confirm the harvested seeds were the product of a backcross between the mutants and the WT. This was done via hygromycin selection by growing the mutant seedlings on agar plates dosed with hygromycin. Following an initial period of 6 hours of light exposure, the plates were wrapped in foil and left for 5 days. The foil was removed, and the mutant seedlings were left to grow in standard conditions. Following 5 days of growth, the mutant populations were compared against a WT control. Comparison showed that all of the mutant populations grew significantly better than WT on hygromycin plates, indicating that the mutant populations were truly hygromycin resistant and that the confirming the crosses between the paternal mutants and maternal WT had taken.

As mentioned above, the assumption was that the gene mutations of interest are loss-of-function single-allele recessive, meaning that 25% of the mutants from the progeny of the backcross would be homozygous recessive. As these mutations would result in the phenotype of eW5-insensitivity, individuals with the smallest hypocotyls would be selected for genome sequencing. Choosing the lower quartile of mutants assumes perfect selection and could result in the selection of false positives. Thus, a higher threshold of 10% was chosen as the selection criterion for individual mutants for genome sequencing. F_2 seeds were grown on agar plates dosed with 200 μM eW5 for 5 days in reduced light, the hypocotyls imaged and measured and the bottom 10% of seedlings were selected. This process was repeated until roughly 100 seedlings per mutant population were obtained.

Next-generation sequencing was chosen for its ability to sequence genomes rapidly. This is done through the parallel sequencing of millions of small fragments of DNA which are then pieced back together using bioinformatic analysis. Through SHOREmapping, a combined mixture of genomes from one single mutant is sequenced and the mutations mapped according to frequency. By selecting seedlings with dwarfed hypocotyls, the causative mutation has been "enriched" for and thus would be present at a much higher frequency (close to 100%), assuming the screening process allowed for perfect selection of the causative mutation. Next-generation sequencing was conducted by Novagene.

4.3.5: Conclusions and Future Work

This chapter outlined the methodology undertaken to identify individuals with a phenotype of interest from an EMS mutant library. The series of initial set of screens selected for 12 eW5-insensitive mutants from a starting pool of over 23,000 seeds. Backcrossing these mutants with WT *Arabidopsis* was

confirmed through hygromycin selection and individuals displaying dwarfed hypocotyls when grown in eW5 were selected for genome sequencing.

Following analysis of genomic data and identification of mutated gene(s) of interest, future work could include gene knockout experiments. These constructs can be created through various gene editing technologies such as CRIPSR/CAS9 and would allow for confirmation that mutation in this gene is causative.

Chapter 5: Experimental

5.1: Biological Procedures

5.1.1: Plant Material

Arabidopsis thaliana wild-type seeds were from laboratory lab stocks of the Columbia (Col-0) and Landsberg erecta (Ler-0). The A. thaliana line expressing RGA-GFP seeds were obtained from Prof. Keith Lindsey (Durham University, UK).

5.1.2: Hypocotyl Assay

Arabidopsis seeds were grown on solid 1 X MS medium agar plates (Murashige and Skoog, 1962). The medium was adjusted to pH 5.8 using 0.1M KOH before adding 8 g of plant tissue culture agar (Sigma-Aldrich, Poole, UK). The medium was then sterilized by autoclaving for 20 minutes at 121 °C, at 10^5 Pa pressure. For the chemically dosed plates, 1.2% (w/v) plant agar was used. Addition of the chemicals was performed following the cooling of MS media to (50 °C). *Arabidopsis* seeds were sterilized in 1 mL 70% ethanol (v/v) by shaking (Labnet Vortex Mixer, Labnet International Inc., Woodbridge, New Jersey, USA) for 5 minutes before being transferred to Whatman filter paper (Whatman^{TM} International Ltd, Kent, UK). The seeds were air-dried in a laminar flow hood before being spread onto solid MS growth medium.

Sterilised seeds were stratified at 4 ℃ for a minimum of 48 hr to achieve synchronous germination. The seeds were then grown vertically wrapped in 4 sheets of A4 paper in a Percival (CU-36L5D, CLF plant climatics, Emersacker, Germany) with a photoperiod of 16/8 h at a light intensity of 150 μmol m^2 s^{-1} and a temperature of 20 ± 1 ℃. Plates were imaged following 5 days of growth using a scanner and hypocotyls were measured using ImageJ software.

5.1.3: RGA-GFP Della assay

GFP:RGA seeds were germinated and grown on 1.2% MS vertically. After 7 days, the seedlings were incubated in chemical solution (at the final concentration of 100 μM). The seedlings were then imaged according to time point of 2h and 24 h. The microscope used was Leica SP5 CLSM FLIM FCCS (Leica Microsystems, Wetzlar, Germany). The laser was Argon, excitation 488 nm (blue) and used at 50%

intensity. Emission spectra were collected through a 585 nm long pass filter. Images were processed using Zen (blue) software.

5.1.4: Hygromycin Selection

Agar medium was prepared in accordance with the procedure outlined in Section 5.1.1. The agar medium was left to cool to 55 ℃ before Hygromycin B was added to make up a final concentration of 40 μg/mL. Seeds were spread onto the solid MS growth medium and stratified in line Section 5.1.1. Following 48-hours, the plates were sealed and exposed to light in the Percival (CU-36L5D, CLF plant climatics, Emersacker, Germany) for 30-minutes. The plates were wrapped in foil and left at this condition for 5d after which the foil was unwrapped. The plates were observed over the following 7-days for germination and growth.

5.2: Chemical Procedures

General Procedure A: Sulfonamide synthesis from sulfonyl chlorides

A DCM solution of the starting sulfonyl chloride was added to a solution of triethylamine (1.20 eq) and the starting amine (1.20 eq) in DCM. The reaction mixture was stirred for 3 hours at room temperature and quenched with 1M $NaHCO_{3\,(aq)}$. Extraction was conducted with DCM (3 x 5 mL) and the combined organic layers were dried over $MgSO_4$ and concentrated. Purification by flash chromatography using the stated solvent system yielded the title compound.

General Procedure B: Boc-deprotection of Boc carbamates

4M HCl in dioxane (1.0 mL) was added to a vial containing the starting Boc-protected compound. The reaction was allowed to stir at room temperature for 3 hours after which volatiles were evaporated to afford the title compound.

General Procedure C: Phenol alkylation

K_2CO_3 (4.00 eq) was added in portions to an acetonitrile solution (0.40 M) of the stated phenol/naphthol/hydroxyaromatic (1.00 eq). The corresponding alkyl halide (4.00 eq) was then added dropwise and the reaction mixture was left to stir under reflux for 16 hours. The reaction mixture was

quenched with sat $NaHCO_{3(aq)}$. Separation of layers and extraction of the aqueous fraction afforded the crude product which was purified as described.

General Procedure D: Formation of sulphonamides from aromatic bromides

n-BuLi (1.10 eq) was added to a solution of the aryl-bromide (1.00 eq), in dry THF (0.2 M) at –78 °C under N_2. The mixture was stirred for 20 min at -78 °C when sulfuryl chloride (1.50 eq) was added. The reaction mixture was then stirred for 30 min at 0 °C after which it was allowed to reach ambient temperature and stirred for a further 1 hour. The reaction was then quenched with ice water, layers separated and the aqueous fraction extracted with Et_2O. The combined organic layers were then dried over $MgSO_4$ and concentrated. The resulting crude sulfonyl chloride intermediate used without further purification, dissolved in DCM and added dropwise to a mixture of N-boc ethylene diamine (1.50 eq) and triethylamine (1.50 eq) in DCM (0.3 M). The reaction was stirred at room temperature for 3 hours before being quenched with sat. $NaHCO_{3(aq)}$, separated and the aqueous fraction extracted with stated solvent. Combined organic layers were dried over $MgSO_4$, concentrated and purified as described.

74. *tert-butyl N-[2'-(naphthalene-1-sulfonamido)ethyl]carbamate*

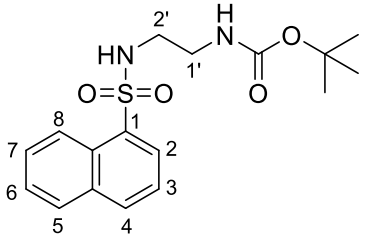

Compound was synthesized according to general procedure D using *1-bromonaphthalene* **93** (1040 mg, 5.00 mmol, 1.00 eq)) and *N-Boc ethylenediamine* (9.50 mL, 6.00 mmol, 1.20 eq). Following separation of the layers, the aqueous layer was extracted with DCM (3 x 20 ml), concentrated and purified by recrystallization (Hex in $CHCl_3$) to yield the title compound as an off-white solid (537 mg, 1.53 mmol, 31%). M.p.: 139-145°C. δ_H (700 MHz, $CDCl_3$) 8.65 – 8.61 (1H, m, 5–H), 8.24 (1H, dd, *J* = 7.3, 1.2, 2–H), 8.07 (1H, dd, *J* = 8.2, 1.2, 4–H), 7.97 – 7.92 (1H, m, 8–H), 7.68 (1H, ddd, *J* = 8.5, 6.9, 1.4, 6–H), 7.60 (1H ddd, *J* = 8.0, 6.9, 1.1, 7–H), 7.54 (1H, dd, *J* = 8.2, 7.3, 3–H), 5.31 (1H, s, 2'–N*H*), 4.70 (1H, s, 1'–N_H), 3.15 (2H, q, *J* = 5.7 Hz, 2'–H_2), 3.01 (1H, q, *J* = 5.7 Hz, 1'–H_2), 1.38 (9H, s, –(CH_3)$_3$). δ_C (176 MHz, $CDCl_3$) 156.2 (C=O), 135.5 (C–2), 134.3 (C–1), 132.9 (C–4a), 129.6 (C–5), 129.1 (C–4), 128.5 (C–7), 126.9 (C–8), 124.3 (C–8a), 124.1 (C–6), 123.3 (C–3), 79.8 (–*C*(CH_3)$_3$), 43.8 (C–2'), 40.7 (C–1'), 28.3 (–(*C*H_3)$_3$). ν_{max} (ATR) 3301 (N–H), 2982, 2928, 2252, 1694 (C=O), 1511, 1316, 1246, 1160, 900 cm^{-1}. *m/z* (LC-MS ESI+) 351.44 $[M+H]^+$, 297.47 [M–*tBu*+2H]$^+$. Data agrees with that as reported in Sukiran.[102]

1. *N-(2-aminoethyl)naphthalene-1-sulfonamide hydroch*loride

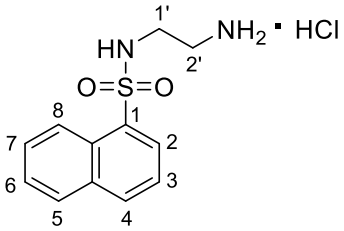

Compound was prepared according to general procedure B using *tert-butyl N-[2'-(naphthalene-1-sulfonamido)ethyl]carbamate* **74** (50mg, 0.143mmol) to yield the title compound as a white solid (39mg, 0.136mmol, 96%). m.p. 178–179 ºC. δ_H (400 MHz, D_2O) 8.36 (1H, dq, *J* = 8.6, 0.9 Hz, 5–H), 8.04 (2H, m, 2–H, 4–H), 7.90 (1H, dd, *J* = 8.1, 1.5 Hz , 8–H), 7.62 (1H, ddd, *J* = 8.6, 6.9, 1.5 Hz, 6–H), 7.54 (1H, ddd, *J* = 8.1, 6.9, 0.9 Hz, 7–H), 7.45 (1H, dd, *J* = 8.3, 7.4 Hz, 3–H), 2.97 (4H, d, *J* = 1.8 Hz, 2'–H_2, 1'–H_2). δ_C (101 MHz, D_2O) 135.2 (C–2), 134.0 (C–1), 131.9 (C–4a), 129.8 (C–5), 129.4 (C–4), 128.7 (C–7), 127.2 (C–8), 127.0 (C–8a), 124.3 (C–6), 123.2 (C–3), 39.7 (C–2'), 39.1 (C–1'). ν_{max} (ATR) 3302 (N–H), 3221 (N–H), 2988, 2945, 1595, 1508, 1243, 1129, 1026, 961 cm^{-1}. *m/z* (LC-MS ESI+) 251.26 $[M+H]^+$, 501.48 $[2M+H]^+$. Data agrees with that as reported in Sukiran.[102]

75a. *tert-butyl N-[2'-(naphthalene-2-sulfonamido)ethyl]carbamate*

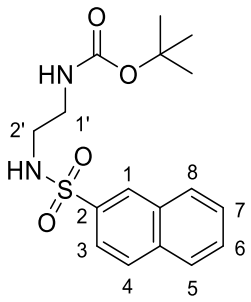

Compound was prepared according to general procedure A using *naphthlene-2-sulfonyl chloride* (50.0 mg, 0.221 mmol, 1.00 eq) and *N-Boc ethylenediamine* (0.042 mL, 0.265 mmol, 1.20 eq). Purification by column chromatography (EtOAc in Hex 0-50%) yielded the title compound as a white amorphous solid (54.9 mg, 0.157 mmol, 71%). δ_H (400 MHz, $CDCl_3$) 8.45 (1H, d, *J* = 1.8 Hz, 1–H), 7.98-7.96 (2H, m, 5–H, 3–H), 7.94 – 7.89 (1H, m, 4–H), 7.85 (1H, dd, *J* = 8.7, 1.9 Hz, 8–H), 7.70 – 7.58 (2H, m, 6–H, 7–H), 5.63 (1H, s, 2'–N*H*), 4.97 (1H, s, 1'–N*H*), 3.25 (2H, t, *J* = 5.8 Hz, 2'–H_2), 3.11 (2H. t, *J* = 5.8 Hz, 1'–H_2), 1.41 (9H, s, –C(CH_3)$_3$). δ_C (101 MHz, $CDCl_3$) 156.6 (C=O), 136.6 (C–2), 134.8 (C–8a), 132.2 (C–4a), 129.6 (C–1), 129.3 (C–5), 128.8 (C–4), 128.4 (C–3), 127.9 (C–8), 127.6 (C–7), 122.3 (C–6), 79.9 (–*C*(CH_3)$_3$), 43.9 (C–2'), 40.3 (C–1'), 28.3 (–(*C*H_3)$_3$). ν_{max} (ATR) 3374 (N–H), 3296 (N–H), 2984, 1680 (C=O), 1513, 1326, 1152, 1087 cm^{-1}. *m/z* (LC-MS ESI+) 251.257 $[M–Boc+H]^+$, 295.305 $[M–tBu+2H]^+$, 351.362 $[M+H]^+$.

75. *N-(2'-aminoethyl)naphthalene-2-sulfonamide hydrochloride*

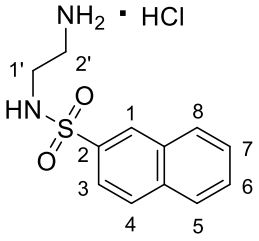

Compound was prepared according to general procedure B, starting with *tert-butyl N-[2'-(naphthalene-2-sulfonamido)ethyl]carbamate* **75a** (20.0 mg, 0.057 mmol, 1.00 eq) to yield the title compound as a white amorphous solid (14.8 mg, 0.052 mmol, 90%). δ_H (400 MHz, MeOD) 8.49 (1H, d, *J* = 1.7 Hz, 1–H), 8.17 – 8.04 (2H, m, 5–H, 3–H), 8.04 – 7.96 (1H, m, 4–H), 7.89 (1H, dd, *J* = 8.5, 1.7 Hz, 8–H), 7.75 – 7.59 (2H, m, 6–H, 7–H), 3.12 (4H, m, 2'–H, 1'–H). δ_C (101 MHz, MeOD) 136.3 (C–2), 135.0 (C–8a), 132.2 (C–4a), 129.5 (C–1), 128.9 (C–5), 128.7 (C–4), 128.1 (C–3), 127.7 (C–8), 127.5 (C–7), 122.0 (C–6) 40.1 (C–2'), 39.4 (C–1'). ν_{max} (ATR) 3268 (*b*, N–H), 3056, 2871, 1584, 1499, 1343, 1149, 1070, 1020 cm^{-1}. *m/z* (LC-MS ESI+) 251.257 $[M+H]^+$, 501.437 $[2M+H]^+$. Accurate mass (ES+) found $[M+H]^+$ 251.0871, $C_{12}H_{15}N_2O_2S$ requires *M* 251.0854.

76a. *tert-butyl N-[2'-(2-fluorobenzenesulfonamido)ethyl]carbamate*

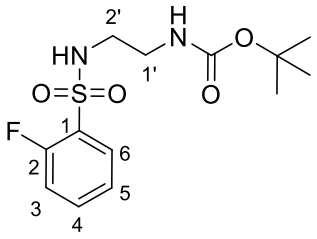

Compound was prepared according to general procedure A using *2-fluorobenzene-1-sulfonyl chloride* (50.0 mg, 0.257 mmol, 1.00 eq) and *N-Boc ethylenediamine* (0.049 mL, 0.308 mmol, 1.20 eq). Purification by column chromatography (EtOAc in Hex 0-50%) yielded the title compound as an off white amorphous solid (66.7 mg, 0.210 mmol, 82%). δ_H (400 MHz, $CDCl_3$) 7.91 (1H, td, *J* = 7.5, 1.8 Hz, 3–H), 7.65 – 7.53 (1H, m, 6–H), 7.35 – 7.27 (1H, m, 4–H), 7.23 (1H, ddd, *J* = 10.2, 8.3, 1.8 Hz, 5–H), 5.42 (1H, s, 2'–NH), 4.88 (1H, s, 2'–NH), 3.28 (2H, t, *J* = 5.8 Hz, 2'–H_2), 3.14 (2H, t, *J* = 5.8 Hz, 1'–H_2), 1.45 (9H, s, –C(CH_3)$_3$). δ_C (101 MHz, $CDCl_3$) 158.7 (d, *J* = 253.0 Hz, C–2), 156.4 (C=O), 135.0 (d, *J* = 8.9 Hz, C–4), 128.6 (C–5), 127.8 (d, *J* = 15.1 Hz, C–1), 124.5 (d, *J* = 4.0 Hz, C–6), 117.0 (d, *J* = 20.3 Hz, C–3), 80.0 (–*C*(CH_3)$_3$), 43.7 (C–2'), 40.4 (C–1'), 28.3 (–(*C*H_3)$_3$). δ_F (376 MHz, $CDCl_3$) –110.45. ν_{max} (ATR) 3371 (N–H), 3300 (N–H), 2977, 1691 (C=O), 1524, 1474, 1336, 1266, 1152, cm^{-1}. *m/z* (LC-MS ESI+) 219.256 $[M–Boc+H]^+$, 263.266 $[M–tBu+2H]^+$, 319.418 $[M+H]^+$. Accurate mass (ES+) found $[M+H]^+$ 319.1113, $C_{13}H_{20}N_2O_4SF$ requires *M* 319.1128.

76. *N-(2'-aminoethyl)-2-fluorobenzene-1-sulfonamide hydrochloride*

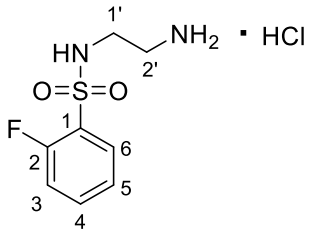

Compound was prepared according to general procedure B, using *tert-butyl N-[2'-(2-fluorobenzenesulfonamido)ethyl]carbamate* **76a** (20.0 mg, 0.063 mmol, 1.00 eq) to yield the title compound as a light yellow amorphous solid (16.0 mg, 0.063 mmol, 100.0%). δ_H (400 MHz, MeOD) 7.92 (1H, td, *J* = 7.6, 1.7 Hz, 3–H), 7.80 – 7.62 (1H m, 6–H), 7.46 – 7.28 (2H, m, 4–H, 5–H), 3.22 (2H, t, *J* = 5.7 Hz, 2'–H_2), 3.08 (2H, t, *J* = 5.7 Hz, 1'–H_2). δ_C (101 MHz, MeOD) 158.9 (d, *J* = 254.7 Hz, C–2) 135.4 (d, *J* = 8.8 Hz, C–4), 130.05 (C–5), 127.4 (d, *J* = 16.5 Hz, C–1), 124.5 (d, *J* = 4.0 Hz, C–6), 116.9 (d, *J* = 22.6 Hz, C–3), 39.9 (C–2'), 39.5 (C–1'). δ_F (376 MHz, MeOD) –111.84. ν_{max} (ATR) 3389 (*b*, N–H), 3077, 2861, 1598, 1513, 1474, 1336, 1144 cm^{-1}. *m/z* (LC-MS ESI+) 219.218 $[M+H]^+$, 437.403 $[2M+H]^+$. Accurate mass (ES+) found $[M+H]^+$ 219.0592, $C_8H_{12}N_2O_2SF$ requires *M* 219.0604.

77a. *tert-butyl N-[2-(3-fluorobenzenesulfonamido)ethyl]carbamate*

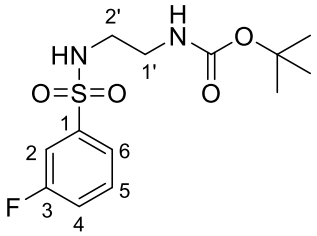

Compound was prepared according to general procedure A using *3-fluorobenzene-1-sulfonyl chloride* (50.0 mg, 0.257 mmol, 1.00 eq) and *N-Boc ethylenediamine* (0.049 mL, 0.308 mmol, 1.20 eq). Purification by column chromatography (EtOAc in Hex 0-50%) yielded the title compound as a white amorphous solid (45.1 mg, 0.142 mmol, 55%). δ_H (400 MHz, $CDCl_3$) 7.65 (1H, dt, *J* = 7.8, 1.7 Hz, 6–H), 7.56 (1H, ddd, *J* = 8.2, 2.6, 1.7 Hz, 4–H), 7.50 (1H, td, *J* = 8.2, 7.8 Hz, 5–H), 7.31 – 7.22 (1H, m, 2-H), 5.61 (1H, s, 2'–NH), 4.90 (1H, s, 1'–NH), 3.24 (2H, q, *J* = 5.5 Hz, 2'–H_2), 3.08 (2H, q, *J* = 5.5 Hz, 1'–H_2), 1.42 (9H, s, –C(CH_3)$_3$). δ_C (101 MHz, $CDCl_3$) 162.5 (d, *J* = 250.5 Hz, C–3), 156.8 (–C=O), 141.9 (d, *J* = 6.9 Hz, C–1), 130.0 (d, *J* = 7.9 Hz, C–5), 122.8, (d, *J* = 3.8 Hz, C–6) 119.9 (d, *J* = 22.3 Hz, C–2), 114.4 (d, *J* = 24.4 Hz, C–4), 80.2 (–*C*(CH_3)$_3$), 44.03 (C–2'), 40.22 (C–1'), 28.3 (–(*C*H_3)$_3$). δ_F (376 MHz, $CDCl_3$) –109.55. ν_{max} (ATR) 3356 (N–H), 3283 (N–H), 2981, 1688 (C=O), 1524, 1279, 1219, 1152, 1081 cm^{-1}. *m/z* (LC-MS ESI+) 219.108 $[M–Boc+H]^+$, 263.266 $[M–tBu+2H]^+$, 319.324 $[M+H]^+$. Accurate mass (ES+) found $[M+H]^+$ 319.1118, $C_{13}H_{20}N_2O_4SF$ requires *M* 319.1128.

77. *N-(2'-aminoethyl)-3-fluorobenzene-1-sulfonamide hydrochloride*

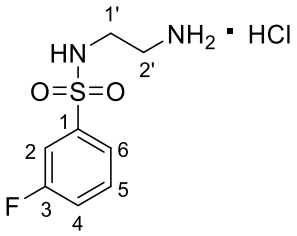

Compound was prepared through general procedure B, using *tert-butyl N-[2'-(3-fluorobenzenesulfonamido)ethyl]carbamate* **77a** (20.0 mg, 0.063 mmol, 1.00 eq) to yield the title compound as an off white amorphous solid (15.8 mg, 0.062 mmol, 99%). δ_H (400 MHz, MeOD) 7.82 – 7.56 (3H, m, 6–H, 4–H, 5–H), 7.44 (1H, m, 2–H), 3.10 (4H, m, 2'–H_2, 1'–H_2). δ_C (101 MHz, MeOD) 162.6 (d, *J* = 248.1 Hz, C–3), 141.7 (d, *J* = 6.4 Hz, C–1), 131.4 (d, *J* = 8.0 Hz, C–5), 122.9 (d, *J* = 2.8 Hz, C–6), 119.7 (d, *J* = 21.3 Hz, C–2), 114.9 (d, *J* = 24.5 Hz, C–4), 40.23 (C–2'), 39.62 (C–1'). δ_F (376 MHz, MeOD) –111.97. ν_{max} (ATR) 3283 (*b*, N–H), 3066, 2977, 2857, 1591, 1457, 1327, 1149, 1064, 1025, 966 cm^{-1}. *m/z* (LC-MS ESI+) 219.218 $[M+H]^+$, 437.441 $[2M+H]^+$. Accurate mass (ES+) found $[M+H]^+$ 219.0603, $C_8H_{12}N_2O_2SF$ requires *M* 219.0604.

78a. *tert-butyl N-[2'-(4-nitrobenzenesulfonamido)ethyl]carbamate*

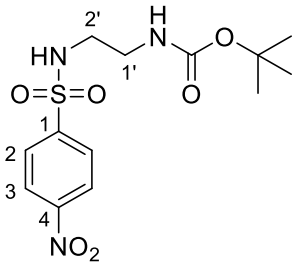

Compound was prepared according to general procedure A *using 4-nitrobenzene-1-sulfonyl chloride* (50.0 mg, 0.226 mmol, 1.00 eq) and *N-Boc ethylenediamine* (0.043 mL, 0.271 mmol, 1.20 eq). Purification by column chromatography (EtOAc in Hex 0-50%) yielded the title compound as a white amorphous solid (45.1 mg, 0.142 mmol, 55%). δ_H (400 MHz, $CDCl_3$) ^{1}H NMR (400 MHz, $CDCl_3$) δ 8.50 – 8.26 (2H, m, 3–H), 8.16 – 8.01 (2H, m, 2–H), 5.83 (1H, s, 2'–N*H*), 4.85 (1H, m, 1'–N*H*), 3.27 (2H, t, *J* = 6.2 Hz, 2'–H_2), 3.20 – 3.07 (2H, t, *J* = 6.2 Hz, 1'–H_2), 1.45 (9H, s, –C(CH_3)$_3$). δ_C (101 MHz, $CDCl_3$) 157.1 (C=O), 150.0 (C–4), 145.9 (C–1). 128.3 (C–3), 124.4 (C–2), 80.5 (–*C*(CH_3)$_3$), 44.5 (C–2'), 40.2 (C–1), 28.8 (–C(*C*H_3)$_3$). ν_{max} (ATR) 3356 (N–H), 3271 (N–H), 2984, 1676 (C=O), 1528, 1336, 1269, 1155, 1084, cm^{-1}. *m/z* (LC-MS ESI+) 246.240 $[M–Boc+H]^+$, 290.288 $[M–tBu+2H]^+$, 346.383 $[M+H]^+$.

78. *N-(2'-aminoethyl)-4-nitrobenzene-1-sulfonamide hydrochloride*

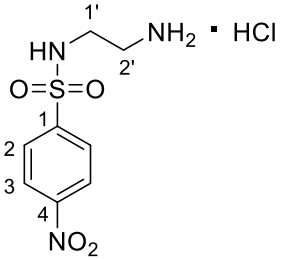

Compound was prepared according to general procedure B, starting with *tert-butyl N-[2'-(4-nitrobenzenesulfonamido)ethyl]carbamate* **78a** (20.0 mg, 0.058 mmol, 1.00 eq) to yield the title compound as a light green solid (16.0 mg, 0.057 mmol, 98%). δ_H (400 MHz, MeOD) 8.44 (2H, d, J = 8.3 Hz, 3–H), 8.13 (2H, d, J = 8.3 Hz, 2–H), 3.13 (4H, m, 2'–H_2, 1'–H_2). δ_C (101 MHz, MeOD) 150.3 (C–4), 145.3 (C–1), 128.31 (C–3), 124.24 (C–2), 40.12 (C–2'), 39.4 (C–1'). ν_{max} (ATR) 3399 (*b*, N–H), 3214, 3044, 2964, 2882, 1606, 1541, 1336, 1152, 1084, 1020, 850 cm^{-1}. *m/z* (LC-MS ESI+) 246.240 $[M+H]^+$. Accurate mass (ES+) found $[M+H]^+$ 246.0546, $C_8H_{12}N_3O_4S$ requires *M* 246.0549.

79a. tert-butyl N-[2-(4-tert-butylbenzenesulfonamido)ethyl]carbamate

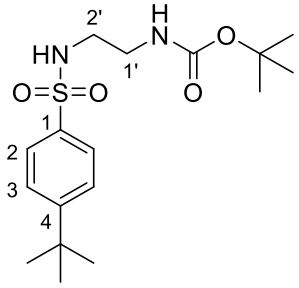

Compound was prepared according to general procedure A using *3-fluorobenzene-1-sulfonyl chloride* (50.0 mg, 0.257 mmol, 1.00 eq) and *N-Boc ethylenediamine* (0.049 mL, 0.308 mmol, 1.20 eq). Purification by column chromatography (EtOAc in Hex 0-50%) yielded the title compound as a white amorphous solid (45.1 mg, 0.142 mmol, 55%). δ_H (400 MHz, $CDCl_3$) 7.86 – 7.72 (2H, m, 2–H_2), 7.63 – 7.43 (2H, m, 3–H_2), 5.38 (1H, s, 2'–N*H*), 4.99 (1H, s, 1'–N*H*), 3.26 (2H, q, J = 5.8 Hz, 2'–H_2), 3.08 (1H, q, J = 5.8 Hz, 1'–H_2), 1.43 (9H, s, –OC(CH_3)$_3$), 1.36 (9H, s, –ArC(CH_3)$_3$). δ_C (101 MHz, $CDCl_3$) 156.5 (C=O), 165.5 (C–1) 136.7 (C–4), 126.9 (C–2), 126.2 (C–3), 79.8 (–O*C*(CH$_3$)$_3$), 43.6 (C–2'), 40.3 (C–1'), 35.2 (–Ar*C*(CH$_3$)$_3$), 31.1 (–ArC(*C*H$_3$)$_3$), 28.4 (–OC(*C*H$_3$)$_3$). ν_{max} (ATR) 3396 (N–H), 3233 (N–H), 2959, 1698 (C=O), 1524, 1326, 1247, 1159, 1067, 985 cm^{-1}. *m/z* (LC-MS ESI+) 257.338 [M–Boc+H]$^+$, 301.386 [M–*tBu*+2H]$^+$, 357.405 $[M+H]^+$. Accurate mass (ES+) found $[M+H]^+$ 357.1857, $C_{17}H_{29}N_2O_4S$ requires *M* 357.1848.

79. N-(2'-aminoethyl)-4-tert-butylbenzene-1-sulfonamide hydrochloride

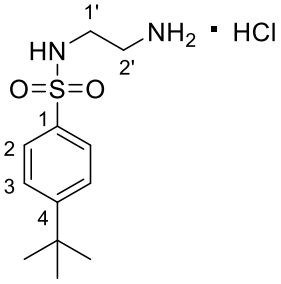

Compound was prepared according to general procedure B, using *tert-butyl N-[2'-(4-tert-butylbenzenesulfonamido)ethyl]carbamate* **79a** (20.0 mg, 0.056 mmol, 1.00 eq) to yield the title compound as a light yellow amorphous solid (13.3 mg, 0.045 mmol, 81.0%). δ_H (400 MHz, MeOD) 7.83 (2H, d, *J* = 8.2 Hz, 2–H), 7.66 (2H, d, *J* = 8.2 Hz, 3–H), 3.17 – 3.02 (4H, m, 2'–H_2, 1'–H_2), 1.37 (9H, s, –*tBu*). δ_C (101 MHz, MeOD) 156.6 (C–1), 136.5 (C–4), 126.7 (C–2), 126.1 (C–3), 40.0 (C–2'), 39.4 (C–1'), 34.7 (–*C*$(CH_3)_3$), 30.1 (–C(*C*$H_3)_3$). ν_{max} (ATR) 3041 (*b*, N–H), 2959, 2864, 1598, 1474, 1311, 1152, 1092, 1031 cm^{-1}. *m/z* (LC-MS ESI+) 257.300 $[M+H]^+$, 513.522 $[2M+H]^+$. Accurate mass (ES+) found $[M+H]^+$ 257.1329, $C_{12}H_{21}N_2O_2S$ requires *M* 257.1324.

80a. *tert-butyl N-(2'-{[1,1''-biphenyl]-4-sulfonamido}ethyl)carbamate*

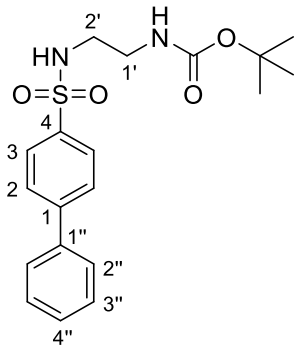

Compound was prepared according to general procedure A using *[1,1'-biphenyl]-4-sulfonyl chloride* (50.0 mg, 0.198 mmol, 1.00 eq) and *N-Boc ethylenediamine* (0.038 mL, 0.237 mmol, 1.20 eq). Purification by column chromatography (EtOAc in Hex 0-60%) yielded the title compound as a white amorphous solid (55.1 mg, 0.146 mmol, 74%). δ_H (400 MHz, $CDCl_3$) 7.96 – 7.92 (2H, m, 2''–H), 7.74 – 7.71 (2H, m, 3''–H), 7.63 – 7.60 (2H, m, 3–H), 7.52 – 7.48 (2H, m, 2–H), 7.47 – 7.42 (2H, m, 4''–H_2, 3–H_2), 5.51 (1H, s, 2'–N*H*), 4.99 (1H, s, 1'–N*H*), 3.29 (2H, t, *J* = 5.8 Hz, 2'–H_2), 3.13 (2H, t, *J* = 5.8 Hz, 1'–H_2), 1.44 (9H, s, –(C$H_3)_3$). δ_C (101 MHz, $CDCl_3$) ^{13}C NMR (101 MHz, $CDCl_3$) 156.6 (C=O), 145.6 (C–4), 139.3 (C–1'), 138.3 (C–1''), 129.1 (C–3), 128.5 (C–4''), 127.8 (C–2), 127.6 (C–2''), 127.3 (C–3''), 80.0 (–*C*$(CH_3)_3$), 43.8 (C–2'), 40.3 (C–1'), 28.4 (–(*C*$H_3)_3$). ν_{max} (ATR) 3361 (N–H), 3279 (N–H), 2984, 1683 (C=O), 1524, 1322, 1276, 1155, 1097, cm^{-1}. *m/z* (LC-MS ESI+) 277.328 [M–

Boc+H]$^+$, 321.338 [M–*tBu*+2H]$^+$, 377.357 [M+H]$^+$. Accurate mass (ES+) found [M+H]$^+$ 377.1534, $C_{19}H_{25}N_2O_4S$ requires *M* 377.1535.

80. *N-(2'-aminoethyl)-[1,1''-biphenyl]-4-sulfonamide hydrochloride*

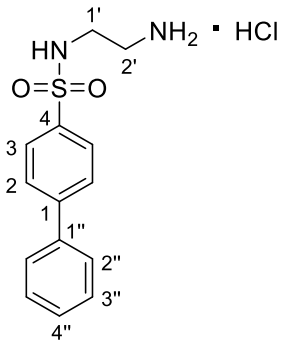

Compound was prepared according to general procedure B, starting with tert-butyl N-(2'-{[1,1''-biphenyl]-4-sulfonamido}ethyl)carbamate **80a** (20.0 mg, 0.053 mmol, 1.00 eq) to yield the title compound as a white amorphous solid (16.5 mg, 0.053 mmol, 99%). δ_H (400 MHz, MeOD) 8.02 – 7.82 (4H, m, 2''–H, 3''–H), 7.75 – 7.67 (2H, m, 3–H), 7.55 – 7.48 (2H, m, 2–H), 7.47 – 7.40 (1H, m, 4''–H), 3.18 – 3.06 (4H, m, 2'–H_2, 1'–H_2). δ_C (101 MHz, MeOD) 145.7 (C–4), 139.1 (C–1'), 138.0 (C–1''), 128.8 (C–3), 128.3 (C–4''), 127.5 (C–2), 127.4 (C–2''), 126.9 (C–3''), 40.0 (C–2'), 39.3 (C–1'). ν_{max} (ATR) 3261 (*b*, N–H), 3038, 2871, 1584, 1489, 1311, 1152, 1099, 1042, 765 cm^{-1}. *m/z* (LC-MS ESI+) 277.290 [M+H]$^+$, 553.461 [2M+H]$^+$. Accurate mass (ES+) found [M+H]$^+$ 277.1014, $C_{14}H_{17}N_2O_2S$ requires *M* 277.1011.

81a. *tert-butyl N-{2'-[2''-(naphthalen-1-yl)ethanesulfonamido]ethyl}carbamate*

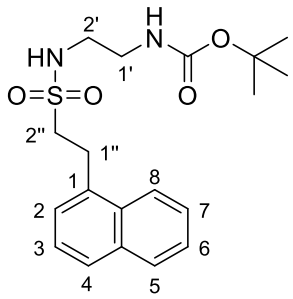

Compound was prepared according to general procedure A using *2'-(naphthalen-1-yl)ethane-1-sulfonyl chloride* (50.0 mg, 0.196 mmol, 1.00 eq) and *N-Boc ethylenediamine* (0.037 mL, 0.236 mmol, 1.20 eq). Purification by column chromatography (EtOAc in Hex 0-65%) yielded the title compound as a colourless oil (47.1 mg, 0.124 mmol, 63%). δ_H (400 MHz, $CDCl_3$) 8.07 – 7.99 (1H, m, 2–H), 7.90 (1H, dd, *J* = 8.0, 1.5 Hz, 5–H), 7.80 (1H, dd, *J* = 7.8, 1.8 Hz, 4–H), 7.60 – 7.51 (2H, m, 7–H, 6–H), 7.47 –

7.37 (2H, m, 8–H, 3–H), 4.99 (2H, m, 2'–N*H*, 1'–N*H*), 3.70 – 3.54 (2H, m, 2'–H_2), 3.50 – 3.36 (2H, m, 1'–H_2), 3.28 – 3.16 (4H, m, 2''–H, 1''–H), 1.42 (9H s, –C(CH_3)$_3$). δ_C (101 MHz, $CDCl_3$) 156.6 (C=O), 133.9 (C–1), 133.9 (C–4a), 131.3 (C–8a), 129.1 (C–2), 127.9 (C–5), 126.7 (C–4), 126.6 (C–7), 126.0 (C–8), 125.6 (C–6), 123.0 (C–3), 80.0 (–*C*(CH_3)$_3$), 53.0 (C–2''), 43.8 (C–2'), 40.8 (C–1'), 28.3 (–(*C*H_3)$_3$), 27.3 (C-1''). ν_{max} (ATR) 3371 (N–H), 3307 (N–H), 2981, 1683 (C=O), 1528, 1322, 1254, 1152, 1127, 1070, 907 cm^{-1}. *m/z* (LC-MS ESI+) 279.343 $[M–Boc+H]^+$, 323.353 $[M–tBu+2H]^+$, 379.371 $[M+H]^+$. Accurate mass (ES+) found $[M+H]^+$ 379.1693, $C_{19}H_{27}N_2O_4S$ requires *M* 379.1693.

81. *N-(2'-aminoethyl)-2''-(naphthalen-1-yl)ethane-1''-sulfonamide hydrochloride*

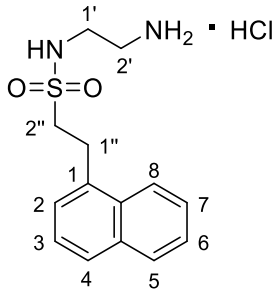

Compound was prepared according to general procedure B, using *tert-butyl N-{2-[2-(naphthalen-1-yl)ethanesulfonamido]ethyl}carbamate* **81a** (20.0 mg, 0.053 mmol, 1.00 eq) to yield the title compound as light brown amorphous solid (15.8 mg, 0.050 mmol, 95.0%). δ_H (400 MHz, MeOD) 8.08 (1H, dd, *J* = 8.4, 2.1 Hz, 2–H), 7.92 (1H, dd, *J* = 8.0, 1.4 Hz, 5–H), 7.81 (1H, dd, *J* = 7.2, 2.1 Hz, 4–H), 7.60 (1H, ddd, *J* = 8.4, 6.8, 1.4 Hz, 7–H), 7.53 (1H, ddd, *J* = 8.0, 6.8, 1.2 Hz, 6–H), 7.49 – 7.40 (2H, m, 8–H, 3–H), 3.63 – 3.46 (4H, m, 2'–H_2, 1'–H_2), 3.40 (2H, t, *J* = 5.7 Hz, 2''–H_2), 3.10 (2H, t, *J* = 5.7 Hz, 1''–H_2). δ_C (101 MHz, MeOD) 134.1 (C–1), 134.0 (C–4a), 131.3 (C–8a), 128.7 (C–2), 127.4 (C–5), 126.3 (C–4), 126.2 (C–7), 125.5 (C–8), 125.3 (C–6), 122.6 (C–3), 51.8 (C–2''), 40.0 (C–2'), 39.8 (C–1'), 26.5 (C–1''). ν_{max} (ATR) 3361 (*b*, N–H), 3208, 2946, 2403, 1598, 1496, 1439, 1329, 1137, 794 cm^{-1}. *m/z* (LC-MS ESI+) 279.305 $[M+H]^+$, 557.490 $[2M+H]^+$. Accurate mass (ES+) found $[M+H]^+$ 279.1169, $C_{14}H_{19}N_2O_2S$ requires *M* 279.1169.

82a. *tert-butyl N-[3'-(naphthalene-1-sulfonamido)propyl]carbamate*

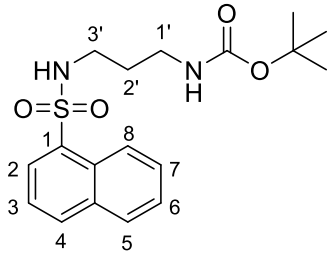

Compound was prepared according to general procedure A using *1-naphthalene sulfonyl chloride* **73** (50.0 mg, 0.221 mmol, 1.00 eq) and *N-(3-aminopropyl)carbamic acid tert-butyl ester* (0.046 mL, 0.265 mmol, 1.20 eq). Purification by column chromatography (EtOAc in Hex 0-50%) yielded the title compound as a colourless oil (68.0 mg, 0.187 mmol, 85%). δ_H (400 MHz, $CDCl_3$) 8.72 (1H, dd, *J* = 8.6, 1.2 Hz, 5–H), 8.25 (1H, dd, *J* = 7.3, 1.3 Hz, 2–H), 8.06 (1H, dd, *J* = 8.2, 1.3 Hz, 4–H), 7.95 (1H, dd, *J* = 8.2, 1.5 Hz, 8–H), 7.69 (1H, ddd, *J* = 8.6, 6.9, 1.5 Hz, 6–H), 7.61 (1H, ddd, *J* = 8.2, 6.9, 1.2 Hz, 7–H), 7.54 (1H, dd, *J* = 8.2, 7.3 Hz, 3–H), 6.04 – 5.88 (1H, m, 3'–N*H*), 4.59-4.65 (1H, m, 1'–N*H*), 3.11 (2H, q, *J* = 6.3 Hz, 3'–H_2), 2.97 (2H, q, *J* = 6.5 Hz, 1'–H_2), 1.61 – 1.46 (2H, m, 2'–H_2), 1.34 (9H, s, –(CH_3)$_3$). δ_C (101 MHz, $CDCl_3$) 156.8 (C=O), 135.3 (C–2), 134.3 (C–1), 134.0 (C–4a), 129.2 (C–5), 129.0 (C–4), 128.4 (C–7), 128.2 (C–8), 126.8 (C–8a), 124.7 (C–6), 124.1 (C–3), 79.6 (–*C*(CH_3)$_3$), 39.8 (C–3'), 36.7 (C–1'), 30.6 (C–2'), 28.6 (–(*C*H_3)$_3$). ν_{max} (ATR) 3374 (N–H), 3293 (N–H), 2977, 2885, 1688, 1513, 1368, 1322, 1254, 1159, 1134 cm^{-1}. *m/z* (LC-MS ESI+) 265.281 $[M–Boc+H]^+$, 309.329 $[M–tBu+2H]^+$, 365.348 $[M+H]^+$. Accurate mass (ES+) found $[M+H]^+$ 365.1525, $C_{18}H_{25}N_2O_4S$ requires *M* 365.1535.

82. *N-(3'-aminopropyl)naphthalene-1-sulfonamide hydrochloride*

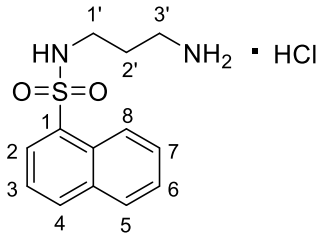

Compound was prepared according to general procedure B, starting with tert-butyl *N-[3-(naphthalene-1-sulfonamido)propyl]carbamate* **82a** (20.0 mg, 0.055 mmol, 1.00 eq) to yield the title compound off white amorphous solid (16.1 mg, 0.054 mmol, 98%). δ_H (400 MHz, MeOD) 8.33 (1H, dd, *J* = 8.6, 1.1 Hz, 5–H), 7.87 (1H. dd, *J* = 7.3, 1.1 Hz, 2–H), 7.82 (1H, dd, *J* = 8.3, 1.1 Hz, 4–H), 7.72 – 7.64 (1-H, m, 8–H), 7.36 (1H, ddd, *J* = 8.6, 6.9, 1.5 Hz, 6–H), 7.32 – 7.22 (2H, m, 7–H, 3–H), 2.60 (4H, m, 3'–H_2, 1'–H_2), 1.51 – 1.39 (2H, m, 2'–H_2). δ_C (101 MHz, MeOD) 136.4 (C–2), 135.9 (C–1), 135.3 (C–4a), 130.2 (C–5), 130.2 (C–4), 129.3 (C–7), 129.2 (C–8), 128.0 (C–8a), 125.7 (C–6), 125.3 (C–3), 40.8 (C–3'), 38.3 (C–1'), 29.1 (C–2'). ν_{max} (ATR) 3396 (*b*, N–H), 2981, 2885, 1382, 1319, 1155, 1134, 1084, 954 cm^{-1}. *m/z* (LC-MS ESI+) 265.281 $[M+H]^+$, 529.482 $[2M+H]^+$. Accurate mass (ES+) found $[M+H]^+$ 265.1021, $C_{13}H_{17}N_2O_2S$ requires *M* 265.1011.

83. *N-[2'-(dimethylamino)ethyl]naphthalene-2-sulfonamide*

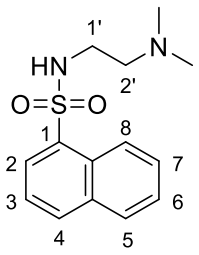

Compound was prepared according to general procedure A using *1-naphthalene sulfonyl chloride* **73** (0.050 g, 0.221 mmol, 1.00 eq) and *N,N dimethyl ethylene diamine* (0.029 mL, 0.265 mmol, 1.20 eq) . Purification was achieved by column chromatography (EtOAc in Hex, 0-100%) to yield the title compound as a light brown oil (0.052 g, 0.187 mmol, 85%). δ_H (400 MHz, $CDCl_3$) 8.69 (1H, d, *J* = 8.6 Hz, 5–H), 8.30 (1H, d, *J* = 7.3 Hz, 2–H), 8.09 (1H, dd, *J* = 8.3, 1.1 Hz, 4–H), 7.97 (1H dd, *J* = 8.2, 1.5 Hz, 8–H), 7.71 (1H, ddd, *J* = 8.6, 6.9, 1.5 Hz, 6–H), 7.63 (1H, dd, *J* = 8.2, 6.9 Hz, 7–H), 7.57 (1H, dd, *J* = 8.3, 7.3 Hz, 3–H), 2.97 – 2.82 (2H, m, 1'–H_2), 2.29 – 2.06 (2H, m, 2'–H_2), 1.90 (6H, s, –N(CH_3)$_2$). δ_C (101 MHz, $CDCl_3$) 134.3 (C–2), 134.2 (C–1), 134.1 (C–4a), 129.9 (C–5), 129.1 (C–4), 128.3 (C–7), 128.2 (C–8), 126.7 (C–8a), 124.5 (C–6), 124.1 (C–3), 56.7 (C–1'), 44.5 (–N(*C*H_3)$_2$), 40.2 (C–2'). ν_{max} (ATR) 3276 (N-H), 2952, 2775, 1461, 1322, 1159, 1134, 747 cm^{-1}. *m/z* (LC-MS ESI+) 279.305 $[M+H]^+$.Accurate mass (ES+) found $[M+H]^+$ 279.1164, $C_{14}H_{19}N_2O_2S$ requires *M* 279.1167.

84. *N-(2-hydroxyethyl)naphthalene-1-sulfonamide*

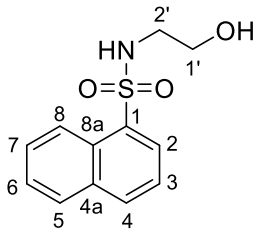

Compound was prepared according to general procedure A using *1-naphthalene sulfonyl chloride* **73** (200 mg, 0.882 mmol, 1.00 eq) and *ethanolamine* (0.080 mL, 1.32 mmol, 1.50 eq). Purified by column chromatography (EtOAc in Hexane, 0-70%) to yield the title compound as a white solid (181 mg, 0.720 mmol, 82%). m.p.: 106-107 °C. δ_H (599 MHz, CD_3OD) 7.17 (1H, dd, *J* = 8.7, 1.1 Hz, 5–H), 6.68 (1H, dd, *J* = 7.3, 1.2 Hz, 2–H), 6.58 (1H, dd, *J* = 8.3, 1.2 Hz, 4–H), 6.45 (1H, dd, *J* = 8.1, 1.4 Hz, 8–H), 6.14 (1H, ddd, *J* = 8.7, 6.9, 1.4 Hz, 6–H), 6.07 (1H, ddd, *J* = 8.1, 6.9, 1.1 Hz, 7–H), 6.03 (1H, dd, *J* = 8.3, 7.3 Hz, 3–H), 1.94 (2H, t, *J* = 6.1 Hz, 1'–H), 1.78 (1H, s, 2'–NH), 1.41 (2H, t, *J* = 6.1 Hz, 2'–H). δ_C (151 MHz, CD_3OD) 135.3 (C–2), 134.4 (C–1), 133.7 (C–4a), 128.7 (C–5), 128.7 (C–4), 128.0 (C–7), 127.6 (C–8), 126.5 (C–8a), 124.4 (C–6), 123.9 (C–3), 60.5 (C–1'), 44.6 (C–2'). ν_{max} (ATR) 3487 (O–H), 3317 (N–H), 2921, 2872, 1428, 1330, 1314, 1160, 1131, 1057, 977 cm^{-1}. m/z (LC-MS ESI+)

252.176 $[M+H]^+$, 503.255 $[2M+H]^+$. Accurate mass (ES+) found $[M+H]^+$ 252.0702, $C_{12}H_{14}NO_3S$ requires *M* 252.0694.

85. *N-(2-methoxyethyl)naphthalene-2-sulfonamide*

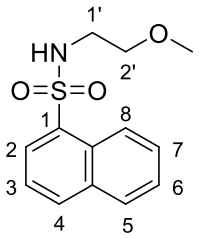

Compound was prepared according to general procedure A using 1-naphthalene sulfonyl chloride **73** (0.050 g, 0.221 mmol, 1.00 eq) and 2-methoxyethan-1-amine (0.023 mL, 0.265 mmol, 1.20 eq). Purification by flash chromatography (EtOAc in Hex, 0-50%) yielded the title compound as a white amorphous solid (51.0 mg, 0.192 mmol, 87%). δ_H (400 MHz, $CDCl_3$) 8.66 (1H dd, *J* = 8.6, 1.2 Hz, 5–H), 8.29 (1H, dd, *J* = 7.3, 1.3 Hz, 2–H), 8.10 (1H, dd, *J* = 8.2, 1.3 Hz, 4–H), 8.01 – 7.94 (1H, m, 8–H), 7.71 (1H, ddd, *J* = 8.6, 6.9, 1.5 Hz, 6–H), 7.63 (1H, ddd, *J* = 8.1, 6.9, 1.2 Hz, 7–H), 7.57 (1H, dd, *J* = 8.2, 7.3 Hz, 3–H), 5.15 (1H, d, *J* = 6.8 Hz, –N*H*), 3.26 (2H, d, *J* = 6.8 Hz, 2'–H_2), 3.15 – 3.07 (5H, m, 1'–H_2, –OCH_3). δ_C (101 MHz, $CDCl_3$) 134.7 (C–2), 134.3 (C–1), 129.5 (C–4a), 129.1 (C–5), 128.4 (C–4), 128.2 (C–7), 128.2 (C–8), 126.9 (C–8a), 124.37 (C–6), 124.2 (C–3), 70.34 (–O*C*H_3), 58.58 (C–2'), 42.9 (C–1'). ν_{max} (ATR) 3296 (N–H), 2984, 2899, 1506, 1322, 1159, 1134, 755 cm^{-1}. *m/z* (LC-MS ESI+) 266.269 $[M+H]^+$. Accurate mass (ES+) found $[M+H]^+$ 266.0869, $C_{13}H_{16}NO_3S$ requires *M* 266.0851.

86a. *tert-butyl N-(2'-methanesulfonamidoethyl)carbamate*

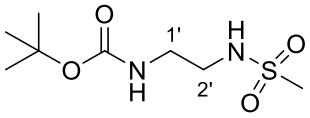

Compound was prepared according to general procedure A using *methanesulfonyl chloride* (0.072 mL, 0.001 mol, 1.50 eq) and *N-Boc-ethylenediamine* (0.099 mL, 0.001 mol, 1.00 eq). Purification by flash chromatography (EtOAc in Hex, 0-50%) yielded the title compound as a white amorphous solid (51.0 mg, 0.192 mmol, 87%). δ_H (400 MHz, $CDCl_3$) 4.86 (2H, s, 2'–N*H* , 1'–N*H*), 3.32 (4H, m, 2'–H_2, 1–H_2) 3.00 (3H, s, –CH_3), 1.47 (9H, s, –C(CH_3)$_3$). δ_C (101 MHz, $CDCl_3$) 156.7 (C=O), 80.1 (–*C*(CH_3)$_3$), 43.7 (C–2'), 40.7 (C–1'), 40.4 (–*C*H_3), 28.4 (–C(*C*H_3)$_3$). ν_{max} (ATR) 3363 (N–H), 3286 (N–H), 2994, 1684 (C=O), 1528, 1450, 1307, 1279, 1140 cm^{-1}. (GC-MS ESI+) 238.1 $[M+H]^+$. Data agrees with that reported in Katsuhito *et al*.[133]

86. *N-(2-aminoethyl)methanesulfonamide*

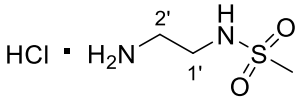

Compound was prepared according to general procedure B, using tert-butyl N-(2'-methanesulfonamidoethyl)carbamate **86a** (15.0 mg, 0.067 mmol, 1.000 eq) to yield the title compound as a colourless oil (10.0 mg, 0.063 mmol, 93.3%). δ_H (400 MHz, MeOD) 3.37 (2H, t, J = 5.8 Hz, 2'–H_2), 3.10 (2H, t, J = 5.9 Hz, 1'–H_2), 3.02 (3H, s, –CH_3). δ_C (101 MHz, MeOD) 40.0 (C–2'), 39.6 (C–1'), 38.0 (–CH$_3$). ν_{max} (ATR) 3361 (N–H), 3176 (N–H), 2974, 1591, 1326, 1286, 1141, 1084 cm^{-1}. *m/z* (LC-MS ESI+) 139.117 $[M+H]^+$. Data agrees with that reported in Yong *et al*.[134]

87a. *tert-butyl N-(2'-cyclohexanesulfonamidoethyl)carbamate*

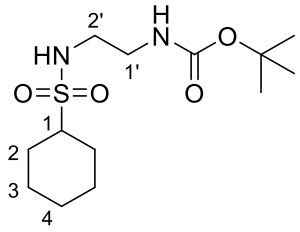

Compound was prepared according to general procedure A using *cyclohexane-sulfonyl chloride* (50.0 mg, 0.274 mmol, 1.00 eq) and *N-Boc ethylenediamine* (0.052 mL, 0.328 mmol, 1.20 eq). Purification by column chromatography (EtOAc in Hex 0-50%) yielded the title compound as a colourless oil (69.4 mg, 0.226 mmol, 82%). δ_H (400 MHz, $CDCl_3$) 4.93 (1H, s, 2'–NH), 4.68 (1H, s, 1'–NH), 3.42 – 3.15 (4H, m, 2'–H_2, 1'–H_2), 2.86 –2.92 (1H, m, 1–H), 2.22 – 1.86 (4H, m, 2–H_2), 1.82 – 1.12 (15H, m, 3–H_4, –C(CH_3)$_3$, 4–H_2). δ_C (101 MHz, $CDCl_3$) 157.1 (C=O), 80.3 (–C(CH$_3$)$_3$), 61.4 (C–1), 44.0 (C–2'), 41.2 (C–1'), 28.4 (–C(CH$_3$)$_3$), 26.5 (C–5), 25.2 (C–3), 25.1 (C–4). ν_{max} (ATR) 3371 (N–H), 3289 (N–H), 2931, 1691 (C=O), 1513 1453, 1311, 1144 cm^{-1}. *m/z* (LC-MS ESI+) 207.284 $[M–Boc+H]^+$, 251.295 $[M–tBu+2H]^+$, 307.428 $[M+H]^+$.

87. *N-(2'-aminoethyl)cyclohexanesulfonamide hydrochloride*

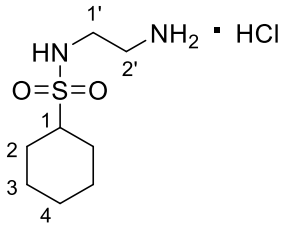

Compound was prepared according to general procedure B, using *tert-butyl N-(2'-cyclohexanesulfonamidoethyl)carbamate* **87a** (20.0 mg, 0.065 mmol, 1.00 eq) to yield the title compound as a colourless oil (15.5 mg, 0.064 mmol, 98%). δ_H (400 MHz, MeOD) 3.35 (2H, m, 2'–H_2), 3.09 – 3.00 (3H, m, 1'–H_2, 1–H), 2.20 – 1.83 (4H, m, 2–H_2)), 1.79 – 1.15 (6H, m, 3–H_2, 4–H_2). δ_C (101 MHz, MeOD) 60.1 (C–1), 40.1 (C–2'), 40.0 (C–1'), 26.2 (C–2), 24.9 (C–4), 24.7 (C–3). ν_{max} (ATR) 3346 (*b*, N–H), 2488, 2077, 1116, 971 cm^{-1}. *m/z* (LC-MS ESI+) 207.284 $[M+H]^+$, 413.498 $[2M+H]^+$. Accurate mass (ES+) found $[M+H]^+$ 207.1166, $C_8H_{19}N_2O_2S$ requires *M* 207.1167.

71a. *tert-butyl N-methyl-N-[2'-(naphthalene-1-sulfonamido)ethyl]carbamate*

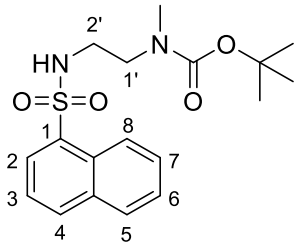

Compound was prepared according to general procedure A using *1-naphthalene sulfonyl chloride* **73** (50.0 mg, 0.221 mmol, 1.00 eq) and *N-(2-aminoethyl)-N,N Boc methyl* (0.047 mL, 0.265 mmol, 1.20 eq). Purification by column chromatography (EtOAc in Hex 0-50%) yielded the title compound as a light brown oil (55.9 mg, 0.153 mmol, 70%). δ_H (400 MHz, $CDCl_3$) 8.66 (1H, d, *J* = 8.6 Hz, 5–H), 8.28 (1H, dd, *J* = 7.3, 1.5 Hz, 2–H), 8.10 (1H, dd, *J* = 8.2, 1.5 Hz, 4–H), 7.97 (1H, dd, *J* = 8.1, 1.5 Hz, 8–H), 7.70 (1H, ddd, *J* = 8.6, 6.8, 1.5 Hz, 6–H), 7.60 (2H, m, 7–H, 3–H), 5.58 (1H, s, 2'–N*H*), 3.31 (2H, t, *J* = 5.8 Hz, 2'–H_2), 3.08 (2H, t, *J* = 5.8 Hz, 1'–H_2), 2.70 (3H, m,–NCH_3), 1.45 (9H, s, –(CH_3)$_3$). δ_C (101 MHz, $CDCl_3$) 157.06 (C=O), 134.3 (C–2), 134.3 (C–1), 130.6 (C–4a), 129.5 (C–5), 129.1 (C–4), 128.5 (C–7), 128.2 (C–8), 127.3 (C–8a), 124.5 (C–6), 124.1 (C–3), 80.3 (–*C*$(CH_3)_3$), 48.2 (–N*C*H_3), 42.03 (C–2'), 35.4 (C–1'), 28.4 (–(*C*H_3)$_3$). ν_{max} (ATR) 3261 (N–H), 2974, 1673 (C=O), 1481, 1393, 1322, 1155, 1131 cm^{-1}. *m/z* (LC-MS ESI+) 265.319 $[M–Boc+H]^+$, 365.338 $[M+H]^+$.

71. *N-[2'-(methylamino)ethyl]naphthalene-1-sulfonamide hydrochloride*

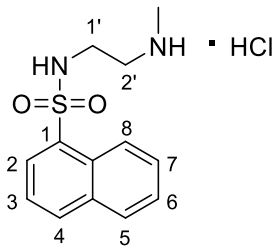

Compound was prepared according to general procedure B, starting with *tert-butyl N-methyl-N-[2'-(naphthalene-1-sulfonamido)ethyl]carbamate* **71a** (20.0 mg, 0.055 mmol, 1.00 eq) to yield the title compound as a white amorphous solid (15.8 mg, 0.053 mmol, 96%). δ_H (400 MHz, MeOD) 8.68 (1H,

dd, *J* = 8.5, 1.0 Hz, 5–H), 8.29 – 8.17 (2H, m, 2–H, 4–H), 8.09 – 8.02 (1H, m, 8–H), 7.73 (1H, ddd, *J* = 8.5, 6.9, 1.5 Hz, 6–H), 7.70 – 7.59 (2H, m, 7–H, 3–H), 3.15 – 3.02 (4H, m, 1'–H_2, 2'–H_2), 2.73 (3H, s, –NHCH_3). δ_C (101 MHz, MeOD) 134.6 (C–2), 134.3 (C–1), 134.0 (C–4a), 129.3 (C–5), 128.9 (C–4), 128.0 (C–7), 127.9 (C–8), 126.8 (C–8a), 124.1 (C–6), 124.0 (C–3'), 48.6 (–NH*C*H_3), 38.6 (C–2'), 32.4 (C–1'). ν_{max} (ATR) 3353 (*b*, N–H), 2981, 2485, 2073, 1116, 974 cm^{-1}. *m/z* (LC-MS ESI+) 265.281 $[M+H]^+$. Accurate mass (ES+) found $[M+H]^+$ 265.1013, $C_{13}H_{17}N_2O_2S$ requires *M* 265.1011.

72a. *tert-butyl N-[2'-(N-methylnaphthalene-1-sulfonamido)ethyl]carbamate*

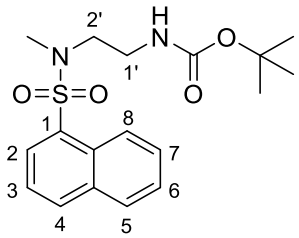

Compound was prepared according to general procedure A using *1-naphthalene sulfonyl chloride* **73** (50.0 mg, 0.221 mmol, 1.00 eq) and *N-Boc-2-methylamino-ethylamine ethylenediamine* (46.1 mg, 0.265 mmol, 1.20 eq). Purification by column chromatography (EtOAc in Hex 0-50%) yielded the title compound as a colourless oil (75.0 mg, 0.206 mmol, 93%). δ_H (400 MHz, $CDCl_3$) 8.75 – 8.57 (1H, m, 5–H), 8.16 (1H, dd, *J* = 7.4, 1.2 Hz, 2–H), 8.07 (1H, dd, *J* = 8.3, 1.2 Hz, 4–H), 7.93 (1H, d, *J* = 8.1 Hz, 8–H), 7.67 (1H, ddd, *J* = 8.6, 6.9, 1.5 Hz, 6–H), 7.59 (1H, ddd, *J* = 8.1, 6.9, 1.2 Hz, 7–H), 7.57 – 7.51 (1H, m, 3–H), 4.82 (1H, s, –N*H*), 3.30 (4H m, 2'–H_2, 1'–H_2), 2.89 (3H, s, –NCH_3), 1.42 (9H, s, –(CH_3)$_3$). δ_C (101 MHz, $CDCl_3$) 156.0 (C=O), 134.5 (C–2), 134.4 (C–1), 133.6 (C–4a), 129.9 (C–5), 129.0 (C–4), 128.8 (C–7), 128.3 (C–8), 127.0 (C–8a), 125.0 (C–6), 124.2 (C–3), 79.6 (–*C*$(CH_3)_3$), 49.2 (–N*C*H_3), 38.4 (C–2'), 34.8 (C–1'), 28.4 (–(*C*H_3)$_3$). ν_{max} (ATR) 3396 (N–H), 2977, 1701, 1509, 1326, 1162, 1131, 979 cm^{-1}. *m/z* (LC-MS ESI+) 265.281 $[M–Boc+H]^+$, 309.291 $[M–tBu+2H]^+$, 365.348 $[M+H]^+$. Accurate mass (ES+) found $[M+H]^+$ 365.1530, $C_{18}H_{25}N_2O_4S$ requires *M* 365.1535.

72. *N-(2'-aminoethyl)-N-methylnaphthalene-1-sulfonamide*

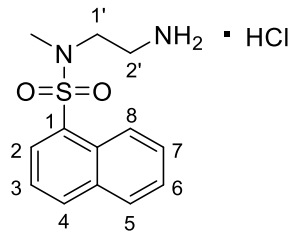

Compound was prepared according to general procedure B, starting with *tert-butyl N-[2'-(N-methylnaphthalene-1-sulfonamido)ethyl]carbamate* **72a** (20.0 mg, 0.055 mmol, 1.00 eq) to yield the title compound as an off white amorphous solid (15.8 mg, 0.053 mmol, 96%). δ_H (400 MHz, MeOD)

8.81 (1H, dd, *J* = 8.6, 1.1 Hz, 5–H), 8.24 (1H, dd, *J* = 8.3, 1.2 Hz, 2–H), 8.18 (1H, dd, *J* = 7.4, 1.1 Hz, 4–H), 8.10 – 8.05 (1H, m, 8–H), 7.77 – 7.62 (3H, m, 6–H, 7–H, 3–H), 3.44 (2H, t, *J* = 5.9 Hz, 2'–H_2), 3.18 (2H, t, *J* = 5.9 Hz, 1'–H_2), 2.98 (3H, s, –NCH_3). δ_C (101 MHz, MeOD) 134.7 (C–2), 134.4 (C–1), 133.1 (C–4a), 129.2 (C–5), 128.9 (C–4), 128.6 (C–7), 127.9 (C–8), 126.8 (C–8a), 124.6 (C–6), 124.1 (C–3), 66.7 (–NCH_3), 37.0 (C–2'), 34.4 (C–1'). ν_{max} (ATR) 3406 (*b*, N–H), 2971, 2917, 1595, 1506, 1322 1155, 1127, 996, 772 cm^{-1}. *m/z* (LC-MS ESI+) 265.281 $[M+H]^+$, 529.482 $[2M+H]^+$. Accurate mass (ES+) found $[M+H]^+$ 265.1010, $C_{13}H_{17}N_2O_2S$ requires *M* 265.1011.

68a. *tert-butyl N-[2'-(4-propylbenzenesulfonamido)ethyl]carbamate*

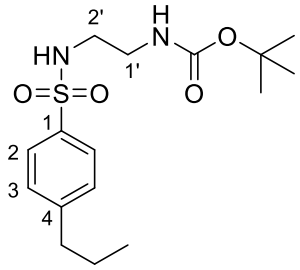

Compound was prepared according to general procedure A using *4-n-propyl-1-sulfonyl chloride* (50.0 mg, 0.229 mmol, 1.00 eq) and *N-Boc ethylenediamine* (0.043 mL, 0.274 mmol, 1.20 eq). Purification by column chromatography (EtOAc in Hex 0-50%) yielded the title compound as a white amorphous solid (48.2 mg, 0.141 mmol, 62%). δ_H (400 MHz, $CDCl_3$) 7.78 (2H d, *J* = 8.4 Hz, 2–H_2), 7.33 (2H, d, *J* = 8.4 Hz, 3–H_2), 5.17 (1H, s, 2'–NH), 4.88 (1H, s, 1'–NH), 3.25 (2H, t, *J* = 5.7 Hz, 2'–H_2), 3.08 (t, *J* = 5.7 Hz, 1'–H_2), 2.67 (2H, t, *J* = 8.5, Hz, –ArCH_2), 1.76 – 1.61 (2H, m, –CH_2CH_3), 1.45 (9H, s, –$(CH_3)_3$), 0.97 (3H, t, *J* = 7.3 Hz, –CH_3). δ_C (101 MHz, $CDCl_3$) 156.6 (C=O), 148.2 (C–1), 137.0 (C–4), 129.2 (C–2), 127.1 (C–3), 79.9 (–$C(CH_3)_3$), 43.7 (C–2'), 40.3 (C–1'), 37.9 (–ArCH_2), 28.3 (–$(CH_3)_3$), 24.2 (–CH_2CH_3), 13.7 (–CH_3). ν_{max} (ATR) 3371 (N–H), 3283 (N–H), 2969, 2872, 1687 (C=O), 1527, 1324, 1269, 1153, 1090 cm^{-1}. *m/z* (LC-MS ESI+) 243.275 $[M–Boc+H]^+$, 287.362 $[M–tBu+2H]^+$, 343.381 $[M+H]^+$. Accurate mass (ES+) found $[M+H]^+$ 343.1683, $C_{16}H_{27}N_2O_4S$ requires *M* 343.1692.

68. *N-(2-aminoethyl)-4-propylbenzene-1-sulfonamide*

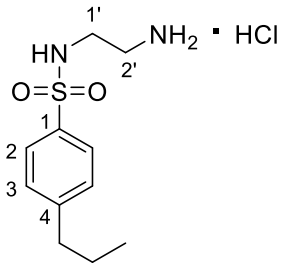

Compound was prepared according to general procedure B, starting with *tert-butyl N-[2'-(4-propylbenzenesulfonamido)ethyl]carbamate* **68a** (20.0 mg, 0.058 mmol, 1.000 eq) to yield the title compound as an off white amorphous solid (16.0 mg, 0.057 mmol, 98%). δ_H (400 MHz, MeOD) 7.81 (2H, d, *J* = 8.2 Hz, 2–H), 7.44 (2H, d, *J* = 8.2 Hz, 3–H), 3.13 – 2.99 (4H, m, 2'–H_2. 1'–H_2), 2.71 (2H, d, *J* = 8.5, Hz, Ar–CH_2), 1.80 – 1.60 (2H, m, –$CH_2CH_2CH_3$), 0.98 (3H, t, *J* = 7.4 Hz, -CH_3). δ_C (101 MHz, MeOD) 148.4 (C–1), 136.7 (C–4), 129.1 (C–2), 126.8 (C–3), 40.0 (C–2'), 39.3 (C–1'), 37.4 (Ar-CH_2), 24.0 (–$CH_2CH_2CH_3$), 12.3 (–CH_3). ν_{max} (ATR) 3396 (*b*, N–H), 2964, 2871, 1595, 1326, 1155, 1092 cm^{-1}. *m/z* (LC-MS ESI+) 243.314$[M+H]^+$, 485.514 $[2M+H]^+$. Accurate mass (ES+) found $[M+H]^+$ 243.1166, $C_{11}H_{19}N_2O_2S$ requires *M* 243.1167.

63a. *tert-butyl N-[2'-(5-chloronaphthalene-1-sulfonamido)ethyl]carbamate*

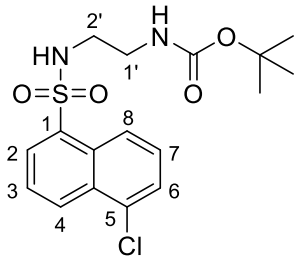

Compound was prepared according to general procedure A using *5-chloro,naphthlene-1-sulfonyl chloride* (50.0 mg, 0.191 mmol, 1.00 eq) and *N-Boc ethylenediamine* (0.036 mL, 0.230 mmol, 1.20 eq). Purification by column chromatography (EtOAc in Hex 0-50%) yielded the title compound as a white amorphous solid (57.2 mg, 0.149 mmol, 78%). δ_H (400 MHz, $CDCl_3$) 8.64-8.60 (2H, m, 8–H, 4–H), 8.32 (1H, dd, *J* = 7.3, 1.2 Hz, 2–H), 7.76 – 7.61 (2H, m, 6–H, 3–H), 7.56 (1H, t, *J* = 8.1 Hz, 7–H), 5.82 (1H, s, 2'–N*H*), 4.86 (1H, s, 1'–N*H*), 3.20 (2H, t, *J* = 5.8 Hz, 2'–H_2), 3.04 (1H, t, *J* = 5.7 Hz, 1'–H_2), 1.40 (9H, s, –C(CH_3)$_3$). δ_C (101 MHz, $CDCl_3$) 156.6 (C=O), 135.1 (C–1), 133.1 (C–5), 131.7 (C–4a), 130.6 (C–4), 130.3 (C–2), 129.4 (C–8a), 128.2 (C–7), 127.4 (C–8), 125.3 (C–6), 123.6 (C–3), 80.0 (–*C*$(CH_3)_3$), 43.9 (C–2'), 40.3 (C–1'), 28.3 (–(*C*H_3)$_3$). ν_{max} (ATR) 3361 (N–H), 3286 (N–H), 2981, 1680 (C=O), 1528, 1332, 1162, 1134, 790 cm^{-1}. *m/z* (LC-MS ESI+) 285.271 $[M(^{35}Cl)–Boc+H]^+$ (100), 287.286 $[M(^{37}Cl)–Boc+H]^+$ (39), 329.243 $[M(^{35}Cl)–tBu+2H]^+$ (76), 331.258 $[M(^{37}Cl)–tBu+2H]^+$ (27). Accurate mass (ES+) found $[M+H]^+$ 385.0991, $C_{17}H_{22}N_2O_4S^{35}Cl$ requires *M* 385.0989.

63. *N-(2'-aminoethyl)-5-chloronaphthalene-1-sulfonamide hydrochloride*

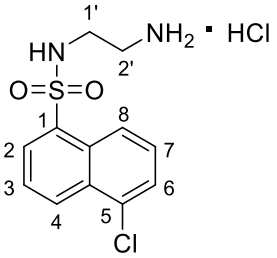

Compound was prepared according to general procedure B, using *tert-butyl N-[2-(5-chloronaphthalene-1-sulfonamido)ethyl]carbamate* **63a** (20.0 mg, 0.052 mmol, 1.00 eq) to yield the title compound as an amorphous white solid (15.0 mg, 0.047 mmol, 90%). δ_H (400 MHz, MeOD) 8.70 (1H, d, *J* = 8.5 Hz, 8–H), 8.63 (1H, d, *J* = 8.4 Hz, 4–H), 8.35 (1H, d, *J* = 7.0 Hz, 2–H), 7.85 – 7.73 (2H, m, 6–H, 3–H), 7.69 (1H, t, *J* = 8.5 Hz, 7–H), 3.07 (4H, m, 2'–H_2, 1'–H_2). δ_C (101 MHz, MeOD) 135.2 (C–1), 132.5 (C–5), 131.5 (C–4a), 130.0 (C–4), 129.9 (C–2), 129.3 (C–8a), 127.9 (C–7), 127.4 (C–8), 125.4 (C–6), 123.7 (C–3), 33.9 (C–1'), 33.5 (C–2'). ν_{max} (ATR) 3271 (*b*, N–H), 2988, 2854, 1591, 1563, 1496, 1319, 1134, 1031 cm^{-1}. *m/z* (LC-MS ESI+) 285.233 $[M(^{35}Cl)+H]^+$ (100), 287.248 $[M(^{37}Cl)+H]^+$ (80). Accurate mass (ES+) found $[M+H]^+$ 285.0467, $C_{12}H_{24}N_2O_2S^{35}Cl$ requires *M* 285.0465.

92. *N,N-diethylbenzenesulfonamide*

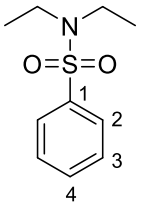

PhMgBr **88** (1.3 mL of a 1M solution in THF, 1.25 mmol, 1.00 eq) was added dropwise to a suspension of *DABSO* **89** (0.481 g, 2.00 mmol, 1.60 eq) in THF (15.0 mL) at –40 °C. The mixture was left stir for 1 h after which SO_2Cl_2 (0.169 g, 1.25 mmol, 1.00 eq) was added and the reaction mixture allowed to attain ambient temperature. The mixture was transferred dropwise to *diethyl amine* (1.3 mL, 12.5 mmol, 10.0 eq) in THF (5 ml) and was allowed to stir at room temperature for 16 hours. The reaction was quenched with water (10 ml), the layers separated, and the aqueous layers extracted with chloroform (3 x 15 ml). The combined organic extracts were dried over $MgSO_4$, concentrated and purified by flash chromatography (EtOAc in Hex, 0-45%) to yield the title compound as a clear oil (0.206 g, 0.967 mmol, 77%). δ_H (400 MHz, $CDCl_3$) 7.85 – 7.81 (2H, m, 2–H), 7.61 – 7.55 (1H, m, 4–H), 7.55 – 7.49 (2H, m, 3–H), 3.27 (4H, q, *J* = 7.2 Hz, –CH_2), 1.15 (6H, t, *J* = 7.2 Hz, –CH_3). δ_C (101 MHz, $CDCl_3$) 140.4 (C–1), 132.23 (C–2), 129.00 (C–3), 126.97 (C–4), 42.02 (–CH_2), 14.1 (–CH_3). m/z (LC-MS ESI+) 214.604 $[M+H]^+$, 427.207 $[2M+H]^+$. Data agrees with that reported in Wei et al.[135]

94. *N,N-diethylnaphthalene-1-sulfonamide*

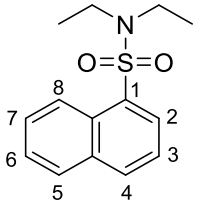

Compound was synthesized according to general procedure B using *1-bromonaphthalene* **93** (2.00 g, 1.4 ml, 5.00 mmol) and *diethyl amine* (3.66 g, 50.0 mmol, 10.0 eq). Following separation of the layers, the aqueous layer was extracted with DCM (3 x 20 ml), concentrated and purified by column chromatography (EtOAc in Hex, 0-45%) to yield the title compound as a clear oil (0.297 g, 1.12 mmol. 23%). δ_H (599 MHz, $CDCl_3$) 8.64 (1H, dq, *J* = 8.7, 0.9 Hz, 5–H), 8.19 (1H, dd, *J* = 7.3, 1.2 Hz, 2–H), 8.03 (1H, dd, *J* = 8.2, 1.2 Hz, 4–H), 7.90 (1H ddd, *J* = 8.1, 1.3, 0.6 Hz, 8–H), 7.63 (1H, ddd, *J* = 8.7, 6.9, 0.6 Hz, 6–H), 7.57 (1H, ddd, *J* = 8.1, 6.9, 0.9 Hz, 7–H), 7.51 (1H, dd, *J* = 8.2, 7.3 Hz, 3–H) 3.40 (4H, q, *J* = 7.1, –CH_2), 1.11 (6H, t, *J* = 7.1, –CH_3). δ_C (151 MHz, $CDCl_3$) 135.4 (C–2), 134.4 (C–1), 133.9 (C–4a), 129.4 (C–5), 128.8 (C–4), 128.6 (C–7), 127.9 (C–8), 126.7 (C–8a), 125.1 (C–6), 124.0 (C–3), 40.8 (–*C*H_2), 13.7 (–*C*H_3). m/z (LC-MS ESI+) 264.25 $[M+H]^+$. Data agrees with that reported in Lai et al.[136]

95. *N-(2'-aminoethyl)quinoline-8-sulfonamide*

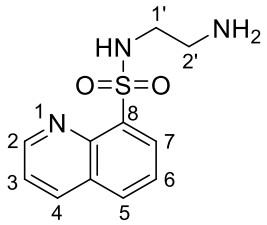

Compound was synthesized according to general procedure C using *8-Bromoquinoline* (0.560g, 2.69 mmol, 1.00 eq) and *N-Boc ethylenediamine* (0.647 g, 4.037 mmol, 1.50 eq). Following quenching with sat. $NaHCO_{3(aq)}$ (15 ml), the aqueous layer was washed with DCM (3 x 15 ml). 3M HCl (10 ml) was added to the aqueous fraction and the mixture was allowed to room temperature for 1 hour. The resulting free amine was then purified with successive washes of hexane (2 x 20 ml), DCM (2 x 20 ml) and ethyl acetate (2 x 20 ml). The aqueous layer was then basified to pH12 using 1M NaOH, extracted with EtOAc (3 x 20 ml) and the combined organic layers were washed with brine (3 x 10 ml) and dried over $MgSO_4$. The resulting mixture was then dissolved in ice water and filtered. The filtrate was collected and dried *in vacuo* to yield the title compound (84mg, 0.322 mmol, 12.9%) as a yellow oil. δ_H (699mHz, $CDCl_3$) 9.03 (1H, dd, *J* = 4.2, 1.8, 2–H), 8.41 (1H, dd, *J* = 7.3, 1.5, 7–H), 8.26 (1H, dd, *J* = 8.3, 1.8, 4–H), 8.04 (1H, dd, *J* = 8.2, 1.5, 5–H), 7.64 (1H, dd, *J* = 8.2, 7.3, 6–H), 7.54 (1H, dd, *J* = 8.3, 4.2 Hz, 3–H), 3.65 (2H, m, *b*, –NH_2) 2.94 (2H, t, *J* = 5.7, 1'–H_2), 2.83 (2H, t, *J* = 5.7, 2'–H_2). δ_C (176 MHz, $CDCl_3$) 151.4 (C–2), 143.2 (C–8a), 137.0 (C–4), 135.8 (C–4a), 133.3 (C–5), 131.2 (C–7), 128.7 (C–8),

125.7 (C–6), 122.3 (C–3), 45.70 (C–1'), 41.28 (C–2'). ν_{max} (ATR) 3370 (N–H), 3257 (N–H), 2933, 2868, 2256, 1489, 1316, 1143, 905 cm^{-1}. m/z (LC-MS ESI+) 252.0 $[M+H]^+$. Data agrees with Del Solar et al.[137]

96a. *tert-butyl N-[2'-(isoquinoline-8-sulfonamido)ethyl]carbamate*

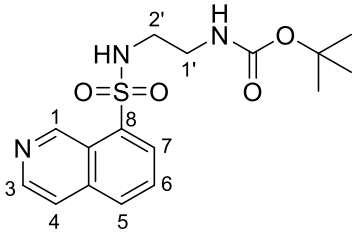

Compound was synthesized according to general procedure C using *8-bromoisoquinoline* (490mg, 2.00 mmol) and *N-Boc ethylenediamine* (0.566 g, 0.004 mol, 1.50 eq). Following separation of the layers, the crude product was isolated by extraction into the aqueous layer with water (3x20ml) basified to pH 12 using 0.1M NaOH. The aqueous layers were then combined and neutralized to pH 7 using 0.1M HCl and extracted with DCM (3x50ml). The combined organic layers were dried over $MgSO_4$, concentrated and purified by column chromatography [(EtOAc: (MeOH:DCM, 1:9), 0-100%) to yield the title compound as an off-white solid (317 mg, 0.774 mmol, 39%) m.p.: 135-137 °C. δ_H (700mHz, $CDCl_3$) 10.15 (1H, s, 1–H), 8.72 (1H, d, *J* = 5.6, 3–H), 8.32 (1H, d, *J* = 7.2, 7–H), 8.05 (1H, d, *J* = 8.2, 5–H), 7.80 (1H, d, *J* = 5.6, 4–H), 7.77 (1H, dd, *J* = 8.2, 7.2, 6–H), 6.98 (1H, s, 2'–N*H*), 4.93 (1H, s, 1'–N*H*), 3.22 (2H, q, *J* = 5.7, 2'–H_2), 3.07 (2H, q, *J* = 5.7, 1'–H_2), 1.36 (9H, s, –$(CH_3)_3$). δ_C (176 MHz, $CDCl_3$) 156.3 (*C*=O), 149.1 (C–1), 143.7 (C–2), 136.9 (C–4a), 136.2 (C–1), 132.5 (C–5), 130.5 (C–7), 128.9 (C–6), 123.2 (C–8a), 121.3 (C–4), 79.8 (–*C*$(CH_3)_3$), 43.5 (C–2'), 40.5 (C–1'), 28.3 (–C(*C*$H_3)_3$). ν_{max} (ATR) 3292 (N–H), 2972, 2917, 2156, 1695 (C=O), 1603, 1510, 1161, 984 cm^{-1}. *m/z* (LC-MS ESI+) 352.03 $[M+H]^+$. Accurate mass (ES+) found $[M+H]^+$ 352.1322, $C_{16}H_{22}N_3O_4S$ requires *M* 352.1331.

96. *N-(2'-aminoethyl)isoquinoline-8-sulfonamide hydrochloride*

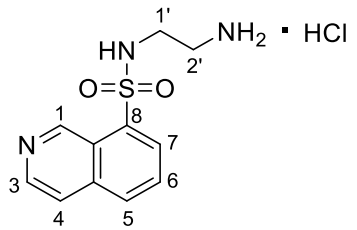

Compound was prepared according to general procedure B, using *tert-butyl N-[2'-(isoquinoline-8-sulfonamido)ethyl]carbamate* **96a** (61.1 mg, 0.174 mmol) to yield the title compound as a light brown amorphous solid (48.0 mg, 0.167 mmol, 96%). δ_H (700 MHz, D_2O) 10.09 (1H, s, 1–H), 8.59 (1H, d, *J* = 6.5 Hz, 3–H), 8.51 – 8.44 (2H, m, 7–H & 5–H), 8.40 (1H, d, *J* = 6.5 Hz, 4–H), 8.16 (1H, dd, *J* = 8.4, 7.4 Hz, 6–H), 3.72 – 3.50 (m (broad), –NH_3^+), 3.14 (2H. dd, *J* = 5.7, 5.1 Hz, 2'–H_2), 3.04 (2H, t, *J* = 5.7 Hz, 1'–H_2). δ_C (176 MHz, D_2O) 143.4 (C–1), 140.5 (C–2), 136.2 (C–4a), 135.1 (C–1), 133.6 (C–5), 133.5 (C–6), 132.9 (C–7), 126.9 (C–8a), 122.4 (C–4), 40.0 (C–2'), 39.2 (C–1'). ν_{max} (ATR) 3345 (N–H), 3260 (N–H), 2980, 2933, 2347, 2112, 1538, 1471, 1382, 1206, 1062, 1019 $cm^{-}1$. *m/z* (LC-MS ESI+) 252.30 $[M+H]^+$. Accurate mass (ES+) found $[M+H]^+$ 252.0810, $C_{11}H_{14}N_3O_2S$ requires *M* 252.0813.

97a. *tert-butyl N-[2'-(isoquinoline-5-sulfonamido)ethyl]carbamate*

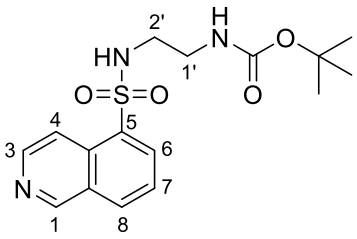

Compound was synthesized according to general procedure C using *5-bromoisoquinoline* (500 mg, 2.40 mmol) and *N-Boc ethylenediamine* (0.578 g, 0.004 mol, 1.50 eq). Following separation of the layers, the crude product was isolated by extraction into the aqueous layer with water (3 x 20 ml) basified to pH 12 using 0.1M NaOH. The aqueous layers were then combined and neutralized to pH 7 using 0.1M HCl and extracted with DCM (3 x 50 ml). The combined organic layers were dried over $MgSO_4$, concentrated and purified by column chromatography (EtOAc in Hex, 0-100%) to yield the title compound as a light-yellow solid (0.290 mg, 0.825 mmol, 29%). m.p.: 118-120 °C. δ_H (700mHz, $CDCl_3$) 9.02 (1H, d, *J* = 8.8, 3–H), 9.00 (1H, d, *J* = 4.2, 1–H), 8.32 (1H, dd, *J* = 8.4, 1.2, 6–H), 8.26 (1H, dd, *J* = 7.4, 1.2, 8–H), 7.76 (1H, dd, *J* = 8.4, 7.4, 7–H), 7.55 (1H, dd, *J* = 8.8, 4.2, 4–H), 5.78 (1H, s, 2'–N*H*), 4.81 (1H, s, 1'–N*H*), 3.19 (2H, q, *J* = 5.6, 2'–H_2), 3.06 (2H, t, *J* = 5.6, 1'–H_2), 1.38 (9H, s, – (CH_3)$_3$). δ_C (176 MHz, $CDCl_3$) 156.8 (*C*=O), 151.1 (C–1), 148.6 (C–3), 135.6 (C–4), 135.1 (C–8a), 133.0 (C–5), 129.5 (C–8), 127.6 (C–7), 124.0 (C–4a), 122.7 (C–6), 80.2 (–*C*(CH_3)$_3$), 44.2 (C–2'), 40.3 (C–1'), 28.3 (– (*C*H_3)$_3$). ν_{max} (ATR) 3269 (N-H), 2989, 2934, 2245, 1695 (C=O), 1601, 1502, 1321, 1156, 1089 cm^{-1}. *m/z* (LC-MS ESI+) 352.795 $[M+H]^+$. Accurate mass (ES+) found $[M+H]^+$ 352.1337, $C_{16}H_{22}N_3O_4S$ requires *M* 352.1331. CHN found: C 54.65; H 5.99; N 11.72. $C_{16}H_{21}N_3O_4S$ requires C 54.68; H 6.02; N 11.96.

97. *N-(2'-aminoethyl)isoquinoline-5-sulfonamide hydrochloride*

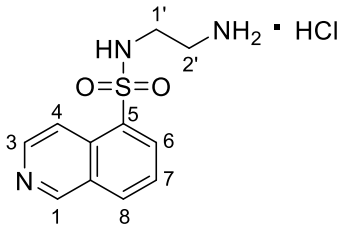

Compound was prepared according to general procedure B, using *tert-butyl N-[2'-(isoquinoline-5-sulfonamido)ethyl]carbamate* **97a** (86.8mg, 0.247mmol) to yield the title compound as a light brown amorphous solid (69.5 mg, 0.242 mmol, 98%). δ_H (700 MHz, D_2O) 9.55 (1H, dd, *J* = 8.9, 1.3 Hz, 3–H), 9.13 (1H, d, *J* = 1.3 Hz, 1–H), 8.41 (1H, dd, *J* = 7.4, 1.2 Hz, 6–H), 8.37 (1H, dd, *J* = 8.7, 1.2 Hz, 8–H), 8.13 – 8.07 (2H, m, 7–H & 4–H), 3.72 – 3.48 (m (broad), –NH_3^+), 3.10 (2H, t, *J* = 5.7 Hz, 2'–H_2), 3.02 (2H t, *J* = 5.7 Hz, 1'-H_2). δ_C (176 MHz, D_2O) 145.6 (C–1), 142.9 (C–3), 139.0 (C–4), 134.9 (C–8a), 133.3 (C–5), 132.2 (C–8), 127.0 (C–7), 124.3 (C–4a), 123.7 (C–6), 39.9 (C–2'), 39.2 (C–1'). ν_{max} (ATR) 3359 (N–H), 3273 (N–H), 2983, 2892, 2111, 2003, 1544, 1334, 1230, 1139, 1031, 953 cm^{-1}. *m/z* (LC-MS ESI+) 252.248 $[M+H]^+$. Accurate mass (ES+) found $[M+H]^+$ 252.0812, $C_{11}H_{14}N_3O_2S$ requires *M* 252.0813.

98a. *tert-butyl N-[2'-(quinoline-5-sulfonamido)ethyl]carbamate*

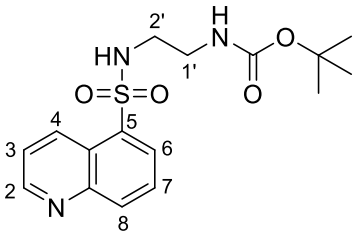

Compound was synthesized according to general procedure C using *5-bromoquinoline* (500mg 2.40mmol) and *N-Boc ethylenediamine* (0.202 mL, 2.643 mmol, 1.10 eq). Following separation of the layers, the crude product was isolated by extraction into the aqueous layer with water (3 x 20 ml) basified to pH 12 using 0.1M NaOH. The aqueous layers were then combined and neutralized to pH 7 using 0.1M HCl and extracted with DCM (3 x 50 ml). The combined organic layers were dried over $MgSO_4$, concentrated and purified by column chromatography (EtOAc in Hex, 0-100%) to yield the title compound as a light yellow amorphous solid (348 mg, 0.990 mmol, 41%). δ_H (700 MHz, $CDCl_3$) 9.01 (1H, d, *J* = 8.7, 8–H), 8.99 (1H, dd, *J* = 4.2, 1.6, 6–H), 8.31 (1H, d, *J* = 8.5, 2–H), 8.25 (1H, dd, *J* = 7.3, 1.6, 4–H), 7.75 (1H, dd, *J* = 8.5, 7.3, 3–H), 7.53 (1H, dd, *J* = 8.7, 4.2, 7–H), 5.92 (1H, s, 2'–N*H*), 4.85 (1H, s, 1'–N*H*), 3.18 (2H, q, *J* = 5.8, 2'–H_2), 3.05 (2H, q, *J* = 5.8, 1'–H_2), 1.37 (9H, s, –C(CH_3)$_3$). δ_C (176 MHz, $CDCl_3$) 156.8 (*C*=O), 151.1 (C–4), 148.6 (C–5), 135.6 (C–2), 135.1 (C–8a), 133.0 (C–8), 129.5 (C–4a), 127.6 (C–3), 124.0 (C–6), 122.7 (C–7), 80.1 (–*C*(CH_3)$_3$), 44.1 (C–2'), 40.3

(C–1'), 28.3 (– (*C*H$_3$)$_3$). ν_{max} (ATR) 3269 (N–H), 3119, 2980, 2934, 1690 (C=O), 1618, 1518, 1492, 1321, 1249, 1161, 1094, 733 cm^{-1}. *m/z* (LC-MS ESI+) 352.04 [M+H]$^+$. Accurate mass (ES+) found [M+H]$^+$ 352.1333, $C_{16}H_{22}N_3O_4S$ requires *M* 352.1331.

98. *N-(2'-aminoethyl)quinoline-5-sulfonamide hydrochloride*

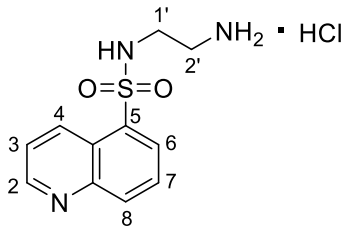

Compound was prepared according to general procedure B, using tert-butyl N-[2'-(quinoline-5-sulfonamido)ethyl]carbamate (**98a**) (86.8 mg, 0.247 mmol) to yield the title compound as a light brown amorphous solid (69.5 mg, 0.24 2mmol, 98%). δ_H (700 MHz, D_2O) 9.53 (1H, dt, *J* = 8.9, 1.4 Hz, 8–H), 9.13 (1H, dd, *J* = 5.3, 1.4 Hz, 6–H), 8.39 (1H, dd, *J* = 7.5, 1.1 Hz, 2–H), 8.35 (1H, dt, *J* = 8.7, 1.1 Hz, 4–H), 8.12 – 8.07 (2H, m, 3-H & 7–H), 3.10 (2H, dd, *J* = 5.8, 5.1 Hz, 2'–H$_2$), 3.02 (2H t, *J* = 5.8 Hz, 1'–H$_2$). δ_C (176 MHz, D_2O) δ 145.6 (C–4), 142.8 (C–5), 138.9 (C–2), 134.9 (C–8a), 133.3 (C–8), 132.3 (C–4a), 127.1 (C–3), 124.2 (C–6), 123.7 (C–7), 39.9 (C–2'), 39.2 (C–1'). ν_{max} (ATR) 3317 (N–H), 3222 (N–H), 2971, 2930, 2350, 2127, 1474, 1375, 1267, 1155, 1015 cm^{-1}. *m/z* (LC-MS ESI+) 252.30 [M+H]$^+$. Accurate mass (ES+) found [M+H]$^+$ 252.0812, $C_{11}H_{14}N_3O_2S$ requires *M* 252.0813.

100a. *tert-butyl N-[2'-(isoquinoline-4-sulfonamido)ethyl]carbamate*

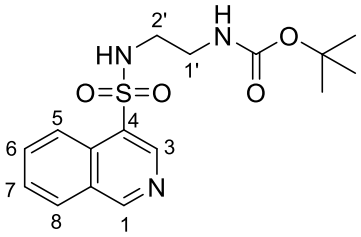

Compound was synthesized according to general procedure C using *4-bromo, isoquinoline* (500 mg, 2.40 mmol) and *N-Boc ethylenediamine* (579.9 mg, 0.004 mol, 1.50 eq). Following separation of the layers, the crude product was isolated by extraction into the aqueous layer with water (3 x 20 ml) basified to pH 12 using 0.1M NaOH. The aqueous layers were then combined and neutralized to pH 7 using 0.1M HCl and extracted with DCM (3 x 50 ml). The combined organic layers were dried over $MgSO_4$, concentrated and purified by column chromatography (EtOAc in Hex 0-100%) to yield the title compound as a light orange solid (516 mg, 1.64 mmol, 61%), m.p. 140-142 ^{o}C. δ_H (599 MHz, $CDCl_3$) 9.40 (1H, s, 1–H), 9.10 (1H, s, 3–H), 8.65 – 8.52 (1H, m, 5–H), 8.09 (1H, dt, *J* = 8.2, 1.0 Hz, 8–H), 7.88 (1H, ddd, *J* = 8.4, 6.9, 1.0 Hz, 6–H), 7.74 (1H, ddd, *J* = 8.2, 6.9, 1.2 Hz, 7–H), 5.90 (1H, s, 2'–N*H*),

4.84 (1H, s, 1'–N*H*), 3.21 (2H, q, *J* = 5.6 Hz, 1'–H_2), 3.10 (2H, q, *J* = 5.6 Hz, 2'–H_2), 1.38 (9H, s, –$(CH_3)_3$). δ_C (151 MHz, $CDCl_3$) 157.9 (C–1), 156.8 (*C*=O), 144.6 (C–3), 132.8 (C–6), 130.8 (C–8a), 129.5 (C–4a), 128.8 (C–8), 128.4 (C–7), 125.7 (C–4) 123.8 (C–5), 80.1 (–*C*$(CH_3)_3$), 44.2 (C–2'), 40.4 (C–1'), 28.2 (–(CH$_3$)$_3$). ν_{max} (ATR) 3282 (N–H), 2983, 2942, 2255, 1694 (C=O), 1592, 1500, 1369, 1259, 1159, 1099, 914 cm^{-1}. m/z (LC-MS ESI+) 353.29 $[M+H]^+$, 296.073 $[M–tBu+2H]^+$, 705.47 $[2M+H]^+$. Accurate mass (ES+) found $[M+H]^+$ 352.1339, $C_{16}H_{22}N_3O_4S$ requires *M* 352.1331.

100. *N-(2-aminoethyl)isoquinoline-4-sulfonamide hydrochloride*

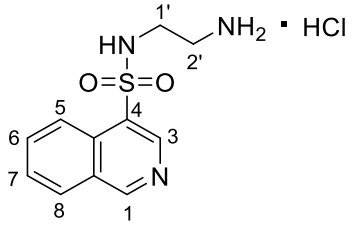

Compound was prepared according to general procedure B, using *tert-butyl N-[2'-(isoquinoline-4-sulfonamido)ethyl]carbamate* **100a** (60.0 mg, 0.171 mmol) to yield the title compound as a light brown solid (48.0 mg, 0.167 mmol, 98%) m.p. 137-139ºC. δ_H (700 MHz, CD_3OD) 9.98 (1H, s, 1–H), 9.11 (1H, s, 3–H), 8.87 (1H, d, J = 8.6 Hz, 5–H), 8.64 (1H, d, J = 8.2 Hz, 8–H), 8.41 – 8.34 (1H, dd, J = 8.6, 7.5 Hz, 6–H), 8.14 (1H, dt, J = 8.2, 7.5 Hz, 7–H), 3.23 (2H, t, J = 5.8 Hz, 2'–H_2), 3.09 (2H, t, J = 5.8 Hz, 1'–H_2). δ_C (176 MHz, CD_3OD) 153.3 (C–1), 137.9 (C–3), 135.1 (C–6), 133.7 (C–8a), 133.1 (C–4a), 131.8 (C–8), 131.1 (C–7), 128.6 (C–4), 124.3 (C–5), 39.9 (C–2'), 39.4 (C–1'). ν_{max} (ATR) 3301 (N–H), 3267 (N–H, 2972, 2926, 2846, 1644, 1484, 1384, 1226, 1136, 1089, 1018 cm-1. *m/z* (LC-MS ESI+) 292.31 $[M+H]^+$. Accurate mass (ES+) found $[M+H]^+$ 252.0817, $C_{11}H_{14}N_3O_2S$ requires *M* 252.0813.

102. *tert-butyl N-[2'-(7-chloro-2,1,3-benzoxadiazole-4-sulfonamido)ethyl]carbamate*

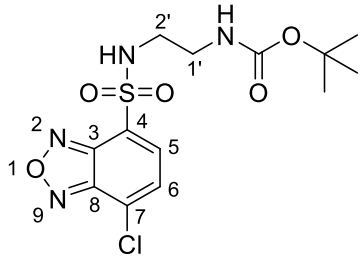

Compound was prepared according to general procedure A using *4-chloro-7-chlorosulfonyl-2,1,3-benzoxadiazole* (150 mg, 0.593 mmol, 1.00 eq) and *N-Boc ethylenediamine* (143 mg, 0.889 mmol, 1.50 eq). Purification by recrystallization (DCM in Hexane) afforded the title compound as a white solid (154 mg, 0.409 mmol, 69%). m.p.: 181-182 ℃. δ_H (599 MHz, $CDCl_3$) 7.99 (d, *J* = 7.3 Hz, 5–H), 7.54 (d, *J* = 7.3 Hz, 6–H), 5.81 (1H. s, 2'–NH), 4.78 (1H, s, 1'–NH), 3.42 – 3.15 (4H, m, 2'–H_2, 1'–

H_2), 1.40 (9H, s, –C(CH_3)$_3$). δ_C (151 MHz, $CDCl_3$) 156.4 (C=O), 148.9 (C–4), 145.0 (C–7), 133.5 (C–5), 129.1 (C–6), 128.0 (C–3), 127.8 (C–8), 80.2 (–*C*(CH$_3$)$_3$), 44.1 (C–2'), 40.3 (C–1'), 28.2 (–C(CH$_3$)$_3$). ν_{max} (ATR) 3325 (N–H), 3087, 2997, 1687 (C=O), 1542, 1336, 1279, 1155, 1098, 1045, 945 cm^{-1}. *m/z* (LC-MS ESI+) 321.178 ([M(^{35}Cl)–*tBu*+2H]$^+$, 100), 323.154 ([M(^{37}Cl)–*tBu*+2H]$^+$, 36), 399.197 ([M+Na (^{35}Cl)]$^+$, 39), 401.163 ([M+Na (^{37}Cl)]$^+$, 14) Accurate mass (ES+) found [M+Na ($_{35}$Cl)]$^+$ 399.0505, $NaC_{13}H_{17}N_4O_5{}^{35}ClS$ requires *M* 399.0506.

103. *tert-butyl N-{2'-[7-(methylamino)-2,1,3-benzoxadiazole-4-sulfonamido]ethyl}carbamate*

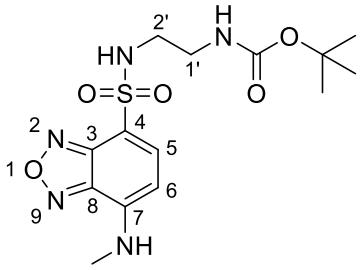

To a sealed flasks under argon, cesium carbonate (277 mg, 0.849 mmol, 4.00 eq) was added in portions to a solution of *tert-butyl N-[2-(7-chloro-2,1,3-benzoxadiazole-4-sulfonamido)ethyl]carbamate* **102** (80.0 mg, 0.212 mmol, 1.00 eq) and methyl amine in THF (2.1 mL, 2.00M, 4.25 mmol, 20.0 eq) in MeOH (2.0 mL). The reaction was left to stir at room temperature for 5 hours, quenched with water (5 ml) concentrated and the resulting aqueous mixture was extracted with DCM (3x10ml). The combined organic layers were then washed with sat. $Na_2CO_{3\,(aq)}$, dried over $MgSO_4$ concentrated and purified by column chromatography (EtOAc in Hexane, 0-60%) to yield the title compound as a yellow solid (66 mg, 0.178 mmol, 84%). m.p: δ_H (400 MHz, MeOD) 8.05 (1H, d, *J* = 7.8 Hz, 5–H), 6.88 (1H, d, *J* = 7.8 Hz, 6–H), 4.15 (3H, s, –NHCH_3), 3.03-3.10 (4H, m, 2'–H_2, 1'–H_2), 1.37 (9H, s, –C(CH_3)$_3$). δ_C (101 MHz, MeOD) 156.9 (C=O), 152.6 (C–7), 145.9 (C–3), 144.9 (C–8), 136.7 (C–5), 120.1 (C–4), 104.7 (C–6), 78.8 (–*C*(CH$_3$)$_3$), 56.4 (–NH*C*H$_3$), 42.3 (C–2'), 39.8 (C–1'), 27.2 (–C(*C*H$_3$)$_3$). ν_{max} (ATR) 3369 (N–H), 3282 (N–H), 2992, 2955, 2504, 2432, 1683 (C=O),1556, 1534, 1428, 1334, 1165, 1146, 1093, 976, 886 cm^{-1}. *m/z* (LC-MS ESI+) 373.297 [M+H]$^+$, 317.238 [M–*tBu*+2H]$^+$, 273.245 [M–Boc+2H]$^+$. Accurate mass (ES+) found [M–Boc+2H]$^+$ 273.0653, $C_9H_{15}N_5O_3S$ requires *M* 273.0658.

104. *7-(methylamino)-N-[2'-(trimethylazaniumyl)ethyl]-2,1,3-benzoxadiazole-4-sulfonamide chloride*

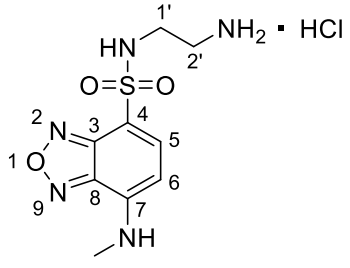

Compound was prepared according to general procedure B, using *tert-butyl N-{2'-[7-(methylamino)-2,1,3-benzoxadiazole-4-sulfonamido]ethyl}carbamate* **103** (38 mg, 0.102 mmol, 1.00 eq) to yield the title compound as a bright yellow amorphous solid (31 mg, 0.100 mmol, 98%). δ_H (700 MHz, CD_3OD) 8.12 (1H, d, J = 7.8 Hz, 5–H), 6.91 (1H, d, J = 7.8 Hz, 6–H), 4.17 (3H, s, –NHCH_3), 3.29 (2H, t, J = 5.9 Hz, 2'–H_2), 3.09 (2H, t, J = 5.9 Hz, 1'–H_2). δ_C (176 MHz, CD_3OD) 152.9 (C–7), 146.0 (C–3), 145.1 (C–8), 137.5 (C–5), 119.1 (C–4), 104.8 (C–6), 56.5 (–NHCH_3), 40.0 (C–2'), 39.4 (C–1'). *m/z* (LC-MS ESI+) 272.703 $[M+H]^+$, 545.071 $[2M+H]^+$. Accurate mass (ES+) found $[M+H]^+$ 272.0820, $C_9H_{14}N_5O_3S$ requires *M* 272.0817.

108b. *1-bromo, 2-methoxynaphthalene*

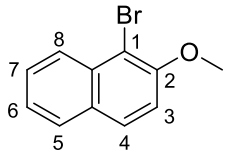

Compound was synthesized according to general procedure C using *1-bromo, naphtha-2-ol* (500 mg, 2.24 mmol) and *iodomethane* (0.558 ml, 8.97 mmol). Following extraction of the aqueous fraction with EtO_2 (3 x 15 ml), the combined organic layers were purified by successive washes with 0.1 M NaOH (3 x 20 ml) and brine (3 x 20 ml). The organic fraction was dried over $MgSO_4$ and concentrated to yield the title compound as a light brown solid (493 mg, 2.08 mmol, 93%). m.p.: 82-83 °C. δ_H (400MHz, $CDCl_3$) 8.24 (1H, dq, J = 8.6, 1.2, 8–H), 7.82 – 7.78 (2H, m, 5–H, 4–H), 7.58 (1H, ddd, J = 8.6, 6.9, 1.3, 7–H), 7.41 (1H ddd, J = 8.1, 6.9, 1.2, 6–H), 7.26 (1H, d, J = 8.9, 3–H), 4.02 (3H, s, –OCH_3). δ_C (101 MHz, $CDCl_3$) 153. (C–2), 133.1 (C–8a), 129.8 (C–4a), 129.0 (C–4), 128.1 (C–5), 127.8 (C–7), 126.1 (C–8), 124.3 (C–6), 113.6 (C–3), 108.6 (C–1), 57.1 (–OCH_3). ν_{max} (ATR) 2927, 2837, 1599, 1351, 1275, 1070, 739 cm^{-1}. *m/z* (LCMS ES+) 237.2 ($[M(^{79}Br)+H]^+$, 100), 239.1 ($[M(^{81}Br)+H]^+$, 100). Data agrees with that reported in Zhao et al.[138]

108c. *tert-butyl N-[2'-(2-methoxynaphthalene-1-sulfonamido)ethyl]carbamate*

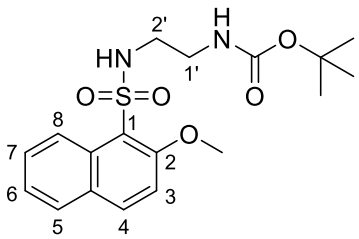

Compound was synthesized according to general procedure C using *1-bromo, 2-methoxynaphthalene* **108b** (486 mg, 2.00 mmol, 1.00 eq) and *N-Boc ethylenediamine* (0.493 g, 3.08 mmol, 1.50 eq). Following separation of the layers and extraction of the aqueous fraction with DCM (3 x 15 ml), the combined organic layers were dried over $MgSO_4$, concentrated and purified by column chromatography

(EtOAc in Hex 0-55%) to yield the title compound as a brown amorphous solid (274 mg, 0.702 mmol, 35%). δ_H (700MHz, $CDCl_3$) 9.20 (1H, dd, *J* = 8.9, 1.1, 8–H), 8.02 (1H, d, *J* = 9.0, 4–H), 7.79 (1H, dd, *J* = 8.0, 1.4, 5–H), 7.59 (1H, ddd, *J* = 8.9, 6.8, 1.4, 7–H), 7.43 (1H, ddd, *J* = 8.0, 6.8, 1.1, 6–H), 7.33 (1H, d, *J* = 9.0, 3–H), 5.90 (1H, t, *J* = 6.3 Hz, 2'–N*H*), 4.92 (1H, s, 1'–N*H*), 4.11 (3H, s, –OCH_3), 3.22 (2H, q, *J* = 6.0, 1'–H_2), 3.04 (2H, q, *J* = 6.0, 2'–H_2), 1.40 (9H, s, –C(CH_3)$_3$). δ_C (176 MHz, $CDCl_3$) 156.1 (C–2) 156.0 (*C*=O), 135.6 (C–4), 131.3 (C–8a), 129.3 (C–4a), 128.8 (C–5), 128.6 (C–7), 124.7 (C–6), 124.30 (C–8), 121.0 (C–1), 113.0 (C–3), 79.6 (–*C*(CH_3)$_3$), 57.7 (–OCH_3), 43.5 (C–2'), 40.4 (C–1'), 21.6 (–C(CH_3)$_3$). ν_{max} (ATR) 3337 (N–H), 2979, 2875, 2255, 1623 (C=O), 1507, 1275, 1251, 1151, 1027 cm^{-1}. *m/z* (LC-MS ESI+) 381.2 $[M+H]^+$. Accurate mass (ES+) found $[M+H]^+$ 381.1472, $C_{18}H_{25}N_2O_5S$ requires *M* 381.1472.

108. *N-(2'-aminoethyl)-2-methoxynaphthalene-1-sulfonamide hydrochloride*

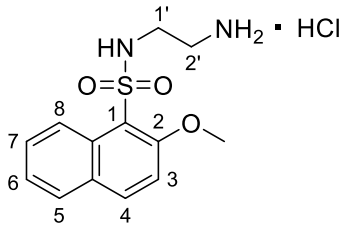

Compound was prepared according to general procedure B, using *tert-butyl N-[2'-(2-methoxynaphthalene-1-sulfonamido)ethyl]carbamate* **108c** (52.0 mg, 0.137 mmol) to yield the title compound as a light brown amorphous solid (0.420 mg, 0.134 mmol, 98%). δ_H (700 MHz, D_2O) 8.66 (1H, d, *J* = 7.9, Hz, 8–H), 7.95 (1H, d, *J* = 9.2 Hz, 4–H), 7.72 (1H, d, *J* = 8.2 Hz, 5–H), 7.48 (1H, dt, *J* = 7.9, 6.8 Hz, 7–H), 7.36 – 7.25 (2H, m, 3–H & 6–H), 3.94 (3H, s, –OCH_3), 3.71 – 3.48 (m (broad), –NH_3^+), 2.99 (4H, s, 2'–H_2 & 1'–H_2). δ_C (176 MHz, D_2O) 156.8 (C–2), 137.0 (C–4), 130.4 (C–8a), 129.2 (C–4a), 129.1 (C–5), 128.7 (C–7), 124.6 (C–6), 122.7 (C–8), 116.7 (C–1), 113.1 (C–3), 57.0 (–OCH_3), 39.8 (C–2'), 39.1 (C–1'). ν_{max} (ATR) 3425 (N–H), 3207 (N–H), 2929, 2872, 2466, 1997, 1725, 1602, 1468, 1430, 1335, 1151, 1024, 986 cm^{-1}. *m/z* (LC-MS ESI+) 281.664 $[M+H]^+$, 561.428 $[2M+H]^+$. Accurate mass (ES+) found $[M+H]^+$ 281.0969, $C_{13}H_{17}N_2O_3S$ requires *M* 281.0960.

109b. *1-bromo, 4-pentoxynaphthalene*

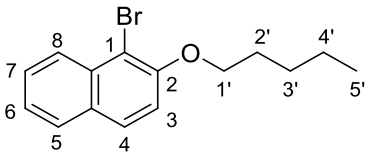

Compound was synthesized according to general procedure C using *1-bromo, naphtha-2-ol* (500 mg, 2.24 mmol) and *1-iodopentane* (1.78 g, 1.2 ml, 8.97 mmol). Following extraction of the aqueous fraction with EtO_2 (3 x 15 ml), the combined organic layers were purified by successive washes with

0.1 M NaOH (3 x 20 ml) and brine (3 x 20 ml). The organic fraction was dried over $MgSO_4$ and concentrated to yield the title compound as a colourless oil (599 mg, 2.042 mmol, 91%). δ_H (700 MHz, $CDCl_3$) 8.22 (1H, dd, *J* = 8.6, 1.1 Hz, 8–H), 7.79 – 7.75 (2H, m, 5–H, 4–H), 7.55 (1H, ddd, *J* = 8.6, 6.8, 1.2 Hz, 7–H), 7.38 (1H, ddd, *J* = 8.0, 6.8, 1.1 Hz, 6–H), 7.26 – 7.23 (1H, m, 3–H), 4.17 (2H, t, *J* = 6.6 Hz, 1'–H_2), 1.92 – 1.82 (2H, m, 2'–H_2), 1.58 – 1.49 (2H, m, 3'–H_2), 1.41 (2H, h, *J* = 7.3 Hz, 4'–H_2), 0.95 (3H, t, *J* = 7.3 Hz, 5'–H_3). δ_C (176 MHz, $CDCl_3$) 153.4 (C–2), 133.2 (C–8a), 129.8 (C–4a), 128.8 (C–4), 128.0 (C–5), 127.6 (C–7), 126.2 (C–8), 124.2 (C–6), 115.2 (C–3), 109.5 (C–1), 70.3 (C–1'), 29.1 (C–2'), 28.2 (C–3'), 22.4 (C–4'), 14.0 (C–5'). ν_{max} (ATR) 2981, 2885, 2260, 1459, 1061, 651 cm^{-1}. *m/z* (LC-MS ESI+) 292.3 ([M(^{79}Br)+H]$^+$, 97), 294.2 ([M(^{81}Br)+H]$^+$, 100). Accurate mass (ES+) found [M+H]$^+$ 292.0471, $C_{15}H_{17}OBr$ requires *M* 292.0463.

109c. *tert-butyl N-[2'-(2-pentoxynaphthalene-1-sulfonamido)ethyl]carbamate*

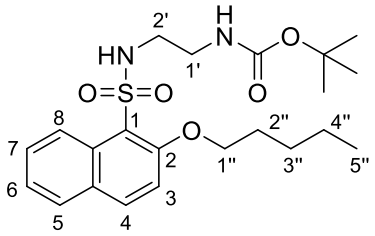

Compound was synthesized according to general procedure C using *1-bromo, 2-pentoxynaphthalene* **109b** (528 mg, 1.80 mmol) and *N-Boc ethylenediamine* (0.433 g, 2.701 mmol, 1.50 eq). Following separation of the layers and extraction of the aqueous fraction with $CHCl_3$ (3 x 15 ml), the combined organic layers were dried over $MgSO_4$, concentrated and purified by column chromatography (EtOAc in $CHCl_3$, 0-15%) to yield the title compound as an off-white amorphous solid (189 mg, 0.433 mmol, 24%). δ_H (700 MHz, $CDCl_3$) 9.22 (1H, d, *J* = 8.6 Hz, 8–H), 8.01 (1H, d, *J* = 9.0 Hz, 4–H), 7.81 (1H dd, *J* = 7.9, 1.4 Hz, 5–H), 7.60 (1H, ddd, *J* = 8.6, 6.8, 1.4 Hz, 7–H), 7.44 (1H, dd, *J* = 7.9, 6.8 Hz, 6–H), 7.32 (1H, d, *J* = 9.0 Hz, 3–H), 5.73 (1H t, *J* = 6.4 Hz, 2'–N*H*), 4.82 (1H, s, 1'–N*H*), 4.29 (2H, t, *J* = 6.9 Hz, 1''–H_2), 3.22 (2H, t, *J* = 6.1 Hz, 1'–H_2), 3.05 (2H, t, *J* = 6.1 Hz, 2'–H_2), 1.95 (2H, p, *J* = 6.9 Hz, 2''–H_2), 1.51 (2H, ddd, *J* = 15.1, 8.6, 6.0 Hz, 3''–H_2), 1.46 – 1.43 (2H, m, 4''–H_2), 1.42 (9H, s, –$C(CH_3)_3$), 0.96 (3H, t, *J* = 7.3 Hz, 5''–H_3). δ_C (176 MHz, $CDCl_3$) 163.2 (C=O), 155.7 (C–2), 135.5 (C–4), 131.4 (C–8a), 129.3 (C–4a), 128.8 (C–5), 128.5 (C–7), 125.0 (C–6) 124.7 (C–8), 121.4 (C–1), 114.2 (C–3), 79.5 (–*C*$(CH_3)_3$), 71.3 (C–1''), 43.4 (C–2'), 40.4 (C–1'), 29.1 (C–2''), 28.3 (–(CH$_3$)$_3$), 28.0 (C–3''), 22.4 (C–4''), 14.0 (C–5''). ν_{max} (ATR) 3465 (N–H), 3319 (N–H), 2981, 2896, 2256, 1707, 1607 (C=O), 1511, 1339, 1160 cm^{-1}. *m/z* (LC-MS ESI+) 437.4 [M+H]$^+$, 381.37 [M–*tBu*+2H]$^+$. Accurate mass (ES+) found [M+H]$^+$ 437.2111, $C_{22}H_{33}N_2O_5S$ requires *M* 437.2110.

109. *N-(2'-aminoethyl)-2-(pentyloxy)naphthalene-1-sulfonamide hydrochloride*

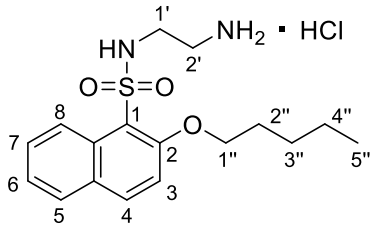

Compound was prepared according to general procedure B using *tert-butyl N-[2'-(2-pentoxynaphthalene-1-sulfonamido)ethyl]carbamate* **109c** (25.0 mg, 0.057 mmol) to yield the title compound as a light brown amorphous solid (21.0 mg, 0.056 mmol, 98%). δ_H (700 MHz, CD_3OD) 9.10 (1H, d, *J* = 8.9 Hz, 8–H), 8.14 (1H, d, *J* = 9.1 Hz, 4–H), 7.88 (1H, d, *J* = 8.2 Hz, 5–H), 7.57 (1H, dd, *J* = 8.9, 6.9 Hz, 7–H), 7.53 (1H, d, *J* = 9.1 Hz, 3–H), 7.44 (1H, dt, *J* = 8.2, 6.9 Hz, 6–H), 4.37 (2H, t, *J* = 7.3 Hz, 1''–H_2), 3.14 (2H, t, *J* = 5.8 Hz, 2'–H_2), 3.07 (1H, t, *J* = 5.8 Hz, 1'–H_2), 1.93 (2H, p, *J* = 7.3 Hz, 2''–H_2), 1.50 (1H, p, *J* = 7.3 Hz, 3''–H_2), 1.42 (2H, h, *J* = 7.3 Hz, 4''–H_2), 0.95 (3H, t, *J* = 7.3 Hz, 5''–H_3). δ_C (176 MHz, CD_3OD) 156.4 (C–2), 135.9 (C–4), 131.2 (C–8a), 129.3 (C–4a), 128.6 (C–5), 128.2 (C–7), 124.2 (C–6), 123.5 (C–8), 119.7 (C–1), 114.3 (C–3), 70.5 (C–1''), 40.1 (C–2'), 39.4 (C–1'), 28.5 (C–2''), 27.6 (C–3''), 22.1 (C–4''), 12.9 (C–5''). ν_{max} (ATR) 3339 (N–H), 2943, 2838, 1607,1511, 1339, 1149 1024 cm^{-1}. *m/z* (LC-MS ESI+) 337.36 $[M+H]^+$, 673.47 $[2M+H]^+$. Accurate mass (ES+) found $[M+H]^+$ 337.1591, $C_{17}H_{25}N_2O_3S$ requires *M* 337.1586.

110b. *1-bromo, 4 methoxynaphthalene*

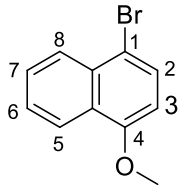

Compound was synthesized according to general procedure D using *1-bromo, naphtha-4-ol* (500 mg, 2.24 mmol) and *iodomethane* (0.558 ml, 8.97 mmol). Following extraction of the aqueous fraction with EtO_2 (3 x 15 ml), the combined organic layers were purified by successive washes with 0.1 M NaOH (3 x 20 ml) and brine (3 x 20 ml). The organic fraction was dried over $MgSO_4$ and concentrated to yield the title compound as a light yellow solid (507 mg, 2.13 mmol, 96%). m.p.: 63-66 °C. δ_H (599 MHz, $CDCl_3$) 8.28 (1H, ddd, *J* = 8.4, 1.3, 0.7 Hz, 5–H), 8.19 – 8.16 (1H, m, 8–H), 7.65 (1H, d, *J* = 8.2 Hz, 2–H), 7.63 – 7.50 (2H, m, 6–H & 7–H), 6.66 (1H, d, *J* = 8.2 Hz, 3–H), 3.97 (3H, s, –OCH_3). δ_C (151 MHz, $CDCl_3$) 155.2 (C–4), 132.4 (C–8a), 129.4 (C–2), 127.7 (C–7), 126.8 (C–1), 126.7 (C–8), 125.9 (C–6), 122.4 (C–5), 113.2 (C–4a), 104.5 (C–3), 55.7 (–OCH_3). ν_{max} (ATR) 2931,2846, 2251, 1588, 1456, 1262, 1089, 651 cm^{-1}. *m/z* (LC-MS ESI+) 237.0 ($[M(^{79}Br)+H]^+$, 100), 239.0 ($[M(^{81}Br)+H]^+$, 100). Data agrees with that reported in Weimar et al.[139]

110c. *tert-butyl N-[2'-(4-methoxynaphthalene-1-sulfonamido)ethyl]carbamate*

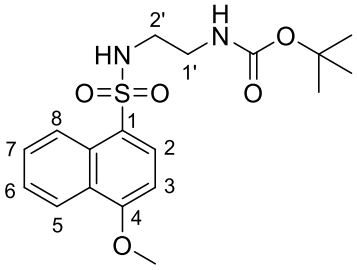

Compound was synthesized according to general procedure C using *1-bromo, 4-methoxynaphthalene* (482 mg, 2.04 mmol) and *N-Boc ethylenediamine* (489.3 mg, 3.054 mmol, 1.50 eq). Following separation of the layers and extraction of the aqueous fraction with $CHCl_3$ (3x15ml), the combined organic layers were dried over $MgSO_4$, concentrated and purified by column chromatography (EtOAc in Hex 0-45%) to yield the title compound as a light-yellow amorphous solid (280 mg, 0.736 mmol, 36%). δ_H (599 MHz, $CDCl_3$) 9.20 (1H, d, *J* = 9.0 Hz, 5–H), 8.02 (1H, d, *J* = 9.1 Hz, 2–H), 7.79 (1H, d, *J* = 8.1 Hz, 8–H), 7.59 (1H, dd, *J* = 9.0, 6.8 Hz, 6–H), 7.43 (1H, dd, *J* = 8.1, 6.8 Hz, 7–H), 7.33 (1H, d, *J* = 8.1 Hz, 3–H), 5.87 (1H, t, *J* = 6.4 2'–N*H*), 4.90 (1H, s, 1'–N*H*), 4.11 (3H, s, –OCH_3), 3.21 (2H, t, *J* = 6.0 Hz, 1'–H_2), 3.04 (2H, q, *J* = 6.4 Hz, 2'–H_2), 1.40 (9H, s, –C(CH_3)$_3$). δ_C (151 MHz, $CDCl_3$), 157.8 (C=O) 156.0 (C–4), 135.6 (C–2), 131.3 (C–1), 129.4 (C–6), 128.8 (C–8a), 128.6 (C–7), 124.8 (C–4a), 124.3 (C–5), 121.0 (C–8), 113.0 (C–3), 79.6 (–*C*(CH_3)$_3$), 57.7 (–O*C*H_3), 43.5 (C–2'), 40.4 (C–1'), 28.3 (–(*C*H_3)$_3$). ν_{max} (ATR) 3370 (N–H), 2990, 2852, 2260, 1604 (C=O), 1511, 1339, 1254, 1155, 1067 cm^{-1}. *m/z* (LC-MS ESI+) 381.4 $[M+H]^+$. Accurate mass (ES+) found $[M+H]^+$ 381.1468, $C_{18}H_{25}N_2O_5S$ requires *M* 381.1484.

110. *N-(2'-aminoethyl)-4-methoxynaphthalene-1-sulfonamide hydrochloride*

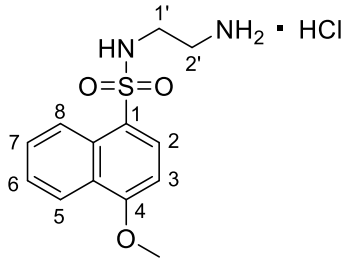

Compound was prepared according to general procedure B, using *tert-butyl N-[2'-(4-methoxynaphthalene-1-sulfonamido)ethyl]carbamate* **110c** (57.1 mg, 0.150 mmol) to yield the title compound as a light brown amorphous solid (47.3 mg, 0.149 mmol, 99%). δ_H (700 MHz, D_2O) 8.69 (1H, d, *J* = 8.9 Hz, 5–H), 7.99 (1H, d, *J* = 9.2 Hz, 2–H), 7.77 – 7.72 (1H, dd, *J* = 8.1, 1.5 8–H), 7.50 (ddd, *J* = 8.9, 6.8, 1.5 Hz, 6–H), 7.37 – 7.30 (2H, m, 7–H & 3–H), 3.96 (3H, s, –OCH_3), 3.71 – 3.47 (m (broad), –NH_3^+), 3.04 – 2.95 (4H, m, 2'–H_2 & 1'–H_2). δ_C (176 MHz, D_2O) 156.8 (C–4), 137.1 (C–2), 130.4 (C–1), 129.2 (C–6), 129.1 (C–8a), 128.7 (C–7), 124.6 (C–4a), 122.7 (C–5), 116.8 (C–8), 113.1 (C–3), 57.0 (–O*C*H_3), 39.8 (C–2'), 39.1 (C–1'). ν_{max} (ATR) 3403 (N–H), 3277 (N–H), 2962, 2857,

2618, 2514, 1716, 1602, 1511, 1335, 1256, 1030 cm^{-1}. *m/z* (LC-MS ESI+) 281.694 $[M+H]^+$, 561.428 $[2M+H]^+$. Accurate mass (ES+) found $[M+H]^+$ 281.0974, $C_{13}H_{17}N_2O_3S$ requires *M* 281.0960.

111b. *1-bromo, 4-pentoxynaphthalene*

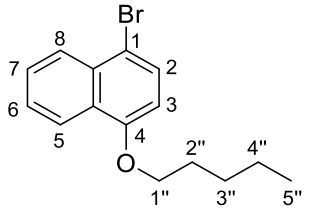

Compound was synthesized according to general procedure D using *4-bromo, naphtha-1-ol* (500 mg, 2.24 mmol) and *1-iodopentane* (1.78g, 1.2 ml, 8.97 mmol). Following extraction of the aqueous fraction with EtO_2 (3 x 15 ml), the combined organic layers were purified by successive washes with 0.1 M NaOH (3 x 20 ml) and brine (3 x 20 ml). The organic fraction was dried over $MgSO_4$ and concentrated to yield the title compound as a light brown oil (608 mg, 2.08 mmol, 93%). δ_H (700 MHz, $CDCl_3$) 8.30 (1H, dd, *J* = 8.4, 1.4, Hz, 5–H), 8.15 (1H, dd, *J* = 8.4, 1.2, Hz, 8–H), 7.63 (1H, d, *J* = 8.2 Hz, 2–H), 7.60 (1H. ddd, *J* = 8.4, 6.8, 1.4 Hz, 7–H), 7.52 (1H, ddd, *J* = 8.4, 6.8, 1.2 Hz, 6–H), 6.66 (1H, d, *J* = 8.2 Hz, 3–H), 4.10 (2H, t, *J* = 6.4 Hz, 1'–H_2), 1.98 – 1.85 (2-H, m, 2'–H_2), 1.54 (2H, m, 3'–H_2), 1.44 (2H, dt, *J* = 14.8, 7.3 Hz, 4'–H_2), 0.96 (3H, t, *J* = 7.3 Hz, 5'–H_3). δ_C (176 MHz, $CDCl_3$) 154.7 (C–4), 132.5 (C–8a), 129.5 (C–2), 127.7 (C–7), 127.0 (C–1), 126.8 (C–8), 125.8 (C–6), 122.5 (C–5), 112.9 (C–4a), 105.2 (C–3), 68.4 (C–1'), 28.9 (C–2'), 28.4 (C–3'), 22.5 (C–4'), 14.0 (C–5'). ν_{max} (ATR) 2981, 2256, 1590, 1375, 1264, 1086, 659 (C-Br) cm^{-1}. *m/z* (LC-MS ESI+) 292.3 ($[M(^{79}Br)+H]^+$ 100), 294.2 ($[M(^{81}Br)+H]^+$, 100). Accurate mass (ES+) found [M+H]+ 292.0470, $C_{15}H_{17}OBr$ requires *M* 292.0463.

111c. *tert-butyl N-[2'-(4-pentoxynaphthalene-1-sulfonamido)ethyl]carbamate*

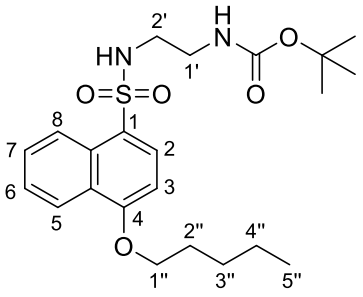

Compound was synthesized according to general procedure C using *1-bromo, 4-methoxynaphthalene* **111b** (530mg, 1.808mmol) and N-Boc ethylenediamine (434.4 mg, 2.711 mmol, 1.50 eq). Following separation of the layers and extraction of the aqueous fraction with $CHCl_3$ (3 x 15 ml), the combined organic layers were dried over $MgSO_4$, concentrated and purified by column chromatography (EtOAc in Hex, 0-20%) to yield the title compound as a light brown oil (307mg, 0.703mmol, 39%). δ_H (599

MHz, $CDCl_3$) 8.54 (1H, dd, *J* = 8.6, 1.1 Hz, 5–H), 8.37 (1H, dd, *J* = 8.5, 1.4 Hz, 8-H), 8.17 (1H, d, *J* = 8.3 Hz, 2–H), 7.66 – 7.59 (1H, m, 6–H), 7.54 (1H, ddd, *J* = 8.5, 6.8, 1.1 Hz, 7–H), 6.76 (1H, d, *J* = 8.3 Hz, 3–H), 5.47 (1H, s, 2'–N*H*), 4.83 (1H, s, 1'–N*H*), 4.17 (2H, t, *J* = 6.4 Hz, 1''–H_2), 3.11 (2H, t, *J* = 5.6 Hz, 2'–H_2), 2.95 (2H, t, *J* = 5.6 Hz, 1'–H_2), 1.99 – 1.88 (2H, m, 2''–H_2), 1.54 (2H, tt, *J* = 14.6, 6.2 Hz, 3''–H_2), 1.43 (2H, dq, *J* = 14.6, 7.3 Hz, 4''–H_2), 1.34 (9H, s, –C(CH_3)$_3$), 0.95 (4-H, t, *J* = 7.3 Hz, 5''–H_3). δ_C (151 MHz, $CDCl_3$) 159.3 (C–4), 156.3 (*C*=O), 131.9 (C–2), 129.3 (C–1), 128.8 (C–6), 126.3 (C–8a), 126.0 (C–7), 125.2 (C–4a), 124.0 (C–5), 123.2 (C–8), 102.4 (C–3), 79.6 (–*C*(CH_3)$_3$) 68.7 (C–1''), 43.4 (C–2'), 40.2 (C–1'), 28.7 (C–2''), 28.3 (C–3''), 28.3 (– (*C*H_3)$_3$), 22.4 (C–4''), 14.0 (C–5''). ν_{max} (ATR) 3444 (N–H), 2976, 2261, 1728, 1606 (C=O), 1507, 1409, 1311, 1224, 1155, 1084, 917 cm^{-1}. *m/z* (LC-MS ESI+) 437.2123 $[M+H]^+$, 381.3630 [M–*tBu*+2H]$^+$. Accurate mass (ES+) found $[M+H]^+$ 437.2122, $[M\text{-Boc}]^+$ 337.1604, $C_{22}H_{33}N_2O_5S$ requires *M* 437.2110.

111. *N-(2'-aminoethyl)-4-(pentyloxy)naphthalene-1-sulfonamide hydrochloride*

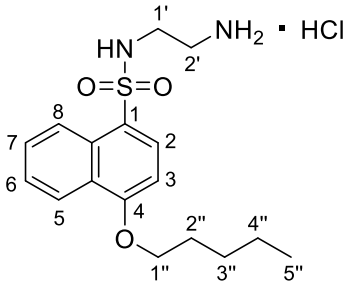

Compound was prepared according to general procedure B, using *tert-butyl N-[2'-(4-pentoxynaphthalene-1-sulfonamido)ethyl]carbamate* **111c** (65.0 mg, 0.149 mmol) to yield the title compound as a light brown amorphous solid (54.0 mg, 0.145 mmol, 97%). δ_H (700 MHz, D_2O) 8.20 (1H, d, *J* = 8.6 Hz, 5–H), 7.86 – 7.76 (2H, m, 2–H & 8–H), 7.31 (1H, dt, *J* = 8.6, 7.6 Hz, 6–H), 7.03 (1H, t, *J* = 7.6 Hz, 7–H), 6.30 (d, *J* = 8.3 Hz, 3–H), 3.51 (2H, t, *J* = 7.2 Hz, 1''–H_2), 2.96 (2H, t, *J* = 5.7 Hz, 2'–H_2), 2.89 (2H, t, *J* = 5.7 Hz, 1'–H_2), 1.34 (2H, d, *J* = 7.2 Hz, 2''–H_2), 1.06 – 0.91 (m, 4H, 3''–H_2, 4''–H_2), 0.57 (3H, t, *J* = 7.2 Hz, 5''–H_3). δ_C (176 MHz, D_2O) 158.8 (C–4), 132.0 (C–2), 128.7 (C–1), 128.5 (C–6), 125.8 (C–8a), 125.5 (C–7), 123.5 (C–4a), 122.3 (C–5), 109.6 (C–8), 102.8 (C–3), 68.4 (C–1''), 39.7 (C–2'), 39.1 (C–1'), 28.0 (C–2''), 27.8 (C–3''), 21.9 (C–4''), 13.4 (C–5''). ν_{max} (ATR) 3314 (N–H) 3267 (N–H), 2977, 2885, 1578, 1330, 1263, 1153, 1091, 819 cm^{-1}. *m/z* (LC-MS ESI+) 337.03 $[M+H]^+$, 673.50 $[2M+H]^+$. Accurate mass (ES+) found $[M+H]^+$ 337.1593, $C_{17}H_{25}N_2O_3S$ requires *M* 337.1586.

112b. *2-bromoanisole*

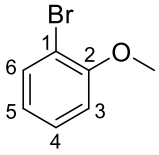

Compound was synthesized according to general procedure D using *2-bromophenol* (0.335 ml, 2.89 mmol) and *iodomethane* (0.720 ml, 11.6 mmol). Following extraction of the aqueous fraction with EtO_2 (3 x 15 ml), the combined organic layers were purified by successive washes with 0.1 M NaOH (3 x 20 ml) and brine (3 x 20 ml). The organic fraction was dried over $MgSO_4$ and concentrated to yield the title compound as a colourless oil (511mg, 2.73mmol, 95%). δ_H (400 MHz, $CDCl_3$) 7.56 (1H, dd, J = 7.8, 1.7 Hz, 3–H), 7.30 (1H, ddd, J = 8.2, 7.4, 1.7 Hz, 5–H), 6.93 (1H, ddd, J = 8.2, 7.8, 1.4 Hz, 4–H), 6.86 (1H, dd, J = 7.4, 1.4 Hz, 6–H), 3.92 (3H, s, –OCH_3). δ_C (101 MHz, $CDCl_3$) 155.9 (C–2), 133.4 (C–3), 128.5 (C–5), 121.8 (C–4), 112.0 (C–6), 111.7 (C–1), 56.2 (–OCH$_3$). V_{max} (ATR) 2929, 2258, 1489, 1254, 1057, 907, 652 cm^{-1}. *m/z* (GC-MS ES+) 186.0 ([M(^{79}Br)+H]$^+$, 100), 188.0 ([M(^{81}Br)+H]$^+$, 98). Data agrees with that as reported in Wang et al.[140]

112c. *tert-butyl N-[2'-(2-methoxybenzenesulfonamido)ethyl]carbamate*

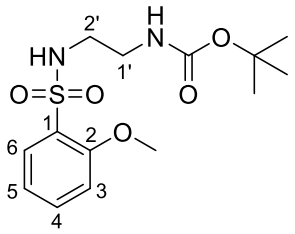

Compound was synthesized according to general procedure C using *2-bromoanisole* **112b** (518 mg, 2.77 mmol) and *N-Boc ethylenediamine* (0.666 g, 4.15 mmol, 1.50 eq). Following separation of the layers and extraction of the aqueous fraction with $CHCl_3$ (3 x 15 ml), the combined organic layers were dried over $MgSO_4$, concentrated and purified by column chromatography (EtOAc in $CHCl_3$ 0-50%) to yield the title compound as a colourless oil (506 mg, 1.53 mmol, 55%). δ_H (700 MHz,$CDCl_3$) 7.88 (1H, dd, J = 7.8, 1.8 Hz, 6–H), 7.53 (1H, ddd, J = 8.3, 7.4, 1.8 Hz, 4–H), 7.05 (1H, ddd, J = 7.8, 7.4, 1.0 Hz, 5–H), 7.02 (1H, dd, J = 8.3, 1.0 Hz, 3–H), 5.34 (1H d, J = 6.8 Hz, 2'–NH), 4.89 (1H, s, 1'–NH), 3.97 (3H, s, –OCH_3), 3.20 (2H, q, J = 5.9 Hz, 1'–H_2), 2.98 (2H, q, J = 5.9 Hz, 2'–H_2), 1.40 (9H, s, –C(CH_3)). δ_C (176 MHz, $CDCl_3$) 156.1 (C–2), 156.0 (C=O), 134.6 (C–4), 130.4 (C–6), 127.7 (C–1), 120.7 (C–5), 112.1 (C–3), 79.6 (–C(CH$_3$)$_3$), 56.4 (–OCH$_3$), 43.3 (C–2'), 40.4 (C–1'), 28.3 (–C(CH$_3$)$_3$. V_{max} (ATR) 3394 (N–H), 2986, 2253, 1678 (C=O), 1596, 1486, 1162, 1072 cm^{-1}. *m/z* (LC-MS ES+) 276.22 [M–*tBu*+2H]$^+$. Accurate mass (ES+) found [M+H]$^+$ 331.1336, $C_{14}H_{23}N_2O_5S$ requires *M* 381.1328.

112. *N-(2'-aminoethyl)-2-methoxybenzene-1-sulfonamide hydrochloride*

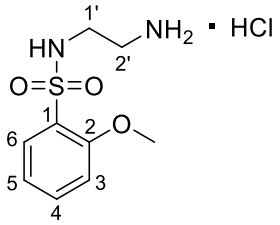

Compound was prepared according to general procedure B, using *tert-butyl N-[2'-(2-methoybenzenesulfonamido)ethyl]carbamate* **112c** (56.0 mg, 0.166 mmol) to yield the title compound as a light brown amorphous solid (42.0 mg, 0.157 mmol, 95%). δ_H (700 MHz, D_2O) 7.84 (1H, dd, J = 7.9, 1.7 Hz, 6–H), 7.71 (1H, ddd, J = 8.5, 7.7, 1.7 Hz, 4–H), 7.26 (1H, ddd, J = 8.5, 7.9, 0.9 Hz, 5–H), 7.15 (1H, td, J = 7.7, 0.9 Hz, 3–H), 3.99 (3H, s, –OCH_3), 3.20 – 3.16 (4H, m, 2'–H_2 & 1'–H_2). δ_C (176 MHz, D_2O) 156.4 (C–2), 136.2 (C–4), 130.1 (C–6), 124.1 (C–1), 120.6 (C–5), 112.9 (C–3), 56.1 (–OCH_3), 39.8 (C–2'), 39.2 (C–1'). V_{max} (ATR) 3369 (N–H), 3257 (N–H), 2124, 1487, 1322, 1288, 1162, 1015 cm^{-1}. *m/z* (LC-MS ESI+) 231.28 $[M+H]^+$, 461.35 $[2M+H]^+$. Accurate mass (ES+) found $[M+H]^+$ 231.0809, $C_9H_{15}N_2O_3S$ requires *M* 231.0803.

113b. *1-bromo, 2-hexoxybenxene*

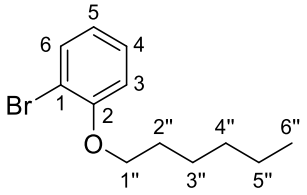

Compound was synthesized according to general procedure D using *2-bromophenol* (650 mg, 3.76 mmol, 1.00 eq), *1-bromohexane* (2.48 g, 2.1 mL, 15.0 mmol, 4.00 eq) and TBAI (14.0 mg, 0.038 mmol, 0.01 eq). Following extraction of the aqueous fraction with EtO_2 (3 x 25 ml), the combined organic layers were purified by successive washes with 0.1 M NaOH (3 x 30 ml) and brine (3 x 30 ml). The organic fraction was dried over $MgSO_4$ and concentrated to yield the title compound as a colourless oil (833 mg, 3.43 mmol, 91%). δ_H (400 MHz, $CDCl_3$) 7.53 (1H, dd, J = 7.9, 1.6 Hz, 6–H), 7.23 (1H, ddd, J = 8.2, 7.6, 1.6, 4–H), 6.88 (1H, ddd, J = 8.2, 7.9, 1.4 Hz, 5–H), 6.81 (td, J = 7.6, 1.4 Hz, 3–H), 4.02 (2H, t, J = 6.5 Hz, 1'–H_2), 1.84 (2H, ddt, J = 9.1, 7.9, 6.5 Hz, 2'–H_2), 1.56 – 1.44 (2H, m, 3'–H_2), 1.39 – 1.29 (4-H, m, 4'–H_2, 5'–H_2), 0.95 – 0.85 (3H, m, 6'–H_3). δ_C (101 MHz, $CDCl_3$) 155.5 (C–2), 133.3 (C–4), 128.4 (C–5), 121.6 (C–6), 113.2 (C–3), 112.3 (C–1), 69.1 (C–1'), 31.5 (C–2'), 29.1 (C–3'), 25.7 (C–4'), 22.6 (C–5'), 14.1 (C–6'). V_{max} (ATR) 2938, 2866, 2253, 1592, 1472, 1249 1032, 903, 728 cm^{-1}. *m/z* (LC-MS ESI+) 292.2 ($[M(^{79}Br)+H]^+$, 100), 294.1 ($[M(^{81}Br)+H]^+$, 100). Data Agrees with that obtained in Hwang et al.[141]

113c. *tert-butyl N-[2'-(2-hexoxybenzenesulfonamido)ethyl]carbamate*

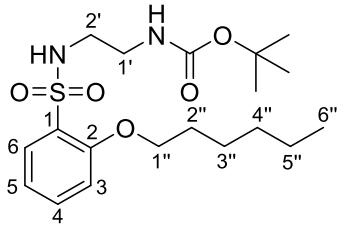

Compound was synthesized according to general procedure C using *1-bromo, 2-hexoxybenzene* **113b** (600 mg, 2.47 mmol) and *N-Boc ethylenediamine* (0.593 g, 3.70 mmol, 1.50 eq). Following separation of the layers and extraction of the aqueous fraction with $CHCl_3$ (3 x 15 ml), the combined organic layers were dried over $MgSO_4$, concentrated and purified by column chromatography (EtOAc in Hex, 0-30%) to yield the title compound as an white amorphous solid (0.397 g, 0.992mmol, 40%). δ_H (700 MHz, $CDCl_3$) 7.85 (1H, dd, *J* = 7.8, 1.7 Hz, 6–H), 7.49 (1H, ddd, *J* = 8.4, 7.4, 1.7 Hz, 4–H), 7.02 (1H, ddd, *J* = 7.8, 7.4, 1.0 Hz, 5–H), 6.99 (1H, dd, *J* = 8.4, 1.0 Hz, 3–H), 5.15 (1H, d, *J* = 6.4 Hz, 2'–N*H*), 4.88 (1H, s, 1'–N*H*), 4.11 (2H, t, *J* = 6.8 Hz, 1''–H_2), 3.19 (2H, q, *J* = 6.0 Hz, 1'–H_2), 2.97 (2H, q, *J* = 6.0 Hz, 2'–H_2), 1.86 (2H, p, *J* = 6.8 Hz, 2''–H_2), 1.51 – 1.43 (2H, m, 3''–H_2), 1.40 (9H, s, –$(CH_3)_3$), 1.37-1.28 (4H, m, 4''–H_2, 5''–H_2), 0.88 (3H, t, *J* = 7.1 Hz, 6''–H_2). δ_C (176 MHz, $CDCl_3$) 156.0 (*C*=O), 155.6 (C–2), 134.5 (C–4), 130.3 (C–6), 127.1 (C–1), 120.5 (C–5), 113.0 (C–3), 79.5 (–*C*$(CH_3)_3$), 69.5 (C–1''), 43.3 (C–2'), 40.4 (C–1'), 31.4 (C–2''), 29.0 (C–3''), 28.3 (–(*C*$H_3)_3$), 25.6 (C–4''), 22.5 (C–5''), 14.0 (C–6''). V_{max} (ATR) 3462 (N–H), 3159 (N–H), 2940, 2877, 2261, 1610 (C=O), 1514, 1334, 1252 1166 cm^{-1}. m/z (LC-MS ESI+) 401.4 $[M+H]^+$, 345.3 [M–*tBu*+2H]$^+$. Accurate mass (ES+) found $[M+H]^+$ 401.2104, $C_{19}H_{33}N_2O_5S$ requires *M* 401.2110.

113. *N-(2'-aminoethyl)-2-(hexyloxy)benzene-1-sulfonamide hydrochloride*

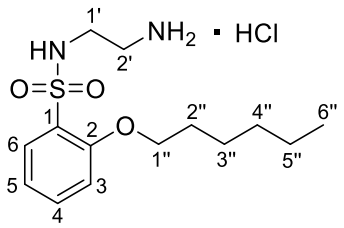

Compound was prepared according to general procedure B, using *tert-butyl N-[2'-(2-hexoxybenzenesulfonamido)ethyl]carbamate* **113c** (40.0 mg, 0.100 mmol) to yield the title compound as a light brown oil (31.0 mg, 0.0920 mmol, 92%). δ_H (700 MHz, D_2O) 7.67 (1H, dt, *J* = 7.9, 1.1 Hz, 6–H), 7.46 (1H, ddt, *J* = 8.4, 7.2, 1.1 Hz, 4–H), 7.00 (1H, dd, *J* = 8.4, 7.9 Hz, 5–H), 6.94 (1H, d, *J* = 7.2 , 3–H), 4.02 (t, *J* = 6.7 Hz, 1''–H_2), 3.05 (2H, t, *J* = 5.8 Hz, 2'–H_2), 3.01 (2H, t, *J* = 5.8 Hz, 1'–H_2), 1.62 (2H, p, *J* = 6.7 Hz, 2''–H_2), 1.23 (2H, p, *J* = 6.7 Hz, 3''–H_2), 1.13 – 1.04 (4H, m, 4''–H_2, 5''–H_2), 0.70 – 0.62 (3H, m, 6''–H_3). δ_C (176 MHz, D_2O) 155.8 (C–2), 135.9 (C–4), 130.1 (C–6), 124.6 (C–1), 120.4

(C–5), 113.7 (C–3), 69.2 (C–1''), 40.0 (C–2'), 39.3 (C–1'), 30.7 (C–2''), 28.0 (C–3''), 24.8 (C–4''), 22.0 (C–5''), 13.3 (C–6''). ν_{max} (ATR) 3364 (N–H), 3254 (N–H), 2940, 2872, 1590, 1473, 1328, 1288, 1154, 1026 cm^{-1}. *m/z* (LC-MS ES+) 302.34 $[M+H]^+$, 602.47 $[2M+H]^+$. Accurate mass (ES+) found $[M+H]^+$ 301.1600, $C_{14}H_{25}N_2O_3S$ requires *M* 301.1586.

114b. *4-bromoanisole*

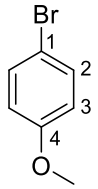

Compound was synthesized according to general procedure D using *4-bromophenol* (500 mg, 2.89 mmol) and *iodomethane* (0.720 ml, 11.6 mmol). Following extraction of the aqueous fraction with EtO_2 (3 x 15 ml), the combined organic layers were purified by successive washes with 0.1 M NaOH (3 x 20 ml) and brine (3 x 20 ml). The organic fraction was dried over $MgSO_4$ and concentrated to yield the title compound as a colourless oil (518 mg, 2.77 mmol, 96%). δ_H (400 MHz, $CDCl_3$) 7.45 – 7.36 (1H, m, 3–H), 6.84 – 6.75 (1H, m, 2–H), 3.81 (3H, s, –OCH_3). δ_C (101 MHz, $CDCl_3$) 158.7 (C–4), 132.3 (C–2), 115.7 (C–3), 112.8 (C–1), 55.5 (–OCH_3). *Vmax* (ATR) 2981, 2258, 1494, 1250, 1073, 907, 726, 648 cm^{-1}**.** *m/z* (GC-MS ES+) 186.0 ($[M(^{79}Br)+H]^+$, 100), 188.0 ($[M(^{81}Br)+H]^+$, 100). Data agrees with that reported in Waterford et al.[142]

114c. *tert-butyl N-[2'-(4-methoxybenzenesulfonamido)ethyl]carbamate*

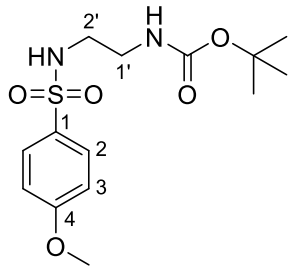

Compound was synthesized according to general procedure C using *4-bromoanisole* **114b** (518 mg, 2.77 mmol) and *N-Boc ethylenediamine* (0.642 g, 4.01 mmol, 1.50 eq). Following separation of the layers and extraction of the aqueous fraction with DCM (3 x 15 ml), the combined organic layers were dried over $MgSO_4$, concentrated and purified by column chromatography (EtOAc in Hex 0-35%) followed by recrystallization ($CHCl_3$:Hex) to yield the title compound as a white solid (388 mg, 117 mmol, 44%). δ_H (599 MHz, $CDCl_3$) 7.86 – 7.69 (2H, m, 2–H_2), 7.05 – 6.85 (2H, m, 3–H_2), 5.08 (1H, s, 2'–N*H*), 4.83 (1H, s, 1'–N*H*), 3.86 (3H, s, –OCH_3), 3.21 (2H, t, J = 5.7 Hz, 1'–H_2), 3.03 (2H, t, J = 5.7 Hz, 2'–H_2), 1.41 (9H, s, –C(CH_3)$_3$). δ_C (151 MHz, $CDCl_3$) 162.9 (C–4), 156.4 (*C*=O), 131.3 (C–1), 129.2 (C–2), 114.3 (C–3), 79.9 (–*C*(CH_3)$_3$, 55.6 (–OCH_3), 43.6 (C–2'), 40.3 (C–1'), 28.3 (–(*C*H_3)$_3$).

ν_{max} (ATR) 3375 (N–H), 3292 (N–H), 2987, 1682 (C=O), 1601, 1526, 1328, 1264, 1155, 1102, 841 cm^{-1}. *m/z* (LC-MS ESI+) 331.3 $[M+H]^+$, 275.3 $[M–tBu+H]^+$, 661.5 $[2M+H]^+$. Accurate mass (ES+) found $[M+H]^+$ 331.1333, $C_{14}H_{23}N_2O_5S$ requires *M* 331.1334.

114. *N-(2'-aminoethyl)-4-methoxybenzene-1-sulfonamide hydrochloride*

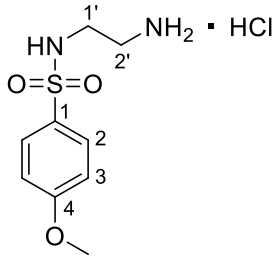

Compound was prepared according to general procedure B, using *tert-butyl N-[2'-(4-methoxybenzenesulfonamido)ethyl]carbamate* **114c** (60.0 mg, 0.182 mmol) to yield the title compound as an off-white amorphous solid (44.0 mg, 0.165 mmol, 91%). δ_H (700 MHz, D_2O) 7.67 – 7.64 (2H, m, 2–H_2), 6.98 – 6.95 (2H, m, 3–H_2), 3.74 (3H, s, –OCH_3), 3.19 – 3.15 (4H, m, 2'–H_2 & 1'–H_2). δ_C (176 MHz, D_2O) 163.1 (C–4), 129.1 (C–1, C–2), 114.8 (C–3), 55.7 (–O*C*H_3), 39.8 (C–2'), 39.1 (C–1'). ν_{max} (ATR) 3353 (N–H), 3296 (N-H), 2953, 2848, 1611, 1507, 1328, 1250 1148, 1021 cm^{-1}. *m/z* (LC-MS ESI+) 231.27 $[M+H]^+$, 461.33 $[2M+H]^+$. Accurate mass (ES+) found $[M+H]^+$ 231.0807, $C_9H_{15}N_2O_3S$ requires *M* 231.0803.

115b. *1-bromo, 4-hexoxybenzene*

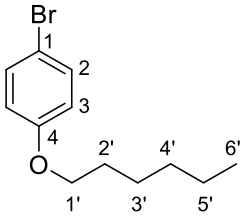

Compound was synthesized according to general procedure D using *4-bromophenol 4-bromophenol* (650 mg, 3.76 mmol, 1.00 eq), *1-bromohexane* (2.48 g, 2.1 mL, 15.0 mmol, 4.00 eq) and TBAI (14.0 mg, 0.038 mmol, 0.01 eq). Following extraction of the aqueous fraction with EtO_2 (3 x 25 ml), the combined organic layers were purified by successive washes with 0.1 M NaOH (3 x 30 ml) and brine (3 x 30 ml). The organic fraction was dried over $MgSO_4$ and concentrated to yield the title compound as a colourless oil (867mg, 3.57 mmol, 95%). δ_H (400 MHz, $CDCl_3$) 7.44 – 7.32 (2H, m, 2–H_2), 6.84 – 6.74 (2H, m, 3–H_2), 3.94 (2H, t, *J* = 6.6 Hz, 1'–H_2), 1.79 (2H dq, *J* = 8.0, 6.6 Hz, 2'–H_2), 1.54 – 1.40 (2H, m, 3'–H_2), 1.35 (4H, m, 4'–H_2, 5'–H_2), 0.98 – 0.85 (3H, m, 6'–H_3). δ_C (101 MHz, $CDCl_3$) 158.3 (C–4), 132.2 (C–2), 116.3 (C–1), 112.5 (C–3), 68.3 (C–1'), 31.6 (C–2'), 29.2 (C–3'), 25.7 (C–4'), 22.6 (C–5'), 14.1 (C–6'). V_{max} (ATR) 2941, 2870, 2258, 1494, 1241, 907, 726 cm^{-1}. *m/z*

(LC-MS ESI+) 256.0 ([M(^{79}Br)+H]$^+$, 100), 258.1 ([M(^{81}Br)+H]$^+$, 100). Data agrees with that reported in Shellaiah et al.[143]

115c. *tert-butyl N-[2'-(4-hexoxybenzenesulfonamido)ethyl]carbamate*

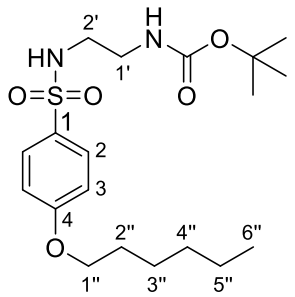

Compound was synthesized according to general procedure C using *1-bromo, 4-hexoxybenzene* **115b** (500 mg, 1.94 mmol) and *N-Boc ethylenediamine* (259.6 mg, 1.620 mmol). Following separation of the layers and extraction of the aqueous fraction with $CHCl_3$ (3 x 15 ml), the combined organic layers were dried over $MgSO_4$, concentrated and purified by column chromatography (EtOAc in Hex, 0-20%) to yield the title compound as an off-white amorphous solid (366 mg, 0.914 mmol, 47%). δ_H (700 MHz, $CDCl_3$) 7.83 – 7.67 (2H, m, 2–H), 6.97 – 6.90 (2H, m, 3–H), 5.16 (1H, s, 2'–NH), 4.87 (1H, s, 1'–N*H*), 3.99 (2H, t, *J* = 6.5 Hz, 1''–H_2), 3.20 (2H, t, *J* = 6.1 Hz, 1'–H_2), 3.05 – 2.95 (2H, t, *J* = 6.1 Hz, 2'–H_2), 1.78 (2H, ddt, *J* = 9.4, 7.9, 6.5 Hz, 2''–H_2), 1.43 (2H, s, 3''–H_2), 1.41 (9H, s, –C(CH_3)$_3$), 1.37 – 1.29 (4H, m, 4''–H_2, 5''–H_2), 0.93 – 0.85 (3H, m, 6''–H_2). δ_C (176 MHz, $CDCl_3$) 162.5 (C–4), 156.5 (*C*=O), 131.0 (C–1), 129.1 (C–2), 114.7 (C–3), 79.8 (–*C*(CH$_3$)$_3$), 68.4 (C–1''), 43.6 (C–2'), 40.2 (C–1'), 31.5 (C–2''), 29.0 (C–3''), 28.3 (– (*C*H$_3$)$_3$), 25.6 (C–4''), 22.5 (C–5''), 14.0 (C–6''). V_{max} (ATR) 3362 (N–H), 2976, 2344, 1639 (C=O), 1375, 1155, 904 cm^{-1}. *m/z* (LC-MS ESI+) 401.5 [M+H]$^+$, 301.3 [M–Boc]$^+$, 435.4 [M–*tBu*+2H]$^+$, 701.8 [2M+H]$^+$. Accurate mass (ES+) found [M+H]$^+$ 401.2110, $C_{19}H_{33}N_2O_5S$ requires *M* 401.2110.

115. *N-(2'-aminoethyl)-4-(hexyloxy)benzene-1-sulfonamide hydrochloride*

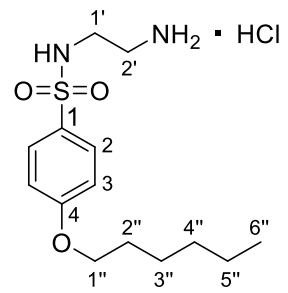

Compound was prepared according to general procedure B, using *tert-butyl N-[2'-(4-hexoxybenzenesulfonamido)ethyl]carbamate* **115c** (50.0 mg, 0.125 mmol) to yield the title compound as a light brown amorphous solid (41mg, 0.122mmol, 97%). δ_H (700 MHz, D_2O) 7.61 (2H, d, *J* = 8.8

Hz, 2–H), 6.83 (2H, d, *J* = 8.8 Hz, 3–H), 3.81 (2H, t, *J* = 6.5 Hz, 1''–H_2), 3.05 – 2.95 (4H, m, 2'–H_2 & 1'–H_2), 1.56 – 1.49 (2H, m, 2''–H_2), 1.25 – 1.17 (2H, m, 3''–H_2), 1.11 (4H, m, 4''–H_2, 5''–H_2), 0.73 – 0.64 (3H, m, 6''–H_2). δ_C (176 MHz, D_2O) 162.4 (C–4), 129.3 (C–1), 129.1 (C–2), 115.0 (C–3), 68.6 (C–1''), 39.8 (C–2'), 39.1 (C–1'), 31.0 (C–2''), 28.4 (C–3''), 25.1 (C–4''), 22.1 (C–5''), 13.4 (C–6''). V_{max} (ATR) 3309 (N–H), 3266 (N–H), 2940, 2848, 1601, 1502, 1328, 1241, 1166, 1096 cm^{-1}. *m/z* (LC-MS ESI+) 302.3 $[M+H]^+$, 601.5 $[2M+H]^+$. Accurate mass (ES+) found $[M+H]^+$ 301.1596, $C_{14}H_{25}N_2O_3S$ requires *M* 301.1586.

116. *N-(2'-aminoethyl)-3-methoxybenzene-1-sulfonamide hydrochloride*

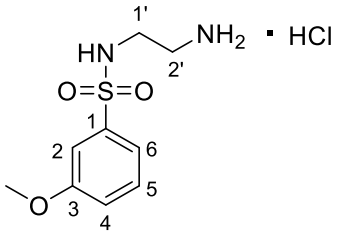

Compound was prepared through general procedure B, starting with *tert-butyl N-[2'-(3-methoxybenzenesulfonamido)ethyl]carbamate* **116c** (20.0 mg, 0.061 mmol, 1.00 eq) to yield the title compound as a white amorphous solid (15.4 mg, 0.058 mmol, 95%). δ_H (400 MHz, MeOD) 7.51 (1H, t, *J* = 7.9 Hz, 5–H), 7.47 – 7.42 (1H, m, 6–H), 7.40 (1H dd, *J* = 2.6, 1.6 Hz, 2–H), 7.21 (1H, ddd, *J* = 8.2, 2.6, 1.1 Hz, 4–H), 3.87 (3H, s, –OC*H*$_3$), 3.07 (4H m, 2'–H, 1'–H). δ_C (101 MHz, MeOD) 160.3 (C–3), 140.6 (C–1), 130.2 (C–6), 118.7 (C–2), 118.4 (C–5), 111.8 (C–4), 54.8 (–O*C*H$_3$), 40.0 (C–2'), 39.3 (C–1'). v_{max} (ATR) 3378 (*b*, N-H), 2502, 1638, 1598, 1481, 1436, 1319, 1247, 1155 cm^{-1}. *m/z* (LC-MS ESI+) 231.266 $[M+H]^+$, 461.458 $[2M+H]^+$. Accurate mass (ES+) found $[M+H]^+$ 231.0811, $C_9H_{15}N_2O_3S$ requires *M* 231.0803

117. *2-ethoxyethyl methanesulfonate*

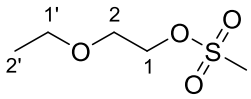

Methanesulfonyl chloride (1.0 mL, 13.3 mmol, 1.20 eq) was added dropwise to a solution of ethoxy-ethanol (1.00 g, 11.1 mmol, 1.00 eq) and triethylamine (1.8 mL, 13.3 mmol, 1.00 eq) in anhydrous dichloromethane (20.0 mL) at 0 °C. The reaction was stirred for 1 hour at 0 °C, and then allowed to warm to room temperature with stirring for 16 hours. The reaction was quenched with water, separated and the organic layer successively washed with 1M HCl (3 x 10 ml), sat. $NaHCO_{3\,(aq)}$ (3 x 10 ml) and brine (3 x 10 ml). The organic layer was then dried over $MgSO_4$ and concentrated to yield the title compound as a colourless oil (1.75 g, 10.4 mmol, 94%). δ_H (400 MHz, $CDCl_3$) 4.45 – 4.30 (2H, m, 1–H_2), 3.75 – 3.65 (2H, m, 2–H_2), 3.55 (2H, q, *J* = 7.0 Hz, 1'–H_2), 3.06 (3H, s, –SC*H*$_3$) 1.21 (1H. t, *J* =

7.0 Hz, 2'–H_3). δ_C (101 MHz, $CDCl_3$) 69.3 (C–1), 68.2 (C–2), 66.8 (C–1'), 37.7 (–S*C*H_3), 15.1 (C–2'). ν_{max} (ATR) 3034, 2985, 2877, 1353, 1225, 1180, 1127, 1019, 970, 921, 802 cm^{-1}. *m/z* (GC-MS ES+) 169.1 $[M+H]^+$. Data agrees with that reported in Ohta *et al*.[144]

118. 1-bromo-2-(2'-ethoxyethoxy)naphthalene

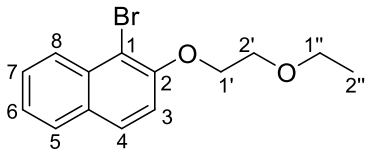

K_2CO_3 (1.58 g, 11.4 mmol, 4.00 eq) was added in portions to a solution of 4-bromonaphth-1-ol (0.700 g, 3.14 mmol, 1.10 eq) in MeCN (10.0 mL). The solution was cooled to 0 °C and *ethoxy-ethylmesolate* **117** (0.480 g, 2.85 mmol, 1.00 eq) was added dropwise over a period of 10 minutes. The reaction was the stirred and heated reflux for 16 h. The reaction was quenched with water and then concentrated to give a aqueous slurry which was extracted with $CHCl_3$ (3 x 20 ml). The combined organic layers were washed with 0.1M NaOH (2 x 25 ml), dried over $MgSO_4$, concentrated and purified by column chromatography ($CHCl_3$ in Hex, 0-55%) to yield the title compound as an off white amorphous solid (0.48 g, 1.63 mmol, 57%). δ_H (700 MHz, $CDCl_3$) 8.24 (1H, dd, *J* = 8.4, 1.1 Hz, 8–H), 7.80 – 7.76 (2H, m, 5–H, 4–H), 7.57 (1H, ddd, *J* = 8.4, 6.8, 1.3 Hz, 7–H), 7.41 (1H, ddd, *J* = 8.1, 6.8, 1.1 Hz, 6–H), 7.29 (1H, d, *J* = 8.9 Hz, 3–H), 4.40 – 4.22 (2H, m, 1'–H), 3.95 – 3.80 (2H, m, 2'–H), 3.68 (2H, q, *J* = 7.0 Hz, 1''–H), 1.26 (3H, t, *J* = 7.0 Hz, 2''–H). δ_c (176 MHz, $CDCl_3$) 153.4 (C–2), 133.2 (C–8a), 130.1 (C–4a), 128.8 (C–4), 128.0 (C–5), 127.6 (C–7), 126.3 (C–8), 124.5 (C–6), 115.9 (C–3), 110.0 (C–1), 70.2 (C–1'), 69.0 (C–2'), 67.1 (C–1''), 15.3 (C–2''). ν_{max} (ATR) 2988, 2939, 2880, 1595, 1378, 1259, 1123, 1091, 805 cm^{-1}. *m/z* (LC-MS, ESI^+) found 295.181 ($[M(^{79}Br)+H]^+$, 70), 297.198 ($[M(^{81}Br)+H]^+$, 71). Accurate mass (ES^+) found $[M+H]^+$ 295.0339, $C_{14}H_{16}O_2{}^{79}Br$ requires *M*, 295.0334

119a. *tert-butyl N-{2'-[2-(2''-ethoxyethoxy)naphthalene-1-sulfonamido]ethyl}carbamate*

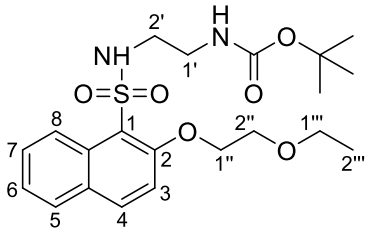

Compound was synthesized according to general procedure B using *1-bromo-2-(2'-ethoxyethoxy)naphthalene* **118** (500 mg, 1.69 mmol, 1.00 eq). Following separation of the layers and extraction of the aqueous fraction with $CHCl_3$ (3 x 20ml), the combined organic layers were dried over $MgSO_4$, concentrated and purified by column chromatography (EtOAc in Hex, 0-40%) to yield the title

compound as a light brown oil (293 mg, 0.699 mmol, 39%). δ_H (599 MHz, $CDCl_3$) 9.23 (1H, d, *J* = 9.0 Hz, 8–H), 8.00 (1H, d, *J* = 9.0 Hz, 4–H), 7.79 (1H, dd, *J* = 8.2, 1.5 Hz, 5–H), 7.60 (1H, ddd, *J* = 9.0, 6.9, 1.5 Hz, 7–H), 7.44 (1H, dd, *J* = 8.2, 6.9 Hz, 6–H), 7.30 – 7.23 (1H, d, *J* = 9.0 Hz, 3–H), 6.89 (1H, s, 2'–NH), 5.17 (1H, s, 1'–NH), 4.39 (2H, t, *J* = 4.2 Hz, 1''–H), 3.93 (2H, t, *J* = 4.2 Hz, 2''–H), 3.71 (2H, q, *J* = 7.1 Hz, 1'''–H), 3.15 – 3.17 (2H, m, 2'–H), 2.97 – 2.99 (2H, m, 1'–H), 1.50 – 1.24 (12H, m, –C(CH_3)$_3$, 2'''–H_3). δ_c (151 MHz, $CDCl_3$) 155.7 (C=O), 154.8 (C–2), 135.4 (C–4), 131.5 (C–8a), 129.5 (C–4a), 128.8 (C–5), 128.5 (C–7), 124.8 (C–6), 124.5 (C–8), 121.6 (C–1), 113.3 (C–3), 79.2 (–*C*(CH_3)$_3$), 69.4 (C–1''), 68.3 (C–2''), 67.3 (C–1'''), 43.5 (C–1'), 40.1 (C–2'), 28.4 (–C(*C*H_3)$_3$), 15.7 (C–2'''). ν_{max} (ATR) 3368 (N–H), 3278 (N–H), 2981, 2930, 2881, 1711 (C=O), 1597, 1513, 1334, 1280 1245, 1151, 1116 1072 cm^{-1}. *m/z* (LC-MS, ESI^+) 439.327 $[M+H]^+$, 383.273 [M–*tBu*+2H]$^+$. Accurate mass (ES^+) found $[M+H]^+$ 439.1886; $C_{21}H_{30}N_2O_6S$ requires *M*, 439.1863.

119. *N-(2'-aminolethyl)-2-(2''-ethoxyethoxy)naphthalene-1-sulfonamide hydrogenchloride*

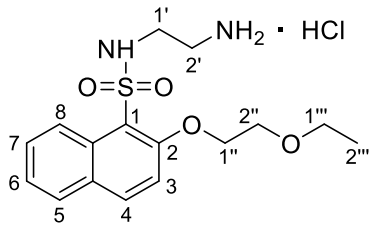

Compound was prepared according to general procedure B, using *tert-butyl N-{2'-[2-(2''-ethoxyethoxy)naphthalene-1-sulfonamido]ethyl}carbamate* **119a** (43.1 mg, 0.098 mmol, 1.00 eq) to yield the title compound as a light brown amorphous solid (36.2 mg, 0.097 mmol, 98%). δ_H (700 MHz, CD_3OD) 8.76 (1H, dd, *J* = 8.9, 0.9 Hz, 8–H), 7.84 (1H, d, *J* = 9.1 Hz, 4–H), 7.58 (1H, dd, *J* = 8.0, 1.4 Hz 5–H), 7.26 (1H, ddd, *J* = 8.9, 6.8, 1.4 Hz, 7–H), 7.21 (1H, d, *J* = 9.1 Hz, 3–H), 7.13 (1H, ddd, *J* = 8.0, 6.8, 0.9 Hz, 6–H), 4.18 – 4.07 (2H, m, 1''–H_2), 3.65 – 3.54 (2H, m, 2''–H_2), 3.38 (q, *J* = 7.0 Hz, 2H), 2.96 (2H, m, 1'–NH_2), 2.70 – 2.73 (4H, m, 2'–H_2, 1'–H_2), 0.97 (3H, t, *J* = 7.0 Hz, 2'''–H_2). δ_c (176 MHz, CD_3OD) 155.5 (C–2), 136.0 (C–4), 131.2 (C–8a), 129.6 (C–4a), 128.6 (C–5), 128.3 (C–7), 124.5 (C–6), 123.6 (C–8), 119.6 (C–1), 114.2 (C–3), 70.2 (C–1''), 68.1 (C–2''), 66.7 (C–1'''), 41.1 (C–2'), 38.8 (C–1'), 14.1 (C–2'''). *m/z* (LC-MS, ESI^+) 339.618 $[M+H]^+$, 677.298 $[2M+H]^+$. Accurate mass (ES^+) found $[M+H]^+$ 339.1382, $C_{16}H_{23}N_2O_4S$ requires *M* 339.1379.

120. *1-bromo-4-(2'-ethoxyethoxy)naphthalene*

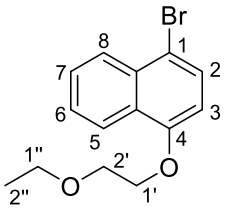

K_2CO_3 (1.57 g, 11.4 mmol, 4.00 eq) was added in portions to a solution of *4-bromonaphth-1-ol* (0.700 g, 3.14 mmol, 1.10 eq) in MeCN (10.0 mL). The solution was cooled to 0 ℃ and *ethoxy-ethylmesolate* **117** (0.480 g, 2.85 mmol, 1.00 eq) was added dropwise over a period of 10 minutes. The reaction was then left to stir heated under reflux for 16 hrs. The reaction was quenched with water (15 ml), concentrated, and the resulting aqueous slurry extracted with $CHCl_3$ (3 x 10 ml). The combined organic layers were washed with 0.1M NaOH (2 x 20 ml), dried over $MgSO_4$ and purified by through flash chromatography (CHCl3 in Hex, 0-55%) to yield the title compound as a clear oil (557.0 mg, 1.887 mmol, 66%). δ_H (700 MHz, $CDCl_3$) 8.34 (1H, dd, *J* = 8.4, 1.4 Hz, 5–H), 8.18 (1H, dt, *J* = 8.4, 1.2 Hz, 8–H), 7.64 (1H, d, *J* = 8.2 Hz, 2–H), 7.61 (1H, ddd, *J* = 8.4, 6.8, 1.4 Hz, 7–H), 7.54 (1H, ddd, *J* = 8.4, 6.8, 1.2 Hz, 6–H), 6.66 (1H, d, *J* = 8.2 Hz, 3–H), 4.28 – 4.19 (2H, m, 1'–H_2), 3.98 – 3.84 (2H, m, 2'–H_2), 3.67 (2H, q, *J* = 7.0 Hz, 1''–H_2), 1.29 (3H, t, *J* = 7.1 Hz, 2''–H_2). δ_c (176 MHz, $CDCl_3$) 154.5 (C–4), 132.5 (C–8a), 129.4 (C–2), 127.8 (C–7), 127.0 (C–1), 126.8 (C–8), 125.9 (C–6), 122.7 (C–5), 113.4 (C–4a), 105.6 (C–3), 68.9 (C–1'), 68.1 (C–2'), 67.0 (C–1''), 15.3 (C–2''). ν_{max} (ATR) 2985, 2873, 1374, 1265, 1129, 809, 647 cm-1. *m/z* (LC-MS, ESI^+) found 295.184 ($[M(^{79}Br)+H]^+$, 91), 297.160 ($[M(^{81}Br)+H]^+$, 100), Accurate mass (ES+) found $[M+H\ (^{79}Br)]^+$ 295.0346, $C_{14}H_{16}O_2{}^{79}Br$ requires *M*, 295.0334

121a. *bis(tert-butylN-{2'-[3-chloro-4-(2''-ethoxyethoxy)naphthalene-1-sulfonamido]ethyl}carbamate)*

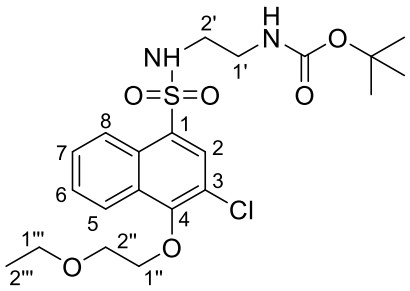

Compound was synthesized according to general procedure C using 1-bromo, *4-ethoxy-ethane* **120** (560 mg, 1.90 mmol, 1.00 eq). Following separation of the layers and extraction of the aqueous fraction with $CHCl_3$ (3 x 15 ml), the combined organic layers were dried over $MgSO_4$, concentrated and purified by column chromatography (EtOAc in Hex 0-30%) to yield the title compound as a to yield the title compound as a brown oil (285 mg, 0.665 mmol, 35%). δ_H (599 MHz, $CDCl_3$) 8.59 – 8.53 (1H, m, 5–H), 8.42 (1H, dd, *J* = 8.2, 1.7 Hz, 8–H), 8.22 (1H, s, 2–H), 7.67 – 7.60 (2H, m, 6–H, 7–H), 5.80 (1H, s,

2’–NH), 4.89 (1H, s, 1’–NH), 4.40 – 4.33 (2H, m, 1’’’–H_2), 3.92 – 3.83 (2H, m, 2’’’–H_2), 3.61 (2H, q, *J* = 7.0 Hz, 1’’’–H_2), 3.19 (1H, t, *J* = 5.6 Hz, 2’–H_2), 3.04 (2H, t, *J* = 5.6 Hz, 1’–H_2), 1.38 (9H, s, –C(CH_3)$_3$), 1.25 (3H, t, *J* = 7.0 Hz, 2’’’–H_3). δ_C (151 MHz, $CDCl_3$) 156.6 (C=O), 155.4 (C–4), 131.6 (C–2), 131.3 (C–1), 130.4 (C–3), 128.7 (C–6), 128.1 (C–8a), 127.5 (C–7), 124.5 (C–5), 123.6 (C–8), 121.3 (C–4a), 79.9 (–*C*(CH$_3$)$_3$), 73.6 (C–1’’), 69.4 (C–2’’), 66.7 (C–1’’’), 43.9 (C–2’), 40.3 (C–1’), 28.3 (–C(*C*H$_3$)$_3$), 15.2 (C–2’’’). ν_{max} (ATR) 3303 (N–H), 3211 (N–H), 3018, 2978, 2877, 1691 (C=O), 1505, 1349, 1220, 1168, 1143, 1075, 966, 866 cm^{-1}. *m/z* (LC-MS ESI+) 473.292 ([M+H (^{35}Cl)]$^+$, 9), 475.249 ([M+H (^{37}Cl)]$^+$, 3), 417.221 ([M(^{35}Cl)–*tBu*+2H]$^+$, 100), 419.186 ([M(^{37}Cl)–*tBu*+2H]$^+$, 39). Accurate mass (ES+) found [M+H]$^+$ 473.1507, $C_{21}H_{30}N_2O_6{}^{35}ClS$ requires *M* 473.1513.

121. *N-(2-aminoethyl)-3-chloro-4-(2-ethoxyethoxy)naphthalene-1-sulfonamide hydrogen chloride*

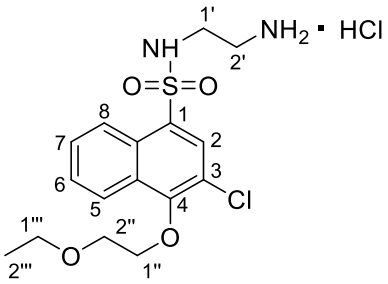

Compound was prepared according to general procedure B using *bis(tert-butyl N-{2’-[3-chloro-4-(2’’-ethoxyethoxy)naphthalene-1-sulfonamido]ethyl}carbamate)* **121a** (101 mg, 0.214 mmol, 1.00 eq) to yield the title compound as a light brown oil (84.3 mg, 0.206 mmol, 96%). δ_H (700 MHz, CD_3OD) 8.30 (1H, dd, *J* = 8.5, 1.2 Hz, 5–H), 8.13 (ddd, *J* = 8.1, 1.4 Hz, 8–H), 7.88 (1H, s, 2-H), 7.41 (1H, ddd, *J* = 8.5, 6.8, 1.4 Hz, 6–H), 7.37 (1H, ddd, *J* = 8.1, 6.8, 1.2 Hz, 7–H), 4.07 – 4.02 (2H, m, 1’’–H_2), 3.54 – 3.49 (2H, m, 2’’–H_2), 3.24 (2H, q, *J* = 7.0 Hz, 1’’’–H_2), 2.97 (m, –NH_3), 2.75 – 2.72 (2H, m, 1’–H_2), 2.69 – 2.71 (2H, m, 2’–H_2), 0.86 (3H, t, *J* = 7.0 Hz, 2’’’–H_3). δ_C (176 MHz, CD_3OD) 155.4 (C–4), 131.2 (C–2), 131.1 (C–1), 130.3 (C–3), 128.5 (C–6), 128.1 (C–8a), 127.4 (C–7), 124.5 (C–5), 123.3 (C–8), 120.8 (C–4a), 73.6 (C–1’’), 69.3 (C–2’’), 66.7 (C–1’’’), 39.7 (C–1’), 39.3 (C–2’), 14.6 (C–2’’’). *m/z* (LC-MS ESI+) 373.121 ([M+H (^{35}Cl)]$^+$, 20), 375.146 ([M+H (^{37}Cl)]$^+$, 7), 745.147 ([2M+H (^{35}Cl)]$^+$, 35), 767.110 ([2M+H (^{37}Cl)]$^+$, 10). Accurate mass (ES+) found [M+H]$^+$ 373.0990, $C_{16}H_{22}N_2O_4{}^{35}ClS$ requires *M* 373.0989

122a. *tert-butyl N-{2'-[4-(2''-ethoxyethoxy)naphthalene-1-sulfonamido]ethyl}carbamate*

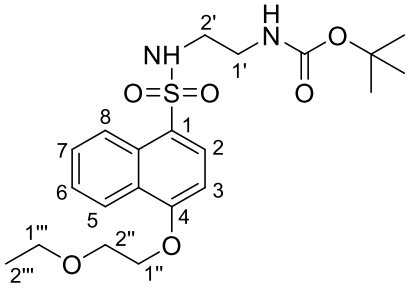

n-BuLi (0.27 mL, 0.68 mmol, 0.95 eq) was added dropwise to a to a solution of the *1-bromo, 4-ethoxy-ethane* **120** (210 mg, 0.71 mmol, 1.00 eq) in THF (4.7 mL) at –78 ℃ under argon. The mixture was allowed to stir for 30 mins to which SO_2Cl_2 (0.055 mL, 0.68 mmol, 0.95 eq) was added. The mixture was allowed to stir for a further 90 minutes from –78 ℃ to room temperature. The reaction was then quenched over ice, separated and the aqueous layer extracted with Et_2O (3 x 15 ml). The crude sulfonyl-chloride intermediate was used without further purification and added dropwise to a solution of triethylamine and *N-Boc ethylenediamine* (0.169 mL, 1.07 mmol, 1.50 eq) in DCM (10.0 ml). The reaction mixture was allowed to stir at room temperature for 3 hours and quenched with water, separated and the aqueous layer extracted with DCM (3 x 15 ml). The combined organic layers were washed with $NaHCO_3$ (3 x 10 ml), dried over $MgSO_4$ and purified by column chromatography (EtOAc in hexane 0-30%) to yield the title compound as a brown amorphous solid (48.2 mg, 0.110 mmol, 15%). δ_H (700 MHz, $CDCl_3$) 8.55 (1H, dd, *J* = 8.7, 1.3 Hz, 5–H), 8.41 (1H, d, *J* = 8.4 Hz, 8-H), 8.19 (1H, d, *J* = 8.3, Hz, 2-H), 7.66 (1H, ddd, *J* = 8.7, 6.9 Hz, 6-H), 7.57 (1H, ddd, *J* = 8.2, 6.9, 1.3 Hz, 7–H), 6.82 (1H, d, *J* = 8.3 Hz, 3–H), 5.30 (1H, s, 2'–NH), 4.74 (1H, s, 1'–NH), 4.36 (1H, t, *J* = 4.8 Hz, 1''–H), 3.95 (2H, t, *J* = 4.8 Hz, 2''–H), 3.67 (2H, q, *J* = 7.0 Hz, 1'''–H), 3.12 (2H, t, *J* = 7.0 Hz, 2'–H), 2.96 (2H, t, *J* = 7.0 Hz, 1'–H), 1.27 (3H, t, *J* = 7.0 Hz, 2'''–H). δ_C (176 MHz, $CDCl_3$) 159.1 (C–4), 156.3 (C=O), 132.1 (C–2), 129.3 (C–1), 128.9 (C–6), 126.2 (C–8a), 126.1 (C–7), 125.7 (C–4a), 124.0 (C–5), 123.3 (C–8), 102.6 (C–3), 79.7 (–*C*$(CH_3)_3$), 69.2 (C–1''), 68.3 (C–2''), 67.0 (C–1'''), 43.5 (C–1'), 40.2 (C–2'), 28.3 (–C(*C*$H_3)_3$), 15.2 (C–2'''). ν_{max} (ATR) 3304 (N–H), 3011, 2974, 2933, 2877, 1694 (C=O), 1573, 1509, 1368, 1324, 1252, 1155, 1094, 966 cm^{-1}. *m/z* (LC-MS, ESI$^+$) found 439.131 $[M+H]^+$, 383.161 [M–*tBu*+2H]$^+$, 877.306 $[2M+H]^+$. Accurate mass (ES$^+$) found $[M+H]^+$ 439.1889; $C_{21}H_{30}N_2O_6S$ requires *M*, 439.1863.

122. *N-(2'-aminoethyl)-4-(2''-ethoxyethoxy)naphthalene-1-sulfonamide hydrogen chloride*

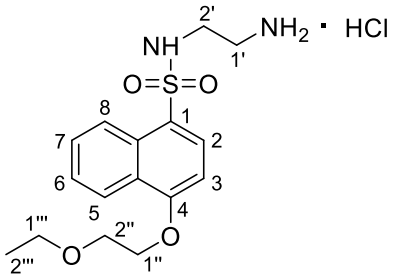

Compound was prepared according to general procedure B, using *tert-butyl N-{2'-[4-(2''-ethoxyethoxy)naphthalene-1-sulfonamido]ethyl}carbamate* **122a** (11.5 mg, 0.026 mmol, 1.00 eq) to yield the title compound as a brown amorphous solid. (9.4 mg, 0.025 mmol, 95%). δ_H (700 MHz, CD_3OD) 8.59 (1H, dd, *J* = 8.6, 0.9 Hz, 5–H), 8.43 (1H, d, *J* = 8.3 Hz, 2–H), 8.20 (1H, dd, *J* = 8.3, 1.4 Hz, 8–H), 7.72 (1H, ddd, *J* = 8.6, 6.8, 1.4 Hz, 6–H), 7.63 (1H, ddd, *J* = 8.3, 6.8, 0.9 Hz, 7–H), 7.04 (1H, d, *J* = 8.3 Hz, 3–H), 4.46 – 4.35 (2H, m, 1''–H), 4.02 – 3.95 (2H, m, 2''–H), 3.68 (2H, q, *J* = 7.0 Hz, 1'''–H), 3.00 (4H, s, 1'–H, 2'–H), 1.25 (3H, t, *J* = 7.0 Hz, 2'''–H). δ_C (176 MHz, CD_3OD) 159.1 (C–4), 131.5 (C–2), 129.1 (C–1), 128.3 (C–6), 126.1 (C–8a), 125.9 (C–7), 125.4 (C–4a), 123.9 (C–5), 122.7 (C–8), 102.6 (C–3), 68.5 (C–1''), 68.3 (C–2''), 66.5 (C–1'''), 39.7 (C–1'), 39.3 (C–2'), 14.0 (C–2'''). *m/z* (LC-MS, ESI^+) 339.158 $[M+H]^+$, 677.243 $[2M+H]^+$. Accurate mass (ES^+) found $[M+H]^+$ 339.1385, $C_{16}H_{23}N_2O_4S$ requires *M* 339.1379.

127a. *1-bromo-4-(methoxy methoxy)naphthalene*

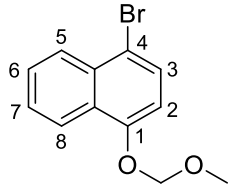

Sodium hydride (49 mg, 1.23 mmol, 1.10 eq) was placed in a round bottom flask under Ar and washed with dry hexane (3 x 10 ml). A suspension was then created with dry THF (8.0 mL) and cooled to 0 ℃. To the suspension, a solution of *4-bromonaphth-1-ol* (250 mg, 1.12 mmol, 1.00 eq) in THF (2.0 ml) was added dropwise and following the emission of H_2, the mixture was allowed to reach ambient temperature and stirred for 30 min. MOM-Cl (0.01 mL, 1.23 mmol, 1.10 eq) was then added and the mixture was allowed to stir at room temperature for 1 h. The reaction mixture was quenched with sat. $NH_4Cl_{(aq)}$ and the aqueous fraction was extracted with EtOAc (3 x 10 ml). The combined organic layers were then washed with 1M NaOH (3 x 10 ml), dried over $MgSO_4$ and purified by column chromatography (Hex: EtOAc, 0-20%) to yield the title compound as a colourless oil (244 mg, 0.91 mmol, 80%). δ_H (400 MHz, $CDCl_3$) 8.30 (1H, dd, *J* = 8.3, 0.9 Hz, 5–H), 8.21 – 8.14 (1H, m, 8–H),

7.69 – 7.59 (2H, m, 2–H, 7–H), 7.55 (1H, ddd, *J* = 8.3, 6.8, 1.3 Hz, 6–H), 6.99 (1H, d, *J* = 8.3 Hz, 3–H), 5.39 (2H, s, –OC*H*$_2$), 3.54 (3H. s, –OC*H*$_3$). δ_C (101 MHz, $CDCl_3$) 152.7 (C-4), 132.6 (C–8a), 129.6 (C–2), 127.7 (C–7), 127.2 (C–1), 127.0 (C–8), 126.2 (C–6), 122.4 (C–5), 114.6 (C–4a), 108.5 (C–3), 94.8 (–O*C*H$_2$), 56.4 (–O*C*H$_3$). *m/z* (LC-MS, ESI$^+$) 234.930 ([M–OMe (^{79}Br)]$^+$, 63), 236.941 ([M–OMe (^{81}Br)]$^+$, 64). Data agrees with that reported in Hoye et al.[145]

127. t*ert-butyl N-{2'-[4-(methoxymethoxy)naphthalene-1-sulfonamido]ethyl}carbamate*

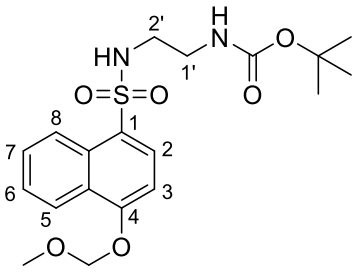

Compound was synthesized according to general procedure C using *1-bromo-4-(methoxy methoxy)naphthalene bromonaphthalene* (**127a**) (0.250 g, 0.936 mmol, 1.00 eq) and N-Boc ethylenediamine (0.222 mL, 1.404 mmol, 1.50 eq). Following separation of the layers and extraction of the aqueous fraction with $CHCl_3$ (3x15ml), the combined organic layers were dried over $MgSO_4$, concentrated and purified by column chromatography (EtOAc in Hex 0-25%) to yield the desired compound as a light brown oil (0.170 g, 0.414 mmol, 44%). δ_H (700 MHz, $CDCl_3$) 8.58 (1H, dd, *J* = 8.6, 0.9 Hz, 5–H), 8.38 (1H, dd, *J* = 8.1, 1.4 HZ, 8–H), 8.18 (1H, d, *J* = 8.3 Hz, 2–H), 7.67 (1H, ddd, *J* = 8.6, 6.8, 1.4 Hz, 6–H), 7.58 (1H, ddd, *J* = 8.1, 6.8, 0.9 Hz, 7–H), 7.09 (1H, d, *J* = 8.3 Hz, 3–H), 5.45 (3H, s, –OCH$_2$, 2'–N*H*), 4.82 – 4.86 (1H, m, 1'–N*H*), 3.55 (3H, s, –OCH$_3$), 3.15 (2H, t, *J* = 6.7 Hz, 2'–H$_2$), 2.97 (2H, t , *J* = 6.7 Hz, 1'–H$_2$), 1.37 (9H, s, –C(C*H*$_3$)$_3$). δ_C (176 MHz, $CDCl_3$) 157.2 (C–4), 156.4 (C=O), 131.5 (C–2), 129.4 (C–1), 128.8 (C–6), 126.7 (C–8a), 126.4 (C–7), 126.3 (C–4a), 124.2 (C–5), 123.0 (C–8), 105.2 (C–3), 94.6 (–OCH$_2$), 80.4 (–*C*(CH$_3$)$_3$), 56.64 (–O*C*H$_3$), 43.5 (C–2'), 40.2 (C–1'), 28.3 (–C(*C*H$_3$)$_3$). *m/z* (LC-MS, ESI$^+$) 411.206 [M+H]$^+$, 355.121 [M–*tBu*+2H]$^+$, 311.196 [M–Boc+2H]$^+$, 821.310 [2M+H]$^+$, 721.296 [2M–Boc+2H]$^+$.

128a. *1-(benzyloxy)-4-bromonaphthalene*

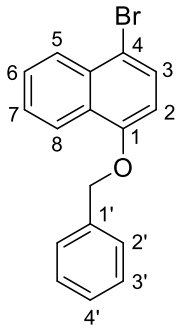

Compound was prepared according to general procedure D using *1-bromonaphth-4-ol* (0.586 g, 2.63 mmol, 1.05 eq) and benzyl bromide (0.297 mL, 2.50 mmol, 1.00 eq). TBAI (34.1 mg, 0.250 mmol, 0.10 eq) was added as a nucleophilic catalyst. The reaction was monitored by TLC (EtOAc in Hex, 0-30%) and upon complete consumption of the starting naphthol, the mixture was concentrated and the resulting residue dissolved in EtO_2 (20 ml). The organic solution was washed with water (3 x 25 ml) and brine (3 x 25 ml), dried over MgSO4, concentrated and purified by column chromatography (EtOAc in Hex, 0-15%) to yield the title compound as colourless amorphous solid (0.698 g, 2.20 mmol, 89%). δ_H (700 MHz, $CDCl_3$) 8.37 (1H, d, J = 8.4 Hz, 8–H), 8.18 (1H, d, J = 8.6 Hz 5–H), 7.67 – 7.60 (2H, m, 3–H, 6–H), 7.54 –7.51 (3H, m, 2'–H, 7–H), 7.44 – 7.36 (43, m, 3'–H, 4'–H), 6.77 (1H, d, J = 8.2 Hz, 2–H) 5.25 (2H, s, $–OCH_2$). δ_C (176 MHz, $CDCl_3$) 154.3(C-1), 136.7 (C–4'), 132.5 (C–4a), 129.4 (C–3), 128.6 (C–2'), 128.1 (C–1'), 127.8 (C–6), 127.4 (C–3'), 127.0 (C–4), 126.9 (C–5), 126.0 (C–7), 122.6 (C–8), 113.5 (C–8a), 105.9 (C–2), 70.7 ($–OCH_2$). ν_{max} (ATR) 2977, 2880, 2186, 1427, 1340, 1162, 1140, 805 cm^{-1}. *m/z* (LC-MS, ESI^+) 313.197 ([M+H (^{79}Br)]$^+$, 36), 315.287 ([M+H (^{81}Br)]$^+$, 34). Data agrees with that as reported in Lowe et al.[146]

129a. *[(4-bromonaphthalen-1-yl)oxy](tert-butyl)dimethylsilane*

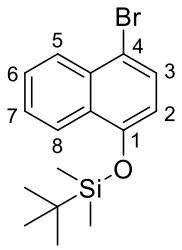

1-bromonaphtha-4-ol (800 mg, 3.59 mmol, 1.00 eq), TBDMS-Cl (610 mg, 3.95 mmol, 1.10 eq) and imidazole (488 mg, 7.18 mmol, 2.00 eq) were dissolved in DMF (35 mL) and the reaction mixture was allowed to stir at room temperature for 16 hours. The reaction was monitored by TLC (EtOAc in Hex, 1:9) and upon completion consumption of the starting naphthol, the mixture was concentrated, and the resulting residue dissolved in EtO_2 (30 ml). Purification was achieved by

successive washes of the organic solution with water (3 x 20 ml), 0.1M NaOH (3 x 20 ml) and brine (3 x 20 ml). The organic layer was dried over $MgSO_4$, concentrated and dried *in vacuo* to yield the desired product as an off white amorphous solid (1140 mg, 3.23 mmol, 93%). δ_H (700 MHz, $CDCl_3$) 8.20 (1H, ddd, *J* = 8.2, 1.3 Hz, 8–H), 8.17 (1H, dd, *J* = 8.4, 1.0 Hz, 5–H), 7.64 – 7.57 (2H, m, 3–H, 6–H), 7.52 (1H, ddd, *J* = 8.2, 6.8, 1.0 Hz, 7–H), 6.74 (1H, d, *J* = 8.1 Hz, 2–H), 1.10 (9H, s, –C(CH_3)$_3$), 0.29 (6H, s, –Si(CH_3)$_2$). δ_C (176 MHz, $CDCl_3$) 151.6 (C–1), 132.9 (C–4a), 129.6 (C–3), 129.2 (C–6), 127.5 (C–4), 127.0 (C–5), 125.9 (C–7), 123.1 (C–8), 113.8 (C–8a), 113.1 (C–2), 25.8 (–C(*C*H_3)$_3$), 18.4 (–*C*(CH$_3$)$_3$), -4.3 (–Si(*C*H_3)$_2$). ν_{max} (ATR) 2961, 2930, 2856, 1592, 1453, 1384, 1254, 1066, 1021, 838 cm^{-1}. *m/z* (LC-MS, ESI^+) 336.226 ([M+H (^{79}Br)]$^+$, 29), 338.203 ([M+H (^{81}Br)]$^+$, 26).

130a. *(2'-{[(4-bromonaphthalen-1-yl)oxy]methoxy}ethyl)trimethylsilane*

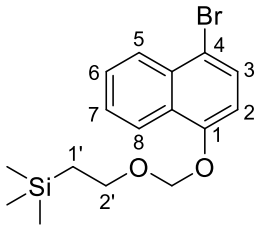

Sodium hydride (29.6 mg, 1.23 mmol, 1.10 eq) was placed in a round bottom flask under argon and washed 3 times with dry hexane. A suspension was then created with dry THF (8.0 mL) and the reaction mixture was cooled to 0 ℃. To the suspension, a solution of *4-bromonaphth-1-ol* (250 mg, 1.12 mmol, 1.00 eq) in THF (2.0 ml) was added dropwise and following the emission of hydrogen gas, the mixture was allowed to stir at this temperature for 30 min. SEM-Cl (205 mg, 0.218 mL, 1.23 mmol, 1.10 eq) was then added and the mixture was allowed to reach ambient temperature and stir 1 h. The reaction was quenched with 1M $NH_4Cl_{(aq)}$ and extraction of the solution was conducted with Et_2O (3 x 10 ml). The combined organic layers were washed with 1M NaOH (3 x 10 ml) and brine (3 x 15 ml), dried over $MgSO_4$, concentrated and purified by column chromatography (EtOAc in Hex, 0-5%) to yield the title compound as a colourless oil (329 mg, 0.931 mmol, 83%). δ_H (400 MHz, $CDCl_3$) 8.31 – 8.26 (1H, dd, *J* = 8.2, 1.4 Hz, 8–H), 8.19 (1H, dd, *J* = 8.4, 1.1 Hz, 5–H), 7.67 (1H, d, *J* = 8.3 Hz, 3–H), 7.62 (1H, ddd, *J* = 8.4, 6.8, 1.4 Hz, 6–H), 7.54 (1H, ddd, *J* = 8.2, 6.8, 1.1 Hz, 7–H), 7.01 (1H, d, *J* = 8.3 Hz, 2–H), 5.43 (2H, s, –OCH_2O), 3.92 – 3.75 (2H, m, 2'–H), 1.02 – 0.96 (1H, m, 1'–H), 0.01 (9H, s, –Si(CH_3)$_3$). δ_C (101 MHz, $CDCl_3$) 153.0 (C–1), 132.6 (C–4a), 129.6 (C–3), 127.7 (C–6), 127.2 (C–4), 127.0 (C–5), 126.0 (C–7), 122.5 (C–8), 114.3 (C–8a), 108.5 (C–2), 93.4 (–O*C*H_2O), 66.7 (C–2'), 18.1 (C–1'), -1.4 (–Si(*C*H_3)$_3$). ν_{max} (ATR) 2990, 1590, 1337, 1252, 1220, 749, 673 cm^{-1}. LCMS (ESI^+) 336.008 ([M–CH_3 (^{79}Br)]$^+$, 7), 338.022 ([M–CH_3 (^{81}Br)]$^+$, 6). Accurate mass (ES+) found 353.0587, $C_{16}H_{22}{}^{79}BrO_2Si$ requires *M* 353.0572.

130. *tert-butyl N-[2'-(4-{[2''-(trimethylsilyl)ethoxy]methoxy}naphthalene-1-sulfonamido) ethyl] carbamate*

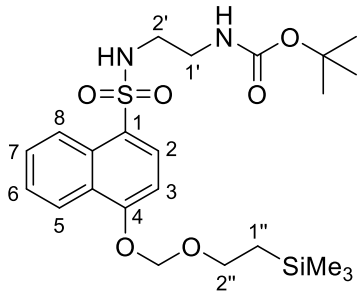

Compound was prepared according to general procedure C using *(2'-{[(4-bromonaphthalen-1-yl)oxy]methoxy}ethyl)trimethylsilane* (**130a**) (1.70 g, 4.81 mmol, 1.00 eq) and N-Boc ethylenediamine (1.1 mL, 7.22 mmol, 1.50 eq). Following separation of the layers, extraction was conducted with Et_2O (3 x 20 ml) and the combined organic extracts were dried over $MgSO_4$ and concentrated. Purification was achieved by flash chromatography (EtOAc in Hex, 0-30%) to yield the title compound as a light orange oil (1.12 g, 2.245mmol, 47%). δ_H (400 MHz, $CDCl_3$) 8.59 (1H, dt, *J* = 8.6, 1.0 Hz, 5–H), 8.41 (1H, dd, *J* = 8.3, 1.4, Hz, 8–H), 8.22 (1H, d, *J* = 8.4 Hz, 2–H), 7.70 (1H, ddd, *J* = 8.6, 6.9, 1.4 Hz, 6–H), 7.61 (1H, ddd, *J* = 8.3, 6.9, 1.0 Hz, 7–H), 7.14 (1H, d, *J* = 8.4 Hz, 3–H), 5.52 (2H, s, $–OCH_2O$), 5.29 (1H, s, 2'–N*H*), 4.78 (1H, s, 1'–N*H*), 3.97 – 3.76 (2H, m, 2''–H), 3.18 (2H, q, *J* = 5.7 Hz, 2'–H), 3.00 (2H, q, *J* = 5.7 Hz, 1'–H), 1.41 (9H, s, $–C(CH_3)_3$), 1.07 – 0.96 (2H, m, 1''–H), 0.02 (9H, s, $–Si(CH_3)_3$). δ_C (101 MHz, $CDCl_3$) 157.6 (C–4), 156.5 (C=O), 131.7 (C–2), 129.4 (C–1), 128.8 (C–6), 126.4 (C–8a), 126.3 (C–7), 126.3 (C–4a), 124.1 (C–5), 123.2 (C–8), 105.3 (C–3), 93.2 ($–OCH_2O$), 79.8 ($–C(CH_3)_3$), 67.2 (C–2''), 43.6 (C–2'), 40.3 (C–1'), 28.3 (C–1''), 18.1 ($–C(CH_3)_3$), -1.4 ($–Si(CH_3)_3$). ν_{max} (ATR) 2949, 1691 (C=O), 1513, 1368, 1251, 1155, 1056, 974 cm^{-1}. *m/z* (LC-MS ESI+) 397.385 $[M–Boc+H]^+$, 441.396 $[M–tBu+2H]^+$, 497.447 $[M+H]^+$. Accurate mass (ES+) found 497.2134, $C_{23}H_{37}N_2O_6SSi$ requires *M* 497.2142.

131. *tert-butyl N-[2'-(4-hydroxynaphthalene-1-sulfonamido)ethyl]carbamate*

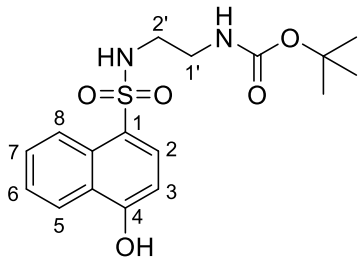

Et_3N (2.8 mL, 21.14 mmol, 15.0 eq) was added dropwise to a solution of *tert-butyl N-[2'-(4-{[2''-(trimethylsilyl)ethoxy]methoxy}naphthalene-1-sulfonamido) ethyl] carbamate* (**130**) (0.70 g, 1.41 mmol, 1.00 eq) in THF (7.0 mL), followed by *tetrabutylammonium fluoride* (21.1 mL, 21.14 mmol, 15.0 eq) added dropwise. The reaction mixture was refluxed at 65 °C for 4 hours. The reaction mixture

was quenched with water and concentrated under reduced pressure. The resulting mixture was dissolved in EtOAc (25ml), washed with sat. $NaHCO_3$ (3 x 20 ml), dried over $MgSO_4$, concentrated and purified by column chromatography (EtOAc in Hex 0-70%) to yield the title compound as a light orange amorphous solid (0.40 g, 1.09 mmol, 78%). δ_H (599 MHz, MeOD) 8.54 (1H, dt, *J* = 8.6, 1.1 Hz, 8–H), 8.39 – 8.27 (1H, m, 5–H), 8.04 (1H, d, *J* = 8.2 Hz, 2–H), 7.64 (1H, ddd, *J* = 8.6, 6.8, 1.4 Hz, 6–H), 7.54 (1H, ddd, *J* = 8.2, 6.8, 1.1 Hz, 7–H), 6.84 (1H, d, *J* = 8.2 Hz, 3–H), 3.00 (2H, t, *J* = 6.4 Hz, 2'–H), 2.82 (2H, t, *J* = 6.4 Hz, 1'–H), 1.33 (9H, s, –C(C*H*$_3$)$_3$). δ_C (151 MHz, MeOD) 158.6 (C–4), 156.9 (C=O), 131.4 (C–2), 129.8 (C–8a), 127.9 (C–7), 125.5 (C–5a), 125.1 (C–6), 124.4 (C–1), 124.0 (C–8), 122.9 (C–5), 105.3 (C–3), 78.8 (–*C*(CH$_3$)$_3$), 42.1 (C–2'), 39.8 (C–1'), 27.2 (–C(*C*H$_3$)$_3$). ν_{max} (ATR) 3463 (*b*, O–H), 3381 (N–H), 3293 (N–H), 2971, 1691 (C=O), 1524, 1364, 1149, 1017 cm^{-1}. *m/z* (LC-MS ESI+) 267.228 [M–Boc+H]$^+$, 311.274 [M–*tBu*+2H]$^+$, 367.324 [M+H]$^+$. Accurate mass (ES+) found 367.1339, $C_{17}H_{23}N_2O_5S$ requires *M* 367.1328.

134. *methyl N-[2-(2'-hydroxyethoxy)ethyl]carbamate*

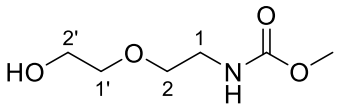

A solution of methyl chloroformate (0.772 mL, 0.011 mol, 1.05 eq) in THF (5 ml) was added dropwise to a sealed flask containing *2-(2-aminoethoxy)ethan-1-ol* (**132**) (1.00 g, 0.010 mol, 1.00 eq) in THF/1M $NaHCO_3$ (1:1, 20 ml) at 0 °C. The mixture was the allowed to reach ambient temperature and stirred for an additional 16 h. Progress was monitored using TLC and upon complete consumption of the starting material, the reaction was quenched with sat. $NaHCO_{3(aq)}$, and the aqueous fraction was extracted with EtOAc (3 x 10 ml). The combined organic layers were dried over $MgSO_4$, concentrated and the residue purified by column chromatography (EtOAc in Hex 0-60%) to yield the title compound as a colourless oil (1.46 g, 0.009 mol, 94%). δ_H (700 MHz, $CDCl_3$) 5.26 (1H, s, –O*H*), 3.74 – 3.69 (2H, m, 2'–H_2), 3.65 (3H, s, –OC*H*$_3$), 3.57-3.53 (4H, m, 1'–H_2, 2–H_2), 3.38-3.36 (2H, m, 1–H_2), 2.44 (1H, s, –N*H*). δ_C (176 MHz, $CDCl_3$) 158.7 (*C*=O), 72.2 (C–1'), 70.5 (C–2), 61.7 (C–2'), 52.1 (–O*C*H$_3$), 40.4 (C–1). ν_{max} (ATR) 3334 (*b*, O–H), 2948, 2877, 1699 (C=O), 1536, 1388, 1261, 1119, 1061 cm^{-1}. *m/z* (GC-MS, EI$^+$) 164.2 [M+H]$^+$, 133.1 [M–OMe]$^+$. Accurate mass (ES+) found [M+H]$^+$ 164.0919, $C_6H_{14}NO_4$ requires *M* 164.0923.

135. *2-[2'-(methylamino)ethoxy]ethan-1-ol*

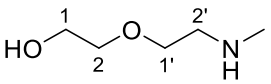

A solution of *methyl N-[2-(2'-hydroxyethoxy)ethyl]carbamate* (**134**) (0.900 g, 5.51 mmol, 1.00 eq) in THF (10 ml) was added dropwise to a stirred suspension of $LiAlH_4$ (0.281 g, 8.27 mmol, 1.50

eq) in THF (30 mL) maintained at 0 ℃. On completion of the addition, the reaction was stirred and heated under reflux for 16 h. The reaction was then cooled to 0 ℃ and quenched with sequential additions of water (1.0 eq), NaOH (1M, 2.0 eq) and water (3.0 eq). A saturated solution of Rochelle salt (15 ml) was added and the resulting mixture was stirred for 15 minutes until all solids had dissolved and the mixture became clear. The layers were separated and the aqueous fraction was extracted with EtOAc (3 x 15 ml). The combined organic layers were dried over $MgSO_4$ and concentrated *in vacuo* to yield the title compound as a light yellow oil (0.626 g, 5.25 mmol, 95%). δ_H (700 MHz, $CDCl_3$) 3.72 – 3.70 (2H, m, 1–H_2), 3.62 – 3.60 (2H, m, 1'–H_2), 3.59 – 3.57 (2H, m, 2–H_2), 2.79 – 2.76 (2H, m, 2'–H_2), 2.68 (1H, s, –O*H*), 2.44 (3H, s, –NCH_3). δ_C (176 MHz, $CDCl_3$) 72.5 (C–2), 69.8 (C–1'), 61.8 (C–1), 51.3 (C–2'), 36.1 (–N*C*H_3). ν_{max} (ATR) 3300 (*b*, O–H), 2933 2870, 1552, 1478, 1386, 1128, 1072 cm^{-1}. *m/z* (LC-MS, ESI^+) 120.217 $[M+H]^+$, Accurate mass (ES+) found $[M+H]^+$ 120.1025, $C_5H_{14}NO_2$ requires *M* 120.1025.

136. *prop-2-en-1-yl N-[2'-(2''-hydroxyethoxy)ethyl]-N-methylcarbamate*

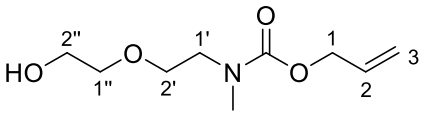

A solution of allyl chloroformate (0.441 g, 4.41 mmol, 1.05 eq) was added dropwise to a solution of *2-[2'-(methylamino)ethoxy]ethan-1-ol* (**135**) (0.500 g, 4.20 mmol, 1.00 eq) in THF/1M $NaHCO_3$ (1:1, 15 ml), at 0 ℃ under N_2. Upon completion of the addition, the reaction mixture was allowed to reach ambient temperature and stirred for an additional 16 hours. The reaction was quenched with sat. $NaHCO_{3(aq)}$ (10 ml), the layers separated and the aqueous layer extracted with EtOAc (3 x 10 ml). The combined organic layers were dried over $MgSO_4$, concentrated and the crude product purified by column chromatography (EtOAc in Hexane 0-90%) to yield the title compound as a light yellow oil (0.655 g, 3.22 mmol, 77%). δ_H (700 MHz, $CDCl_3$) 5.94 (1H, ddt, *J* = 17.2, 11.5, 5.5 Hz, 2–H), 5.30 (1H, dd, *J* = 17.2, 3.4 Hz, 3–H_Z), 5.20 (1H, dd, *J* = 11.5, 3.4 Hz, 3–H_E), 4.59 (2H, d, *J* = 5.5, 1–H_2), 3.71 (2H, t, *J* = 4.5 Hz, 2''–H_2), 3.68 – 3.56 (4H, m, 1''-H_2, 2'–H_2), 3.48 (2H, d, *J* = 7.5 Hz, 1'–H_2), 2.98 (3H, s, –NCH_3), 2.19 – 1.98 (1H, s, –O*H*). δ_C (176 MHz, $CDCl_3$) 156.3 (C=O), 133.1 (C–2), 117.2 (C–3), 72.2 (C–1''), 69.3 – 69.0 (C–2'), 66.0 (C–1), 61.8 (C–2''), 48.8 – 48.4 (C–1'), 35.7 – 35.0 (–N*C*H_3). ν_{max} (ATR) 3425 (*b*, O–H), 3086, 2940, 2873, 1686 (C=O), 1478, 1462, 1399, 1169, 1127, 1060, 771 cm^{-1}. m/z (LC-MS, ESI^+) 226.325 $[M+Na]^+$, 204.195 $[M+H]^+$. Accurate mass (ES+) found $[M+H]^+$ 204.1242, $C_9H_{18}NO_4$ requires *M* 204.1236.

140. *prop-2-en-1-yl N-(pent-4'-yn-1'-yl)-N-[2''-(2'''-hydroxyethoxy)ethyl]carbamate*

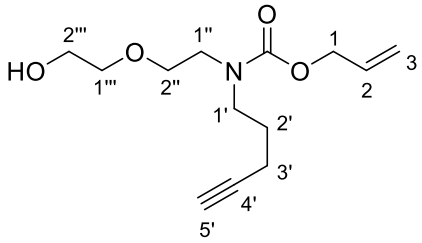

DMSO (4.8 mL, 67.5 mmol, 2.50 eq) in 10 mL CH_2Cl_2 was added dropwise over 10 minutes to a stirred solution of oxalyl chloride (2.5 mL, 30.0 mol, 1.10 eq) in 50 mL DCM under argon at –78 °C. After stirring for a further 30 min, a solution of *4-pentyn-1-ol* (**137**) (2.5 mL, 27.0 mmol, 1.00 eq) in DCM (20 mL) was added dropwise and stirred at –78 °C for a further 1 h. Et_3N (20ml) was then added and the mixture was maintained at –78 °C for 1.5 h after which it was allowed to warm to ambient temperature and stirred for a further 3 h. The reaction mixture was then diluted with DCM (30 ml) and washed with water (3 x 30 ml), $NaHCO_3$ (3 x 30 ml) and brine (3 x 30 ml). The organic layer was then dried over $MgSO_4$ and concentrated using a rotary evaporator, maintaining the water bath temperature ≤ 20 °C to yield crude aldehyde **138** as a yellow oil.

A dry MeOH (5ml) solution of crude aldehyde **138** was added dropwise to a flask containing *2-(2-aminoethoxy)ethan-1-ol* (**132**) (3.00 g, 2.9 ml, 28.4 mmol, 1.05 eq) in dry MeOH (50ml) and 4Å molecular sieves under N_2. After 30 min, $NaCNBH_3$ (5.34 g, 81.0 mmol, 3.00 eq) was added and the reaction mixture was allowed to stir for a further 48 hours at room temperature. The reaction mixture was the concentrated and the crude residue was suspended in cold MeOH. The mixture was filtered and the filtrate concentrated in vacuo to yield crude secondary amine **139** as a yellow oil which was used without further purification.

A solution of allyl chloroformate (4.02g, 40.5 mmol, 1.50 eq) in THF (10 ml) was added dropwise to a sealed flask containing crude secondary amine **139** in THF/1M $NaHCO_3$ (1:1, 50 ml) at 0 °C under N_2. Upon completion of addition, the reaction mixture was allowed to reach ambient temperature and stirred for an additional 16 hours. The reaction was quenched with sat. $NaHCO_{3(aq)}$ (25 ml), the layers separated and the aqueous layer extracted with EtOAc (3 x 30ml). The combined organic layers were dried over $MgSO_4$, concentrated and the crude product purified by column chromatograph (EtOAc in Hex 0-95%) to yield the title compound as a colourless oil (2.49 g, 9.75 mmol, 36% (over 3 steps)). δ_H (700 MHz, $CDCl_3$) 5.93 (1H, ddt, J = 17.2, 10.5, 5.5, 2–H), 5.29 (1H, dd, J = 17.2, 3.5 Hz, 3–H_Z), 5.20 (1H, dd, J = 10.5, 3.5 Hz, 3–H_E), 4.58 (2H, d, J = 5.5, Hz, 1–H_2), 3.75 – 3.68 (2H, m, 2'''–H_2), 3.67 – 3.44 (4H, m, 1'''–H, 2''–H_2), 3.47 – 3.44 (2H, m, 1'–H_2) 3.44 – 3.36 (2H, m, 1''–H_2), 2.26 – 2.14 (2H, m, 3'–H_2), 1.97 (1H, t, J = 2.7 Hz, 5'–H), 1.81-1.79 (2H, m, 2'–H_2). δ_C (176 MHz, $CDCl_3$) 156.3 (C=O), 133.1 (C–2), 117.3 (C–3), 82.6 (C–4'), 72.3 – 72.1 (C–1'''), 69.7 (C–5') 69.3 (C–2''), 66.9 – 66.8 (C–1), 66.0

– 65.8 (C–1'), 61.8 (C–2'''), 47.7 – 47.0, (C–1'') 27.3 – 26.8 (C–3'), 15.2 (C–2'). ν_{max} (ATR) 3448 (*b*, O–H), 3305, 3076, 2949, 2875, 1689 (C=O), 1483, 1421, 1283, 1227, 1128, 1060, 997, 774 cm^{-1}. m/z (LC-MS, ESI^+) 256.310 $[M+H]^+$, 226.325 $[M+Na]^+$. Accurate mass (ES+) found $[M+H]^+$ 256.1539, $C_{13}H_{22}NO_4$ requires *M* 256.1549.

142. *methyl 3-tert-butylbenzoate*

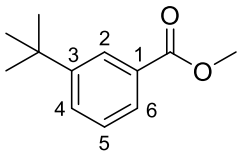

K_2CO_3 (1.55 g, 11.2 mmol, 4.00 eq) was added in portions to a solution of *3-tertbutylbenzoic acid* (**141**) (0.500 g, 2.81 mmol, 1.00 eq) in MeCN (11.2 mL). The mixture was allowed to stir at room temperature for 15 mins after which MeI (0.699 mL, 11.2 mmol, 4.00 eq) was added. Following the addition of the electrophile, the reaction mixture was allowed to stir under reflux for 16 hours. Volatiles were evaporated and the resulting mixture was dissolved in 1M $NaHCO_3$ (15 ml). Extraction of the aqueous solution was conducted with DCM (3 x 10 ml) and the combined organic layers were washed with 1M NaOH (3 x 20 ml), dried over $MgSO_4$ and concentrated to yield the title compound as a light brown oil (0.407 g, 2.12 mmol, 76%). δ_H (400 MHz, $CDCl_3$) 8.08 (1H, t, *J* = 1.9 Hz, 2–H), 7.85 (1H, dt, *J* = 7.8, 1.9 Hz, 6–H), 7.59 (1H, dd, *J* = 7.8, 1.9 Hz, 4–H), 7.37 (1H, t, *J* = 7.8 Hz, 5–H), 3.92 (3H, s, $–OCH_3$), 1.35 (9H, s, $–(CH_3)_3$). δ_C (101 MHz, $CDCl_3$) 167.5 (C=O), 151.5 (C–1), 130.0 (C–2), 129.9 (C–3), 128.1 (C–6), 126.8 (C–5), 126.5 (C–4), 52.1 ($–OCH_3$), 34.8 ($–C(CH_3)_3$), 31.3 ($–(CH_3)_3$). *m/z* ($ASAP^+$) 193.121 $[M+H]^+$. Data agrees with that reported in Fournier et al.[147]

143. *methyl 3-tert-butyl-5-hydroxybenzoate*

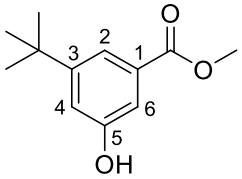

A vial was charged with the B_2Pin_2 (634.0 mg, 2.497 mmol, 1.20 eq), dtbpy (55.8 mg, 0.208 mmol, 0.10 eq), $[Ir(COD)(OMe)]_2$ (69.0 mg, 0.104 mmol, 0.05 eq) and *methyl 3-tertbutylbenzoate* (**142**) (400.0 mg, 2.08 mmol, 1.00 eq) and subjected to 3 N_2-purge refill cycles. MTBE (2.1 mL) was added and the mixture was allowed to stir at room temperature for 16 hours after which volatiles were evaporated and the resulting crude material was dissolved in a 1:1 mixture of acetone and water (10 mL). Oxone (1279.0 mg, 2.08 mmol, 1.00 eq) was added and the mixture was left to stir at room temperature for 30 minutes. Upon complete conversion of the boronate ester, the reaction was quenched with Na_2SO_3 (10 mL). Volatiles were evaporated and the resulting aqueous mixture was buffered to

pH5 using 0.1M HCl and extracted with DCM (3 x 15 mL). The combined organic layers were dried over MgSO4 and concentrated. Purification was achieved by column chromatography (EtOAc in Hex 0-45%) to yield the title compound as a yellow amorphous solid (270.0 mg, 1.30 mmol, 62%). δ_H (599 MHz, $CDCl_3$) 7.64 (1H, t, *J* = 1.6 Hz, 2–H), 7.42 (1H, dd, *J* = 2.5, 1.6 Hz, 6–H), 7.12 (1H, dd, *J* = 2.5, 1.6 Hz, 4–H), 6.54 (1H, s, –O*H*), 3.91 (3H, s, –OCH_3), 1.43 (9H, s, –(CH_3)$_3$). δ_C (151 MHz, $CDCl_3$) 168.0 (C=O), 156.0 (C–5), 153.7 (C–1), 130.9 (C–3), 119.2 (C–2), 118.0 (C–4), 113.7 (C–6), 52.5 (–O*C*H_3), 34.9 (–*C*(CH_3)$_3$), 31.3 (–(*C*H_3)$_3$). ν_{max} (ATR) 3406 (O–H), 2956, 2864, 1701 (C=O), 1595 (C–O), 1432, 1326, 1297, 1254, 1116, 1000, 879, 769 cm^{-1}. *m/z* (LC-MS, ESI^+) 209.146 $[M+H]^+$. Accurate mass (ES+) found 209.1179, $C_{12}H_{17}O_3$ requires *M* 209.1178.

144. *methyl 3-tert-butyl-5-(pent-4'-yn-1'-yloxy)benzoate*

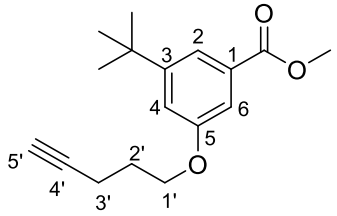

1-chloropent-4-yne (0.153 mL, 1.441 mmol, 2.00 eq) was added to a prestirred mixture of K_2CO_3 (398 mg, 2.88 mmol, 4.00 eq), TBAI (39.9 mg, 0.108 mmol, 0.15 eq) and *methyl 3-tert-butyl-5-hydroxybenzoate* (**143**) (150.0 mg, 0.720 mmol, 1.00 eq) in MeCN (7.2 mL). The mixture was allowed to stir under reflux for 16 hours after which it was quenched with $NaHCO_3$ (10 mL) and the organic layer was extracted with $CHCl_3$ (3 x 10 mL). The extracts were combined, dried over $MgSO_4$ and concentrated. Purification was achieved by column chromatography (0-20% EtOAc in Hex) to yield the title compound as a colourless oil (153.0 mg, 0.558 mmol, 77%). δ_H (599 MHz, $CDCl_3$) 7.68 (1H, t, *J* = 1.6 Hz, 2–H), 7.36 (1H, dd, *J* = 2.6, 1.6 Hz, 6–H), 7.13 (1H, dd, *J* = 2.6, 1.6 Hz, 4–H), 4.10 (2H, t, *J* = 6.1 Hz, 1'–H_2), 3.90 (3H, s, –OCH_3), 2.41 (2H, td, *J* = 7.0, 2.7 Hz, 3'–H_2), 2.00 (2H, tt, *J* = 7.0, 6.1 Hz, 2'–H_2), 1.97 (1H, t, *J* = 2.7 Hz, 5'–H), 1.32 (9H, s, –(CH_3)$_3$). δ_C (151 MHz, $CDCl_3$) 167.5 (C=O), 158.9 (C–5), 153.3 (C–1), 131.1 (C–3), 119.7 (C–2), 118.1 (C–4), 111.1 (C–6), 83.6 (C–4'), 69.1 (C–5'), 66.4 (C–1'), 52.3 (–O*C*H_3), 35.0 (–*C*(CH_3)$_3$), 31.4 (–(*C*H_3)$_3$), 28.4 (C-2'), 15.3 (C-3'). ν_{max} (ATR) 2952, 2255, 1730 (C=O), 1588, 1375, 1180, 1131, 904 cm^{-1}. *m/z* (LC-MS, ESI^+) 275.276 $[M+H]^+$. Accurate mass (ES+) found 275.1634, $C_{17}H_{23}O_3$ requires *M* 275.1647.

145. *3-tert-butyl-5-(pent-4-yn-1-yloxy)benzoic acid*

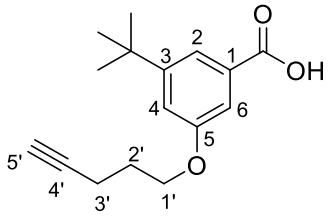

LiOH (0.436 g, 18.22 mmol, 5.00 eq) was added in portions to a solution of *methyl 3-tert-butyl-5-(pent-4'-yn-1'-yloxy)benzoate* (**144**) (1.00 g, 3.645 mmol, 1.00 eq) in a 5:1 mixture of THF (23.5 mL), water (4.7 mL), and 1 drop of MeOH. The reaction was allowed to stir at room temperature for 40 hours after which volatiles were evaporated. The remaining aqueous mixture was redissolved in 0.1M HCl (30 ml) and organic extraction was conducted with EtOAc (3 x 25 ml). The combined organic fractions were dried over $MgSO_4$ and concentrated to yield the title compound as a white amorphous solid (0.898 g, 3.449 mmol, 95%). δ_H (599 MHz, $CDCl_3$) 7.77 (1H, t, J = 1.6 Hz, 2–H), 7.44 (1H, dd, J = 2.5, 1.6 Hz, 6–H), 7.19 (1H, dd, J = 2.5, 1.6 Hz, 4–H), 4.13 (2H, t, J = 6.1 Hz, 1'–H_2), 2.43 (2H, td, J = 7.0, 2.6 Hz, 3'–H_2), 2.03 (2H, tt, J = 7.0, 6.1 Hz, 2'–H_2), 1.98 (1H, t, J = 2.6 Hz, 5'–H), 1.33 (9H, s, 9H, –(CH_3)$_3$). δ_C (151 MHz, $CDCl_3$) 172.1 (C=O), 158.8 (C–5), 153.3 (C–1), 130.0 (C–3), 120.2 (C–2), 118.9 (C–4), 111.4 (C–6), 83.3 (C–4'), 69.0 (C–5'), 66.3 (C–1'), 34.9 (–*C*(CH_3)$_3$), 31.2 (–(*C*H_3)$_3$), 28.1 (C–2'), 15.2 (C–3'). ν_{max} (ATR) 3279 (O–H), 2967, 2952, 1683 (C=O), 1602, 1414, 1332, 1304, 1059, 662 cm^{-1}. *m/z* (LC-MS, ESI^-) 259.411 $[M–H]^-$. Accurate mass (ES–) found 259.1356, $C_{16}H_{19}O_3$ requires *M* 259.1334

149. tert-butyl, N - {2'-[4-(2'''''-{2''''-[(pent-4'''-yn-1'''-yl) [(prop-2''-en-1''-yloxy) carbonyl] amino] ethoxy} ethoxy) naphthalene-1-sulfonamido] ethyl} carbamate

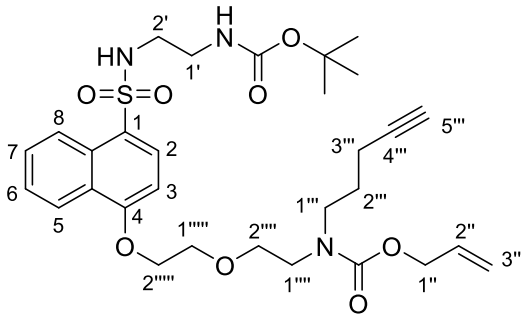

To a solution of *prop-2-en-1-yl N-(pent-4'-yn-1'-yl)-N-[2''-(2'''-hydroxyethoxy)ethyl]carbamate* (**140**) (90.0 mg, 0.353 mmol, 1.00 eq) in anhydrous dichloromethane (0.635 mL) (0.635 mL) and triethylamine (0.056 mL, 0.423 mmol, 1.20 eq) cooled to 0 ℃, methanesulfonyl chloride (0.033 mL, 0.423 mmol, 1.20 eq) was added dropwise. The reaction was stirred for 1 hour at 0 ℃, and then allowed to warm to room temperature with stirring for 16 hours. Following quenching with water, the organic layer underwent successive washes with HCl (3 x 10 ml), NaHCO3 (3 x 10 ml) and brine (3 x

10 ml). The organic layer was then dried over $MgSO_4$ and concentrated to yield intermediate mesylate **146** as a clear oil. *m/z* (ASAP+) 334.117 $[M+H]^+$.

K_2CO_3 (24.9 mg, 0.180 mmol, 1.50 eq) was added to a MeCN (1 mL) solution of *tert-butyl N-[2'-(4-hydroxynaphthalene-1-sulfonamido)ethyl]carbamate* (**131**) (50.0 mg, 0.136 mmol, 1.14 eq). To a separate flask, TBAI (7.4 mg, 0.020 mmol, 0.167 eq) was added to a MeCN solution (1 mL) of the intermediary mesylate (**146**) (40.0 mg, 0.120 mmol, 1.00 eq) and allowed to stir at room temperature for 30 mins. This mixture was then added to the naphthol and the mixture was stirred under reflux for 16 hours. Upon complete consumption of the starting mesylate, volatiles were evaporated and the resulting mixture was redissolved in 0.1M NaOH (15 ml) and organic extraction was conducted with DCM (3 x 10 ml). The combined organic layers were dried over $MgSO_4$ and concentrated to yield the crude material as a dark brown oil. Purification was achieved by column chromatography (EtOAc in Hex 0-50%) to yield the title compound as a dark yellow oil (42.0 mg, 0.070 mmol, 58%). δ_H (599 MHz, $CDCl_3$) 8.54 (1H, d, *J* = 8.5 Hz, 5–H), 8.37 (1H, d, *J* = 8.5 Hz, 2–H), 8.17 (1H, d, *J* = 8.3 Hz, 8–H), 7.65 (1H, dd, *J* = 8.5, 6.8 Hz, 6–H), 7.55 (1H, dd, *J* = 8.3, 6.8 Hz, 7–H), 6.80 (1H, d, *J* = 8.5 Hz, 3–H), 5.90 (1H, ddt, *J* = 16.2, 10.7, 5.4 Hz, 2''–H), 5.33 (1H, s, 2'–N*H*), 5.30 – 5.22 (1H, m, 3''–H_Z), 5.16 (1H, dd, *J* = 10.7, 5.4 Hz, 3''–H_E), 4.56 (2H, d, *J* = 5.4 Hz, 1''–H_2), 4.34 (2H, t, *J* = 4.8 Hz, 2'''''–H_2), 3.96 (2H, t, *J* = 4.8 Hz, 1'''''–H_2), 3.79 – 3.65 (2H, m, 2''''–H_2), 3.54 – 3.46 (2H, m, 1''''–H_2), 3.40 (2H, t, *J* = 5.8 Hz, 2'–H_2), 3.12 (2H, t, *J* = 5.8 Hz, 1'–H_2), 2.95 (2H, m, 1'''–H_2), 2.13 (2H, m, 3'''–H_2), 1.89 (1H, t, *J* = 2.6 Hz, 5'''–H), 1.76 (2H, m, 2'''–H_2), 1.36 (9H, s, –(C*H*$_3$)$_3$). *δC* (151 MHz, $CDCl_3$) 158.9 (C–4), 156.3 (1''''NH*C*=O), 156.1 – 155.9 (1'NH*C*=O), 133.1 – 132.9 (C–2''), 131.6 (C–8), 129.3 (C–1), 128.9 (C–6), 126.2 (C–7), 126.1 (C–8a) 125.8 (C–4a), 124.0 (C–5), 123.2 (C–2), 117.2 (C–3''), 102.6 (C–3), 83.4 (C–4'''), 79.7 (–*C*$(CH_3)_3$), 70.3 (C–2''''), 69.8 (C–5'''), 69.2 (C–1'''''), 68.8 (C–1''''), 68.2 (C–2'''''), 65.9 (C–1''), 47.8 – 47.4 (C–1'''), 43.5 (C–1'), 40.2 (C–2'), 28.3 (–(C*H*$_3$)$_3$), 27.3 – 26.8 (C–2'''), 15.8 (C–3'''). ν_{max} (ATR) 3304 (N–H), 2981, 2885, 1696, 1683, 1574, 1509, 1418, 1155, 1134, 1092, 910 cm^{-1}. *m/z* (LC-MS, ESI^+) 604.535 $[M+H]^+$, 504.477 $[M\text{-}Boc+H]^+$, 548.483 [M–*tBu*+2H]$^+$. Accurate mass (ES+) found 604.2714, $C_{30}H_{42}N_3O_8S$ requires *M* 604.2693

152. *N-[2''-(2'-hydroxyethoxy)ethyl]pent-4-ynamide*

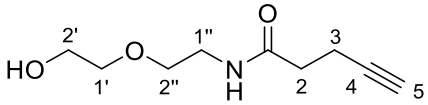

A solution of *4-pentynoic acid* (**151**) (0.443 g, 4.518 mmol, 0.95 eq) and one drop of DMF in DCM (47.6 mL) was cooled to 0 ℃. Oxalyl chloride (0.387 mL, 4.518 mmol, 0.95 eq) was added dropwise and the mixture was allowed to reach ambient temperature and stirred until gas evolution has stopped. Volatiles were evaporated using a rotavapor with the water bath set to 20 ℃. The resulting residue was taken up in DCM (47.6 mL) and cooled to 0 ℃. A mixture of *2-(2-aminoethoxy)ethan-1-*

ol (**132**) (0.500 g, 4.756 mmol, 1.00 eq) and Et_3N (0.695 mL, 5.231 mmol, 1.10 eq) in DCM (50 mL) was then added dropwise. The mixture was allowed to reach ambient temperature and stirred for 3 hours. Upon completion, volatiles were evaporated and the resulting material was purified by column chromatography (EtOAc in Hex 0-100%) to yield the title compound as a colourless oil (0.643 g, 3.471 mmol, 73%). δ_H (599 MHz, $CDCl_3$) 6.52 (1H, m, –N*H*), 3.70 (2H, q, *J* = 4.4 Hz, 2'–H_2), 3.54 (4H, m, 1'–H_2, 2''–H_2), 3.45 (2H, m, 1''–H_2), 2.49 (2H, dt, *J* = 7.3, 2.3 Hz, 3–H_2), 2.38 (2H, t, *J* = 7.3, 2–H_2), 1.98 (1H, t, *J* = 2.3 Hz, 5–H). δ_C (151 MHz, $CDCl_3$) 171.4 (C–1), 83.0 (C–4), 72.2 (C–1'), 69.8 (C–2''), 69.3 (C–5), 61.6 (C–2'), 39.3 (C–1''), 35.2 (C–2), 14.8 (C–3). ν_{max} (ATR) 3307 (*b*, O–H), 2927, 2874, 2247, 1651 (C=O), 1549, 1127, 1067, 907 cm^{-1}. m/z (LC-MS, ESI^+) 186.153 $[M+H]^+$. Accurate mass (ES+) found $[M+H]^+$ 186.1132, $C_9H_{16}NO_3$ requires *M* 186.1130.

153. 3-tert-butyl-N-[2''-(2'''-hydroxyethoxy)ethyl]-N-(pent-4'-yn-1'-yl)benzamide

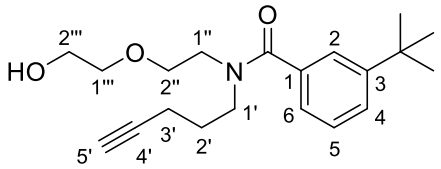

A solution of *N-[2''-(2'-hydroxyethoxy)ethyl]pent-4-ynamide* (**152**) (0.510 g, 2.75 mmol, 1.00 eq) in THF (4.0 ml) was added dropwise to a suspension of $LiAlH_4$ (0.374 g, 11.0 mmol, 4.00 eq) in THF (5 mL) at 0 ℃. The mixture was allowed to reach ambient temperature and stirred for 16 hours after which it was heated at 50 ℃ for a further 4 hours. The mixture was then cooled to 0 ℃ and quenched with successive additions of water (1.0 eq), 4M NaOH (2.0 eq) and water (3.0 eq) and left to stir at room temperature for a further 30 mins. The mixture was filtered, volatiles evaporated and the resulting residue redissolved in THF (10 ml). The THF solution was dried over $MgSO_4$ and concentrated to yield intermediary secondary amine (**139**) as a bright orange oil (0.452 g) m/z (LC-MS, ESI^+) 172.318 $[M+H]^+$.

Oxalyl chloride (0.115 mL, 1.35 mmol, 1.20 eq) was added at 0 ℃ to a solution of 3-tertbutyl benzoic acid (0.200 g, 1.122 mmol, 1.00 eq) and 1 drop of DMF in DCM (11.2 mL). Upon completion of addition, the mixture was allowed to reach ambient temperature and stirred until gas evolution had stopped. Volatiles were evaporated and the resulting residue was taken up in DCM and added to a solution of secondary amine **139** and Et_3N (0.224 mL, 1.68 mmol, 1.50 eq) in DCM (11.2 mL) at 0 ℃. The mixture was allowed to reach ambient temperature and stirred for 3 hours after which it was quenched with 1M $NaHCO_3$ (10 mL). Extraction was conducted with EtOAc (3 x 15 ml) and the combined organic extracts were dried over $MgSO_4$ and concentrated. Purification was achieved by column chromatography (EtOAc in Hex, 0-100%) to yield the title compound as a colourless oil (0.164 g, 0.495 mmol, 44% (over 2 steps)). δ_H (599 MHz, $CDCl_3$) 7.44 – 7.39 (1H, m, 6–H), 7.37 (1H, m, 2–

H), 7.31 – 7.29 (1H, m, C–5), 7.17 – 7.15 (1H, m, 4–H), 3.85 – 3.29 (10H, m, 2’’’–H_2, 1’’’–H_2, 1’’–H_2, 2’’–H_2, 1’–H_2), 2.31 (1H, s, –O*H*) 2.03 – 1.91 (3H, m, 3’–H_2, 5’–H), 1.79 (2H, m, 2’–H_2), 1.31 (9H, s, –(CH_3)$_3$). δ_C (151 MHz, $CDCl_3$) 172.8 (C=O), 151.4 (C–1), 136.3 (C–3), 128.1 (C–5), 126.4 (C–6), 123.7 (C–4), 123.5 (C–2), 82.6 (C–4’), 72.4 (C–1’’), 69.1 (C–5’), 69.1 (C–2’’’), 61.8 (C–1’’’), 49.3 (C–1’), 45.1 (C–2’’), 34.8 (–*C*(CH$_3$)$_3$), 31.2 –(*C*H$_3$)$_3$), 27.5 – 26.2 (C–2’), 16.1 – 15.7 (C–3’). ν_{max} (ATR) 3410 (O–H), 3300, 2956, 2871, 1619 (C=O), 1461, 1428, 1414, 1364, 1124, 1059 cm^{-1}. m/z (LC-MS, ESI^+) 332.360 $[M+H]^+$, 355.390 $[M+Na]^+$, 663.662 $[2M+H]^+$. Accurate mass (ES+) found $[M+H]^+$ 332.2233, $C_{20}H_{30}NO_3$ requires *M* 332.2226.

154a. *tert-butyl N-{2’-[4-(2’’’’-{2’’’’-[1’’-(3’’-tert-butylphenyl)-N-(pent-4’’’-yn-1’’’-yl)formamido] ethoxy} ethoxy) naphthalene-1-sulfonamido] ethyl} carbamate*

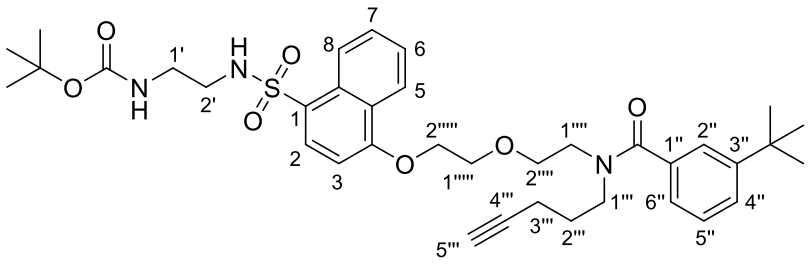

Mesylate chloride (0.020 mL, 0.253 mmol, 1.20 eq) was added dropwise to a solution of *3-tert-butyl-N-[2’’-(2’’’-hydroxyethoxy)ethyl]-N-(pent-4’-yn-1’-yl)benzamide* (**153**) (0.070 g, 0.211 mmol, 1.00 eq) and Et_3N (0.034 mL, 0.253 mmol, 1.20 eq) in DCM (1.1 mL) at 0 °C. The mixture was allowed to reach ambient temperature and stirred for 16 hours after which it was quenched with 1M $NaHCO_3$ (5 mL). The layers were separated, and the aqueous layer extracted with DCM (3 x 5 mL). The combined organic extracts were washed with brine, dried over $MgSO_4$ and concentrated to yield the intermediate mesylate as a dark brown oil (0.086 g). m/z ($ASAP^+$) 410.187 $[M+H]^+$.

A pre-stirred solution of the mesylate (0.025 g, 0.061 mmol, 1.00 eq) and TBAI (0.011 g, 0.031 mmol, 0.50 eq) in MeCN (0.3 mL) was added to a solution of *tert-butyl N-[2’-(4-hydroxynaphthalene-1-sulfonamido)ethyl]carbamate* (**131**) (0.025 g, 0.067 mmol, 1.10 eq) and K_2CO_3 (0.013 g, 0.092 mmol, 1.50 eq) in MeCN (0.3 mL). The mixture was allowed to stir under reflux for 48 hours after which volatiles were evaporated and the resulting residue was taken up in 0.1M NaOH (5 mL). Extraction was conducted with DCM (3 x 5 mL) and the combined organic layers were dried over $MgSO_4$ and concentrated to afford the crude mixture as a dark brown oil. Purification by reverse phase chromatography (C18, MeCN in H_2O, 0-80%) yielded the title compound as a light brown oil (0.015 g, 0.022 mmol, 36%). δ_H (599 MHz, $CDCl_3$) 8.56 (1H, d, *J* = 7.7 Hz, 5–H), 8.41 – 8.33 (1H, m, 2–H), 8.19 (1H, d, *J* = 8.2 Hz, 8–H), 7.66 (1H, t, *J* = 7.7 Hz, 6–H), 7.59 – 7.56 (1H, m, 7–H), 7.42 – 7.35 (2H, m, 6’’–H, 2’’–H), 7.20 – 7.08 (2H, m, 5’’–H, 4’’–H), 6.82 (1H, d, *J* = 8.4 Hz, 3–H), 5.30 (1H, s, 2’–

N*H*), 4.76 (1H, s, 1’–N*H*), 4.41 – 4.33 (2H, m, 2’’’’’–H_2), 4.13 – 4.03 (2H, m, 1’’’’’–H_2), 3.77 – 3.66 (4H, m, 2’’’’–H_2, 1’’’’–H_2), 3.41 – 3.37 (2H, m, 1’’’–H_2), 3.13 (2H, q, *J* = 5.8 Hz, 2’–H_2), 2.96 (2H, q, *J* = 5.8 Hz, 1’–H_2), 2.04 (1H, s, 5’’’–H), 2.00 – 1.90 (2H, m, 2’’’–H_2), 1.76 – 1.70 (2H, m, 3’’’–H_2), 1.38 (9H, s, –OC(CH_3)$_3$), 1.28 (9H, s, –(CH_3)$_3$). δ_C (151 MHz, $CDCl_3$) 172.7 (C=O *amide*), 158.9 (C–4) 156.6 (C=O *carbamate*), 151.4 (C–1’’), 136.3 (C–3’’), 131.6 (C–8), 129.4 (C–1), 128.9 (C–6), 128.1 (C–5’’), 126.3 (C–6’’), 126.2 (C–8a), 126.2 (C–7), 124.0 (C–5), 123.9 (C–4a), 123.4 (C–2’’) 123.4 (C–4’’), 123.2 (C–2), 102.6 (C–3). 83.3 (C–4’’’), 79.7 (–O*C*$(CH_3)_3$), 69.6 (C–5’’’), 69.6 (C–2’’’’’) 69.2 (C–1’’’’’), 69.0 (C–1’’’’), 68.2 (C–2’’’’), 49.5 (C–1’’’), 43.6 (C–1’), 40.2 (C–2’), 34.7 (–*C*$(CH_3)_3$), 31.2 (–(CH_3)$_3$), 28.3 (–OC(*C*H_3)$_3$), 21.0 (C–2’’’), 14.2 (C–3’’’). ν_{max} (ATR) 3441 (N–H), 3349 (N–H), 2952, 2861, 2247, 1711 (C=O, *carbamate*), 1616 (C=O, *amide*), 1364, 1262, 1219, 1112, 914 cm^{-1}. m/z (LC-MS, ESI^+) 680.534 $[M+H]^+$, 580.480 $[M\text{-}Boc+H]^+$, 624.485 [M–*tBu*+2H]$^+$. Accurate mass (ES+) found $[M+H]^+$ 680.3380, $C_{37}H_{50}N_3O_7S$ requires *M* 680.3369.

154. *N-{2-[2-({4-[(2-aminoethyl)sulfamoyl]naphthalen-1-yl}oxy)ethoxy]ethyl}-3-tert-butyl-N-(pent-4-yn-1-yl)benzamide hydrochloride*

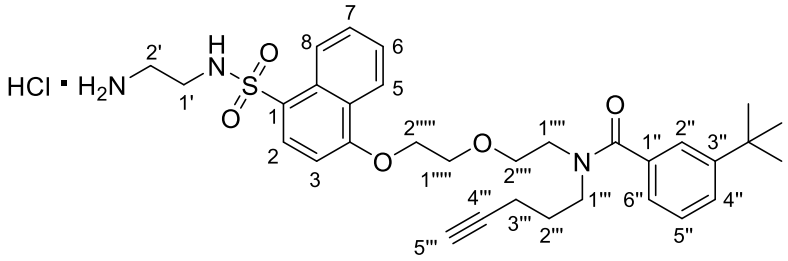

Compound was prepared according to general procedure B using *tert-butyl N-{2’-[4-(2’’’’-{2’’’’-[1’’-(3’’-tert-butylphenyl)-N-(pent-4’’’-yn-1’’’-yl)formamido] ethoxy} ethoxy) naphthalene-1-sulfonamido] ethyl} carbamate* (**154a**) (12.0 mg, 0.018 mmol, 1.00 eq) to yield the title compound as a light brown oil (10.0 mg, 0.017 mmol, 98%). δ_H (599 MHz, MeOD) 8.56 (1H, *J* = 8.4 Hz, 5–H), 8.43 – 8.32 (1H, m, 2–H), 8.17 (1H, d, *J* = 7.4 Hz, 8–H), 7.73 – 7.50 (2H, m, 6–H, 7–H), 7.43 – 7.31 (2H, m, 6’’–H, 2’’–H), 7.26 – 7.08 (2H, m, 5’’–H, 4’’–H), 7.03 – 6.99 (1H, m, 3–H), 4.41 – 4.30 (2H, m, 2’’’’’–H_2), 4.08 – 3.66 (6H, m, 1’’’’’–H_2, 2’’’’–H_2, 1’’’’–H_2), 3.57 – 3.47 (2H, m, 1’’’–H_2), 3.05 – 2.96 (4H, s, 2’–H, 1’–H), 2.20 – 2.11 (1H, m, 5’’’–H), 2.03 – 1.82 (2H, m, 2’’’–H), 1.78 – 1.51 (2H, m, 3’’’–H_2), 1.25 – 1.18 (9H, s, –(CH_3)$_3$). δ_C (151 MHz, MeOD) 173.3 (C=O), 159.0 (C–4), 151.3 (C–1’’), 136.0 (C–3’’), 131.5 (C–8), 129.2 (C–1), 128.4 (C–6), 128.0 (C–5’’), 127.9 (C–6’’), 126.1 (C–7), 126.1 (C–8a), 124.0 (C–5), 123.7 (C–4a), 123.6 (C–2’’), 123.1 (C–4’’), 122.9 (C–2), 102.8 (C–3), 81.9 (C–4’’’), 72.1 (C–5’’’), 71.02 (C–2’’’’’), 68.8 (C–1’’’’’), 66.7 (C–1’’’’), 60.8 (C–2’’’’), 49.4 (C–1’’’), 39.8 (C–2’), 39.4 (C–1’), 34.1 (–*C*$(CH_3)_3$), 30.2 (–(CH_3)$_3$), 27.1 (C–2’’’), 15.4 – 14.9 (C–3’’’). ν_{max} (ATR) 3318 (N–H), 2971, 2148, 1623 (C=O), 1506, 1371, 1322, 1276, 1155, 1134 cm^{-1}. m/z (LC-MS, ESI^+) 580.419 $[M+H]^+$. Accurate mass (ES+) found $[M+H]^+$ 580.2850, $C_{32}H_{42}N_3O_5S$ requires *M* 580.2845.

156a. *tert-butyl N-(2'-{4-[2''''-(2'''-{1''-[3''-tert-butyl-5''-(pent-4'''-yn-1'''-yloxy)phenyl]-N-methylformamido} ethoxy) propyl] naphthalene-1-sulfonamido} ethyl)carbamate*

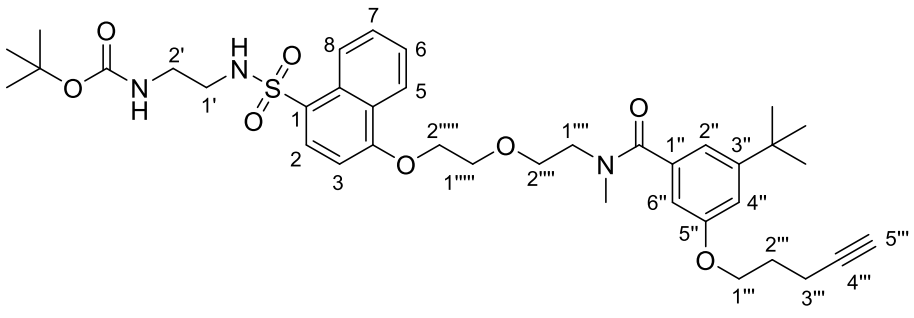

Oxalyl chloride (0.067 mL, 0.784 mmol, 1.20 eq) was added at 0 ℃ to a solution of *3-tert-butyl-5-(pent-4-yn-1-yloxy)benzoic acid* (**145**) (0.170 g, 0.653 mmol, 1.00 eq) and 1 drop of DMF in DCM (6.5 mL). Upon completion of addition, the mixture was allowed to reach ambient temperature and stirred until gas evolution had stopped. Volatiles were evaporated and the resulting residue was taken up in THF (3.5 mL) and added to a solution of *2-[2'-(methylamino)ethoxy]ethan-1-ol* (**135**) (0.093 g, 0.784 mmol, 1.200 eq) and Et_3N (0.173 mL, 1.306 mmol, 2.00 eq)in THF (3.0 mL) at 0 ℃. The mixture was allowed to reach ambient temperature and stirred for 3 hours after which it was quenched with 1M $NaHCO_3$ (10 mL). The layers were separated and the aqueous layer was extracted with DCM (3 x 15 mL). The combined organic extracts were dried over $MgSO_4$, concentrated to yield intermediate amide **155** as a light brown oil (0.102 g). m/z (LC-MS, ESI^+) 362.421 $[M+H]^+$, 723.739 $[2M+H]^+$.

To a solution of amide **155**, (0.090 g, 0.249 mmol, 1.00 eq) in anhydrous dichloromethane (0.449 mL) and triethylamine (0.040 mL, 0.299 mmol, 1.20 eq) cooled to 0 ℃, methanesulfonyl chloride (0.023 mL, 0.299 mmol, 1.20 eq) was added dropwise. The reaction was stirred for 1 hour at 0 ℃, and then allowed to warm to room temperature with stirring for 16 hours. Following quenching with water (5 ml), the organic layer underwent successive washes with HCl (3 x 10 ml), $NaHCO_3$ (3 x 10 ml) and brine (3 x 10ml). The organic layer was then dried over $MgSO_4$ and concentrated to yield the intermediary mesylate (**155a**) as a dark orange oil (0.102 g). m/z ($ASAP^+$) 440.205 $[M+H]^+$.

A pre-stirred solution of the intermediate mesylate **155a** (100 mg, 0.227 mmol, 1.00 eq) and TBAI (84.0 mg, 0.227 mmol, 1.00 eq) in MeCN was added to a solution of *tert-butyl N-[2'-(4-hydroxynaphthalene-1-sulfonamido)ethyl]carbamate* (**131**) (125.0 mg, 0.341 mmol, 1.50 eq) and K_2CO_3 (62.9 mg, 0.455 mmol, 2.00 eq) in MeCN (2.3 mL). The mixture was allowed to stir under reflux for 16 hours after which volatiles were evaporated and the resulting residue was taken up in 0.1M NaOH (5 mL). Extraction was conducted with EtOAc (3 x 10 mL) and the combined organic layered were dried over $MgSO_4$ then concentrated. Purification was achieved through HPLC reverse phase chromatography (MeCN in H_2O 0-55%) to yield the title compound as a light brown oil (39.7

mg, 0.056 mmol, 25% (over 3 steps)). δ_H (599 MHz, $CDCl_3$) 8.54 (1H, m, 5–H), 8.34 (1H, m, 2–H), 8.18 – 8.17 (1H, m, 8–H), 7.65 (1H, m, 6–H), 7.54 (1H, m, 7–H), 6.99 – 6.62 (2H, m, 2’’–H, 6’’–H), 6.80 – 6.79 (1H, m, 3–H), 6.74 (1H, s, 4’’–H), 5.22 (1H, m, 2’–N*H*), 4.74 (1H, m, 1’–N*H*), 4.37 – 4.36 (2H, m, 2’’’’’–H_2), 4.04 – 4.01 (2H, m, 1’’’’’–H_2), 3.92 – 3.77 (4H, m, 1’’’–H_2, 2’’’’–H_2), 3.72 – 3.45 (2H, m, 1’’’’–H_2), 3.17 – 3.01 (4H, m, 2’–H_2, 3’’’–H_2), 2.96 – 2.94 (2H, m, 1’–H_2), 2.37 – 2.34 (2H, m, 2’’’–H_2), 2.16 (1H, m, 5’’’–H), 1.97 – 1.95 (3H, m,–NCH_3), 1.37 (9H, s, –OC(CH_3)$_3$), 1.26 – 1.24 (9H, m, –C(CH_3)$_3$). δ_C (151 MHz, $CDCl_3$) 172.2 (C=O, amide), 159.1 (C–5’’), 158.7 (C–4), 156.3 (C=O, *carbamate*), 153.2 (C–1’’), 131.6 (C–8), 129.8 (C–3’’), 129.3 (C–1), 128.9 (C–6), 126.2 (C–8a), 126.2 (C–7), 125.9 (C–4a), 124.0 (C–5), 123.1 (C–2), 116.5 (C–2’’), 113.8 (C–6’’), 109.3 (C–4’’), 102.6 (C–3), 83.4 (C–4’’’), 79.7 ((–O*C*(CH$_3$)$_3$), 69.7 (C–1’’’’’), 69.5 (C–1’’’’), 69.2 (C–5’’’), 68.9 (C–2’’’’’), 66.2 (C–1’’’), 66.2 (C–2’’’’), 43.6 (C–1’), 40.2 (C–2’), 39.1 (C–3’’’), 34.8 (–*C*(CH$_3$)$_3$), 31.2 (–C(*C*H$_3$)$_3$), 28.3 (–OC(*C*H$_3$)$_3$), 28.1 (–NC*H*$_3$), 15.1 (C–2’’’). ν_{max} (ATR) 3307 (N–H), 2977, 2924, 1701 (C=O, *carbamate*), 1616 (C=O, *amide*), 1588, 1513, 1247, 1155, 1087 cm^{-1}. m/z (LC-MS, ESI$^+$) 233.138 [M+H]$^+$. m/z (LC-MS, ESI$^+$) 710.515 [M+H]$^+$, 610.501 [M-Boc+H]$^+$. Accurate mass (ES+) found [M+H]$^+$ 710.3497, $C_{38}H_{52}N_3O_8S$ requires *M* 710.3475.

156. *N-{2’’’’-[2’’’’’-({4-[(2’-aminoethyl)sulfamoyl]naphthalen-1-yl}oxy)ethoxy]ethyl}-3’’-tert-butyl-N-methyl-5’’-(pent-4’’’-yn-1’’’-yloxy)benzamide hydrochloride*

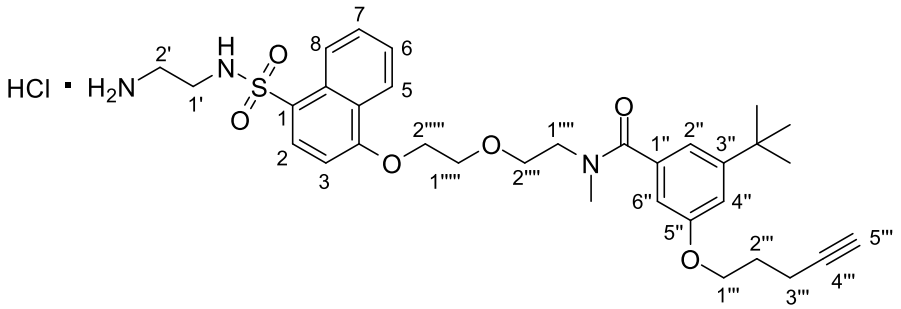

Compound was prepared according to general procedure B, using *tert-butyl N-(2’-{4-[2’’’’’-(2’’’’-{1’’-[3’’-tert-butyl-5’’-(pent-4’’’-yn-1’’’-yloxy)phenyl]-N-methylformamido} ethoxy) propyl] naphthalene-1-sulfonamido} ethyl)carbamate* (**156a**) (0.015 g, 0.021 mmol, 1.00 eq) to yield the title compound as a light brown amorphous solid (0.013 g, 0.020 mmol, 95%). δ_H (400 MHz, MeOD) 8.60 – 8.58 (1H, m, 5–H), 8.43 – 8.40 (1H, m, 2–H), 8.22 – 8.20 (1H, m, 8–H), 7.75 – 7.69 (1H, m, 6–H), 7.66 – 7.52 (1H, m, 7–H), 7.13 – 6.91 (m, 3H), 7.10 – 6.94 (3H, m, 2’’–H, 6’’–H, 3–H), 6.78 – 6.75 (1H, m, 4’’–H), 4.45 (2H, s, 2’’’’’–H_2), 4.08 – 4.01 (2H, m, 1’’’’’–H_2), 3.97 – 3.76 (4H, m, 1’’’–H_2, 2’’’’–H_2), 3.75 – 3.63 (2H, m, 1’’’’–H_2), 3.62 – 3.52 (2H, m, 3’’’–H_2), 3.13 – 3.06 (2H, m, 2’–H_2), 3.00 (3H, s, –NCH_3) 2.42 – 2.19 (3H, m, 1’–H_2, 5’’’–H), 1.97 – 1.75 (3H, m, 2’’’–H_2), 1.32 – 1.17 (9H, m, –C(CH_3)$_3$). δ_C (101 MHz, MeOD) 172.8 (C=O), 159.2 (C–5’’), 157.2 (C–4), 153.5 (C–1’’), 131.5 (C–3’’), 131.1 (C–8) 130.4 (C–1), 129.2 (C–6), 128.4 (C–8a) 126.1 (C–7), 125.4 (C–4a), 124.0 (C–5),

122.8 (C–2), 118.7 (C–2’’), 113.2 (C–6’’), 109.4 (C–4’’) 102.9 (C–3), 82.7 (C–4’’’), 69.2 (C–1’’’’’), 69.1 (C–1’’’’), 68.7 (C–5’’’), 68.6 (C–2’’’’’) 66.0 (C–1’’’), 65.9 (C–2’’’’), 40.1 (C–2’), 39.7 (–*C*$(CH_3)_3$), 39.3 (C–3’’’), 38.6 (C–1’) 30.1 (–C(*C*$H_3)_3$), 27.9 (–NC*H*$_3$) 14.3 (C–2’’’). ν_{max} (ATR) 3399 (N–H), 3293 (N–H), 2956, 2871, 2513, 1616 (C=O), 1509, 1428, 1322, 1149, 1127, 1092 cm^{-1}. m/z (LC-MS, ESI^+) 610.539 $[M+H]^+$, 1219.798 $[2M+H]^+$. Accurate mass (ES+) found $[M+H]^+$ 610.2955, $C_{33}H_{44}N_3O_6S$ requires *M* 610.2951.

160. *methyl 3-formylbenzoate*

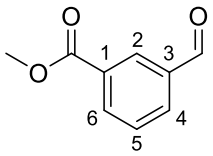

MeOH (0.337 mL, 8.34 mmol, 1.250 eq) was added to a stirred DCM (66.6 mL) solution of DMAP (0.134 g, 1.10 mmol, 0.165 eq), *3-formylbenzoic acid* (**159**) (1.00 g, 6.66 mmol, 1.00 eq) and DCC (2.749g, 13.3 mmol, 2.00 eq) at room temperature under N_2. The reaction mixture was left to stir for 24 hours until the formation of a white precipitate. The precipitate was filtered, and the filtrate was concentrated and purified by column chromatography (EtOAc in Hex 0-30%) to yield the title compound as a white solid (0.976 g, 5.94 mmol, 89%). m.p: 52-53 °C. δ_H (400 MHz, $CDCl_3$) 10.08 (1H, s, –HC=O), 8.53 (1H, td, *J* = 1.8, 0.6 Hz, 2–H), 8.30 (1H, ddd, *J* = 7.8, 1.8, 1.3 Hz, 4–H), 8.09 (1H, ddd, *J* = 7.8, 1.3, 0.6 Hz, 6–H), 7.65 (1H, t, J=7.8, 5–H), 3.97 (3H, s, –OC*H*$_3$). δ_C (101 MHz, $CDCl_3$) 191.4 (3–*C*=O), 166.0 (1–*C*=O), 136.6 (C–3), 135.2 (C–2), 133.9 (C–6), 131.4 (C–4), 131.2 (C–1), 129.3 (C–5), 52.6 (–O*C*H_3). ν_{max} (ATR) 2966, 2867, 2757, 1721 (C=O), 1696 (C=O), 1621, 1444, 1388, 1285, 1195, 1116, 977 cm^{-1}. m/z (LC-MS, ESI^+) 165.176 $[M+H]^+$, 133.139 $[M–OMe]^+$. Accurate mass (ES+) found 165.0545, $C_9H_9O_3$ requires *M* 165.0552. Data agrees with that reported in Jiang et al.[148]

161. *methyl 3-(2’,2’,2’-trifluoroacetyl)benzoate*

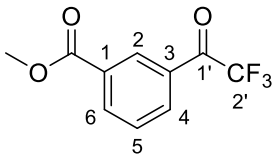

$TMSCF_3$ (1.1 mL, 7.31 mmol, 1.20 eq) was added to a DMF solution (12.2 mL) of *methyl 3-formylbenzoate* (**160**) (1.00 g, 6.09 mmol, 1.00 eq) and K_2CO_3 (8.4 mg, 0.061 mmol, 0.01 eq). The reaction was allowed to stir at room temperature and upon complete consumption of the benzaldehyde, 1M HCl (7.3 mL, 7.30 mmol, 1.20 eq) was added and the mixture was allowed to stir for a further 3 hours. The reaction was quenched with water (25 ml) and extraction of the aqueous layer was conducted

with EtO_2 (3 x 20 ml). The combined organic layers were dried over $MgSO_4$, concentrated and the resulting mixture dissolved in EtOAc (24.4 mL). IBX (4873.6 mg, 12.2 mmol, 2.0 eq) was added and the mixture was stirred under reflux for 16 hours, filtered and the filtrate washed with water (3 x 15 ml). The filtrate was concentrated and purification was achieved by column chromatography (EtOAc in Hex 0-15%) to yield the title compound as a colourless oil (885 mg, 3.81 mmol, 63%). δ_H (599 MHz, $CDCl_3$) 8.72 (1H, dd, *J* = 1.8, 0.9 Hz, 2–H), 8.38 (1H, dd, *J* = 7.8, 1.8 Hz, 6–H), 8.25 (1H, dd, *J* = 7.8, 1.8 Hz, 4–H), 7.66 (1H, t, *J* = 7.8 Hz, 5–H), 3.98 (3H, s, –OC*H*$_3$). δ_C (151 MHz, $CDCl_3$) 179.9 (q, *J* = 34.7 Hz, C–1'), 165.5 (C=O), 136.1 (C–6), 133.9 (q, *J* = 2.1 Hz, C–4), 131.4 (C–1), 131.1 (q, *J* = 2.7 Hz, C–2), 130.2 (C–3), 129.4 (C–5), 116.4 (q, *J* = 289.1, C–2'), 52.6 (–O*C*H$_3$). δ_F (376 MHz, $CDCl_3$) -71.58 (2'–F). ν_{max} (ATR) 2959, 1719 (C=O), 1602, 1432, 1279, 1141, 946 cm^{-1}. m/z (LC-MS, ESI^+) 233.138 $[M+H]^+$. Accurate mass (ES+) found 233.0422, $C_9H_8O_3F_3$ requires *M* 165.0552. Data agrees with that reported in Inglis *et al*.[149]

167. *methyl 3-[2',2',2'-trifluoro-1-(hydroxyimino)ethyl]benzoate*

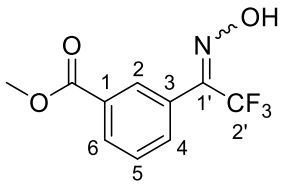

Hydroxylamine hydrochloride (598.6 mg, 8.62 mmol, 4.00 eq) was added in portions to a solution of the *methyl 3-(2',2',2'-trifluoroacetyl)benzoate* (**161**) (500.0 mg, 2.15 mmol, 1.00 eq) in pyridine (5.4 mL). The reaction was allowed to stir at 70 ℃ for 3 hours after which volatiles were evaporated. The resulting residue was taken up in EtOAc (20 ml) and washed with 0.01M HCl (8 x 15 ml) and H_2O (3 x 15 ml). The organic layer was dried over $MgSO_4$ and concentrated to yield the title compound as a mixture of *cis* and *trans* isomers as an amorphous white solid (511.0 mg, 2.07 mmol, 96%). δ_H (599 MHz, MeOD) 8.15 – 8.03 (2H, m, 2–H, 6–H), 7.71 – 7.68 (1H, m, 4–H), 7.61 – 7.49 (1H, m, 5–H), 3.92 – 3.90 (3H, m, –OC*H*$_3$). δ_C (151 MHz, MeOD) 166.2 (C=O), 144.6 (q, *J* = 31.4 Hz, C–1'), 144.5 (q, *J* = 29.3 Hz, C–1') 133.0 (C–4), 132.4 (C–4), 131.5 (C–1), 130.5 (C–2), 130.3 (C–1), 130.2 (C–6), 129.4 (C–6), 128.8 (C–2), 128.4 (C–5), 128.4 (C–5), 127.6 (C–3), 121.0 (q, *J* = 273.0 Hz, C–2'), 118.6 (q, *J* = 284.7, C–2'), 51.4 (–O*C*H$_3$). δ_F (376 MHz, MeOD) -63.89 (2'–F_a), -67.64 (2'–F_b). ν_{max} (ATR) 3311 (O–H), 2964, 2861, 1691 (C=O), 1609, 1449, 1301, 1169, 1127, 982, 954 cm^{-1}. m/z (LC-MS, ESI^+) 248.217 $[M+H]^+$, 260.303 $[M+Na]^+$. Accurate mass (ES+) found 248.0542, $C_{10}H_9NO_3F_3$ requires *M* 248.0535. Data agrees with that reported in Andrews et al.[150]

169. *methyl 3-[1'-(trifluoromethyl)diaziridin-1-yl]benzoate*

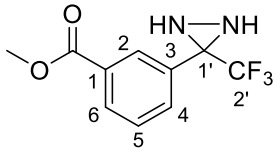

p-toluenesulfonylchloride (347.1 mg, 1.82 mmol, 1.50 eq) was added in portions to a pyridine solution (4.9 mL) of the *methyl 3-[2',2',2'-trifluoro-1-(hydroxyimino)ethyl]benzoate* (**167**) (300.0 mg, 1.21 mmol, 1.00 eq). The reaction was allowed to stir at 60 ℃ for 3 hours after which volatiles were evaporated. The resulting mixture was taken up in DCM (5 mL) and washed with 1M $NaHCO_3$ (3 x 5 mL). The organic layer was dried over $MgSO_4$ and concentrated to yield intermediary tosylate **168** as a light yellow oil. m/z (ASAP$^+$) 402.049 $[M+H]^+$.

In a sealed thick-walled tube, the tosylate intermediate (**168**) was dissolved in Et_2O (1.2 mL) and the solution was cooled to -78 ℃ after which liquid ammonia (1.2 mL, 53.40 mmol, 107.16 eq) was added via canula. Upon completion of addition, the mixture was allowed to reach room temperature and stirred for 6 hours after which it was cooled to -78 ℃ before the cap was removed to release excess ammonia. The remaining volatiles were evaporated and purification was achieved by flash chromatography ($CHCl_3$ in Hex, 0-30%) to yield the title compound as a white amorphous solid (95.4 mg, 0.388 mmol, 32% (over 2 steps)). δ_H (599 MHz, $CDCl_3$) 8.33 – 8.22 (1H, m, 2–H), 8.11 (1H, ddd, J = 7.8, 1.7, 1.2 Hz, 6–H), 7.88 – 7.76 (1H, m, 4–H), 7.51 (1H, td, J = 7.8, 0.6 Hz, 5–H), 3.93 (3H, s, –OCH_3), 2.85 (1H, m, N–*H*), 2.27 (1H, m, N–*H*). δ_C NMR (151 MHz, $CDCl_3$) 166.1 (C=O), 132.5 (C–4), 132.2 (C–1), 131.3 (C–6), 130.9 (C–3), 129.3 (C–2), 129.0 (C–5), 123.3 (q, J = 277.9 Hz, C–2'), 57.8 (q, J = 39.5 Hz, C–1') 52.4 (–O*C*H$_3$). δ_F (376 MHz, $CDCl_3$) -75.48. ν_{max} (ATR) 3258 (N–H), 2967, 1723 (C=O), 1446, 1272, 1159, 914 cm^{-1}. m/z (LC-MS, ESI$^+$) 247.266 $[M+H]^+$, 288.350 $[M+MeCN+H]^+$. Accurate mass (ES+) found 247.0688, $C_{10}H_{10}N_2O_2F_3$ requires M 247.0694.

170. *methyl 3-[3'-(trifluoromethyl)-diazirin-3'-yl]benzoate*

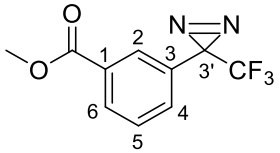

I_2 (0.739 g, 2.91 mmol, 1.20 eq) was added in portions to a solution of *methyl 3-[1'-(trifluoromethyl)diaziridin-1-yl]benzoate* (**169**) (0.600 g, 2.43 mmol, 1.00 eq) and Et_3N (0.484 mL, 3.64 mmol, 1.50 eq) in MTBE (24 mL) at 0 degrees. The mixture was stirred at this condition for 1 hour. The reaction was then allowed to reach room temperature and the flask was wrapped in aluminum foil to block out ambient light. Following a further 4 hours of stirring, the reaction mixture was quenched with Na_2SO_3 solution (20 ml). Organic extraction was conducted with ether (3 x 25 ml) and

the combined organic extracts were dried over $MgSO_4$ and concentrated. Purification was achieved by column chromatography ($CHCl_3$ in Hex, 0-15%) to yield the title compound as a colourless oil (0.452 g, 1.85 mmol, 76%). δ_H (400 MHz, $CDCl_3$) 8.11 (1H, dt, *J* = 7.6, 1.5 Hz, 6–H), 7.85 (1H, dd, *J* = 1.5, 0.7 Hz, 2–H), 7.56 – 7.42 (2H, m, 4–H, 5–H), 3.95 (3H, s, –OCH_3). δ_C (101 MHz, $CDCl_3$) 165.9 (C=O), 131.0 (C–1), 130.8 (q, *J* = 1.1 Hz, C–2), 130.8 (C–6), 129.6 (C–3), 129.1 (C–5), 127.6 (q, *J* = 1.1 Hz, C–4), 121.9 (q, *J* = 274.5 Hz, –CF_3), 52.5 (–OCH_3), 28.3 (q, *J* = 39.7 Hz, C–3'). δ_F (376 MHz, $CDCl_3$) -65.25 (–CF_3). Data agrees with that reported in Andrews et al.[150]

158. *3-[3'-(trifluoromethyl)-diazirin-3'-yl]benzoic acid*

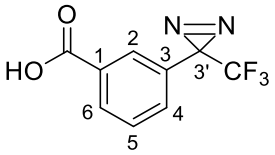

LiOH (0.067 g, 2.78 mmol, 4.00 eq) was added in portions to a solution of the *methyl 3-[3'-(trifluoromethyl)-diazirin-3'-yl]benzoate* (**170**) (0.170 g, 0.696 mmol, 1.00 eq) in a 1:1 mixture of Methanol and water (15 ml). The mixture was stirred at room temperature in the absence of ambient light for 16 hours after which it was quenched with 1M HCl (5 mL). Volatiles were evaporated and extraction was conducted with EtOAc (3 x 15 ml). The combined organic extracts were dried over MgSO4 and concentrated to yield the title compound as an amorphous white solid (0.152 g, 0.660 mmol, 95%). δ_H (400 MHz, $CDCl_3$) 8.20 (1H, d, *J* = 7.4 Hz, 6–H), 7.95 (1H, s, 2–H), 7.58 – 7.54 (2H, m, 5–H, 4–H). δ_C (101 MHz, $CDCl_3$) 171.0 (C=O), 131.7 (C–1), 131.4 (C–2), 130.0 (C–6), 129.9 (C–3), 129.3 (C–5), 128.2 (C–4), 121.8 (q, *J* = 272.3 Hz, –CF_3) , 28.3 (q, *J* = 39.3 Hz, C–3'). δ_F (376 MHz, $CDCl_3$) -65.18 (–CF_3). Data agrees with that reported in Andrews et al.[150]

178. *tert-butyl 3-bromobenzoate*

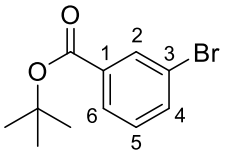

LiOH (5.57 g, 116.0 mmol, 5.00 eq) was added in portions to a solution of *methyl, 3-bromobenzoate* (**177**) (5.00 g, 23.2 mmol, 1.00 eq) dissolved in a 5:1 mixture of THF (150 mL) and water (30.0 mL) at room temperature. The reaction was allowed to stir at room temperature for 3 hours after which volatiles were evaporated. The remaining mixture was acidified to pH 1 using 3M HCl and the aqueous layer was extracted with EtOAc (3 x 30 ml). The combined organic layers were dried over $MgSO_4$ and concentrated to give crude 3-bromobenzoic acid as a white solid. The solid was dissolved in THF (75 ml) and DMAP (0.57 g, 4.65 mmol, 0.10 eq), followed by the dropwise

addition of a solution of Boc_2O (25.37 g, 116 mmol, 2.50 eq) in THF (75 ml). Upon completion of addition, the reaction mixture was stirred and heated under reflux for a further 4 hours and was quenched with ice water (40 ml). The layers were separated, and the aqueous fraction was extracted with Et_2O. (3 x 30 ml). The combined organic layers were dried over $MgSO_4$, concentrated and purified by column chromatography (EtOAc in Hex, 0-5%) to yield the title compound as a colourless oil (4.27 g, 16.6 mmol, 71%). δ_H (400 MHz, $CDCl_3$) 8.11 (1H, td, *J* = 1.8, 0.5 Hz, 2–H), 7.92 (1H, ddd, *J* = 8.0, 1.8, 1.1 Hz, 6–H), 7.64 (1H, ddd, *J* = 8.0, 1.8, 1.1 Hz, 4–H), 7.29 (1H td, *J* = 8.0, 0.5 Hz, 5–H), 1.59 (9H, s, –*tBu*). δ_C (101 MHz, $CDCl_3$) 164.4 (*C*=O), 135.9 (C–2), 134.0 (C–1), 132.5 (C–4), 130.3 (C–5), 128.6 (C–6), 122.3 (C–3), 82.6 (–*C*(CH_3)), 28.2 (–C(*C*H_3)). ν_{max} (ATR) 2984 (C–H), 1719 (C=O), 1369, 1300, 1254, 1162, 1123, 744 cm^{-1}. *m/z* (GC-MS, EI^+) 256.1 ([M+H (^{79}Br)]$^+$, 11), 258.1 ([M+H (^{81}Br)]$^+$, 11), 183.0 ([M-OtBu (^{79}Br)]$^+$, 39), 185.0 ([M-OtBu (^{79}Br)]$^+$, 41). Data agrees with that reported in La *et al*.[151]

179. *tert-butyl 3-bromo-5-hydroxybenzoate*

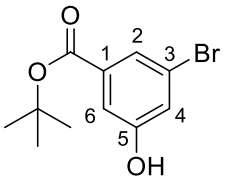

A sealed microwave vial was charged with *tert-butyl 3-bromobenzoate* (**178**) (2.00 g, 7.78 mmol, 1.00 eq) and subjected to three N_2 purge/refill cycles. A separate Schlenk tube was charged with B_2Pin_2 (2.37 g, 9.33 mmol, 1.20 eq), $[Ir(COD)(OMe)]_2$ (0.077 g, 0.117 mmol, 0.015 eq) and dtbpy (0.063 g, 0.233 mmol, 0.030 eq) and also subjected to 3 N_2 purge/refill cycles. To this, degassed MTBE (8 ml) was added, leading to a black solution. The catalyst cocktail was transferred to the sealed reaction vial and was monitored via GC-MS. Following the completion of the reaction, volatiles were evaporated, and the resulting crude product was redissolved in a 1:1 mixture of acetone and water (50 ml). Oxone (9.56 g, 15.6 mmol, 2.00 eq) was added and the reaction was allowed to stir at room temperature for 20 minutes. The reaction was quenched with sat. $NaS_2O_{3(aq)}$, concentrated and the resulting aqueous mixture was extracted with DCM (3 x 30 ml). The combined organic layers were washed with brine (3 x 10 ml), dried over $MgSO_4$, concentrated and purified by column chromatography (EtOAc in Hex, 0-45%) to yield the title compound as light yellow oil which upon drying at reduced pressure solidified into an off white amorphous solid. (1.87 g, 6.85 mmol, 88%). δ_H (700 MHz, $CDCl_3$) 7.64 (1H, t, *J* = 1.6 Hz, 2–H), 7.55 (1H, dd, *J* = 2.4, 1.6 Hz, 6–H), 7.22 (1H. dd, *J* = 2.4, 1.6 Hz, 4–H), 6.76 (1H, s, –O*H*), 1.59 (9H, s, –C(CH_3)$_3$). δ_C (176 MHz, $CDCl_3$) 165.0 (C=O), 157.0 (C–5), 133.8 (C–1), 124.6 (C–2), 123.1 (C–3), 122.7 (C–4), 115.6 (C–6), 82.6 (–*C*(CH_3)$_3$), 28.1 (–C(*C*H_3)$_3$). ν_{max} (ATR) 3443 (O–H), 2990, 1696 (C=O), 1598, 1455, 1375, 1306, 1157, 974, 762 cm^{-1}. *m/z* (LC-MS, ESI^-)

271.245 ([M–H (^{79}Br)]$^-$, 100), 273.222 ([M–H (^{81}Br)]$^-$, 96). Accurate mass (ES–) found [M-H (^{79}Br)]$^-$ 270.9963, $C_{11}H_{12}O_3{}^{79}Br$ requires *M* 270.9970.

180. *tert-Butyl 3-bromo-5-{[5'-(trimethylsilyl)pent-4'-yn-1'-yl]oxy}benzoate*

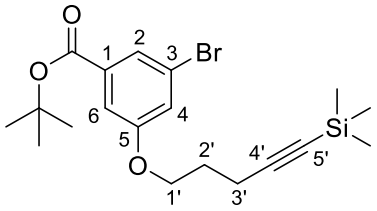

Cs_2CO_3 (7.16 g, 22.0 mmol, 4.00 eq) was added in portions to a solution of tert-butyl 3-bromo-5-hydroxybenzoate (1.50 g, 5.49 mmol, 1.00 eq) and TBAI (0.200 g, 0.549 mmol, 0.100 eq) in MeCN (18.0 mL). (5-chloropent-1-yn-1-yl)trimethylsilane (1.92 g, 11.0 mmol, 2.00 eq) was then added dropwise and the reaction mixture was stirred and heated under reflux for 16 hours. The reaction was quenched with sat. $NaHCO_{3\,(aq)}$ (20 ml) and concentrated before the resulting aqueous solution was extracetd with Et_2O (3 x 20 ml). The combined organic layers were dried over $MgSO_4$, concentrated and purified by column chromatography (EtOAc in Hex, 0-15%) followed by reverse phase chromatography (MeCN in H_2O, 0-100%) to yield the title compound as a colourless oil (1.37 g, 3.33 mmol, 61%). δ_H (599 MHz, $CDCl_3$) 7.68 (1H, t, *J* = 1.6 Hz, 2–H), 7.44 (1H, dd, *J* = 2.5, 1.6 Hz, 6–H), 7.21 (1H, dd, *J* = 2.5, 1.6 Hz, 4–H), 4.08 (2H, t, *J* = 6.1 Hz, 1'–H_2), 2.43 (2H, t, *J* = 7.0 Hz, 3'–H_2), 2.02 – 1.95 (2H, m, 2'–H_2), 1.58 (9H, s, –C(CH_3)$_3$), 0.14 (9H, s, –*TMS*). δ_C (151 MHz, $CDCl_3$) 164.24 (C=O), 160.0 (C–5), 134.6 (C-1), 125.7 (C-2), 122.5 (C-3), 121.9 (C-4), 114.7 (C-6), 105.8 (C-5'), 85.4 (C-4'), 81.8 (–*C*(CH_3)$_3$, 66.8 (C–1'), 28.1 (–C(*C*H_3)$_3$), 28.1 (C–2') 16.49 (C–3'), -0.12 (–Si(*C*H_3)$_3$). ν_{max} (ATR) 2968, 2182, 1719 (C=O), 1581, 1289, 1254, 1169, 1054, 848, 763 cm^{-1}. m/z (LC-MS, ESI$^+$) 334.369 [M–Br+H]$^+$. Accurate mass (ES+) found [M–*tbu*+2H (^{79}Br)]$^+$ 355.0347, $C_{15}H_{20}O_3{}^{79}BrSi$ requires *M* 355.0365.

183. *(5-chloropent-1-yn-1-yl)tris(propan-2'-yl)silane*

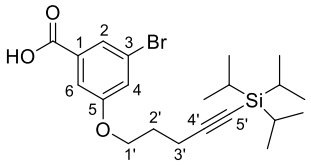

nBuLi (6.1 mL, 0.015 mol, 1.05 eq) was added to a solution of *1-chloropent-4-yne* (**182**) (1.50 g, 0.015 mol, 1.00 eq) in THF (20.0 mL) at -78 °C under nitrogen. After stirring at -78 °C for 30 minutes, a solution of TIPS-Cl (4.1 mL, 0.019 mol, 1.30 eq) in THF (5 ml) was added dropwise over 30 minutes. Upon completion of addition, the reaction mixture was allowed to reach ambient temperature and stirred for a further 2 hours. The reaction was quenched with sat. $NH_4Cl_{(aq)}$ (15 ml), separated and the resulting

aqueous fraction extracted with Et_2O (3 x 20 ml). The combined organic layers were dried over $MgSO_4$, concentrated and purified by column chromatography ($CHCl_3$ in Hexane, 0-2%) to yield the title compound as a colourless oil (3.11 g, 0.012 mol, 82%). δ_H (599 MHz, $CDCl_3$) 3.68 (2H, t, J = 6.4 Hz, 5–H_2), 2.45 (2H, t, J = 6.7 Hz, 3–H_2), 1.98 (2H, tt, J = 6.7, 6.4 Hz, 4–H_2), 1.16 – 0.92 (21H, m, *–iPr*). δ_C (151 MHz, $CDCl_3$) 106.9 (C–1), 81.7 (C–2), 43.7 (C–5), 31.7 (C–3), 20.4 (C–2'), 17.5 (C–4), 11.6 (C–1',C–3'). ν_{max} (ATR) 2944, 2869, 2176, 1462, 1290, 1039, 997, 884, 659 cm^{-1}. m/z (ASAP) 258.124 ([M+H(^{35}Cl)]$^+$, 100), 260.143 ([M+H(^{37}Cl)]$^+$, 32). Accurate mass (ES+) found [M+H(^{35}Cl)] 258.1440, $C_{14}H_{27}{}^{35}ClSi$ requires *M* 285.1571.

185. *methyl 3-bromo-5-({5'-[tris(propan-2''-yl)silyl]pent-4'-yn-1'-yl}oxy)benzoate*

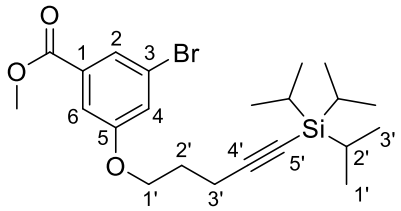

A vial was charged with $[Ir(cod)(OMe)]_2$ (92.5 mg, 0.140 mmol, 0.015 eq), dtbpy (74.9 mg, 0.279 mmol, 0.030 eq), B2Pin2 (2834.1 mg, 11.160 mmol, 1.20 eq) and methyl, *3-bromobenzoate* (**177**) (2000.0 mg, 9.300 mmol, 1.00 eq), sealed and subjected to 3 N_2 purge/refill cycles. To the sealed vial, degassed MTBE (9.3 mL) was added and the reaction mixture was allowed to stir at room temperature for 16 hoursrt. Upon completion, the crude boronate ester was obtained following the evaporation of volatiles. The resulting mixture was then redissolved in a 1:1 mixture of acetone and water (20 ml) and oxone (1715.3 mg, 2.790 mmol, 0.30 eq) was added. The reaction was monitored by TLC and when completed was quenched with sat. Na_2SO_3 solution (10 ml). Volatiles were evaporated and the resulting aqueous mixture was basified to pH 10 using 0.1M NaOH solution. The aqueous layer was washed with EtOAc (3 x 20 mL) and was neutralised using 0.1M HCl. Organic extraction was conducted using EtOAc (3 x 25 ml). The combined organic extracts were dried over $MgSO_4$ and concentrated to yield crude phenol (**184**) as a brown oil (1.81g). m/z (LC-MS ESI+) 231.115 ([M+H(^{79}Br)]$^+$, 13.5), 233.125 ([M+H(^{81}Br)]$^+$, 13.9).

K_2CO_3 (5.38 g, 39.0 mmol, 6.00 eq) was added in portions to a solution of the crude phenol and TBAI (0.240 g, 0.649 mmol, 0.100 eq) in MeCN (21.6 mL). *(5-chloropent-1-yn-1-yl)triisopropylsilane* (**183**) (2.52 g, 9.74 mmol, 1.50 eq) was then added dropwise and the reaction mixture was stirred and heated under reflux for 54 hours. The reaction was monitored by TLC and upon complete consumption of the starting phenol, volatiles were evaporated and the resulting residue was redissolved in 0.1M NaOH (25ml). The aqueous mixture was extracted with EtOAc (3 x 15 ml). The combined organic layers were dried over $MgSO_4$, concentrated and purified by column chromatography (EtOAc in Hex, 0-15%) to yield the title compound as a colourless oil (2.14 g, 5.21 mmol, 80%). δ_H (599 MHz, $CDCl_3$)

7.75 (1H t, *J* = 1.4 Hz, 2–H), 7.48 (1H, dd, *J* = 2.5, 1.4 Hz, 6–H), 7.23 (1H, dd, *J* = 2.5, 1.4 Hz, 4–H), 4.13 (2H t, *J* = 6.1 Hz, 1'–H_2), 3.91 (3H, s, –OCH_3), 2.47 (t, *J* = 6.9 Hz, 3'–H_2), 2.00 (2H, tt, *J* = 6.9, 6.1 Hz, 2'–H_2), 1.09 – 0.96 (21H, m, *–iPr*). δ_C (151 MHz, $CDCl_3$) 165.7 (C=O), 158.8 (C–5), 132.6 (C–1), 124.9 (C–2), 122.7 (C–3), 122.5 (C–4), 114.2 (C–6), 107.6 (C–5'), 81.4 (C–4'), 67.4 (C–1'), 52.4 (–O*C*H_3), 28.2 (C–2'), 18.7 (–Si*C*$(CH_3)_2$, 16.5 (C–3'), 11.4 (–SiC(*C*$H_3)_2$. *m/z* (ASAP) 453.138 ([M(^{79}Br)+H]$^+$, 100), 455.138 ([M(^{81}Br)+H]$^+$, 98), 411.101 ([M–3(CH_3)(^{79}Br)]$^+$, 53), 413.100 ([M–3(CH_3)(^{81}Br)]$^+$, 53) Accurate mass (ASAP+) found [M+H (^{79}Br)]$^+$ 453.1466, $C_{22}H_{34}O_3{}^{79}$BrSi requires *M* 453.1461.

186. *3-bromo-5-{[5'-(triisopropylsilyl)pent-4'-yn-1'-yl]oxy}benzoic acid*

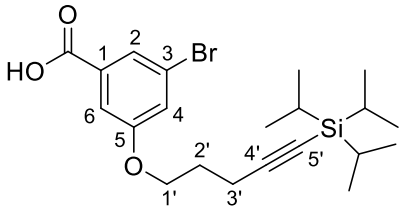

To a solution of the *methyl 3-bromo-5-{[5'-(triisopropylsilyl)pent-4'-yn-1'-yl]oxy}benzoate* (**185**) (2.50 g, 0.006 mol, 1.00 eq) dissolved in a 5:1 mixture of THF and water (42 ml), LiOH (0.660 g, 0.028 mol, 5.00 eq) was added in portions. The reaction was allowed to stir at room temperature for 3 hours after which following evaporation of volatiles, the remaining aqueous mixture was redissolved in 0.1M HCl (30 ml). Organic extraction was conducted with EtOAc (3 x 25 ml) and the combined organic fractions were dried over $MgSO_4$ and concentrated to yield the title compound as a white solid (2.42 g, 0.006 mol, 100%). δ_H (599 MHz, MeOD) 7.68 (1H, t, *J* = 1.5 Hz, 2–H), 7.49 (1H, dd, *J* = 2.1, 1.5 Hz, 6–H), 7.29 (1H, t, *J* = 2.1 Hz, 4–H), 4.17 (2H, t, *J* = 6.5 Hz, 1'–H_2), 2.48 (2H, t, *J* = 6.5 Hz, 3'–H), 1.97 (2H, p, *J* = 6.5 Hz, 2'–H_2), 1.09 – 0.83 (21H, m, *–iPr*). δ_C (151 MHz, MeOD) 166.7 (C=O), 159.9 (C–5), 133.6 (C–1), 124.4 (C–2), 122.6 (C–3), 121.8 (C–4), 114.1 (C–6), 107.5 (C–5'), 80.6 (C–4'), 66.6 (C–1'), 27.7 (C–2'), 17.6 (–CH(*C*$H_3)_2$), 15.6 (C–3'), 11.0 (–*C*H$(CH_3)_2$). ν_{max} (ATR) 3271 (O–H), 2939, 2861, 2170, 1691 (C=O), 1574, 1461, 1418, 1294, 1052, 1002 cm^{-1}. m/z (LC-MS, ESI$^-$) 437.400 [M(^{79}Br)–H]$^-$, 479.378 [M(^{81}Br)–H]$^-$. Accurate mass (ES–) found [M–H (^{79}Br)]$^-$ 437.1145, $C_{21}H_{30}O_3{}^{79}$BrSi requires *M* 437.1148.

188. *methyl 5-(pent-4-yn-1-yloxy)-3-(2'',2'',2''- trifluoro-1''-(hydroxyimino)ethyl)benzoate*

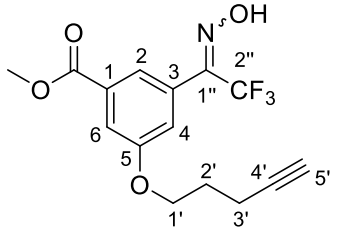

Bu_2Mg (7.7 mL, 3.846 mmol, 0.52 eq) was added dropwise to *3-bromo-5-{[5'-(triisopropylsilyl)pent-4'-yn-1'-yl]oxy}benzoic acid* (**186**) (3.250 g, 7.395 mmol, 1.00 eq) in THF (37.0 mL) at –40 °C. Upon the formation of a white precipitate, nBuLi (3.3 mL, 8.135 mmol, 1.100 eq) was added at this condition and the mixture was stirred for a further 30 minutes. $EtOOCCF_3$ (1.8 mL, 14.791 mmol, 2.00 eq) was then added and the reaction mixture was allowed to reach ambient temperature where it was stirred for a further 2 hours. The mixture was quenched with sat. $NH_4Cl_{(aq)}$ (20 ml) and extraction was conducted with EtOAc (3 x 20 ml). The combined organic layers were washed with 1M HCl (3 x 35 ml) dried over $MgSO_4$ and concentrated to yield crude trifluromethyl ketone **186** as a bright yellow oil (2.960 g) which was used without further purification. m/z (LC-MS, ESI^-) 455.569 $[M–H]^-$.

K_2CO_3 (4.843 g, 0.035 mol, 4.00 eq) was added in portions to a solution of the crude trifluoromethyl ketone (**186**) (2.96 g) in MeCN. After stirring at room temperature for 15 minutes, MeI (2.2 mL, 0.035 mol, 4.00 eq) was added and the mixture was stirred under reflux for 16 hours. Volatiles were then evaporated, the resulting mixture was dissolved in 0.1M NaOH (30 mL) and organic extraction was carried out with DCM (3 x 25 mL). The combined organic layers were dried over $MgSO_4$ and concentrated to yield the crude ester as a bright yellow oil (3.770 g) which was used without further purification. m/z (ASAP+) 471.569 $[M+H]^+$.

1M TBAF in THF (39.3 ml) was added dropwise to a sealed flask containing the crude ester (3.77 g). The mixture was allowed to stir at room temperature for 2 hours. Upon completion of the reaction, volatiles were evaporated and the resulting mixture was redissolved in $CHCl_3$ (30 ml) and washed with 1M $NaHCO_3$ (3 x 25 ml). The organic layer was then dried over MgSO4 and concentrated to yield crude deprotected alkyne **187** as a bright yellow oil (1.930 g) which was used without further purification. m/z (LC-MS, ESI^+) 315.356 $[M+H]^+$.

Hydroxylamine·HCl (0.884 g, 12.728 mmol, 4.00 eq) was added in portions to a solution of the deprotected alkyne (**187**) (1.93 g) in pyridine (8.0 mL). The reaction was allowed to stir at 70 °C for 3 hours after which volatiles were evaporated. The resulting residue was taken up in EtOAc (25 ml) and washed with 0.01M HCl (3 x 15 ml) and water (3 x 15 ml). The organic layer was dried over $MgSO_4$ and concentrated. Purification was achieved through column chromatography (EtOAc in Hex, 0-60%) to yield the title compound as a mixture of cis-trans isomers as a white amorphous solid (0.606 g, 1.840 mmol, 25% (over 4 steps). δ_H (599 MHz, MeOD) 7.72 – 7.59 (2H, m, 2–H, 6–H)), 7.25 – 7.24 (1H, m, 4–H), 4.17 – 4.14 (2H, m, 1'–H_2), 3.92 (3H, m, –OCH_3), 2.42 – 2.38 (2H, m 2'–H_2), 2.27 – 2.25 (1H, m, 5'–H), 2.05 – 1.92 (2H, m, 3'–H_2). δ_C (151 MHz, MeOD) 166.1 (C–5), 166.1 (C=O), 159.0 (C=O), 144.5 (q, J = 33.1 Hz, C–2''), 144.3 (q, J = 30.4 Hz, C–2''), 132.6 (C–1), 131.5 q, J = 15.4 Hz, C–3), 121.5 (C–2), 121.2 (C–2), 121.0 (q, J = 274.0 Hz, C–2''), 119.6 (C–4), 118.9 (C–4), 118.7 (q, J = 282.3 Hz, C–2''), 115.9 (C–6), 115.6 (C–6), 82.5 (C–4'), 68.7 (C–5'), 68.7 (C–5'), 66.5 (C–1'), 66.5 (C–1'),

51.5 (–O*C*H$_3$), 51.5 (–O*C*H$_{3b}$), 27.8 (C–3'), 14.3 (C–2'), 14.3 (C–2'). δ_F (376 MHz, MeOD) -63.82 (2''–F), -67.57 (2''–F). ν_{max} (ATR) 3289 (O–H), 2956, 1701 (C=O), 1595, 1461, 1432, 1290, 1131, 974 cm^{-1}. m/z (LC-MS, ESI$^+$) 330.250 $[M+H]^+$, 352.588 $[M+Na]^+$. Accurate mass (ES+) found $[M+H]^+$ 330.0955, $C_{15}H_{15}O_4NF_3$ requires *M* 330.0953.

190. *methyl 5-(pent-4'-yn-1'-yloxy)-3-[3''-(trifluoromethyl)diaziridin-3''-yl]benzoate*

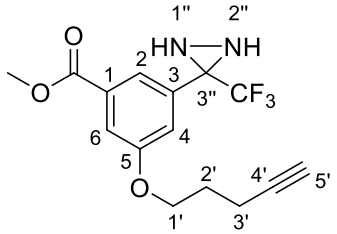

TsCl (0.130 g, 0.683 mmol, 1.500 eq) was added in portions to a solution of *methyl 5-(pent-4-yn-1-yloxy)-3-(2'',2'',2''- trifluoro-1''-(hydroxyimino)ethyl)benzoate* (**188**) (0.150 g, 0.456 mmol, 1.00 eq) in pyridine (4.6 mL). The mixture was allowed to stir at 60 °C for 4 hours after which volatiles were evaporated to afford the crude oxime tosylate (**189**). Without further purification, the resulting residue was taken up in EtO_2 (4.6 mL) and sealed in a thick-walled vial. In a separate flask containing NaOH (10.00 g) and NH_4Cl (10.00 g), water was added dropwise. The evolved gas was passed through a drying tube and collected into another thick-walled vial cooled to –78 °C and sealed. The condensed ammonia (1 mL) was then transferred via canula to the vial containing the oxime tosylate and the reaction mixture was allowed to reach ambient temperature and stirred for 3 hours. The mixture was then cooled to –78 °C and the vial unsealed. The vial was then allowed to reach ambient temperature to allow excess ammonia to evaporate and quenched with water (3 ml). The remaining volatiles were evaporated and the resulting aqueous mixture was extracted with DCM (3 x 5 mL). The combined organic layers were dried over $MgSO_4$ and concentrated. Purification was achieved through column chromatography (EtOAc in Hex, 0-30%) to yield the title compound as a white amorphous solid (0.103 g, 0.314 mmol, 69%). δ_H (599 MHz, $CDCl_3$) 7.86 (1H, d, *J* = 1.4 Hz, 2–H), 7.63 (1H, dd, *J* = 2.1, 1.4 Hz, 6–H), 7.35 (1H, d, *J* = 2.1 Hz, 4–H), 4.13 (2H, t, *J* = 6.9 Hz, 1'–H_2), 3.92 (3H, s, –OC*H*$_3$), 2.81 (1H, m, N–H), 2.41 – 2.40 (2H, m, 2'–H_2), 2.24 (1H, m, N–*H*), 2.05 – 1.99 (2H, m, 3'–H_2), 1.97 (1H, t, *J* = 2.6 Hz, 5'–H). δ_C (151 MHz, $CDCl_3$) 166.0 (C–5), 159.1 (C=O), 133.4 (C–1), 132.2 (C–3), 123.3 (q, *J* = 278.3 Hz, –CF_3), 121.4 (C–2), 119.4 (C–4), 116.5 (C–6), 83.1 (C–4'), 69.1 (C–5'), 66.6 (C–1'), 57.8 (q, *J* = 36.1 Hz, C–3''), 52.4 (–O*C*H$_3$), 27.9 (C–3'), 15.1 (C–2'). δ_F (376 MHz, $CDCl_3$) -75.35. ν_{max} (ATR) 3261 (N–H), 2952, 1719 (C=O), 1559, 1432, 1326, 1283, 1216, 1149, 1059, 910 cm^{-1}. m/z (LC-MS, ESI$^+$) 329.319 $[M+H]^+$, 370.364 $[M+H+MeCN]^+$.

194. *1-(4-bromonaphthalen-1-yl)ethan-1'-one*

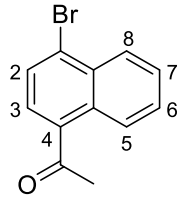

$AlCl_3$ (0.805 g, 6.04 mmol, 2.50 eq) was added in portions to a solution of 1-bromonaphthalene (**93**) (0.500g, 2.42 mmol, 1.00 eq) and acetyl chloride in DCE (24.1 mL). The mixture was left to stir at room temperature for 16 hours after which it was quenched by the addition of ice water. The organic layer was extracted with Et_2O (3 x 15 mL) and the combined organic extracts were dried over $MgSO_4$ and concentrated to yield the crude mixture as a brown oil (0.574 g, 2.30 mmol, 95%). δ_H (400 MHz, $CDCl_3$) 8.72 (1H, dd, *J* = 7.4, 3.2 Hz, 5–H), 8.40 – 8.29 (1H, m, 8–H), 7.83 (1H, d, *J* = 7.7 Hz, 3–H), 7.75 (1H, d, *J* = 7.7 Hz, 2–H), 7.66 – 7.63 (2H, m, 6–H, 7–H), 2.74 (3H, s, $–CH_3$). δ_C (101 MHz, $CDCl_3$) 201.3 (C=O), 135.4 (C–4), 132.4 (C–4a), 131.2 (C–8a), 128.8 (C–3), 128.7 (C–2), 128.4 (C–5), 128.3 (C–1), 127.9 (C–6), 127.6 (C–7), 126.44 (C–8), 30.2 ($–CH_3$). *m/z* (LC-MS, ESI^+) 249.166 ($[M(^{79}Br)+H]^+$, 82), 251.143 ($[M(^{81}Br)+H]^+$, 100). Data agrees with that reported in Wu *et al*.[152]

197. *4-[tris(propan-2'-yl)silyl]but-3-yn-1-ol*

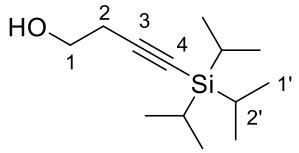

nBuLi (12.5 mL, 31.4 mmol, 2.10 eq) was added dropwise to a solution of but-3-yn-ol (**196**) (1.1 mL, 14.3 mmol, 1.00 eq) in THF (30 mL) at –78 °C. The mixture was stirred at this condition for 30 minutes after which TIPS-Cl (1.05 ml, 5.79 mmol, 2.1 eq) was added. The reaction was allowed to reach ambient temperature and stirred for a further 3 hours. The reaction mixture was quenched with sat. NH_4Cl solution (100 mL) and extracted with Et_2O (3 x 50 mL). The organic extracts were combined and concentrated to yield the crude protected alkyne. The resulting residue was taken up in THF and 3M HCl (126.6 mL, 379.7 mmol, 10.00 eq) was added. The mixture was stirred vigorously at room temperature for 16 hours after which volatiles were evaporated and the organic layer extracted with DCM (3 x 50 ml). Purification was achieved through column chromatography (EtOAc in Hex, 0-60%) to yield the title compound as a colourless oil (5.910 g, 26.10 mmol, 69%). δ_H (400 MHz, $CDCl_3$) 3.75 (2H, t, *J* = 6.2 Hz, 1–H_2), 2.56 (2H, t, *J* = 6.2 Hz, 2–H_2), 1.21 – 0.98 (21H, m, 1'–H_3, 2'–H). δ_C (101 MHz, $CDCl_3$) 104.9 (C–3), 83.1 (C–4), 61.2 (C–1), 24.4 (C–2), 18.6 (C–2'), 11.2 (C–1'). ν_{max} (ATR) 3261 (N–H), 2952, 1719 (C=O), 1559, 1432, 1326, 1283, 1216, 1149, 1059, 910 cm^{-1}. m/z ($ASAP^+$) 227.179 $[M+H]^+$. Data agrees with that reported in Tan *et al*.[153]

199. *Ethyl 2-({4'-[tris(propan-2''-yl)silyl]but-3'-yn-1'-yl}oxy)acetate*

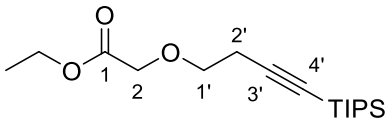

A suspension of NaH (1.06 g, 26.5 mmol, 1.20 eq) and TBAI (1.223 g, 3.31 mmol, 0.15 eq) in THF (20 mL) under N_2 was cooled to 0 °C and a solution of *4-[tris(propan-2'-yl)silyl]but-3-yn-1-ol* (**197**) (5.00 g, 22.08 mmol, 1.00 eq) in THF (25 mL) was added dropwise. The mixture was stirred at this condition for 30 minutes after which ethyl bromoacetate (3.7 mL, 33.12 mmol, 1.50 eq) was added dropwise. The mixture was allowed to reach ambient temperature and stirred for 4 hours after which it was diluted with THF (30 mL). The solution was left to settle, decanted, concentrated and purified by column chromatography (EtOAc in Hex, 0-20%) to yield the title compound as a light yellow oil (3.90 g, 12.5 mmol, 57%). δ_H (599 MHz, $CDCl_3$) 4.21 (2H, q, J = 7.1 Hz, –OCH_2CH$_3$), 4.12 (2H, s, 2–H$_2$), 3.68 (2H, t, J = 7.4 Hz, 1'–H$_2$), 2.58 (2H, t, J = 7.4 Hz, 2'–H$_2$), 1.27 (3H, t, J = 7.1 Hz, –OCH$_2$CH_3), 1.04 (21H, m, –(*iPr*)$_3$). δ_c (151 MHz, $CDCl_3$) 170.2 (C=O), 104.6 (C–3'), 81.9 (C–4'), 70.2 (C–1'), 68.4 (C–2), 60.9 (–O*C*H$_2$CH$_3$), 21.2 (C–2'), 18.6 (–CH(*C*H$_3$)$_2$), 14.2 (–OCH$_2$*C*H$_3$), 11.2 (–*C*H(CH$_3$)$_2$). ν_{max} (ATR) 2942, 2864, 2173, 1754, 1464, 1205, 1131, 907 cm^{-1}. *m/z* (LC-MS ESI+) 313.218 [M+H]$^+$. Accurate mass (ES+) found [M+H]$^+$ 285.1873, $C_{17}H_{33}O_3Si$ requires *M* 313.2177.

200. *2-({4'-[tris(propan-2''-yl)silyl]but-3'-yn-1'-yl}oxy)acetic acid*

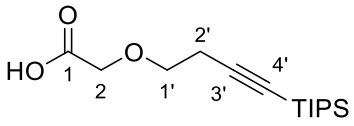

Ethyl 2-({4'-[tris(propan-2''-yl)silyl]but-3'-yn-1'-yl}oxy)acetate (**199**) (5.30 g, 16.7 mmol, 1.00 eq) was added to a solution of LiOH (2.03 g, 84.79 mmol, 5.00 eq) in a 5:1 mixture of THF:H_2O (200 mL). The mixture was stirred vigorously at room temperature for 16 hours after which it was quenched with 3M HCl (50 mL). Extraction was conducted with EtOAc (3 x 50 ml). The combined organic layers were dried over $MgSO_4$ and concentrated to yield the title compound as a white oil (4.43 g, 15.6 mmol, 92%). δ_H (599 MHz, $CDCl_3$) 4.17 (2H, s, 2–H$_2$), 3.72 (2H, t, J = 6.8 Hz, 1'–H$_2$), 2.60 (2H, t, J = 6.8 Hz, 2'–H$_2$), 1.06 (21H, m, –(*iPr*)$_3$). δ_C (151 MHz, $CDCl_3$) 172.8 (C=O), 104.3 (C–4'), 82.5 (C–3'), 70.3 (C–1'), 68.0 (C–1), 21.2 (C–2'), 18.5 (–CH(*C*H$_3$)$_2$), 11.1 (–*C*H(CH$_3$)$_2$). ν_{max} (ATR) 3229 (O–H, *b*) 2939, 2867, 2173, 1730, 1461, 1244, 1137, 907 cm^{-1}. *m/z* (ASAP+) 285.188 [M+H]$^+$. Accurate mass (ES+) found [M+H]$^+$ 285.1873, $C_{15}H_{29}O_3Si$ requires *M* 285.1886.

203. *(4-bromonaphthalen-1-yl)trimethylsilane*

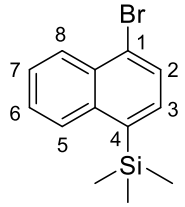

nBuLi (1.4 mL, 3.50 mmol, 1.00 eq) was added to a solution of the 1,4-dibromonaphthalene (**202**) (1.000 g, 3.50 mmol, 1.00 eq) in THF (7.0 mL) under N_2 at –78 °C. The mixture was allowed to stir at this condition for 30 minutes after which $SiMe_3Cl$ (0.888 mL, 6.94 mmol, 2.00 eq) was added. The mixture was then allowed to reach ambient temperature and stirred for a further 3 hours. The reaction mixture was quenched with sat NH_4Cl solution (15 mL) and extracted with EtO_2 (3 x 25 mL). The combined organic extracts were dried over MgSO4 and concentrated. Purification was achieved by column chromatography (EtOAc in Hex, 0-10%) to yield the title compound as a light grey amorphous solid (0.874 g, 3.13 mmol, 90%). δ_H (599 MHz, $CDCl_3$) 8.41 – 8.25 (1H, m, 8–H), 8.17 – 8.01 (1H, m, 5–H), 7.75 (1H, d, J = 7.4 Hz, 2–H), 7.60 – 7.53 (2H, m, 6–H, 7–H), 7.49 (1H, d, J = 7.4 Hz, 3–H), 0.46 (9H, s, –Si(CH_3)$_3$). δ_C (151 MHz, $CDCl_3$) 138.5 (C–8a), 138.1 (C–1), 133.3 (C–3), 131.8 (C–4a), 129.3 (C–2), 128.5 (C–5), 128.1 (C–8), 126.7 (C–6), 126.4 (C–7), 125.2 (C–4a), 0.16 (–Si(*C*H_3)$_3$). ν_{max} (ATR) 3073, 2952, 1503,m 1254, 872 cm^{-1}. *m/z* (ASAP+) 285.188 [M(^{79}Br)+H]$^+$, [M(^{81}Br)+H]$^+$. Accurate mass (ES+) found [M(^{79}Br)+H]$^+$ 278.0131, $C_{13}H_{15}Si^{79}Br$ requires *M* 278.0126. Data agrees with that reported in Offner *et al*.[113]

204. *N-methoxy-N-methyl-2-({4'-[tris(propan-2''-yl)silyl]but-3'-yn-1'-yl}oxy)acetamide*

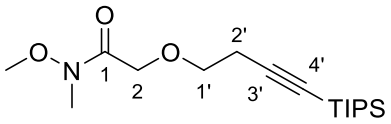

N,O-Dimethylhydroxylamine (0.257 g, 2.64 mmol, 1.50 eq) was added to a solution of DMAP (0.043 g, 0.35 mmol, 0.20 eq), *2-({4'-[tris(propan-2''-yl)silyl]but-3'-yn-1'-yl}oxy)acetic acid* (**200**) (0.500 g, 1.75 mmol, 1.00 eq), triethylamine (0.934 mL, 7.031 mmol, 4.00 eq) and DCC (0.544 g, 2.64 mmol, 1.50 eq) in DCM (7.0 mL). The reaction mixture was left to stir at room temperature for 24 hours until the formation of a precipitate. The mixture was then filtered and concentrated. Purification was achieved by column chromatography (EtOAc in Hex, 0-55%) to yield the title compound as a light brown oil (0.414 g, 1.264 mmol, 72%). δ_H (599 MHz, $CDCl_3$) 4.32 (2H, s, 2–H_2), 3.71 (2H, t, J = 7.5 Hz, 1'–H_2), 3.68 (3H, s, –OCH_3), 3.19 (3H, s, –NCH_3), 2.61 (2H, t, J = 7.5 Hz, 2'–H_2), 1.05 (21H, m, –(*iPr*)$_3$). δ_C (151 MHz, $CDCl_3$) 171.1 (C=O), 110.2 (C–4'), 104.8 (C–3'), 81.7 (C–1'), 70.3 (–OCH_3), 68.4 (C–2), 61.4 (–NCH_3), 21.2 (C–2'), 18.6 (–CH(*C*H_3)$_2$), 11.2 (–*C*H(CH$_3$)$_2$). ν_{max} (ATR) 2942, 2864, 2173,

1683 (C=O), 1464, 1144, 992 cm^{-1}. *m/z* (ASAP+) 328.230 $[M+H]^+$. Accurate mass (ES+) found $[M+H]^+$ 328.2294, $C_{17}H_{34}NO_3Si$ requires *M* 328.2308.

209. *4-(4'-bromonaphthalen-1'-yl)-4-oxobutyl acetate*

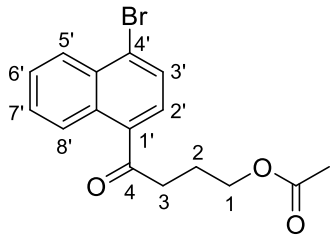

n-BuLi (6.6 mL, 16.61 mmol, 0.95 eq) was added dropwise to a solution of 1,4-dibromonaphthalene (**202**) in THF (35.0 mL) at –78 °C. After stirring at 10 minutes at this condition, γ-butyrolactone (**206**) (4.0 mL, 52.45 mmol, 3.00 eq) was added and the mixture was allowed to reach ambient temperature and stirred for a further 4 hours. The reaction was quenched with sat. $NH_4Cl_{(aq)}$ solution. Extraction of the organic layer was conducted with EtOAc (3 x 30 ml) and the combined organic extracts were dried over $MgSO_4$ and concentrated to give the intermediary alcohol as a mixture. The light-yellow oil was used in subsequent steps without further purification. ν_{max} (ATR) 3403 (O–H), 2954, 2927, 2863, 1711 (C=O), 1216, 1056, 752 cm^{-1}. *m/z* (LC-MS, ESI^+) 293.329 ($[M+H(^{79}Br)]^+$, 27), 295.267 ($[M+H(^{81}Br)]^+$, 43).

AcCl was added dropwise to a solution of alcohol **208** (5.00 g, 17.06 mmol, 1.00 eq) and triethylamine (3.4 mL, 25.58 mmol, 1.50 eq) in DCM (85.3 mL) at 0 °C. Upon completion of addition, the mixture was allowed to reach ambient temperature and stirred for 16 hours. The reaction mixture was quenched with sat. $NaHCO_{3(aq)}$ and extracted with DCM (3 x 20 ml). The combined organic extracts were dried over $MgSO_4$ and concentrated. Purification was achieved through column chromatography (EtOAc in Hex, 0-25%) to yield the title compound as an off-white amorphous solid (1.887 g, 5.630 mmol, 33.0%). δ_H (400 MHz, $CDCl_3$) 8.55 (1H, m, 2'–H), 8.39 – 8.26 (1H, m, 3'–H), 7.84 (1H, d, *J* = 7.8 Hz, 8'–H), 7.73 – 7.57 (3H. m, 5'–H, 7'–H, 6'–H), 4.20 (2H, t, *J* = 6.3 Hz, 1–H_2), 3.13 (2H, t, *J* = 7.2 Hz, 3–H_2), 2.16 (2H, tt, *J* = 7.2, 6.3 Hz, 2–H_2), 2.04 (3H, s, –CH_3). δ_C (101 MHz, $CDCl_3$) 202.8 (–ArC=O), 171.1 (C=O), 135.9 (C–1'), 132.4 (C–8a'), 131.2 (C–4a'), 128.7 (C–2', C–3'), 128.0 (C–8', C–4'), 127.7 (C–5'), 127.2 (C–7'), 126.2 (C–6'), 63.7 (–*C*H_3), 38.6 (C–1), 23.5 (C–3), 21.0 (C–2). *m/z* (LC-MS, ESI^+) 335.252 ($[M+H(^{79}Br)]^+$, 14), 337.267 ($[M+H(^{81}Br)]^+$, 18).

210. *3-[2-(4-bromonaphthalen-1-yl)-1,3-dioxolan-2-yl]propan-1-ol*

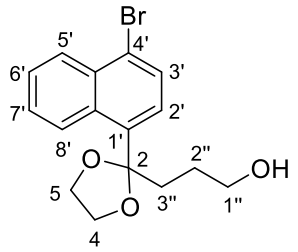

Ethylene glycol (2.9 mL, 52.21 mmol, 5.00 eq) was added to a solution of the starting *4-(4'-bromonaphthalen-1'-yl)-4-oxobutyl acetate* (**209**) (3.50 g, 10.44 mmol, 1.00 eq) and TsOH (0.01 g, 0.522 mmol, 0.05 eq) in Toluene (52.2 mL). The mixture was stirred under reflux for 8 hours using a Dean-Stark trap. Upon completion, the volatiles were evaporated and the resulting mixture was taken up in 1M $NaHCO_3$ solution (25 ml) and extracted with DCM (3 x 30 ml). The combined organic extracts were dried over $MgSO_4$ to yield crude *3-[2-(4'-bromonaphthalen-1'-yl)-1,3-dioxolan-2-yl]propyl acetate* as a light yellow oil which was used without further purification. *m/z* (LC-MS, ESI^+) 379.347 ($[M+H\ (^{79}Br)]^+$, 78), 381.323 ($[M+H\ (^{81}Br)]^+$, 80). Accurate mass (ES+) found $[M+H]^+$ 379.0550, $C_{18}H_{20}O_4{}^{79}Br$ requires *M* 328.2308.

NaOH (0.888 g, 15.82 mmol, 2.00 eq) was added in portions to a solution of the crude acetate in Methanol and water (1:1, 70 ml). The reaction mixture was allowed to stir at room temperature for 1 hour after which volatiles were evaporated and extraction was conducted with DCM (3 x 25ml). The combined organic extracts were dried over MgSO4 and concentrated. Purification was achieved through column chromatography (EtOAc in Hex, 0-75%) to yield the title compound as a light yellow oil (1.447 g, 4.291 mmol, 54%). δ_H (400 MHz, $CDCl_3$) 8.65 (1H, d, *J* = 8.1 Hz, 2'–H), 8.32 (1H, d, *J* = 8.1 Hz, 3'–H), 7.76 (1H, d, *J* = 7.9 Hz, 8'–H), 7.59 (3H, m, 5'–H, 7'–H, 6'–H), 4.21 – 3.78 (4H, m, 4–H_2, 5–H_2), 3.68 (2H, t, *J* = 6.2 Hz, 1''–H_2), 3.46 (2H, t, *J* = 9.7 Hz, 3''–H), 2.25 (2H, tt, *J* = 9.7, 6.2 Hz, 2''–H). δ_C (101 MHz, $CDCl_3$) 137.7 (C–1'), 132.7 (C–8a'), 131.8 (C–4a'), 129.0 (C–2'), 127.8 (C–3'), 126.9 (C–8'), 126.7 (C–4'), 126.6 (C–5'), 125.0 (C–7'), 123.9 (C–4'), 110.9 (C–6'), 71.6 (C–4) 70.9 (C–5), 64.5 (C–2), 61.8 (C–1''), 36.4 (C–3''), 24.1 (C–2''). *m/z* (LC-MS, ESI^+) 337.300 ($[M+H\ (^{79}Br)]^+$, 33), 339.314 ($[M+H\ (^{81}Br)]^+$, 31). Accurate mass (ES+) found $[M+H]^+$ 337.0437, $C_{16}H_{18}O_3{}^{79}Br$ requires *M* 337.0439.

Volume I Bibliography:

1. Kodadek, L. B. and T. Target Identification Overview in Chemical Genetics: The (Often) Missing Link. *Artif. Intell. Med.* **11**, ARTMED1118 (2010).

2. Kwok, Trevor C.Y., Ricker, Nicole, Fraser, Regina Chan, Allen W. Burns, Andrew Stanley, Elise F. McCourt, Peter Cutler, Sean R. Roy, Peter J. A small-molecule screen in C. elegans yields a new calcium channel antagonist. *Nature* **441**, 91–95 (2006).

3. Antoni, Regina Gonzalez-Guzman, Miguel Rodriguez, Lesia Peirats-Llobet, Marta Pizzio, Gaston A. Fernandez, Maria A. De Winne, Nancy De Jaeger, Geert Dietrich, Daniela Bennett, Malcom J. Rodriguez, Pedro L. PYRABACTIN RESISTANCE1-LIKE8 plays an important role for the regulation of abscisic acid signaling in root. *Plant Physiol.* **161**, 931–941 (2013).

4. Serrano, M., Kombrink, E. & Meesters, C. Considerations for designing chemical screening strategies in plant biology. *Front. Plant Sci.* **6**, 1–19 (2015).

5. Tóth, R. R. A. L. van der H. Emerging principles in plant chemical genetics. *Trends Plant Sci.* **15**, 81–88 (2009).

6. McCourt, P. & Desveaux, D. Plant chemical genetics. *New Phytol.* **185**, 15–26 (2010).

7. Ares, J. M. B., Ďurañ-Pena, M. J., Hernández-Galán, R. & Collado, I. G. Chemical genetics strategies for identification of molecular targets. *Phytochem. Rev.* **12**, 895–914 (2013).

8. Castoreno AB, E. U. Small molecule probes of cellular pathways and networks. *ACS Chem Bio* **6**, 86–94 (2011).

9. Altmann, Karl Heinz, Buchner, Johannes, Kessler, Horst, Diederich, François, Kräutler, Bernhard, Lippard, Stephen J., Liskamp, Rob, Müller, Klaus, Nolan, Elizabeth M., Samorì, Bruno, Schneider, Gisbert, Schreiber, Stuart L., Schwalbe, Harald, Toniolo, Claudio van Boeckel, Constant A.A., Waldmann, Herbert, Walsh, Christopher T. The state of the art of chemical biology. *ChemBioChem* **10**, 16–29 (2009).

10. Ziegler, S., Pries, V., Hedberg, C. & Waldmann, H. Target identification for small bioactive molecules: Finding the needle in the haystack. *Angew. Chemie - Int. Ed.* **52**, 2744–2792 (2013).

11. Das, Raj Kumar, Samanta, Animesh, Ghosh, Krishnakanta, Zhai, Duanting, Xu, Wang, Su, Dongdong, Leong, Cheryl, Chang, Young-Tae. Target Identification: A Challenging Step in Forward Chemical Genetics. *Interdiscip. Bio Cent.* **3**, 3.1-3.16 (2011).

12. Zhou, X., Sun, Q., Kini, R. M. & Sivaraman, J. A universal method for fishing target proteins from mixtures of biomolecules using isothermal titration calorimetry. *Protein Sci.* **17**, 1798–1804 (2008).

13. Kawasumi, M. & Nghiem, P. Chemical genetics: Elucidating biological systems with small-molecule compounds. *J. Invest. Dermatol.* **127**, 1577–1584 (2007).

14. Garbaccio, R. M. & Parmee, E. R. The Impact of Chemical Probes in Drug Discovery: A Pharmaceutical Industry Perspective. *Cell Chem. Biol.* **23**, 10–17 (2016).

15. Arrowsmith, Cheryl H., Audia, James E., Austin, Christopher, Baell, Jonathan, Bennett, Jonathan, Blagg, Julian, Bountra, Chas, Brennan, Paul E., Brown, Peter J., Bunnage, Mark E., Buser-Doepner, Carolyn, Campbell, Robert M., Carter, Adrian J., Cohen, Philip, Copeland, Robert A., Cravatt, Ben, Dahlin, Jayme L., Dhanak, Dashyant, Edwards, Aled M., Frye, Stephen V., Gray, Nathanael, Grimshaw, Charles E., Hepworth, David, Howe, Trevor, Huber, Kilian V.M., Jin, Jian, Knapp, Stefan, Kotz, Joanne D., Kruger, Ryan G., Lowe, Derek, Mader,

Mary M., Marsden, Brian, Mueller-Fahrnow, Anke, Müller, Susanne, O'Hagan, Ronan C., Overington, John P., Owen, Dafydd R., Rosenberg, Saul H., Roth, Brian, Ross, Ruth, Schapira, Matthieu, Schreiber, Stuart L., Shoichet, Brian, Sundström, Michael, Superti-Furga, Giulio, Taunton, Jack, Toledo-Sherman, Leticia, Walpole, Chris, Walters, Michael A., Willson, Timothy M., Workman, Paul, Young, Robert N., Zuercher, William J.. The promise and peril of chemical probes. *Nat. Chem. Biol.* **11**, 536–541 (2015).

16. Leslie, B. J. & Hergenrother, P. J. Identification of the cellular targets of bioactive small organic molecules using affinity reagents. *Chem. Soc. Rev.* **37**, 1347–1360 (2008).

17. Zhang, Chunhua, Brown, Michelle Q., Van De Ven, Wilhelmina, Zhang, Zhi Min, Wu, Bin, Young, Michael C., Synek, Lukáš, Borchardt, Dan, Harrison, Reed, Pan, Songqin, Luo, Nan, Huang, Yu Ming M., Ghang, Yoo Jin, Ung, Nolan, Li, Ruixi, Isley, Jonathan, Morikis, Dimitrios, Song, Jikui, Guo, Wei, Hooley, Richard J., Chang, Chia En A., Yang, Zhenbiao, Zarsky, Viktor, Muday, Gloria K., Hicks, Glenn R, Raikhel, Natasha V.. Endosidin2 targets conserved exocyst complex subunit EXO70 to inhibit exocytosis. *Proc. Natl. Acad. Sci. U. S. A.* **113**, E41–E50 (2016).

18. Uehara, Takahiro N., Mizutani, Yoshiyuki, Kuwata, Keiko, Hirota, Tsuyoshi, Sato, Ayato, Mizoi, Junya, Takao, Saori, Matsuo, Hiromi, Suzuki, Takamasa, Ito, Shogo, Saito, Ami N., Nishiwaki-Ohkawa, Taeko, Yamaguchi-Shinozaki, Kazuko, Yoshimura, Takashi, Kay, Steve A., Itami, Kenichiro, Kinoshita, Toshinori, Yamaguchi, Junichiro, Nakamichi, Norihito. Casein kinase 1 family regulates PRR5 and TOC1 in the Arabidopsis circadian clock. *Proc. Natl. Acad. Sci. U. S. A.* **166**, 11528–11536 (2019).

19. Knippschild, Uwe, Krüger, Marc, Richter, Julia, Xu, Pengfei, Balbina García-Reyes, Peifer, Christian, Halekotte, Jakob, Bakulev, Vasiliy, Bischof, Joachim. The CK1 family: Contribution to cellular stress response and its role in carcinogenesis. *Front. Oncol.* **4 MAY**, 1–32 (2014).

20. Saito, Ami N., Matsuo, Hiromi, Kuwata, Keiko, Ono, Azusa, Kinoshita, Toshinori, Yamaguchi, Junichiro, Nakamichi, Norihito. Structure–function study of a novel inhibitor of the casein kinase 1 family in Arabidopsis thaliana. *Plant Direct* **3**, 1–12 (2019).

21. Kyoko Morimoto, R. A. L. van der H. The Increasing Impact of Activity-Based Protein Profiling in Plant Science. *Plant Cell Physiol.* **57**, 446–461 (2016).

22. Kovács, J. & van der Hoorn, R. A. L. Twelve ways to confirm targets of activity-based probes in plants. *Bioorganic Med. Chem.* **24**, 3304–3311 (2016).

23. Benjamin F Cravatt, Aaron T Wright, J. W. K. Activity-based protein profiling: from enzyme chemistry to proteomic chemistry. *Annu. Rev. Biochem.* **77**, 383–414 (2008).

24. Morimoto, Kyoko, Cole, Kyle S., Kourelis, Jiorgos, Witt, Collin H., Brown, Daniel, Krahn, Daniel, Stegmann, Monika, Kaschani, Farnusch, Kaiser, Markus, Burton, Jonathan, Mohammed, Shabaz, Yamaguchi-Shinozaki, Kazuko, Weerapana, Eranthie, van der Hoorn, Renier A.L. Triazine probes target ascorbate peroxidases in plants. *Plant Physiol.* **180**, 1848–1859 (2019).

25. Shannon, D. A. & Weerapana, E. Covalent protein modification: The current landscape of residue-specific electrophiles. *Curr. Opin. Chem. Biol.* **24**, 18–26 (2015).

26. Sadakane, Y. & Hatanaka, Y. Photochemical fishing approaches for identifying target proteins and elucidating the structure of a ligand-binding region using carbene-generating photoreactive probes. *Anal. Sci.* **22**, 209–218 (2006).

27. Yulin Tian and Qing Lin. Recent Development of Photo-Cross_Linkers as Tools for

Biomedical Research. *Bioorthogonal Chem.* **72**, 758–763 (2018).

28. A. Fleming, S. Chemical reagents in photoaffinity labeling. *Tetrahedron* **51**, 12479–12520 (1995).

29. Leslie, B. J. & Hergenrother, P. J. Identification of the cellular targets of bioactive small organic molecules using affinity reagents. *Chem. Soc. Rev.* **37**, 1347–1360 (2008).

30. Vodovozova, E. L. PhotoaffinityLabeling and Its Application in Structural Biology. *Biochem.* **72**, 1–20 (2007).

31. Jörg, M. & Scammells, P. J. Guidelines for the Synthesis of Small-Molecule Irreversible Probes Targeting G Protein-Coupled Receptors. *ChemMedChem* 1488–1498 (2016) doi:10.1002/cmdc.201600066.

32. Dorman, G.; Prestwich, G. D. Benzophenone Photophores in Biochemistry. *Biochemistry* **33**, 5661–5673 (1994).

33. Dormán, G; Prestwich, G. . Using photolabile ligands in drug discovery and development. *Trends Biotechnol.* **18**, 64–77 (2000).

34. Dormán, G., Nakamura, H., Pulsipher, A. & Prestwich, G. D. The Life of Pi Star: Exploring the Exciting and Forbidden Worlds of the Benzophenone Photophore. *Chem. Rev.* **116**, 15284–15398 (2016).

35. Weber, P. J. A. & Beck-Sickinger, A. G. Comparison of the photochemical behavior of four different photoactivatable probes. *J. Pept. Res.* **49**, 375–383 (1997).

36. Young, Travis S., Young, Douglas D., Ahmad, Insha, Louis, John M., Benkovic, Stephen J., Schultz, Peter G. Evolution of cyclic peptide protease inhibitors. *Proc. Natl. Acad. Sci. U. S. A.* **108**, 11052–11056 (2011).

37. Garcia, Galo, Chiara, David C., Nirthanan, Selvanayagam, Hamouda, Ayman K., Stewart, Deirdre S., Cohen, Jonathan B.. [3H]benzophenone photolabeling identifies state-dependent changes in nicotinic acetylcholine receptor structure. *Biochemistry* **46**, 10296–10307 (2007).

38. Liu, M. T. H. The thermolysis and photolysis of diazirines. *Chem. Soc. Rev.* **11**, 127–140 (1982).

39. Rosenberg, M. G. & Brinker, U. H. Constrained carbenes. *European J. Org. Chem.* 5423–5440 (2006)

40. Hill, J. R. & Robertson, A. A. B. Fishing for Drug Targets: A Focus on Diazirine Photoaffinity Probe Synthesis. *J. Med. Chem.* **61**, 6945–6963 (2018).

41. Modarelli, D. A., Morgan, S. & Platz, M. S. Carbene Formation, Hydrogen Migration, and Fluorescence in the Excited States of Dialkyldiazirines. *J. Am. Chem. Soc.* **114**, 7034–7041 (1992).

42. Li, Z. *et al.* Design and synthesis of minimalist terminal alkyne-containing diazirine photo-crosslinkers and their incorporation into kinase inhibitors for cell- and tissue-based proteome profiling. *Angew. Chemie - Int. Ed.* **52**, 8551–8556 (2013).

43. Das, J. Aliphatic diazirines as photoaffinity probes for proteins: Recent developments. *Chem. Rev.* **111**, 4405–4417 (2011).

44. Yang, Y., Song, H. & Chen, P. R. Genetically encoded photocrosslinkers for identifying and mapping protein-protein interactions in living cells. *IUBMB Life* **68**, 879–886 (2016).

45. Chin, J. W., Martin, A. B., King, D. S., Wang, L. & Schultz, P. G. Addition of a photocrosslinking amino acid to the genetic code of Escherichia coli. *Proc. Natl. Acad. Sci. U.*

S. A. **99**, 11020–11024 (2002).

46. Mori, H. & Ito, K. Different modes of SecY-SecA interactions revealed by site-directed in vivo photo-cross-linking. *Proc. Natl. Acad. Sci. U. S. A.* **103**, 16159–16164 (2006).

47. Smith, R. A. G.; Knowles, J. R. Aryldiazirines. Potential Reagents for Photolabeling of Biological Receptor Sites. *J. Am. Chem. Soc* **95**, 5072–5073 (1973).

48. Richard A. G. Smith, J. R. K. The Preparation and Photolysis of 3-Aryl-3H-diazirines. *J. Chem. Soc.* **2**, 686–694 (1975).

49. Brunner, J., Senn, H. & Richards, F. M. 3-Trifluoromethyl-3-phenyldiazirine. A new carbene generating group for photolabeling reagents. *J. Biol. Chem.* **255**, 3313–3318 (1980).

50. Song, M. & Sheridan, R. S. Regiochemical Substituent Switching of Spin States in Aryl(trifluoromethyl)carbenes. *J. Am. Chem* **133**, 19688–19690 (2011).

51. Leyva, E., de Loera, D. & Leyva, S. Photochemistry of 7-azide-1-ethyl-3-carboxylate-6,8-difluoroquinolone: a novel reagent for photoaffinity labeling. *Tetrahedron Lett.* **49**, 6759–6761 (2008).

52. Peng, Q. *et al.* Synthesis of a photoactivatable phospholipidic probe containing tetrafluorophenylazide. *Tetrahedron Lett.* **46**, 5893–5897 (2005).

53. Li, W. *et al.* Development of Photoaffinity Probe for the Discovery of Steviol Glycosides Biosynthesis Pathway in Stevia rebuadiana and Rapid Substrate Screening. *ACS Chem. Biol.* **13**, 1944–1949 (2018).

54. Fujii, T., Manabe, Y., Sugimoto, T. & Ueda, M. Detection of 210 kDa receptor protein for a leaf-movement factor by using novel photoaffinity probes. *Tetrahedron* **61**, 7874–7893 (2005).

55. Shigemori, H.; Sakai, N.; Miyoshi, E.; Shizuri, Y.; Yamamura, S. BIOACTIVE SIBSTAWCES FROM LESPEDEZA CulEATA L. G. DON AND THEIR BIOLOGICAL ACTIVITIES. *Tetrahedron* **46**, 383–394.

56. Shoji, M. *et al.* Bioorganic studies on plant movement, from natural products to its receptor. *Chem. Rec.* **6**, 344–355 (2006).

57. Okada, M., Matsubara, A. & Ueda, M. Synthesis of photoaffinity probe based on the leaf-opening factor from genus Albizzia. *Tetrahedron Lett.* **49**, 3794–3796 (2008).

58. Gray, W. M. Hormonal regulation of plant growth and development. *PLoS Biol.* **2**, (2004).

59. Ecker, J. R. & Davis, R. W. Plant defense genes are regulated by ethylene. *Proc. Natl. Acad. Sci.* **84**, 5202–5206 (1987).

60. Kermode, A. R. Role of abscisic acid in seed dormancy. *J. Plant Growth Regul.* **24**, 319–344 (2005).

61. Nemhauser, J. L., Mockler, T. C. & Chory, J. Interdependency of brassinosteroid and auxin signaling in Arabidopsis. *PLoS Biol.* **2**, (2004).

62. Park, S. S.-Y. *et al.* Abscisic Acid Inhibits Type 2C. *Science (80-.).* **324**, 1068–1069 (2009).

63. Cao, M. *et al.* An ABA-mimicking ligand that reduces water loss and promotes drought resistance in plants. *Cell Res.* **23**, 1043–1054 (2013).

64. Cutler, S. R., Rodriguez, P. L., Finkelstein, R. R. & Abrams, S. R. *Abscisic Acid: Emergence of a Core Signaling Network*. *Annual Review of Plant Biology* vol. 61 (2010).

65. Klingler, J. P., Batelli, G. & Zhu, J. K. ABA receptors: The START of a new paradigm in phytohormone signalling. *J. Exp. Bot.* **61**, 3199–3210 (2010).

66. Lyer, L. M. Adaptations of the helix-grip fold for ligand binding and catalysis in the START domain superfamily. *Proteins* **43**, 134–144 (2001).

67. Sun, D. *et al.* Crystal structures of the Arabidopsis thaliana abscisic acid receptor PYL10 and its complex with abscisic acid. *Biochem. Biophys. Res. Commun.* **418**, 122–127 (2012).

68. Melcher, K. *et al.* A gate-latch-lock mechanism for hormone signalling by abscisic acid receptors. *Nature* **462**, 602–608 (2009).

69. Nishimura, N. *et al.* PYR/PYL/RCAR family members are major in-vivo ABI1 protein phosphatase 2C-interacting proteins in Arabidopsis. *Plant J.* **61**, 290–299 (2010).

70. Miyazono, K. I. *et al.* Structural basis of abscisic acid signalling. *Nature* **462**, 609–614 (2009).

71. Peng, J. *et al.* The Arabidopsis GAI gene defines a signaling pathway that negatively regulates gibberellin responses. *Genes Dev.* **11**, 3194–3205 (1997).

72. Pysh, L. D., Wysocka-Diller, J. W., Camilleri, C., Bouchez, D. & Benfey, P. N. The GRAS gene family in Arabidopsis: Sequence characterization and basic expression analysis of the SCARECROW-LIKE genes. *Plant J.* **18**, 111–119 (1999).

73. Schweighofer, A., Hirt, H. & Meskiene, I. Plant PP2C phosphatases: Emerging functions in stress signaling. *Trends Plant Sci.* **9**, 236–243 (2004).

74. Yoshida, R. *et al.* The regulatory domain of SRK2E/OST1/SnRK2.6 interacts with ABI1 and integrates abscisic acid (ABA) and osmotic stress signals controlling stomatal closure in Arabidopsis. *J. Biol. Chem.* **281**, 5310–5318 (2006).

75. Umezawa, T. *et al.* Molecular basis of the core regulatory network in ABA responses: Sensing, signaling and transport. *Plant Cell Physiol.* **51**, 1821–1839 (2010).

76. Yoshida, R. *et al.* ABA-activated SnRK2 protein kinase is required for dehydration stress signaling in Arabidopsis. *Plant Cell Physiol.* **43**, 1473–1483 (2002).

77. K Melcher, Y Xu, L M Ng, X E Zhou, F F Soon, V. C. Identification and mechanism of ABA receptor antagonism. *Nat Struct. Biol* **17**, 1102–1108 (2010).

78. Rigal, A., Ma, Q. & Robert, S. Unraveling plant hormone signaling through the use of small molecules. *Front. Plant Sci.* **5**, 1–20 (2014).

79. Anier, K. & Kalda, A. Epigenetics in the Central Nervous System. *Curr. Geriatr. Reports* **1**, 190–198 (2012).

80. Takeuchi, Jun, Okamoto, Masanori, Akiyama, Tomonori, Muto, Takuya, Yajima, Shunsuke, Sue, Masayuki, Seo, Mitsunori, Kanno, Yuri, Kamo, Tsunashi, Endo, Akira, Nambara, Eiji, Hirai, Nobuhiro, Ohnishi, Toshiyuki, Cutler, Sean R., Todoroki, Yasushi. Designed abscisic acid analogs as antagonists of PYL-PP2C receptor interactions. *Nat. Chem. Biol.* **10**, 477–482 (2014).

81. Wilen, Ronald W, Hays, Dirk B, Mandel, Roger M, Abrams, Suzanne R, Moloney, Maurice M, Wilen, Ronald W, Hays, Dirk B, Mandel, Roger M, Abrams, Suzanne R., Moloney, Maurice M. Competitive Inhibition of Abscisic Acid-Regulated Gene Expression by Stereoisomeric Acetylenic Analogs of Abscisic Acid Published by : American Society of Plant Biologists (ASPB) Linked references are available on JSTOR for this article : Competitive In. **101**, 469–476 (2020).

82. Gupta, R. & Chakrabarty, S. K. Gibberellic acid in plant: Still a mystery unresolved. *Plant Signal. Behav.* **8**, (2013).

83. Hedden, P. & Phillips, A. L. Manipulation of hormone biosynthetic genes in transgenic plants.

Curr. Opin. Biotechnol. **11**, 130–137 (2000).

84. Tyler, Ludmila Thomas, Stephen G, Hu, Jianhong, Dill, Alyssa, Alonso, Jose M, Ecker, Joseph R, Sun, Tai-ping, Tyler, Ludmila, Thomas, Stephen G, Hu, Jianhong, Dill, Alyssa, Alonso, Jose M, Ecker, Joseph R. DELLA Proteins and Gibberellin-Regulated Seed Germination and Floral Development in Arabidopsis Published by : American Society of Plant Biologists (ASPB) Linked references are available on JSTOR for this article : DELLA Proteins and Gibberellin-Regulat. **135**, 1008–1019 (2004).

85. Ueguchi-Tanaka, M., Hirano, K., Hasegawa, Y., Kitano, H. & Matsuoka, M. Release of the repressive activity of rice DELLA protein SLR1 by gibberellin does not require SLR1 degradation in the gid2 mutant. *Plant Cell* **20**, 2437–2446 (2008).

86. Griffiths, Jayne, Murase, Kohji, Rieu, Ivo, Zentella, Rodolfo, Zhang, Zhong Lin, Powers, Stephen J., Gong, Fan, Phillips, Andrew L., Hedden, Peter, Sun, Tai Ping, Thomas, Stephen G.. Genetic characterization and functional analysis of the GID1 gibberellin receptors in Arabidopsis. *Plant Cell* **18**, 3399–3414 (2006).

87. Iuchi, Satoshi, Suzuki, Hiroyuki, Kim, Young Cheon, Iuchi, Atsuko, Kuromori, Takashi, Ueguchi-Tanaka, Miyako, Asami, Tadao, Yamaguchi, Isomaro, Matsuoka, Makoto, Kobayashi, Masatomo, Nakajima, Masatoshi. Multiple loss-of-function of Arabidopsis gibberellin receptor AtGID1s completely shuts down a gibberellin signal. *Plant J.* **50**, 958–966 (2007).

88. Sun, Xiaolin, Jones, William T., Harvey, Dawn, Edwards, Patrick J.B., Pascal, Steven M., Kirk, Christopher, Considine, Thérèse, Sheerin, David J., Rakonjac, Jasna, Oldfield, Christopher J., Xue, Bin, Dunker, A. Keith, Uversky, Vladimir N.. N-terminal domains of DELLA proteins are intrinsically unstructured in the absence of interaction with GID1/gibberellic acid receptors. *J. Biol. Chem.* **285**, 11557–11571 (2010).

89. Lee, Sorcheng, Cheng, Hui, King, Kathryn E, Wang, Weefuen, He, Yawen, Hussain, Alamgir, Lo, Jane, Harberd, Nicholas P, Peng, Jinrong. Gibberellin regulates. *Genes Dev.* **16**, 646–658 (2002).

90. Dill, A., Jung, H. S. & Sun, T. P. The DELLA motif is essential for gibberellin-induced degradation of RGA. *Proc. Natl. Acad. Sci. U. S. A.* **98**, 14162–14167 (2001).

91. Gomi, Kenji, Sasaki, Akie, Itoh, Hironori, Ueguchi-Tanaka, Miyako, Ashikari, Motoyuki, Kitano, Hidemi, Matsuoka, Makoto. GID2, an F-box subunit of the SCF E3 complex, specifically interacts with phosphorylated SLR1 protein and regulates the gibberellin-dependent degradation of SLR1 in rice. *Plant J.* **37**, 626–634 (2004).

92. Hirano, Ko, Asano, Kenji, Tsuji, Hiroyuki, Kawamura, Mayuko, Mori, Hitoshi, Kitano, Hidemi, Ueguchi-Tanaka, Miyako, Matsuoka, Makoto Characterization of the molecular mechanism underlying gibberellin perception complex formation in rice. *Plant Cell* **22**, 2680–2696 (2010).

93. Mcginnis, Karen M, Thomas, Stephen G, Soule, Jonathan D, Strader, Lucia C, Zale, Janice M, Sun, Tai-ping, Steber, Camille M, Mcginnis, Karen M, Thomas, Stephen G, Soule, Jonathan D, Strader, Lucia C, Zale, C Janice M, Sun, Tai-ping, Steberas, Camille M The Arabidopsis SLEEPY1 Gene Encodes a Putative F-Box Subunit of an SCF E3 Ubiquitin Ligase Published by : American Society of Plant Biologists (ASPB) **15**, 1120–1130 (2013).

94. Steber, C. M., Cooney, S. E. & McCourt, P. Isolation of the GA-response mutant sly1 as a suppressor of ABI1-1 in Arabidopsis thaliana. *Genetics* **149**, 509–521 (1998).

95. Li, Kunlun, Yu, Renbo, Fan, Liu Min, Wei, Ning, Chen, Haodong, Deng, Xing Wang. DELLA-mediated PIF degradation contributes to coordination of light and gibberellin signalling in Arabidopsis. *Nat. Commun.* **7**, (2016).

96. De Lucas, Miguel, Davière, Jean Michel, Rodríguez-Falcón, Mariana, Pontin, Mariela, Iglesias-Pedraz, Juan Manuel, Lorrain, Séverine, Fankhauser, Christian, Blázquez, Miguel Angel, Titarenko, Elena, Prat, Salomé. A molecular framework for light and gibberellin control of cell elongation. *Nature* **451**, 480–484 (2008).

97. Achard, P. & Genschik, P. Releasing the brakes of plant growth: How GAs shutdown della proteins. *J. Exp. Bot.* **60**, 1085–1092 (2009).

98. No Title. in *Encyclopedia of Food Sciences and Nutrition (Second Edition)* (ed. Caballero, B.) 5729–5733 (Academic Press, 2003).

99. Ritzel, M., Geissman, T. A., Phinney, B. O., Physiology, S. P. & Mar, N. Tannins as Gibberellin Antagonists Published by : American Society of Plant Biologists (ASPB) Linked references are available on JSTOR for this article : Tannins as Gibberellin Antagonistsl. **49**, 323–330 (1972).

100. Li, Y, Zhang, D., An, N., Fan, S., Zuo, X., Zhang, X., Zhang, L., Gao, C., Han, M., Xing, L. Transcriptomic analysis reveals the regulatory module of apple (Malus × domestica) floral transition in response to 6-BA. *BMC Plant Biol.* **19**, 1–17 (2019).

101. Kaplan, B., Davydov, O., Knight, H., Galon, Y., Knight, M., Fluhr, R., Fromm, H. Rapid transcriptome changes induced by cytosolic Ca2+ transients reveal ABRE-related sequences as Ca2+-responsive cis elements in Arabidopsis. *Plant Cell* **18**, 2733–2748 (2006).

102. Sukiran, N. A. Exploring plant hormonal signalling through chemical perturbation. (2018).

103. Morris, J. Genes, genetics, and epigenetics: a correspondence. *Science (80-.).* **293**, 1103–1105 (2001).

104. Hayashi, Ken ichiro, Jones, Alan M., Ogino, Kentaro, Yamazoe, Atsushi, Oono,Yutaka, Inoguchi, Masahiko, Kondo, Hirokiyo, Nozaki, Hiroshi. Yokonolide B, a novel inhibitor of auxin action, blocks degradation of AUX/IAA factors. *J. Biol. Chem.* **278**, 23797–23806 (2003).

105. Woolven, H., González-Rodríguez, C., Marco, I., Thompson, A. L. & Willis, M. C. DABCO-bis (sulfur dioxide), DABSO, as a convenient source of sulfur dioxide for organic synthesis: Utility in sulfonamide and sulfamide preparation. *Org. Lett.* **13**, 4876–4878 (2011).

106. Kosugi, Y., Akakura, M. & Ishihara, K. Kinetic resolution of racemic alcohols catalyzed by minimal artificial acylases derived from l-histidine. *Tetrahedron* **63**, 6191–6203 (2007).

107. Lehmann, J., Richers, J., Pöthig, A. & Sieber, S. A. Synthesis of ramariolide natural products and discovery of their targets in mycobacteria. *Chem. Commun.* **53**, 107–110 (2017).

108. Rennhack, Andreas, Jumpertz, Thorsten, Ness, Julia, Baches, Sandra, Pietrzik, Claus U., Weggen, Sascha, Bulic, Bruno. Synthesis of a potent photoreactive acidic γ-secretase modulator for target identification in cells. *Bioorganic Med. Chem.* **20**, 6523–6532 (2012).

109. Dolman, S. J., Gosselin, F., Shea, D. O. & Davies, I. W. mediated by lithium tributylmagnesiate. **62**, 5092–5098 (2006).

110. Kato, S., Nonoyama, N., Tomimoto, K. & Mase, T. Non-cryogenic metalation of aryl bromides bearing proton donating groups: Formation of a stable magnesio-intermediate. *Tetrahedron Lett.* **43**, 7315–7317 (2002).

111. Elisabeth A. Dixon, Alfred Fischer. A. F. P. R. Preparation of a series of substituted fluoromethylnaphthalenes. *Can. J. Chem.* **59**, 2629–2641 (1981).

112. Muthusamy, S., Babu, S. A. & Gunanathan, C. Indium triflate: A mild and efficient Lewis acid catalyst for O-H insertion reactions of α-diazo ketones. *Tetrahedron Lett.* **43**, 3133–3136 (2002).

113. Dubarle, J., Schnakenburg, G., Rose, E. & D, K. H. Heterobimetallic Dibenzoindenyl (Cr (CO) 3 À Re (CO) 3) Complexes and Molecular Structures. *Inorg. Chem.* 8153–8157 (2011).

114. Lee, S., Bae, H. Y. & List, B. Can a Ketone Be More Reactive than an Aldehyde? Catalytic Asymmetric Synthesis of Substituted Tetrahydrofurans. *Angew. Chemie - Int. Ed.* **57**, 12162–12166 (2018).

115. Greene, Elizabeth A., Codomo, Christine A., Taylor, Nicholas E., Henikoff, Jorja G. Till, Bradley J., Reynolds, Steven H., Enns, Linda C., Burtner, Chris, Johnson, Jessica E. Odden, Anthony R., Comai, Luca, Henikoff, Steven. Spectrum of chemically induced mutations from a large-scale reverse-genetic screen in Arabidopsis. *Genetics* **164**, 731–740 (2003).

116. Qu, L. J. & Qin, G. Generation and identification of arabidopsis EMS mutants. *Methods Mol. Biol.* **1062**, 225–239 (2014).

117. Kim Y., Schumaker K.S., Z. J. EMS Mutagenesis of Arabidopsis. in *Arabidopsis Protocols. Methods in Molecular Biology™, vol 323* (2006).

118. Singer, B. Mutagenesis from a chemical perspective: Nucleic acid reactions, reair, translation and transcription. in *Molecular and Cellular Mechanism of Mutagenesis* (ed. J. F. Lemontt, W. M. G.) 1–42 (New York: Plenum Publishing Cor, 1982).

119. Lawley, P. D. & Thatcher, C. J. Methylation of Deoxyribonucleic Acid in Cultured Mammalian Cells by N-Methyl-N′-nitro-N-nitrosoguanidine. *Biochem. J.* **116**, 693–707 (1970).

120. Settles, M. A. EMS Mutagenesis of Maize Pollen. in *Plant Embryogenesis: Methods In Molecular Biology* (2020). doi:10.1007/978-1-0716-0342-0_3.

121. Hequan Sun, K. S. SHOREmap v3.0: Fast and Accurate Identification of Causal Mutations from Forward Genetic Screens. in *Methods in Molecular Biology* 381–395 (2015).

122. Schneeberger, K., Sun, H. SHOREmap: Simultaneous mapping and mutation identification by deep sequencing. *Nat. Methods* **6**, 550–551 (2009).

123. Jander, G., Baerson, S., Hudack, J., Gonzalez, K., Gruys, K., Last, R. Ethylmethanesulfonate saturation mutagenesis in Arabidopsis to determine frequency of herbicide resistance. *Plant Physiol.* **131**, 139–146 (2003).

124. Zhang, X. C., Millet, Y., Ausubel, F. M. & Borowsky, M. Next-gen sequencing-based mapping and identification of ethyl methanesulfonate-induced mutations in Arabidopsis thaliana. *Curr. Protoc. Mol. Biol.* **2014**, 7.18.1-7.18.16 (2014).

125. Naoyuki Uchida, Tomoaki Sakamoto, Masao Tasaka, T. K. Identification of EMS-induced causal mutations in Arabidopsis thaliana by next-generation sequencing. *Methods Mol. Biol.* **1062:259**–**7**, (2014).

126. Josh T. Cuperus, Taiowa A. Montgomery, Noah Fahlgren, Russell T. Burke, Tiffany Townsend, Christopher M. Sullivan, J. C. C. Identification of MIR390a precursor processing-defective mutants in Arabidopsis by direct genome sequencing. *Proc. Natl. Acad. Sci.* **107**, 466–471 (2010).

127. Damian R. Page, U. G. The art and design of genetic screens: Arabidopsis thaliana. *Nat. Rev. Genet.* **3**, 124–136 (2002).

128. Yu, L., Nie, Y., Jiao, J., Jian, L. & Zhao, J. The sequencing-based mapping method for effectively cloning plant mutated genes. *Int. J. Mol. Sci.* **22**, (2021).

129. Rao, R. N., Allen, N., Hobbs, J., Alborn, W., Kirst, H., Paschal, J. Genetic and enzymatic basis of hygromycin B resistance in Escherichia coli. *Antimicrob. Agents Chemother.* **24**, 689–695 (1983).

130. Harrison, S. J., Mott, E., Parsley, K., Aspinall, S., Gray, J., Cottage, A. A rapid and robust method of identifying transformed Arabidopsis thaliana seedlings following floral dip transformation. *Plant Methods* **2**, 1–7 (2006).

131. W Lukowitz, C S Gillmor, W. R. S. Positional cloning in Arabidopsis. Why it feels good to have a genome initiative working for you. *Plant Physiol.* **123**, 795–805 (2020).

132. Capilla-Perez, L. Solier, V., Portemer, V., Chambon, A., Hurel, A., Guillebaux, A., Vezon, D., Cromer, L., Grelon, M., Mercier, R. The hem lines: a new library of homozygous arabidopsis thaliana ems mutants and its potential to detect meiotic phenotypes. *Front. Plant Sci.* **9**, 1–9 (2018).

133. Sakai Nozomumomose Yu, Murase Katshito. Patent. H. M. EP1486490 (A1). (2004).

134. Yong, H. The new preparation of aliphatic amines with sulphonyl group and their salts. 1–14 (2011).

135. Wei, W., Liu, C., Yang, D., Wen, J., You, Y., Wang, H. Metal-free direct construction of sulfonamides via iodine- mediated coupling reaction of sodium sulfinates and amines at room temperature. *Adv. Synth. Catal.* **357**, 987–992 (2015).

136. Lai, J., Chang, L. & Yuan, G. I2/TBHP Mediated C-N and C-H Bond Cleavage of Tertiary Amines toward Selective Synthesis of Sulfonamides and β-Arylsulfonyl Enamines: The Solvent Effect on Reaction. *Org. Lett.* **18**, 3194–3197 (2016).

137. Del Solar, Virginia, Quiñones-Lombraña, Adolfo, Cabrera, Silvia, Padrón, José M., Ríos-Luci, Carla, Alvarez-Valdés, Amparo, Navarro-Ranninger, Carmen, Alemán, José. Expanding the synthesis of new trans-sulfonamide platinum complexes: Cytotoxicity, SAR, fluorescent cell assays and stability studies. *J. Inorg. Biochem.* **127**, 128–140 (2013).

138. Zhao, Y., Li, Z., Yang, C., Lin, R. & Xia, W. Visible-light photoredox catalysis enabled bromination of phenols and alkenes. *Beilstein J. Org. Chem.* **10**, 622–627 (2014).

139. M. Weimar, G. Durner, J. W. Bats, M. W. G. Enantioselevtive snthesis of (+)-Estrone Exploiting a Hydrogen Bond-Promoted Diels-Alder Reaction. *J. Org. Chem.* **75**, 2718–2721 (2010).

140. Wang, D. Y., Yang, Z. K., Wang, C., Zhang, A. & Uchiyama, M. From Anilines to Aryl Ethers: A Facile, Efficient, and Versatile Synthetic Method Employing Mild Conditions. *Angew. Chemie - Int. Ed.* **57**, 3641–3645 (2018).

141. Jong, Yeon Hwang, Arnold, Leggy A., Zhu, Fangyi, Kosinski, Aaron, Mangano, Thomas J., Setola, Vincent, Roth, Bryan L., Guy, R. Kiplin. Improvement of pharmacological properties of irreversible thyroid receptor coactivator binding inhibitors. *J. Med. Chem.* **52**, 3892–3901 (2009).

142. Waterford, M., Saubern, S. & Hornung, C. H. Evaluation of a Continuous-Flow Photo-Bromination Using N -Bromosuccinimide for Use in Chemical Manufacture. *Aust. J. Chem.* **74**, 569–573 (2021).

143. Shellaiah, M., Rajan, Y. C. & Lin, H. C. Synthesis of novel triarylamine-based dendrimers with N 4,N 6-dibutyl-1,3,5-triazine-4,6-diamine probe for electron/energy transfers in H-bonded donor-acceptor-donor triads and as efficient Cu 2+ sensors. *J. Mater. Chem.* **22**, 8976–8987 (2012).

144. Ohta, Hiroshi, Ishizaka, Tomoko, Tatsuzuki, Makoto, Yoshinaga, Mitsukane, Iida, Izumi, Yamaguchi, Tomomi, Tomishima, Yasumitsu, Futaki, Nobuko, Toda, Yoshihisa, Saito, Shuji. Imine derivatives as new potent and selective CB2 cannabinoid receptor agonists with an analgesic action. *Bioorganic Med. Chem.* **16**, 1111–1124 (2008).

145. Hoye, T. R. & Chen, M. Studies of Palladium-Catalyzed Cross-Coupling Reactions for Preparation of Highly Hindered Biaryls Relevant to the Korupensamine / Michellamine Problem. **3263**, 7940–7942 (1996).

146. Lowe, John A., Qian, Weimin, Drozda, Susan E., Volkmann, Robert A., Nason, Deane, Nelson, Robert B., Nolan, Charles, Liston, Dane, Ward, Karen, Faraci, Steve, Verdries, Kim, Seymour, Pat, Majchrzak, Michael, Villalobos, Anabella, White, W. Frost Structure-Activity Relationships of Potent, Selective Inhibitors of Neuronal Nitric Oxide Synthase Based on the 6-Phenyl-2-aminopyridine Structure. *J. Med. Chem.* **47**, 1575–1586 (2004).

147. Fournier, D. & Poirier, D. Chemical synthesis and evaluation of 17α-alkylated derivatives of estradiol as inhibitors of steroid sulfatase. *Eur. J. Med. Chem.* **46**, 4227–4237 (2011).

148. Jiang, J., Wang, P. & Cai, M. Diphosphino-functionalised MCM-41-supported palladium complex: An efficient and recyclable catalyst for the formylation of aryl halides. *J. Chem. Res.* **38**, 218–222 (2014).

149. Inglis, Steven R., Zervosen, Astrid, Woon, Esther C.Y., Gerards, Thomas, Teller, Nathalie, Fischer, Delphine S., Luxen, André, Schofield, Christopher J. Synthesis and evaluation of 3-(dihydroxyboryl)benzoic acids as D,D-carboxypeptidase R39 inhibitors. *J. Med. Chem.* **52**, 6097–6106 (2009).

150. Andrews, Mark David; Bagal, Sharanjeet Kaur; Gibson, Karl Richard; Omoto, Kiyoyuki; Ryckmans, Thomas; Skerratt, Sarah Elizabeth; Stupple, P. A. Wo 2012/137089. vol. WO 2012/13 (2012).

151. La, M. T. & Kim, H. K. A fast and practical synthesis of tert-butyl esters from 2-tert-butoxypyridine using boron trifluoride·diethyl etherate under mild conditions. *Tetrahedron* **74**, 3748–3754 (2018).

152. Wu, Jianglong, Liu, Yan, Ma, Xiaowei, Liu, Ping, Gu, Chengzhi, Dai, Bin Cu(II)-Catalyzed Ligand-Free Oxidation of Diarylmethanes and Second Alcohols in Water. *Chinese J. Chem.* **35**, 1391–139 (2017).

153. Tan, E., Zanini, M. & Echavarren, A. M. Iridium-Catalyzed β-Alkynylation of Aliphatic Oximes as Masked Carbonyl Compounds and Alcohols. *Angew. Chemie - Int. Ed.* **59**, 10470–10473 (2020).

Volume II: Ir Catalysed Aromatic C–H Activation

Chapter 1: Introduction to Ir Catalysed C–H Borylation

1.1 Volume II Introduction

A separate line of research investigated the application of Ir catalysed C–H activation to discrete problems. This volume will briefly outline the rationale behind the two lines of study and discuss the results obtained. Chapter 1 briefly outlines Ir catalysed C–H borylation, with a focus on the borylation of heteroaromatic systems. Chapter 2 discusses a study into the formation of trifunctional pyridines through Ir C–H activation of 2-halo nicotinates. Chapter 3 outlines a systematic study of the borylation of fluoroarenes, namely how substitution patterns and source of boron impact regioselectivity. Chapter 4 provides detailed experimental methods and results along with NMR spectra.

1.2 Ir Catalysed Borylation

The last 40 years has seen the development of organoboron compounds into important intermediates in organic synthesis due to their abilities to undergo a wide range of transformations.[154] First reported in 1981, the Suzuki-Miyaura cross-coupling between organoboron compounds and organohalides to form sp^2-sp^2 C–C bonds is widely used in the fields of medicinal chemistry and natural product synthesis.[155] Aromatic organoboron intermediates have historically been accessed via metalation of a C–H or C–X bond. These approaches are often limited due to the harsh conditions employed, by the requirement of aryl halide intermediates or by the need for substituents with suitable directing groups to facilitate metalation.[156] Direct conversion of C–H bonds to C–B bonds presents a simple solution to these issues and thus has been studied extensively with transition metals such as Pd, Fe, Ru, Pt, Rh, Mn, and Ir having been shown to catalyse this process.[154,157–159] The development of this transformation has been especially beneficial to late-stage functionalization of compounds in drug discovery and to the drive towards sustainable chemistry with its high atom economy and ability to reduce synthetic steps. Arguably, Ir-catalysed methods of C–H borylation have become dominant, and as such, this review will only discuss these transformations.

Initial reports of Ir catalysed C–H borylation were published in 2002 describing two catalytic systems; Ir(Ind)(cod) as a precatalyst and DMPE as a ligand by Smith *et al*. and $[Ir(cod)(Cl)]_2$ as a precatalyst and 2,2'–bipyridine (bpy) as the ligand by Hartwig, Ishiyama and Miyaura *et al*.[160,161] The latter

methodology using an OMe ligand in place of Cl has now become the standard catalyst system and has found wide-spread applications. Significantly, many functional groups such as amides, esters, amines, and nitrile groups are compatible with the reaction, providing a broad scope for its use.[154]

In the mechanism for Ir-borylation (Scheme 53), the active catalyst species cycles between Ir^{III} and Ir^{V}.[162,163] Resting species **217** is first formed from following the combination of the starting Ir precatalyst $[Ir(cod)(OMe)]_2$, solvent, boron reagent and ligand. Following ligand exchange, cod is reduced to cyclooctene (coe) and the boron reagent facilitates oxidisation of the precatalyst to form Ir^{III} species **217**. The weakly bound coe dissociates, forming pentacoordinate species (**218**) to which an aromatic C–H bond can oxidatively add into. Ar-BPin can then reductively eliminate from Ir^{V} species (**219**), resulting in a Ir^{III} bisboryl hydride **220**. Active species **217** is regenerated by an oxidative addition of the boron species into **221** followed by the reductive elimination of HBpin or H_2.

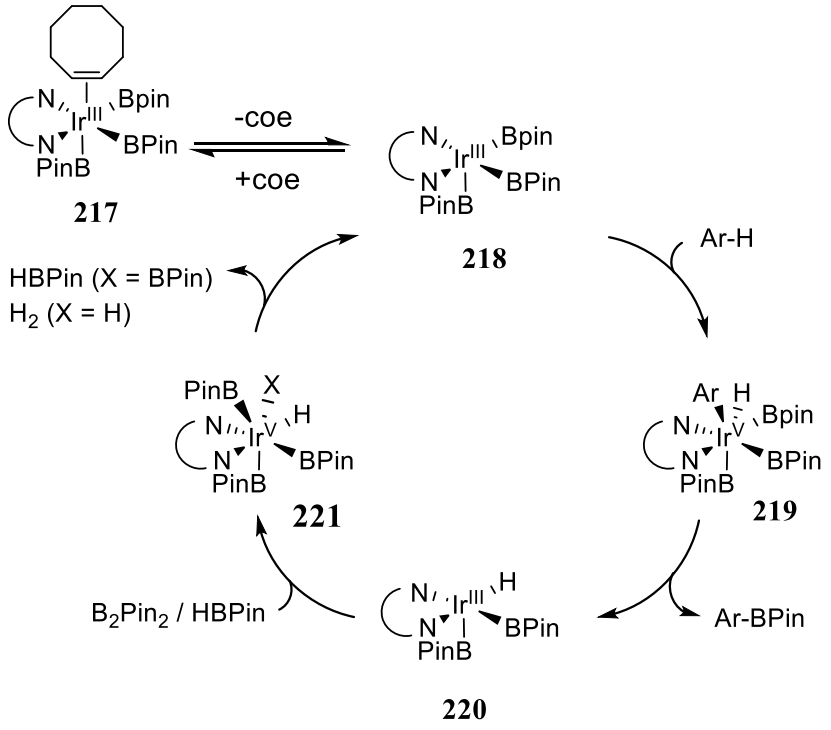

Scheme 53: Catalytic cycle of Ir catalysed C–H borylation

Compounds containing heteroaromatics are very prevalent in natural products, pharmaceuticals, bioactive compounds, and agrochemicals making the ability to synthesise these molecules efficiently and economically commercially attractive. In general, electron-deficient aromatics are more reactive towards C–H activation due to the increased ability to oxidatively add into the active Ir species (**218**)[162] As a result, the borylation of many heteroaromatics has been described, with these generally proving to be excellent substituents.[164] Examples of such borylations include pyrroles and indoles, which

selectively borylate in the α-position and (iso)quinolines, which typically borylate in the ring containing the heteroatom (Scheme 54).[165,166]

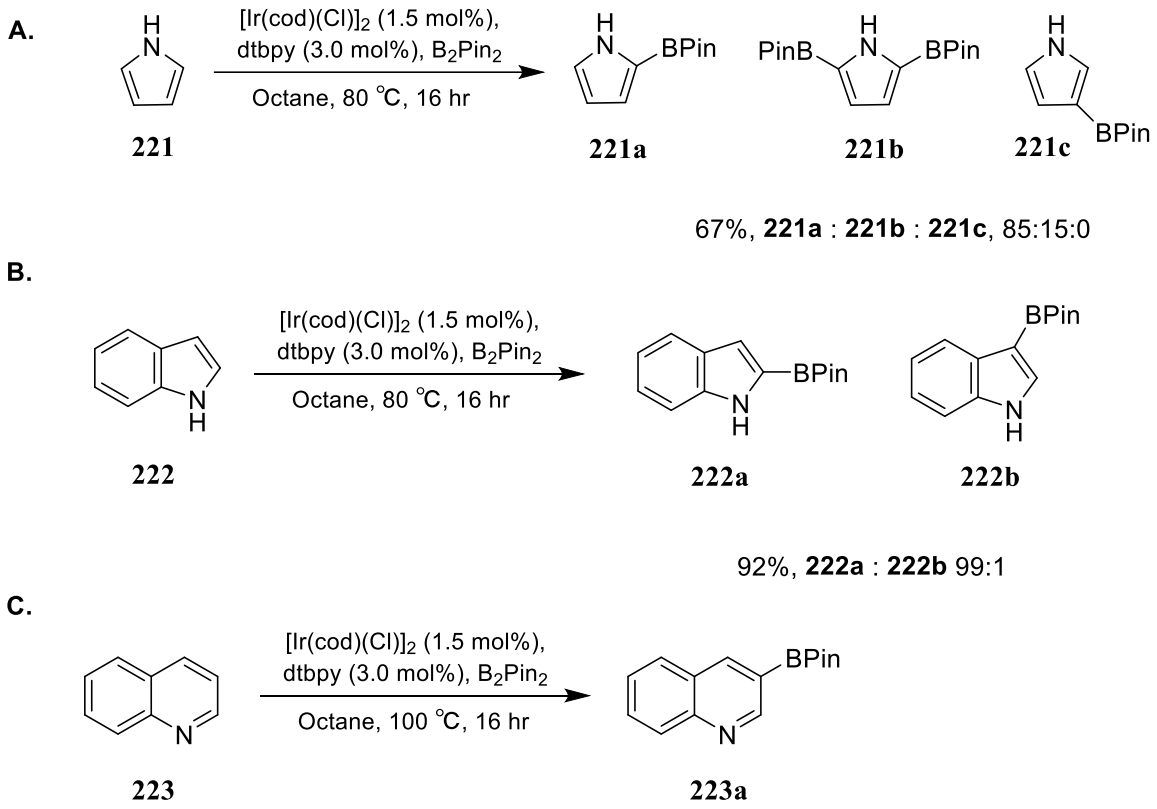

Scheme 54: Ir catalysed borylation of selected heteroaromatic substrates

Given the crowded nature of the 7-coordinate intermediate (**219**, Scheme 53), the selectivity of Ir-catalysed borylation is predominantly sterically controlled. Despite this, there are examples of selectivity being controlled electronically. One notable example is the borylation of benzodioxole which affords the more hindered boronate ester (**224a**), indicating C-H acidity may also play a role in regioselectivity (Scheme 55, **A**).[167] In the borylation of (substituted) heteroaromatics both factors are often observed contributing to the determination of regioselectivity. An example of this is in the C–H activation of indazoles where free N–H indazoles do not borylate potentially due to the ability of the azinyl nitrogen to inhibit the catalyst but N-substituted indazoles have shown to be good substrates. N-methyl-2H-indazole (**225**) borylates selectively in the ring containing the heteroatoms, forming the C–3 boronate ester **225a** but the introduction of a 4-bromo-substitutent results in the formation of C–6 boronate ester (**226a**) as steric constraints are introduced at the *peri*-position (Scheme 55, **B** and **C**).[168]

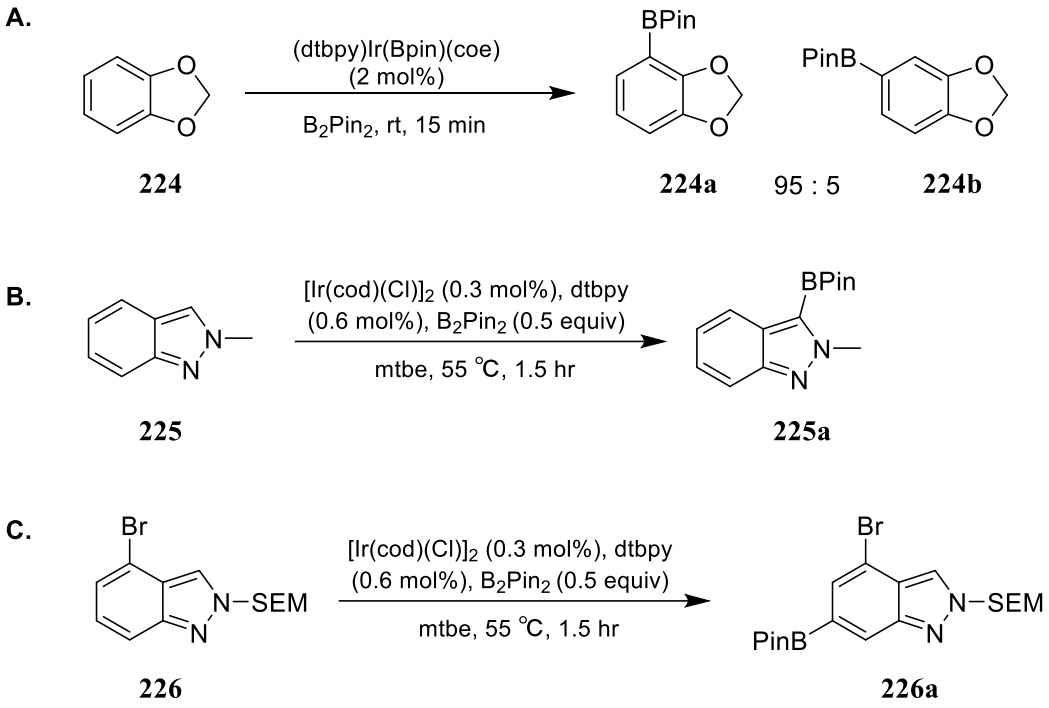

Scheme 55: Electronic and sterically controlled Ir catalysed borylation

Chapter 2: C–H Activation of 2-Halopyridines.

2.1: Introduction to Ir borylation of pyridines

Although electron deficient, the borylation of pyridines has proven to be unusually challenging, often requiring high temperatures and prolonged reaction times.[164] This has been attributed to the ability of the azinyl nitrogen to coordinate to the active catalytic species, inhibiting further reaction. The borylation of pyridines are further challenged by the propensity of the desired products to undergo rapid protodeborylation.[169,170,171] Other challenges include the electronic inhibition to C–H activation at the position α-to the azinyl nitrogen.

Most methods of accessing substituted pyridine rings involve the *de novo* construction of the aromatic ring, limiting the ability to introduce structural and substituent diversity. As a component of a project exploring the use of C–H borylation chemistry in the late-stage functionalisation of heteroarenes, previous work in the group explored the use of 2-halo pyridines. The 2-halo substituent serves two purposes in this transformation; as a steric blocker preventing coordination to the active Ir species, and to reduce the Lewis basicity of the nitrogen lone pair, reducing the probability of protodeborylation. The resultant boronate esters are valuable intermediates, allowing for derivatisation via a number of transformations.

2.2: Results and Discussion

In earlier work, this strategy had been validated with a series of 2-halonicotinates used as primary substrates for borylation. Due to the inability to isolate the boronate esters a one-pot two-step process was developed where the afforded boronate esters are used crude in the subsequent cross-coupling reaction (Scheme 56). For the tandem Suzuki-Miyaura step, 4-iodonitrobenzene, 4-iodotoluene and 1-iodo, 4-triflouromethyl benzene were the main coupling partners employed in this study, affording the desired bi-aryl compounds in good yields.

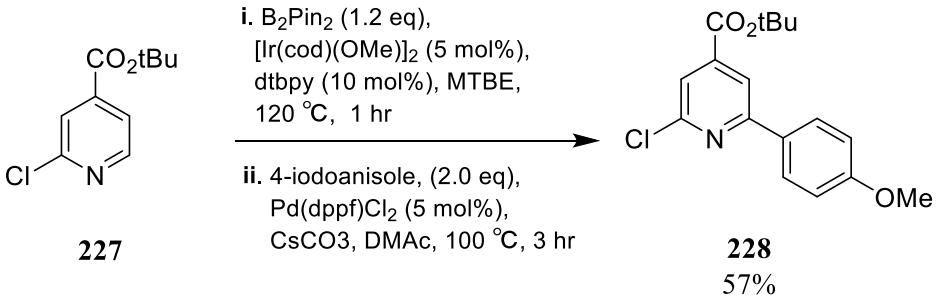

Scheme 56: Tandem Ir borylation-Suzuki Miyaura synthesis of trifunctional pyridines

Further functionalisation was achieved by S_NAr using aliphatic amines to obtain trifunctional pyridines. 2-chloropyridines were dissolved in neat amine and irradiated using microwaves to facilitate the substitution whilst 2-fluoropyridines were able to undergo substitution under much milder conditions with heating at 80 °C in dioxane being sufficient (Scheme 57). Despite the increased reactivity of the fluoropyridines, S_NAr was still not possible with anilines. Further attempts of this reaction using microwave irradiation also failed, indicating a stronger base such as NaH may be required to facilitate this reaction.

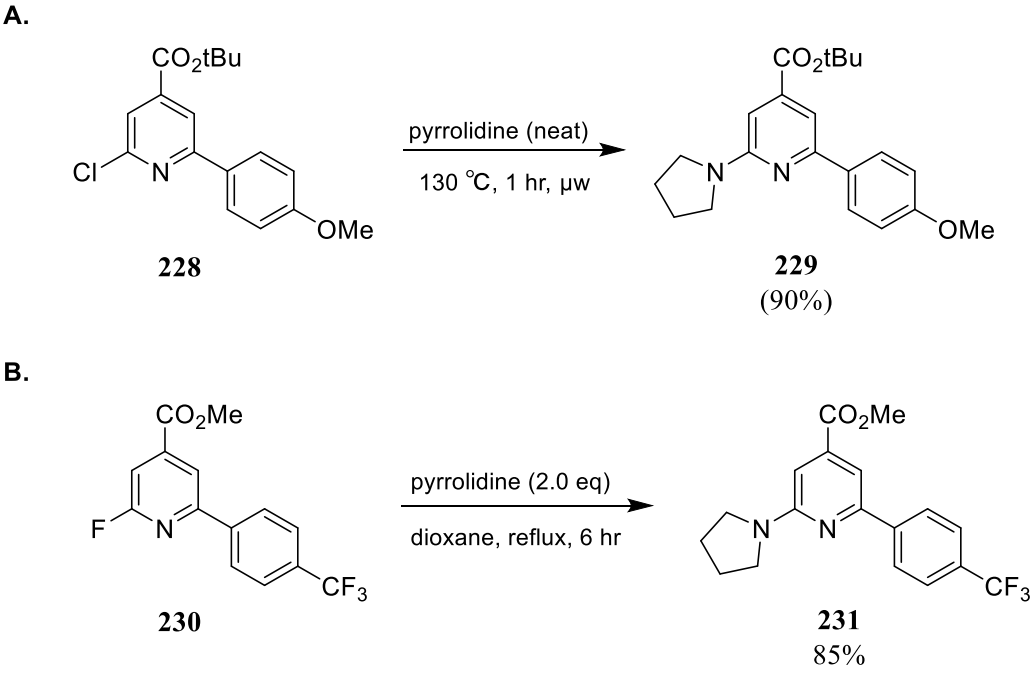

Scheme 57: S_NAr using pyrrolidine on 2-chloro (A.) and 2-fluoro (B.) nicotinates.

In order to complete this study, additional examples, expanding the variation that is possible from the halo-nicotinate scaffold were required. To fulfil this need, a further generation of examples were

prepared, including a second Suzuki-Miyaura cross coupling with a boronic acid (Scheme 58, **B**), reduction of the halo-substituent (Scheme 58, **A**) and functionalisation of the ester through amide coupling with amino acid **236** (Scheme 58, **C**).

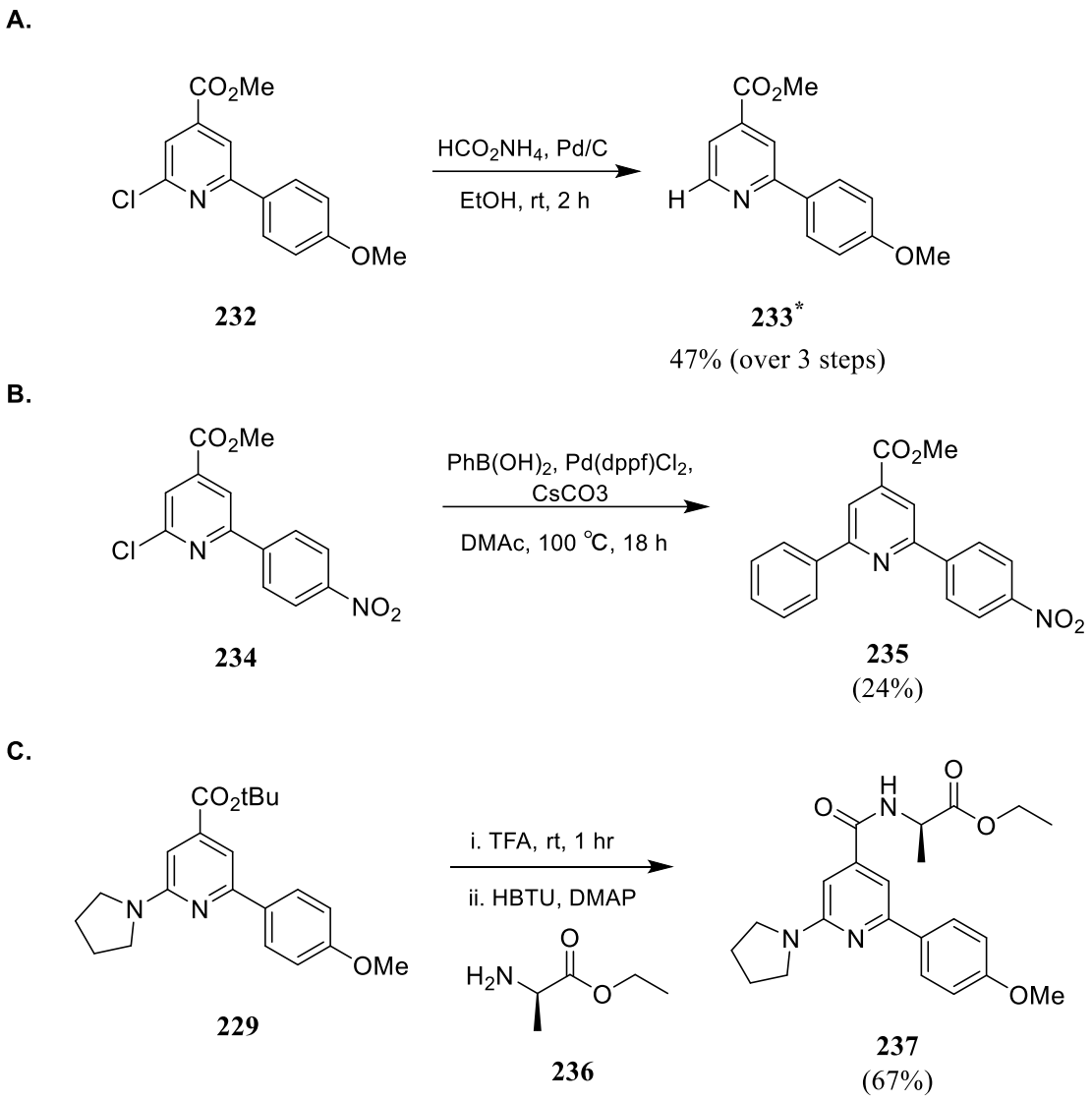

Scheme 58: Further functionalisation of trifunctional pyridines.

Ultimately, a total of 32 examples were described.[2] Full results and experimental data were reported in Steel *et al*. (2020)[172] and are presented in Appendix D.

[2] Compounds include those prepared earlier by Omar A. Salih, Scott. A. Sadler, and Carys L. Thomas.

Chapter 3 Borylation of Fluoroarenes

3.1 Introduction to Fluoroarenes

In the second line of study, an investigation of the steric and electronic effects of fluoroarenes on Ir catalysed C–H activation was undertaken. The introduction of fluorine atoms into molecules is widely observed in the field of medicinal chemistry with fluorinated analogues possessing distinctive chemical and physical properties such as increased lipophilicity.[173] However, accessing these compounds remains challenging as the highly electron withdrawing properties of fluorine deactivate the ring to standard electrophilic strategies of aromatic derivatisation. In contrast, the electron-deficient nature of these arenes naturally lends itself towards C–H activation.[174] The directing abilities of fluorine on C–H activation remain to be evaluated. Earlier work in the group by Mingyan Dan had been shown that F-substituents are highly activating, with fluoroaromatic substrates often borylating at room temperature (Section 3.2, Scheme 59). Additionally, in the process of studying the regioselectivity in the C–H activation of 1,3-difluoro benzene, it was observed that the ratio of products obtained would vary depending on the boron source employed. Further data was needed to support these observations and an investigation into the electronic and steric effects of Ir catalysed C–H activation was employed to systematically study the role of fluorine substituents and boron sources and their relation to observed results. This work was done in collaboration with Mingyan Ding, Mark Fox and Andrew C. Hones, full experimental data and NMR spectra can be found in Chapter 4 of this volume.

3.2 Results and Discussion

Previous studies have indicated that the regioselectivity of C–H borylation is primarily dictated by steric effects but the small size of the fluorine atom does allow for ortho-borylation to occur should other sites be blocked.[171] At low temperatures, electronic effects were observed with ortho fluorine proving to be highly activating, especially in the borylation of tetra fluorobenzene. This observation was rationalised through computational analysis where an ortho fluorine was estimated to increase the stability of the M–C bond over the original C–H bond in the late transition state that typifies these reactions.

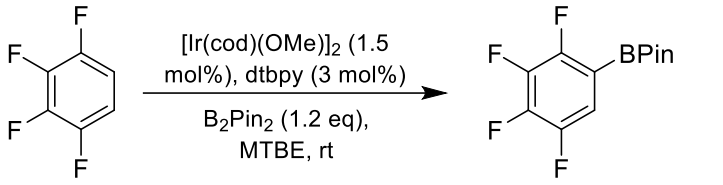

338 **338a**
42%, 96% conversion

Scheme 59: Borylation of 1,2,3,4-tetrafluorobenzene at room temperature

With fluoroarenes readily borylating at room temperatures, complex mixtures from the result of poly-borylation were often observed, especially in compounds that contained multiple di-*ortho* fluorine C–H positions. In these cases, lowering the stoichiometry of the borylating agent allowed for selectivity of C–H activation to be observed. In addition to demonstrating *ortho* borylation to aromatic fluorines is facile, it was also observed that there was a small yet distinct difference in selectivity depending on the boron source used. This effect was initially seen by Minyang Dan in the borylation of 1,3-trifluorobenzene where the use of HBPin resulted in a greater proportion of the 5-borylated product when normalising the ratios to factor for bis-borylation. This was surprising given that the accepted mechanism involved the same catalytic species and rate determining step. Product analysis was complicated by the fact that HBPin is formed as the by-product from the initial reaction with B_2Pin_2. Building on reports that triethylamine is able to coordinate to HBPin, it was proposed that the addition of the tertiary amine would be able to return selectivity with 0.6 eq B_2Pin_2 to resemble that observed with excess B_2Pin_2. Although addition of 1 eq of NEt_3 did not result in the same levels of ortho-selectivity as obtained with excess B_2Pin_2 (Table 5, Entry 3), the subtle yet distinct change from 0.6 eq B_2Pin_2 does indicate that it was able to sequester some HBPin, again demonstrating the slight differences in selectivity obtained by using differing boron sources.

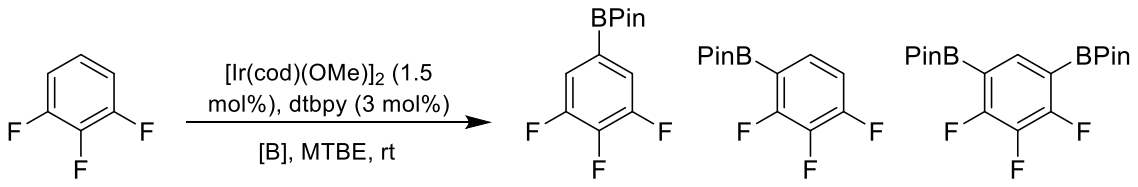

339 **339a** **339b** **339c**

Entry	[B]	Time	Conversion / %	Product distribution (**a** : **b** : **c**)[#]	Adjusted ratio (5:1/3)
1	HBPin (3.0 eq)	16 hr	100	28:10:62	44:56
2	B_2Pin_2 (0.6 eq)[*]	14 hr	86	26:48:26	41:59

3	B_2Pin_2 (0.6 eq), 1eq (NEt_3)	6 hr	60	21:66:13	35:65
4	B_2Pin_2 (3.0 eq)	6 hr	100	19:0:68	32:68

Table 5: Borylation of 1,2,3-trifluorobenzene. [#]Determined by ^{19}F-NMR analysis of crude mixture. [*]Data obtained by Dan Minyang

To investigate further the interplay between electronic and steric control, borylation was carried out on various 2-substituted, 1,3-difluoroarene substrates. This was undertaken in a similar fashion as above with both HBPin and B_2Pin_2 source and ratios of the boronate esters were calculated using ^{19}F-NMR.

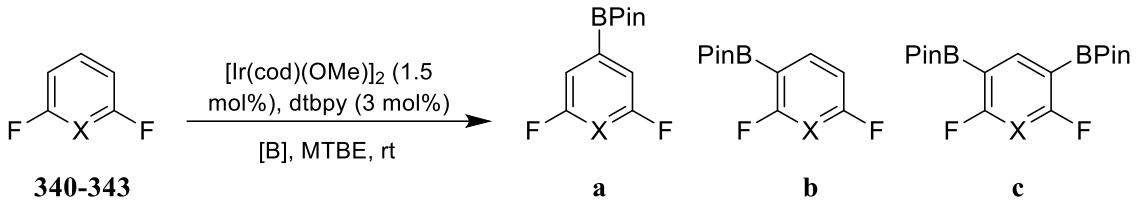

340-343 **a** **b** **c**

Entry	Compound	X	[B]	Equiv.	Time / h	Conv / %	Ratio **a** : **b** : **c**, (**a** : **b** + **c**)[#]
1	**340**	N	HBPin	3.0	5	100	78 : 12 : 10 (88 : 12)
2		N	B_2Pin_2	0.6[*]	3	95	77 : 19 : 4 (87 : 13)
3		N	B_2Pin_2	3.0	4	100	71 : 0 : 29 (83 : 17)
4	**341**	C–Me	HBPin	3.0	16	82	67 : 29 : 4 (80 : 20)
5		C–Me	B_2Pin_2	0.6[*]	14	86	63 : 31 : 6 (77 : 23)
6		C–Me	B_2Pin_2	0.6[#]	16	93	60 : 38 : 2 (75 : 25)
7		C–Me	B_2Pin_2	3.0	6	99	57 : 26 : 16 (73 : 27)
8	**342**	C–OMe	HBPin	3.0	16	80	44 : 46 : 10 (63 : 37)
9		C–OMe	B_2Pin_2	0.6[♯]	16	74	42 : 50 : 8 (59 : 41)
10		C–OMe	B_2Pin_2	3.0	5	100	39 : 0 : 61 (56 : 44)
11	**343**	C–CO_2Me	HBPin	3.0	24	85	72 : 24 : 4, (84 : 16)
12		C–CO_2Me	B_2Pin_2	0.6[*]	19	92	70 : 23 : 7, (82 : 18)
13		C–CO_2Me	B_2Pin_2	3.0	5	100	63 : 0 : 37, (77 : 33)

Table 6: Borylation of 1,3-difluoro substrates. [#]Determined by ^{19}F-NMR analysis of crude mixture. [*]Data obtained by Dan Minyang. [♯] + 1.0 eq NEt_3.

Conversion of the 1,3-difluoro substrates into the respective boronate esters was achieved in excellent yields at room temperature. Of the substituted benzenes (Entries 4-13), the proportion of 4-borylated to 5-borylated product seem to correspond with the electron-withdrawing ability of the 2-substituent with the 5-borylated product being increasingly favoured as substituent electron-withdrawing nature increases. This is also somewhat reflected in the borylation of 2,6-difluoropyridine (Entries 1-3) where a significant increase in the proportion of 5-borylated product was observed when compared to 2,6-difluorotoluene. As with 1,2,3-trifluorobenzene, distinct differences in selectivity were observed depending on the boron source with *ortho* borylation at C–4 being favoured with the use of B_2Pin_2. As mentioned above, Ir catalysed borylation of pyridines present challenges and high temperatures and prolonged periods are often employed to form the boronate ester. As such, literature reports on the regioselectivity of unsubstituted pyridines shows little preference between C-3 and C-4 borylation and most substituted pyridines lead to the 4-borylated product, reflecting simple steric effects. In contrast, borylation of sterically unlimited 2,6-difluoropyridine was able to be carried out at room temperature, leading to selectivity being observed. The ratios of the products followed the general trends observed with the other 1,3-difluoro substrates where employing excess B_2Pin_2 resulted in an increased amount of the C-3 (*ortho* to –F) boronate ester.

To further explore this observation, the scope of the investigation was extended to see if the electronic effects observed with 2,6-difluoropyridine were replicated in other fluorinated pyridines. As before, these substrates were converted to the respective boronate esters at room temperature in good yields, further demonstrating the reactive nature of electron deficient heteroaromatics to Ir catalysed C–H activation. In the three substrates that were chosen (**344**-**346**), borylation occurred preferentially at C–4. Despite ortho fluorine substituents being present in **344** and **345**, this trend was observed regardless. Unlike 2,6-difluoropyridine which showed a distinctive trend in borylation products in relation to the boron source, attempts to rationalise the observed product ratios with **346** as the substrate was inconclusive.

A

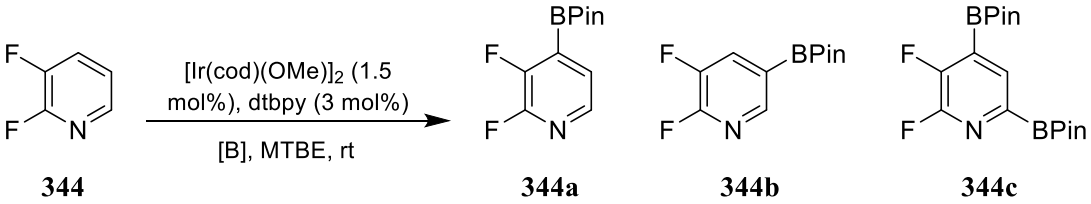

344 **344a** **344b** **344c**

Entry	[B]	Time	Conversion / %	Product distribution (**a** : **b** : **c**) [#]	Adjusted ratio (**b** : **a**+**c**)
1	HBPin (3.0 eq)	5 hr	100	71 : 15 : 14	15 : 85
2	B_2Pin_2 (0.6 eq)	5 hr	97	62 : 20 : 18	20 : 80
3	B_2Pin_2 (3.0 eq)	5 hr	100	67 : 24 : 76	24 : 76

B

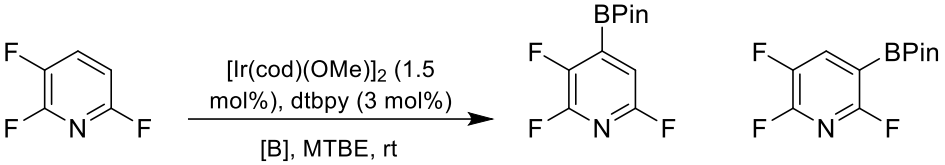

345 **345a** **345b**

Entry	[B]	Time	Conversion / %	Product distribution (**a** : **b**) [#]
1	HBPin (3.0 eq)	5 hr	100	89 : 11
2	B_2Pin_2 (0.6 eq)	4 hr	95	88 : 12
3	B_2Pin_2 (3.0 eq)	4 hr	100	94 : 6

C

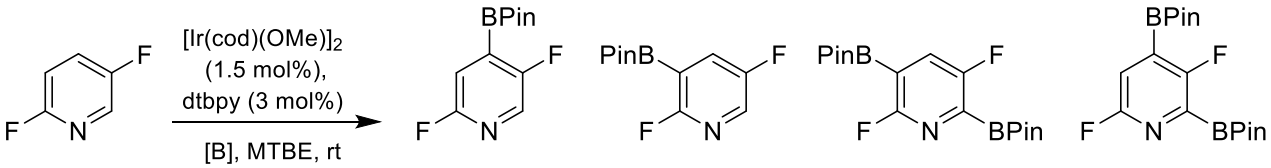

346 **346a** **346b** **346c** **346d**

Entry	[B]	Time	Conversion / %	Product distribution (**a** : **b** : **c** : **d**)[#]	Adjusted ratio (**b**+**c** : **a**+**d**)
1	HBPin (3.0 eq)	5 hr	100	76 : 15 : 4 : 5	19 : 81
2	B_2Pin_2 (0.6 eq)	5 hr	98	77 : 19 : 2 : 2	21 : 79
3	B_2Pin_2 (3.0 eq)	4 hr	100	52 : 0 : 32 : 16	16 : 84

Table 7: Borylation of fluoropyridines. [#]Determined by ^{19}F-NMR analysis of crude mixture.

To evaluate if the differences in boronate ester ratios when differing boron sources are employed was simply down to steric considerations, a model experiment was devised using a smaller source of boron. Thus, B_2eg_2 (**348**) was synthesized using conditions described by Eck *et al*.[175] where $B_2(NMe_2)_4$ (**347**) was treated with ethylene glycol in 6M HCl in ether. Purification by sublimation gave the desired compound as white crystals as characterised by a single peak in ^{1}H–NMR δ 3.50 (8H, s) corresponding to the aliphatic $–CH_2$ protons.

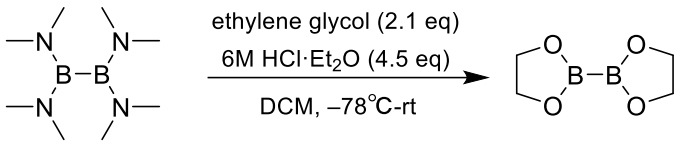

347 **348**

Scheme 60: Synthesis of B_2eg_2

Surprisingly, borylation using B_2eg_2 (**348**) as a boron source proved challenging primarily due to its poor solubility and low reactivity of the associated Ir complex. Borylation of anilines using B_2eg_2 (**340**) and 2.0 eq. of NEt_3 at 80 °C a had been described previously by Smith III *et al*. [176] These conditions were modified to borylate 2,6-difluoropyridine (**340**). Pervious reports on the use of B_2eg_2 in borylations also comment on the inherent instability of the resulting boronate esters. As such, the reaction was conducted in a Young's tap NMR tube in D_8-THF. As the use of elevated temperatures challenges comparisons with earlier reactions, control experiments were conducted in parallel using HBPin and B_2Pin_2.

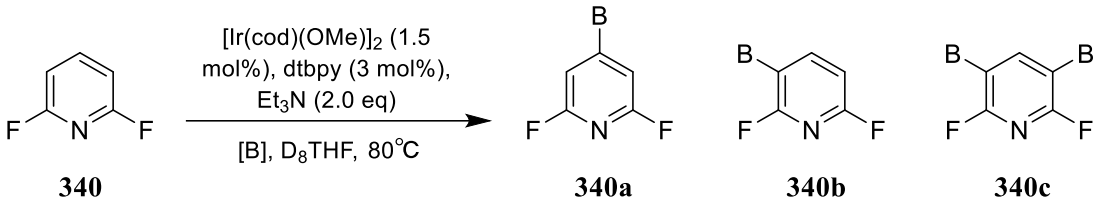

Entry 1: B = Beg
Entry 2,3: B=BPin

Entry	[B]	Time	Conversion / %	Product distribution (**a** : **b** : **c**)	Adjusted ratio (**a** : **b** + **c**)
1	B_2eg_2 (3.0 eq)	8 hr	23	85 : 12 : 0	93 : 7
2	$HBpin_2$ (3.0 eq)	8 hr	89	26 : 15 : 59	26 : 74
3	B_2Pin_2 (3.0 eq)	6 hr	100	4 : 12 : 84	27 : 73

Table 8: Borylation of 2,6-difluoropyridine using B_2eg_2. #Determined by ^{19}F-NMR analysis of crude mixture.

Despite the low conversion, borylation using B_2eg_2 also resulted in preferential C–4 borylation. Although it was unsurprising that no difference in regioselectivity was observed between B_2pin_2 and HBpin at 80 °C, the reversal of regioselectivity to form majority C–3 borylated product was unexpected. In comparing the ^{19}F–NMR spectra of entries 1 and 2 (Figure 61), there were slight differences in the observed chemical shifts was attributed to the two spectra being run in different solvents. Interestingly, a new peak in the reaction with B_2eg_2 (**348**) was observed at δ –75.15 which was speculated to correspond to a B_2eg_2–pyridine complex. It was thus hypothesised that the regioselectivity observed when using B_2eg_2 as the boron source was a result of this complexation which would enhance the electron withdrawing abilities of the azinyl nitrogen, further activating the C–4 position.

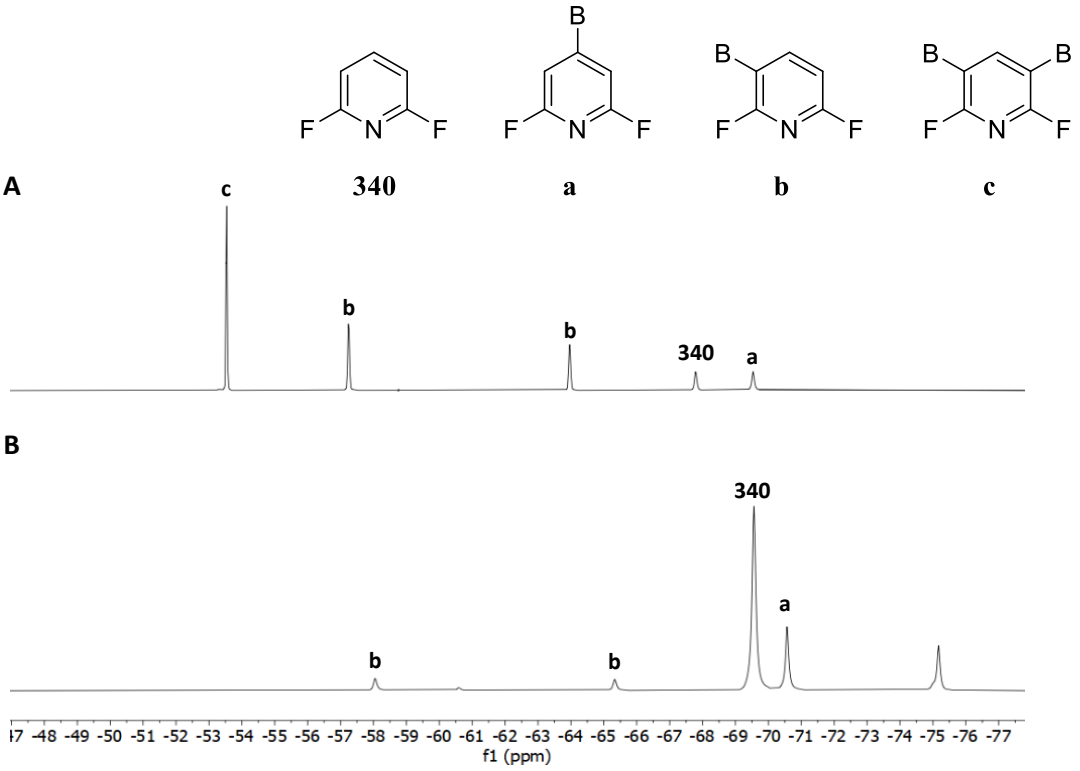

Figure 61: Crude ^{19}F-NMR spectrum in the borylation of 2,6-difluoropyridine using (**A.**) B_2Pin_2 and (**B.**) B_2eg_2.

To support this hypothesis, an additional experiment was conducted where 1 eq of B_2eg_2 and 2,6-difluoro pyridine were prestirred for 1 hour at 80 °C before the addition of B_2pin_2 and the catalytic cocktail. From this reaction, it was observed that borylation preferentially occurred at C–4, supporting the proposal that B_2eg_2 is able to enhance the electron withdrawing abilities of the azinyl nitrogen via the formation of a "complex."

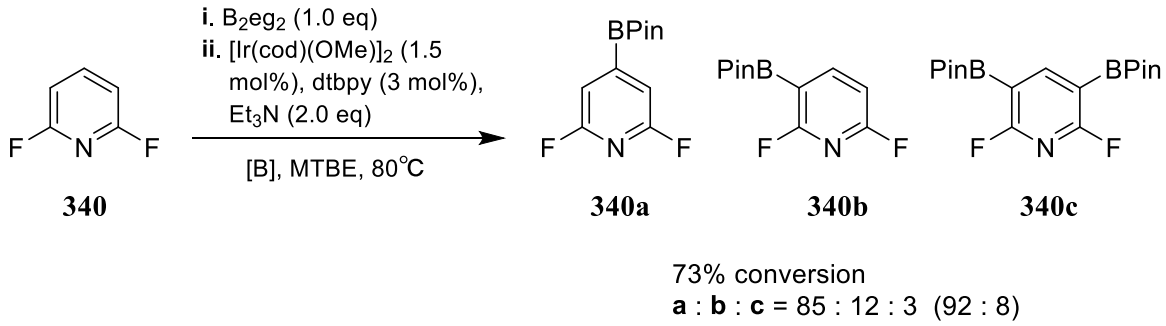

Scheme 61: Borylation of 2,6-difluoropyridine using B_2Pin_2 in the presence of B_2eg_2. Ratios determined by ^{19}F-NMR analysis of crude mixture.

Ultimately, when considering the non-basic nature of the substrate, this observation was surprising. A two fluoro-substituent reduces the pKa to -0.22 from 5.17 of unsubstituted pyridine and it can be reasonably assumed that 2,6-difluoropyridine (**340**) would be even less basic, making the formation of the B_2eg_2-**340** "complex" unlikely. Conversely, experimental data does indicate some interaction increasing the electronic selectivity of borylation. With B_2eg_2 being significantly less sterically demanding than B_2pin_2, one possible explanation is that the small size and increased Lewis acidic nature increase the probability of it forming an interaction with the azinyl nitrogen.

3.3 Conclusions and future work

This study was able to demonstrate the highly reactive nature of fluoroarenes to Ir catalysed C–H borylation, with all substrates reacting readily at room temperature. Whereas steric considerations normally dominate, the small size of the fluorine atom means that electronics can also play a major role in the determination of regioselectivity. This work also showed that differences in regioselectivity can arise depending on the boron source employed. A general trend was observed where increasing the stoichiometry of B_2Pin_2 resulted in more *ortho*-borylation. Sterics was proposed as an explanation to these observations but subsequent experiments with the smaller B_2eg_2 were only achievable at 80 °C, erasing the stereoselectivity observed at room temperature.

As illustrated in Scheme 53, HBPin and B_2Pin_2 are used interchangeably in the catalytic cycle, forming the same active species. The observations reported above challenges this accepted mechanism as the differences in regioselectivity indicate a slight divergence in the mechanism depending on the boron source employed. This conjecture is supported in a recent report by Smith and Maleczka et al.[177] where modification of the steric and electronic properties of the ligand were able to generate even greater differences in selectivity between HBPin and B_2Pin_2.

Although further investigation is required, the possible complexation of B_2eg_2 to the azinyl nitrogen raises interesting possibilities surrounding the regioselective control in the Ir catalysed borylation of pyridines. Future work could explore various Lewis acids that can complex with the azinyl nitrogen and are also compatible with Ir borylation. Building on the observations from the study outlined above, this could be an alternative method in increasing the selectivity of borylation to the C–4 position.

Chapter 4: Volume II Experimental Methodology and NMR Data

4.1: General Procedure for the borylation of fluoro-arenes.

An oven-dried Biotage microwave vial was sealed and subjected to three N_2 evacuation/refill cycles, followed by the addition of the corresponding fluoroarene (1.00 mmol, 1.0 equiv.). In a separate oven-dried Schlenk tube was charged with $[Ir(COD)(OMe)]_2$ (9.9 mg, 1.5 mol%), dtbpy (8.1 mg, 3.0 mol%), and bis(pinacolato)diboron (B_2pin_2) / pinacolborane (HBPin) / 2-(1,3,2-dioxaborolan-2-yl)-1,3,2-dioxaborolane (B_2eg_2) (0.6 equiv. 3 equiv). The vessel was sealed and subjected to three N_2 evacuation/refill cycles before anhydrous MTBE (1.0 mL) was added. Once the solids were completely dissolved, this black active catalyst solution was transferred into the microwave vial using a syringe. For reactions using B_2eg_2, the corresponding fluoroarene was added to a sealed vial containing the catalytic cocktail and 1.0 eq of NEt_3.The reaction was stirred at the temperature stated before being monitored by ^{19}F-NMR or GC-MS. Upon completion, the volatiles were then removed *in vacuo* and the desired borylated product was isolated following purification by flash column chromatography with the appropriate solvent system.

348. *2-(1,3,2-dioxaborolan-2-yl)-1,3,2-dioxaborolane (B_2eg_2)*

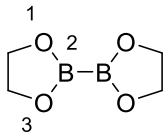

Conc. H_2SO_4 (20.0 mL, 0.375 mol) was added dropwise to $CaCl_2$ (20.0 g, 0.180 mol) in a sealed, oven dried flask. The generated HCl was then pumped into dry ether (400 ml) kept at 0°C. The ether was allowed to warm to room temperature, allowing the pressure to equalized and cooled again to repeat the gas passing procedure until the titrated concentration of the etherified HCl was between 5.5 and 6M. To a flask charged with $B_2(NMe_2)_4$ (1.0 mL, 0.005 mol, 1.00 eq) in DCM (10.8 mL), ethylene glycol (0.593 mL, 0.011 mol, 2.10 eq) was added and the mixture was cooled to -78 °C. The etherified HCl was precooled to -78 °C and added dropwise to the mixture over a period of 1 hour. The mixture was stirred at the condition until the formation of ammonium salt precipitates were observed after which it was allowed to reach ambient temperature and stirred overnight. Upon completion of the reaction, volatiles were evaporated, and the resulting residue was taken up in toluene. The mixture was then filtered and the filtrate was washed with additional portions of toluene. The resulting mixture was concentrated, resulting in a light-yellow solid which was purified via sublimation to yield the title compound as a white crystal (0.20 g, 0.001 mol, 28%). δ_H (400 MHz, $CDCl_3$) 4.23 (4–H_2). δ_C (101

MHz, $CDCl_3$) 65.6 (C–4). δ_B (128 MHz, $CDCl_3$) 30.9 (B–2). Data agrees with that as reported in Eck *et al*.[175]

4.2: ^{19}F-NMR:

Ratios were calculated using crude ^{19}F-NMR spectra which are presented below. Full characterisation of boronate esters was carried out by Mingyan Dang.

348. *2-(1,3,2-dioxaborolan-2-yl)-1,3,2-dioxaborolane*

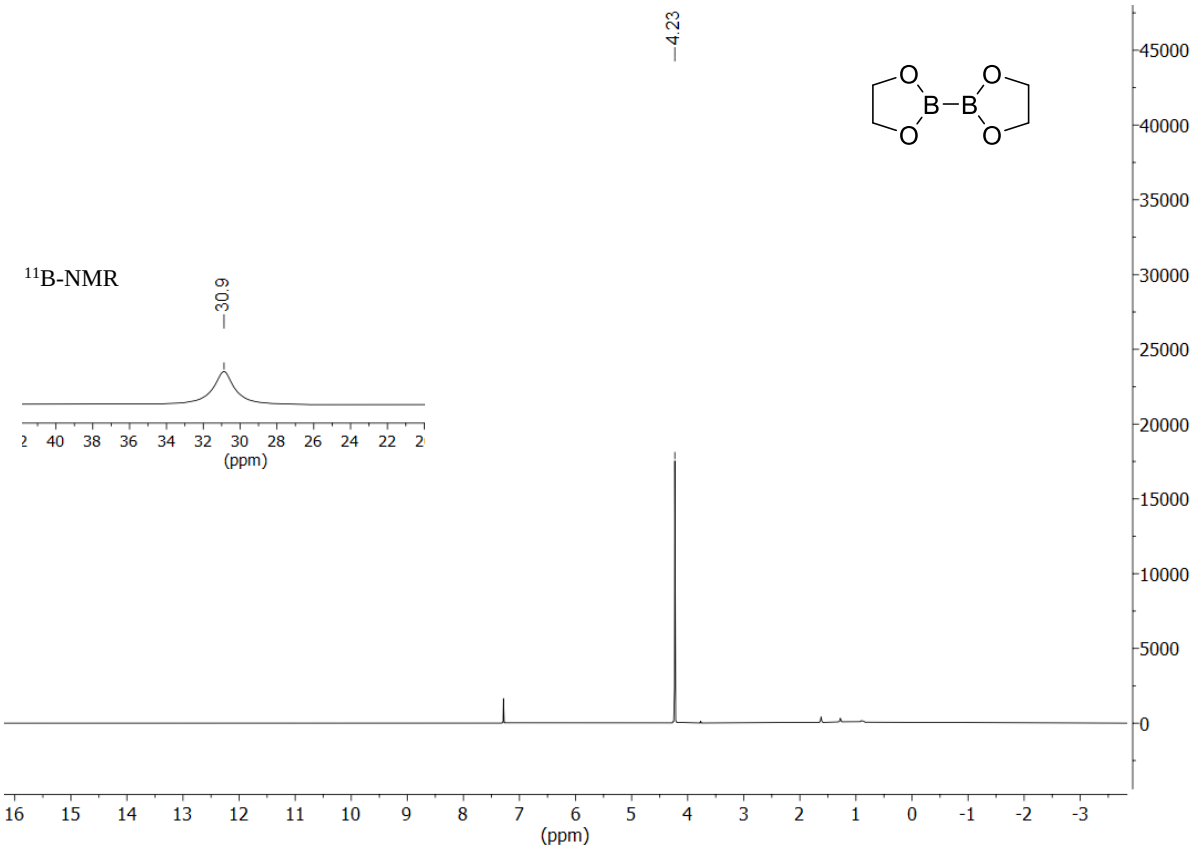

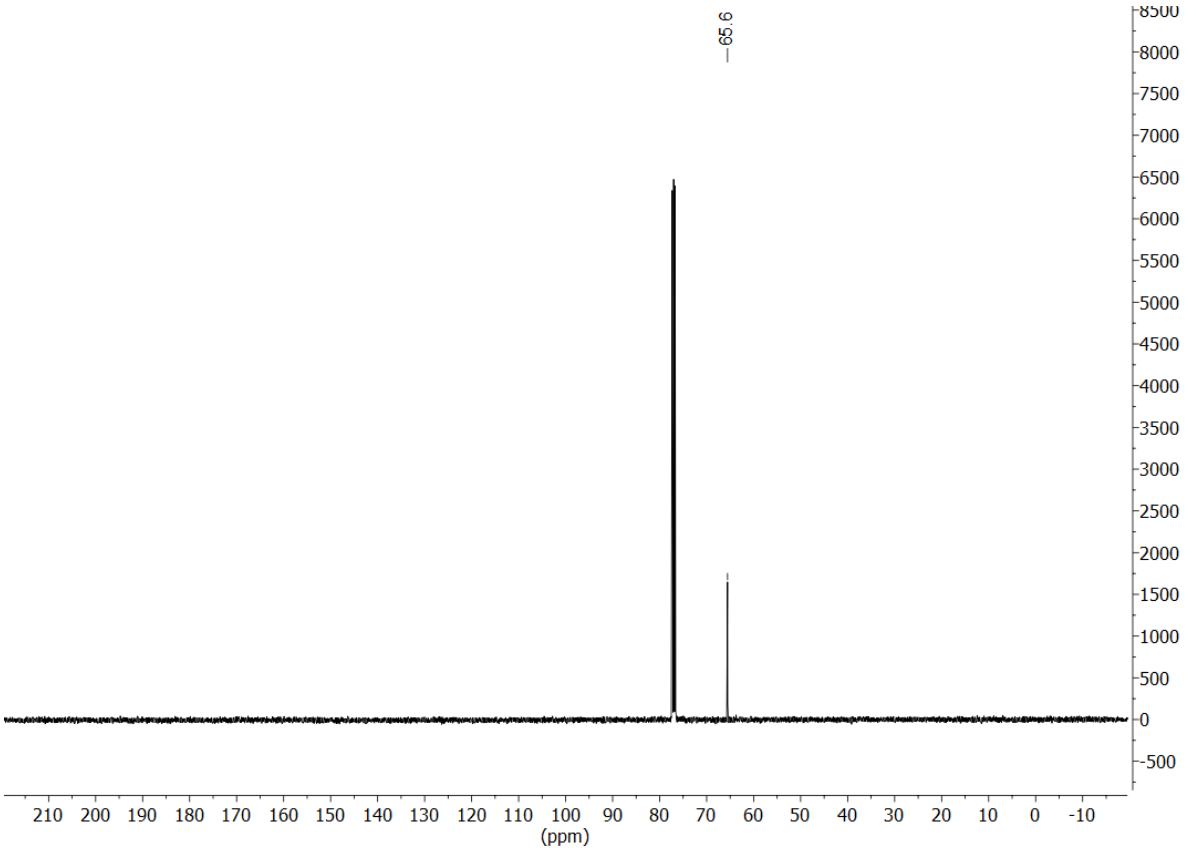

Table 5: Entry 1

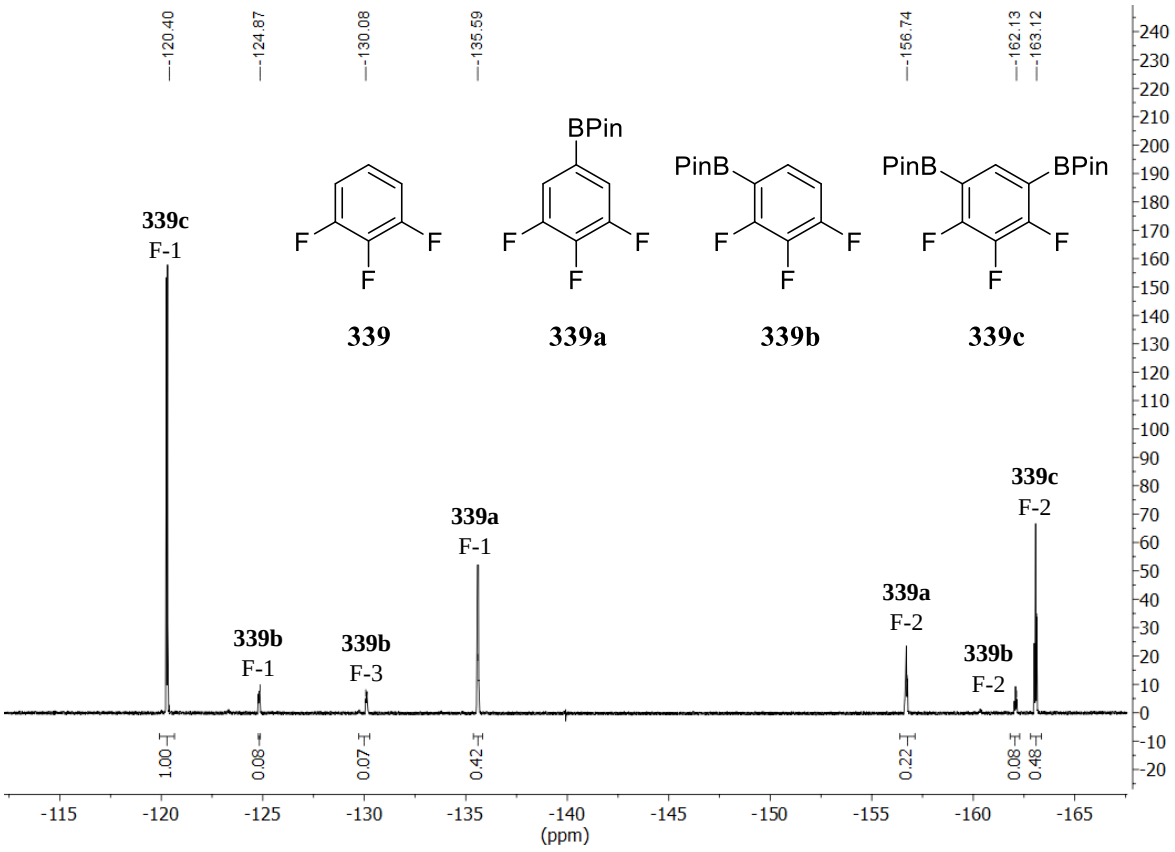

Table 5: Entry 3

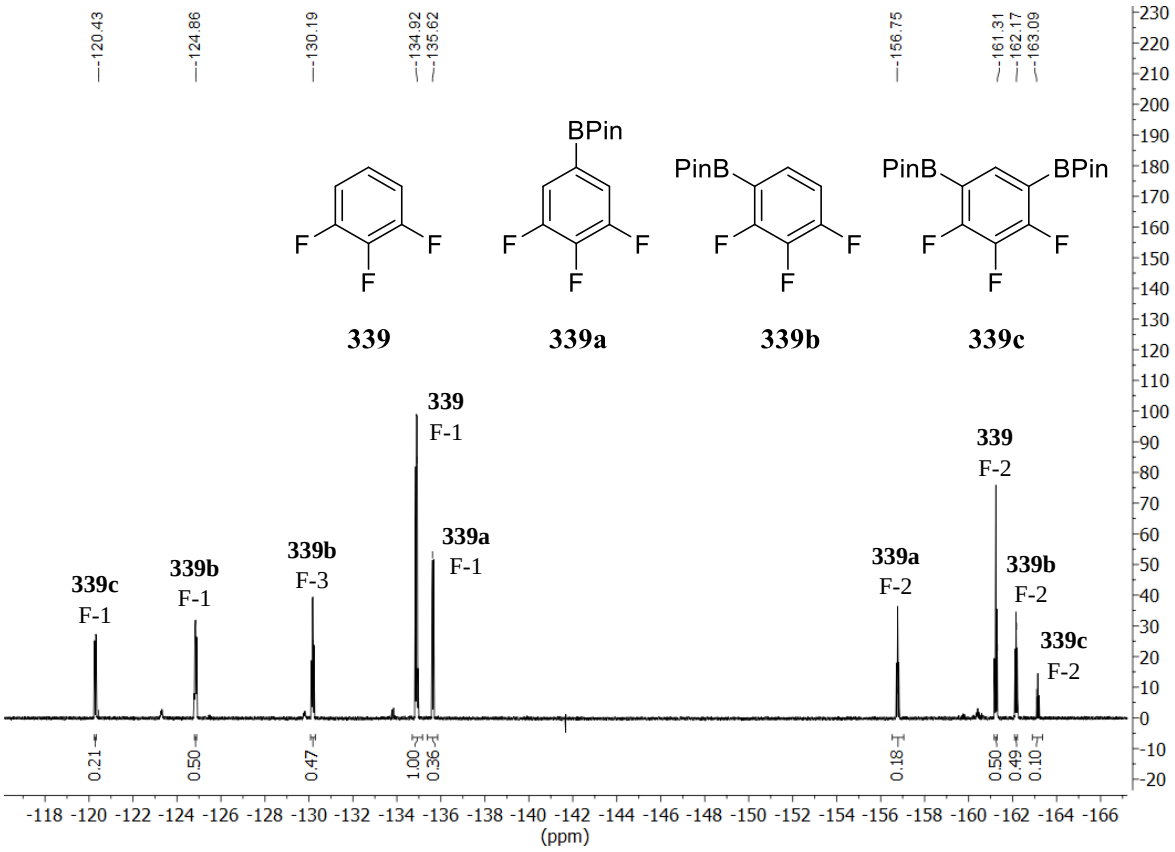

Table 5: Entry 4

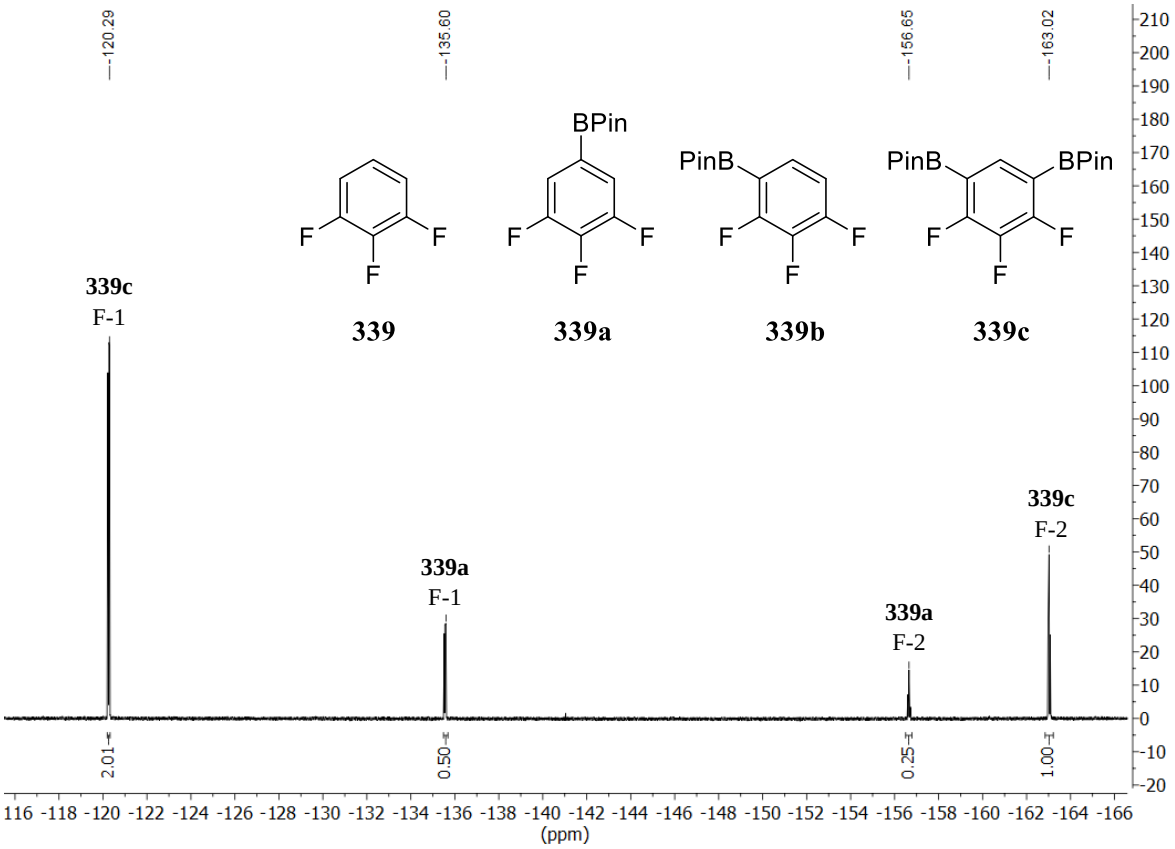

Table 6: Entry 1

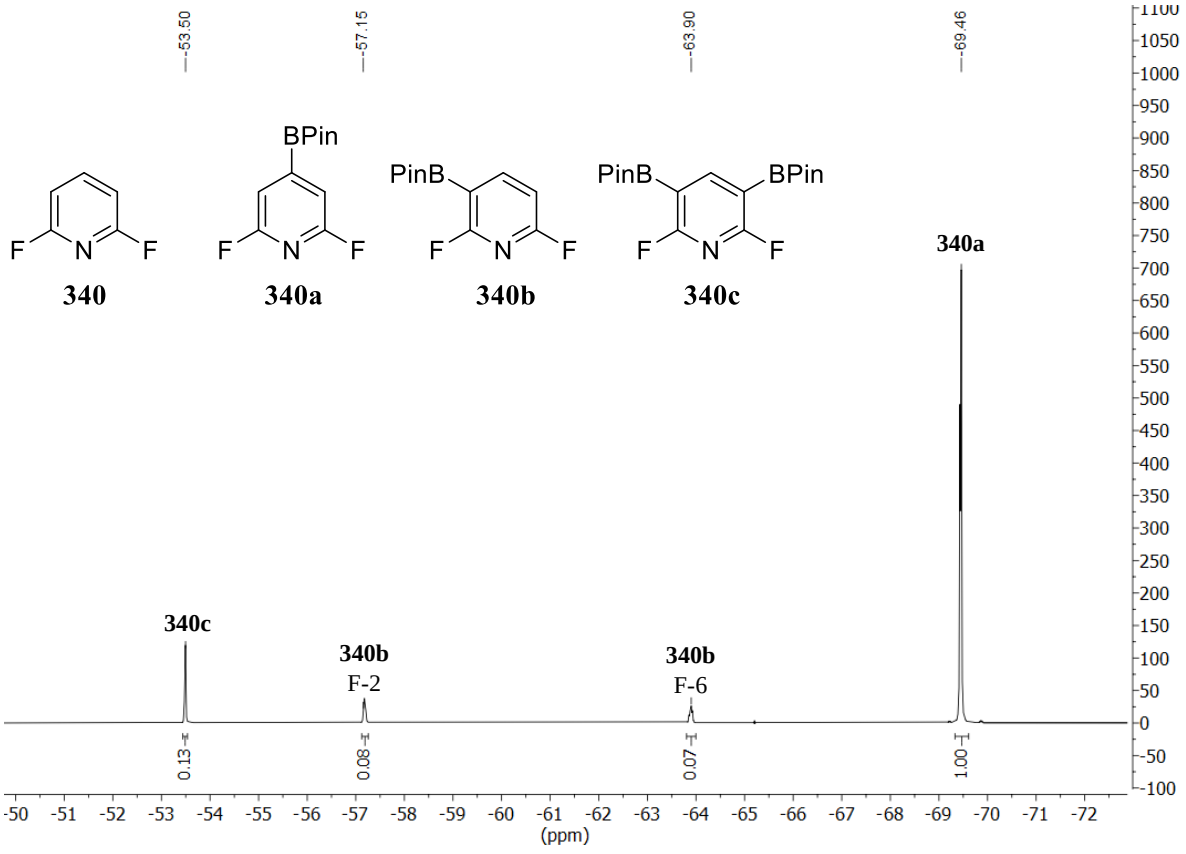

Table 6: Entry 3

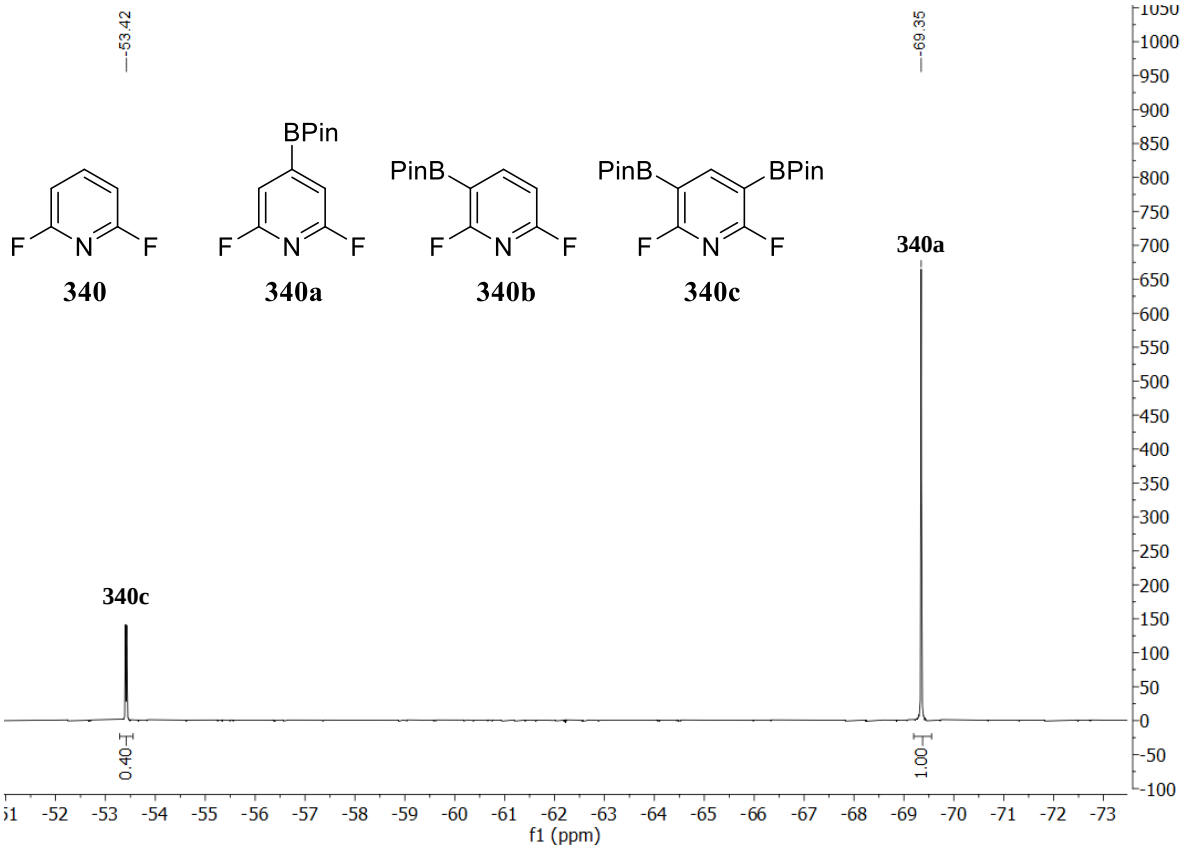

Table 6:Entry 4

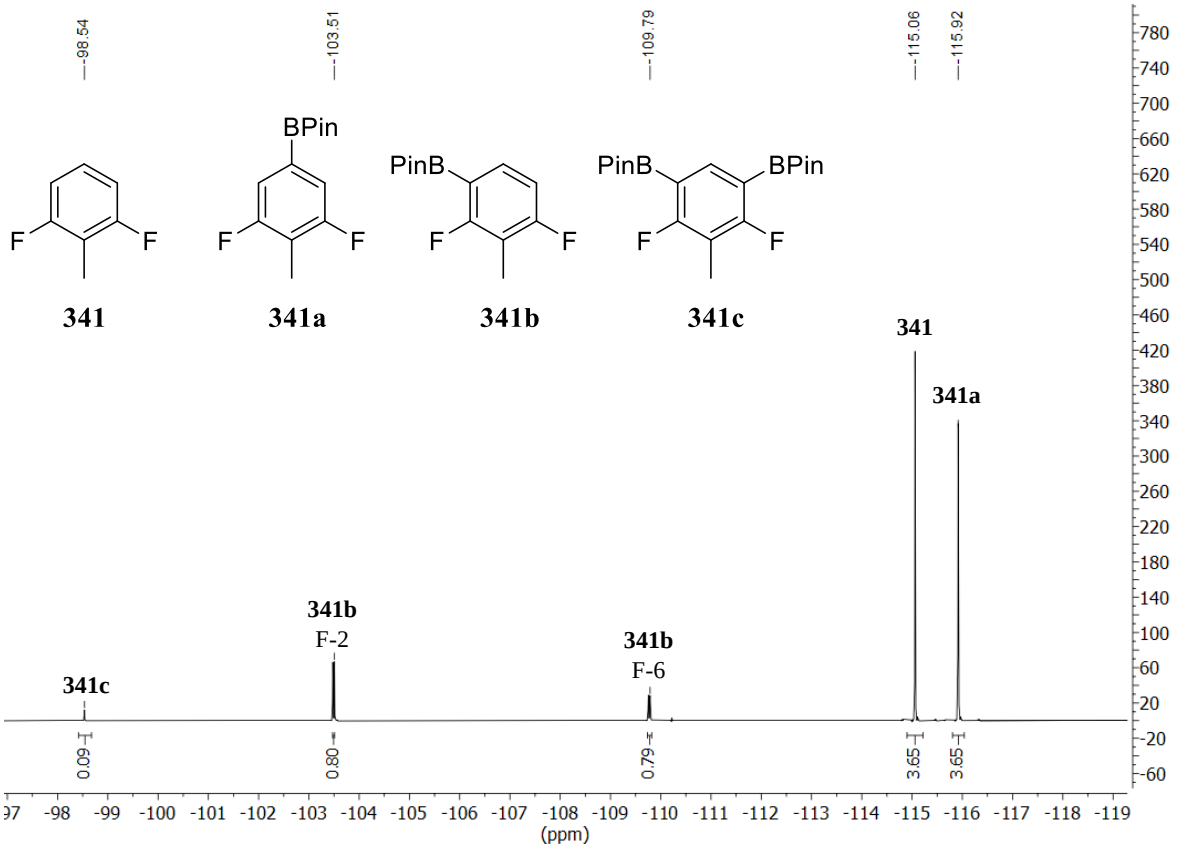

Table 6: Entry 6

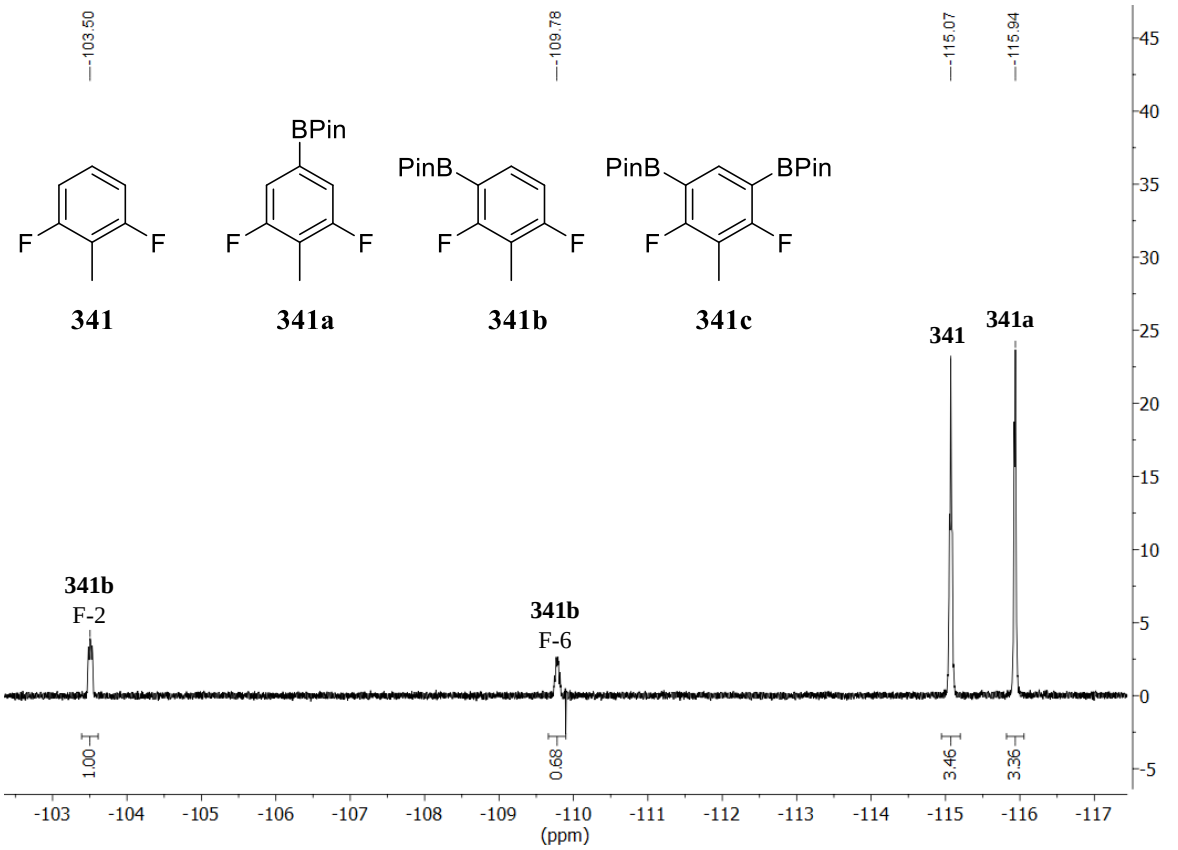

Table 6: Entry 7

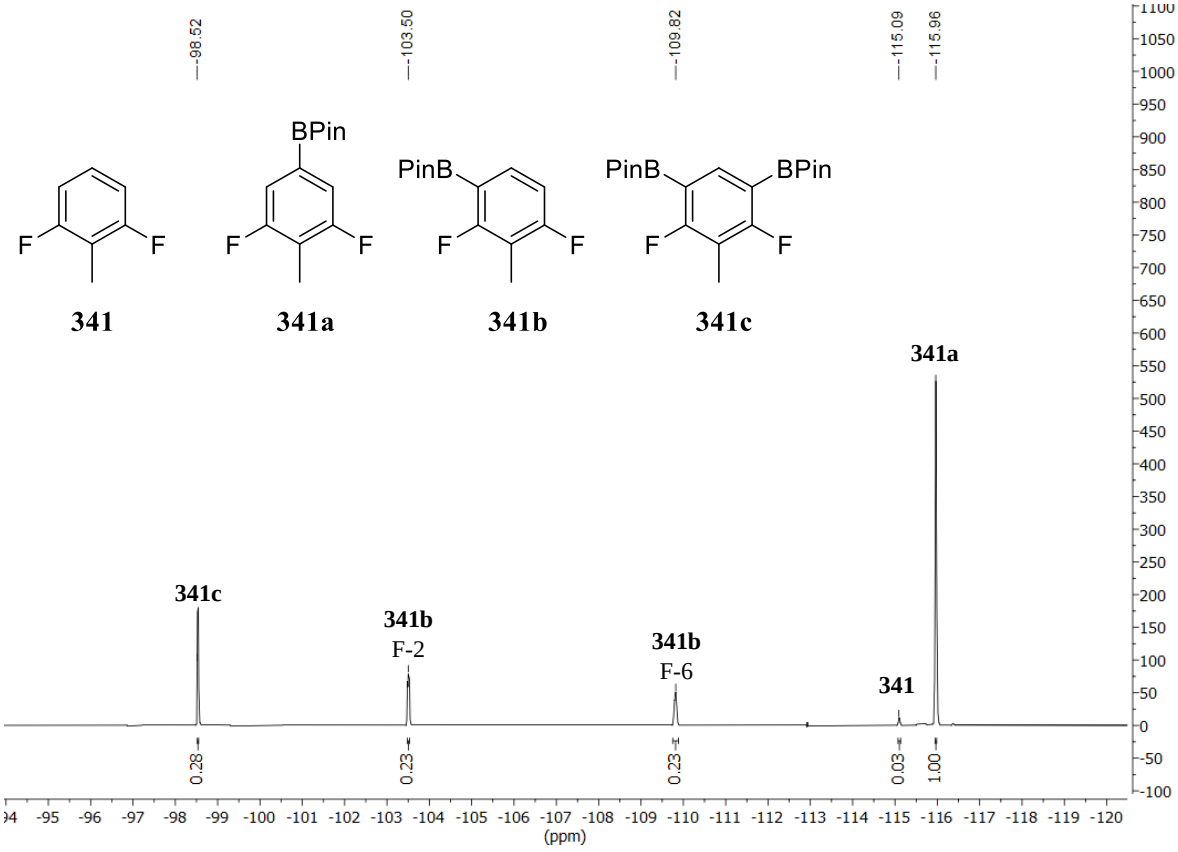

Table 6: Entry 8

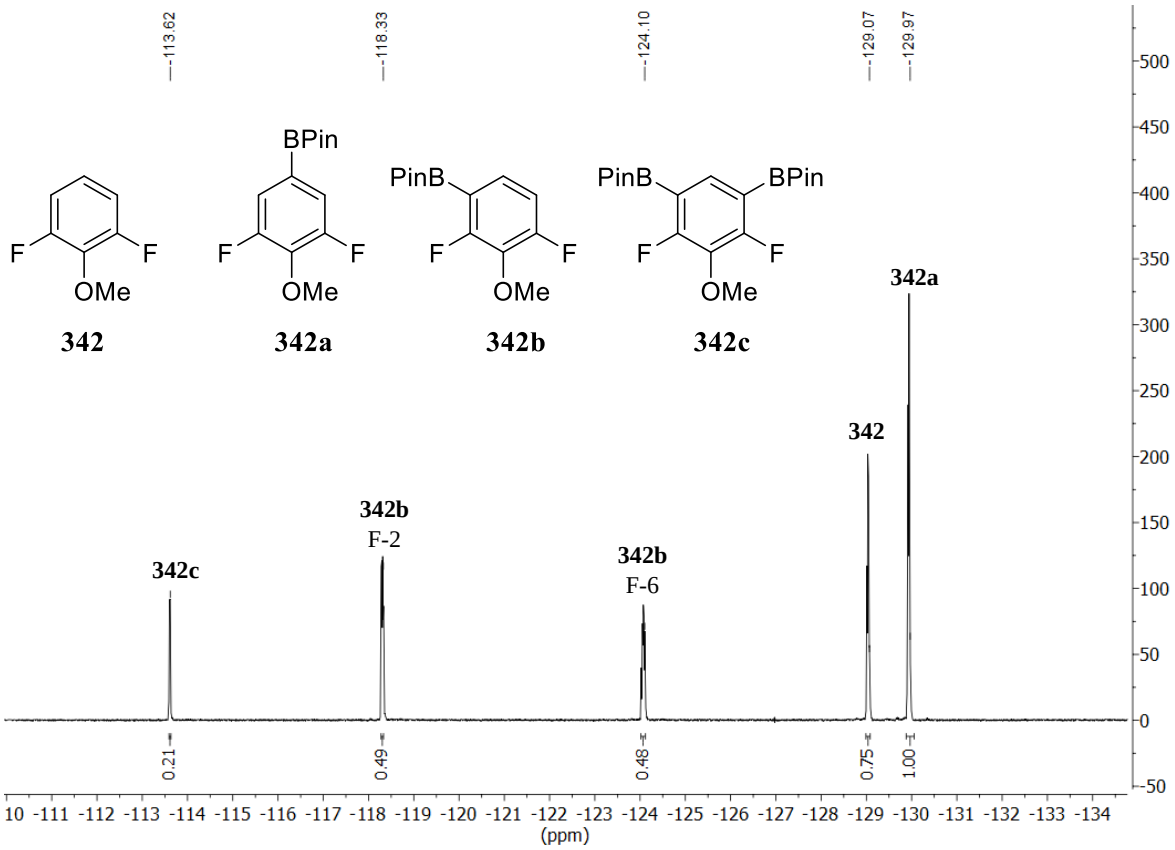

Table 6: Entry 10

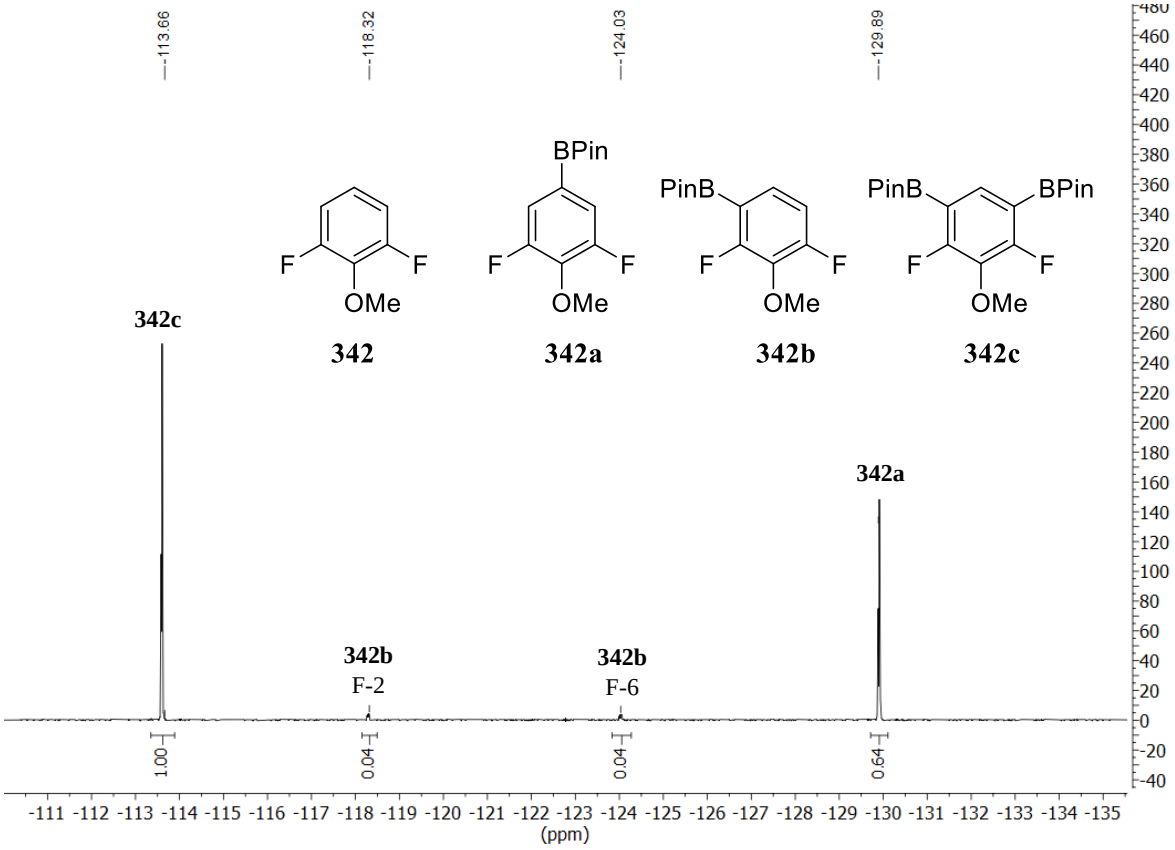

Table 6: Entry 11

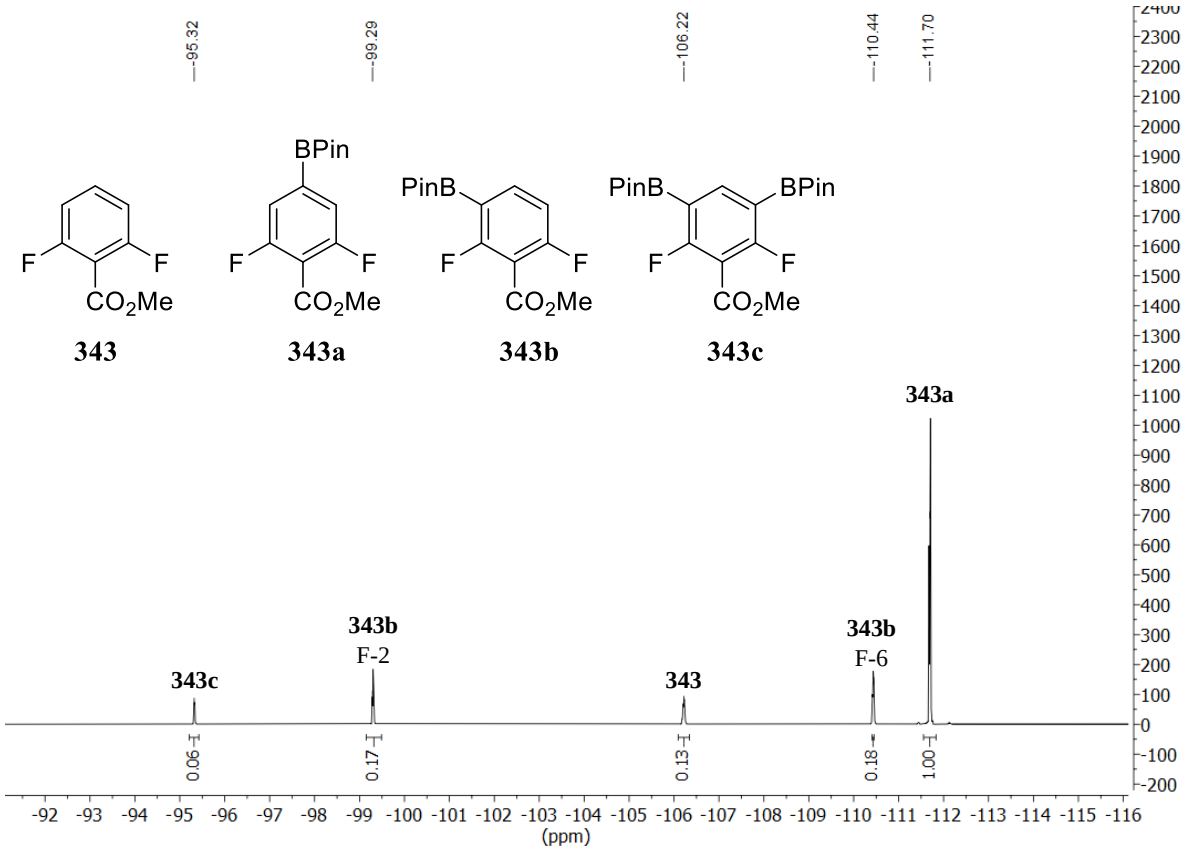

Table 6: Entry 13

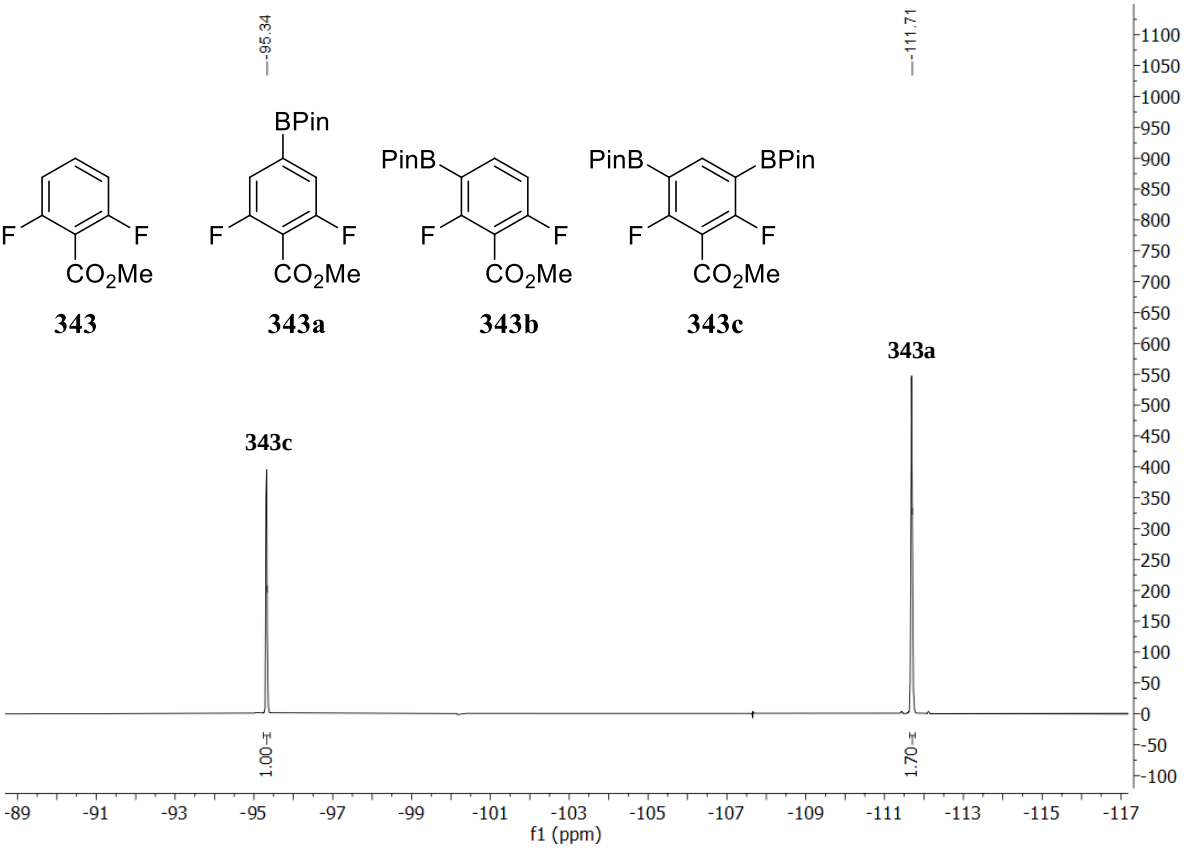

Table 7 (**A**): Entry 1

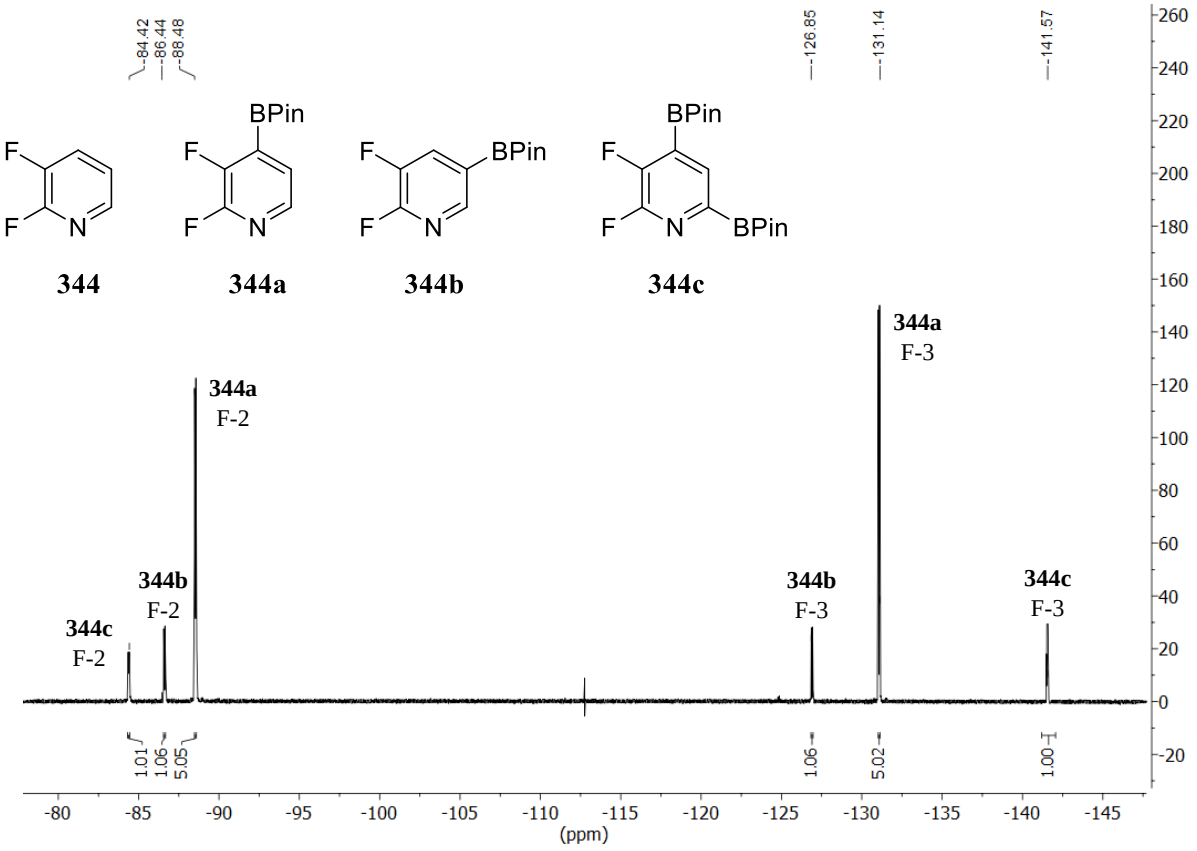

Table 7 (**A**): Entry 2

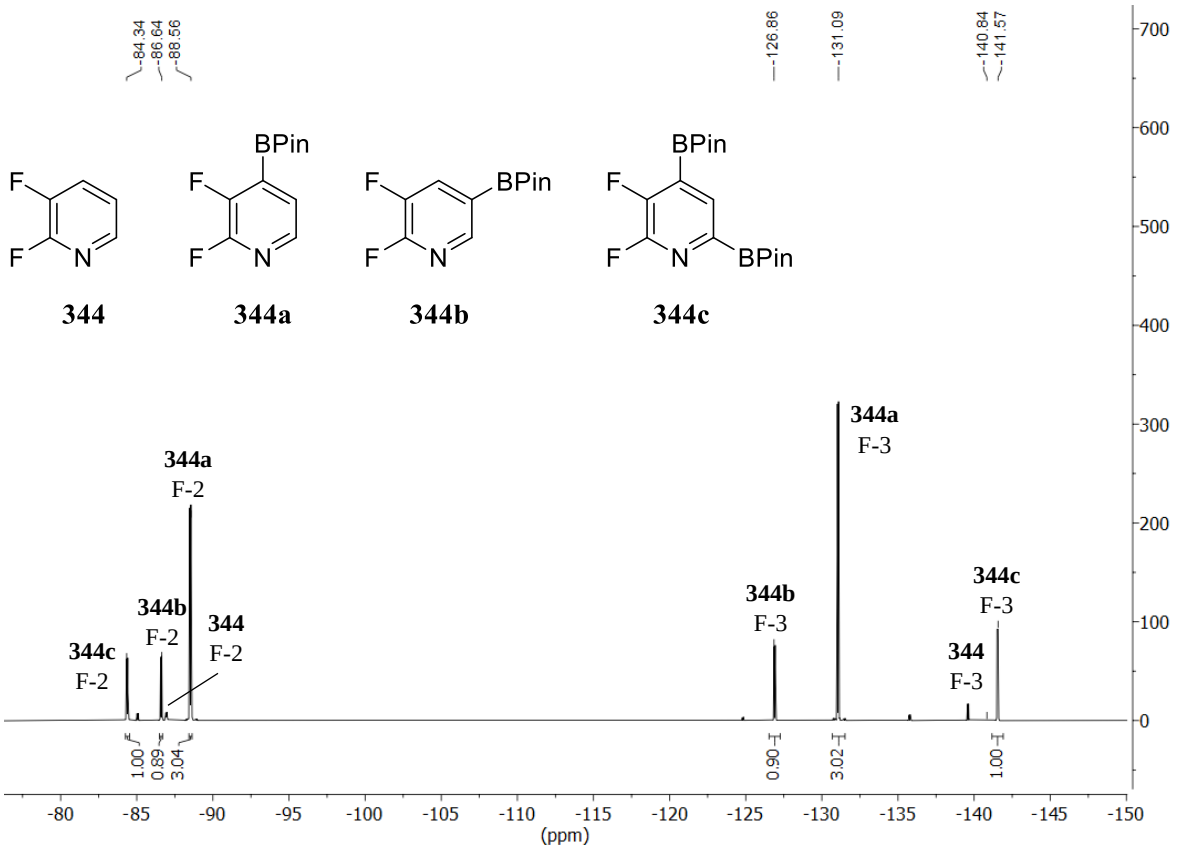

Table 7 (**A**): Entry 3

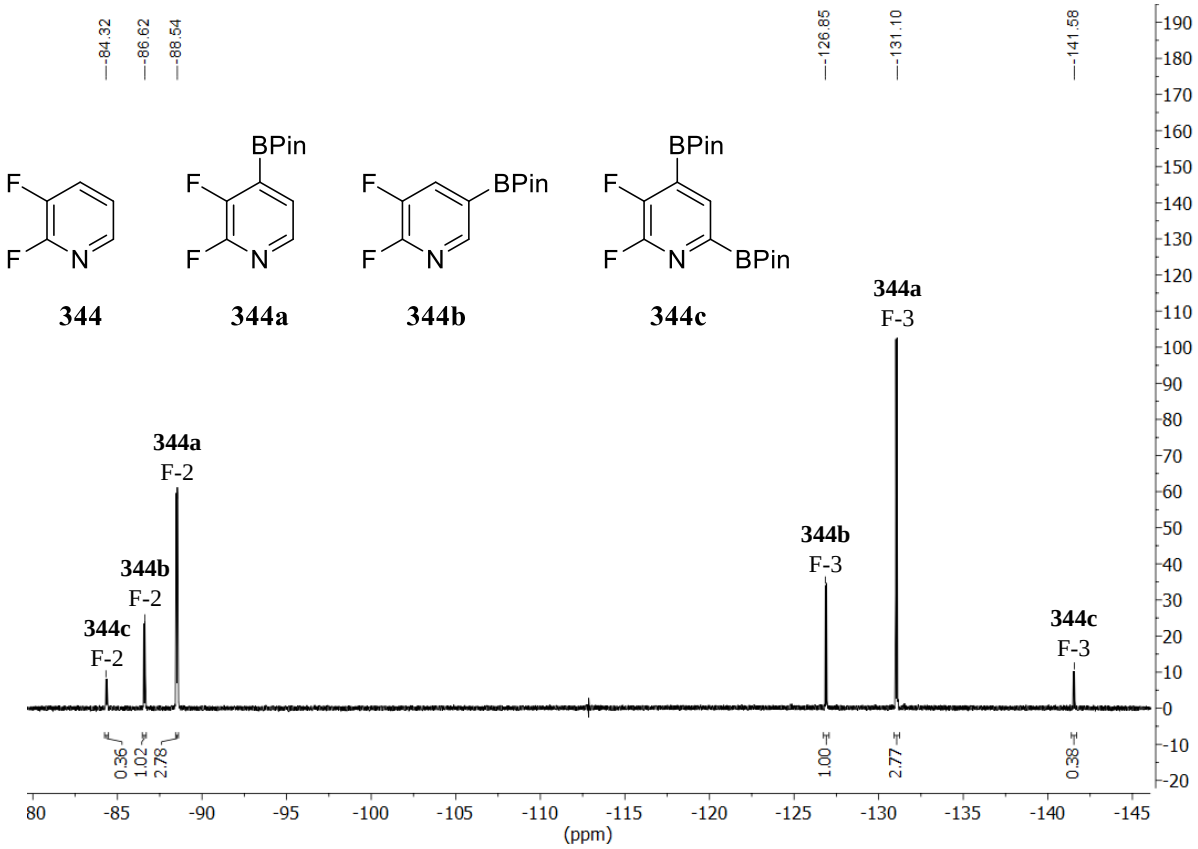

Table 7 (**B**): Entry 1

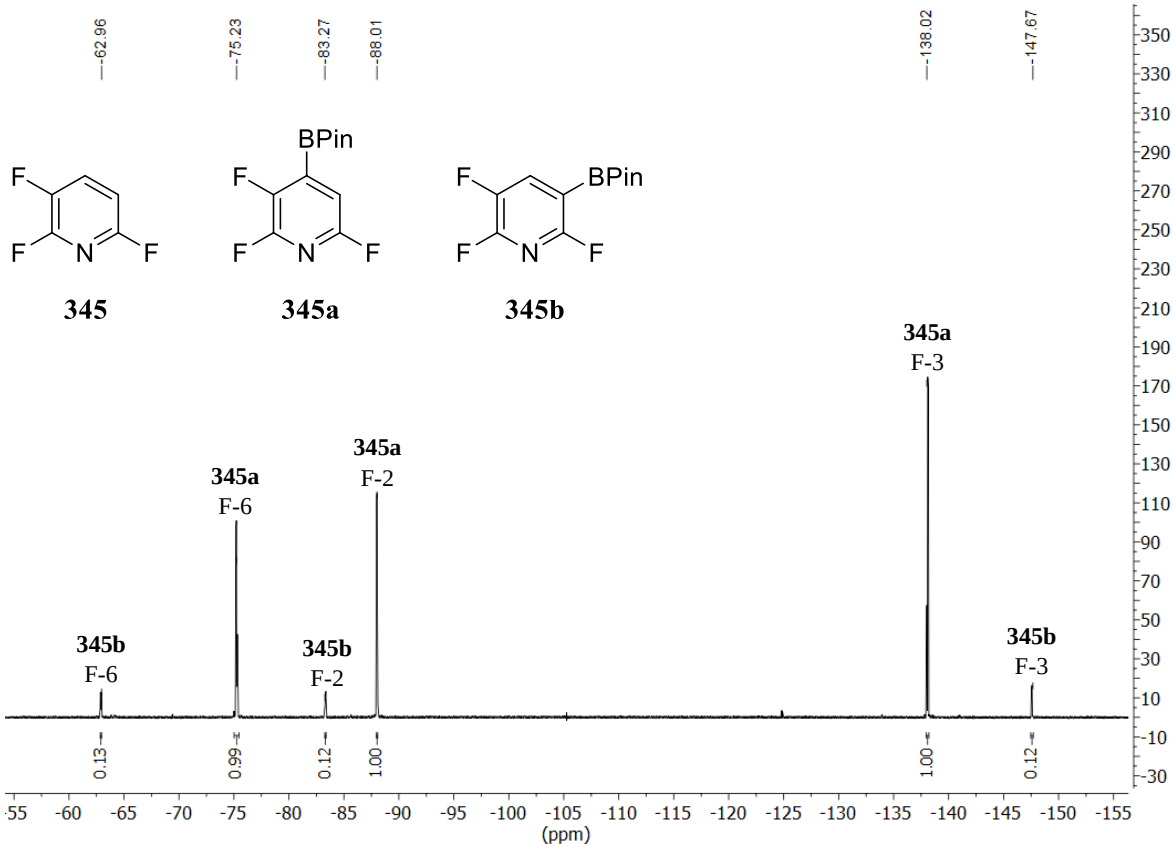

Table 7 (**B**): Entry 2

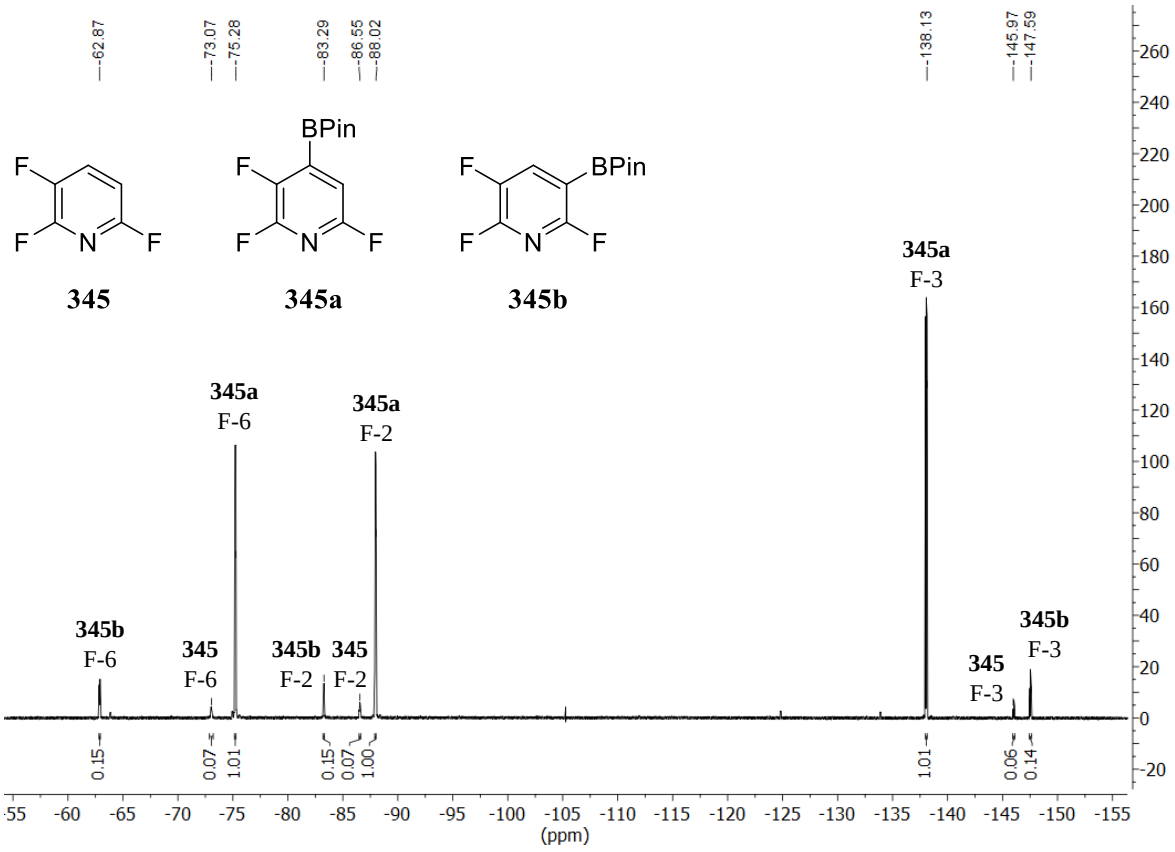

Table 7 (**B**): Entry 3

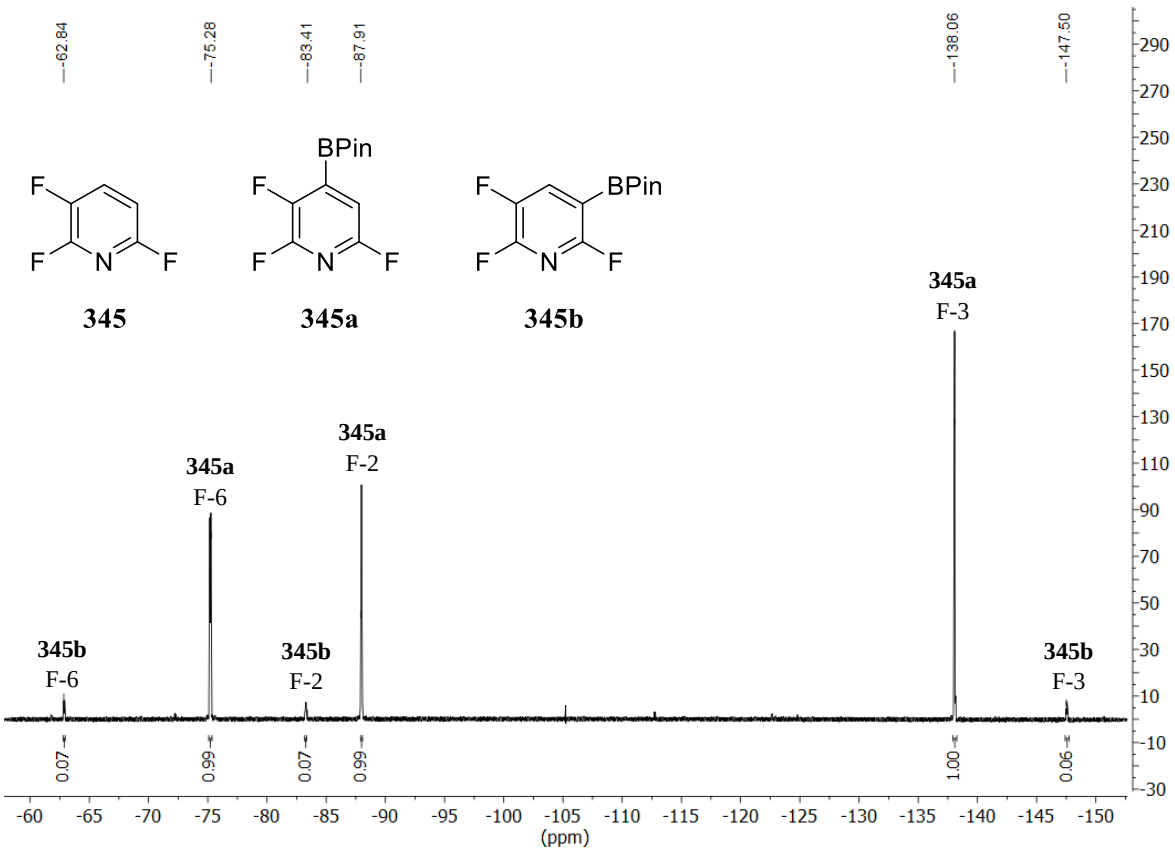

Table 7 (**C**): Entry 1

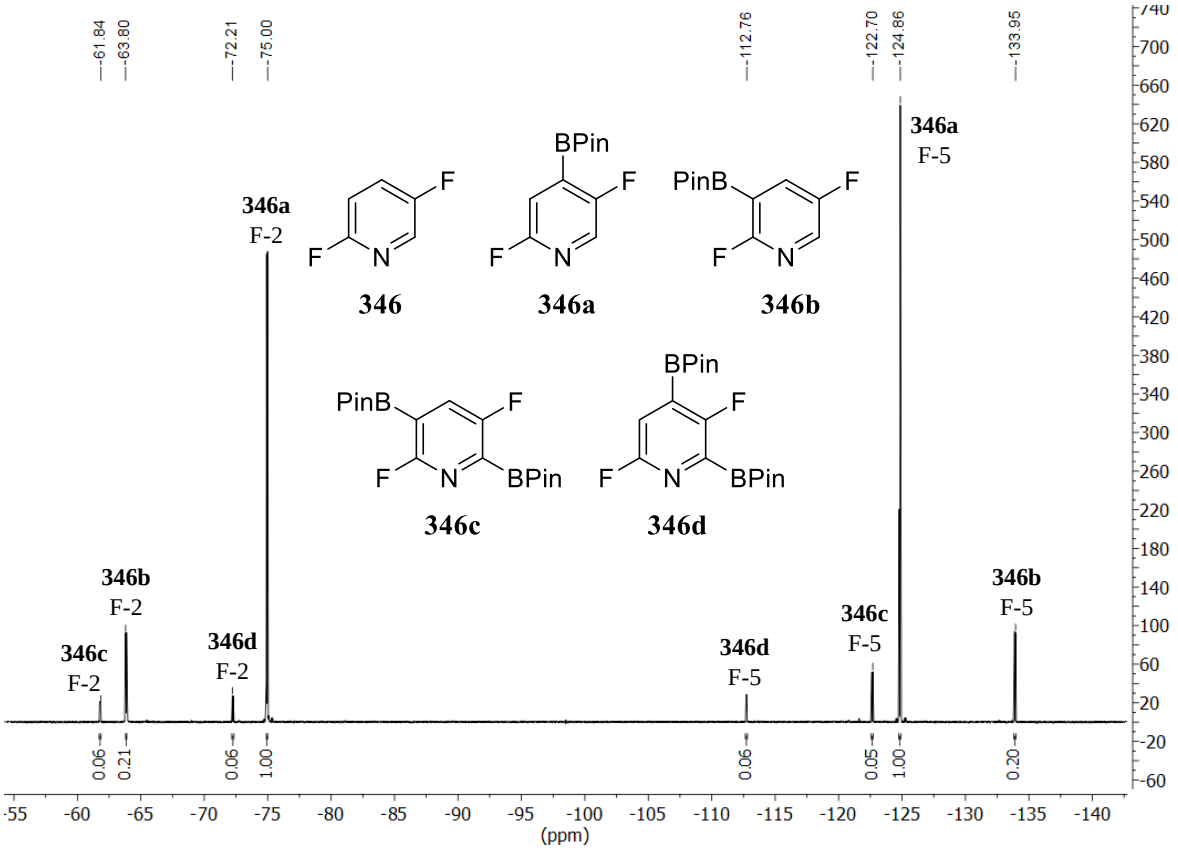

Table 7 (**C**): Entry 2

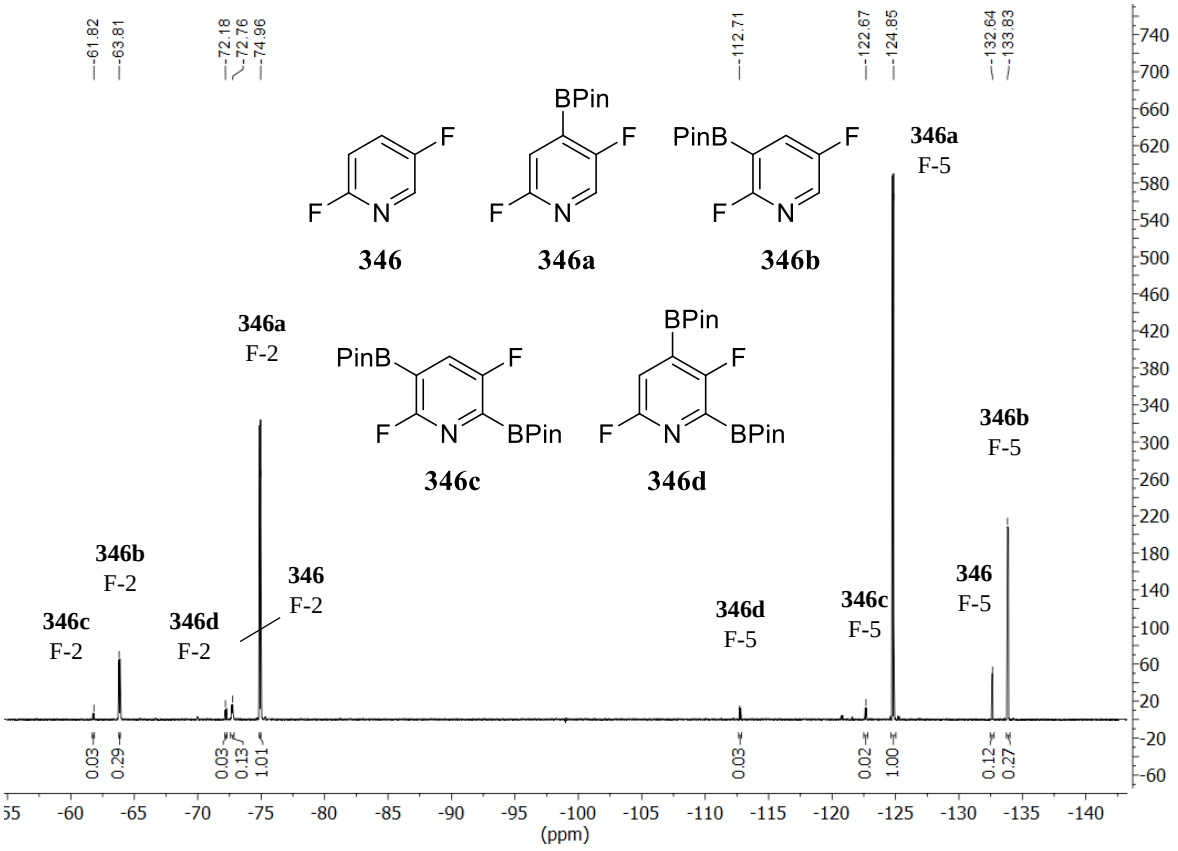

Table 7 (**C**): Entry 3

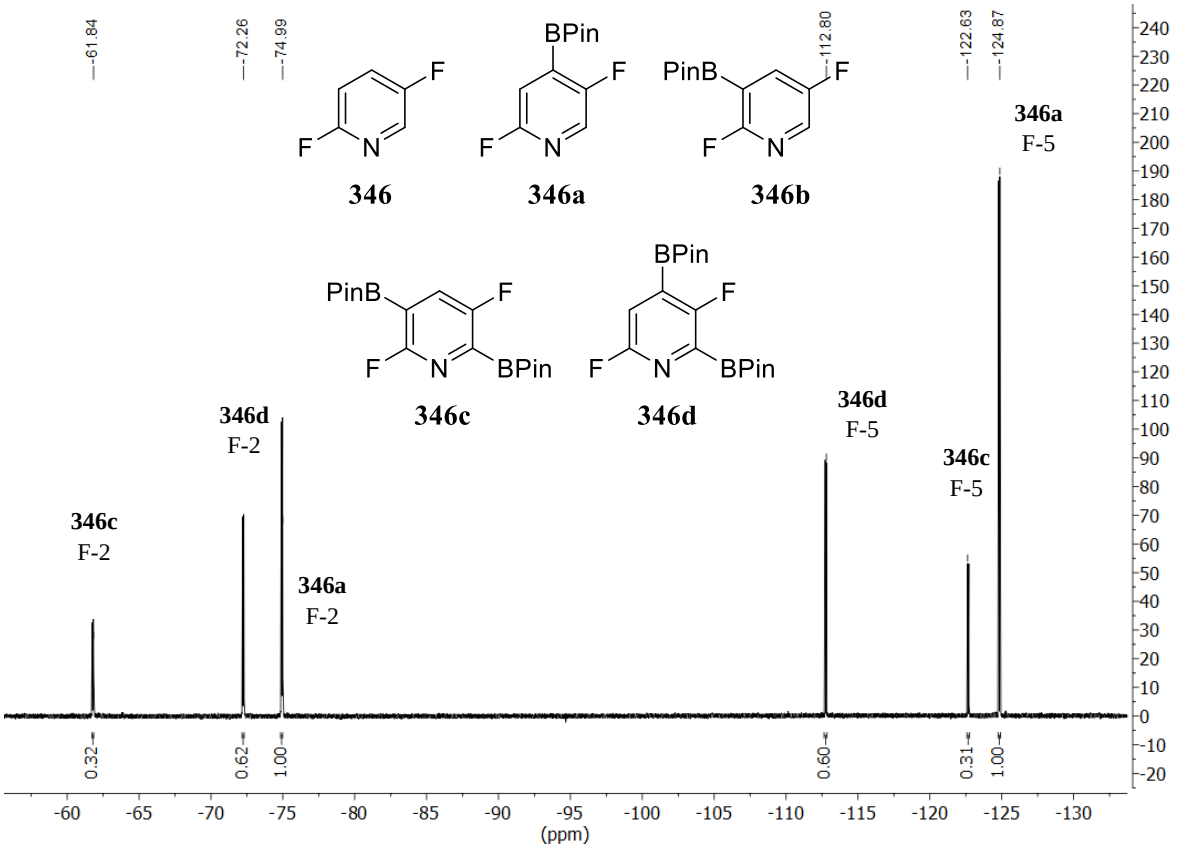

Table 8: Entry 1

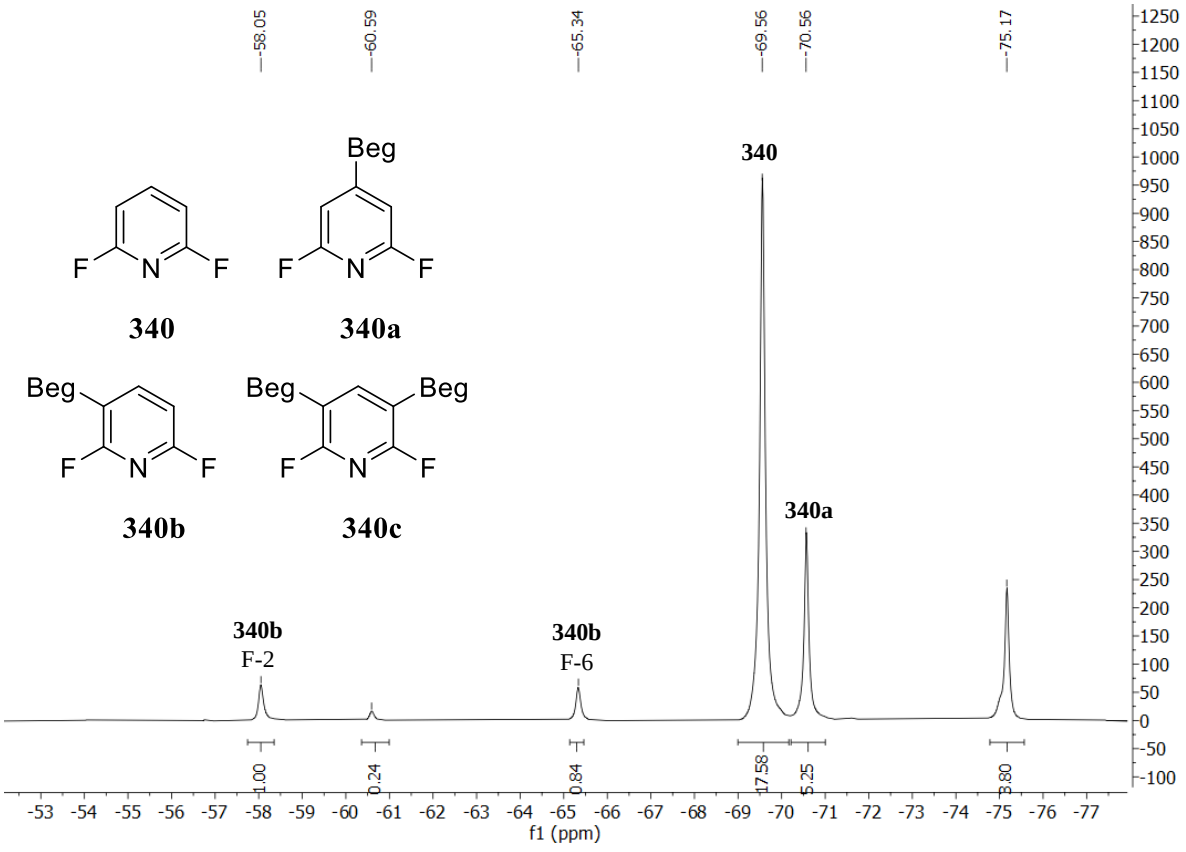

Table 8: Entry 2

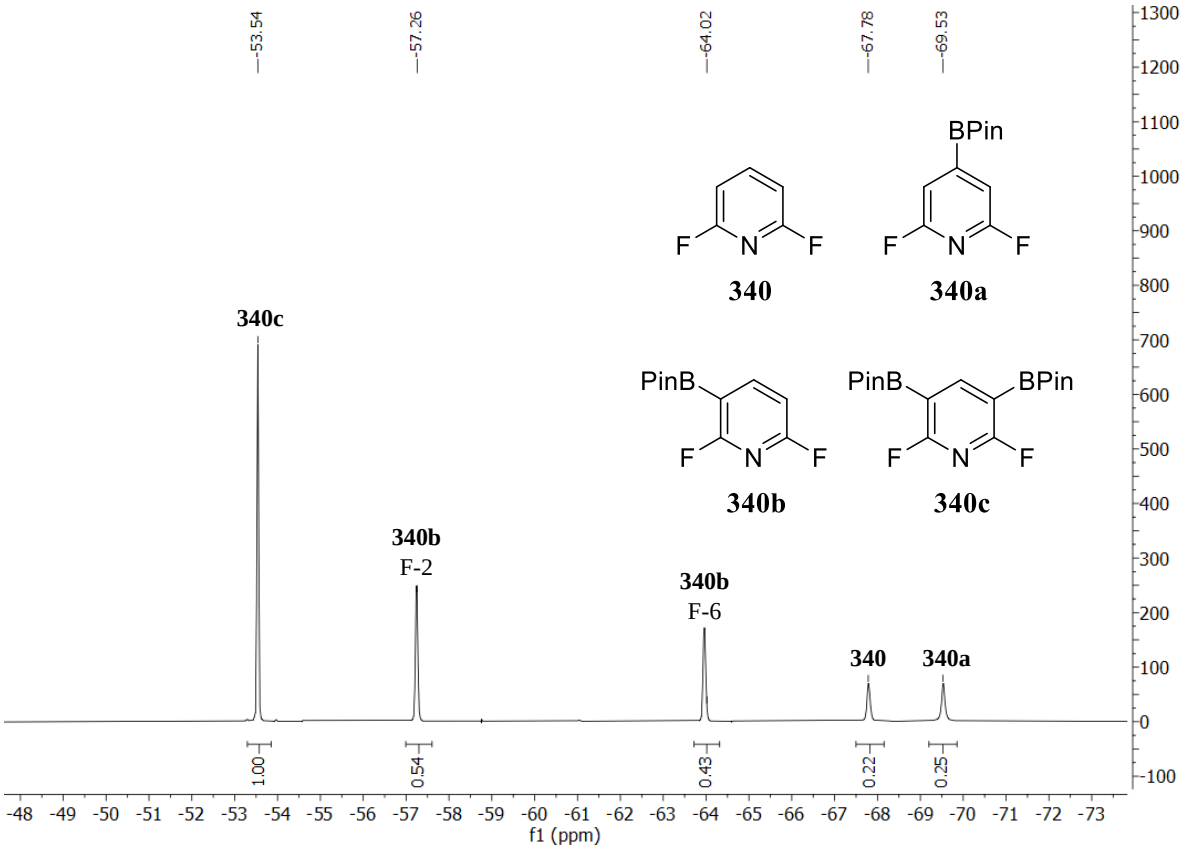

Table 8: Entry 3

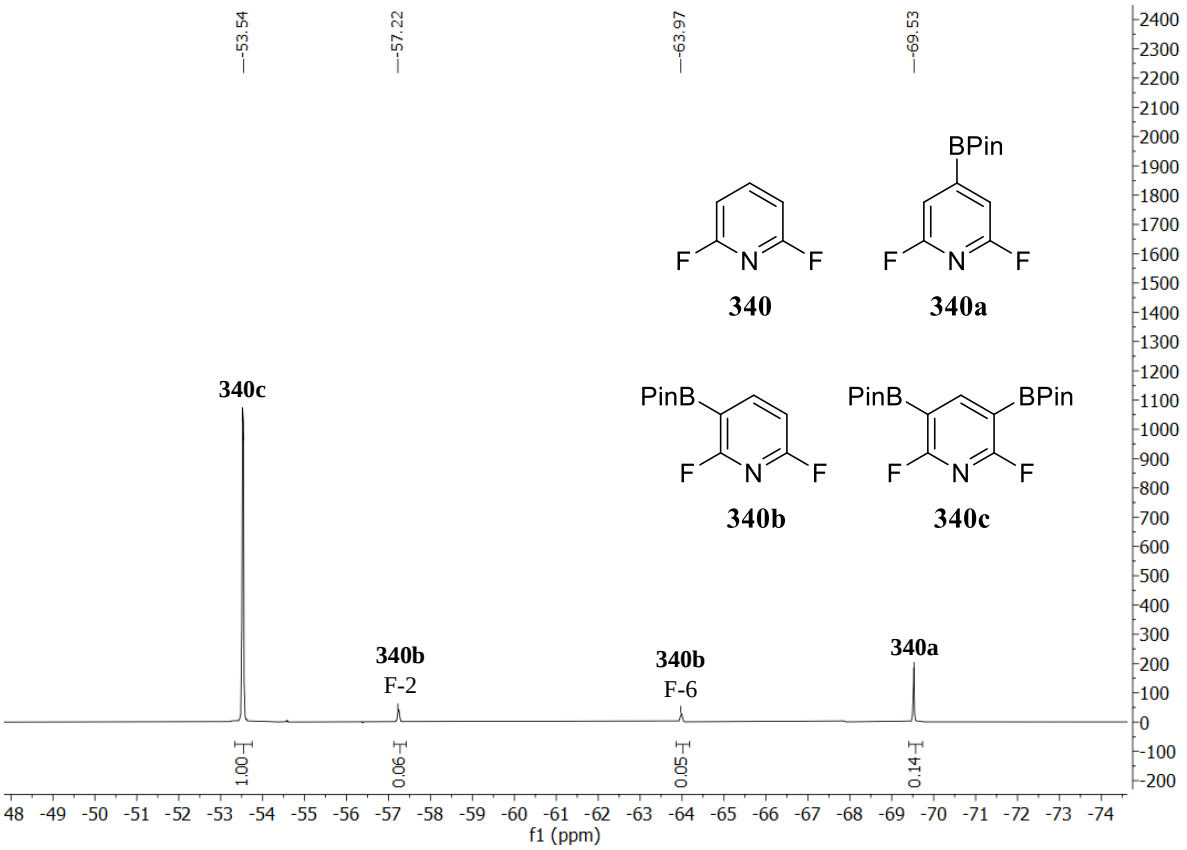

Scheme 61:

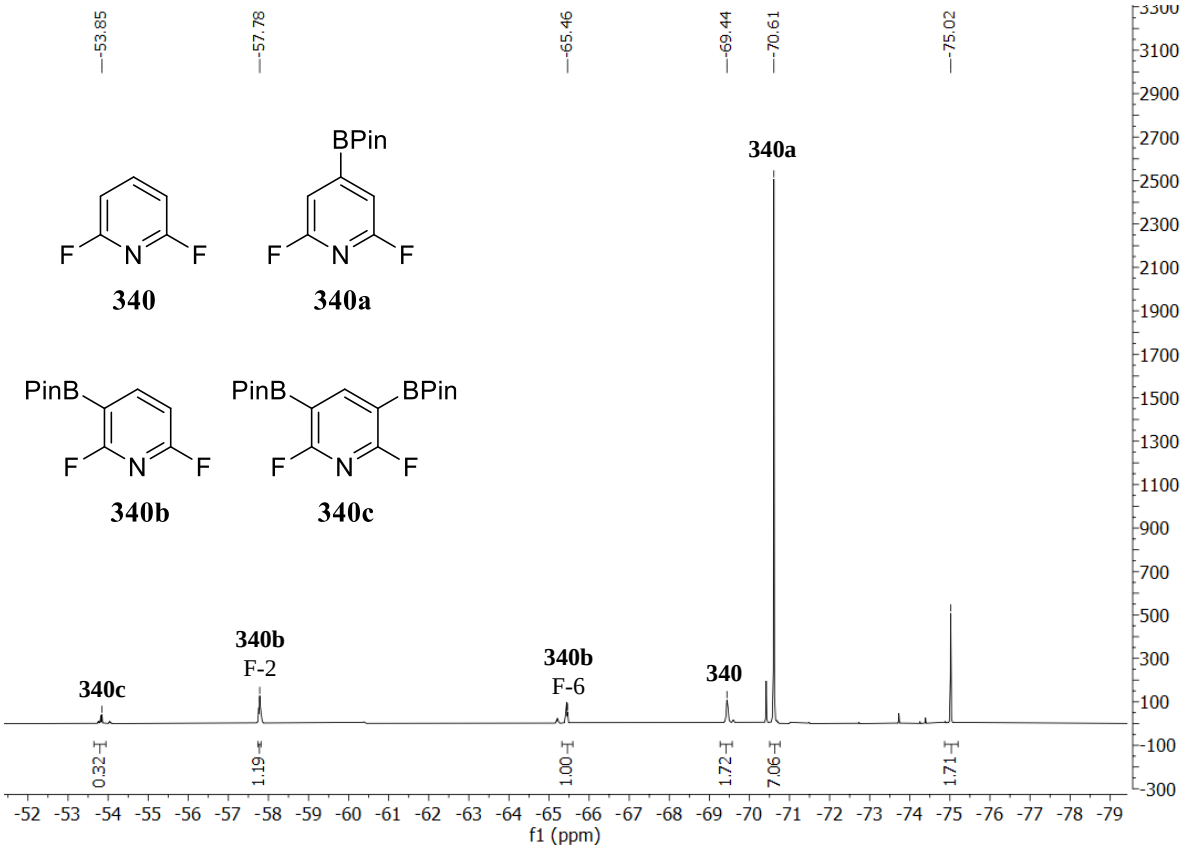
-53.85
-57.78
-65.46
-69.44
-70.61
-75.02
BPin
340
340a
PinB
BPin
340b
340c
340a
340b
F-2
340b
F-6
340
340c
0.32
1.19
1.00
1.72
7.06
1.71
-52 -53 -54 -55 -56 -57 -58 -59 -60 -61 -62 -63 -64 -65 -66 -67 -68 -69 -70 -71 -72 -73 -74 -75 -76 -77 -78 -79
f1 (ppm)
3300 3100 2900 2700 2500 2300 2100 1900 1700 1500 1300 1100 900 700 500 300 100 -100 -300

Volume II Bibliography:

154. Wright, J. S., Scott, P. J. H. & Steel, P. G. Iridium-Catalysed C À H Borylation of Heteroarenes : Balancing Steric and Electronic Regiocontrol. Angewandte. 2796–2821 (2021) doi:10.1002/anie.202001520.

155. Brown, D. G. Analysis of Past and Present Synthetic Methodologies on Medicinal Chemistry: Where Have All the New Reactions Gone? (2016)

156. Morgan, J. & Pinhey, J. T. Reaction of Arylboronic Acids and their Derivatives with Lead Tetra-acetate. The Generation. (2006).

157. Hartwig, J. F. Regioselectivity of the borylation of alkanes and arenes. *Chem. Soc. Rev.* **40**, 1992–2002 (2011).

158. Furukawa, T., Tobisu, M. & Chatani, N. C-H Functionalization at Sterically Congested Positions by the Platinum-Catalyzed Borylation of Arenes. *J. Am. Chem. Soc.* **137**, 12211–12214 (2015).

159. Bheeter, C. B., Chowdhury, A. D., Adam, R., Jackstell, R. & Beller, M. Efficient Rh-catalyzed C-H borylation of arene derivatives under photochemical conditions. *Org. Biomol. Chem.* **13**, 10336–10340 (2015).

160. Cho, A. J. *et al.* Remarkably Selective Iridium Catalysts for the Elaboration of Aromatic C-H Bonds. *Science (80-.).* **295**, 305–308 (2002).

161. Di, V. *et al.* Mild Iridium-Catalyzed Borylation of Arenes . High Turnover Numbers , Room Temperature Reactions , and Isolation of a Potential Intermediate. JACS Communications. 124, 3. 2001–2002 (2002).

162. Boller, Timothy M, Murphy, Jaclyn M, Hapke, Marko, Ishiyama, Tatsuo, Miyaura, Norio, Hartwig, John F. Mechanism of the Mild Functionalization of Arenes by Diboron Reagents Catalyzed by Iridium Complexes . Intermediacy and Chemistry of Bipyridine-Ligated Iridium Trisboryl Complexes. 14263–14278 (2005).

163. Tamura, H., Yamazaki, H., Sato, H. & Sakaki, S. Iridium-Catalyzed Borylation of Benzene with Diboron. Theoretical Elucidation of Catalytic Cycle Including Unusual Iridium(V) Intermediate. *J. Am. Chem. Soc.* **125**, 16114–16126 (2003).

164. Takagi, J., Sato, K., Hartwig, J. F. & Miyaura, N. Iridium-catalyzed C – H coupling reaction of heteroaromatic compounds with bis (pinacolato) diboron : regioselective synthesis of heteroarylboronates. *Tetrahedron Lett.* **43**, 5649–5651 (2002).

165. Paul, Sulagna, Chotana, Ghayoor A., Holmes, Daniel, Reichle, Rebecca C., Maleczka, Robert E., Smith, Milton R.. Ir-catalyzed functionalization of 2-substituted indoles at the 7-position: Nitrogen-directed aromatic borylation. *J. Am. Chem. Soc.* **128**, 15552–15553 (2006).

166. Takagi, J., Sato, K., Hartwig, J. F., Ishiyama, T., and N. M. Iridium-catalyzed C-H coupling reaction of heteroaromatic compounds with bis(pinacolato)diboron: regioselective synthesis of heteroarylboronates. *Tetrahedron Lett.* **43**, 5649–5651 (2002).

167. Vanchura, B. A. *et al.* Electronic effects in iridium C-H borylations: Insights from unencumbered substrates and variation of boryl ligand substituents. *Chem. Commun.* **46**, 7724–7726 (2010).

168. Egan, B. A. & Burton, P. M. Synthesis of 3-aryl-1H-indazoles via iridium-catalysed C-H borylation and Suzuki-Miyaura coupling. *RSC Adv.* **4**, 27726–27729 (2014).

169. Larsen, M. A. & Hartwig, J. F. Iridium-Catalyzed C − H Borylation of Heteroarenes : Scope ,

Regioselectivity , Application to Late-Stage Functionalization , and Mechanism. *J. Am. Chem. Soc* (2014). 136, 4287-4299.

170. Albesa-jove, D., Batsanov, A. S., Howard, J. A. K., Perutz, R. N. & Marder, T. B. Ir-Catalyzed Borylation of C À H Bonds in N-Containing Heterocycles: Regioselectivity in the Synthesis of Heteroaryl Boronate Esters**. Angewandte. 489–491 (2006)

171. Chotana, G. A., Rak, M. A. & Smith, M. R. Sterically Directed Functionalization of Aromatic C - H Bonds : Selective Borylation Ortho to Cyano Groups in Arenes and Heterocycles. *J. Am. Chem. Soc*, 127, 10539–10544 (2005).

172. Reuven, J. A., Salih, O. A., Sadler, S. A., Thomas, C. L. & Steel, P. G. Exploiting C–H borylation for the multidirectional elaboration of 2-halopyridines. *Tetrahedron* **76**, 130836 (2020).

173. Wang, Jiang, Luis, Jose, Pozo, Carlos, Sorochinsky, Alexander E, Fustero, Santos, Soloshonok, Vadim A, Liu, Hong. Fluorine in Pharmaceutical Industry : Fluorine-Containing Drugs Introduced to the Market in the Last Decade (2001 − 2011). Chemical Reviews, 114, 2432-2506, (2014).

174. Tian, Ya-ming, Guo, Xiao-ning, Kuntze-fechner, Maximilian W, Krummenacher, Ivo, Braunschweig, Holger, Radius, Udo, Ste, Andreas, Marder, Todd B Selective Photocatalytic C − F Borylation of Poly fl uoroarenes by Rh/ Ni Dual Catalysis Providing Valuable Fluorinated Arylboronate Esters. *J. Am. Chem. Soc*, 140, 17612-17623, (2018).

175. B, B Eck, Martin, Würtemberger-pietsch, Sabrina, Eichhorn, Antonius, Berthel, Johannes H J, Bertermann, Rüdiger, Paul, Ursula S D, Schneider, Heidi, Friedrich, Alexandra, Kleeberg, Christian, Marder, Todd B. B–B bond activation and NHC ring-expansion reactions of diboron(4) compounds, and accurate molecular structures of B2(NMe2)4, B2eg2, B2neop2 and B2pin2. Dalton Trans. 46, 3661–3680 (2017)

176. Smith, Milton R, Bisht, Ranjana, Haldar, Chabush, Pandey, Gajanan, Jonathan, E, Ghaffari, Behnaz, Maleczka, Robert E, Chattopadhyay, Buddhadeb. Achieving High Ortho Selectivity in Aniline C – H Borylations by Modifying Boron Substituents. *J. Am. Chem. Soc*, 8, 7, 6216-6223.

177. Miller, S. L. *et al.* C-H Borylation Catalysts that Distinguish between Similarly Sized Substituents like Fluorine and Hydrogen. *Org. Lett.* **21**, 6388–6392 (2019).

Appendix A: Volume 1 NMR Spectrum

74. *tert-butyl N-[2'-(naphthalene-1-sulfonamido)ethyl]carbamate*

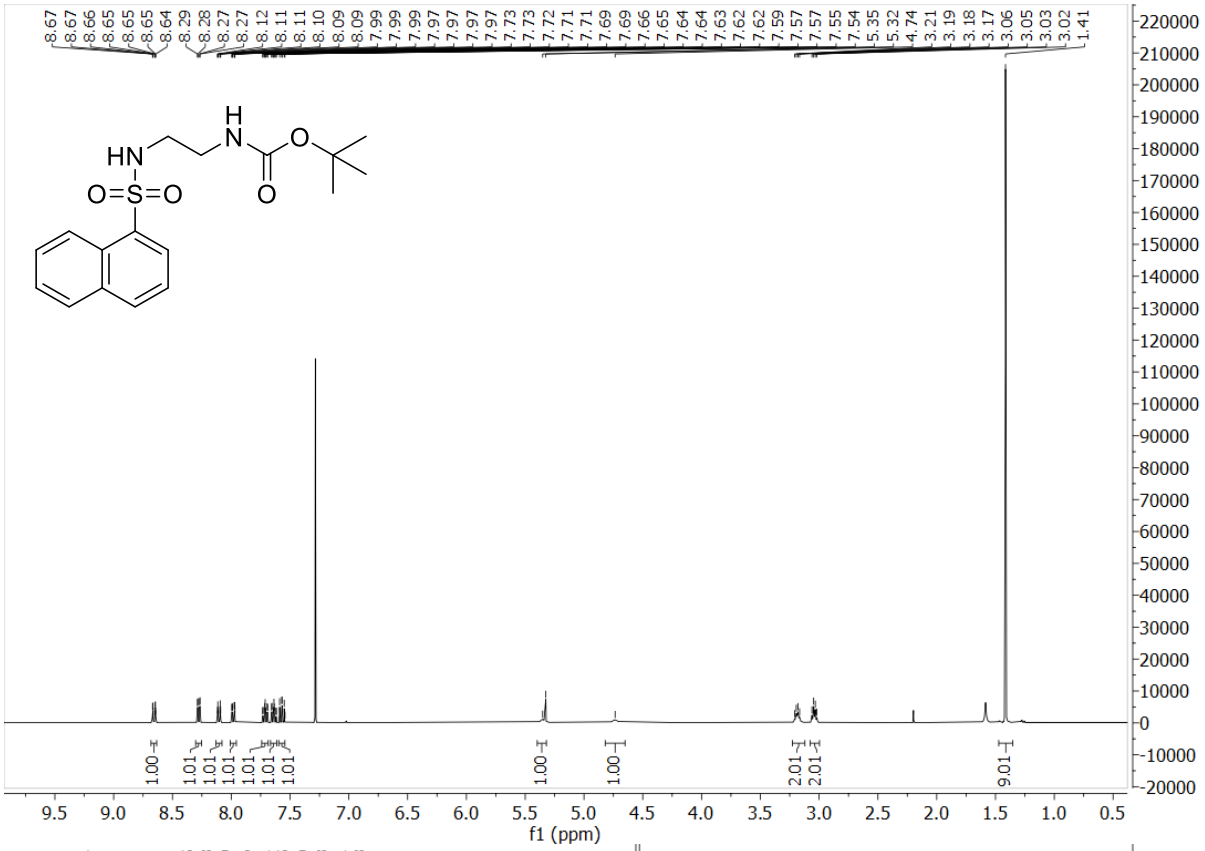

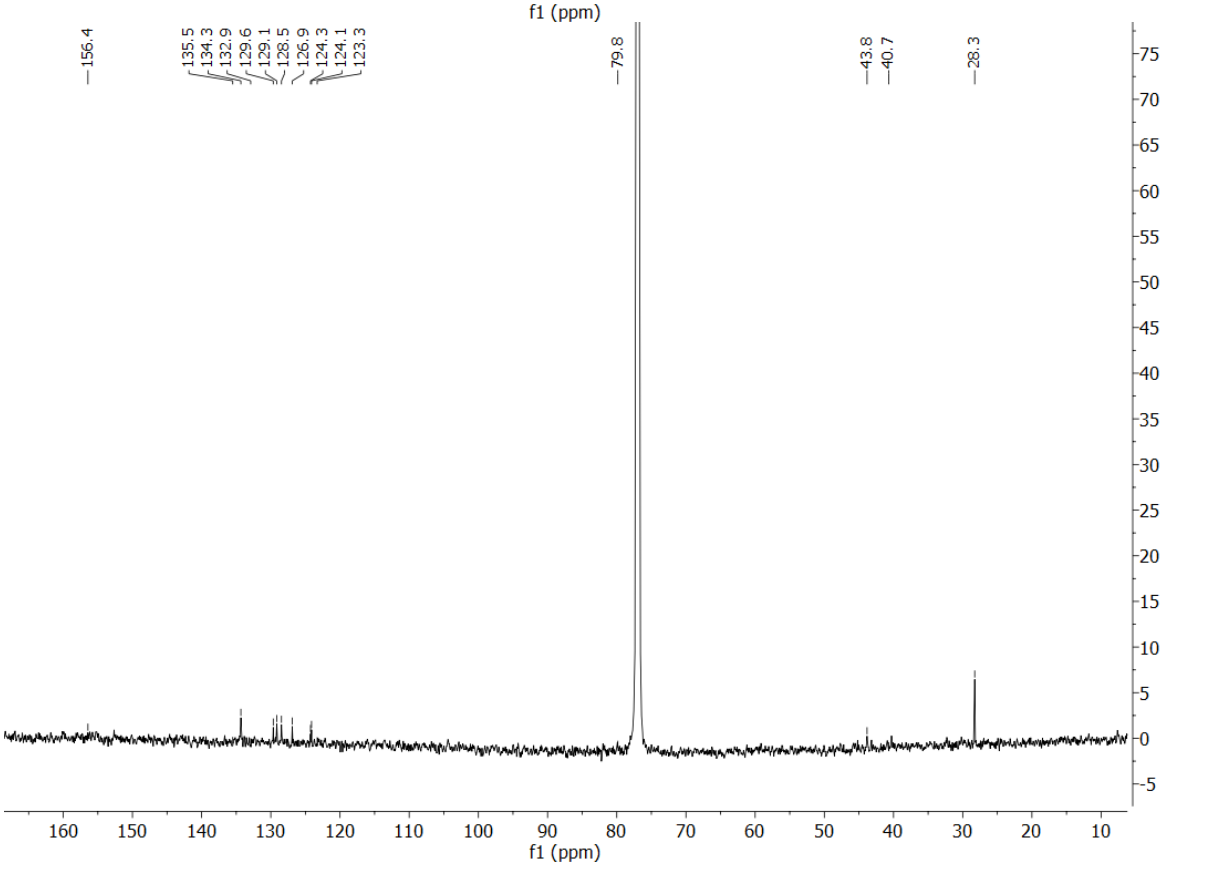

1. *N-(2-aminoethyl)-naphthalene-1-sulfonamide hydrogen chloride*

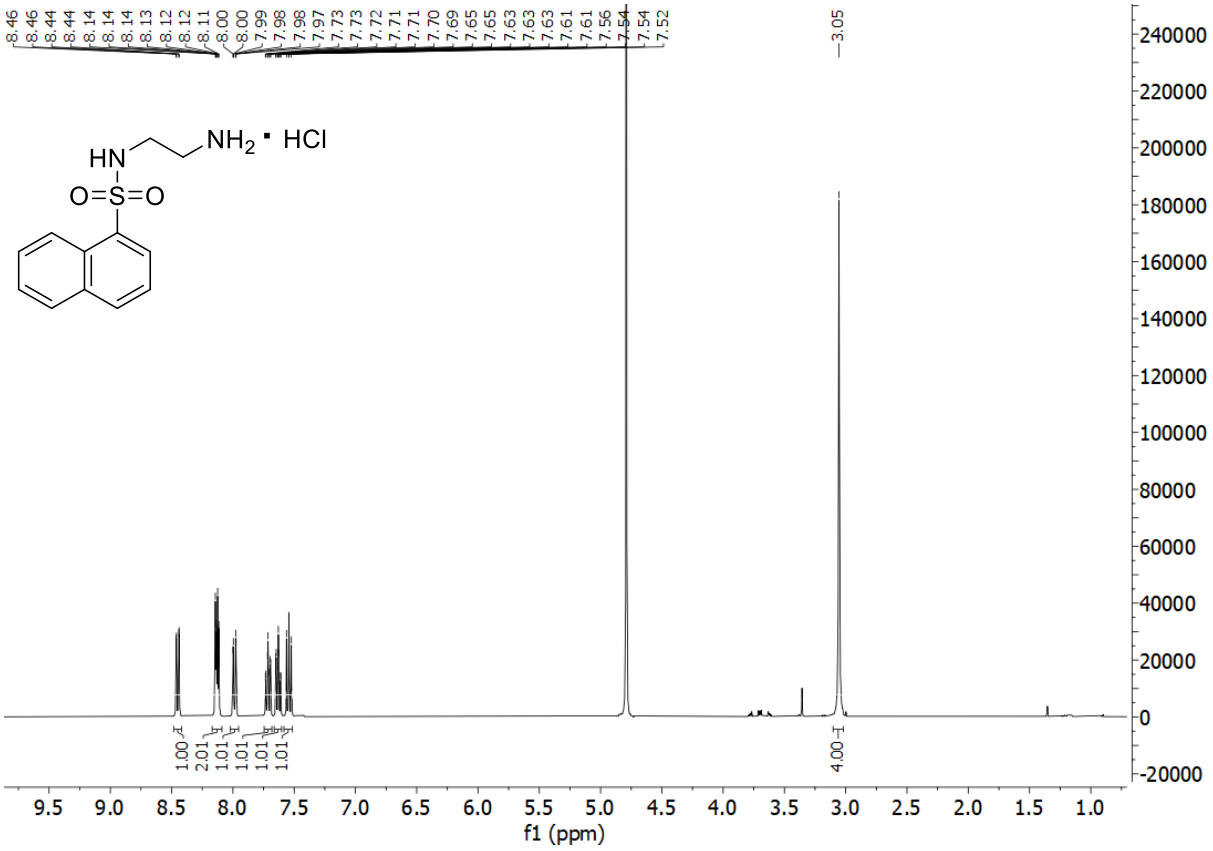

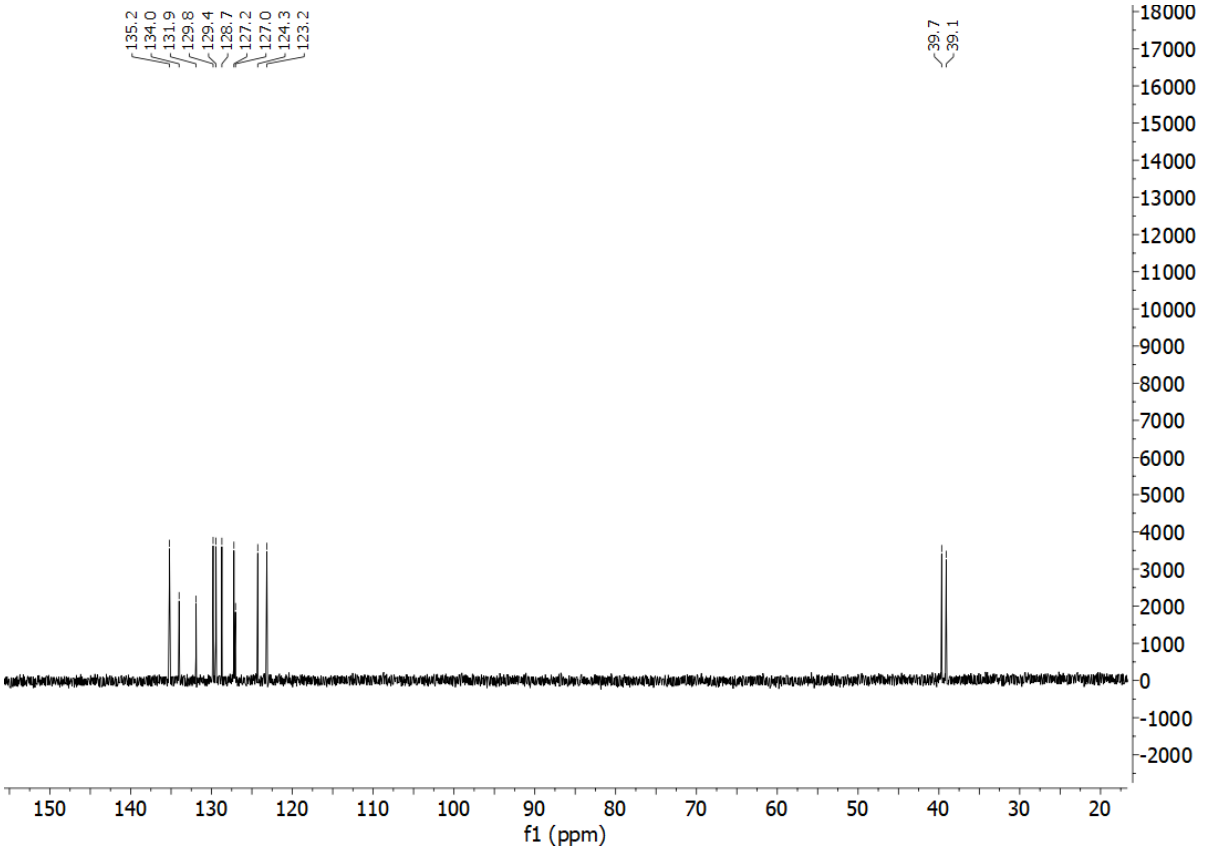

75a. *tert-butyl N-[2'-(naphthalene-2-sulfonamido)ethyl]carbamate*

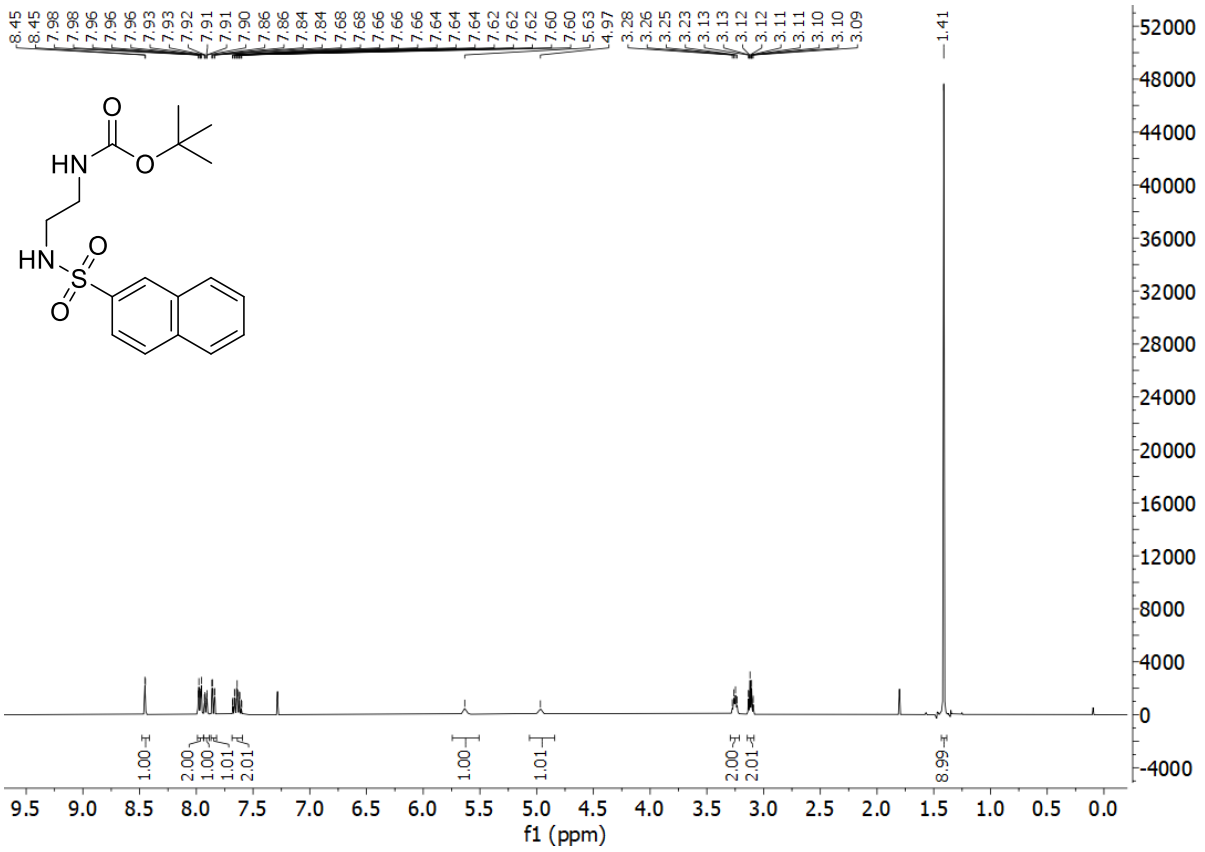

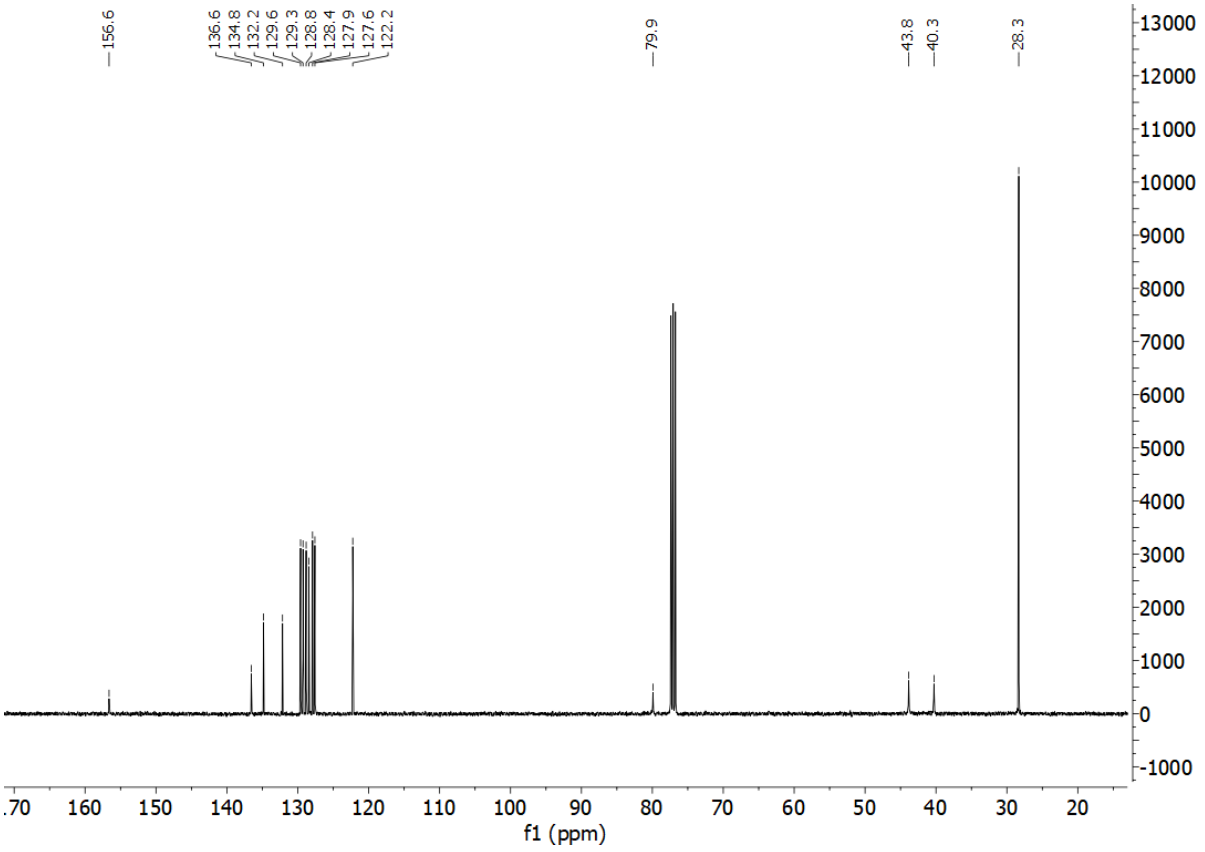

75. *N-(2'-aminoethyl)naphthalene-2-sulfonamide hydrochloride*

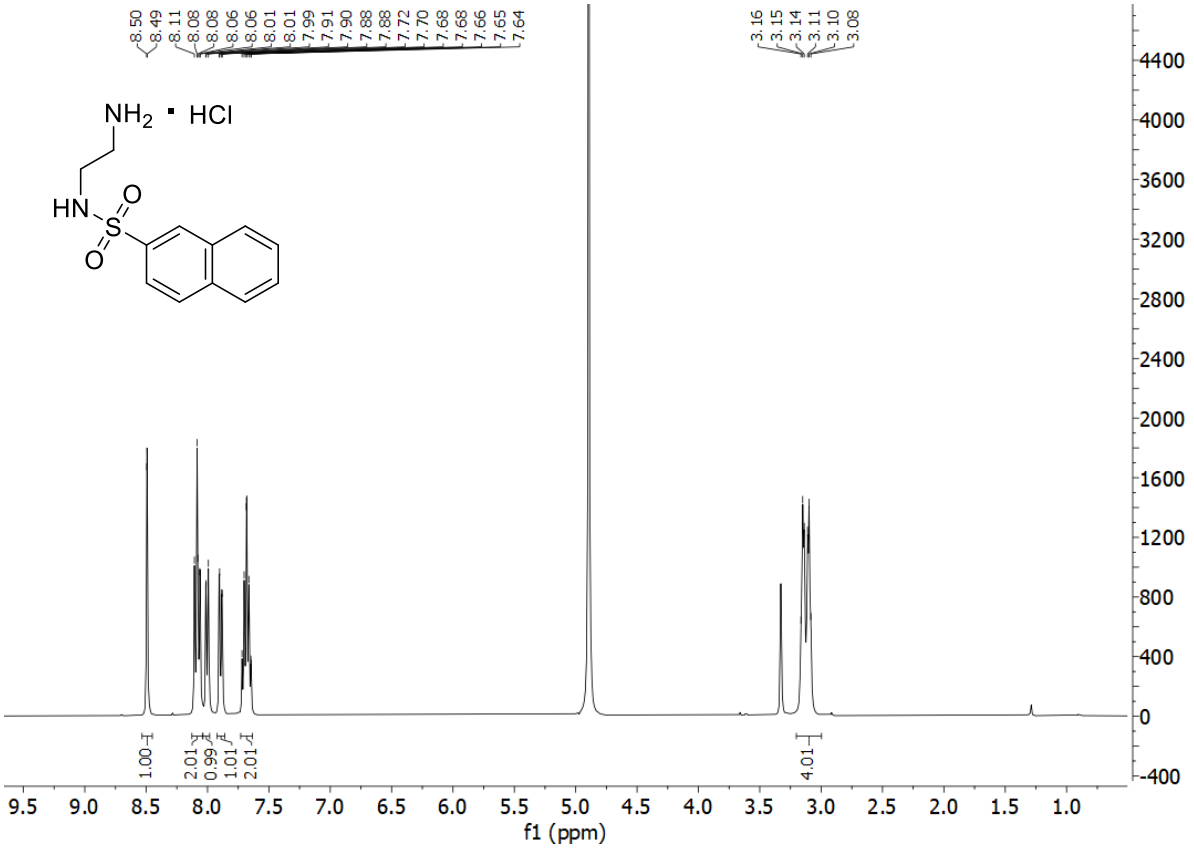

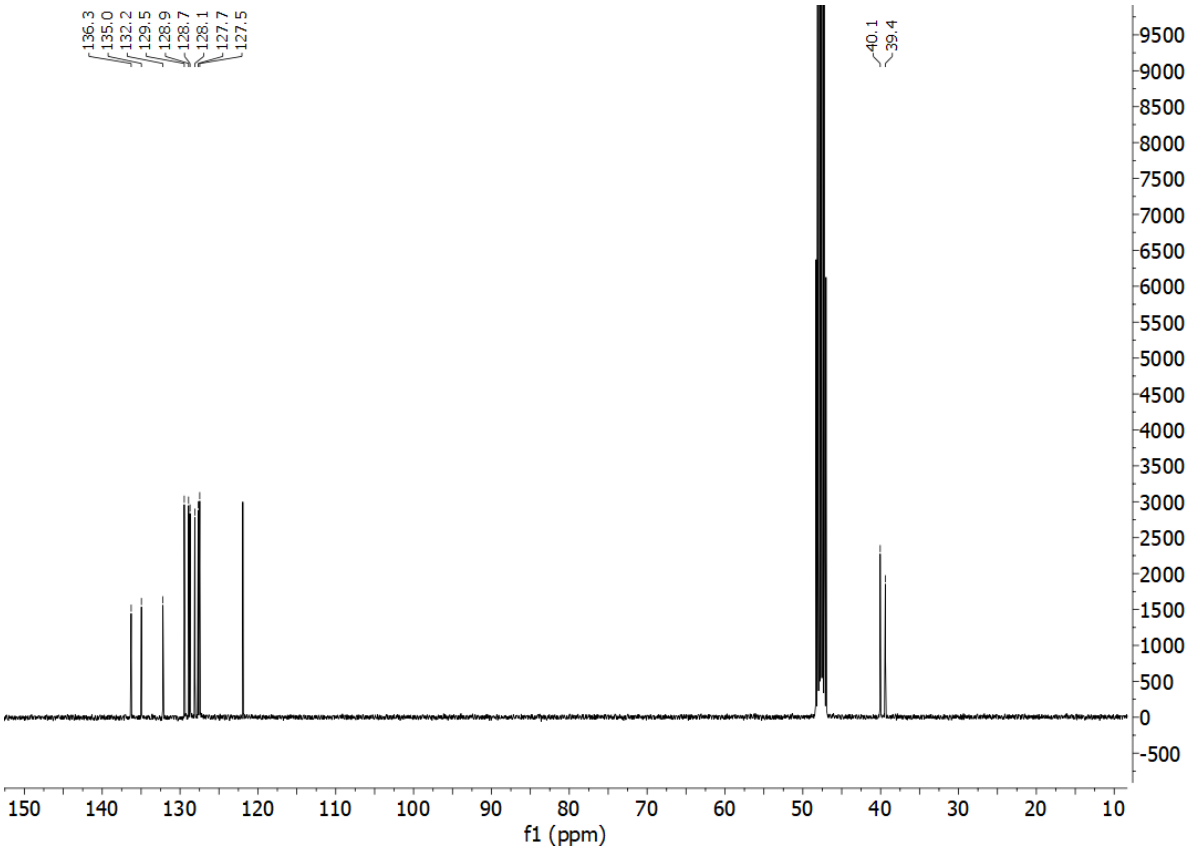

76a. *tert-butyl N-[2'-(2-fluorobenzenesulfonamido)ethyl]carbamate*

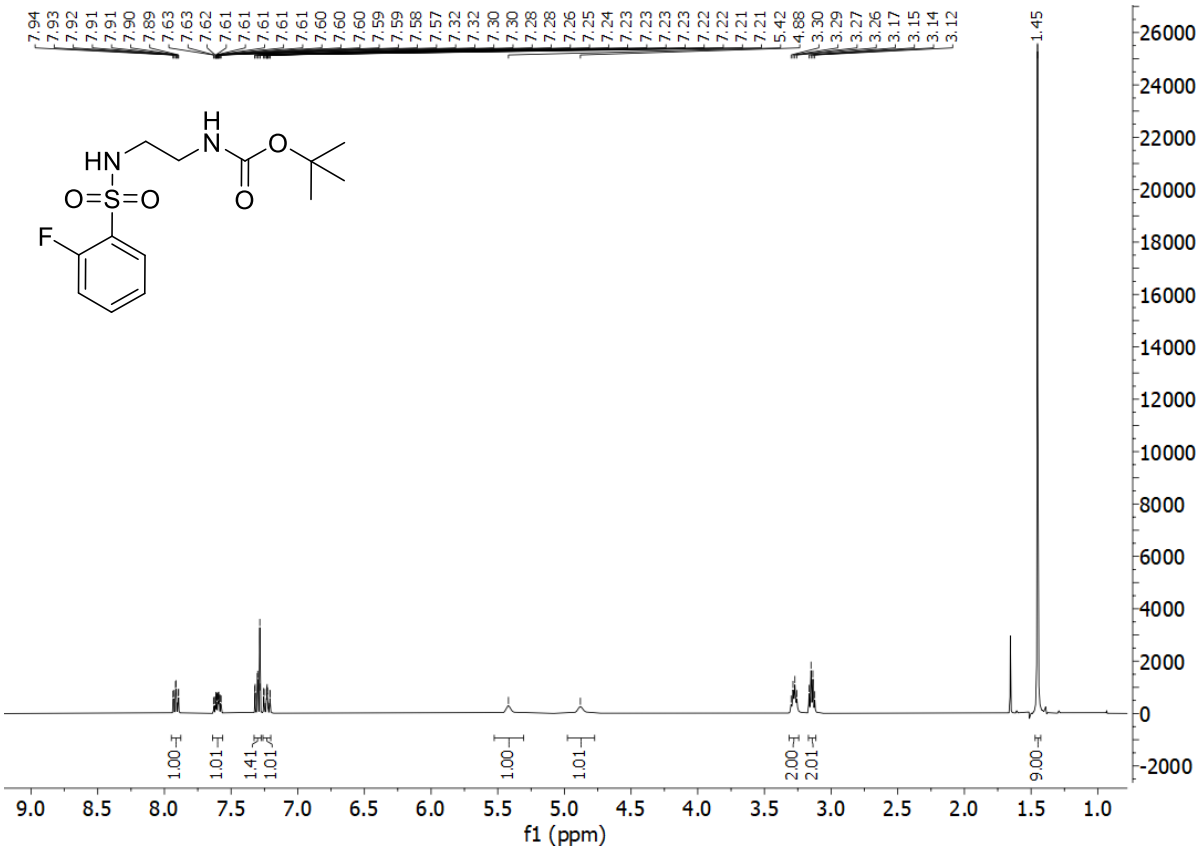

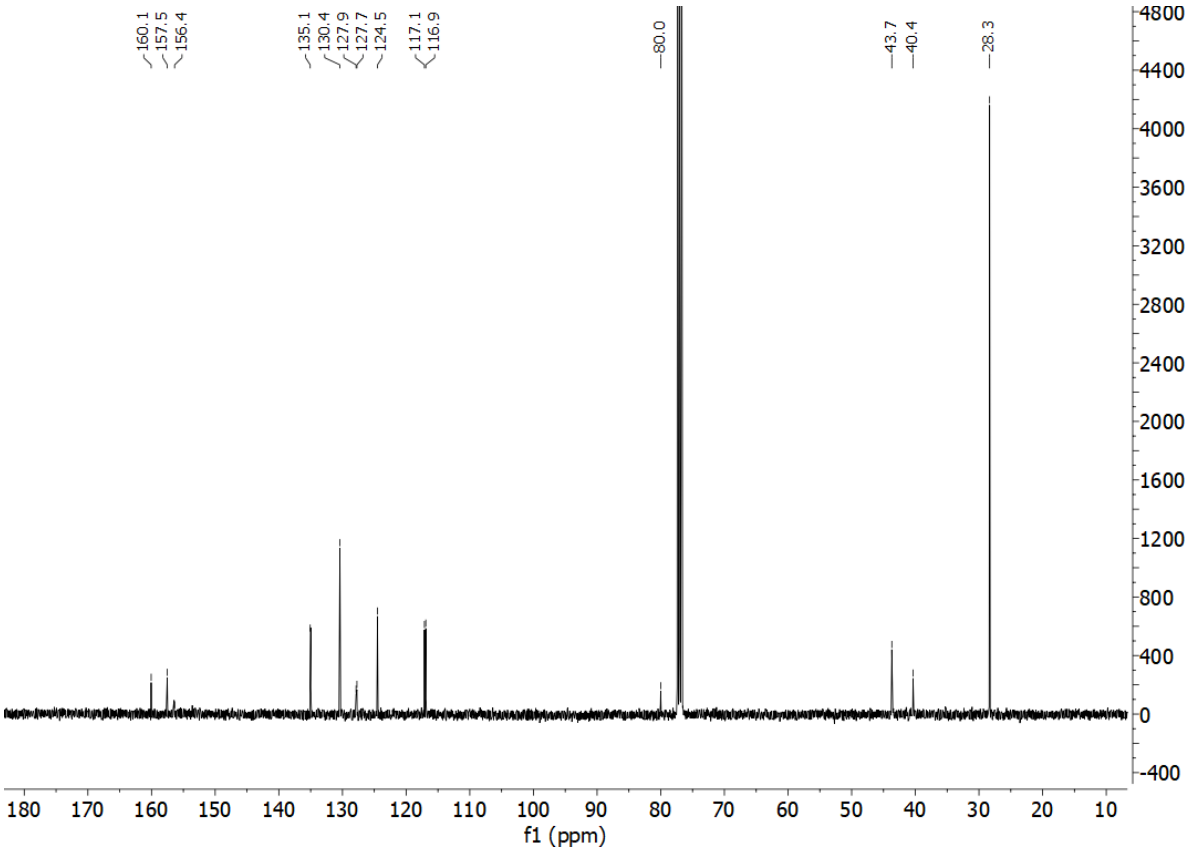

76. *N-(2'-aminoethyl)-2-fluorobenzene-1-sulfonamide hydrochloride*

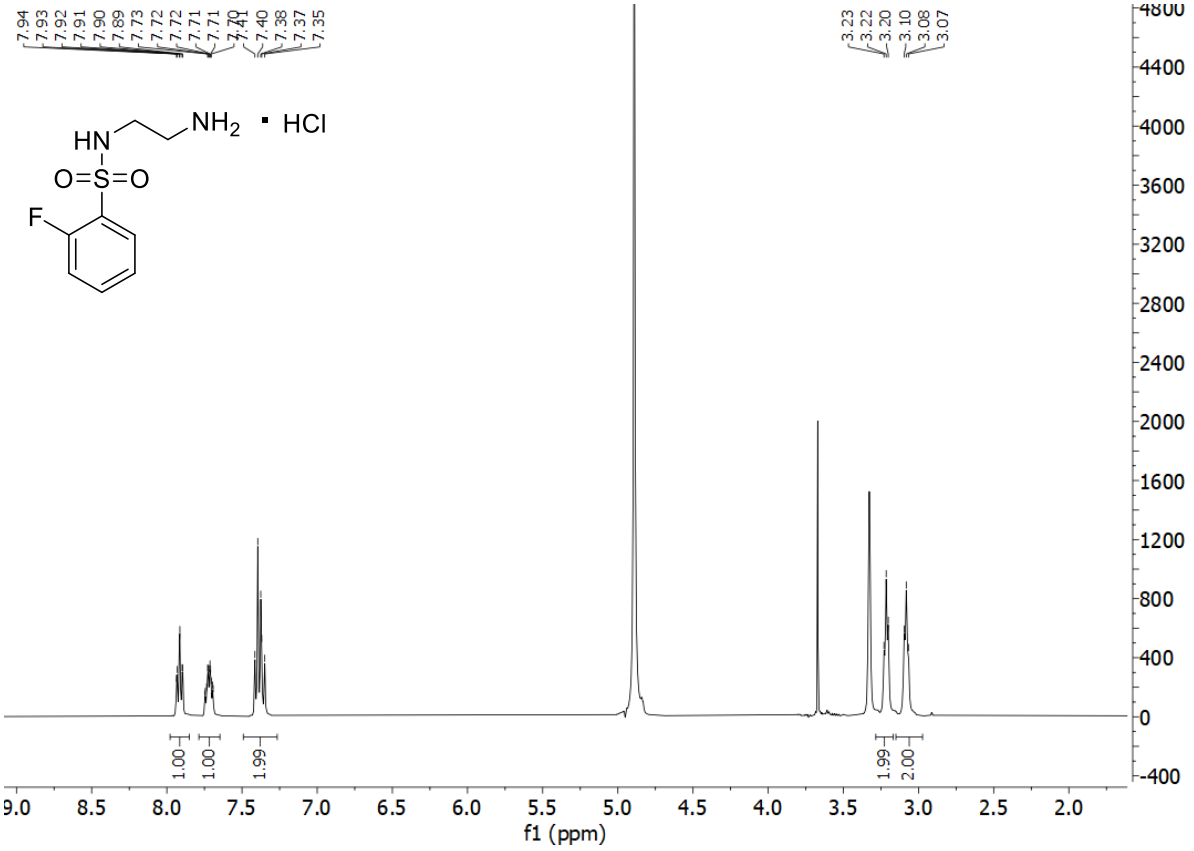

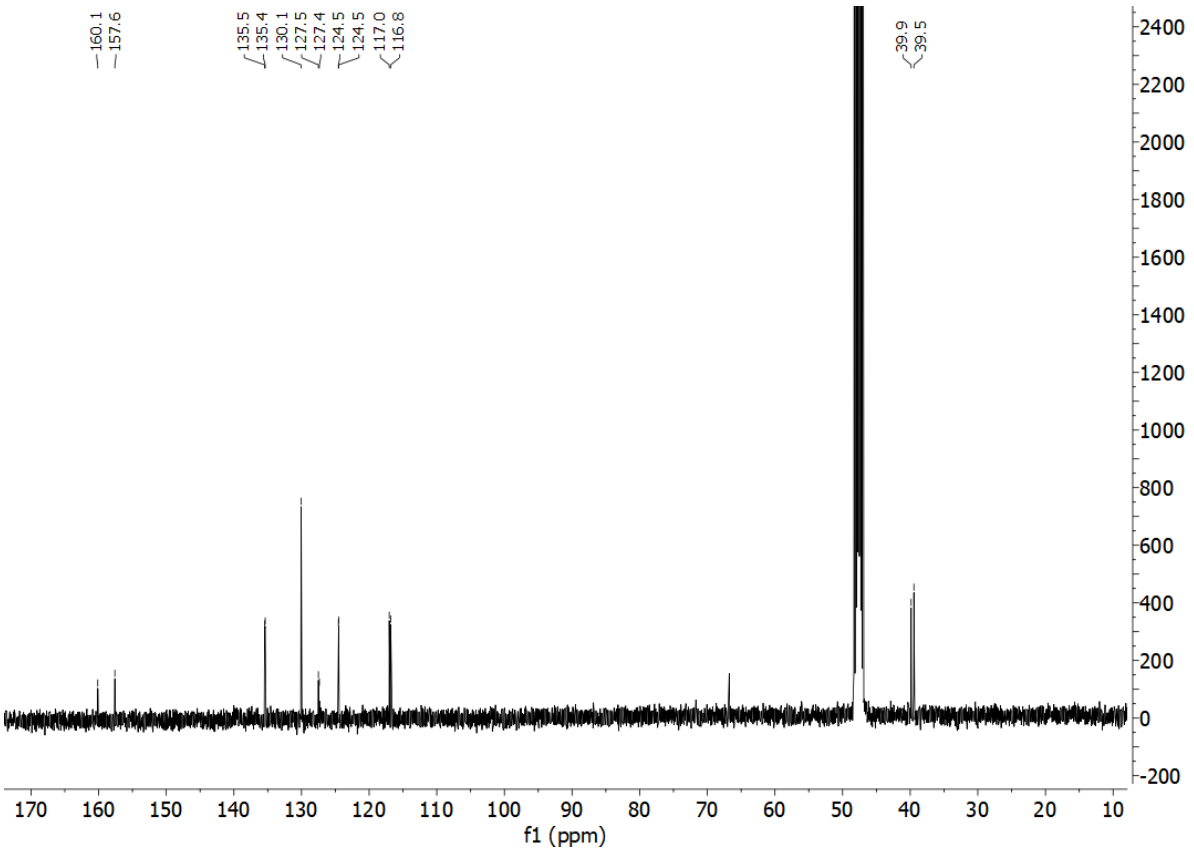

77a. *tert-butyl N-[2-(3-fluorobenzenesulfonamido)ethyl]carbamate*

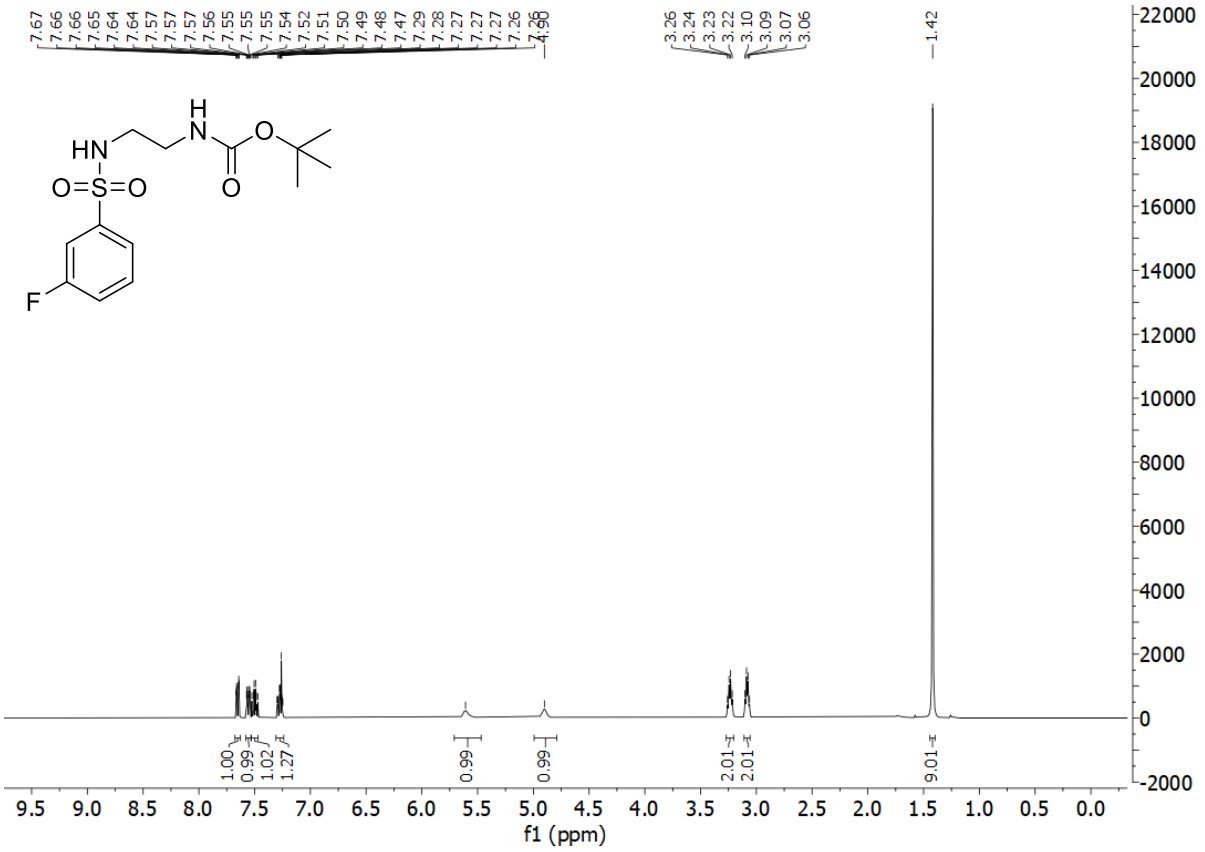

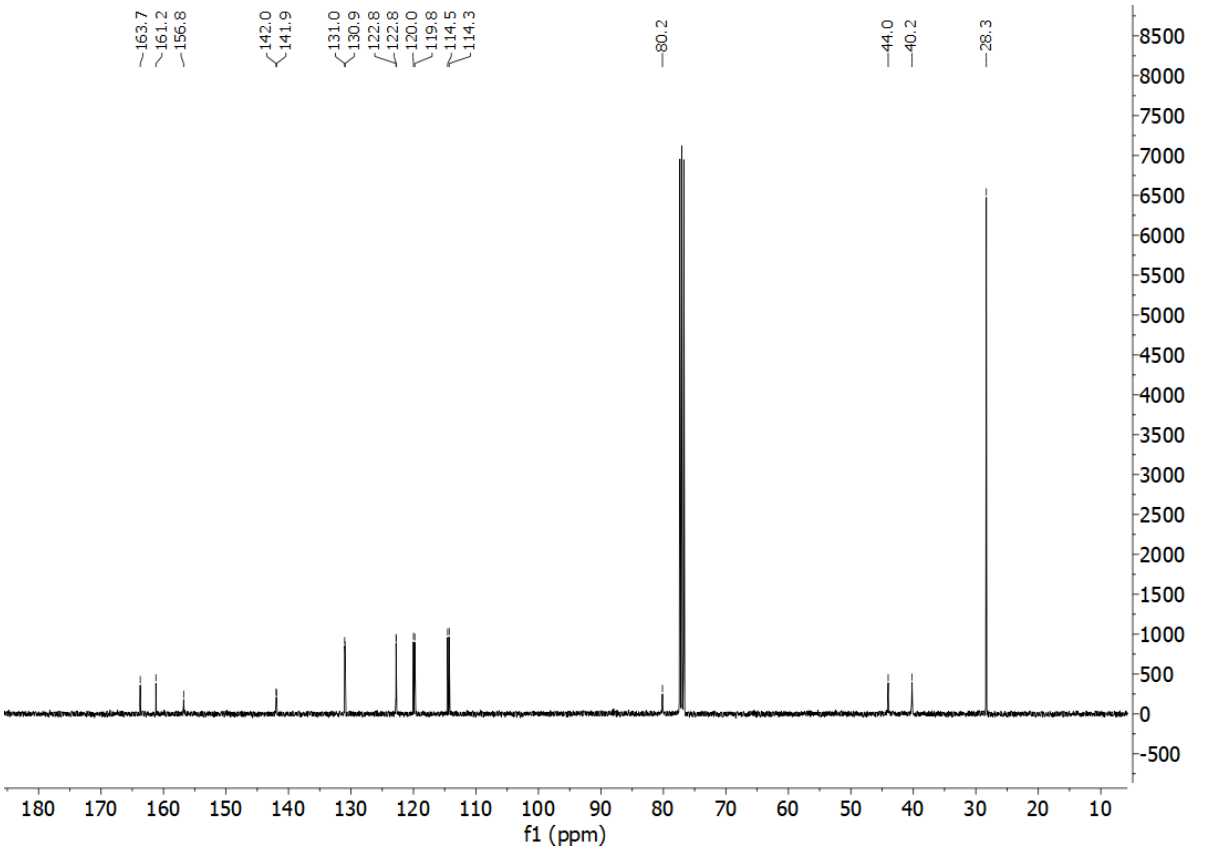

77. *N-(2'-aminoethyl)-3-fluorobenzene-1-sulfonamide hydrochloride*

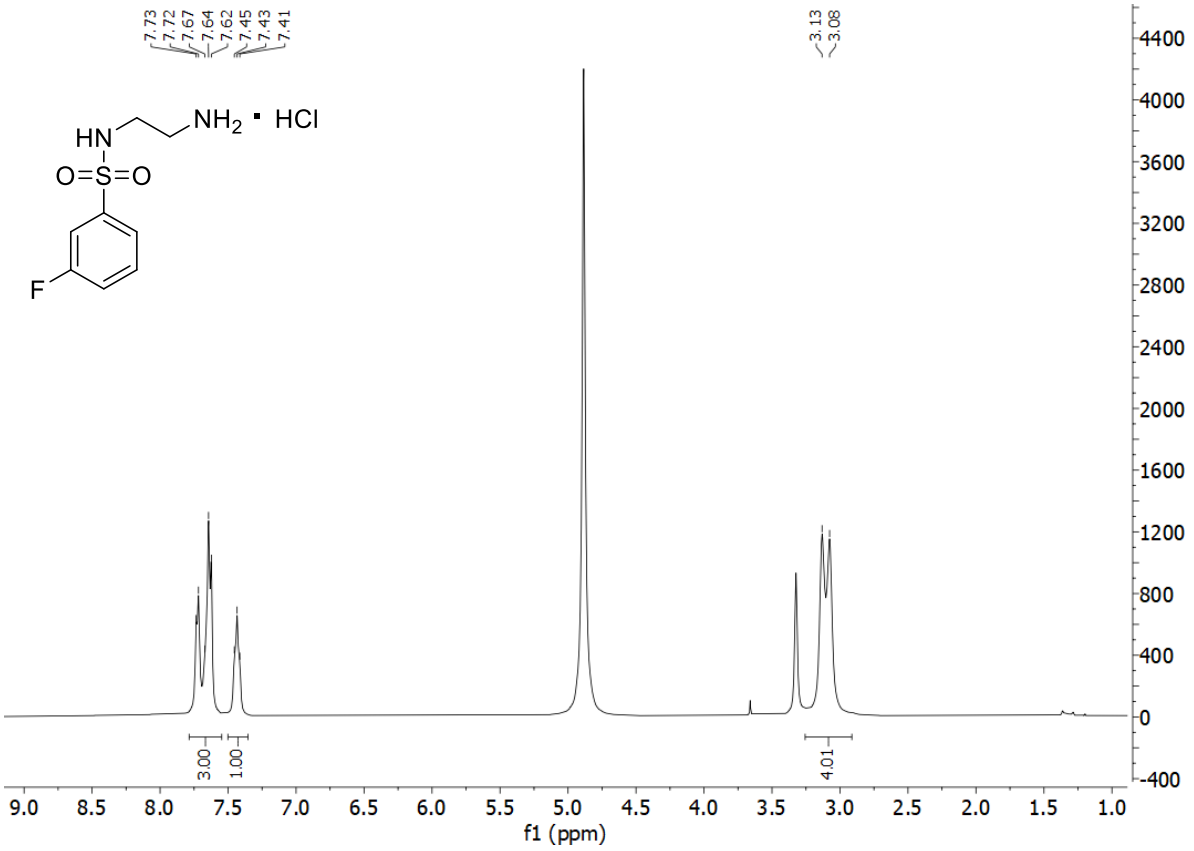

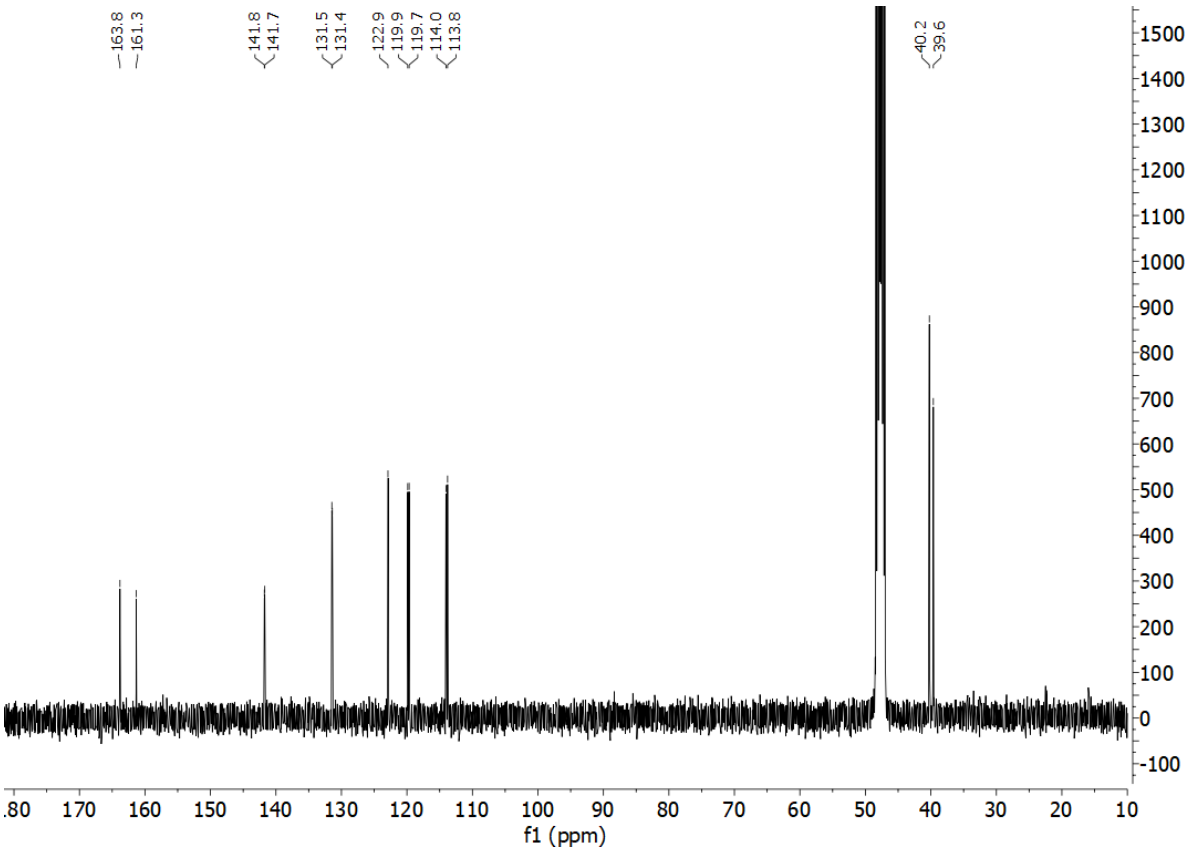

78a. *tert-butyl N-[2'-(4-nitrobenzenesulfonamido)ethyl]carbamate*

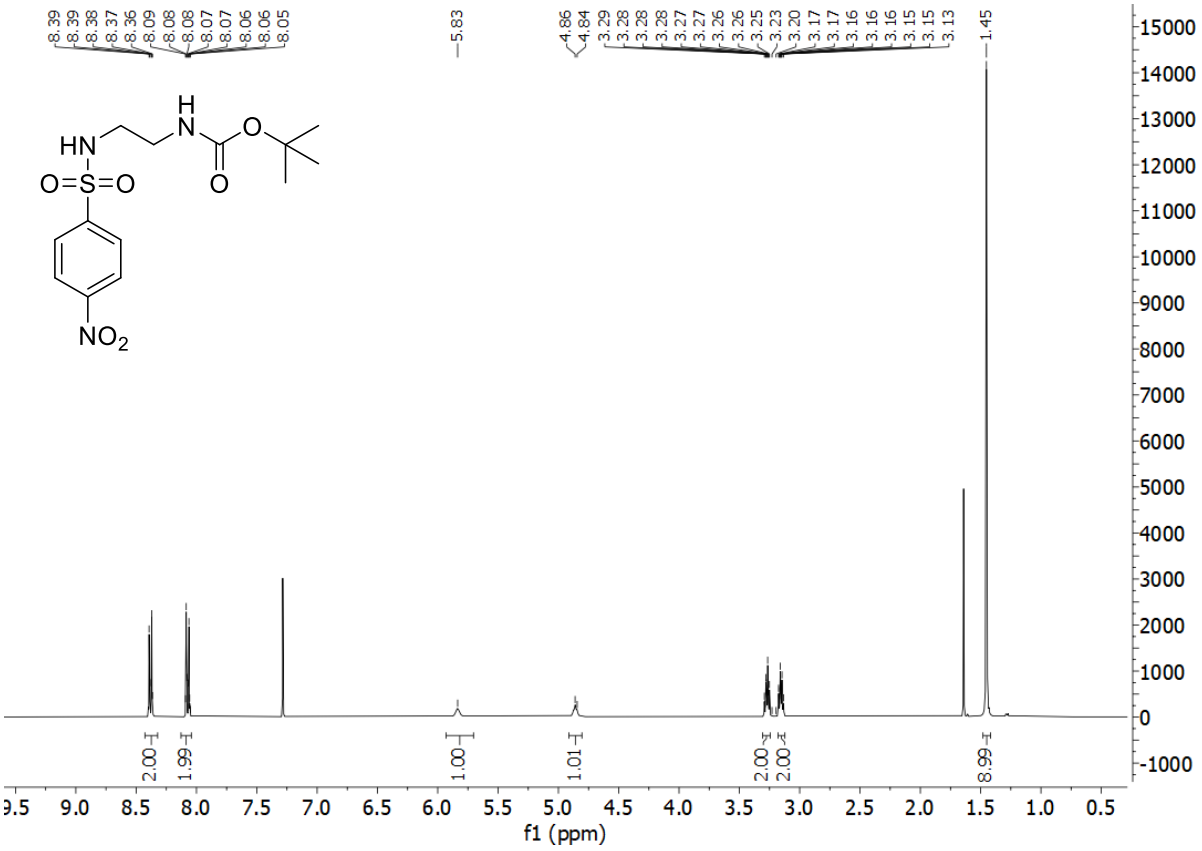

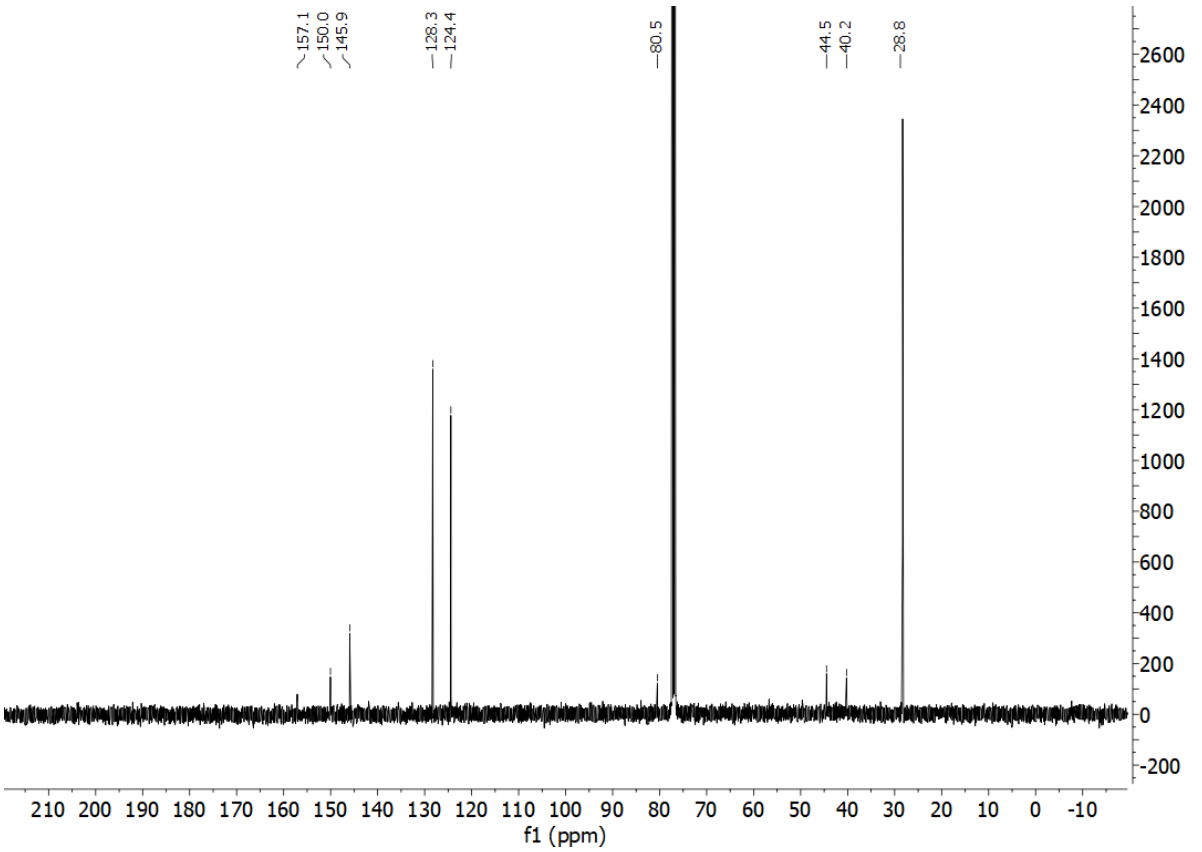

78. *N-(2'-aminoethyl)-4-nitrobenzene-1-sulfonamide hydrochloride*

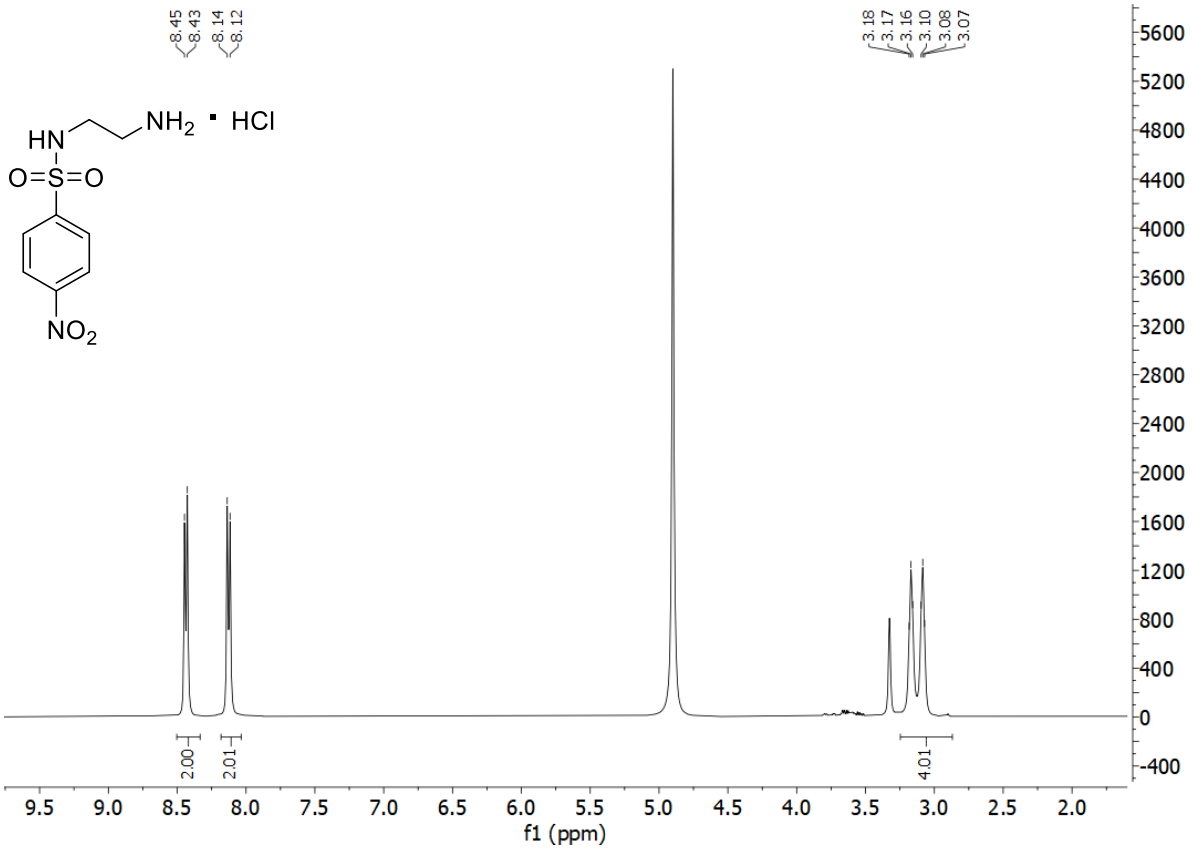

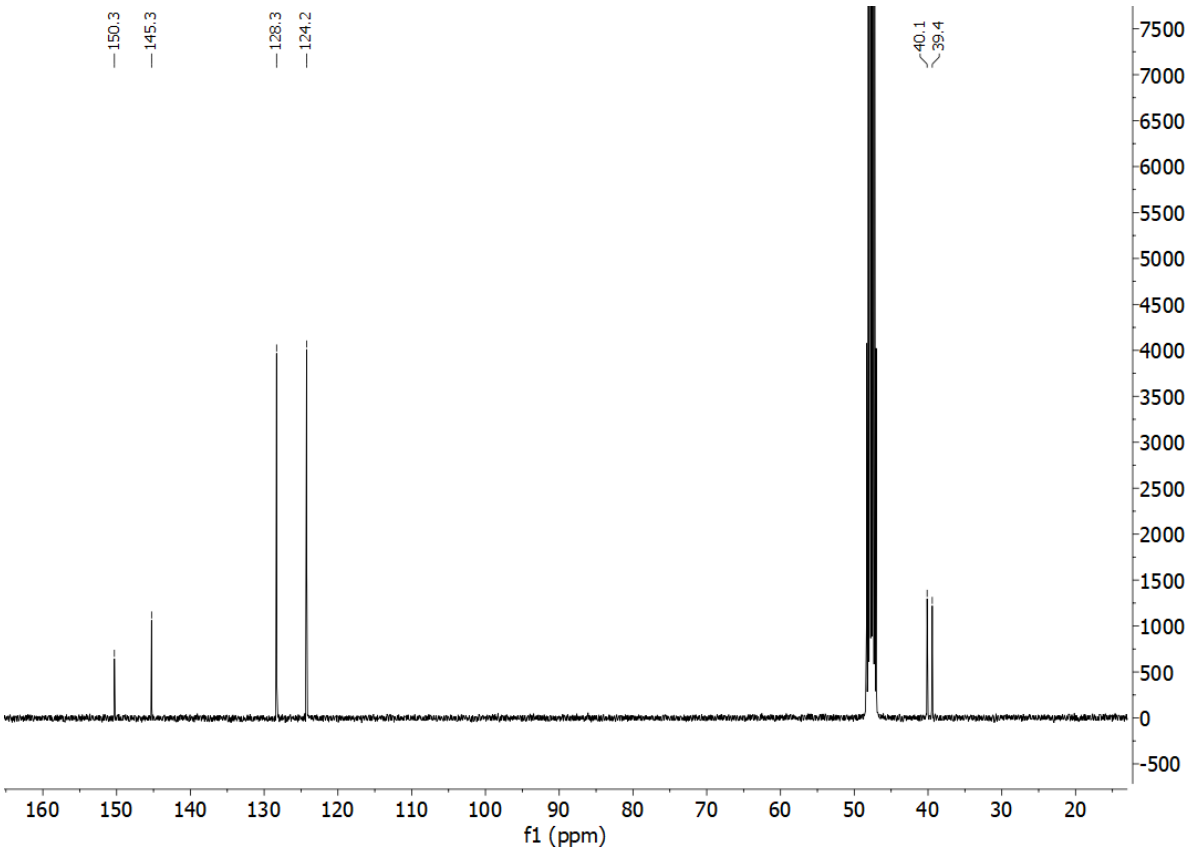

79a. *tert-butyl N-[2-(4-tert-butylbenzenesulfonamido)ethyl]carbamate*

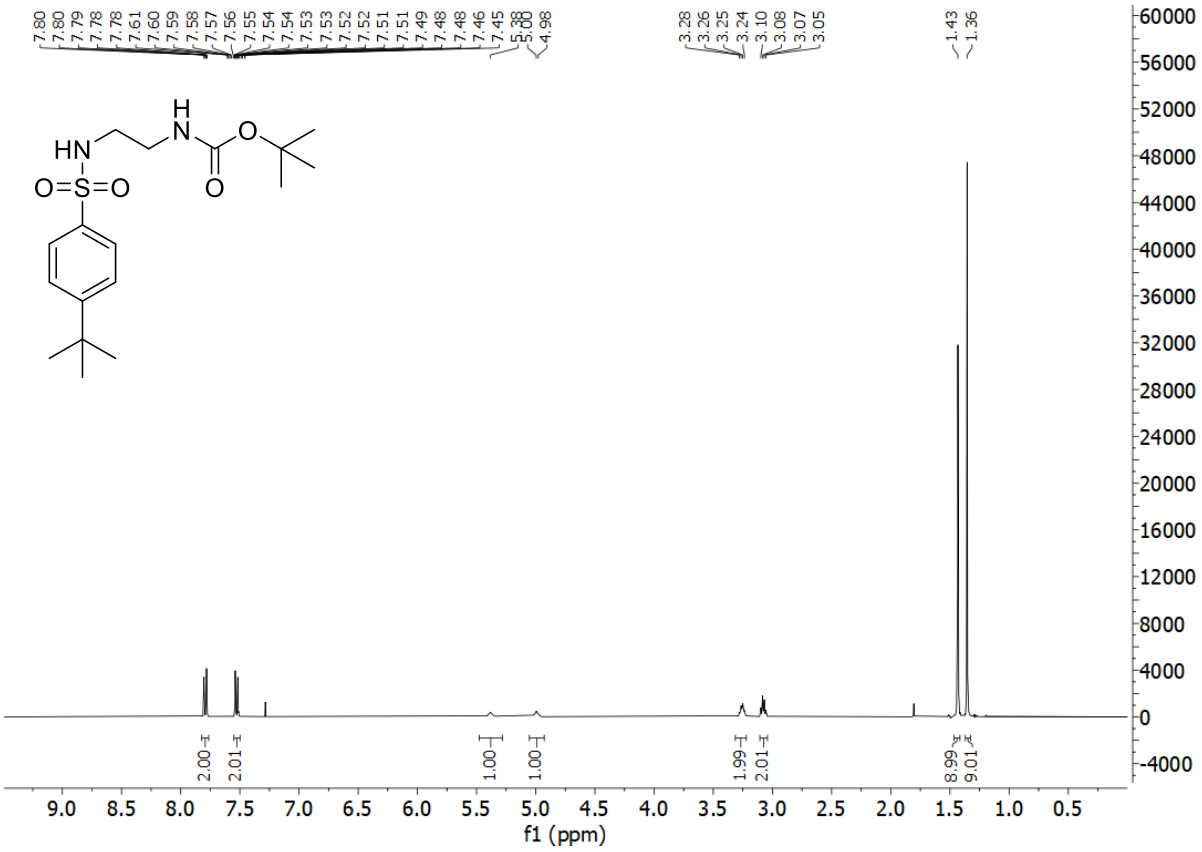

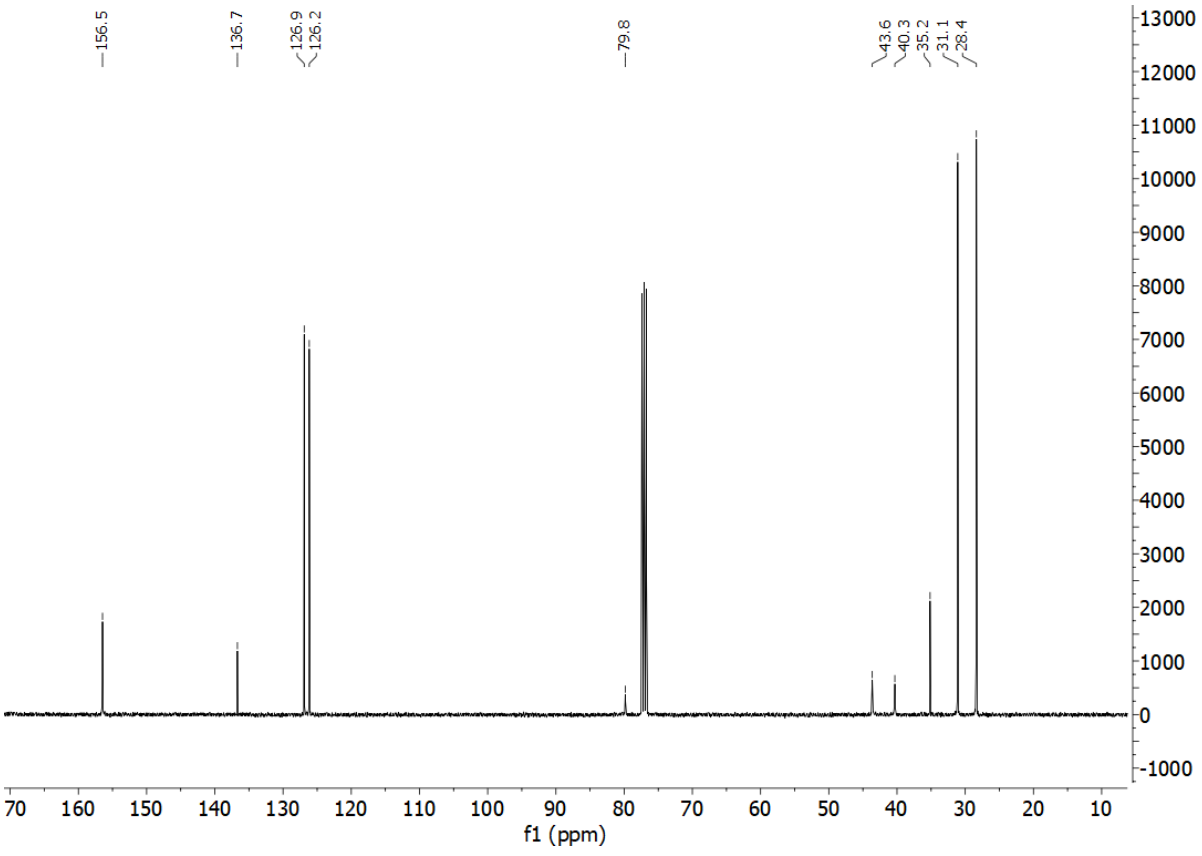

79. *N-(2'-aminoethyl)-4-tert-butylbenzene-1-sulfonamide hydrochloride*

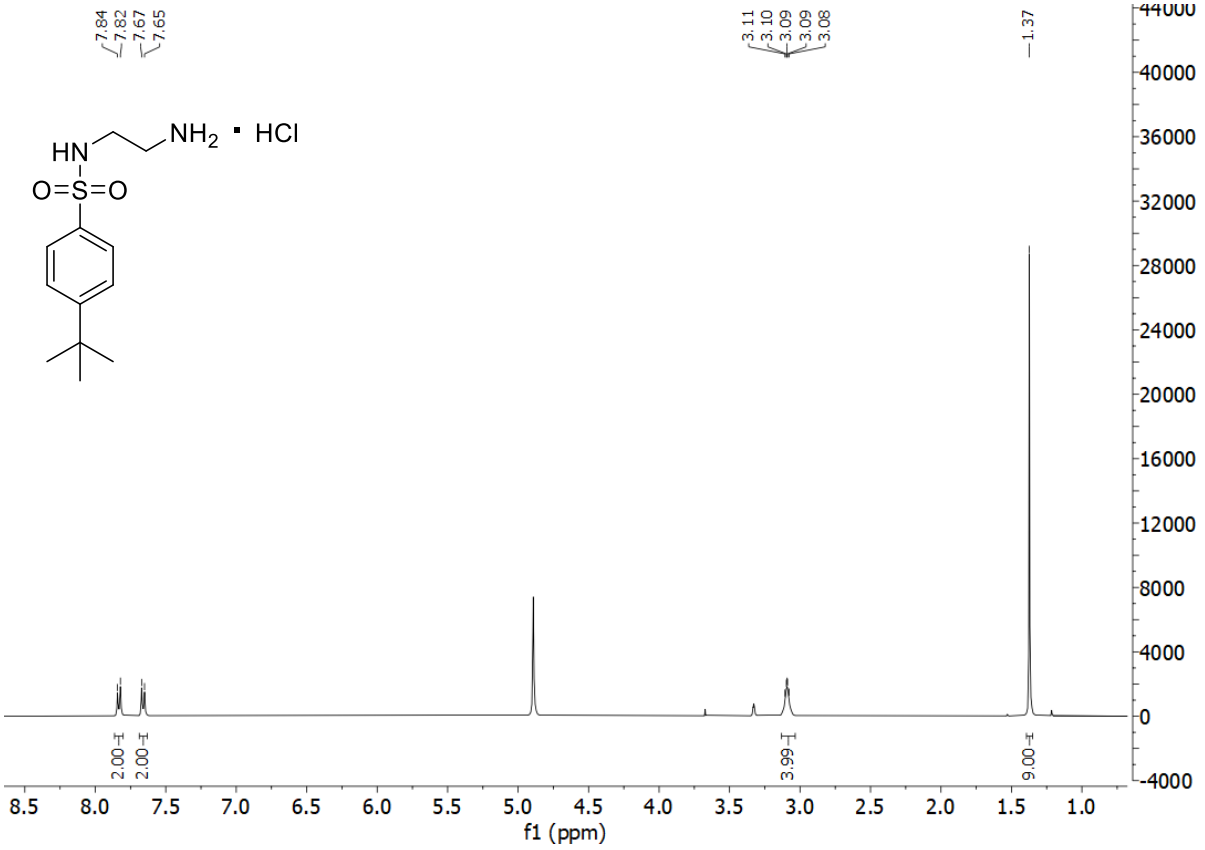

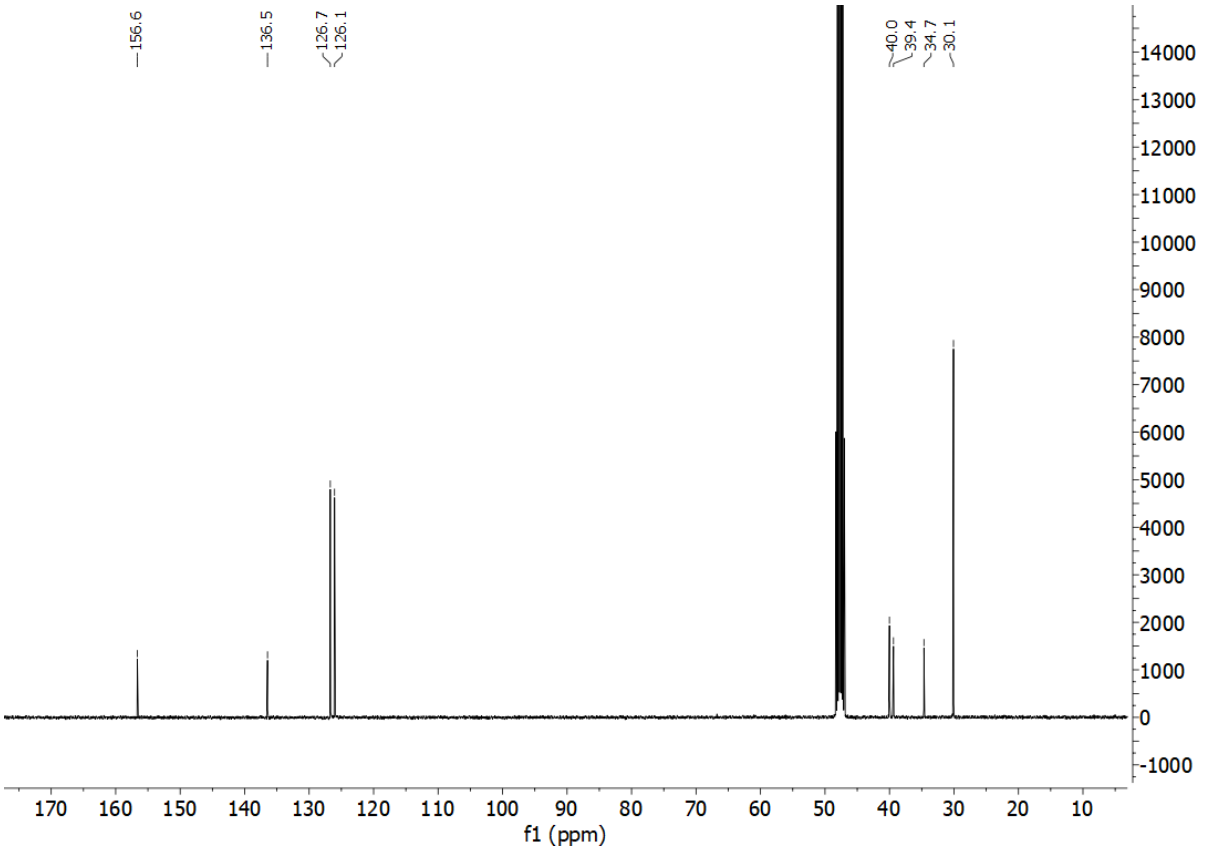

80a. *tert-butyl N-(2'-{[1,1''-biphenyl]-4-sulfonamido}ethyl)carbamate*

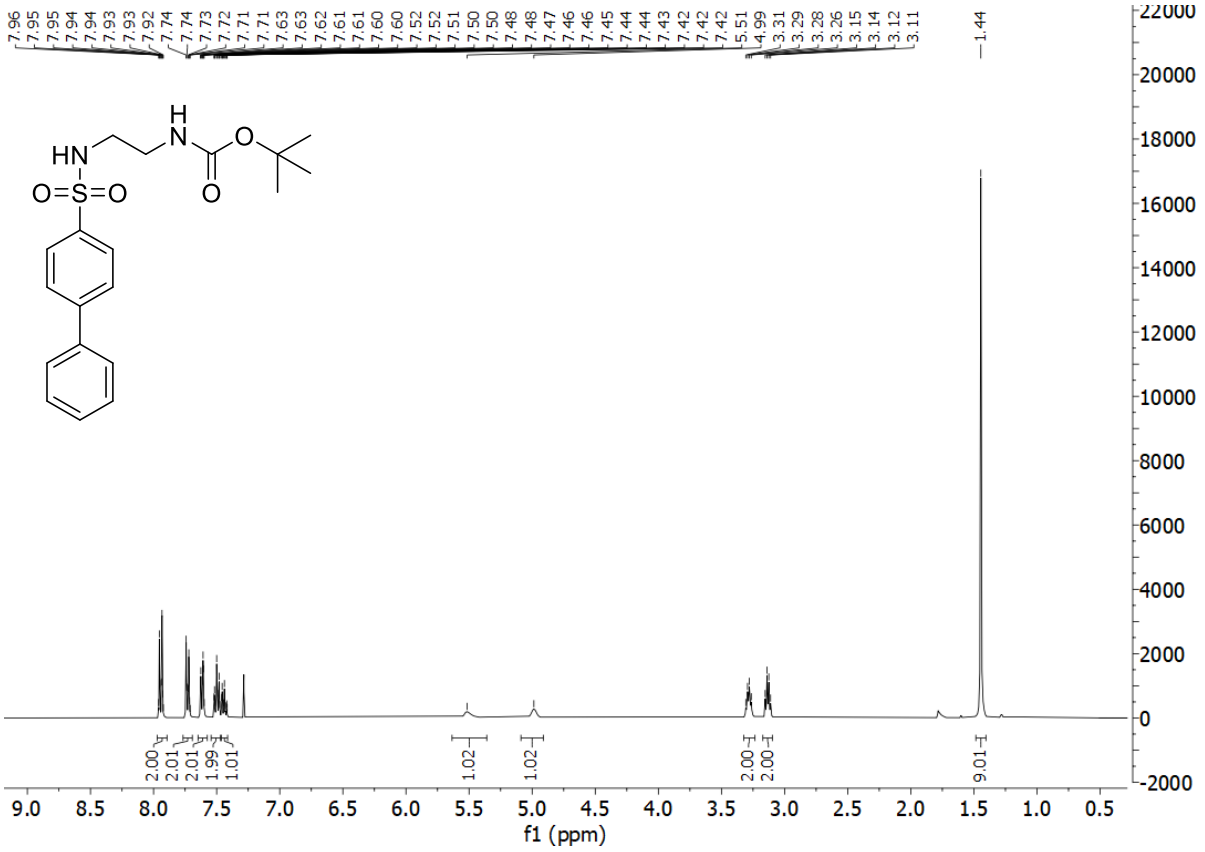

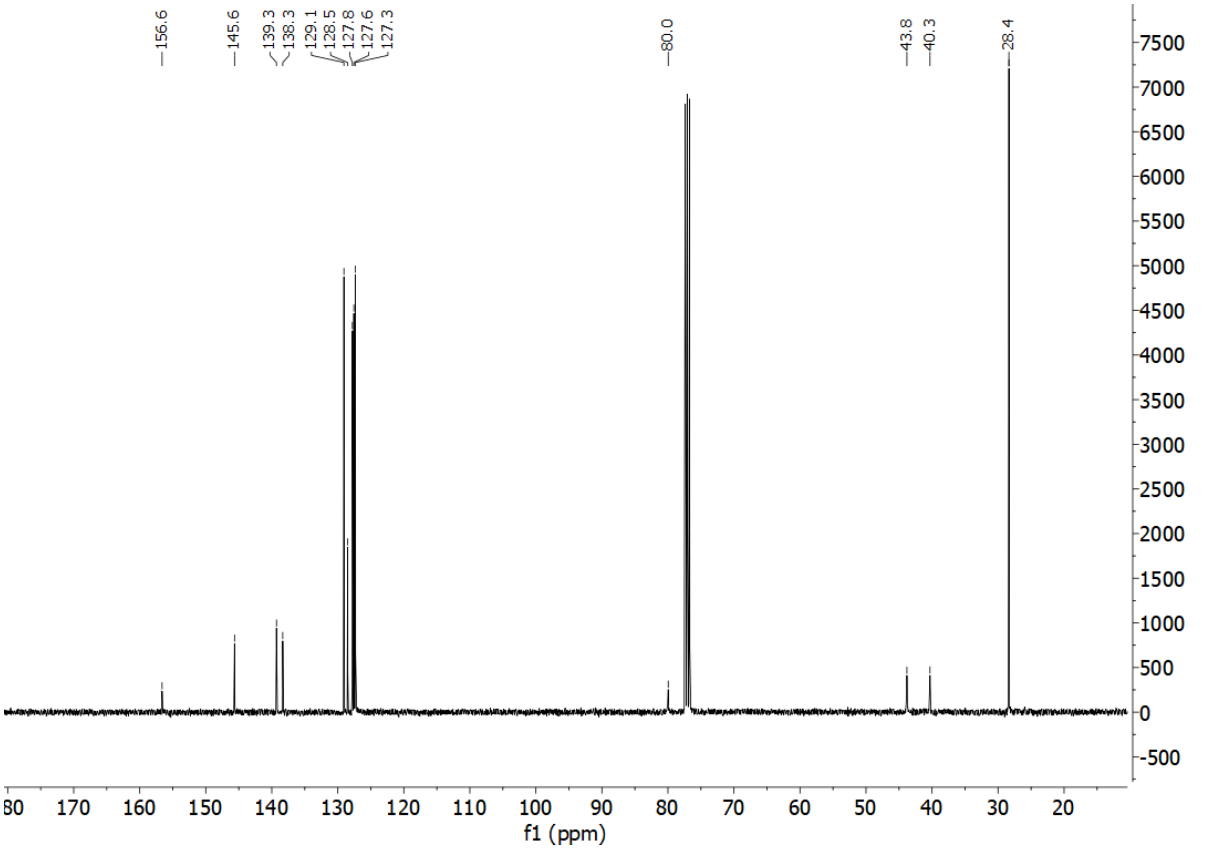

80. *N-(2'-aminoethyl)-[1,1''-biphenyl]-4-sulfonamide hydrochloride*

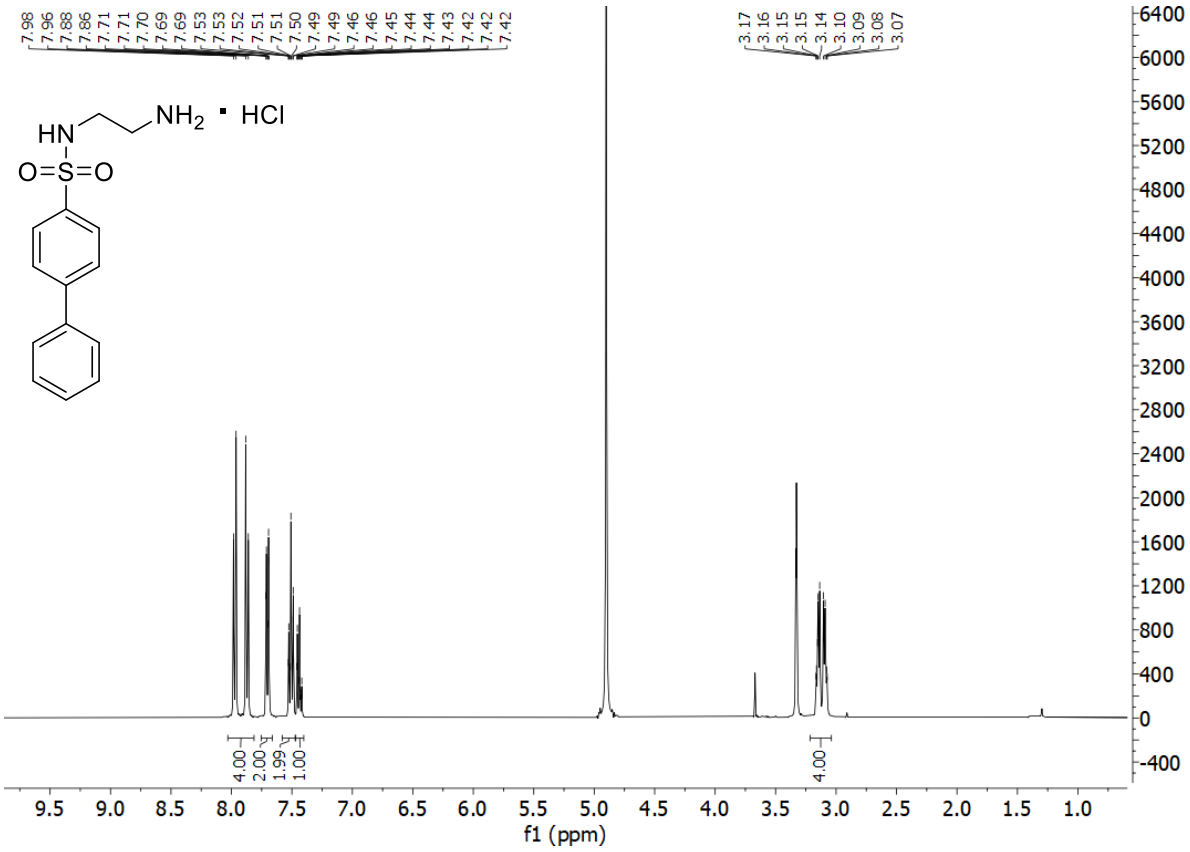

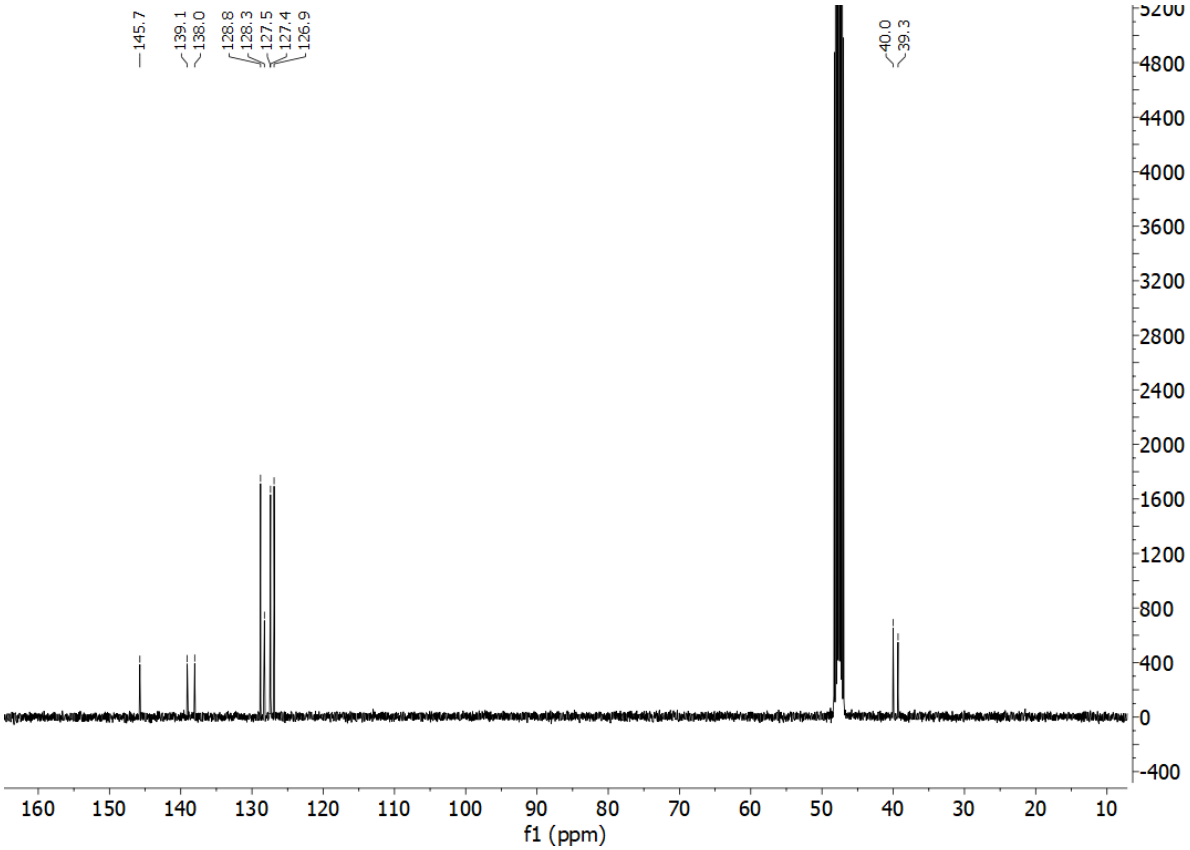

81a. *tert-butyl N-{2'-[2''-(naphthalen-1-yl)ethanesulfonamido]ethyl}carbamate*

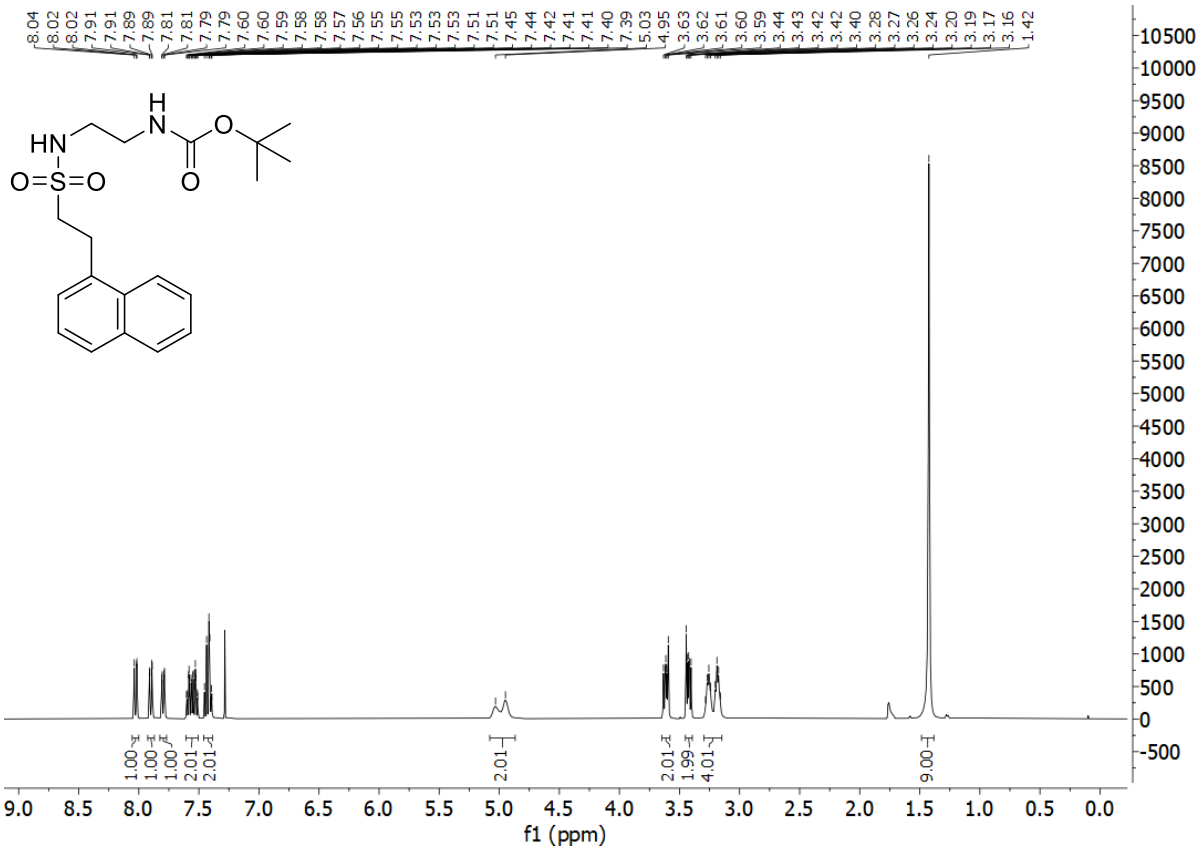

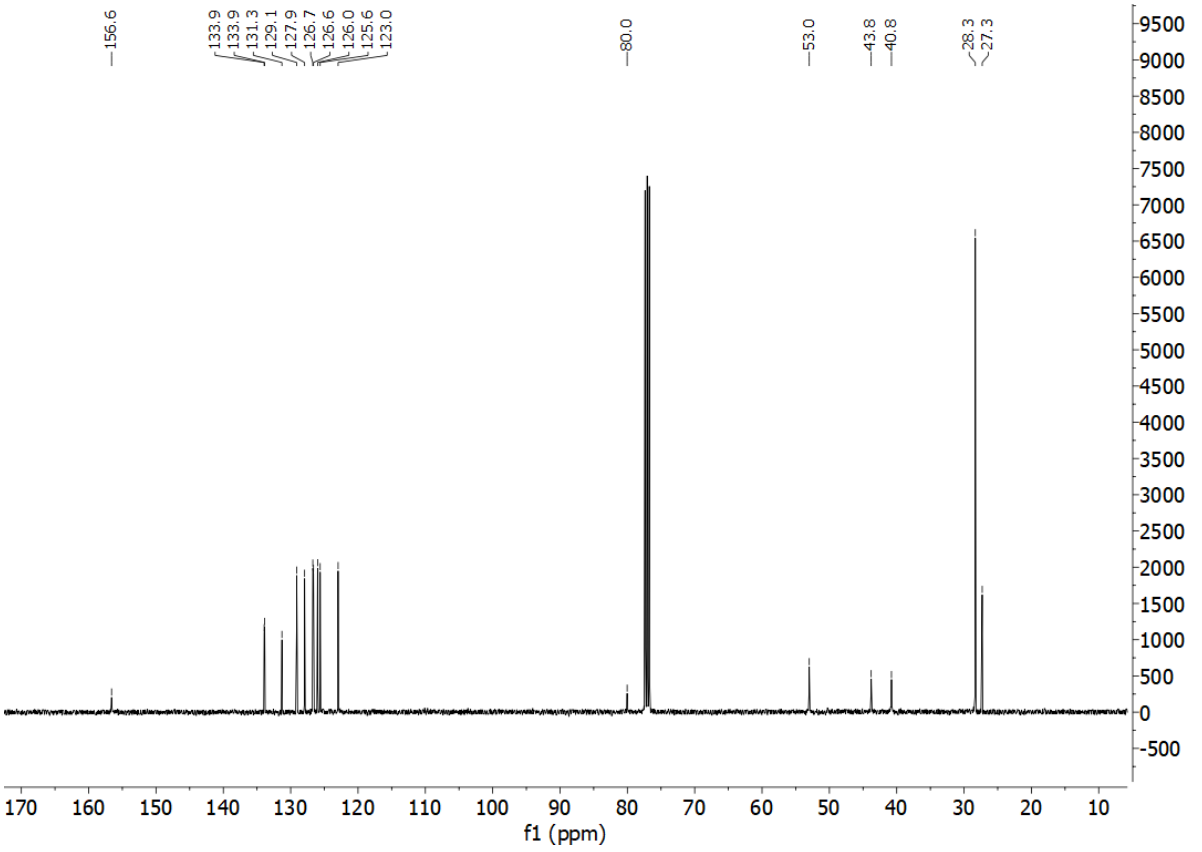

81. *N-(2'-aminoethyl)-2''-(naphthalen-1-yl)ethane-1''-sulfonamide hydrochloride*

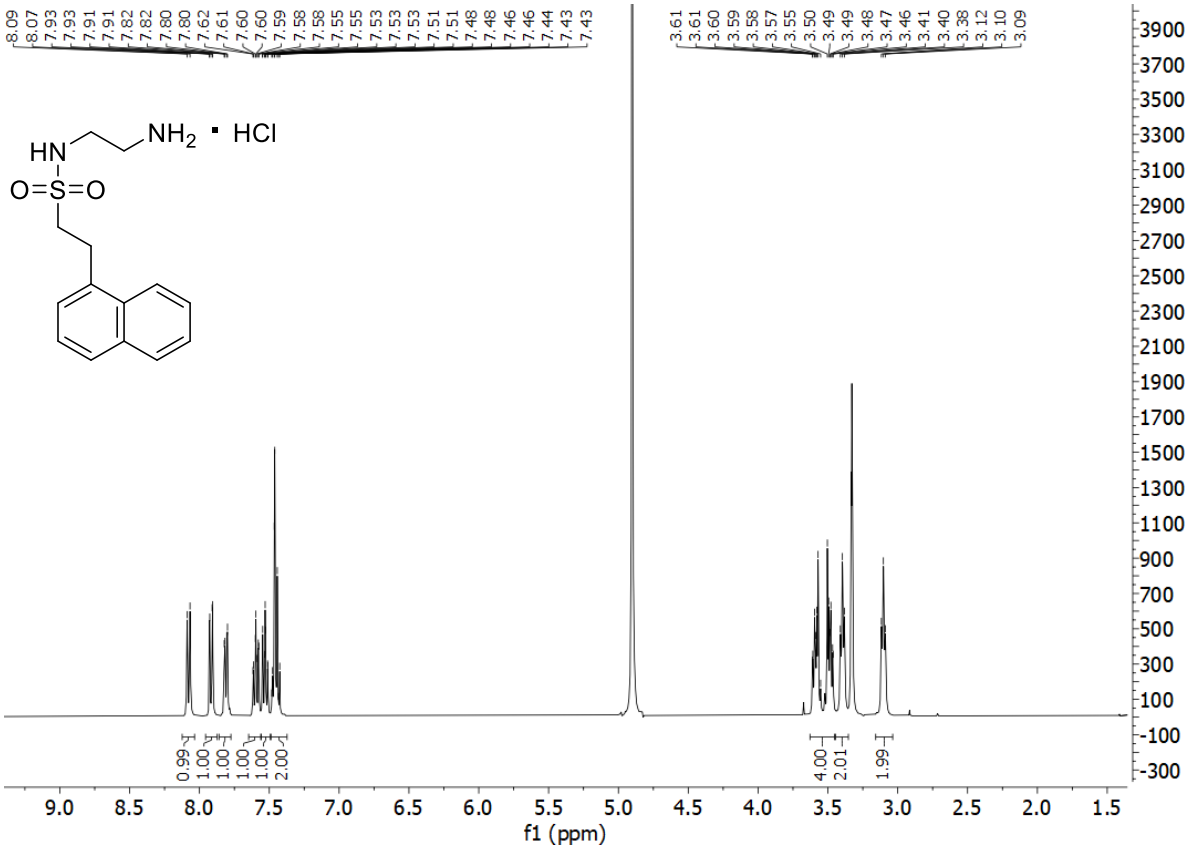

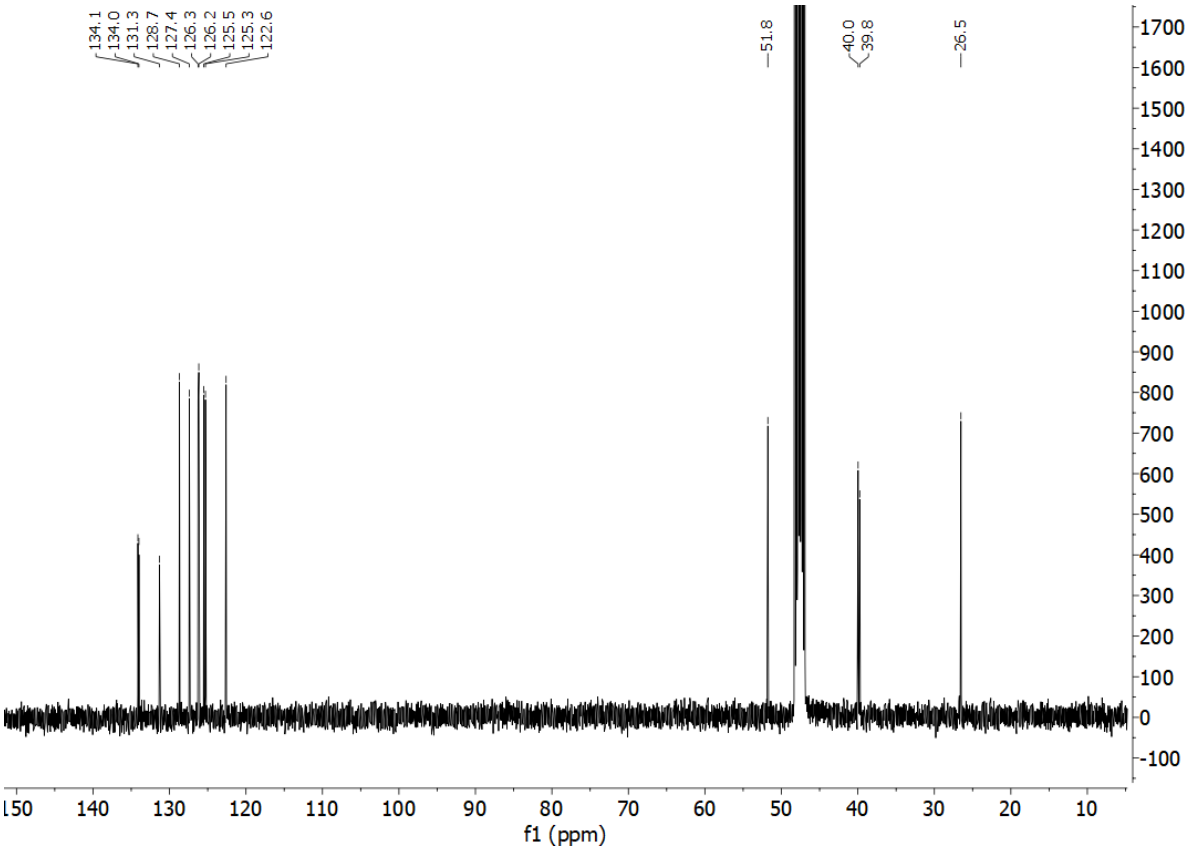

82a. *tert-butyl N-[3'-(naphthalene-1-sulfonamido)propyl]carbamate*

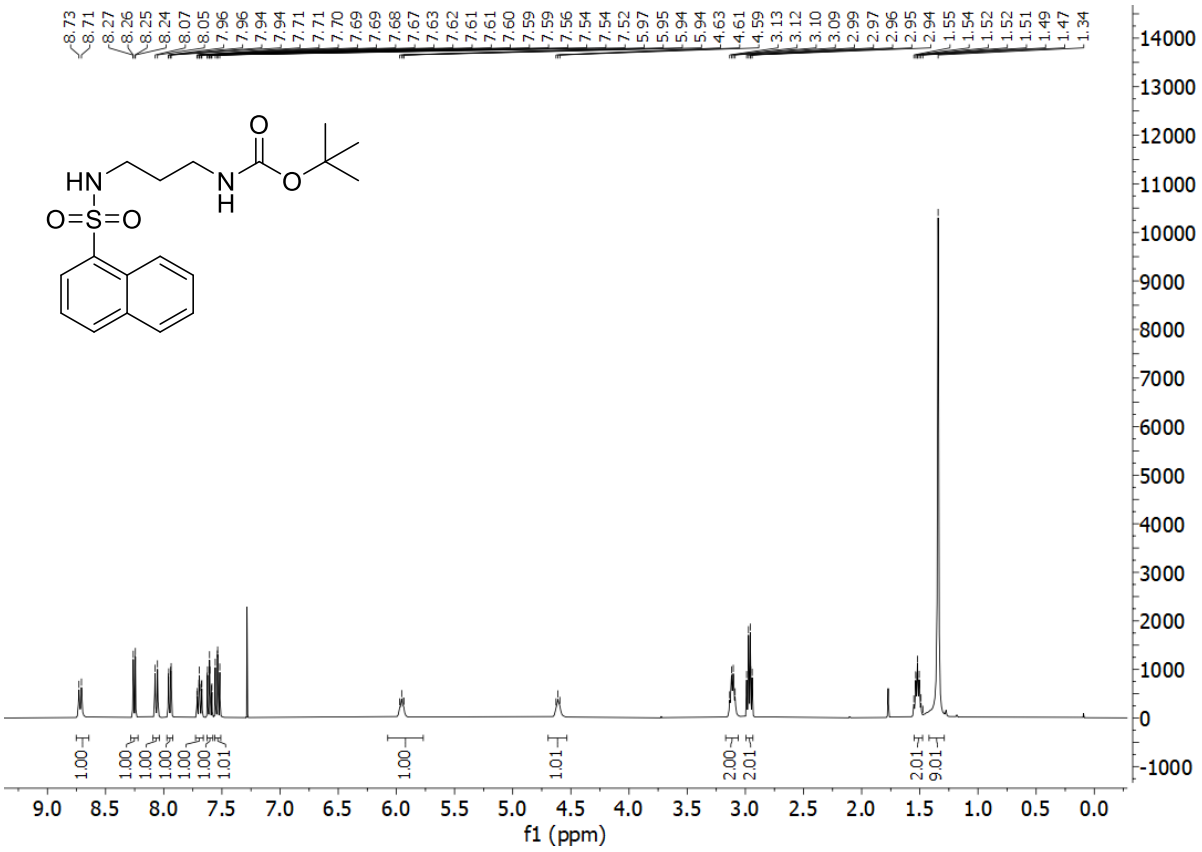

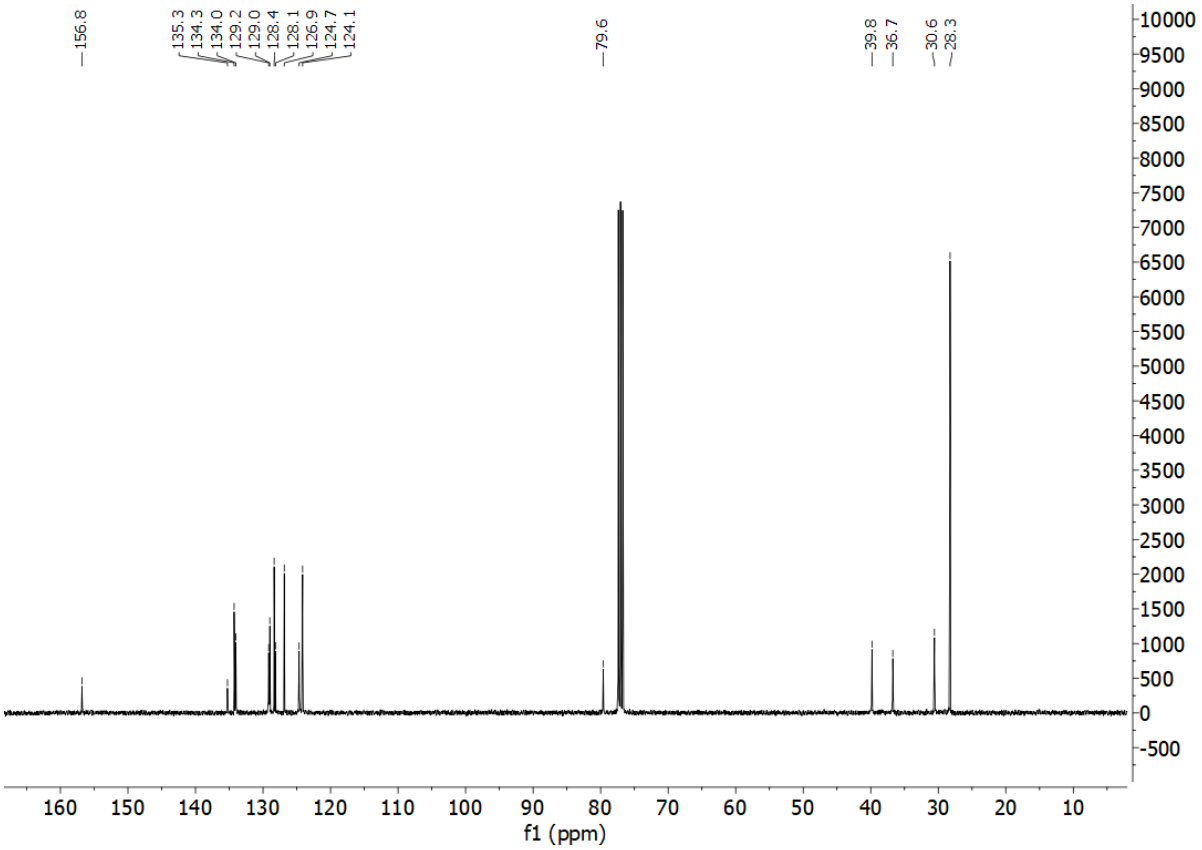

82. *N-(3'-aminopropyl)naphthalene-1-sulfonamide hydrochloride*

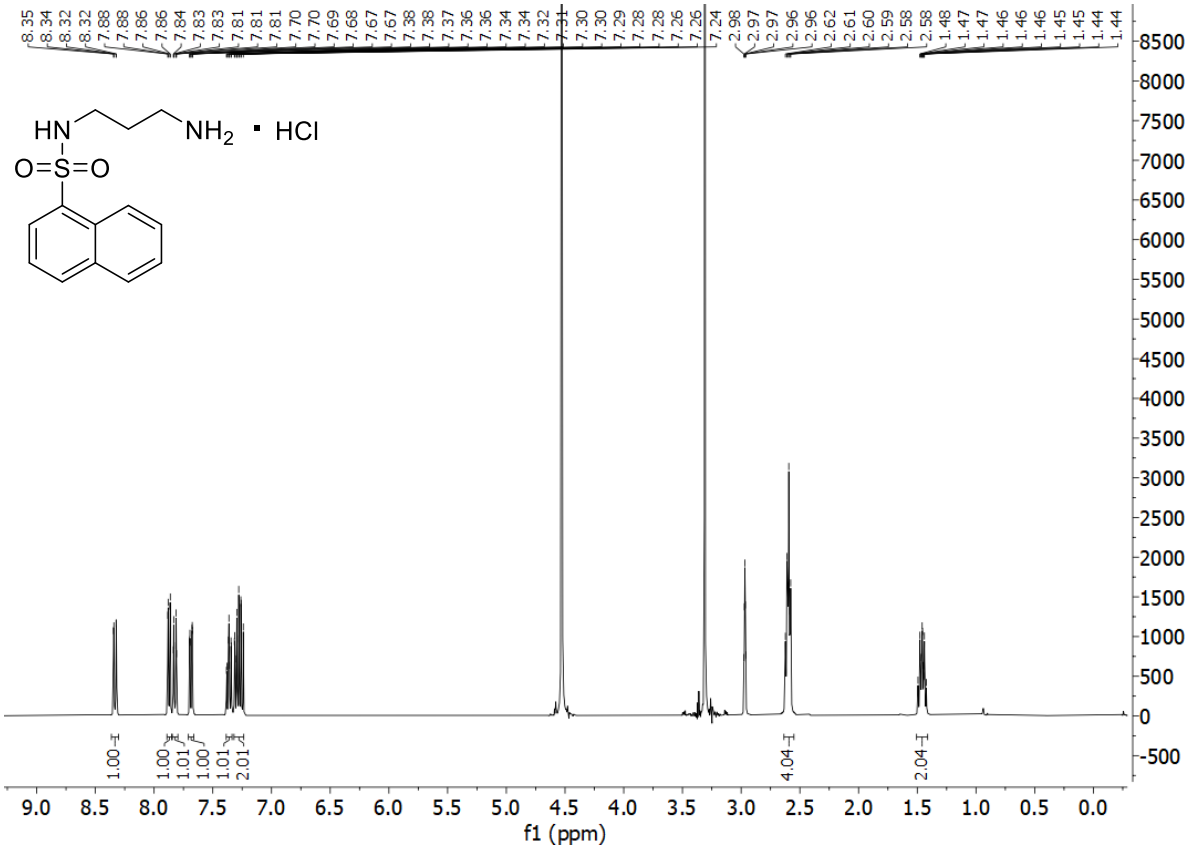

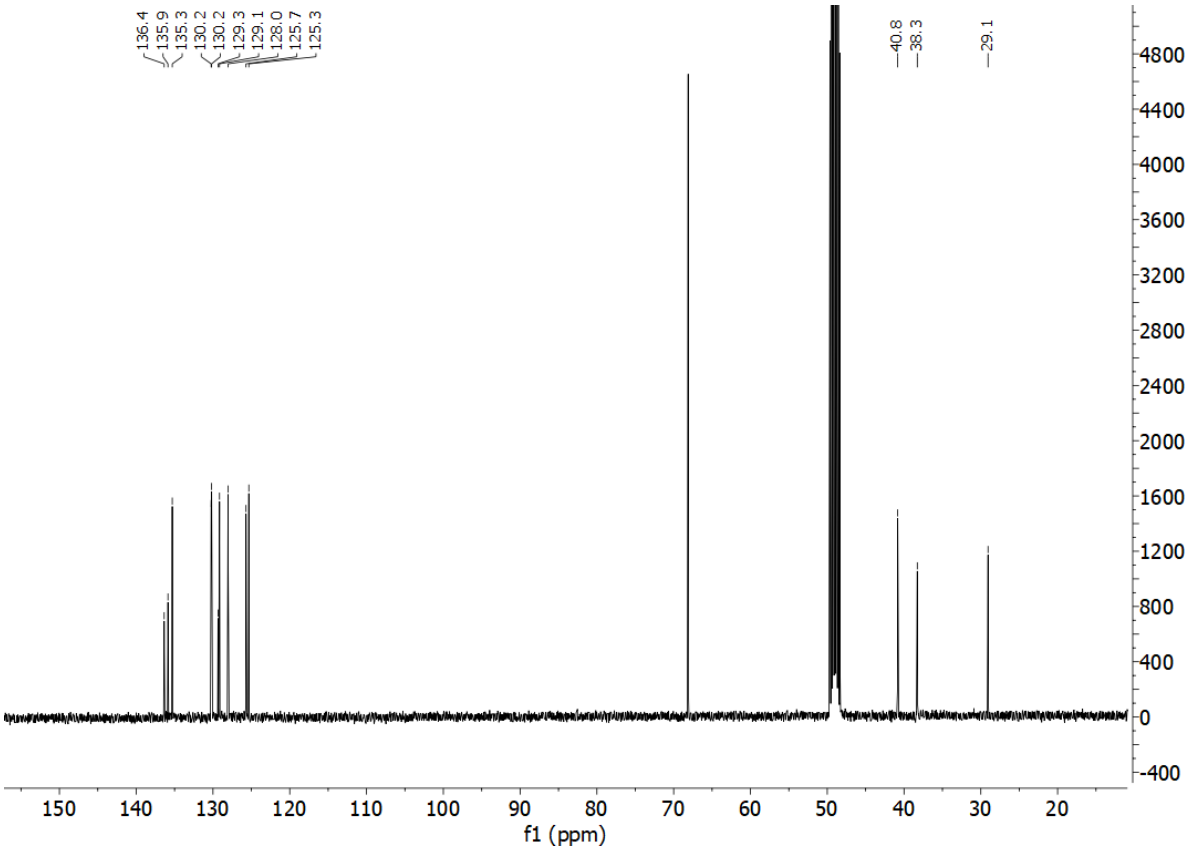

83. *N-[2'-(dimethylamino)ethyl]naphthalene-2-sulfonamide*

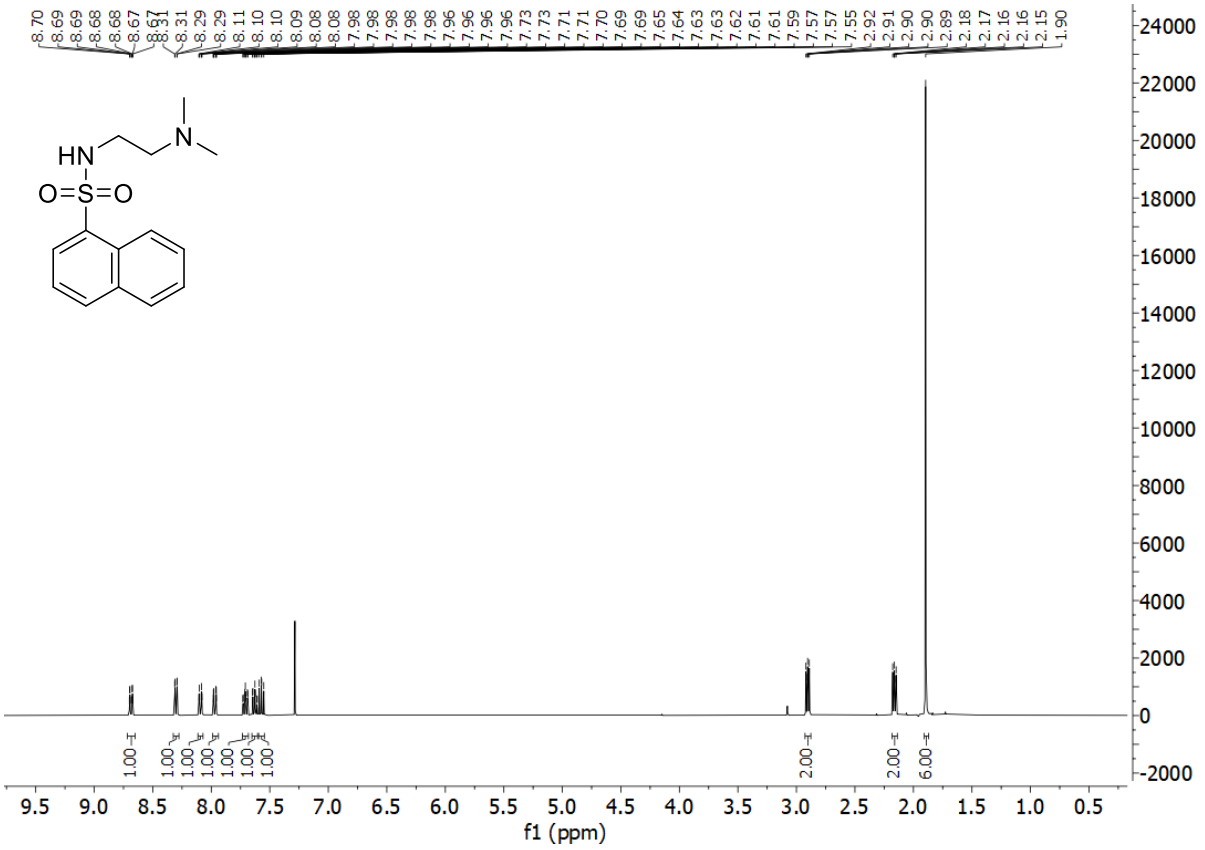

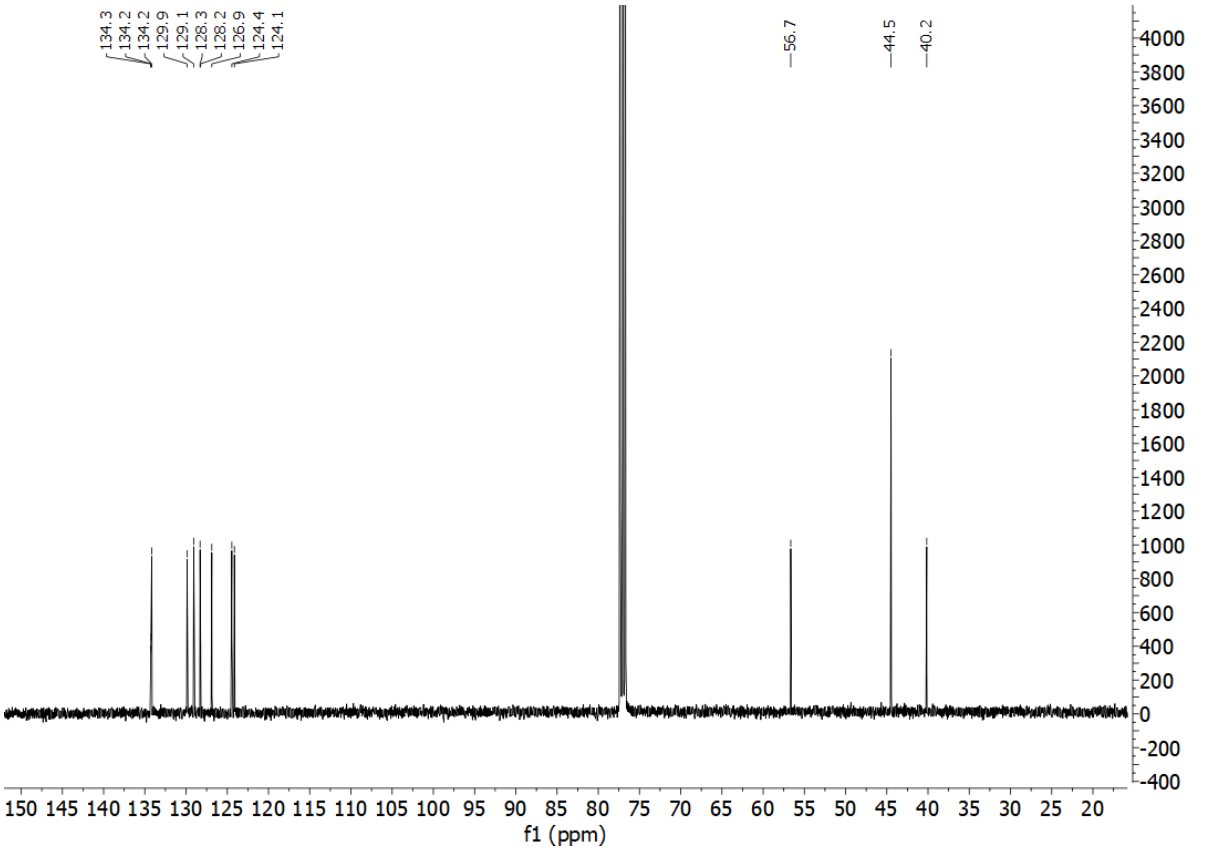

84. *N-(2-hydroxyethyl)naphthalene-1-sulfonamide*

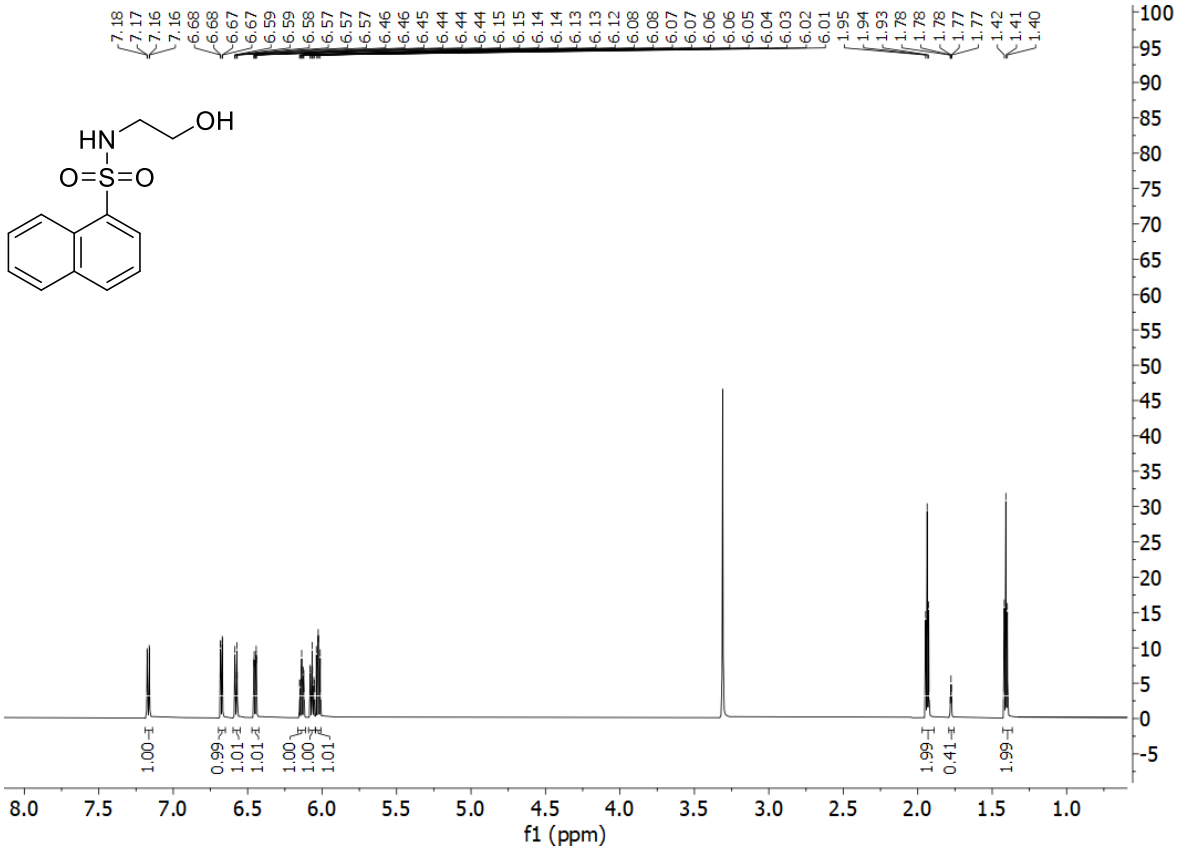

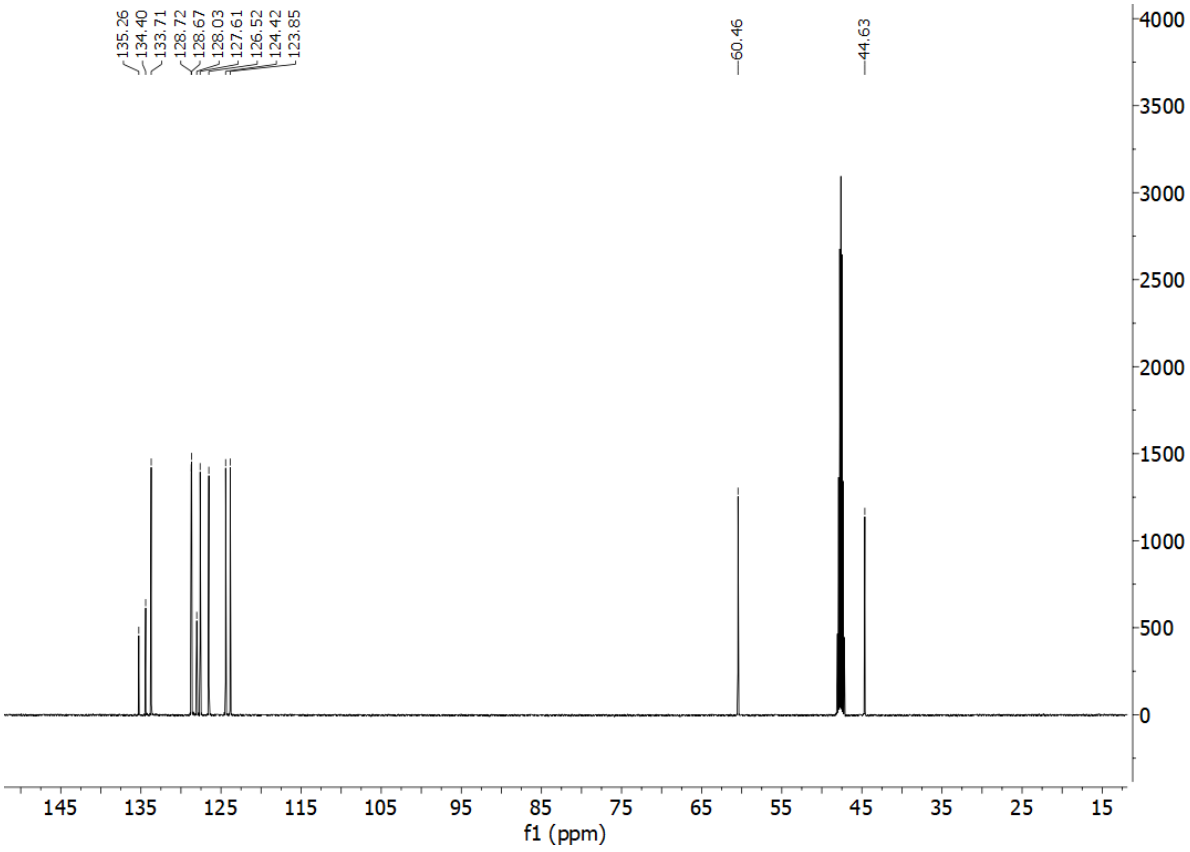

85. *N-(2-methoxyethyl)naphthalene-2-sulfonamide*

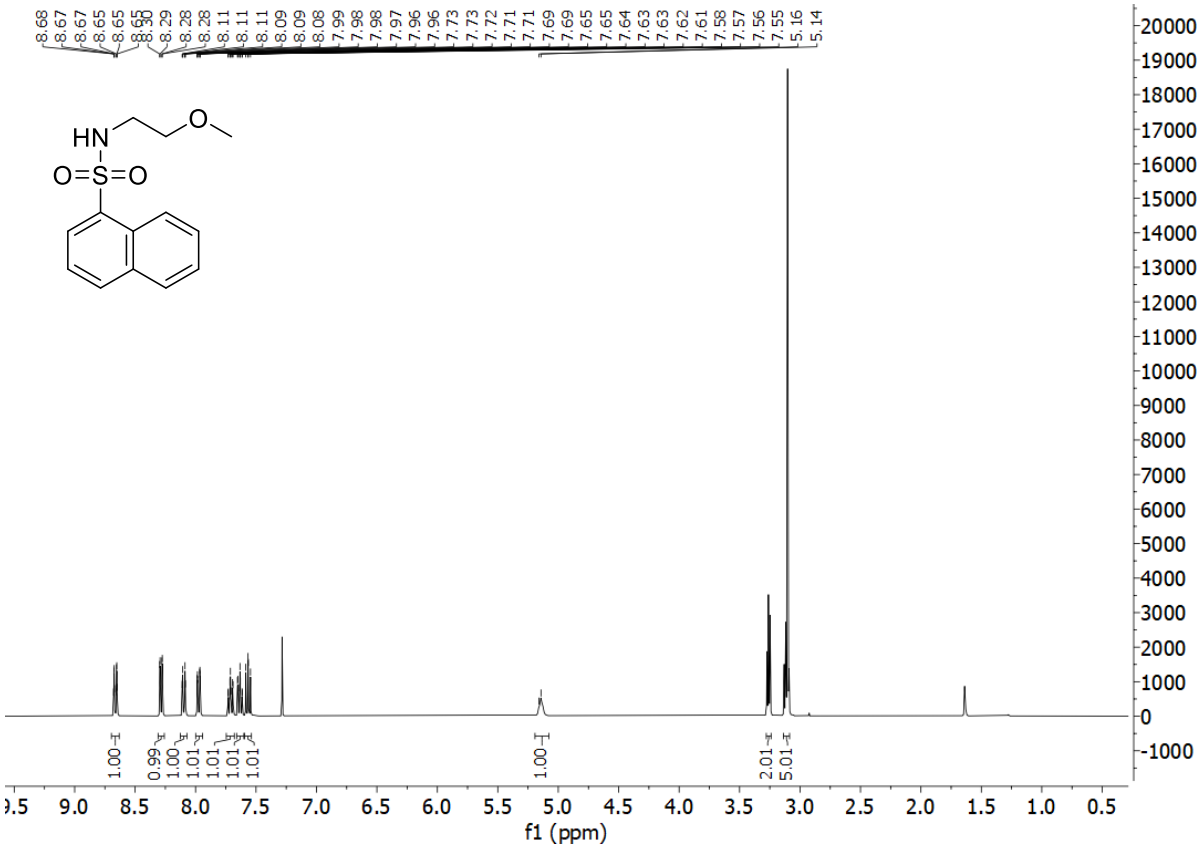

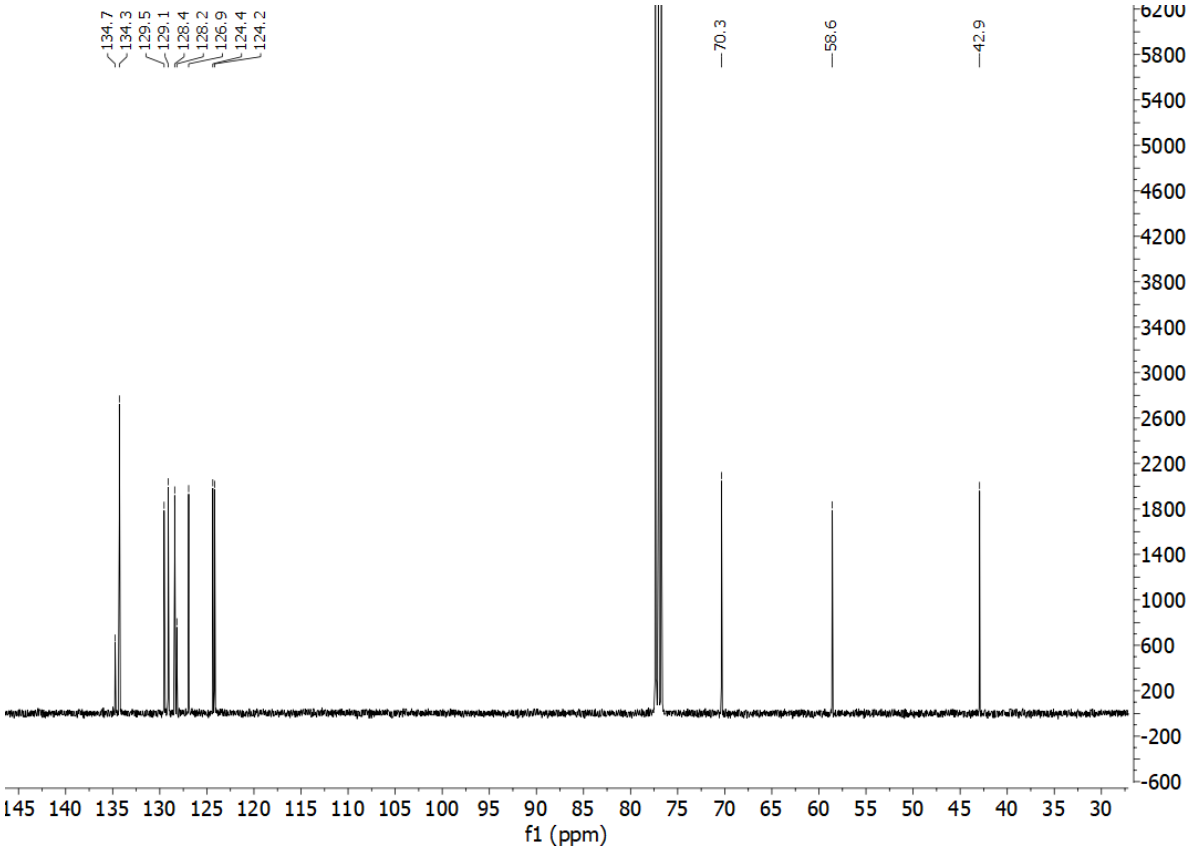

86a. *tert-butyl N-(2'-methanesulfonamidoethyl)carbamate*

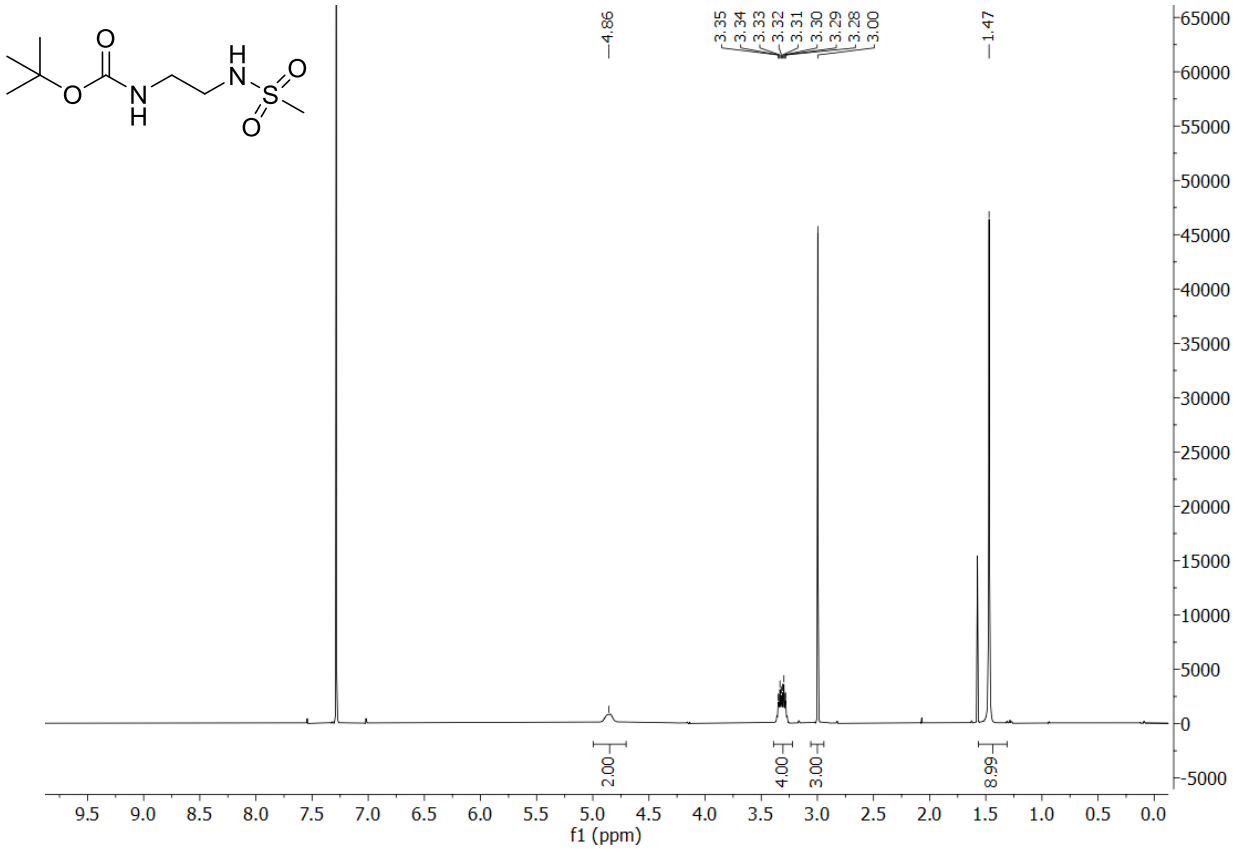

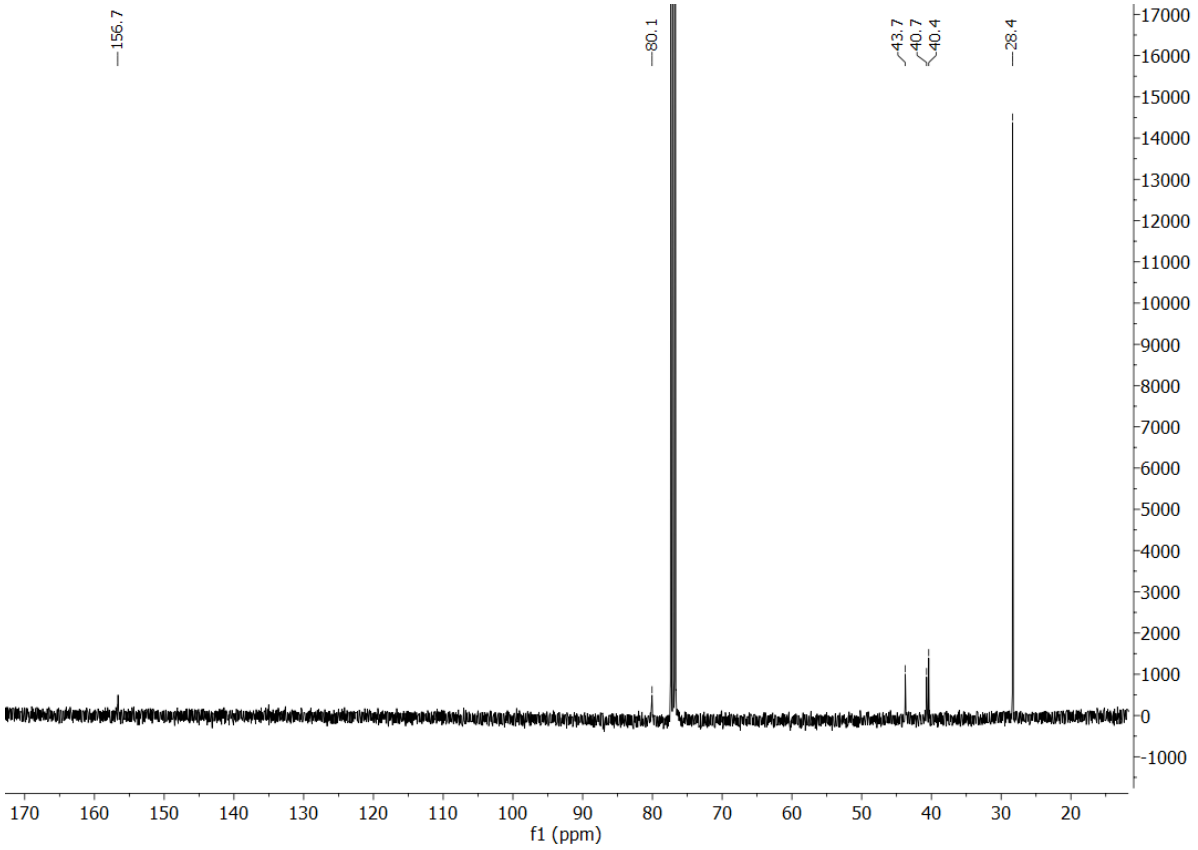

86. *N-(2-aminoethyl)methanesulfonamide*

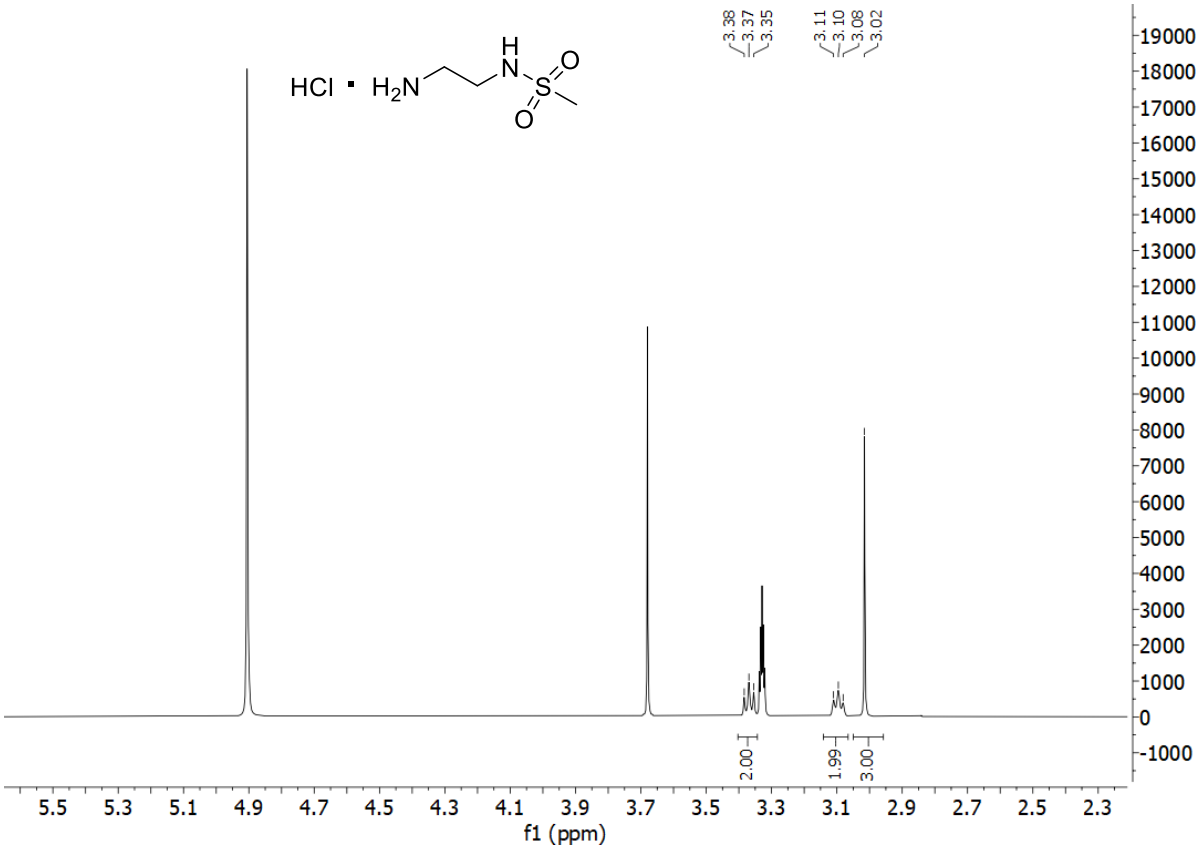

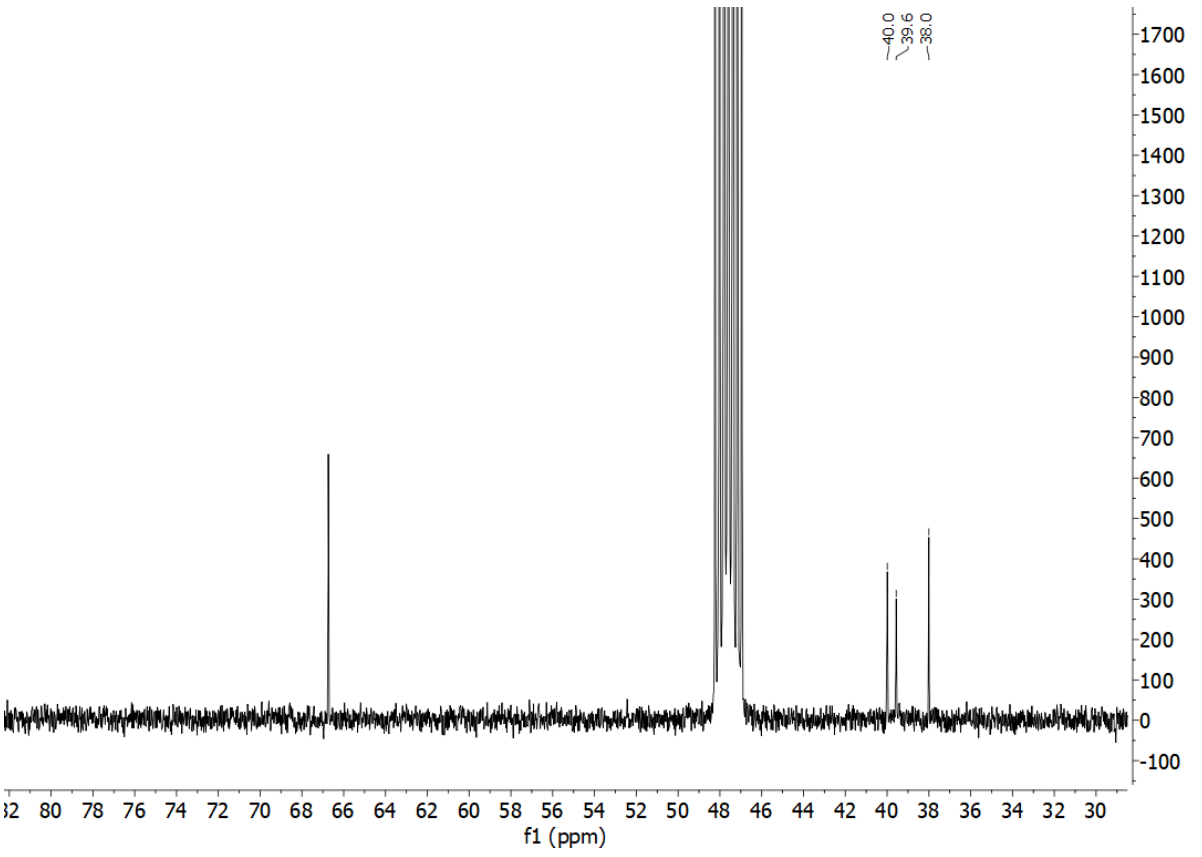

87a. *tert-butyl N-(2'-cyclohexanesulfonamidoethyl)carbamate*

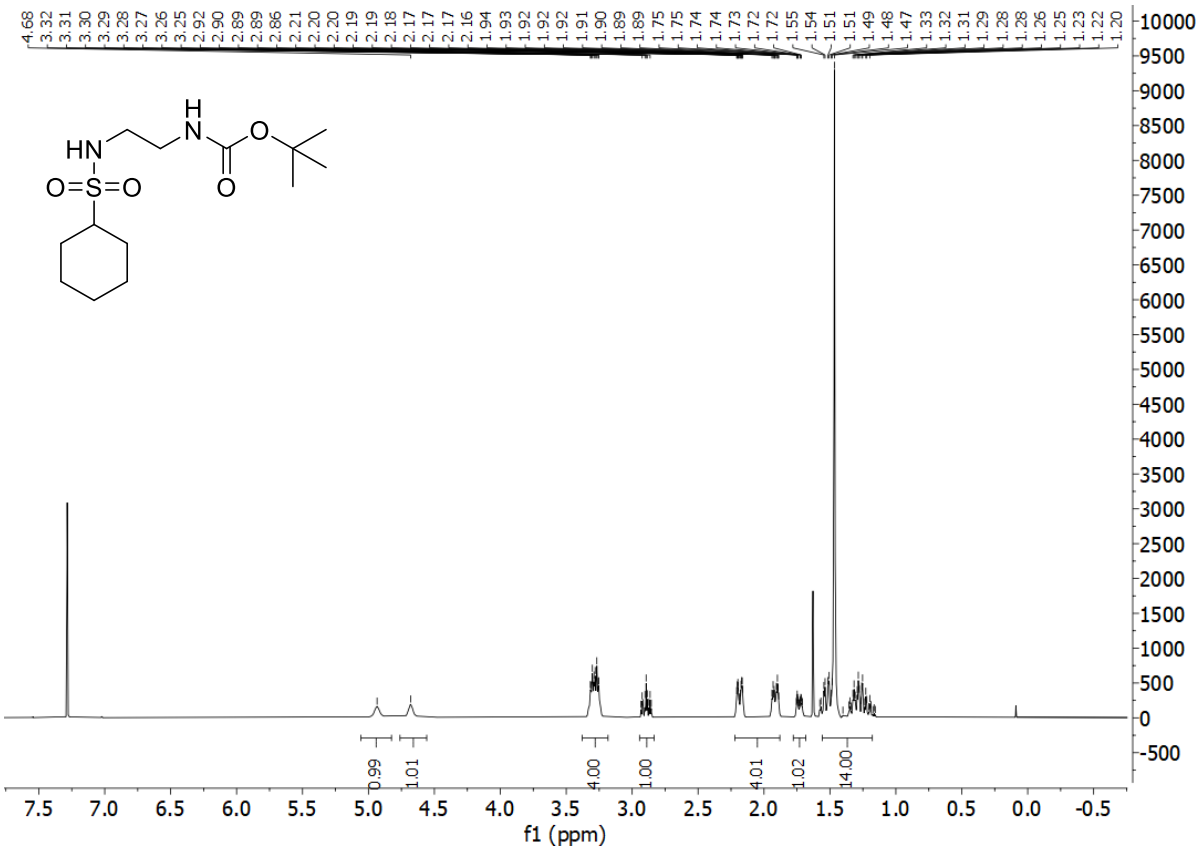

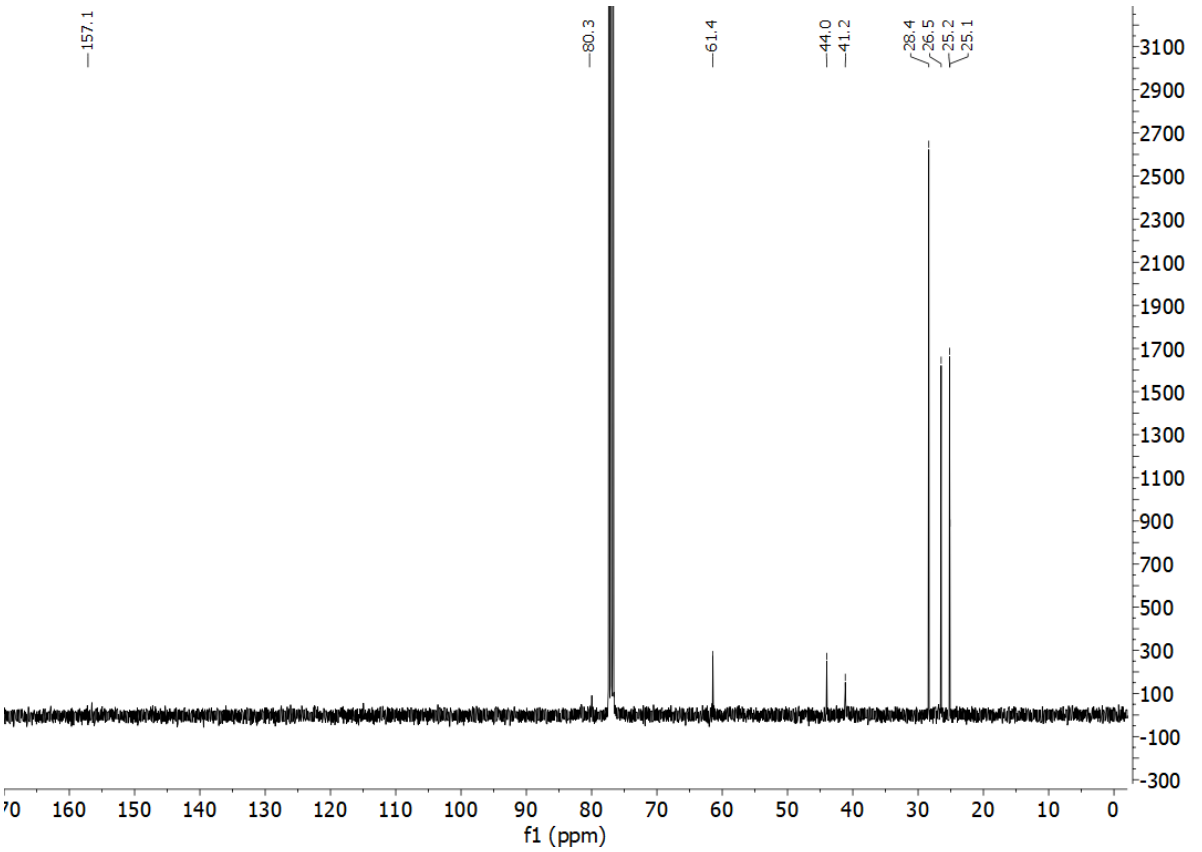

87. *N-(2'-aminoethyl)cyclohexanesulfonamide hydrochloride*

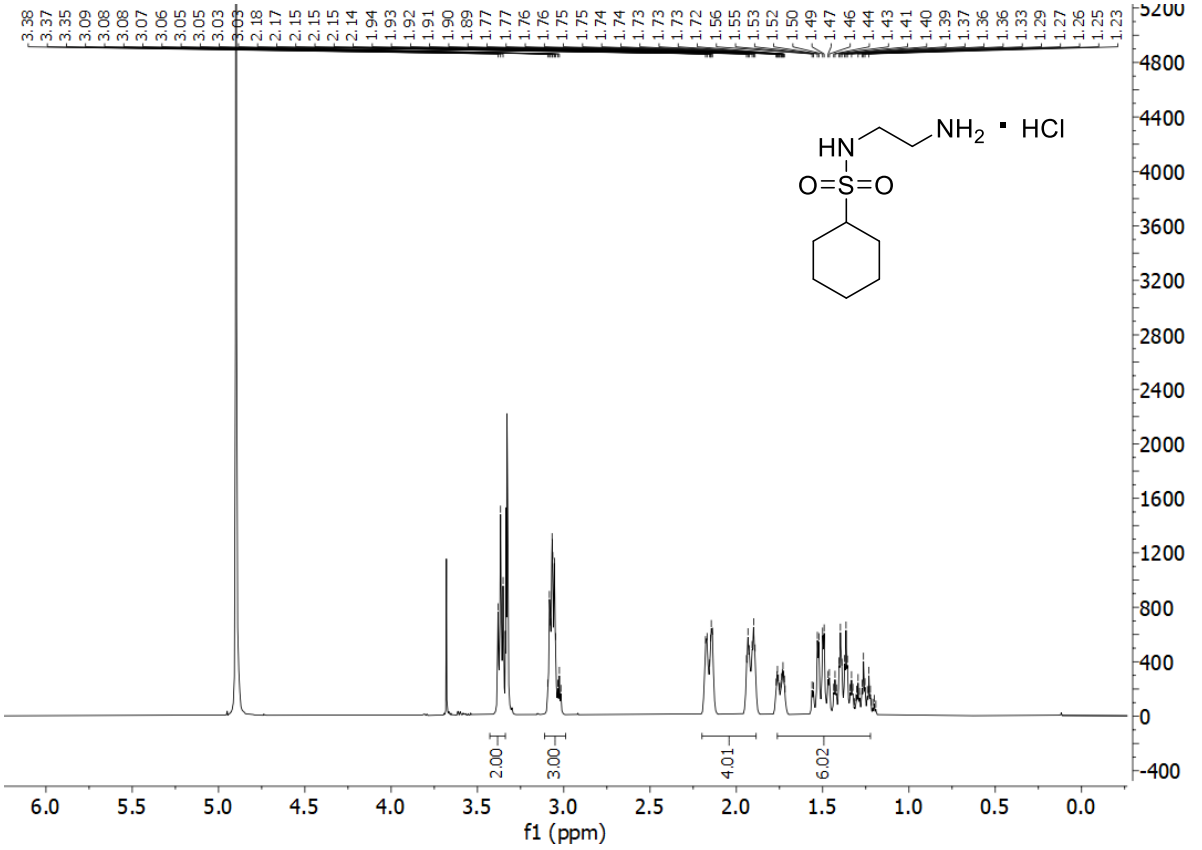

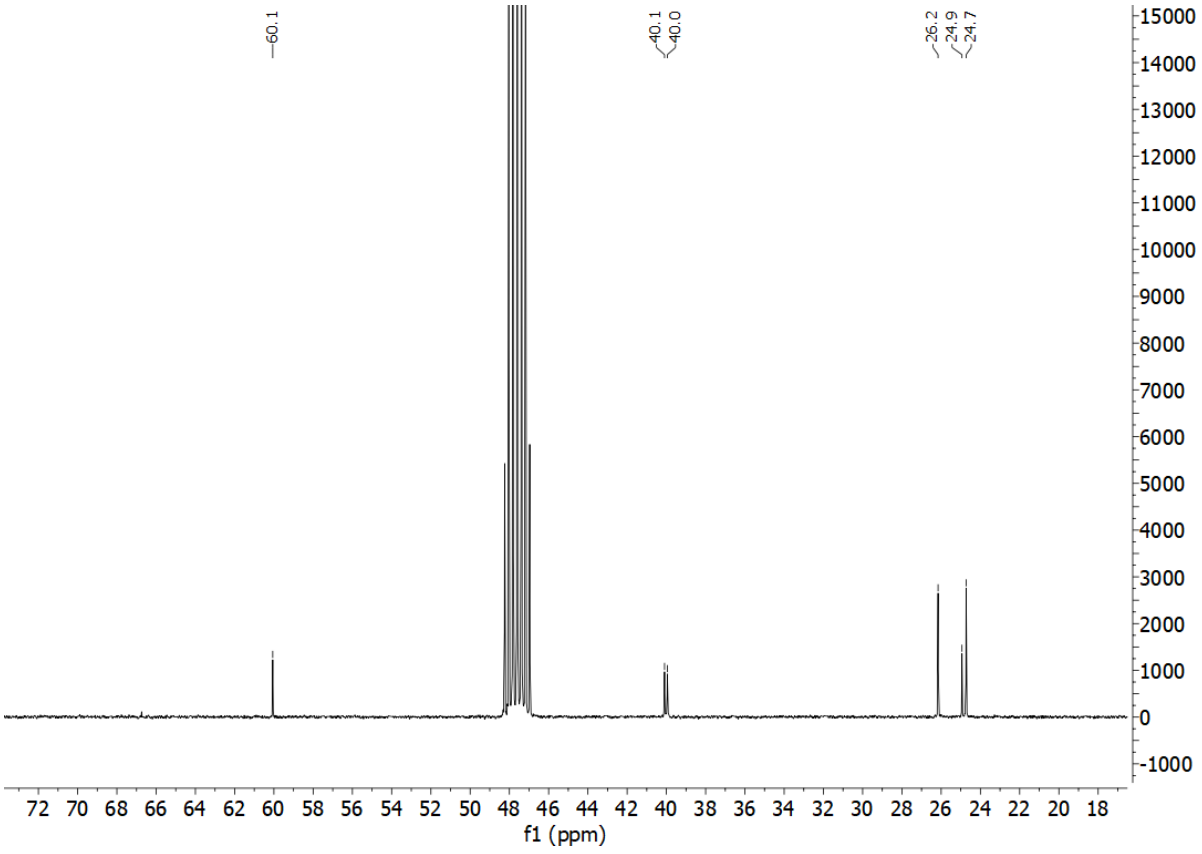

71a. *tert-butyl N-methyl-N-[2'-(naphthalene-1-sulfonamido)ethyl]carbamate*

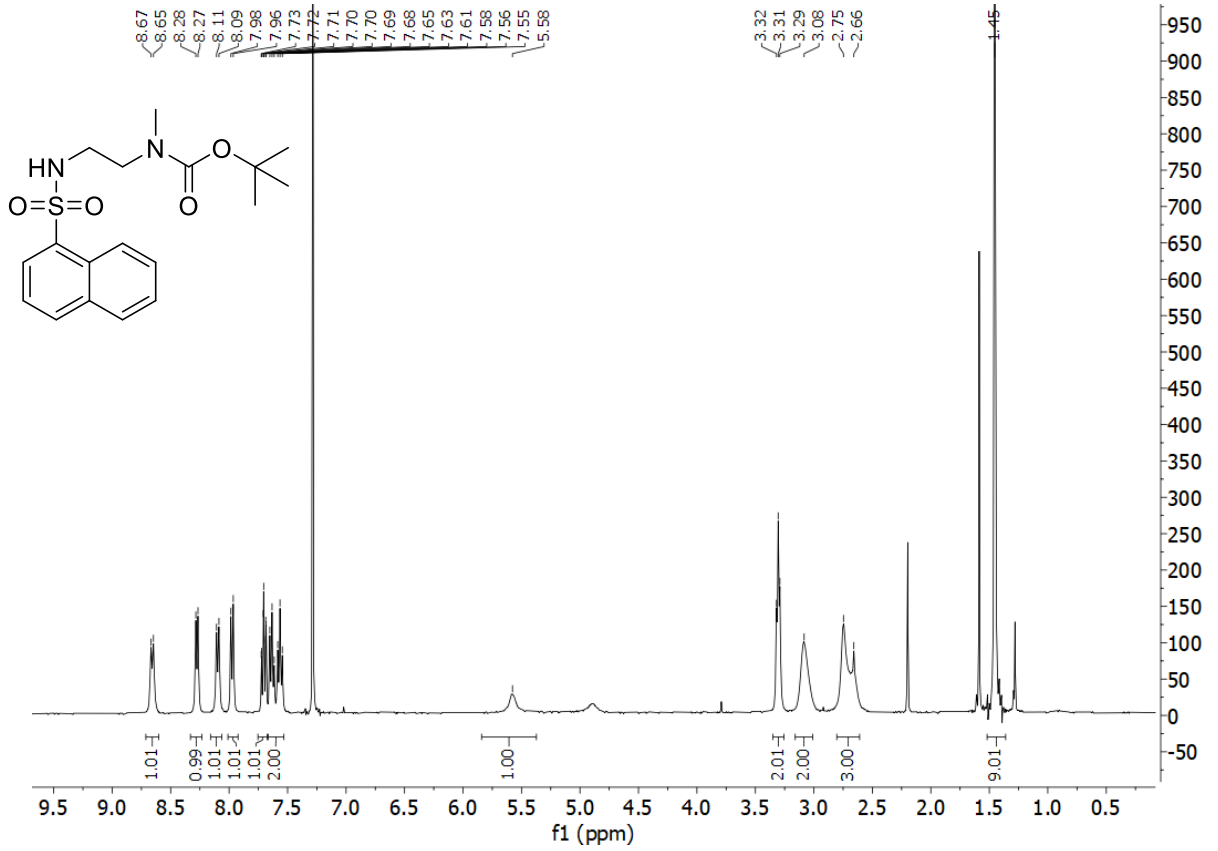

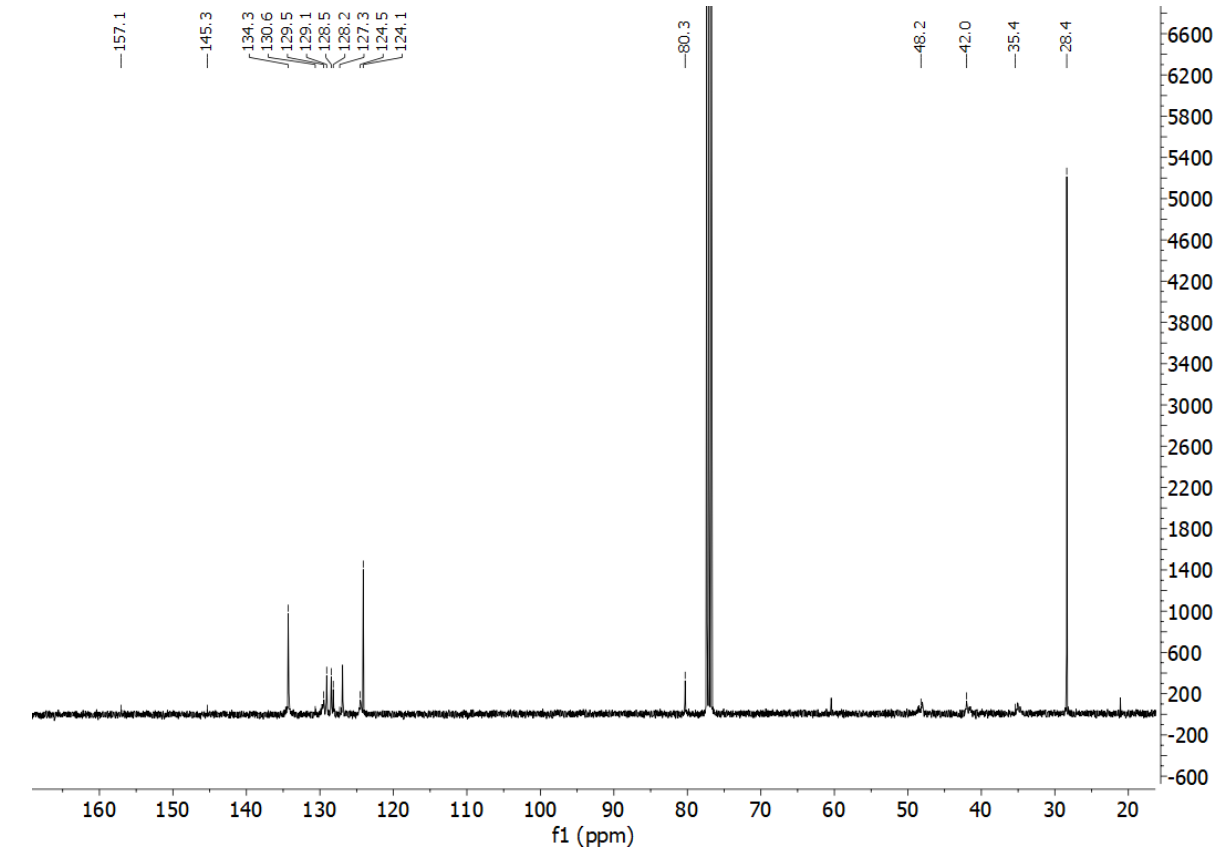

71. *N-[2'-(methylamino)ethyl]naphthalene-1-sulfonamide hydrochloride*

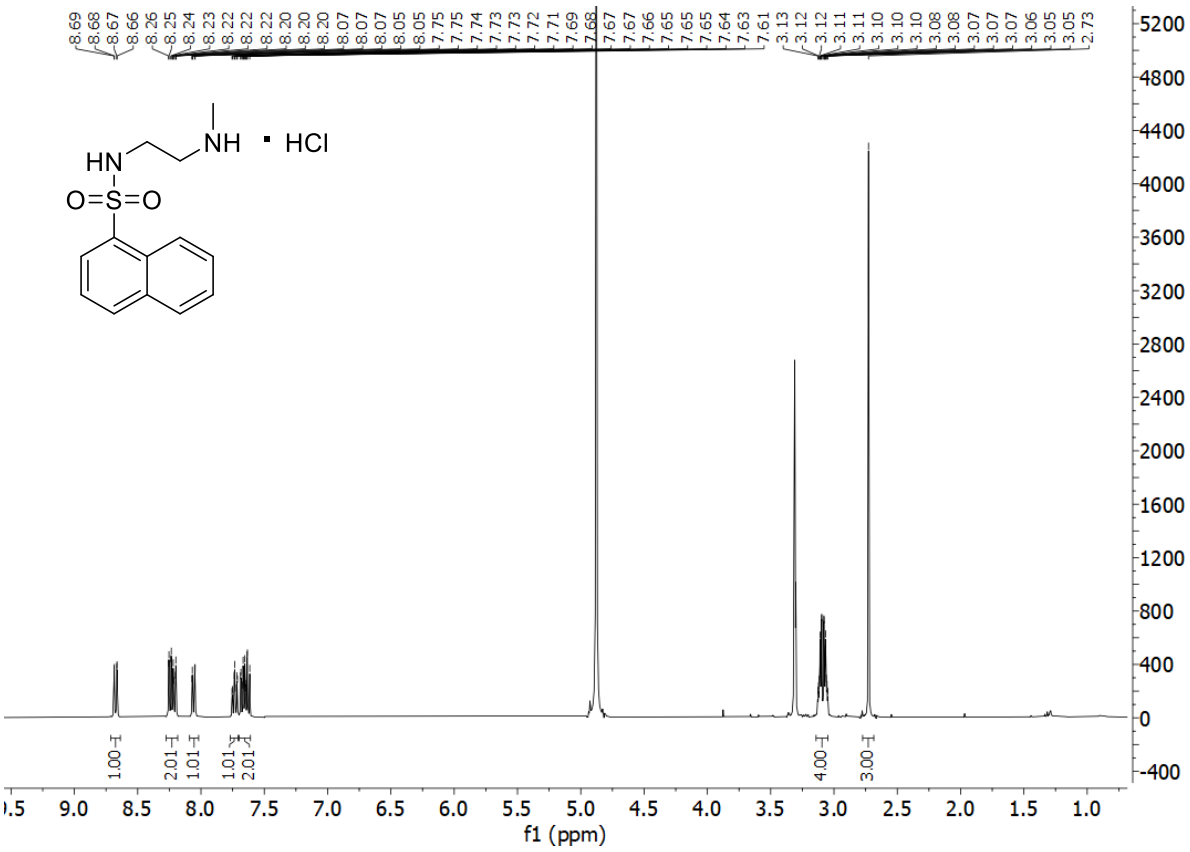

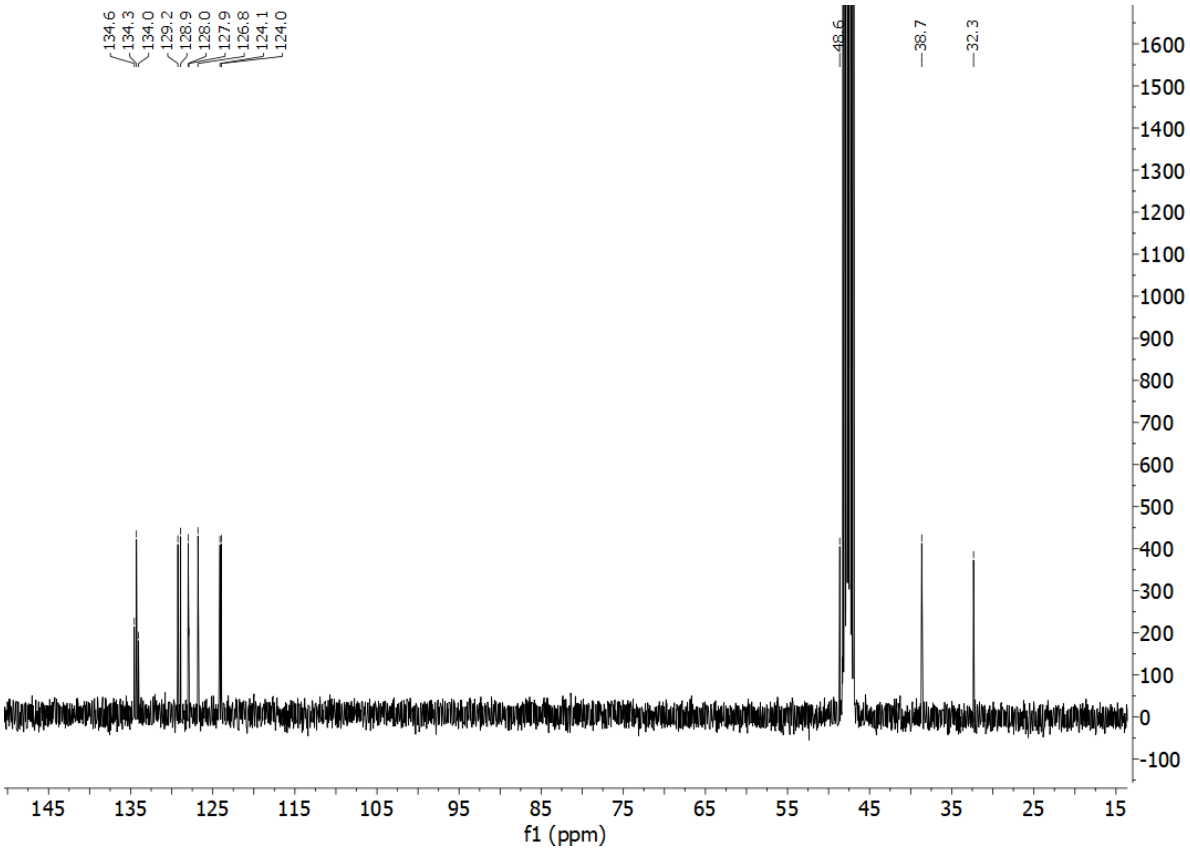

72a. *tert-butyl N-[2'-(N-methylnaphthalene-1-sulfonamido)ethyl]carbamate*

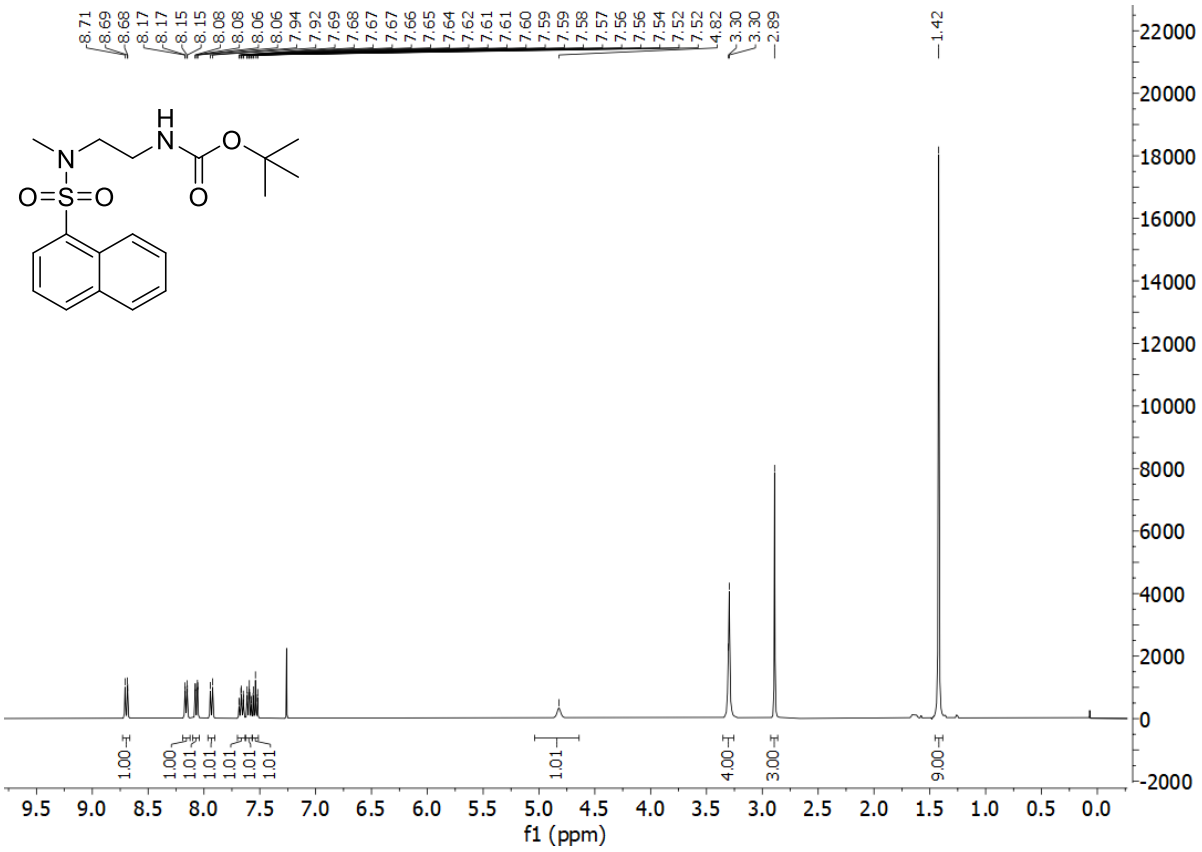

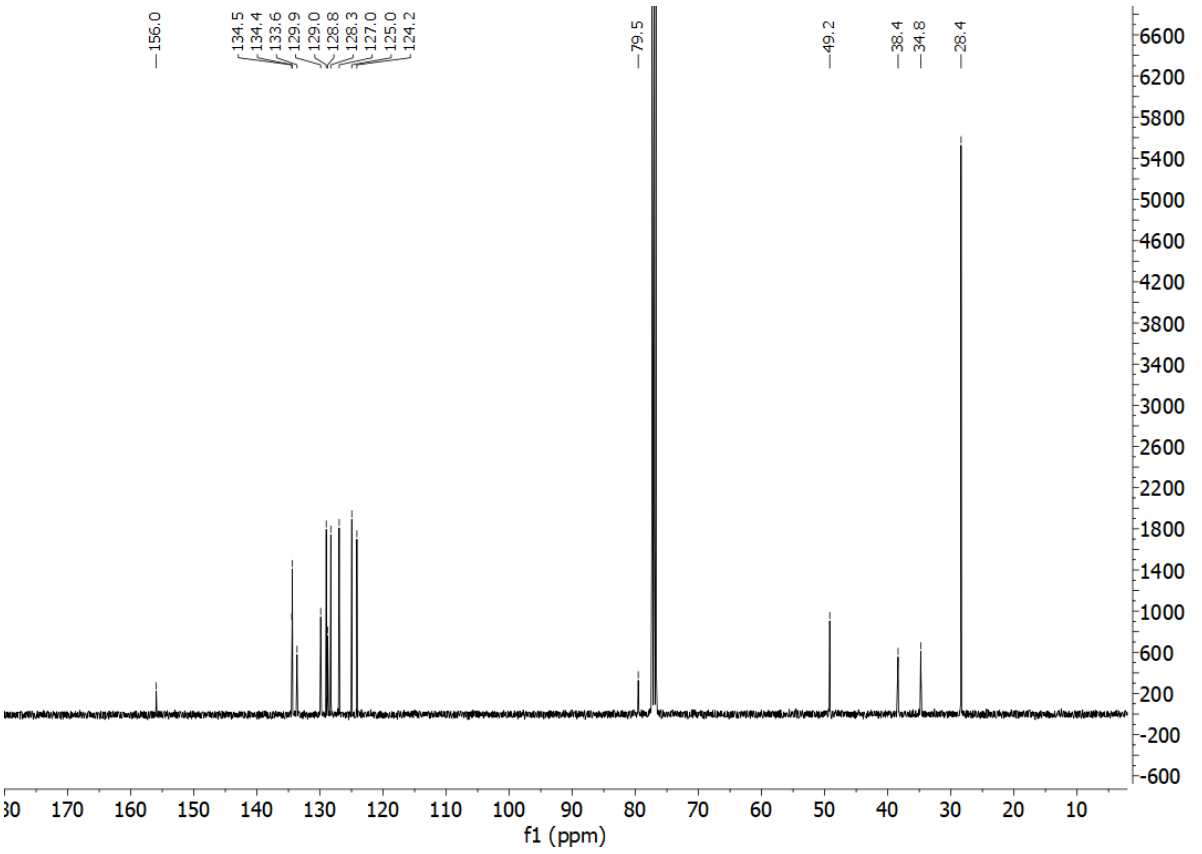

72. *N-(2'-aminoethyl)-N-methylnaphthalene-1-sulfonamide*

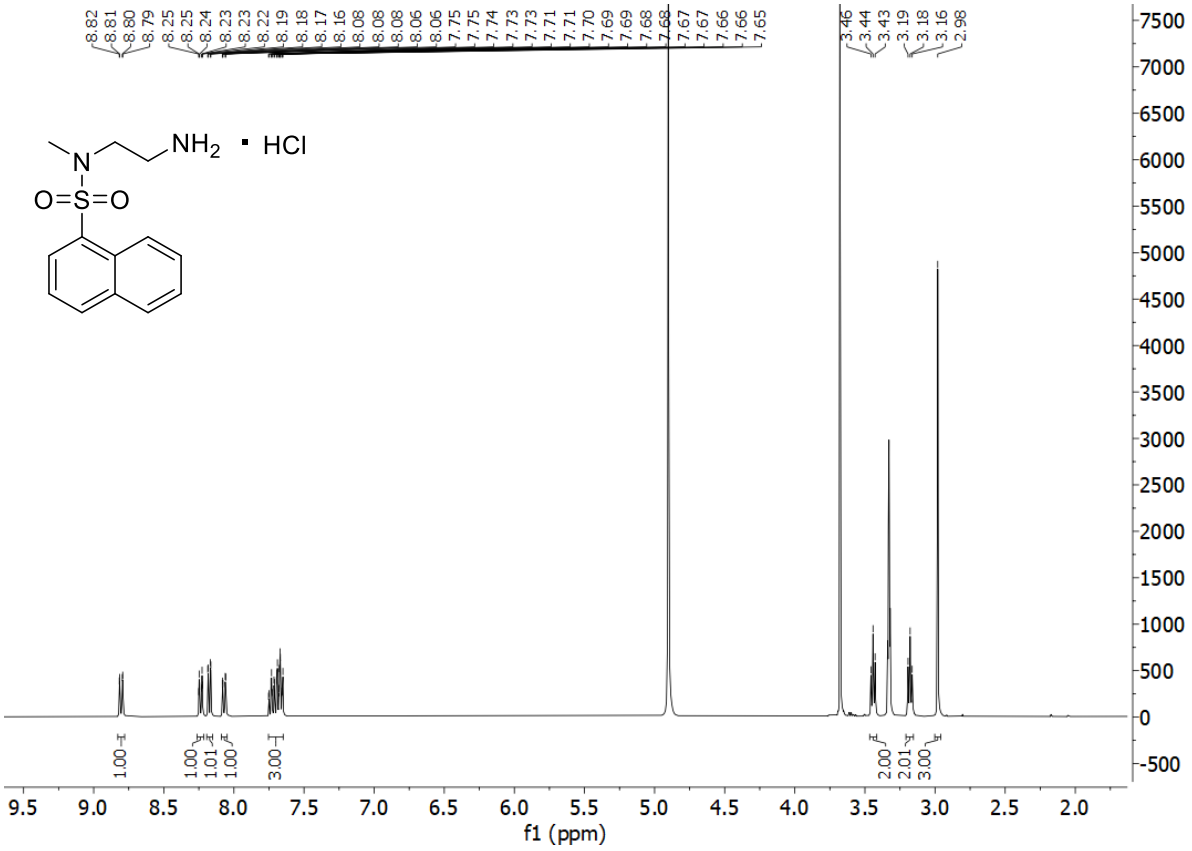

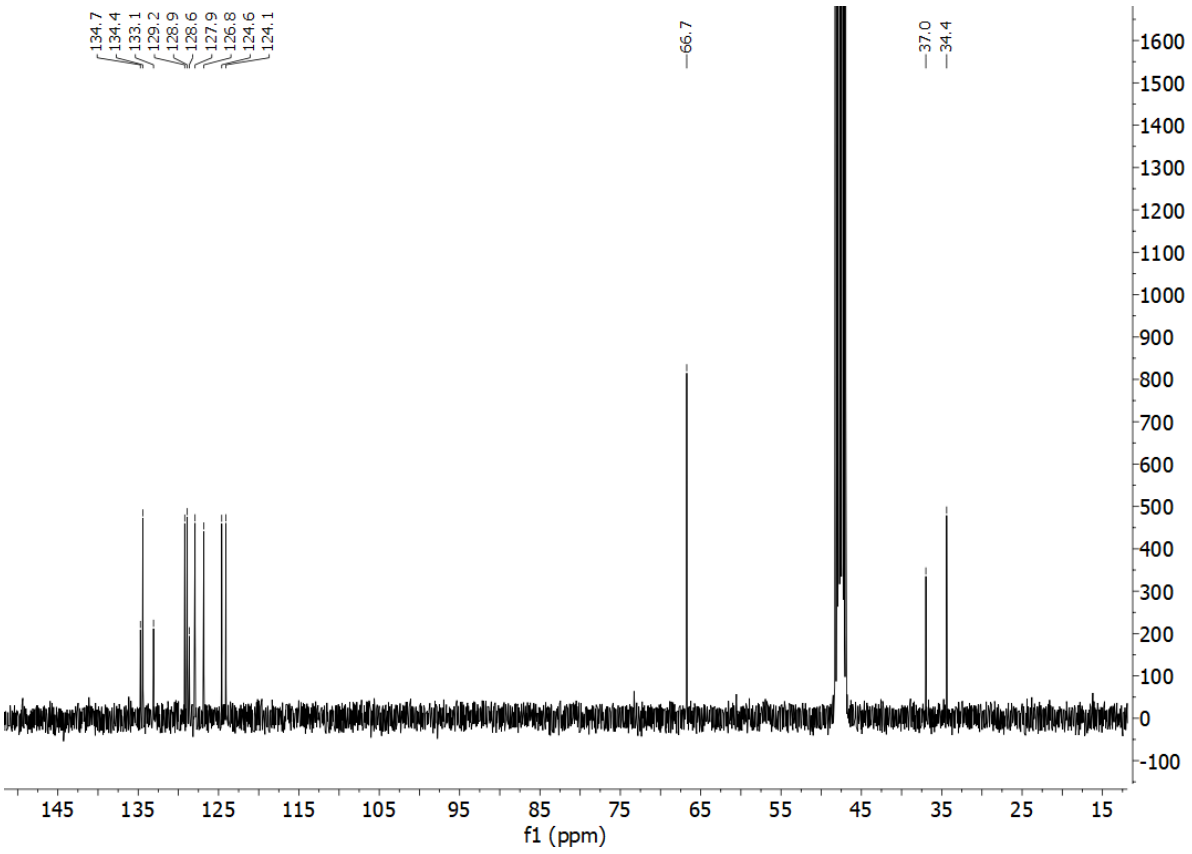

68a. *tert-butyl N-[2'-(4-propylbenzenesulfonamido)ethyl]carbamate*

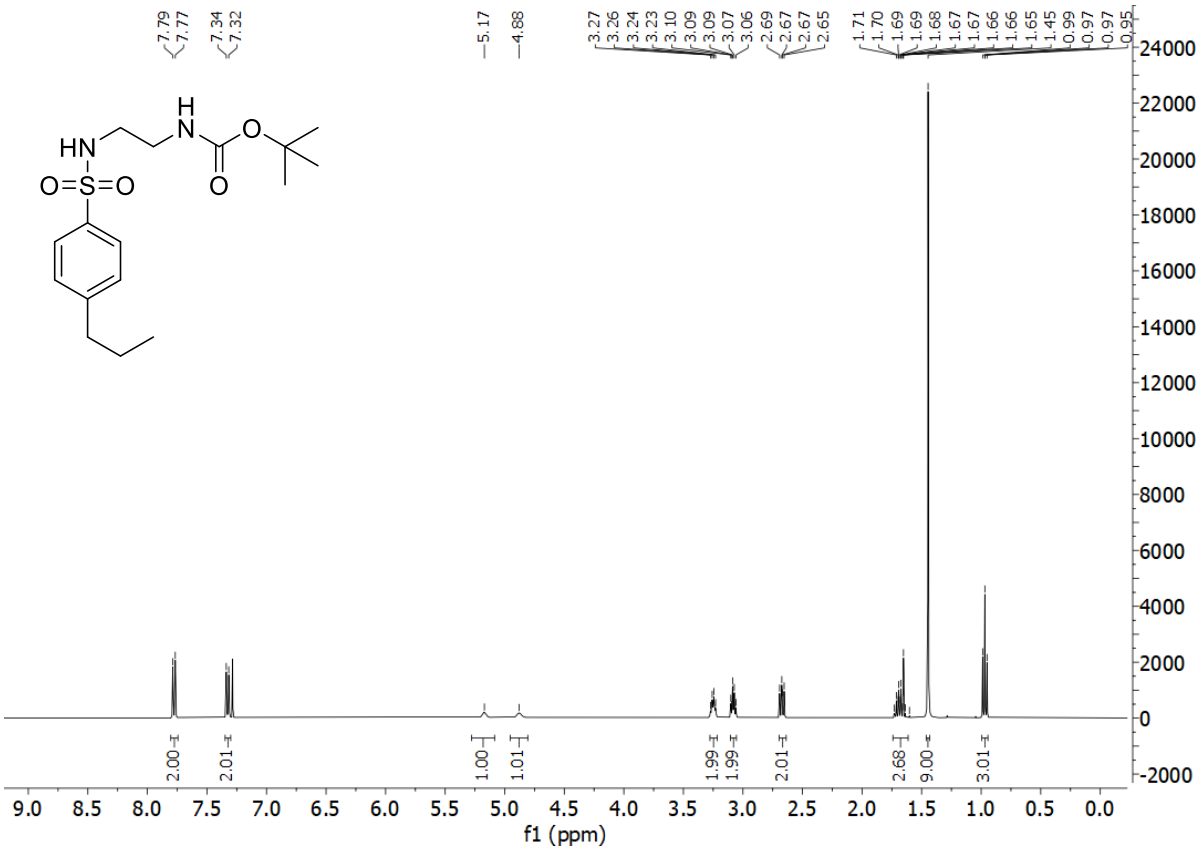

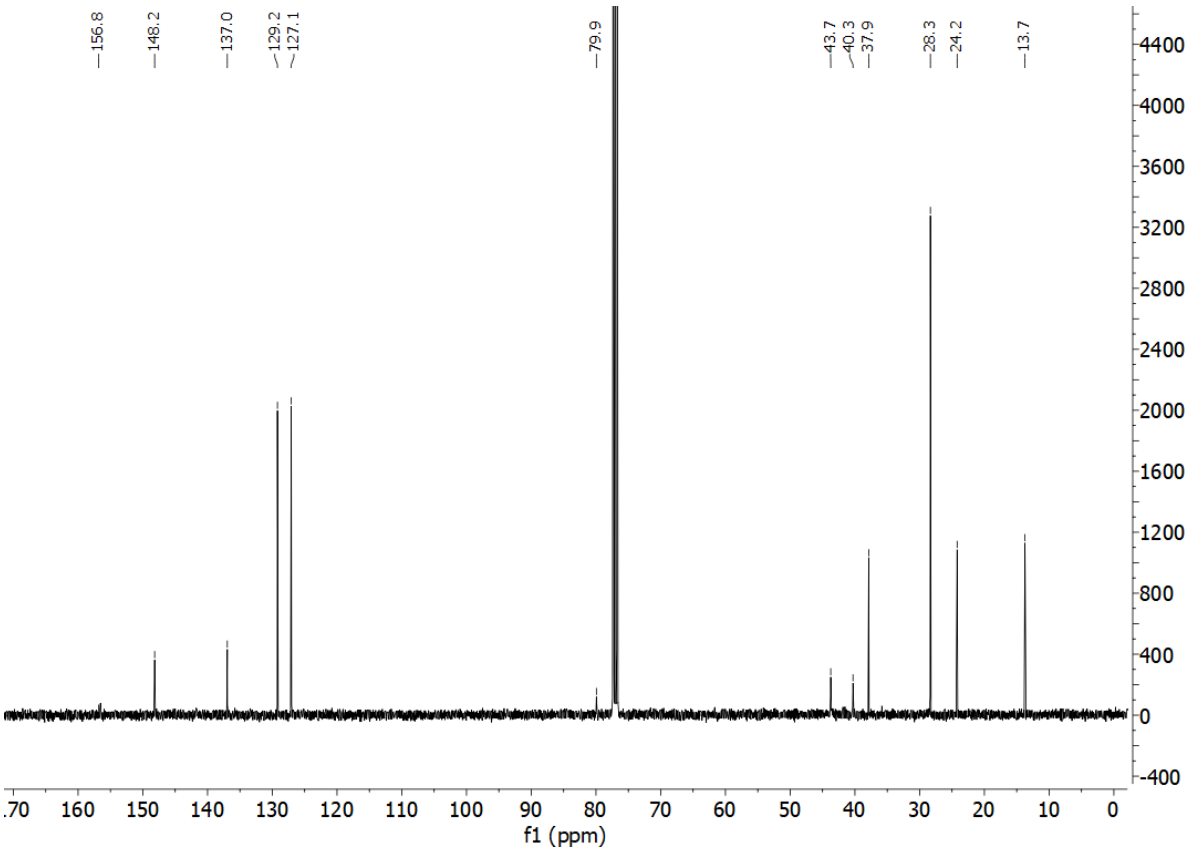

68. *N-(2'-aminoethyl)-4-propylbenzene-1-sulfonamide*

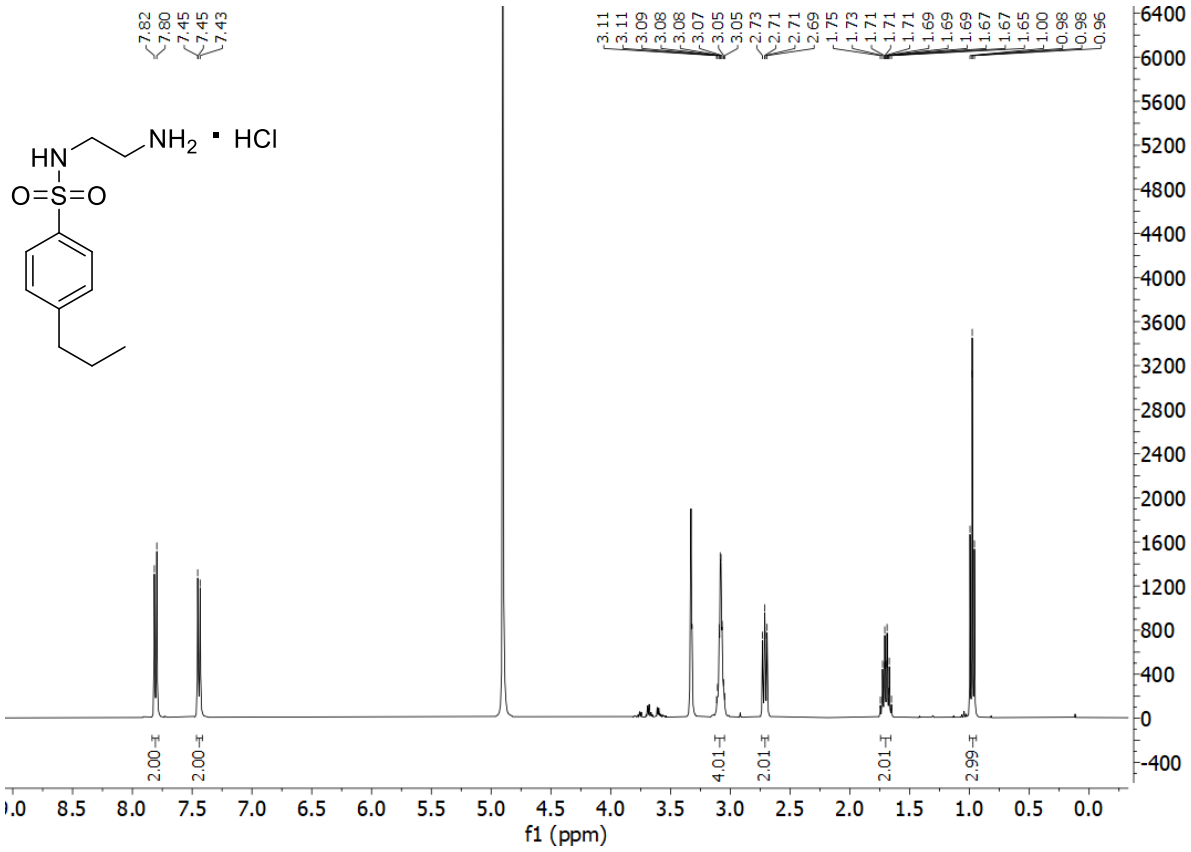

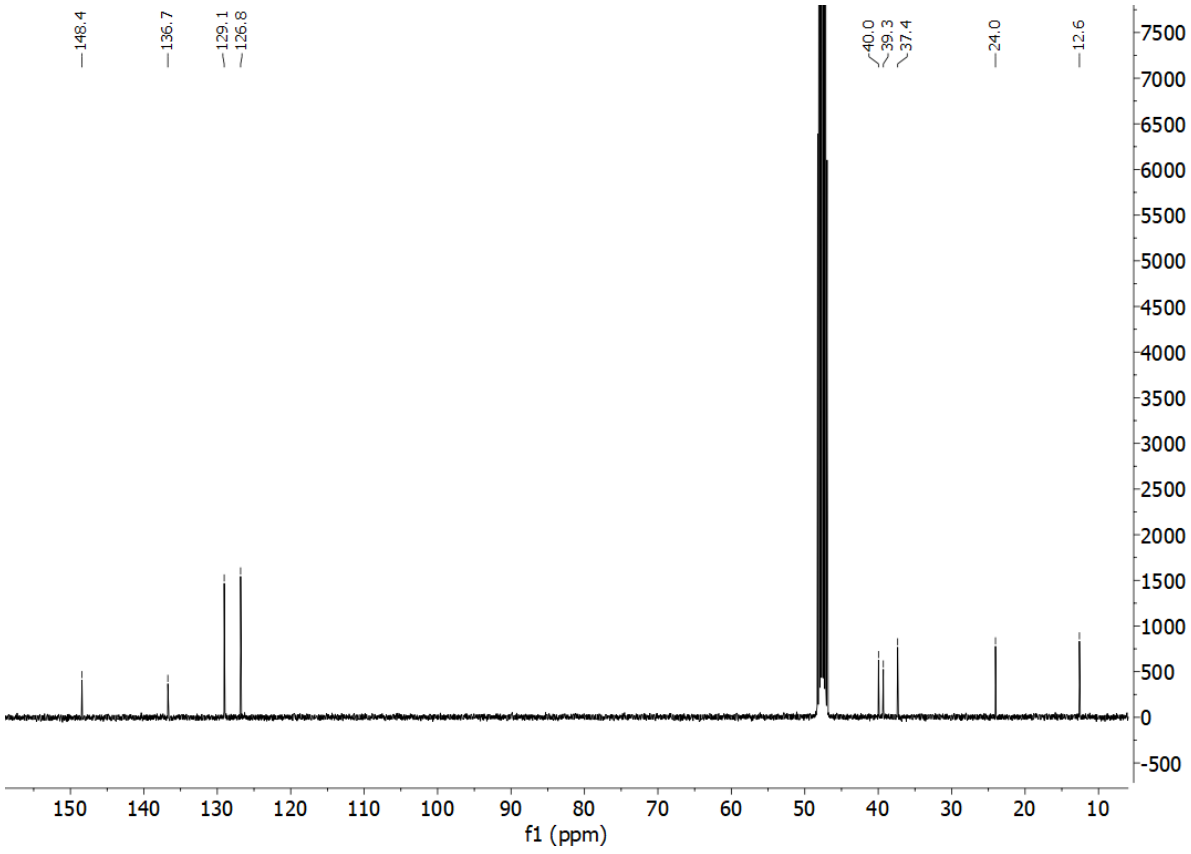

63a. *tert-butyl N-[2'-(5-chloronaphthalene-1-sulfonamido)ethyl]carbamate*

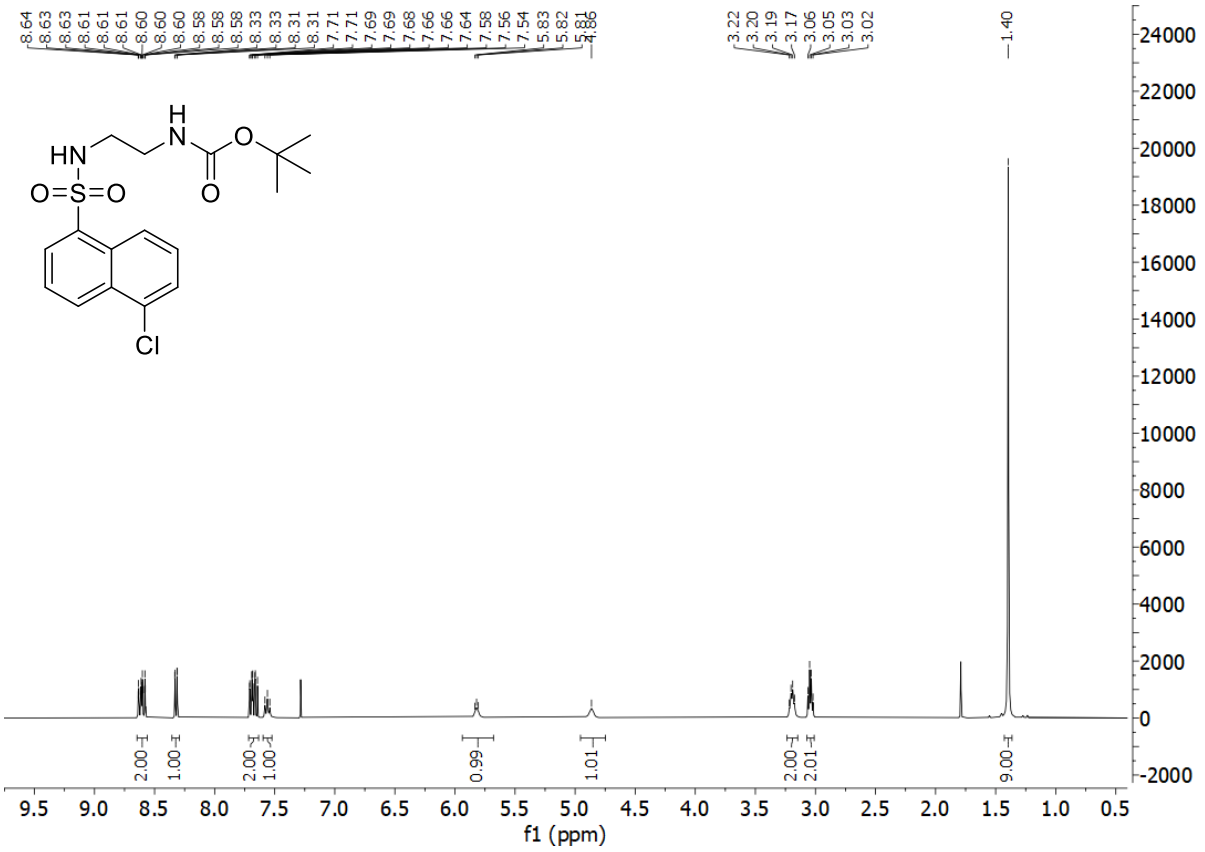

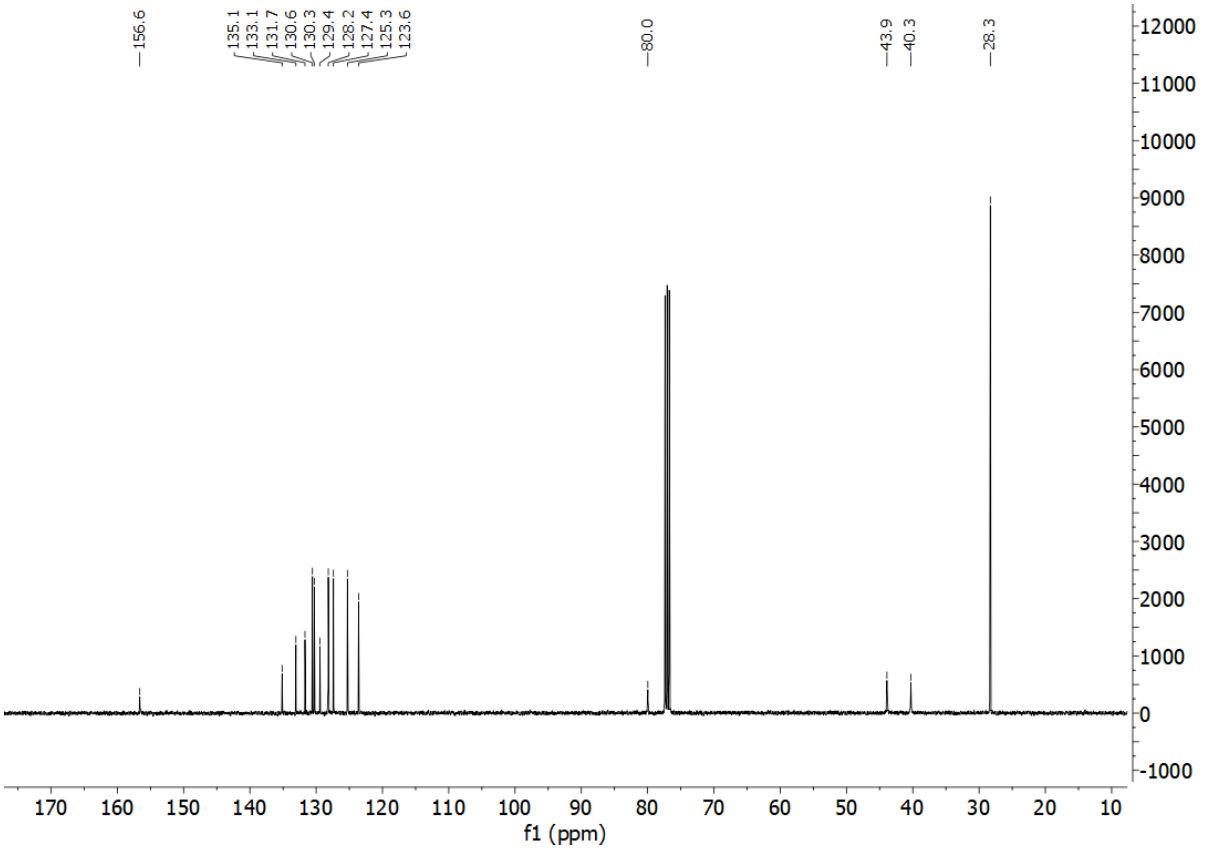

63. *N-(2'-aminoethyl)-5-chloronaphthalene-1-sulfonamide hydrochloride*

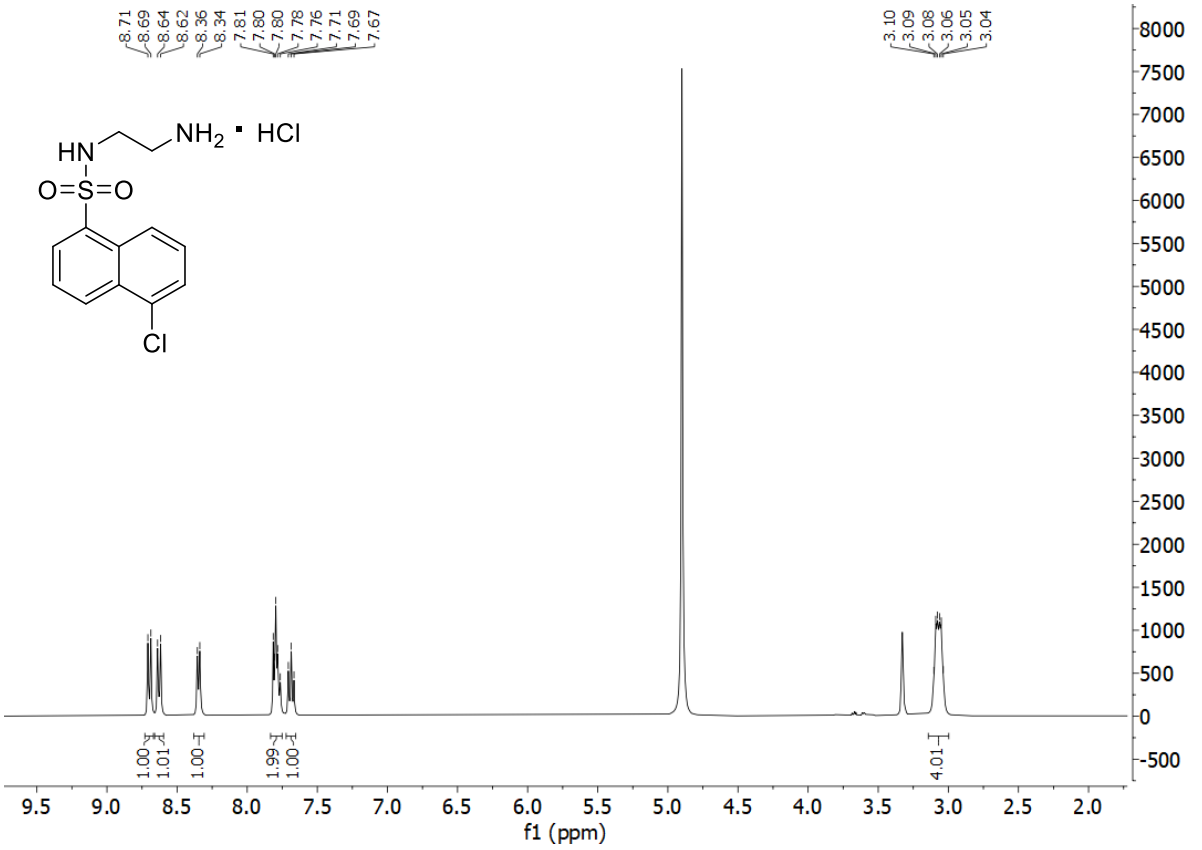

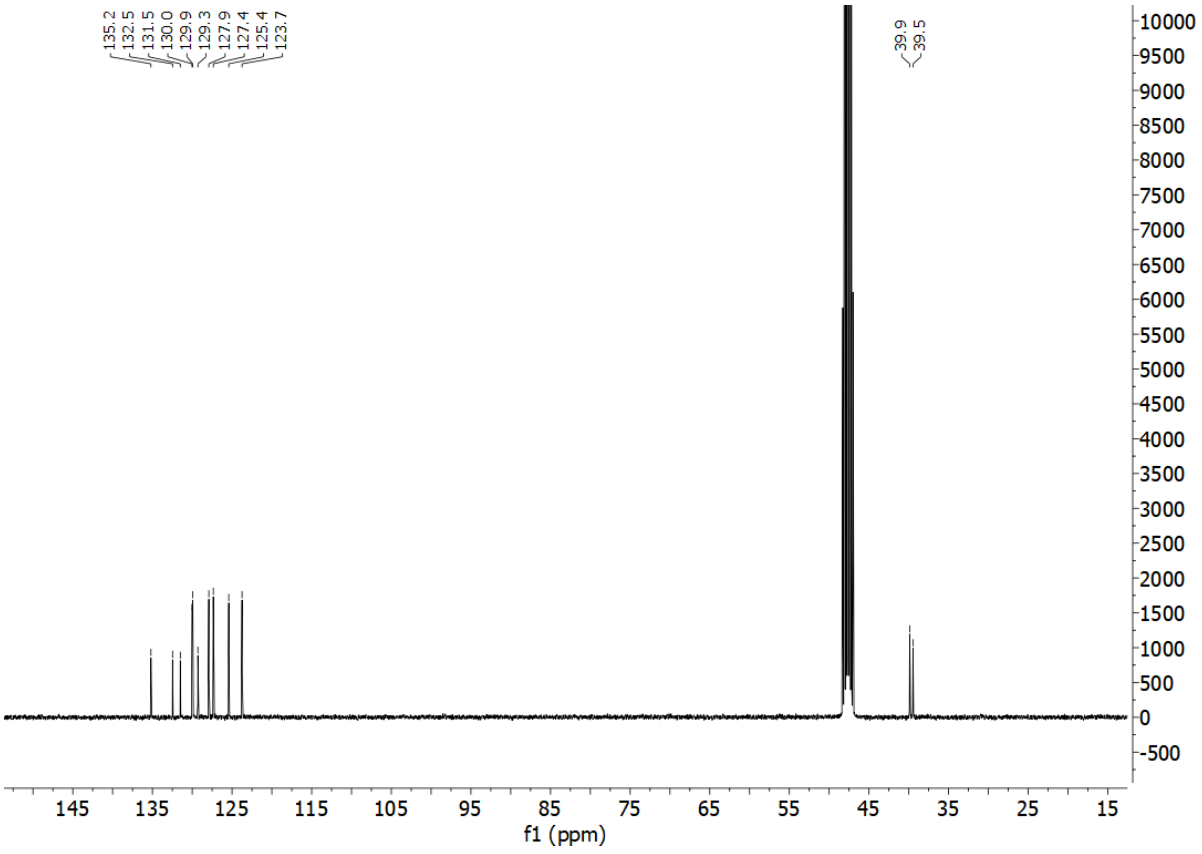

92. *N,N-diethylbenzenesulfonamide*

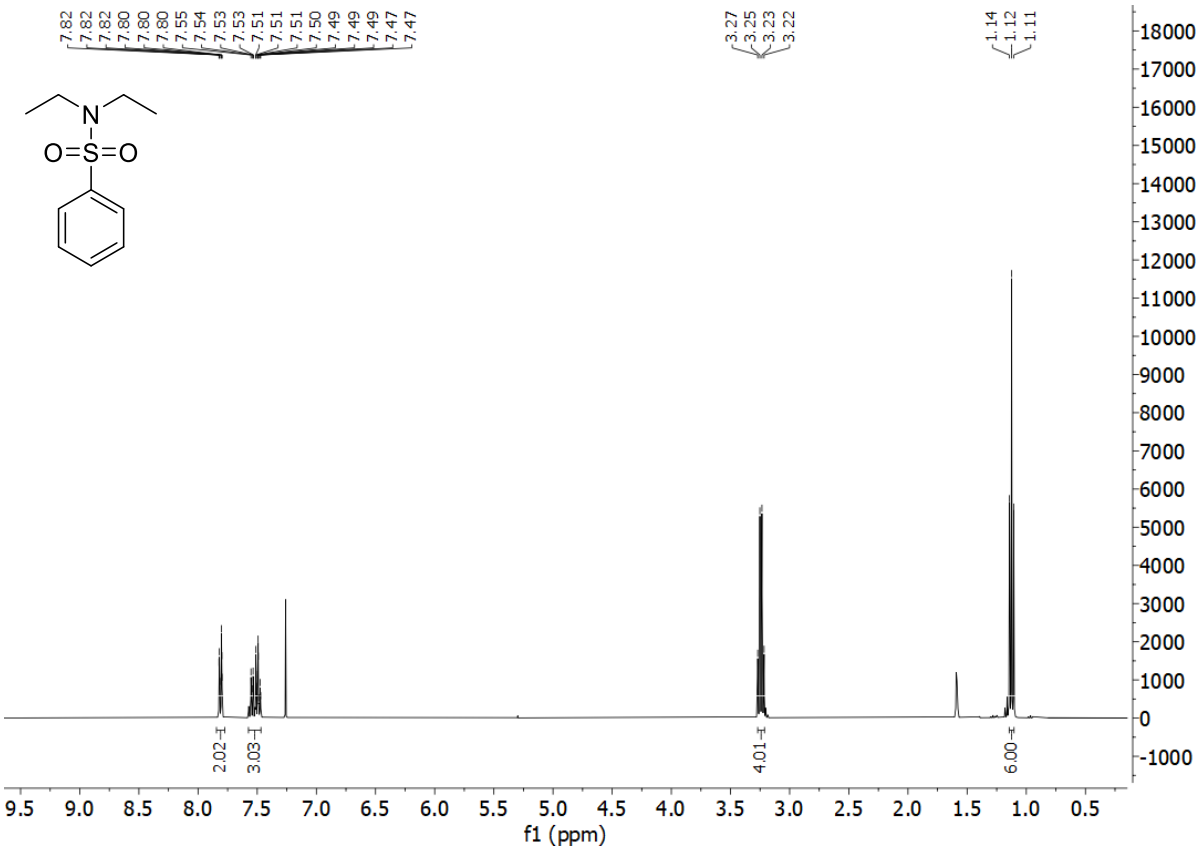

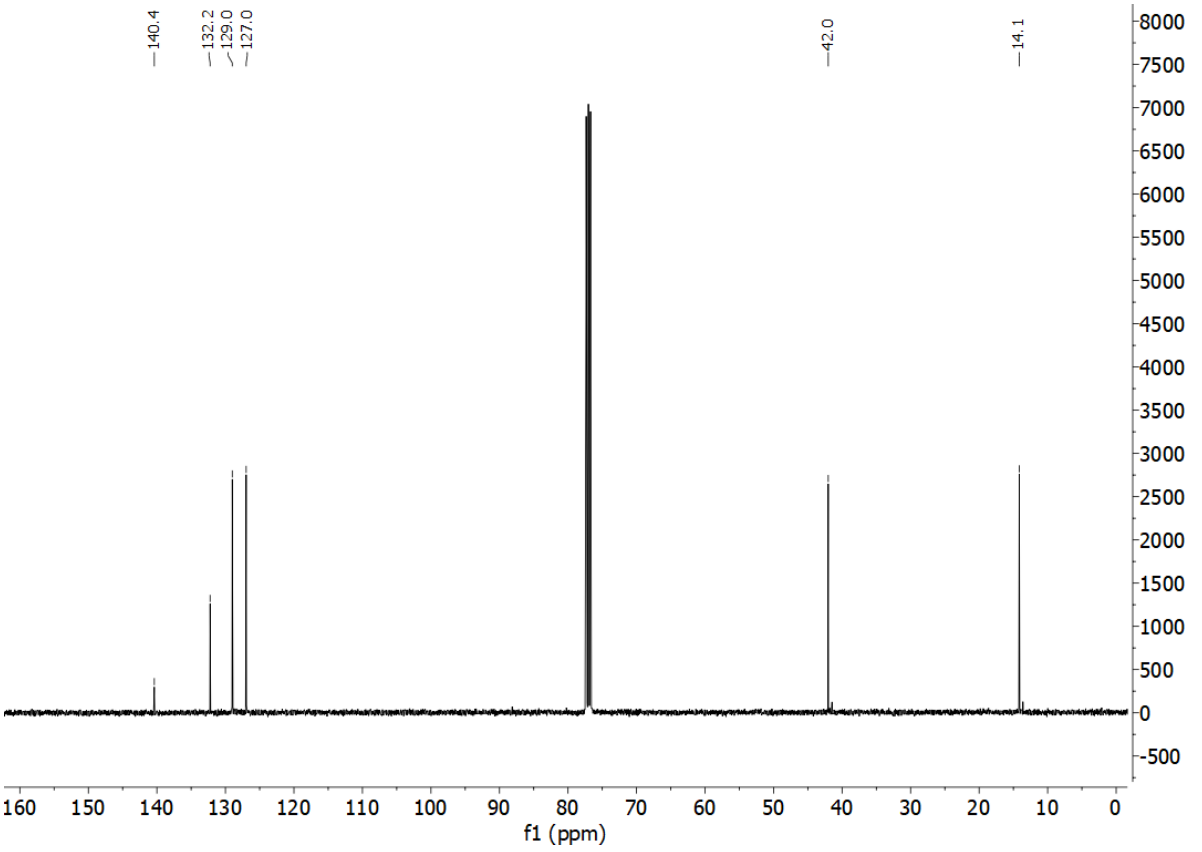

94. *N,N-diethylnaphthalene-1-sulfonamide*

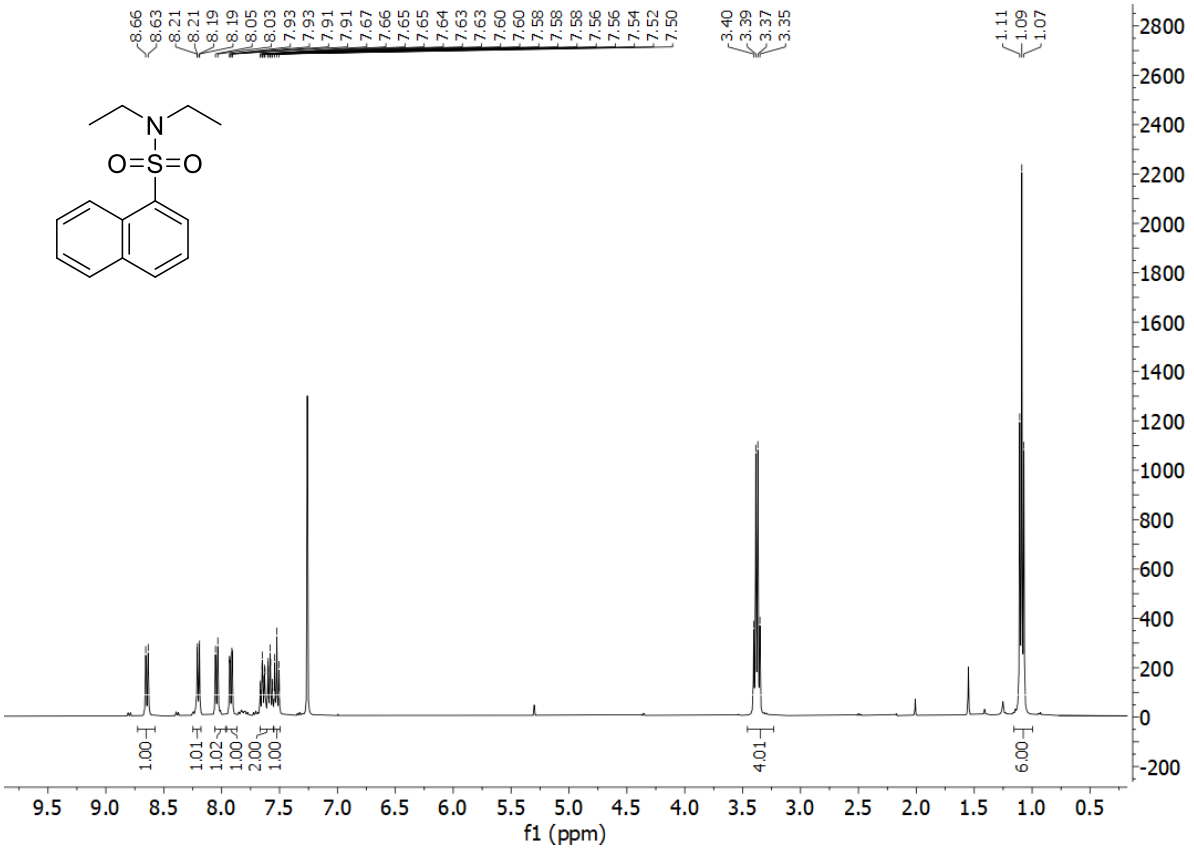

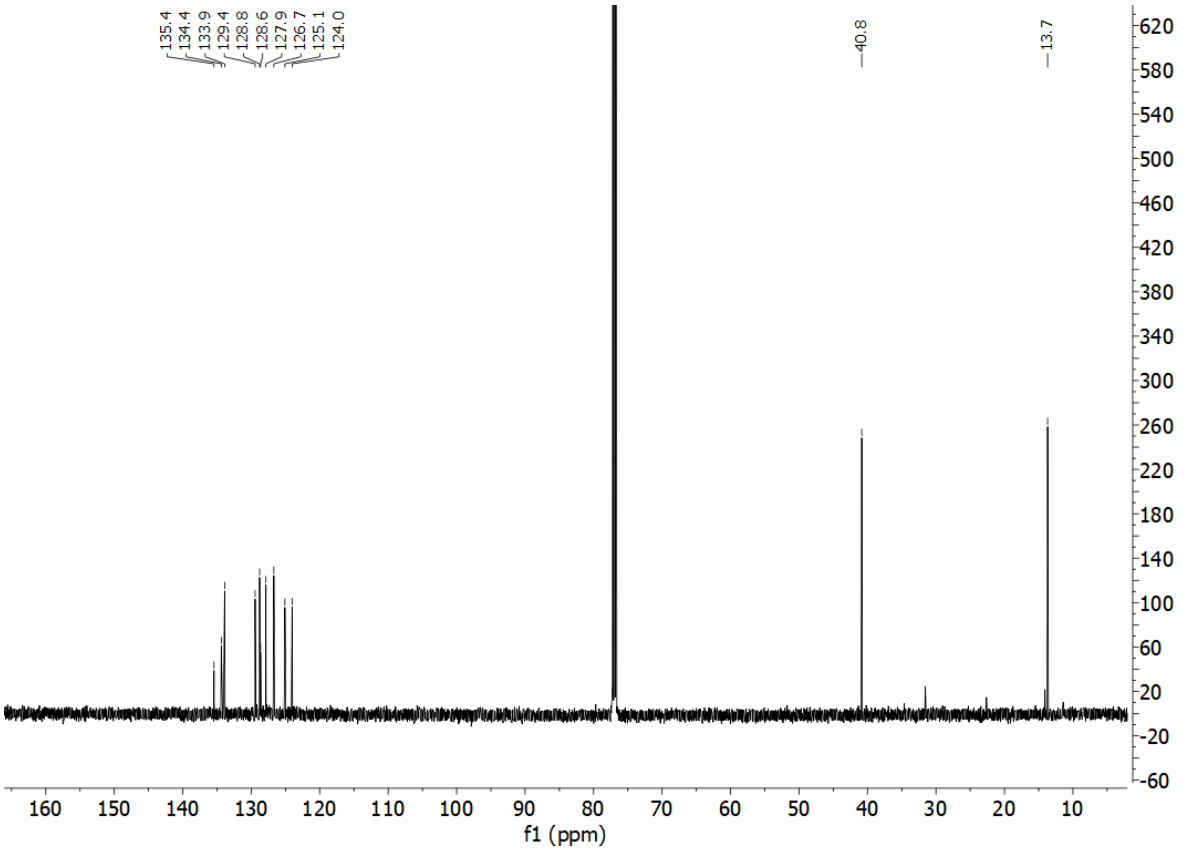

95. *N-(2'-aminoethyl)quinoline-8-sulfonamide*

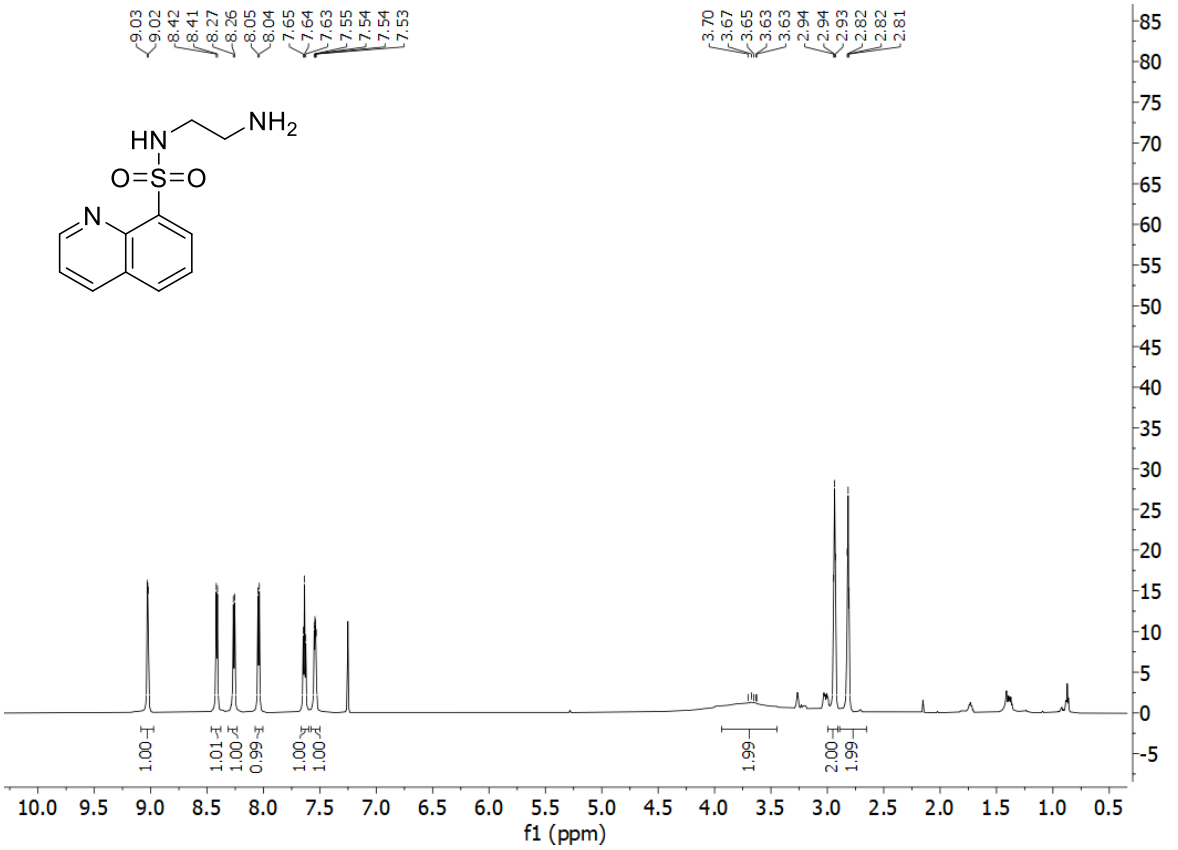

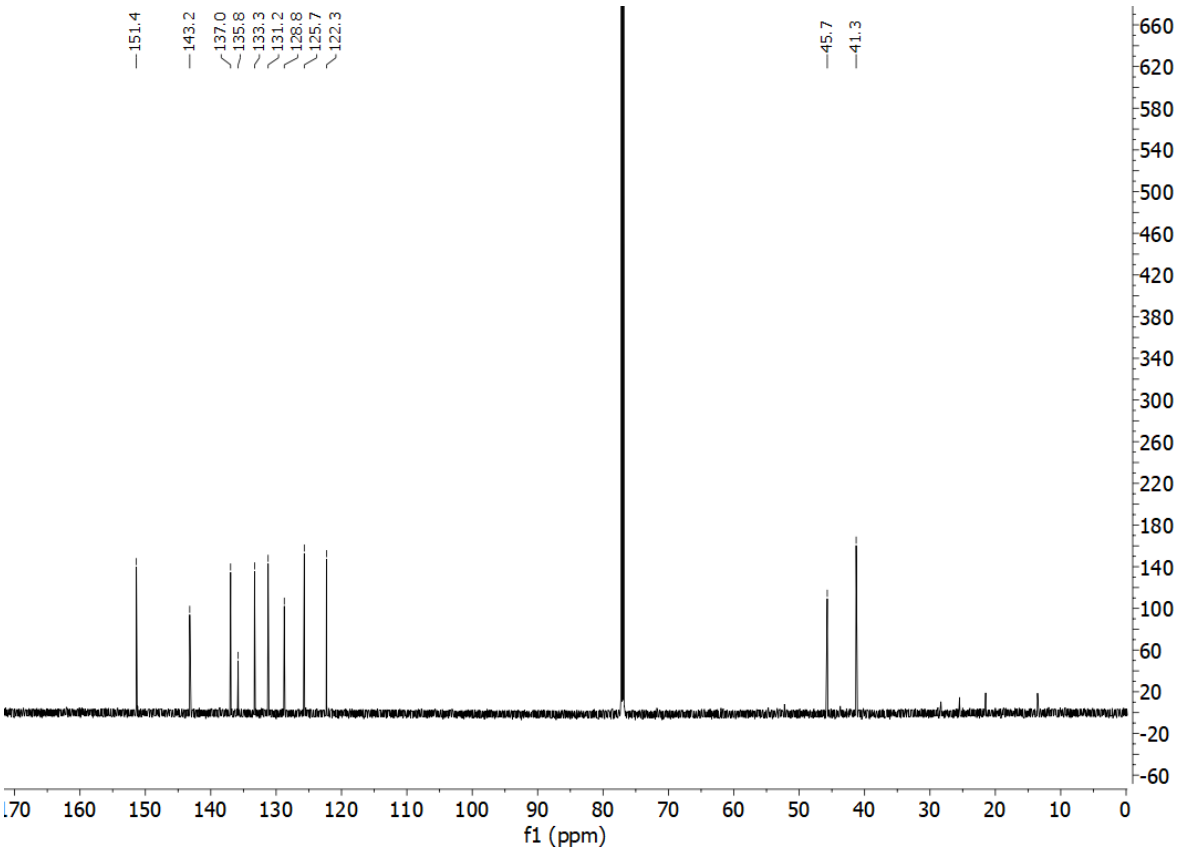

96a. *tert-butyl N-[2'-(isoquinoline-8-sulfonamido)ethyl]carbamate*

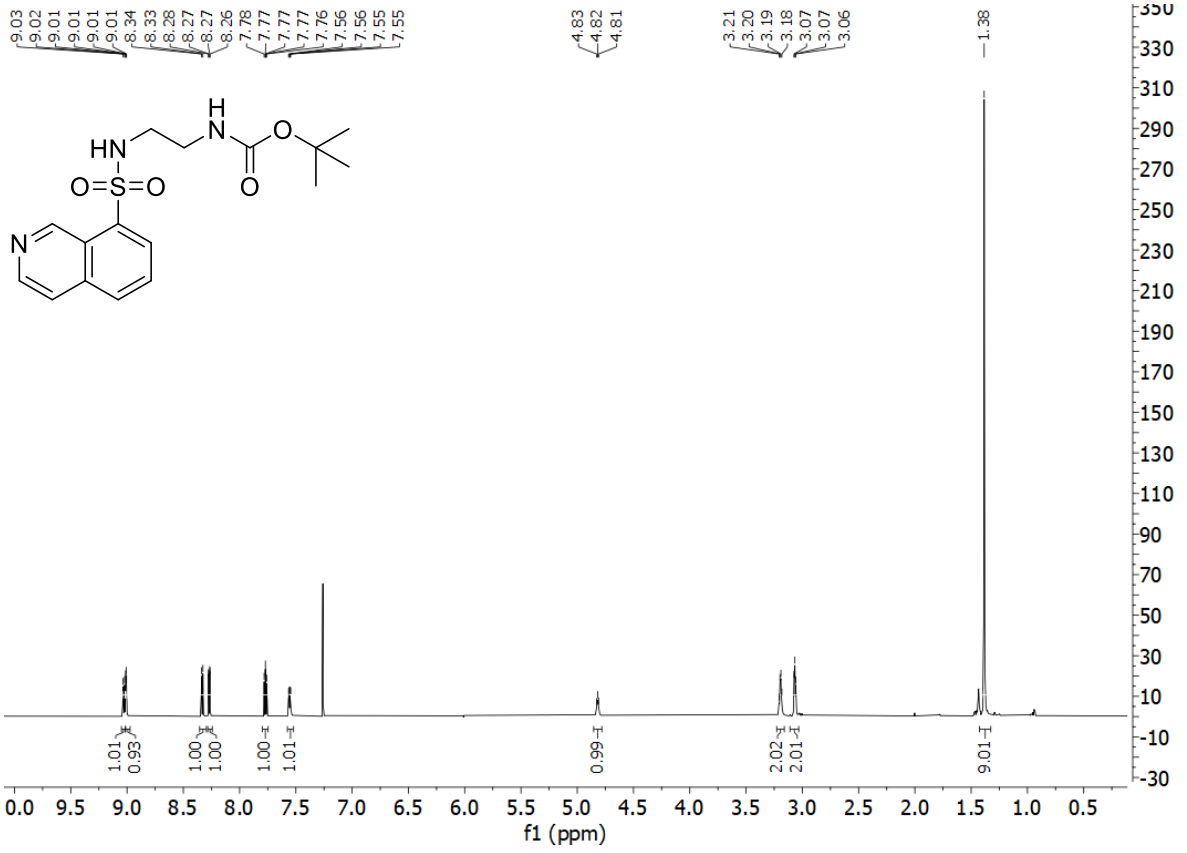

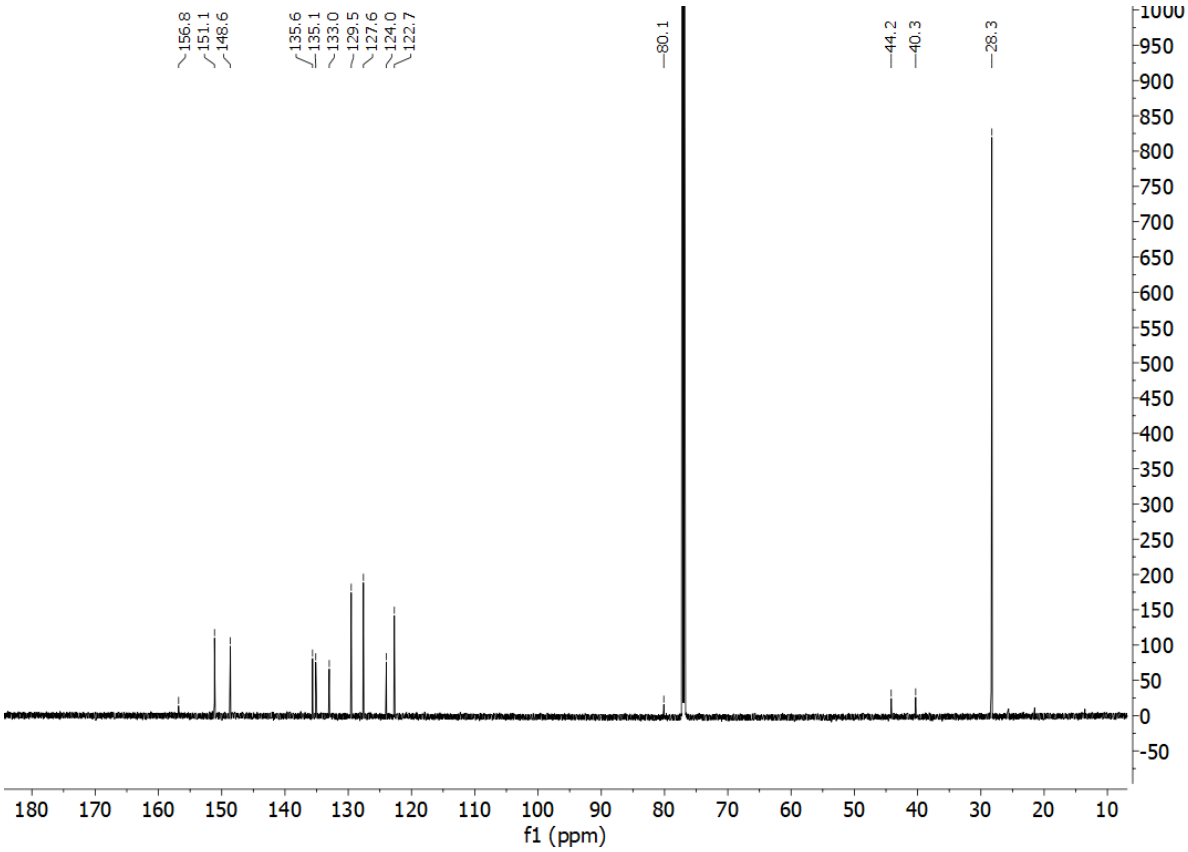

96. *N-(2'-aminoethyl)isoquinoline-8-sulfonamide hydrochloride*

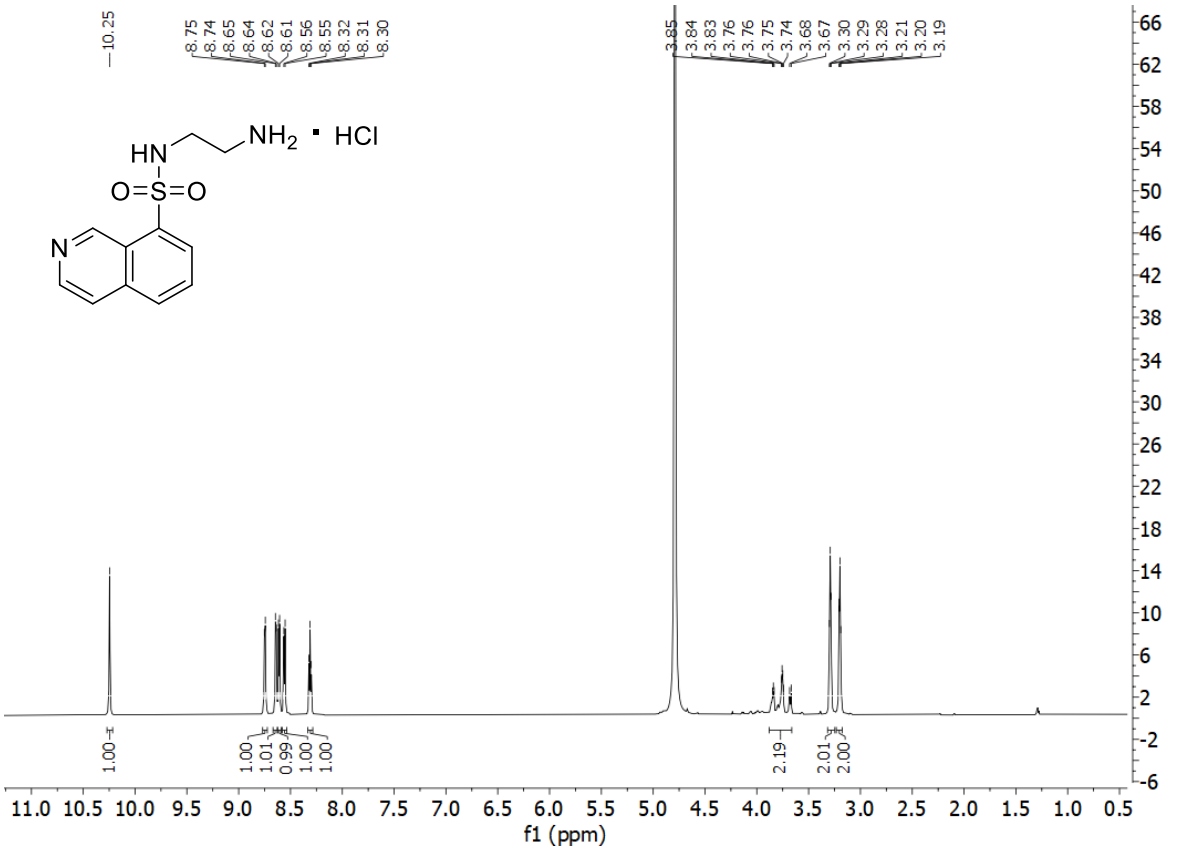

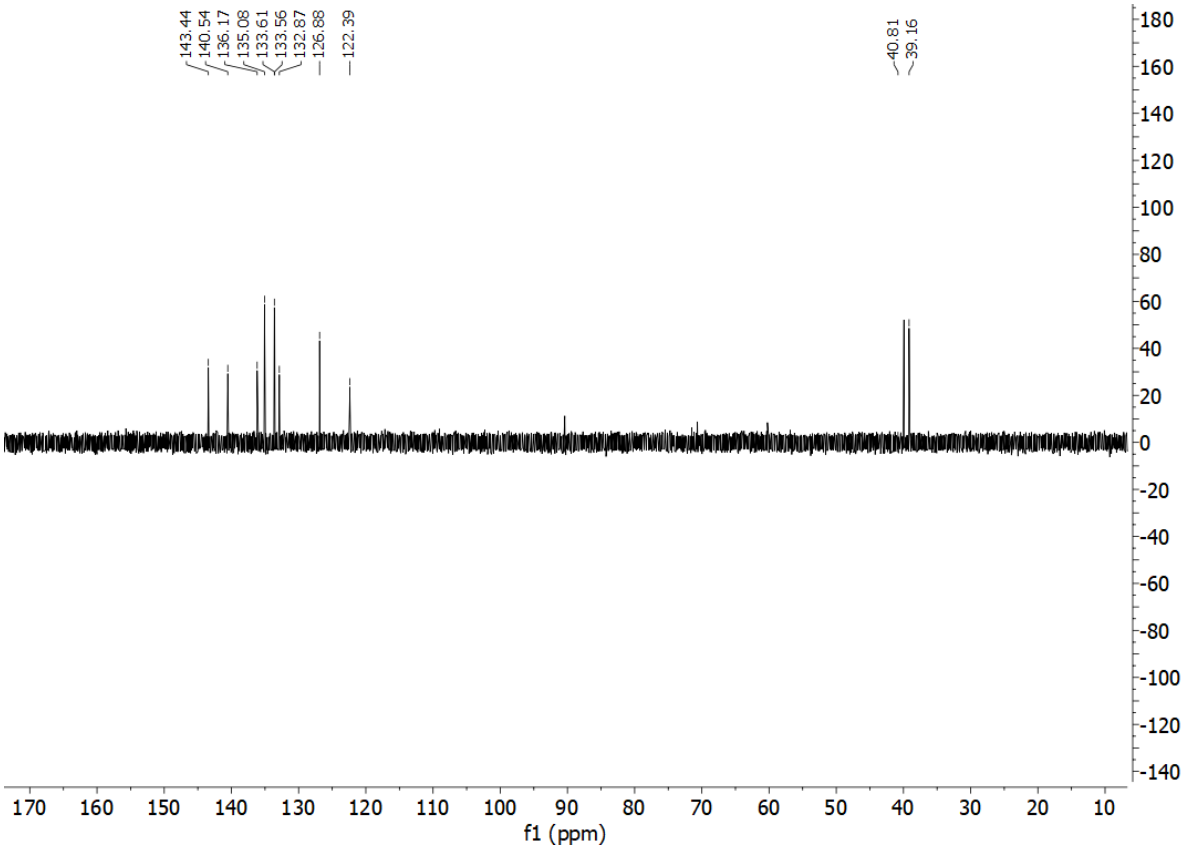

97a. *tert-butyl N-[2'-(isoquinoline-5-sulfonamido)ethyl]carbamate*

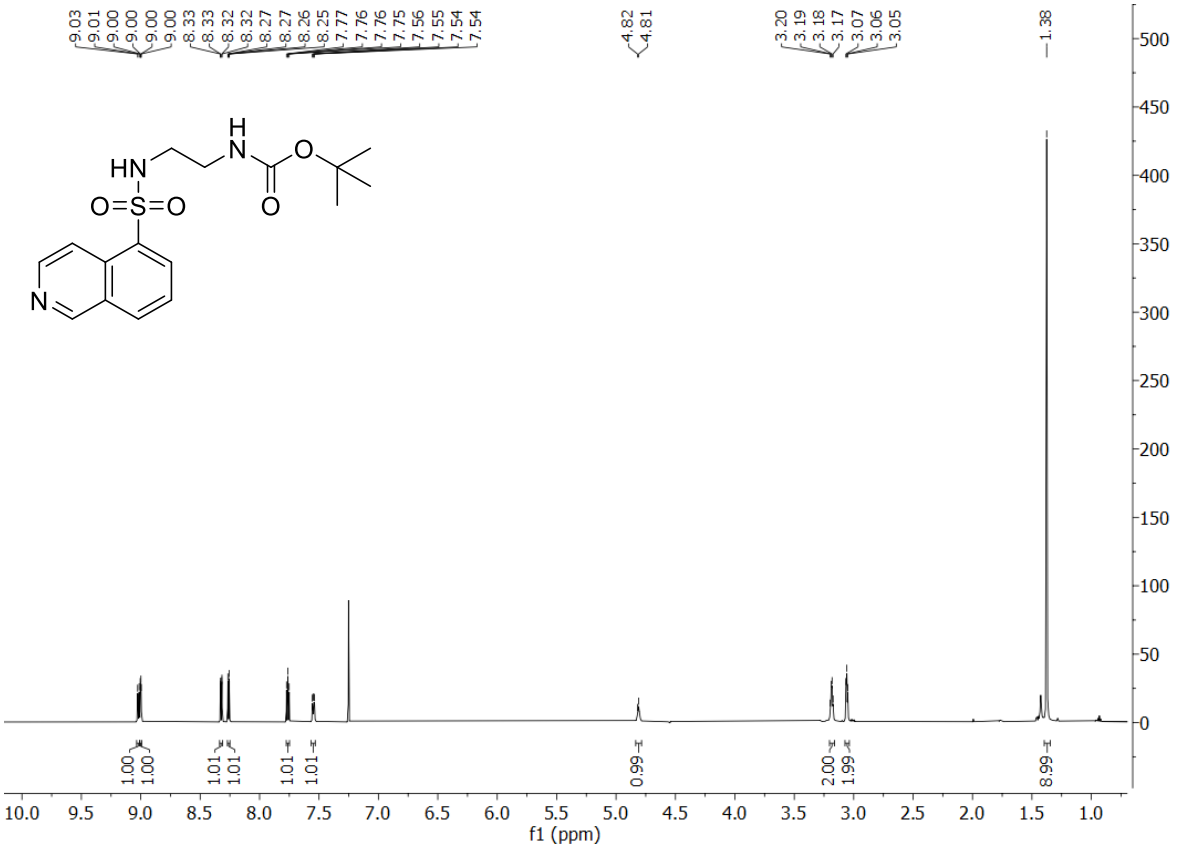

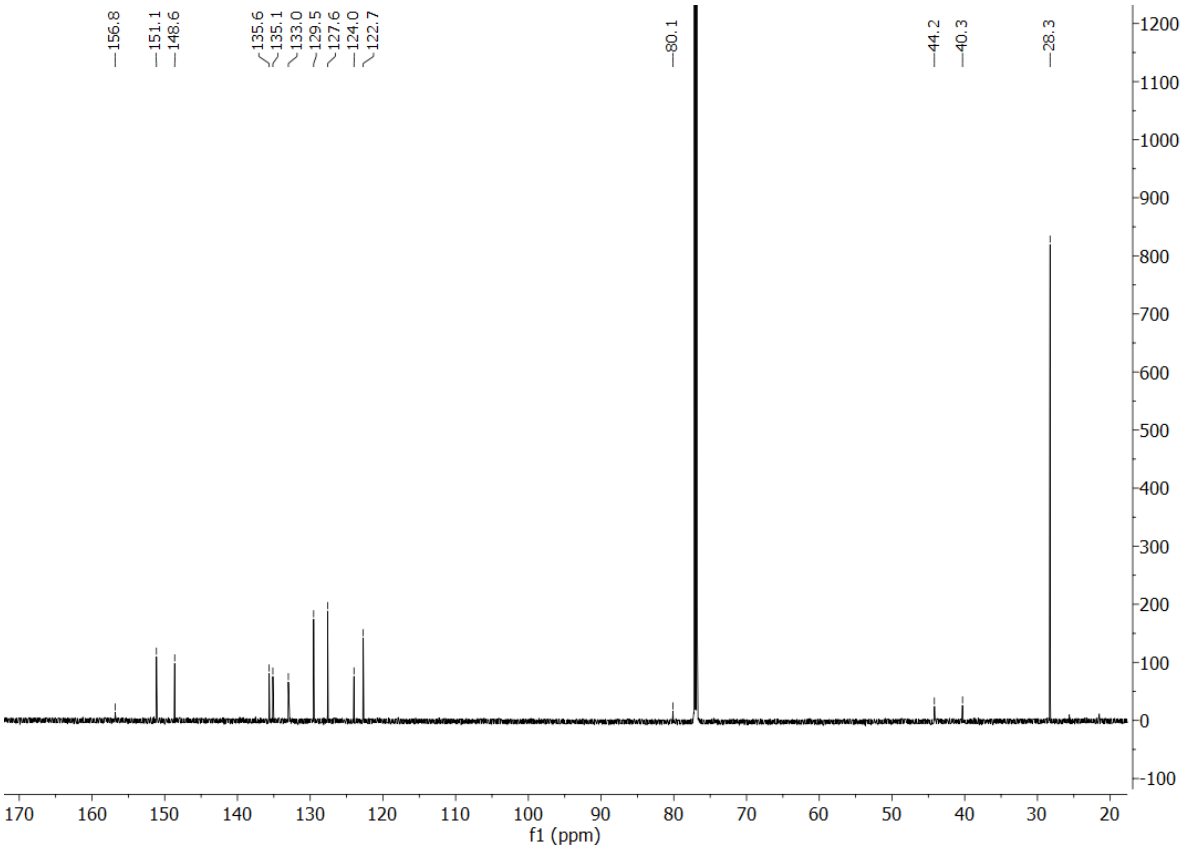

97. *N-(2'-aminoethyl)isoquinoline-5-sulfonamide hydrochloride*

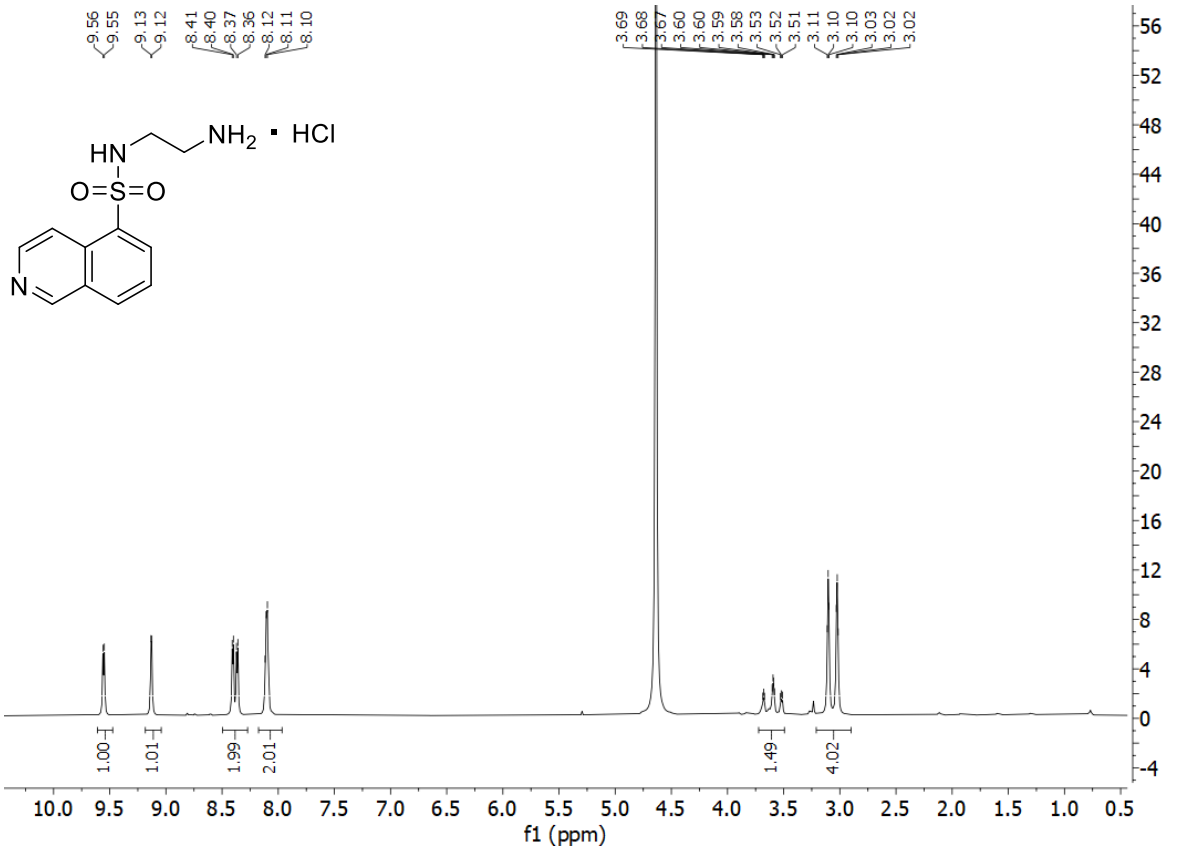

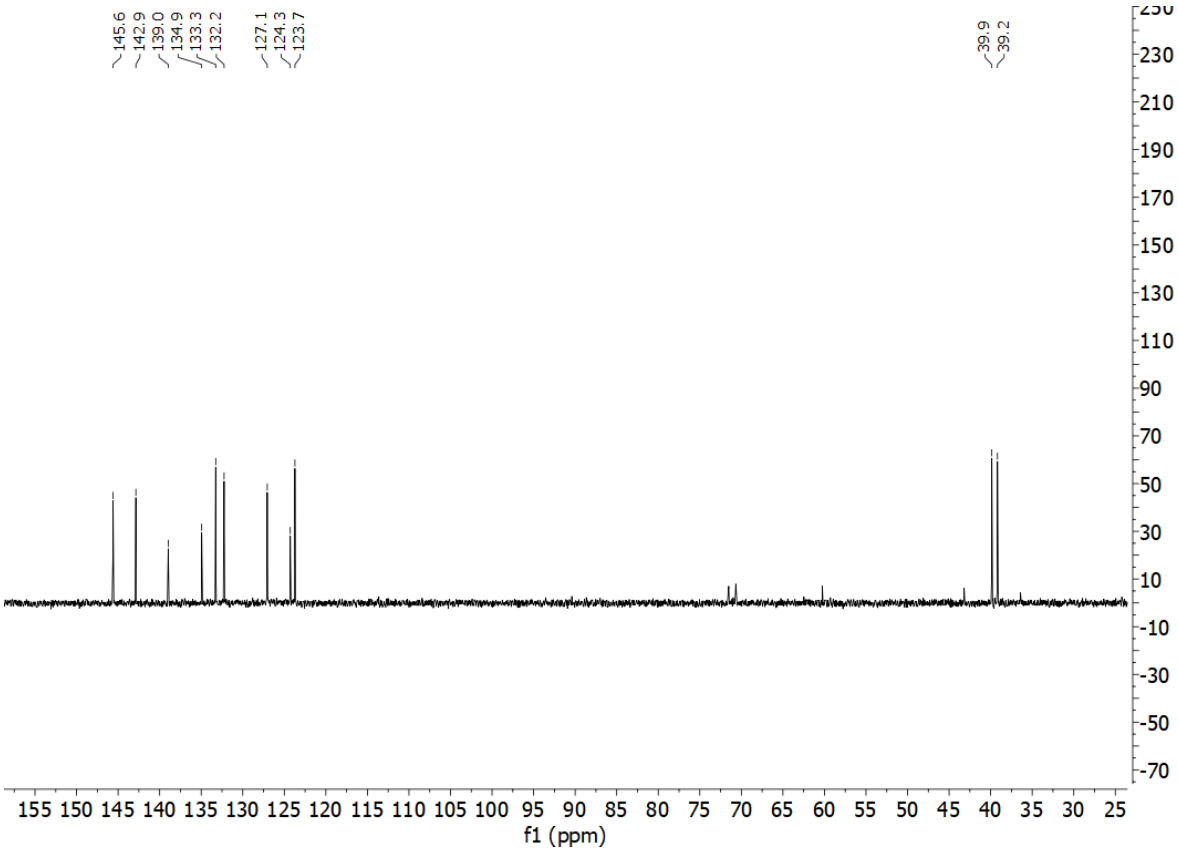

98a. *tert-butyl N-[2'-(quinoline-5-sulfonamido)ethyl]carbamate*

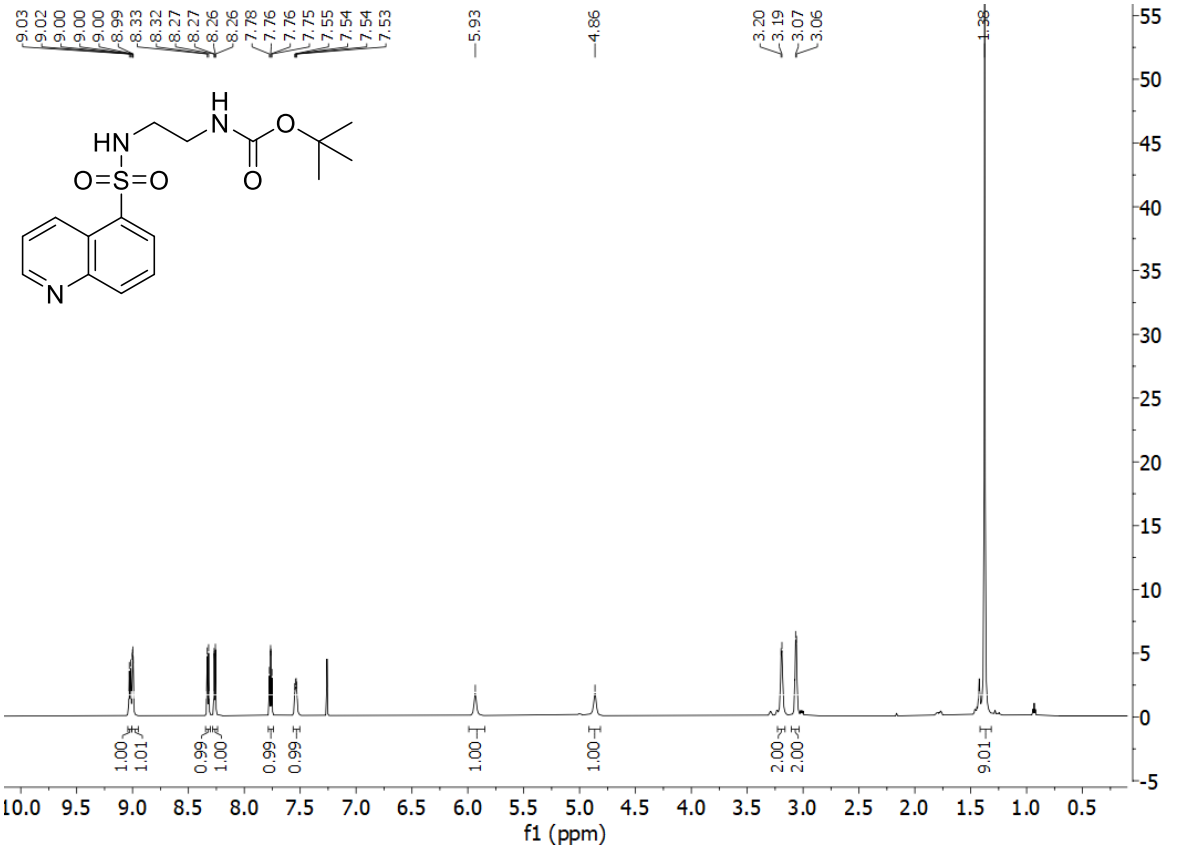

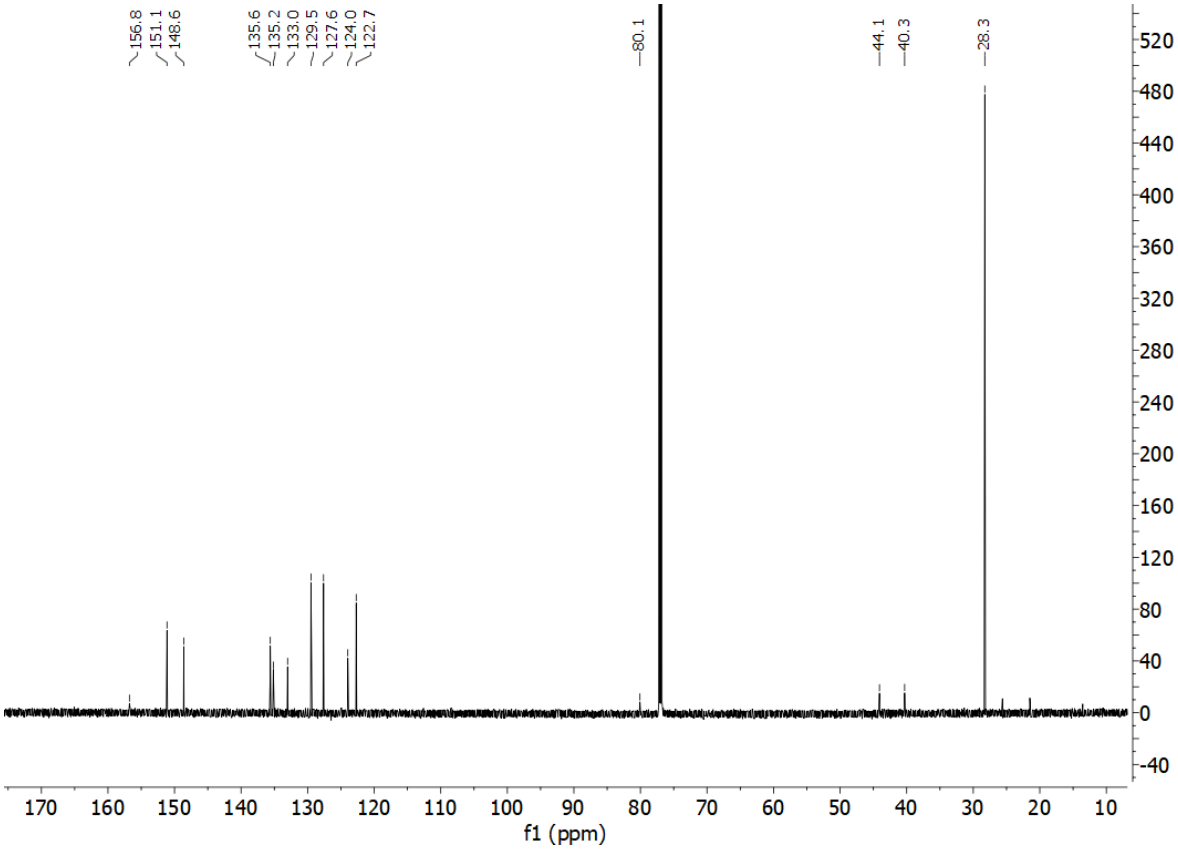

98. *N-(2'-aminoethyl)quinoline-5-sulfonamide hydrochloride*

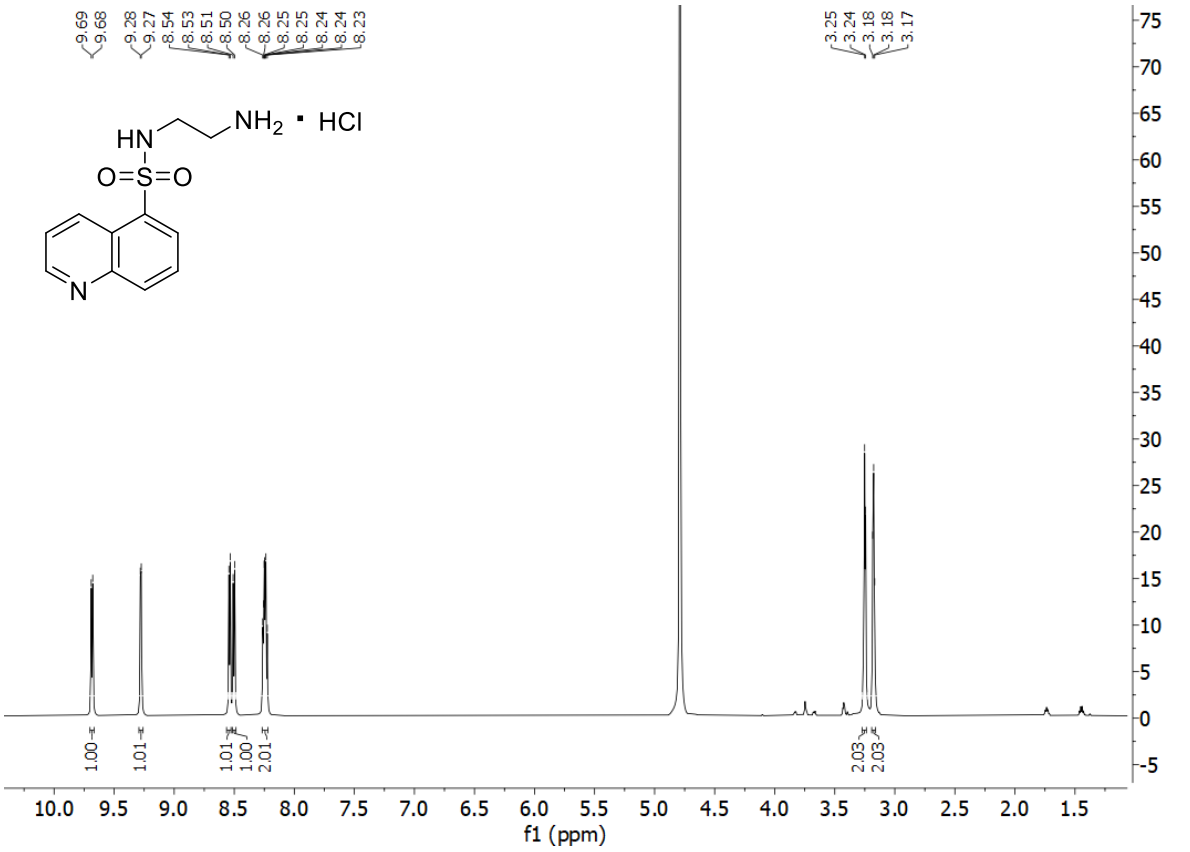

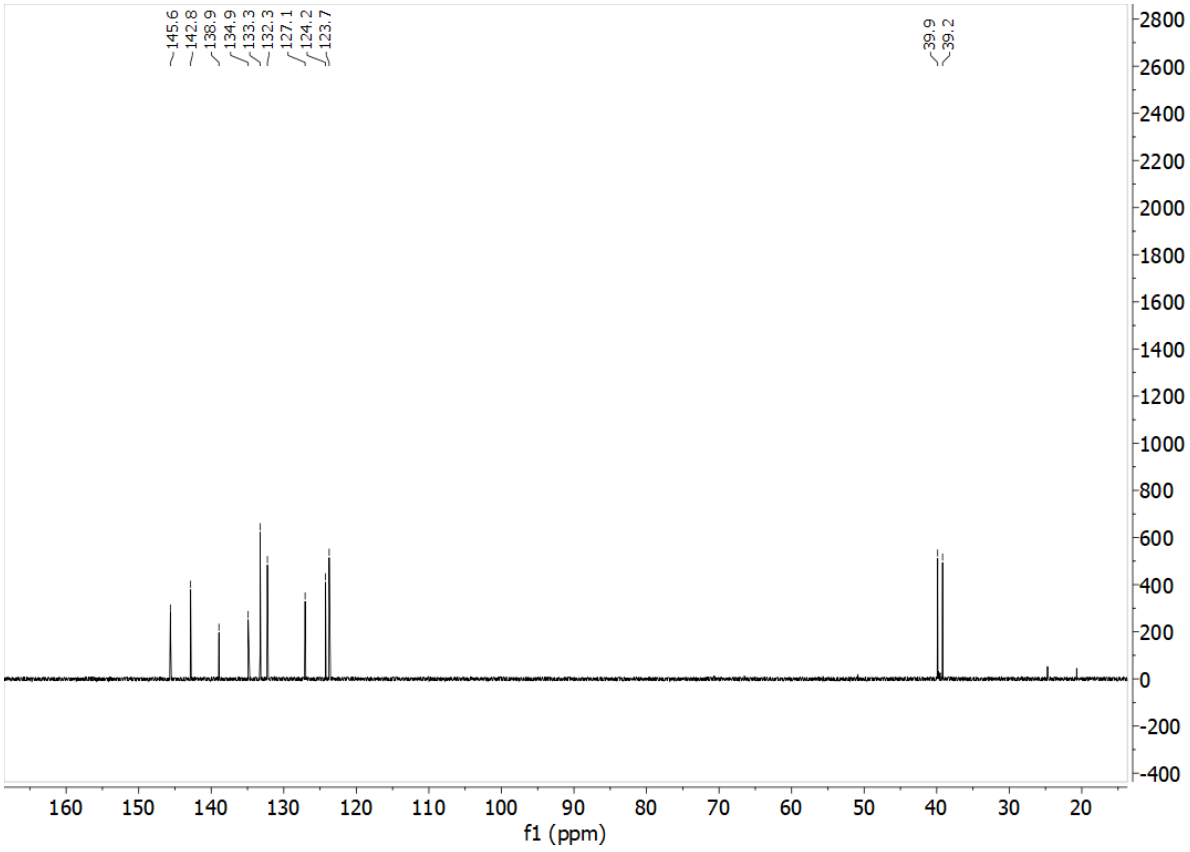

100a. *tert-butyl N-[2'-(isoquinoline-4-sulfonamido)ethyl]carbamate*

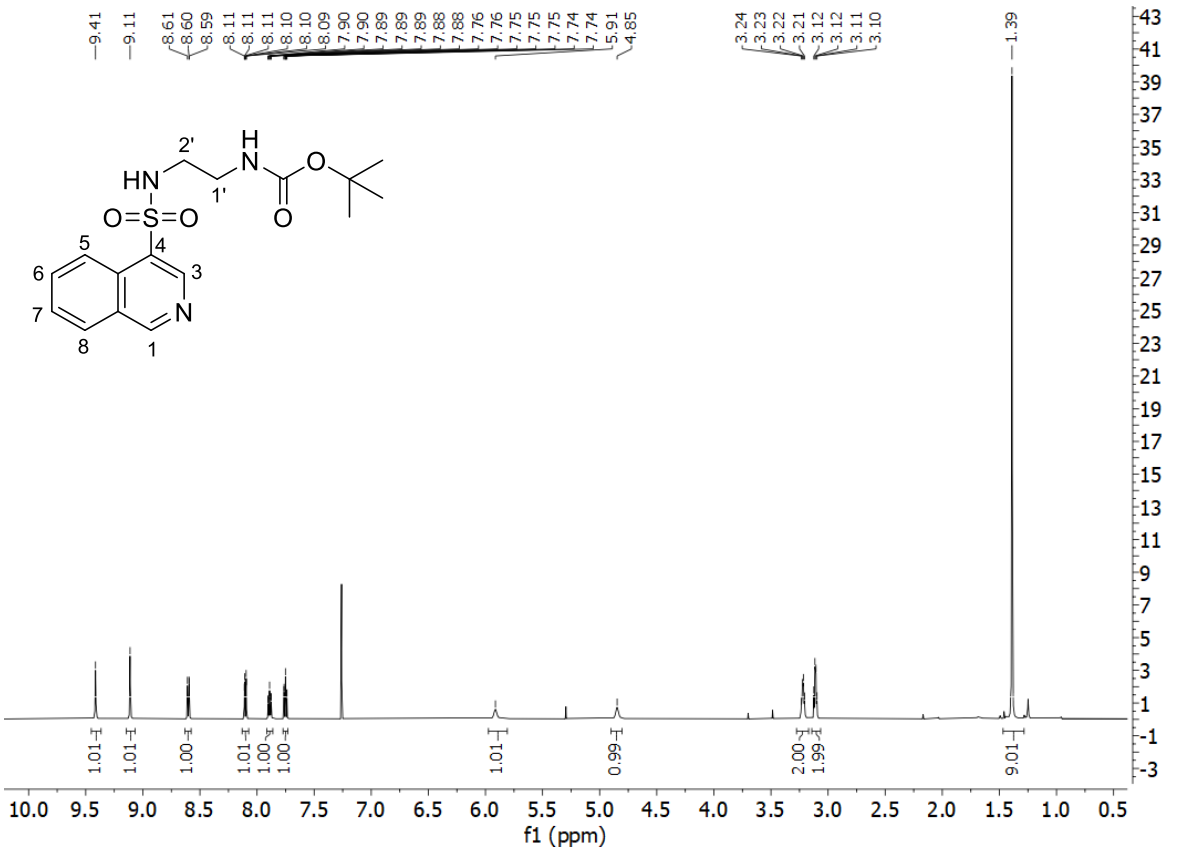

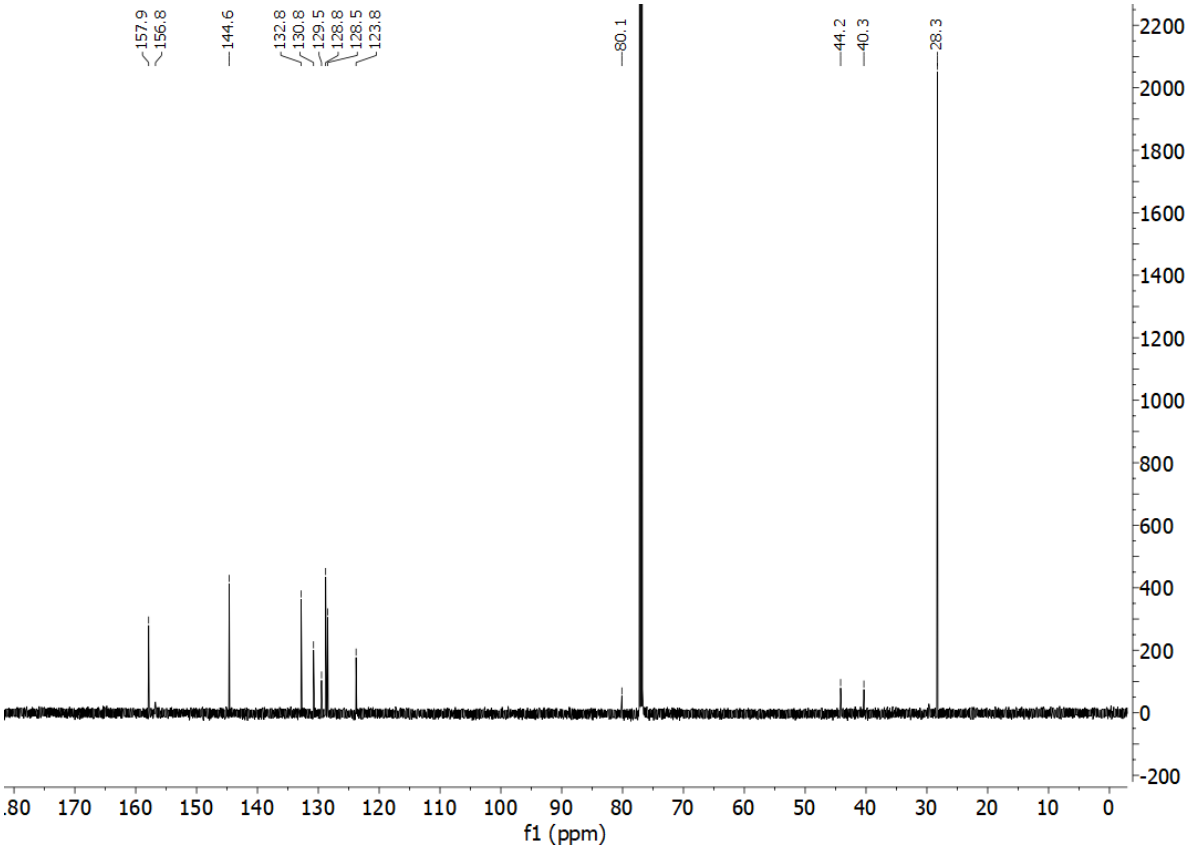

100. *N-(2-aminoethyl)isoquinoline-4-sulfonamide hydrochloride*

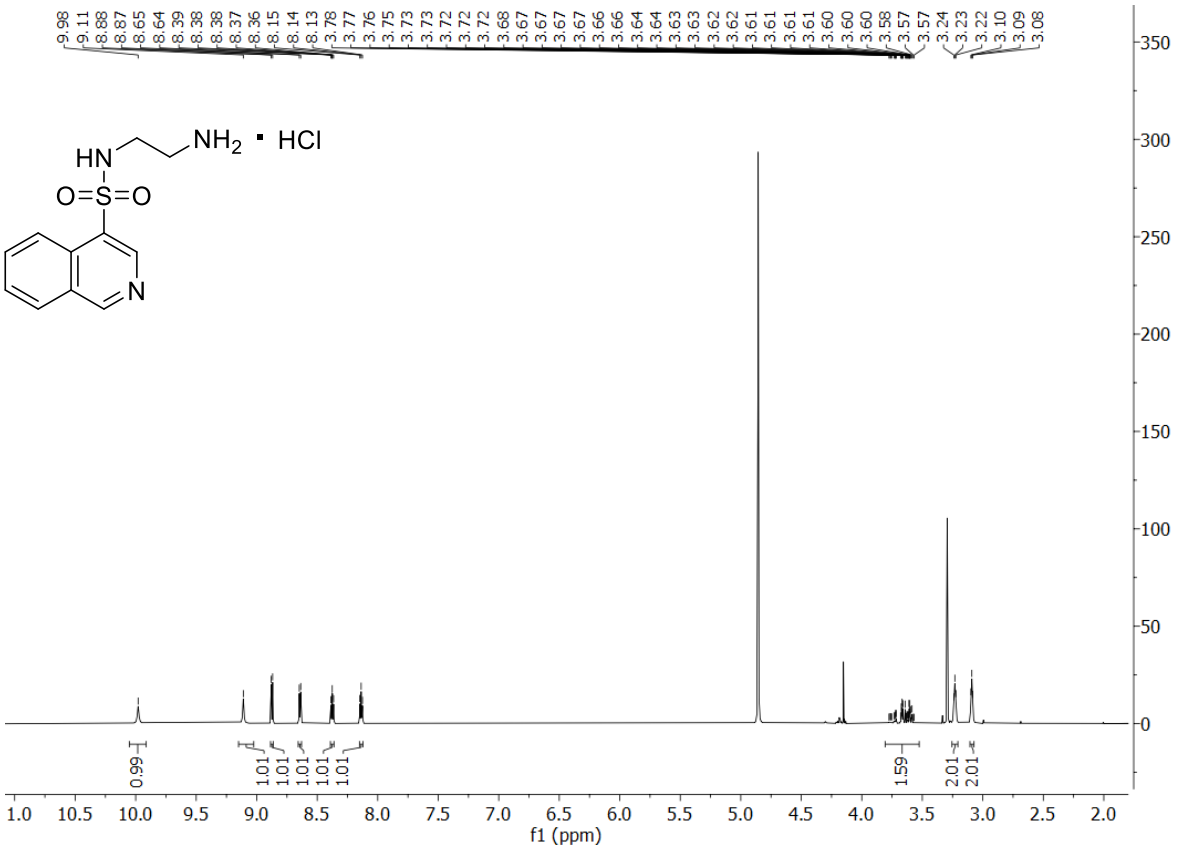

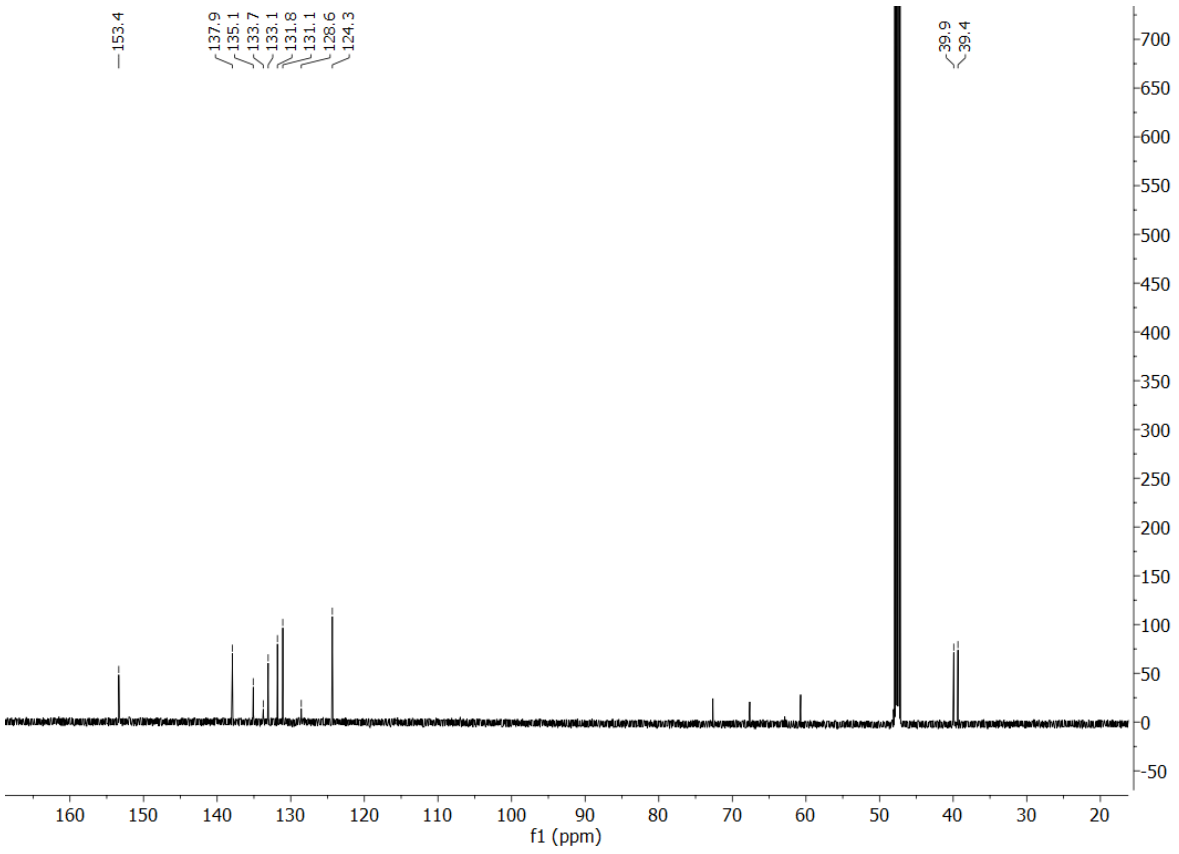

102. *tert-butyl N-[2'-(7-chloro-2,1,3-benzoxadiazole-4-sulfonamido)ethyl]carbamate*

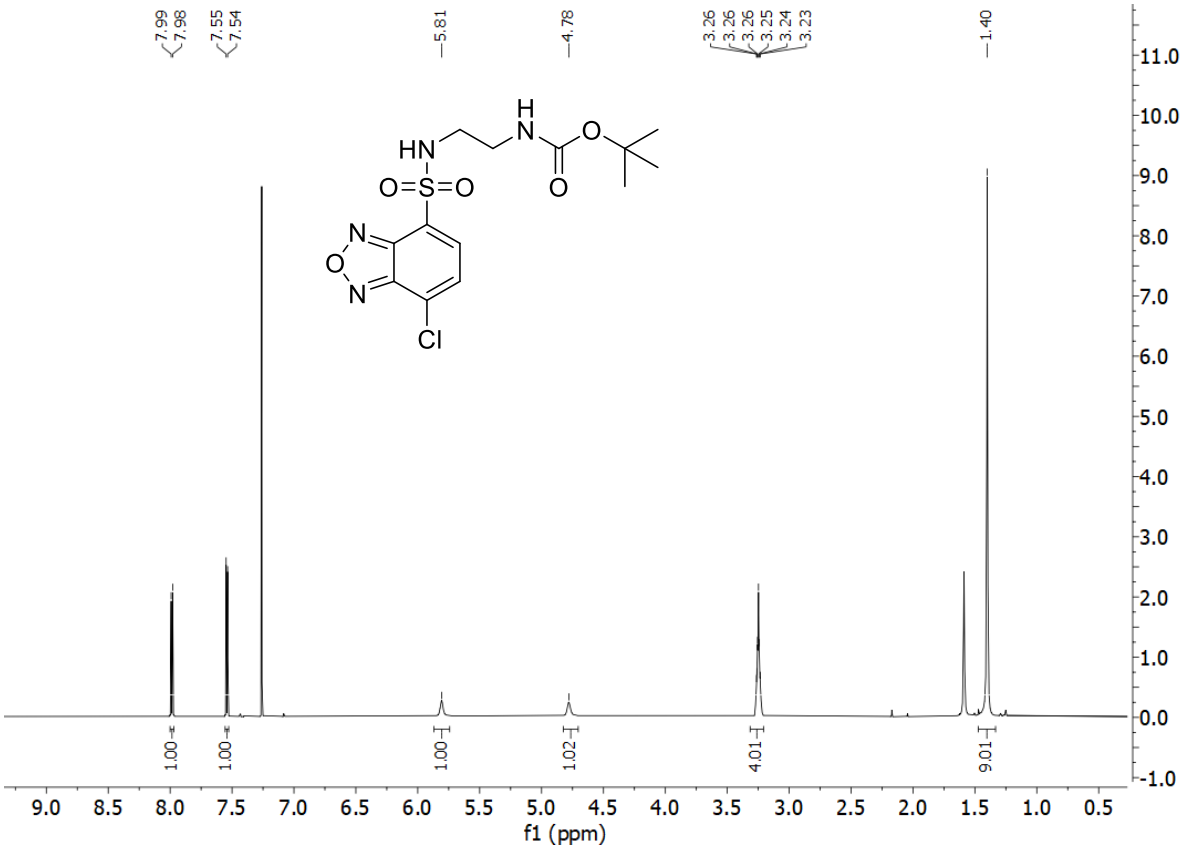

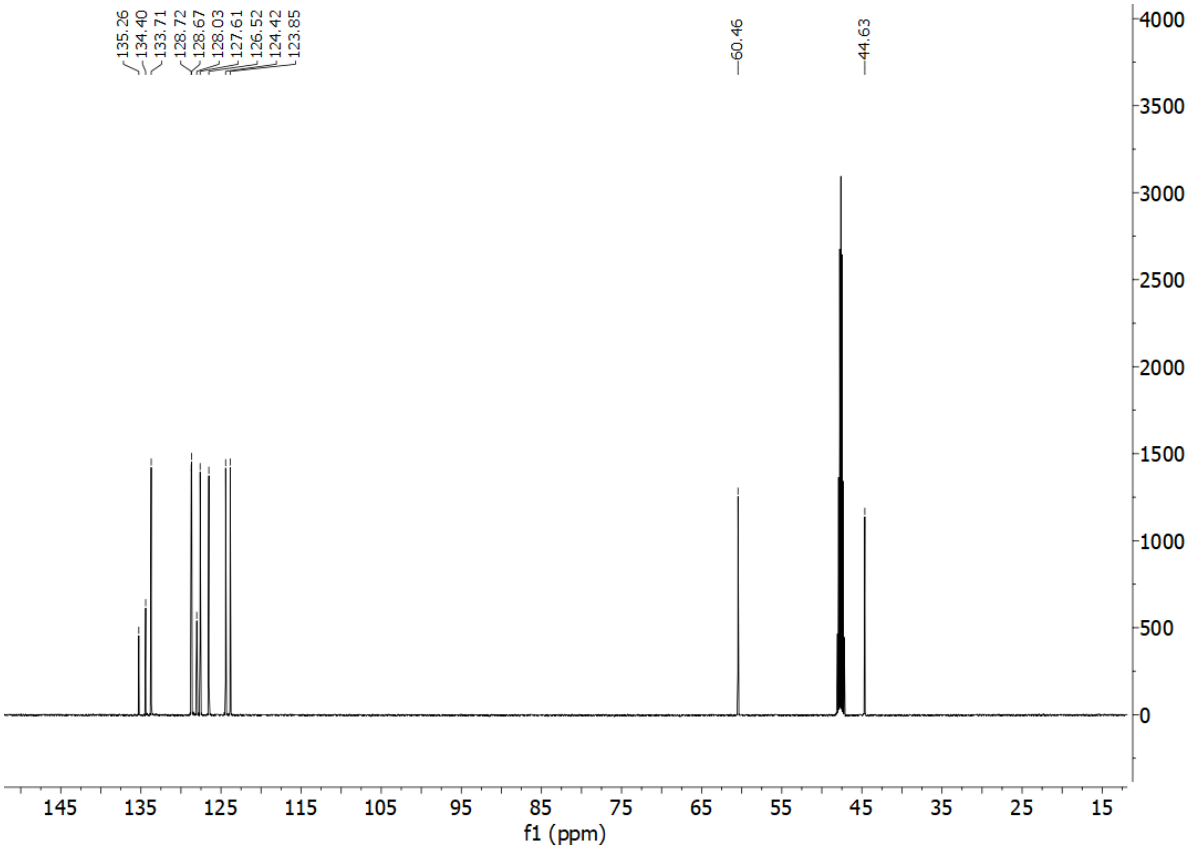

103. *tert-butyl N-{2'-[7-(methylamino)-2,1,3-benzoxadiazole-4-sulfonamido]ethyl}carbamate*

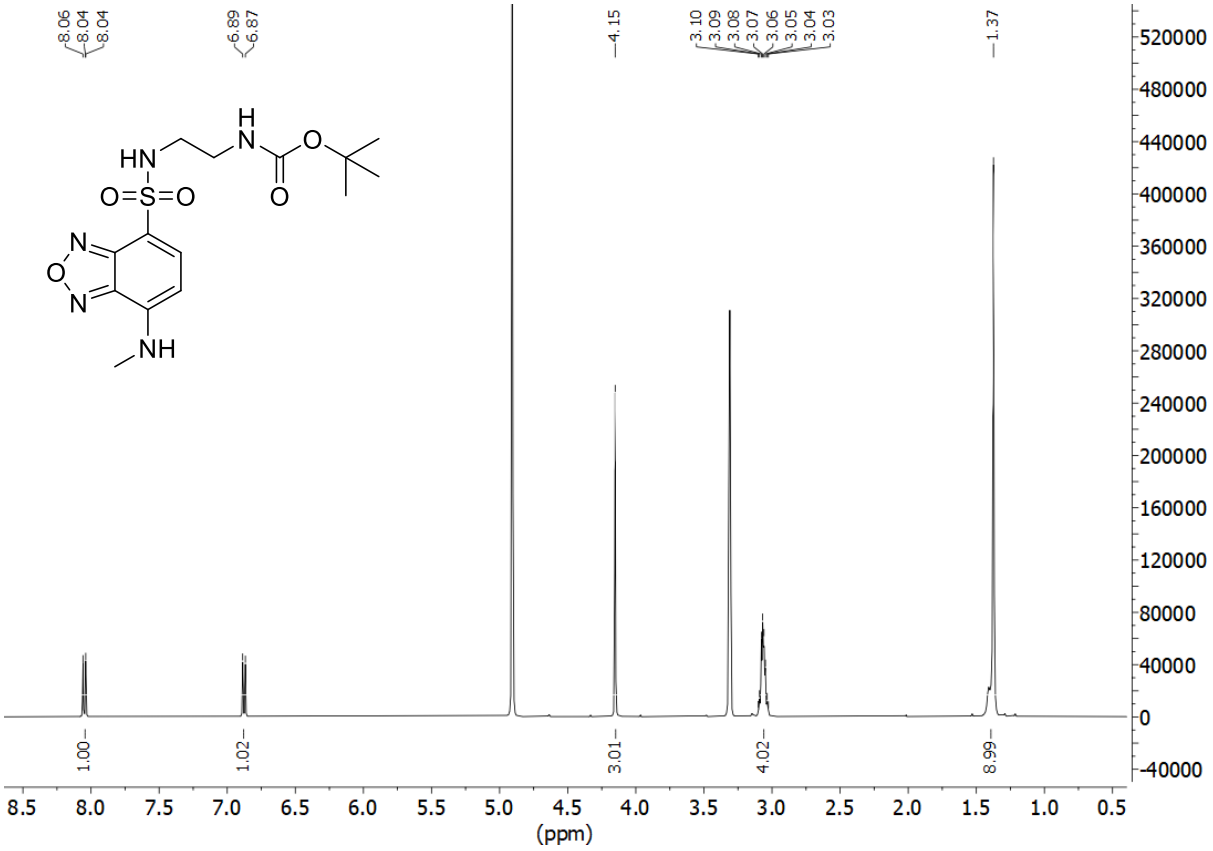

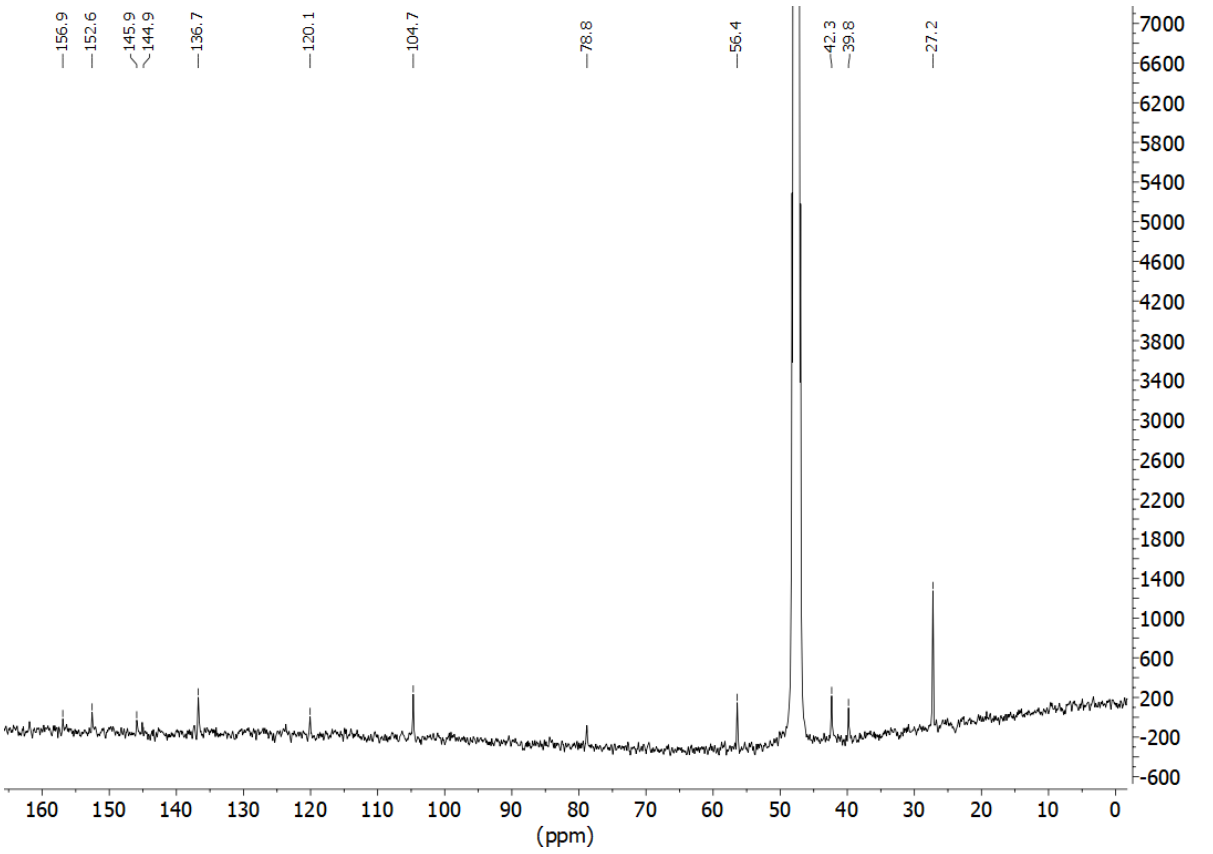

104. *7-(methylamino)-N-[2'-(trimethylazaniumyl)ethyl]-2,1,3-benzoxadiazole-4-sulfonamide chloride*

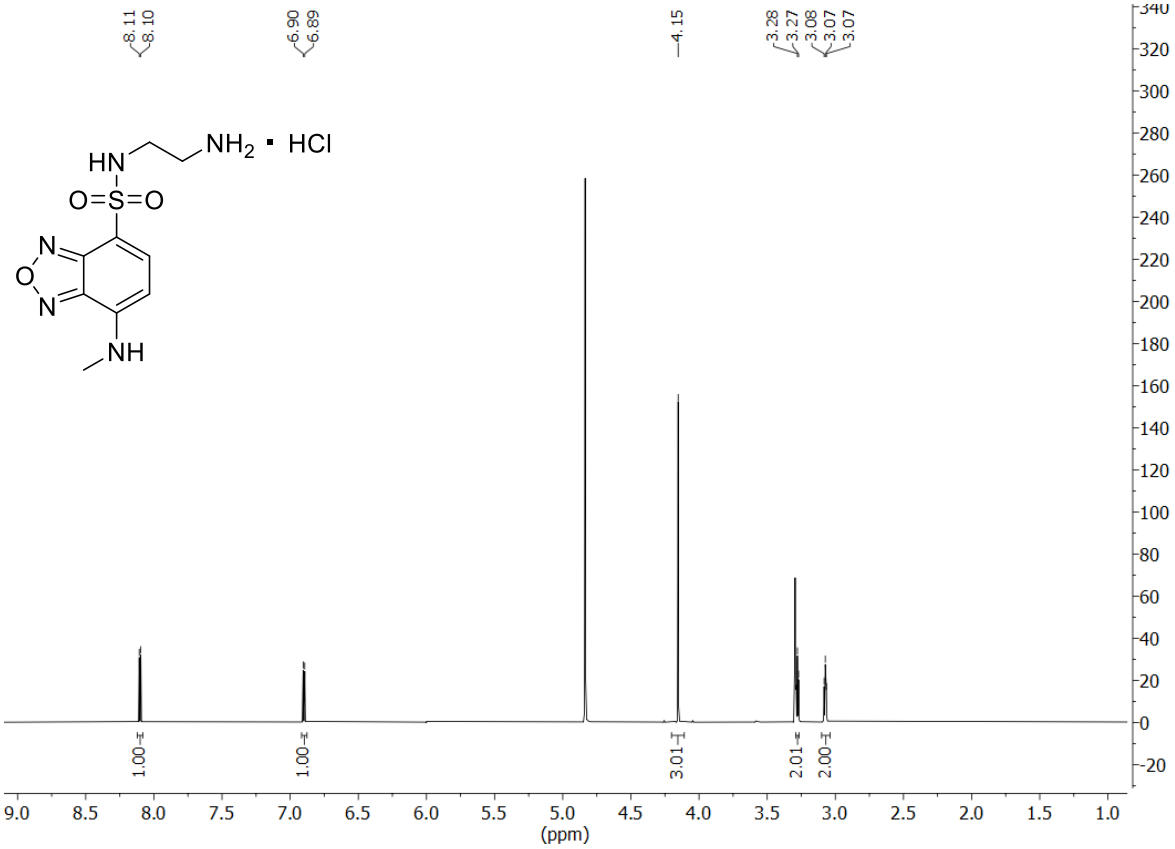

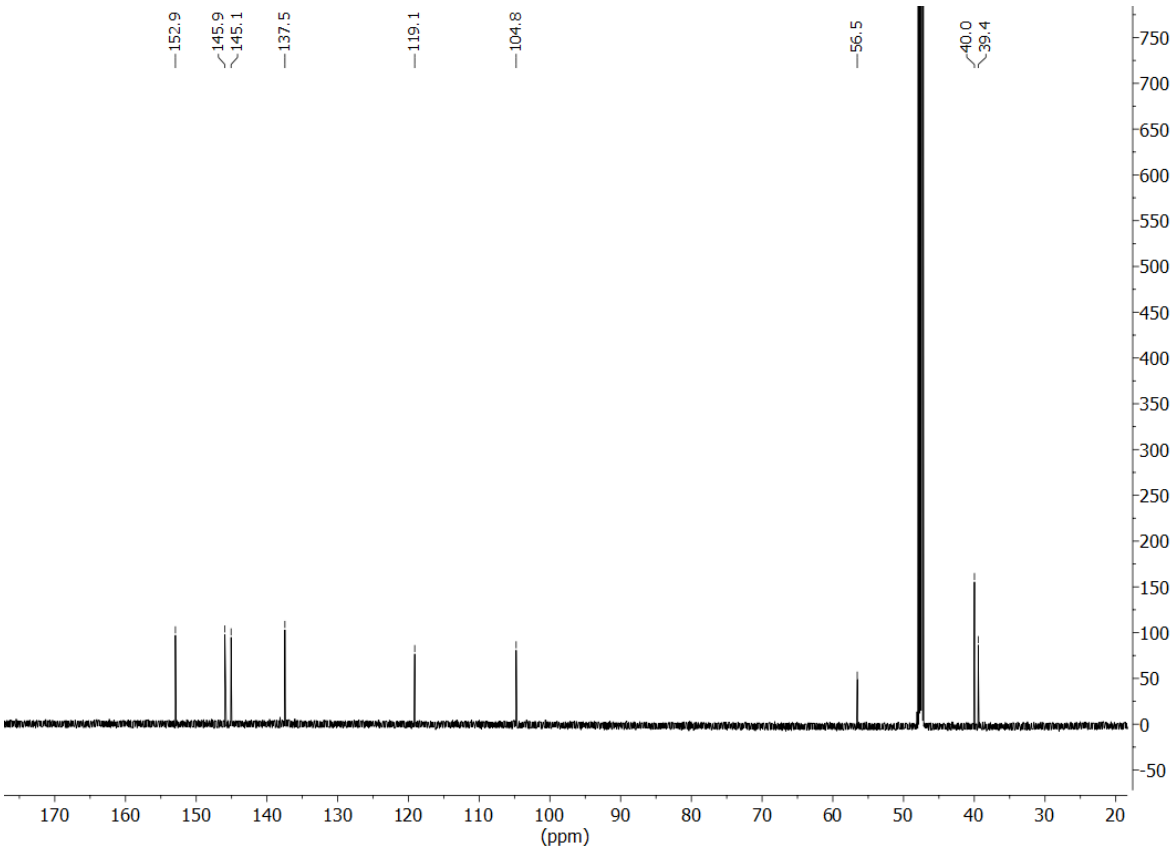

108b. *1-bromo, 2-methoxynaphthalene*

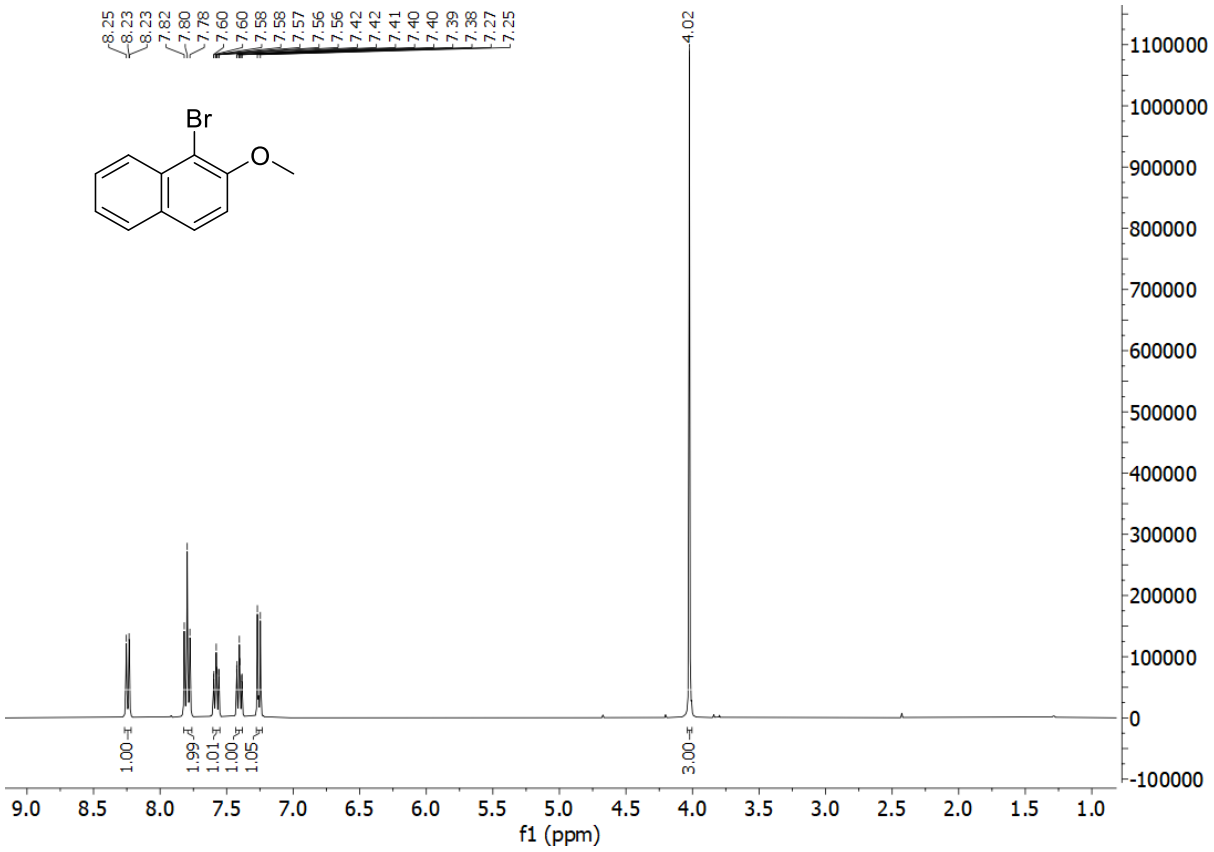

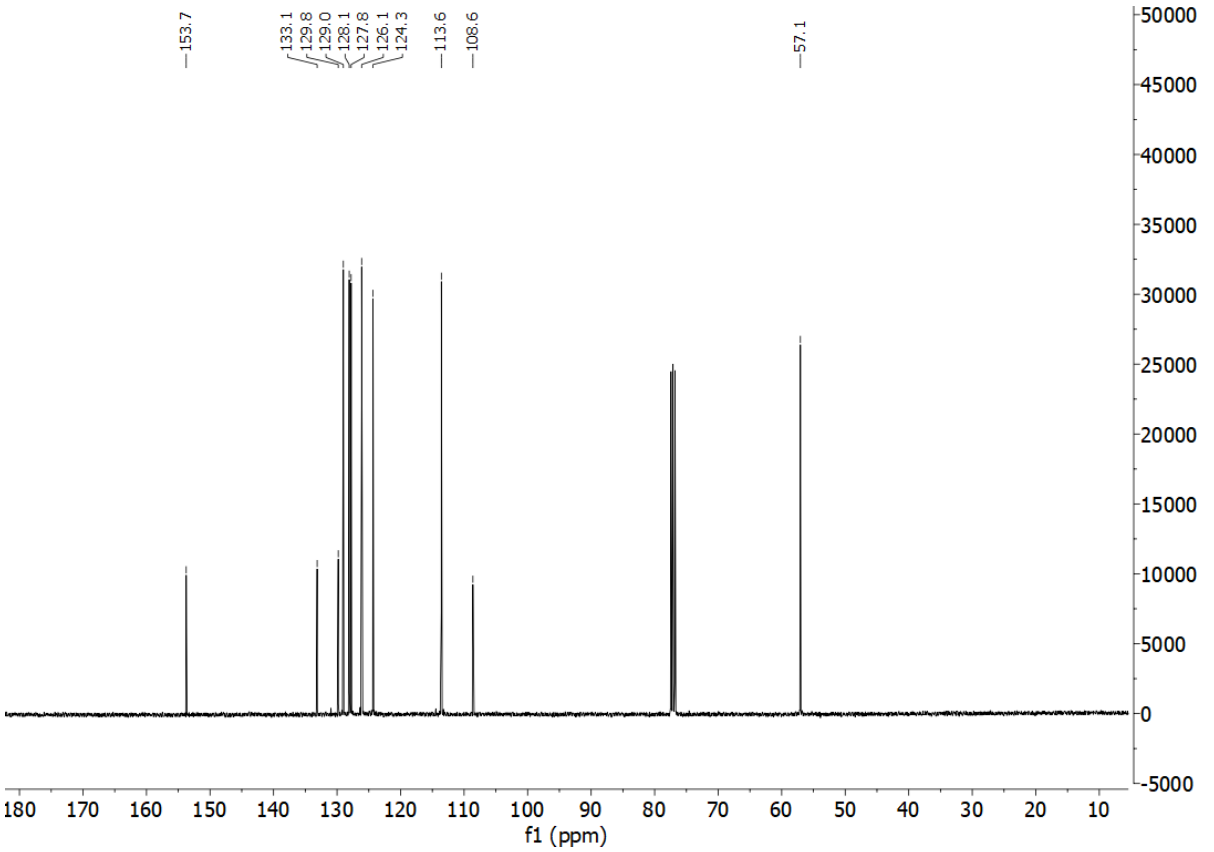

108c. *tert-butyl N-[2'-(2-methoxynaphthalene-1-sulfonamido)ethyl]carbamate*

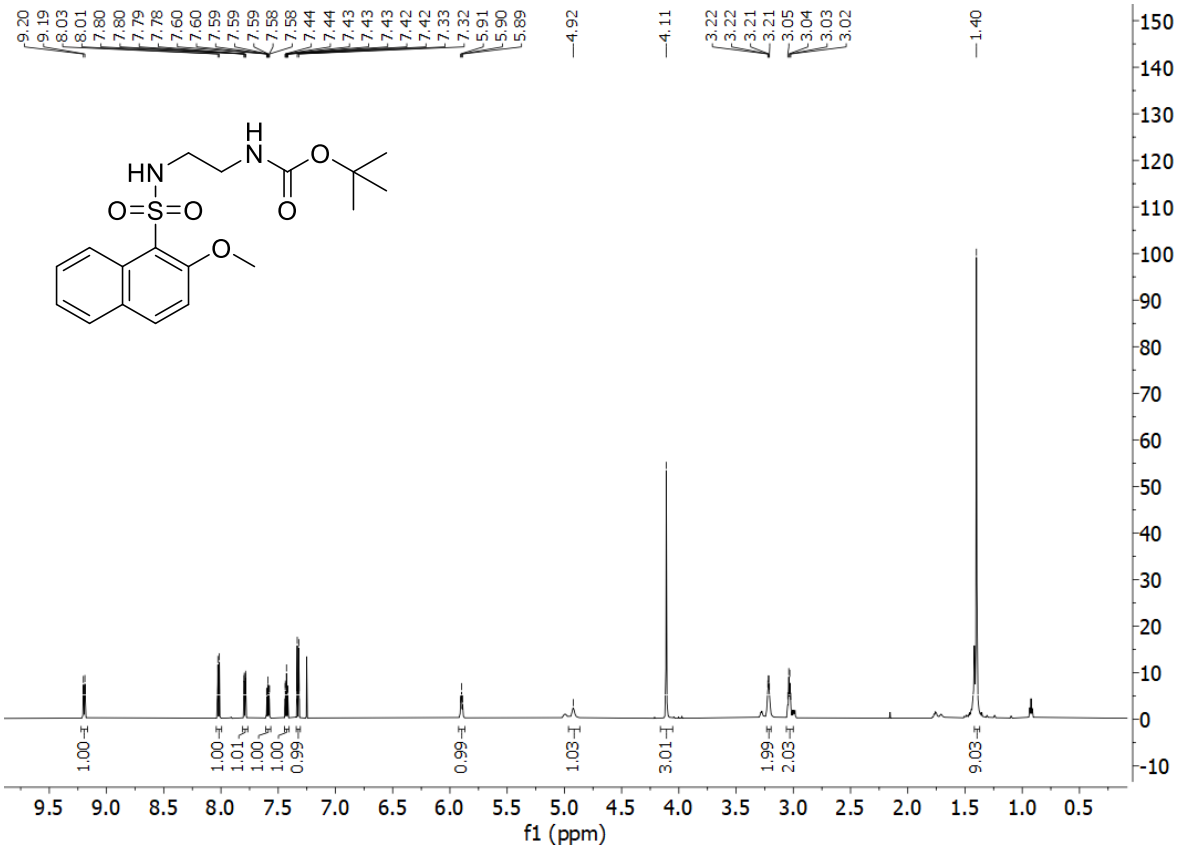

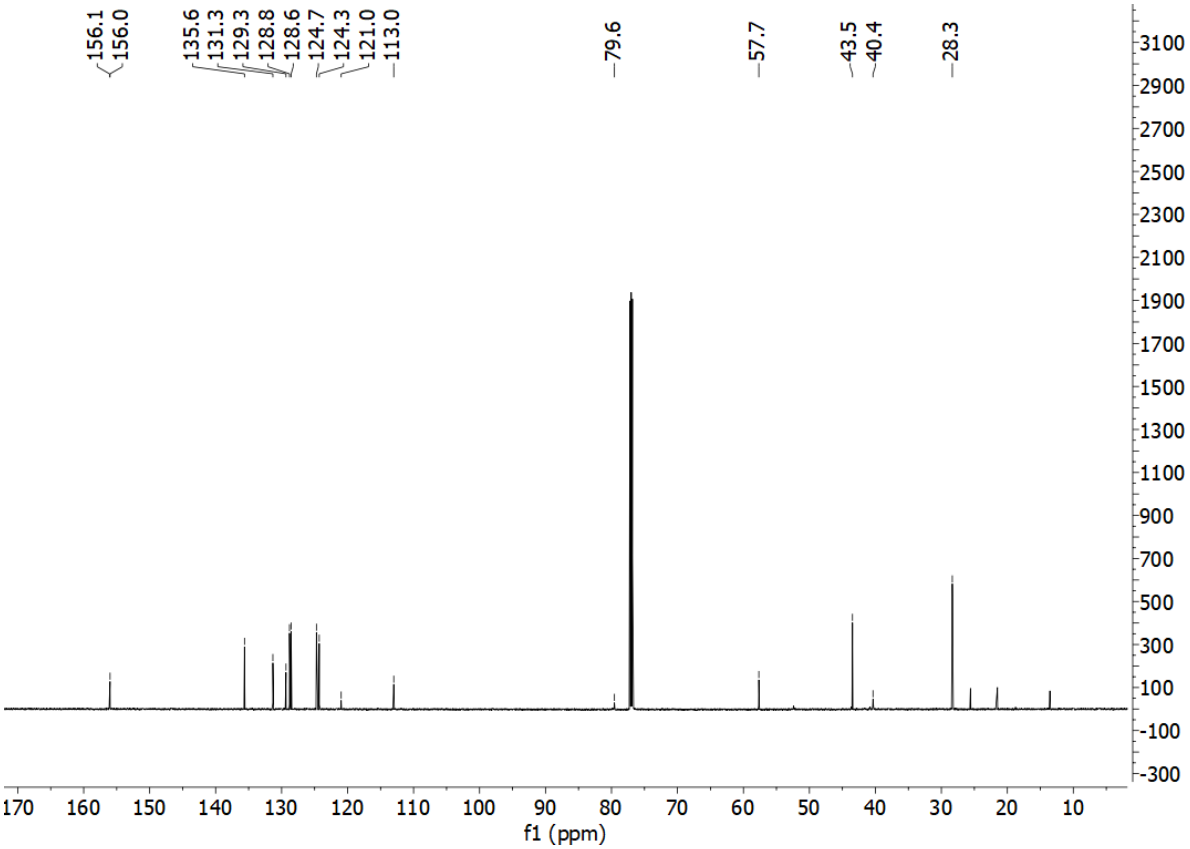

108. *N-(2'-aminoethyl)-2-methoxynaphthalene-1-sulfonamide hydrochloride*

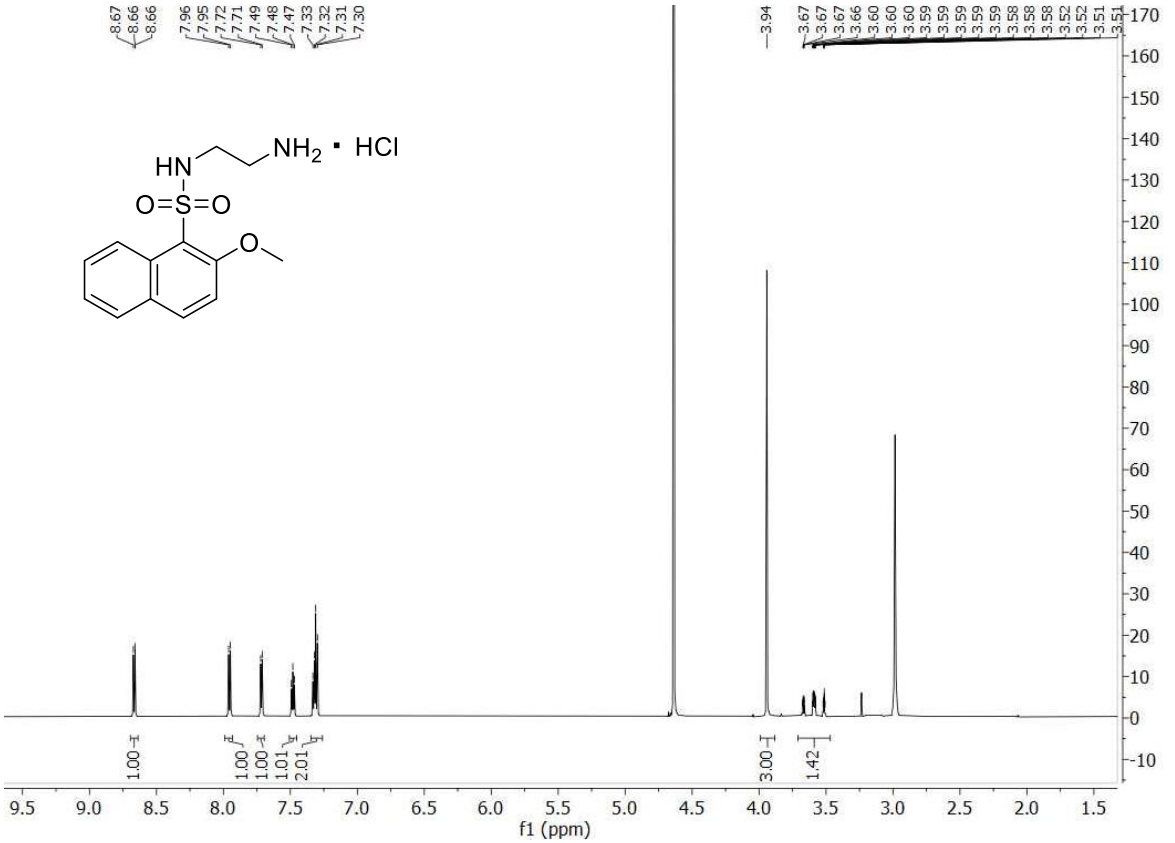

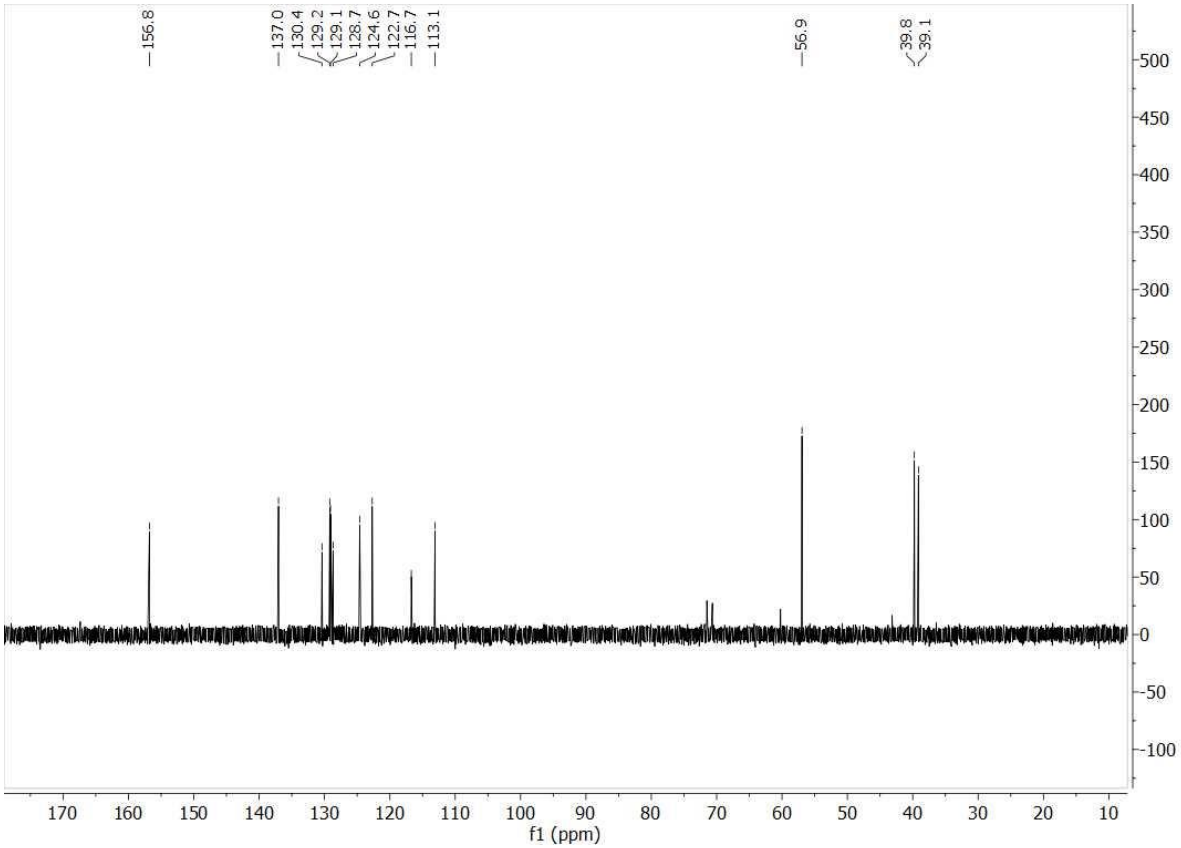

109b. *1-bromo, 4-pentoxynaphthalene*

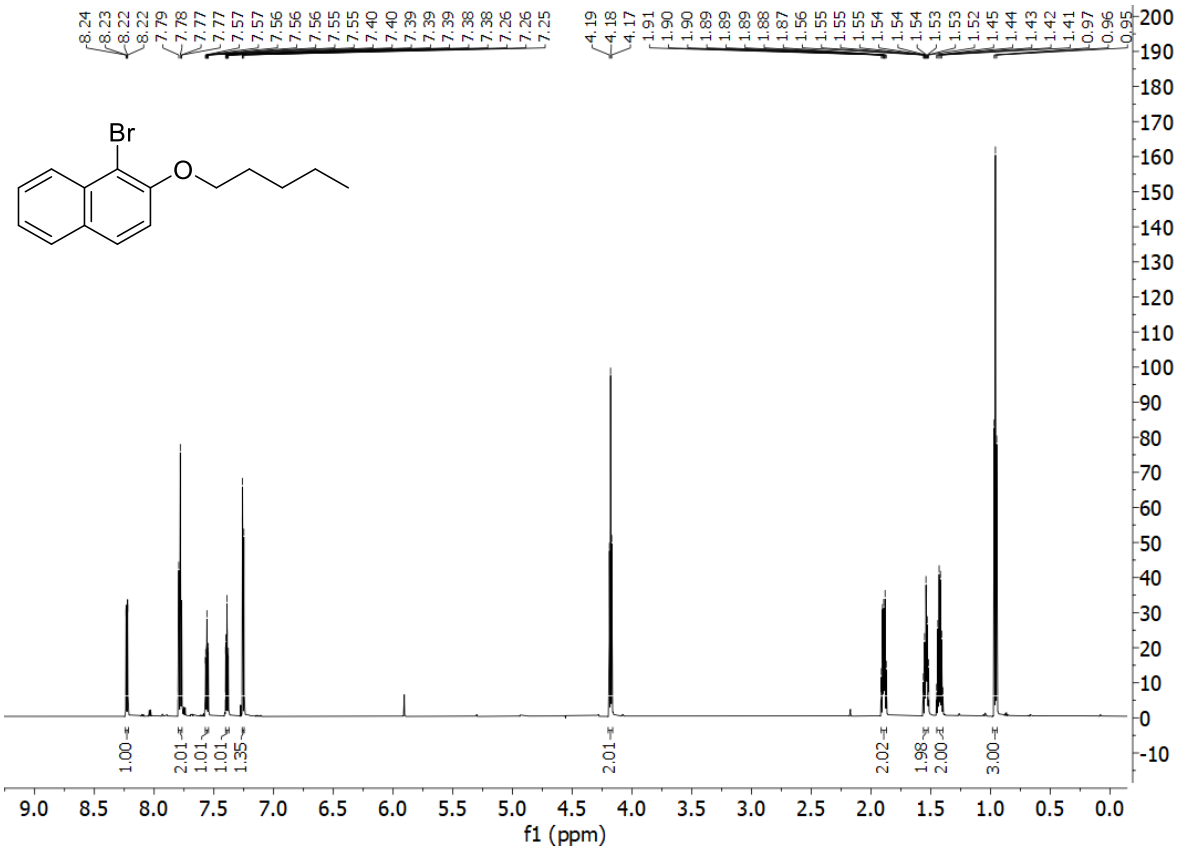

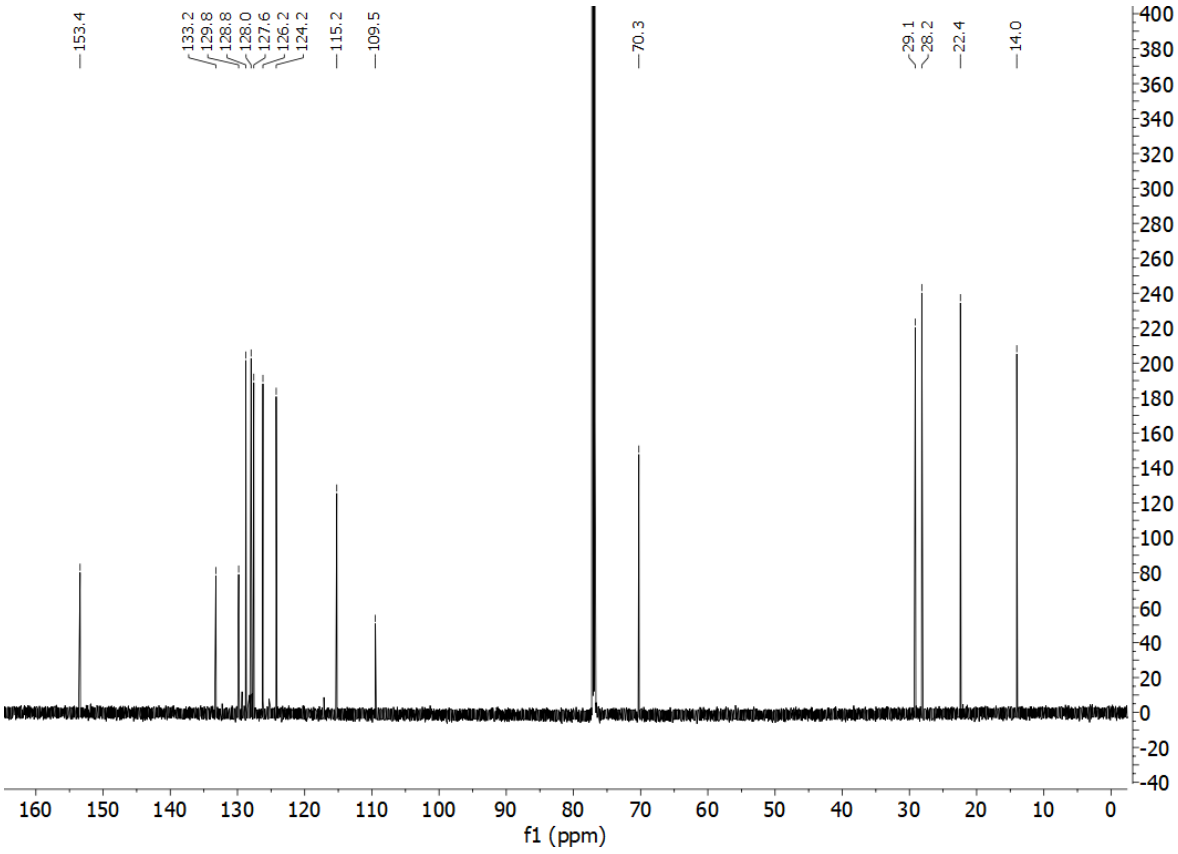

109c. *tert-butyl N-[2'-(2-pentoxynaphthalene-1-sulfonamido)ethyl]carbamate*

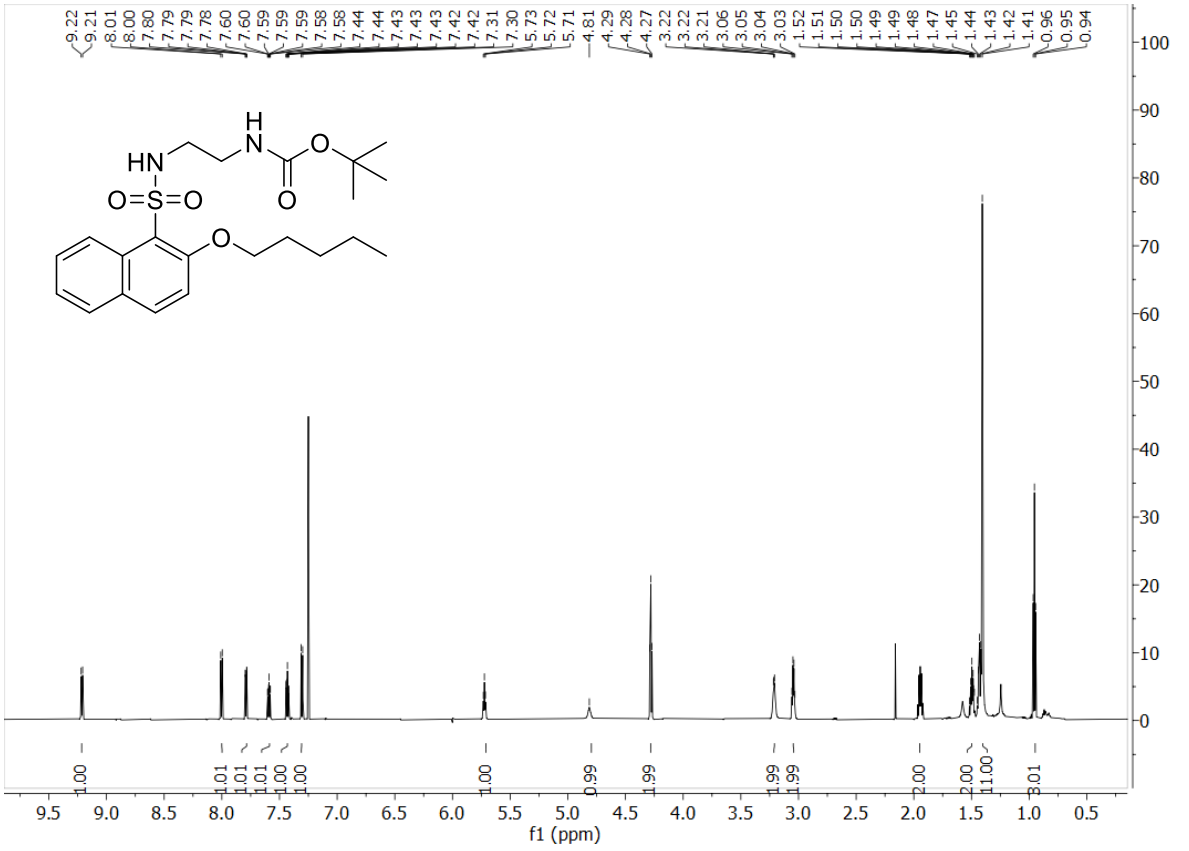

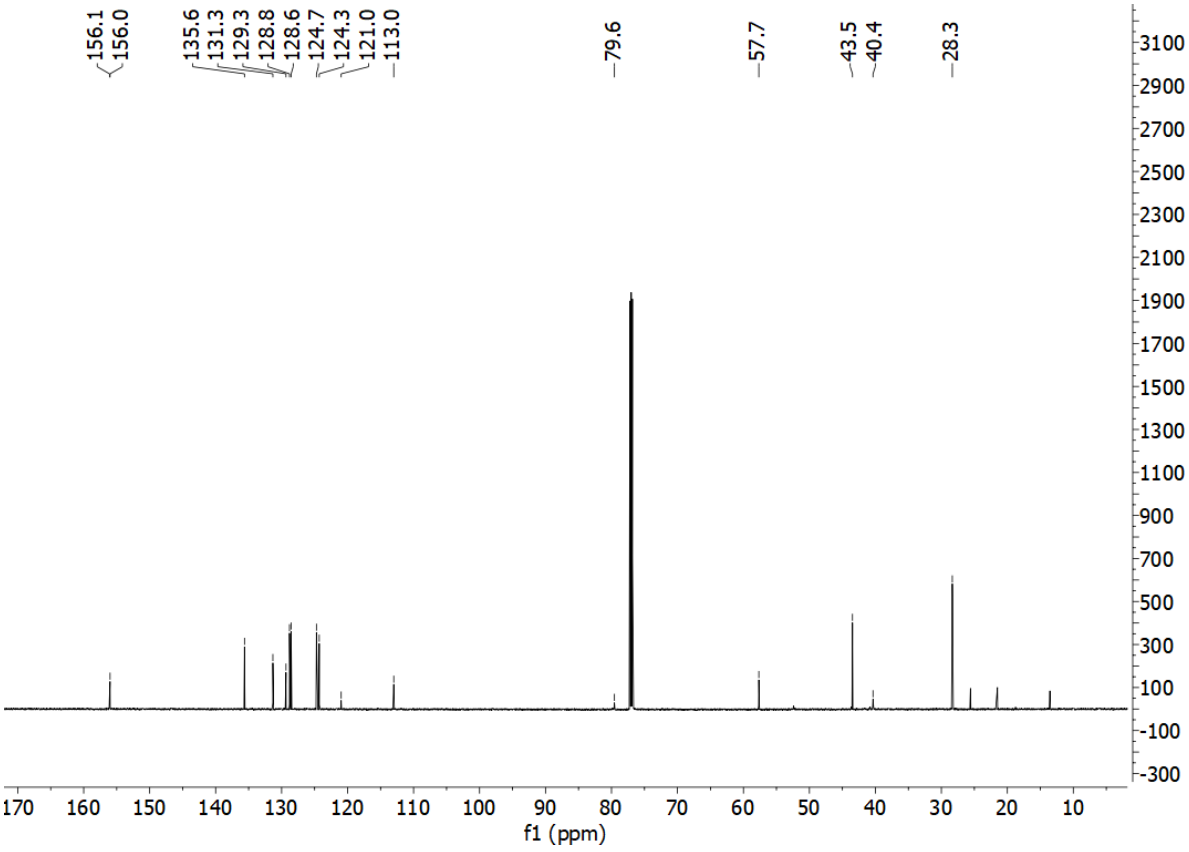

109. *N-(2'-aminoethyl)-2-(pentyloxy)naphthalene-1-sulfonamide hydrochloride*

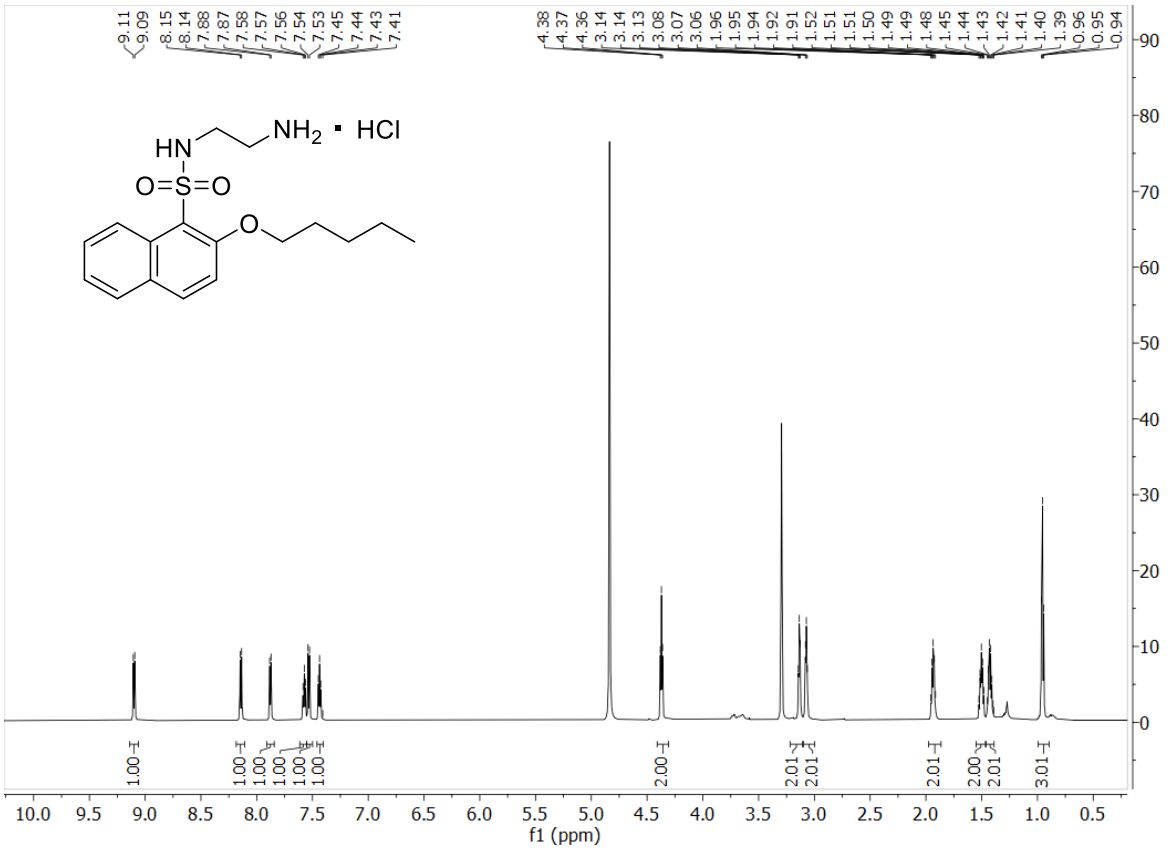

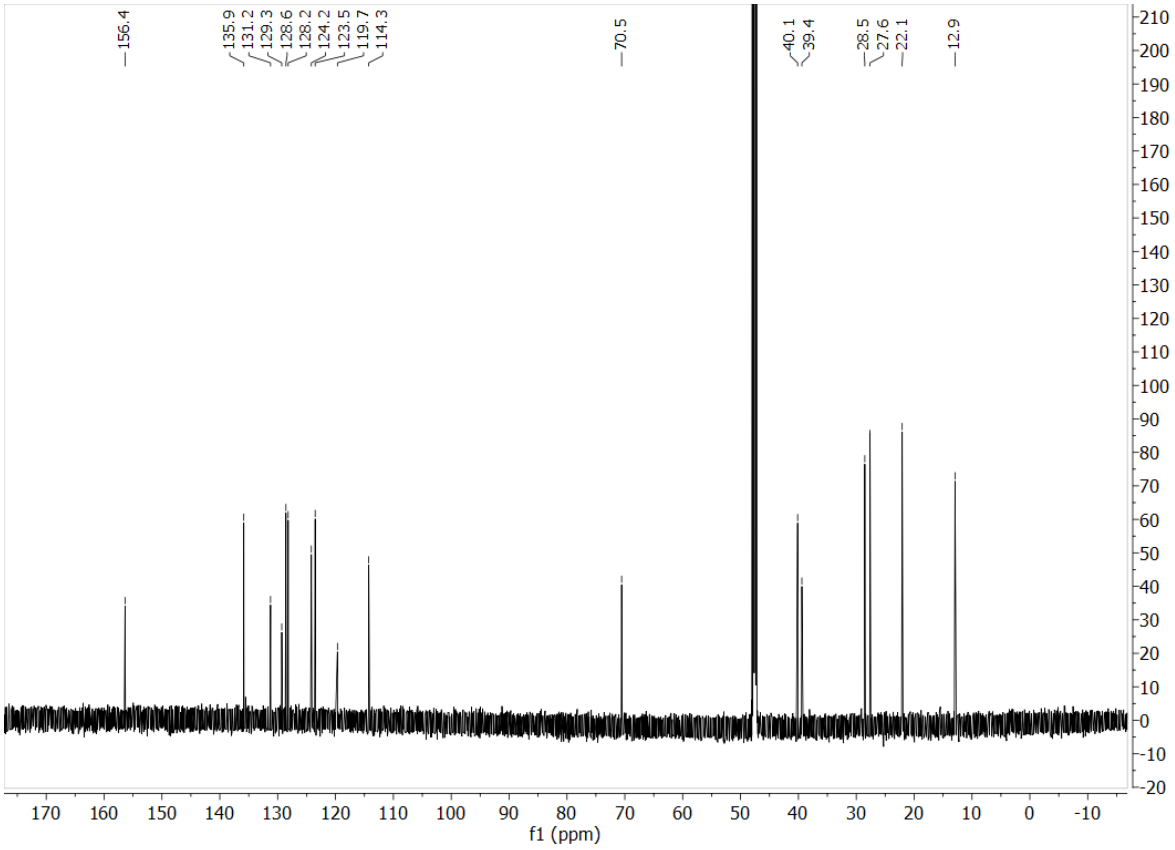

110b. *1-bromo, 4 methoxynaphthalene*

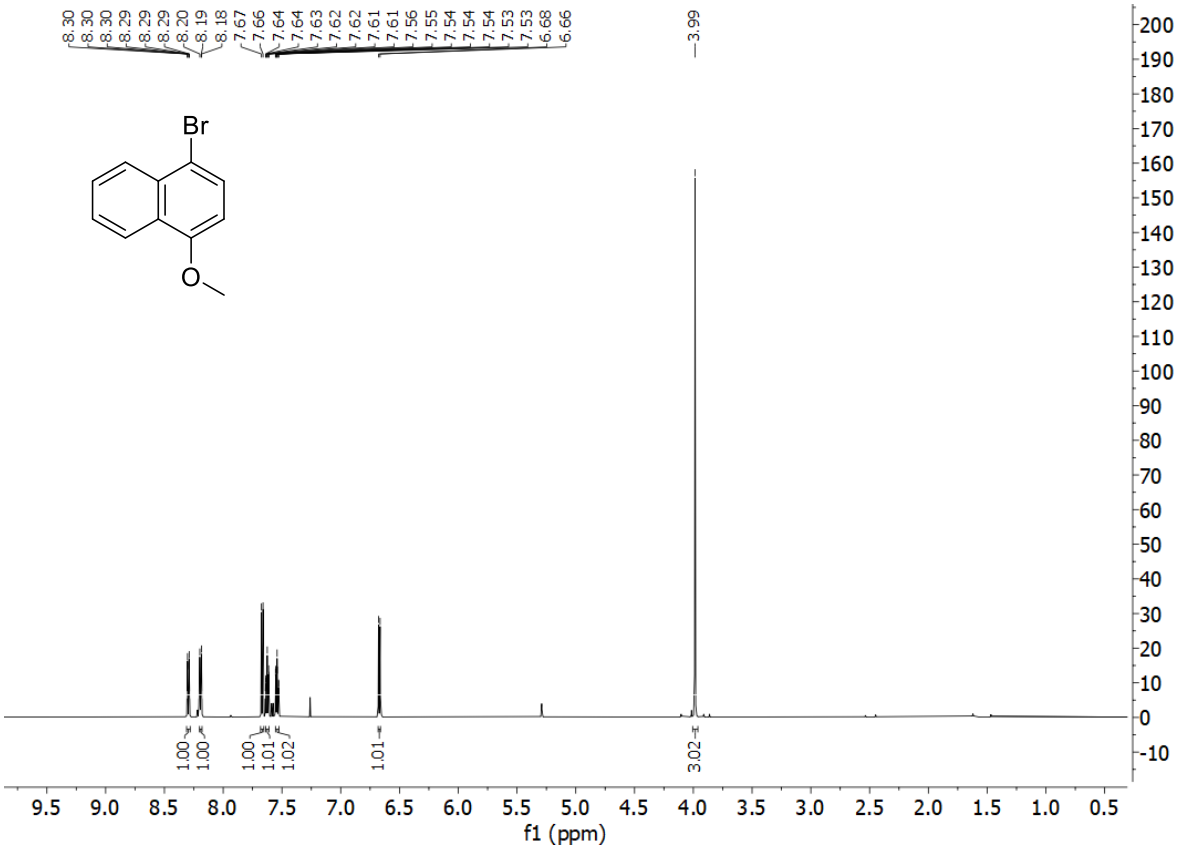

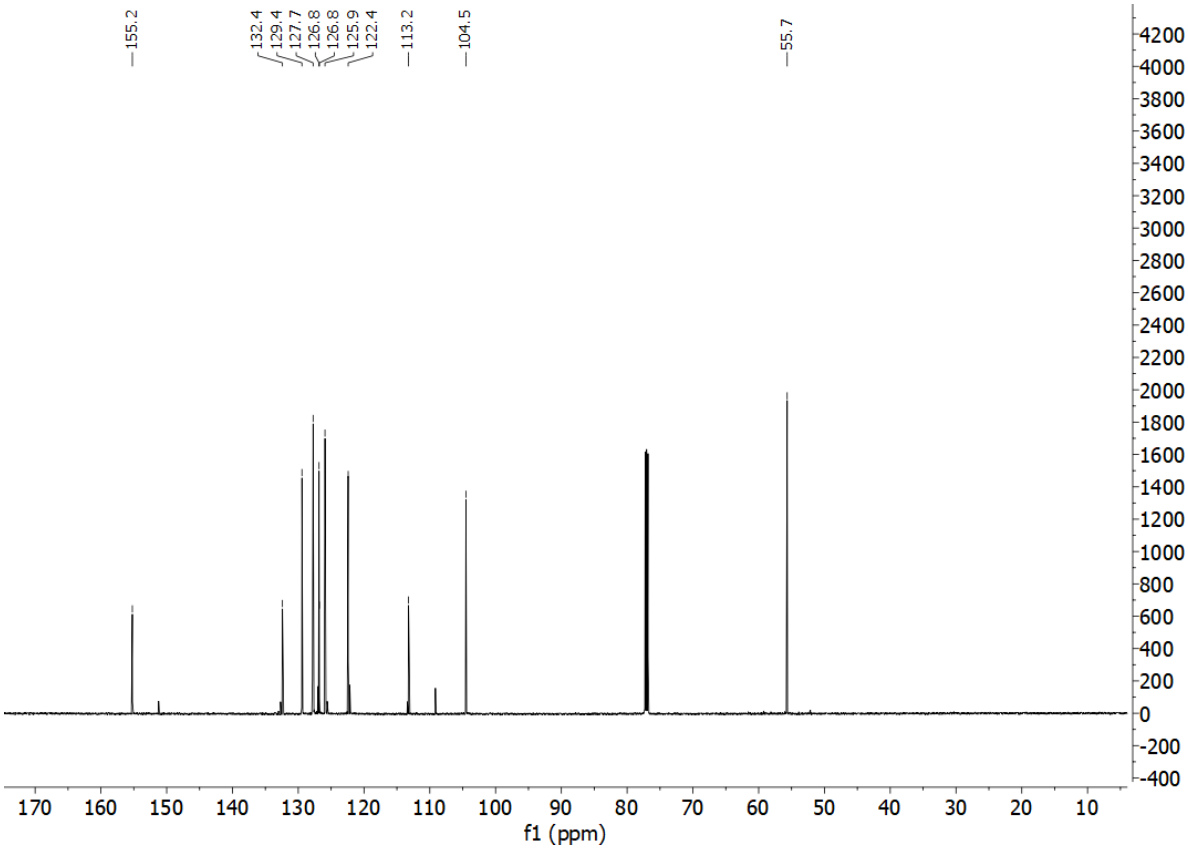

110c. *tert-butyl N-[2'-(4-methoxynaphthalene-1-sulfonamido)ethyl]carbamate*

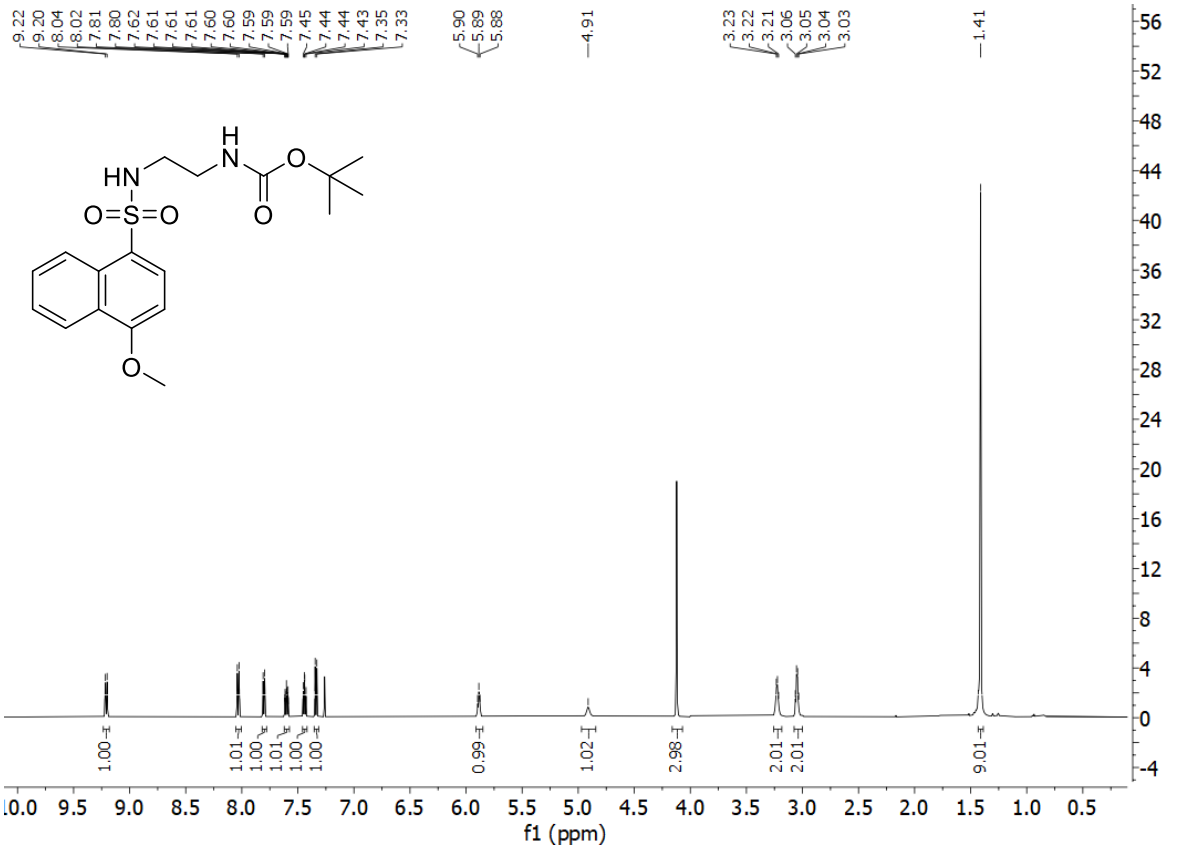

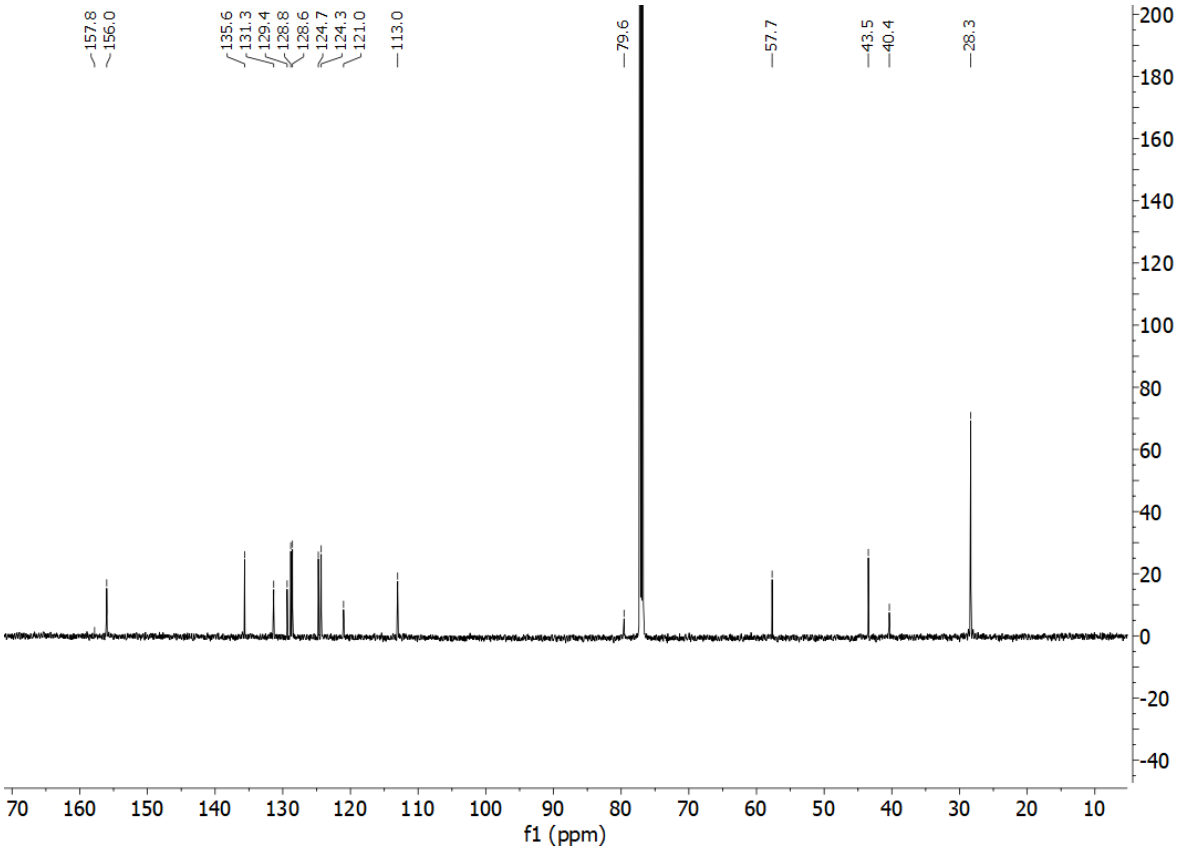

110. *N-(2'-aminoethyl)-4-methoxynaphthalene-1-sulfonamide hydrochloride*

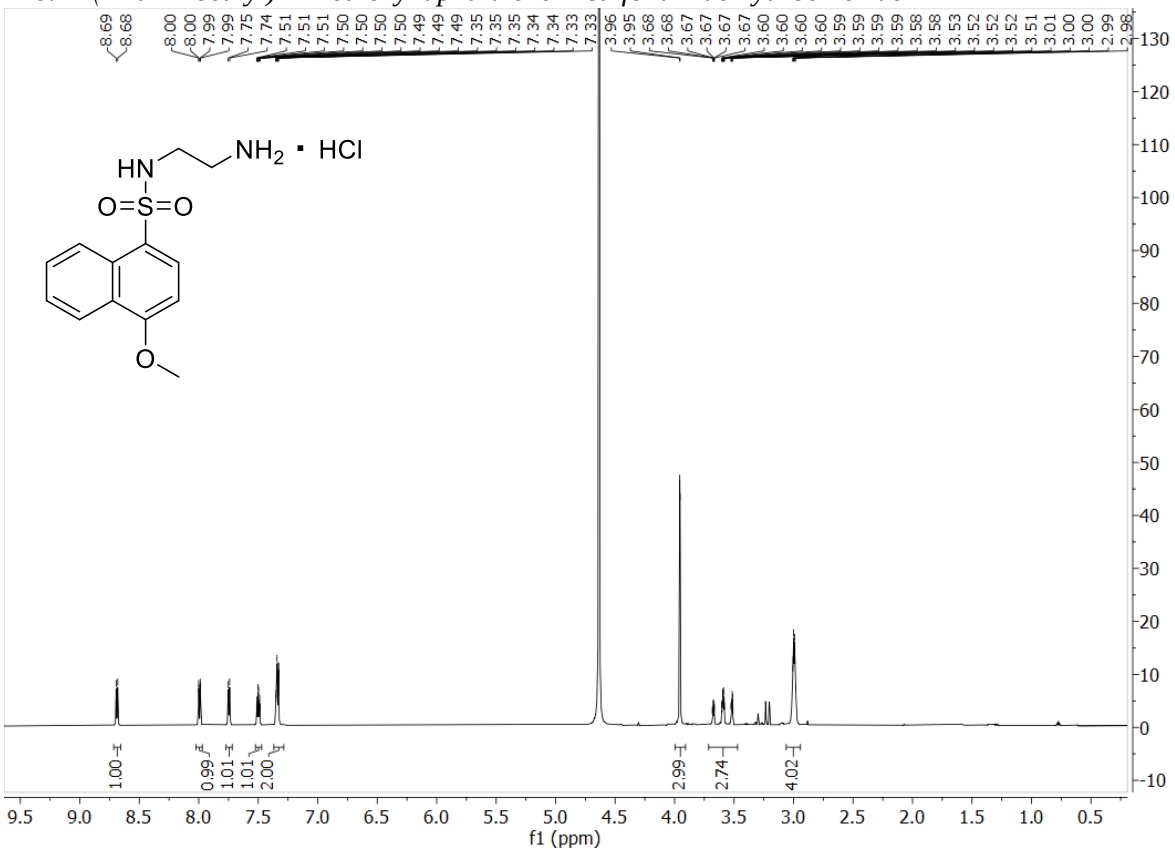

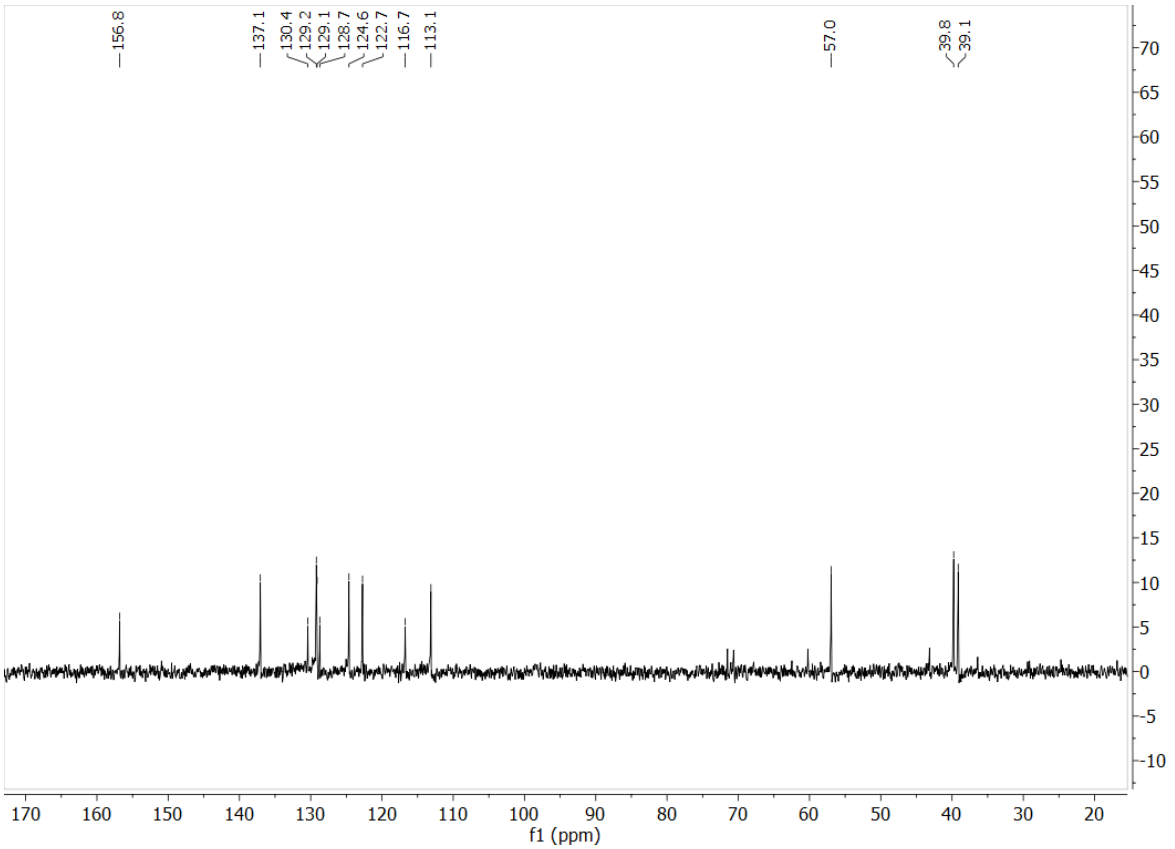

111b. *1-bromo, 4-pentoxynaphthalene*

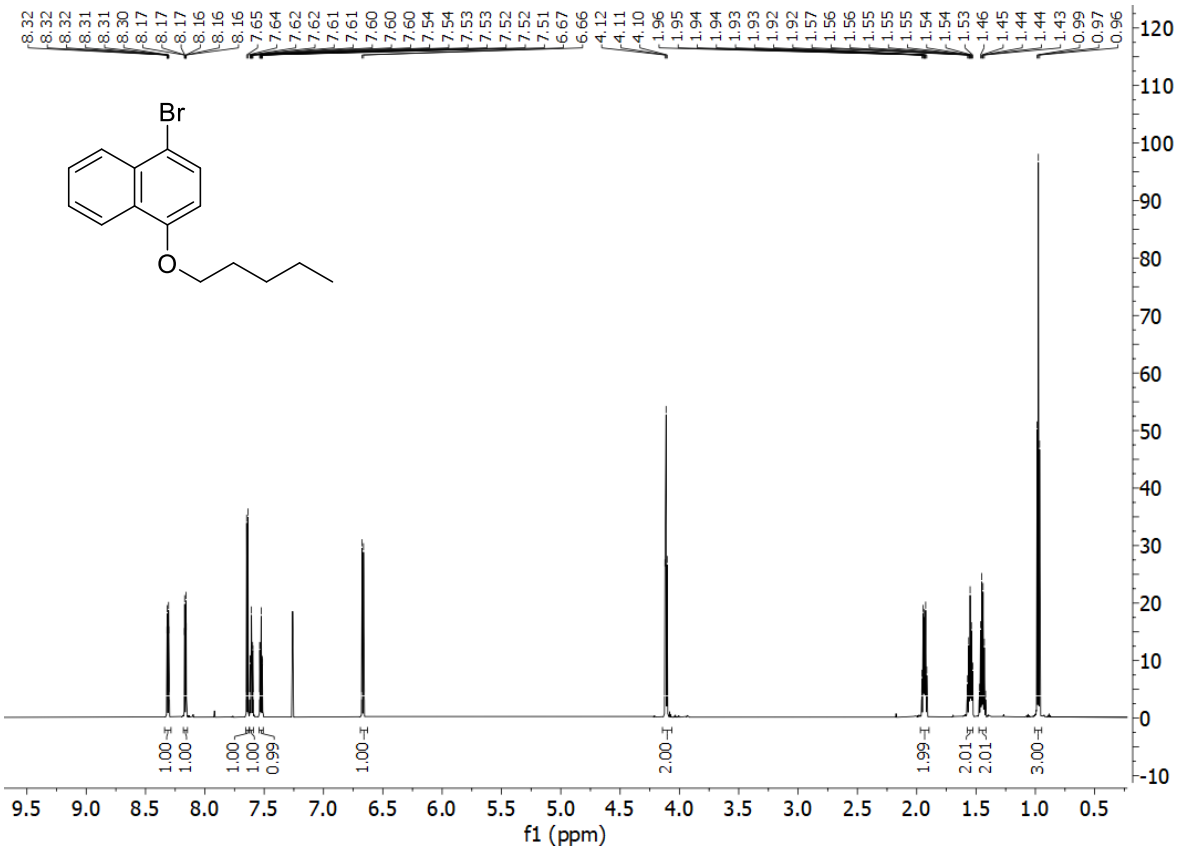

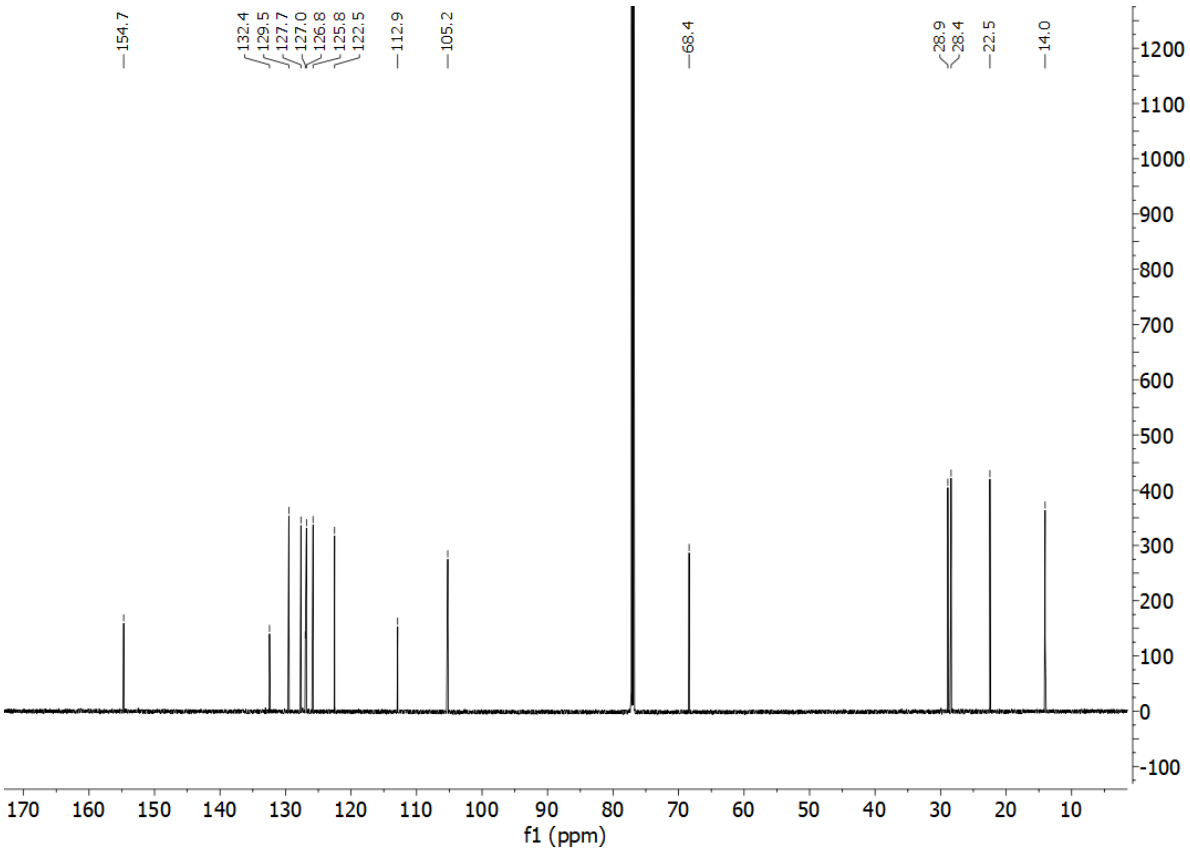

111c. *tert-butyl N-[2'-(4-pentoxynaphthalene-1-sulfonamido)ethyl]carbamate*

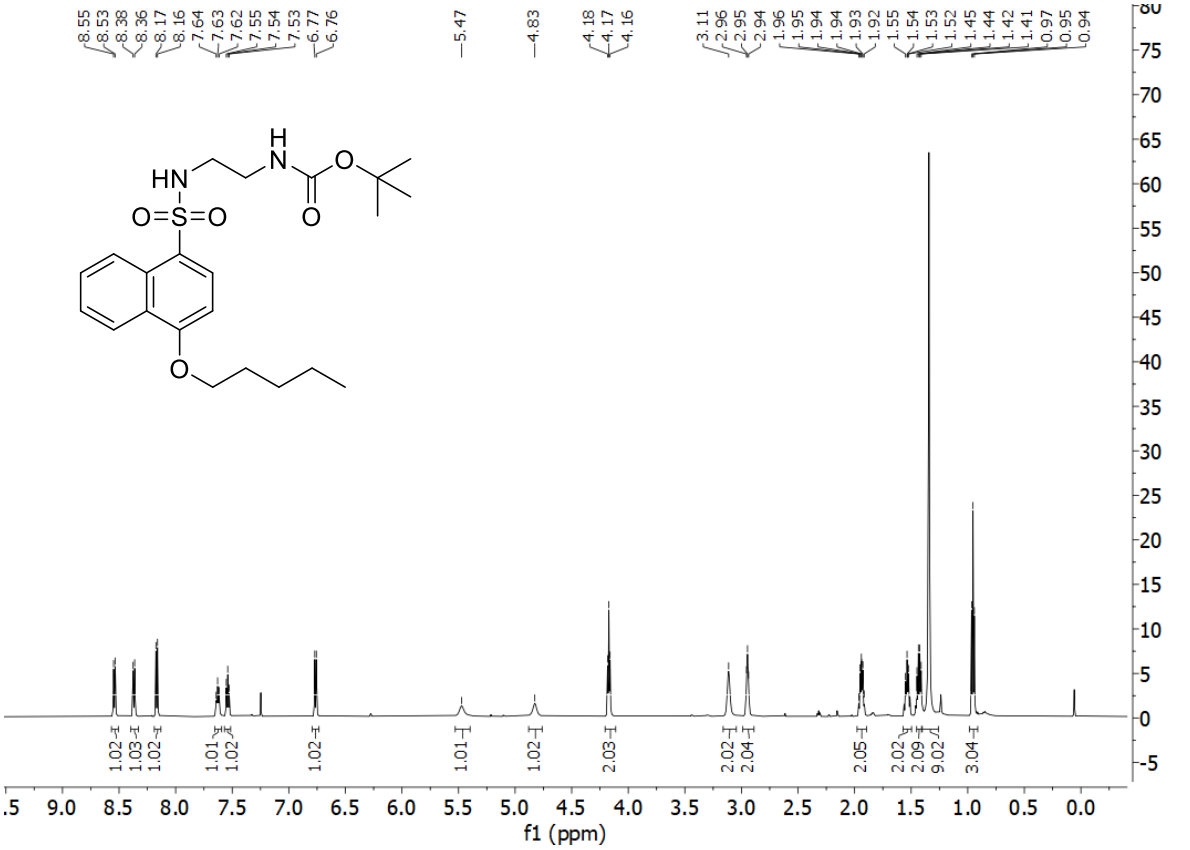

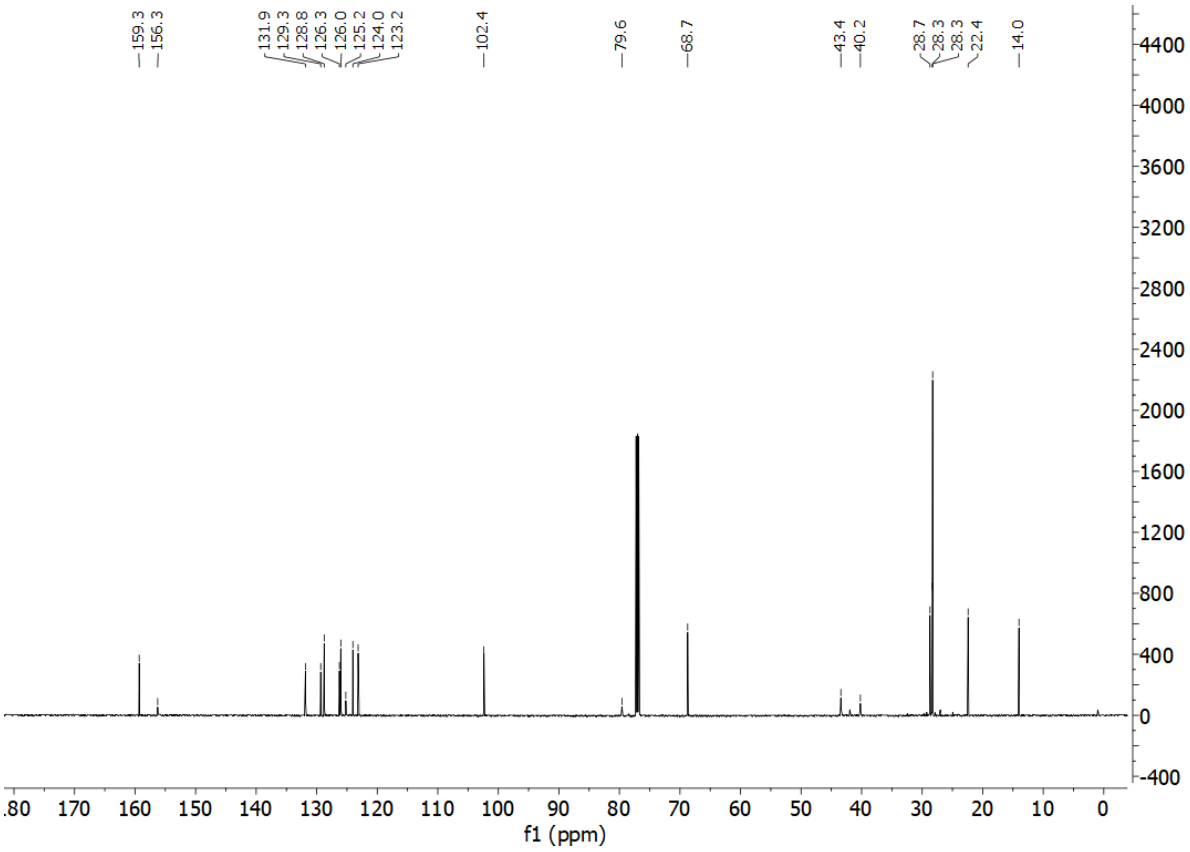

111. *N-(2'-aminoethyl)-4-(pentyloxy)naphthalene-1-sulfonamide hydrochloride*

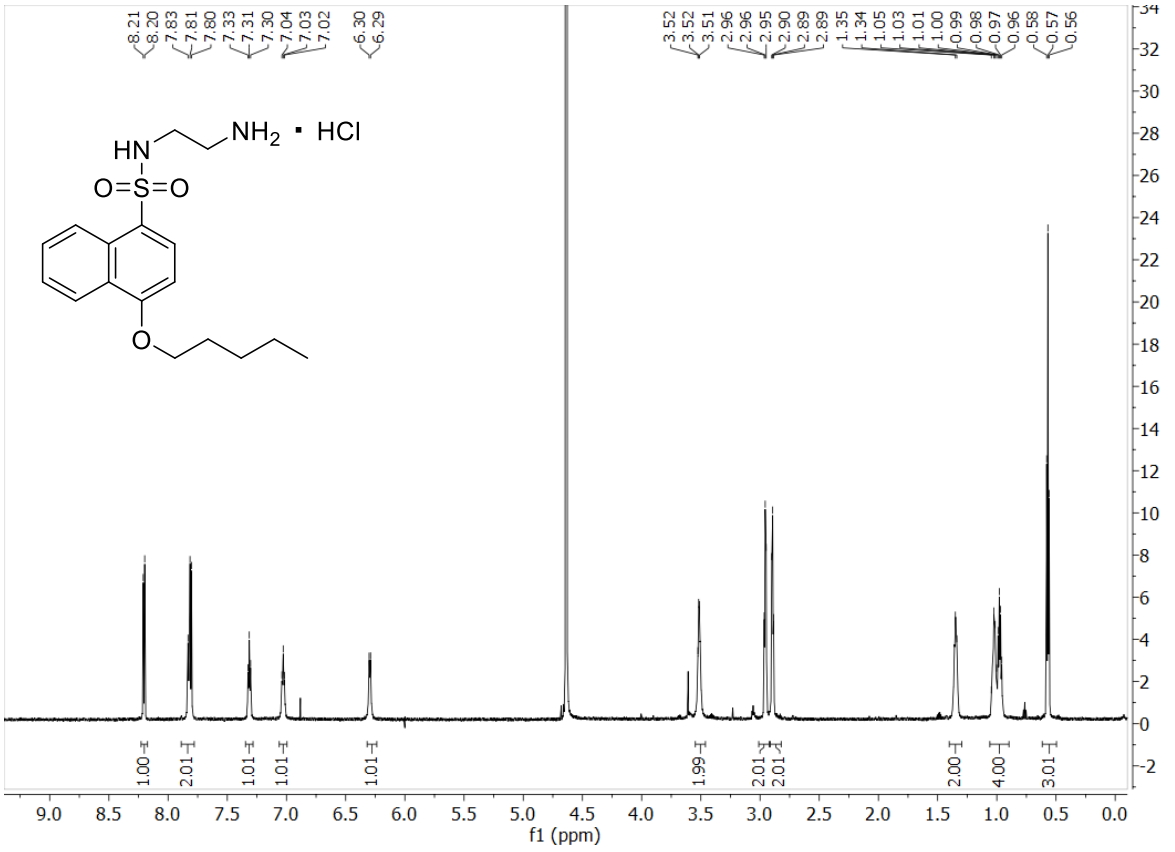

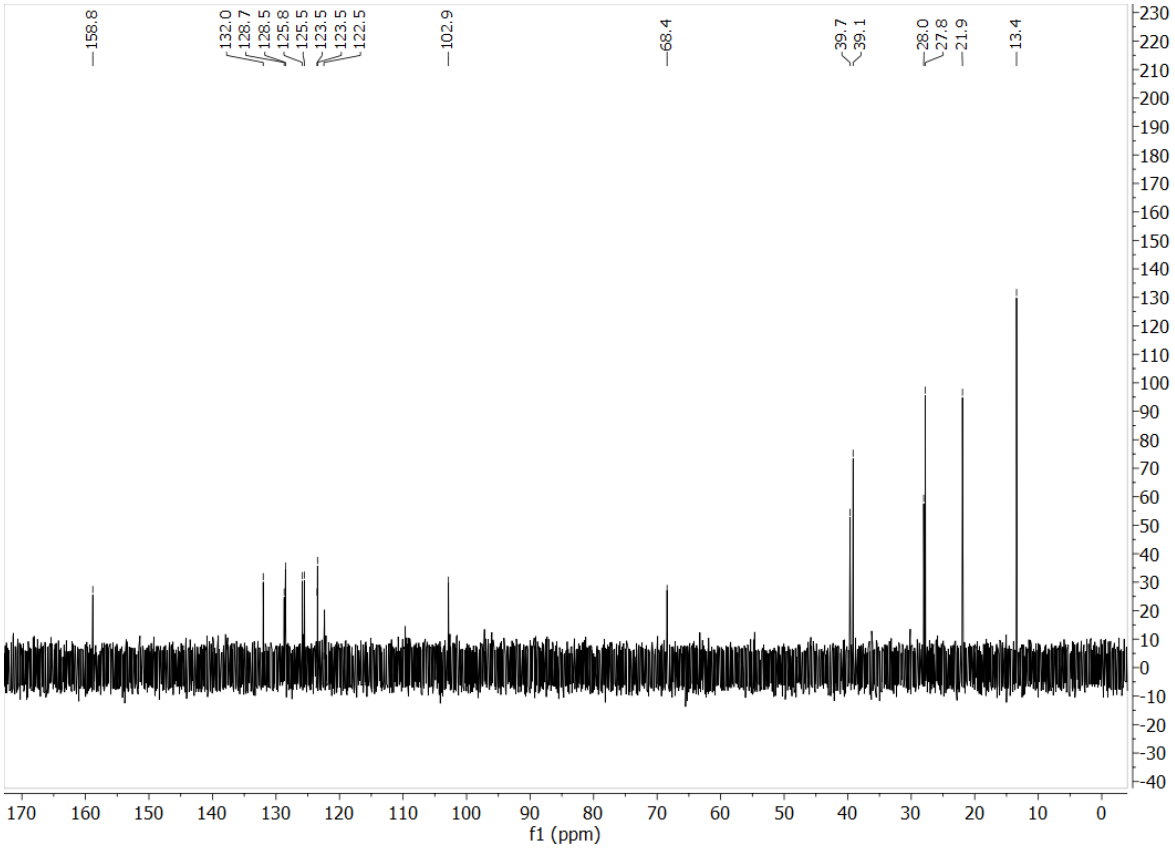

112b. *2-bromoanisole*

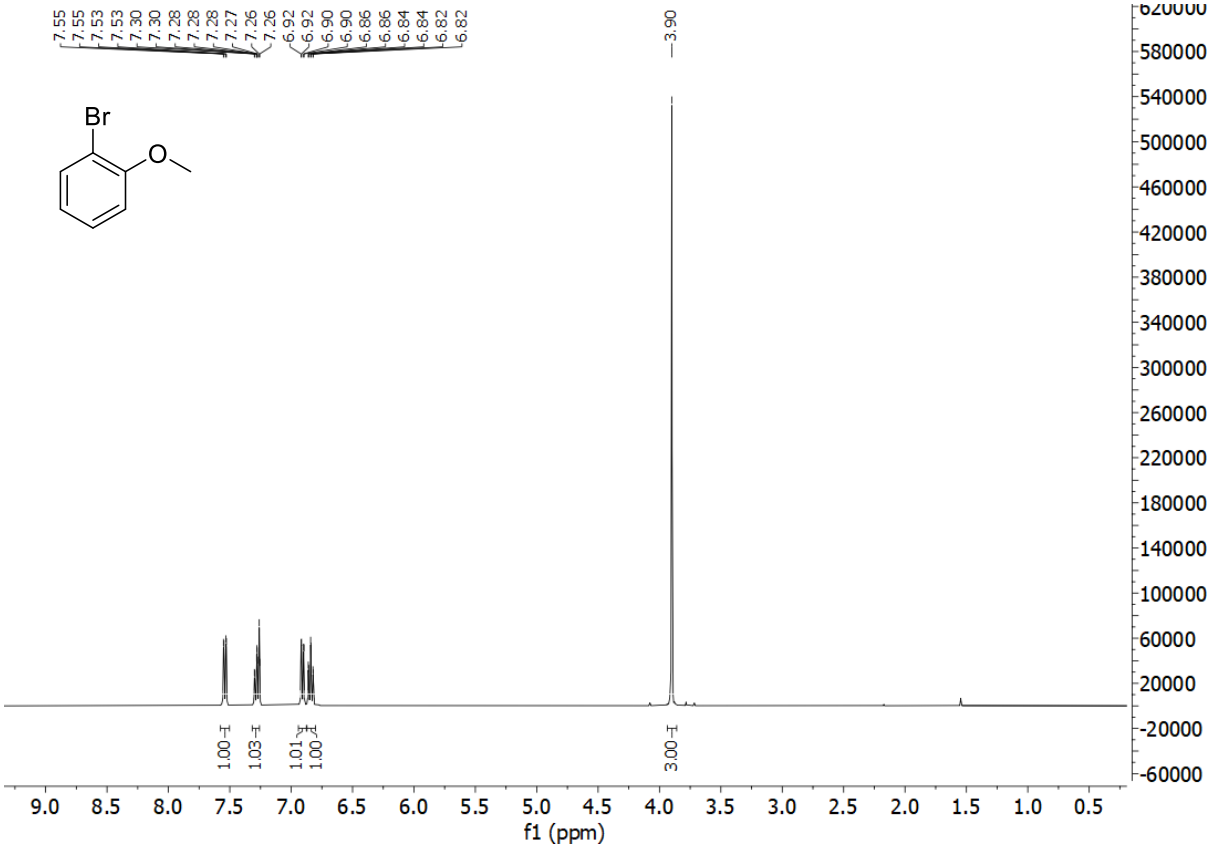

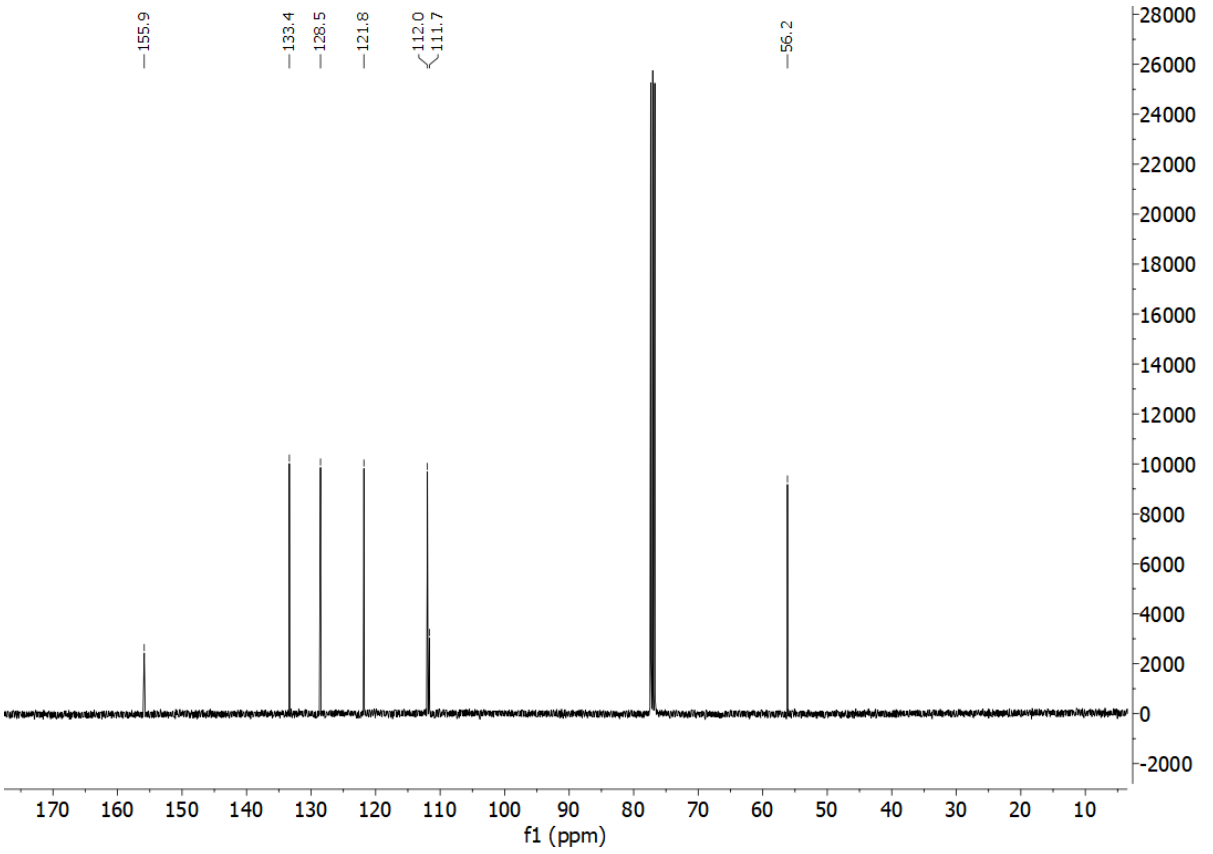

112c. *tert-butyl N-[2'-(2-methoxybenzenesulfonamido)ethyl]carbamate*

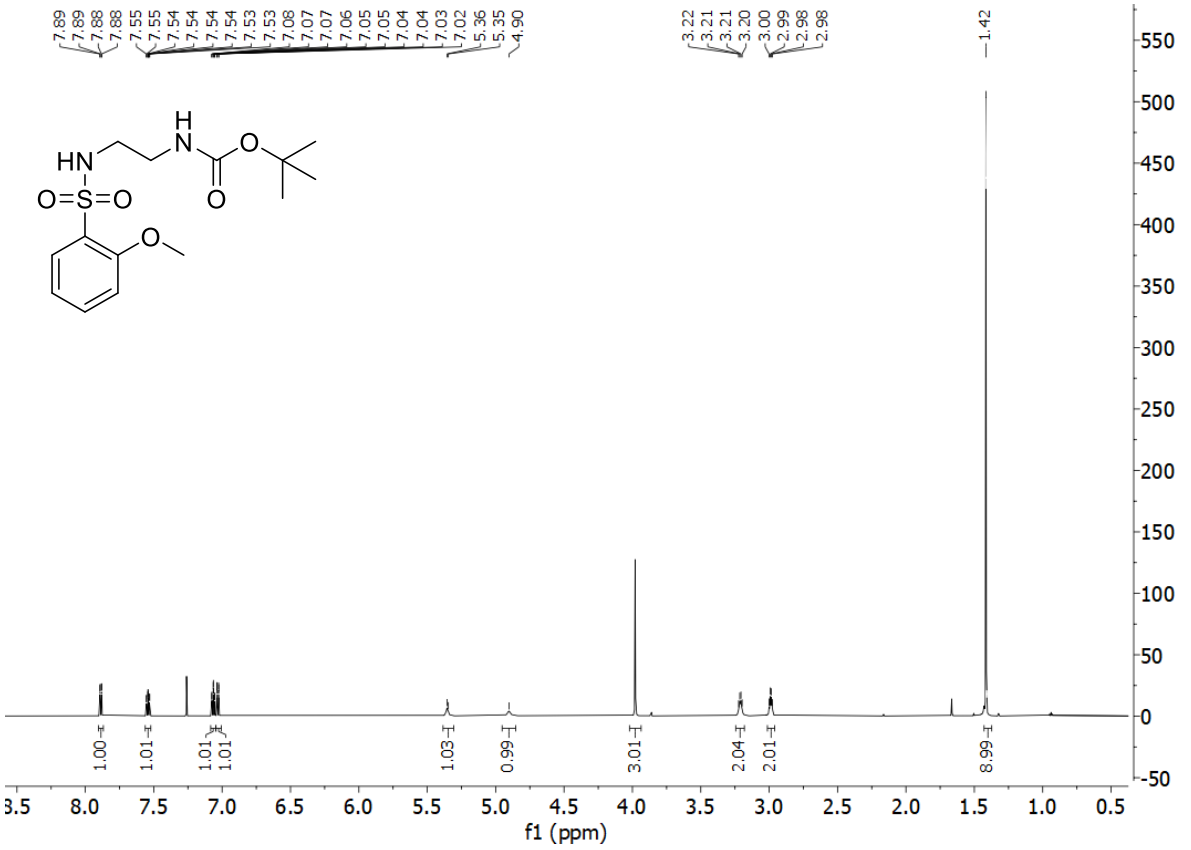

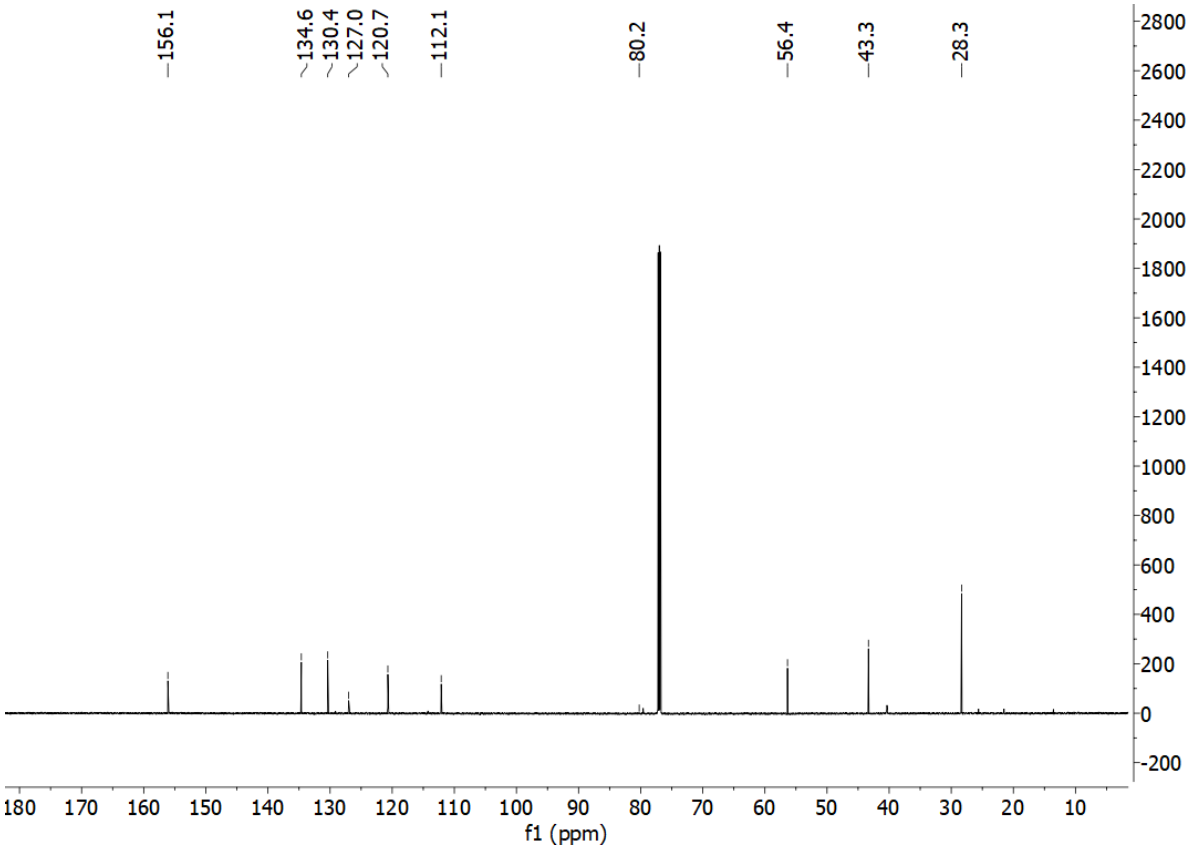

112. *N-(2'-aminoethyl)-2-methoxybenzene-1-sulfonamide hydrochloride*

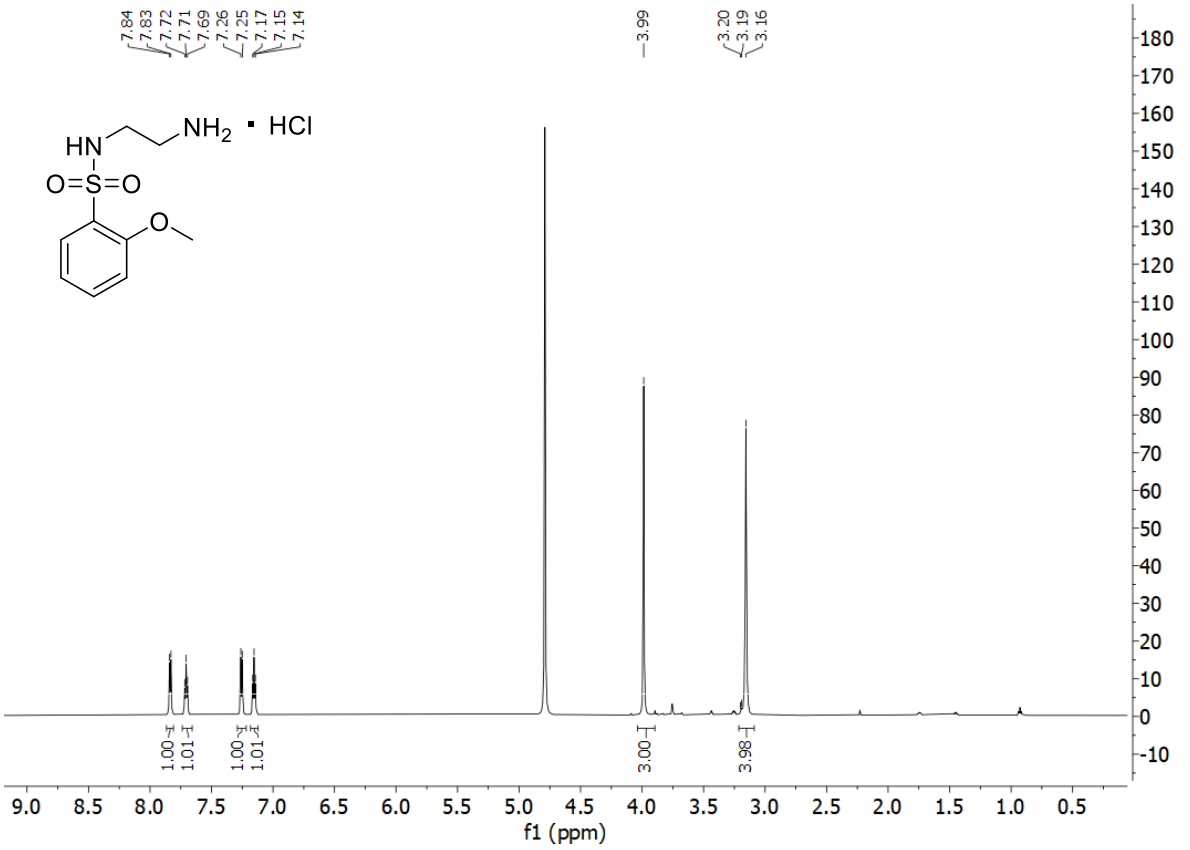

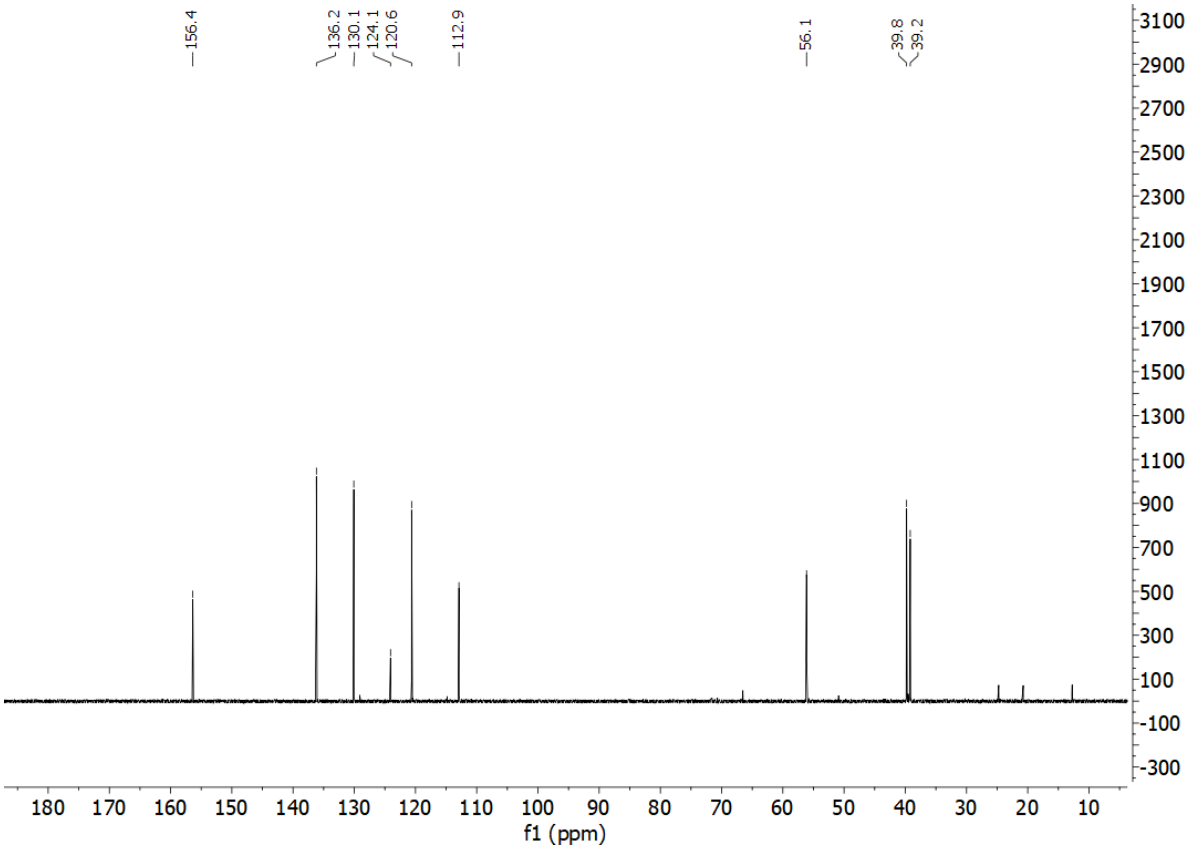

113b. *1-bromo, 2-hexoxybenxene*

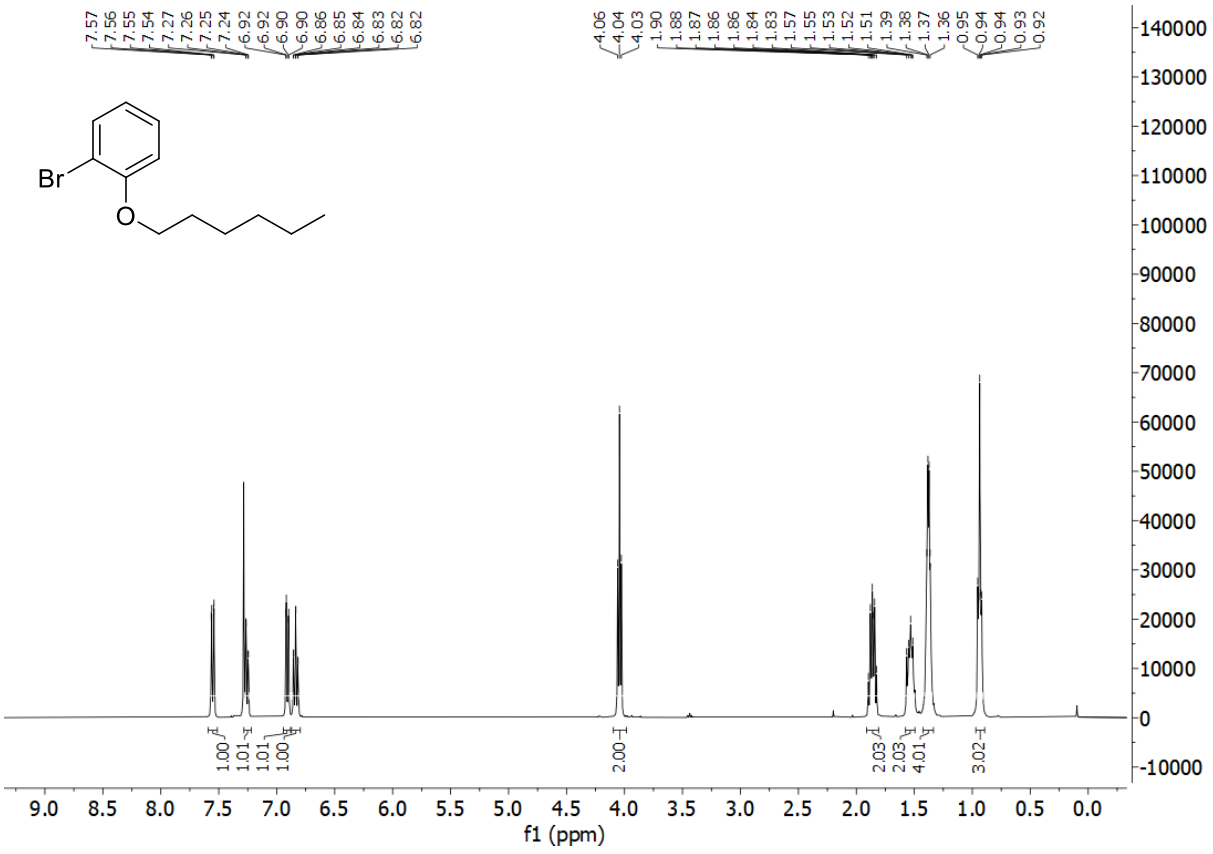

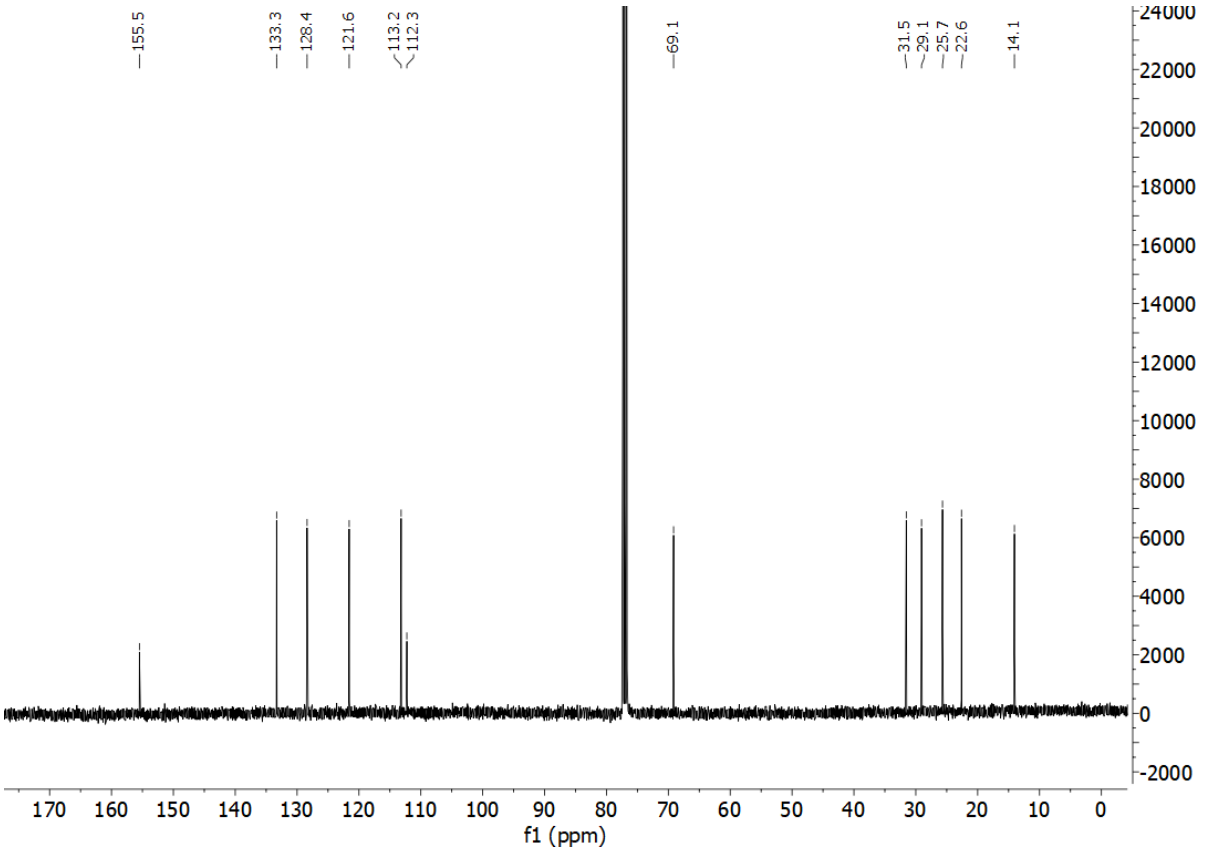

113c. *tert-butyl N-[2'-(2-hexoxybenzenesulfonamido)ethyl]carbamate*

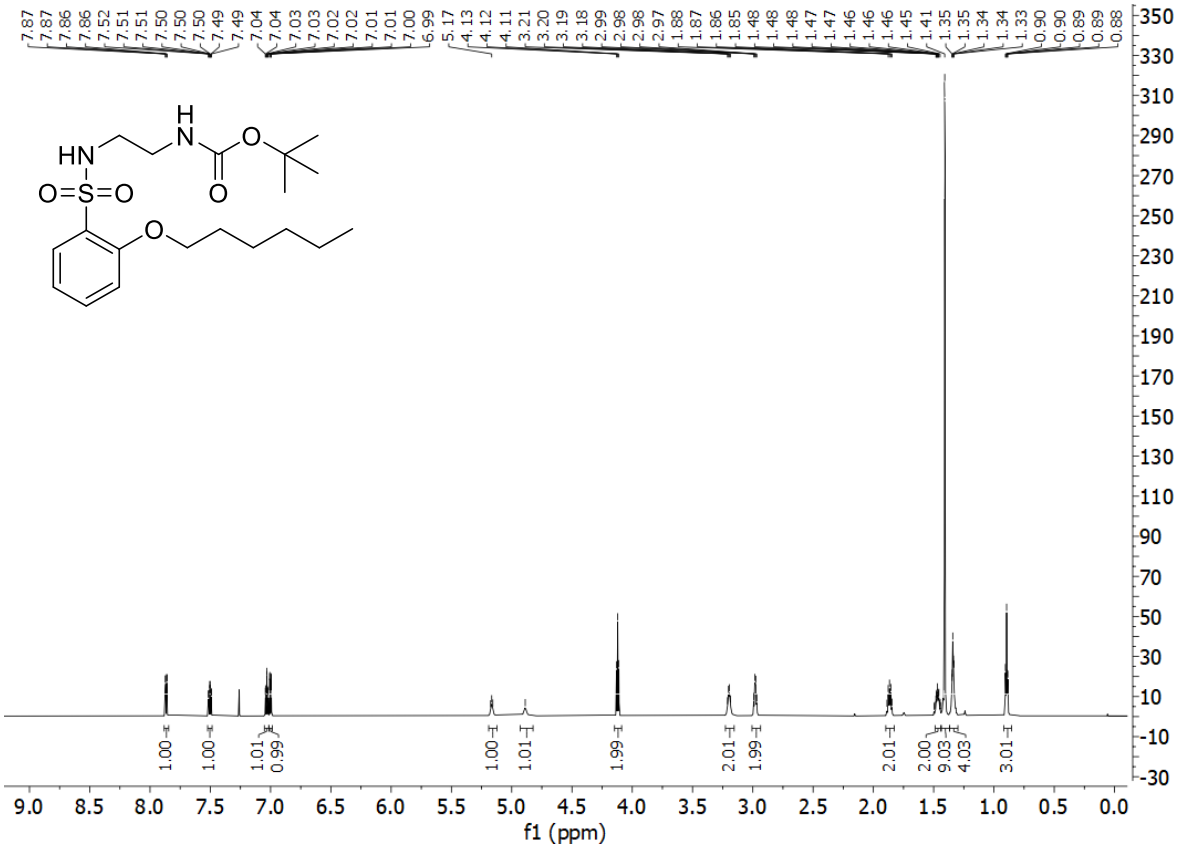

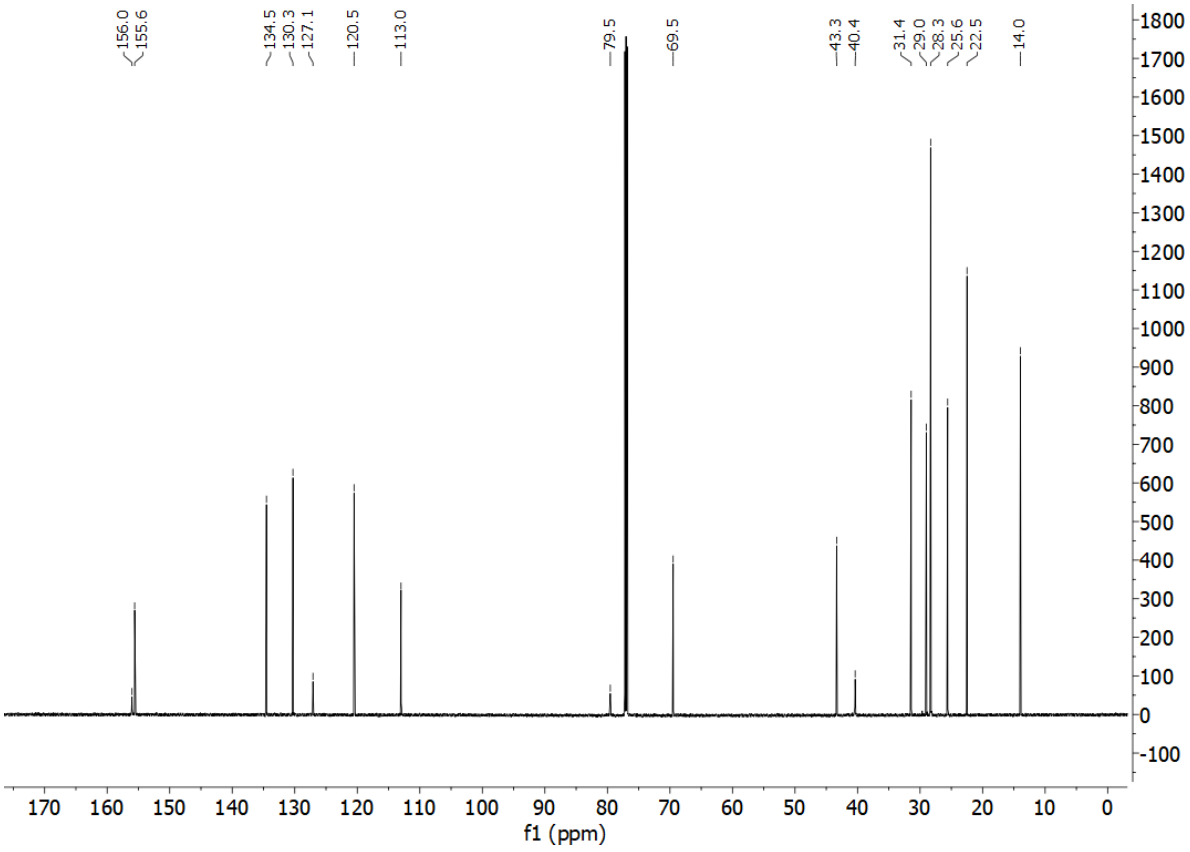

113. *N-(2'-aminoethyl)-2-(hexyloxy)benzene-1-sulfonamide hydrochloride*

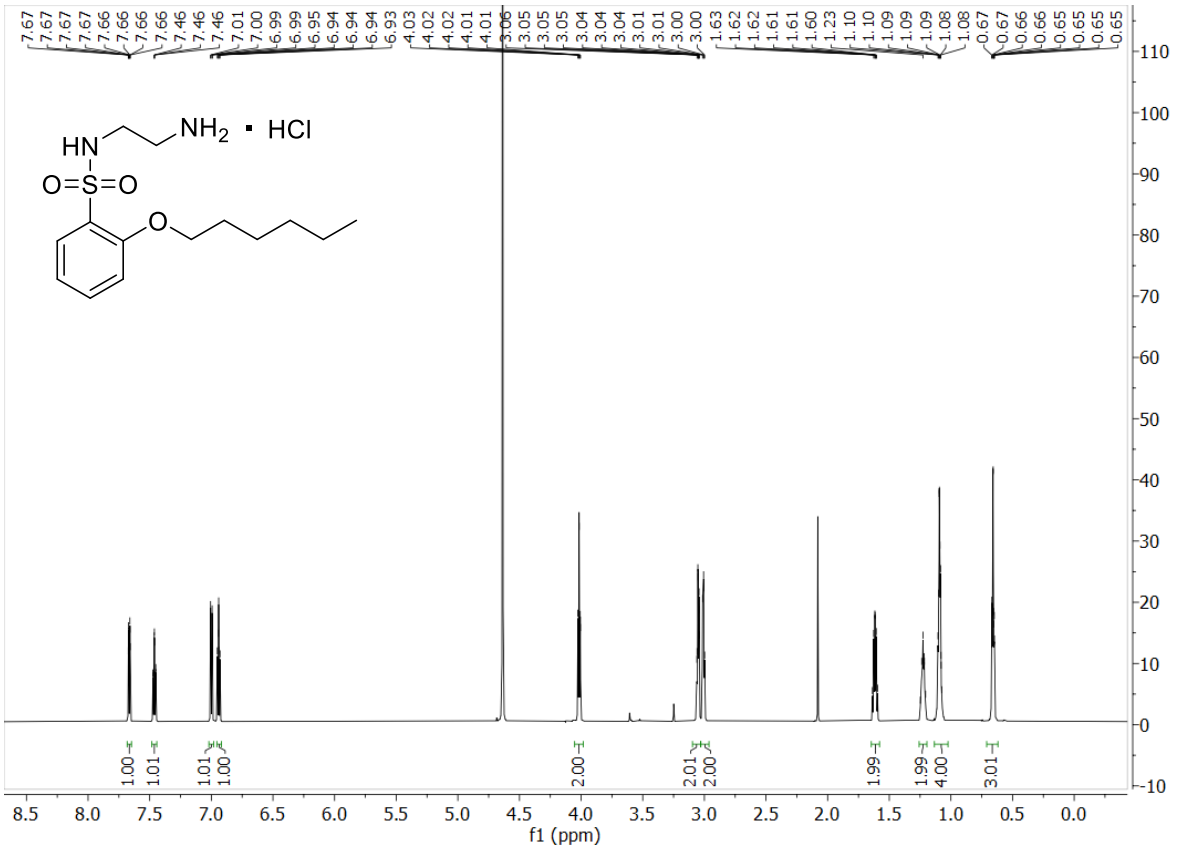

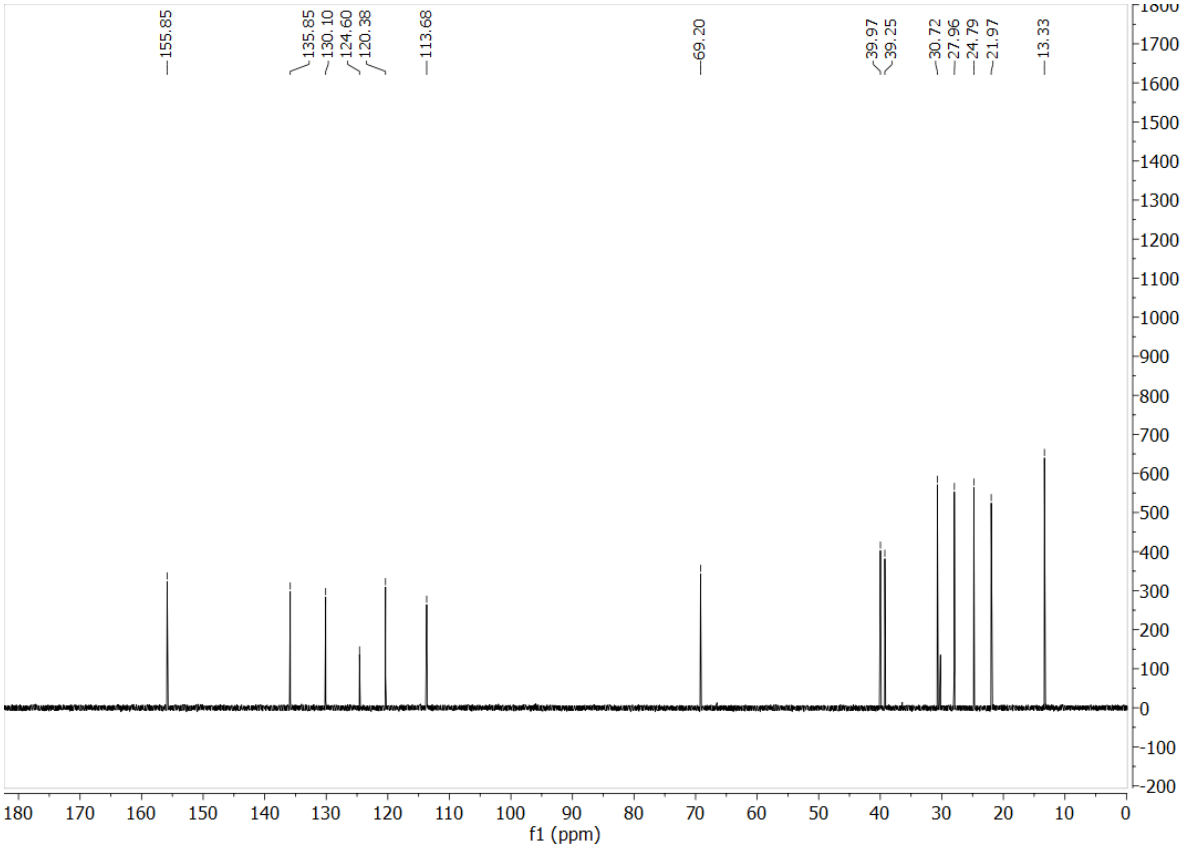

114b. *4-bromoanisole*

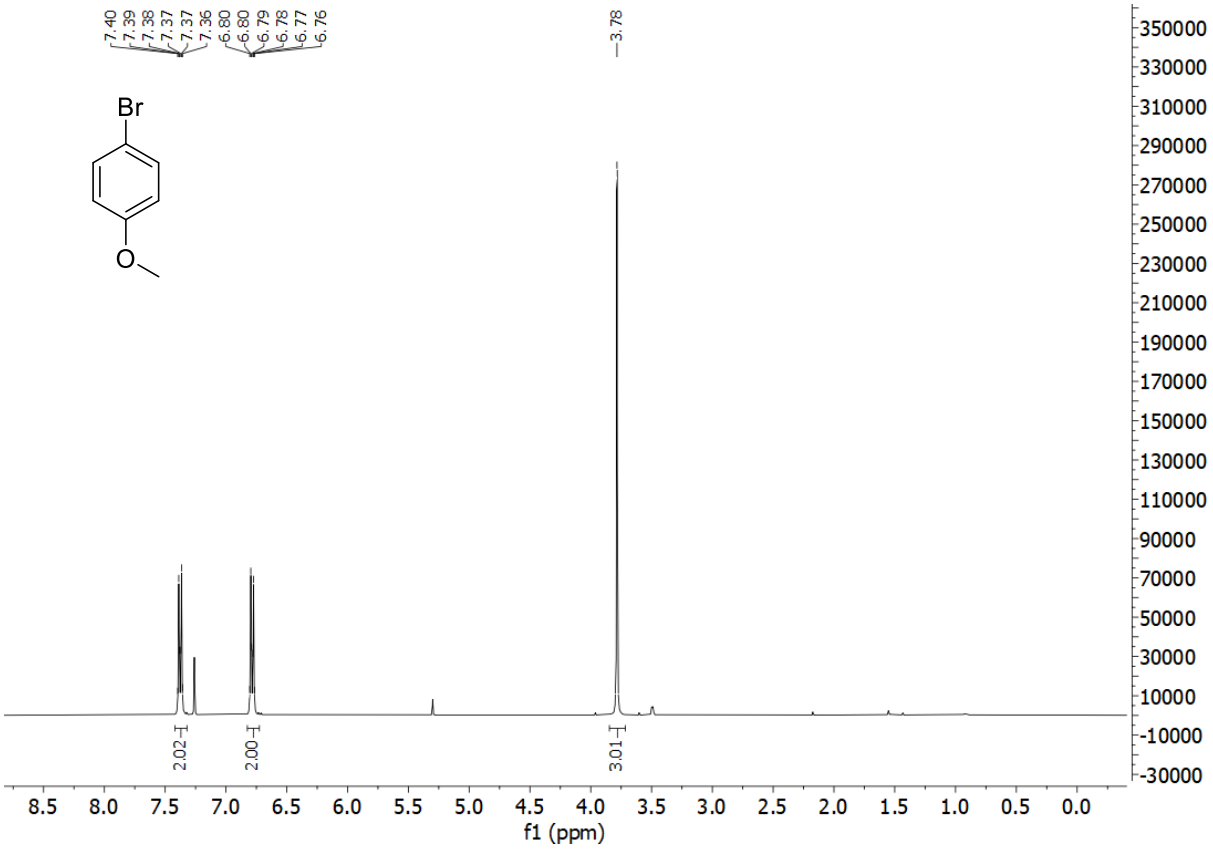

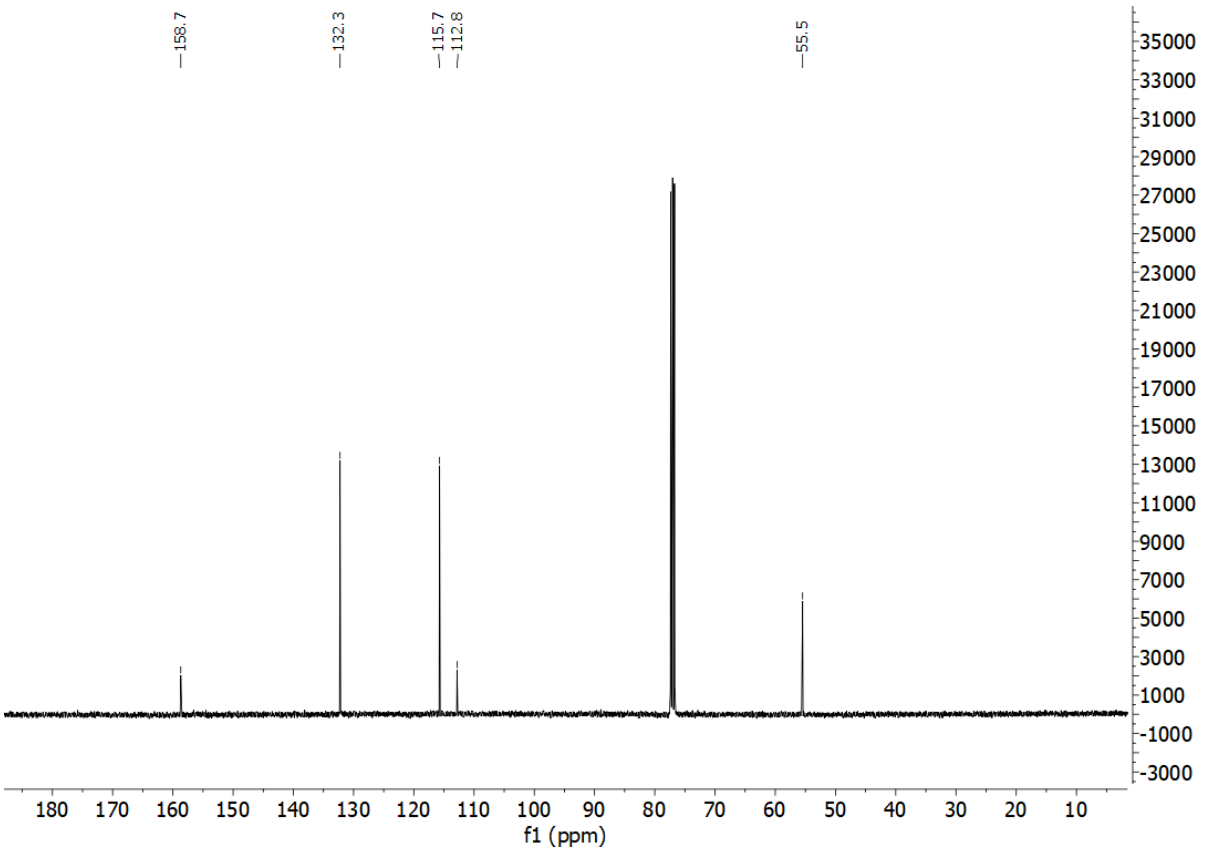

114c. *tert-butyl N-[2'-(4-methoxybenzenesulfonamido)ethyl]carbamate*

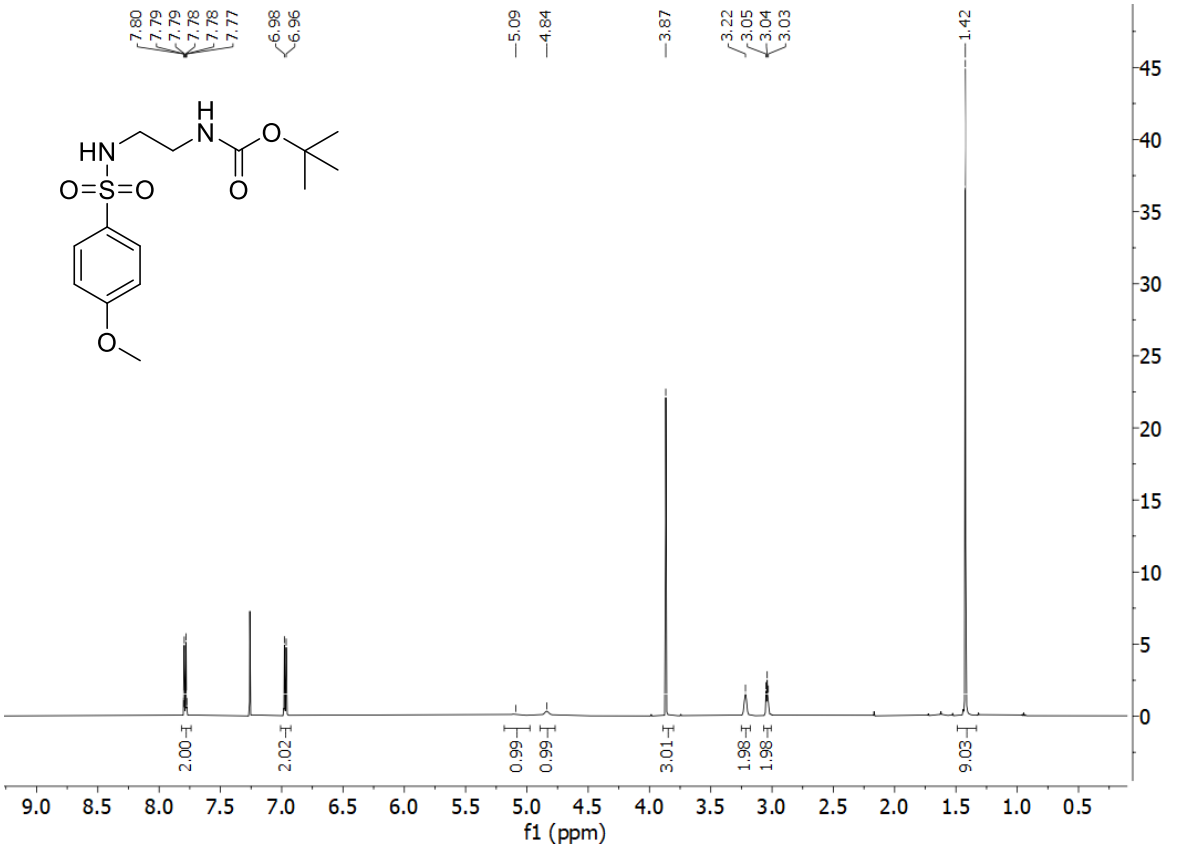

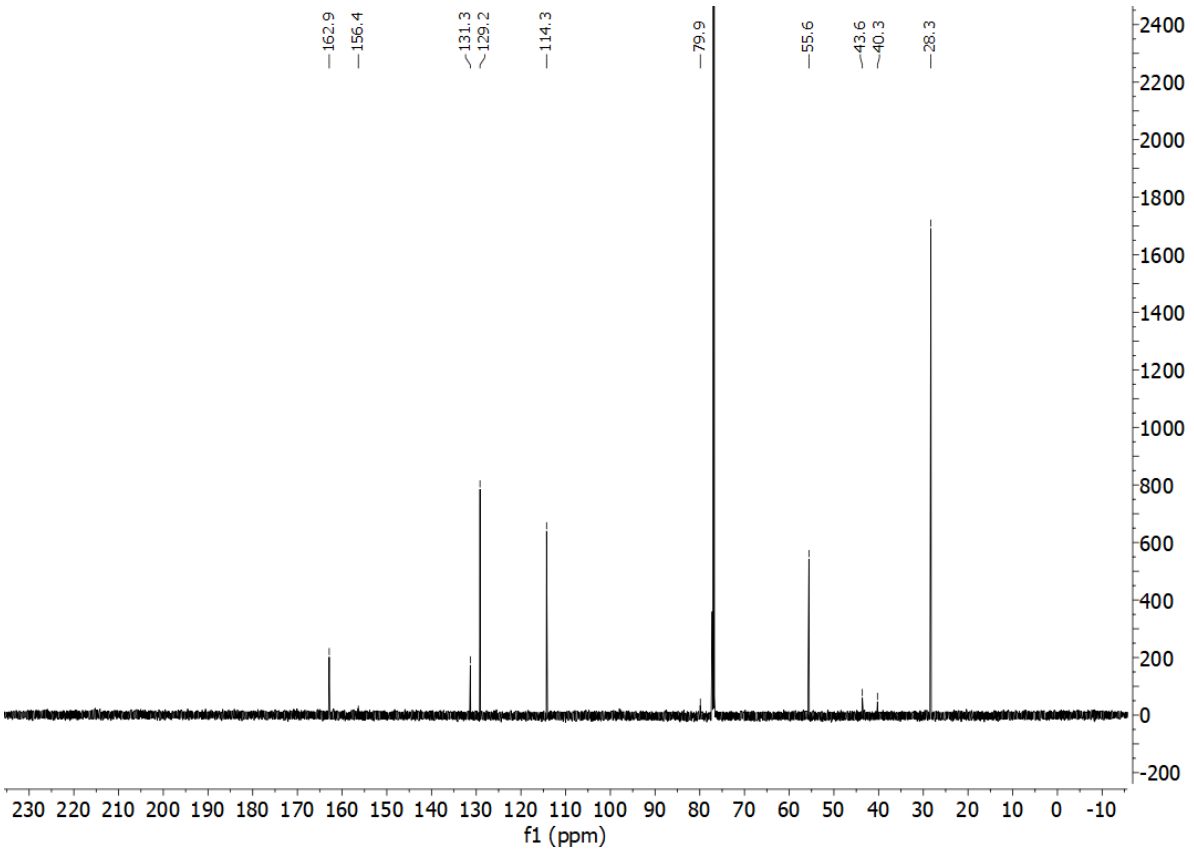

114. *N-(2'-aminoethyl)-4-methoxybenzene-1-sulfonamide hydrochloride*

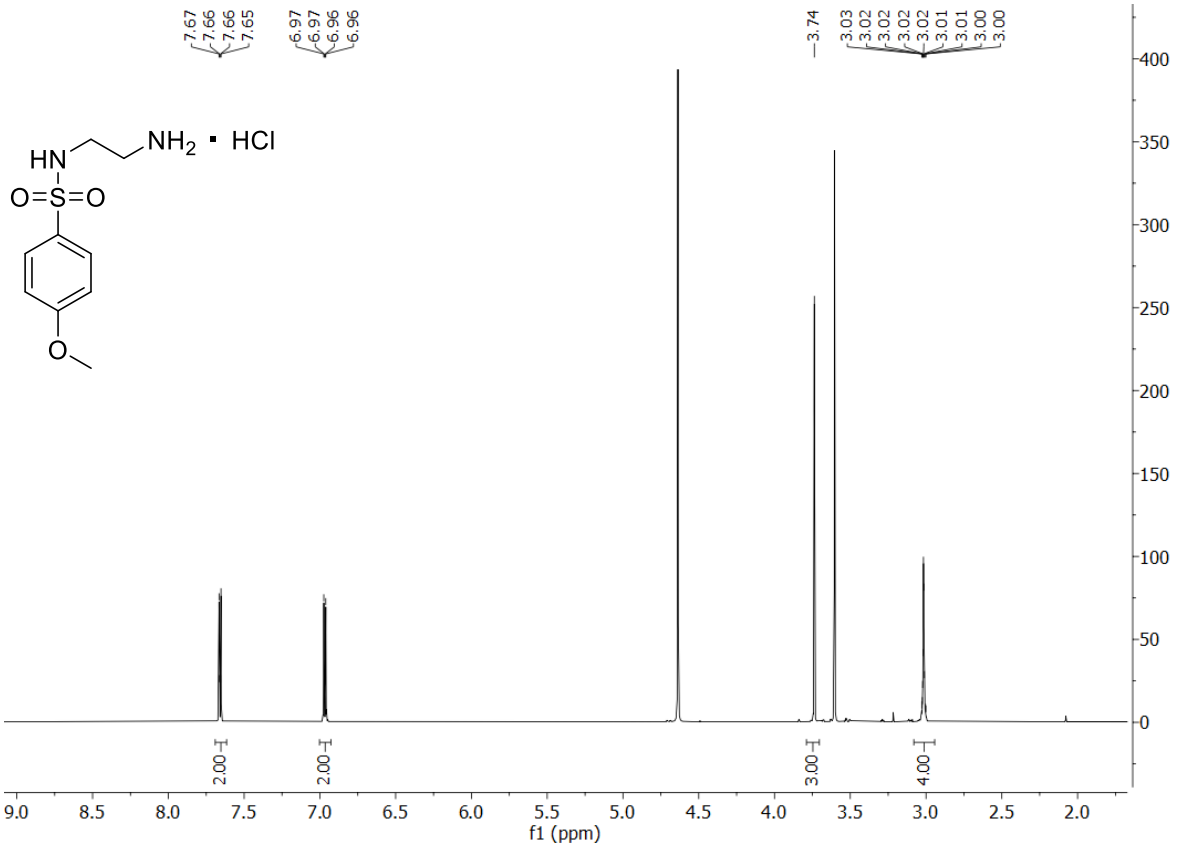

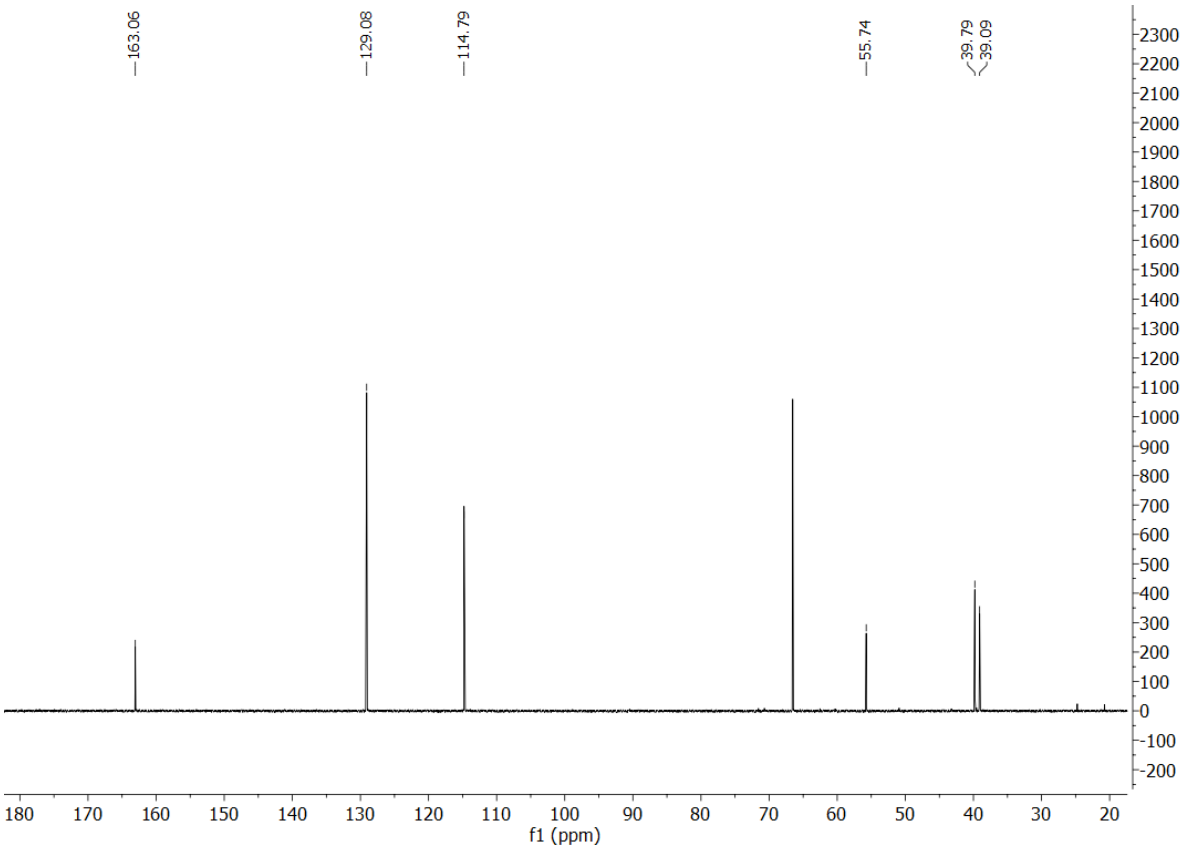

115b. *1-bromo, 4-hexoxybenzene*

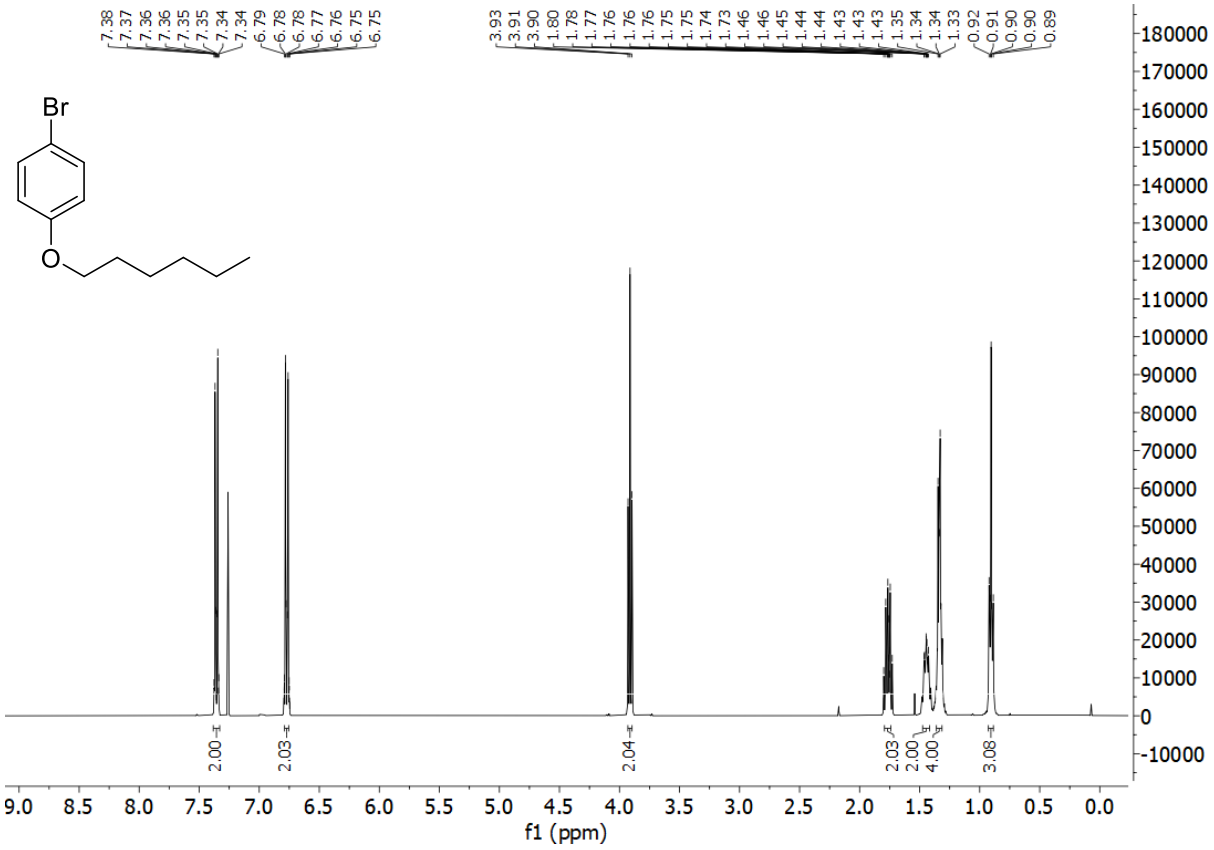

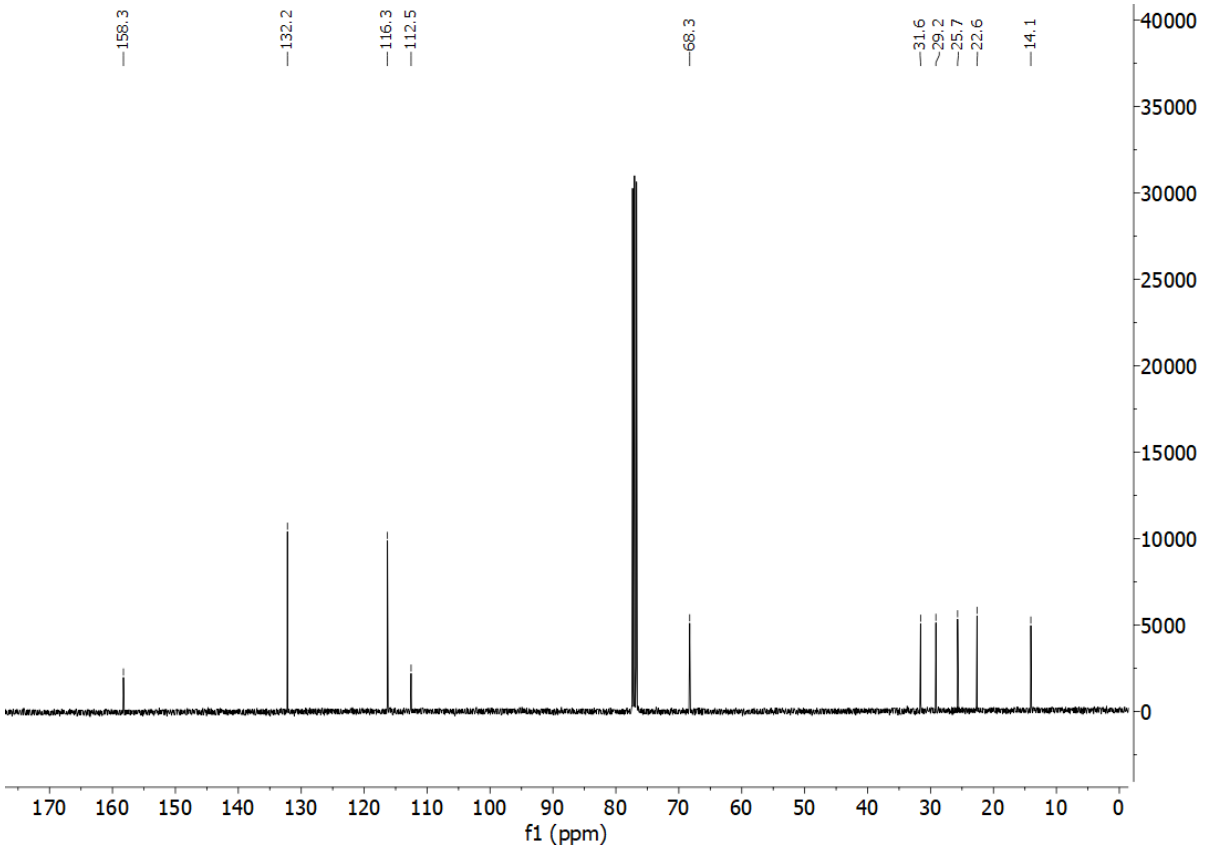

115c. *tert-butyl N-[2'-(4-hexoxybenzenesulfonamido)ethyl]carbamate*

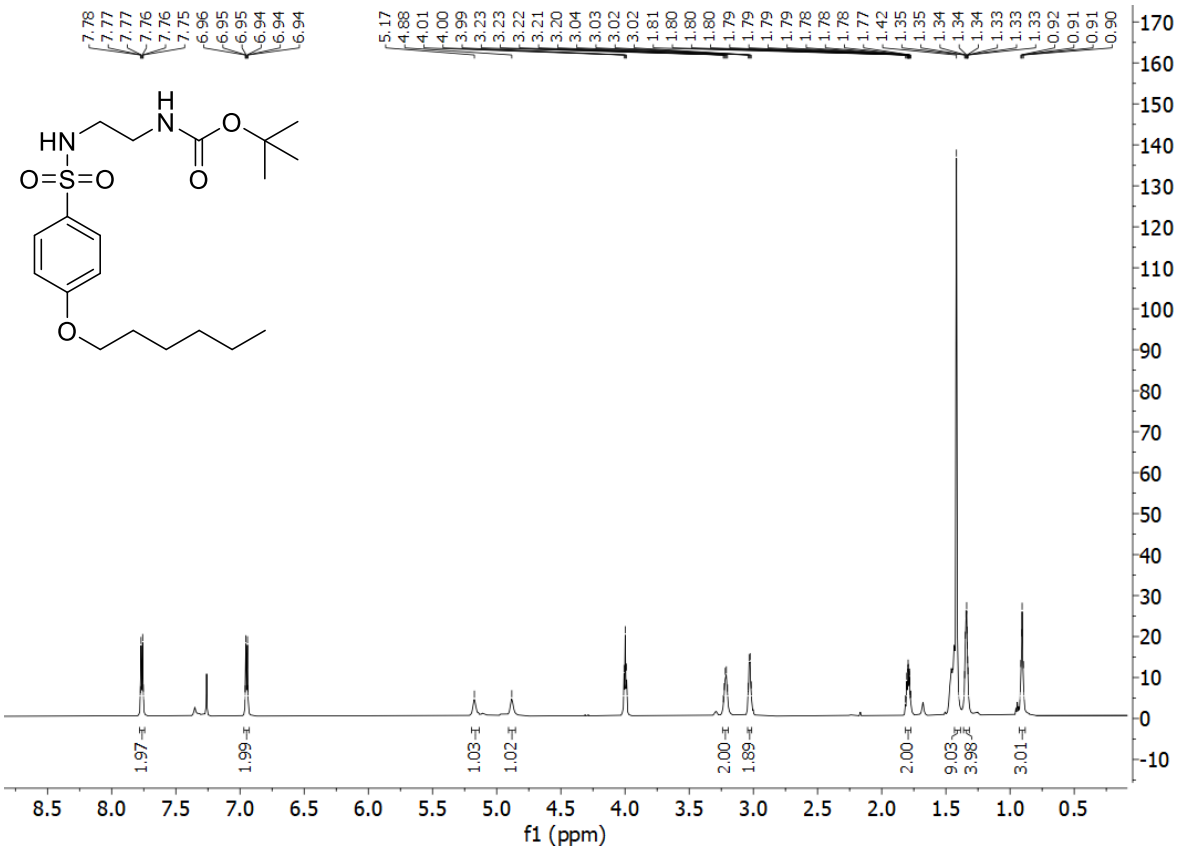

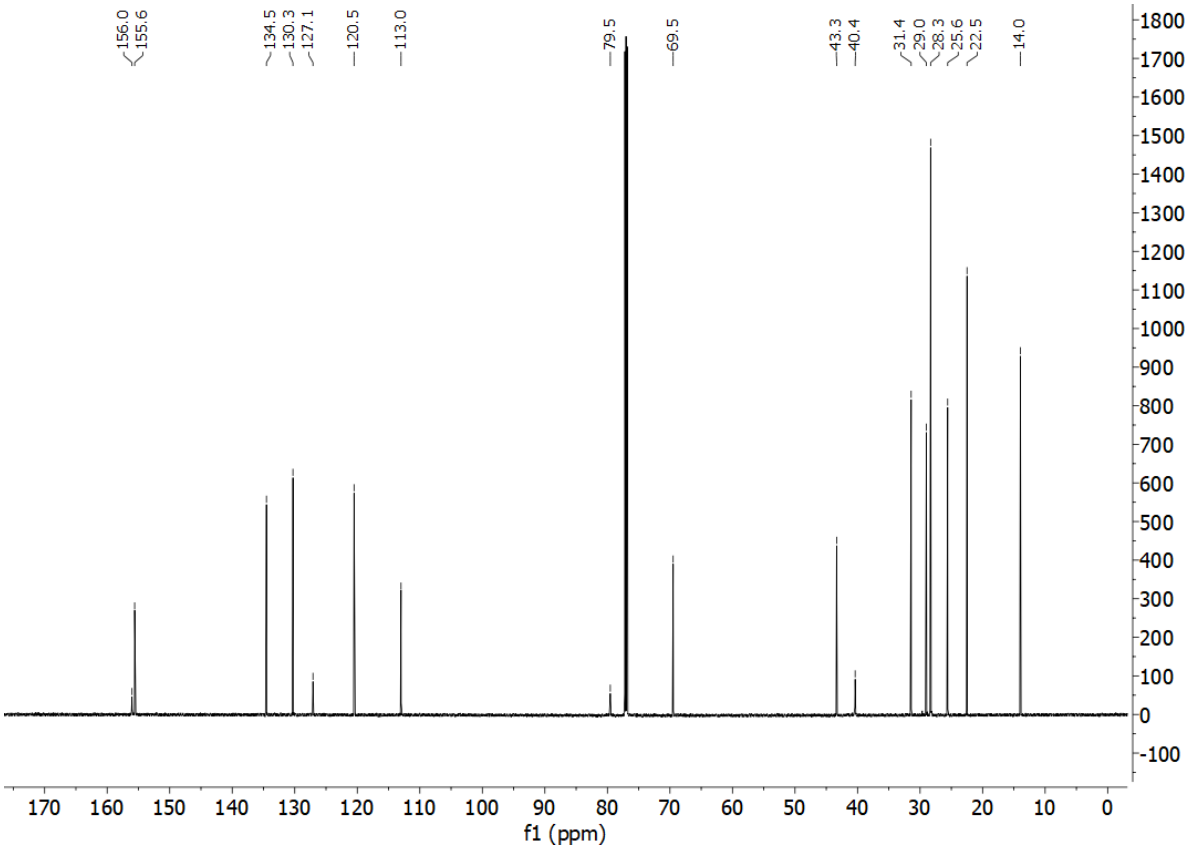

115. *N-(2'-aminoethyl)-4-(hexyloxy)benzene-1-sulfonamide hydrochloride*

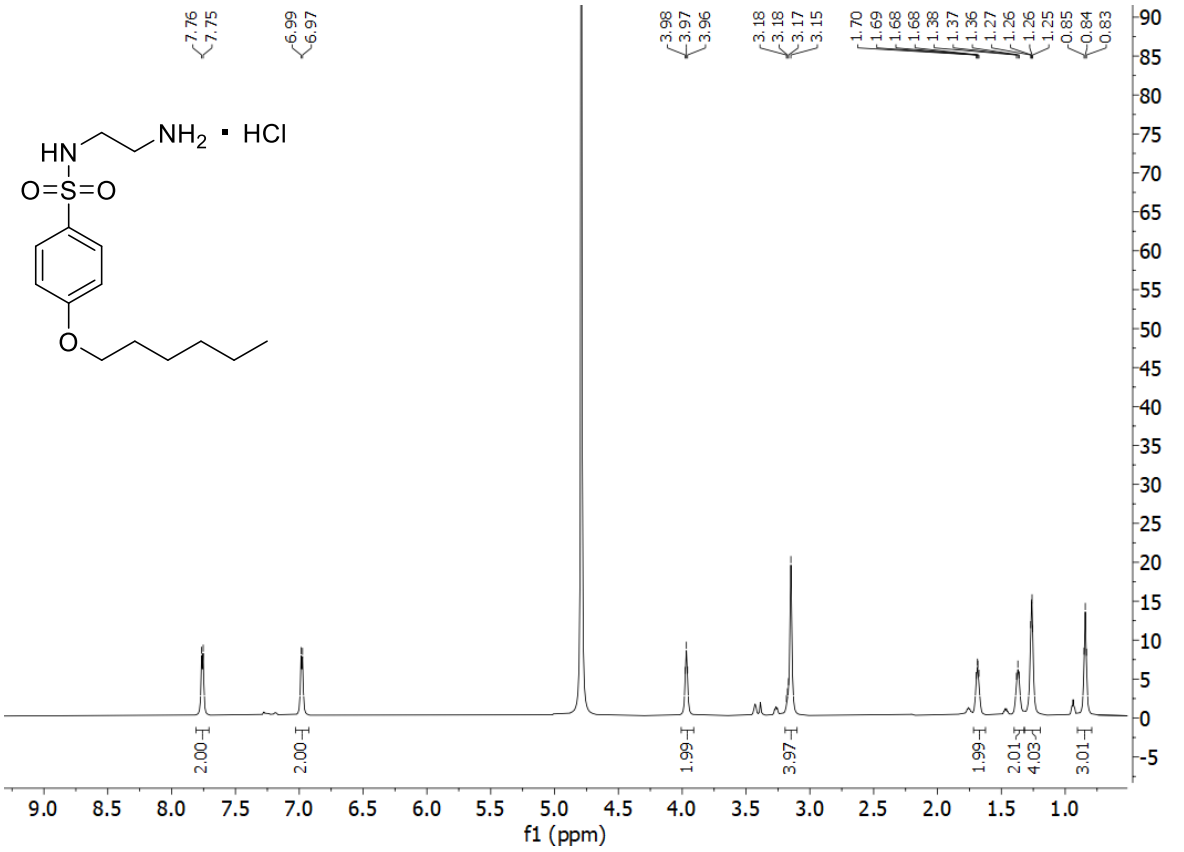

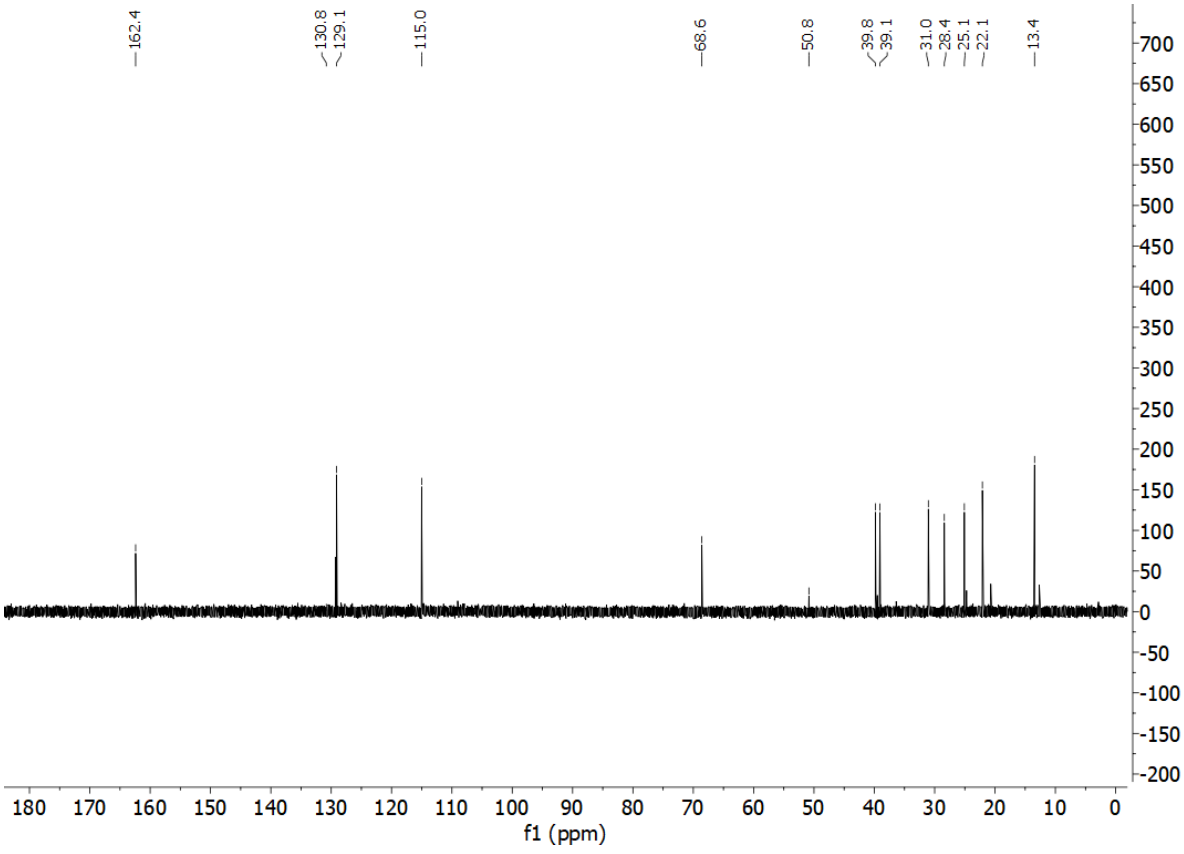

116. *N-(2'-aminoethyl)-3-methoxybenzene-1-sulfonamide hydrochloride*

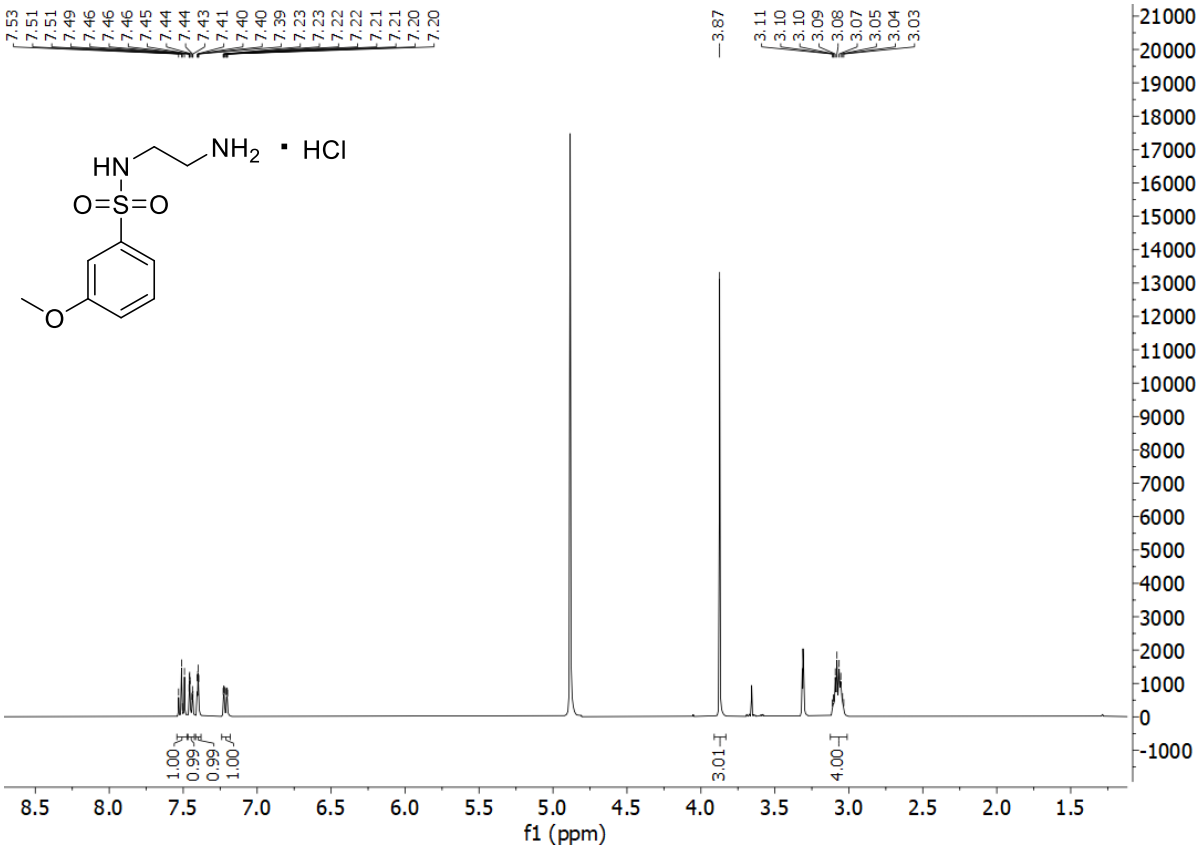

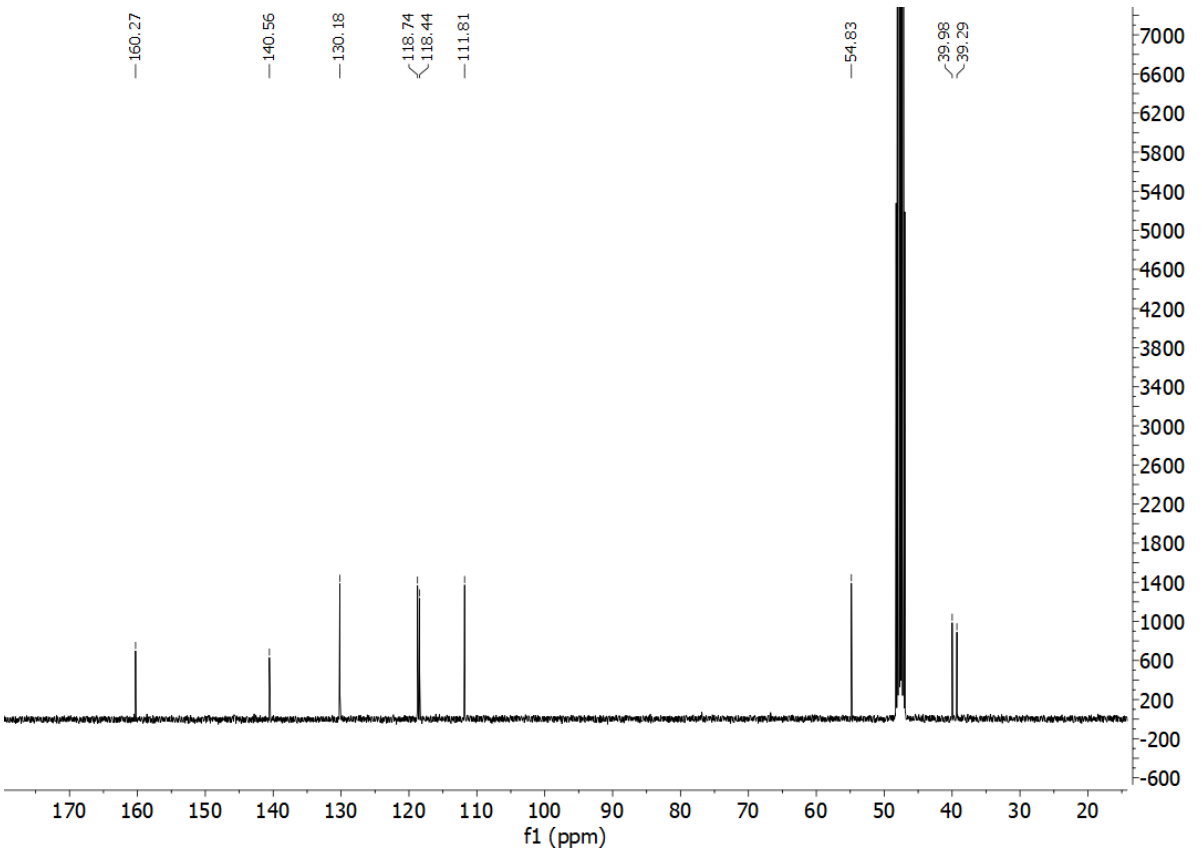

117. *2-ethoxyethyl methanesulfonate*

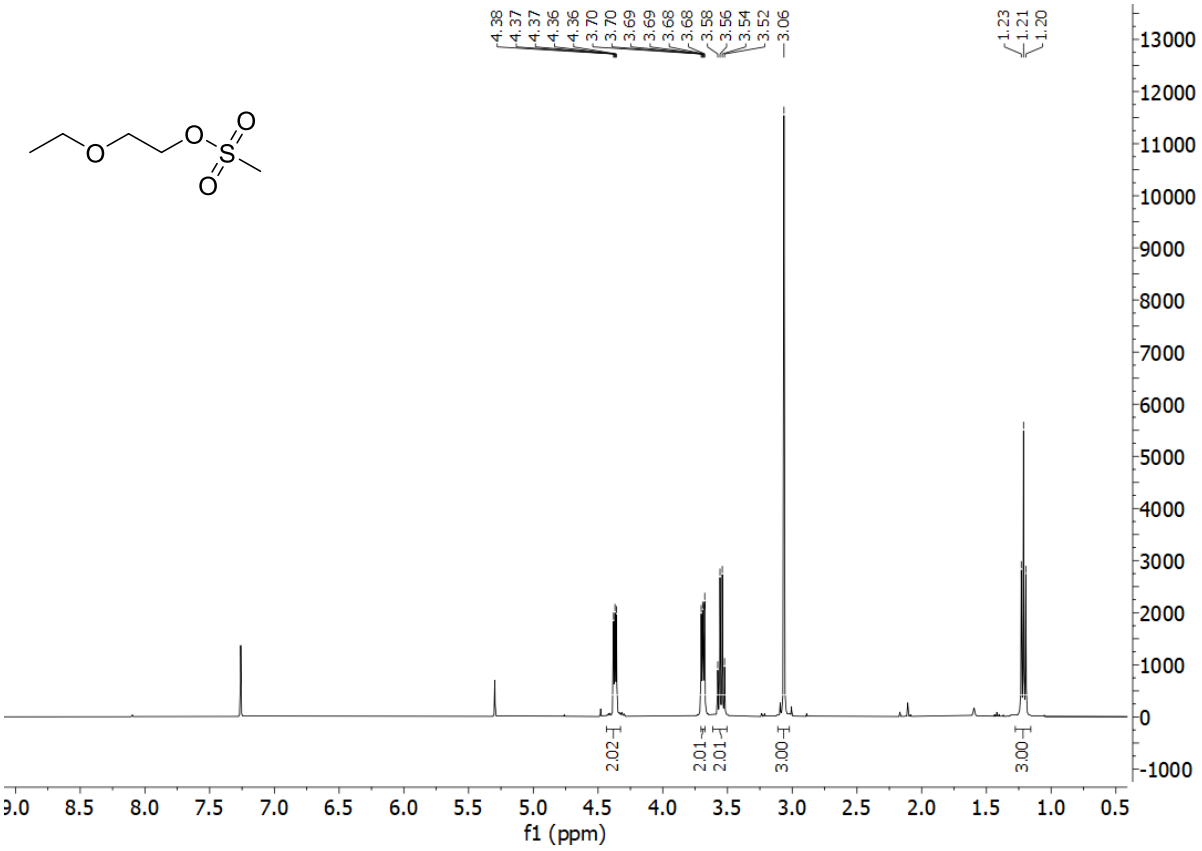

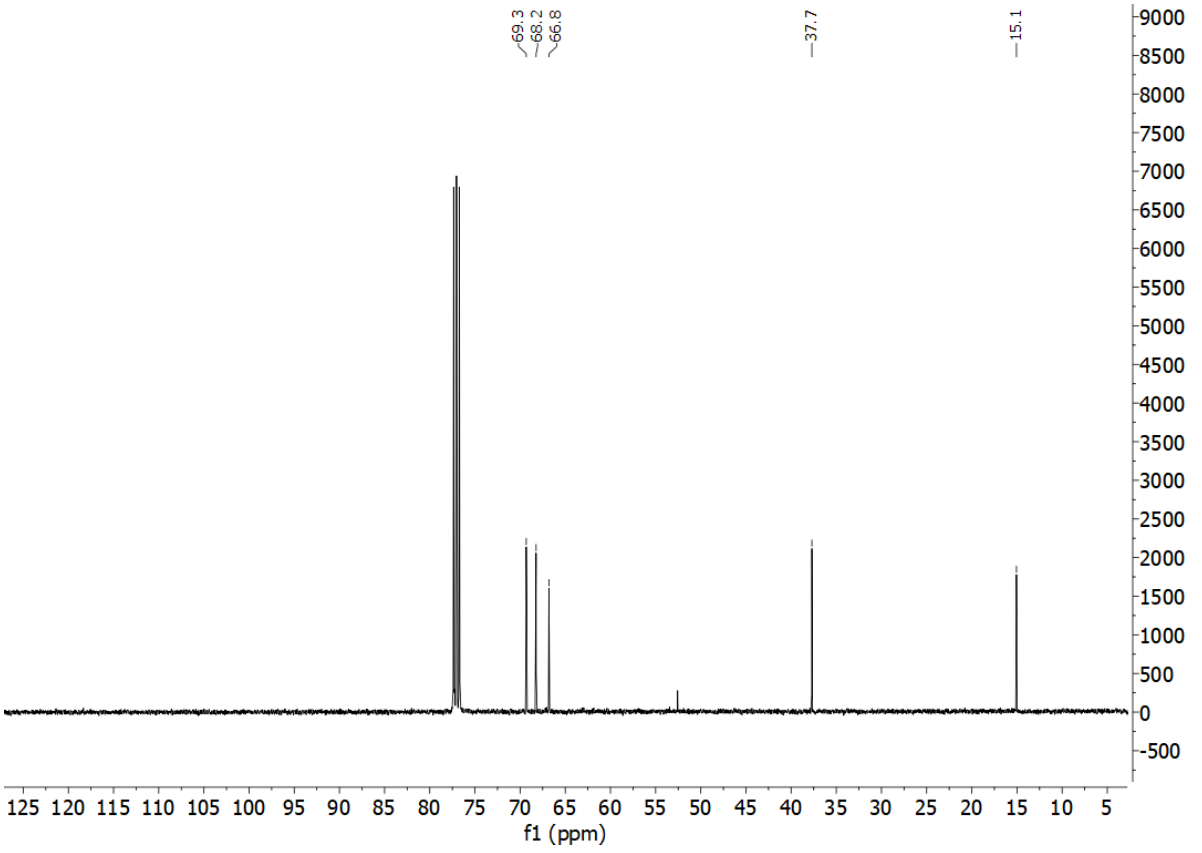

118. *1-bromo-2-(2'-ethoxyethoxy)naphthalene*

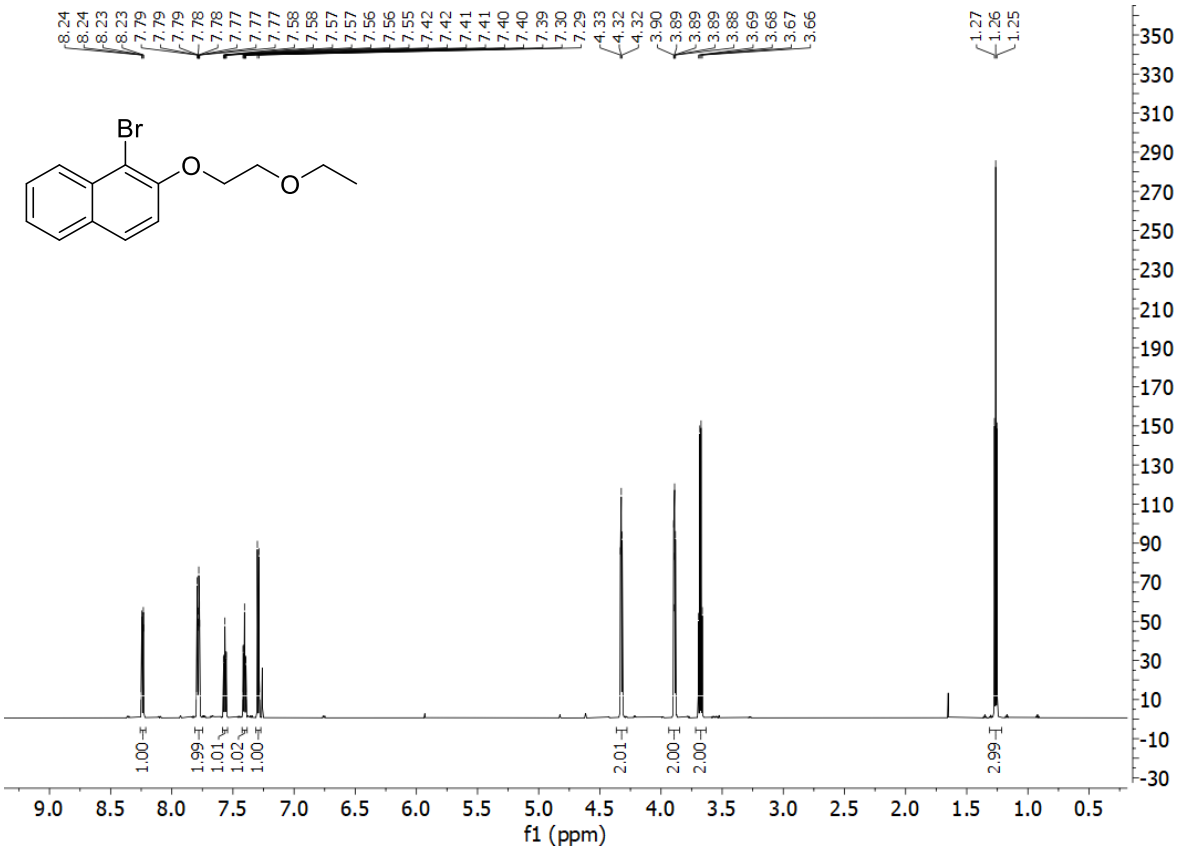

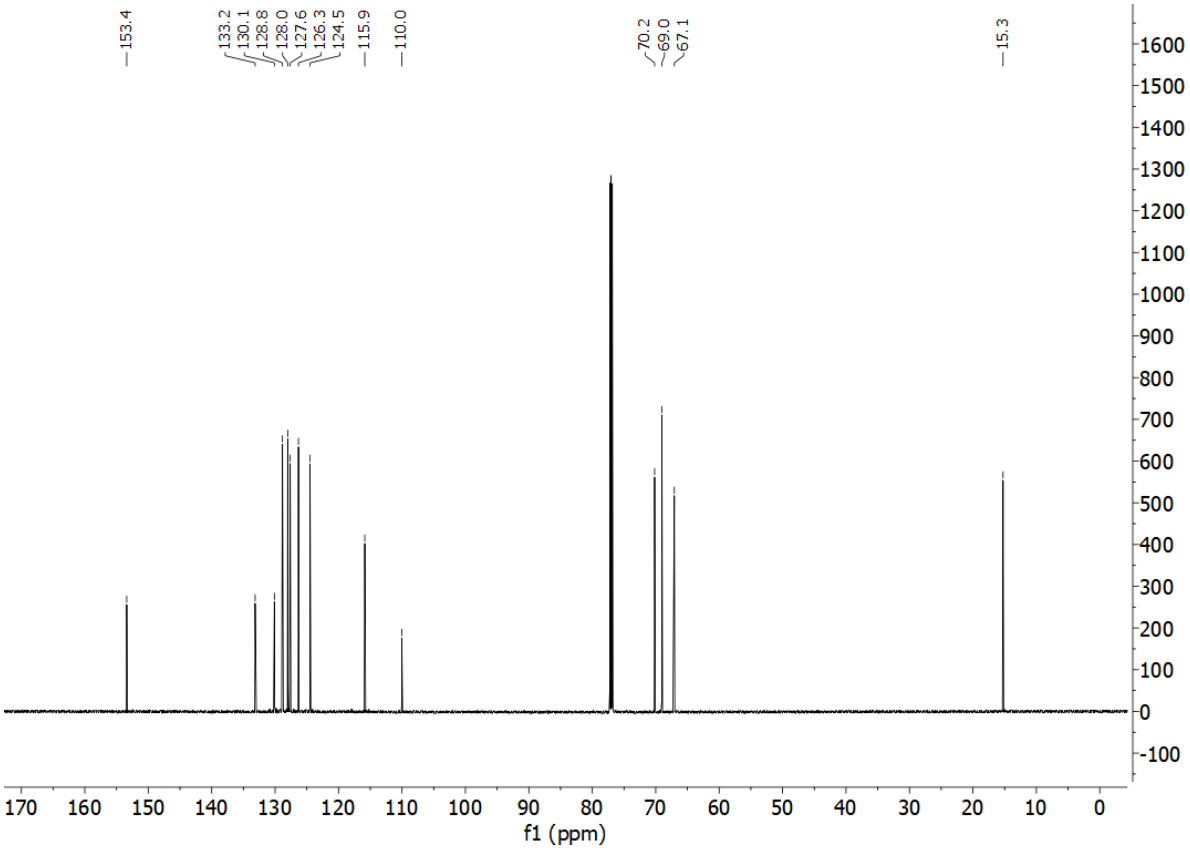

119a. *tert-butyl N-{2'-[2-(2''-ethoxyethoxy)naphthalene-1-sulfonamido]ethyl}carbamate*

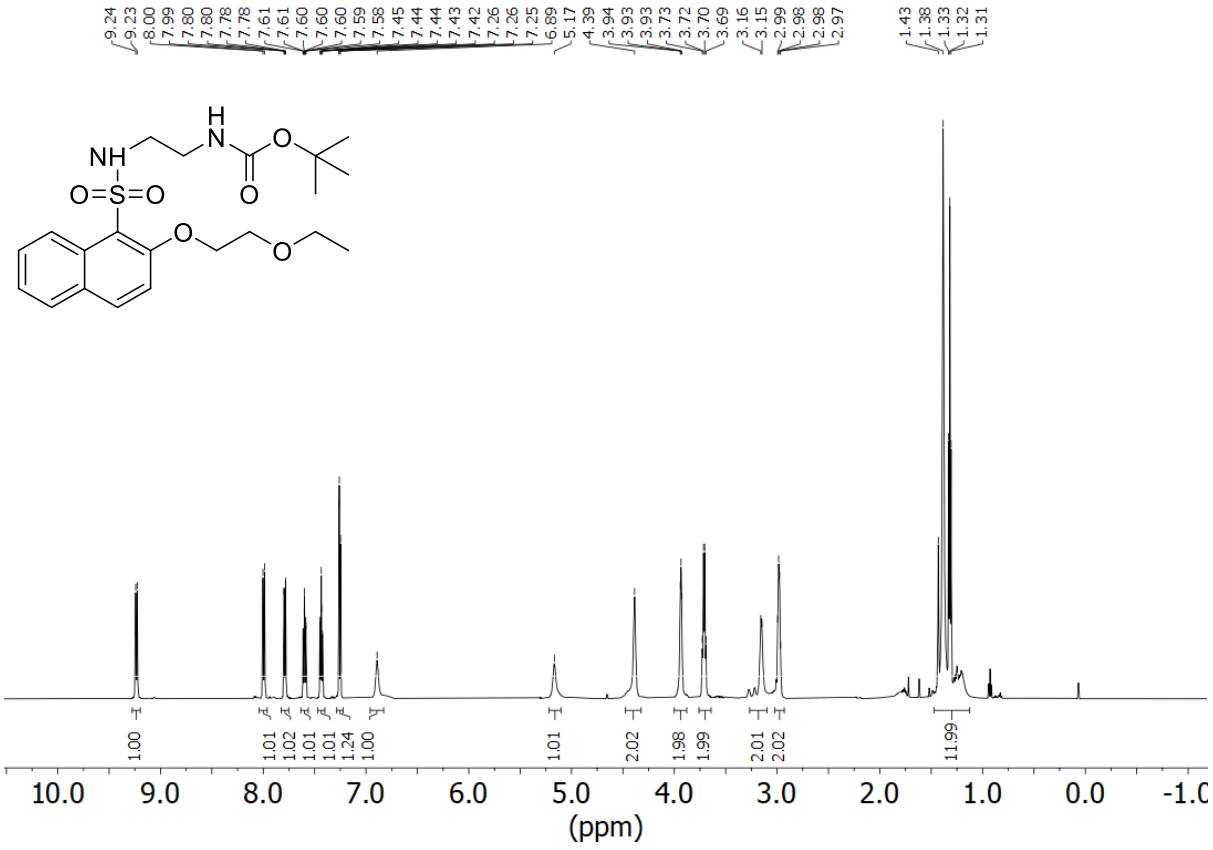

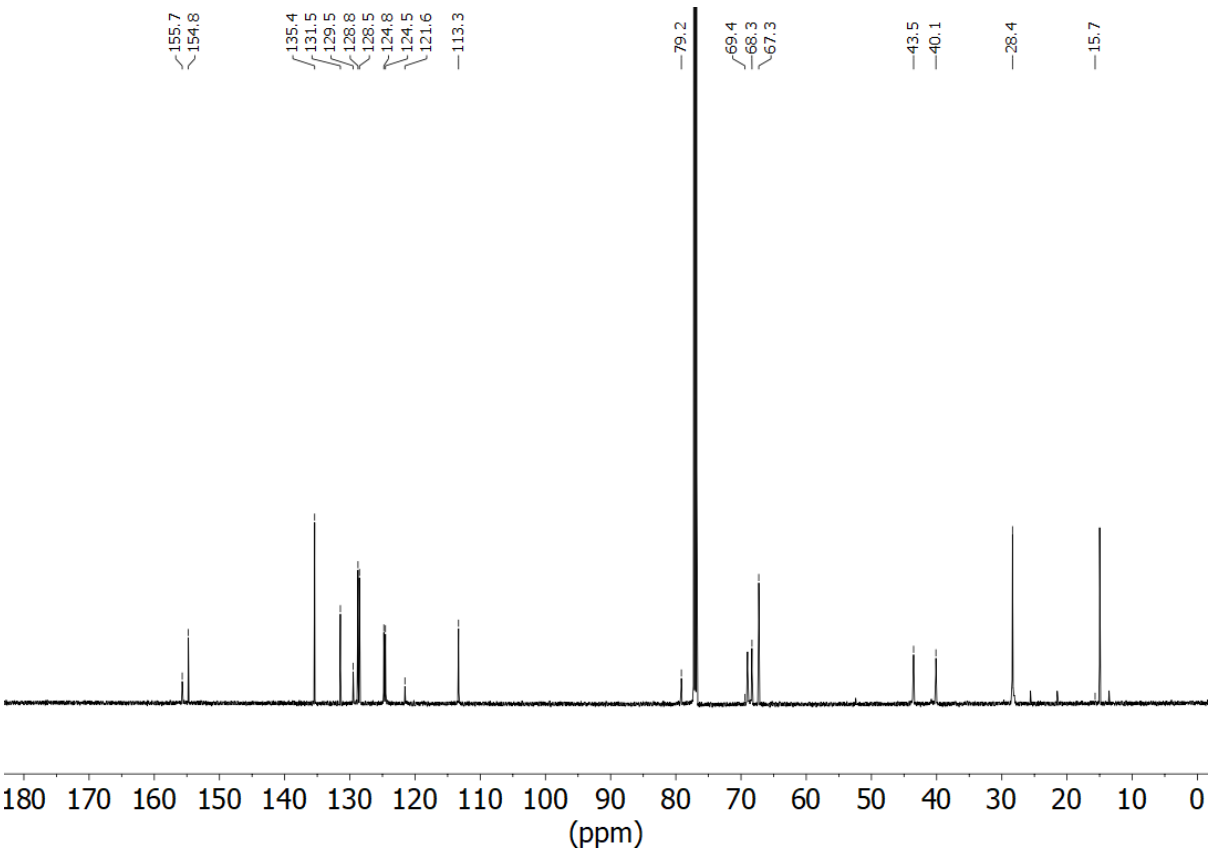

119. *N-(2'-aminolethyl)-2-(2''-ethoxyethoxy)naphthalene-1-sulfonamide hydrogenchloride*

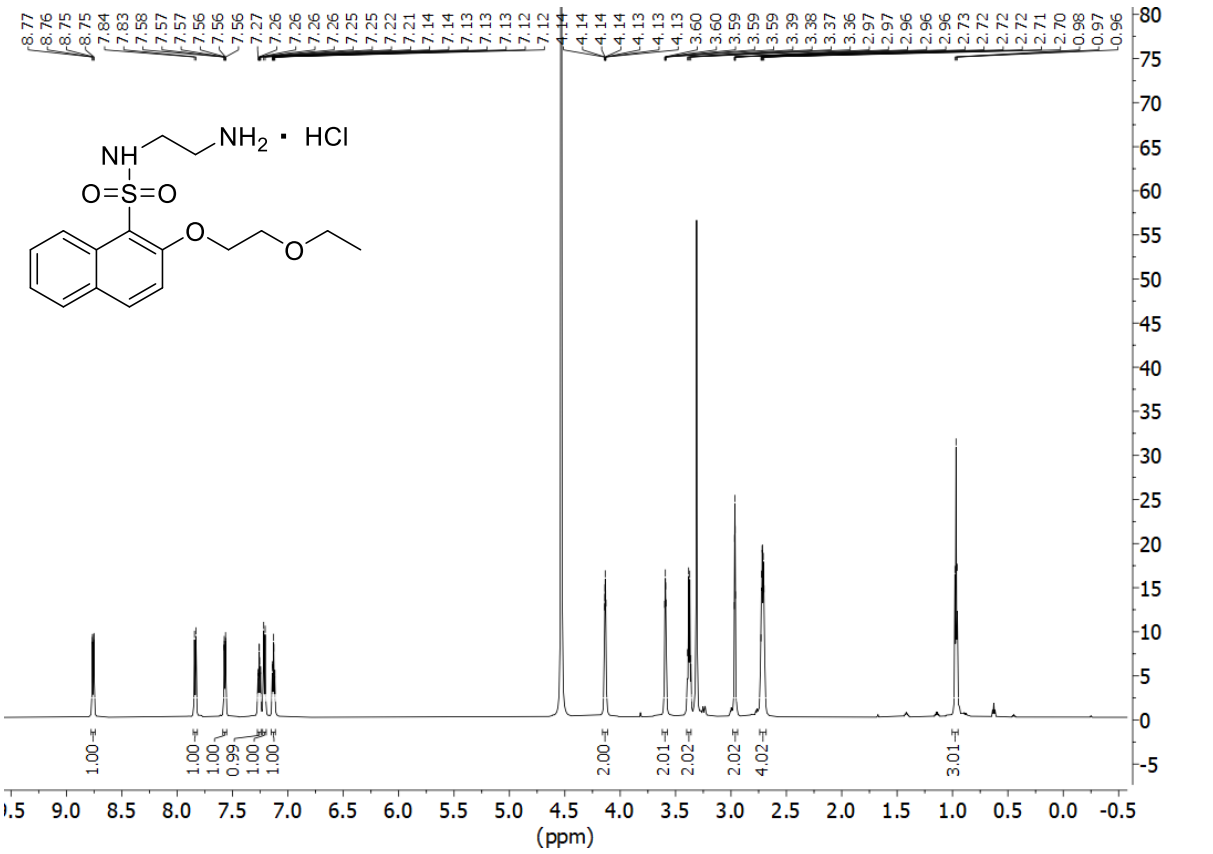

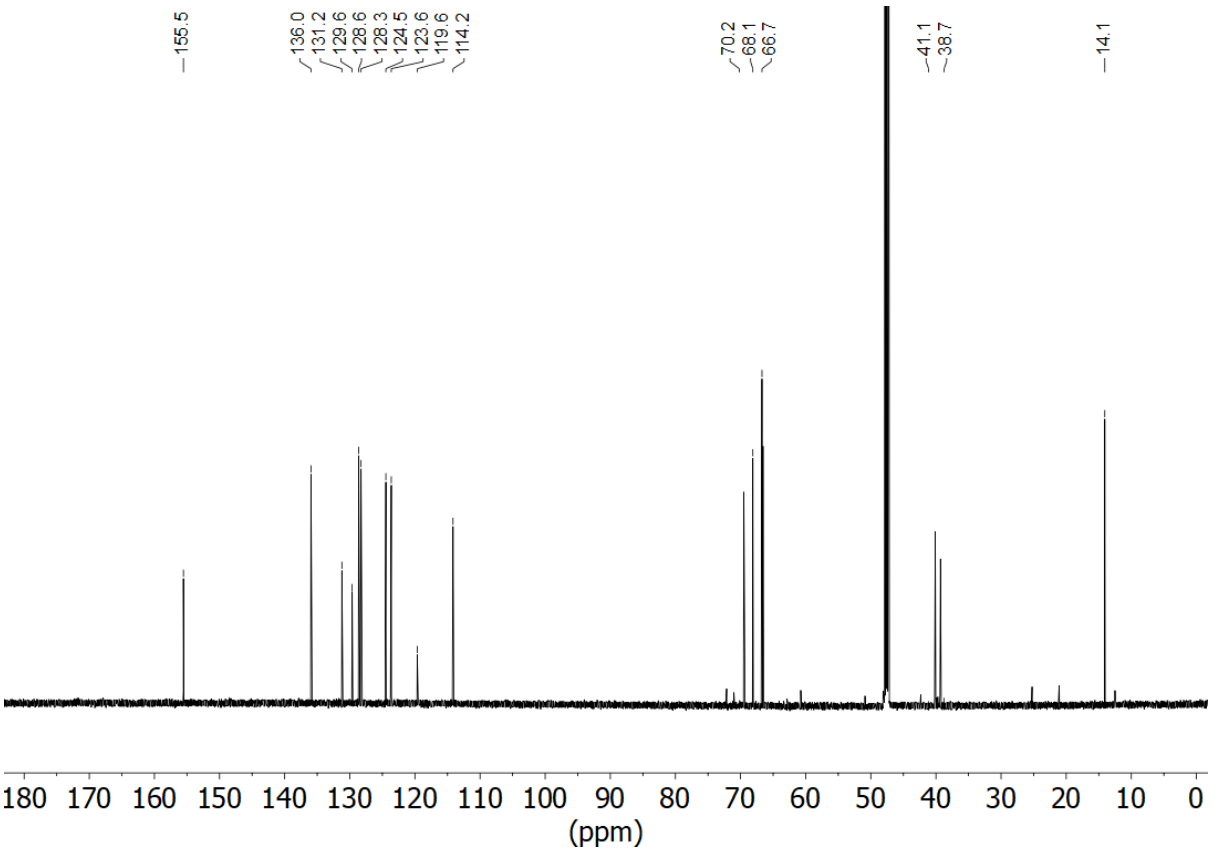

120. *1-bromo-4-(2'-ethoxyethoxy)naphthalene*

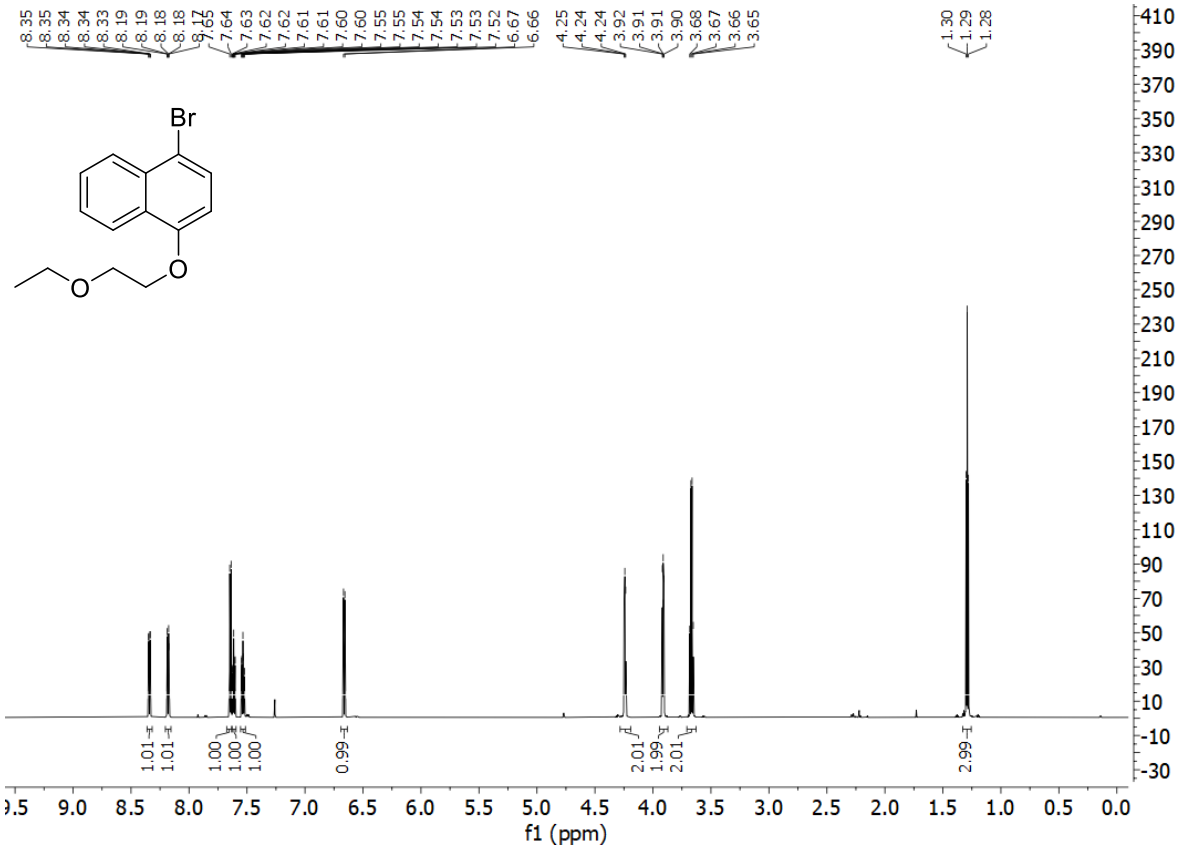

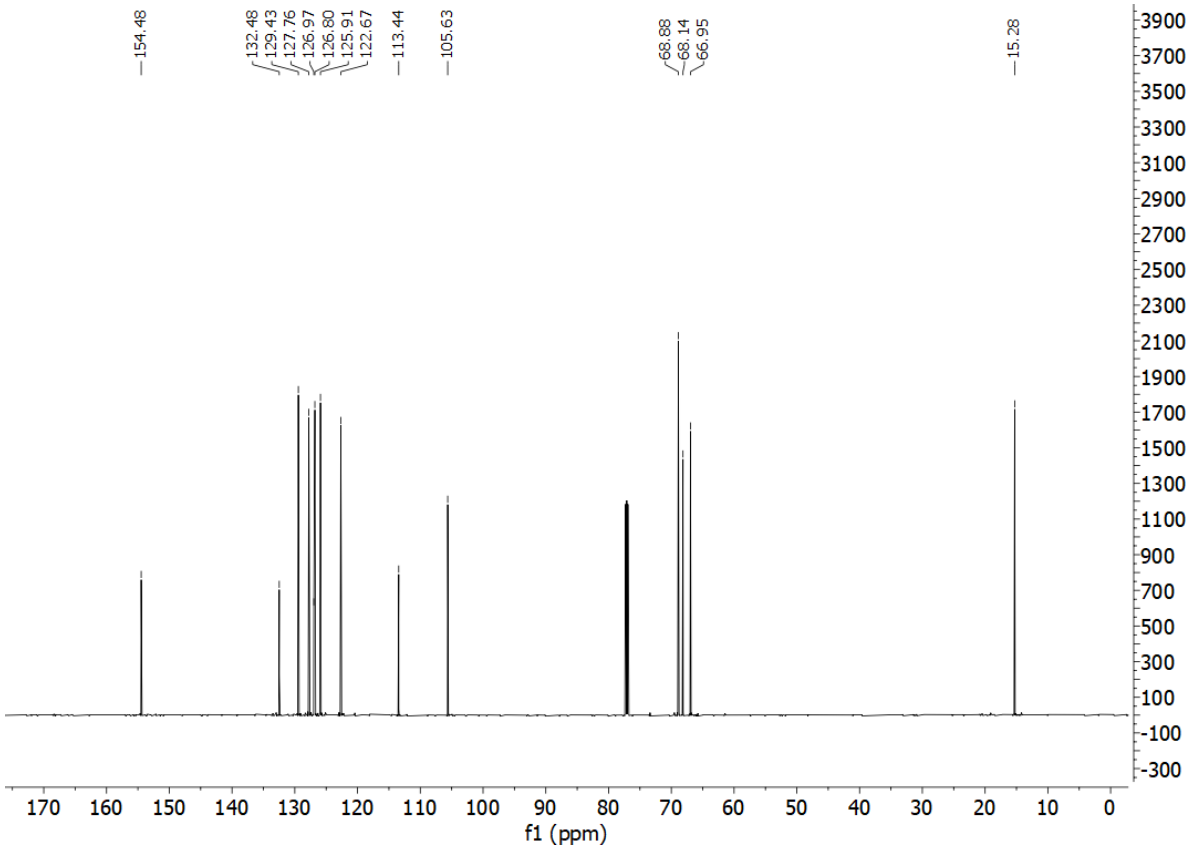

121a *bis(tert-butyl N-{2'-[3-chloro-4-(2''-ethoxyethoxy)naphthalene-1-sulfonamido]ethyl}carbamate)*

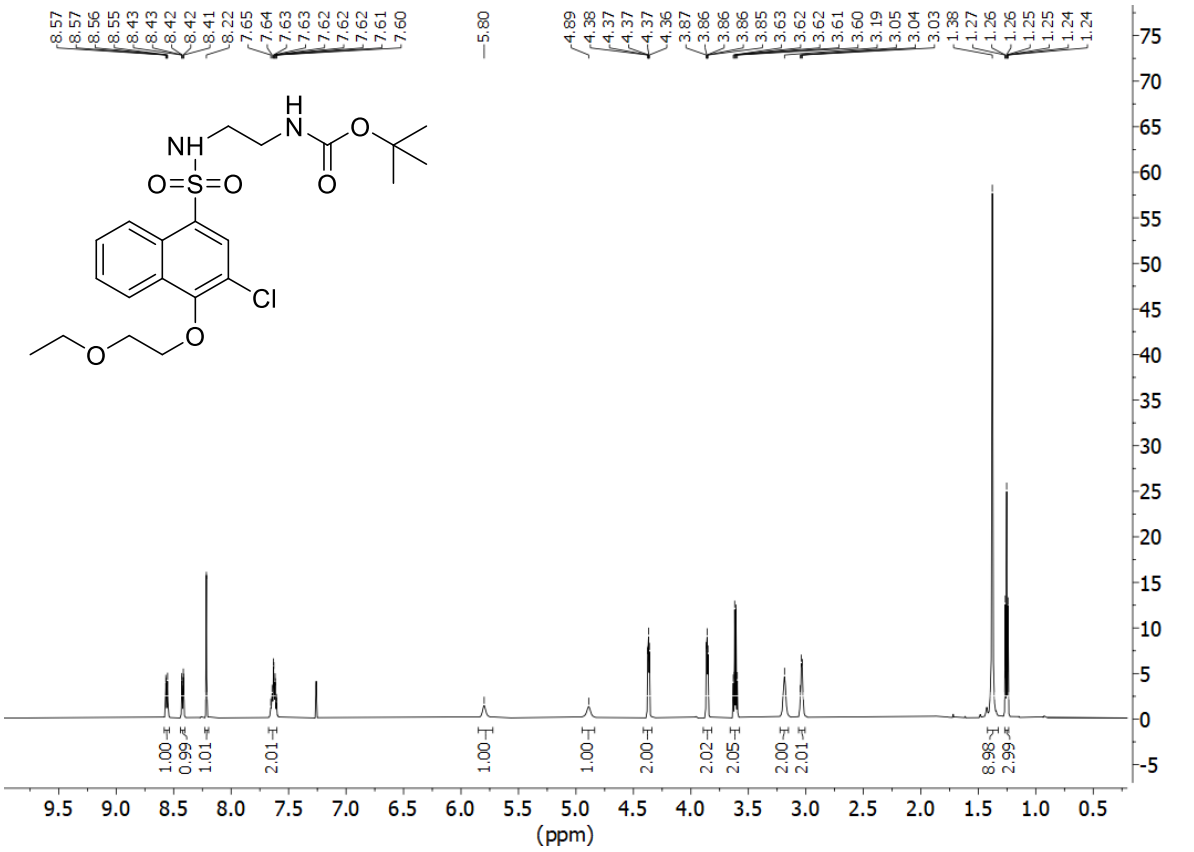

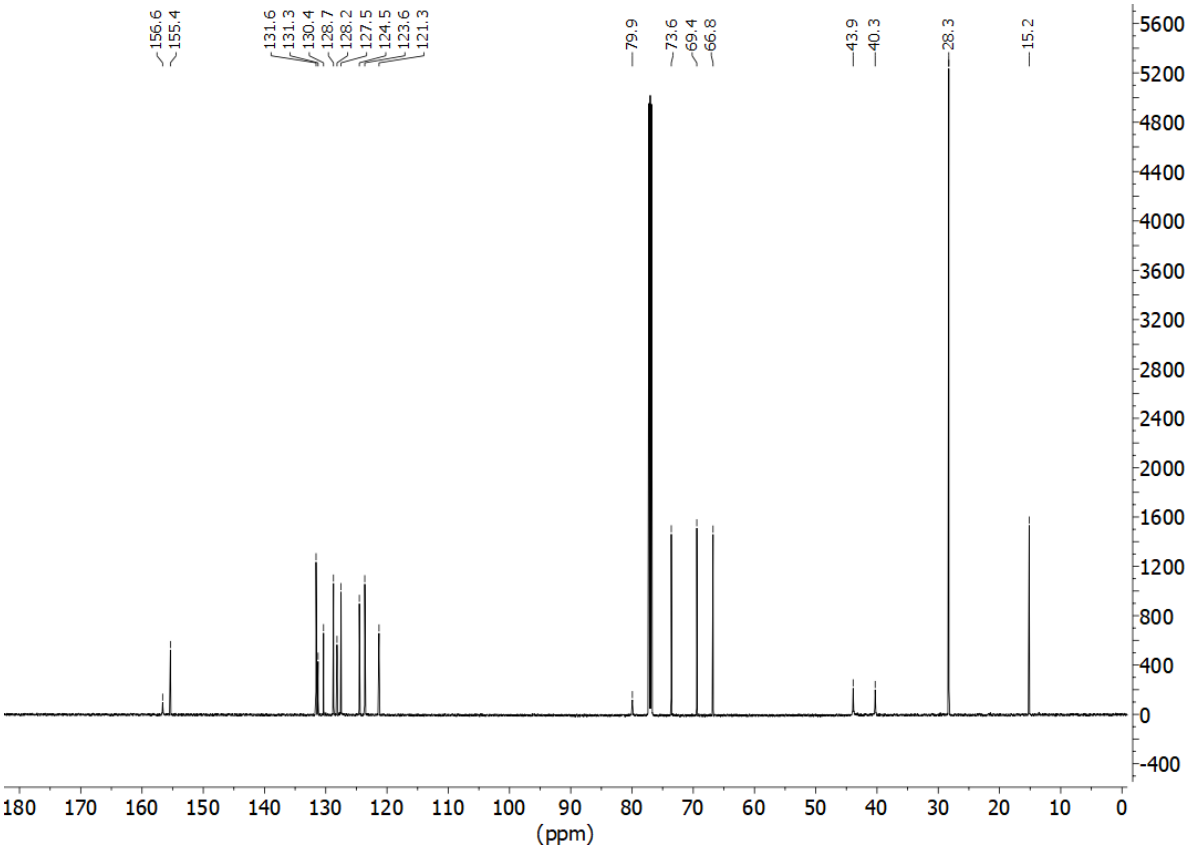

121. *N-(2-aminoethyl)-3-chloro-4-(2-ethoxyethoxy)naphthalene-1-sulfonamide hydrogen chloride*

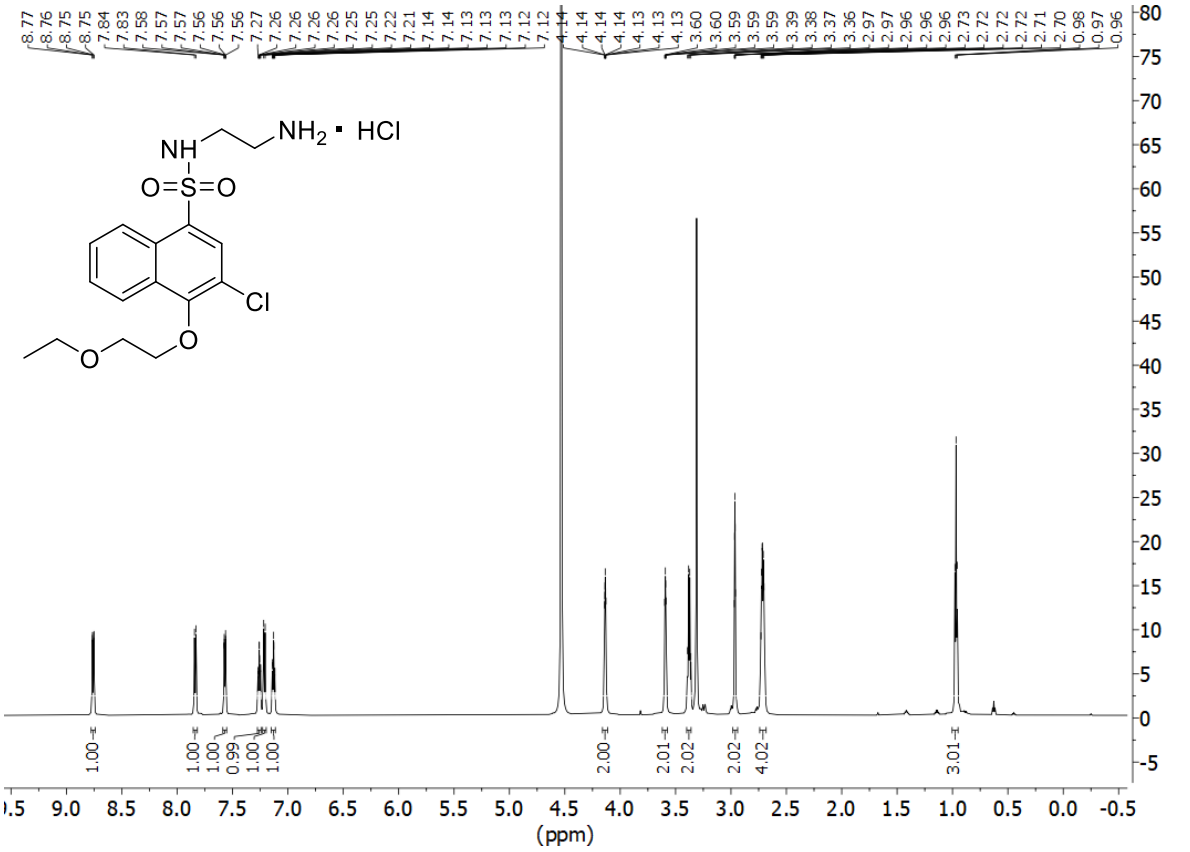

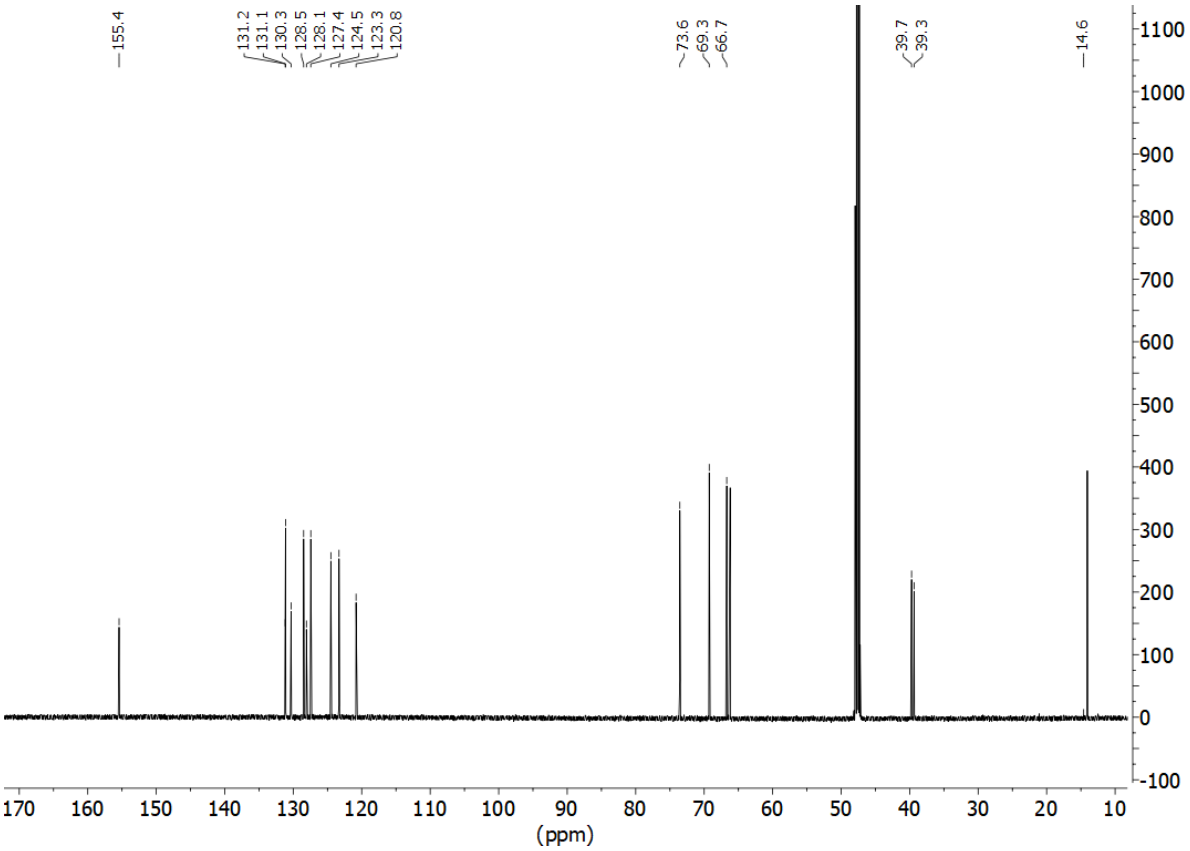

122a. *tert-butyl N-{2'-[4-(2''-ethoxyethoxy)naphthalene-1-sulfonamido]ethyl}carbamate*

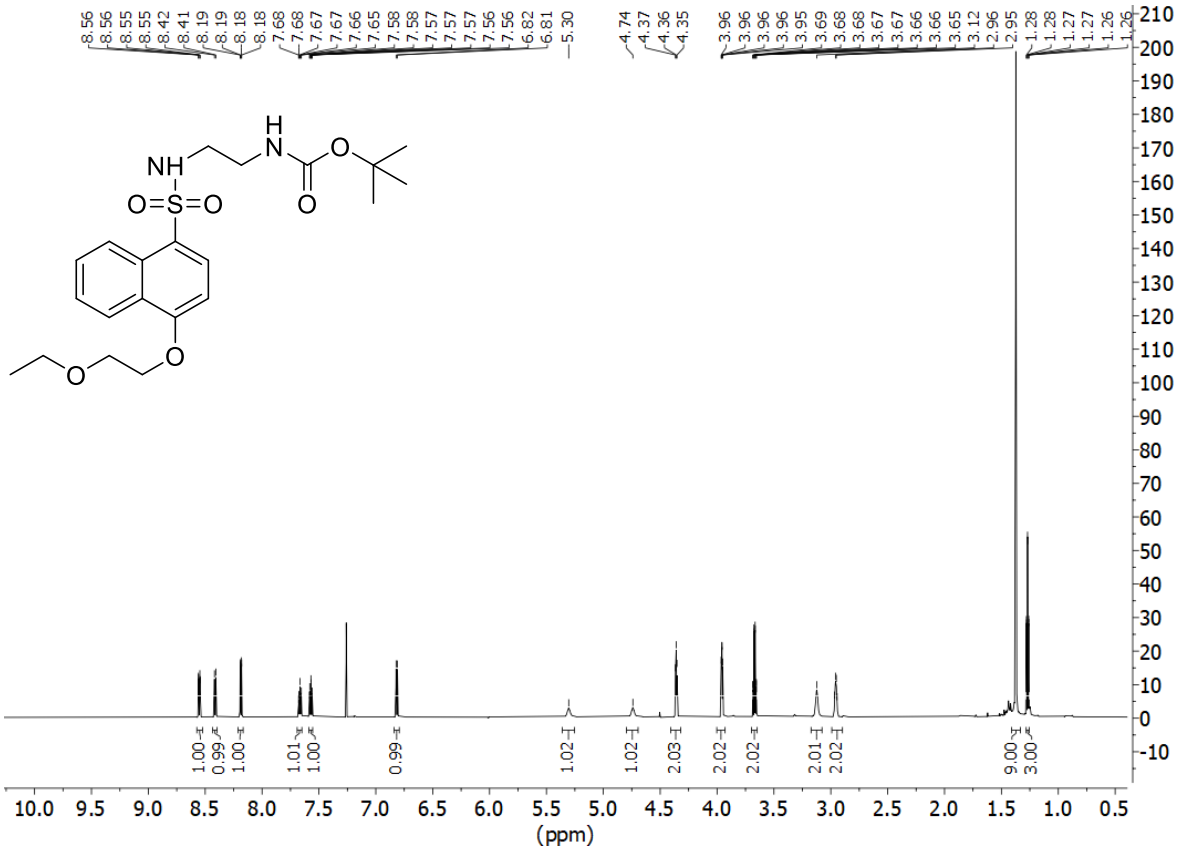

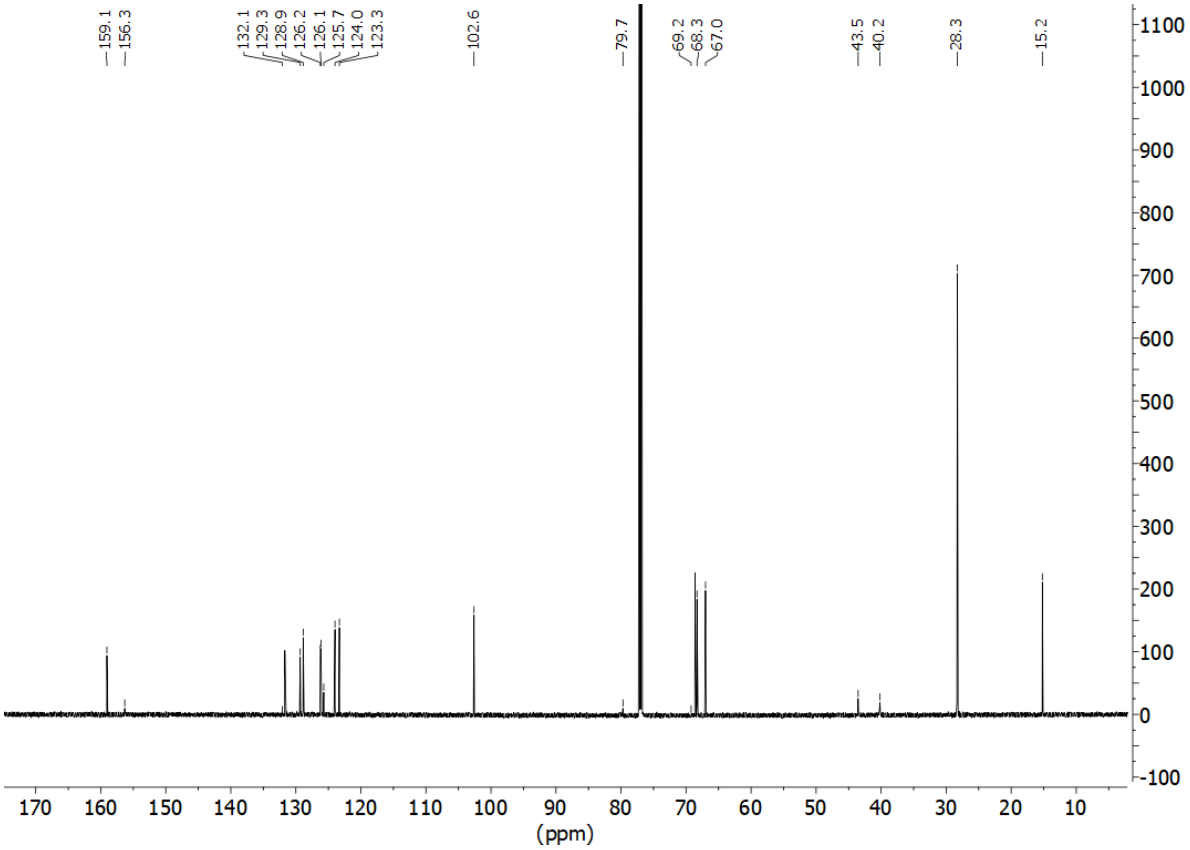

122. *N-(2'-aminoethyl)-4-(2''-ethoxyethoxy)naphthalene-1-sulfonamide hydrogen chloride*

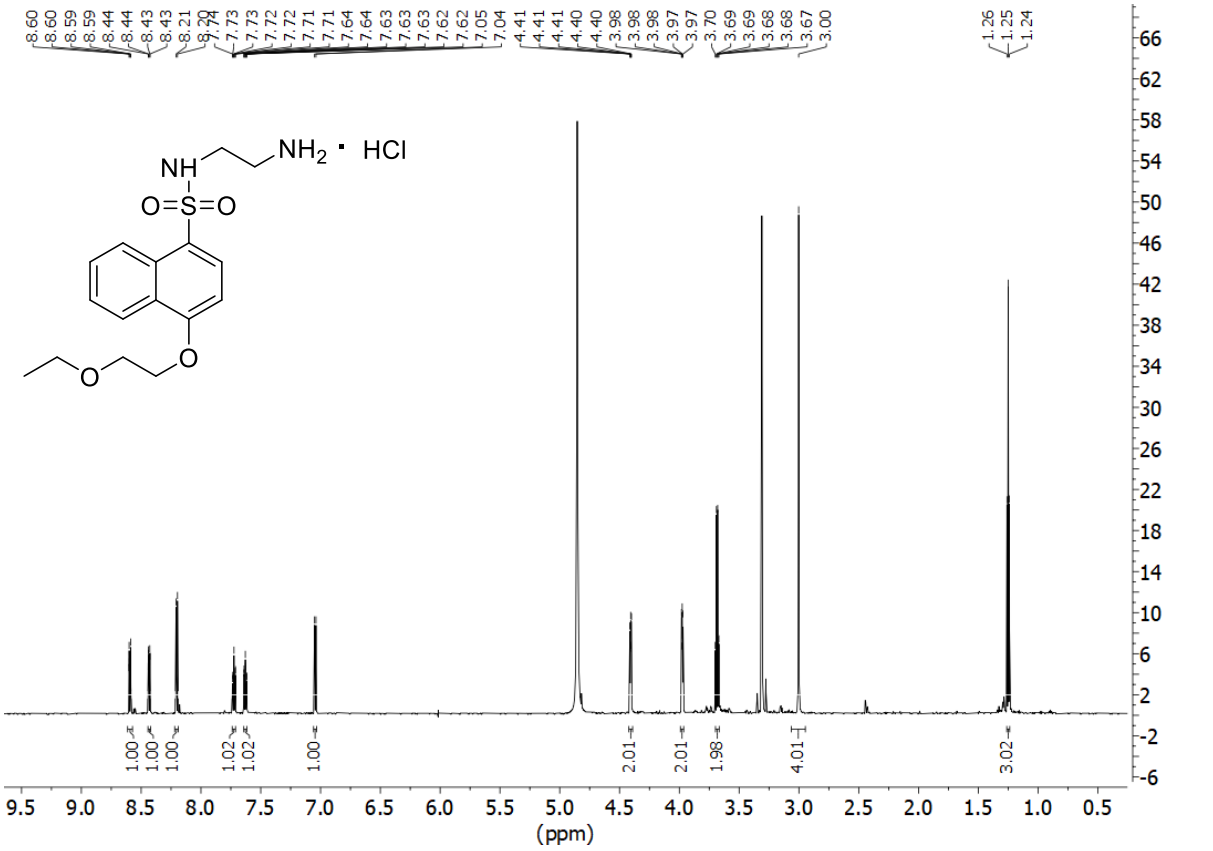

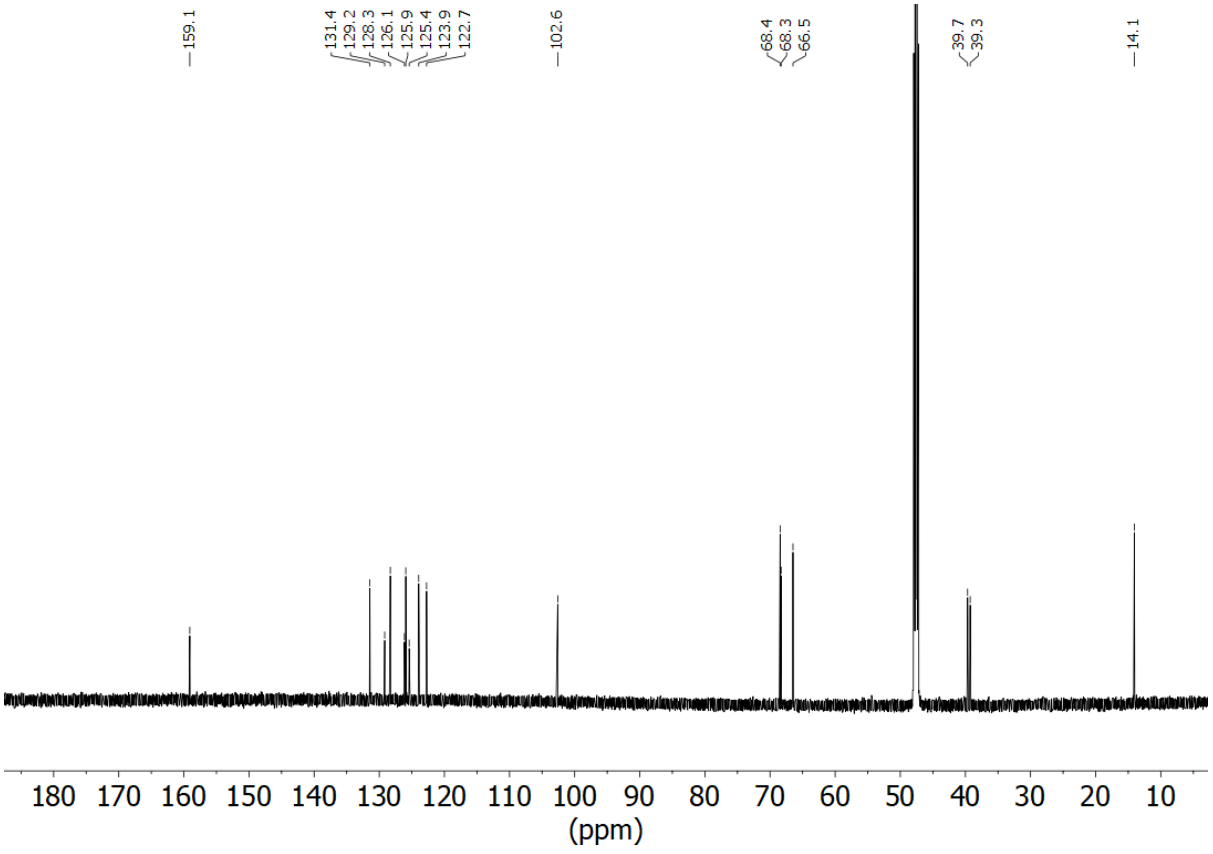

127a. *1-bromo-4-(methoxy methoxy)naphthalene*

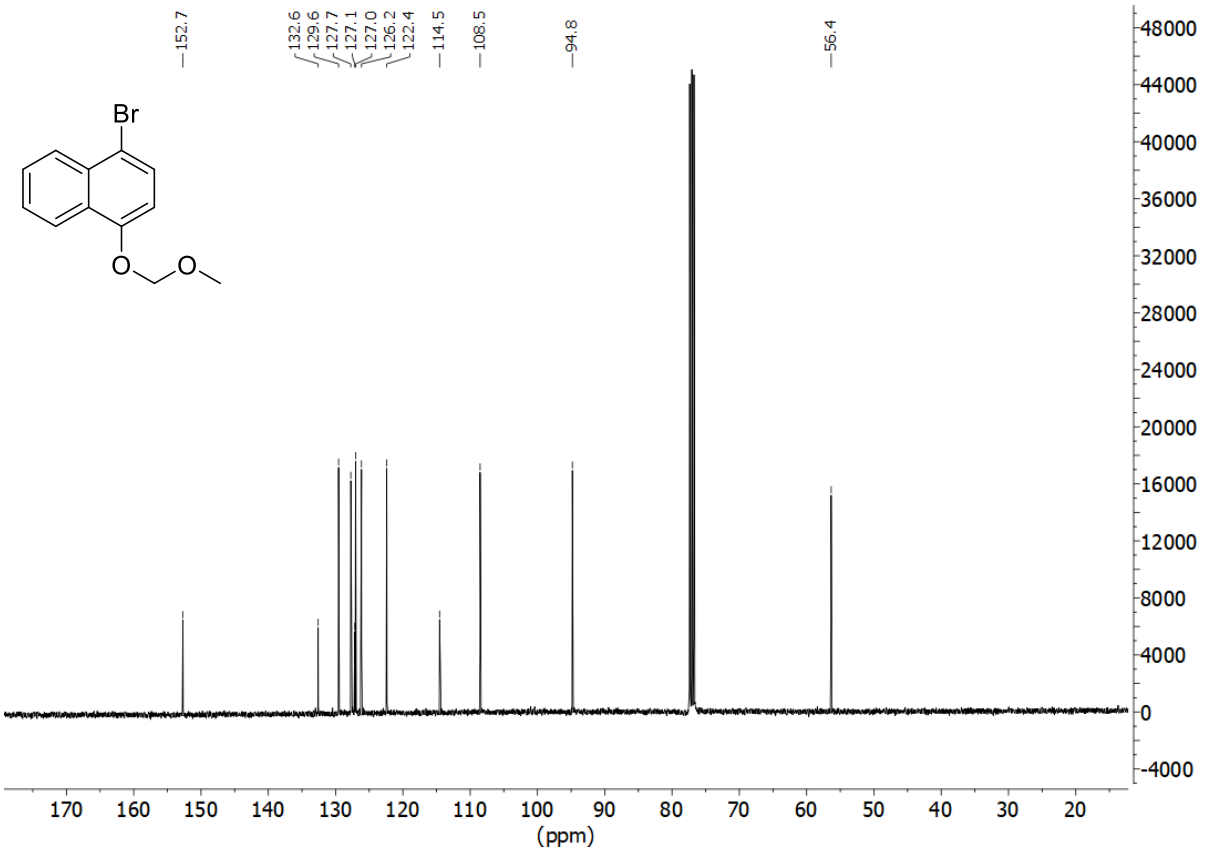

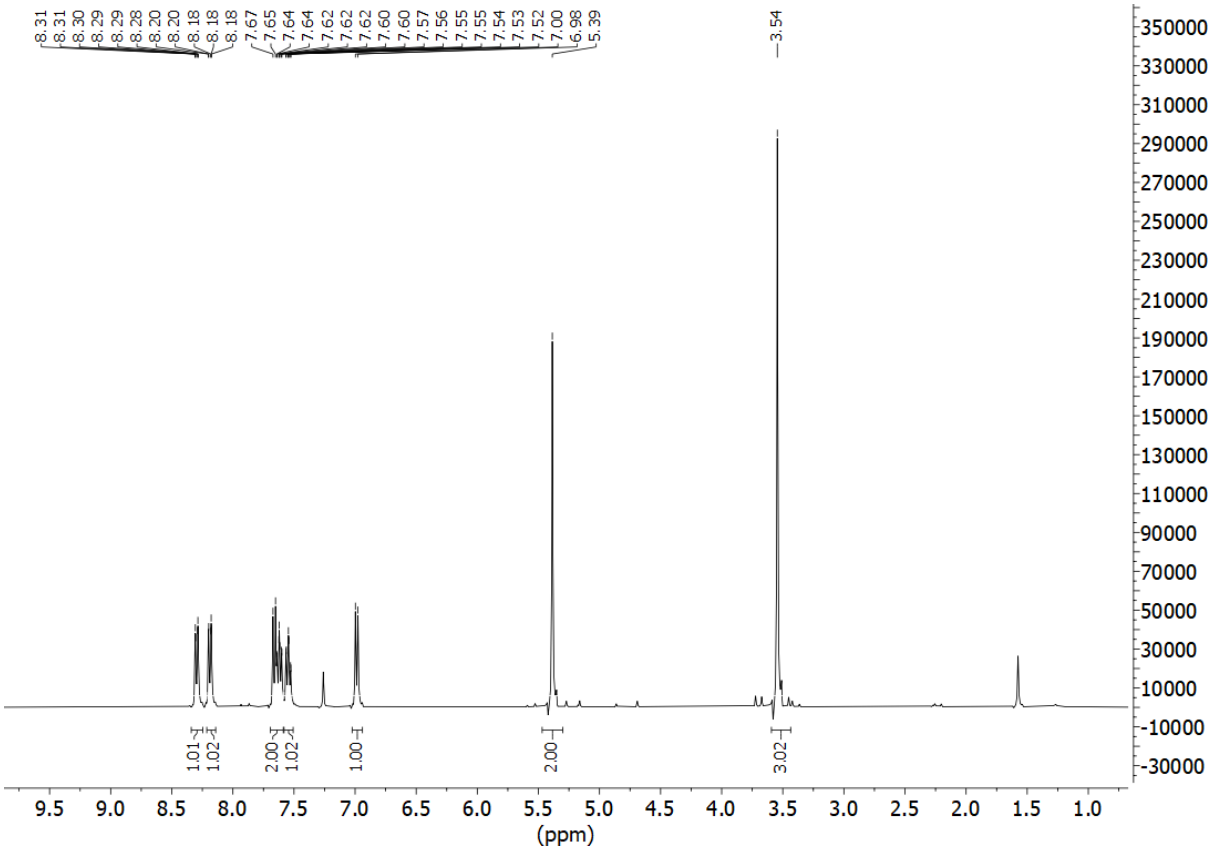

127. *tert-butyl N-{2'-[4-(methoxymethoxy)naphthalene-1-sulfonamido]ethyl}carbamate*

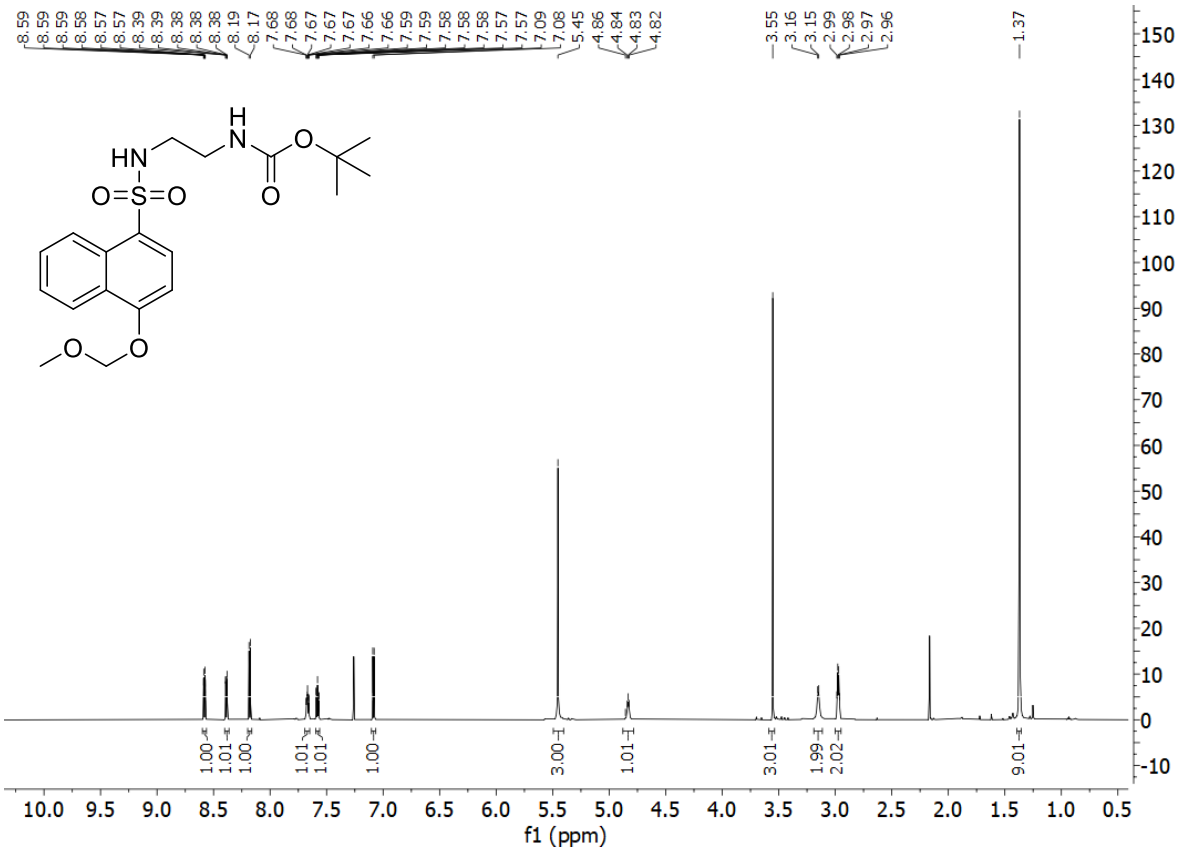

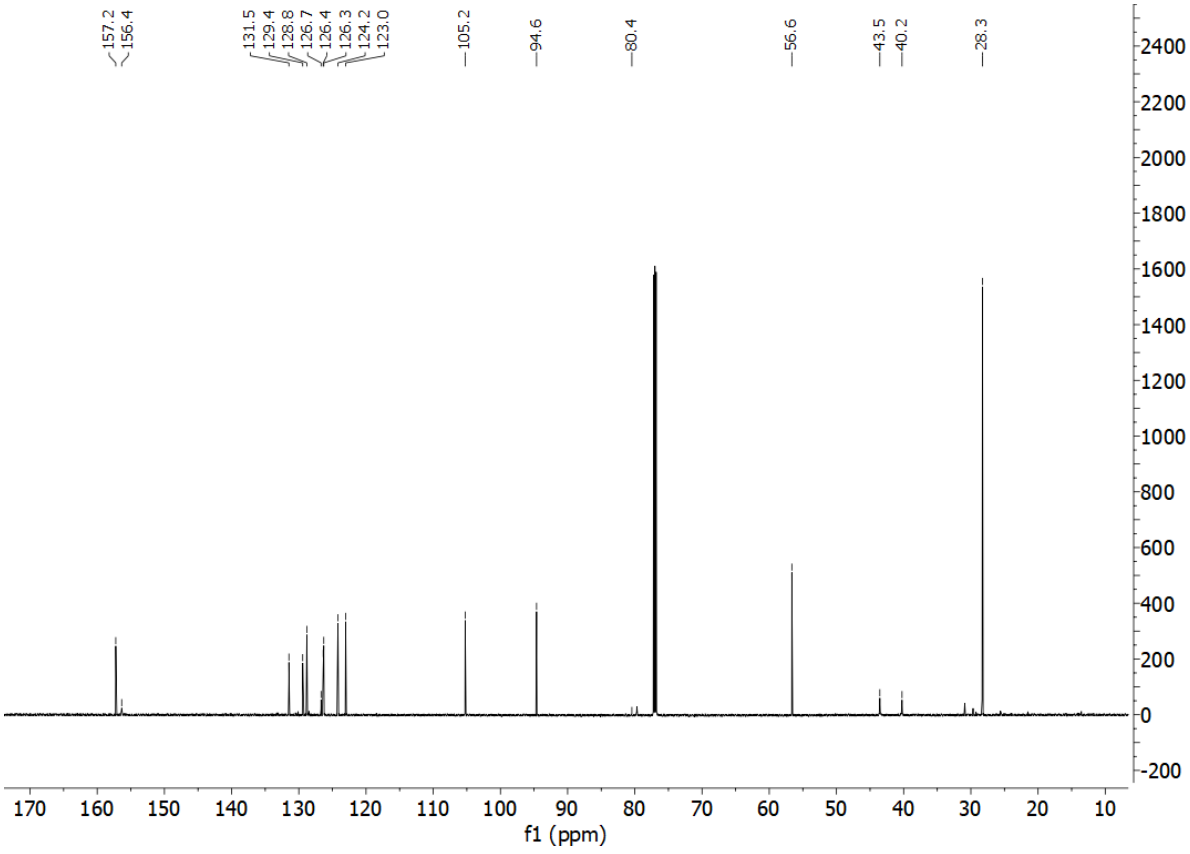

128a. *1-(benzyloxy)-4-bromonaphthalene*

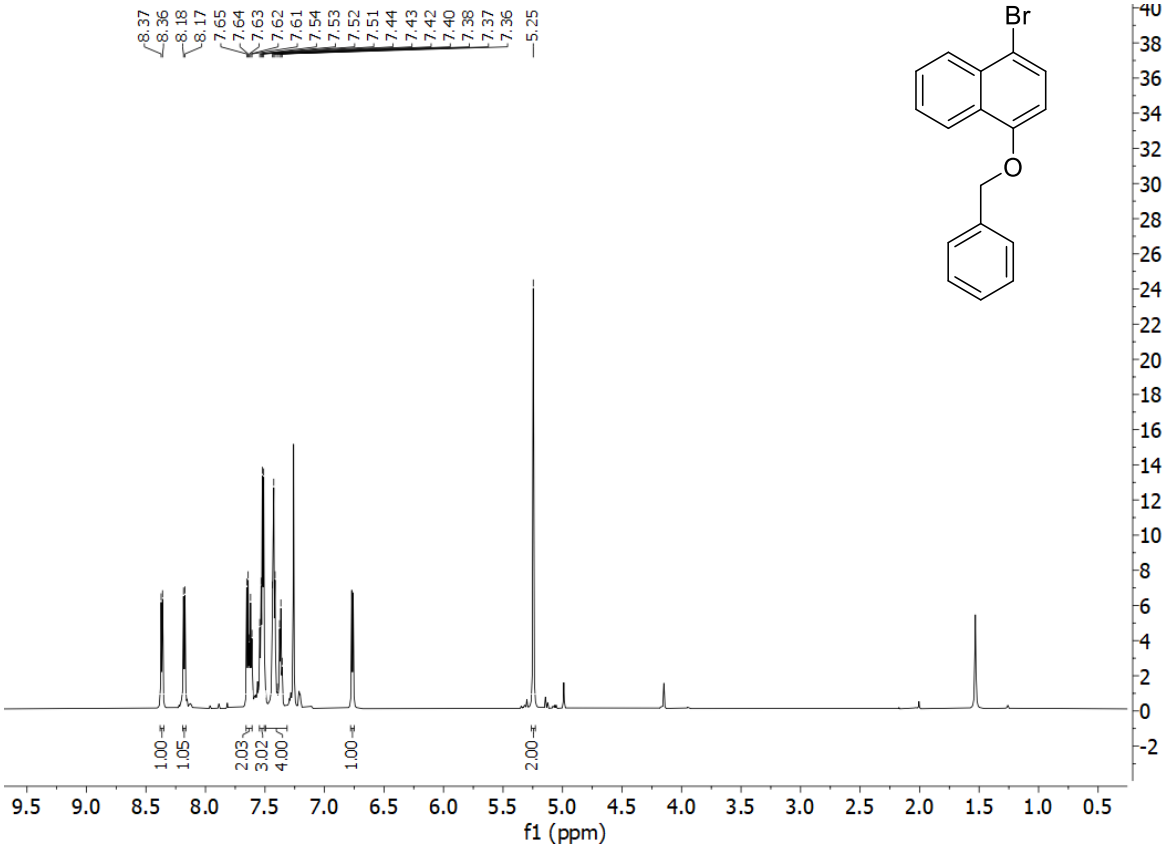

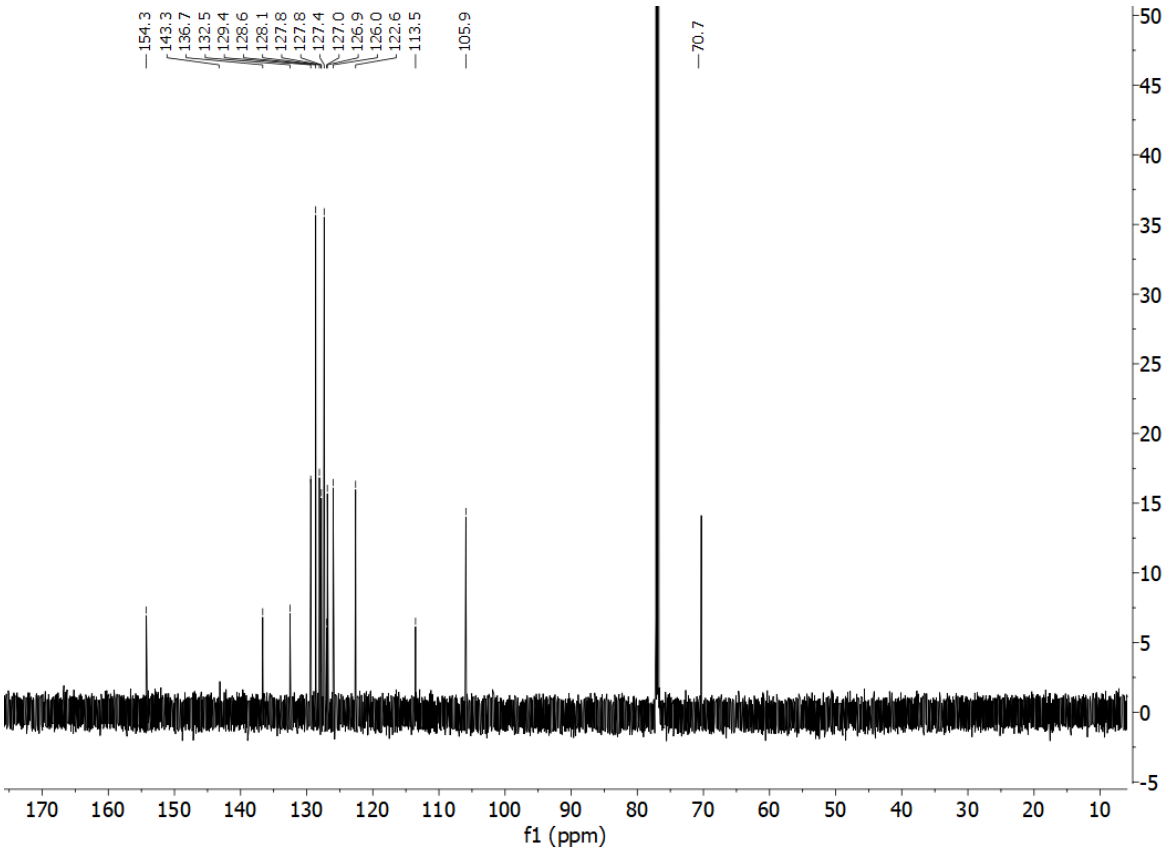

129a. *[(4-bromonaphthalen-1-yl)oxy](tert-butyl)dimethylsilane*

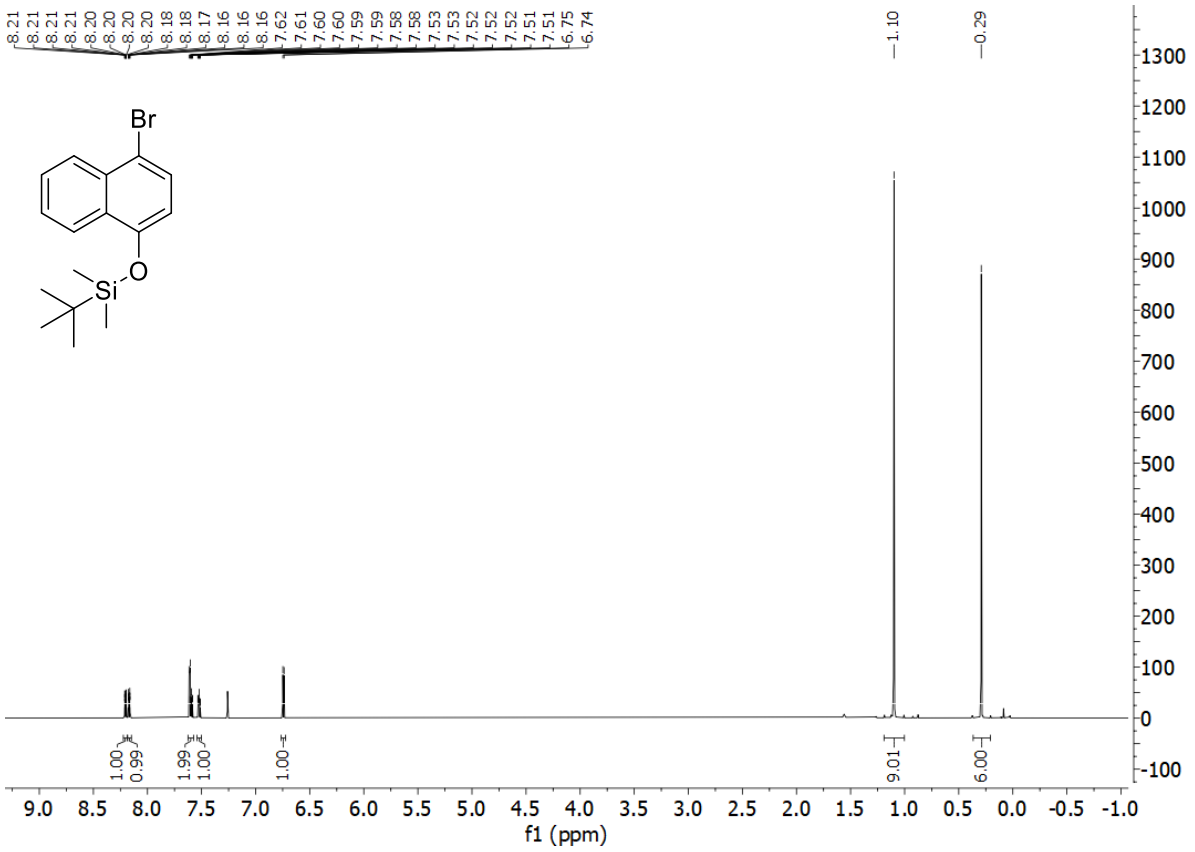

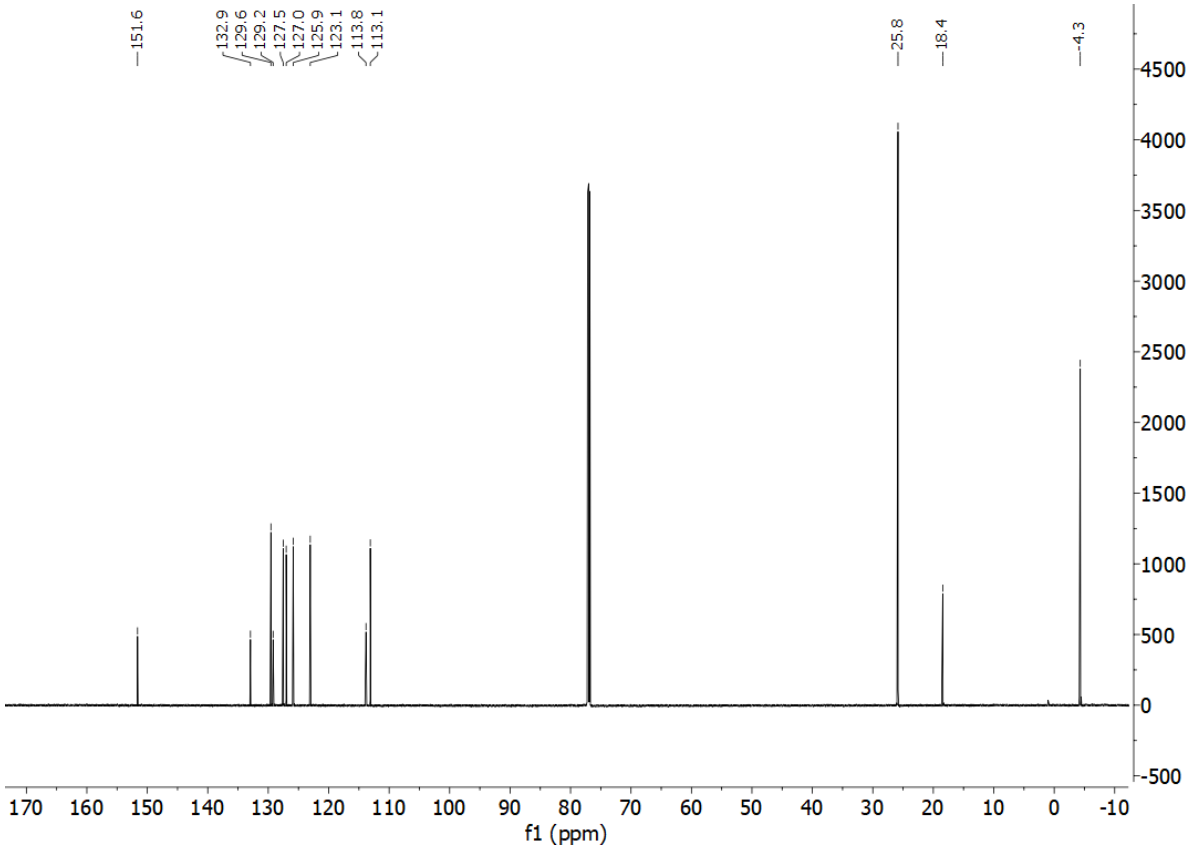

130a. *(2'-{[(4-bromonaphthalen-1-yl)oxy]methoxy}ethyl)trimethylsilane*

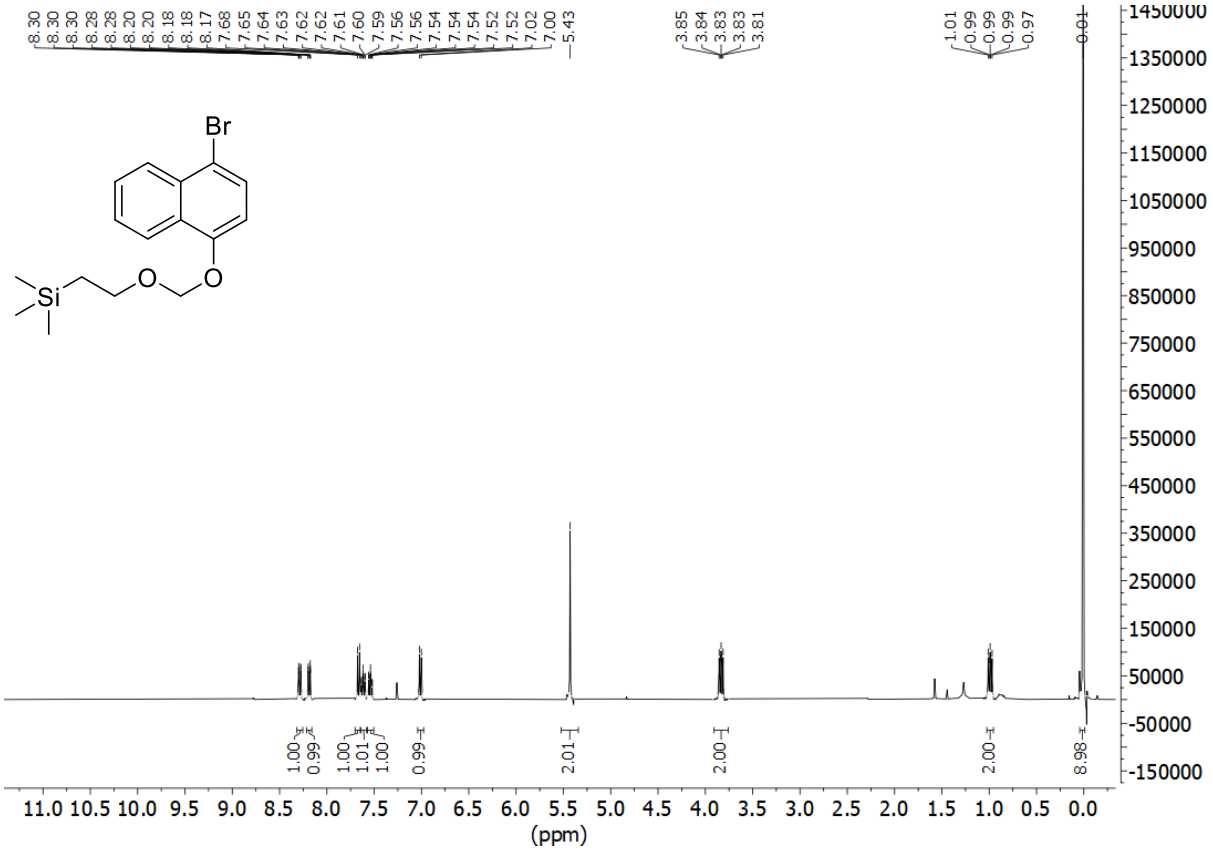

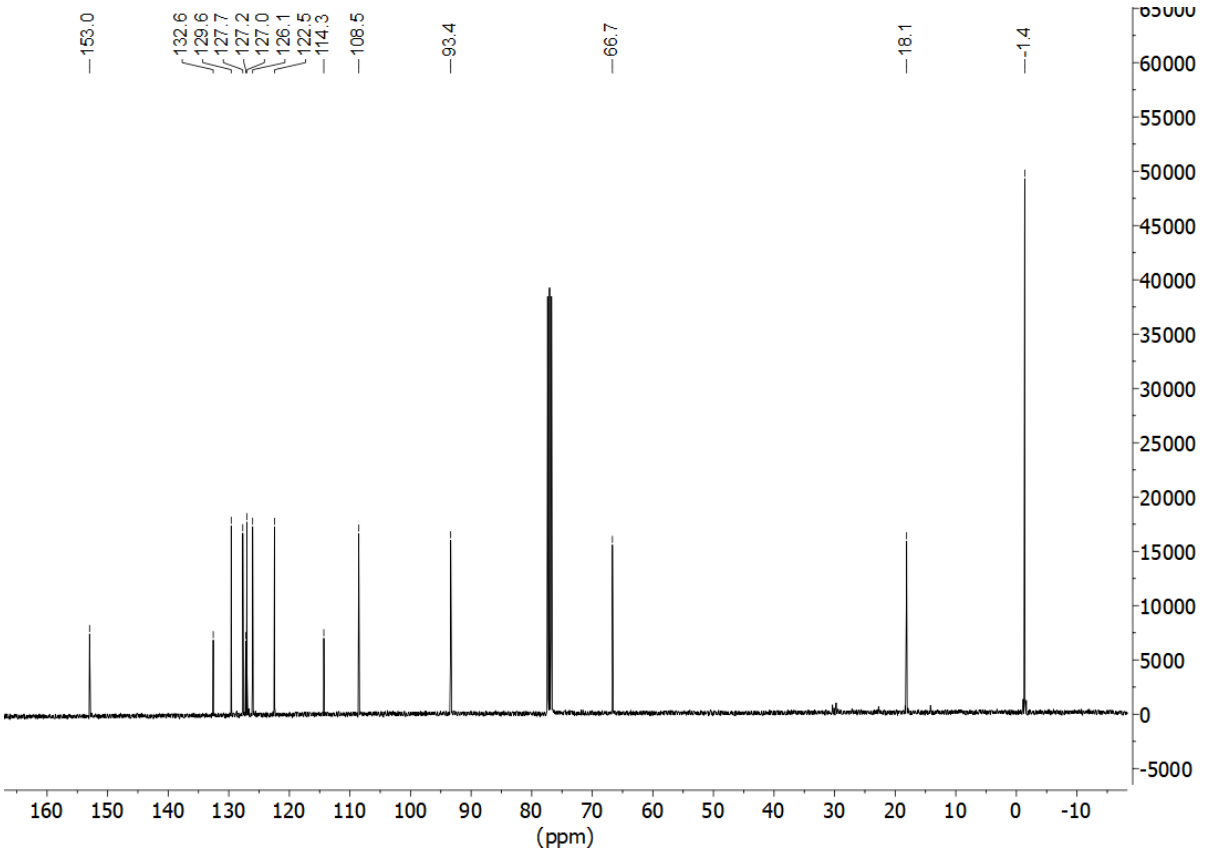

130. tert-butyl N-[2'-(4-{[2''-(trimethylsilyl)ethoxy]methoxy}naphthalene-1-sulfonamido) ethyl] carbamate

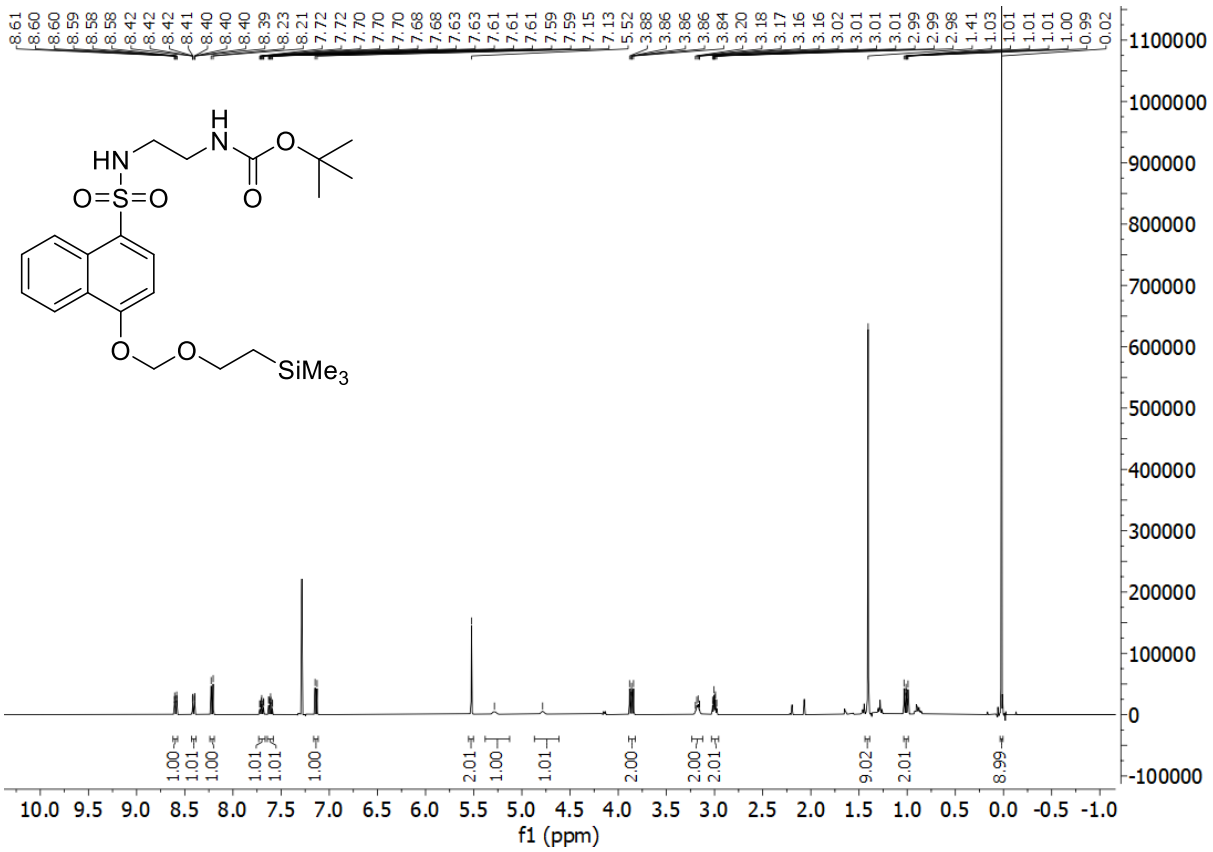

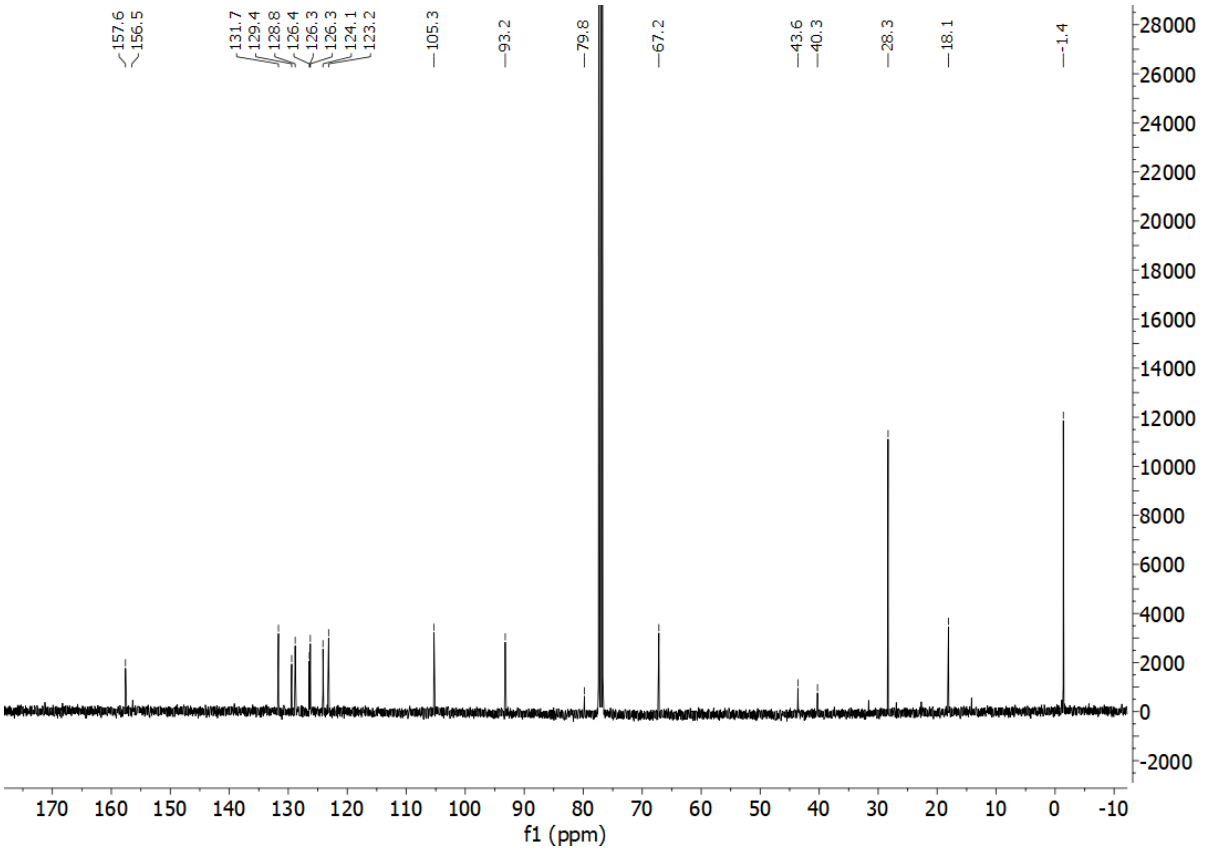

131. *tert-butyl N-[2'-(4-hydroxynaphthalene-1-sulfonamido)ethyl]carbamate*

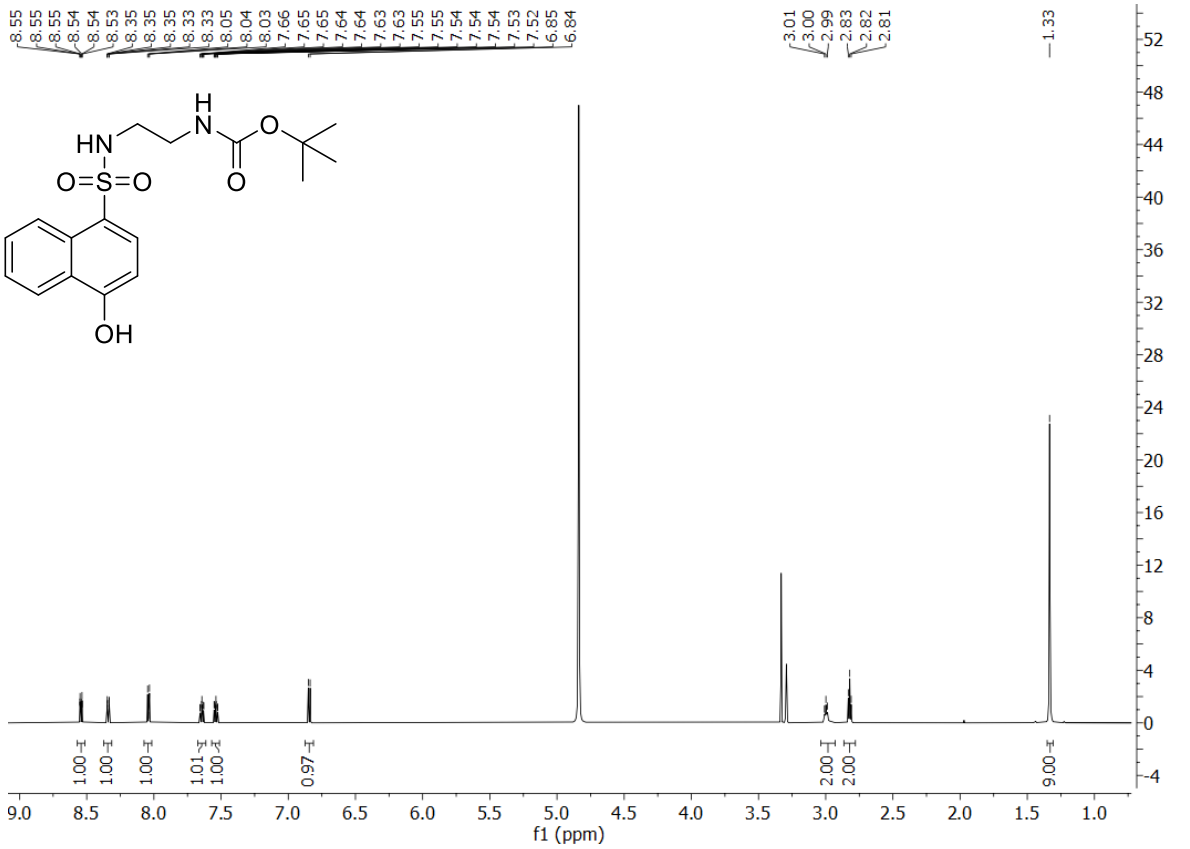

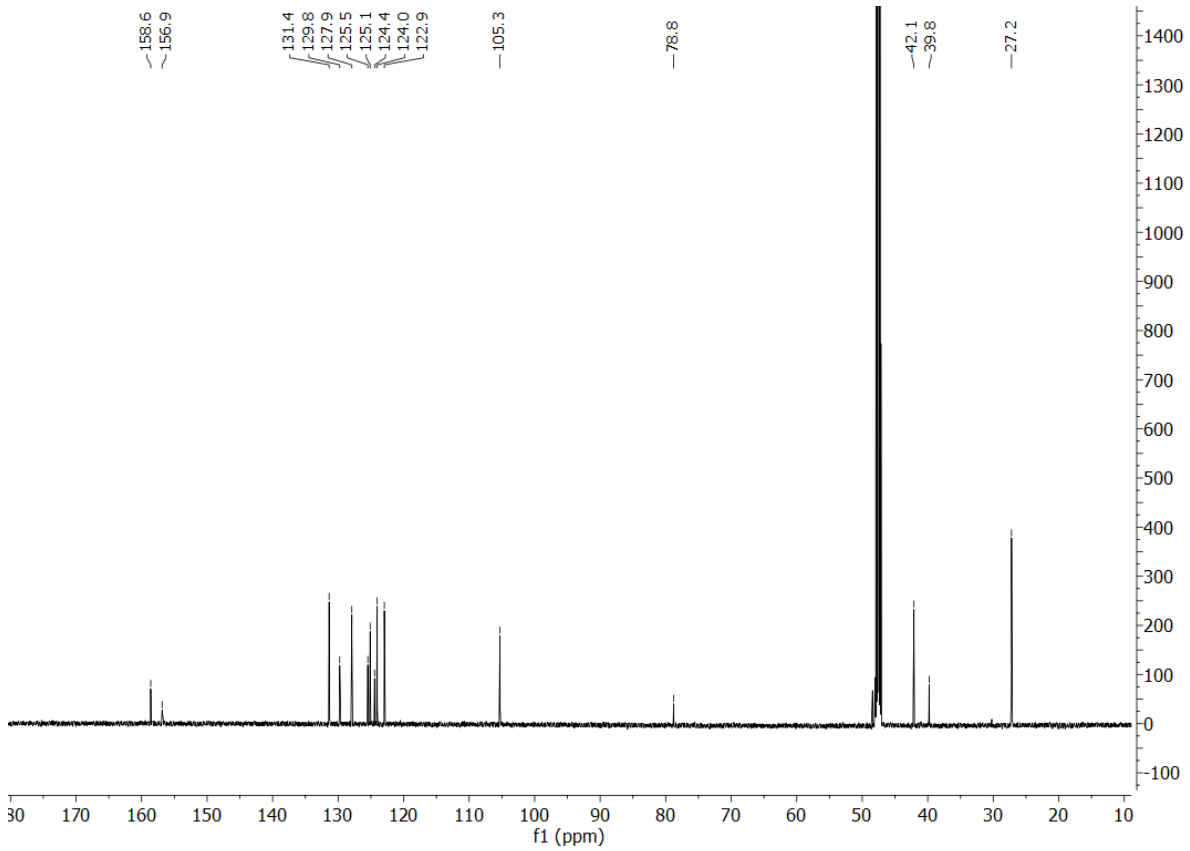

134. *methyl N-[2-(2'-hydroxyethoxy)ethyl]carbamate*

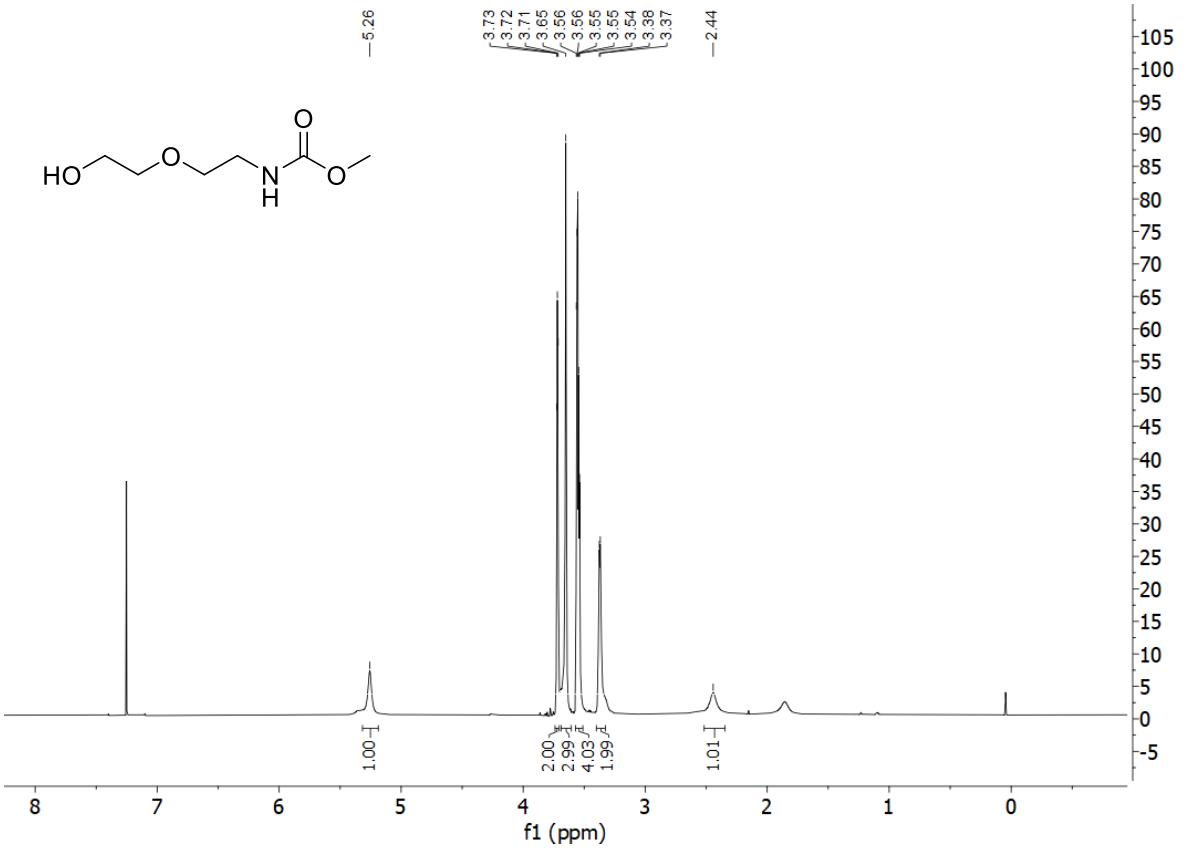

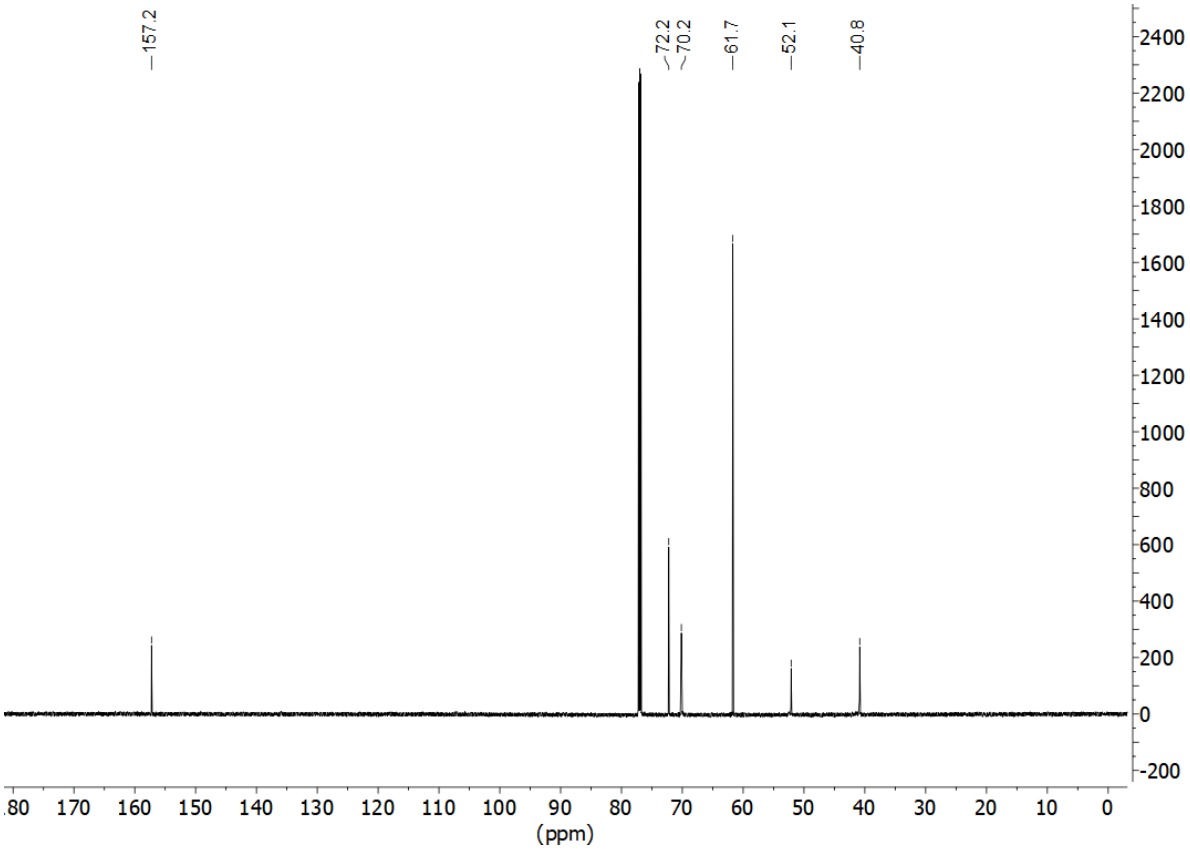

135. *2-[2'-(methylamino)ethoxy]ethan-1-ol*

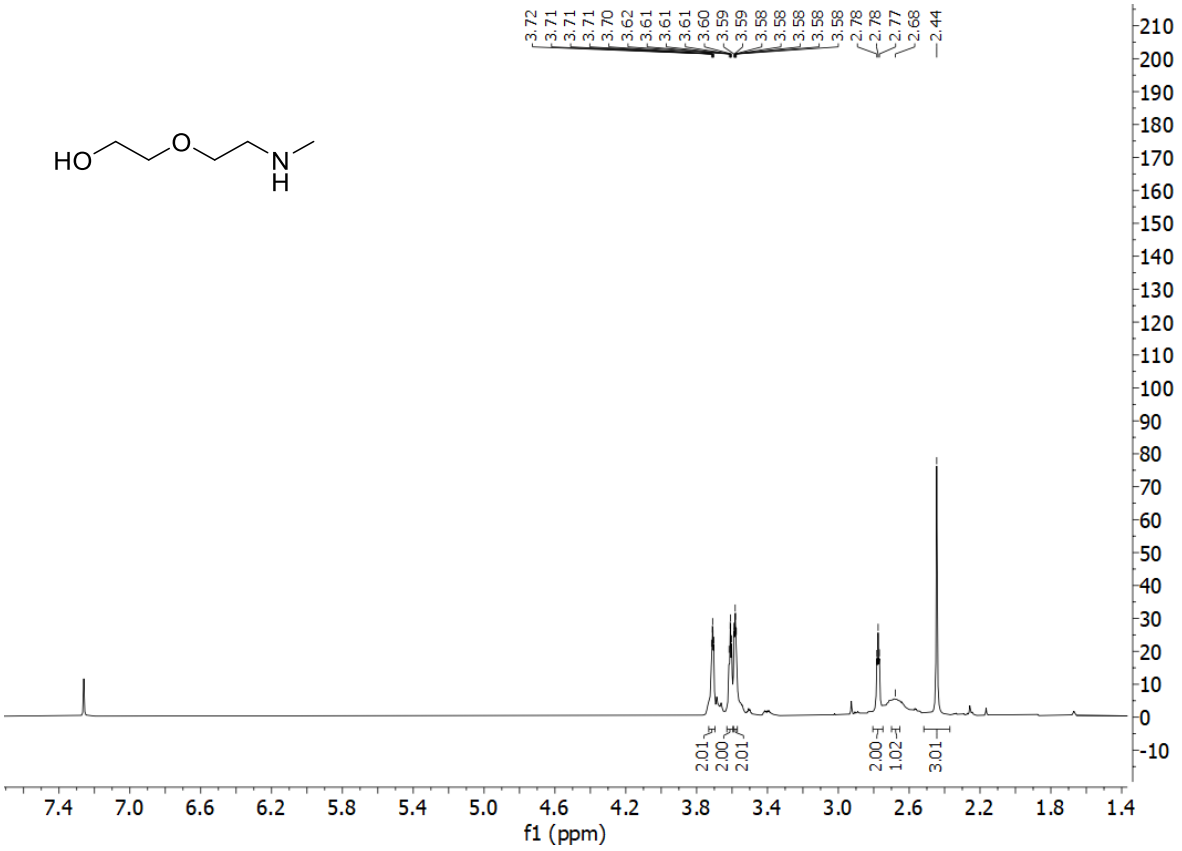

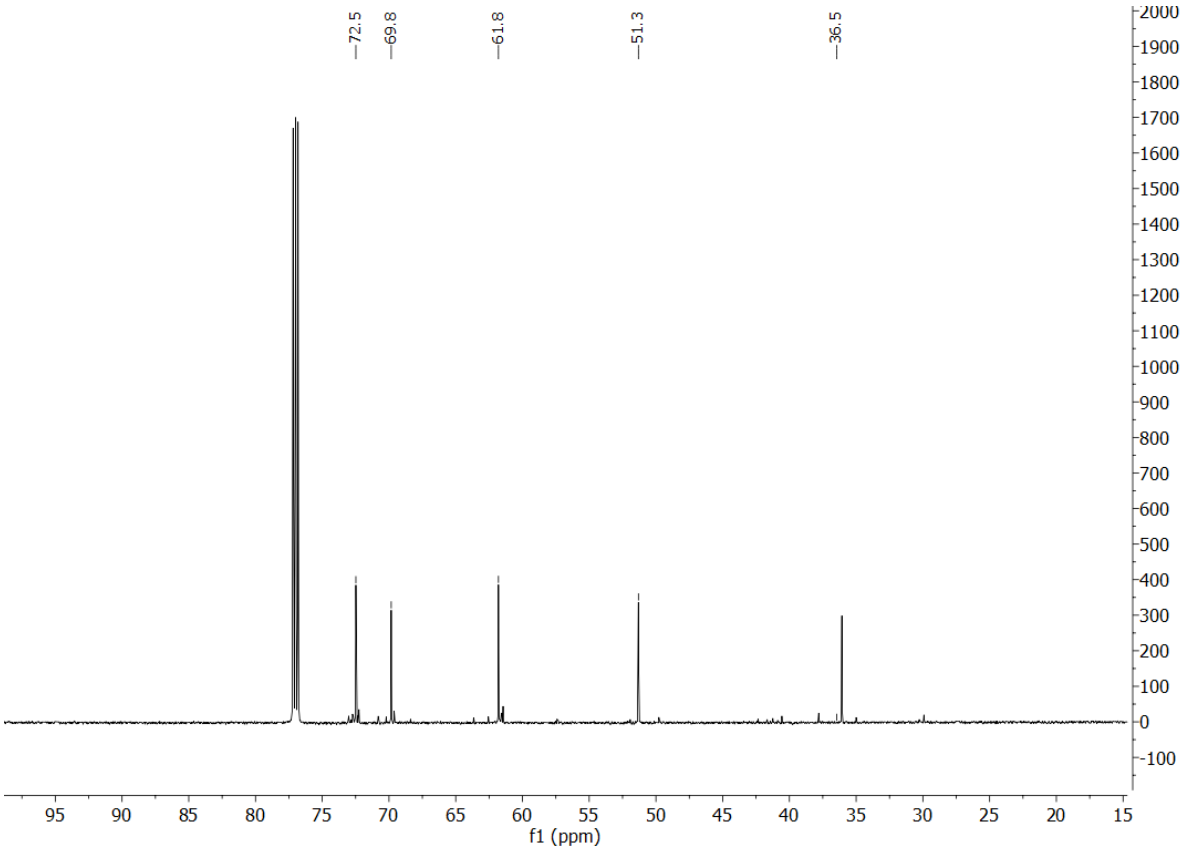

136. *prop-2-en-1-yl N-[2'-(2''-hydroxyethoxy)ethyl]-N-methylcarbamate*

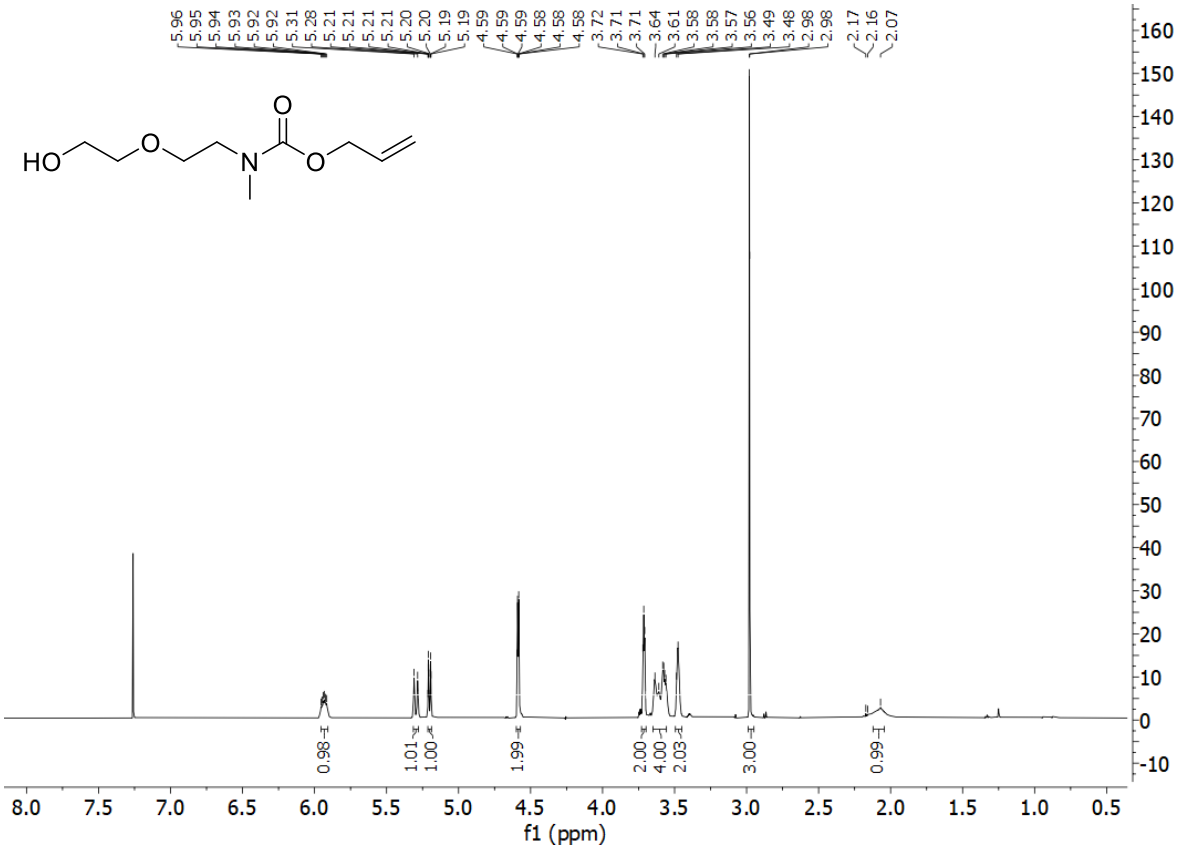

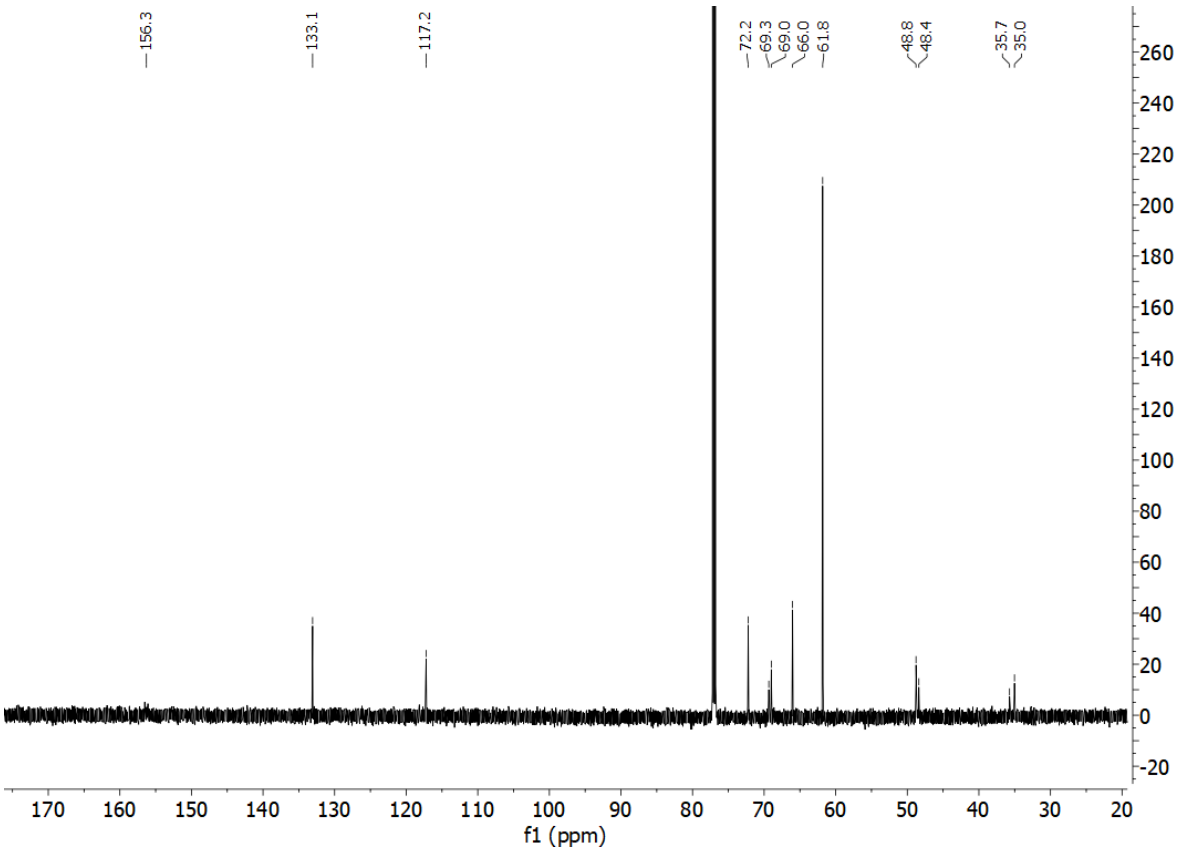

140. *prop-2-en-1-yl N-(but-3'-yn-1-yl)-N-[2''-(2'''-hydroxyethoxy)ethyl]carbamate*

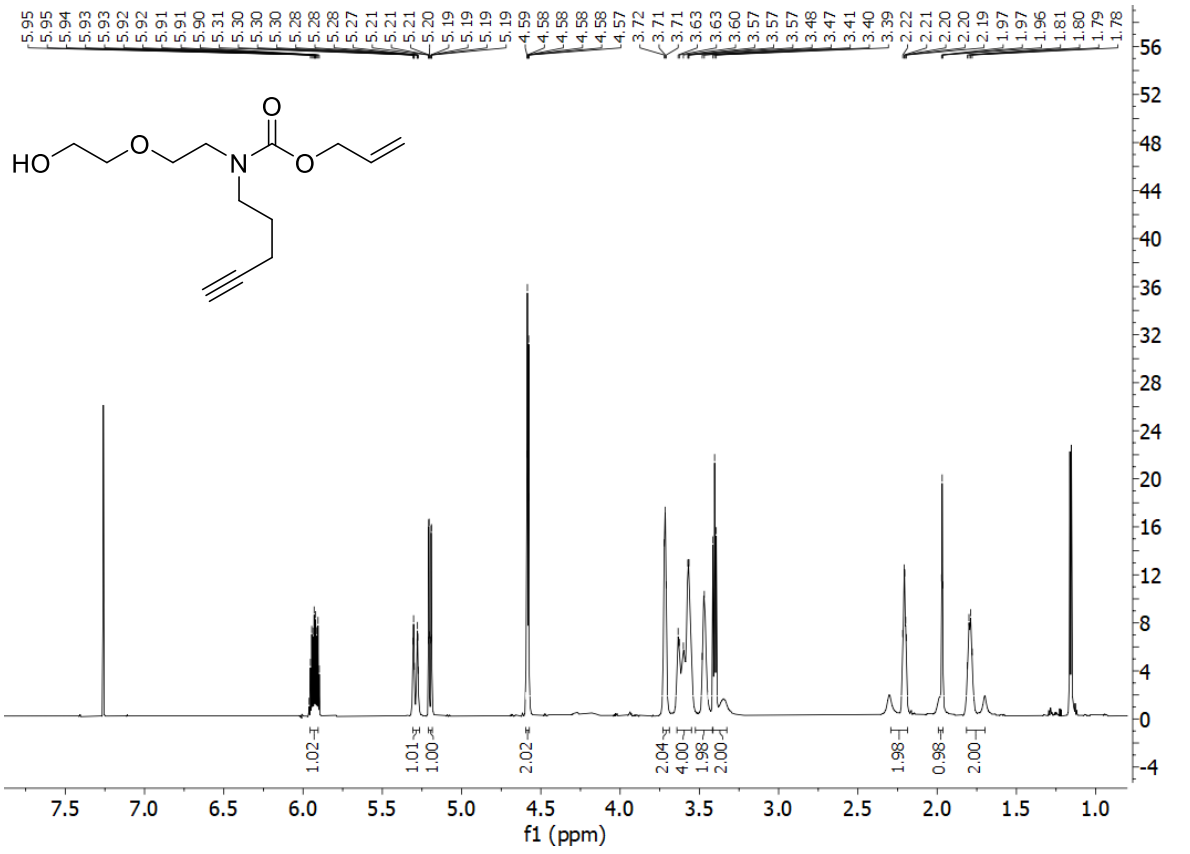

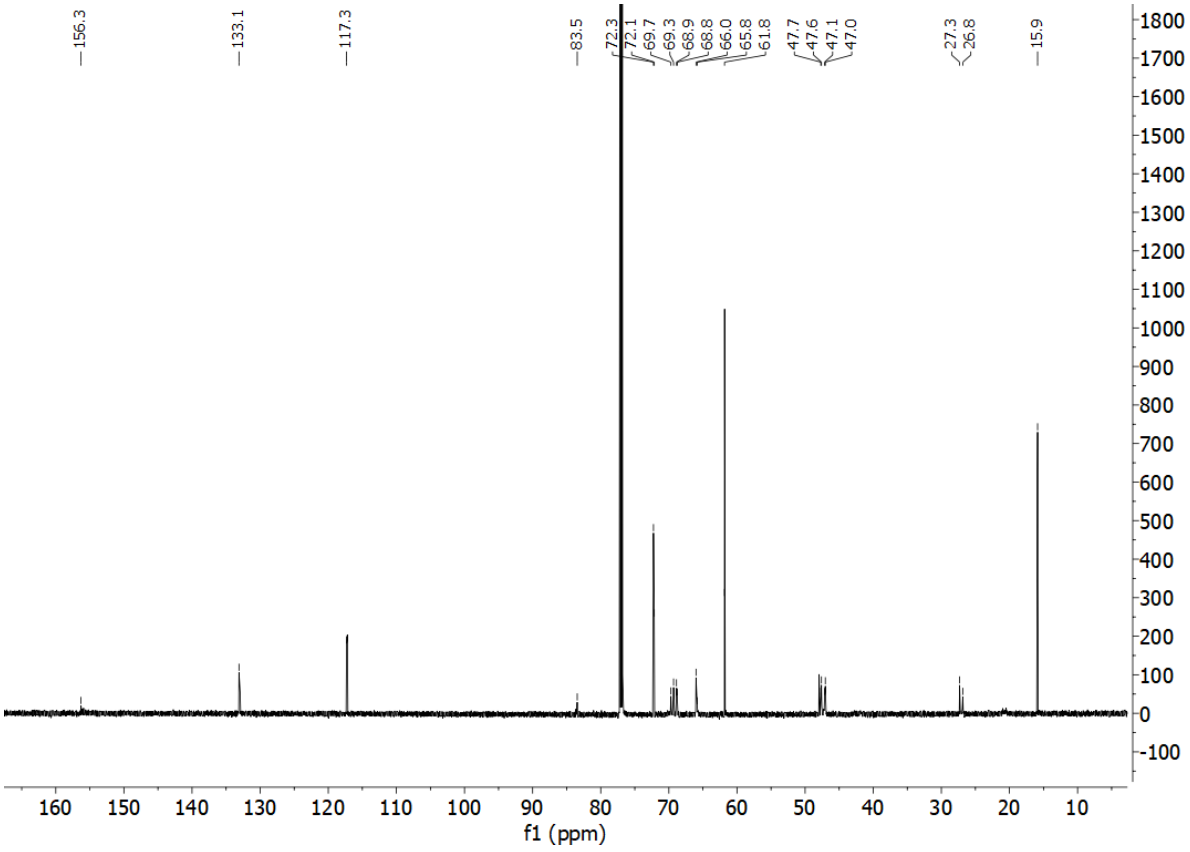

142. *methyl 3-tert-butylbenzoate*

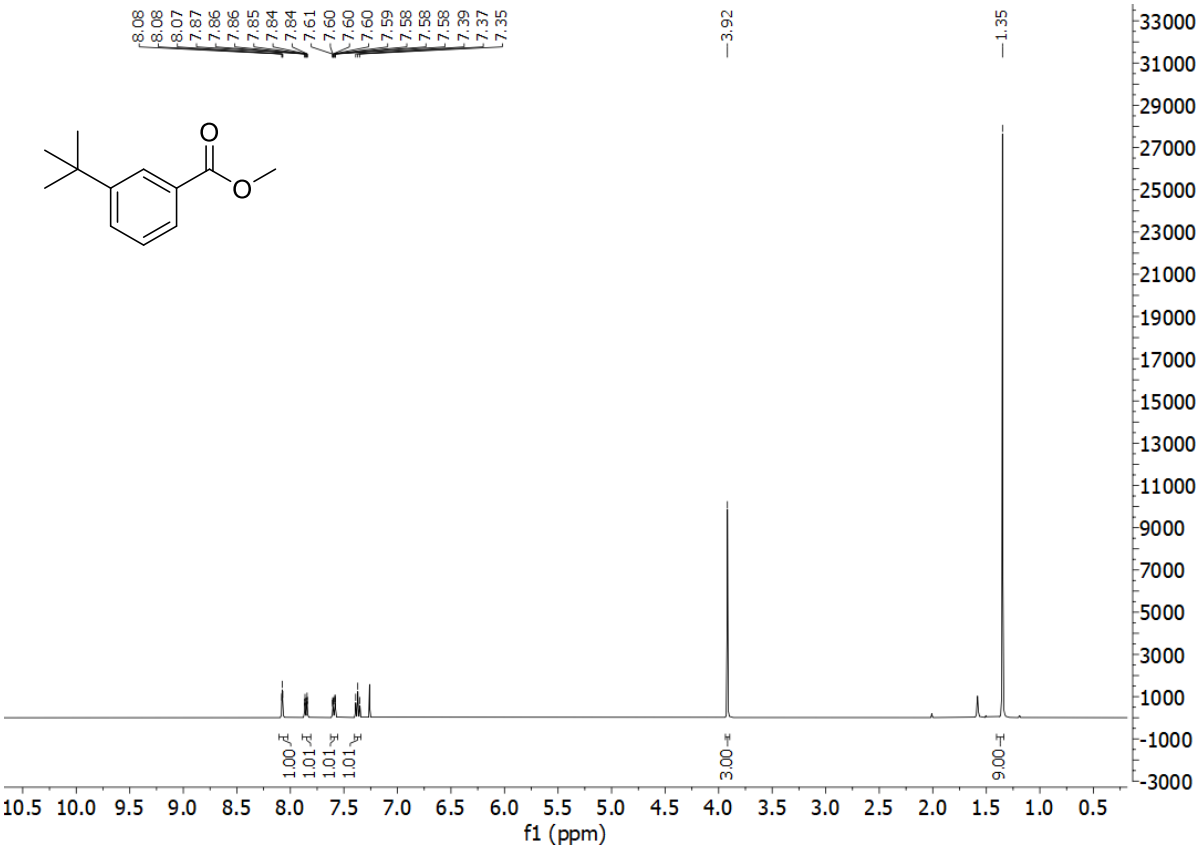

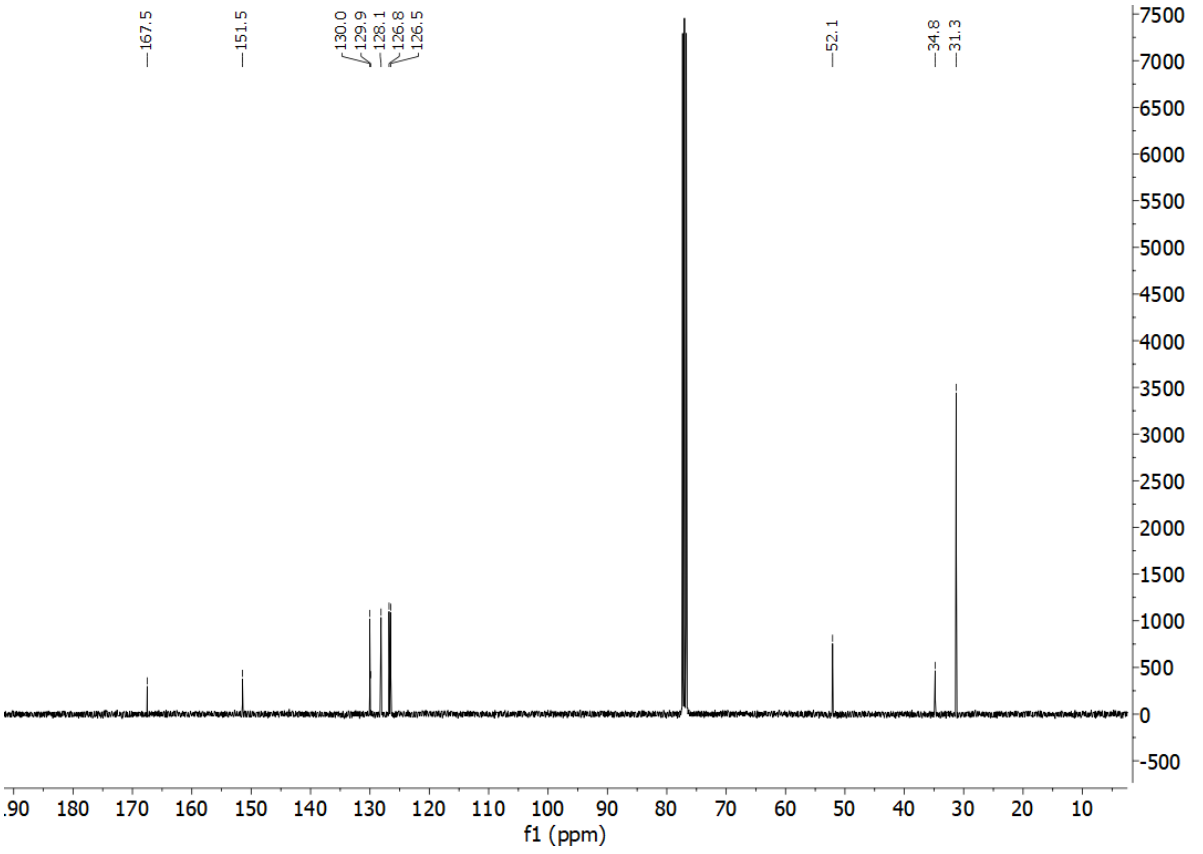

143. *methyl 3-tert-butyl-5-hydroxybenzoate*

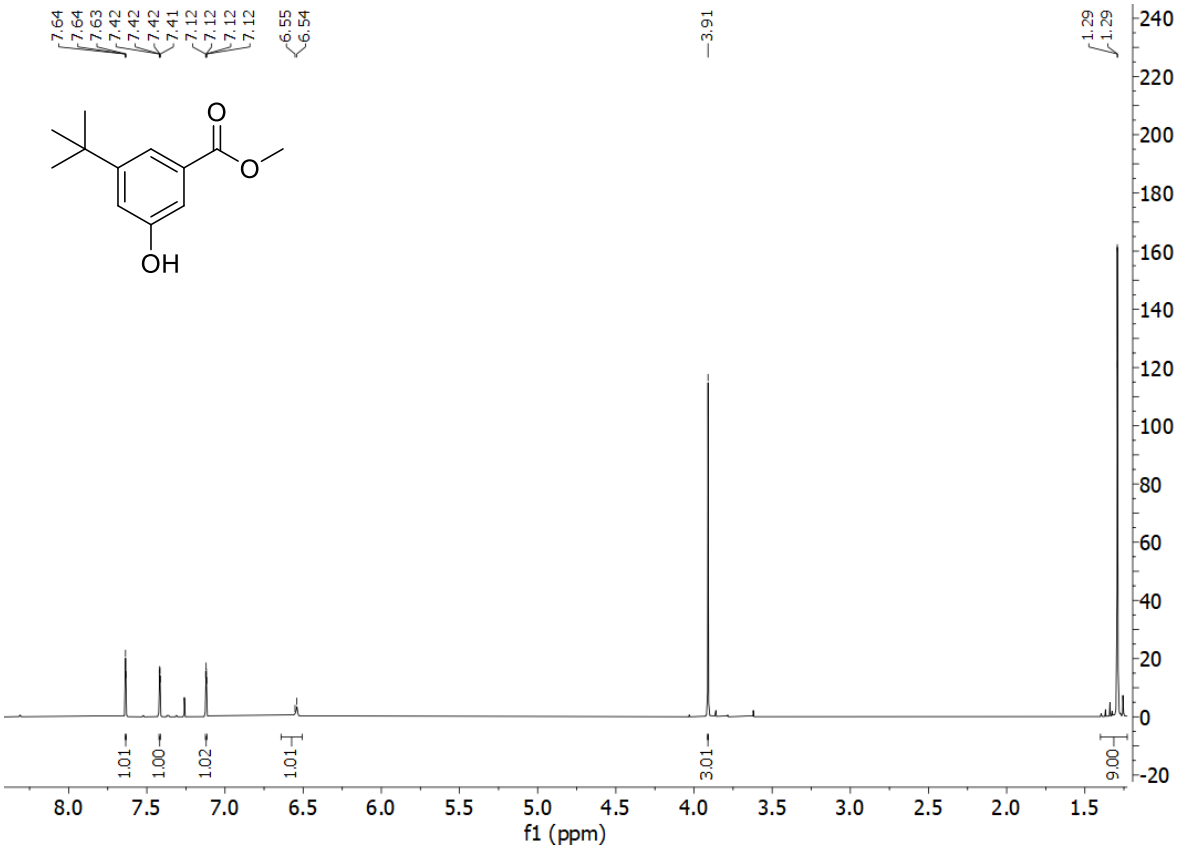

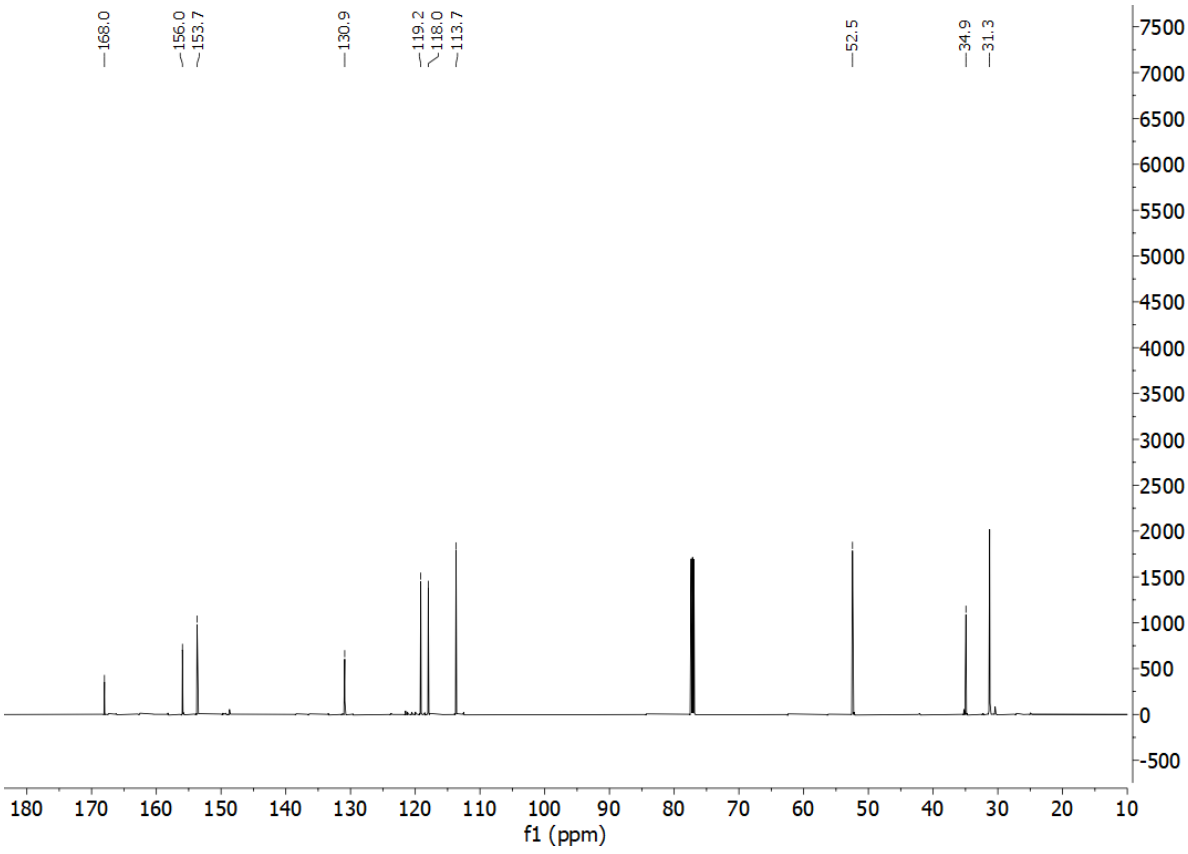

144. *methyl 3-tert-butyl-5-(pent-4'-yn-1'-yloxy)benzoate*

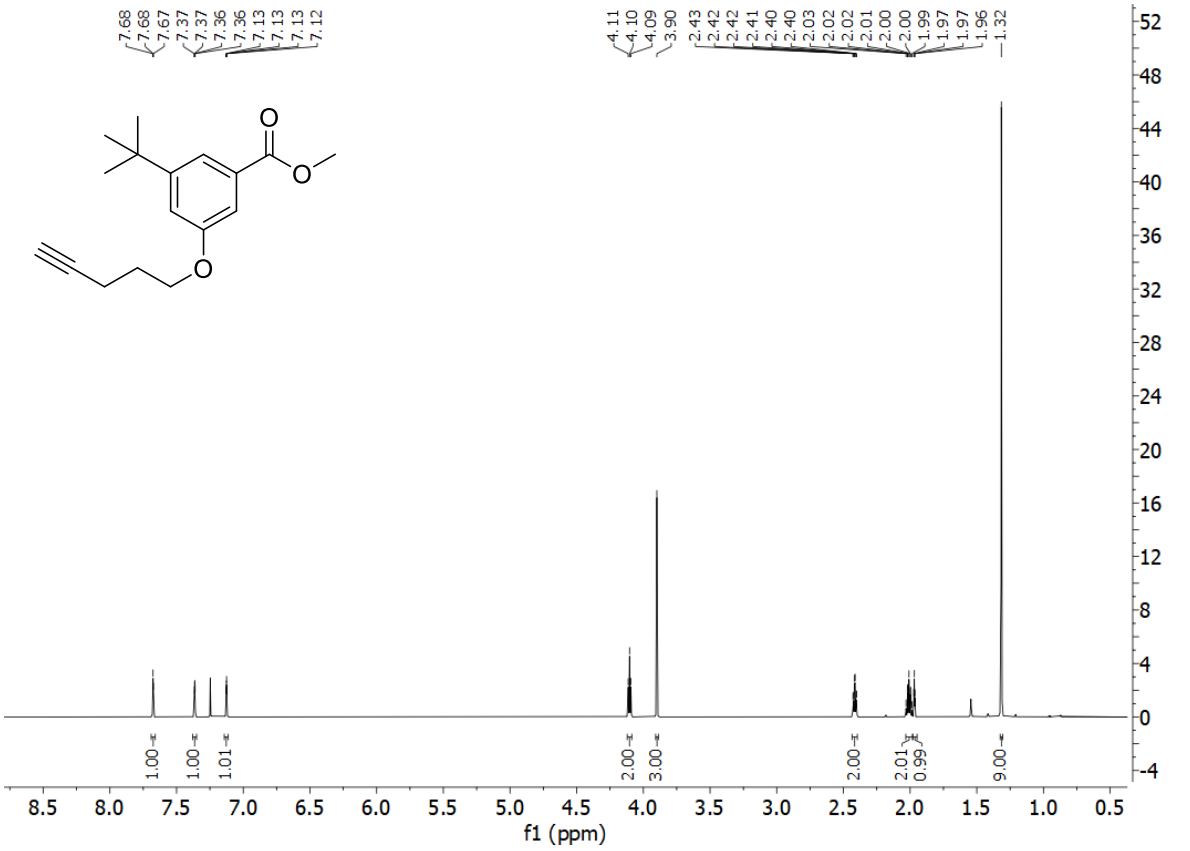

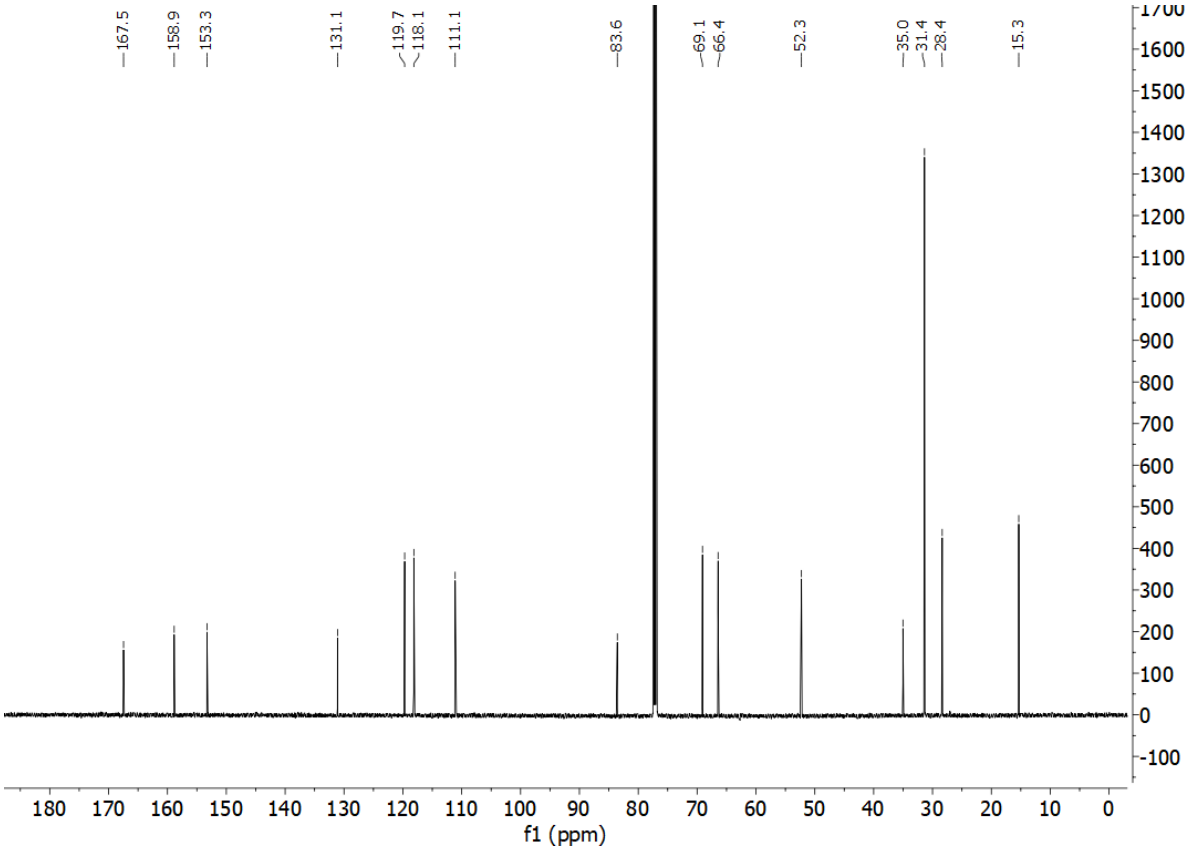

145. *3-tert-butyl-5-(pent-4-yn-1-yloxy)benzoic acid*

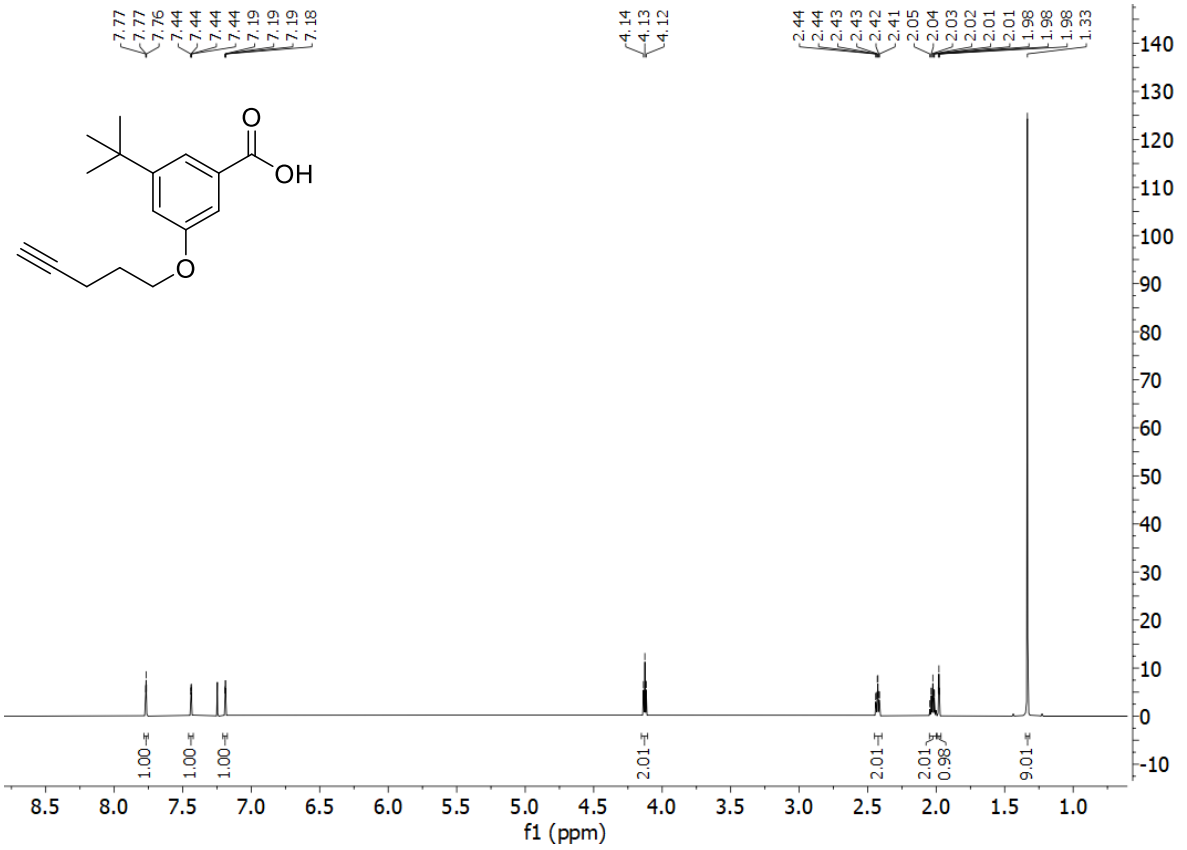

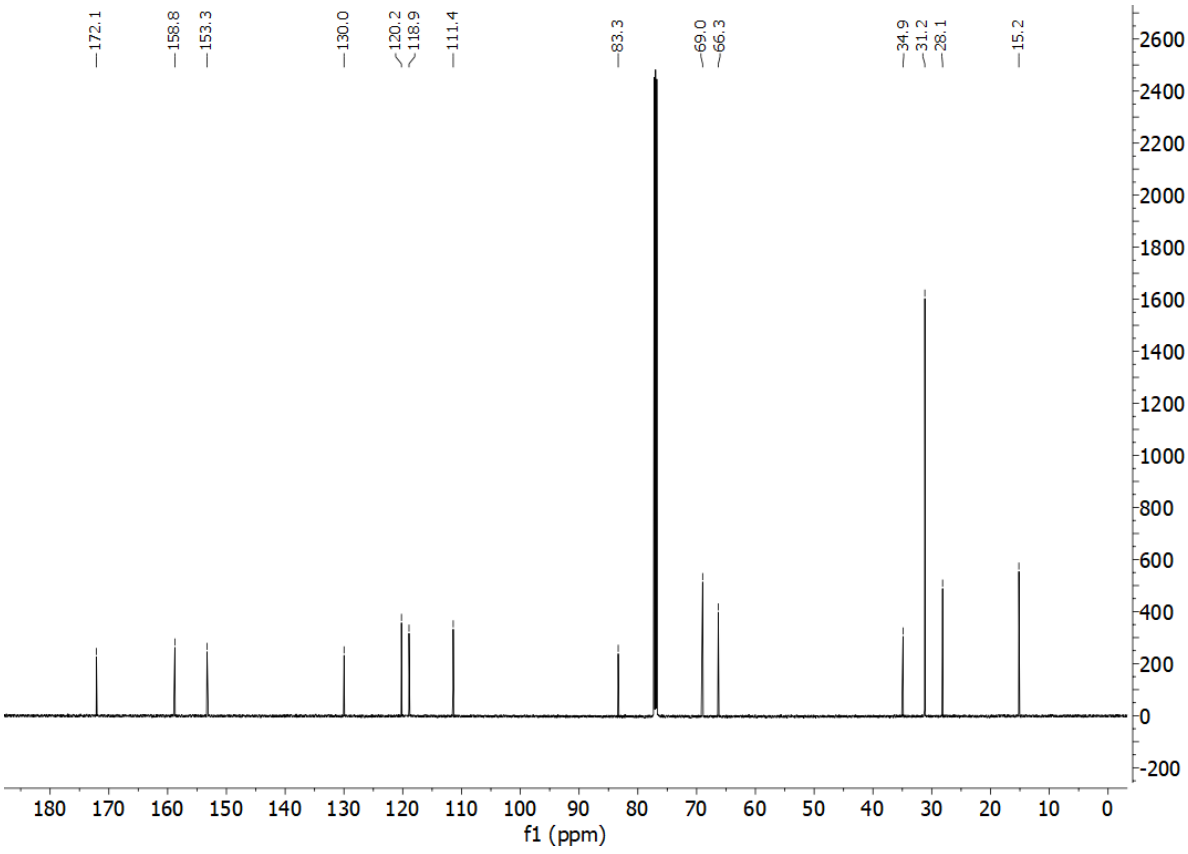

149. *tert-butyl, N - {2'-[4-(2''''-{2''''-[(pent-4'''-yn-1'''-yl) [(prop-2''-en-1''-yloxy) carbonyl] amino] ethoxy} ethoxy) naphthalene-1-sulfonamido] ethyl} carbamate*

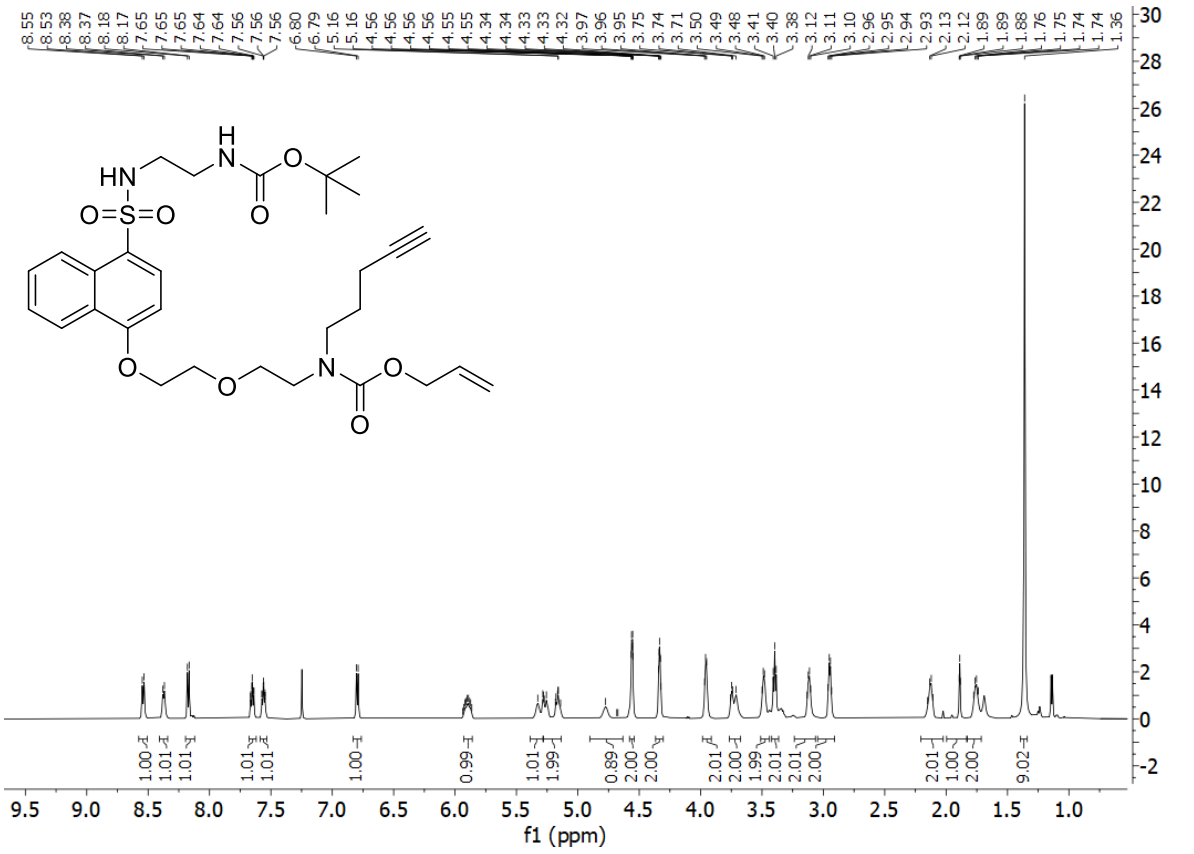

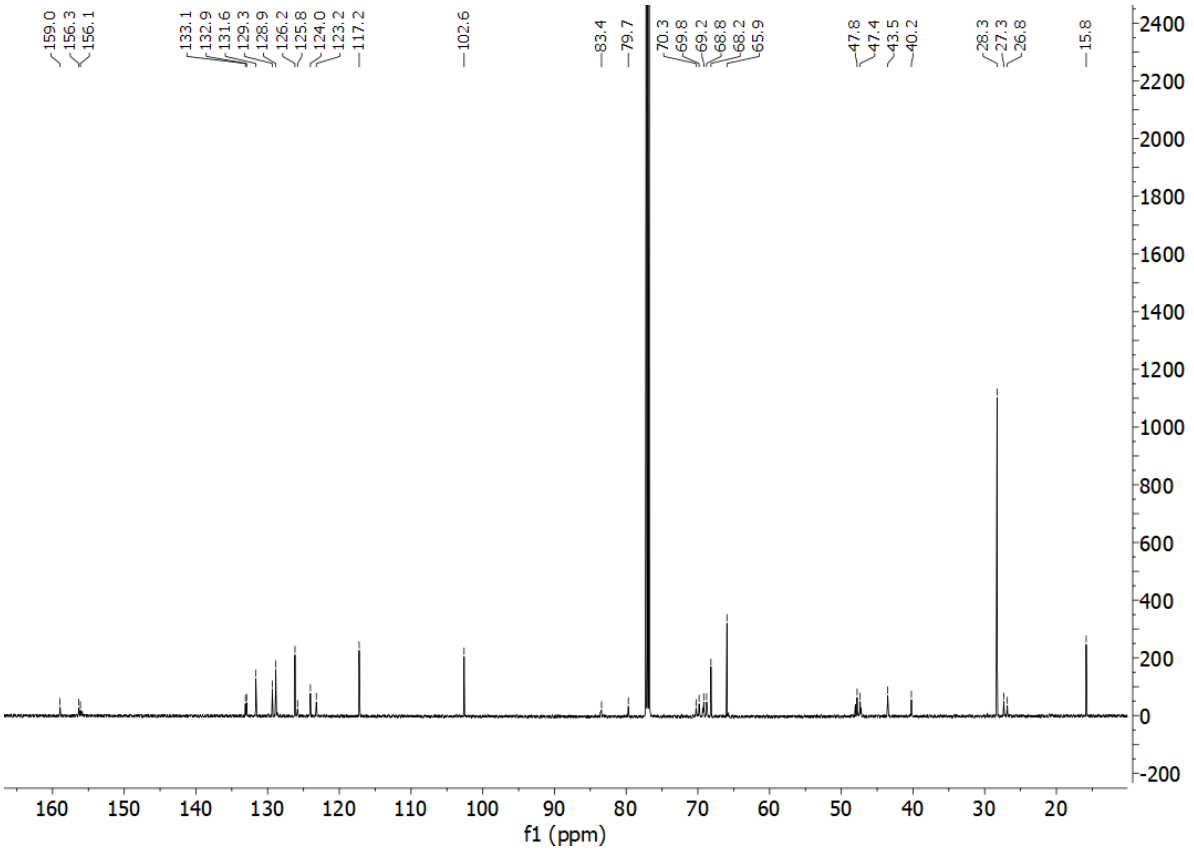

152. *N-[2''-(2'-hydroxyethoxy)ethyl]pent-4-ynamide*

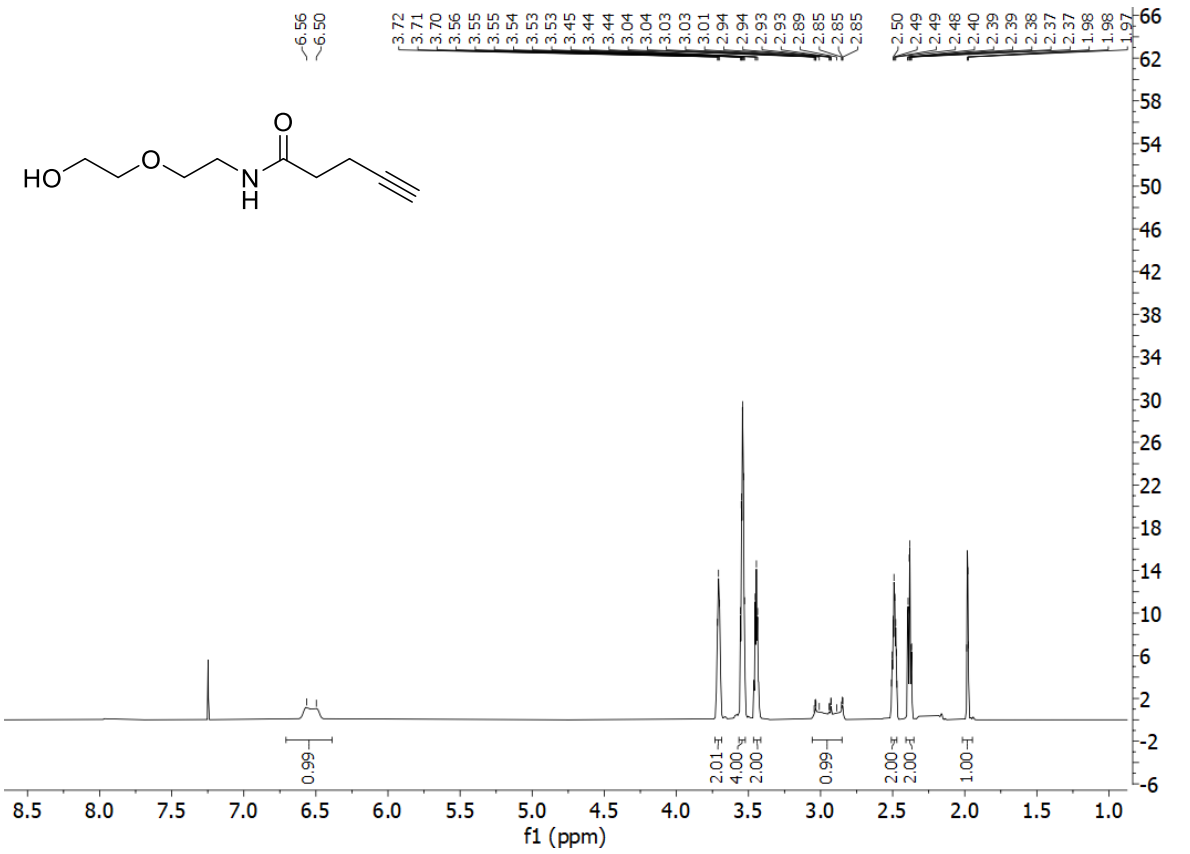

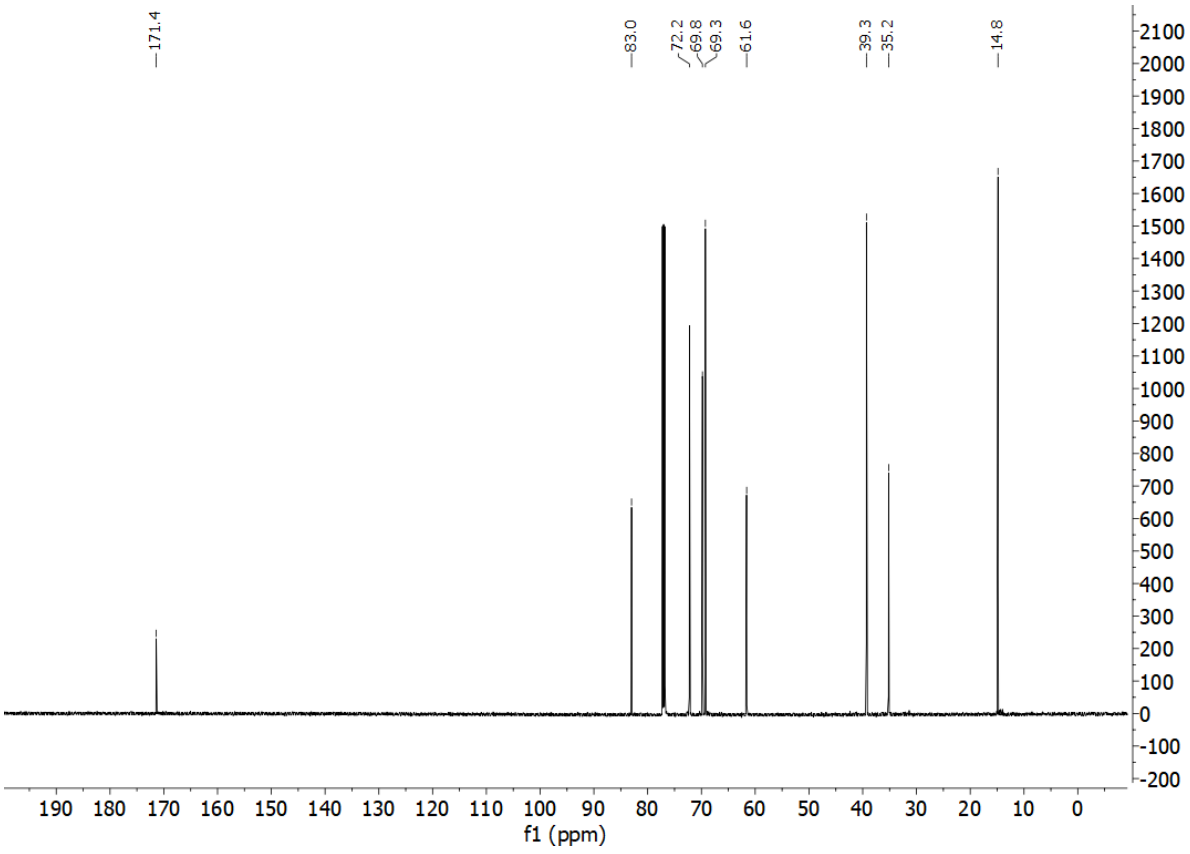

153. *3-tert-butyl-N-[2’’-(2’’’-hydroxyethoxy)ethyl]-N-(pent-4’-yn-1’-yl)benzamide*

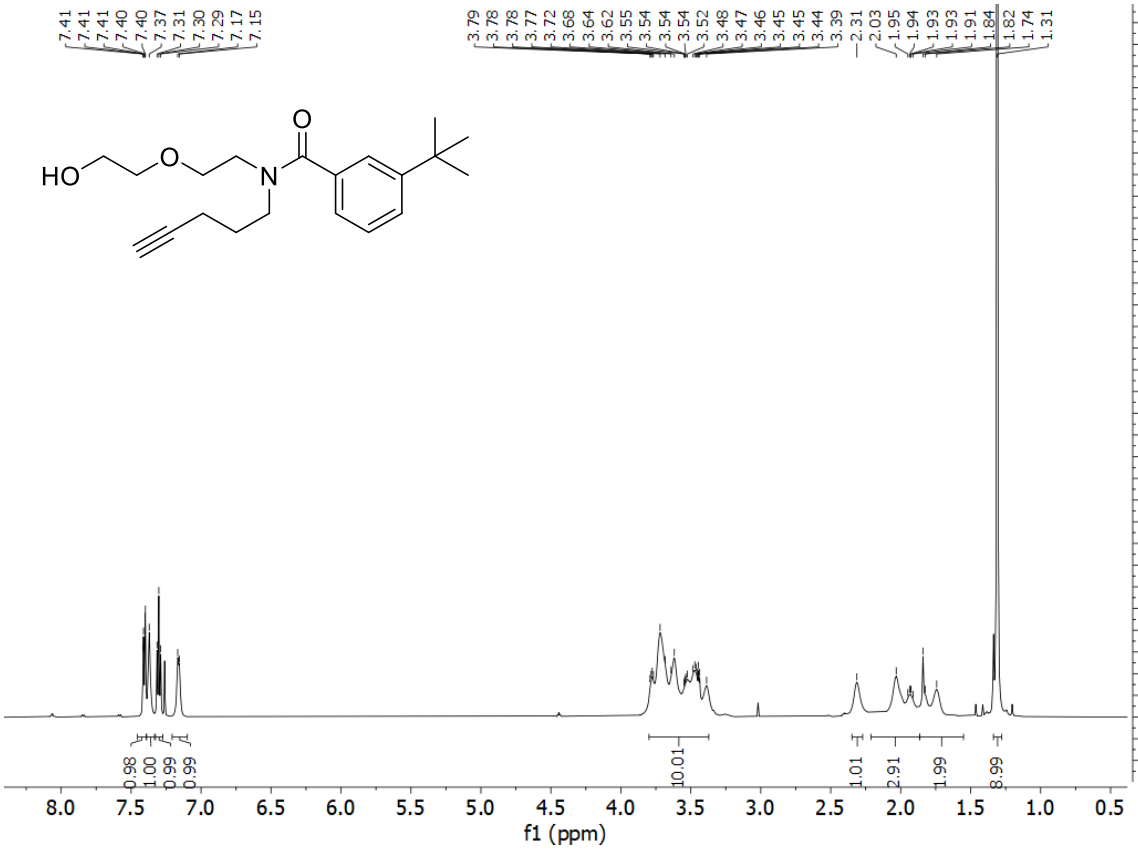

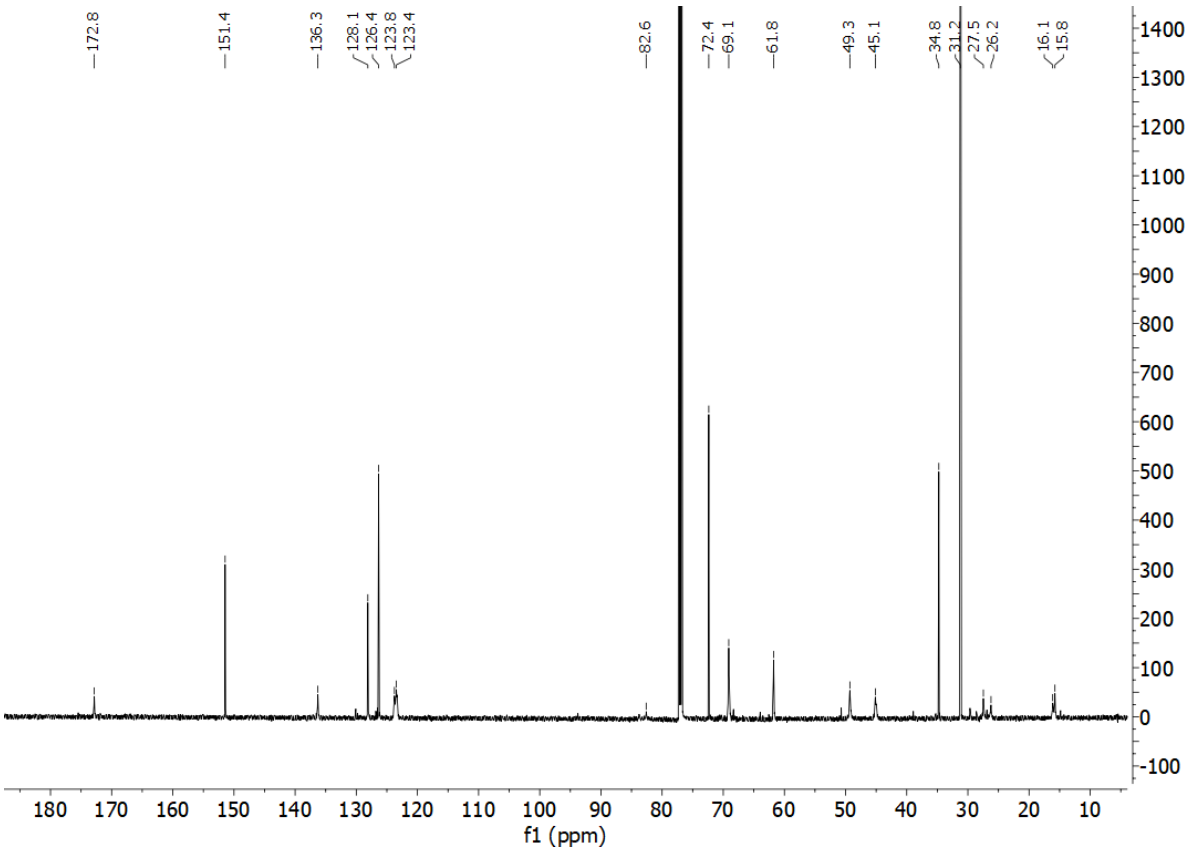

154a. *tert-butyl N-{2'-[4-(2''''-{2''''-[1''-(3''-tert-butylphenyl)-N-(pent-4'''-yn-1'''-yl)formamido] ethoxy} ethoxy) naphthalene-1-sulfonamido] ethyl} carbamate*

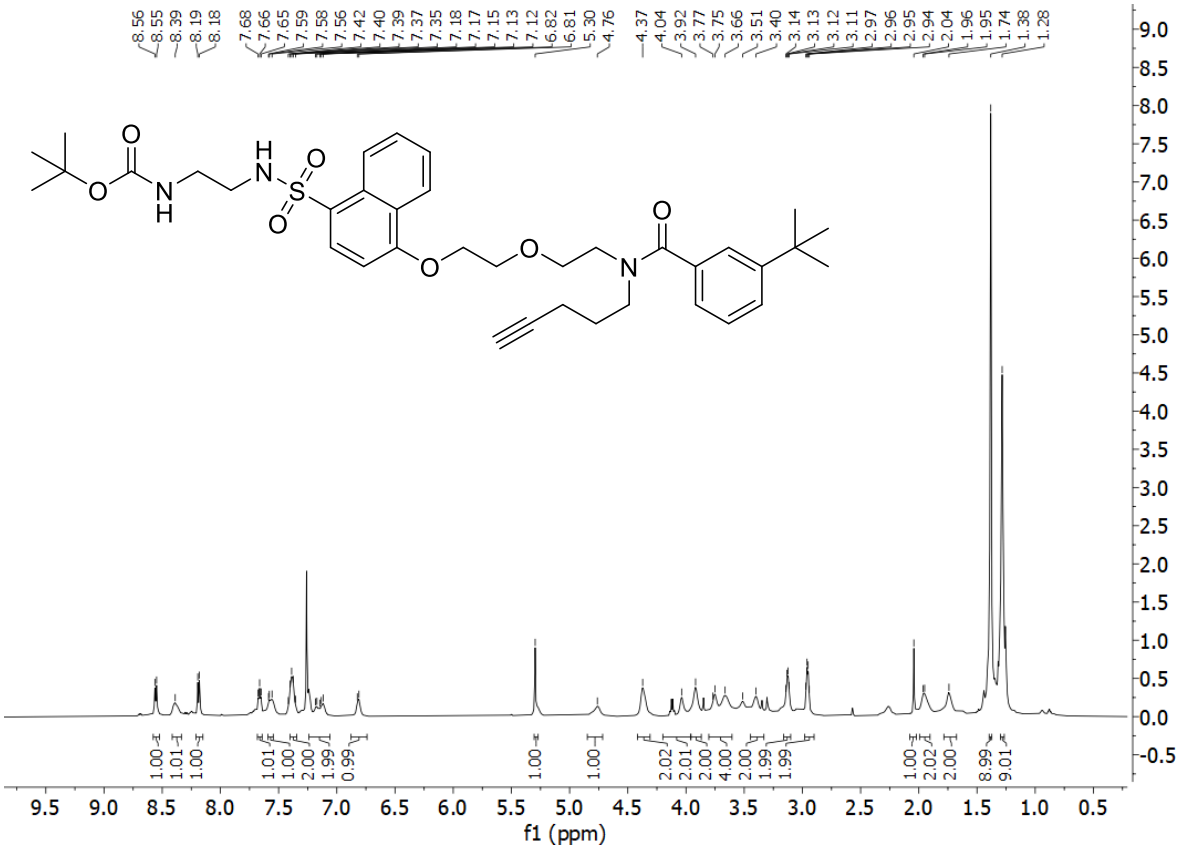

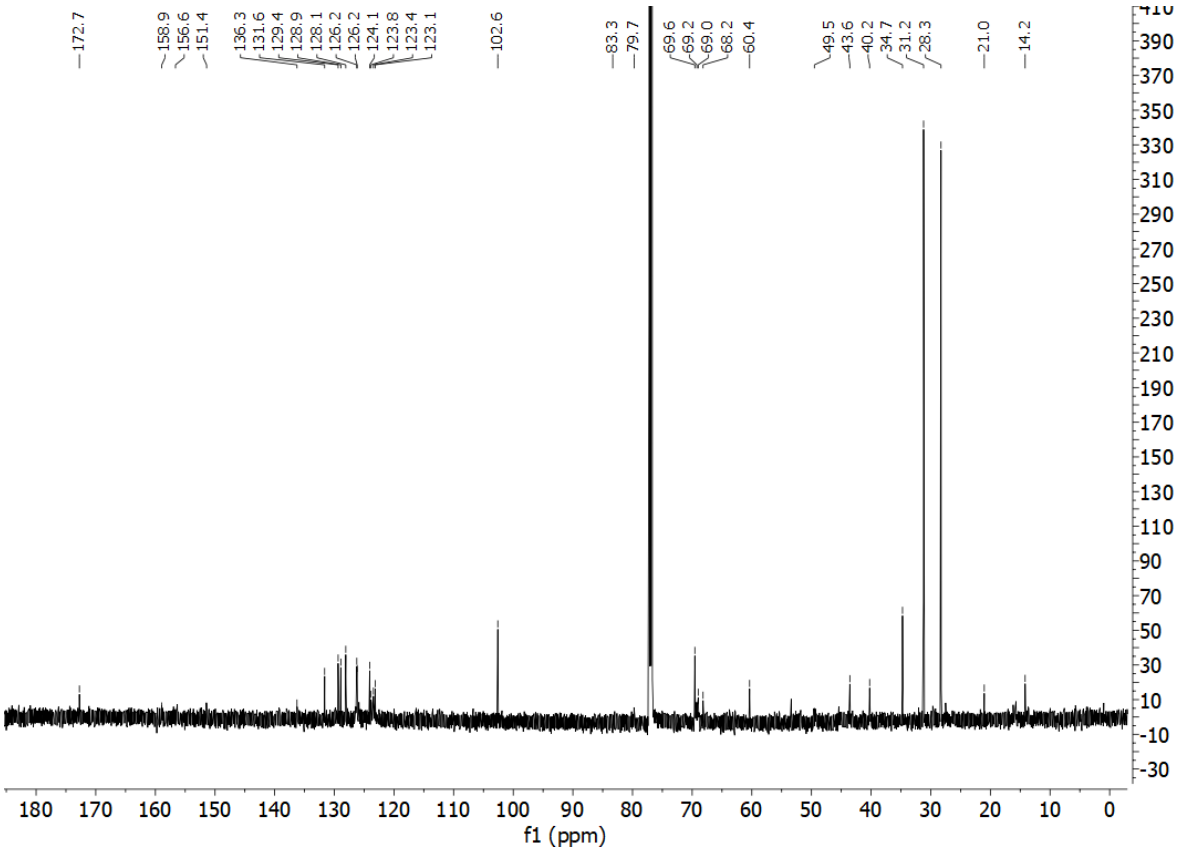

154. *N-{2-[2-({4-[(2-aminoethyl)sulfamoyl]naphthalen-1-yl}oxy)ethoxy]ethyl}-3-tert-butyl-N-(pent-4-yn-1-yl)benzamide hydrochloride*

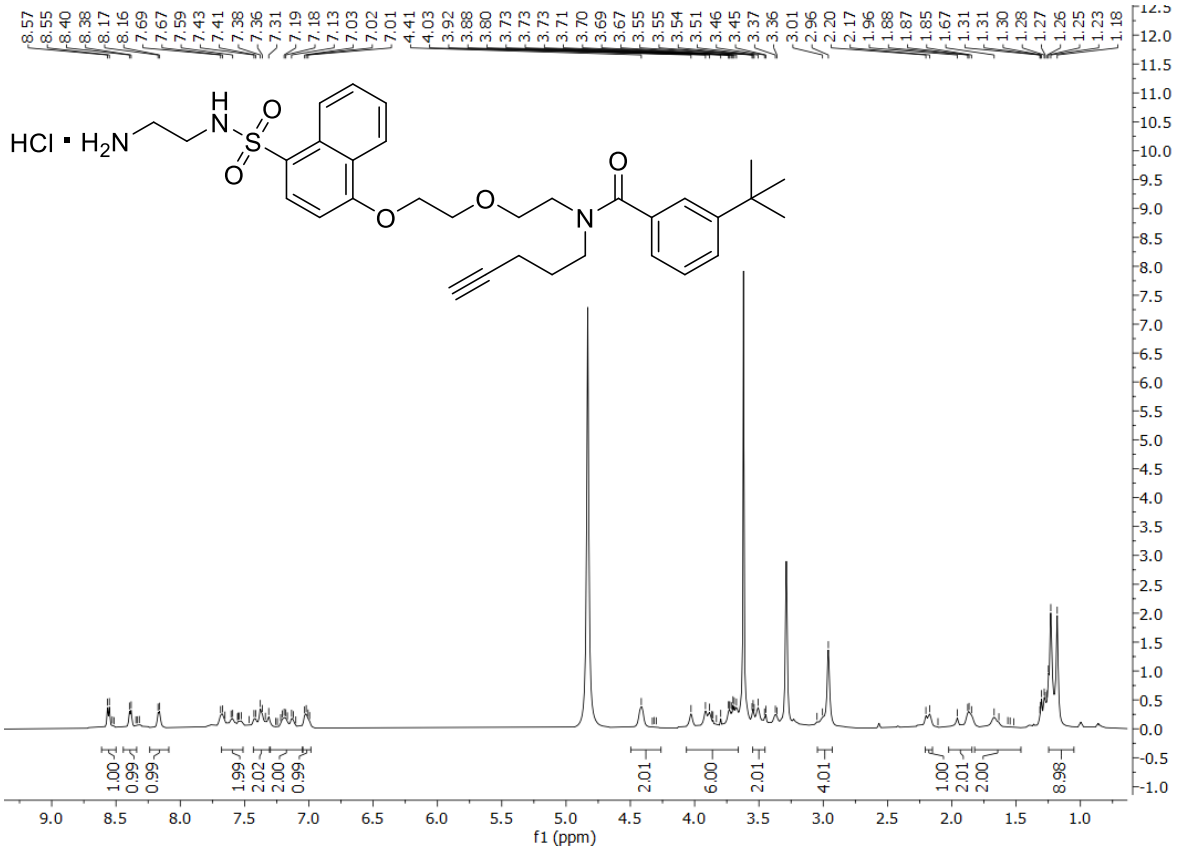

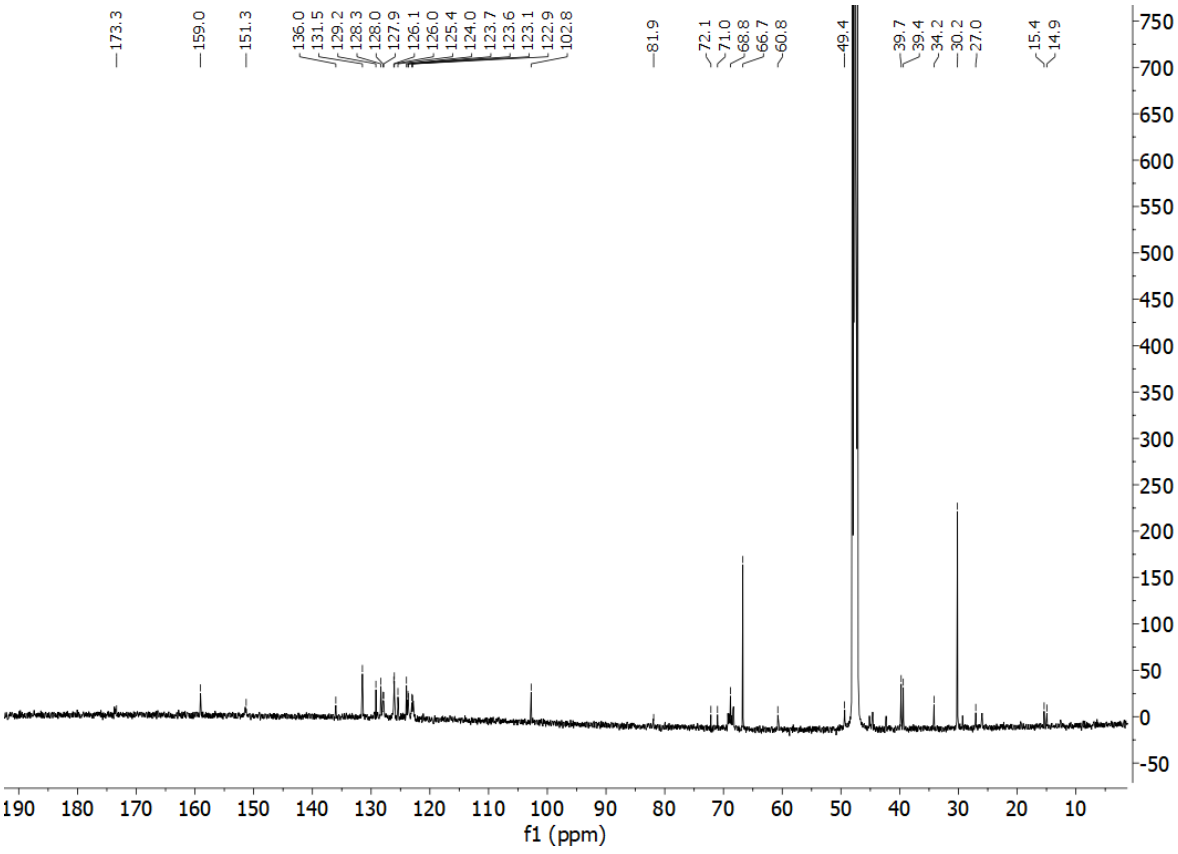

156a. *N-{2’’’’-[2’’’’’-({4-[(2’-aminoethyl)sulfamoyl]naphthalen-1-yl}oxy)ethoxy]ethyl}-3’’-tert-butyl-N-methyl-5’’-(pent-4’’’-yn-1’’’-yloxy)benzamide hydrochloride*

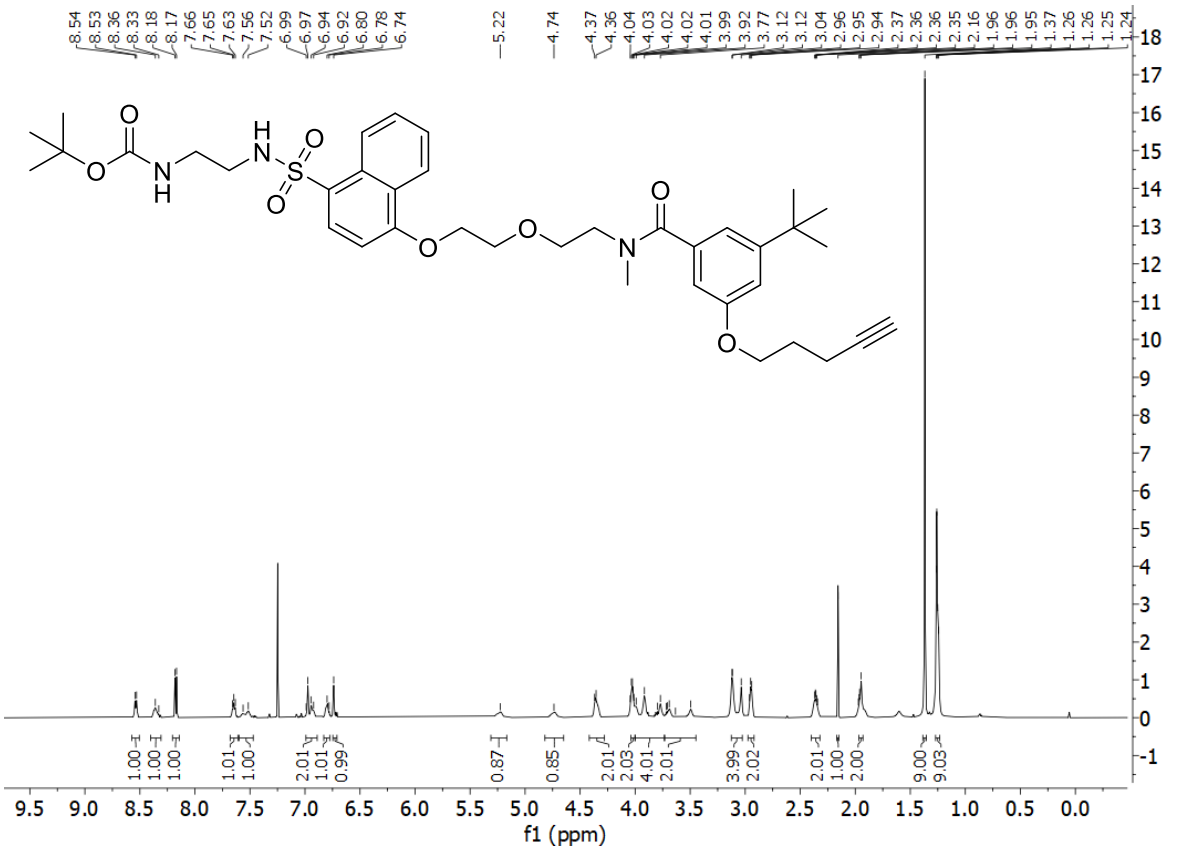

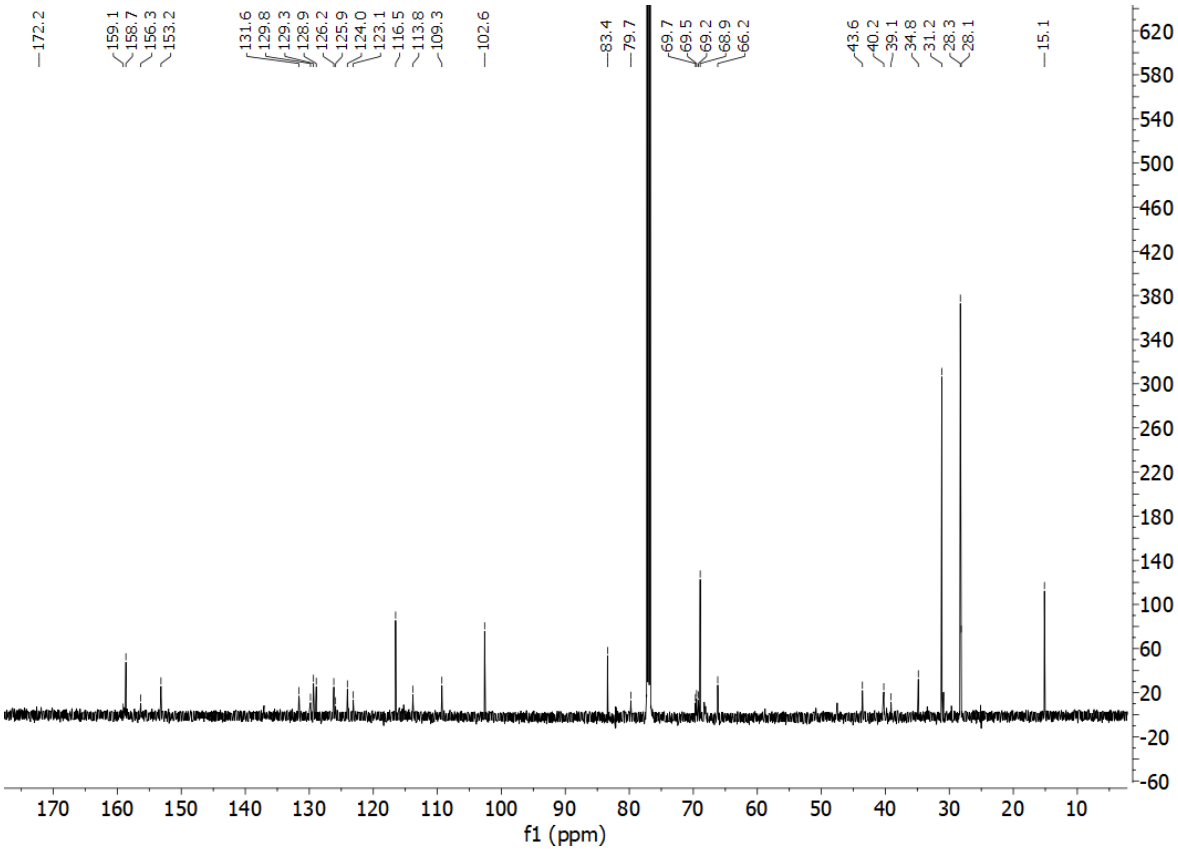

156. *N-{2’’’’-[2’’’’’-({4-[(2’-aminoethyl)sulfamoyl]naphthalen-1-yl}oxy)ethoxy]ethyl}-3’’-tert-butyl-N-methyl-5’’-(pent-4’’’-yn-1’’’-yloxy)benzamide hydrochloride*

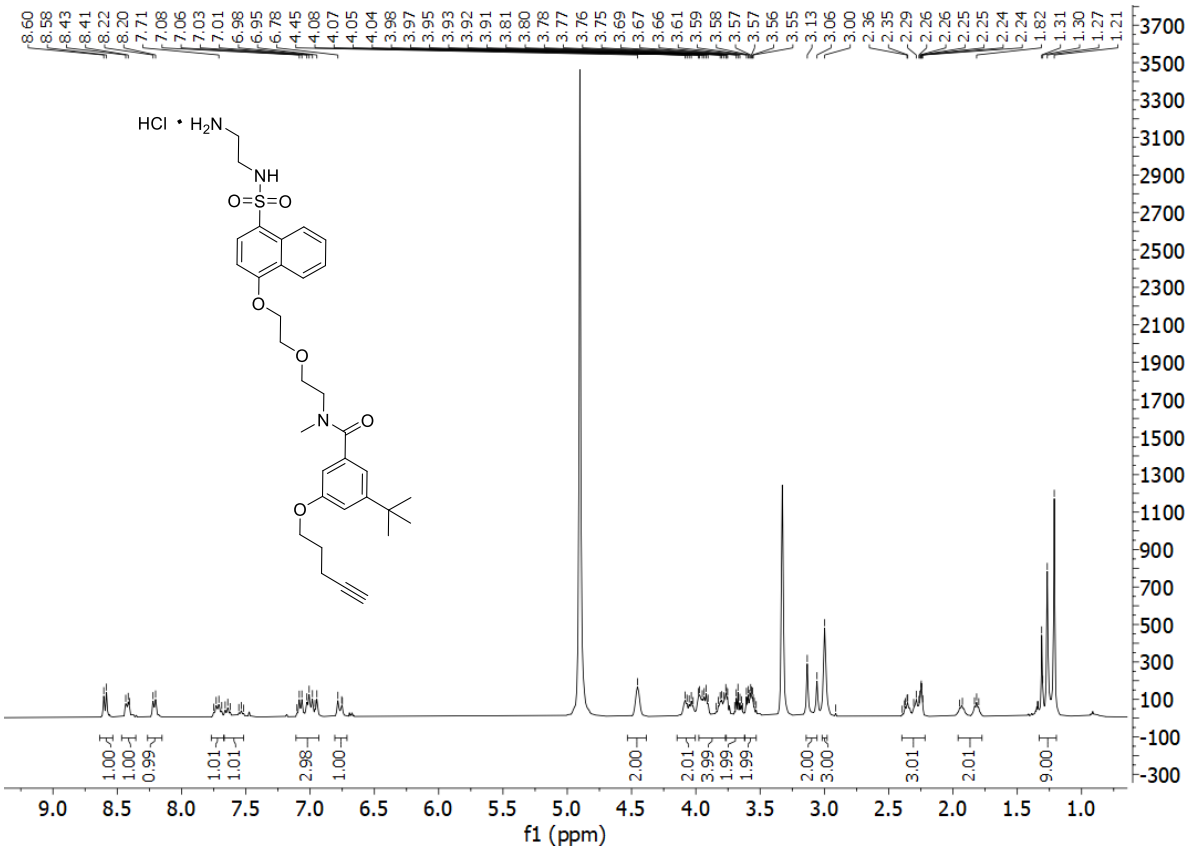

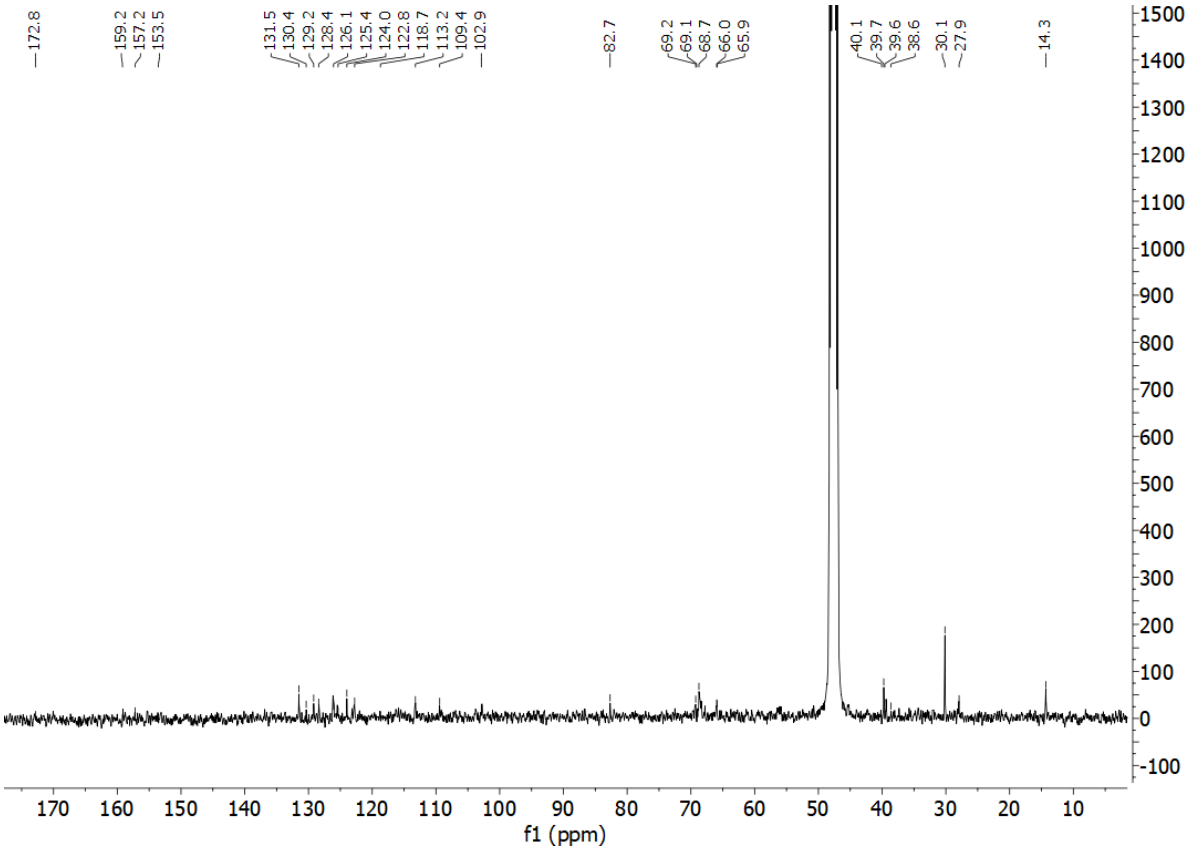

160. *methyl 3-formylbenzoate*

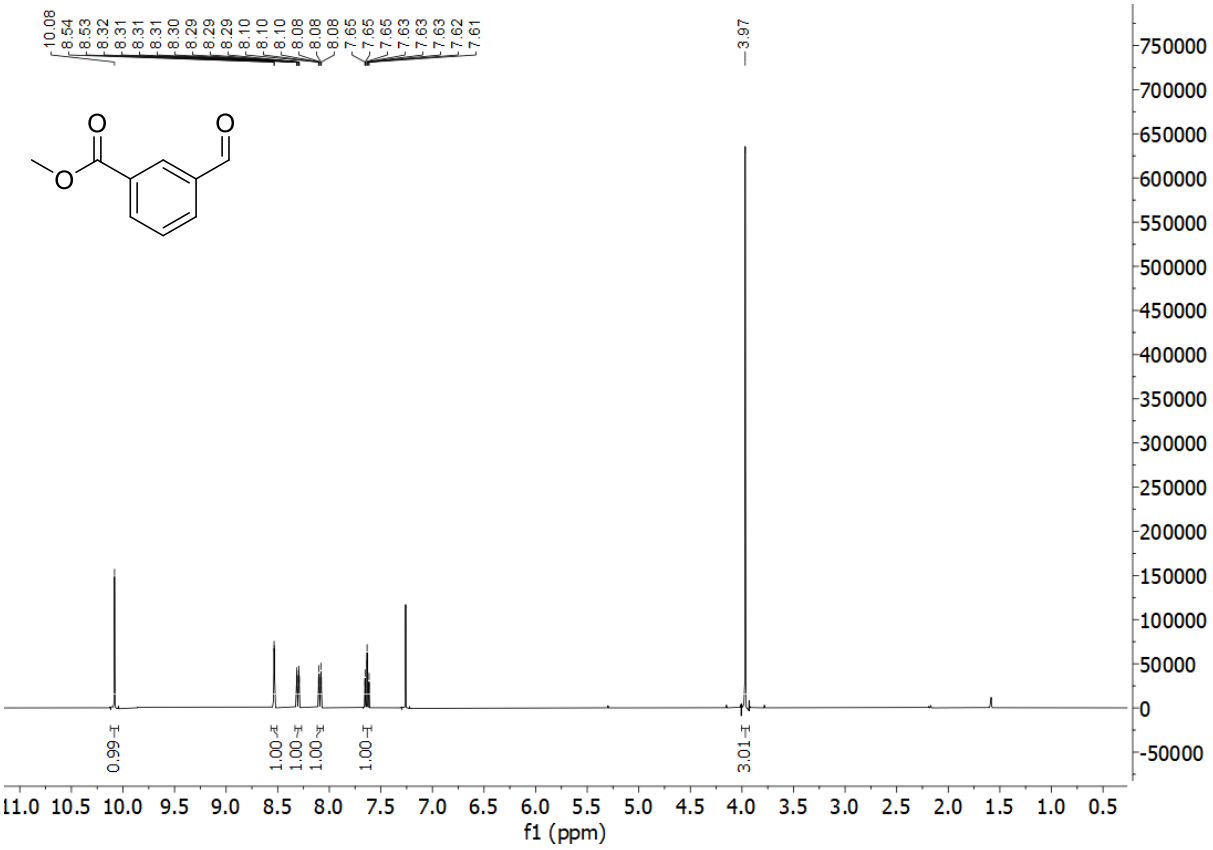

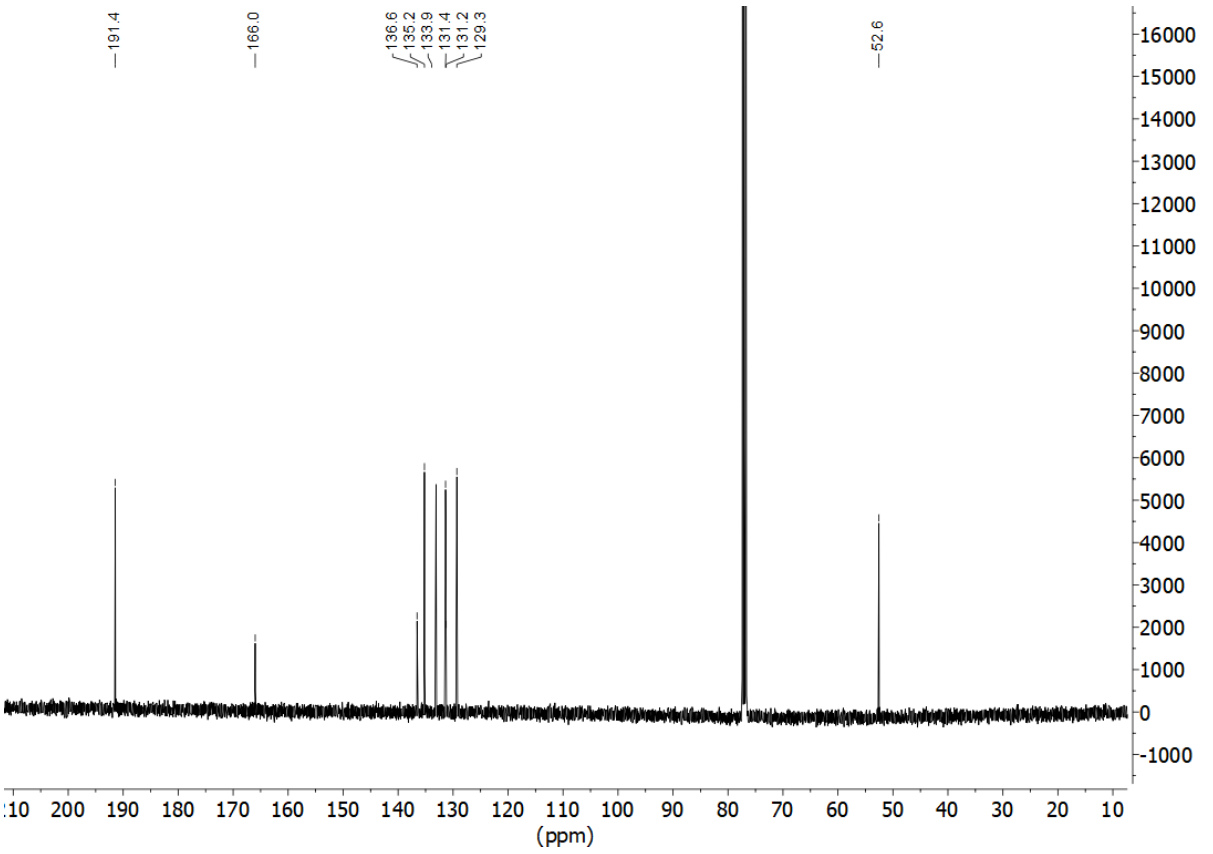

161. *methyl 3-(2',2',2'-trifluoroacetyl)benzoate*

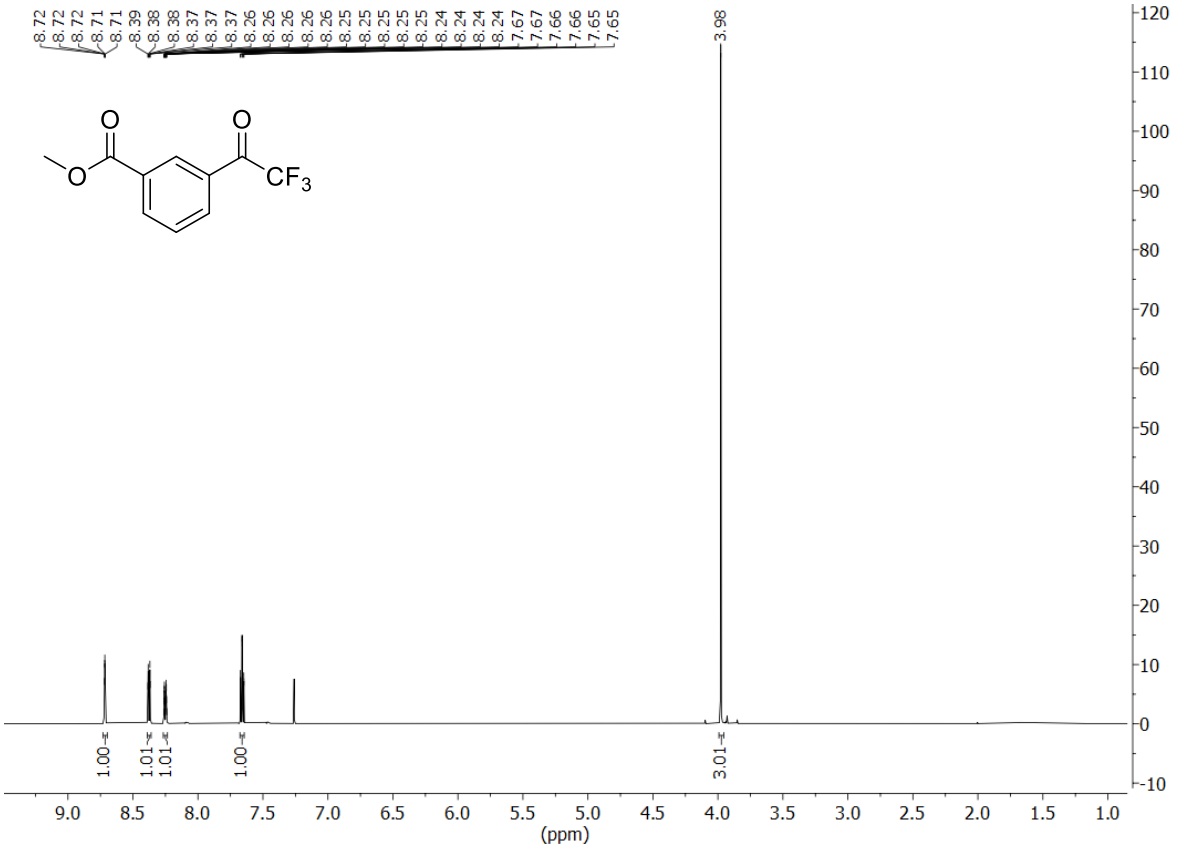

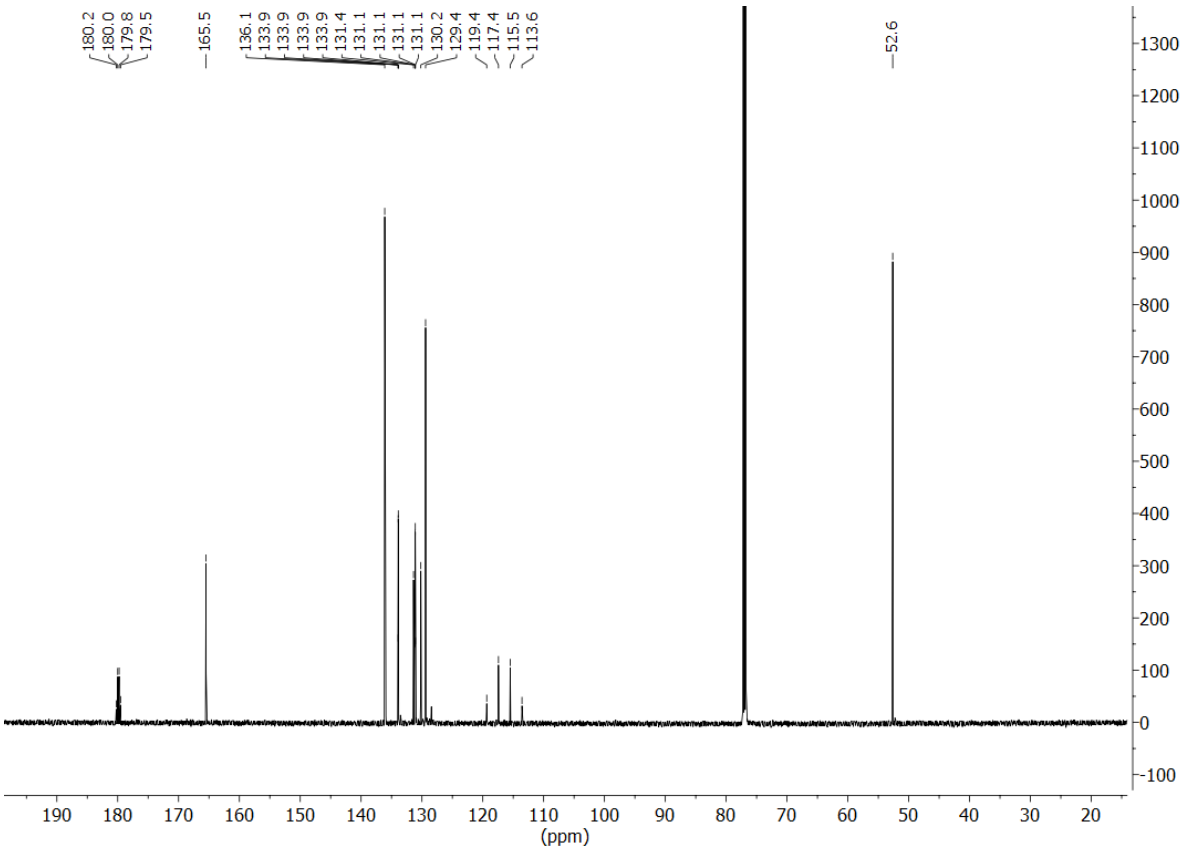

167. *methyl 3-[2',2',2'-trifluoro-1-(hydroxyimino)ethyl]benzoate*

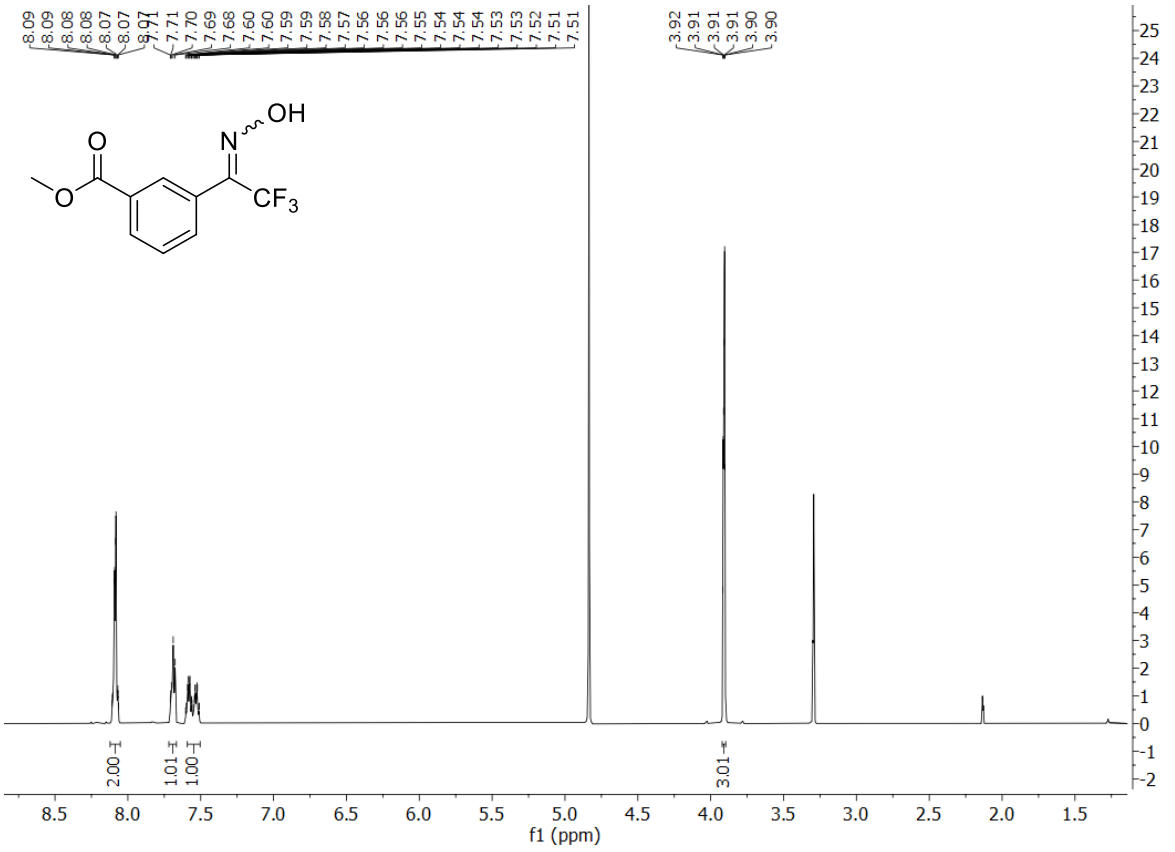

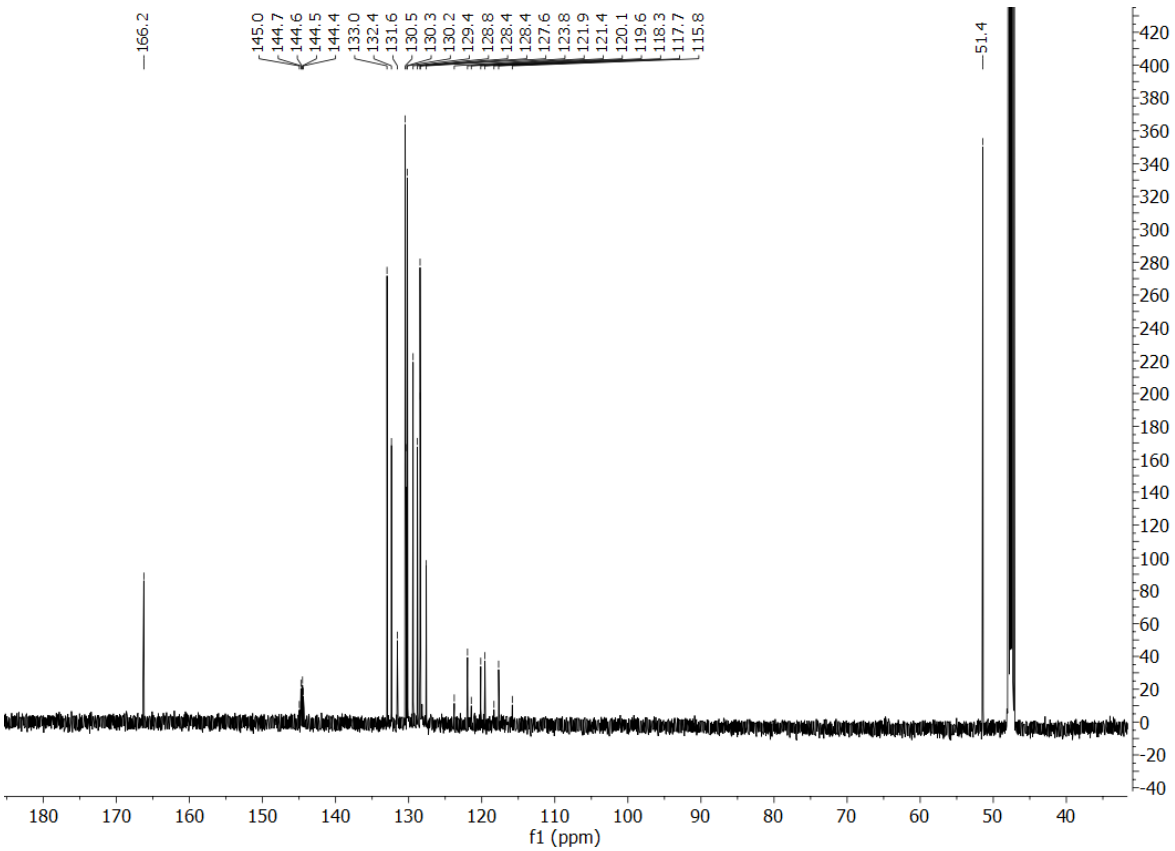

169. *methyl 3-[1'-(trifluoromethyl)diaziridin-1-yl]benzoate*

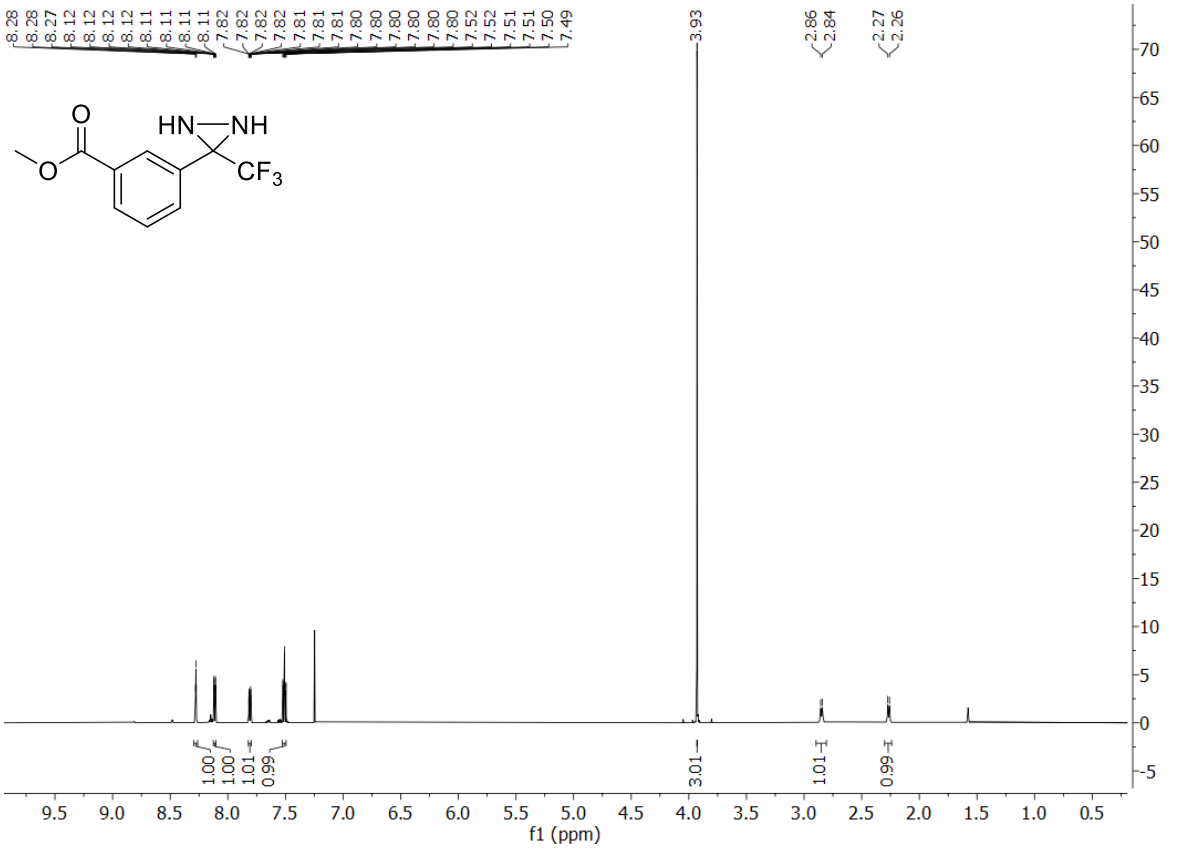

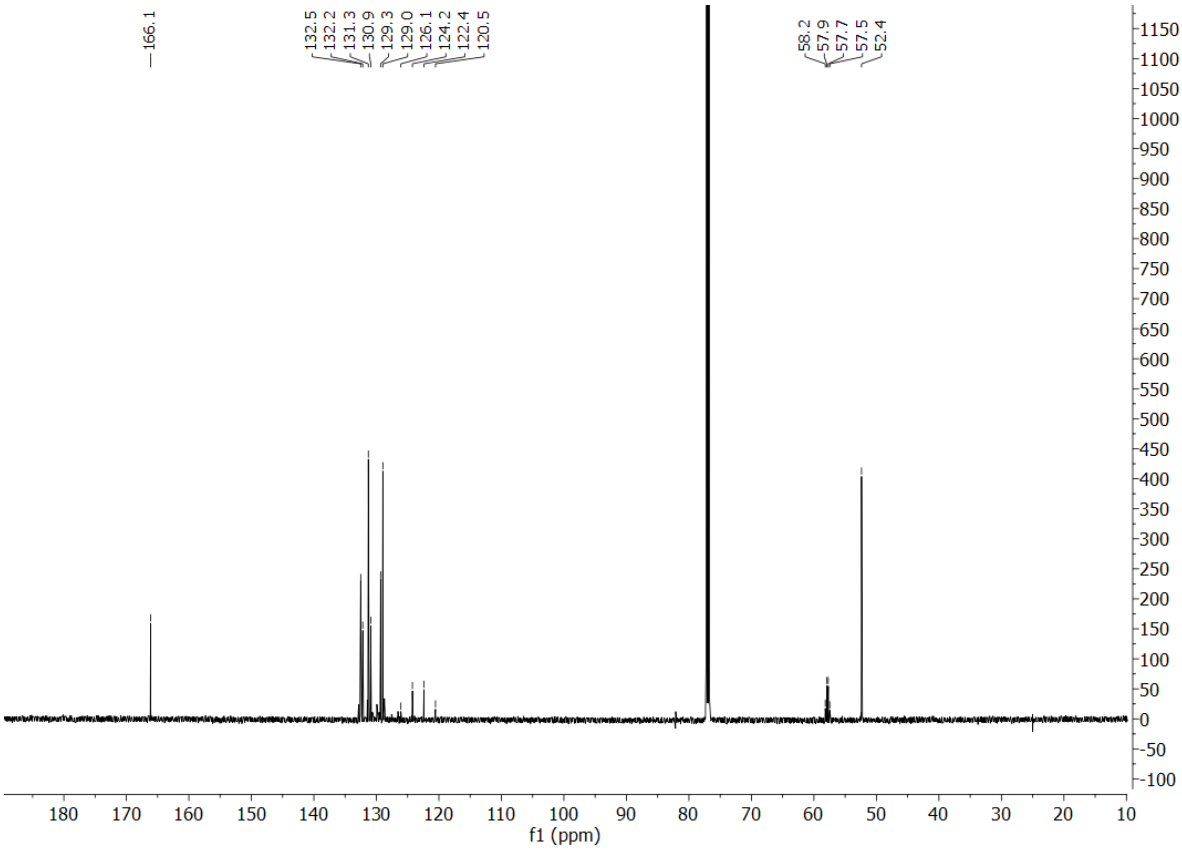

170. *methyl 3-[3'-(trifluoromethyl)-diazirin-3'-yl]benzoate*

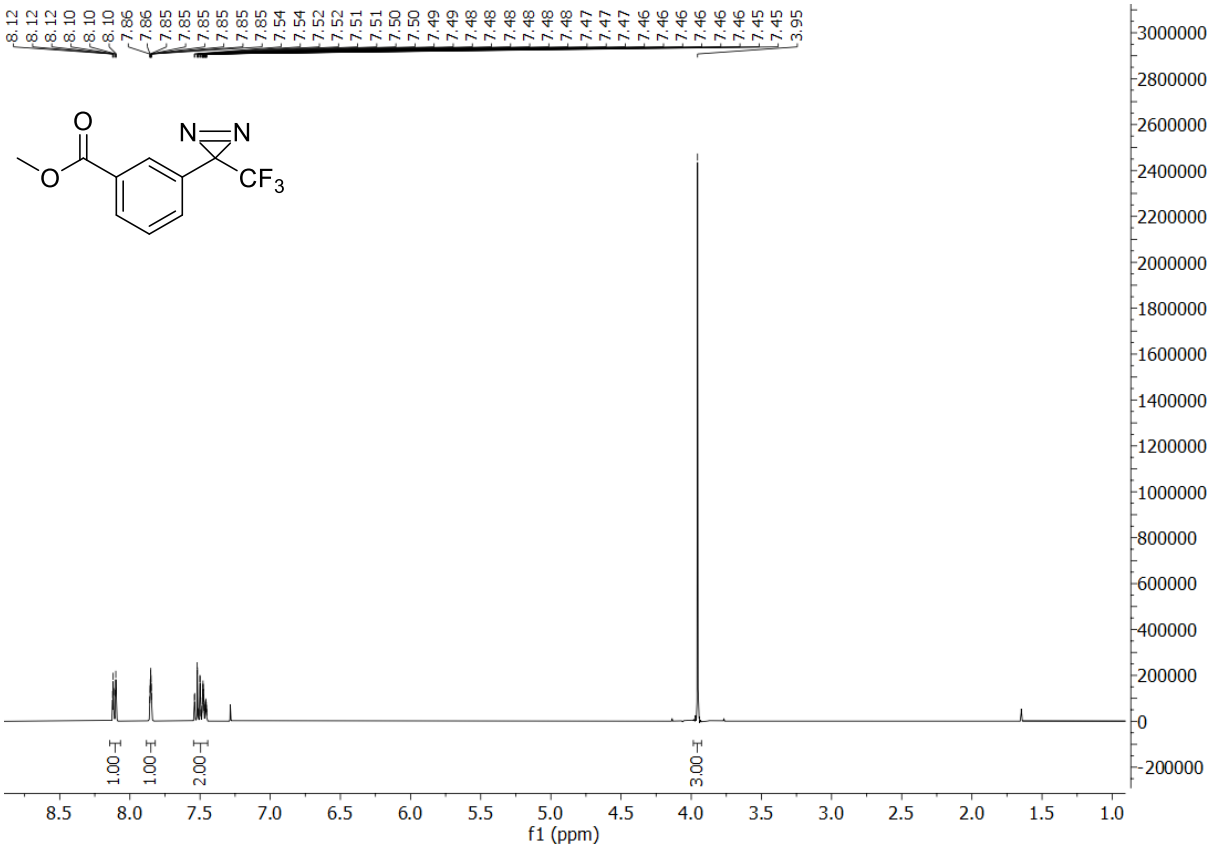

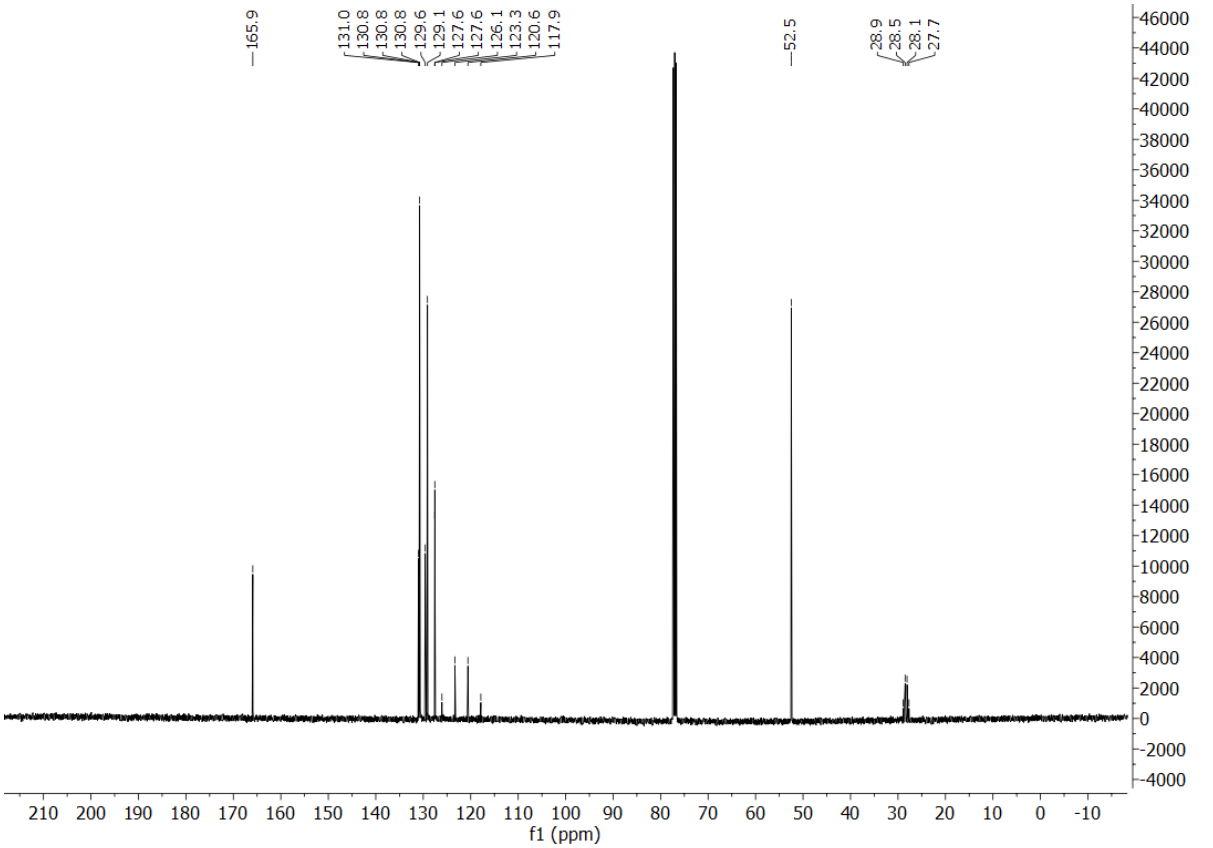

158. *3-[3'-(trifluoromethyl)-diazirin-3'-yl]benzoic acid*

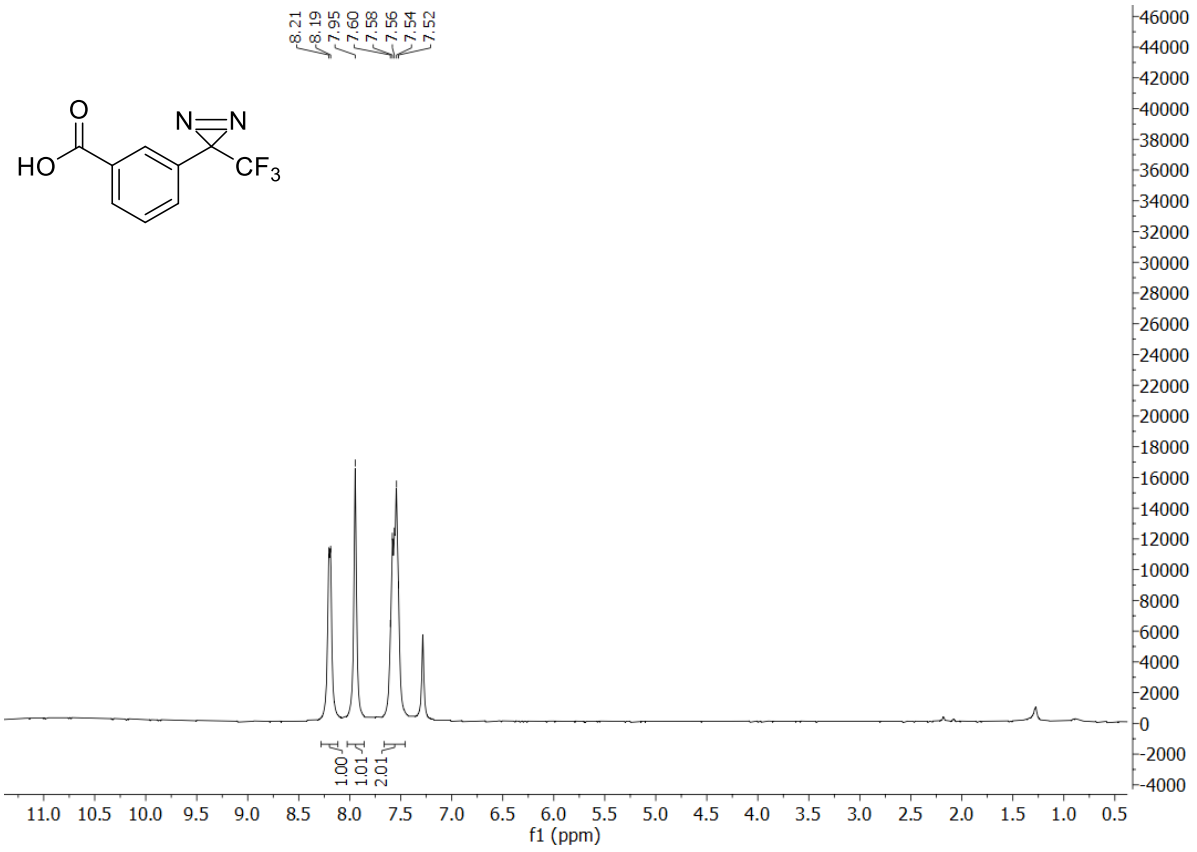

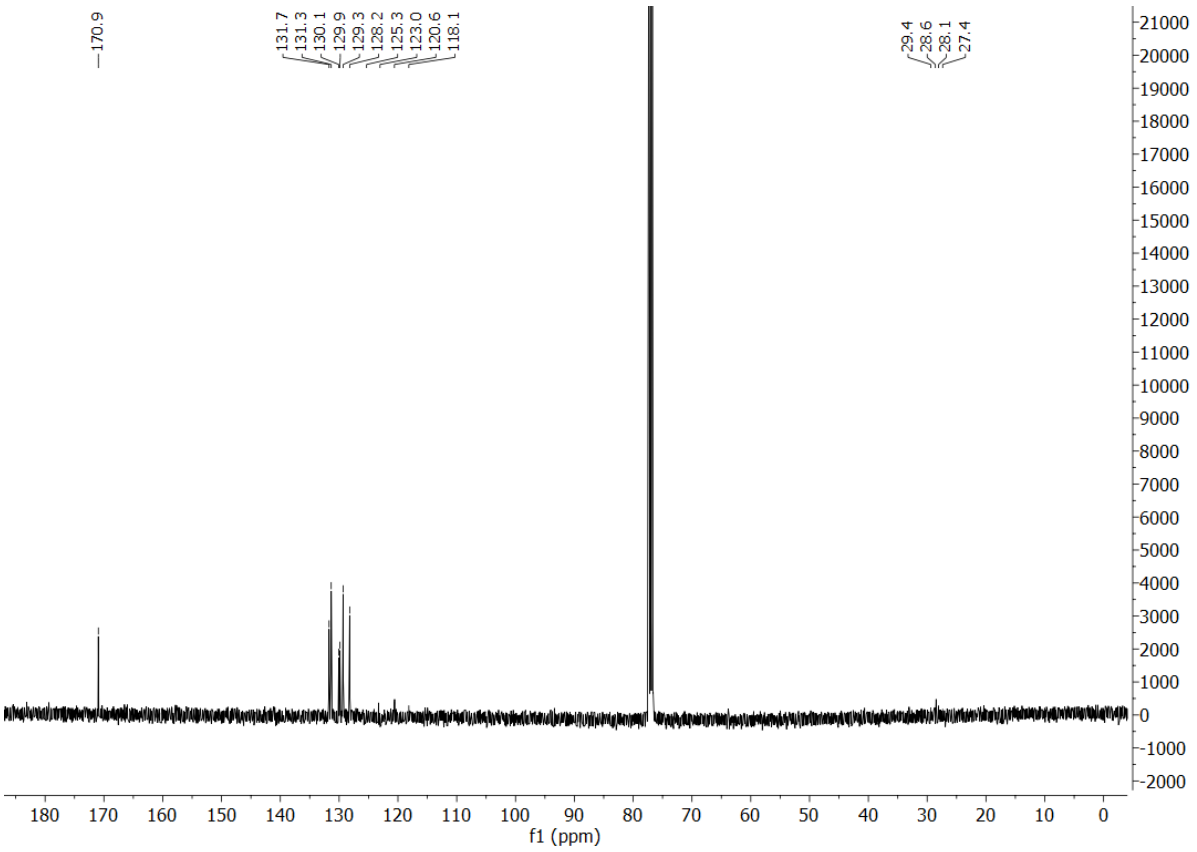

178. *tert-butyl 3-bromobenzoate*

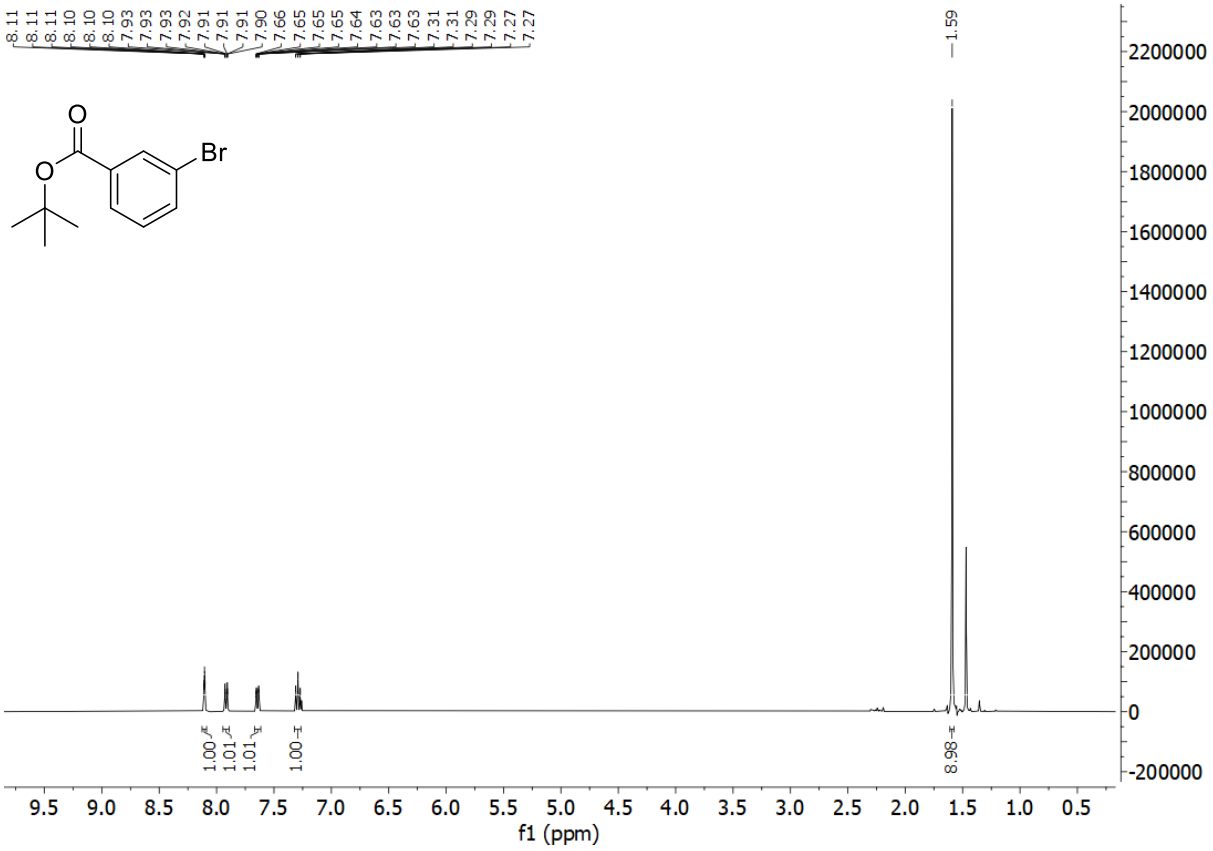

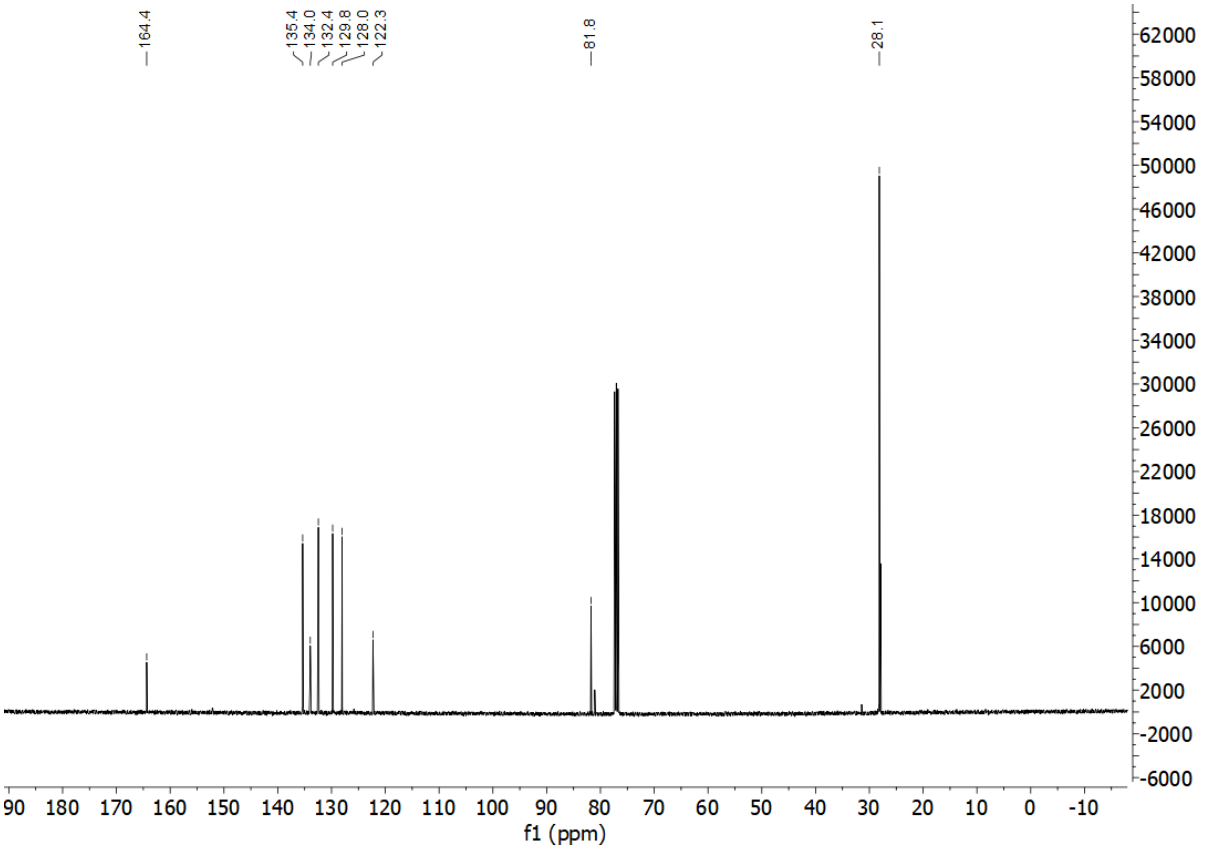

179. *tert-butyl 3-bromo-5-hydroxybenzoate*

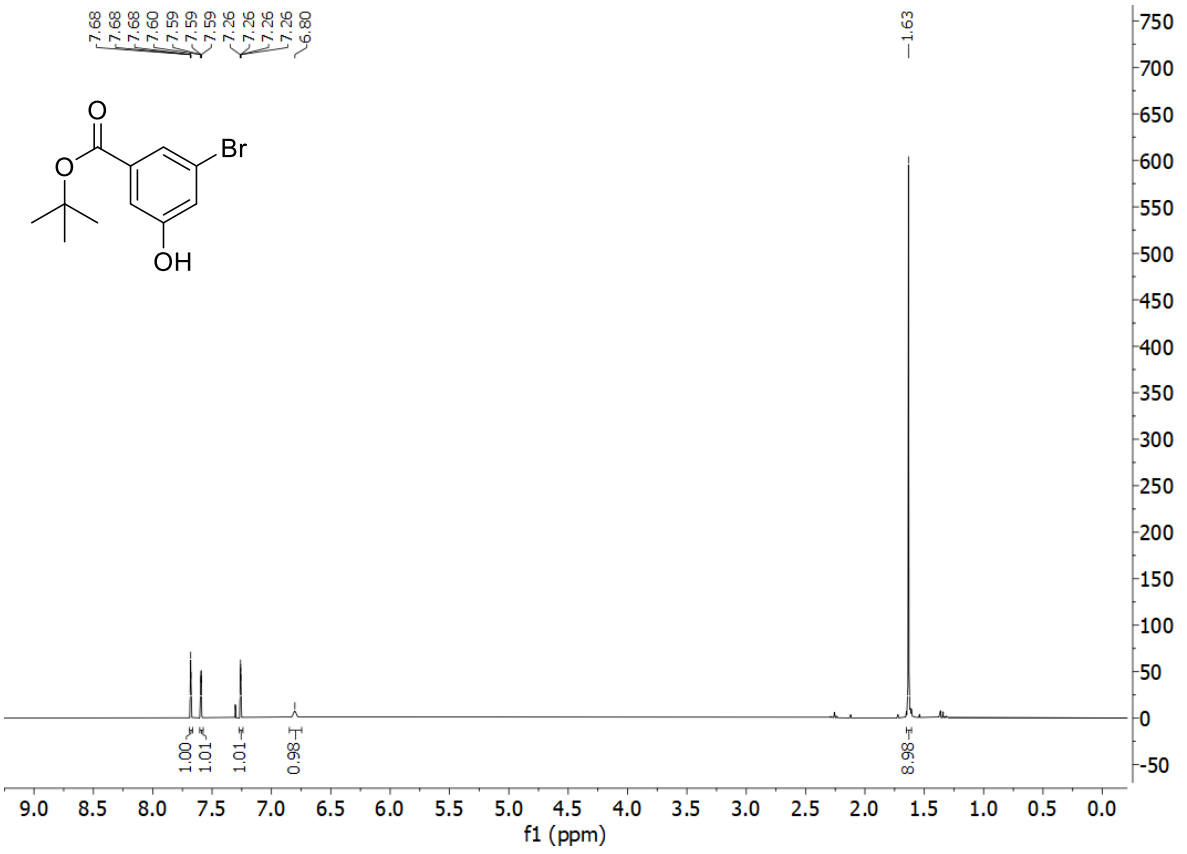

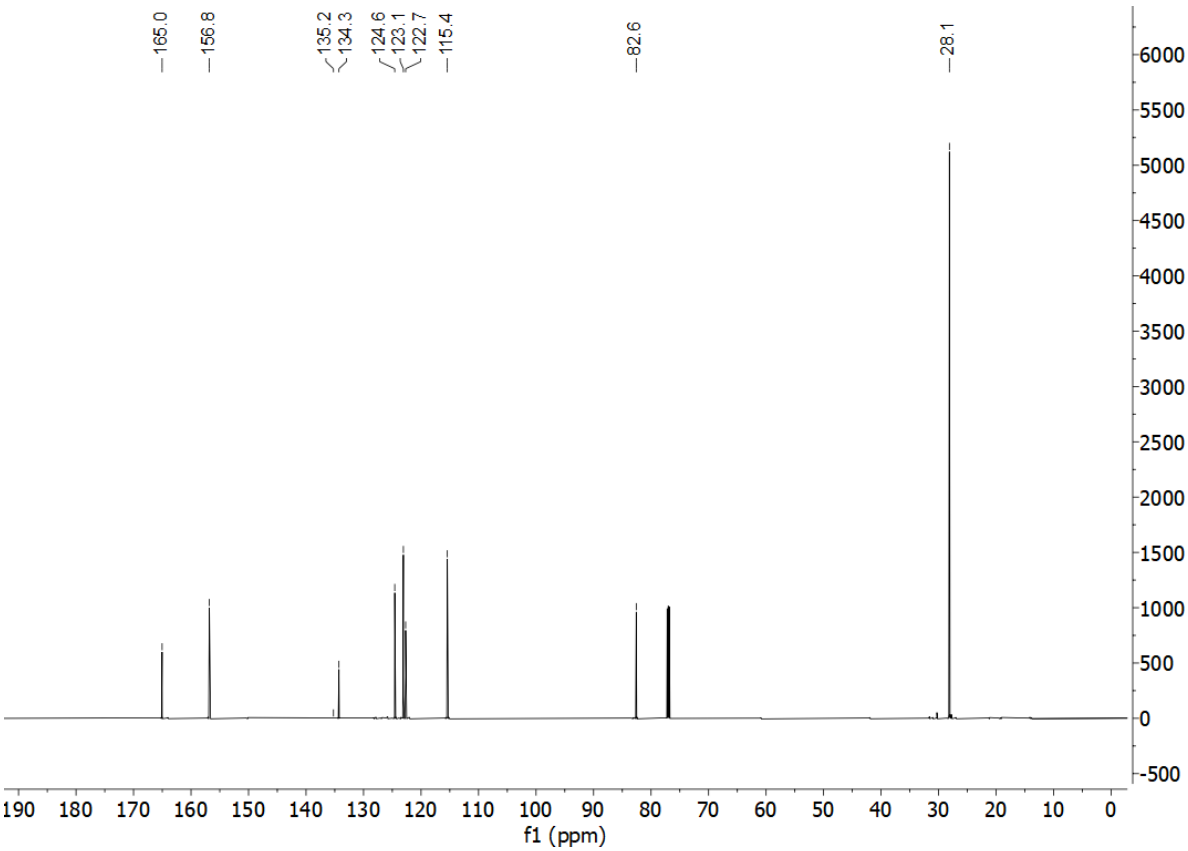

180. *tert-butyl 3-bromo-5-{[5'-(trimethylsilyl)pent-4'-yn-1'-yl]oxy}benzoate*

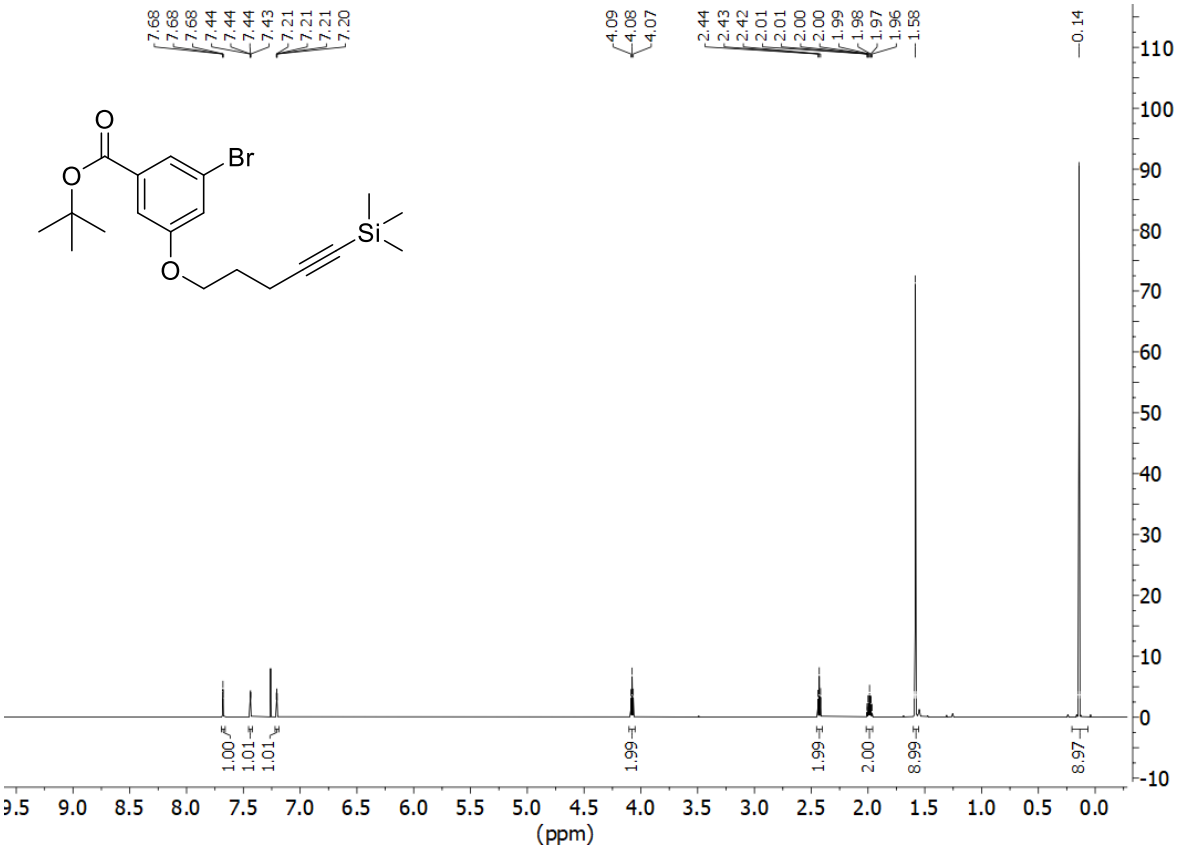

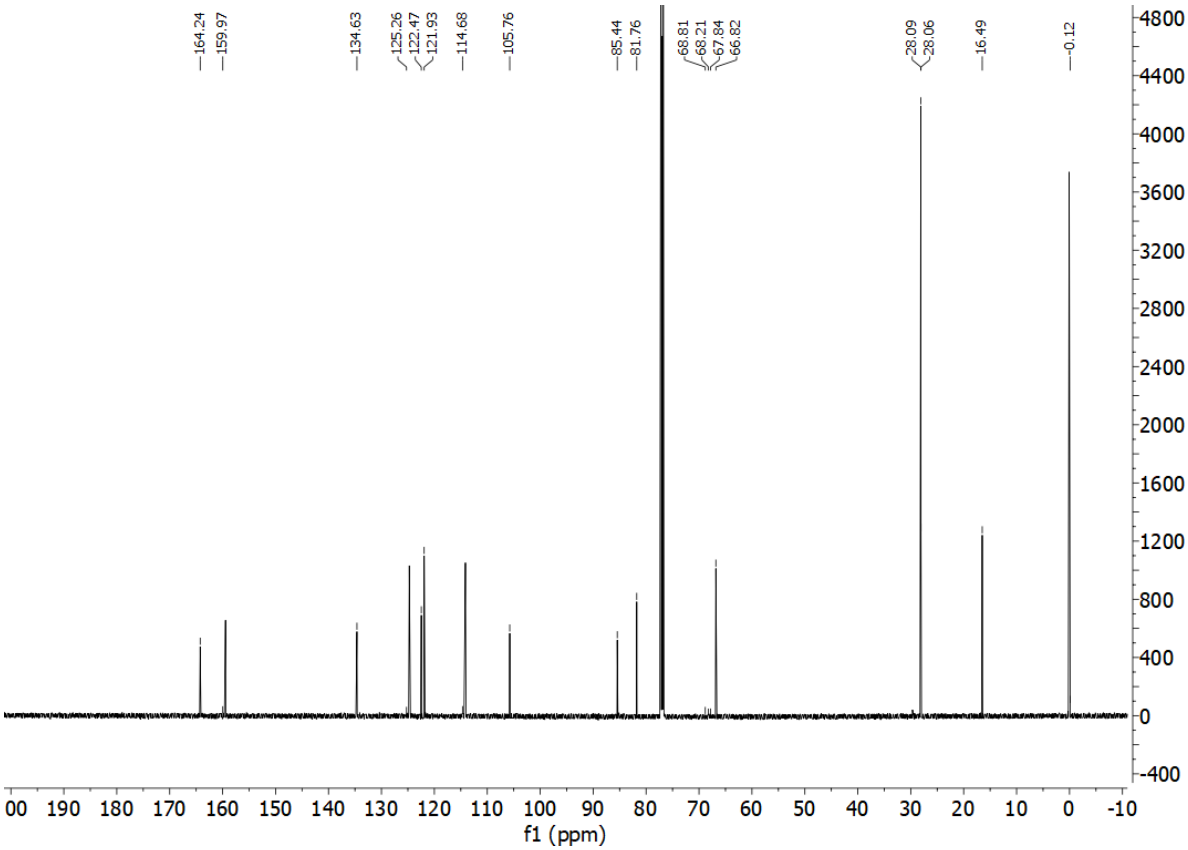

183. *(5-chloropent-1-yn-1-yl)tris(propan-2'-yl)silane*

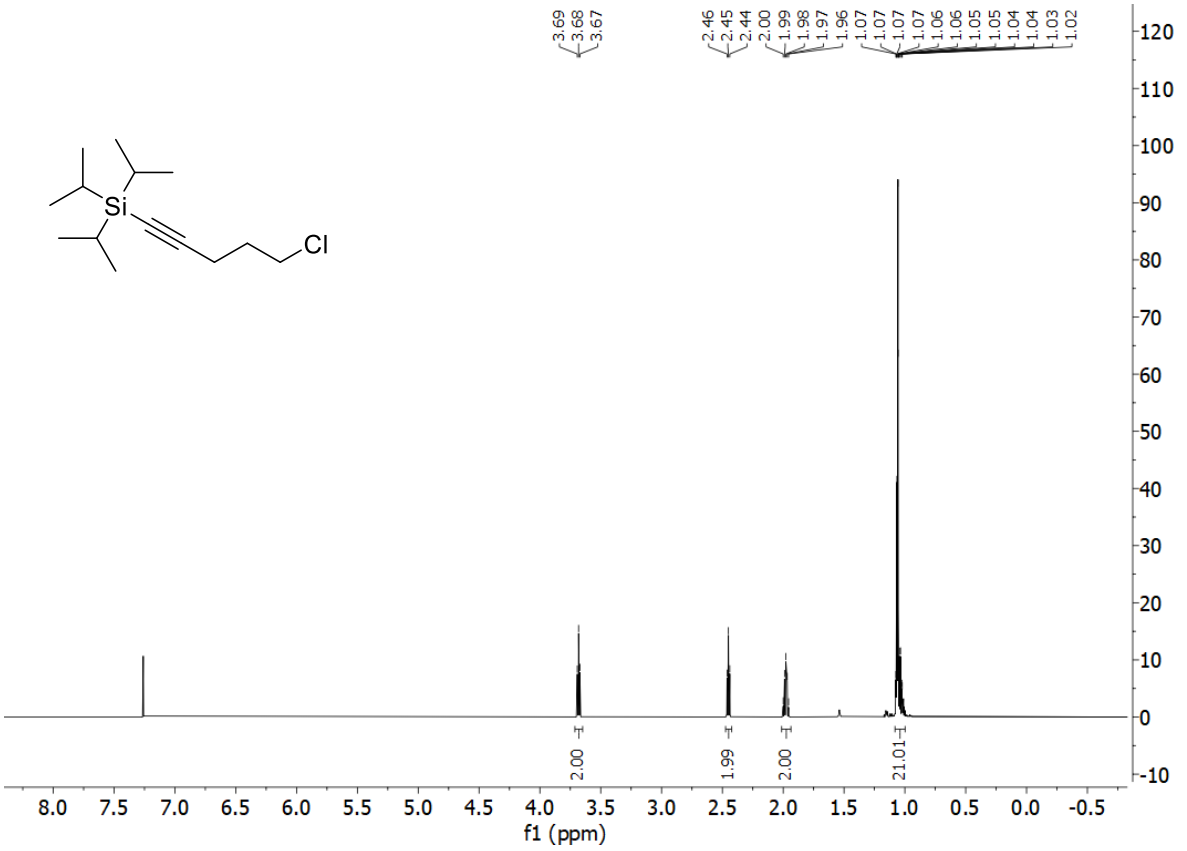

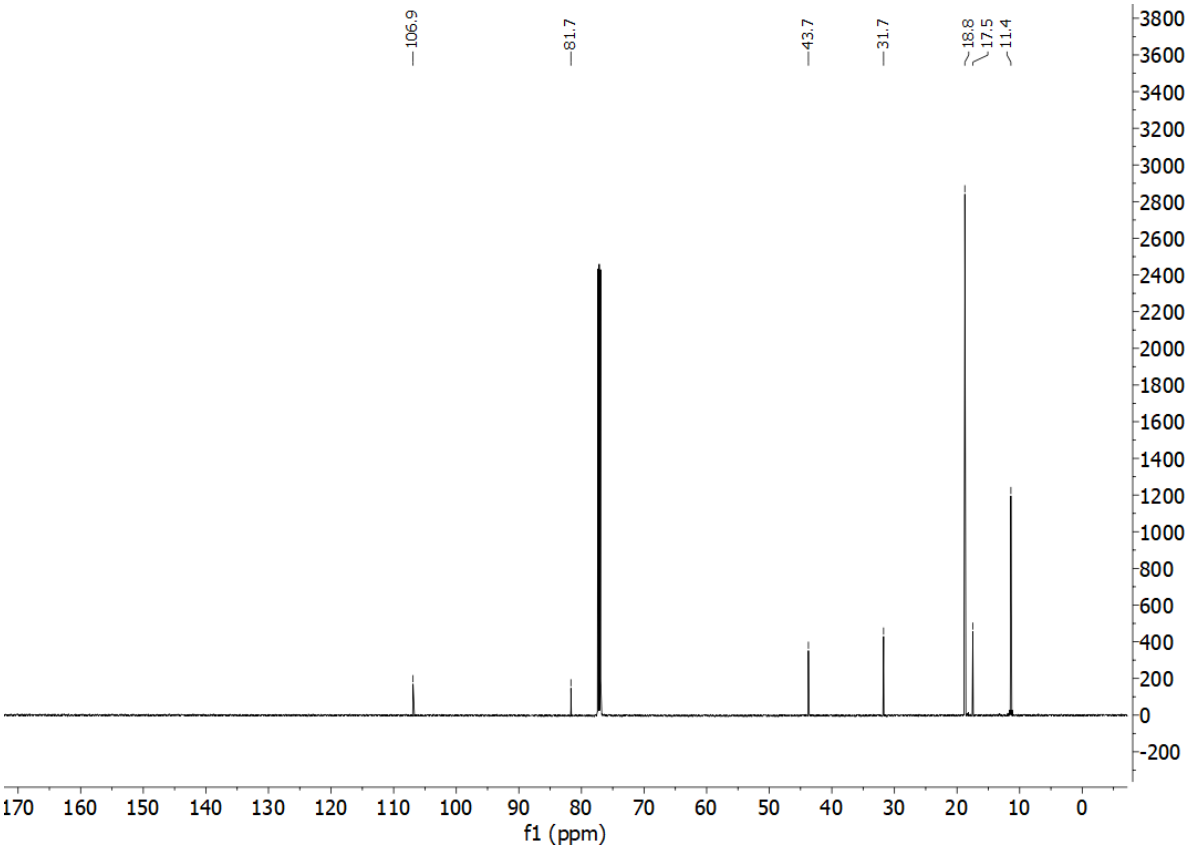

185. *methyl 3-bromo-5-({5'-[tris(propan-2''-yl)silyl]pent-4'-yn-1'-yl}oxy)benzoate*

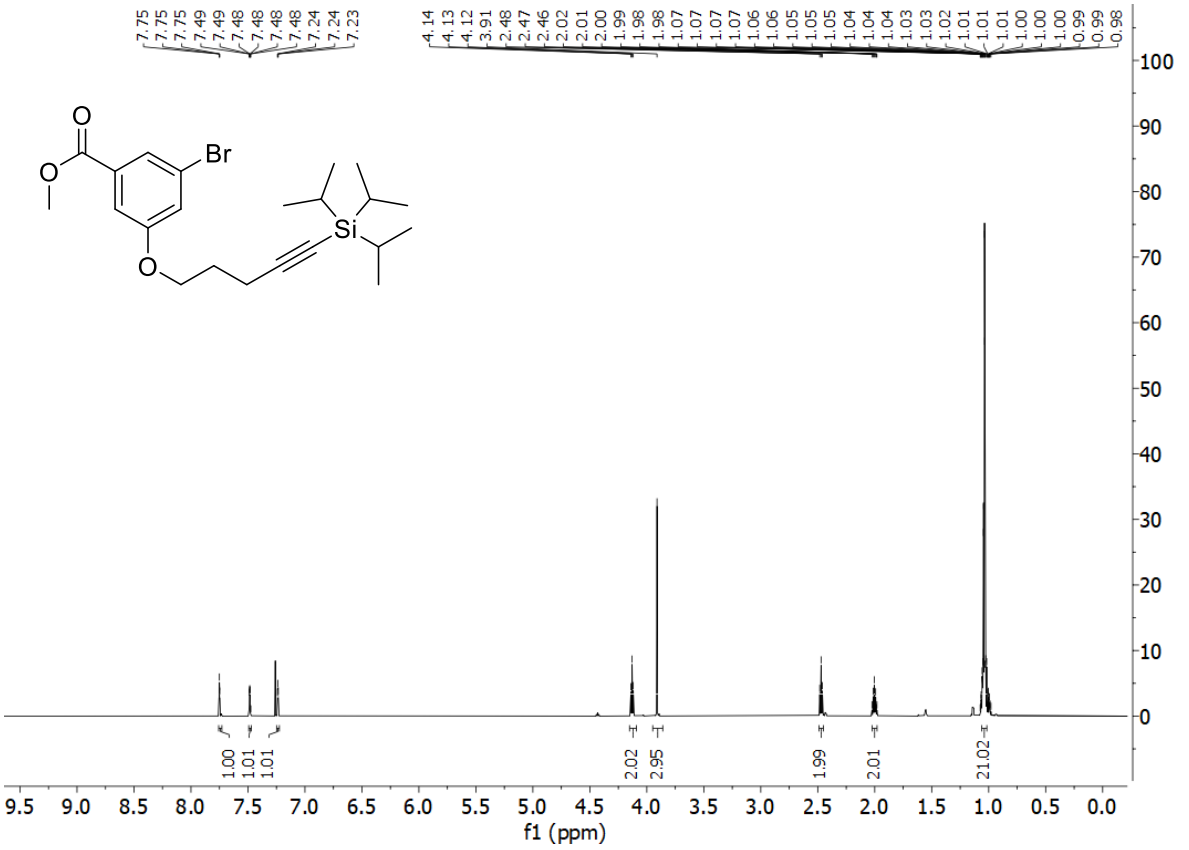

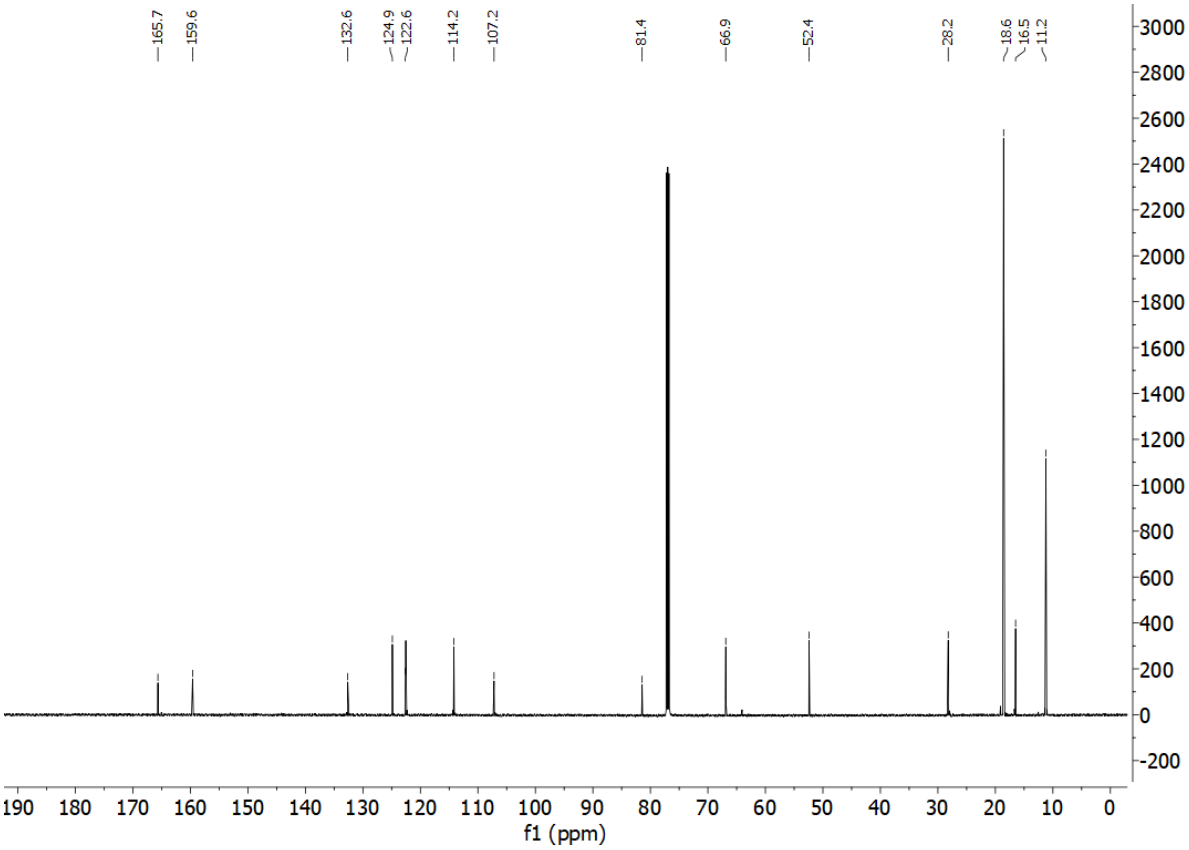

186. *3-bromo-5-{[5'-(triisopropylsilyl)pent-4'-yn-1'-yl]oxy}benzoic acid*

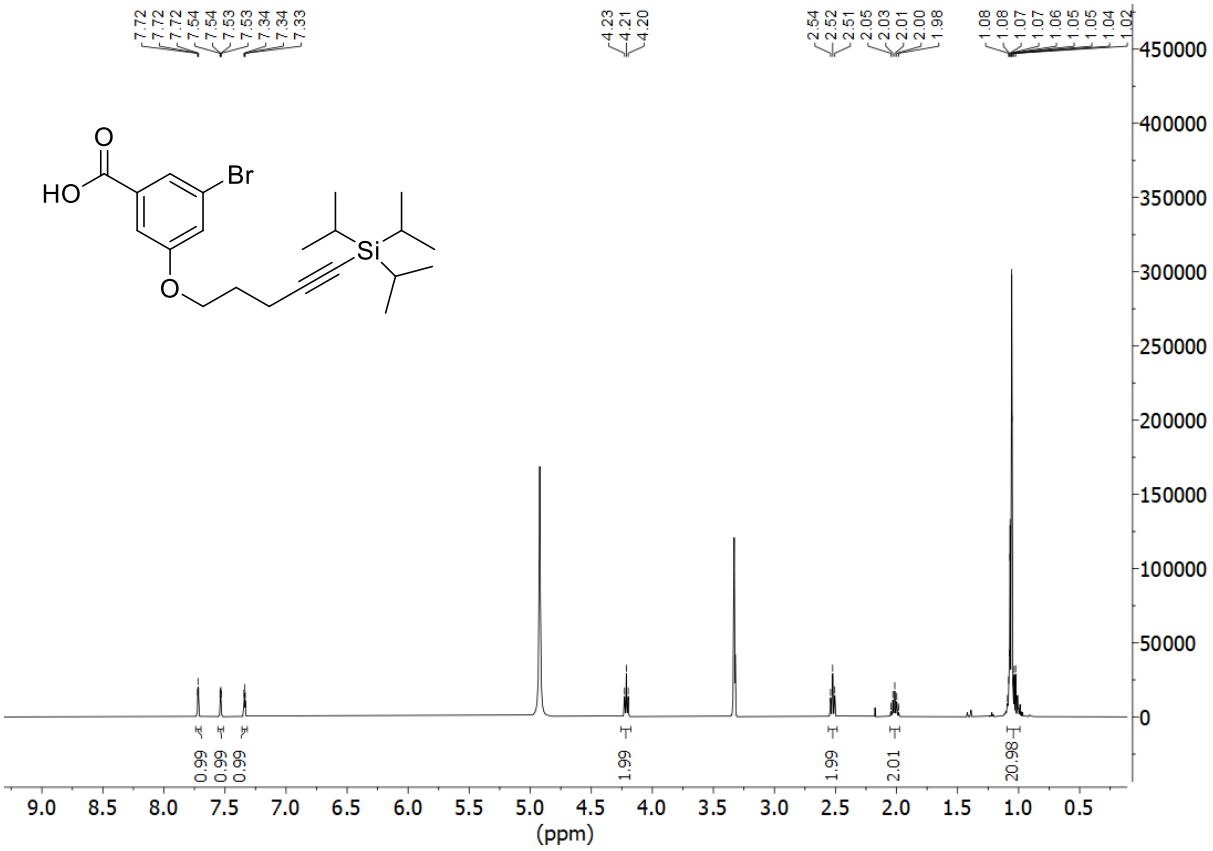

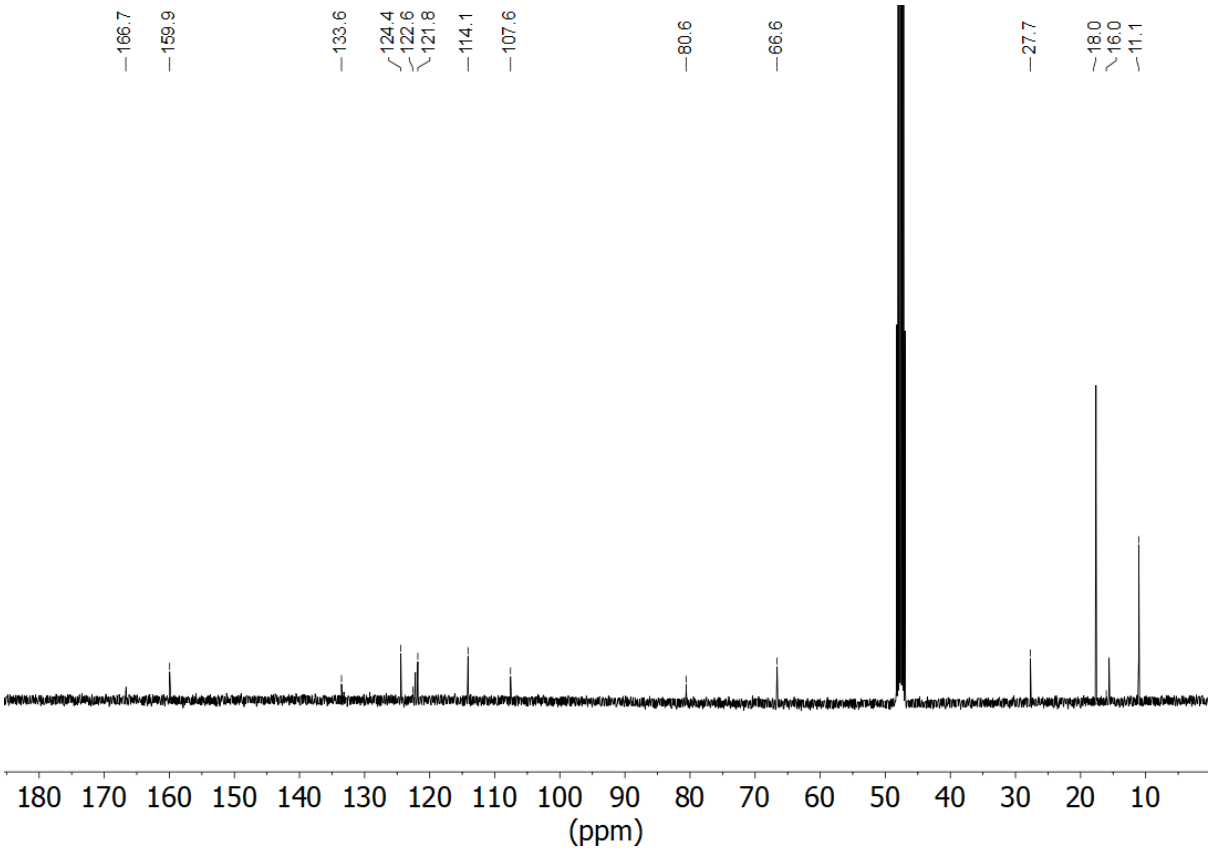

188. *methyl 3-(pent-4-yn-1-yloxy)-5-(2'',2'',2''- trifluoro-1''-(hydroxyimino)ethyl)benzoate*

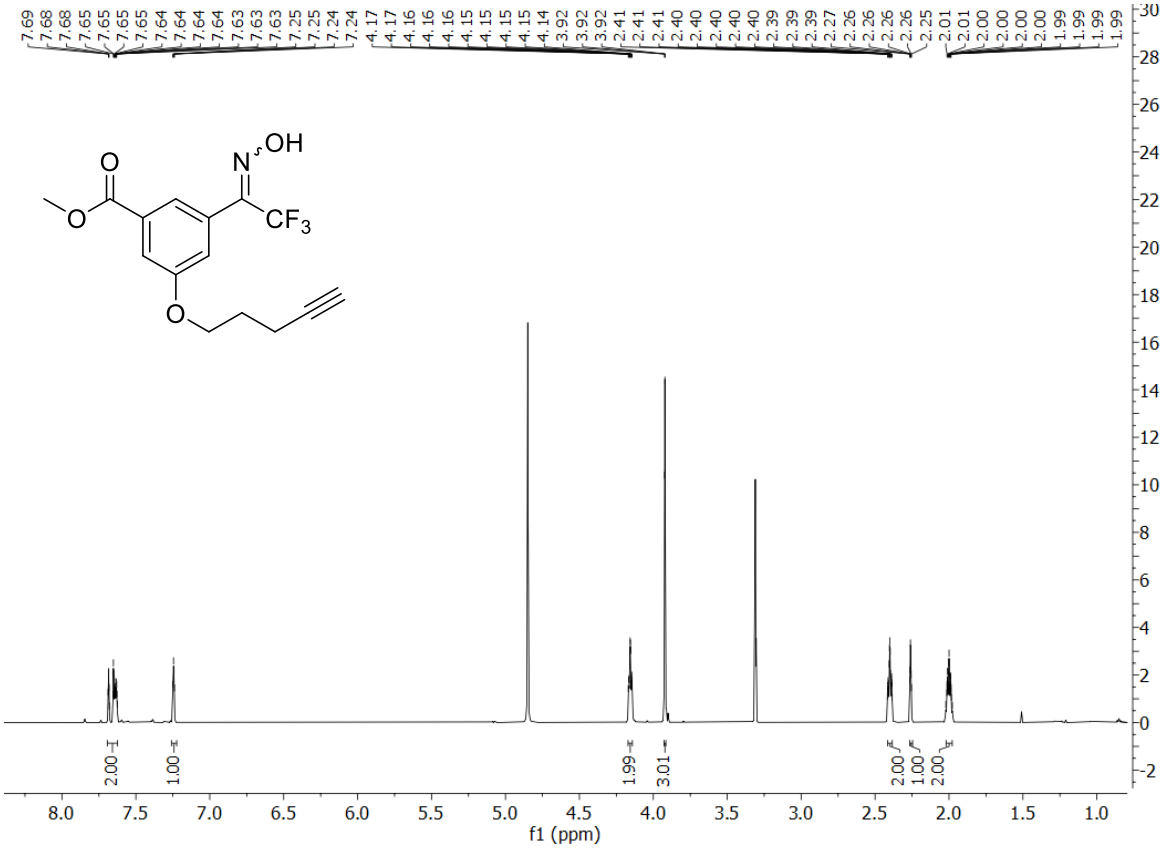

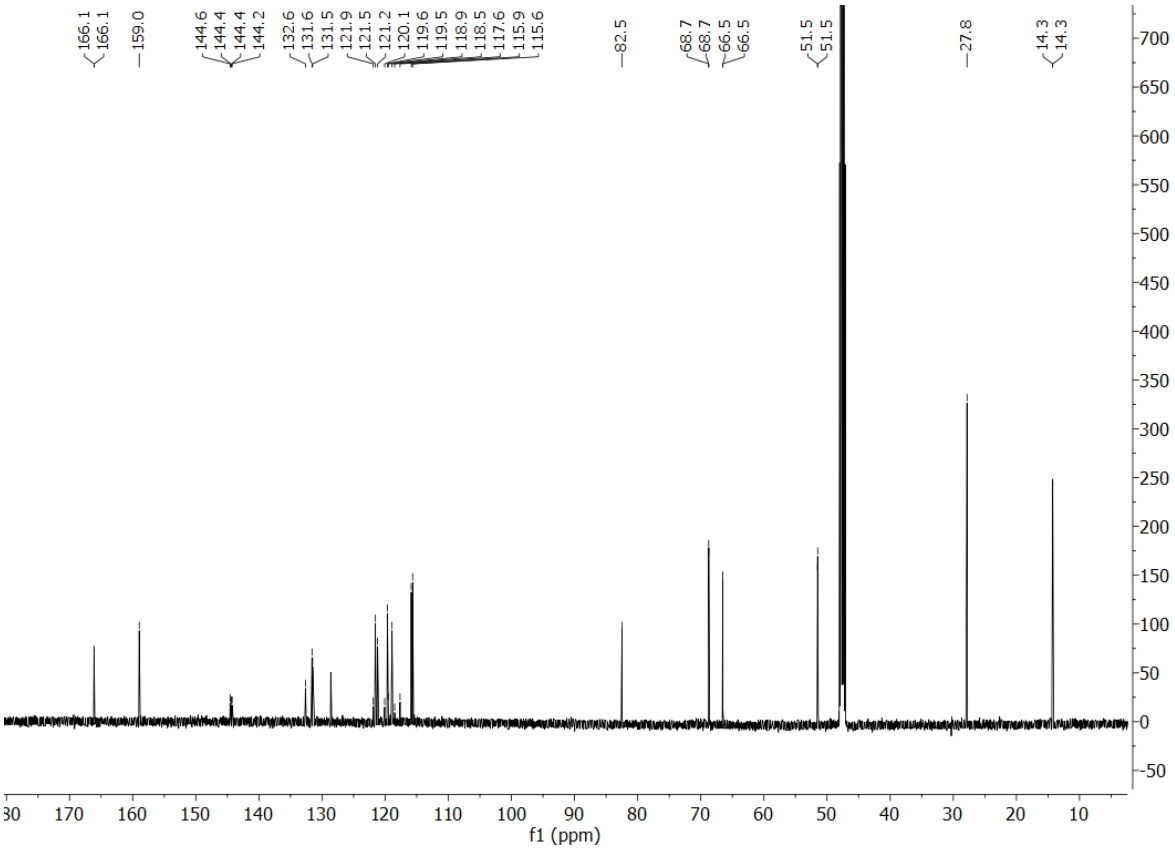

190. *methyl 5-(pent-4'-yn-1'-yloxy)-3-[3''-(trifluoromethyl)diaziridin-3''-yl]benzoate*

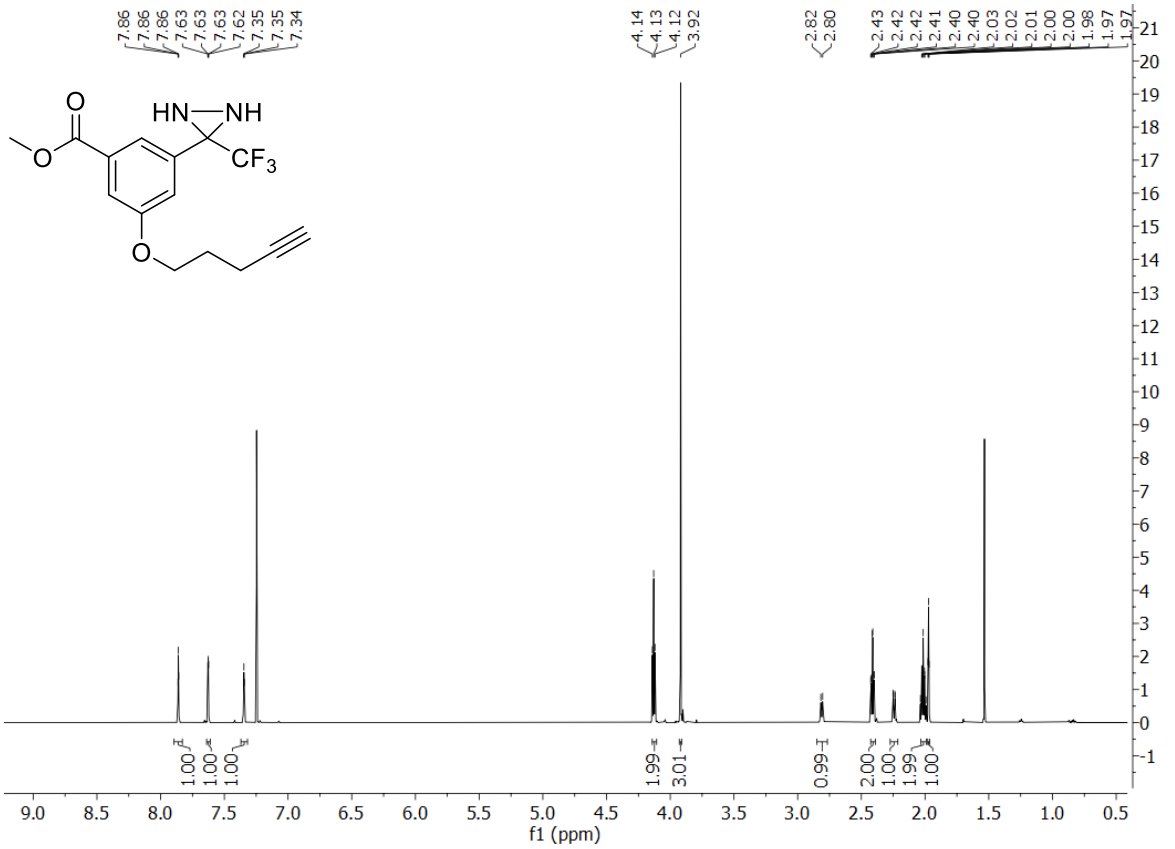

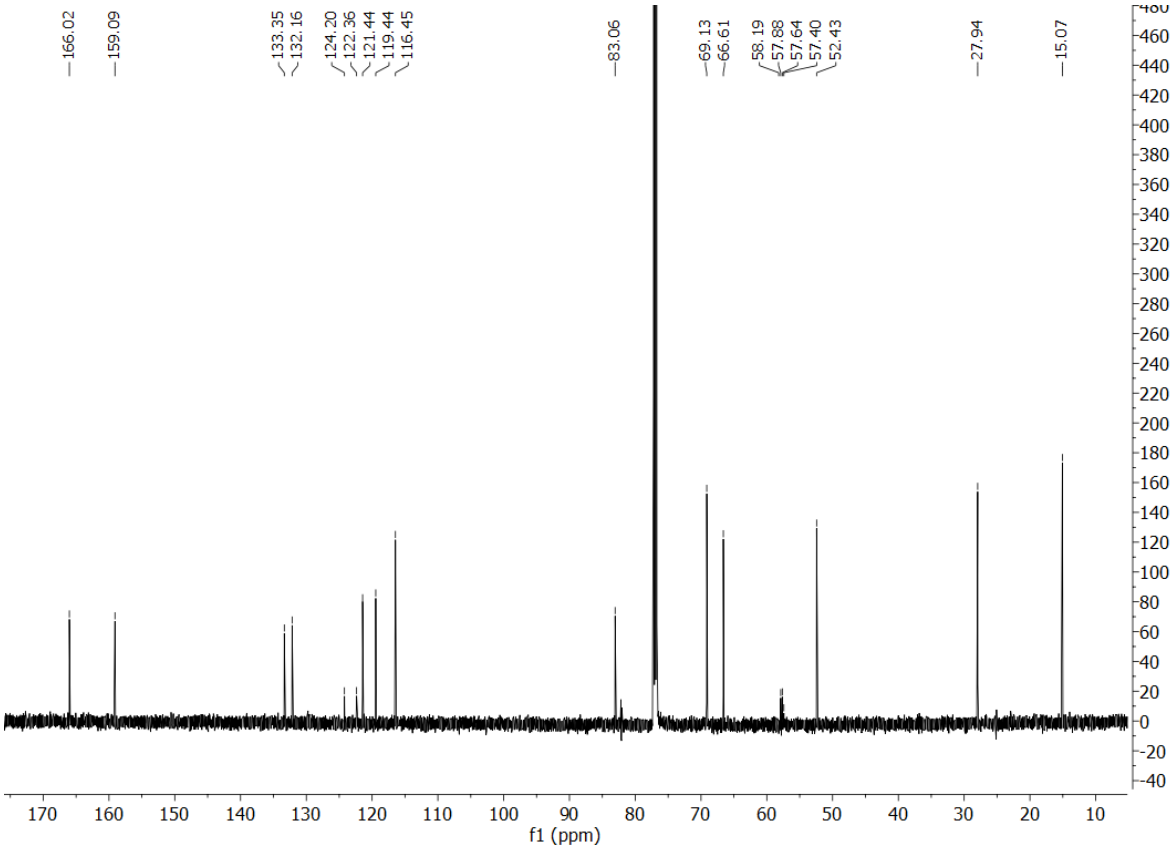

194. *1-(4-bromonaphthalen-1-yl)ethan-1'-one*

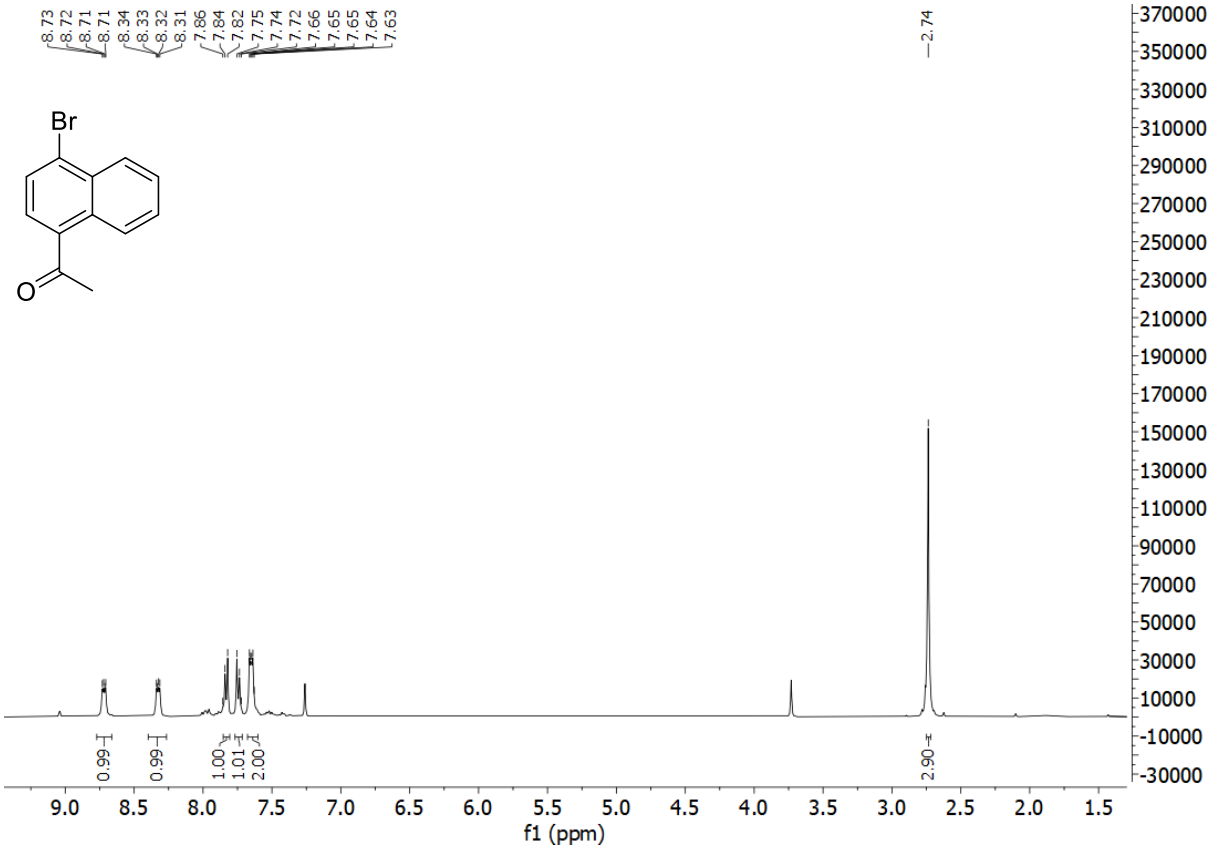

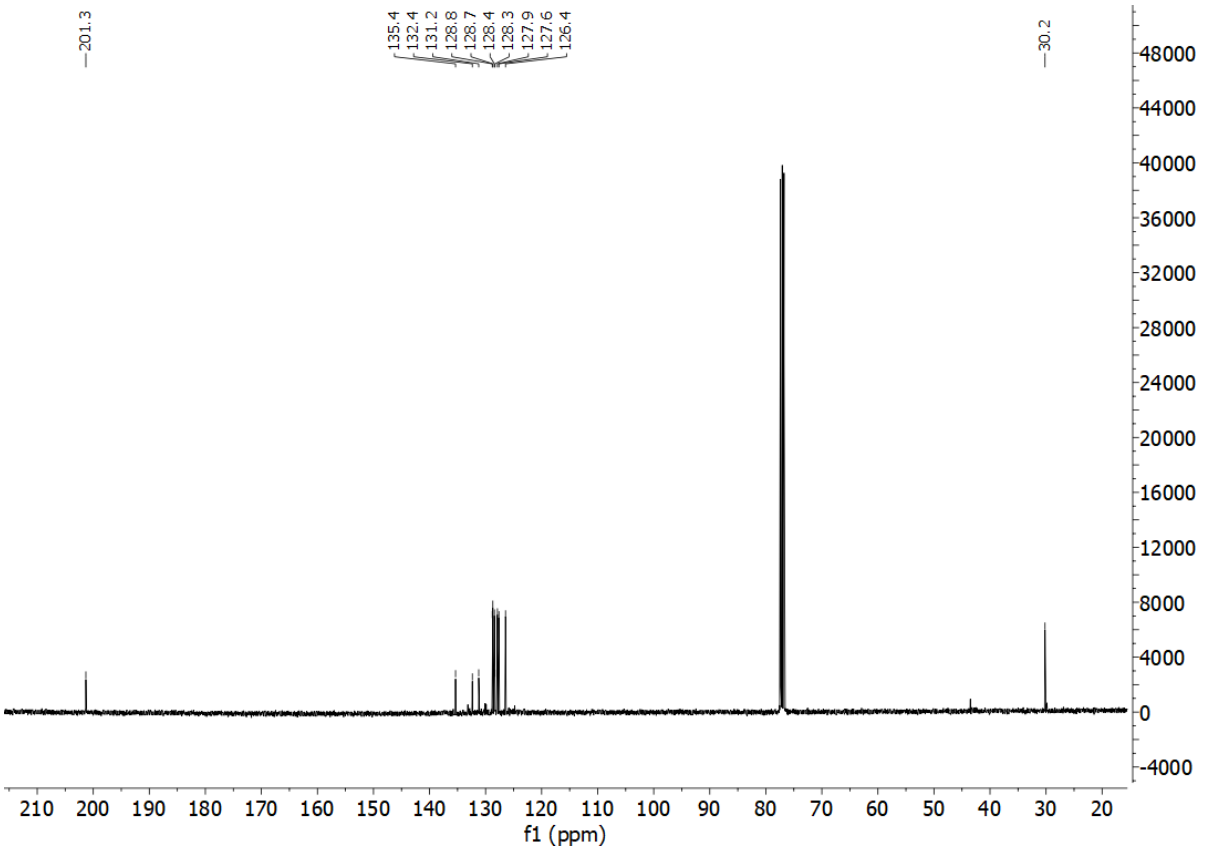

197. *4-[tris(propan-2'-yl)silyl]but-3-yn-1-ol*

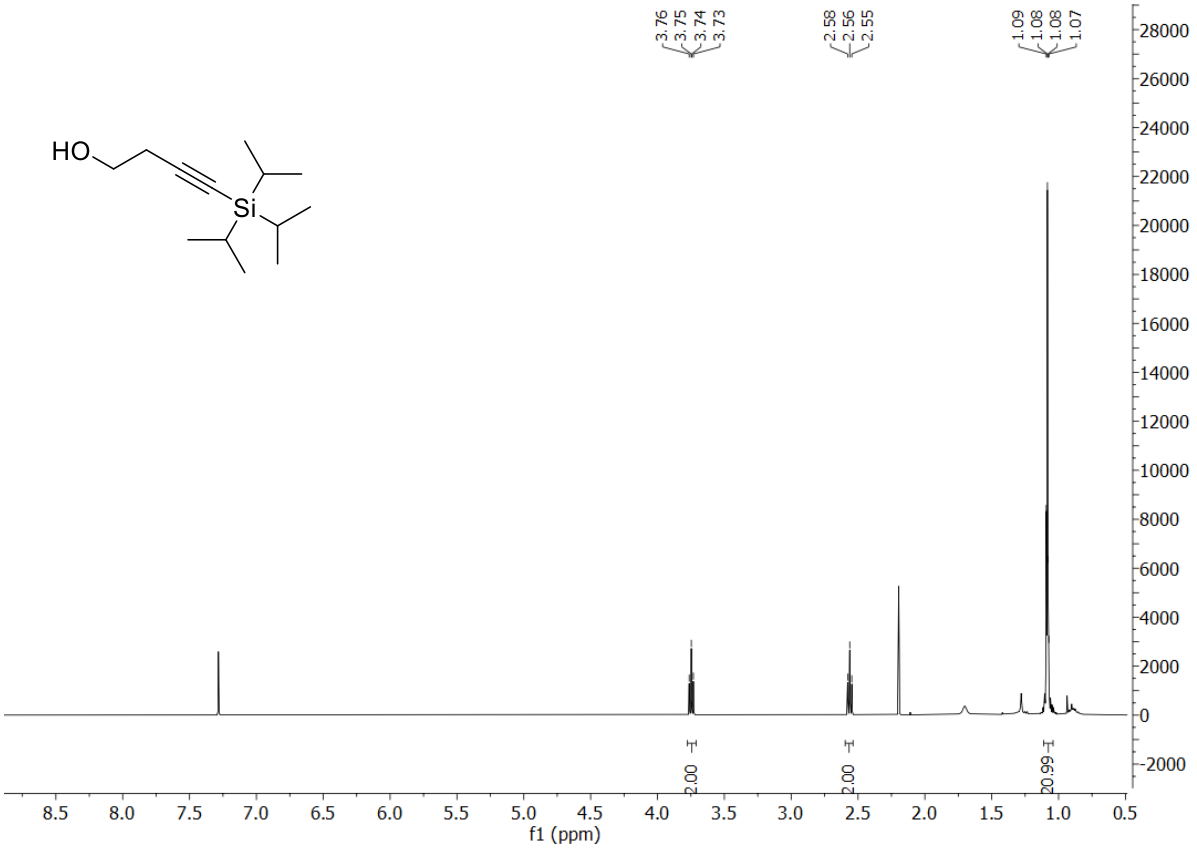

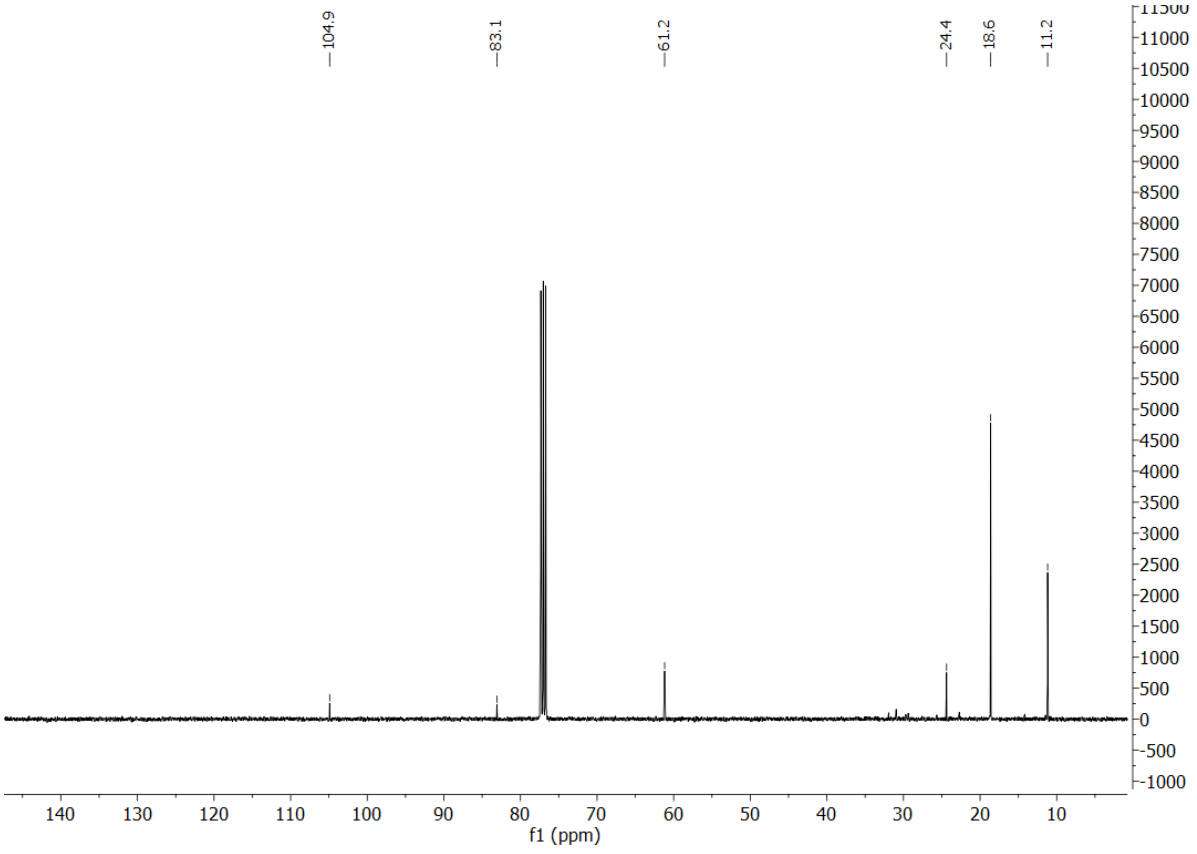

199. *Ethyl 2-({4'-[tris(propan-2''-yl)silyl]but-3'-yn-1'-yl}oxy)acetate*

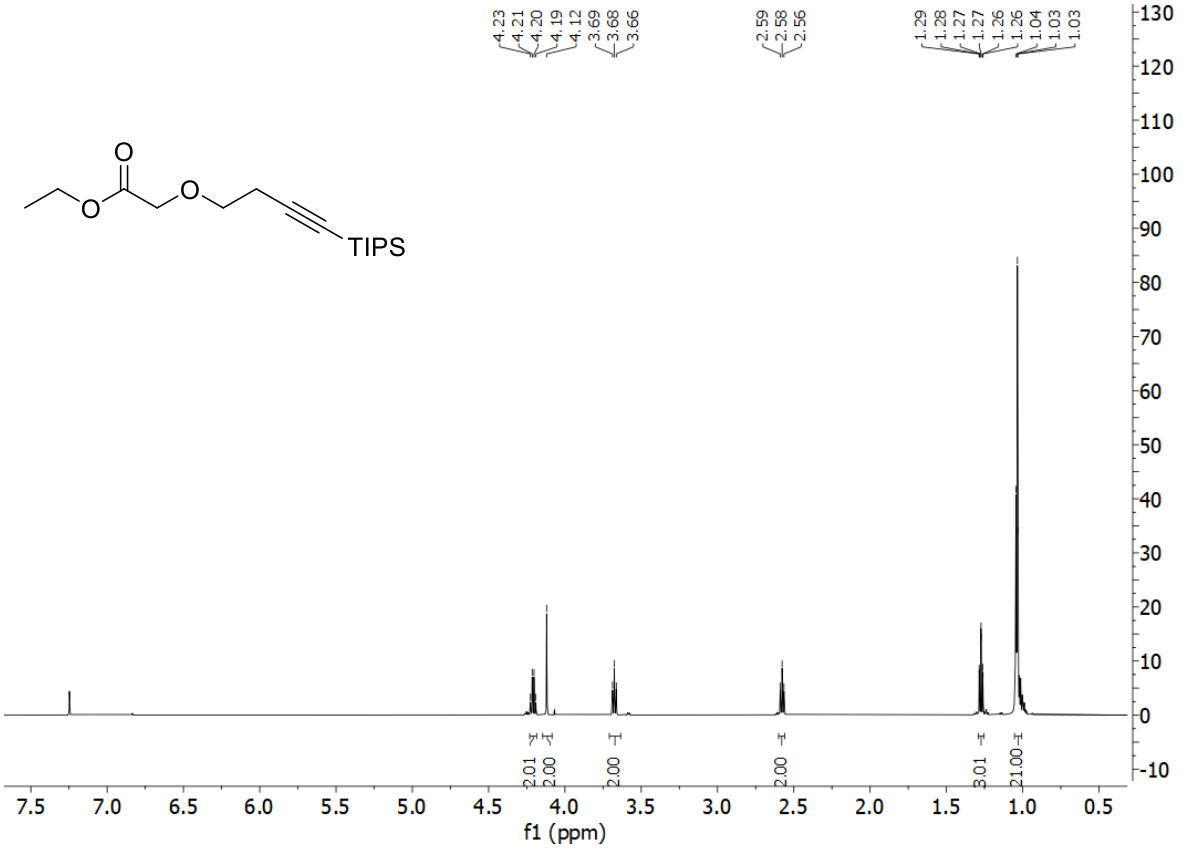

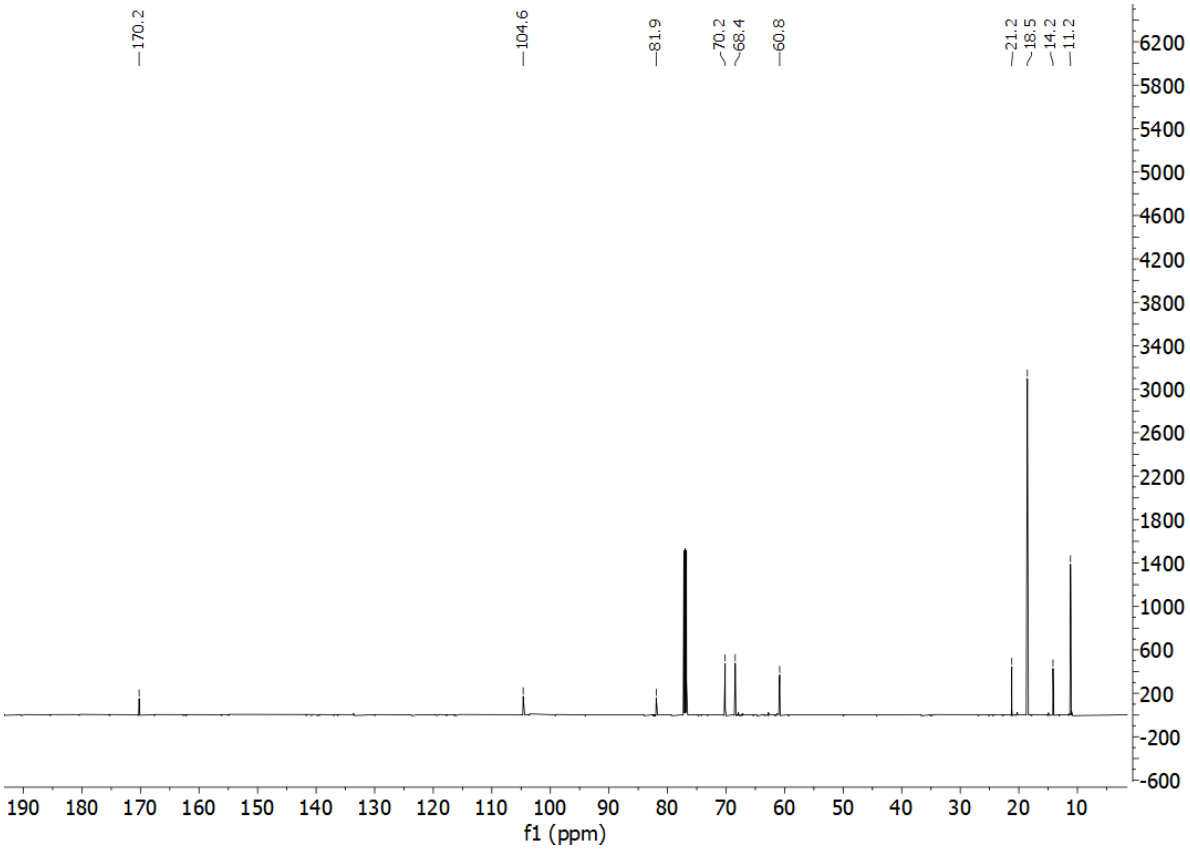

200. *2-({4'-[tris(propan-2''-yl)silyl]but-3'-yn-1'-yl}oxy)acetic acid*

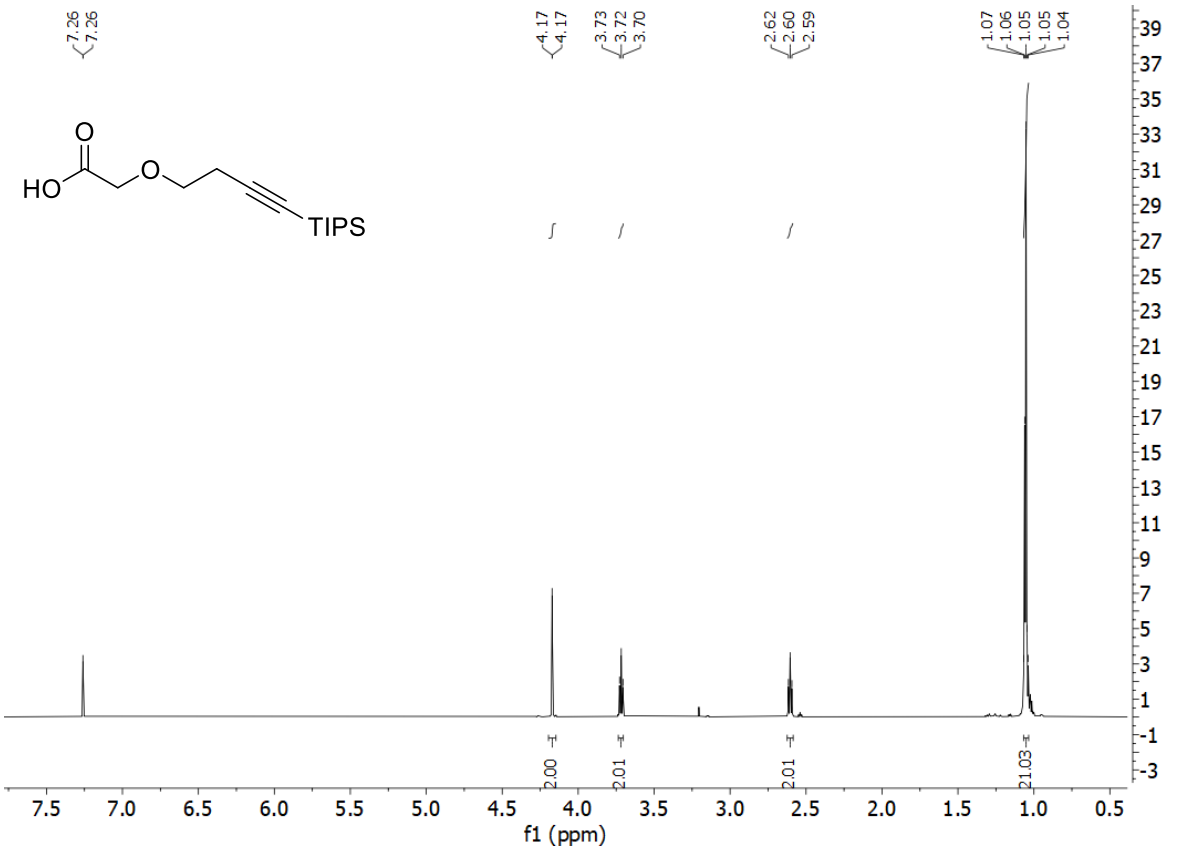

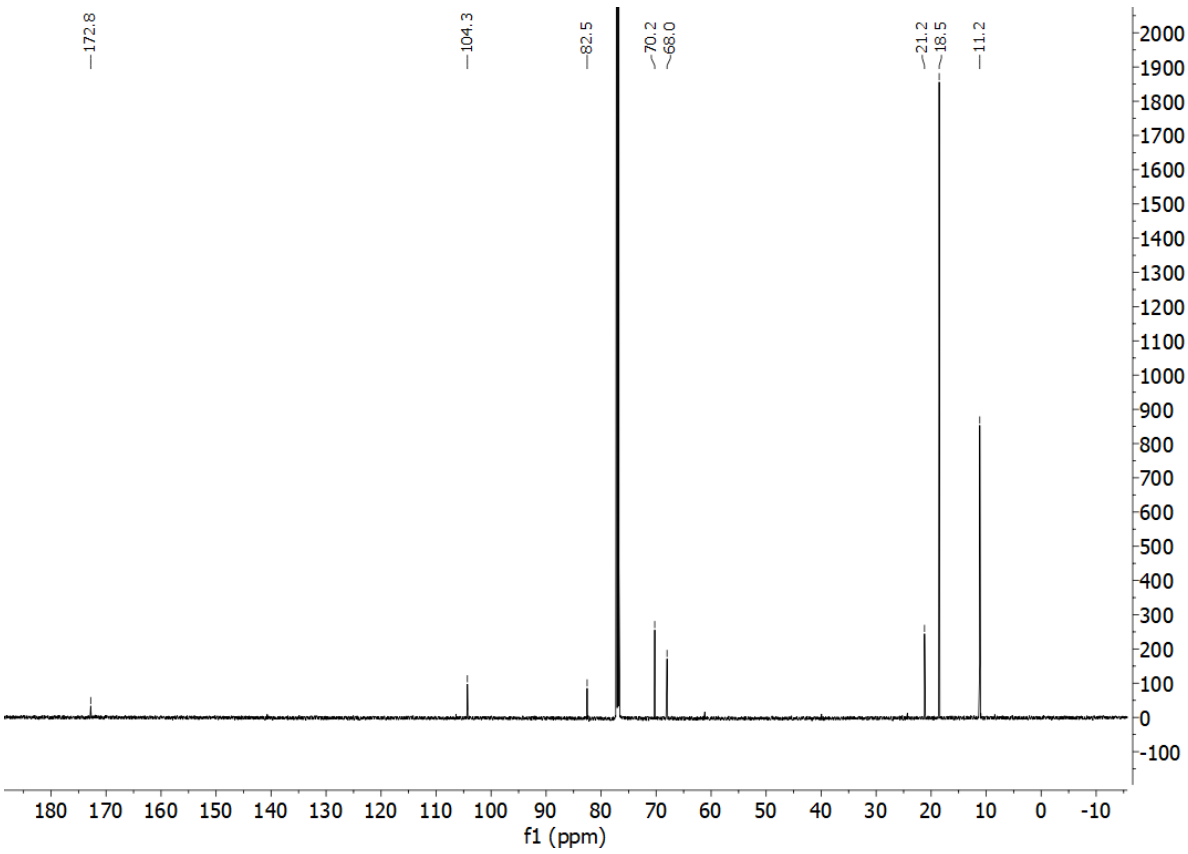

203. *(4-bromonaphthalen-1-yl)trimethylsilane*

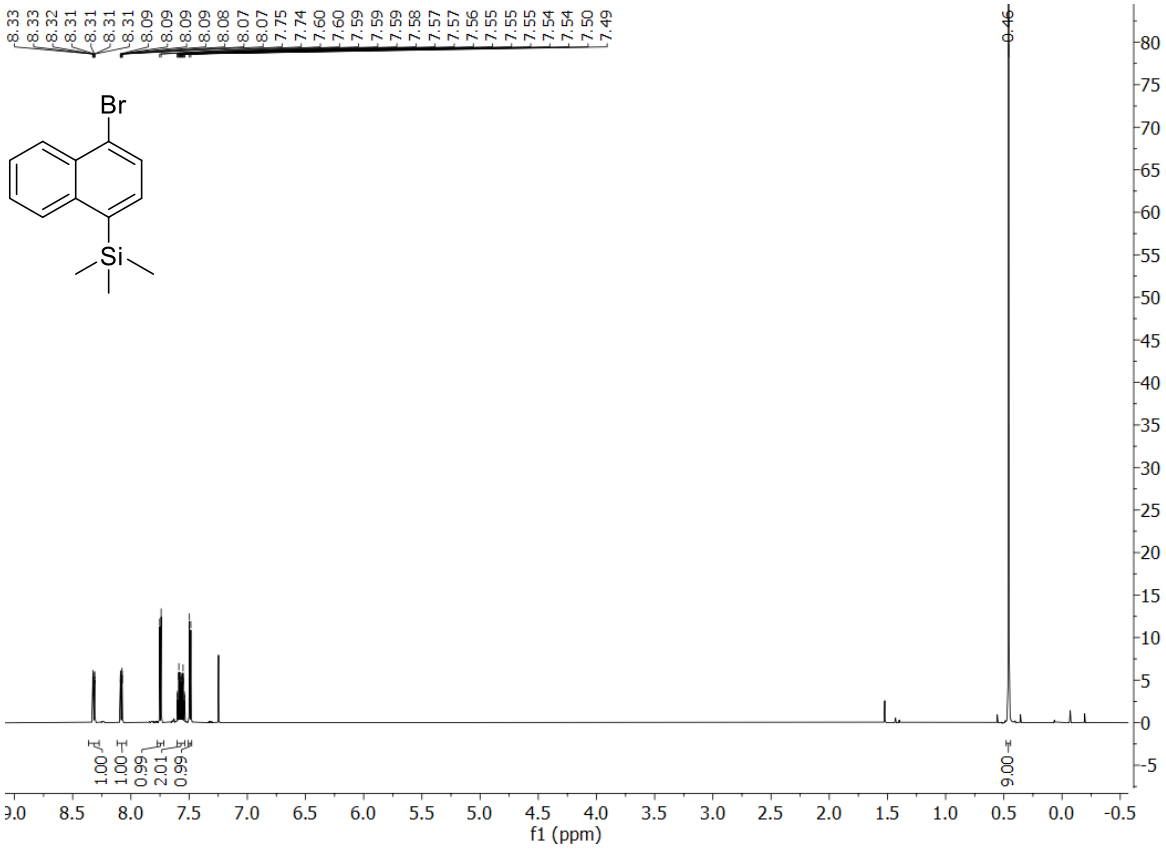

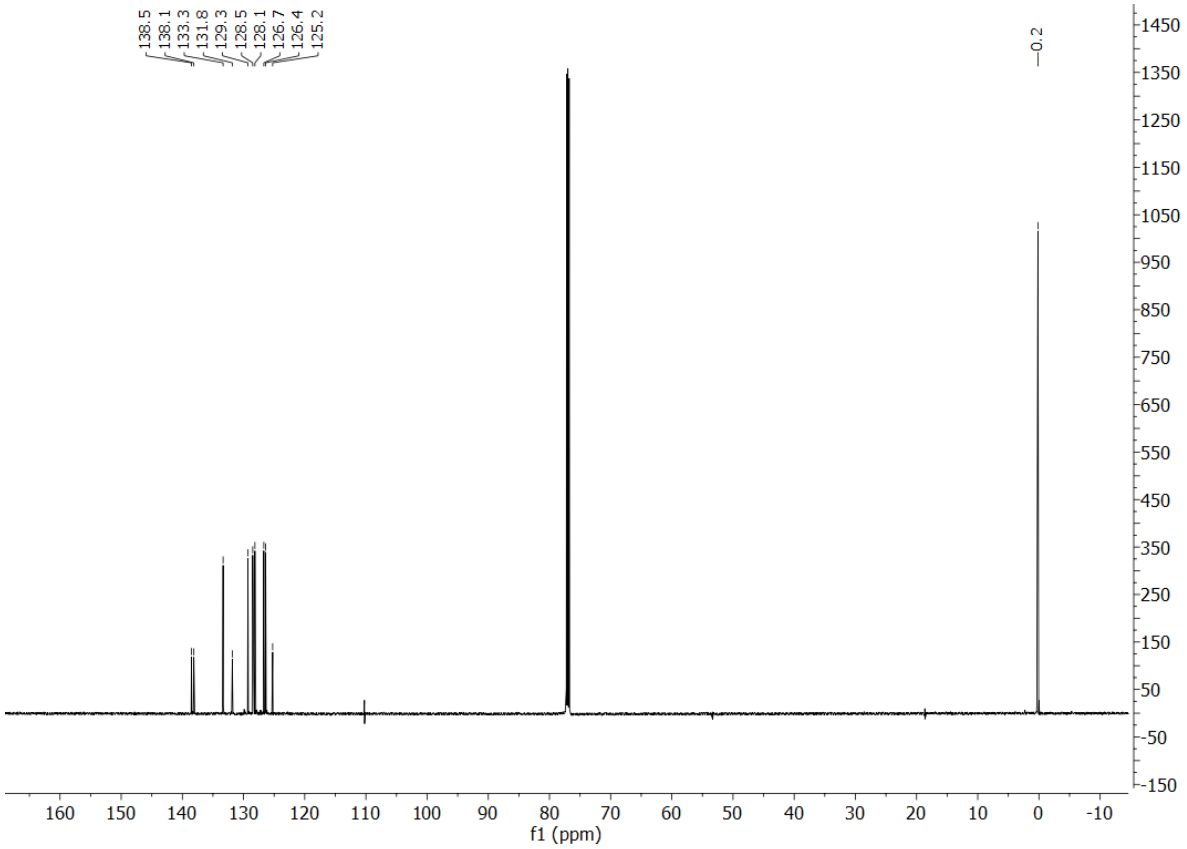

204. *N-methoxy-N-methyl-2-({4'-[tris(propan-2''-yl)silyl]but-3'-yn-1'-yl}oxy)acetamide*

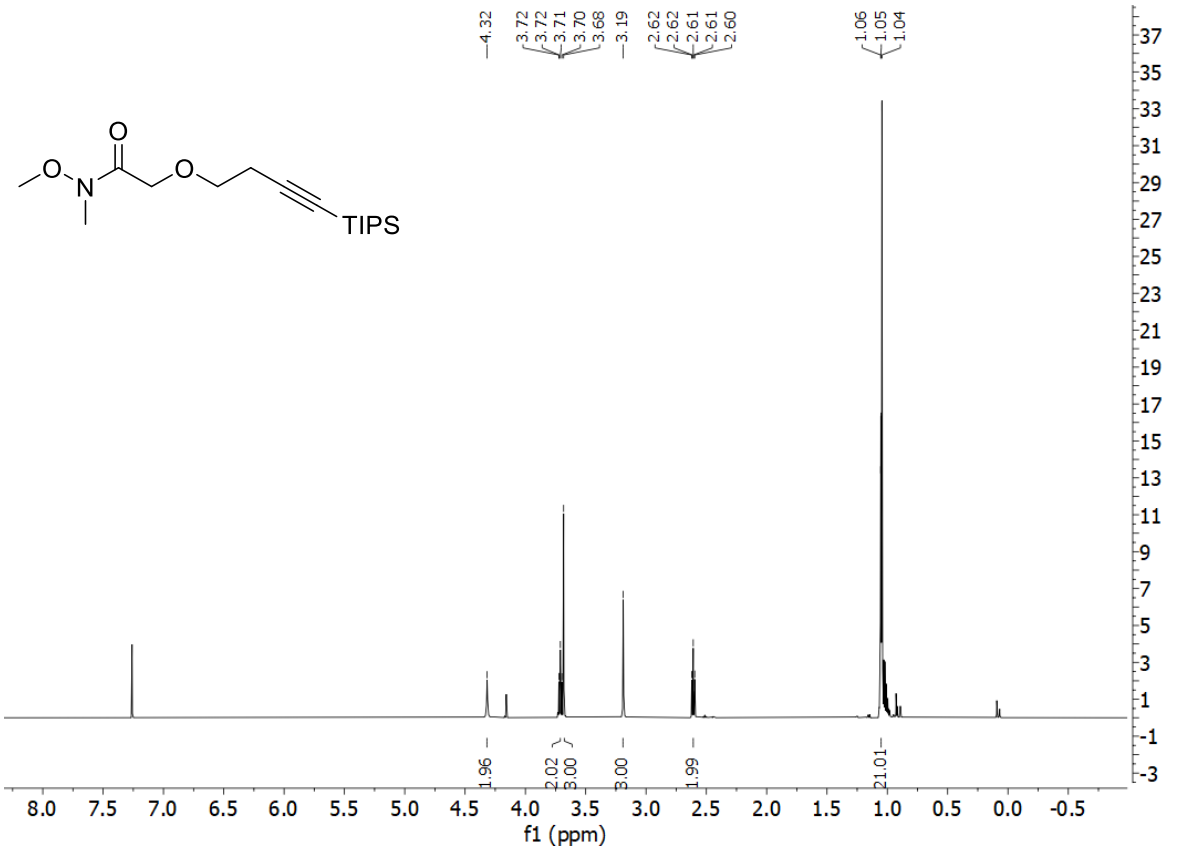

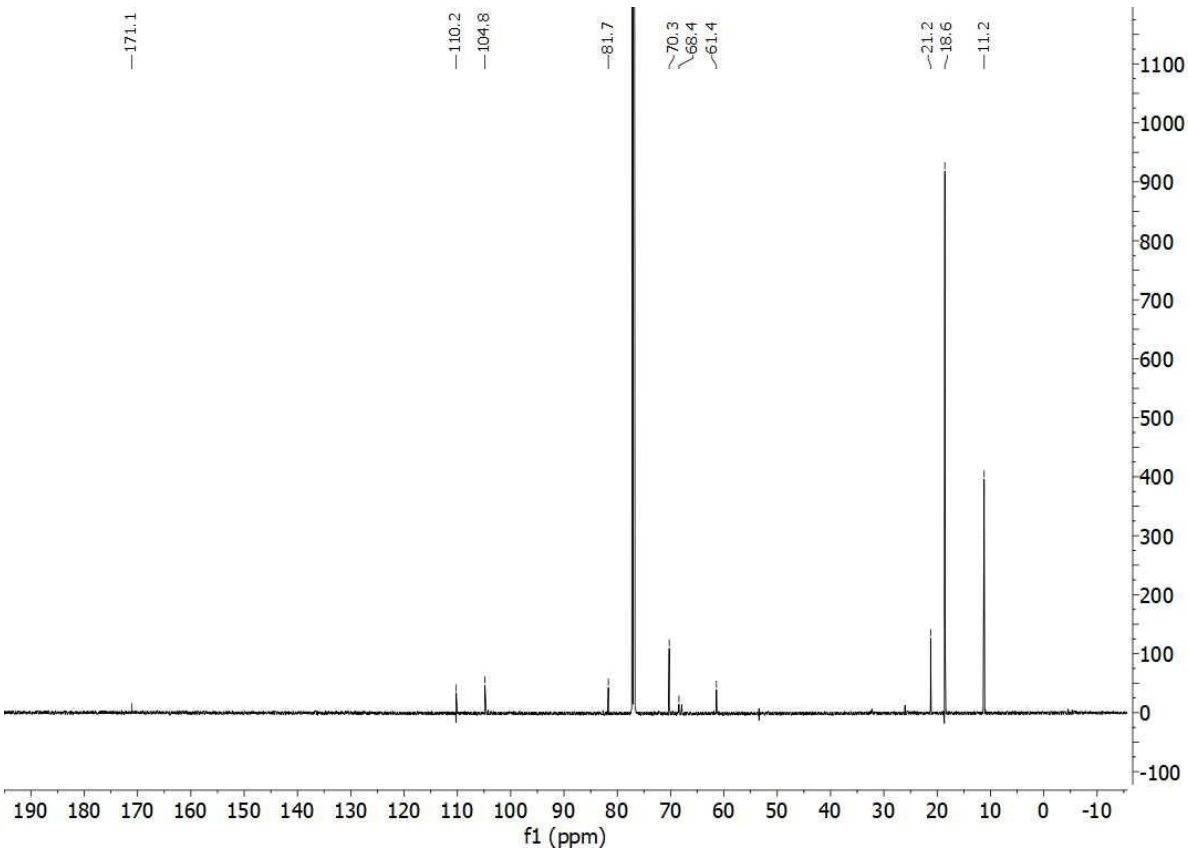

209. *4-(4'-bromonaphthalen-1'-yl)-4-oxobutyl acetate*

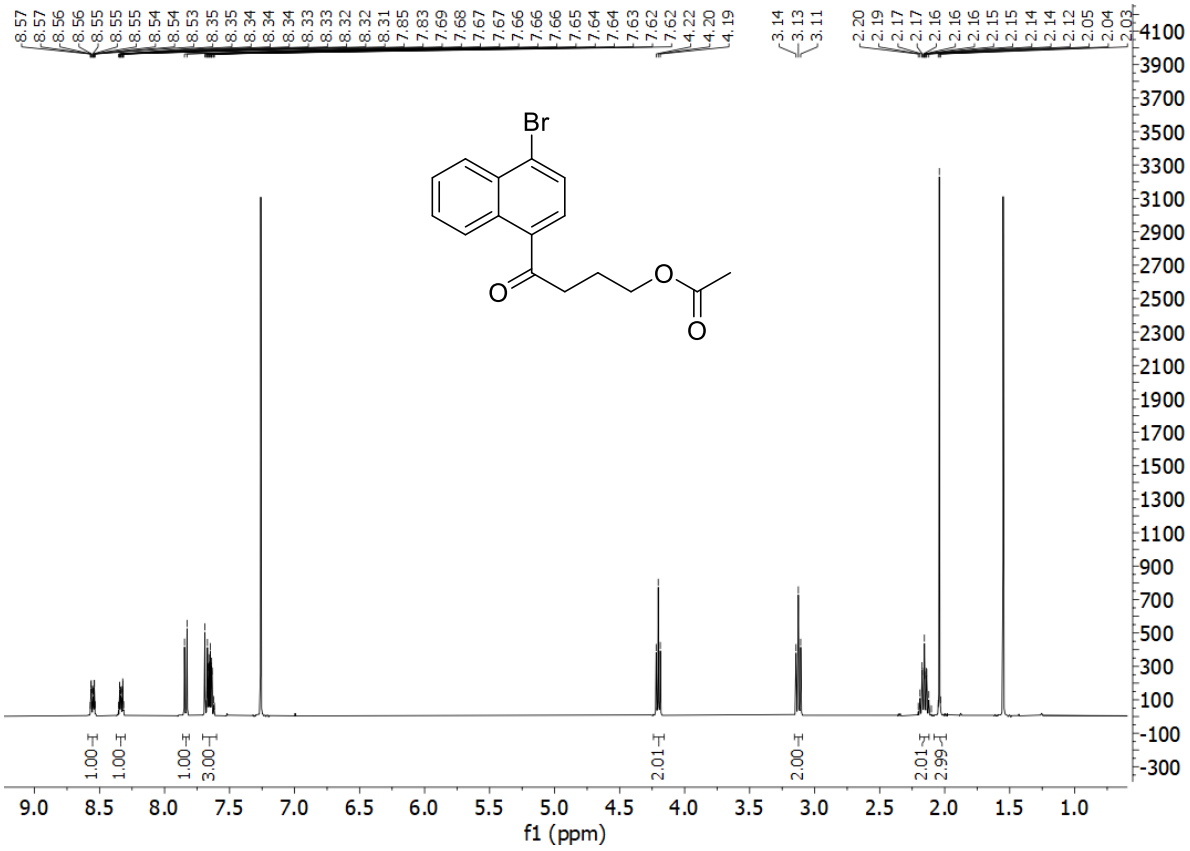

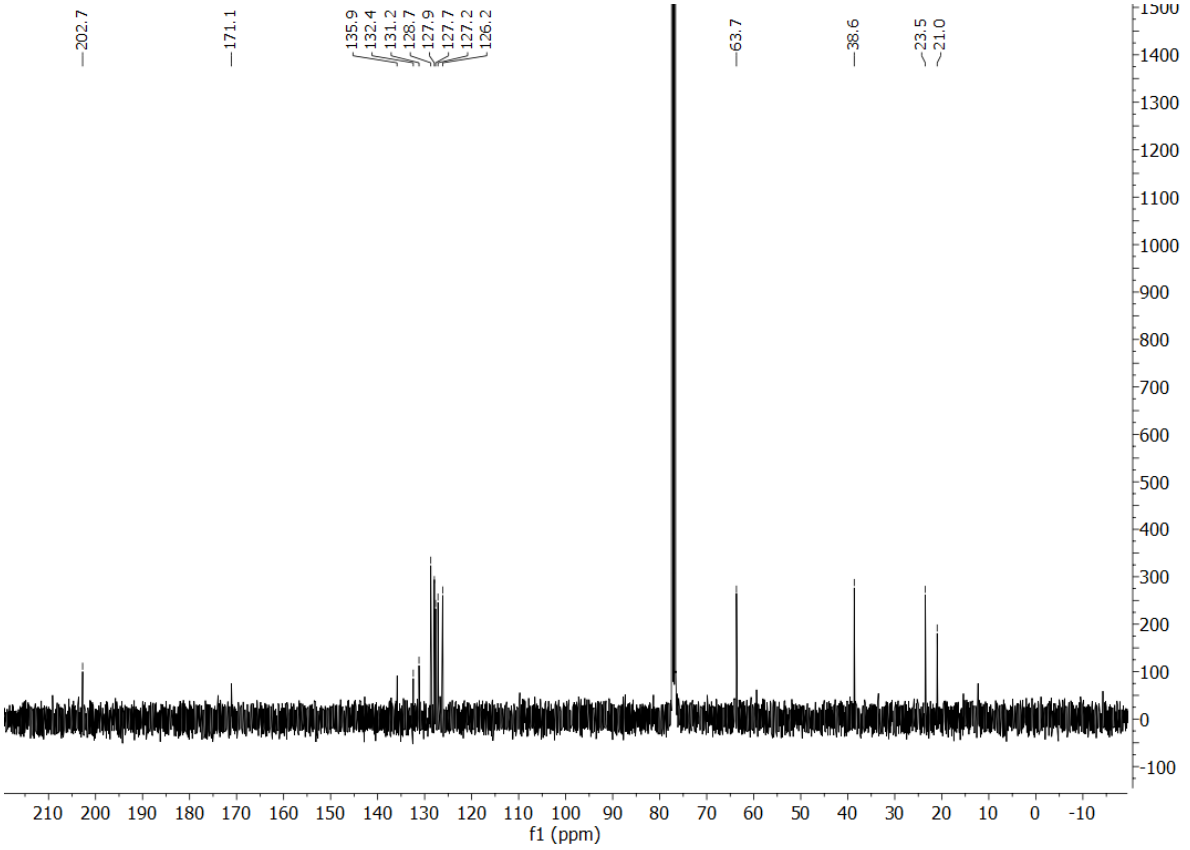

210. *3-[2-(4-bromonaphthalen-1-yl)-1,3-dioxolan-2-yl]propan-1-ol*

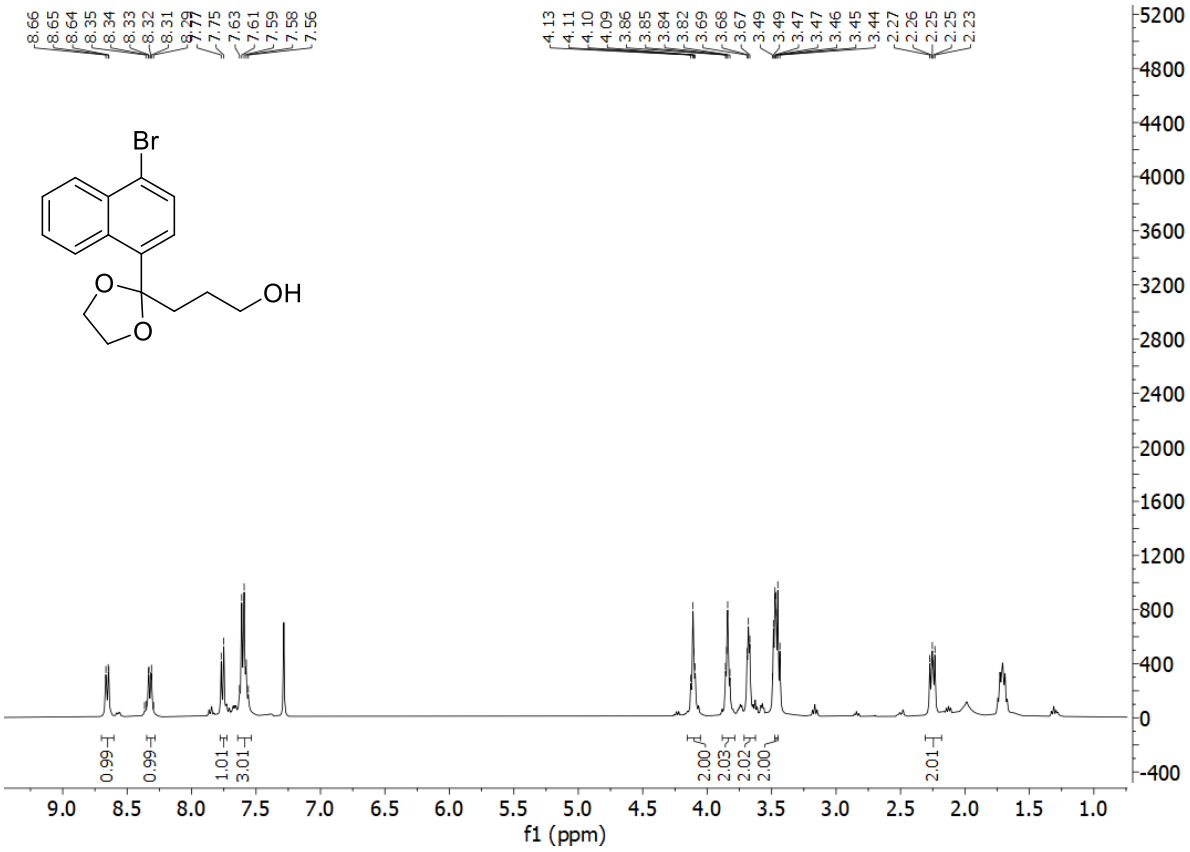

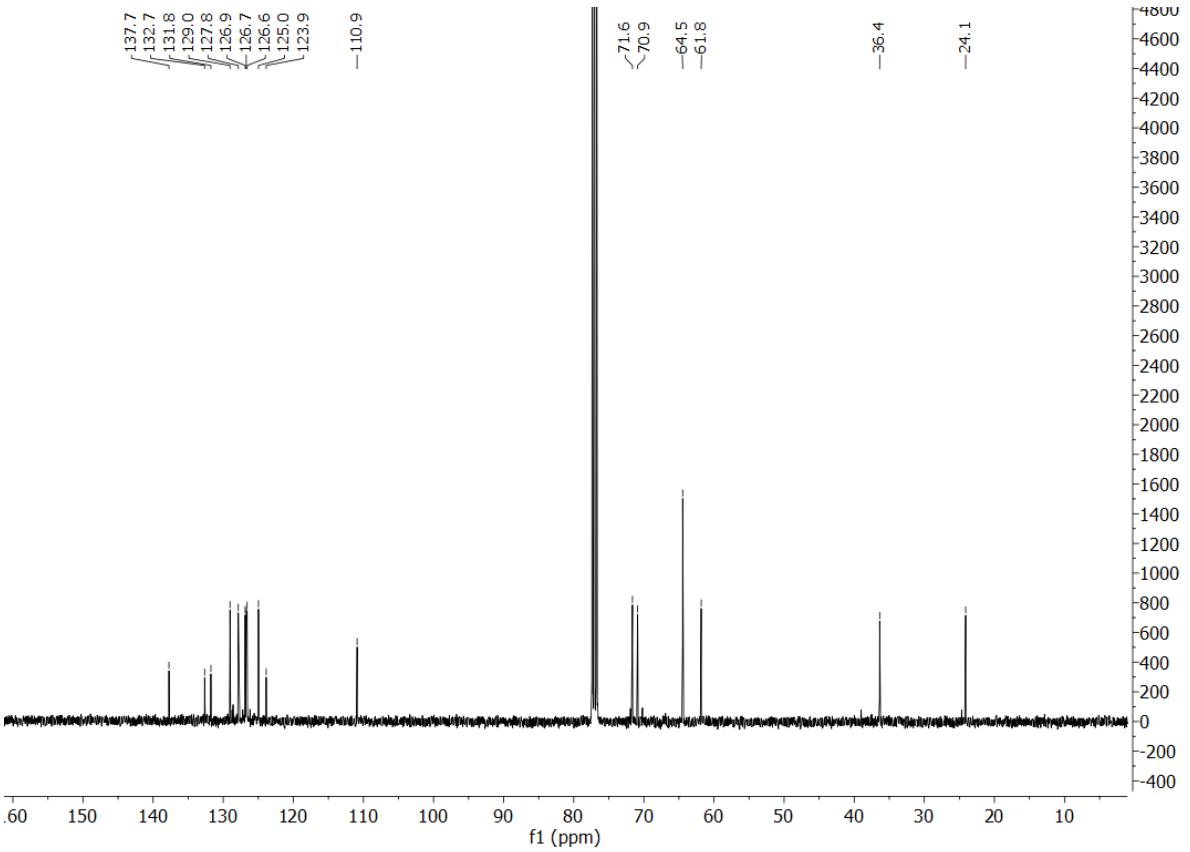

Appendix B: Full hypocotyl data

B.1 Chapter 2 SAR Data (100 µM)

Trial	Compound	Structure	1st Rep	2nd Rep	3rd Rep	Average	SD	SE	R.G. DMSO	Error	R.G. eW5	Error
1	**DMSO**		0.726	0.664	0.667	0.686	0.151	0.0871	0	0	0	0
1	**1**	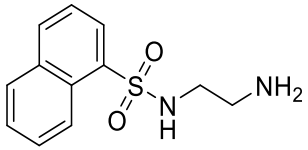	0.984	0.866	0.926	0.925	0.131	0.0755	0.350	0.0528	0	0
1	**75**	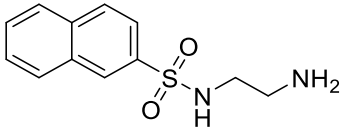	0.786	0.642	0.669	0.699	0.148	0.0857	0.019	0.0034	-0.245	0.0361
1	**76**	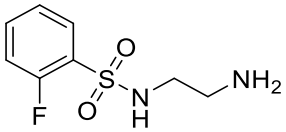	0.818	0.887	0.822	0.842	0.154	0.0891	0.229	0.0378	-0.090	0.0145
1	**77**	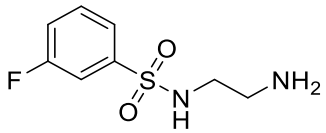	0.895	0.847	0.887	0.877	0.154	0.0891	0.279	0.0454	-0.053	0.0077
1	**78**	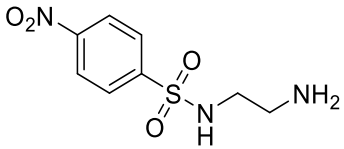	0.895	0.853	0.864	0.871	0.144	0.0832	0.270	0.0429	-0.059	0.0082
1	**79**	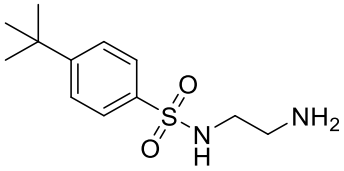	0.823	0.851	0.940	0.871	0.121	0.0697	0.271	0.0407	-0.058	0.0073

1	**80**	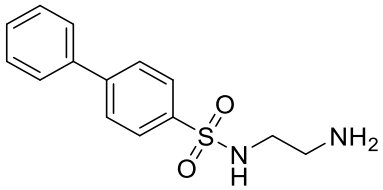	0.782	0.733	0.816	0.777	0.147	0.0847	0.134	0.0224	-0.160	0.0217
1	**81**	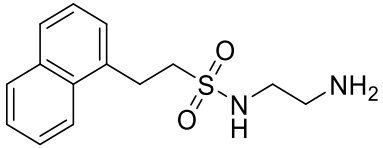	0.708	0.666	0.699	0.691	0.136	0.0786	0.008	0.0013	-0.253	0.0399
1	**82**	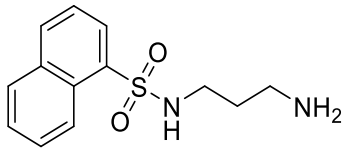	0.818	0.780	0.823	0.807	0.103	0.0596	0.177	0.0261	-0.128	0.0173
1	**83**	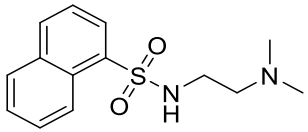	0.617	0.589	0.597	0.601	0.182	0.1052	-0.123	0.0266	-0.350	0.0665
1	**85**	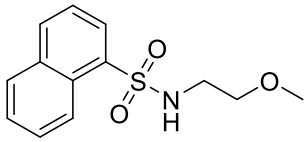	0.536	0.549	0.565	0.550	0.121	0.0701	-0.197	0.0355	-0.405	0.0878
1	**86**	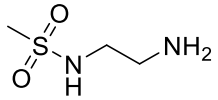	0.651	0.657	0.623	0.644	0.118	0.0679	-0.061	0.0100	-0.304	0.0503
1	**87**	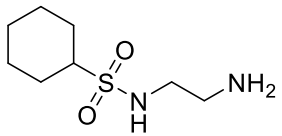	0.627	0.645	0.732	0.668	0.152	0.0878	-0.026	0.0047	-0.278	0.0468
1	**71**	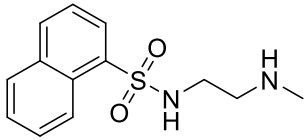	0.879	0.912	0.900	0.897	0.089	0.0517	0.309	0.0430	-0.031	0.0044

1	**72**	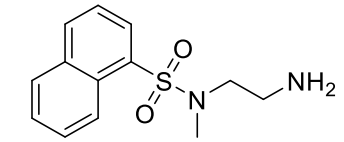	0.796	0.828	0.861	0.828	0.103	0.0596	0.209	0.0304	-0.105	0.0096
1	**68**	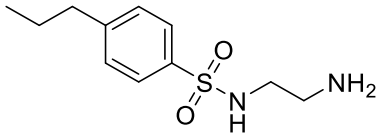	0.944	0.928	0.944	0.939	0.177	0.1021	0.369	0.0618	0.014	0.0019
1	**63**	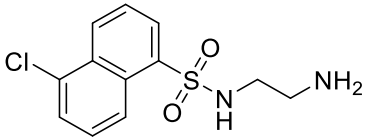	0.585	0.581	0.600	0.589	0.115	0.0663	-0.141	0.0240	-0.364	0.0569
1	**116**	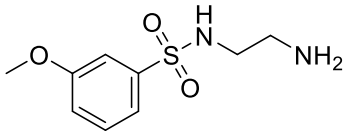	0.836	0.850	0.804	0.830	0.089	0.0619	0.211	0.0310	-0.103	0.0139
2	**DMSO**		0.207	0.242	0.255	0.235	0.056	0.0323	0	0	0	0
2	**1**	eW5	0.317	0.318	0.319	0.318	0.072	0.0416	0.353	0.0670	0	0
2	**92**	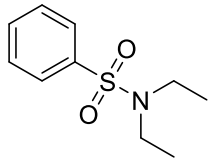	0.175	0.164	0.161	0.167	0.069	0.0397	-0.291	0.0800	-0.476	0.1293
2	**94**	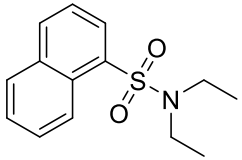	0.154	0.150	0.148	0.151	0.041	0.0238	-0.358	0.0749	-0.525	0.1502
2	**95**	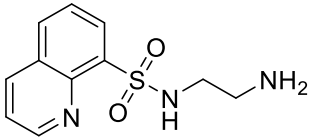	0.223	0.213	0.201	0.212	0.046	0.0266	-0.098	0.0182	-0.333	0.0672

2	**96**	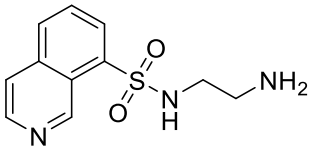	0.288	0.274	0.260	0.274	0.073	0.0421	0.166	0.0342	-0.138	0.0274
2	**97**	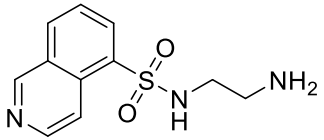	0.204	0.185	0.217	0.202	0.029	0.0167	-0.140	0.0226	-0.365	0.0637
2	**98**	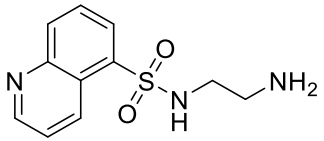	0.316	0.343	0.340	0.333	0.100	0.0577	0.417	0.0923	0.047	0.0091
2	**100**	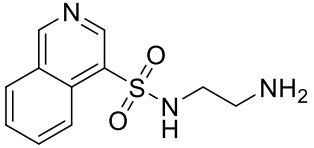	0.325	0.311	0.326	0.321	0.079	0.0454	0.365	0.0721	0.009	0.0020
2	**108**	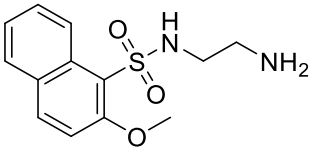	0.330	0.325	0.332	0.329	0.068	0.0393	0.400	0.0728	0.035	0.0064
2	**110**	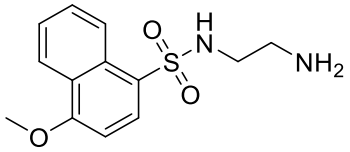	0.280	0.294	0.322	0.299	0.056	0.0325	0.271	0.0475	-0.061	0.0099
3	**DMSO**		0.249	0.240	0.234	0.241	0.026	0.0152	0	0	0	0
3	**1**	eW5	0.323	0.325	0.318	0.322	0.031	0.0180	0.336	0.0283	0	0
3	**109**	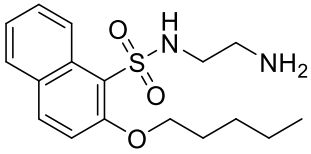	0.198	0.197	0.196	0.197	0.033	0.0192	-0.183	0.0212	-0.388	0.0436

3	**111**	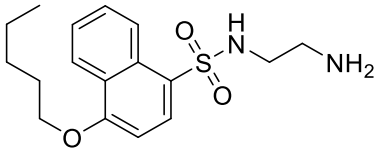	0.191	0.137	0.191	0.173	0.042	0.0241	-0.282	0.0431	-0.463	0.0787
3	**112**	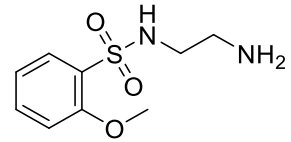	0.310	0.317	0.320	0.316	0.033	0.0188	0.311	0.0269	-0.019	0.0028
3	**113**	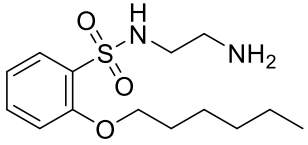	0.209	0.207	0.190	0.202	0.041	0.0239	-0.162	0.0217	-0.373	0.0494
3	**114**	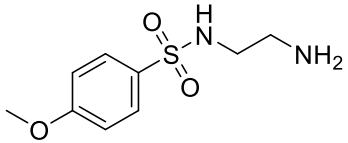	0.311	0.300	0.382	0.331	0.029	0.0167	0.373	0.0301	0.028	0.0036
3	**115**	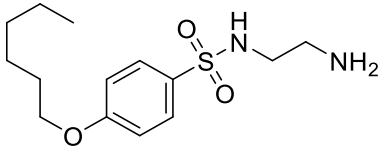	0.192	0.189	0.202	0.195	0.036	0.0207	-0.191	0.0236	-0.394	0.0464
4	**DMSO**		0.403	0.417	0.387	0.402	0.102	0.0587	0	0	0	0
4	**1**	eW5	0.596	0.601	0.621	0.606	0.187	0.1078	0.506	0.1163	0	0
4	**84**	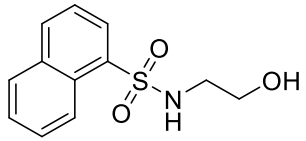	0.259	0.296	0.293	0.283	0.059	0.0343	-0.297	0.0565	-1.143	0.2462
4	**119**	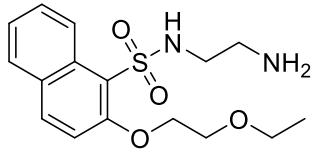	0.592	0.612	0.598	0.601	0.145	0.0836	0.493	0.0993	-0.009	0.0016

4	**121**	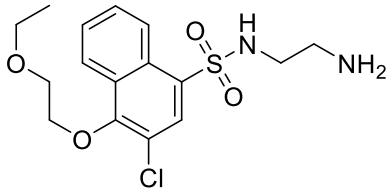	0.456	0.415	0.445	0.439	0.116	0.0669	0.090	0.0191	-0.381	0.0787
4	**122**	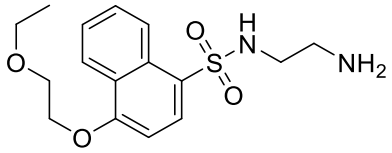	0.607	0.685	0.635	0.642	0.155	0.0894	0.597	0.1203	0.057	0.0118
4	**104**	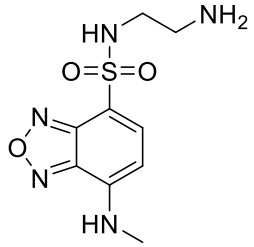	0.295	0.292	0.267	0.285	0.079	0.0456	-0.292	0.0634	-1.128	0.2394

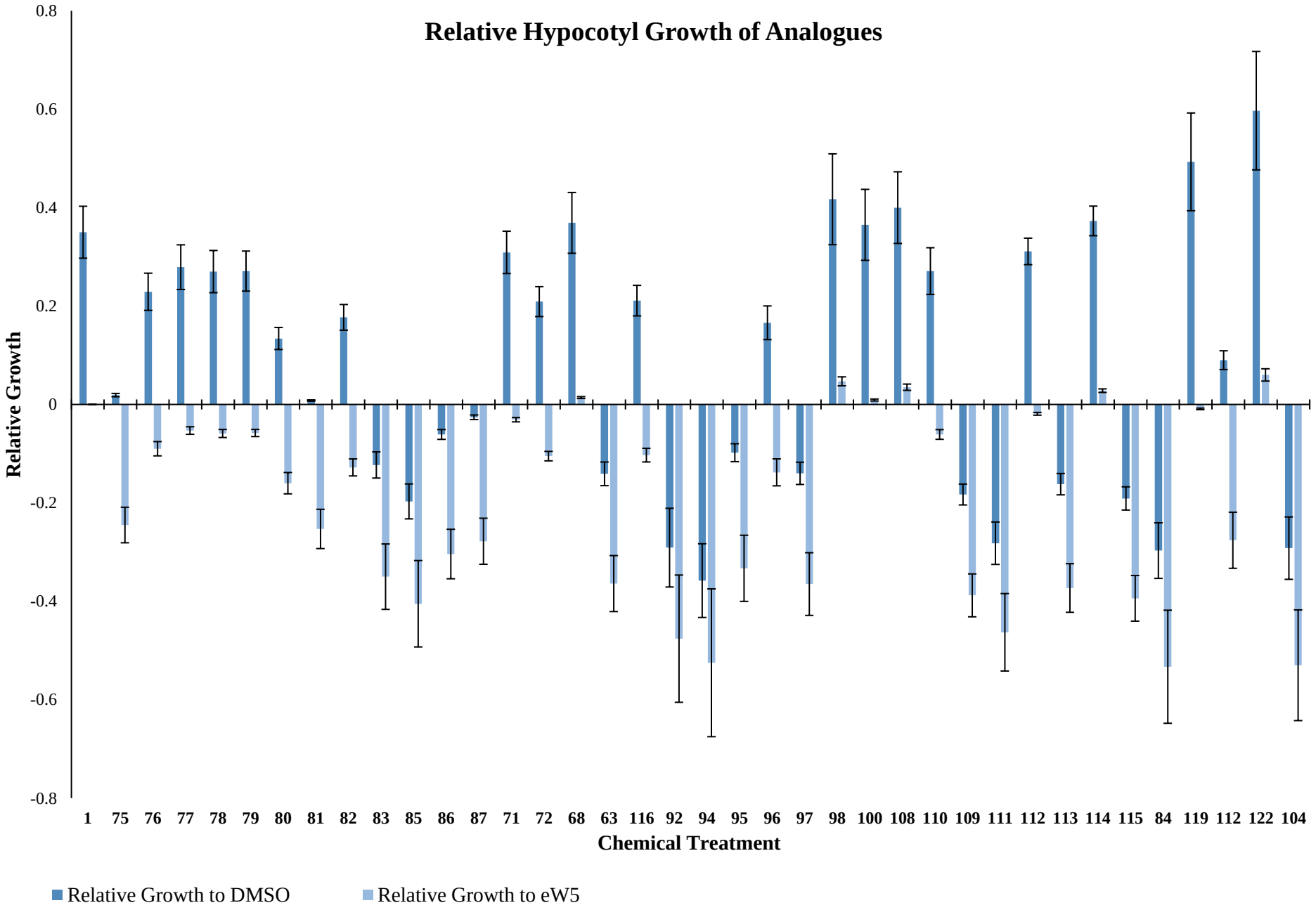
Relative Hypocotyl Growth of Analogues
Relative Growth
0.8
0.6
0.4
0.2
0
-0.2
-0.4
-0.6
-0.8
1 75 76 77 78 79 80 81 82 83 85 86 87 71 72 68 63 116 92 94 95 96 97 98 100 108 110 109 111 112 113 114 115 84 119 112 122 104
Chemical Treatment
Relative Growth to DMSO
Relative Growth to eW5

B.2 Concentration Gradient of Alkoxy Substituents 109 & 111

Compound	Concentration	1st Rep	2nd Rep	3rd Rep	Average	SD	SE
DMSO	100 μM	0.387	0.377	0.386	0.381	0.103	0.0595
DMSO	50 μM	0.356	0.391	0.384	0.377	0.119	0.0687
DMSO	25 μM	0.377	0.394	0.396	0.389	0.0951	0.0549
eW5 (**1**)	100 μM	0.620	0.611	0.587	0.606	0.082	0.0475
eW5 (**1**)	50 μM	0.534	0.533	0.502	0.523	0.142	0.0816
eW5 (**1**)	25 μM	0.438	0.454	0.461	0.451	0.121	0.0700
109	100 μM	0.199	0.240	0.224	0.221	0.0629	0.0363
109	50 μM	0.344	0.385	0.372	0.367	0.119	0.0689
109	25 μM	0.602	0.598	0.585	0.595	0.178	0.103
111	100 μM	0.248	0.269	0.245	0.254	0.0560	0.0323
111	50 μM	0.587	0.515	0.566	0.556	0.109	0.0629
111	25 μM	0.621	0.632	0.640	0.631	0.146	0.0842

B.3 Model Probe 154 & 156 (100 μM)

Compound	1st Rep	2nd Rep	3rd Rep	Average	SD	SE
DMSO	0.202	0.232	0.210	0.215	0.0396	0.0229
eW5	0.273	0.271	0.281	0.275	0.0503	0.0290
156	0.259	0.272	0.252	0.261	0.0490	0.0283
154	0.234	0.240	0.252	0.242	0.0384	0.0222

B.4 Concentration Gradient of eW5 (Chapter 4)

Compound	Concentration	1st Rep	2nd Rep	3rd Rep	Average	SD	SE
DMSO	300	0.415	0.377	0.399	0.397	0.108	0.0624
DMSO	200	0.404	0.351	0.342	0.366	0.122	0.0704
DMSO	100	0.387	0.377	0.386	0.381	0.103	0.0595
DMSO	50	0.356	0.391	0.384	0.377	0.119	0.0687
DMSO	25	0.377	0.394	0.396	0.389	0.0951	0.0549
eW5 (**1**)	300	0.736	0.722	0.801	0.753	0.196	0.113
eW5 (**1**)	200	0.749	0.711	0.733	0.731	0.187	0.108
eW5 (**1**)	100	0.62	0.611	0.587	0.606	0.082	0.0475
eW5 (**1**)	50	0.534	0.533	0.502	0.523	0.142	0.0816
eW5 (**1**)	25	0.438	0.454	0.461	0.451	0.121	0.0700

Appendix C: EMS Mutant Screen Data

C.1: Generation 1 (M_2) Selected Mutants

Trial 1:

Line	Label	Hypocotyl Length / cm
3439	38	0.131
3778	168	0.13
3778	51	0.125
3778	124	0.123
3778	112	0.135
3778	170	0.115
3439	34	0.132
3776	77	0.132
4136	81	0.123
3439	81	0.137
4122	38	0.138
3439	79	0.096
3793	88	0.131
3793	128	0.267
3447	29	0.13
3447	121	0.131
3447	66	0.092
3447	70	0.112
3447	51	0.097
3447	16	0.117
3447	80	0.123
3761	20	0.099
7452	34	0.113
3762	94	0.133
3762	87	0.125
3762	14	0.137
3762	93	0.121
3753	27	0.137
3753	88	0.12
3753	78	0.199
3753	30	0.11
3438	30	0.119
7452	133	0.126
3438	32	0.122
3778	64	0.105
3778	140	0.084
3778	34	0.083
3778	98	0.099
3778	13	0.09
3750	55	0.056
3447	58	0.126
3447	71	0.129
3447	74	0.134
3447	44	0.12
3447	31	0.115
3447	62	0.137
3447	97	0.131
3447	55	0.13
3796	24	0.118
3771	150	0.137
3750	69	0.077
3771	108	0.122
7452	128	0.115
7452	91	0.085
3750	52	0.114
3750	83	0.128
3750	78	0.128
3124	104	0.086
3759	100	0.107
3433	43	0.107
3433	109	0.098
3438	79	0.125
3438	74	0.138
4123	7	0.136
4123	34	0.136
4123	84	0.125
4123	72	0.136
4123	87	0.12
4123	10	0.11
3747	2	0.136
3747	105	0.079
3747	16	0.087
3438	90	0.124
3746	74	0.087
3746	23	0.123
3802	71	0.122
3802	135	0.123
3802	18	0.134
3802	7	0.106
3802	72	0.138
4124	12	0.122
3438	77	0.128
4124	3	0.124
4124	31	0.124
4124	42	0.127
4124	26	0.134
4124	48	0.137
3438	145	0.085
3803	16	0.101
3438	99	0.114
3803	121	0.115
3440	88	0.132
3440	32	0.375
3438	80	0.128
3440	122	0.11
3438	109	0.129
3752	120	0.122
4133	86	0.138
3438	117	0.129
3752	12	0.186
3438	76	0.148
3438	65	0.137
3438	131	0.134
3438	134	0.134
3438	98	0.138
3748	45	0.094
3748	167	0.103

Trial 2:

Line	Label	Hypocotyl Length / cm
4144	91	0.282
3794	45	0.269
4124	10	0.056
3764	19	0.274
3784	61	0.118
3784	147	0.232
3784	143	0.219
3784	146	0.188
3784	149	0.238
3784	12	0.259
3784	9	0.277
4144	69	0.279
3784	150	0.277
3784	148	0.278
3784	155	0.279
3784	145	0.28
3784	115	0.241
3784	62	0.203
3766	29	0.275
3766	77	0.135
3760	108	0.224
3760	97	0.255
3728	12	0.262
3760	33	0.267
3760	58	0.252
3434	79	0.226
4140	52	0.119
3790	50	0.093506
3790	54	0.122078
3726	98	0.749
3786	98	0.249
3726	136	0.262
3726	10	0.11
3728	116	0.206
3726	62	0.278
4147	36	0.222
4147	96	0.071
3794	101	0.204
3794	61	0.244
3794	71	0.222

Trial 3:

Line	Label	Hypocotyl Length / cm
3450	118	0.106
3731	54	0.114
3767	12	0.095
3731	165	0.06
3767	24	0.117
3767	96	0.114
3767	65	0.112
3767	22	0.097
3779	46	0.107
3779	48	0.115
3779	19	0.097
3450	124	0.113
3779	14	0.1
3787	76	0.103
3783	60	0.075
3783	72	0.083
3783	123	0.095
3755	112	0.095
3755	102	0.08
3777	113	0.115
3450	150	0.11
3788	38	0.103
3788	57	0.109
3788	65	0.116
3788	113	0.117
3791	58	0.107
3731	61	0.111

Trial 4:

Line	Label	Hypocotyl Length / cm
3798	99	0.176
3798	85	0.239
3798	179	0.183
3789	157	0.231
3454	146	0.229
4142	125	0.191
3744	16	0.124
4135	93	0.213
4135	97	0.222
4135	39	0.218
3758	37	0.2
3758	57	0.095
3758	61	0.142
3758	69	0.145
3758	20	0.229
3758	164	0.171
3758	41	0.196
3758	47	0.193
3758	130	0.212
3758	75	0.161
3758	121	0.204
4129	86	0.241
3758	19	0.199
3769	54	0.221
3444	48	0.181
3134	36	0.128
3134	37	0.164
3134	44	0.188
3134	66	0.182
3134	55	0.184
3758	124	0.176
3134	35	0.214
3134	74	0.21
3134	62	0.24
3134	97	0.219
3134	113	0.213
3134	105	0.221
3134	115	0.22
3134	18	0.108
3745	55	0.203
3745	56	0.215
3745	80	0.165
3772	133	0.242
3450	66	0.157
3450	155	0.164
3450	87	0.195
3450	139	0.179
3450	161	0.224
3450	103	0.182

Trial 5:

Line	Label	Hypocotyl Length / cm
3748	75	0.093
3744	19	0.089
3730	145	0.121
3741	92	0.11
3809	149	0.12
3786	152	0.127
3790	17	0.12
3744	32	0.118
3790	29	0.122
3786	88	0.124
3786	2	0.104
3741	82	0.129
3790	19	0.129
3744	100	0.111
3744	183	0.129
3744	166	0.125
3786	144	0.089
3786	118	0.172
3809	91	0.097
3809	55	0.129
3730	171	0.125
3748	45	0.094
3748	167	0.103
3744	16	0.124

Trial 6:

Line	Label	Hypocotyl Length / cm
3766	168	0.125
3782	10	0.139
3774	83	0.136
3781	155	0.126
3748	9	0.159
3793	169	0.153
3754	83	0.161
3777	194	0.096
3777	199	0.155
3777	201	0.112
3441	166	0.145
3766	78	0.137
3441	125	0.147
3801	68	0.149
3783	94	0.147
3783	95	0.119
3783	92	0.108
3783	109	0.151
3783	39	0.096
3783	159	0.123
3783	172	0.152
3783	138	0.151
3766	170	0.107
3783	161	0.157
3755	54	0.138
3783	72	0.149
3755	57	0.159
3755	75	0.149
3748	30	0.126
3748	5	0.14
3748	18	0.146
3748	62	0.145
3748	124	0.145
3748	89	0.159
3790	49	0.147
3749	77	0.133
3753	81	0.158
3753	80	0.099
3753	60	0.139
4138	89	0.148
3782	150	0.148
3749	98	0.154
3752	65	0.16
3752	87	0.128
3446	30	0.139
3446	38	0.124
3446	39	0.145
3446	11	0.139
3446	53	0.136
3446	149	0.13
3446	145	0.137
3446	82	0.124
4130	6	0.146
3446	59	0.145
3446	159	0.15
3446	27	0.154
3446	23	0.16
3727	128	0.14
3727	144	0.134
3769	99	0.157
3769	29	0.121
3769	147	0.158
3769	139	0.153
3780	5	0.158
4130	118	0.131
3780	33	0.121
4130	46	0.138
4130	123	0.156
4130	93	0.161
3729	13	0.154
3752	9	0.13
3752	34	0.135

C.2: Generation 2 (M_3) Selected Mutants

1st Replicate*:

Line	label	eW5 mean Hypocotyl length / cm	eW5 S.D.	DMSO mean Hypocotyl length / cm	DMSO S.D.	t-statistic	t-test p value	Mean difference
3726	10	0.1229	0.0293	0.2660	0.0699	21.0398	1.72E-54	0.143096
4123	72	0.3160	0.0619	0.5137	0.1107	18.4992	5.01E-50	0.197653
3794	45	0.0844	0.0166	0.1406	0.0301	16.3545	1.34E-39	0.056202
3784	146	0.2629	0.0611	0.4742	0.1029	16.9844	1.57E-39	0.211332
3778	51	0.3234	0.0728	0.1948	0.0397	-15.8740	4.52E-38	-0.12864
3778	168	0.3692	0.0714	0.2562	0.0536	-14.7928	1.53E-36	-0.11298
3758	47	0.4498	0.0881	0.2687	0.0509	-15.9351	5.32E-34	-0.18112
7452	128	0.4477	0.1043	0.2867	0.0517	-14.6685	5.82E-34	-0.16095
3788	65	0.2345	0.0485	0.3469	0.0847	13.4708	5.21E-32	0.112386
3134	36	0.1379	0.0405	0.2860	0.0796	14.7231	2.66E-30	0.148146
3446	38	0.3625	0.0886	0.2464	0.0470	-12.6574	2.28E-28	-0.11604
4140	52	0.2694	0.0580	0.4254	0.0973	13.2528	4.45E-28	0.155982
3446	53	0.3656	0.1004	0.2582	0.0543	-11.9353	4.67E-27	-0.10741
4123	7	0.2221	0.0490	0.3889	0.0873	13.6786	9.70E-27	0.166804
4130	118	0.3692	0.0940	0.2774	0.0689	-11.4837	1.09E-26	-0.0918
3780	33	0.4747	0.1175	0.2979	0.0717	-12.2774	3.01E-26	-0.17682
3752	12	0.3679	0.0658	0.2741	0.0640	-11.7468	5.19E-26	-0.09379
3438	65	0.2677	0.0695	0.3935	0.0866	11.8046	3.84E-25	0.125868
4123	34	0.3225	0.0624	0.4324	0.0854	11.3271	4.32E-24	0.109886
3752	34	0.3182	0.0867	0.4340	0.1222	10.5543	5.83E-23	0.11586
3788	113	0.2616	0.0541	0.3652	0.0842	11.0789	6.15E-23	0.103534
3783	60	0.2402	0.0375	0.1208	0.0349	-14.2601	6.32E-23	-0.11942
3782	150	0.3488	0.0820	0.2346	0.0488	-11.0974	3.28E-22	-0.1142
4130	6	0.2742	0.0442	0.3604	0.0918	10.3192	2.63E-21	0.086202
3446	149	0.4049	0.1015	0.2889	0.0674	-10.2512	7.14E-21	-0.11603
3447	71	0.3279	0.0831	0.2137	0.0404	-10.5927	8.33E-20	-0.11426
3790	17	0.2070	0.0366	0.1572	0.0382	-9.9842	1.18E-19	-0.04979
3726	62	0.3520	0.0758	0.2668	0.0619	-9.8042	2.12E-19	-0.08523
3790	19	0.2598	0.0674	0.3903	0.1133	9.9367	2.40E-19	0.130469
3438	117	0.2422	0.0419	0.4177	0.1205	10.8158	3.44E-19	0.175457
4130	123	0.2763	0.0382	0.4333	0.0876	10.0428	8.08E-19	0.156962
3446	159	0.2997	0.0504	0.4002	0.0930	9.7100	1.06E-18	0.100492
3767	24	0.3246	0.0673	0.2172	0.0456	-10.1282	1.28E-17	-0.10745
3744	19	0.1970	0.0504	0.3002	0.0854	9.2437	8.38E-17	0.103198
3446	30	0.2849	0.0790	0.4408	0.1113	9.4477	1.21E-16	0.155831
3779	19	0.3353	0.0630	0.2362	0.0365	-9.4170	1.46E-15	-0.09904
3779	46	0.4008	0.0959	0.3091	0.0630	-8.2255	1.66E-14	-0.09166
3748	9	0.3993	0.0778	0.3098	0.0689	-8.2682	2.53E-14	-0.08952
3798	99	0.2770	0.0702	0.1824	0.0443	-8.7012	3.86E-14	-0.09458
3727	144	0.3273	0.0882	0.4294	0.1169	7.9819	4.20E-14	0.102115

4142	125	0.1912	0.0422	0.2636	0.0671	8.2094	6.08E-14	0.072384
3767	12	0.3546	0.0861	0.2788	0.0575	-7.8635	1.66E-13	-0.07578
3788	57	0.2463	0.0515	0.3048	0.0643	7.6042	5.09E-13	0.058518
3793	88	0.1123	0.0238	0.2553	0.0627	9.1135	7.40E-13	0.143024
3447	62	0.2961	0.0650	0.2104	0.0450	-8.1004	7.80E-13	-0.08567
3726	98	0.1895	0.0552	0.3094	0.0748	8.4510	8.19E-13	0.119939
3438	134	0.2707	0.0557	0.3317	0.0637	7.5207	1.37E-12	0.060956
3777	194	0.3291	0.0901	0.4276	0.0839	7.5598	1.95E-12	0.09855
3440	122	0.2708	0.0485	0.3697	0.0989	7.4833	6.76E-12	0.09885
3447	29	0.2922	0.0668	0.2286	0.0531	-7.2104	1.34E-11	-0.06368
3446	145	0.3449	0.0863	0.4574	0.1032	7.1024	3.60E-11	0.112531
3790	29	0.2519	0.0702	0.1544	0.0499	-7.5216	5.45E-11	-0.09748
3790	54	0.2870	0.0641	0.2353	0.0489	-6.8404	7.64E-11	-0.05173
3766	29	0.3514	0.0823	0.2861	0.0689	-6.6594	1.87E-10	-0.06532
3750	55	0.3094	0.0764	0.2427	0.0586	-6.6275	3.58E-10	-0.06668
3758	75	0.3078	0.0747	0.3994	0.1078	6.5419	6.03E-10	0.091575
3748	75	0.1790	0.0346	0.2359	0.0543	6.6271	1.10E-09	0.056928
3809	149	0.1247	0.0350	0.1565	0.0403	6.3486	1.18E-09	0.03174
3447	80	0.2548	0.0487	0.2053	0.0531	-6.2996	2.58E-09	-0.04946
3446	59	0.2308	0.0545	0.3440	0.0910	6.3282	2.64E-09	0.113226
4135	39	0.3070	0.0775	0.2477	0.0665	-6.1985	2.64E-09	-0.05935
3755	112	0.3107	0.0596	0.3645	0.0798	6.1308	3.20E-09	0.053787
3741	82	0.2418	0.0690	0.3246	0.1031	6.1942	3.91E-09	0.082867
3752	9	0.3565	0.0967	0.2837	0.0554	-6.1193	5.39E-09	-0.07284
3802	18	0.3372	0.0573	0.2700	0.0658	-6.2304	6.09E-09	-0.06712
3783	159	0.3569	0.1069	0.4648	0.1283	5.9471	1.32E-08	0.107825
3809	55	0.2390	0.0622	0.3000	0.0749	5.9345	1.48E-08	0.061043
4130	46	0.2331	0.0392	0.2660	0.0488	5.7293	2.79E-08	0.032874
3747	2	0.3765	0.0594	0.2106	0.0714	-7.2473	3.11E-08	-0.16587
3450	124	0.2762	0.0759	0.3331	0.0703	5.6980	3.90E-08	0.056859
7452	133	0.2416	0.0510	0.1816	0.0496	-5.7766	5.95E-08	-0.06
3745	55	0.2345	0.0695	0.3622	0.1190	5.9366	8.15E-08	0.127706
3762	94	0.3013	0.0633	0.2536	0.0603	-5.5425	9.01E-08	-0.04776
3760	33	0.3041	0.0696	0.3743	0.0824	5.5678	1.23E-07	0.070196
3752	65	0.3680	0.0862	0.3019	0.0774	-5.4583	1.45E-07	-0.06608
3782	10	0.3473	0.0825	0.2819	0.0745	-5.4718	1.52E-07	-0.06539
3753	80	0.3676	0.0959	0.3067	0.0701	-5.2190	4.17E-07	-0.06083
4135	93	0.2132	0.0504	0.2731	0.0787	5.3000	4.36E-07	0.059931
4124	10	0.1271	0.0349	0.1083	0.0249	-5.1677	4.53E-07	-0.01876
3727	128	0.3780	0.0920	0.3209	0.0643	-5.2138	4.56E-07	-0.05717
3780	5	0.2053	0.0654	0.2774	0.0806	5.3238	5.16E-07	0.072154
3748	89	0.3535	0.1062	0.2896	0.0834	-5.1007	6.93E-07	-0.06392
3134	55	0.2997	0.0753	0.3653	0.1137	5.1049	7.27E-07	0.065617
3790	50	0.2783	0.0631	0.1374	0.0488	-5.4755	1.07E-06	-0.14084
3758	61	0.2913	0.0742	0.2258	0.0719	-5.0318	1.46E-06	-0.06546
3450	139	0.4322	0.1133	0.2920	0.0739	-5.2989	2.89E-06	-0.14024

3728	116	0.1473	0.0278	0.1298	0.0272	-4.7784	3.20E-06	-0.01752
3758	20	0.1871	0.0416	0.2182	0.0503	4.7879	3.27E-06	0.031063
3783	39	0.1757	0.0353	0.2162	0.0455	4.9335	3.39E-06	0.040528
3446	23	0.3507	0.0789	0.3089	0.0617	-4.6855	4.38E-06	-0.04185
3772	133	0.2497	0.0597	0.2034	0.0558	-4.7695	4.58E-06	-0.04624
3801	68	0.2518	0.0587	0.3052	0.0686	4.7432	5.53E-06	0.053445
3766	77	0.3032	0.0671	0.2588	0.0632	-4.6195	7.26E-06	-0.04441
3758	69	0.2429	0.0649	0.2884	0.0644	4.6220	7.33E-06	0.04548
3787	76	0.3582	0.0899	0.3117	0.0780	-4.5607	7.56E-06	-0.04646
3784	155	0.2418	0.0574	0.2037	0.0372	-4.5986	9.84E-06	-0.03811
3778	13	0.2824	0.0728	0.2440	0.0723	-4.4710	1.13E-05	-0.03844
3784	148	0.2453	0.0581	0.2074	0.0538	-4.5096	1.16E-05	-0.03791
3786	144	0.2670	0.0876	0.1946	0.0712	-4.5493	1.52E-05	-0.07247
3447	121	0.2475	0.0593	0.2132	0.0444	-4.4085	1.81E-05	-0.03437
4144	91	0.2227	0.0482	0.3203	0.1040	4.6406	1.89E-05	0.09757
3769	99	0.2583	0.0603	0.3075	0.0721	4.3748	2.36E-05	0.049223
3730	171	0.2284	0.0626	0.1718	0.0651	-4.4126	2.65E-05	-0.05664
3778	170	0.2035	0.0374	0.1780	0.0398	-4.1037	6.57E-05	-0.0255
3764	19	0.2115	0.0507	0.2449	0.0536	4.0818	7.00E-05	0.033417
3784	9	0.3094	0.0719	0.2635	0.0835	-4.0523	7.42E-05	-0.04585
3438	74	0.2983	0.0641	0.2511	0.0544	-4.0973	8.30E-05	-0.04722
3750	52	0.2649	0.0625	0.2216	0.0514	-4.0254	0.000104	-0.04328
3794	71	0.2708	0.0683	0.2219	0.0493	-4.0286	0.000115	-0.04886
3796	24	0.4293	0.1052	0.3774	0.0860	-3.8699	0.000146	-0.05193
3802	72	0.3059	0.0685	0.2677	0.0587	-3.8786	0.000151	-0.03814
3730	145	0.3232	0.0770	0.2446	0.1099	-3.9575	0.000153	-0.07866
WT	WT	0.3875	0.1289	0.2693	0.0927	-3.9543	0.000211	-0.11815
3767	22	0.3363	0.0751	0.3752	0.0843	3.6989	0.000271	0.03892
3784	143	0.0915	0.0224	0.1115	0.0383	3.6998	0.000306	0.020016
3438	32	0.2774	0.0446	0.2482	0.0565	-3.6521	0.000353	-0.02924
3728	12	0.1203	0.0262	0.0980	0.0235	-3.6903	0.000357	-0.02226
3781	155	0.2370	0.0538	0.2043	0.0437	-3.6597	0.00038	-0.03271
3771	150	0.2588	0.0527	0.2185	0.0559	-3.6722	0.00039	-0.04031
3760	108	0.1619	0.0498	0.1944	0.0334	3.5963	0.000449	0.032514
3438	80	0.3286	0.0699	0.2941	0.0625	-3.5612	0.00047	-0.03458
3798	179	0.3932	0.0903	0.4456	0.0833	3.5515	0.000521	0.052464
3447	66	0.3352	0.0708	0.3747	0.0850	3.5121	0.000553	0.039534
3794	101	0.1239	0.0326	0.1058	0.0338	-3.5126	0.000558	-0.01814
3744	100	0.2152	0.0479	0.2443	0.0616	3.4241	0.000778	0.029065
3774	83	0.3386	0.0916	0.3014	0.0755	-3.3733	0.00086	-0.03723
3785	5	0.1065	0.0285	0.0953	0.0186	-3.3699	0.000899	-0.01116
3784	9	0.4041	0.0947	0.3533	0.0770	-3.3809	0.000943	-0.05077
3766	168	0.2952	0.0742	0.2521	0.0589	-3.3871	0.000984	-0.04314
3784	61	0.2187	0.0418	0.2510	0.0733	3.3423	0.001052	0.03233
4136	81	0.0985	0.0191	0.0826	0.0191	-3.3978	0.001156	-0.01596
3783	72	0.3761	0.0777	0.3373	0.0816	-3.2719	0.001282	-0.03872

3760	97	0.2937	0.0811	0.3332	0.0987	3.2265	0.00144	0.039507
4129	86	0.2821	0.0634	0.3257	0.0735	3.2562	0.001468	0.043579
3748	62	0.3563	0.0951	0.3002	0.0998	-3.2195	0.001568	-0.05608
3767	65	0.3161	0.0624	0.3413	0.0768	3.0379	0.002608	0.025212
3784	147	0.2544	0.0572	0.2292	0.0502	-3.0199	0.002936	-0.02526
3783	123	0.3237	0.0691	0.3521	0.0773	3.0041	0.002948	0.02846
3450	161	0.2705	0.0708	0.3140	0.0741	3.0241	0.002993	0.043506
3754	83	0.3075	0.0731	0.2762	0.0718	-2.9700	0.003362	-0.03126
3446	39	0.3260	0.0862	0.2955	0.0883	-2.8907	0.004155	-0.03053
3450	150	0.1100	0.0514	0.3058	0.0610	2.8025	0.005488	0.020493
3769	25	0.3161	0.0862	0.2743	0.0725	-2.8188	0.00562	-0.04171
3783	92	0.4084	0.1158	0.3678	0.0929	-2.7932	0.005711	-0.04066
3779	14	0.3521	0.0832	0.3824	0.0871	2.7710	0.006023	0.03029
3753	60	0.2685	0.0869	0.3271	0.1305	2.7635	0.006776	0.058608
3778	**140**	**0.3626**	**0.1036**	**0.3924**	**0.1052**	**2.7087**	**0.007057**	**0.029846**
3783	**94**	**0.3617**	**0.0676**	**0.3933**	**0.0813**	**2.7131**	**0.007374**	**0.031578**
3798	**85**	**0.2229**	**0.0429**	**0.2523**	**0.0812**	**2.7131**	**0.007503**	**0.029344**
3748	**18**	**0.1150**	**0.0306**	**0.1030**	**0.0209**	**-2.6579**	**0.008783**	**-0.01199**
3786	2	0.1739	0.0337	0.1517	0.0389	-2.6625	0.009487	-0.02217
3440	32	0.3233	0.0890	0.3595	0.0867	2.6139	0.009774	0.036172
3758	**57**	**0.3546**	**0.1175**	**0.3120**	**0.1243**	**-2.5864**	**0.010358**	**-0.04254**
4124	12	0.3041	0.0607	0.3285	0.0714	2.5363	0.012001	0.024387
3793	**169**	**0.2170**	**0.0402**	**0.1973**	**0.0438**	**-2.5429**	**0.012309**	**-0.01967**
3446	**82**	**0.3167**	**0.0717**	**0.3408**	**0.0743**	**2.4795**	**0.013896**	**0.024172**
3748	**5**	0.0748	0.0216	0.0841	0.0252	2.4700	0.014581	0.009305
3783	**161**	**0.4178**	**0.1289**	**0.4526**	**0.1000**	**2.4565**	**0.014582**	**0.034831**
3438	74	0.3683	0.0724	0.3424	0.0889	-2.4551	0.014809	-0.02593
3433	**43**	**0.2672**	**0.0669**	**0.2989**	**0.0802**	**2.4615**	**0.015107**	**0.031636**
3783	172	0.2163	0.0423	0.2001	0.0349	-2.4524	0.015457	-0.01618
3778	**98**	**0.3131**	**0.0787**	**0.3398**	**0.0990**	**2.2801**	**0.023507**	**0.026669**
4123	**84**	**0.2721**	**0.0733**	**0.2282**	**0.0829**	**-2.2739**	**0.026334**	**-0.04389**
3726	**136**	**0.2739**	**0.0770**	**0.2484**	**0.0694**	**-2.2318**	**0.026991**	**-0.02551**
3447	16	0.2747	0.0988	0.3072	0.1048	2.1968	0.029211	0.03251
3134	18	0.1889	0.0508	0.2276	0.0528	2.2099	0.032239	0.038655
3778	**64**	**0.3128**	**0.0756**	**0.2848**	**0.0789**	**-2.1279**	**0.034956**	**-0.02796**
3758	**124**	**0.3130**	**0.0803**	**0.3461**	**0.0900**	**2.0474**	**0.043004**	**0.033139**
3444	48	0.1761	0.0493	0.1470	0.0417	-2.0668	0.04511	-0.0291
3438	**131**	**0.1387**	**0.0267**	**0.1619**	**0.0397**	**2.0113**	**0.047936**	**0.023197**
3758	19	0.1838	0.0517	0.2331	0.0362	2.1658	0.049508	0.0493
3446	**11**	**0.3766**	**0.1025**	**0.3513**	**0.0832**	**-1.9531**	**0.052091**	**-0.02532**
3134	**115**	**0.2716**	**0.0705**	**0.2972**	**0.0899**	**1.9135**	**0.057654**	**0.025583**
3779	**48**	**0.1320**	**0.0256**	**0.0920**	**0.0101**	**-2.5131**	**0.065838**	**-0.04**
3134	**105**	**0.3332**	**0.0691**	**0.3506**	**0.0782**	**1.8206**	**0.06994**	**0.017416**
3766	**78**	**0.2963**	**0.0817**	**0.2793**	**0.0738**	**-1.7727**	**0.07743**	**-0.01697**
3447	**97**	**0.3180**	**0.0653**	**0.3347**	**0.0675**	**1.7673**	**0.078728**	**0.016708**
3741	**92**	**0.1847**	**0.0349**	**0.1938**	**0.0395**	**1.7652**	**0.07894**	**0.009103**

3758	**164**	**0.2153**	**0.0494**	**0.2283**	**0.0517**	**1.7285**	**0.085605**	**0.013028**
3766	170	0.2131	0.0523	0.1882	0.0309	-1.7494	0.088296	-0.02491
3786	**118**	**0.2189**	**0.0463**	**0.2069**	**0.0570**	**-1.7078**	**0.089107**	**-0.01207**
3450	**87**	**0.2484**	**0.0312**	**0.2061**	**0.0479**	**-1.7618**	**0.103541**	**-0.04229**
4135	**97**	**0.1409**	**0.0464**	**0.1291**	**0.0467**	**-1.5994**	**0.111714**	**-0.01175**
3802	135	0.2886	0.0650	0.3094	0.0690	1.4978	0.137465	0.020772
3788	**38**	**0.1189**	**0.0236**	**0.1143**	**0.0280**	**-1.4894**	**0.137535**	**-0.00463**
3438	**109**	**0.1824**	**0.0363**	**0.2025**	**0.0938**	**1.4867**	**0.140513**	**0.020103**
3450	**66**	**0.2113**	**0.0386**	**0.1998**	**0.0451**	**-1.4240**	**0.157383**	**-0.01146**
3783	109	0.2260	0.0458	0.2133	0.0485	-1.3566	0.177897	-0.01275
3790	**49**	**0.1641**	**0.0576**	**0.1368**	**0.0482**	**-1.3480**	**0.189276**	**-0.0273**
3450	**103**	**0.2900**	**0.0589**	**0.3071**	**0.0662**	**1.2858**	**0.201683**	**0.017129**
3450	**66**	**0.2524**	**0.0561**	**0.2307**	**0.0510**	**-1.1962**	**0.239657**	**-0.02168**
3134	**66**	**0.2784**	**0.0701**	**0.2949**	**0.0771**	**1.1698**	**0.244651**	**0.016497**
3450	**118**	**0.3371**	**0.0898**	**0.3208**	**0.0797**	**-1.1213**	**0.264048**	**-0.01629**
3439	38	0.2427	0.0484	0.2672	0.0865	1.1136	0.271495	0.024448
3438	**79**	**0.2664**	**0.0759**	**0.2776**	**0.0567**	**1.0825**	**0.28064**	**0.011219**
3729	**13**	**0.2800**	**0.0549**	**0.2924**	**0.0789**	**1.0761**	**0.283376**	**0.012428**
3750	**78**	**0.2602**	**0.0711**	**0.2830**	**0.0748**	**0.9736**	**0.336599**	**0.022789**
3446	**27**	**0.2410**	**0.0607**	**0.2284**	**0.0547**	**-0.9584**	**0.340821**	**-0.01263**
3783	**172**	**0.2987**	**0.0626**	**0.2902**	**0.0649**	**-0.9368**	**0.349978**	**-0.00843**
3791	**58**	**0.2006**	**0.0744**	**0.1793**	**0.0369**	**-0.7811**	**0.444869**	**-0.0213**
3134	**35**	**0.2775**	**0.0648**	**0.2676**	**0.0749**	**-0.7351**	**0.463919**	**-0.00991**
3440	**88**	**0.3583**	**0.0948**	**0.3689**	**0.1023**	**0.6885**	**0.492137**	**0.010627**
3761	**20**	**0.2826**	**0.0732**	**0.2897**	**0.0759**	**0.6749**	**0.500491**	**0.007092**
3784	**115**	**0.2152**	**0.0465**	**0.2101**	**0.0496**	**-0.6595**	**0.510615**	**-0.00515**
3769	**147**	**0.1881**	**0.0311**	**0.1912**	**0.0326**	**0.5610**	**0.575781**	**0.003117**
3447	58	0.3132	0.0794	0.3063	0.0892	-0.5561	0.578782	-0.00684
3762	**14**	**0.2796**	**0.0695**	**0.2738**	**0.0817**	**-0.5183**	**0.604862**	**-0.00584**
3778	**34**	**0.3024**	**0.0828**	**0.2964**	**0.0862**	**-0.5173**	**0.605506**	**-0.00591**
3750	**83**	**0.3333**	**0.0784**	**0.3426**	**0.1106**	**0.4812**	**0.631483**	**0.009238**
3767	**96**	**0.3321**	**0.0774**	**0.3357**	**0.0738**	**0.3957**	**0.692609**	**0.003605**
3758	**130**	**0.1763**	**0.0702**	**0.1926**	**0.0726**	**0.3970**	**0.696966**	**0.016365**
3748	**124**	**0.2678**	**0.0594**	**0.2699**	**0.0526**	**0.3768**	**0.706547**	**0.002129**
3446	**39**	**0.2152**	**0.0653**	**0.2227**	**0.0693**	**0.3581**	**0.722189**	**0.007569**
3777	**199**	**0.1961**	**0.0416**	**0.2009**	**0.0380**	**0.3524**	**0.726089**	**0.004825**
3746	**23**	**0.2526**	**0.0803**	**0.2466**	**0.0518**	**-0.3000**	**0.7654**	**-0.00596**
3758	**37**	**0.2168**	**0.0444**	**0.2189**	**0.0522**	**0.2780**	**0.781358**	**0.002092**
3784	145	0.2313	0.0510	0.2295	0.0494	-0.2414	0.809503	-0.00181
3753	**30**	**0.2503**	**0.0713**	**0.2539**	**0.0690**	**0.1916**	**0.848763**	**0.003593**
3744	**16**	**0.1970**	**0.0370**	**0.1982**	**0.0459**	**0.1851**	**0.853333**	**0.001117**
3783	**138**	**0.1139**	**0.0325**	**0.1146**	**0.0332**	**0.1350**	**0.892746**	**0.00066**
3749	**77**	**0.2570**	**0.0710**	**0.2579**	**0.0562**	**0.1192**	**0.90519**	**0.000925**
3438	**99**	**0.2877**	**0.0491**	**0.2894**	**0.1178**	**0.1057**	**0.916007**	**0.001705**
7452	**91**	**0.2499**	**0.0755**	**0.2477**	**0.0630**	**-0.0965**	**0.923705**	**-0.00221**
3745	**56**	**0.2073**	**0.0367**	**0.2071**	**0.0511**	**-0.0342**	**0.972742**	**-0.00023**

3450	**155**	**0.0850**	**0.0193**	**0.0849**	**0.0171**	**-0.0101**	**0.991923**	**-3.63E-05**
3447	**70**	**0.2419**	**0.0469**	**0.2419**	**0.0633**	**0.0027**	**0.997823**	**2.19E-05**

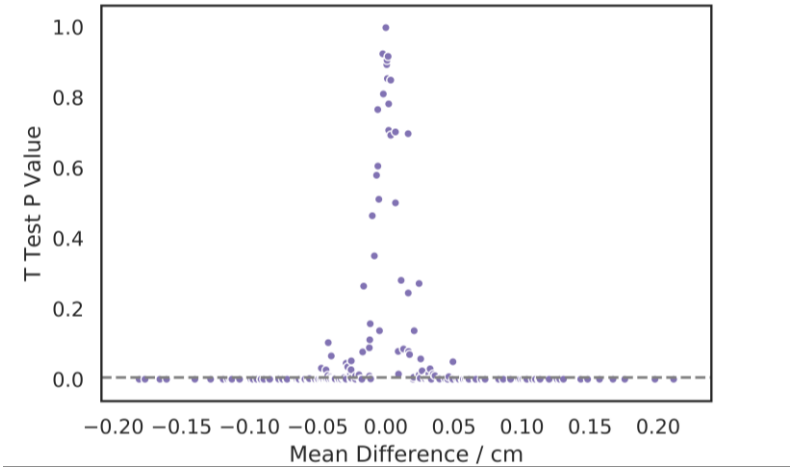

Figure C.2.1: Mean hypocotyl length difference between DMSO and eW5 against T-test P value for 1st replicate

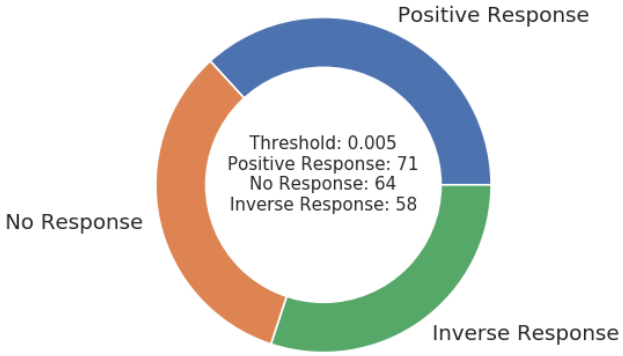

Figure C.2.2: Distribution of responses of selected EMS mutant populations to eW5 compared to DMSO for 1st replicate. Threshold selected for "No response" = p<0.005. "Positive response" populations have positive mean hypocotyl length difference and "inverse response" populations have negative mean hypocotyl length difference

2nd Replicate*:

Line	label	eW5 mean Hypocotyl length / cm	eW5 S.D.	DMSO mean Hypocotyl length / cm	DMSO S.D.	t-statistic	t-test p value	Mean difference
3726	136	0.2961	0.0650	0.2104	0.0450	-8.1004	7.80E-13	-0.08567
3758	37	0.3291	0.0901	0.4276	0.0839	7.5598	1.95E-12	0.09855
3769	147	0.2331	0.0501	0.2873	0.0481	7.1925	1.87E-11	0.054217
3786	118	0.3026	0.0803	0.4294	0.0971	7.3173	4.90E-11	0.126771
3446	39	0.3151	0.1020	0.2186	0.0520	-6.1323	1.36E-08	-0.09652
3762	14	0.2431	0.0503	0.2992	0.0780	5.1995	6.94E-07	0.056114

3748	124	0.2202	0.0387	0.2504	0.0423	4.9754	1.48E-06	0.030233
3783	138	0.1757	0.0353	0.2162	0.0455	4.9335	3.39E-06	0.040528
3450	66	0.3297	0.0815	0.2738	0.0669	-4.7538	4.48E-06	-0.05592
3134	105	0.2518	0.0587	0.3052	0.0686	4.7432	5.53E-06	0.053445
3750	78	0.4278	0.1002	0.3507	0.0863	-4.6009	1.02E-05	-0.07712
3729	13	0.1945	0.0390	0.2443	0.0540	4.4052	2.59E-05	0.049839
3741	92	0.2983	0.0641	0.2511	0.0544	-4.0973	8.30E-05	-0.04722
3793	169	0.2708	0.0683	0.2219	0.0493	-4.0286	0.000115	-0.04886
3450	87	0.1917	0.0444	0.2244	0.0407	3.9966	0.000118	0.032705
WT	WT	0.3875	0.1289	0.2693	0.0927	-3.9543	0.000211	-0.11815
3758	124	0.4041	0.0947	0.3533	0.0770	-3.3809	0.000943	-0.05077
3729	13	0.2952	0.0742	0.2521	0.0589	-3.3871	0.000984	-0.04314
4135	97	0.0985	0.0191	0.0826	0.0191	-3.3978	0.001156	-0.01596
3438	109	0.2224	0.0484	0.2496	0.0444	3.0890	0.002548	0.027224
3440	88	0.2893	0.0550	0.2599	0.0553	-3.0563	0.002654	-0.02938
3758	57	0.2705	0.0708	0.3140	0.0741	3.0241	0.002993	0.043506
3767	96	0.3545	0.0755	0.3987	0.0973	2.9393	0.003825	0.044251
3753	30	0.3188	0.0708	0.2858	0.0641	-2.9373	0.003834	-0.03301
3450	103	0.3136	0.0777	0.2324	0.0565	-3.0839	0.004931	-0.08119
3778	34	0.2704	0.0816	0.3295	0.0881	2.8946	0.00512	0.059149
3433	43	0.3161	0.0862	0.2743	0.0725	-2.8188	0.00562	-0.04171
3798	85	0.2229	0.0429	0.2523	0.0812	2.7131	0.007503	0.029344
3438	79	0.2551	0.0538	0.2891	0.0847	2.7106	0.007669	0.034039
3748	18	0.2657	0.0501	0.2459	0.0527	-2.6741	0.008139	-0.01973
3784	115	0.1722	0.0331	0.1899	0.0392	2.6121	0.010232	0.017741
3788	38	0.2767	0.0539	0.2956	0.0587	2.4913	0.013471	0.018879
3778	98	0.3153	0.0660	0.2563	0.0547	-2.6301	0.013521	-0.05897
3746	23	0.2161	0.0493	0.1440	0.0664	-2.6653	0.014864	-0.07206
3766	**78**	**0.2163**	**0.0423**	**0.2001**	**0.0349**	**-2.4524**	**0.015457**	**-0.01618**
3748	**5**	**0.1889**	**0.0508**	**0.2276**	**0.0528**	**2.2099**	**0.032239**	**0.038655**
3758	**164**	**0.3130**	**0.0803**	**0.3461**	**0.0900**	**2.0474**	**0.043004**	**0.033139**
3134	**66**	**0.1387**	**0.0267**	**0.1619**	**0.0397**	**2.0113**	**0.047936**	**0.023197**
3446	**27**	**0.2700**	**0.0617**	**0.2395**	**0.0520**	**-2.0114**	**0.049198**	**-0.03046**
4123	**84**	**0.2131**	**0.0523**	**0.1882**	**0.0309**	**-1.7494**	**0.088296**	**-0.02491**
3783	**172**	**0.2701**	**0.0725**	**0.2883**	**0.0654**	**1.6390**	**0.103281**	**0.018257**
3783	**161**	**0.2260**	**0.0458**	**0.2133**	**0.0485**	**-1.3566**	**0.177897**	**-0.01275**
3758	**130**	**0.1641**	**0.0576**	**0.1368**	**0.0482**	**-1.3480**	**0.189276**	**-0.0273**
3779	**48**	**0.2900**	**0.0589**	**0.3071**	**0.0662**	**1.2858**	**0.201683**	**0.017129**
3450	**66**	**0.2524**	**0.0561**	**0.2307**	**0.0510**	**-1.1962**	**0.239657**	**-0.02168**
7452	**91**	**0.2439**	**0.0806**	**0.2209**	**0.0745**	**-1.1858**	**0.240242**	**-0.023**
3447	**70**	**0.3268**	**0.1037**	**0.3118**	**0.0915**	**-1.1262**	**0.261355**	**-0.015**
3447	**97**	**0.2800**	**0.0549**	**0.2924**	**0.0789**	**1.0761**	**0.283376**	**0.012428**
3134	**35**	**0.2650**	**0.0863**	**0.2260**	**0.0627**	**-1.0504**	**0.307419**	**-0.039**
3744	**16**	**0.2788**	**0.0565**	**0.2667**	**0.0659**	**-1.0252**	**0.307597**	**-0.01202**
3745	**56**	**0.2602**	**0.0711**	**0.2830**	**0.0748**	**0.9736**	**0.336599**	**0.022789**
3783	**94**	**0.2410**	**0.0607**	**0.2284**	**0.0547**	**-0.9584**	**0.340821**	**-0.01263**

3791	**58**	**0.2006**	**0.0744**	**0.1793**	**0.0369**	**-0.7811**	**0.444869**	**-0.0213**
3446	**11**	**0.3583**	**0.0948**	**0.3689**	**0.1023**	**0.6885**	**0.492137**	**0.010627**
3134	**35**	**0.1976**	**0.0364**	**0.1935**	**0.0245**	**-0.6416**	**0.522612**	**-0.00406**
3778	**140**	**0.1881**	**0.0311**	**0.1912**	**0.0326**	**0.5610**	**0.575781**	**0.003117**
3761	**20**	**0.3369**	**0.0836**	**0.3439**	**0.0839**	**0.5464**	**0.585471**	**0.007018**
3438	**131**	**0.2270**	**0.1179**	**0.2562**	**0.0421**	**0.5214**	**0.616188**	**0.0292**
3450	**118**	**0.2074**	**0.0435**	**0.2118**	**0.0349**	**0.4888**	**0.626378**	**0.004338**
3134	**115**	**0.3333**	**0.0784**	**0.3426**	**0.1106**	**0.4812**	**0.631483**	**0.009238**
3777	**199**	**0.2742**	**0.0747**	**0.2814**	**0.0624**	**0.4202**	**0.675774**	**0.007199**
3790	**49**	**0.2152**	**0.0653**	**0.2227**	**0.0693**	**0.3581**	**0.722189**	**0.007569**
3778	**64**	**0.1961**	**0.0416**	**0.2009**	**0.0380**	**0.3524**	**0.726089**	**0.004825**
3438	**99**	**0.1934**	**0.0330**	**0.1883**	**0.0642**	**-0.1514**	**0.884616**	**-0.00507**
3450	**155**	**0.1931**	**0.0300**	**0.1923**	**0.0381**	**-0.1352**	**0.892644**	**-0.00078**
3750	**83**	**0.2425**	**0.0481**	**0.2420**	**0.0567**	**-0.0546**	**0.956572**	**-0.00055**
3749	**77**	**0.2073**	**0.0367**	**0.2071**	**0.0511**	**-0.0342**	**0.972742**	**-0.00023**
3446	**82**	**0.0850**	**0.0193**	**0.0849**	**0.0171**	**-0.0101**	**0.991923**	**-3.63E-05**

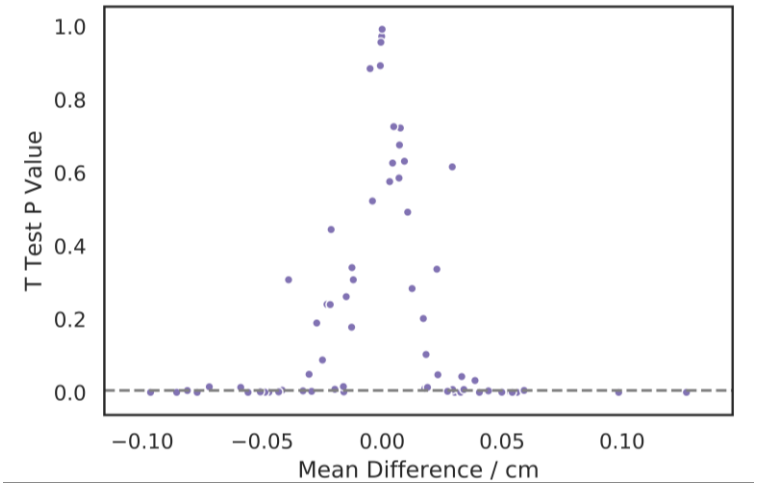

Figure C.2.3: Mean hypocotyl length difference between DMSO and eW5 against T-test P value for 2nd replicate

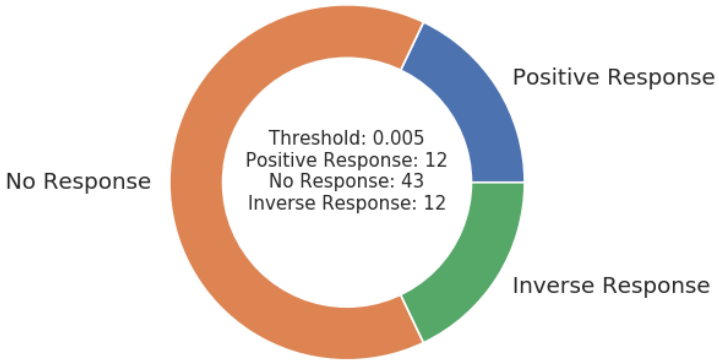

Figure C.2.4: Distribution of responses of selected EMS mutant populations to eW5 compared to DMSO for 2nd replicate. Threshold selected for "No response" = p<0.005. "Positive response" populations have positive mean hypocotyl length difference and "inverse response" populations have negative mean hypocotyl length difference.

3rd Replicate*:

Line	label	eW5 mean Hypocotyl length / cm	eW5 S.D.	DMSO mean Hypocotyl length / cm	DMSO S.D.	t-statistic	t-test p value	Mean difference
3446	11	0.2717	0.0523	0.1993	0.0396	-9.1390	5.38E-16	-0.07244
3741	92	0.2014	0.0489	0.2763	0.0739	8.2710	2.73E-14	0.074862
3779	48	0.2369	0.0727	0.1670	0.0347	-7.8524	4.81E-13	-0.06987
3777	199	0.5548	0.1394	0.4168	0.1175	-6.9259	9.35E-11	-0.13809
3447	97	0.1941	0.0307	0.1644	0.0235	-6.4355	1.95E-09	-0.02974
3750	83	0.2750	0.0673	0.3997	0.1279	6.3765	4.48E-09	0.124682
3749	77	0.1766	0.0245	0.1428	0.0205	-6.4005	1.45E-08	-0.03379
WT	WT	0.2692	0.0607	0.1932	0.0610	-6.1499	1.82E-08	-0.07601
3788	38	0.2119	0.0454	0.2388	0.0509	4.7440	3.31E-06	0.026904
3783	94	0.1844	0.0511	0.2394	0.0623	4.5376	1.52E-05	0.055044
3758	130	0.2235	0.0707	0.3177	0.0780	4.6541	2.15E-05	0.094198
3783	172	0.3556	0.0958	0.4130	0.0848	4.3174	2.56E-05	0.057344
3134	35	0.1849	0.0362	0.2424	0.0574	4.3427	7.24E-05	0.057519
3450	118	0.2990	0.0717	0.2225	0.0715	-4.1185	0.000113	-0.07648
3438	99	0.3676	0.0801	0.3281	0.0800	-3.5603	0.00046	-0.03955
3758	164	0.2014	0.0333	0.1771	0.0324	-3.5432	0.000626	-0.0243
3783	94	0.2074	0.0492	0.1755	0.0281	-3.4995	0.000815	-0.03191
7452	91	0.2172	0.0360	0.1968	0.0322	-3.2859	0.001336	-0.0204
3134	35	0.1739	0.0236	0.1946	0.0323	3.1900	0.002059	0.020683
4123	**84**	**0.2153**	**0.0523**	**0.1669**	**0.0329**	**-3.2514**	**0.002647**	**-0.04834**
3783	161	0.1622	0.0226	0.1845	0.0271	2.9756	0.003818	0.022293
3748	5	0.1641	0.0473	0.2007	0.0620	2.8045	0.006518	0.036615
3134	**66**	**0.1910**	**0.0319**	**0.2174**	**0.0472**	**2.7575**	**0.007291**	**0.026423**
3778	64	0.1974	0.0462	0.2253	0.0485	2.3053	0.024684	0.027939
3761	**20**	**0.3485**	**0.0911**	**0.3211**	**0.0901**	**-1.8582**	**0.06509**	**-0.02736**
3450	**66**	**0.1962**	**0.0462**	**0.2358**	**0.0396**	**1.9494**	**0.069001**	**0.039556**
3745	**56**	**0.2153**	**0.0776**	**0.2480**	**0.0743**	**1.4909**	**0.142822**	**0.032696**
3766	**78**	**0.2043**	**0.0613**	**0.2243**	**0.0632**	**1.3199**	**0.191099**	**0.020008**
3438	**131**	**0.2079**	**0.0375**	**0.2222**	**0.0487**	**1.3086**	**0.194727**	**0.014317**
3790	**49**	**0.1598**	**0.0099**	**0.1460**	**0.0337**	**-0.8775**	**0.403037**	**-0.0138**
3791	**58**	**0.2741**	**0.0775**	**0.3065**	**0.0864**	**0.7342**	**0.472257**	**0.032438**
3446	**82**	**0.2173**	**0.0525**	**0.2105**	**0.0499**	**-0.7203**	**0.472742**	**-0.00678**
3450	**155**	**0.2069**	**0.0277**	**0.2110**	**0.0429**	**0.6594**	**0.510799**	**0.0041**
3446	**27**	**0.2018**	**0.0397**	**0.2034**	**0.0409**	**0.2722**	**0.785791**	**0.001592**

* Bold individuals represent mutants taken forward.

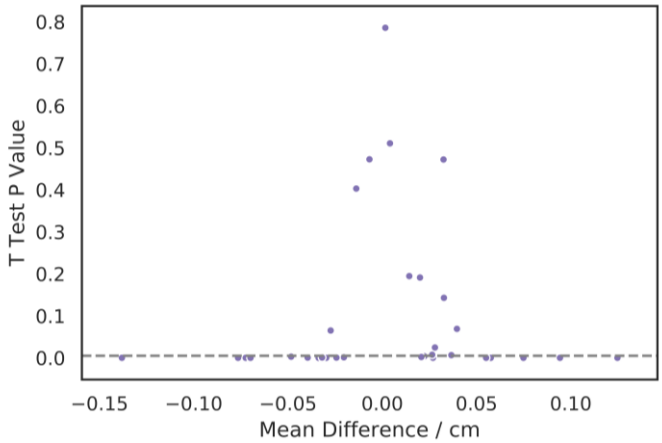

Figure C.2.5: Mean hypocotyl length difference between DMSO and eW5 against T-test P value for 3rd replicate

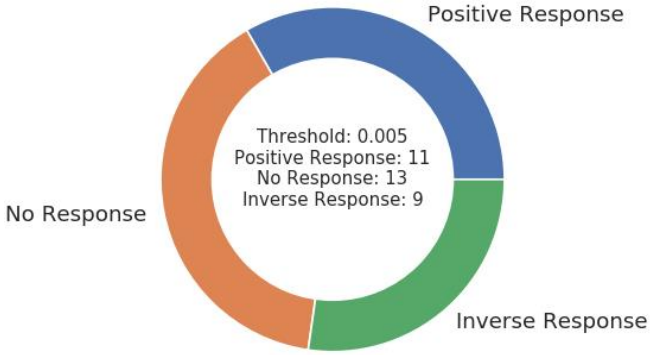

Figure C.2.4: Distribution of responses of selected EMS mutant populations to eW5 compared to DMSO for 3rd replicate. Threshold selected for "No response" = $p<0.005$. "Positive response" populations have positive mean hypocotyl length difference and "inverse response" populations have negative mean hypocotyl length difference.

C.3: Generation 3 (F_2) Successful Crosses:

3761-20
3745-56
3450-155
3446-82
3790-49
3766-78

Appendix D: Exploiting C–H Borylation for the Multidirectional Elaboration of 2-Halopyridines

Jonathan A. Reuven[a], Omar A. Salih[a,b], Scott. A. Sadler[a], Carys L. Thomas[a], and Patrick G. Steel[a,*]

[a]Department of Chemistry, University of Durham, Science Laboratories, Lower Mountjoy, South Road, Durham, DH1 3LE

[b] Department of Chemistry, College of Education for Pure Sciences, Mosul University, Iraq

[*] Corresponding author

Graphical Abstract

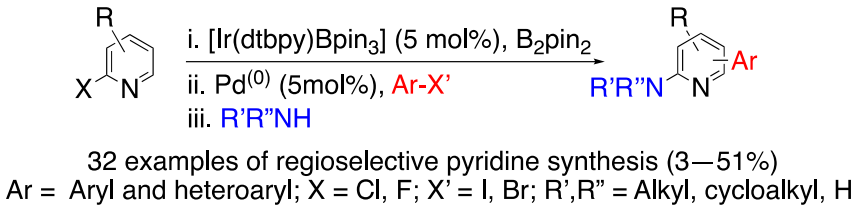

Abstract

Regioselectively polysubstituted pyridines can be efficiently accessed from 2-halopyridines via a sequence involving C-H borylation, Suzuki-Miyaura cross-coupling and nucleophilic aromatic substitution chemistry.

Dedication

Dedicated to Professor Steve Davies in recognition of his outstanding contributions to advancing organic chemistry though both his teaching and his research.

Keywords

Pyridine; C-H Borylation; Suzuki-Miyaura; Multidirectional synthesis

Introduction

The pyridine ring represents an essential structural component of many functional molecules including sensors, pharmaceuticals, agrochemicals, ligands for catalysis etc and is also found in numerous natural products (Fig. 1). [1,2,3,4]

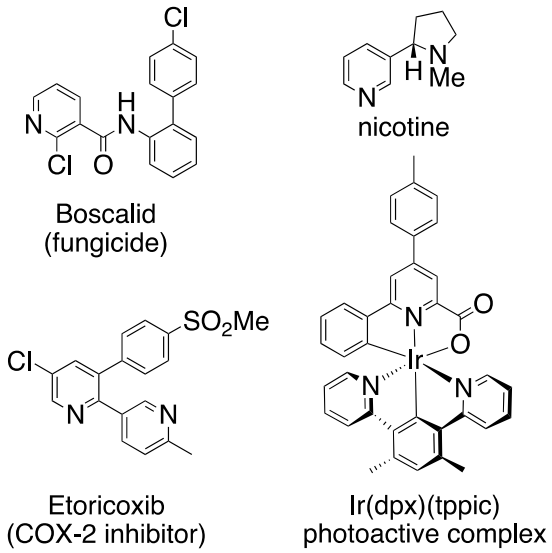

Figure 1. Representative functional pyridines

As such, methods to synthesise functionalised pyridines are of great value and much effort has been applied towards this effect.[5-11] Given the low reactivity of the electron deficient azinyl ring towards electrophilic aromatic substitution, most routes to substituted pyridines involve *de novo* synthesis with substituents and substitution patterns determined by the building blocks employed. However, the ability to manipulate a preformed pyridine ring is particularly valuable for late stage diversification. Among the various strategies for preparing polyfunctionalised pyridines in this way are ring metalation with various strong bases,[12,13] radical substitution[14,15] and transition metal mediated C-H activation. [16,11] Whilst each has its merit, the last is particularly attractive providing both high atom and step efficiency and represent the ideal for green sustainable processes. Reflecting the versatility of the resulting arylboronate esters for further downstream transformations and the functional group tolerance of the process, Ir catalysed C-H borylation is a particularly attractive option for elaboration of a preformed pyridine ring.[17,11] First reported by Miyaura and Ishiyama in 2002,[18,19] the borylation of pyridine is challenged by the Lewis basicity of the azinyl nitrogen atom which can coordinate to and inhibit the catalytically active species. Moreover, the azinyl nitrogen also affects both the regiochemistry of pyridine borylation disfavouring substitution at the 2 and 6 positions and also rendering the products unstable with respect to protodeborylation.[20-23] In recent work we have shown this effect can be

modulated by the presence of an electron withdrawing 2-halo substituent which, not only sterically protects the catalyst by blocking co-ordination to the iridium centre but also lowers the basicity of the azinyl lone pair enhancing reactivity at the α-positions and increasing stability to protodeborylation.[24] The resultant 2-halopyridine boronate esters are versatile building blocks for multi-directional elaboration and in this report we demonstrate this concept with the synthesis of a diverse set of trifunctional pyridine scaffolds.

Results & Discussion

Building on our earlier work, initial studies focused on the borylation of simple 2,4-disubstituted pyridines. The borylation of 2-chloro-4-trifluoromethyl- and 2-chloro-4-*tert*butylpyridine **1** and **2** (Table 1), using $[Ir(cod)OMe]_2$ (1.5 mol%), dtbpy (3 mol%) and B_2Pin_2 in THF, occurred as predicted at the sterically uninhibited 6-position. Although adjacent to the azinyl nitrogen atom, the stabilising effect of the 2-chloro substituent allowed the isolation of the boronate ester which could be identified by a characteristic downfield shift of the signal for the adjacent 5-hydrogen in the ^{1}H NMR spectrum. Whilst sufficiently stable to be analysed as a crude product, attempts to chromatographically purify this compound were complicated by significant protodeborylation and it was more effective to use the crude reaction mixture directly in subsequent steps. Using the Suzuki-Miyuara reaction as a classic exemplar transformation, reaction with 4-iodo-nitrobenzene (1.5 equiv) in the presence of $PdCl_2$(dppf) (5 mol%) as the precatalyst afforded the desired biaryl **5z** in 58% yield over the two steps (Table 1, entry 1). A range of arenes and heteroarenes (Fig. 2a), including those containing both electron withdrawing and donating substituents, proved viable giving moderate to good yields under these standard conditions. Having exploited the ability of the halogen to enable and direct the C-H borylation, it was then of interest to use this as a handle for further functionalisation. Using pyrrolidine as a test substrate, efficient reaction could be achieved by simply heating the halopyridine with an excess of the amine in THF in a sealed microwave vessel for 60 minutes. This proved to be a general observation and was extended to include a range of amines (Fig. 2b), including primary, secondary cyclic and acyclic alkyl amines but not aniline. Attempts to carry out the whole sequence in a single operation were possible (Table 1 entry 6) but generally lead to more complex crude reaction mixtures and slightly lower overall yields.

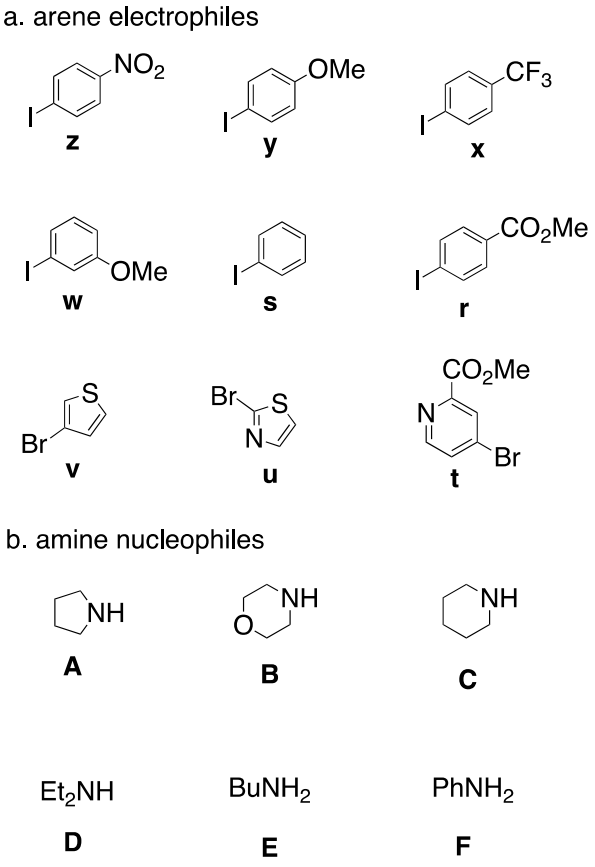

Figure 2. Arenes and amines employed in this study

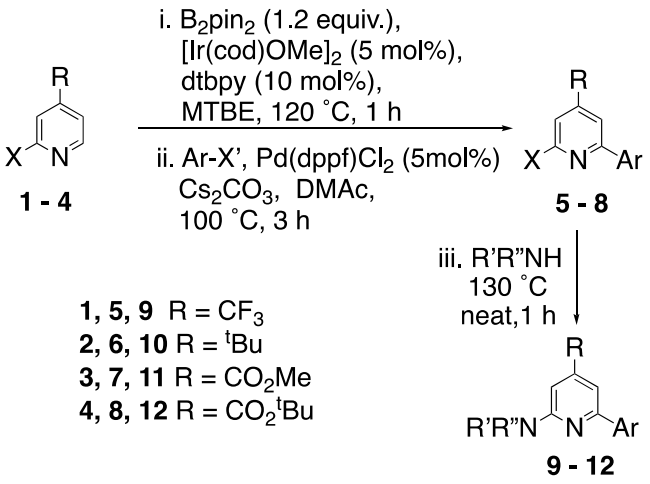

Entry	1 - 4	X	Ar-X'	5-8 (%)[i]	R'R"NH	9-12 (%)[ii]
1	1	Cl	z	**5z** (58)%	A	**9zA** (78)
2	1	Cl	z	**5z**	B	**9zB** (92)
3	1	Cl	z	**5z**	D	**9zD** (61)
4	1	Cl	z	**5z**	E	**9zE** (75)
5	1	Cl	z	**5z**	F	**9zF** (0)
6	1	Cl	y	**5y** (36)	A	**9yA** (20)[iii]
7	1	Cl	w	**5w** (51)	-	-
8	2	Cl	z	**6z** (40)	A	**10zA** (31)
9	2	Cl	y	**6y** (44)	-	-
10	2	Cl	v	**6v** (67)	-	-
11	2	Cl	u	**6u** (66)	-	-
12	2	Cl	t	**6t** (42)	-	-
13	3	Cl	z	**7z** (45)	-	-
14	3	Cl	y	**7y** (48)	-	-
15	3	F	y	**7'y** (55)	A	**11yA** (85)[iv]
16	3	F	x	**7'x** (50)	B	**11xB** (83)[iv]
17	3	F	x	**7'x**	E	**11xE** (64)[iv]
18	4	Cl	z	**8z** (61)	B	**12zB** (78)
19	4	Cl	y	**8y** (57)	A	**12yA** (90)
20	4	Cl	y	**8y**	F	**12yF** (0)
21	4	Cl	x	**8x** (39)	A	**12xA** (91)

i. Yield of isolated purified product from **1-4** in a one-pot two-step process; ii. Yield of isolated purified **9-12** based on **5-8**; iii.yield for a one-pot three-step process from **1**.; iv. Step iii. conditions: R'R"NH (2 equiv), dioxane, reflux, 6 h

Table 1: Sequential borylation cross-coupling amination of 2-halopyridines

Turning to the corresponding isonicotinates (Table 1, entries 13-21) initial attempts were hampered by inefficient borylation of the corresponding esters **2** and **3** under the "standard" conditions (~68% conversion compared with >90% for the other substrates). Attributing this to competitive coordination of the Lewis acidic active catalyst, this could be simply addressed by increasing the catalyst loading to 5 mol% which enabled conversions in excess of 90% to be routinely achieved. As with the earlier

examples, cross-coupling of the resultant pyridyl boronate esters occurred efficiently. However initial attempts to employ methyl ester **7z** in the S_NAr step led to the formation of the corresponding amide **13**. Two strategies to circumvent this problem were developed. Simply replacing the methyl ester by a *tert*-butyl ester enabled the amino esters to be isolated in moderate yields (Table 1 entries 18-21) although aromatic amines were still not tolerated (Table 1, entry 20). Alternatively, using the more reactive 2-fluoropyridine starting material enhanced the facility of the S_NAr reaction enabling lower reaction temperatures to be employed, leading to selective reaction at C-2 even in the presence of the methyl ester (Table 1 entries 13-17).

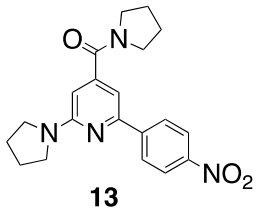

13

Figure 3: Structure of amide 13.

Having demonstrated the possibility for multidirectional approaches around a pyridine template it was of interest to explore other starting pyridine substitution patterns. Retaining a 2-halo substituent, as the borylation enabling (coordination blocking) but labile group, both 2,3- and 2,5-nicotinates were then explored (Table 2). As expected borylation of the 2,5-isomers **14** and **15** occurred preferentially at the sterically unencumbered C-5 site removed from the azinyl nitrogen.[20-24] However small amounts (6-9%) of the □-azinyl (C-6) boronate ester could be observed in the crude reaction mixture but underwent rapid protodeborylation and was not isolable or detectable following the *in situ* cross coupling reaction. With the 2,3-isomer **16**, similar sterically directed borylation led exclusively to the 3-borylated product. For this group of compounds use of the smaller 2-fluoro starting material led to a faster reaction consistent with other observations describing fluorine to act as a C-H activation enhancing group.[25,26,27] In both cases whilst the major boronate esters were isolable, it was more efficient to carry out a 'one-pot' process to afford the corresponding biaryl (**17-19**) in acceptable yields following application of the standard cross coupling conditions. As before S_NAr chemistry with a variety of amines proved facile with anilines again requiring the use of the more reactive fluorine leaving group. With the 2,3 series use of a diamine enabled double substitution to afford the pyridodiazepinone **23** (Scheme 1a). For these substrates, reflecting the higher stability of a non □-azinyl boronate ester, the alternative order of events involving initial displacement with the amine and then borylation of the corresponding 2-amino-pyridine proved to be equally effective (Scheme 1b).

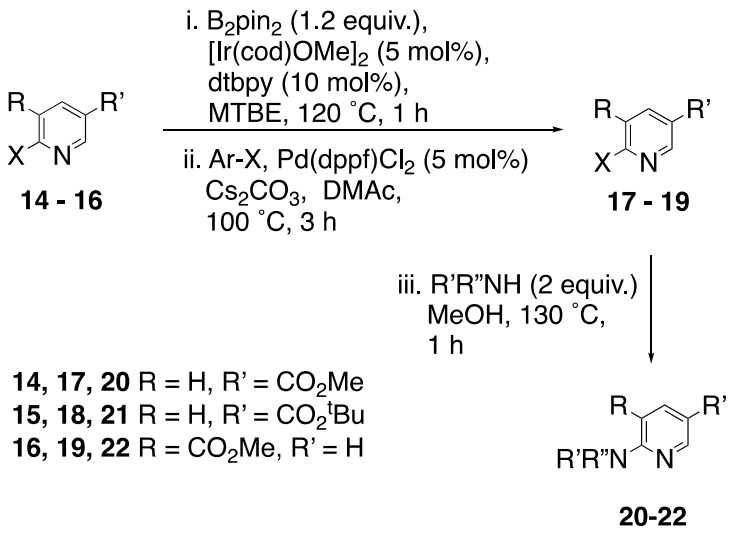

Entry	14-16	X	Ar-X	17-19 (%)[i]	R'R"NH	20-22 (%)[ii]
1	14	Cl	w	17w (32)	-	-
2	14	F	y	17'y (58)	B	20yB (88)[iii]
3	14	Cl	y	17y (61)	A	20yA (71)
4	14	Cl	x	17x (55)	A	20xA (84)
5	15	Cl	y	18y (44)		21yA (75)[iv]
6	15	Cl	y	18y	B	21yB (87)[iv]
7	15	Cl	y	18y	F	21yF (0)[iv]
8	15	Cl	x	18x (32)	B	21xB (82)[iv]
9	16	Cl	z	19z	A	22zA (32)[v]
10	16	Cl	y	19y (20)	B	22yB (93)
11	16	Cl	y	19y	C	22yC (89)
12	16	Cl	y	19y	E	22yE (60)
13	16	F	y	19'y (62)	-	-
14	16	OMe	y	19"y (81)	-	-
15	16	Cl	x	19x (24)	A	22xA (50)
16	16	Cl	x	19x	B	22xB (43)
17	16	Cl	x	19x	C	22xC (13)
18	16	Cl	v	19v (19)	-	-
19	16	Cl	s	19s (38)	-	-
20	16	Cl	r	19r (65)	A	22rA (81)

i. Yield of isolated purified product from **1-4** in a one-pot two-step process; ii. Yield of isolated purified **9-12** based on **5-8**; iii. Step iii conditions: R'R"NH (2 equiv), dioxane, reflux, 6 h; iv. Step iii conditions: R'R"NH (neat), 130 ^{o}C, 1 h; v. yield for a one-pot three -step process from **16.**

Table 2: Sequential borylation cross-coupling amination of 2-halonicotinates

Further extension of the levels of diversity possible can be realised through other standard functional group transformations (Scheme 1). For example, rather than exploit the 2-halo substituent through S_NAr chemistry other options exist using further metal catalysed transformations, with simple reduction using

ammonium formate giving ester **25** (Scheme 1c) or via a second Suzuki-Miyaura reaction, the diarylpyridine **26** (Scheme 1d). Similarly, the ester substituents can easily be converted to the corresponding acid and hence provides a simple handle for the introduction of further variation into the reaction sequence (Scheme 1e).

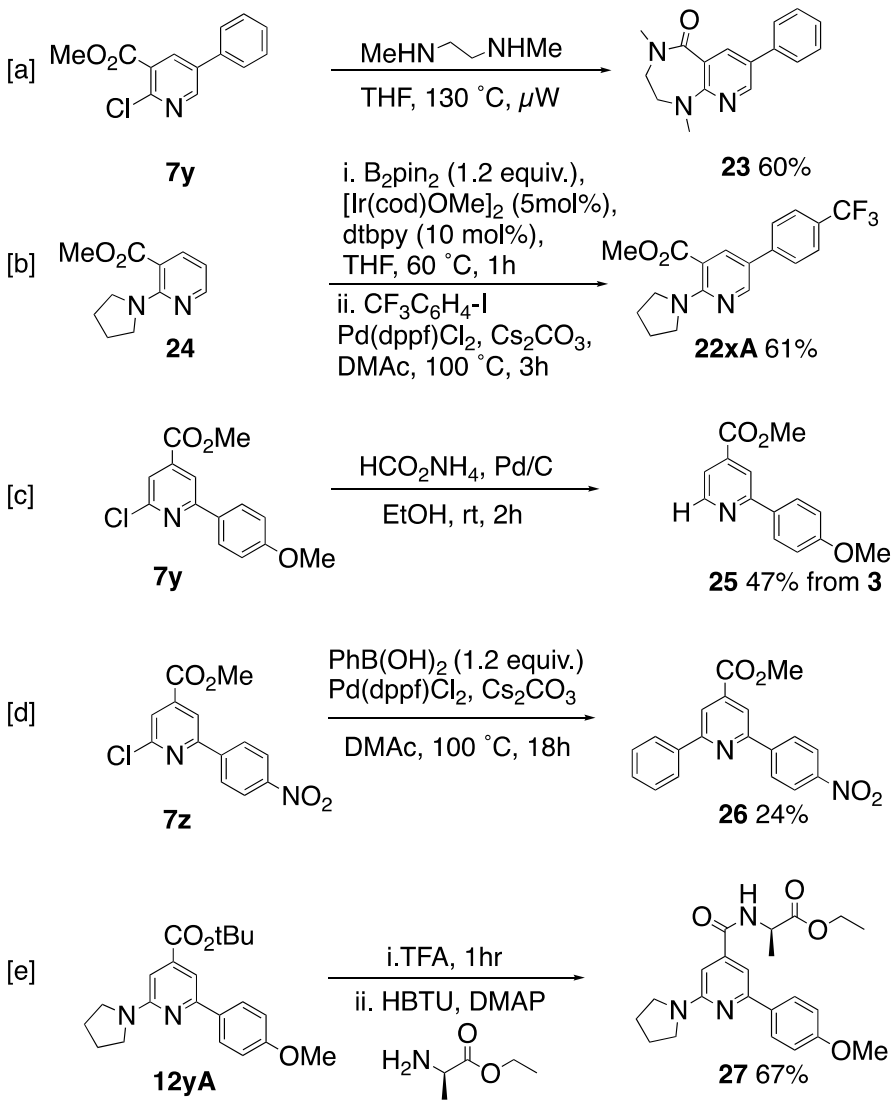

Scheme 1: Exemplar diversity synthesis of pyridines enabled by C-H borylation

Conclusion

In this report we have demonstrated that the combination of iridium catalysed C-H borylation and S_NAr chemistry provide a very simple method to elaborate a 2-halopyridine ring and provide substitution patterns that would be difficult to achieve using traditional heterocycle synthesis. The functional group tolerant nature of the borylation reaction allows many alternative diverse elements to be incorporated in this sequence with minimal impact on the chemistry enabled. Given the wide scope for elaboration

of the intermediate boronate ester the potential of the approach to generate diversity extends beyond the examples presented. Overall this study provides further testimony for the use of C-H borylation as a powerful means to generating otherwise challenging pyridine, and other heterocycle, substitution patterns.

Experimental

General Procedure A: Tandem C-H Borylation-Suzuki-Miyaura Cross-Coupling Sequence:

A solution of $[Ir(COD)OMe]_2$ (5mol%), dtbpy (5mol%) and B_2pin_2 (1.2mol %) in MTBE (0.4M) was prepared in a sealed vial and an aliquot then added to a thick-walled microwave synthesis vial containing the starting pyridine . The vessel was sealed with a crimp top septum cap and shaken until all of the substrate was dissolved. The reaction mixture was stirred on a magnetic stirring block or irradiated in a microwave reactor for the stated time and temperature. Upon completion, the volatiles were removed *in vacuo* to afford the crude borylated product.

To the crude mixture under N_2, was added palladium catalyst (5 mol%), base (2 eq.), aryl halide (1.1 – 2.0 eq.) and the stated solvent. The reaction was heated at the stated temperature for the stated time. The reaction mixture was diluted with water and extracted into EtOAc. The organic phase was dried over $MgSO_4$, filtered and concentrated *in vacuo* to give the crude product. This was dry-loaded onto silica gel and purified by silica gel flash column chromatography using the stated solvent system.

General Method B S_NAr substitution of 2-fluorinated pyridines:

A mixture of the 2-fluorinated pyridine derivatives (1 eq.), K_2CO_3 (2 eq.) and amine (2 eq.) were heated under reflux in dioxane for 6 h. The reaction was cooled to room temperature and filtered through Celite. Purification was achieved by flash column chromatography using EtOAc in hexane.

General method C S_NAr substitution of 2-chlorinated pyridines (-CO_2Me substituted):

To a sealed, evacuated and N_2 backfilled vial containing the 2-chloropyridine derivative, methanol was added. To this solution, the amine was added and the reaction mixture was irradiated in a microwave reactor at 130 ^oC for 30 mins. Following evaporation of volatiles, the resulting mixture was redissolved in DCM and washed with $NaHCO_3$. Purification through column chromatography using EtOAc in hexane yielded the title compound.

General Method D S_NAr substitution of 2-chlorinated pyridines (non -CO_2Me substituted):

2-Chloropyridine derivatives were transferred to microwave vessel which was then sealed, evacuated and backfilled with N_2. The amine (2ml) was then added and the reaction mixture was irradiated in a microwave reactor at 130 ºC for 30 mins. Following the reaction, the resulting mixture was dissolved in DCM and washed with $NaHCO_3$. Purification was achieved by flash column chromatography using EtOAc in Hexane.

(5z) *4-Trifluoromethyl-6-chloro-2(4'-nitrophenyl)-pyridine*

Following general procedure A and purification using toluene in hexane (0-50%) yielded the title compound as a white solid (175 mg, 58 %). mp 120-121 ºC. δ_H (700 MHz, $CDCl_3$) 8.36-8.33 (2H, m, 3',5'-H), 8.24-8.20 (2H, m, 2',6'-H), 7.9 (1H, s, 3-H), 7.6 (1H, s, 5- H); δ_C (176 MHz, $CDCl_3$) 156.9 (C-2), 153.0 (C-6), 149.2 (C-4'), 142.3 (q, *J* = 34.7 Hz, C-4), 142.1 (C-1'), 128.2 (C-2',6'), 124.3 (C-3',5'), 122.1 (q, *J* = 274 Hz, CF_3), 120.3 (q, *J* = 3.6 Hz, C-5), 115.4 (q, *J* = 3.4 Hz, C-3). υ_{max} (ATR) 1601, 1564, 1516, 1409, 1350, 1328, 1263, 1173, 1140, 1101, 1071, 860, 873, 818, 760, 707, 696, 675 cm^{-1}. m/z (GC-MS, EI^+) 304 ([M] (^{37}Cl)]$^+$, 31%), 302 ([M] (^{35}Cl)]$^+$, 100%). Accurate mass (ES^+) *m/z* found $[MH]^+$ 303.0138; $C_{12}H_7{}^{35}ClF_3N_2O_2$ requires *M*, 303.0148.

(9zA) *4-Trifluoromethyl-6-(N-pyrrolidin-yl)-2(4'-nitrophenyl)-pyridine*

Following general procedure D and purification using EtOAc in hexane (0-8%) yielded the title compound as a yellow solid (263 mg, 78 %). mp 212-213 ºC. δ_H (700 MHz, $CDCl_3$) 8.31-8.27 (2H, m, 3',5'-*H*), 8.22-8.18 (2H, m, 2',6'-*H*), 7.19 (1H, s, 3-*H*), 6.57 (1H, s, 5-*H*), 3.63-3.59 (4H, m, 2",5"-H_2), 2.11-2.04 (4H, m, 3", 4"-H_2); δ_C (176 MHz, $CDCl_3$) 157.16 (*C*6), 154.3 (*C*-2), 148.3 (*C*-4'), 145.1 (*C*-1'), 140.39 (q, *J* = 32.9, *C*-4), 127.7 (*C*-2',6'), 123.9 (*C*-3',5'), 123.43 (q, *J* = 273 Hz, *C*F_3), 103.6 (q, *J* = 3.3 Hz, *C*-3), 102.44 (q, *J* = 4.0 Hz, *C*-5), 47.1 (*C*-2",5"), 25.6 (*C*-3",4"); υ_{max} (ATR) 1616, 1601, 1564, 1519, 1492, 1480, 1443, 1390, 1344, 1322, 1290, 1249, 1159, 1108, 1093, 1010, 972, 849, 826, 756, 722, 694, 671 cm^{-1}. *m/z* (GC-MS, EI^+) 337 ([M]$^+$ 39%), 308 ([M-C_2H_5]$^+$ 100%), Accurate Mass (ESI) *m/z* found $[M+H]^+$ 338.1105; $C_{16}H_{15}F_3N_3O_2$ requires *M*, 338.1116.

(9zB) *4-Trifluoromethyl-6-(N-morpholin-yl)-2(4'-nitrophenyl)-pyridine*

Following general procedure D and purification using EtOAc in hexane (0-12%) yielded the title compound as a yellow solid (325 mg, 92 %). mp 268-269 ºC. δ_H (700 MHz, $CDCl_3$) 8.35-8.26 (2H, m, 3',5'-*H*), 8.23-8.12 (2H, m, 2',6'-*H*), 7.33 (1H, s, 3-*H*), 6.85 (1H, s, 5-*H*), 3.9-3.86 (4H, m, 3",5"-H_2), 3.71-3.67 (4H, m, 2",6"-H_2); δ_C (176 MHz, $CDCl_3$) 159.4 (*C*-6), 154.4 (*C*-2), 148.5 (C-4'), 144.6 (C-

1'), 141.3 (q, *J* = 33.0 Hz, *C*-4), 127 (*C*-2', 6'), 124.1 *(C*-3', 5'), 123.2 (q, *J* = 273 Hz, *C*F_3), 106.1 (q, *J* = 3.3 Hz, *C*-3), 102.6 (q, *J* = 4.0 Hz, *C*-5), 66.7 (*C*-3",5"), 45.4 (*C*-2",6"). υ_{max} (ATR) 1603, 1567, 1517, 1438, 1324, 1302, 1242, 1161, 1111, 982, 967, 847, 825, 757, 711, 695, 675 cm^{-1}. *m/z* (GC-MS, EI^+) (353 $[M]^+$), 68%, (334 $[M-F]^+$, 17%), 308 ($[MH-NO_2]^+$, 24%). Accurate Mass (ESI) *m/z* found $[M+H]^+$ 354.1067; $C_{16}H_{15}F_3N_3O_3$ requires *M*, 354.1066.

(9zD) *Diethyl-[6-(4'-nitrophenyl)-4-trifluoromethylpyridine-2-yl]amine*

Following general procedure D, and purification using EtOAc in hexane (0-8%) yielded the title compound as a yellow solid (207 mg, 61 %). mp 88-89 °C. δ_H (700 MHz, $CDCl_3$) 8.32-8.27 (2H, m, 3',5'-*H*), 8.21-8.15 (2H, m, 2',6'-*H*), 7.20 (1H, s, 3-*H*), 6.7 (1H, s, 5-*H*), 3.63-3.59 (4H, q, *J* = 7.1 Hz, 2",4"-H_2), 1.26 (6H, t, *J* = 7.1 Hz, 3",5"-H_3); δ_C (176 MHz, $CDCl_3$) 157.5 (*C*-6), 154.3 (*C*-2), 148.3 (*C*-4'), 145.2 (*C*-1'), 140.7 (q, *J* = 32.7, *C*-4), 127.6 (*C*-2',6'), 124.0 (*C*-3',5'), 123.4 (q, *J* = 273 Hz, *C*F_3), 103.5 (q, *J* = 3.3 Hz, *C*-3), 101.4 (q, *J* = 4.0 Hz, *C*-5), 43.13 (*C*-2",4"), 12.9 (*C*-3",5"). υ_{max} (ATR) 1616, 1601, 1566, 1516, 1503, 1442, 1349, 1344, 1332, 1263, 1249, 1175, 1123, 1110, 979, 853, 829, 758, 710, 695, 676 cm^{-1}. *m/z* (GC-MS, EI^+) 339 ($[M]^+$, 43%), 324 ($[M-CH_3]^+$, 64%), 310 ($[M-C_2H_5]^+$, 100%). Accurate Mass (ESI) *m/z* found $[M+H]^+$ 340.1270; $C_{16}H_{17}F_3N_3O_2$ requires *M*, 340.1273.

(9zE) *Butyl-[6-(4'-nitrophenyl)-4-trifluoromethylpyridine-2-yl]amine*

Following general procedure D, and purification using EtOAc in hexane (0-8%) yielded the title compound as a yellow solid (255 mg, 75 %), mp = 163-164 °C. δ_H (700 MHz, $CDCl_3$) 8.31-8.26 (2H, m, 3',5'-*H*), 8.18-8.11 (2H, m, 2',6'-*H*), 7.2 (1H, d, *J* = 0.6 Hz, 3-*H*), 6.6 (1H, s, 5-*H*), 4.9 (1H, s broad, *NH*), 3.44-3.39 (2H, m, 1"-H_2), 1.69-1.64 (2H, m, 2"-H_2), 1.51.44 (2H, m, 3"-H_2), 1.0 (3H, t, *J* = 7.4 Hz, 4"-H_3); δ_C (176 MHz, $CDCl_3$) 159.1 (*C*-6), 154.7 (*C*-2'), 148.4 (*C*-4'), 144.7 (*C*-1'), 140.8 (q, *J* = 33.2 Hz, *C*-4), 127.7 (*C*-2',6'), 124.0 *(C*3',5'), 123.2 (q, *J* = 273 Hz, *C*F_3), 105.3 (q, *J* = 3.3 Hz, *C*-3), 102.8 (*C*-5), 42.0 (*C*-2"), 31.6 (*C*-3"), 20.3 (*C*-4"), 14.0 (*C*-5"). υ_{max} (ATR) 3401 (*N*H), 1625, 1604, 1573, 1533, 1459, 1413, 1396, 1331, 1257, 1158, 1117, 1096, 860, 830, 757, 723, 695, 678, 639 cm^{-1}. *m/z* (GC-MS, EI^+) 339 ($[M]^+$, 31%), 310 ($[M-C_2H_5]^+$, 52%), 296 ($[M-C_3H_7]^+$, 100%). Accurate Mass (ESI) *m/z* found $[M+H]^+$ 340.1276; $C_{16}H_{17}F_3N_3O_2$ requires *M*, 340.1273.

(5y) *4-Trifluoromethyl-6-chloro-2-(4'-methoxyphenyl)-pyridine*

Following general procedure A, and purification using Et_2O in hexane (0-5%) yielded the title compound as a yellow oil (105 mg, 36 %). δ_H (700 MHz, $CDCl_3$) 7.99-7.94 (2H, m, 2',6'-H), 7.73 (1H, d, *J* = 0.6 Hz, 3-H), 7.37 (1H, d, *J* = 0.6 Hz, 5-H), 6.99-6.94 (2H, m, 3',5'-H), 3.85 (3H, s, OCH_3); δ_C (176 MHz, $CDCl_3$) 161.7 (C-4'), 159.1 (C-2), 151.2 (C-6), 141.5 (q, *J* = 34.1 Hz, C-4), 129.0 (C-1'), 128.6 (C-2',6'), 122.4 (q, *J* = 273 Hz, CF_3), 117.0 (q, *J* = 3.7 Hz, C-5), 114.4 (C-3',5'), 113.4 (q, *J* = 3.7 Hz, C-3), 55.4 (O-CH_3). υ_{max} (ATR) 1606, 1557, 1518, 1408, 1394, 1331, 1265, 1253, 1175, 1135, 1098, 1072, 1031, 830, 694, 665, 581 cm^{-1}. m/z (GC-MS, EI^+) 289 [M (^{37}Cl)]$^+$, 33%, 287 ([M (^{35}Cl)]$^+$, 100%). Accurate mass (ES^+) *m/z* found $[MH]^+$ 288.0401; $C_{13}H_{10}{}^{35}ClF_3NO$ requires *M*, 288.0403.

(9yA) *4-Trifluoromethyl-6-(N-pyrrolidin-yl)-2-(4'-methoxyphenyl)pyridine*

Following general procedure D, the crude mixture of 4-trifluoromethyl-6-chloro-2-(4'methoxyphenyl)-pyridine in (~1.0 mmol) and pyrrolidine (0.46 ml, 5.5 mmol) were combined at 130 °C for 30 min. Purification through flash chromatography using EtOAc in hexane (0-5%) yielded the title compound as an off white solid (65 mg, 20 % (over 3 steps)). mp 103-104 °C. δ_H (700 MHz, $CDCl_3$) 8.06-8.00 (2H, m, 2', 6'-*H*), 7.11 (1H, s, 3*H*), 7.01-6.96 (2H, m, 3',5'-*H*), 6.42 (1H, s, 5-*H*), 3.86 (3H, s, OCH_3), 3.64-3.53 (4H, m, 2",5"-H_2), 2.08-2.00 (4H, m, 3",4"-H_2); δ_C (176 MHz, $CDCl_3$) 160.7 (*C*-4'), 157.0 (*C*-6), 156.6 (*C*-2), 140.0 (q, *J* = 32.4 Hz, *C*-4), 132.0 (*C*-1'), 128.3 (*C*-2',6'), 123.77 (q, *J* = 273 Hz, *C*F_3), 114.0 (*C*-3',5'), 102.1 (q, *J* = 3.4 Hz, *C*-3), 100.0 (q, *J* = 4.0 Hz, *C*-5), 55.4 (O-*C*H_3), 46.9 (*C*-2",5"), 25.6 (*C*-3",4"). υ_{max} (ATR) 1613, 1563, 1497, 1460 1439, 1408, 1389, 1351, 1333, 1304, 1293,1246, 1183, 1157, 1120, 1105, 1097, 1051, 1032, 1014, 1004, 842, 825, 804, 782, 711, 680, 671, 648, 637, 618, 586, 522, 504 cm^{-1}. *m/z* (GC-MS, EI^+) 323 $[MH]^+$, 7%, 322 $[M]^+$, 42%, 293 $[MHOCH_3]^+$, 100%; Accurate Mass (ESI) *m/z* found $[M+H]^+$ 323.1364; $C_{17}H_{18}F_3N_2O$ requires *M*, 323.1371.

(5w) *2-Chloro-4-(trifluoromethyl)-6-(3'-methoxyphenyl)pyridine*

Following general procedure A, and purification using Et_2O in heptane (0-3%) yielded the title compound as an off-white amorphous solid (147 mg, 51%). δ_H (700 MHz, $CDCl_3$) 7.83 (1H, s, 5-*H*), 7.59 (1H, t, *J* = 2.3, 2'-*H*), 7.58 (1H, d, *J* = 7.9, 6'-*H*), 7.48 (1H, s, 3-*H*), 7.41 (1H, t, *J* = 7.9, 5'-*H*), 7.03 (1H, dd, *J* = 7.9, 2.3, 4'-*H*), 3.91 (3H, s, OCH_3); δ_C (176 MHz, $CDCl_3$) 160.4 (*C*-3'), 159.4 (*C*-6), 152.4 (*C*-2), 141.8 (q, *J* = 34.3, *C*-4), 138.0 (*C*-1'), 130.2 (*C*-5'), 122.3 (q, *J* = 274.0, *C*F_3), 119.6 (*C*-6'), 118.7 (q, *J* = 3.7, *C*-3), 116.6 (*C*-4'), 114.8 (q, *J* = 3.5, *C*-5), 112.6 (*C*-2'), 55.6 (O*C*H_3); δ_F (376 MHz, $CDCl_3$) −64.7 (s); ν_{max} (ATR) 1600, 1561, 1459, 1400, 1333, 1274,

1221, 1177, 1142, 1102 cm^{-1}; Accurate Mass (ASAP) *m/z* found $[M]^+$ 287.0330; $C_{13}H_9{}^{35}ClF_3NO$ requires *M*, 287.0325.

(6z) *4-Tert butyl-6-chloro-2-(4'-nitrophenyl)pyridine*

Following general procedure A and purification using EtOAc in hexane (0-6%) yielded the title compound as an off white solid (117 mg, 40 %). mp 192-193 ºC. δ_H (700 MHz, $CDCl_3$) 8.33-8.27 (2H, m, 3',5'-H) 8.19-8.12 (2H, m, 2',6'-H), 7.69 (1H, d, *J* = 1.5 Hz, 3-H), 7.34 (1H, d, *J* = 1.5 Hz, 5-H), 1.38 (9H, s, 4-C(C*H*$_3$)$_3$); δ_C (176 MHz, $CDCl_3$) 164.8 (C-4), 155.3 (C-2), 152.3 (C-6), 148.5 (C-4'), 144.3 (C-1'), 128.0 (C-2',6'), 124.1 (C-3',5'), 121.4 (C-5), 117.2 (C-3), 35.5 (4-*C*), 30.6 (*C*H_3) υ_{max} (ATR), 1588, 1533, 1509, 1410, 1338, 1171, 1104, 856, 813, 762, 731, 698, 644 cm^{-1}. Accurate mass (ES^+) *m/z* found $[MH]^+$ 291.0904; $C_{15}H_{16}{}^{35}ClN_2O_2$ requires *M*, 291.0900.

(10zA) *4-Tert butyl-6-(N-pyrrolidinyl)-2-(4'-nitrophenyl)pyridine*

Following general procedure D and purification using EtOAc in hexane (0-8%) yielded the title compound as a red solid (100 mg, 31 %), mp 180.5-182.5 ºC. δ_H (700 MHz, $CDCl_3$) 8.3-8.23 (2H, m, 3',5'-*H*), 8.21-8.17 (2H, m, 2',6'-*H*), 7.09 (1H, d, *J* = 1.3 Hz, 3-*H*), 6.38 (1H, d, *J* = 1.3 Hz, 5-*H*), 3.55-3.60 (4H, m, 2",5"-*H*$_2$), 2.06-2.01 (4H, m, 3",4"-*H*$_2$), 1.35 (9H, s, C*H*$_3$); δ_C (176 MHz, $CDCl_3$) 161.9 (*C*4),157.7 (*C*-6), 152.6 (*C*-2), 147.7 (*C*-4'), 146.9 (*C*-4'), 127.6 (*C*-2',6'), 123.8 (*C*-3',5'), 107.03 (*C*-3), 103.4 (*C*-5), 47.0 (*C*-2",5"), 35.12 (*4-C*), 30.8 (4-C-(*C*H$_3$)$_3$)), 25.7 (*C*-3", 4"). υ_{max} (ATR) 1597, 1549, 1501, 1476, 1456, 1323, 1107, 1101, 1011, 865, 850, 842, 832, 760, 698, 659, 631, 495 cm^{-1}; *m/z* (GC-MS, EI^+) 326 ($[MH]^+$, 16%), 325 ($[M]^+$, 78%). Accurate Mass (ESI) *m/z* found $[M+H]^+$ 326.1869; $C_{19}H_{24}N_3O_2$ requires *M*, 326.1869.

(6y) *4-Tert butyl-6-chloro-2-(4'-methoxyphenyl)pyridine*

Following general procedure A and purification using Et_2O in hexane (0-5%) yielded the title compound as a colourless oil (121 mg, 44 %). δ_H (700 MHz, $CDCl_3$) 7.96-7.92 (2H, m, 2', 6'-H), 7.55 (1H, d, *J* = 1.5 Hz, 3-H), 7.18 (1H, d, *J* = 1.5 Hz, 5-H), 7.00-6.95 (2H, m, 3',5'-H), 3.86 (3H, s, OCH_3), 1.35 (9H, s, 4-C(C*H*$_3$)$_3$); δ_C (176 MHz, $CDCl_3$) 164.0 (C-4), 160.9 (C-4'), 157.7 (C-2), 151.6 (C-6), 131.0 (C-1'), 128.5 (C-2', 6'), 119.0 (C-5), 115.5 (C3), 114.2 (C-3', 5'), 55.5 (OCH_3), 36.3 (4-*C*), 30.6 (*C*H_3). υ_{max} (ATR) 1607, 1591, 1535, 1514, 1462, 1410, 1385, 1303, 1247, 1175, 1111, 1074, 1031, 878, 831, 780, 650, 585, 507 cm^{-1}. m/z (GC-MS, EI^+) 277 ([M (^{37}Cl)]$^+$, 31%), 275 ([M (35Cl)]$^+$, 100%). Accurate mass (ES^+) *m/z* found $[MH]^+$ 276.1159; $C_{16}H_{19}{}^{35}ClNO$ requires *M*, 276.1155.

(6v) *4-Tertbutyl-6-chloro-2-(3'-thiophenyl) pyridine*

Following general procedure A and purification using EtOAc in hexane (0-7%) yielded the title compound as a white solid (168 mg, 67%). mp 50-51 ºC. δ_H (700 MHz, $CDCl_3$) 8.95 (1H, dd, *J* = 3.0, 1.3 Hz, 2'-H), 7.6 (1H, dd, *J* = 5.0, 1.3 Hz, 4'-H), 7.5 (1H, d, *J* = 1.5 Hz, 3- H), 7.3 (1H, dd, *J* = 5.0, 3.0 Hz, 5'-H), 7.18 (1H, d, *J* = 1.5 Hz, 5-H), 1.35 (9H, s, C*H*$_3$); δ_C (176 MHz, $CDCl_3$) 164.2 (C-4), 153.9 (C-2), 151.6 (C-6), 141.2 (C-3'), 126.5 (C-5'), 126.3 (C-4'), 124.5 (C-2'), 119.4 (C-5), 116.1 (C-3), 35.3 (4-C), 30.6 (*C*H_3). υ_{max} (ATR) 1591, 1540, 1477, 1434, 1422, 1362, 1346, 1287, 1200, 1165, 1079, 1062, 861, 831, 794, 774, 731, 671 cm^{-1}. Accurate mass (ES^+) *m/z* found $[MH]^+$ 252.0596; $C_{13}H_{15}{}^{35}ClNS$ requires *M*, 252.0614.

(6u) *4-Tertbutyl-6-chloro-2-(2'-thiazolyl)pyridine*

Following general procedure A and purification using EtOAc in hexane (0-10%) yielded the title compound as an off white solid (106 mg, 42%). mp. 96.5-97.5 ºC. δ_H (700 MHz, $CDCl_3$) 8.12 (1H, d, *J* = 1.5 Hz, 3-H) 7.9 (1H, d, J = 3.1 Hz, 5'-H), 7.5 (1H, d, *J* = 3.1 Hz, 4'-H), 7.3 (1H, d, *J* = 1.5 Hz, 5-H), 1.36 (9H, s, C*H*$_3$); δ_C (176 MHz, $CDCl_3$) 168.2 (C-2'), 165.0 (C-4), 151.6 (C-2), 151.4 (C-6), 144.1 (C-5'), 122.2 (C-5), 122.0 (C-4'), 115.6 (C-3), 35.5 (4-C), 30.6 (*C*H_3). υ_{max} (ATR) 1591, 1541, 1500, 1478, 1440, 1381, 1242, 1168, 1151, 1048, 874, 863, 794, 770, 745, 723, 620, 583, 515 cm^{-1}. m/z (GC-MS, EI^+) 254 ([M (^{37}Cl)]$^+$, 24%), 252 ([M (^{35}Cl)]$^+$, 65%). Accurate mass (ES^+) *m/z* found $[MH]^+$ 253.0584; $C_{12}H_{15}{}^{35}ClN_2S$ requires *M*, 253.0566.

(6t) *4-Tertbutyl-6-chloro-2,2'-bipyridinyl-4'-carboxylic acid methyl ester*

Following general procedure A and purification using EtOAc in chloroform (0-5%) yielded the title compound as a white solid (200 mg, 66 %). mp. 103-104 ºC. δ_H (600 MHz, $CDCl_3$) 8.9 (1H, bs, 3'-H) 8.8 (1H, d, *J* = 5.0 Hz, 6'-H), 8.4 (1H, d, J = 1.6 Hz, 3-H), 7.86 (1H, dd, *J* = 5.0, 1.6 Hz, 5'-H), 7.3 (1H, d, J = 1.6 Hz, 5-H), 4.0 (3H, s, OCH_3), 1.38 (9H, s, C(C*H*$_3$)$_3$); δ_C (151 MHz, $CDCl_3$) 165.8 (C=O), 164.7 (C-4), 156.3 (C-2'), 155.7 (C-2), 151.5 (C-6), 150.0 (C-6'), 138.7 (C-4'), 123.3 (C-5'), 122.0 (C-5), 121.0 (C-3'), 117.2 (C-3), 52.8 (O*C*H_3), 35.5 (4-*C*), 30.6 (C*C*H_3). υ_{max} (ATR), 1726 (C=O), 1585, 1532, 1478, 1438, 1373, 1365, 1356, 1315, 1294, 1268, 1165, 1133, 1100, 966, 891, 859, 769, 751, 694, 674, 650 cm^{-1}. m/z (GC-MS, EI^+) 306 ([M(^{37}Cl)]$^+$, 8%), 304 ([M (^{35}Cl)]$^+$, 25%), 291 ([M (^{37}Cl)-CH_3]$^+$, 37%), 289 ([M (^{35}Cl)-CH_3]$^+$, 100%). Accurate mass (ES^+) *m/z* found $[MH]^+$ 305.1065; $C_{16}H_{17}{}^{35}ClN_2O_2$ requires *M*, 305.1057.

(7z) *Methyl-6-chloro-2-(4'-nitrophenyl)pyridine-4-carboxylate*

Following general procedure A and purification using DCM in toluene (0-30%) yielded the title compound as a yellow solid (130 mg, 45 %), mp 166-167 °C. δ_H (700 MHz, $CDCl_3$) 8.36-8.33 (2H, m, 3',5'-*H*), 8.3 (1H, d, *J* = 1.1 Hz, 3-*H*), 8.3-8.23 (2H, m, 2',6'-*H*), 7.9 (1H, d, *J* = 1.1 Hz, 5-*H*), 4.0 (3H, s, OC*H*$_3$). δ_C (176 MHz, $CDCl_3$) 164.3 (*C*=O), 156.9 (*C*-2), 152.9 (*C*-6), 149.0 (*C*-4'), 142.8 (*C*1'), 141.5 (*C*-4), 128.1 (*C*-2',6'), 124.3 (*C*-3',5'), 123.8 (*C*-3), 119.0 (*C*-5), 53.4 (*OC*H$_3$). υ_{max} (ATR) 1733 (C=O), 1591, 1557, 1514, 1439, 1404, 1340, 1317, 1252, 1244, 1156, 1104, 982, 857, 818, 770, 755, 742, 722, 689 cm^{-1}; *m/z* (GC-MS, EI$^+$) 294 ([M (^{37}Cl)]$^+$, 33%), 292 ([M (^{35}Cl)]$^+$, 100%). Accurate mass (ES$^+$) *m/z* found [MH]$^+$ 293.0344; $C_{13}H_{10}{}^{35}ClN_2O_4$ requires *M*, 293.0329.

(7y) *Methyl-6-chloro-2-(4'-methoxyphenyl)-pyridine-4-carboxylate*

Following general procedure A and purification using EtOAc in hexane (0-10%) yielded the title compound as a white solid (134.5 mg, 48 %). mp. 102-103 °C. δ_H (700 MHz, $CDCl_3$) 8.11 (1H, d, *J* = 1.2 Hz, 3- H), 8.03-7.96 (2H, m, 2',6'-H), 7.7 (1H, d, *J* = 1.2 Hz, 5-H), 7.01-6.93 (2H, m, 3',5'-H), 4.0 (3H, s, CO_2CH_3), 3.86 (3H, s, 4'-OC*H*$_3$); δ_C (176 MHz, $CDCl_3$) 164.8 (C=O), 161.4 (C-4'), 158.7 (C-2), 152.0 (C-6), 140.8 (C-4), 129.6 (C-1'), 128.6 (C-2',6'), 121.1 (C-5), 117.3 (C3), 114.4 (C-3',5'), 55.5 (4'-O*C*H$_3$), 53.1 (CO_2CH_3) υ_{max} (ATR) 1734 (C=O), 1606, 1597, 1583, 1549, 1519, 1441, 1404, 1390, 1302, 1256, 1180, 1161, 1113, 1071, 1021, 981, 824, 761, 732, 615, 585 cm^{-1}. m/z (GC-MS, EI$^+$) 279 ([M (^{37}Cl)]$^+$, 32%), 277 ([M (^{35}Cl)]$^+$, 100%). Accurate mass (ES$^+$) *m/z* found [MH]$^+$ 278.0600; $C_{14}H_{13}{}^{35}ClNO_3$ requires *M*, 278.0584.

(7'y) *methyl 2-fluoro-6-(4'-methoxyphenyl)pyridine-4-carboxylate*

Following general procedure A and purification using EtOAc in hexanes (0-20%) yielded the title compound as a colourless oil (157 mg, 55%). δ_H (700 MHz, $CDCl_3$) 8.13 (1H, m, 5-*H*), 8.03 (2H, m, 2', 6'-*H*), 7.32 (1H, m, 3-*H*), 7.00 (2H, m, 3', 5'-*H*), 4.00 (3H, s, CO_2CH_3), 3.88 (3H, s, COC*H*$_3$); δ_C (176 MHz, $CDCl_3$) 164.8 (d, *J* = 4.2, *C*O_2CH$_3$), 162.3 (d, *J* = 247.0, *C*-2), 161.5 (*C*-4'), 157.2 (d, *J* = 14.0, *C*-6), 143.4 (d, J = 8.0, *C*-4), 129.5 (*C*-1'), 128.6 (*C*-2', 6'), 116.3 (d, J = 5.0, *C*-5), 114.4 (*C*-3', 5'), 106.7 (d, J = 40.0 Hz, *C*-3), 55.6 (CO_2CH_3), 53.1 (O*C*H$_3$); δ_F (376 MHz, $CDCl_3$) -66.2 (s); ν_{max} (ATR) 1733, 1608, 1568, 1520, 1420, 1396, 1352, 1252, 1206 1177 cm^{-1}; GC/MS (EI) *m/z* 261 [M]$^+$, 246 [M−CH$_3$]$^+$, 230 [M−OCH$_3$]. Accurate Mass (ASAP) *m/z* found [M]$^+$ 261.0811; $C_{14}H_{12}FNO_3$ requires *M*, 261.0801.

(11yA) *Methyl 2-(4'-methoxyphenyl)-6-(pyrrolidin-1''-yl)pyridine-4-carboxylate*

Following general procedure B and purification using EtOAc in hexane (0-15%) yielded the title compound as a white amorphous solid (32 mg 85%) δ_H (600 MHz, $CDCl_3$) 8.02 (2H, d, *J* = 8.8 Hz, 2', 6'-H), 7.46 (1H, d, *J* = 1.2 Hz, 3-H), 6.95 (2H, d, *J* = 8.8 Hz, 3', 5'-H), 6.83 (1H. d, *J* = 1.2 Hz, 5-H), 3.93 (3H, s, CO_2CH_3), 3.84 (3H, s, 4'-OCH_3), 3.54-3.62 (4H, m, 2'',5''-H_2), 2.11 – 1.92 (4H, m, 3''H, 4''-H_2). δ_C (151 MHz, $CDCl_3$) 166.86 (C=O), 161.08 (C-4'), 157.22 (C-2), 156.11 (C-2), 155.8 (C-6), 132.1 (C-1'), 139.08 (C-4), 128.1 (C-2', 6'), 113.8 (C-3', 5'), 105.8 (C-3), 104.2 (C-5), 55.31 (4'-OCH_3), 52.36 (CO_2CH_3), 46.9 (C-2'', 5''), 25.5 (C-3'', 4''). ν_{max} (ATR) 2949, 2848, 1719, 1611, 1554, 1444, 1243, 1030, 1178, 766 cm^{-1}. GC/MS (EI) *m/z* 313.1 $[M+H]^+$ (100%). Accurate Mass (ES^+) *m/z* found $[M+H]^+$ 313.1562, $C_{18}H_{21}N_2O_3$ requires *M*, 313.1552.

(7'x) *Methyl 2-fluoro-6-(4'-trifluoromethylphenyl) pyridine-4-carboxylate*

Following general procedure A and purification using C18 reverse phase chromatography (H_2O: MeCN, 0-100%) to yield the title compound as a white amorphous solid (151 mg, 50%). δ_H (700 MHz, $CDCl_3$) 8.22 (1H, dd, *J* = 2.0, 0.8 Hz, 5-H), 8.15 (2H, d, *J* = 8.4, 2',6'-H), 7.74 (2H, d, *J* = 8.4, 3',5'-H), 7.46 (1H. dd, 0.8, 0.4 Hz, 3-H), 4.01 (3H, s, -OCH_3). δ_C (176 MHz, $CDCl_3$) 164.3 (d, *J* = 4.1 Hz C=O), 163.8 (d, *J* = 241.1 Hz, C-2), 155.5 (d, *J* = 14.0 Hz, C-6) 143.7 (d, *J* = 6.9 Hz, C-4), 139.92 (C-1'), 131.8 (q, *J* = 32.2 Hz, C-6'), 127.3 (C-2', 6'), 125.8 (C-3', 5'), 124.0 (q, *J* = 263.3 Hz, -CF_3), 117.3 (d, *J* = 4.7 Hz C-5), 108.8 (d, *J* = 39.7 Hz, C-3) 53.1 (-OCH_3). δ_F (376 MHz, $CDCl_3$) -62.78 (-CF_3), -65.15 (Ar-F). ν_{max} (ATR) 2957, 2256, 1741, 1578, 1329, 1255, 1136, 905, 731 cm^{-1}. GC/MS (EI) *m/z* found $[M+H]^+$ 300.0, $[M+MeCN+H]^+$ 341.1. Accurate Mass (ES^+) *m/z* found $[M+H]^+$ 300.0670, $C_{14}H_{10}F_4NO_2$ requires *M* 300.0648.

(11xB) *Methyl 2-(morpholin-4''-yl)-6-[4'-(trifluoromethyl)phenyl]pyridine-4-carboxylate*

Following general procedure B and purification using EtOAc in hexane (0-15%) yielded the title compound as an off white solid (28 mg, 83%). mp. 272-273 ^oC (ethanol). δ_H (599 MHz, $CDCl_3$) 8.14 (2H, d, *J* = 8.3 Hz, 3', 5'-H), 7.70 (2H, d, *J* = 8.3 Hz, 2', 6'-H), 7.69 (1H, d, *J* = 1.0 Hz, 3-H), 7.25 (1H, d, *J* = 1.0 Hz, 5-H), 3.97 (3H, s, -OCH_3), 3.90 – 3.83 (2H, m, 3'', 5''-H_2), 3.71 – 3.64 (1H, m, 2'', 6''-H_2). δ_C (151 MHz, $CDCl_3$) 166.1 (C=O), 159.54 (C-2), 154.6 (C-4), 142.3 (C-6), 140.0 (C-1'), 130.9 (q, *J* = 30.7 Hz, C-4') 127.1 (C-2'', 6''), 125.5 (q, *J* = 4.0 Hz C-3'', 5''), 124.2 (q, *J* = 271.0 Hz -CF_3), 109.42 (C-3), 106.1 (C-5), 66.7 (C-3'', 5''), 52.6 (-OCH_3), 45.5 (C-2'', 6''). δ_F (376 MHz, $CDCl_3$) -62.56. ν_{max} (ATR) 2960, 2860, 2259, 1734, 1604, 1563, 1444, 1237, 1124 cm^{-1}. GC/MS (EI) *m/z* found $[M+H]^+$ 367.1. Accurate Mass (ES^+) *m/z* found $[M+H]^+$ 367.1279, $C_{18}H_{18}F_3N_2O_3$ requires *M* 367.1270.

(11xE) *methyl 2-(butylamino)-6-[4'-(trifluoromethyl)phenyl]pyridine-4-carboxylate*

Following general procedure B and purification using EtOAc in hexane (0-40%) yielded the title compound as a light yellow oil (36 mg, 64%). δ_H (700 MHz, $CDCl_3$) 8.10 (1H, d, *J* = 7.6 Hz, 2', 6'-H), 7.71 (2H, d, *J* = 7.6 Hz, 3', 5'H), 7.55 (1H, d, *J* = 1.1 Hz, 3-H), 6.98 (1H, d, *J* = 1.1 Hz, 5-H), 3.95 (3H, s, -OCH_3), 3.39 (2H, q, *J* = 6.7 Hz, 1''-H_2), 1.70 – 1.62 (2H, m, 2''-H_2), 1.46 (1H, m, 3''-H_2), 0.97 (3H, t, *J* = 7.4 Hz, 4''-C*H*$_3$). δ_C (176 MHz, $CDCl_3$) 166.1 (C=O), 166.0 (C-2), 158.98 (C-6), 154.3 (C-4) 140.0 (C-1'), 130.8 (q, *J* = 30.8 Hz, C-4') 127.1 (C-2', 6') , 125.5 (q, *J* = 3.8 Hz, C-3', 5'), 124.1 (q, *J* = 272.0 Hz -CF_3), 108.6 (C-3), 106.1 (C-5), 52.6 (-OCH_3), 42.0 (C-1''), 31.5 (C-2''), 20.2 (C-3''), 13.8 (C-4''). δ_F (376 MHz, $CDCl_3$) -62.58 (-CF_3). ν_{max} (ATR) 3423, 2960, 2259, 1724, 1571, 1329, 1249, 1124 cm^{-1}. GC/MS (EI) *m/z* found $[M+H]^+$ 353.5. Accurate Mass (ES^+) *m/z* found $[M+H]^+$ 353.1484, $C_{18}H_{20}F_3N_2O_2$ requires *M* 353.1477.

(8z) *Tert butyl 2-chloro-6-(4'-nitrophenyl)pyridine-4-carboxylate*

Following general procedure A and purification using $CHCl_3$ in hexane (0-60%) yielded the title compound as a bright yellow solid (203 mg, 61%). mp 141-142 °C (methanol). δ_H (599 MHz, $CDCl_3$) 8.32 (2H, d, *J* = 8.9 Hz, 3',5'-H), 8.23 – 8.19 (3H, m, 2',6', 5-H), 7.81 (1H, d, *J* = 1.1 Hz, 3-H), 1.62 (9H, s, OC(*CH*$_3$)$_3$). δ_C (151 MHz, $CDCl_3$) 162.5 (C=O), 156.0 (C-6), 152.5 (C-2), 148.7 (C-4'), 143.32 (C-4), 142.8 (C-1'), 127.9 (C-2', 6'), 124.1 (C-3', 5'), 123.6 (C-3), 118.9 (C-5), 83.7 (O*C*$(CH_3)_3$), 28.0 ((*C*H_3)$_3$). ν_{max} (ATR) 2984, 1719, 1593, 1548, 1524, 1346, 1160, 861 cm^{-1}. GC/MS (EI) *m/z* found 325.3 ($[M (^{35}Cl)+H]^+$ 100%), 327.3 ($[M (^{37}Cl)+H]^+$ 31%). Accurate Mass (ES^+) *m/z* found $[M (^{35}Cl)+H]^+$ 335.0803 , $[M-tBu+H]^+$ 279.0191, $C_{16}H_{16}{}^{35}ClN_2O_4$ requires *M* 335.0799.

(12zB) *Tert butyl 2-(morpholin-4''-yl)-6-(4'-nitrophenyl)pyridine-4-carboxylate*

Following general procedure D and purification using EtOAc in hexane (0-15%) yielded the title compound as a bright yellow solid (27 mg, 78%). mp 216-217 °C (ethanol)**.** δ_H (600 MHz, $CDCl_3$) 8.30 (2H, d, *J* = 8.9 Hz, 3', 5'-H), 8.19 (2H, d, *J* = 8.9 Hz, 2', 6'-H), 7.66 (1H, d, *J* = 1.0 Hz, 3-H), 7.24 (1H, d, *J* = 1.0 Hz, 5-H), 3.88 (4H, t, *J* = 4.9 Hz, 3'', 5''-H_2), 3.69 (4H, t, *J* = 4.9 Hz, 2'', 6''-H_2), 1.63 (9H, s, -$(CH_3)_3$). δ_C (151 MHz, $CDCl_3$) 164.4 (C=O) , 159.5 (C-2), 153.3 (C-4'), 148.1 (C-1'), 145.0 (C-6), 142.1 (C-4), 127.6 (C-2', 6'), 123.8 (C-3', 5'), 110.0 (C-3), 106.8 (C-5), 82.6 (-*C*$(CH_3)_3$), 66.6 (C-3'', 5''), 45.6 (C-2'', 6''), 28.1 (-$(CH_3)_3$). ν_{max} (ATR) 2982, 2863, 1717, 1596, 1563, 1516, 1433, 1341, 1251, 998 cm^{-1}. GC/MS (EI) *m/z* found 386.1 ($[M+H]^+$ 100%), 330.1 ($[M-tBu+H]^+$ 62%). Accurate Mass (ES^+) *m/z* found $[M+H]^+$ 386.1726, $C_{20}H_{24}N_3O_5$ requires *M* 386.1716.

(8y) *Tert butyl 2-chloro-6-(4'-methoxyphenyl)pyridine-4-carboxylate*

Following general procedure A and purification using $CHCl_3$ in hexane (0-55%) yielded the title compound as an off white solid (182 mg, 57%). mp, 119-120 °C (methanol). δH (600 MHz, $CDCl_3$) 8.07 (1H, d, *J* = 1.2 Hz, 3-H), 8.01 – 7.96 (2H, m, 2', 6'-H), 7.63 (1H, d, *J* = 1.1 Hz, 5-H), 7.01 – 6.95

(2H, m, 3',5'-H), 3.85 (3H, s, -OCH_3), 1.61 (9H, s, -$(CH_3)_3$). δ_C (151 MHz, $CDCl_3$)163.2 (C=O), 161.2 (C-4'), 158.4 (C-6), 151.8 (C-2), 142.7 (C-4), 129.7 (C-1'), 128.5 (C-5), 121.0 (C-2', 6'), 117.3 (C-3), 114.22 (C-3' 5'), 83.01 (-*C*$(CH_3)_3$, 55.37 (-OCH_3), 28.0 ($OC(CH_3)_3$). ν_{max} (ATR) 2986, 2874, 1728, 1595, 1548, 1415, 1323, 1238, 1147, 1027 cm^{-1}. GC/MS (EI) *m/z* found 320.6 ([M(^{35}Cl)+H]$^+$ 72%), 322.5 ([M(^{37}Cl)+H]$^+$ 21%). Accurate Mass (ES^+) *m/z* found [M(^{35}Cl)+H]$^+$ 320.1071, $C_{17}H_{19}NO_3{}^{35}Cl$ requires *M* 320.1053.

(12yA) *Tert butyl 2-(4'-methoxyphenyl)-6-(pyrrolidin''-yl)pyridine-4-carboxylate*

Following general procedure D and purification using EtOAC in hexane (0-20%) yielded the title compound as an off white amorphous solid (41 mg, 90%). δ_H (600 MHz, $CDCl_3$) 8.01 (2H, d, *J* = 8.7 Hz, 2', 6'-H), 7.40 (1H, d, *J* = 1.1 Hz, 3-H), 6.98 (2H, d, *J* = 8.7 Hz, 3', 5'-H), 6.82 (1H, d, *J* = 1.1 Hz, 5-H), 3.86 (3H, s, -OCH_3), 3.57-3.63 (4H, m, 3'', 4''-H_2), 2.13 – 1.93 (4H, m, 2'',5''-H_2), 1.61 (9H, s, -$(CH_3)_3$). δ_C (151 MHz, CDC_3) 165.4 (C=O), 160.3 (C-4'), 155.5 (C-2) 141.0 (C-6), 128.2 (C-2',6'), 124.6 (C-1'), 121.6 (C-4), 113.8 (C-3',5'), 106.0 (C-3), 104.2 (C-5), 81.7 (-*C*$(CH_3)_3$), 55.3 (-OCH_3), 47.0 (C-2'',5''), 28.1 (C(CH_3)$_3$), 25.5 (C-3'',4''). ν_{max} (ATR) 2972, 2859, 1714, 1607, 1557, 1459, 1382, 1246, 1030 cm^{-1}. GC/MS (EI) *m/z* found 356.3 ([M+H]$^+$ 100%), Accurate Mass (ES^+) *m/z* found ([M+H]$^+$ 355.2022, $C_{21}H_{27}N_2O_3$ requires *M* 355.2022.

(8x) *tert-butyl 2-chloro-6-(4-triflurometh-lphenyl)pyridine-4-carboxylate*

Following general procedure A and purification using C18 reverse phase chromatography (H_2O: MeCN, 0-100%) yielded the title compound as a light brown amorphous solid (140 mg, 39%). δH (700 MHz, $CDCl_3$) 8.19 (1H, d, *J* = 1.1 Hz, 3-H), 8.18 – 8.15 (2H, d, *J* = 1, 2', 6'-H), 7.79 (1H, d, *J* = 1.1 Hz, 5-H), 7.74 (2H, d, *J* = 8.1 Hz m, 3', 5'-H), 1.63 (9H, s, -$(CH_3)_3$). δC (176 MHz, $CDCl_3$) 162.7 (C=O), 157.0 (C-2), 152.3 (C-1'), 143.1 (C-4), 140.4 (C-6), 127.4 (C-2', 6'), 125.8 (q, *J* = 3.9 Hz, C-3', 5'), 123.9 (q, *J* = 272.2 Hz, -CF_3), 123.0 (C-5), 118.5 (C-3), 83.4 (-*C*$(CH_3)_3$), 28.0 (-$(CH_3)_3$). δF (376 MHz, $CDCl_3$) -62.72 (-CF_3). ν_{max} (ATR) 2975, 2887, 1726, 1557, 1471, 1382, 1326, 1261, 1131, 950 cm^{-1}. GC/MS (EI) *m/z* found 358.1 ([M(^{35}Cl)+H]$^+$ 100%), 360.1 ([M(^{37}Cl)+H]$^+$ 39%). Accurate Mass (ES^+) *m/z* found [M(^{35}Cl)+H]$^+$ 358.0826, [M(^{35}Cl)-tBu+H]$^+$ 302.0210, $C_{17}H_{16}{}^{35}ClF_3NO_2$ requires *M* 358.0822.

(12xA) *tert-butyl 2-(pyrrolidin-1-yl)-6-[4-(trifluoromethyl)phenyl]pyridine-4-carboxylate*

Following general procedure D and purification using EtOAC in hexane (0-10%) yielded the title compound as a white solid (39 mg, 90%). mp 168-169 °C (ethanol). δH (600 MHz, $CDCl_3$) 8.19 – 8.15 (2H, d, *J* = 8.2 Hz, 2', 6'-H), 7.69 (2H, d, *J* = 8.2 Hz, 3', 5'-H), 7.48 (1H, d, *J* = 1.1 Hz, 3-H), 6.92 (1H, d, *J* = 1.1 Hz, 5-H), 3.62-3.58 (4H, m, 2'', 5''-H), 2.02-2.07 (4H, m, 3', 4'H), 1.62 (9H, s, -$(CH_3)_3$). δC (151 MHz, $CDCl_3$) 165.1 (C=O), 157.36 (C-2), 154.32 (C-6), 142.81 (C-4), 141.2 (C-1'), 130.4 (q, *J* =

32.6 Hz C-4), 127.1 (C-2',6'), 125.3 (q, *J* = 3.8 Hz C-3', 5'), 124.3 (q, *J* = 273.4 Hz, -CF_3), 107.0 (C-3), 106.0 (C-5), 82.0 (-*C*$(CH_3)_3$), 46.9 (C-2'', 5'', 28.1 (-$(CH_3)_3$), 25.5 (C-3'', 4''). δF (376 MHz, $CDCl_3$) -62.49 (-CF_3). ν_{max} (ATR) 2972, 2839, 2259, 1734, 1604, 1566, 1443, 1326, 1251, 1124 cm^{-1}. GC/MS (EI) *m/z* found 393.5 ($[M+H]^+$ 100%), Accurate Mass (ES^+) *m/z* found $[M+H]^+$ 393.1785, $C_{21}H_{24}F_3N_2O_2$ requires *M* 393.1789.

13 *2-(4'-nitrophenyl)-6-(pyrrolidin-1''-yl)-4-(pyrrolidine-1'''-carbonyl)pyridine*

Following procedure D and purification using EtOAc in hexane (0-50%) yielded the title compound as a yellow solid (275 mg, 75 %). mp 239.5-240.5 °C. δ_H (500 MHz, $CDCl_3$) 8.29-8.21 (2H, m, 3',5'-*H*), 8.21-8.14 (2H, m, 2',6'-*H*), 7.1 (1H, s, 3-*H*), 6.4 (1H, s, 5-*H*), 3.7 (2H, t, *J* = 7.0 Hz, 2'''-H_2), 3.60-3.49 (4H, m, 2'',5''-H_2), 3.43 (2H, t, *J* = 6.7 Hz, 5'''-H_2), 2.06-2.01 (4H, m, 3'',4''-H_2), 2.0 (2H, p, *J* = 7.0 Hz, 3'''-H_2), 1.9 (2H, p, *J* = 6.7 Hz, 4'''-H_2); δ_C (125 MHz, $CDCl_3$) 168.4 (*C*=O), 157.2 (*C*-6), 153.3 (*C*-2), 148.0 (*C*-4'), 146.9 (*C*-4), 145.8 (*C*-1'), 127.5 (*C*-2',6'), 123.8 (*C*-3',5'), 106.0 (*C*-3), 104.1 (*C*-5), 49.4 (*C*-5''), 46.9 (C-2'',5''), 46.2 (*C*-2'''), 26.4 (*C*-4'''), 25.6 (*C*-3'',4''), 24.5 (*C*-3'''); ν_{max} 1618, 1616, 1598, 1541, 1512, 1478, 1456, 1442, 1419, 1344, 1322, 1102, 858, 755, 702, 513 cm^{-1}; *m/z* (LC-MS, ES^+) 1121 ($[M_3Na]^+$, 38%), 755 ($[M_2Na]^+$, 81%), 366 ($[M]^+$, 100%); Accurate mass (ES^+) *m/z* found $[MH]^+$ 367.1781; $C_{20}H_{23}N_4O_3$ requires *M*, 367.1770.

(17w) *Methyl 6-chloro-5-(3-methoxyphenyl)pyridine-3-carboxylate*

Following general procedure and purification using EtOAc in heptane (0-15%) yielded the title compound as a white amorphous solid (229 mg, 76%). δ_H (700 MHz, $CDCl_3$) 8.49 (1H, d, *J* = 2.2, 6-*H*), 8.34 (1H, d, *J* = 2.2, 4-*H*), 7.48 (2H, m, 2', 6'-*H*), 7.00 (2H, m, 3', 5'-*H*), 4.10 (3H, s, 2-COCH_3), 3.93 (3H, s, CO_2CH_3), 3.86 (3H, s, 4'-OCH_3); δ_C (176 MHz, $CDCl_3$) 165.7 (CO_2CH_3), 161.4 (*C*-2), 159.7 (*C*-4'), 148.2 (*C*-6), 139.7 (*C*-4), 129.8 (*C*-5), 129.3 (*C*-1'), 128.0 (*C*-2', 6'), 114.7 (*C*-3', 5'), 113.9 (*C*-3), 55.5 (4'-OCH_3), 54.6 (2-COCH_3), 52.5 (CO_2CH_3); ν_{max} (ATR) 1732, 1606, 1563, 1519, 1474, 1417, 1327, 1285, 1245, 1181, 1087, 1060, 1014 cm^{-1}; Accurate Mass (ASAP) *m/z* found $[M+H]^+$ 274.1075; $C_{15}H_{16}NO_4$ requires *M*, 274.1079.

(17'y) *Methyl 6-fluoro-5-(4'-methoxyphenyl)pyridine-3-carboxylate*

Following general procedure A and purification using EtOAc in hexane (0-50%) yielded the title product as a pale yellow amorphous solid (107 mg, 58%). δ_H (600 MHz, $CDCl_3$) 8.77 (1H, m, 6-*H*), 8.45 (1H, m, 4-*H*), 7.54 (2H, d, *J* = 8.6, 2', 5'-*H*), 7.01 (2H, d, *J* = 8.6, 3', 5'-*H*), 3.96 (3H, s, CO_2CH_3), 3.86 (3H, s, OCH_3); δ_C (151 MHz, $CDCl_3$) 165.0 (CO_2CH_3), 162.6 (d, *J* = 246.2, *C*-6), 160.3 (*C*-4'), 147.8 (dd, *J* = 16.7, 5.1, *C*-6), 141.5 (d, *J* = 6.4, *C*-4), 130.2 (d, *J* = 6.4, *C*-2', 6'), 125.1 (m, *C*-1'), 123.7

(d, *J* = 28.6, *C*-3), 114.5 (*C*-3', 5'), 55.5 (O*C*H$_3$), 52.7 (CO$_2$*C*H$_3$); δ_F (376 MHz, CDCl$_3$) −65.4 (s); ν_{max} (ATR) 1725, 1609, 1518, 1434, 1411, 1313, 1250, 1200, 1181, 1120, 1047, 1029 cm^{-1}; Accurate Mass (ASAP) *m/z* found [M]$^+$ 261.0819; $C_{14}H_{12}FNO_3$ requires *M*, 261.0801.

(20yB) *Methyl 5-(4'-methoxyphenyl)-6-(morpholin-4''-yl)pyridine-3-carboxylate*

Following general procedure B and purification using EtOAc in hexane (0-20%) yielded the title compound as a light yellow solid (22 mg, 88%). mp 242-243 ºC. δ_H (599 MHz, CDCl$_3$) 8.78 (1H, d, *J* = 2.3 Hz, 6-H), 7.97 (1H, d, *J* = 2.3 Hz, 4-H), 7.44 (2H, d, *J* = 8.3 Hz, 3', 5'-H), 6.95 (2H, d, *J* = 8.3 Hz, 3', 6'-H), 3.88 (3H, s, CO$_2$C*H*$_3$), 3.84 (3H. s, 4'-OC*H*$_3$), 3.62 (4H, t, *J* = 4.5 Hz, 3'', 5''-H$_2$), 3.24 (4H, t, *J* = 4.5 Hz, 2'', 6''-H$_2$). δ_C (151 MHz, CDCl$_3$) 159.2 (C=O), 147.9 (C-4'), 140.7 (C-2), 131.4 (C-3), 128.7 (C-4), 127.8 (C-2', 6'), 125.8 (C-1') , 124.8 (C-6), 118.5 (C-4), 114.4 (C-3', 5'), 66.6 (-OCH$_3$), 55.3 (CO$_2$*C*H$_3$), 51.9 (C-2'', 6''), 48.7 (C-3'', 5''). ν_{max} (ATR) 2967, 2854, 1717, 1596, 1509, 1411, 1361, 1249, 1234, 1100 cm^{-1}. *m/z* (LC-MS, ES$^+$) 329.1 ([M+H]$^+$, 100%), Accurate mass (ES$^+$) *m/z* found [M+H]$^+$ 329.1511; $C_{18}H_{21}N_2O_4$ requires *M*, 329.1501.

(17y) *Methyl 6-chloro-5-(4'-methoxyphenyl)pyridine-3-carboxylate*

Following general procedure A and purification using CHCl$_3$ in hexane (0-50%) yielded the title compound as an off white solid (169 mg, 61%). mp 171-172 ºC. δH (700 MHz, CDCl$_3$) 8.93 (1H, d, *J* = 2.3 Hz, 6-H), 8.24 (1H, d, *J* = 2.3 Hz, 4-H), 7.42 (2H, d, *J* = 8.7 Hz, 2', 6'-H), 6.99 (2H, d, *J* = 8.7 Hz, 3', 5'-H), 3.95 (3H, s, CO$_2$C*H*$_3$), 3.86 (3H, s, -OCH$_3$). δC (176 MHz, CDCl$_3$) 165.0 (C=O), 159.9 (C-4'), 153.8 (C-2), 148.9 (C-6), 140.2 (C-4), 136.5 (C-3), 130.5 (C-2', 6'), 128.7 (C-1'), 125.2 (C-5), 113.9 (C-3', 5'), 55.3 (4'-OCH$_3$), 52.6 (CO$_2$*C*H$_3$). ν_{max} (ATR) 2960, 2849, 1726, 1614, 1591, 1523, 1446, 1394, 1317, 1252, 1181 cm^{-1}. *m/z* (LC-MS, ES$^+$) 279.0 ([M(^{35}Cl)+H]$^+$, 100%), 281.1 ([M(^{37}Cl)+H]$^+$, 28%), Accurate mass (ES$^+$) *m/z* found [M(^{35}Cl)+H]$^+$ 278.0601, $C_{14}H_{13}NO_3{}^{35}Cl$ requires *M* 278.0584.

(20yA) *Methyl 5-(4'-methoxyphenyl)-6-(pyrrolidin-1''-yl)pyridine-3-carboxylate*

Following general procedure B and purification using EtOAC in hexane (0-15%) yielded the title compound as a light yellow amorphous solid (24 mg, 71%). δ_H (599 MHz, CDCl$_3$) 8.03 (2H, *J* = 8.8 Hz, 3', 5'-H), 7.46 (1H, d, *J* = 1.2 Hz, 6-H), 6.97 (2H, d, *J* = 8.8 Hz, 2', 6'-H), 6.86 (1H, , d, *J* = 1.2 Hz, 4-H), 3.95 (3H, s, CO$_2$C*H*$_3$), 3.85 (2H, s, 4'-OCH$_3$), 3.62 (2H, m, 2'', 5''-H$_2$), 2.08 – 2.01 (1H, m, 3'', 4''-H$_2$). δC (151 MHz, CDCl$_3$) 166.7 (C=O), 160.5 (C-4'), 157.0 (C-2), 155.6 (C-3), 139.1 (C-4), 128.3 (C-2', 6'), 113.8 (C-3', 5'), 113.1 (C-1'), 105.9 (C-6), 104.4 (C-4), 55.3 (-OCH$_3$), 52.4 (CO$_2$*C*H$_3$), 47.0 (C-2'', 5''), 25.5 (C-3'', 4''). ν_{max} (ATR) 2972, 1731, 1607, 1557, 1518, 1477, 1459, 1246, 1216,

1178, 1030 cm^{-1}. *m/z* (LC-MS, ES^+) 313.1 ($[M+H]^+$, 100%), Accurate mass (ES^+) *m/z* found $[M+H]^+$ 313.1571, $C_{18}H_{21}N_2O_3$ requires *M* 313.1552.

(17x) *Methyl 6-chloro-5-[4'-(trifluoromethyl)phenyl]pyridine-3-carboxylate*

Following General procedure A and purification using C18 reverse phase chromatography (H_2O: MeCN, 0-100%) yielded the title compound as an off white amorphous solid (173 mg, 55%). δ_H (599 MHz, $CDCl_3$) 9.02 (1H, d, *J* = 2.3 Hz, 6-H), 8.27 (1H, d, *J* = 2.3 Hz, 4-H), 7.85 – 7.67 (2H, m, 3', 5'-H), 7.65 – 7.53 (2H, m, 2', 6'-H), 3.98 (3H, s, CO_2CH_3). δ_C (151 MHz, $CDCl_3$) 164.6 (C=O), 153.5 (C-2), 150.0 (C-6), 140.2 (C-4), 140.0 (C-1'), 135.5 (C-2), 131.01 (q, *J* = 32.8 Hz, C-4') 129.7 (C-2', 6'), 127.7 (C-4), 125.5 (q *J* = 3.7 Hz C-3',5'), 123.8 (q, *J* = 269.4 Hz, -CF_3) 52.7 (CO_2CH_3). δ_F (376 MHz, $CDCl_3$) -62.73 (-CF_3). ν_{max} (ATR) 3070, 2964, 1714, 1596, 1397, 1323, 1261, 1169, 1124, 1071 cm^{-1}. *m/z* (LC-MS, ES^+) 316.4 ($[M(^{35}Cl)+H]^+$, 72%), 318.3 ($[M(^{37}Cl)+H]^+$, 22%), Accurate mass (ES^+) *m/z* found $[M(^{35}Cl)+H]^+$ 316.0359, $C_{14}H_{10}{}^{35}ClF_3NO_2$ requires *M* 316.0352.

(20xA) *Methyl 6-(pyrrolidin-1''-yl)-5-[4'-(trifluoromethyl)phenyl]pyridine-3-carboxylate*

Following general procedure C and purification using EtOAc in hexane (0-15%) yielded the title compound as a light yellow amorphous solid (36 mg, 88%). δ_H (599 MHz, $CDCl_3$) 8.16 (2H, d, *J* = 8.1 Hz, 3', 5'-H), 7.68 (2H, d, *J* = 8.1 Hz, 2', 6'-H), 7.53 (1H, d, *J* = 1.2 Hz, 6-H), 6.95 (1H, d, *J* = 1.2 Hz, 4-H), 3.95 (3H, s, CO_2CH_3), 3.59 (4H, d, *J* = 6.4 Hz, C-2'', 5''-H_2), 2.09 – 1.97 (4H, m, C-3'', 4''-H_2). δ_C (151 MHz, $CDCl_3$) 166.44 (C=O), 157.3 (C-2), 154.50 (C-5), 142.6 (C-3), 139.2 (C-1'), 130.7 (q, *J* = 32.6 Hz C-6'), 127.1 (C-3', 5'), 125.35 (C-2', 6'), 124.1 (q, *J* = 263.78 Hz, CF_3), 106.9 (C-6), 106.1 (C-4), 52.5 (-OCH_3), 47.0 (C-2'', 5''), 25.5 (C-3'', 4''). δ_F (376 MHz, $CDCl_3$) δ -62.52. ν_{max} (ATR) 2966, 2863, 1723, 1609, 1560, 1477, 1446, 1323, 1238, 1112 cm^{-1}. *m/z* (LC-MS, ES^+) 351.1 ($[M+H]^+$, 100%), Accurate mass (ES^+) *m/z* found $[M+H]^+$ 351.1308, $C_{18}H_{18}F_3N_2O_2$ requires *M* 351.1320.

(18y) *Tert butyl 6-chloro-5-(4'-methoxyphenyl)pyridine-3-carboxylate*

Following General procedure A and purification using EtOAc in hexane yielded the title compound as an off white solid (140 mg 44%). mp. 177-178 °C (methanol). δ_H (599 MHz, $CDCl_3$) 8.86 (1H, d, *J* = 2.5 Hz, 6-H), 8.16 (1H, d, *J* = 2.4 Hz, 4-H), 7.39 (2H, d, *J* = 9.1, 2', 6'-H), 6.99 (2H, d, *J* = 9.1 Hz, 3', 5'-H), 3.86 (3H, s, 4'-OCH_3), 1.59 (9H, s, $(CH_3)_3$). δ_C (151 MHz, $CDCl_3$) 163.6 (C=O), 159.9 (C-4'), 153.3 (C-2), 148.9 (C-6), 140.1 (C-4), 136.3 (C-3), 130.5 (C-2', 6'), 129.0 (C-1'), 126.9 (C-5), 113.9 (C-3' 5'), 82.5 (-$C(CH_3)_3$), 55.3 (-OCH_3), 28.1 ($C(CH_3)_3$). ν_{max} (ATR) 2987, 2830, 2164, 1726, 1593, 1400, 1258, 1136, 1033 cm^{-1}. *m/z* (LC-MS, ES^+) 320.1 ($[M(^{35}Cl)+H]^+$, 46%), 322.1 ($[M(^{37}Cl)+H]^+$, 18%), 264.0 ($[M(^{35}Cl)$-tBu+$H]^+$, 100%), 266.0 ($[M(^{37}Cl)$-tBu+$H]^+$, 38%) Accurate mass (ES^+) *m/z* found $[M(^{35}Cl)+H]^+$ 320.1075, $C_{17}H_{19}{}^{35}ClNO_3$ requires *M* 320.1053.

(21yA) *Tert butyl 5-(4'-methoxyphenyl)-6-(pyrrolidin-1''-yl)pyridine-3-carboxylate*

Following general procedure D and purification using EtOAC in hexane (0-20%) yielded the title compound as a light yellow solid (26 mg, 75%). mp 248-249 ºC (ethanol). δ_H (700 MHz, CDCl3) 8.73 (1H, d, *J* = 2.2 Hz, 6-H), 7.83 (d, *J* = 2.2 Hz, 1H), 7.24 – 7.20 (2H, m, 2', 6'-H), 6.91 – 6.87 (2H, m, 3', 5'-H), 3.83 (3H, s, 4'-OCH_3), 3.17 – 3.23 (4H, m, 2'', 5''-H_2), 1.79 – 1.75 (4H, m, 3'', 4''-H_2), 1.54 (9H, s, C(CH_3)$_3$). δ_C (176 MHz, $CDCl_3$) 165.3 (C=O), 158.6 (C-4'), 148.2 (C-6), 140.6 (C-4), 132.4 (C-1') 130.1 (C-2', 6'), 128.3 (C-2), 127.8 (C-3), 116.7 (C-5) 113.4 (C-3', 5'), 80.5 (*C*(CH_3)$_3$), 55.7 (-OCH_3), 50.3 (C-2'', 5''), 28.3 (C(*C*H_3)$_3$), 25.6 (C-3'', 4''). ν_{max} (ATR) 2985, 2880, 2256, 1699, 1598, 1513, 1459, 1308, 1251, 1166 cm^{-1}. *m/z* (LC-MS, ES^+) 355.2 ($[M+H]^+$, 100%), Accurate mass (ES^+) *m/z* found $[M+H]^+$ 355.2033, $C_{21}H_{27}N_2O_3$ requires *M* 355.2022

(21yB) *Tert butyl 5-(4'-methoxyphenyl)-6-(morpholin-4''-yl)pyridine-3-carboxylate*

Following general procedure D and purification using EtOAC in hexane (0-20%) yielded the title compound as a light yellow amorphous solid (30 mg, 87%). δ_H (700 MHz, $CDCl_3$) 8.74 (1H, d, *J* = 2.3 Hz, 6-H), 7.92 (1H, d, *J* = 2.3 Hz, 4-H), 7.45 (2H, d, *J* = 8.7 Hz, 2', 6'-C), 6.95 (2H, d, *J* = 8.7 Hz, 3', 5--H), 3.84 (3H, s, 4'-OCH_3), 3.61 (4H, t, *J* = 4.7 Hz, 3'', 5''-H_2), 3.21 (4H, t, *J* = 4.7 Hz, 2'', 6''-H_2), 1.56 (9H, s, C(CH_3)$_3$). δ_C (176 MHz, $CDCl_3$) 164.9 (C=O), 159.1 (C-4'), 147.7 (C-5), 140.5 (C-4), 131.6 (C-1'), 128.8 (C-2'', 6''), 125.7 (C-2), 124.7 (C-3), 120.4 (C-5), 114.3 (C-3'', 5''), 81.1 (*C*(CH_3)$_3$), 66.6 (C-2'', 6''), 55.3 (-OCH_3), 48.8 (C-3'', 5''), 28.3 (C(CH_3)$_3$). ν_{max} (ATR) 2967, 2246, 1731, 1569, 1414, 1320, 1112 cm^{-1}. *m/z* (LC-MS, ES^+) 371.2 ($[M+H]^+$, 100%), Accurate mass (ES^+) *m/z* found $[M+H]^+$ 371.2000, $C_{21}H_{26}N_2O_4$ requires *M* 371.1971.

(18x) *Tert butyl 6-chloro-5-[4'-(trifluoromethyl)phenyl]pyridine-3-carboxylate*

Following General procedure A and purification using C18 reverse phase chromatography (H_2O: MeCN, 0-100%) yielded the title compound as a white solid (177 mg, 32%). mp 105-106 ºC. δ_H (700 MHz, $CDCl_3$) 8.95 (1H, d, *J* = 2.3 Hz, 6-H), 8.18 (1H, d, *J* = 2.3 Hz, 3-H), 7.78 – 7.71 (2H, m, 2',6'-H), 7.61 – 7.56 (2H, m, 3'-5'-H), 1.61 (9H, s, C(CH_3)$_3$). δ_C (176 MHz, $CDCl_3$) 163.2 (C=O), 152.9 (C-2), 150.0 (C-6), 140.24 (C-1'), 140.1 (C-4), 135.2 (C-3), 130.8 (q, *J* = 32.7 Hz, C-4') 129.7 (C-2'', 6''), 127.1 (C-5), 125.4 (q, *J* = 3.7 Hz, C-3'', 5'') 123.8 (q, *J* = 272.6 Hz, -CF_3) 82.9 (*C*(CH_3)$_3$), 28.1 (C(*C*H_3)$_3$). δF (376 MHz, $CDCl_3$) -62.70 (-CF_3). ν_{max} (ATR) 2983, 2930, 1723, 1623,1598, 1392, 1320, 1261, 1112 cm^{-1}. *m/z* (LC-MS, ES^+) 358.1 ($[M(^{35}Cl)+H]^+$, 42%), 360.1 ($[M(^{37}Cl)+H]^+$, 15%), 302.0 ($[M(^{35}Cl)$-tBu+$H]^+$, 100%), 304.0 ($[M(^{37}Cl)$-tBu+$H]^+$, 38%) Accurate mass (ES^+) *m/z* found $[M(^{35}Cl)+H]^+$ 358.0828, $C_{17}H_{16}{}^{35}ClNO_2F_3$ requires *M* 358.0822.

(21xB) *Tert butyl 6-(morpholin-4''-yl)-5-[4'-(trifluoromethyl)phenyl]pyridine-3-carboxylate*

Following general procedure D and purification using EtOAC in hexane (0-20%) yielded the title compound as an off white amorphous solid (41 mg, 82%) δ_H (599 MHz, $CDCl_3$) 8.80 (1H, d, *J* = 2.2 Hz, 6-H), 7.95 (1H, d, *J* = 2.2 Hz, 4-H), 7.67 (4H, m, Ar-H), 3.60 (4H, t, *J* = 4.7 Hz, 3'', 5''-H_2), 3.20 (4H, t, *J* = 4.7 Hz, 2'', 6''-H_2), 1.56 (9H, s, C(CH_3)$_3$). δ_C (151 MHz, $CDCl_3$) 164.6 (C=O), 160.8 (C-2), 149.1 (C-6), 143.26 (C-1'), 140.8 (C-4), 129.9 (q, *J* = 33.1 Hz C-4')), 127.9 (C-2', 6'), 125.9 (q, *J* = 3.7 Hz, C-3', 5'), 123.9 (q, *J* = 278.0 Hz, -CF_3) 120.47 (C-5), 81.3 (-C(CH_3)$_3$, 66.4 (C-3'', 5''), 49.1 (C-2'', 6''), 28.2 (C(CH_3)$_3$). δ_F (376 MHz, $CDCl_3$) -62.55 (-CF_3). ν_{max} (ATR) 2950, 2829, 1729, 1678, 1610, 1497, 1343, 1265, 1184 cm^{-1}. *m/z* (LC-MS, ES^+) 409.1 ($[M+H]^+$, 100%), 353.1 ($[M-tBu+H]^+$, 52%), Accurate mass (ES^+) *m/z* found $[M+H]^+$ 409.1750, $C_{21}H_{24}F_3N_2O_3$ requires *M* 409.1739.

(22zA) *Methyl 5-(4'-nitrophenyl)-2-(pyrrolidin-1''-yl)pyridine-3-carboxylate*

Following general procedure A gave the crude aryl-nicotinate intermediate which was used without further purification according to general procedure C to yield, upon purification using EtOAc in hexane (0-25%) the title compound as a dark yellow amorphous solid (62 mg, 32%), δ_H (700 MHz, $CDCl_3$) 8.58 (1H, d, *J* = 2.5 Hz, 6-H), 8.27 (2H, d, *J* = 8.8 Hz, 3', 5'-H), 8.17 (1H, d, *J* = 2.5 Hz, 3-H), 7.67 (2H, d, *J* = 8.8 Hz, 2', 6'-H), 3.93 (3H, s, CO_2CH_3), 3.51 (4H, d, *J* = 6.6 Hz, 2'', 5''-H_2), 1.99 (4H, d, *J* = 6.6 Hz, 3'', 4''-H_2). δ_C (176 MHz, $CDCl_3$) 167.2 (C=O), 155.42 (C-2), 152.92 (C-3), 146.6 (C-4'), 130.41 (C-6), 129.00, 126.2, (C-2'', C-6''), 124.4 (C-3', 5'), 121.5 (C-5), 117.48 (C-1'), 52.49 (CO_2CH_3), 50.30 (C-2'', 5''), 25.58 (C-3'', 4''). ν_{max} (ATR) 2925, 2291, 1970, 1757, 1669, 1561, 1533, 1371, 1280, 1168 cm^{-1}. *m/z* (LC-MS, ES^+) 328.1 ($[M+H]^+$, 100%), Accurate mass (ES^+) *m/z* found $[M+H]^+$ 328.1291, $C_{17}H_{18}N_3O_4$ requires *M* 328.1297.

(19y) *Methyl 2-chloro-5-(4'-methoxyphenyl)pyridine-3-carboxylate*

Following general procedure A and purification using EtOAc in hexane (0-25%) yielded the title compound as a white amorphous solid. Purification using (0-35% EtOAc-hexane,) afforded the title compounds as an amorphous white solid (55 mg, 20%) δ_H (700 MHz, $CDCl_3$) 8.71-8.64 (1H, m, 6-H), 8.30 (1H, d, *J* = 2.5, 4-H), 7.54-7.50 (2H, m, 2-H), 7.04-6.98 (2H, m, 3',5'-H), 3.98 (3H, s, CO_2CH_3), 3.86 (3H, s, 4'-OCH_3); δ_C (176 MHz, $CDCl_3$) 165.1 (C=O), 160.3 (C-2), 149.5 (C-6), 147.8 (C-5), 137.9 (C-4), 135.2 (C-1), 128.2 (C-2'), 127.7 (C-1'), 126.4 (C-3), 114.8 (C-3'), 55.4 (5'-OCH_3), 52.9 (CO_2CH_3); ν_{max} (ATR) 3019, 2961, 2933, 2839, 1737 (s) (C=O), 1608, 1582, 1552, 1515, 1324, 1310, 1293, 1226, 1184, 1064, 1054, 1033, cm^{-1}. *m/z* (LC-MS, ES^+) $[M+H]^+$ 279.8 (100), Accurate mass (ES^+) *m/z* found $[M+H]^+$ 278.0583, $C_{14}H_{13}NO_3Cl$ requires *M* 278.0584.

(22yB) *Methyl 5-(4''-methoxyphenyl)-2-(morpholin-4'-yl)pyridine-3-carboxylate*

Following general method C and purification using EtOAc in heptane (20-30%) yielded the title product as a white amorphous solid (141 mg, 93%). δ_H (700 MHz, $CDCl_3$) 8.51 (1H, s, 6-*H*), 8.20 (1H, s, 4-*H*), 7.47 (2H, d, *J* = 8.0, 2'',6''-*H*), 6.98 (2H, d, *J* = 8.0, 3'', 5''-*H*), 3.91 (3H, s, CO_2CH_3), 3.85 (7H, m, OCH_3, 3', 5'-H_2), 3.44 (4H, m, 2', 6'-H_2); δ_C (176 MHz, $CDCl_3$) 167.5 (CO_2CH_3), 159.3 (*C*-4''), 158.2 (*C*-2), 148.4 (*C*-6), 138.8 (*C*-4), 129.5 (*C*-1''), 127.6 (*C*-5), 127.4 (*C*-2'', 6''), 114.5 (*C*-3'', 5''), 113.6 (*C*-3), 66.9 (*C*-3', 5'), 55.4 (OCH_3), 52.2 (CO_2CH_3), 49.9 (*C*-2'', 6''); ν_{max} (ATR) 1717, 1601, 1472, 1440, 1246, 1212, 1182, 1114, 1087 cm^{-1}; Accurate Mass (ESI) *m/z* found $[M+H]^+$ 329.1510; $C_{18}H_{21}N_2O_4$ requires *M*, 329.1501.

(22yC) *Methyl 5-(4''-methoxyphenyl)-2-(piperidin-1'-yl)pyridine-3-carboxylate*

Following general procedure C and purification using EtOAc in heptane yielded the title compound as a yellow amorphous solid (57 mg, 89%). δ_H (700 MHz, $CDCl_3$) 8.47 (1H, d, *J* = 2.4, 6-*H*), 8.11 (1H, d, *J* = 2.4, 4-*H*), 7.45 (2H, d, *J* = 8.6, 2'', 6''-*H*), 6.97 (2H, d, *J* = 8.6, 3'', 5''-*H*), 3.91 (3H, s, CO_2CH_3), 3.84 (3H, s, OCH_3), 3.39 (4H, m, 2', 6'-H_2), 1.68 (6H, m, 3', 4', 5'-H_2); δ_C (176 MHz, $CDCl_3$) 168.4 (CO_2CH_3), 159.2 (*C*-4''), 158.6 (*C*-2), 148.3 (*C*-6), 138.7 (*C*-4), 130.0 (*C*-1''), 127.5 (*C*-2'', 6''), 126.4 (*C*-5) 114.6 (*C*-3'', 5''), 113.4 (*C*-3), 55.5 (OCH_3), 52.3 (CO_2CH_3), 50.7 (*C*-2', 6'), 26.1 (Alk*C*), 24.7 (Alk*C*); υ_{max} (ATR) 1716, 1694, 1608, 1441, 1247, 1180 cm^{-1}; Accurate Mass (ESI) *m/z* found $[M+H]^+$ 327.1701; $C_{19}H_{23}N_2O_3$ requires *M*, 327.1709.

(22yE) *Methyl 2-(butylamino)-5-(4'-methoxyphenyl)pyridine-3-carboxylate*

Following general procedure C and purification using EtOAC in hexane (0-20%) yielded the title compound as a yellow amorphous solid (38 mg, 60%). δ_H (700 MHz, $CDCl_3$) 8.50 (1H, d, *J* = 2.5 Hz, 6-H), 8.32 (1H, d, *J* = 2.5 Hz, 4-H), 7.42 (2H, d, *J* = 8.7 Hz, 2', 6'-H), 6.96 (2H, d, *J* = 8.7 Hz, 3', 5'-H), 3.89 (3H, s, CO_2CH_3), 3.83 (3H, s, 4'-OCH_3), 3.60-3.52 (2H, m, 1''-H_2), 1.71 – 1.63 (2H, m, 2''-H_2), 1.52 – 1.42 (2H, m, 3''-H_2), 0.97 (3H, t, *J* = 7.4 Hz, 4''-H_3). δ_C NMR (176 MHz, $CDCl_3$) 162.6 (C=O), 159.0 (C-4'), 152.9 (C-2), 146.4 (C-6), 138.6 (C-4), 131.0 (C-1'), 127.1 (C-2', 6'), 123.9 (C-5), 117.8 (C-4), 114.4 (C-3', 5'), 67.1 (C-1''), 55.4 (-OCH_3), 52.0 (CO_2CH_3), 31.6 (C-2''), 20.3 (C-3''), 13.9 (C-4''). υ_{max} (ATR) 3381, 2960, 2259, 1693, 1611, 1504, 1243, 1036 cm^{-1}. *m/z* (LC-MS, ES^+) 313.3 ($[M-H]^-$, 100%), Accurate mass (ES^+) *m/z* found $[M+H]^+$ 315.1705, $C_{18}H_{23}N_2O_3$ requires *M* 315.1709.

(19'y) *Methyl 2-fluoro-5-(4-methoxyphenyl)pyridine-3-carboxylate*

Following general procedure A, and purification using EtOAc in heptane (0-20%) yielded the title product as an off-white amorphous solid (715 mg, 62%). δ_H (700 MHz, $CDCl_3$) 8.51 (2H, m, 4, 6-*H*), 7.50 (2H, m, 2', 6'-*H*), 7.01 (2H, m, 3', 5'-*H*), 3.98 (3H, s, CO_2CH_3), 3.86 (OCH_3); δ_C (176 MHz, $CDCl_3$) 164.0 (d, *J* = 8.1, CO_2CH_3), 160.5 (d, *J* = 249.8, *C*-2), 160.3 (*C*-4'), 149.1 (d, *J* = 15.4, Ar*C*), 141.7 (d, *J* = 1.6, Ar*C*), 135.0 (*C*-5), 128.3 (*C*-2', 6'), 128.0 (*C*-1'), 114.9 (*C*-3, 5'), 113.4 (d, *J* = 25.6, *C*-3), 55.6 (OCH_3), 53.0 (CO_2CH_3); δ_F (376 MHz, $CDCl_3$) −66.3 (s); ν_{max} (ATR) 1722, 1603, 1459, 1446, 1327, 1292, 1249, 1179, 1089, 1042, 977 cm^{-1}; Accurate Mass (ASAP) *m/z* found $[M]^+$ 261.0824; $C_{14}H_{12}FNO_3$ requires *M*, 261.0801

(19''y) *Methyl 2-methoxy-5-(4-methoxyphenyl)pyridine-3-carboxylate*

Following general procedure A and purification using EtOAc in heptane (0-15%) yielded the title compound as a white amorphous solid (229 mg, 76%). δ_H (700 MHz, $CDCl_3$) 8.49 (1H, d, *J* = 2.2, 6-*H*), 8.34 (1H, d, *J* = 2.2, 4-*H*), 7.48 (2H, m, 2', 6'-*H*), 7.00 (2H, m, 3', 5'-*H*), 4.10 (3H, s, 2-OCH_3), 3.93 (3H, s, CO_2CH_3), 3.86 (3H, s, 4'-OCH_3); δ_C (176 MHz, $CDCl_3$) 165.7 (CO_2CH_3), 161.4 (*C*-2), 159.7 (*C*-4'), 148.2 (*C*-6), 139.7 (*C*-4), 129.8 (*C*-5), 129.3 (*C*-1'), 128.0 (*C*-2', 6'), 114.7 (*C*-3', 5'), 113.9 (*C*-3), 55.5 (4'-$COCH_3$), 54.6 (2-$COCH_3$), 52.5 (CO_2CH_3); ν_{max} (ATR) 1732, 1606, 1563, 1519, 1474, 1417, 1327, 1285, 1245, 1181, 1087, 1060, 1014 cm^{-1}. Accurate Mass (ASAP) *m/z* found $[M+H]^+$ 274.1075; $C_{15}H_{16}NO_4$ requires *M*, 274.1079.

(19x) *Methyl 2-chloro-5-[4'-(trifluoromethyl)phenyl]pyridine-3-carboxylate*

Following general procedure A and purification using EtOAc in hexane (0-15%) to yield the title compound as a white amorphous solid (64 mg, 24%); δ_H (700 MHz, $CDCl_3$) 8.74 (1H, m, 6-H), 8.,37 (1H, d, *J* = 2.1, 4-H), 7.77 (2H, d, *J* = 8.1, C-2', 6'), 7.70 (2H, d, *J* = 8.1, C-3', 5'), 4.00 (3H, s, CO_2CH_3). δ_C (176 MHz, $CDCl_3$) δ 164.9 (C=O), 149.9 (C-2), 149.8 (C-6), 139.1 (C-5), 138.9 (C-4), 134.2 (C-1'), 131.2 (q, *J*=33.2 Hz, C-4'), 127.7 (C-2', 6'), 126.5 (q, *J*=3.8 Hz, C-3', 5')), 124.0 (q, *J*=272.0 Hz, -CF_3), 121.5 (C-3), 53.2 (CO_2CH_3), δ_F (376 MHz, $CDCl_3$) δ -62.83 (-CF_3); ν_{max} (ATR) 2174, 1982, 1730 (C=O), 1555, 1520, 1414, 1224, 1111, 1052, 1033, 962, cm^{-1}; *m/z* (LCMS-ESI) 318 ($[M(^{37}Cl)]^+$, 31 %), 316 ($[M(^{35}Cl)+H]^+$), 100), Accurate Mass (ESI-TOF) *m/z* Found $[M+H]^+$ 316.0345, $C_{14}H_{20}NO_2F_3{}^{35}CI$ requires *M* 316.0352.

(22xA) *Methyl 2-(pyrrolidin-1''-yl)-5-[4'-trifluoromethylphenyl]pyridine-3-carboxylate*

Following general procedure C and purification using EtOAc in hexane (0-20%) yielded the title compound as an amorphous white solid (23 mg, 50%). δ_H (700 MHz, $CDCl_3$) 8.53 (1H, bs, 6-H), 8.11 (1H, d, *J* = 2.2, 4-H), 7.69-7.61 (4H, m, Ar), 3.92 (3H, s, CO_2CH_3), 3.47-3.45 (4H, m, 2'', 5''-H_2), 1.97-

1.94 (4H, m, 3",4"-*H*$_2$); δ_C (176 MHz, $CDCl_3$) 167.7 (C=O), 155.3, 148.7, 141.1, 138.0 128.7, 126.6, 126.1, 124.4, 122.7, 110.8, 52.4, 49.9, 25.8; δ_F (564 MHz, $CDCl_3$) -62.42; ν_{max} (ATR) 2979, 2954, 2876, 1710 (C=O) , 1599, 1546, 1488, 1479, 1321, 1244, 1211, 1160, 1137, 1116, 1100,cm^{-1}; *m/z* (LCMS-ESI) 350 ($[M]^+$, 86 %), 351 ($[M+H]^+$, 100%), Accurate Mass (ESI-TOF) *m/z* Found $[M+H]^+$ 351.1300, $C_{18}H_{19}N_2O_2F_3$ requires *M* 351.1320.

(22xB) *Methyl 2-(morpholin-4"-yl)-5-[4'-(trifluoromethyl)phenyl]pyridine-3-carboxylate*

Following general procedure C and purification using EtOAc in DCM (0-20%) yielded the title compound as a white amorphous solid (16 mg, 43%) ; δ_H, (700 MHz, $CDCl_3$) 8.56-8.54 (1H, m, 6-H), 8.25 (1H, d, J 2.5 Hz, 4-H), 7.71-7.63 (4H, m, Ar), 3.93 (3H, s, CO_2CH_3), 3.85-3.81 (4H, m, 3", 5"-H_2), 3.52-3.49 (4H, m, 2", 6"-H_2); δ_C (176 MHz, $CDCl_3$) 167.3 (C=O), 158.6 (C-2), 148.7 (C-6), 140.6 (C-1'), 139.5 (C-4) 129.4 (q, *J* = 32.4 Hz, C-4'), 126.4 (C-2',6'), 126.0 (q, *J* = 33.1 Hz, C-3', 5'), 124.1 (q, *J* = 272.2 Hz, CF_3), 123.1 (C-5) 113.1 (C-3), 66.8 (C-3", 5"), 52.4 (CO_2CH_3), 49.6 (C-2", 6"); δ_F (376 MHz, $CDCl_3$) -62.47 (CF_3); ν_{max} 2957, 2925, 2847, 1707 (C=O), 1599, 1537, 1526, 1478, 1452, 1441, 1422, 1324, 1252, 1213, 1162, 1109, 1098, 1073, 1052, 1043, 1016 cm^{-1}, *m/z* (LCMS-ESI) 367 ($[M+H]^+$, 100%). Accurate Mass (ESI-TOF) *m/z* Found $[M+H]^+$ 367.1265, $C_{18}H_{18}N_2O_3F_3$ requires *M* 367.1270

(22xC) *Methyl 2-(piperidin-1"-yl)-5-[4'-(trifluoromethyl)phenyl]pyridine-3-carboxylate*

Following general procedure C and purification using EtOAc in DCM (0-20%) yielded the title compound as a white amorphous solid; (5 mg, 13%); δ_H (700 MHz, $CDCl_3$) 8.52 (1H, d, *J* = 2.5, 6-H), 8.17 (1H, d, *J* = 2.5, 4-H), 7.70-7.61 (4H, m, Ar), 3.91 (3H, s, CO_2CH_3), 3.45 (4H, bs, 2", 6"-H_2), 1.69 (6H, bs, 3",4" ,5"-H_2); δ_C (176 MHz, $CDCl_3$) 168.0, 157.3, 148.6, 141.0, 139.3, 129.4, 126.4, 126.0, 125.2, 123.6, 112.9, 52.4, 50.4, 26.0, 24.7; δ_F (376 MHz, $CDCl_3$) -62.42 (-CF_3); ν_{max} 2952, 2876, 2360, 1711 (C=O), 1599, 1541, 1489, 1480, 1461, 1448, 1434, 1322, 1244, 1211, 1160, 1138, 1102, 1086, 1071, 1052, 1014 cm^{-1}; *m/z* (LCMS-ESI) 364 ($[M]^+$, 60%), 365 ($[M+H]^+$, 100%), Accurate Mass (ESI-TOF) *m/z* Found $[M+H]^+$ 365.1464, $C_{19}H_{21}N_2O_2F_3$ requires *M* 365.1477.

(19v) *Methyl 2-chloro-5-(thiophen-3'-yl)pyridine-3-carboxylate*

Following general procedure A and purification using EtOAc in hexane (0-35%) yielded the title compound as an off white amorphous solid (55 mg, 19%). δ_H (400 MHz, $CDCl_3$) 8.72 (1H, m, 6-H), 8.32 (1H, d, J = 2.4, 4-H), 7.58 (1H, dd, *J* = 3.0, 1.4, 4'-H), 7.47 (1H, dd, *J* = 5.0, 3.0, 3'-H), 7.38 (1H, dd, *J* = 5.0, 1.4, 2'-H), 3.98 (3H, s, CO_2CH_3); δ_C (101 MHz, $CDCl_3$) 168.0 (C=O), 159.6, 157.3, 150.1, 143.2, 140.8, 136.5, 127.8, 125.7, 123.1, 53.0 (CO_2CH_3). ν_{max} (ATR) 3091, 2960, 2360, 1738, 1722 (C=O), 1596 , 1562, 1525, 1432, 1418, 1404, 1327, 1296, 1242, 1194, 1134, 1101, 1064, 918, 776 cm^{-1}.

m/z (GC-MS, ES^+) 222 ($[M\text{-}OMe]^+$), 253 ($[M]^+$); Accurate Mass (ESI-TOF) *m/z* Found $[M+H]^+$ 254.0048, $C_{11}H_9NO_2S^{35}CI$ requires *M* 254.0043.

(19s) *Methyl 2-chloro-5-phenylpyridine-3-carboxylate*

Following general procedure A and purification using EtOAc in hexane (0-35%) yielded the title compound as an off white amorphous solid (27 mg, 38%); δ_H, (700 MHz, $CDCl_3$) 8.71 (1H, d, *J* = 2.6, 6-H), 8.35 (d, *J* = 2.6, 1H, 4-H), 7.58 (2H, m, 2',6'-H), 7.50 (2H, m, 3',4'-H), 7.45 (1H, t, *J* = 7.4, 4'-H), 3.99 (3H, s, CO_2CH_3); δc (176 MHz, $CDCl_3$) 165.0 ($3\text{-}CO_2CH_3$, 149.9 (C-6), 138.5 (C-4), 135.6, 135.4, 129.3, 129.3 (C- 3'), 128.9 (C-4), 127.0 (C-2'), 126.5, 52.9 ($3\text{-}CO_2CH_3$); ν_{max} (ATR) 2359, 2184, 1731 (C=O), 1425, 1317, 1255, 1129, 1064 cm^{-1}. *m/z* (LCMS-ESI) 247 ($[M]^+$, 67%), 248 ($[M+H]^+$, 100).

(19r) Methyl 2-chloro-5-[4'-(methoxycarbonyl)phenyl]pyridine-3-carboxylate

Following general procedure A and purification using EtOAc in hexane (0-35%) yielded the title compound as a white amorphous solid (57 mg, 65 %); δ_H (700 MHz, $CDCl_3$) 8.76 (1H, bs, 6-H), 8.39 (1H, d, *J* = 2.4, 4-H), 8.17 (2H, d, *J* = 8.3, Ar-H), 7.66 (2H, d, J = 8.3, Ar -H), 4.00 (3H, s, $4'\text{-}CO_2CH_3$), 3.96 (3H, s, $3\text{-}CO_2CH_3$); δc (176 MHz, $CDCl_3$) 166.4 ($4'\text{-}CO_2CH_3$), 164.8 ($3\text{-}CO_2CH_3$) 149.9 (C-6), 149.5 (C-2), 139.7 (C-4), 138.7 (C-3), 130.5 (C-3',5'), 130.5 (C-4'), 127.0 (C-5), 123.3 (C-2', 6'), 121.8 (C-1'), 53.0 ($3\text{-}CO_2CH_3$), 52.3 ($4'\text{-}CO_2CH_3$); ν_{max} (ATR) 2364, 1711 (C=O), 1427 , 1275, 1108, 1060, 767, 421 cm^{-1}. *m/z* (LCMS-ESI); 306 ($[M+H]^+$ 100 %), 307 ($[M+2]^+$, 32%), 328 ($[M+Na]^+$, 9%); Accurate Mass (ESI-TOF) *m/z* Found $[M+H]^+$ 306.0540, $C_{15}H_{13}ClNO_4$ requires *M* 306.0533.

(22rA) *Methyl 5-[4'-(methoxycarbonyl)phenyl]-2-(pyrrolidin-1''-yl)pyridine-3-carboxylate*

Following general procedure C and purification using EtOAC in hexane (0-20%) yielded the title compound as an off white amorphous solid (19 mg, 81%). δ_H (700 MHz, $CDCl_3$) 8.56 (1H, d, *J* = 2.5 Hz, 6-H), 8.15 (1H, d, *J* = 2.5 Hz, 4-H), 8.07 (1H d, *J* = 8.4 Hz, 2', 6'-H), 7.59 (2H, d, *J* = 8.4 Hz, 3', 5'-H), 3.89-3.94 (6H, m, CO_2Me), 3.48 (4H, t, *J* = 7.0, 2'', 5''-H_2), 1.97 (4H, t, *J* = 7.0, 3'', 4''-H_2); δ_C (176 MHz, $CDCl_3$) 168.9 (4'-C=O), 166.9 (3-C=O), 144.1, 142.0, 138.3, 138.2, 134.0, 130.3, 128.4, 125.6, 122.8, 52.3, 52.1, 49.9, 25.6. ν_{max} (ATR) 3025, 2957, 1719, 1591, 1536, 1477, 1462, 1438, 1326, 1273, 1089 cm^{-1}. *m/z* (LCMS-ESI); 341.2 ($[M+H]^+$ 100 %), Accurate mass (ES^+) *m/z* found $[M+H]^+$ 341.1509, $C_{19}H_{21}N_2O_4$ requires *M* 341.1501.

(23) *1,4-dimethyl-7-phenyl-1H,2H,3H,4H,5H-pyrido[2,3-e][1,4]diazepin-5-one*

Following general procedure C and purification with EtOAc in DCM (0-10%), yielded the title compound as a white amorphous solid (10 mg, 60 %); δ_H (700 MHz, $CDCl_3$) 8.56 (1H, m, 6-H)), 8.29 (1H, d, *J* = 2.8, 8-H), 7.56 (2H, dd, *J* = 8.2, 1.4, 2'-H, 6'-H), 7.43 (2H, td, *J* = 7.5, 8.2, 3', 5'-H), 7.33 (1H, td, *J* = 7.5, 1.4 Hz , m , 4'-H), 3.67-3.58 (4H, m, 2-H_2, 3-H_2), 3.22 (3H, s, 4''-H), 3.13 (3H, s, 1''-H); δ_C (176 MHz, $CDCl_3$) 169.3, 153.9, 149.5, 146.0, 139.5, 130.6, 129.3, 127.8, 127.7, 127.6, 126.7, 118.8, 52.6, 48.4, 39.4, 36.0. ν_{max} 2925, 1716, 1632 (C=O) , 1599 , 1513, 1450, 1412, 1379, 1312, 1260, 1054, 1028 cm^{-1}. *m/z* (LC-MS, ES^+) 268 ($[M+H]^+$, 100), Accurate Mass (ESI-TOF) *m/z* found $[M+H]^+$ 268.1456, $C_{16}H_{13}N_3O$ requires [M+H] 268.1450.

(24) *Methyl 2-(pyrrolidin-1'-yl)pyridine-3-carboxylate*

Following general procedure C and purification by 3 successive washes of the organic layer with water, the title compound was isolated as an orange oil (492 mg, 80%); δ_H (700 MHz, $CDCl_3$) 8.21-8.17 (1H, m, 6-H), 7.80 (1H, m, 5-H), 6.53 (1H, m, 4H), 3.82 (3H, s, CO_2CH_3), 3.35 (4H, t, *J* = 6.3, 2',5'-H_2), 1.87 (4H, m, 3',4'-H_2). δ_C (176 MHz, $CDCl_3$) 167.9 (*C*=O), 155.8 (C-2), 150.4 (C-6), 139.5 (C-5), 110.9 (C-4), 110.7 (C-3), 52.0 (OCH_3), 49.5 (C-2',5'), 25.6 (C-3', 4'); ν_{max} 2948, 2872, 1709 (C=0), 1585, 1549, 1470, 1444, 1284, 1247, 1220, 1114, 1083, 1053, 764, 746 cm^{-1}; *m/z* (LCMS-ESI) 175 ($[M-OMe]^+$, 75%), 206, ($[M]^+$, 65%), 208 ($[M+2H]^+$, 100%), 209 ($[M+3H]^+$, 20%) Accurate Mass (ESI-TOF) *m/z* found $[M+H]^+$ 207.1124, $C_{11}H_{15}N_2O_2$ requires *M*, 207.1134

(25) *Methyl 2-(4'-methoxyphenyl)pyridine-4-carboxylate*

Following general procedure A, the crude cross-coupling reaction product used without further purification and was dissolved in ethanol (20 mL) to which ammonium formate (2.5 g, 40 mmol) was added. The reaction vessel was evacuated and backfilled with nitrogen (3 cycles) before 10% Pd/C (106 mg, 0.1 mmol) was slowly added under a positive pressure of nitrogen. The reaction was stirred at room temperature for 2 h then filtered through a plug of Celite and absorbed onto silica. Purification using EtOAc in hexane (0-20%) yielded the title compound as a white amorphous solid (230 mg, 47%). δ_H (700 MHz, $CDCl_3$) 8.77 (1H, d, *J* = 5.0 6-*H*), 8.22 (1H, s, 3-*H*), 8.01 (2H, m, 2', 6'-*H*), 7.69 (1H, d, *J* = 5.0, 5-*H*), 7.00 (2H, m, 3', 5'-*H*), 3.97 (3H, s, CO_2CH_3), 3.86 (3H, s, OCH_3); δ_c (176 MHz, $CDCl_3$) 166.0 (CO_2CH_3), 161.0 (*C*-4'), 158.2 (*C*-2), 150.4 (*C*-6), 138.1 (*C*-4), 131.2 (*C*-1'), 128.4 (*C*-2', 6'), 120.4 (*C*-5), 119.0 (*C*-3), 114.3 (*C*-3', 5'), 55.5 (OCH_3), 52.8 (CO_2CH_3); ν_{max} (ATR) 1730, 1607, 1580, 1557, 1516, 1467, 1436, 1421, 1390, 1301, 1274, 1249, 1176, 1111, 1060, 1031 cm^{-1}; Accurate Mass (ASAP) *m/z* found $[M+H]^+$ 244.0957; $C_{14}H_{14}NO_3$ requires *M*, 244.0974.

(26) *methyl 2-(4'-nitrophenyl)-6-phenylpyridine-4-carboxylate*

Methyl 2-chloro-6-(4-nitrophenyl)pyridine-4-carboxylate (**2cz**) (130 mg, 0.45mmol, 1equiv.) was combined with phenyl boronic acid (1.2 equiv)) and $CsCO_3$ (1.5 equiv) and was subjected to 3 N_2 purge/refill cycles. DMAC (0.5M) was added and the vial was subjected to microwave irradiation for 18 hours at 100 °C. Purification using C18 reverse phase chromatography yielded the title compound as a yellow oil (36 mg, 24%). δ_H (700 MHz, $CDCl_3$) 8.40 – 8.35 (4H, m), 8.33 (1H, d, *J* = 1.2 Hz), 8.31(1H, d, *J* = 1.2 Hz), 8.21 – 8.18 (2H, m), 7.54 (2H dd, *J* = 8.2, 6.7 Hz), 7.49 (1H, d, *J* = 6.7 Hz,), 4.04 (3H, s, OC*H*$_3$). δ_c (176 MHz, $CDCl_3$) 165.5, 158.5, 155.3, 148.4, 144.4, 139.6, 138.0, 129.9, 128.9, 127.9, 127.1, 124.0, 119.3, 118.5, 53.0. ν_{max} (ATR) 2970, 2801, 2299, 1731, 1662, 1572, 1496, 1331, 1271, 1146 cm^{-1}. *m/z* (LCMS-ESI) 335.1 ($[M+H]^+$, 100%), Accurate Mass (ES^+) *m/z* found $[M+H]^+$ 335.1046, $C_{19}H_{15}N_2O_4$ requires *M*, 335.1032.

(27) *Ethyl 2-{[2-(4'-methoxyphenyl)-6-(pyrrolidin-1''-yl)pyridin-4-yl]formamido}propanoate*

Tert butyl 2-(4-methoxyphenyl)-6-(pyrrolidin-1-yl)pyridine-4-carboxylate (**3dyA**) (38 mg, 0.1mmol, 1equiv.) was treated with TFA for 1 hour when the reaction was concentrated in a stream of nitrogen. The crude residue was combined with HBTU (1.1equiv.), DMAP (1.1equiv.) and DCM (0.1M). The mixture was allowed to stir for 16 hours and quenched with water and extracted with DCM. Purification by column chromatography using EtOAc in Hexane (0-70%) afforded the title compound as a light yellow oil (31 mg, 67% (over 2 steps)). δ_H (700 MHz, $CDCl_3$) 8.01 (2H, d, *J* = 8.8 Hz, 2', 6'-H), 7.16-7.20 (1H, m, 3-H), 6.95 (2H, d, *J* = 8.8 Hz, 3', 5'-H), 6.60-6.68 (1H, m, 5-H), 4.76 (1H, q, *J* = 7.2 Hz), 4.25 (2H, q, *J* = 7.1 Hz, OC*H*$_2$), 3.84 (3H, s, OC*H*$_3$), 3.56-3.60 (4H, m, 2'', 5''-H), 1.99-2.03 (4H, m, 3'', 4''-*H*$_2$), 1.54 (3H, d, *J* = 7.2 Hz, C□CH$_3$), 1.31 (t, *J* = 7.1 Hz, CH_2CH_3). δ_C (176 MHz, $CDCl_3$) 173.0 (NH*C*=O), 166.5 (O*C*=O), 165.9 (C-4'), 160.5 (C-2), 143.4 (C-6), 131.0 (C-3), 128.4 (C-2', 6'), 128.3 (C-5), 127.8 (C-4), 125.8 (C-1'), 113.8 (C-3', 5'), 61.7 (-OCH_2), 55.3 (O*C*H$_3$), 48.6 (C□) 48.2 (C-2'', 5''), 25.5 (C-3'', 4''), 18.2 (C□*C*H$_3$), 14.1 (CH_2CH_3). ν_{max} (ATR) 3227, 2975, 2259, 1738, 1655, 1604, 1518, 1456, 1349, 1026 cm^{-1}. *m/z* (LCMS-ESI) 398.7 ($[M+H]^+$, 100%), Accurate Mass (ES^+) *m/z* found $[M+H]^+$ 398.2079, $C_{22}H_{28}N_3O_4$ requires *M*, 398.2080

Acknowledgments

We thank the Higher Committee for Education Development in Iraq and Astra Zeneca and the EPSRC for studentships to OAS and SAS, respectively.

References and Notes,

1. Keller, P. A. In *Comprehensive Heterocyclic Chemistry III;* Katritzky, A. R.; Ramsden, C. A.; Scriven, E. F. V.; Taylor, R. J. K. Eds.; Elsevier: Oxford, 2008; pp. 215.

2. Guan, A. Y.; Liu, C. L.; Sun, X. F.; Xie, Y.; Wang, M. A. *Bioorg. Med. Chem.* **2016,** *24*, 342.
3. Williams, J. A. G. *Chem. Soc. Rev.* **2009,** *38*, 1783.
4. O'Hagan, D. *Nat. Prod. Rep.* **2000,** *17*, 435.
5. Henry, G. D. *Tetrahedron* **2004,** *60*, 6043.
6. Schlosser, M.; Mongin, F. *Chem. Soc. Rev.* **2007,** *36*, 1161.
7. Bagley, M. C.; Glover, C.; Merritt, E. A. *Synlett* **2007**, 2459.
8. Hill, M. D. *Chem. Eur. J.* **2010,** *16*, 12052.
9. Allais, C.; Grassot, J. M.; Rodriguez, J.; Constantieux, T. *Chem. Rev.* **2014,** *114*, 10829.
10. Karadeniz, E.; Zora, M.; Kilicaslan, N. Z. *Tetrahedron* **2015,** *71*, 8943.
11. Stephens, D. E.; Larionov, O. V. *Tetrahedron* **2015,** *71*, 8683.
12. Balkenhohl, M.; Knochel, P. *Synopen* **2018,** *2*, 78.
13. Gros, P. C.; Fort, Y. *Eur. J. Org. Chem.* **2009**, 4199.
14. Fujiwara, Y.; Dixon, J. A.; O'Hara, F.; Funder, E. D.; Dixon, D. D.; Rodriguez, R. A.; Baxter, R. D.; Herle, B.; Sach, N.; Collins, M. R.; Ishihara, Y.; Baran, P. S. *Nature* **2012,** *492*, 95.
15. Minisci, F.; Vismara, E.; Fontana, F. *Heterocycles* **1989,** *28*, 489.
16. Murakami, K.; Yamada, S.; Kaneda, T.; Itami, K. *Chem. Rev.* **2017,** *117*, 9302.
17. Mkhalid, I. A. I.; Barnard, J. H.; Marder, T. B.; Murphy, J. M.; Hartwig, J. F. *Chem. Rev.* **2010,** *110*, 890.
18. Ishiyama, T.; Nobuta, Y.; Hartwig, J. F.; Miyaura, N. *Chem. Commun.* **2003**, 2924.
19. Takagi, J.; Sato, K.; Hartwig, J. F.; Ishiyama, T.; Miyaura, N. *Tetrahedron Lett.* **2002,** *43*, 5649.
20. Chotana, G. A.; Rak, M. A.; Smith, M. R., III. *J. Am. Chem. Soc.* **2005,** *127*, 10539.
21. Mkhalid, I. A. I.; Coventry, D. N.; Albesa-Jove, D.; Batsanov, A. S.; Howard, J. A. K.; Perutz, R. N.; Marder, T. B. *Angew. Chem. Int. Ed.* **2006,** *45*, 489.
22. Murphy, J. M.; Liao, X.; Hartwig, J. F. *J. Am. Chem. Soc.* **2007,** *129*, 15434.
23. Larsen, M. A.; Hartwig, J. F. *J. Am. Chem. Soc.* **2014,** *136*, 4287.
24. Sadler, S. A.; Tajuddin, H.; Mkhalid, I. A. I.; Batsanov, A. S.; Albesa-Jove, D.; Cheung, M. S.; Maxwell, A. C.; Shukla, L.; Roberts, B.; Blakemore, D. C.; Lin, Z. Y.; Marder, T. B.; Steel, P. G. *Org. Biomol. Chem.* **2014,** *12*, 7318.
25. Robbins, D. W.; Hartwig, J. F. *Org. Lett.* **2012,** *14*, 4266.
26. Ding, M.-Y.; Steel, P. G. *unpublished results*.
27. Pabst, T. P.; Obligacion, J. V.; Rochette, E.; Pappas, I.; Chirik, P. J. *J. Am. Chem. Soc.* **2019**, *141*, 15378.